Power Systems

Naser Mahdavi Tabatabaei
Ersan Kabalci
Nicu Bizon *Editors*

Microgrid Architectures, Control and Protection Methods

Springer

Power Systems

Electrical power has been the technological foundation of industrial societies for many years. Although the systems designed to provide and apply electrical energy have reached a high degree of maturity, unforeseen problems are constantly encountered, necessitating the design of more efficient and reliable systems based on novel technologies. The book series Power Systems is aimed at providing detailed, accurate and sound technical information about these new developments in electrical power engineering. It includes topics on power generation, storage and transmission as well as electrical machines. The monographs and advanced textbooks in this series address researchers, lecturers, industrial engineers and senior students in electrical engineering. ** Power Systems is indexed in Scopus**

More information about this series at http://www.springer.com/series/4622

Naser Mahdavi Tabatabaei ·
Ersan Kabalci · Nicu Bizon
Editors

Microgrid Architectures, Control and Protection Methods

Springer

Editors
Naser Mahdavi Tabatabaei
Department of Electrical Engineering
Seraj Higher Education Institute
Tabriz, Iran

Nicu Bizon
Faculty of Electronics, Communications and Computers
University of Pitesti
Pitesti, Arges, Romania

Ersan Kabalci
Electrical and Electronics Engineering Department, Faculty of Engineering and Architecture
Nevsehir Haci Bektas Veli University
Nevsehir, Turkey

ISSN 1612-1287 ISSN 1860-4676 (electronic)
Power Systems
ISBN 978-3-030-23722-6 ISBN 978-3-030-23723-3 (eBook)
https://doi.org/10.1007/978-3-030-23723-3

This Springer imprint is published by the registered company Springer Nature Switzerland AG
The registered company address is: Gewerbestrasse 11, 6330 Cham, Switzerland

Dedicated to
all our teachers and colleagues
who enabled us to write this book,
and our family and friends
for supporting us all along

Foreword

There are specific interests for the integration of distributed generation systems and reliable consuming networks in the microgrid architectures. The microgrid topologies are designed as the innovative electrical systems, power distribution networks and also independent small power grids. The nature of microgrid operations includes ownership, reliability and locality. The microgrid development is mostly dependent on microprocessors and communication technologies to provide more complicated inverters and load controllers and also offer adequate bandwidth.

Microgrid control and protection based on different interfaces are also important concepts in combining power balancing, optimization and smart activating as grid-connected or islanded modes. The microgrid control and protection include the regulation of voltage and frequency and managing of real and reactive power for the generation units and energy storages.

The book generally explains the fundamentals and contemporary materials in microgrid architectures, control and protection. It will be very efficient for electrical engineers and researchers to have the book which contains important subjects in considering modeling, analysis and practice related to microgrids. The book comprises knowledge, theoretical and practical issues as well as up-to-date contents in these issues and methods for designing, controlling and protecting of AC–DC microgrid networks.

Some textbooks and monographs are previously presented for people who want to learn more on the microgrids. The worth of the present book is that it tries to put forward some practical ways for microgrid planning and modeling, control, protection, infrastructure, converters, energy storage systems, efficiencies, assessments and quality issues which are now more organized. The editors wisely designated the topics to be preserved, and the chapters written by well-recognized experts in the field are placed in three parts.

The book introduces the reader to the modeling, analysis, operation, control and protection of the microgrids. Then, the main subjects related to planning, converters, hybrid energy resources, energy management, adaptive and modified control and protection are presented and explained. The book also includes informative case studies and many instances.

The book can be used in the classroom, to teach microgrid courses to graduate students, and be suggested as further reading to undergraduate students in engineering sciences. It will also be a valuable information resource for the researchers and engineers concerned with microgrid issues or involved in the development of distributed generation applications.

May 2019

Academician Arif M. Hashimov
Institute of Physics
Azerbaijan National Academy of Sciences
Baku, Azerbaijan

Preface

The microgrid researches have been extensively increased and widespread since the last decade. The enhanced use of distributed generation, distributed energy resources, renewable energy sources, energy storage technologies and increased power requirements has promoted microgrid researches. The improvements and outcomes of microgrid researches facilitate to overcome power system problems related to resiliency, flexibility, stability, efficiency and capacity limitations. A crucial component of this new grid type is apparently power electronics devices interfacing sources and utility grid. This interface is required to provide control and protection features depending on device topologies and control software.

Moreover, the generated and converted power should meet the grid codes and should comply with international standards in terms of power quality, efficiency and sustainability. The purpose of this book is to present a broader view of emerging microgrid architectures, control and protection methods and communication systems, approaching the following subjects: (1) presenting detailed surveys for a wide variety of microgrid architectures and emerging microgrid approaches; (2) concepts and visualization of microgrid concepts and related power electronics applications for improved microgrids; (3) providing detailed knowledge on wireless and emerging communication methods used for control and protection issues in microgrids; (4) presenting the virtual inertia and energy storage systems that are key components of microgrid integration to utility grid; (5) contents on relation of smart grid and microgrid applications along IoT and wireless communication systems; and (6) discussions on the issues related to deployment and development of control, protection and communication technologies at future microgrid scope.

Microgrid Architectures, Control and Protection Methods is a book aimed to highlight the microgrid operation and planning issues using different methods which include planning and modeling, AC and DC hybrid microgrid, microgrid infrastructure, power electronic converters in microgrid, energy storage systems in microgrid, energy management in microgrids, PV microgrids, microgrid control strategies, intelligent and adaptive control in microgrid, optimal microgrid

operational planning, microgrid protection and automations, adaptive protection systems in microgrid, IEC 61850-based protection systems and also control and protection of smart microgrids.

A large number of specialists are joined as the authors of the chapters to provide their potentially innovative solutions and research related to microgrid operation, in order to be useful in developing updated approaches in electric power analysis, design and operational strategies. Several theoretical researches, case analysis and practical implementation processes are put together in this book that aims to act as research and design guides to help the graduates, postgraduates and researchers in electric power engineering and energy systems. The book presents significant results obtained by leading professionals from the industry, research and academic fields that can be useful to the variety of groups in specific areas analyzed in this book.

This book comprises 31 chapters structured in three parts as follows: Part I introduces in 12 chapters the microgrid architectures and the used power converters; Part II makes in 12 chapters a deep presentation of microgrid control systems; Part III highlights in 7 chapters the current issues of the microgrid protection systems. A brief introduction for readers on the contents of all chapters will be made below.

AC and DC microgrids and converters consisting of their modeling and operation are discussed in the chapters of Part I.

Chapter 1 presents an overview of microgrid concept, modeling, architectures and operation by presenting the main type of distributed energy resources (DERs) and networks based on renewable energy sources (RESs). The chapter also comprises a brief review of microgrid modeling studies based on the microgrid architectures and operation types in AC, DC and hybrid microgrid models.

Chapter 2 details the microgrid concepts by introducing the fundamentals of microgrids, with focus on microgrid planning and energy management considering the variability of the RES power due to environmental and weather conditions. The RES power is modeled using several different probability distributions, and the optimization strategies for microgrid planning have been proposed based on stochastic programming and deterministic mathematical models.

Chapter 3 explains the advantages and disadvantages of the microgrid architectures based on DC bus, AC bus, or hybrid DC and AC bus using modeling and case studies. The chapter consists of two parallel operated AC and DC microsystems including renewable AC sources of power, and AC–DC loads and power sources.

Chapter 4 details the DER concept and potential issues due to high penetration of DER-based microgrids with their technical characteristics in electrical power systems (EPSs) by presenting and discussing the main models for DER-based microgrids proposed in the literature.

Chapter 5 studies how the DERs dispersed throughout the network can be brought together based on the concept of virtual power plant (VPP), which turns them into active resources that function as a single centralized generating power plant, with the capacity to respond intelligently to variable load demand. The VPP

is a technical, operational and economic concept that is located in the digital part of the microgrids and provides facilities that allow greater flexibility of the EPS.

The power electronic converters have been detailed in Chaps. 6 and 7 in terms of AC–DC rectifiers, inverters (DC–AC converters) and DC–DC converters used in DC and AC microgrids. So, Chap. 6 analyzes the main types, circuit structures and functions of power electronic converters used in DC microgrid and highlights the major advantage of DC microgrids compared to AC microgrids. Then, Chap. 7 analyzes the main power electronic converters used in AC microgrid and highlights the major advantage of AC microgrids compared to DC microgrids. The chapters review the main performance indicators and standards for DC and AC microgrids, respectively, and the conclusions are supported by simulation performed for some topologies.

Chapter 8 explains the important role of the energy storage system (ESS) in enhancing the stability of grid-connected and islanded microgrid by modeling the power flow balance on DC or AC buses and including appropriate case studies. The standards IEC/ISO 62264 and IEEE 2000 related to interconnection of the wind turbine farms and photovoltaic systems into microgrids have been presented as well.

Chapter 9 shows the design and experimental investigations of a fuel cell (FC)–electrolyzer-based energy storage system integrated into a microgrid. The hydrogen-based ESS based on proton-exchange membrane (PEM) FC system and solid polymer electrolyzer seem to be the best alternative to store energy due to their simple structure, high power density, quick start, no moving parts and superior reliability and durability, low operating temperature and environmental aspects.

Chapter 10 analyzes the requirements for the energy management system (EMS), which are identified as follows: (1) determining the amount of produced/consumed energy by the generation units/consumers; (2) ensuring the generation and consumption balance; (3) ensuring compliance and implementation of the rules for connecting the microgrid to the upper distribution system; (4) optimal utilization of its existing resources; (5) minimizing the overall operational costs; (6) separating the microgrid from the upper grid in case of emergencies; and (7) providing convenient control strategy for re-connecting to the upper network after the islanded operation. The role of subsystems of the energy management system (such as communication systems and smart meters) is also discussed in the frame of the main EMSs proposed in the literature, highlighting the pro and cons of the centralized and decentralized EMSs. The supervisory control and data acquisition (SCADA) system can be a solution for decentralized EMSs.

Chapter 11 proposes a technical solution to improve the efficiency of a photovoltaic (PV) power plant within an area of seventy hectares through control, surveillance, metering and monitoring of the system from distance. The SCADA system offers information in real time for the control system about total and daily energy delivered (kWh), weather info, alarms, etc. The received information can be compared with the data stored in the same period of the past years, in order to establish the productive efficiency of the PV power plant.

Chapter 12 analyzes the extremum seeking control (ESC)-based global maximum power point tracking (GMPPT) control for PV microgrids under partially shaded conditions. The influence of photovoltaic array topologies to multimodal PV characteristic and new materials like ferrite nano-core–shell (NCS) multilayer used to construct efficient PV cells based on thin-film transistors are also highlighted.

Part II includes the control of AC and DC microgrids and related strategies, requirements and challenges.

Chapter 13 emphasizes on the current controlling strategies of power converters operating in different modes with AC microgrids, which has the main advantage of compatibility with the existing AC EPS. So, from control point of view, converters are classified as grid forming, grid supporting and grid feeding converter. Anyway, the complexity of reactive power control and frequency issues as stability and synchronization make the DC to be very attractive.

Chapter 14 introduces the centralized, decentralized and distributed DC microgrid architectures and their control. Also, the most used standards related to DC microgrids and cyber-physical system (CPS) related to the power system field are presented. The advanced control of the utility converter has been developed and simulated.

Chapter 15 deals with the basic principles of microgrid control analyzing the local control, central control and emergency control. Also, being the most used control into the microgrids, the hierarchical control is presented. Since centralized control to split the reactive and active power is costly and difficult to be implemented, the decentralized and distributed control techniques will be analyzed in the next chapters.

Chapter 16 discusses the advantages of the hierarchical control in the frame of distributed control systems used in microgrids. The droop-based control algorithms are analyzed, being considered to be the most effective in terms of the stability of network voltage and reactive power sharing.

Chapter 17 analyzes different intelligent and adaptive control techniques proposed in the literature as a response to the difficulty of controlling highly complex and indeterminate nonlinear systems. The chapter provides new designs, at the cutting edge of true intelligent control, and shows directions for future research to improve the real-world applications of the intelligent and adaptive control.

Chapter 18 deals with the basic principles of operating the microgrid in emergency conditions, by analyzing the load shedding, emergency and local control considering uncertainties. The chapter focuses on developing a coordination control algorithm using emergency demand response (EDR) resources and under-frequency load shedding (UFLS) methods considering various probabilistic scenarios. It is worth to mention that the emergence of smart metering system (SMS) has been implemented at the level of majority of distribution grid operators (DGOs) as real-time information about the consumed and produced electricity to take technical measures for efficiently operating the microgrid.

Chapter 19 analyzes the aforementioned solutions to be implemented in smart metering-based strategies for improving energy efficiency in microgrids. The new methods proposed for load modeling, phase load balancing and voltage control are tested using real microgrids.

Chapter 20 proposes the optimal microgrid operational planning (OMOP) approach for DERs, considering wind and photovoltaic power generations, combined heat and power generation units, electrical energy storages and interruptible loads. The OMOP based on a two-level optimization under system uncertainties has been detailed in this chapter.

Chapter 21 analyzes the outage problem that occurs due to weaknesses of the power system infrastructure or the occurrence of human or natural faults in the EPS. The self-healing is presented in this chapter as one of the main abilities of the smart grids to automatically retrieve system after fault occurrence or keep away system from critical conditions. So, the definition, requirements and challenges of self-healing are introduced, and some tools and methods like demand response, load shedding, distributed energy resources and autonomous microgrids which can facilitate self-healing process are assessed.

Chapter 22 further analyzes various droop-based control strategies and shows simulation of some prevalent ones to assess the strength and weakness of each approach. The droop control does not require communication infrastructure and reduces the complexity for implementation, less cost for system maintenance, which improves the reliability indices. Besides the droop controllers, the fuzzy logic (FL)-based controllers have been markedly developed in order to be used in various microgrid applications due to their simple structure, easy implementation and adaptive behavior.

Chapter 23 analyzes in detail the adaptive controlling mechanisms and dynamic efficiencies based on FL-based PID controller. Different control strategies based on fuzzy PID-type controller for controlling microgrids are also described and discussed in this chapter.

Chapter 24 proposes an innovative control structure of the reinforcement learning (RL) based on PID controller to enhance the frequency fluctuations of a hybrid microgrid with a high RESs penetration. The RL algorithms can be used to learn the optimal control policy from interaction with the environment of the system. It is worth mentioning the new applications of RL algorithms in EPS control.

As it was mentioned before, the chapters in Part III focus on microgrid protection techniques.

Chapter 25 introduces the microgrid protection techniques highlighting the close connection between the Internet of things (IoT) and the development of the smart grids. The methods for increasing the microgrid resilience to extreme disruptions and shocks posed by natural, man-made or random events are presented. The chapter presents protection solutions closely with international standards for both DC and AC networks, considering the technical requirements of the microgrids and by using different topology. Therefore, the conventional protection and control systems need to be improved to overcome current difficulties, offering reliable

protection and control for grid-connected and islanded microgrids, as will be shown in the next chapters.

Chapter 26 deals with the protection and automation requirements of the microgrids in the frame of smart grid, including the protection schemes and developments in the related fields. The chapter concentrates on devolution of power generation and the conversion of the radial distribution network into a microgrid. It also discusses on the protection and control requirements of a microgrid, islanding detection and management scheme.

Chapter 27 presents the fault detection methods and protection devices in low-voltage DC (LVDC), medium-voltage DC (MVDC) and high-voltage DC (HVDC) grids. The main protection schemes are presented regarding DC microgrids. The fault detection methods are surveyed considering voltage prediction, disturbance detection, and fault classification and locating methods.

Chapter 28 analyzes the solutions for protecting smart grids using the protocol IEC 61850 based on intelligent electronic devices (IEDs). Based on case studies, the chapter presents the remote-controlled reclosed scheme, the adaptive protection of a distributed system based on the loop automation scheme and the main advantages for the consumers by implementing the restoration scheme.

Chapter 29 presents the protection techniques based on the IEC 61850 protocol using case studies for data communication systems between substations. The IEC 61850 is implemented for real-time communication between IEDs based on Generic Object Oriented Substation Event (GOOSE) messages.

Chapter 30 highlights the main power quality issues in the microgrid, and solutions to handle these issues and their operating principle are explained. Load pulses are frequently encountered in microgrid and need to be mitigated using appropriate control of hybrid energy storage system (ESS) based on different power storage devices such as the ultracapacitors (UCs) stacks, superconducting magnetic energy storage (SMES) devices and high-speed flywheel energy systems (FESs).

Chapter 31 approaches the control and protection of the smart microgrids using the concepts from IoT and highlights the IoT role in creating and developing smart microgrids, including benefits, challenges and risks, in order to reveal a variety of mechanisms, methods and procedures built to control and protect smart microgrids. Thus, microgrids must benefit by large opportunity to implement the IoT mechanisms, because they are composed of equipment that demands sensing, connectivity and analytics technologies to operate at the highest level.

Therefore, the proposed book tries to clear the aforementioned approaches, by presenting intuition explanations about principles and application of microgrid structure and operation. Moreover, the book tries to put forward some practical ways for microgrid analysis.

Moreover, the book will be helpful for the future research to be done in the field of electrical engineering and communication engineering. It also explores the recent progress on several microgrid control and protection technologies and their performance evaluation. The book has the wider coverage ranging the topics from essentials of microgrids to enhanced communication systems such as wireless and Internet of things (IoT). It can also help in understanding the role of emerging

communication systems such as the Internet of things (IoT), wireless communication and IEC 61850-based networks in microgrids.

We hope that this book will be helpful for young researchers and practitioners in the area of electrical engineering. The editors and authors made all efforts to have a good book and hope interested readers to enjoy by reading this book and to be satisfied by its content.

Tabriz, Iran — Naser Mahdavi Tabatabaei
Nevsehir, Turkey — Ersan Kabalci
Pitesti, Romania — Nicu Bizon

Contents

Contributors

Ali Jafari Aghbolaghi Zanjan Electric Energy Distribution Company, Zanjan, Iran;
Sanat Modern AfRaTech Sobhan Company, Zanjan, Iran;
Andishmand Shomal-Gharb Engineering Consultancy, Zanjan, Iran;
Electrical Engineering Department, Seraj Higher Education Institute, Tabriz, Iran

Farid Hamzeh Aghdam Electrical Engineering Department, Faculty of Engineering, Azarbaijan Shahid Madani University, Tabriz, Iran

Horia Andrei Doctoral School of Engineering Sciences, University Valahia of Targoviste, Targoviste, Romania

Paul Cristian Andrei Department of Electrical Engineering, Polytechnic University of Bucharest, Bucharest, Romania

Iulian Nicusor Arama Department of Automation and Electrical Engineering, Dunarea de Jos University of Galati, Galati, Romania

Morteza Kalantari Azad Sanat Modern AfRaTech Sobhan Company, Zanjan, Iran;
Andishmand Shomal-Gharb Engineering Consultancy, Zanjan, Iran

Florin Babarada Department of Electronic Devices, Circuits and Architectures, Faculty of Electronics, Telecommunications and Information Technology, Polytechnic University of Bucharest, Bucharest, Romania

Cristian Andrei Badea Interface Engineering, Bucharest, Romania

Javier Bilbao Applied Mathematics Department, University of the Basque Country, Bilbao, Spain

Fernando Georgel Birleanu Faculty of Electronics, Communications and Computers, Doctoral School, University of Pitesti, Pitesti, Romania

Nicu Bizon Department of Electronics, Computers and Electrical Engineering, Faculty of Electronics, Communications and Computers, University of Pitesti, Pitesti, Romania;
Polytechnic University of Bucharest, Bucharest, Romania

Amin Mokari Bolhasan Electrical Engineering Department, Faculty of Engineering, Azarbaijan Shahid Madani University, Tabriz, Iran

Narges Sadat Boushehri Department of Management, Taba Elm International Institute, Tabriz, Iran

Eugenio Bravo Applied Mathematics Department, University of the Basque Country, Bilbao, Spain

Razvan Buhosu Department of Automation and Electrical Engineering, Dunarea de Jos University of Galati, Galati, Romania

Mrudurajsinh Chudasama Marwadi University, Rajkot, India

Florentina Magda Enescu Department of Electronics, Computers and Electrical Engineering, Faculty of Electronics, Communications and Computers, University of Pitesti, Pitesti, Romania

Marian Gaiceanu Department of Automation and Electrical Engineering, Dunarea de Jos University of Galati, Galati, Romania

Olatz Garcia Applied Mathematics Department, University of the Basque Country, Bilbao, Spain

Naci Genc Department of Electrical and Electronics Engineering, Van Yuzuncu Yil University, Van, Turkey

Alireza Ghafouri Electrical Engineering Department, Sari Branch, Islamic Azad University (IAU), Sari, Iran

Iulian Ghenea Doctoral School of Fundamental and Engineering Sciences, Dunarea de Jos University of Galati, Galati, Romania

Gheorghe Grigoras Power System Department, Electrical Engineering Faculty, "Gheorghe Asachi" Technical University of Iasi, Iasi, Romania

Alireza Heidari School of Electrical Engineering and Telecommunication, University of New South Wales, Sydney, Australia

Ioan Cristian Hoarca National Research and Development Institute for Cryogenics and Isotopic Technologies, Râmnicu Vâlcea, Romania

Ires Iskender Department of Electrical and Electronics Engineering, Cankaya University, Ankara, Turkey

Ovidiu Ivanov Power System Department, Electrical Engineering Faculty, "Gheorghe Asachi" Technical University of Iasi, Iasi, Romania

Rajendrasinh Jadeja Marwadi University, Rajkot, India

Ersan Kabalci Department of Electrical and Electronics Engineering, Faculty of Engineering and Architecture, Nevsehir Haci Bektas Veli University, Nevsehir, Turkey

Navid Taghizadegan Kalantari Electrical Engineering Department, Faculty of Engineering, Azarbaijan Shahid Madani University, Tabriz, Iran

Pragma Kar Department of Information Technology, Jadavpur University, Kolkata, India

Ahmet Karaarslan Department of Electrical and Electronics Engineering, Yildirim Beyazit University, Ankara, Turkey

Ogtay Zaur oglu Karimov Cleaner Production and Energy Efficiency Center, Baku, Azerbaijan

Gagandipsinh Khanduja Marwadi University, Rajkot, India

Naser Mahdavi Tabatabaei Electrical Engineering Department, Seraj Higher Education Institute, Tabriz, Iran;
Department of Management, Taba Elm International Institute, Tabriz, Iran

Elena Manea National Institute for Research and Development in Microtechnologies—IMT Bucharest, Bucharest, Romania

Ioan Marinescu Doctoral School of Engineering Sciences, University Valahia of Targoviste, Targoviste, Romania

Adriana Marinoiu National Center for Hydrogen and Fuel Cell, National Research and Development Institute for Cryogenics and Isotopic Technologies, Râmnicu Vâlcea, Romania

Dan Eduard Mihaiescu Department of Organic Chemistry "Costin Nenitescu", Faculty of Applied Chemistry and Material Science, Polytechnic University of Bucharest, Bucharest, Romania

Mohammad Moradzadeh Electrical Engineering Department, Shahid Rajaee Teacher Training University, Tehran, Iran

Bogdan Constantin Neagu Power System Department, Electrical Engineering Faculty, "Gheorghe Asachi" Technical University of Iasi, Iasi, Romania

Moein Aldin Parazdeh Electrical Engineering Department, Shahid Rajaee Teacher Training University, Tehran, Iran

Catalin Parvulescu National Institute for Research and Development in Microtechnologies—IMT Bucharest, Bucharest, Romania

Mircea Raceanu National Center for Hydrogen and Fuel Cell, National Research and Development Institute for Cryogenics and Isotopic, Râmnicu Vâlcea, Romania; Polytechnic University of Bucharest, Bucharest, Romania

Ainollah Rahimi Sadegh Faculty of Electrical Engineering, Shahid Beheshti University, A.C., Tehran, Iran

Nariman Rahmanovich Rahmanov Cleaner Production and Energy Efficiency Center, Baku, Azerbaijan

Sajad Najafi Ravadanegh Electrical Engineering Department, Faculty of Engineering, Azarbaijan Shahid Madani University, Tabriz, Iran

Cristian Ravariu Department of Electronic Devices, Circuits and Architectures, Faculty of Electronics, Telecommunications and Information Technology, Polytechnic University of Bucharest, Bucharest, Romania

Carolina Rebollar Applied Mathematics Department, University of the Basque Country, Bilbao, Spain

M. Emrah Seker Department of Electrical and Electronics Engineering, Yildirim Beyazit University, Ankara, Turkey

Mehrdad Setayesh Nazar Faculty of Electrical Engineering, Shahid Beheshti University, A.C., Tehran, Iran

Hossein Shayeghi Department of Electrical Engineering, University of Mohaghegh Ardabili, Ardabil, Iran

Maria Stanca Department of Organic Chemistry "Costin Nenitescu", Faculty of Applied Chemistry and Material Science, Polytechnic University of Bucharest, Bucharest, Romania

Marilena Stanculescu Department of Electrical Engineering, Polytechnic University of Bucharest, Bucharest, Romania

Mozhgan Tarantash Sanat Modern AfRaTech Sobhan Company, Zanjan, Iran

Tapankumar Trivedi Marwadi University, Rajkot, India

Omer Usta Istanbul Technical University and Entes Electronics, Istanbul, Turkey

Concepcion Varela Applied Mathematics Department, University of the Basque Country, Bilbao, Spain

Mihai Varlam National Center for Hydrogen and Fuel Cell, National Research and Development Institute for Cryogenics and Isotopic Technologies, Râmnicu Vâlcea, Romania

Amit Ved Marwadi University, Rajkot, India

Abdollah Younesi Department of Electrical Engineering, University of Mohaghegh Ardabili, Ardabil, Iran

Pegah Zafari Electrical Engineering Department, Shahid Rajaee Teacher Training University, Tehran, Iran

Ali Zangeneh Electrical Engineering Department, Shahid Rajaee Teacher Training University, Tehran, Iran

Mehmet Zile Mersin University, Mersin, Turkey

Abbreviations and Acronyms

5G	5th Generation
AAFC	Aqueous Alkaline Fuel Cell
AC	Alternative Current
ACE	Area Correction Error
ACMG	Alternating Current Microgrid
ACS	Ant Colony System
ADC	Analog-to-Digital Converter
ADM	Alternating Direction Method
ADN	Active Distribution Network
AE	Aqua Electrolyzer
AES	All-Electric Ship
AFC	Alkaline Fuel Cell
AGC	Automatic Generation Control
AHC	Adaptive Heuristic Critic
AI	Artificial Intelligence
AMI	Advanced Metering Infrastructure
ANN	Artificial Neural Network
ANSI	American National Standards Institute
aPESC	Asymptotic PESC
aPESCH1	Asymptotic PESC based on FFT
APP	Auxiliary Problem Principle
AR	Average Reward
ARR	Automatic Release of Reserve
AS	Ancillary Services
ATS	Automatic Transfer Switch
AVR	Automatic Voltage Regulator
BCBG	Bottom-Contact Bottom Gate
BESS	Battery Energy Storage Systems
BOS	Balance of System
BPDC	Bipolar DC

BPF	Band-Pass Filter
BTC	Bay Template Configurator
CAA	Central Agent Architecture
CAES	Compressed Air Energy Storage
CAULSC	Centralized Adaptive UFLS Controller
CB	Circuit Breaker
CC	Central Controller
CCM	Continuous Transmission Mode
CDF	Cumulative Distribution Function
CEI	Italian Electrotechnical Committee
CEMS	Central Energy Management System
CHP	Combined Heat and Power
CIU	Communication Interface Unit
CNT	Carbon Nanotube
CPP	Critical Peak Pricing
CPS	Cyber-Physical System
CPU	Central Processing Unit
CRM	Critical Transmission Mode
CS	Centralized System
CSI	Current Source Inverter
CT	Current Transformer
CU	Control Unit
CUF	Current Unbalance Factor
DA	Day Ahead
DA	Distribution Automation
DAA	Decentralized Agent Architecture
DAB	Dual Active Bridge
DC	Direct Current
DCM	Discontinuous Conduction Mode
DCMG	Direct Current Microgrid
DCS	Distributed Control System
DDoS	Distributed Denial of Service
DE	Differential Evolution
DEG	Diesel Engine Generator
DER	Distributed Energy Resource
DES	Distributed Energy Storage
DFIG	Double-Fed Induction Generator
DG	Distributed Generation
DGR	Distributed Generation Resource
DLC	Direct Load Control
DLS	Dynamic Light Scattering
DLSC	Determined Load Shedding Calculator
DMMA	Data Model Manager Application
DMS	Distribution Management System
DN	Distribution Network

DNO	Distribution Network Operator
DNP	Distributed Network Protocol
DO	Distribution Operator
DOD	Depth of Discharge
DOE	Department of Energy
DOR	Directional Overload Relay
DoS	Denial of Service
DOS	Density of States at a Semiconductor Surface
DP	Disconnection Priority
DPC	Direct Power Control
DR	Demand Response
DRPs	Demand Response Programs
DS	Decentralized System
DS	Distribution System
DSE	Distribution State Estimator
DSG	Dispersed Storage and Generation
DSI	Distributed Signaling Interface
DSM	Demand-Side Management
DSO	Distribution System Operator
DSS	Decision Support System
DSTATCOM	Distribution STATCOM
DVR	Dynamic Voltage Restorer
E/P	Energy-to-Power Ratio
EA	Energy Arbitrage
EA	Evolutionary Algorithms
EDG	Electric Distribution Grid
EDP	Economic Dispatch Problem
EDR	Emergency Demand Response
EDS	Electrical Distribution System
ELZ	Electrolyzer
EMI	Electromagnetic Interference
EMS	Energy Management System
EN	European Standard
ENS	Energy Not Supplied
ENSC	Energy Not-Supplied Cost
EPRI	Electric Power System Research Institute
ES	Expert System
ESC	Extremum Seeking Control
ESD	Energy Storage Device
ESM	Energy Surety Microgrid™ Technology
ESS	Electrical Storage System
ESS	Energy Storage System
EU	European Union
EUE	Maximum Permissible Level of Unmet Power
EV	Electrical Vehicle

FAR	Frequency Ancillary Reserves
FB	Full Bridge
FC	Fuel Cell
FCAS	Frequency Control Ancillary Services
FCTS	Fuel Cell Test Stand
FEH	Fire Emblem Heroes
FESS	Flywheel Energy Storage System
FET	Field-Effect Transistor
FFT	Fast Fourier Transform
FL	Fuzzy Logic
FLC	Fuzzy Logic Controller
FLES	Flywheel Energy System
FLISR	Fault Location Isolation Service Restoration
FLL	Frequency-Locked Loop
FPID	Fuzzy PID
FTD	Frequency's First Time Derivative
GA	Genetic Algorithm
GAAS	Gallium Arsenide
GAPC	Grid Active Power Converter
GaPESC	Global aPESC scheme based on one BPF
GaPESCbpf	Global aPESC scheme based on two BPFs
GaPESCd	Global aPESC scheme based on derivative operator
GaPESCH1	Global aPESC scheme based on FFT
GCI	Grid-connected Inverter
Gd	Signal which modulates the dither
GDB	Governor Dead Band
GIO	Generic Inputs/Outputs
GMPP	Global Maximum Power Point
GMPPT	Global Maximum Power Point Tracking
GOOSE	Generic Object Oriented Substation Event
GPS	Global Positioning System
GRC	Generation Rate Constraint
GTG	Gas Turbine Generator
GTO	Gate Turn-Off Thyristor
GUI	Graphical User Interface
H1	First Harmonic of a Signal
HAA	Hierarchical Agent Architecture
HAN	Home Area Network
HC	Hill Climbing
HEM	Home Energy Management
HERIC	High-Efficiency Reliable Inverter Concept
HESS	Hybrid Energy Storage System
HFAC	High-Frequency AC
HHVCB	Hybrid HV Circuit Breaker
HMG	Hybrid Microgrid

HMI	Human–Machine Interface
HOMO	Highest Occupied Molecular Orbital
HPF	High-Pass Filter
H-PLB	Heuristic Phase Load Balancing
HPS	Hybrid Power System
HRE	High Reliable and Efficient Power Inverter
HR-ZVR	Hybrid Zero-Voltage Rectifier
HSFES	High-Speed Flywheel Energy Storage
HSS	Hybrid Storage System
HV	High Voltage
HVAC	Heating, Ventilation, and Air Conditioning
HVDC	High-Voltage DC
IBP	Incentive-Based Program
IC	Incremental Conductance
ICC	Incremental Cost Consensus
ICCB	Isolated Case CB
ICP	Internet Communication Protocol
ICT	Information and Communication Technology
IEA	International Energy Agency
IEC	International Electrotechnical Commission
IED	Intelligent Electronic Device
IEEE	Institute of Electrical and Electronics Engineers
IGBT	Insulated-Gate Bipolar Transistor
ILs	Interruptible Loads
IO	Inputs/Outputs
IoT	Internet of Things
IP	Internet Protocol
IT	Information Technology
ITAE	Integral of Time Multiplied by Absolute Error
ITOC	Inverse Time Overcurrent
LC	Local Control
LCA	Life Cycle Assessment
LD	Logic Device
LED	Light-Emitting Diode
LF	Load Flow
LFAC	Low-Frequency AC
LFC	Load Frequency Controller
LMPP	Local Maximum Power Point
LN	Logical Node
LP	Linear Programming
LQR	Linear–Quadratic Regulator
LS	Load Shedding
LSFES	Low-Speed Flywheel Energy Storage
LUMO	Lowest Unoccupied Molecular Orbital
LV	Low Voltage

LVDC	Low-Voltage DC
LVG	Low-Voltage Grid
LVRT	Low Voltage Ride Through
M2M	Machine to Machine
MAC	Media Access Control
MACCB	Mechanical AC Circuit Breaker
MAPE	Mean Absolute Percentage Error
MAS	Multi-Agent System
MC	Microgeneration Control
MCB	Mechanical Circuit Breaker
MCCB	Molded Case CB
MCCS	Microgrid Central Control System
MCFC	Molten Carbonate Fuel Cell
MCL	MiCOM Configuration Language
MCS	Microsource Control System
MCT	MOS-Controlled Thyristor
MDMS	Meter Data Management System
MEC	Microgrid Emergency Control
MEMS	Microgrid Energy Management System
MF	Membership Function
MG	Microgrid
MGCC	Microgrid Central Controller
MGMS	Microgrid Management System
MGO	Microgrid Operator
MGOS	Microgrid Operation State
MILP	Mixed Integer Linear Programming
MINLP	Mixed Integer Nonlinear Programming
MLI	Multilevel Inverter
MMC	Multi-Modular Converter
MMS	Manufacturing Messaging Specification
MN	Micro-Network
MOSFET	Metal–Oxide–Semiconductor Field-Effect Transistor
MP	Multilayer Perception
MPC	Model Prediction Control
MPI	Message Passing Interface
MPP	Maximum Power Point
MPPT	Maximum Power Point Tracking
MU	Merging Unit
MUT	Master User Terminal
MV	Mean Value
MV	Medium Voltage
MVA	Mega-Volt-Ampere
MVDC	Medium-Voltage DC
NCS	Nano-Core–Shell
NCS-TFT	Thin Film Transistors with Nano-Core-Shell materials

NLP	Nonlinear Programming
NOCT	Normal Cell Operating Temperature
NPC	Neutral Point Diode Clamped
OC	Operating and Contingency
OECD	Organisation for Economic Co-operation and Development
oH5	Optimized H5
OMOP	Optimal Microgrid Operational Planning
OPF	Optimal Power Flow
OPL	Overhead Power Line
OSC	Organic Solar Cell
OSI	Open Systems Interconnection
OTFT	Organic Thin-Film Transistor
P&O	Perturb and Observation
PABA	Para-Aminobenzoic Acid
PAFC	Phosphoric Acid Fuel Cell
PBP	Price-Based Program
PC	Primary Control
PCC	Point of Common Coupling
PCE	Power Conversion Efficiency
PCPM	Predictor-Corrective Proximal Multiplier Method
PD	Physical Device
PDF	Probability Density Function
PE	Protective Earth
PEM	Proton-Exchange Membrane
PEMFC	Proton-Exchange Membrane Fuel Cell
PESC	Perturbed-Based Extremum Seeking Control
PEV	Plug-in Electric Vehicle
PFC	Power Factor Correction
PFR	Primary Frequency Regulating
PG	Power Grid
PHC	Percent of the Hit Count
PHES	Pumped Heat Electrical Storage
PI	Proportional–Integral
PID	Proportional–Integrative–Derivative
PLC	Power Line Communication
PLL	Phase-Locked Loop
PLSC	Pre-determined Load Shedding Calculator
PMSG	Permanent Magnet Synchronous Generator
PMU	Phasor Measurement Unit
PP	Pre-disturbance Preparation
PPI	Payment Protection Insurance
PQ	Power Quality
PR	Proportional Resonance
PS	Power System
PSC	Partially Shaded Condition

PSCC	Power System Control Center
PSH	Pumped-Storage Hydropower
PSO	Particle Swarm Optimization
PV	Photovoltaic
P-V	Power–Voltage
PVGIS	Photovoltaic Geographical Information System
PWM	Pulse-Width Modulation
QE.EXCITON	Absorbed Photon Fraction that Generates Singlet Excitons
QPSK	Quadrature Phase Shift Keying
R&D	Research and Development
RA	Requirement Analysis
RAM	Random Access Memory
RAR	Rapid Auto-Reclosure
RCC	Ripple Correlation Control
RCISS	Reference Control Input and Support System
RCMU	Residual Current Monitoring Unit
RCP	Reactive Power Compensation Process
RER	Renewable Energy Resource
RES	Renewable Energy Source
RL	Reinforcement Learning
RMS	Root-Mean-Square
RMSE	Root-Mean-Square Error
ROCOF	Rate of Change of Frequency
RS	Regulation Service
RT	Real Time
RTP	Real-Time Pricing
RTU	Remote Terminal Unit
S.DISSOC	Singlet Dissociation Model
SA	Simulated Annealing
SAIDI	System Average Interruption Duration Index
SAIFI	System Average Interruption Frequency Index
SAS	Substation Automation System
SBO	Select Before Operation
SC	Short Circuit
SC	SuperCapacitor
SCADA	Supervisory Control and Data Acquisition
SCL	Substation Configuration Language
SEM	Scanning Electron Microscopy
SF	State Feedback
SFCL	Superconductive Fault Current Limiter
SFR	System Frequency Response
SFRF	Stator Flux Reference Frame
SG	Smart Grid
SGF	Sensible Ground Fault
SGS	Smart Grid System

SiC	Silicon Carbide
SLPM	Standard Liter Per Minute
SM	Smart Meter
SMES	Superconducting Magnetic Energy Storage
SMS	Smart Metering System
SNL	Sandia National Laboratories
SNTP	Simple Network Time Protocol
SoC	State of Charge
SOFC	Solid Oxide Fuel Cell
SP	Supply Point
SPWM	Sinusoidal Pulse Width Modulation
SQGA	Species-based Quantum Particle Swarm Optimization
SR	Spinning Reserve
SRH	Shockley–Read–Hall Recombination Rate Model
SSA	Salp Swarm Algorithm
SSCB	Solid-State Circuit Breaker
STPS	Solar Thermal Power Station
SVM	Space Vector Modulation
SV-PWM	Space Vector Pulse-Width Modulation
SVRF	Stator Voltage Reference Frame
TC57	Technical Committee 57
TCP/IP	Transmission Control Protocol/Internet Protocol
TFT	Thin-Film transistor
THD	Total Harmonic Distortion
TLP	Typical Load Profile
ToUT	Time-of-Use Tariff
TP	Touch Panel
TP-GAPC	Three-Phase Grid Active Power Converter
TS	Transformer Station
UC	UltraCapacitor
UFLS	Under-Frequency Load Shedding
UPDC	Unipolar DC
UPQC	Unified Power Quality Conditioner
UPS	Uninterruptible Power Supply
V2G	Vehicle-to-Grid
VCO	Voltage-Controlled Oscillator
VDC	Voltage Droop Control
VIC	Virtual Inertia Control
VLAN	Virtual Local Area Network
VOC	Voltage Oriented Control
VPD/FQB	P-V Droop Controller with Q-f Boost
VPP	Virtual Power Plant
VSC	Voltage Source Converter
VSI	Voltage Source Inverter
VT	Voltage Transformer

WACS	Wide Area Control System
WAMPAC	Wide Area Monitoring, Protection and Control Systems
WAMS	Wide-Area Measurement Systems
WAMS	Wide-Area Monitoring Systems
WAN	Wide Area Network
WAPS	Wide Area Protection Systems
WECS	Wind Energy Conversion System
WG	Wind Generator
WPD	Weibull Probability Distribution
WRIG	Wound Rotor Induction Generator
WSN	Wireless Sensor Network
WSOS	Windows Switchgear Operating System
WT	Wind Turbine
WTG	Wind Turbine Generation
WWTP	Wastewater Treatment Plant
XCBR	Class Defines the Properties of a Breaker
XML	Extensible Markup Language
ZVR	Zero Voltage Regulation
ZVS	Zero-Voltage Switch

Part I
Microgrid Architectures and Power Electronics

Chapter 1
Overview of Microgrid

Naser Mahdavi Tabatabaei, Ersan Kabalci and Nicu Bizon

Abstract The gradual decrement of fossil fuels, low energy efficiency and environmental problems met all over the world has led to several power system researches. These problems have promoted researches on alternative energy sources such as wind energy, solar photovoltaic, fuel cells, combined heat and power (CHP) systems, and micro turbines on the contrary of conventional resources. Moreover, the integration of renewable energy sources (RESs) to existing power grid is taken into account as a reliable and robust solution to aging generation, transmission and distribution systems. The innovative researches have brought a new concept as on-site generation or distributed generation at load sites. The utilized resources in this generation concept are later called as distributed energy resources (DERs) implying for a wide variety of power sources, and the generation type is named as distributed generation (DG). This chapter presents an introduction to microgrid concept by including distributed generation and active distribution networks, several DERs such as synchronous generator based and RES based resources, microgrid architectures, operation principles of microgrid, microgrid modeling studies, control and protection issues of microgrid.

Keywords Microgrid · Active distribution network · Renewable energy sources · Distributed generation · Information and communication technologies · Hierarchical control

N. Mahdavi Tabatabaei (✉)
Electrical Engineering Department, Seraj Higher Education Institute, Tabriz, Iran
e-mail: n.m.tabatabaei@gmail.com

E. Kabalci
Department of Electrical and Electronics Engineering, Faculty of Engineering and Architecture, Nevsehir Haci Bektas Veli University, Nevsehir, Turkey
e-mail: kabalci@nevsehir.edu.tr

N. Bizon
Department of Electronics, Computers and Electrical Engineering, Faculty of Electronics, Communications and Computers, University of Pitesti, Pitesti, Romania
e-mail: nicu.bizon@upit.ro

N. Mahdavi Tabatabaei et al. (eds.), *Microgrid Architectures, Control and Protection Methods*, Power Systems,
https://doi.org/10.1007/978-3-030-23723-3_1

1.1 Introduction

The microgrid is defined as a group of power generating sources and loads that are operated in a separated network where they can be used in island mode or by integrating to utility grid. The grid connection and disconnection are performed according to economical and technical requirements. The distributed energy resources (DERs) along a microgrid are comprised by numerous independently controlled power generating sources in order to constitute a reliable and flexible grid infrastructure. This operation perspective ensures the sustainability of microgrid even though some of the sources leave from generation cycle. The excessive generation is managed by using energy storage systems (ESSs) and power feeding to utility grid. The installed power capacity of microgrids vary from a few kilowatts to megawatts. The main installation aim on microgrids is providing power to consumers at remote areas, critical industrial and military plants. The decreasing fossil fuels, power quality issues, resiliency and flexibility problems of existing grid infrastructure, and degraded network structures have promoted grid improvements and microgrid researches. The appropriately designed microgrids are key infrastructures to improve reliability and resiliency of utility grid by generating a back-up system against grid faults. The fundamental components of microgrids are isolation and protection devices at point of common coupling (PCC), DERs including regular rotating machines and renewable energy sources (RESs) as solar, wind, fuel cell, and combined heat and power (CHP) plants, and microgrid controllers that are responsible for local and distributed control operations [1–3].

The microgrids are classified into five categories as commercial, community, campus, military, and remote microgrids. The commercial or industrial microgrids are generally designed to operate in grid-connected mode to decrease demand and costs. They also provide a backup system to prevent effects of faulty operation conditions. The community microgrids are improved to enhance stability of utility grid while campus microgrids are installed by individual institutions such as colleges, hospitals, and industrial plants due to featured load types and uninterruptible power supply requirements. The military microgrids are implemented in the places where physical and cyber security are required. These types of microgrids can be remote as others installed in rural places where utility grid is not available. Most of the remote microgrids are operated in islanded mode and supplied with diesel generators in addition to RESs. Although each microgrid types are improved to meet particular requirements, the grid connection should be performed by following several international standards. The IEEE Std 1547-2003 (*Standard for Interconnecting Distributed Resources with Electric Power Systems*) is one of the forthcoming international standards that microgrids should comply for interconnection. The IEEE Std 1547-2003 standard provides guidance for voltage and frequency control operations, grounding requirements, islanding preventions, performance operations, test conditions, and maintenance requirements [1, 4].

An approach called Integrated Grid Benefit-Cost Analysis Framework for Microgrids has been proposed by Electric Power Research Institute (EPRI) for guidance

on DER sizing and technology use in microgrid desings. The framework model of EPRI has been improved for advicing on technical and financial analysis of microgrid modelling based on layered infrastructure. The microgrid design requires comprehensive controllers in addition to DERs that are comprising the infrastructure. The microgrid controllers also should comply with several international standards that IEEE Std 2030.7 (*IEEE Standard for the Specification of Microgrid Controllers*) is one of the most widely followed one. The IEEE Std 2030.7 defines technical requirements for microgrid controllers and fundamental specifications of microgrid energy management system (MEMS). Therefore, this standard provides guidance for two main control functions of transition and dispatch areas. The core control functions that are defined for microgrids enable them to operate in autonomous islanded operation mode or grid-connected operation mode. The microgrid control system should provide instantaneous control and energy management features to provide automatic transition between grid-connected and islanded operation modes. The transition from islanded mode to grid-connected operation mode should be managed by resynchronization and reconnection controls. The power controls are also required to manage active and reactive power generation and consumption that are managed by energy management systems [1, 5].

The controllers are involved to operate microgrids in a standardized, interoperable and scalable infrastructure. The international standards ensure interoperability of various microgrids that are structured by using wide variety of sources, controllers, and commercial devices. The integration or disconnection of sources and loads to microgrid also require dedicated central and local controllers to ensure distributed generation (DG) along microgrid. Therefore, another standardization is required to evaluate performance of microgrid controllers. IEEE Std 2030.8 (*Standard for the Testing of Microgrid Controllers*) provides guidance on controller testing equipments, controller functions in grid-connected and islanded operation modes, power flow managements, local control functions, and load management issues [1].

The block diagram of a typical microgrid infrastructure is illustrated in Fig. 1.1. The dc and ac DERs are integrated to ac bus of microgrid by using appropriate power converter devices. Each source is associated with a circuit breaker (CB) to ensure disconnection control for any maintenance or fault situation. The critical loads and DERs are individually controlled by microgrid central controller (MGCC) that improves overall efficiency and reliability of entire microgrid. The MGCCs are classified into two types as AC controllers and DC controllers considering their operation area along the microgrid.

This chapter presents distribution network structure and active distribution network structures that comprise the microgrid infrastructure. The DERs such as synchronous generator-based sources and RES based sources such as wind turbines, solar power plants, biomass plants, fuel cells, and ESSs are also presented in the following sections of this chapter.

Afterwards, the microgrid architectures and operation types are reviewed in AC, DC and hybrid microgrid models. A bried review of microgrid modelling studies have also been presented in this chapter.

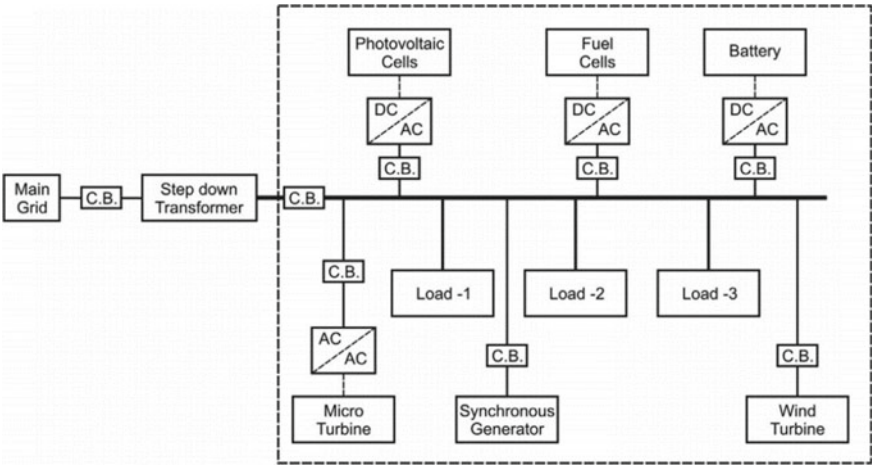

Fig. 1.1 A typical microgrid with sources and control structure [6]

1.2 Distributed Generation and Active Distribution Network

It is obvious that the use of fossil fuel-based energy sources adversely effects the environment by increasing global warming risk. Therefore, the use rate of conventional power generation systems that are based on fossil-fuels is targeted to be decreased to prevent pollution and global warming. The governments and authorities confirming that RES utilization decreases this risk encourage power generation industry and individuals to participate in DG cycle. The RESs are key component of DG infrastructure since they can be integrated to any system at desired scales from a few kWs to MW levels. Although there is a wide variety of RES option could be considered for installing a DG plant, the wind and solar power plants are the most suitable sources among others. The particular requirements of wind and solar plants are remarkably lower than other sources and it is easy to tackle dependencies of these sources. Thus, wind and solar power plants dominate DER type in any microgrid infrastructure. This situation has been also verified by Global Status Report of REN21 Secretariat as shown in Fig. 1.2. The installed RES capacity in China is around 258 GW that is massively comprised by wind and solar photovoltaic (PV) systems. Similarly, wind power-based RES plants cover 27% electricity demand of Ireland, 24% of Portugal, and 19.7% of Cyprus. On the other hand, solar PV based plants cover 7.3% of electricity demand in Italy and 6.4% demand in Germany [7].

On the other hand, share of wind power among other sources was over than 50% of Denmark in 2015 [8]. It is known that the technical challenges and environmental effects of aging convention grid can be tackled by implementing large scale, sophisticated and heterogeneous power plants. Thus, the drawbacks of centralized generation can also be eliminated owing to flexibility and resiliency of distributed generation

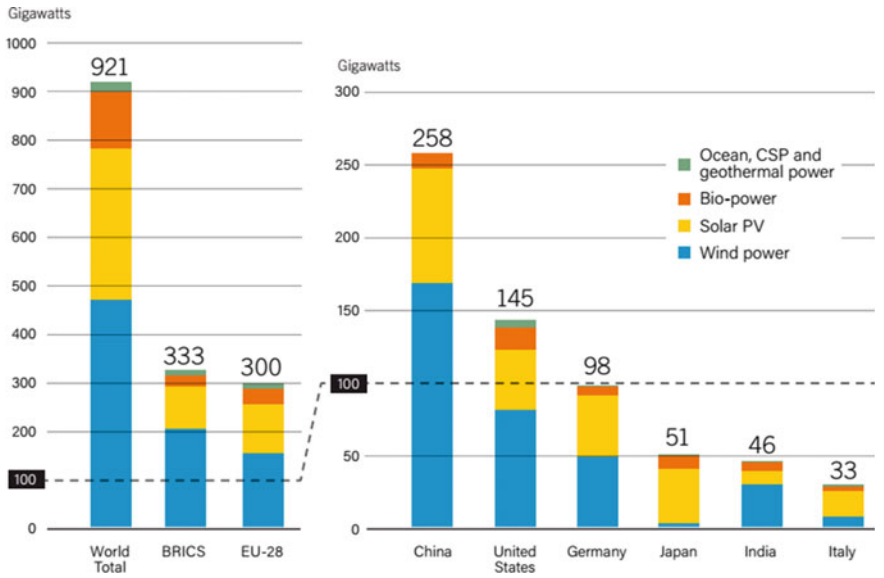

Fig. 1.2 RES capacities and diversity around the world [7]

systems. The contributions of DERs and DG systems are achieved by improving microgrid infrastructures [9].

The conventional utility grid has been planned to operate in any type of radial, mesh or network distribution networks. Each distribution network includes advantages and drawbacks in terms of cost, operational features, fault conditions, and control options. It is required to select most appropriate model considering microgrid structure and load types where mesh type networks are more appropriate selections for microgrid infrastructures since it provides a distribution network crossing over any consumer area and completes the network at generation section [2]. The improved control methods, decision making algorithms, bidirectional communication and power flow enhancements have transformed the conventional distribution networks from passive structure to active distribution networks. The integration of communication and control features have promoted DG connections, RES and demand side management (DSM) controls and ESS integration to existing and recently improved microgrids.

The main contribution of active distribution networks is its efficient response to consumer demands in terms of active and reactive power management. On the other hand, developed information and communication technology (ICT) plays crucial role on sustainability and management of microgrids. The active distribution network (ADN) is comprised by power plants, ICT infrastructure, centralized and decentralized controllers, and several microgrids that are connected to bidirectional power and communication medium [10, 11]. The block diagram of an AND that is comprised by several microgrids and controllers connected to distribution network is

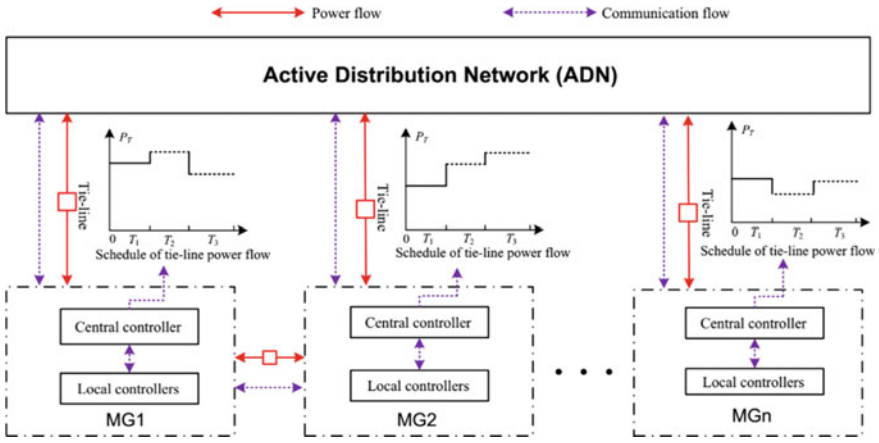

Fig. 1.3 Microgrid integration to active distribution networks [12]

illustrated in Fig. 1.3. Each microgrid includes its own central and local controllers for each power plants located inside the microgrid. On the other hand, dedicated controllers that are responsible to detect and manage the power demand coordinates power flow and control commands between microgrids and ADN.

The control commands enable distribution network to interconnect with upper distribution networks and it allows to operate ADNs in isolated island mode if it is necessary [10, 11].

1.3 Distributed Energy Resources in Microgrid

The conventional and RES used in microgrids are known as DERs. It is targeted to use advantages of each power source along the microgrid and thus, the efficiency and reliability of entire microgrid infrastructure is increased. While the conventional CHPs and synchronous generator based power plants are widely used in high scale microgrid networks, the RES penetration is also preferred to increase variety of sources in a microgrid structure. This section presents introduction to synchronous generator-based sources and RESs as wind turbines and solar PV systems. On the other hand, fuel cells are also presented in brief.

1.3.1 Synchronous Generator Based Sources

A rotational machine driven by a moving engine or turbine is generally named as conventional generation source. The moving engine is a prime mover that transforms the

energy generated by fuel to kinetic energy and thus it is used to rotate shaft of electric machine. On the other hand, any turbine can also rotate the shaft due to kinetic energy obtained from any water or steam source. In the both scenario, synchronous machines are widely used to convert kinetic energy to electric energy by benefiting electromagnetic fields. The DERs named as synchronous generator-based sources are used in steam turbines, hydroelectric plants, diesel generators and thermal power conversion plants such as CHP. Both of the prime mover and synchronous generators require controllers to operate generator with desired voltage/speed, frequency and synchronization controls. The frequency and speed control of synchronous generator-based systems are performed by using speed-droop control or fixed frequency operating methods. On the other hand, the synchronous generator should be equipped with an excitation system that is comprised by a dc voltage source for regulating output voltage [13].

The microgrid should generate reference values of voltage and frequency in islanded operation mode. Therefore, there are several hierarchical control methods have been improved that the primary control substitutes for droop control of synchronous generators. The active and reactive power sharing of any source along microgrid requires more accurate and rapid control methods comparing conventional ones. The virtual synchronous generator (VSG) unifies advantages of ESS and synchronous generator operation by using power electronics. The VSG infrastructure generated by power converters operates as a model of conventional synchronous generator and governor structure without requiring any mechanical components. The sophisticated control algorithms can be applied to VSG systems and power and frequency controls are facilitated due to contributions of power electronics. Figure 1.4 illustrates block diagram of a VSG control system where voltage and current controllers, frequency controllers, and secondary controllers exist. The inertia of synchronous generator is mimicked by VSG controller to eliminate frequency disturbances and to construct virtual impedance control. The phase locked loop (PLL) controller is required to provide secondary frequency control [14, 15].

1.3.2 Wind Turbines

The wind turbines are improved regarding to electromechanical systems that are based on air density rotating the rotor blades. The commercial wind turbines are implemented in 1980s as fixed speed operation principle that is also known as Danish concept. The preliminary wind turbines were capable to generate a few kWs of power regarding to their electromechanical configurations. The fixed speed wind turbines have been improved by using squirrel cage induction generators and the power conversion system was based on soft starter devices to prevent inrush currents as shown in Fig. 1.5a. The improvements of power electronics and power devices have leveraged wind turbine technology for variable speed operations. The recent wind turbine technologies enabled to operate generators under fluctuating wind speeds and to increase the overall efficiency. The improvements have required to classify wind

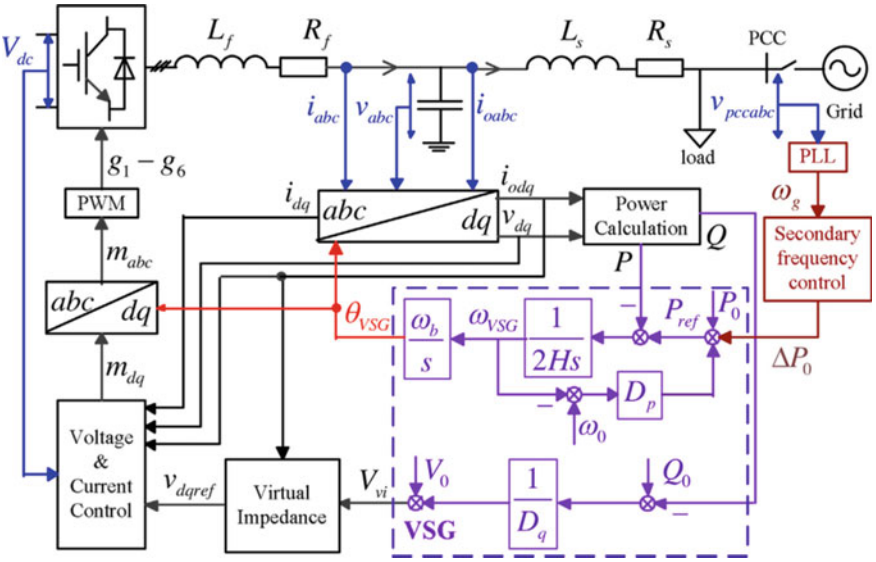

Fig. 1.4 Block diagram of a VSG system [14]

turbine types as Type B, type C, and type D as seen in Fig. 1.5b–d, respectively. The variable speed wind turbines are equipped with sophisticated controllers at rotor side and grid side to accommodate mechanical and electrical control requirements. The rotor side controllers are configured to manage tip speed ratios and blade angles to increase yielded mechanical power that is the base function for electricity generation. The grid side controllers are responsible for power flow control in terms of active and reactive power control in addition to voltage and frequency control for decreasing possible disturbances transferred to utility grid [16].

The mechanical output power (P_m) of a wind turbine is depended to a few parameters as shown in (1.1) where C_p is rotor efficiency, α is pitch angle in degree, β is the peak velocity ratio, ρ is air density in kg/m^3, A is rotor swept area, and v is wind speed in m/s.

$$P_m = \frac{1}{2} C_p(\alpha, \beta) \cdot \rho \cdot A \cdot v^3 \tag{1.1}$$

The output power of a wind turbine is tracked as seen in Fig. 1.6 where the transitions are defined with cut-in speed, average speed, rated speed, and cut-out speed regions. The cut-in speed, or namely starting speed, is the minimum rate of wind speed that gets rotor to move before rotating and wind turbine starts to slightly generate output power in this region. The cut-in speed of a wind turbine is mostly provided around 3 m/s by vendors while the average speed between cut-in and rated speed is around 9 m/s. The rated power of a wind turbine is obtained at around 12 m/s in this scale. The output power arrives to its maximum limit of generator

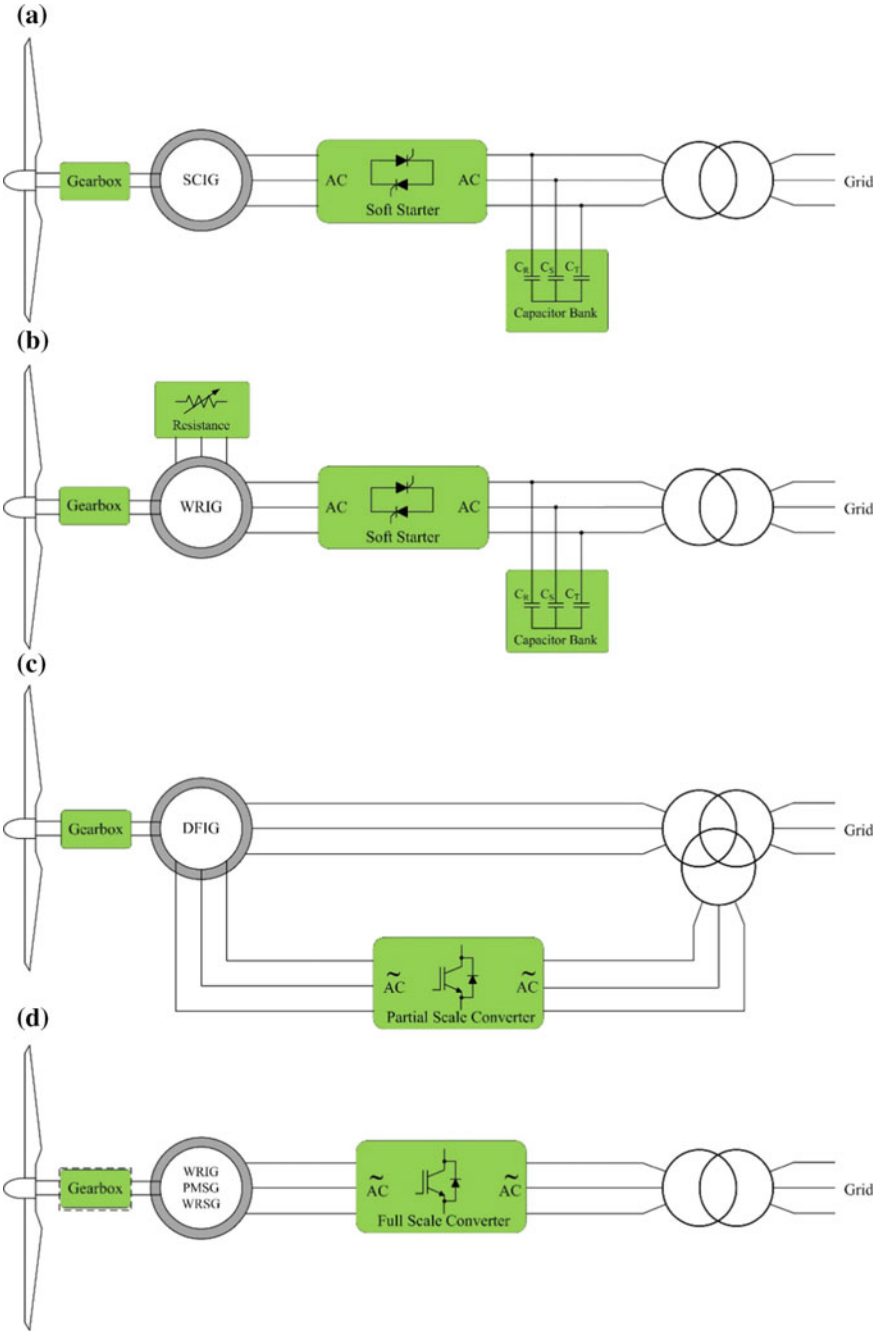

Fig. 1.5 Block diagrams of wind turbines, **a** Type A, **b** Type B, **c** Type C, **d** Type D

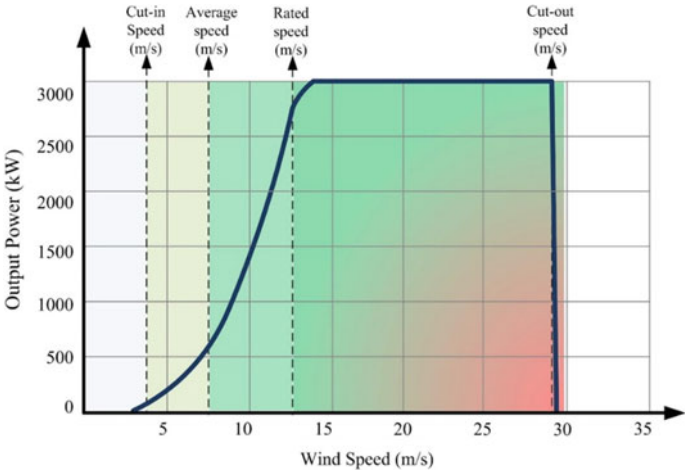

Fig. 1.6 Power curve of a wind turbine at 3 MW rated power

from rated speed to cut-off speed. The cut-off limit denotes the stopping speed that may cause physical damages on wind turbine. The cut-off speed range is fixed around 25–30 m/s. The significant parameters in terms of power control intervals of a WT are seen in Fig. 1.6 together where cut-in speed is set to 4 m/s while average speed at 8 m/s, rated speed at 12 m/s, and cut-out speed at 28 m/s.

The output power of wind turbines is controlled by full-scale or partial-scale power converters that are mainly designed regarding to full bridge power converters. The full-scale concept defines that the power converter is located between wind turbine and utility grid as seen in Type D configuration in Fig. 1.5d, while the partial-scale converter that is shown in Fig. 1.5c is operated at slip power ratio since it has been connected to rotor windings that provides 30% of rated power.

1.3.3 Solar Power Plants

The preliminary solar PV studies have been widespread with the decreased costs around 1980s. The analytical model of a solar PV cell is comprised by using electrical equivalent as shown in Fig. 1.7. The equivalent model is obtained by using (1.2) where output power is generated by depending output current and voltage. The generated power is also affected by short-circuit current (I_{sc}), ideality factor of diode (η), the shunt resistance (R_{sh}), and series resistance (R_S) of PV cell.

$$I_O = I_L - I_{Rs}\left(\left[\exp\left(\frac{V_O + I_o R_s}{\eta_I V_T}\right) - 1\right] - \frac{V_O + I_O R_S}{R_{sh}}\right) \tag{1.2}$$

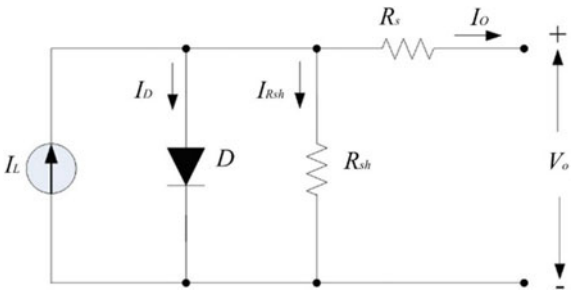

Fig. 1.7 Electrical equivalent of a solar cell

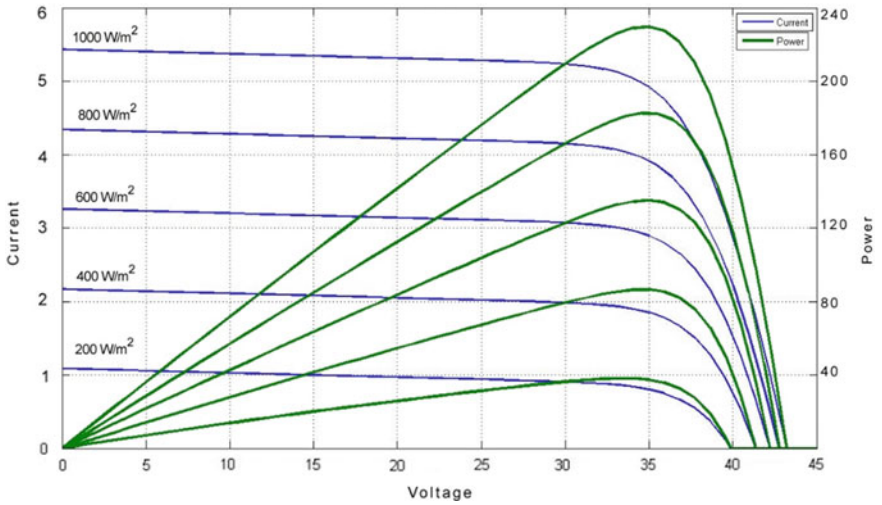

Fig. 1.8 *I-V* and *P-V* curves of a PV module [17]

The I_L denotes the generated current due to illumination rate while V_T is thermal voltage and V_O is output voltage. This equation plays vital role on solar power plant modelling studies since it provides related analysis data for current and power variations against the output voltage of solar module. The *I-V* and *P-V* curves that is shown in Fig. 1.8. for a commercial PV module are used to detect maximum power point (MPP) according to fluctuating irradiations. The MPP tracking (MPPT) algorithms are implemented to achieve possible maximum output of a solar PV module and PV plant under partial shading and other circumstances. Therefore, PV plant modelling is one of the most important topics in microgrid planning and operation analyses. The output current and output current of a PV module have been generated by increasing solar irradiation rate from 200 to 1000 W/m^2 that cause increment on output power [17, 18].

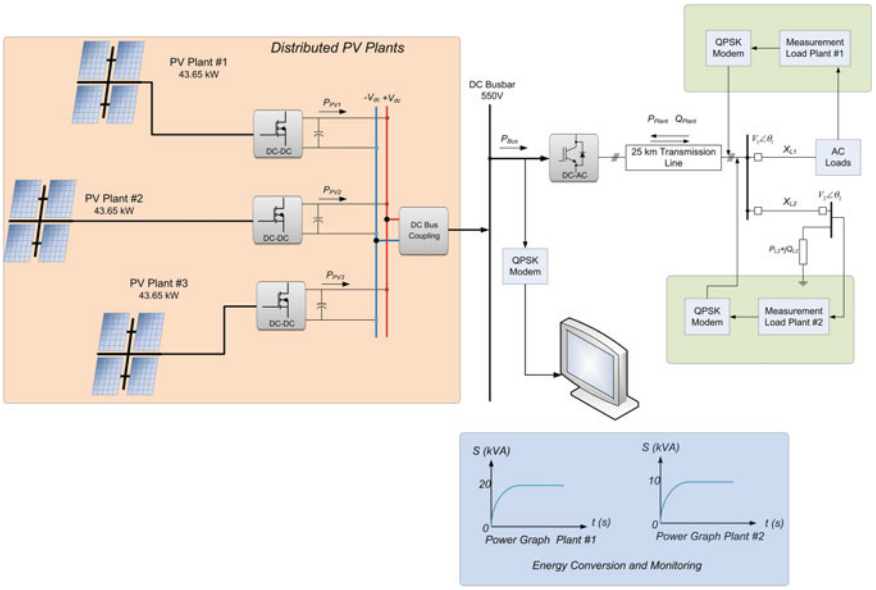

Fig. 1.9 Block diagram of a distributed solar PV microgrid with remote monitoring

Block diagram of a distributed solar PV microgrid has been illustrated in Fig. 1.9 where three different plants are coupled on dc-busbar and the generated power has been converted to ac by a central inverter [19]. Such a modelling study provides several measurement and control opportunities before installing a power plant and microgrid model. In the reviewed study, each solar plant is modelled according to different irradiation and climate conditions since they all are assumed to be installed at various geographical areas. The maximum output power of each power plant is ensured by using a decentralized MPPT algorithm in this model since dc-dc converters are configured in decentralized structure. This type of microgrid scheme is known as dc coupled microgrid due to power plants are connected to a single dc bus. The stabilized dc bus voltage is applied to a central inverter that can be operated with optional MPPT algorithm or a grid side controller. The inverter is responsible for adjusting active and reactive power control in addition to voltage and frequency stabilization. Moreover, the inverter can also be used as a VSG in this schematic since solar PV plants do not provide inertia and reactive power requirements are met by inverter [20].

The inverter topology is comprised by using a regular three-phase full bridge inverter that is controlled with Sinusoidal Pulse Width Modulation (SPWM). Although the modulation algorithm is controlled by PLL and reactive power controllers, the modulator is effective on eliminating power disturbances and distortions such as total harmonic distortion (THD) of current and voltage waveforms. In addition to harmonic elimination, the modulator is used to adjust power factor of entire microgrid [19].

The output of inverter comprises an ADN to feed several loads and utility grid connection. The communication requirement of ADN is met by a power line communication (PLC) infrastructure in this application model. The PLC system is comprised by using Quadrature Phase Shift Keying (QPSK) algorithm that is based on m-ary application of regular PSK modulation where m is four. The wireless communication methods can also be used in remote monitoring and remote-control applications of microgrids. This kind of procedures are presented in the following related chapters of this book.

1.4 The Microgrid Architecture

The microgrid infrastructure is comprised by power sources that have been discussed earlier as DERs, microgrid controllers, and utility connection. It became mandatory to use intelligent power electronics between microgrid and generation sources. A microgrid control infrastructure is composed of a number of central and distributed controllers. The central controllers are connected to MGCC for improving and enhancing operation features of microgrid. The MGCC determines demand power, enhancement conditions and load capacities considering the auxiliary services of distribution system. The defined enhancement and operating scenarios are performed by transmitting control signals to controllable field loads and microgrid controllers. The non-critical and flexible loads can be shedded from grid if it is required. Moreover, active and reactive power measurements should be performed instantly. In the complete distributed control approach, microgrid controllers cooperate with other controllers to transfer the available maximum power to grid by considering market conditions. This approach is improved to tackle MGCC problems met in the systems where many DG sources exist and decisions are made locally.

The general structure of control methods used in microgrid operations is illustrated in Fig. 1.10. The presented microgrid model is controlled by a microsource control system (MCS) in this scenario. The load controllers (LCs) are used to manage controllable loads located in load models as its name implies. A central controller (CC) is located between microgrid and distribution management system (DMS) or distribution system operator (DSO) for each microgrid infrastructure. These controllers are responsible to perform medium voltage (MV) and low voltage (LV) controls in systems where more than single microgrid exists. Several control loops and layers as in conventional utility grids also comprise the microgrids. This hierarchical control scheme meets fundamental infrastructure and dynamic interface requirements in addition to providing integrity through central and distributed control systems.

The local control includes primary control systems such as voltage and current control loops that are used in DG and RES integration. The secondary control is essential to regulate frequency and average voltage fluctuations caused load or source variations. The secondary control is also responsible for local auxiliary services. Central and emergency control layer operates featured protection and emergency control protocols against unexpected events in the context of microgrid reliability.

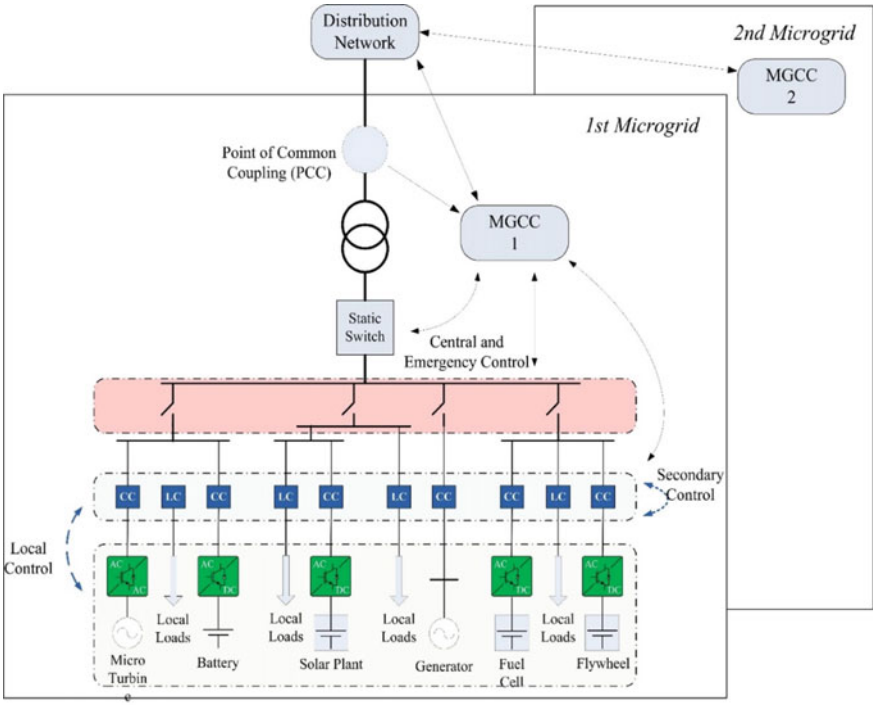

Fig. 1.10 A general view of microgrid and control structure

The emergency control techniques perform fault estimations by realizing protective and regulative measurements. The general control ensures economical operating conditions of microgrids by arranging the organization between microgrids and distribution networks. The general control infrastructure seen in Fig. 1.10 operates as a distribution network interface for MGCC and manages the power flow control. This control interface provides power distribution at predicted values by controlling the microgrid infrastructure. In spite of local control, the secondary, general and emergency control infrastructures require communication channel [6, 11, 21, 22].

A microgrid infrastructure can be designed according to single-phase or three-phase grid networks, and it can be connected to low voltage (LV) or medium voltage (MV) distribution systems regarding to its power scale. The grid-connected operation mode of microgrid is also known as normal operation mode. The microgrid architecture can be dc, ac or hybrid of both grid types due to its DER configurations. In any microgrid type, there can be dc or ac microgrid zones where dc sources are coupled on a dc busbar and integrated to ac microgrid by using an inverter as presented in previous section. The dc microgrids are comprised by dc sources, ESSs, dc loads and RES with dc outputs [23].

The micro sources and controllable loads used in a microgrid infrastructure may cause complexity and latencies due to numbers of DG source comprising the micro-

grid. The sources and loads are mostly distributed along the microgrid and they operate with low bandwidth communication system in low voltage level. The low bandwidth may cause message transmission problems when high ordered control hierarchy is used. Therefore, the complexity of control system should be considered to prevent missing of control commands and communication messages. The decision on microgrid control that are defined by different system operators can increase the node number in addition to technical complexities. Another important issue to be considered is data communication level that can be defined by different system operators to decide which parameters will be used and whether there will be any prevention policy. The details of hierarchical control concept of microgrid are presented in Chap. 15.

1.5 Operation Types of Microgrids

The microgrids can provide two fundamental operation modes as normal mode and islanded mode. However, their connection with neighbouring microgrids generate multi-microgrid infrastructure and requires several operation controls together. In this regard, grid connection control, management procedures, active DSM, and DG control are required to ensure appropriate operation. A large number of DERs and microgrid connection comprise a complex structure including LV and MV connections that should be coordinated. The effective management of such a multi-microgrid system requires hierarchical control architecture with central management controllers. These controllers are located at MV substations to manage MV/HV connection and distribution system operators (DSOs) are responsible to operate these controllers. Thus, the complexity of interconnections is managed by a single center and communication systems are integrated to system for data acquisition and control operations [11]. Since the hierarchical control and other control systems of microgrids are presented, these types will be presented in detail in particular chapters of this book.

1.6 Conclusion

This chapter presents fundamental introduction of microgrid concept. The improvements of power electronics and power devices have promoted widespread use of distributed generation. On the other hand, the decreasing fossil fuels and aging power generation plants have leveraged microgrid researches. The renewable energy sources and implemented power plants such as wind turbines, solar PV plants, and energy storage systems enabled distribution system operators and consumers to install DG plants. The commercial or industrial microgrids are generally designed to operate in grid-connected mode to decrease demand and costs. They also provide a backup system to prevent effects of faulty operation conditions. The international standards providing guidance for microgrids have been presented in this chapter. Moreover,

active distribution networks and required control and source infrastructures have been introduced in the second title of this chapter.

The conventional synchronous generator based power plant approach and most widely used renewable energy sources such as wind turbines and solar PV plants have been presented in brief following the active distribution networks. The basic control principles are presented in classification of local control, secondary control, central and emergency control, and general control methods that are related with hierarchical control concept. The hierarchical control concept has been introduced in brief but not detailed since it will be presented in a dedicated chapter in the context of this book.

The features and selection criteria of central and distributed control schemes are presented in the last sections. The presented researches have outlined that intelligent control systems are much more efficient on power control operations as well as the voltage and frequency controls. The improved control methods are widely researched to enhance power quality and operation conditions of microgrids interacting neighbor microgrids and utility grid that are mentioned at the last part of this chapter.

References

1. A. Maitra et al., Microgrid controllers: expanding their role and evaluating their performance. IEEE Power Energy Mag. **15**(4), 41–49 (2017)
2. E. Hossain, E. Kabalci, R. Bayindir, R. Perez, Microgrid testbeds around the world: state of art. Energy Convers. Manag. **86**, 132–153 (2014)
3. E. Kabalci, Y. Kabalci, *Smart Grids and Their Communication Systems* (Springer, Berlin, 2018)
4. T.S. Basso, R.D. DeBlasio, IEEE P1547-Series of Standards for Interconnection (2003), pp. 556–561
5. IEEE Standard for the Specification of Microgrid Controllers (IEEE, New York, 2017). Standard ISBN 978-1-5044-4608-2
6. A. Kaur, J. Kaushal, P. Basak, A review on microgrid central controller. Renew. Sustain. Energy Rev. **55**, 338–345 (2016)
7. REN21 Secretariat, Renewables 2017: Global Status Report. Paris, France (2017)
8. F. Blaabjerg, Y. Yang, D. Yang, X. Wang, Distributed power-generation systems and protection. Proc. IEEE **105**(7), 1311–1331 (2017)
9. M.S. Mahmoud, F.M.A.L. Sunni, M. Saif Ur Rahman, Review of microgrid architectures—a system of systems perspective. IET Renew. Power Gener. **9**(8), 1064–1078 (2015)
10. S. Chowdhury, S.P. Chowdhury, P. Crossley, *Microgrids and Active Distribution Networks* (Institution of Engineering and Technology, Stevenage, 2009)
11. N. Hatziargyriou, *Microgrid: Architectures and Control* (Wiley, India, 2014)
12. Z. Xiao, J.M. Guerrero, J. Shuang, D. Sera, E. Schaltz, J.C. Vasquez, Flat tie-line power scheduling control of grid-connected hybrid microgrids. Appl. Energy **210**, 786–799 (2018)
13. T. Chang, F. Katiraei, Modeling and analysis of synchronous generator based distributed energy resources for dynamic impact studies, in *IEEE Power and Energy Society General Meeting*, Detroit, MI, USA (2011), pp. 1–6
14. M. Chen, X. Xiao, Hierarchical frequency control strategy of hybrid droop/VSG-based islanded microgrids. Electr. Power Syst. Res. **155**, 131–143 (2018)
15. N. Mahdavi Tabatabaei, A. Jafari Aghbolaghi, N. Bizon, F. Blaabjerg, *Reactive power control in AC power systems* (Springer International Publishing, Cham, 2017)

16. I. Colak, E. Kabalci, Control methods applied in renewable energy systems, in *Use, Operation and Maintenance of Renewable Energy Systems*, ed. by M.A. Sanz-Bobi (Springer International Publishing, Cham, 2014), pp. 205–246
17. E. Kabalci, An islanded hybrid microgrid design with decentralized DC and AC subgrid controllers. Energy **153**, 185–199 (2018)
18. E. Kabalci, Design and analysis of a hybrid renewable energy plant with solar and wind power. Energy Convers. Manag. **72**, 51–59 (2013)
19. E. Kabalci, A smart monitoring infrastructure design for distributed renewable energy systems. Energy Convers. Manag. **90**, 336–346 (2015)
20. N. Bizon, N. Mahdavi Tabatabaei, F. Blaabjerg, E. Kurt, *Energy harvesting and energy efficiency* (Springer International Publishing, Cham, 2017)
21. A. Kwasinski, W. Weaver, R.S. Balog, *Microgrids and other Local Area Power and Energy Systems* (Cambridge University Press, Cambridge, 2016)
22. N. Mahdavi Tabatabaei, S. Najafi Ravadanegh, N. Bizon, *Power Systems Resilience—Modeling, Analysis and Practice* (Springer International Publishing, Cham, 2018)
23. S.A. Hosseini, H.A. Abyaneh, S.H.H. Sadeghi, F. Razavi, A. Nasiri, An overview of microgrid protection methods and the factors involved. Renew. Sustain. Energy Rev. **64**, 174–186 (2016)

Chapter 2
Microgrid Planning and Modeling

Ali Jafari Aghbolaghi, Naser Mahdavi Tabatabaei, Morteza Kalantari Azad, Mozhgan Tarantash and Narges Sadat Boushehri

Abstract Due to a number of financial and operational difficulties that have lately been faced by power plants, the electricity industry is exploring a concept as the smart grid to address the problems in the future. There will be significant differences in the conventional power system in the transmission into a smart network, such that when the demand increases, the system does not necessarily generate more electricity to meet consumption needs. In other words, power generation will not be directly dependent on consumption; instead, it will function through reducing losses, managing user demand and cooperating with consumers in order to optimize the load. All of the proposed approaches ensure that the balance between generation and consumption is increased without creating inevitable generation. The smart grid is capable of improving the operation of its components via reducing power costs, reducing additional charges, ensuring maintenance and saving costs of electricity generation, meeting demand and helping to protect the environment. Smart grid

The original version of this chapter was revised: Abstract has been updated. The correction to this chapter can be found at https://doi.org/10.1007/978-3-030-23723-3_32

A. J. Aghbolaghi (✉)
Zanjan Electric Energy Distribution Company, Zanjan, Iran
e-mail: ali.jafari.860@gmail.com

A. J. Aghbolaghi · M. K. Azad · M. Tarantash
Sanat Modern AfRaTech Sobhan Company, Zanjan, Iran
e-mail: kalantariazad@yahoo.com

M. Tarantash
e-mail: tarantashm@yahoo.com

A. J. Aghbolaghi · M. K. Azad
Andishmand Shomal-Gharb Engineering Consultancy, Zanjan, Iran

A. J. Aghbolaghi · N. M. Tabatabaei
Electrical Engineering Department, Seraj Higher Education Institute, Tabriz, Iran
e-mail: n.m.tabatabaei@gmail.com

N. M. Tabatabaei · N. S. Boushehri
Department of Management, Taba Elm International Institute, Tabriz, Iran
e-mail: nargesboush@yahoo.com

N. Mahdavi Tabatabaei et al. (eds.), *Microgrid Architectures, Control and Protection Methods*, Power Systems,
https://doi.org/10.1007/978-3-030-23723-3_2

energy systems have been developing constantly in order to be able to integrate renewable energy resources, energy storage systems, diesel generators, loads, control systems, etc., which are called microgrids or hybrid power systems, where energy management and planning are of critical importance. There are several functions that are to be considered when dealing with the planning of microgrids, such as load forecasting, the uncertainty of renewable sources, reduction of CO_2 emissions, etc.

Keywords Fundamentals of microgrids · Microgrid planning · Energy management · Solar and wind energy modeling · Optimization models for microgrid planning

2.1 Introduction

Regarding the monetary and operational difficulties that the electrical utilities are recently confronting, the electric industry has set off for seeking innovations toward settling such issues in the future, a future seen as smart grid era. There will be fundamental differences in the conventional power system and the smart grid. As such, when the demand rises, the favored arrangement would not be necessarily generating more electricity to fulfill the consumption requirements. In other words, generation of electricity will not directly be dependent on consumption; rather it will be a function of losses minimization, end-user demand management and collaboration with customers in order to optimize the load. All of the approaches mentioned earlier ensure striking the balance between generation and consumption without the generation having inevitably been increased. The smart grid will have the capacity to improve the utilization of its own components, lessen power losses, diminish superfluous loads, guarantee maintainability and cost-effectiveness of the electricity produced, meet the demand, and help to preserve the environment.

In the last century, the only information that was needed to see if the generation was sufficient or not in the conventional power system was the voltage and frequency of power system, which varied in relation to the demand. Therefore, such a load-following system confronted unabated growth on the demands and was no longer able to keep up with it regarding the reliability considerations. Utility companies were not able to expand their generation capacities due to the increasing cost of electricity production, the unstoppable growth of demand and stagnant revenues. In addition to the mentioned monetary issues, the negative effects of the emission of greenhouse gases on the environment have urged the electric utility to transform from the paradigm of "load-following" to "generation-following", and that is the reason why smart grids and then microgrids were developed [1].

Smart grid energy systems have been developing constantly in order to be able to integrate renewable energy resources, energy storage systems, diesel generators, loads, control systems etc., which are called microgrids or hybrid power systems. Connecting several distributed generation and storage sources to several other loads microgrids are a small version of traditional distribution systems mostly via low-

voltage distribution networks. Moreover, with the invention of microgrids, remote communities have become capable of been supplied by electricity which was uneconomical before. Furthermore, the microgrid concept has been considered one of the best solutions for incorporating more renewable energy resources into the existing power system, as they can be operated in a grid-connected and isolated mode, which can bright plenty of reliability both for customers and for the power system [2].

As the number of distributed generation units and the penetration level of renewable energy resources increase, the new distribution network cannot be neglected for being a passive appendage to the power transmission system, but an integrated unit. Moreover, multi-management approaches should be undertaken for operation and planning of such complex systems, which are thought as a cluster of renewable and non-renewable energy resources and loads of different profiles. All this complexity has plenty of benefits in its favor, such as reduction of power losses, increased efficiency by using combined heat and power generators, increased local reliability, the correction of voltage sag etc.

In this chapter, following an introduction to the fundamentals and definition of microgrids, the focus is taken on microgrid planning and energy management that explores modeling random variables for wind and solar energy. Then, solar and wind energy modeling using several different probability distributions are explained. Afterward, the optimization models for microgrid planning has been proposed elaborately using stochastic programming and deterministic mathematical models.

2.2 Fundamentals of Microgrids

The present power system is practically built to conduct electricity from power plants, which are mostly far away from load centers, to consumers centralized at industrial and domestic sites. In addition, having been using an assortment of compound innovations to guarantee the uppermost productivity in power plants, the process of combustion loses almost 70% of the fuel as lost heat. Moreover, because in the conventional power system generation follows consumption, there are 20% extra capacity in power plants to meet the consumers' electricity only at peak demand time. Another drawback regarding the present power system will be a vulnerability of complete blackouts throughout the network in case of mass interruptions somewhere within the network. All the mentioned downsides have forced scientists to come up with an idea to address the problems to have a stable, more efficient, and cost-effective electric system [1].

The cutting-edge smart grid is to address the significant weaknesses of the current network and to give the service companies full perceivability over operating all the components and services that they provide. Smart grids are also expected to be more resilient in case of any kind of failure and engage all the stakeholders in a cheap and reliable empowerment industry and meticulous energy transactions. Figure 2.1 is a depiction comparing smart grids with the conventional power system highlighting the key differences in hierarchies, technologies and operational strategies [1].

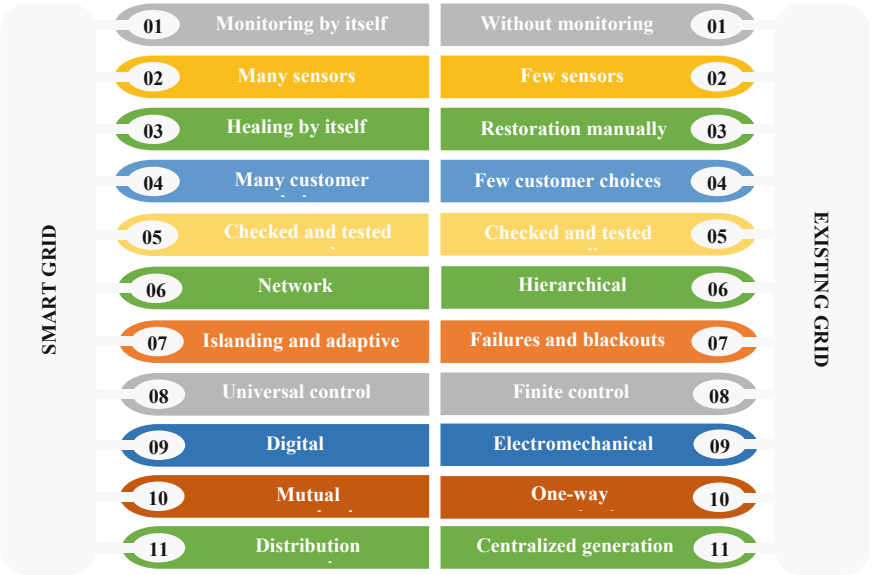

Fig. 2.1 Comparison of a conventional and a smart grid [1]

2.2.1 Definition of Microgrids

Microgrids are interrelated structures of loads and local power plants that can function independently of the network called islanded mode, or be connected to it, considered as a grid-tied mode. Microgrids basically embody virtually all the fundamental components of the conventional network, such as power plants and consumers in a more compact structure. The power plants are closely located in the neighborhood of loads so that no transmission system resembling the existing one is required any longer. Moreover, the local power plants may be able to meet the local demand, otherwise, the deficiency of electricity will be compensated by a larger grid connecting microgrids altogether. In other words, microgrids are just a scaled-down version of the existing network, which is also recognized as smart microgrids if a sophisticated command and control system is incorporated into them [1].

There are also some other diverse terms attached to the general definition of microgrids, each being posed by different communities, all of which seek their own advantages. Some believe microgrids should integrate renewable energy sources for environmental concerns, whereas the others think energy surety and reliability are essential factors to be taken into consideration which demand microgrids to be connected to a firmer grid. Following apprehensions about the latter, energy storage systems are to be added into microgrids in order to mitigate the impacts of uncertain nature of renewable energy resources. In addition, there are imposing concerns about the cyber protection of smart microgrids as there are interconnected components included into microgrids to have them fully manageable, which likewise stresses

incorporating defensive structures into them in case of intrusions. Last but not least, energy efficiency and cost effectiveness of microgrids come as high priorities, without which there will not be any justification for devising such state-of-the-art technologies [1].

It is worth bearing in mind that an interconnected set of loads and generations do not need to inevitably be smart in order to be called a microgrid. In other words, the mere fact that the grid is a scaled-down version of the conventional grid which is a generation-following system rather than a load-following one suffice for being called a microgrid. Nevertheless, a smart microgrid is designed as a structure in which loads are fed by local generation connected to or disconnected from a larger grid, same as a microgrid, that a level of intelligence has been incorporated into it in order to make it efficiently manageable and optimizable. It should be noted that the intelligence can be applied to all of the components of microgrids, such as power generation, load, and accessibility management etc., or a few of them, which the total level of smartness of microgrids are defined based on [1].

2.2.2 Architecture of Microgrids

As discussed earlier, there are several basic building blocks which are indispensable gears of smart microgrids, such as different types of power generation sources, including renewables, a wide variety of loads having different consumption profiles, and interconnected levels of networked intelligence including all the components needed for the command and control system to be devised (Fig. 2.2). This abridged graph underlines the way that the fundamental parts of a smart microgrid are incorporated through two autonomous yet interrelated connections. The first one relates to the conventional straight energy flow interrelation, transferring electricity from local power plants to the consumers. The second one refers to a mutually connected system collecting different sets of sensory, alarm etc. data and making energy management feasible through the channels of communication to the components and parameters of microgrids. In addition, the energy management system of microgrids can be central or distributed according to the size of microgrids to completely fulfill the control requirements of microgrids in relation to the complexity of them [1].

2.3 Microgrid Planning and Energy Management

Energy management and planning are of critical importance when it comes to integrating microgrids, equipped with renewable energy resources, into the network. There are several functions that are to be considered when dealing with the planning of microgrids, such as load forecasting, the uncertainty of renewable sources, reduction of CO_2 emissions etc. In addition, electricity should be consumed almost as soon as it is generated and system operators and planners should devise such

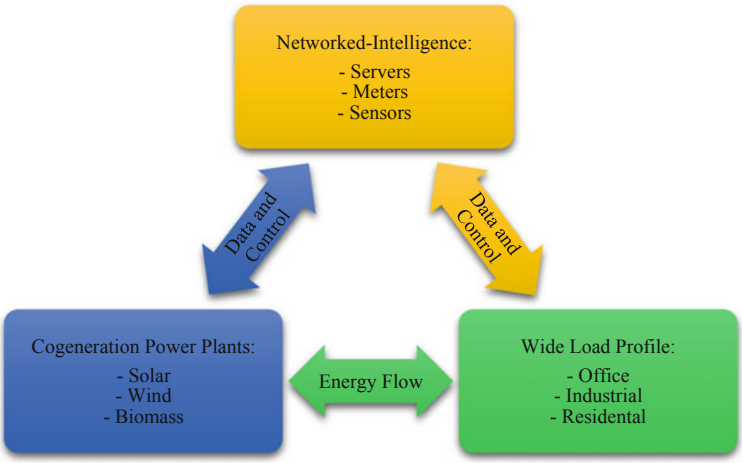

Fig. 2.2 Basic building blocks of microgrids [1]

complex processes in order to make generation meet consumption promptly. As the uncontrollability of renewable energy resources is an important issue to be tackled, one way is to incorporate them with controllable generators and power storage solutions and come up with Hybrid Power Systems (HPS). The main conclusion to be drawn is that it is a very challenging task to develop a right strategy to combine renewable resources with the conventional network and storage systems in order to meet the demand while struggling with the uncertain nature of power sources. Hence, all the parameters that have a part in the planning of microgrids should be modeled in details mathematically to avail of picking the best approaches where microgrid planning and energy management jut out [2].

2.3.1 Modeling Random Variables for Wind Energy

The penetration of wind power, which is a means of electricity production utilizing the kinetic energy of wind, has been growing dramatically since the beginning of the 21st century. The total capacity of wind power installed globally increased considerably from 18 GW at the end of 2000 to 238 GW at the end of 2011, having 41 GW installed in 2011 alone. Regarding the amount of penetration of renewable sources of energy, it is highly essential to investigate power generation in the presence of such sources. As for Wind Turbines, achieving an accurate assessment of the electrical system is not simply conceivable only by analyzing deterministically. However, the power injected into the network can be calculated using the wind turbines' power curve and the probabilistic distribution of wind speed [3].

2.3.1.1 Characteristics of Wind Turbines

The output power of wind turbines is generally established by two parameters as mean hourly wind speed and the output characteristics of wind turbines. To have a careful assessment of the output power of wind turbines, specific evaluations should be made on the hourly-logged data of wind speed as converting them to the pertinent values at the height of hubs. It is feasible to calculate the data at the height of hubs through Eq. (2.1) as:

$$v = v_{hr}\left(\frac{h}{h_r}\right)^{\gamma} \tag{2.1}$$

where h_r is the wind speed at a reference height, h is the wind speed at a pre-defined hub height, v_{hr} is wind speed at reference height in m/s, v is wind speed in m/s, and γ represents the power law exponent [4].

The model that is used to calculate the wind turbine output power (P_{WT}) has been given by Eqs. (2.2) and (2.3) as follows:

$$P_{WT} = \begin{cases} a.v^3 - b.P_R & v_{ci} < v < v_r \\ P_R & v_r < v < v_{co} \\ 0 & \text{otherwise} \end{cases} \tag{2.2}$$

subject to:

$$\begin{cases} a = \frac{P_R}{v_r^3 - v_{ci}^3} \\ b = \frac{v_{ci}^3}{v_r^3 - v_{ci}^3} \end{cases} \tag{2.3}$$

where P_R is rated the power of wind turbine in kW, v_{co} is cutoff speed, v_{ci} is the cut-in speed of wind turbine in m/s and v_r signifies the rated velocity of the wind turbine in m/s [4].

Figure 2.3 is related to one of the common wind turbines that is used in a few microgrid-related projects called Whisper 3 kW (Southwest Wind Power), which its output power curve is established based on Eqs. (2.1), (2.2) and (2.3). In addition, the output power curve for most of the wind turbines follow almost the same path as Whisper 3 kW (Southwest Wind Power) does. However, the selection process of wind turbines also is dependent on the data of average annual wind speed and economic considerations both for specific locations.

2.3.1.2 Probability Distributions for Wind Speed Modeling

The mathematical expressions given by Eqs. (2.4) and (2.5) are the Weibull Probability Distribution formulas that model hourly wind speed as a random variable, which

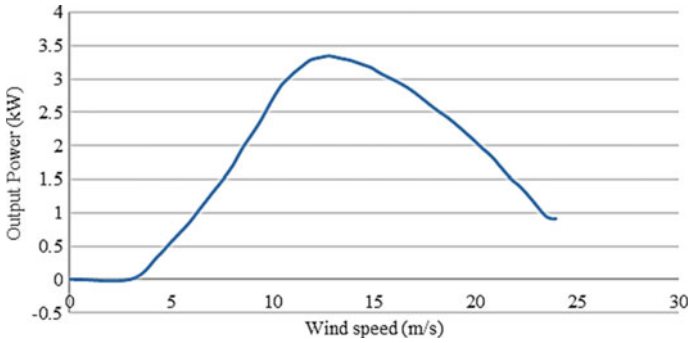

Fig. 2.3 Power curve for Whisper 3 kW wind turbine

makes the prediction of wind speed at a given location feasible for the planners to make an estimation of the wind power available to inject into the grid [5].

$$f(v) = \frac{r}{c}\left(\frac{v}{c}\right)^{r-1} \exp\left[-\left(\frac{v}{c}\right)^{r}\right] \tag{2.4}$$

subject to:

$$\begin{cases} r = \left(\frac{\sigma}{v_{mean}}\right)^{-1.086} \\ c = \frac{v_{mean}}{\Gamma\left(1+\frac{1}{r}\right)} \quad \text{where,} \ \ \Gamma(n) = (n-1)! \end{cases} \tag{2.5}$$

where $f(v)$ is the wind speed, v_{mean} is the mean speed and σ is the standard deviation of the wind speed for a specific location, then the Cumulative Distribution Function (CDF) can be characterized mathematically by Eq. (2.6) [5].

$$F(v) = 1 - \exp\left[\left(-\frac{v}{c}\right)^{r}\right] \tag{2.6}$$

2.3.2 Modeling Random Variables for Solar Energy

Another environmentally friendly means of energy production is photovoltaic systems that are operated without the smallest amount of emissions. What make them an ideal solution for both urban and rural utilizations are little maintenance requirements and long lifespan when used as independent systems. Moreover, transmission and distribution costs can be effectively reduced when generator systems are located in close proximate to consumers, in which context PV systems can be taken efficiently into the consideration. However, extensive adoption of PV systems confronts a major barrier as the high cost of their deployment.

It is practicable to predict solar radiation at a particular location based on the logged data for a certain period that are usually measured per unit area on a horizontal surface in Wh/m^2. In other words, the solar radiation that a surface receives is depended on the angle of the surface with respect to the sun, of which astronomical parameters and the surface orientation decide. More on this, there are two main steps to radiation conversion as decomposition and transposition. The former refers to the decomposition of the radiation into two separate components as beam and diffuse. The latter denotes transposition of the beam and diffuse onto the inclined panel. Thus, the overall radiation consists of the two components and the radiation reflected by the ground. The main process in the estimation of diffuse radiation, which is the most important step, is the clearness index expressing extraterrestrial solar radiation caused by the atmosphere. Just as the other renewable sources of energy and the varying solar insolation from day to day comparing the same hours, there is a desperate need to develop a comprehensive method to deal with the uncertainty of solar energy.

2.3.2.1 Characteristics of Photovoltaic Panels

Several investigative models presenting the current-voltage relations that are developed based on the electrical characteristics of PV panels can be used for calculating the hourly output power. Belfkira presented one comprehensive model in 2009 that is taken into consideration for this chapter. It is applicable, using a maximum power point tracker (MPPT), to determine PV panel current (I_{mpp}) and voltage (V_{mpp}) at the maximum power point based on the mentioned model. In addition, the models comprise the properties of panel temperature and radiation level on the output power as shown by Eqs. (2.7)–(2.14) [6].

$$I_{mpp} = I_{SC}\left[1 - C_1\left[\exp\left(\frac{V_{\max}}{C_2 V_{OC}}\right) - 1\right]\right] + \Delta I \tag{2.7}$$

$$V_{mpp} = V_{\max} + \mu_{V,OC} \cdot \Delta T \tag{2.8}$$

where I_{SC} is short circuit current of solar panel in Amps, , is temperature constant for open circuit voltage in V/degC, V_{OC} and $V_{\max}$ are open circuit voltage of PV panel and maximum voltage of PV panel at the reference operating condition in Volts, respectively.

The output power of PV panel at the extreme power point, P_{mpp}, is expressed as:

$$P_{mpp} = V_{mpp} \cdot I_{mpp} \tag{2.9}$$

subject to:

$$C_1 = \left(1 - \frac{I_{\max}}{I_{SC}}\right)\exp\left(-\frac{V_{\max}}{C_2 V_{OC}}\right) \tag{2.10}$$

$$C_2 = \left(\frac{V_{\max}}{V_{OC}} - 1\right)\left[\ln\left(1 - \frac{I_{\max}}{I_{SC}}\right)\right]^{-1} \tag{2.11}$$

$$\Delta I = I_{SC}\left(\frac{G_T}{G_{ref}} - 1\right) + \mu_{I,SC} \cdot \Delta T \tag{2.12}$$

$$\Delta T = T_c - T_{c,ref} \tag{2.13}$$

where $I_{\max}$ is the maximum amount for current of the PV panel at the reference working condition, $\mu_{I,SC}$ is temperature coefficient at reference operating conditions for short circuit current. G_{ref} and G_T are irradiance at reference operating conditions equal to 1000 W/m^2 hourly and irradiance on tilted surface in W/m^2, respectively, and T_c and T_{ref} are PV panel operating temperature and reference temperature in degree Celsius, respectively. T_c can be presented as follows:

$$T_c = T_a + \frac{NOCT - 20}{800} \cdot G_T \tag{2.14}$$

where *NOCT* denotes the Normal Cell Operating Temperature. In addition, *NOCT* refers to the cell temperature when the PV panel is being operated under 800 W/m^2 of solar irradiance and the ambient temperature of 20 °C and also it is usually between 42 and 46 °C [6].

As discussed before, there are two determining factors to the output power produced by solar panels as the irradiation and the angle between the panel and the sun, while solar irradiation data is what most of the sources make available. More on that, when the sunlight and solar panel are perpendicular to each other, the output power is at its maximum level, whereas the power delivered by sunlight to a fixed module is less than the maximum amount due to the changing nature of the sun angle. In addition, when the tilt angle is equal to the latitude of the location, the panel will provide the maximum output power over a course of a year. Nevertheless, lower tilt angles are optimized for summer times as greater fraction of sunlight will be transferred into electricity, while steeper tilt angles being the best choice for winter times as for large winter loads.

2.3.3 Non-linear Dependence Structures for Modeling Random Variables

Wind and solar power having been the most accessible sources of renewable energy, the uncertainty connected cause them not to be able to meet the demand completely. In other words, there is a high variability in output power when it comes to wind power because of the ever-changing nature of wind, while solar power following a more known pattern showing large changes in output power compared to the slight changes in solar radiation. In general, there is a correlation between the spatial dependencies, non-Gaussian and non-linear nature of wind speeds, where Kumaraswamy

distribution model is one of the best models to be utilized. Moreover, three main advantages justify using Kumaraswamy distribution as its comparable characteristics with beta distribution, simple analytical formulations for convenient calculations as well as its simple integration with copulas. Most of the existing literature refer to wind farms as a feasible means of smoothing wind power that also have a great effect on stability and reliability enhancement of renewable energy generation [7].

More on copulas, it is one of the most appropriate methodologies of modeling non-linear, non-normal and complex dependency structures, which is widely used in the field of finance. In addition, one of the most significant advantages of copulas is their power in demonstrating the dependency structure autonomously of the marginal distributions of the contributing variables, which comes to a great importance for planners when finding the output of wind power at different locations independently of their behavior. An estimation can be made for the correlation between the locations through separation distance and averaging period, which makes it feasible to produce a precise model of dependency structure via basic information about the location of wind turbines. Therefore, it is highly important to select an appropriate copula function in order to have the least unacceptable errors. Generation of scenarios is one of the most important usages of wind power modeling using copulas, which are inseparable parts of scholastic programming as a common decision-making tools in power system analysis. Moreover, it has already been proven that wind speeds are non-normally distributed and non-linearly dependent. Hence, while the multivariate data not being distributed normally, the quantiles of margins' sums cannot be calculated from sums of variances and covariance [8].

2.4 Microgrid Planning—Solar and Wind Energy Modeling

As solar and wind energy are site-dependent, zero emissions and non-depletable, they have always been considered to be the most important sources of renewable energy, although their unpredictable nature being of utmost concern. In general, the time distribution of the demand does not necessarily fit with the variations of wind and solar energy, which makes the designs costly and not reliable if they are devised independently. This section introduces mathematical solutions for modeling wind and solar-based renewable sources of energy, which will be investigated to understand their characteristics in order to design microgrids that are more reliable. In order to comprehend the correlation between renewable energy sources and their spatial properties, novel approaches using copulas have been examined through leading us to avoid over-designed as well as under-designed systems [9].

2.4.1 *Probability Distributions for Modeling PV, Solar and Wind Energy*

The amount of solar radiation reaching the ground depends on the climate conditions as well as spatial properties such as latitude and altitude, but it has been proven by many studies that the irradiation difference between on the ground and outside the atmosphere depends mainly on the cloudiness. In addition, solar irradiation can precisely be modeled by Hollands and Huggets distribution, while Weibull probability distribution models wind speed as a random variable quite well and Kumaraswamy distribution presents a general tool for modeling all the parameters at once that will be taken for consideration.

2.4.1.1 Kumaraswamy Distribution

There are two main reasons for using the Kumaraswamy distribution for modeling renewable resources of energy as its ability to model non-linear transformation of energy resources in order to be integrated with copulas and a much simpler form than the Beta distribution that is also computationally faster. The Kumaraswamy distribution is given by Eqs. (2.15) and (2.16), which is an alternative two-parameter distribution on (0, 1). Having some more advantages in terms of traceability, it possesses the same properties as the beta distribution [10].

$$\begin{cases} f(x) = abx^{a-1}(1-x^a)^{b-1} \\ a, b > 0 \\ x \in [0, 1] \end{cases} \tag{2.15}$$

$$F(x) = [1 - (1 - x^a)^b] \tag{2.16}$$

where $f(x)$ is the probability density functions and $F(x)$ is the cumulative density functions.

Furthermore, Kumaraswamy distribution can be used not only for resource modeling in general but also for demand modeling effectively. It is also important to note that the copulas that are used to model the dependency structure of the wind power are of more interest to the system planners rather than the ones modeling only wind speed. Regarding modeling wind power, standard benchmark wind turbines, such as 3 kW Turbine based on HOMER, are taken into consideration in order to come up with the best parametric fit for wind power at each location. One best way to fit wind power to the distribution is to take advantage of the double bounded Kumaraswamy distribution due to its general nature and simplicity, and then the marginal for all the locations will be obtained and dependence structure can be established through Vine Copulas. Moreover, non-Gaussian nature of wind power and high dimensionality of wind data at different locations makes it virtually impossible to be captured completely using correlation means as well as adequate copula functions, where solutions such as Pair Copula Constructions (PCC) approaches come up [11, 12].

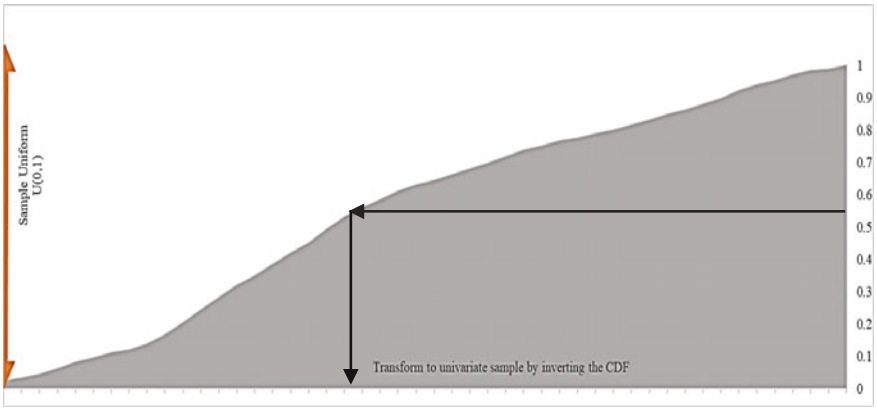

Fig. 2.4 Drawing a random sample from a CDF

2.4.1.2 The Theory of Copulas

A copula, in probability theory and statistics, is a multivariate probability distribution for which the marginal probability distribution of each variable is uniform, which is used to describe the dependence between random variables. In other words, combining univariate distributions is possible through copula functions in order to obtain a joint distribution with particular dependence structure. Most simplified demonstrations of copulas derive from the way copulas are used on distributions, of which knowing the way a cumulative density function (CDF) contributing in generating a random sample is a necessity. In general, sampling from a uniform distribution would be the first step through drawing a value from a particular distribution, which is called the CDF of a variable, and then a sample can be obtained from a PDF as shown in Fig. 2.4. Moreover, several different distributions are extended this method such as Sklar's theorem, which states that for a given joint multivariate distribution function and the marginal distributions related; a copula function can be found that relates them [13].

2.4.1.3 Sklar's Theorem

Sklar's theorem has been considered the foundation of most of the applications of copulas theory in statistics, which clarifies the role of copulas in the joint connection between multivariate distribution functions and their univariate margins. This theorem first appeared in [13], which the name "copula" was chosen to emphasize the manner in which a copula "couples" a joint distribution function to its univariate margins. Thus, the brief explanation of Sklar's theorem is as the following [14]:

Let H be a joint distribution function with margins F and G. Then there exists a copula C such that for all x, y in $\overline{\mathbf{R}}$,

$$H(x, y) = C(F(x), G(y)) \tag{2.17}$$

If F and G are continuous, then C is unique; otherwise, C is uniquely determined on RanF×RanG. Conversely, if C is a copula and F and G are distribution functions, then the function H defined by Eq. (2.17) *is a joint distribution function with margins F and G.*

C is a copula if $C{:}[0,1]^2 \rightarrow [0,1]$ *and,*

1. $C(0, u_m) = C(v_m,0) = 0$
2. $C(1, u_m) = C(u_m, 1) = u_m$
3. $C(u_{m2}, v_{m2}) - C(u_{m1}, v_{m2}) - C(u_{m2}, v_{m1}) + C(u_{m1}, v_{m1}) \geq 0$ *for all* $v_{m1} < v_{m2}$, $u_{m1} < u_{m2}$
4. *If C is differentiable once in its first argument and once in its second then, C is equivalent to* $\int_{v_{m1}}^{v_{m2}} \int_{u_{m1}}^{u_{m2}} \frac{\partial^2 C}{\partial u_m \partial v_m} du_m dv_m \geq 0$ *for all* $v_{m1} < v_{m2}$, $u_{m1} < u_{m2}$

The above-mentioned definition shows that copulas can be counted as independent distribution functions which are defined on $[0, 1]^2$ with uniform marginal. In addition, probabilities of one-dimensional events can be produced by each of the marginal distributions taken by copula functions and projected to a joint probability and having the relationship enforced on them. Overall, it is very efficient to use copulas in order to create multivariate distributions as they help segregate selection of dependence and marginal from one another, Sklar's theorem being one of the easiest ways for the formation of copulas. More on this, if $F(x)$ and $G(y)$ are the marginal distributions and the copula can be given by Eq. (2.18) [14].

$$C(u_m, v_m) = H_{u_m v_m}(F^{-1}(u_m), G^{-1}(v_m)) \tag{2.18}$$

2.4.1.4 The Right Copula Selection

Making the right choice when it comes to modeling data through distribution means is of utmost importance, considering wide verity of distributions and copulas available. The selection of copulas is mostly based on two factors as familiarity and tractability whereby Gumbel copula being the best for extreme distributions, Gaussian the rightest for linear correlations, which is obtained from normal distribution, and t-copula for the dependence in tails etc. Moreover, in order to generate a copula incorporating marginal distributions of two variables, distributions such as lognormal and Kumaraswamy with (μ, σ) and (a, b) as their parameters, respectively, a copula from Frank family can be taken advantage of which is given by Eq. (2.19) [14, 15].

$$C(u_m, v_m) = -\frac{1}{\delta} \ln\left(1 + \frac{\left(e^{-\delta u_m} + 1\right)\left(e^{-\delta v_m} - 1\right)}{\left(e^{-\delta} - 1\right)}\right) \tag{2.19}$$

where δ is a coefficient determining the degree of dependence between marginal.

A lot of work having been carried out on acquiring marginal distributions and different methods having been proven efficient for different cases such as empirical distribution or parametric best fit, empirical distribution is where to start often, but in order to obtain a smooth curve, it is efficient to apply kernel smoothing or cubic splines. Likewise, Eq. (2.20) presents t-copula as for modeling tails, which compared with Gaussian copula enables for joint fat tails and an increased probability of joint extreme events [16, 17].

$$C_{\rho,\vartheta}(u_m, v_m) = \int_{-\infty}^{t_\vartheta^{-1}(u_m)} \int_{-\infty}^{t_\vartheta^{-1}(v_m)} \frac{1}{2\pi\left(1-\rho^2\right)^{\frac{1}{2}}} \left\{1 + \frac{x^2 - 2\rho xy + y^2}{\vartheta\left(1-\rho^2\right)}\right\}^{\frac{-(\vartheta+2)}{2}} dsdt \tag{2.20}$$

where, t_ϑ^{-1} is the inverse of the standard univariate t-copula with ϑ degrees of freedom, ρ and ϑ are the factors of the copula, and expectation 0 and variance $\frac{\vartheta}{\vartheta-2}$. An additional parameter was introduced by t-copula compared to Gaussian copula as ϑ, which an increase in it decreases the tendency to exhibit extreme co-movements [18].

There is another copula called Gumbel copula, which is an asymmetric one (given by Eq. (2.21)) and shows superior dependency in the positive tail than in the negative [17].

$$C_\delta(u_m, v_m) = \exp\left(-\left[(-\log u_m)^\delta + (-\log v_m)^\delta\right]^{1/\delta}\right) \tag{2.21}$$

where δ is a coefficient controlling the degree of dependence.

It is understood that no any particular distribution presented in this chapter or in all the other addressed references fit the output power generated by wind turbines and solar panels quite well. On the other hand, Kumaraswamy distribution has proven a better efficiency on modeling the dependence regarding wind and solar power, and it is also one of the best probabilistic approaches to model uncertainty in the resources. Furthermore, to better model the association between uncertain parameters, the idea of modeling dependence seems to be of great importance where copulas come to use to model wind power in relation to the spatial domain.

2.5 Optimization Models for Microgrid Planning

The penetration of renewable energy sources is typically high in an isolated microgrid system with a small amount of carbon footprint, in which removing interruptions is of great importance. Although the capital investment on such power systems is high and the uncertain nature of such sources of energy is a serious challenge to be met, they are significantly appreciated from the environmental aspects. Besides, there are several basic and sophisticated optimization models in order to include and consider

all of the possible energy generation and cost scenarios in the microgrid planning problem such as deterministic optimization model, scholastic programming etc., which are discussed in this section.

2.5.1 Deterministic Optimization Models

Designing a cost-effective and reliable capacity for Hybrid Power Systems (HPS) has been studied from different aspects of view, for which heuristic approaches are applied to choose the best system configurations and cost minimization policies for the most economical operational purposes. However, the operational planning and HPS was conventionally formulated as a single objective function, denoting to the minimization of total cost considering certain reliability factors. In addition, there are other objectives recently incorporated into the general one as reliability maximization, losses, and emissions minimization etc. Just as many other optimization problems, there are several contradictory objectives combined into one which requires multi-objective optimization methods to be used [19].

The optimization procedure is a repetitive process starting from selecting system configurations randomly, and then conducting the related simulations by static rules and choosing operational policies to minimize costs. The iterative process obtains the fitness of system configurations and ranks them, and then a new set of variables are produced and applied to the system using evolutionary algorithms, which carries on until the best solution is found according to the stopping criteria for the algorithm. Additionally, there are plenty of simulation tools such as HOMER and HYBRIDS available to apply to the designed systems and make various comparisons on them in order to come up with the best operational strategies when facing contrasting scenarios. The correlation between the operational planning of HPS and the capacity design is well understood by the simulation approach, although the optimal systems configurations might not found during the process because of the limitations posed by unnecessary constraints and possible suboptimal points found by the heuristic algorithm. Therefore, it is important to hire an optimization method that tackles all the hurdles and comes up with the best solution for the HPS designing. Equations (2.22)–(2.38) represent the mathematical functions for an approach that simultaneously finds an optimal operating plan and system configurations for the HPS problem incorporated as a Multi-objective Linear Programming optimization problem [19].

2.5.1.1 Objective Function

The combined objective function to be minimized is given by Eq. (2.22).

$$\text{Objective: } w_c \cdot TDC + (1 - w_c) \cdot TDE \tag{2.22}$$

$$TDC = \sum_{i=\{dg,pv,wt\}} \left[N_i \left(\frac{IC_i}{T_i} + OM_i \right) \right] + \frac{IC_b}{T_b} \cdot \frac{\sum_{t=1}^{24} \sum_{m=1}^{12} Ch_b(t,m)}{12 \cdot C_{\max}} + FC_{dg} \cdot \frac{\sum_{t=1}^{24} \sum_{m=1}^{12} O_{dg}(t,m)}{12} \tag{2.23}$$

$$TDE = \sum_{i=\{dg,pv,wt\}} \left[\frac{N_i \cdot EE_i}{T_i} \right] + \frac{EE_b}{T_b} \cdot \frac{\sum_{t=1}^{24} \sum_{m=1}^{12} Ch_b(t,m)}{12 \cdot C_{\max}} + DE_{dg} \cdot \frac{\sum_{t=1}^{24} \sum_{m=1}^{12} O_{dg}(t,m)}{12} \tag{2.24}$$

where w_c is a factor denoting the weight of the cost minimization objective function, N_i and IC_i represent the number of power storage units and generation and initial cost per storage unit and power generation of type i in US$. T_i and OM_i are expected life and maintenance and daily operations costs for a storage or generation unit of type i in days and US$/day, respectively. $Ch_b(t, m)$ is all batteries' charging power in kW, $O_{dg}(t, m)$ and $C_{\max}$ are and the output power from DG sources in kW and the maximum available charge of a battery in kWh [19].

2.5.1.2 Constraints

The ideal answer must meet a set of constraints presented in the following:

A. Supply-demand balance: Power demand equals the sum of unmet load and power supply at any time interval:

$$\left(\begin{array}{c} D(t,m) + Ch_b(t,m) \le O_{dg}(t,m) + N_{pv} \cdot O_{pv}(t,m) + N_{wt} \cdot O_{wt}(t,m) \\ + DCh_b(t,m) + D_{us}(t,m) \\ \forall t, m \end{array} \right) \tag{2.25}$$

where, $D(t, m)$ is the amount of peak demand in kW and $D_{us}(t, m)$ is the unmet load in kW. $Ch_b(t, m)$ (kW) and $DCh_b(t, m)$ (kWh) are the charging power and the power shared by the storage system (batteries), respectively. $O_{dg}(t, m)$, $O_{pv}(t, m)$ and $O_{wt}(t, m)$ are the output power from generation sources in kW, and N_i is the quantity of power storage/generation units [19].

B. The output limit of diesel generator: diesel generators' output power must not be larger than their rated capacity:

$$\left(\begin{array}{c} O_{dg}(t,m) + SR(t,m) \le N_{dg} \cdot RC_{dg} \\ \forall t, m \end{array} \right) \tag{2.26}$$

where, $SR(t, m)$ is the available spinning reserve in kW and RC_{dg} is the rated capacity of diesel generator [19].

C. The State of Charge (SoC) of batteries: A restraint presenting the linkage between energy storage in the battery and the process of discharging and charging.

$$\left(\begin{array}{c} C(t+1,m) = C(t,m)(1-\gamma_{sd}) + Ch_b(t,m) - \frac{Dch_b(t-1,m)}{\gamma_d} \\ \forall t, m \end{array} \right) \tag{2.27}$$

where, $C(t, m)$ is the stored energy in the batteries in kWh, γ_{sd} and γ_d are the efficiencies of hourly self-discharging and discharging for batteries in %/hour and %, respectively, while m is the month of the year and t is the hour of the day [19].

D. Capacity limits of batteries: There is an upper limit for batteries regarding their SoC:

$$\left(\begin{array}{c} (1 - DOD_{\max}) \cdot C_{\max} \cdot N_b \leq C(t,m) \leq C_{\max} \cdot N_b \\ \forall t, m \end{array} \right) \tag{2.28}$$

where DOD is the maximum value of depth of discharge in a cycle considering the fact that discharging and charging electricity to or from the battery must be less than or equal to its rated capacity [19].

$$\left(\begin{array}{c} Ch_b(t,m) \leq N_b \cdot RC_b \\ \forall t, m \end{array} \right) \tag{2.29}$$

$$\left(\begin{array}{c} DCh_b(t,m) \leq N_b \cdot RC_b \\ \forall t, m \end{array} \right) \tag{2.30}$$

E. The requirements of spinning reserve (SR): Diesel generators must be capable of responding promptly to any changes and possible failures in the power generation units.

$$\left(\begin{array}{c} SR(t,m) \geq SR_{\min} D(t,m) \\ \forall t, m \end{array} \right) \tag{2.31}$$

where, $SR(t, m)$ representing spinning reserve available in kW and the requirements of spinning reserve is considered as a fraction of total demand. Moreover, it has been assumed that no limits have been imposed on the ramp up/down of generators and their output power can be changed immediately [19].

F. Cycle repeatability: The SoC of batteries, in the beginning, should equal to the one at the end of the cycle, which guarantees the optimal cycle is repeatable [19].

$$\left(\begin{array}{c} C(24,m)(1-\gamma_{sd}) + Ch_b(1,m) - \frac{Dch_b(1,m)}{\gamma_d} = C(1,m) \\ \forall m \end{array} \right) \tag{2.32}$$

G. The maximum permissible level of unmet power (*EUE*): To maintain the acceptable service being delivered, the amount of energy not being supplied, as *EUE*, must not exceed a predefined extent.

$$\sum_{t=1}^{24} \sum_{m=1}^{12} D_{us}(t,m) \leq EUE_{\max} \tag{2.33}$$

In addition, reliability assessment is done through considering the ability of storage units and generators to meet the demand completely whereby an accurate planning of resources will ensure perfect reliability ($EUE = 0$) [19].

H. Budget and/or resource limitations: In order to assure that the solution is practical from the monetary point of view, the following constraints are applied to the objective function, which denotes the budget by means of RES numbers [19].

$$N_{pv,\min} \leq N_{pv} \leq N_{pv,\max} \tag{2.34}$$

$$N_{wt,\min} \leq N_{wt} \leq N_{wt,\max} \tag{2.35}$$

$$N_{b,\min} \leq N_b \leq N_{b,\max} \tag{2.36}$$

I. Prevention of simultaneous discharging and charging: To prevent the process of charging and discharging from happening at the same time the following constraint is applied to the objective function [19].

$$\left(\begin{array}{c} Ch_b(t,m) \times DCh_b(t,m) = 0 \\ \forall t, m \end{array} \right) \tag{2.37}$$

J. Energy to Power Ratio (E/P): Batteries' capacity is determined via E/P ratio for any given power rating, which represents an association between energy size and power for a particular storage system. The former notes to the maximum sum of energy that the storage system can store for a certain duration, while the latter represents the rate at which charging and discharging processes can be continually run.

$$\left(\begin{array}{c} \underline{EPR} \cdot N_b \cdot RC_b \leq C(t,m) \leq \overline{EPR} \cdot N_b \cdot RC_b \\ \forall t, m \\ \text{where: } EPR \text{ or} \frac{E}{P} = \frac{\text{Energy Capacity (kWh)}}{\text{Power Rating (kWh)}} \end{array} \right) \tag{2.38}$$

2.5.2 Two-Stage Stochastic Programming Grounded Model

One of the lately developed approaches for operating and planning of the distributed energy systems is the two-stage stochastic programming model, which has been demonstrated to be efficient and flexible when it comes to dealing with uncertainty in microgrids. In addition, Monte Carlo Simulation (MCS) is the most common way for generating stochastic variable scenarios for two-stage stochastic programming, and the risk cost can be enormously reduced by all the possible realizations having been considered. There are several problems that the two-stage stochastic programming has been applied on, such as a stochastic model for optimal energy management with the goal of cost and emission minimization, two-stage SP strategy for energy and reserve scheduling with demand response, two-stage SP method for the optimal design of distributed energy system etc. Equations (2.39)–(2.54) represent the mathematical formulation for the problem of microgrid planning and operation using the two-stage stochastic programming method [19, 20].

2.5.2.1 Objective Function

The combined objective function to be minimized is given by Eq. (2.39).

$$\begin{aligned}&\overline{N}_{pv}\left(IC_{pv}+OM_{pv}(N_{pv})\right)+\overline{N}_{wt}(IC_{wt}+OM_{wt}(N_{wt}))\\&\quad+N_{dg}\left(IC_{dg}+OM_{dg}(O_{dg})\right)+\overline{N}_{b}(IC_{b}+OM_{b})\\&\quad+\frac{1}{n_s}\left(\sum_{t}\sum_{s}\left(C_{us}D^{s}_{ust}\right)+FC_{dg}\sum_{s}\sum_{t}\left(O^{s}_{dg_t}\right)+\sum_{s}\sum_{t}O^{s}_{dg_t}\cdot C_{tax}\cdot C_{int}\right)\end{aligned} \tag{2.39}$$

where, N_{dg}, N_{wt}, and N_{pv} are the total numbers of non-renewable generators, wind turbines and PV panels, respectively. $IC_{pv}, IC_{dg}, IC_{wt}$ and IC_b are the levelized annual installation cost of PV panels, diesel generation, wind turbines and batteries in $, correspondingly. OM_{dg}, OM_{pv}, OM_{wt}, and OM_b are expressed as levelized annual management and operation cost for generation sources and FC_{dg} is the fuel cost in $/kWh. D and D_{us} are the demand in kW and the unserved demand in kW, respectively. C_{us}, C_{tax} and C_{int} are unserved power's cost in $/kW, the tax of carbon in ($/kg) and intensity of CO2 in kg/kW, correspondingly. O_{dg}, O_{pv} and O_{wt} are the output power from generation sources in kW and n_s refers to the total number of scenarios where $s \in n_s$ and $t \in 1\ldots8760$ and t is in hours, respectively. There are two sets of variables for any two-stage stochastic programming as recourse and here-and-now variables, the former denoting the decisions to be made in case of uncertainty happening in the operational phase and latter referring to the decisions to be made in the planning phase. More on that, planning phase includes the installation of batteries, diesel generators, solar panels and wind turbines, while operational phase embodying the

real-time output power of batteries (DCh_b) and diesel generators (O_{dg}) and also the unsupplied load (D_{us}) [19].

2.5.2.2 Constraints

The ideal answer must meet a set of constraints presented in the following:

A. Supply-demand balance: Power demand equals to the sum of unmet load and power supply from renewable energy sources at any time interval, while the storage might not have the capacity for the power produced which should be dumped or a specific amount of energy might remain unsupplied [19].

$$\begin{pmatrix} D(t,s) = O_{dg}(t,s) + N_{pv} \cdot O_{pv}(t,s) + N_{wt} \cdot O_{wt}(t,s) \\ +DCh_b(t,s) + D_{us}(t,s) - Ch_b(t,s) \\ \forall t \in 1 \ldots t, s \in 1 \ldots n_s \end{pmatrix} \tag{2.40}$$

B. The output limit of diesel generator: the output power of diesel generators must not be larger than their rated capacity. In order to insure that the desired amount of power is available for all of the scenarios, the spinning reserve has been considered a function of variable s.

$$\begin{pmatrix} O_{dg}(t,s) + SR(t,s) \leq N_{dg} \cdot RC_{dg} \\ \forall t \in 1 \ldots t, s \in 1 \ldots n_s \end{pmatrix} \tag{2.41}$$

C. The State of Charge (SoC) of batteries: A constraint presenting the linkage between energy storage in the battery and the process of charging and discharging [19].

$$\begin{pmatrix} C(t,s) = C(t-1,s) \cdot (1-\gamma_{sd}) + Ch_b(t,s) - \frac{DCh_b(t,s)}{\gamma_d} \\ \forall t \in 1 \ldots t, s \in 1 \ldots n_s \end{pmatrix} \tag{2.42}$$

where C is the stored energy in the batteries in kWh, γ_{sd} and γ_d are the efficiencies of hourly self-discharging and discharging for batteries in %/hour and %, respectively. Ch_b (kW) and DCh_b (kWh) are the charging power and the power shared by the storage system (batteries), respectively [19].

D. Capacity limits of batteries: There is an upper limit for batteries regarding their SoC:

$$\begin{pmatrix} (1 - DOD_{\max}) \cdot C_{\max} \cdot N_b \leq C(t,s) \leq C_{\max} \cdot N_b \\ \forall s \in 1 \ldots n_s \end{pmatrix} \tag{2.43}$$

where $DOD_{\max}$ is the maximum amount of depth of discharge in a cycle considering the fact that charging and discharging electric power to or from the battery must be less than or equal to its rated capacity [19].

$$\begin{pmatrix} Ch_b(t,s) \le N_b \cdot RC_b \\ \forall t, s \end{pmatrix} \tag{2.44}$$

$$\begin{pmatrix} DCh_b(t,s) \le N_b \cdot RC_b \\ \forall t, s \end{pmatrix} \tag{2.45}$$

where The rated capacity of batteries is given by RC_b in kW.

E. The maximum permissible level of unmet power (EUE): To maintain the acceptable service being delivered, the amount of energy not being supplied, as EUE, must not exceed a predefined extent [19].

$$\begin{pmatrix} \frac{\sum_{t=1}^{9760} D_{us_t}^s}{\sum_{t=1}^{9760} D_t^s} \le EUE_{\max} \\ \forall s \in 1 \ldots n_s \end{pmatrix} \tag{2.46}$$

F. Budget and/or resource limitations: In order to assure that the solution is practical from the monetary point of view, the following constraints are applied to the objective function, which denotes the budget by means of RES numbers.

$$N_{pv,\min} \le N_{pv} \le N_{pv,\max} \tag{2.47}$$

$$N_{wt,\min} \le N_{wt} \le N_{wt,\max} \tag{2.48}$$

$$N_{b,\min} \le N_b \le N_{b,\max} \tag{2.49}$$

G. The initial state of batteries in each scenario: The initial state of batteries in each scenario is as the following:

$$\begin{pmatrix} C_t^s = \frac{C_{\max} \times N_b}{2} \\ \forall S \in 1 \ldots n_s, t = 1 \end{pmatrix} \tag{2.50}$$

Renewable energy penetration is one of the most important components, which needs to be taken into consideration when modeling two-stage stochastic programming for the sake of microgrids planning. In addition, as the initial investment needed for installation of diesel generation is much lower than renewable sources of energy, it is quite cost-effective to provide all the energy from them, which is not the case. Therefore, the contribution percentage for renewable resources of energy should be determined and optimized considering a particular reliability measures as the following.

H. Minimum penetration levels of Renewable Energy Sources: In order to make the planner and optimizer to ensure a particular percentage of renewable resources energy penetration, the following constraint should be applied to the objective function [19].

$$\left(\begin{array}{c} \sum_{t=1}^{t} N_{wt} O_{wt}(t,s) + \sum_{t=1}^{t} N_{pv} O_{pv}(t,s) \geq RP \sum_{t=1}^{t} (D(t,s) - D_{us}(t,s)) \\ \forall s \in 1 \ldots n_s \end{array} \right) \quad (2.51)$$

where RP is the factor specifying the penetration level.

I. The requirements of spinning reserve (SR): Diesel generators must be capable of responding promptly to any changes and possible failures in the power generation units.

$$\left(\begin{array}{c} SR(t,s) \geq SR_{\min} D(t,s) \\ \forall t \in 1 \ldots 8760, s \in 1 \ldots n_s \end{array} \right) \quad (2.52)$$

J. Prevention of simultaneous discharging and charging: To prevent the process of charging and discharging from happening at the same time the following constraint is applied to the objective function.

$$\left(\begin{array}{c} Ch_b(t,s) \times DCh_b(t,s) = 0 \\ \forall t, s \end{array} \right) \quad (2.53)$$

K. Energy to Power Ratio (E/P): Batteries' energy capacity is determined via E/P ratio for any given power rating, which represents an association between energy size and power for a particular storage system. The former notes to the maximum sum of energy that the storage system can store for a certain duration, while the latter represents the rate at which charging and discharging processes can be continually run.

$$\left(\begin{array}{c} \underline{EPR} \cdot N_b \cdot RC_b \leq C(t,s) \leq \overline{EPR} \cdot N_b \cdot RC_b \\ \forall t, m \\ \text{where: } EPR \text{ or} \frac{E}{P} = \frac{\text{Energy Capacity (kWh)}}{\text{Power Rating (kWh)}} \end{array} \right) \quad (2.54)$$

2.5.3 *Two-Stage Stochastic Programming Model—Risk Averse*

One of the most important problems to be dealt with in modeling and planning microgrids that involve uncertainty is the risk investigations and exposure to economic and environmental risk cannot be avoided when it comes to planning power transmission and distribution systems for microgrids. Moreover, ideas of portfolio optimization by Markowitz [21] can be used in order to extend the two-stage stochastic programming model to consider risk investigations [19]. As there is a variance in the second-stage variables, the evaluation of the variance should be applied to them as well. The new objective function incorporating risk investigations is expressed as Eqs. (2.55) and (2.56).

$$\text{minimize}\, A + \theta_r \sqrt{Var(B)} \tag{2.55}$$

$$Var(B) = E\left[B^2\right] - (E[B])^2 \tag{2.56}$$

where B is the second-stage objective function, $(E[B])^2$ is the square of the objective function and $E[B^2]$ is as the following:

$$E[B^2]_s = \sum_{s=1}^{n} B_s^2 \times \Pr(s) \tag{2.57}$$

where B is the objective function and $\Pr(s)$ is the possibility function expressing the incidence of state s.

The new objective function to be minimized is a non-linear objective function incorporating risk investigations as Eq. (2.58).

$$\text{minimize}\, E[A + B] + \theta_r \sqrt{Var(B)} \tag{2.58}$$

where,

$$\begin{aligned} A = {} & \overline{N}_{pv}(IC_{pv} + OM_{pv}(N_{pv})) + \overline{N}_{wt}(IC_{wt} + OM_{wt}(N_{wt})) \\ & + N_{dg}(IC_{dg} + OM_{dg}(O_{dg})) + \overline{N}_b(IC_b + OM_b) \end{aligned} \tag{2.59}$$

$$B = \frac{1}{n_s}\left(\sum_t \sum_s (C_{us} D^s_{us_t}) + FC_{dg}\left(\sum_s \sum_t O^s_{dg_t}\right) + \sum_s \sum_t O^s_{dg_t} C_{tax} C_{int}\right) \tag{2.60}$$

It should be noted that all the constraints for two-stage stochastic programming stay the same for the new risk-averse objective function, while the objective function incorporates the variance for the uncertainties explicitly.

2.6 Conclusion

Smart grids are the solution for the traditional power system confronting operational and monetary difficulties, which has fundamental differences comparing to the conventional one. As such, when the demand rises, the favored arrangement would not be necessarily generating more electricity to fulfill the consumption requirements. In other words, generation of electricity will not directly be dependent on consumption; rather it will be a function of losses minimization, end-user demand management and collaboration with customers in order to roll back the load. Furthermore, microgrids are a compact version of traditional power system connection multiple distributed sources to multiple loads, which draws the interest of power system planners as they can be of great importance when it comes to electrifying remote areas. In this

chapter, following an introduction to the fundamentals and definition of microgrids, the focus was taken on microgrid planning and energy management that explored modeling random variables for wind and solar energy. Then, solar and wind energy modeling using several different probability distributions were explained. Finally, the optimization models for microgrid planning has been proposed elaborately using stochastic programming and deterministic mathematical models.

References

1. H. Farhangi, *Smart Microgrids—Lessons from Campus Microgrid Design and Implementation* (CRC Press, New York, 2017)
2. H. Bevrani, B. Francois, T. Ise, *Microgrid Dynamics and Control* (Wiley, USA, 2017)
3. M. Lydia, S.S. Kumar, A.I. Selvakumar, G.E. Prem Kumar, A comprehensive review on wind turbine power curve modeling techniques. Renew. Sustain. Energy Rev. **30**, 452–460 (2014)
4. A. Kaabeche, M. Belhamel, R. Ibtiouen, Sizing optimization of grid-independent hybrid photovoltaic/wind power generation system. Energy **36**, 1214–1222 (2011)
5. G. Tina, S. Gagliano, S. Raiti, Hybrid solar/wind power system probabilistic modelling for long term performance assessment. Solar Energy **80**, 578–588 (2006)
6. R. Belfkira, L. Zhang, G. Barakat, Optimal sizing study of hybrid wind-PV-diesel power generation unit. Solar Energy **85**, 100–110 (2011)
7. A. Abdollahi, M.P. Moghaddam, Investigation of economic and environmental-driven demand response measures incorporating UC. IEEE Trans. Smart Grid **3**, 12–25 (2012)
8. O. Grothe, J. Schnieders, Spatial dependence in wind and optimal wind power allocation—a copula based analysis. Energy Policy **39**, 4742–4754 (2011)
9. G. Tina, S. Gagliano, V.A. Doria, Probability analysis of weather data for energy assessment of hybrid solar-wind power system, in *4th IASME/WSEAS International Conference on Energy, Environment, Ecosystems and Sustainable Development* (2008), pp. 217–223
10. M. Jones, Kumaraswamy's distribution a beta-type distribution with some tractability. Stat. Methodol. **6**, 70–81 (2009)
11. P. Kumaraswamy, A generalized probability density function for double-bounded random processes. J. Hydrol. **46**, 79–88 (1980)
12. E.C. Brechmann, U. Schepsmeier, Modeling dependence with C- and D-vine copulas the R package CDVine. J. Stat. Softw. **52**(3) (2013)
13. A. Sklar, *Distribution Functions of N Dimensions and Margins*, vol. 8 (Publications of the Institute of Statistics of the University of Paris, 1959), pp. 229–231
14. R.B. Nelsen, *An Introduction to Copulas* (Springer, 2006)
15. A. Seifi, K. Ponnambalam, J. Vlach, A unified approach to statistical design centering of integrated circuits with correlated parameters. IEEE Trans. Circuits Syst. Fundam. Theory Appl. **46**, 190–196 (1999)
16. A.E. Gelfand, A.F.M. Smith, Sampling-based approaches to calculating marginal densities. J. Am. Stat. Assoc. **85**, 398–409 (1990)
17. H. Joe, *Multivariate Models and Multivariate Dependence Concepts* (Springer-Science and Business Media, B.V., 1997)
18. S. Demarta, A.J. McNeil, *The t Copula and Related Copulas* (Department of Mathematics, Federal Institute of Technology, Zurich, 2004)
19. A. Saif, K.G. Elrab, H.H. Zeineldin, S. Kennedy, J.L. Kirtley, Multi-objective capacity planning of a PV-wind-diesel-battery hybrid power system, in *IEEE International Energy Conference* (2010)

20. Z. Li, C. Zang, P. Zeng, H. Yu, H. Li, Two-stage stochastic programming based model predictive control strategy for microgrid energy management under uncertainties, in *IEEE—PMAPS* (2016)
21. H. Markowitz, Portfolio selection. J. Financ. **7**, 77–91 (1952)

Chapter 3
AC and DC Combined Microgrid, Modeling and Operation

Nariman Rahmanovich Rahmanov and Ogtay Zaur oglu Karimov

Abstract In this chapter, we present modeling of a combined microgrid which is made by integration of two subsystems as AC bus microgrid and DC bus microgrid. To the contrary of existing AC and DC microgrids the combined microgrid has advantages in efficient provision of local customers with ecologically clean, digital quality and reliable energy supply. This is achieved by special circuit design, whereby AC bus subsystem is connected with sources of power and loads which traditionally producing and consuming subsequently AC current. DC bus subsystem of combined microgrid connected with sources of power and loads which traditionally producing and consuming subsequently DC current. Both subsystems are interconnected by means of two-way inverter. In case of power deficiency in any of subsystems the control unit may change the direction of power flow and provide stable operation of combined microgrid using minimal number of conversion devices. Two study cases—for parallel operation of combined microgrid with Main grid as well as islanded operation of combined microgrid are presented. This chapter consists of the sections including introduction, structure of combined AC-DC microgrid, modeling of combined microgrid, energy storage, integration, conclusion, reference.

Keywords AC microgrid · DC microgrid · AC-DC microgrid · Renewable sources · Wind generator · PV-Solar unit · Energy storage · Power flow

3.1 Introduction

Traditionally electrical energy is generated by large power plants in close vicinity of fuel sources and then electrical energy is transferred to the centers of consumption. To reduce energy losses power transformers are used to increase voltage level to

N. R. Rahmanov (✉) · O. Z. Karimov
Cleaner Production and Energy Efficiency Center, Baku, Azerbaijan
e-mail: nariman@cpee.az

O. Z. Karimov
e-mail: okerimov@yahoo.com

N. Mahdavi Tabatabaei et al. (eds.), *Microgrid Architectures, Control and Protection Methods*, Power Systems,
https://doi.org/10.1007/978-3-030-23723-3_3

220–1150 kV and then reduce it on the consumption side to the level of distribution network 35/10/0.4 kV. Such practice has existed for more than 100 years and considered the most effective. In regional distribution networks power flow usually directed to the one end—from substation to the customer. But until the recent time the distribution network (DN) as a part of the Grid considered as a passive due to absence of sources of electrical energy in it.

Therefore, DN did not take part in power regulation; the situation didn't change even when some sources of renewable energy were introduced into the circuit. Application of RS (regulation services) as well as other traditional sources of power in DN resulted in losses reduction and voltage profile improvement [1, 2]. But with increased usage of RS connected to the grid it becomes inevitable to take them into account analyzing steady state or dynamic processes in the energy system as it becomes available with advance technology devices for measurement and registration. Despite the fact that future energy systems will rely mainly on central power plants as before, nevertheless it will be more dependent on increasing RS, electrical energy storing devices, DG, electro mobiles, intellectual devices measuring energy, phase censoring devices and communication equipment. In the contemporary period of time further improvement of energy efficiency and increased reliability may be reached by using the conception of smart grid or its first study—intellectual network [3].

The concept of distributed generation is realized in the form of microgrid, which is in essence a group of interconnected loads and distributed renewable power sources that act as a single controllable system. As a matter of fact, microgrid is a small scale power grid, which producing electrical energy on site and supply local loads.

It is well known that diesel and gas turbine generators as a distributed power source were used in remote places, or as back-up power supply units in small local network called now as microgrid. Microgrid includes renewable power sources as wind power generator, PV-solar units, fuel cells, biogas units, hydro and some other systems, as well as conventional micro gas turbine, diesel generator and energy storage systems and control.

Application of new technologies with renewable sources of power may reduce operating expenses; improve reliability and system efficiency by reducing losses compared to conventional generation.

The conception of microgrid permits:

- to switch from radial supply circuit to ring, providing reliable connection of the end users with energy sources;
- short electrical connections between on-site sources of power and loads minimizing line losses;
- modular application of low voltage power unit and storage devices providing flexibility and ease in microgrid projection and construction;
- to replace electromechanical system by digital, providing necessary data needed by informational and automatic systems;

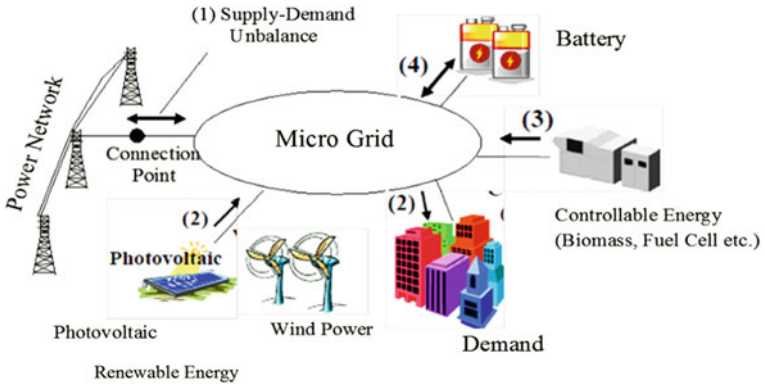

Fig. 3.1 Microgrid

– provide two-way communication inside the energy system to create conditions for end users to switch from passive to the active participation on the energy market (providing demand side management).

In this connection novel idea of power supply for residential area, for example house or small premises for commercial sector and local community buildings was studied. It is suggested to supply customers of the microgrid from two buses. One bus has standard 10/0.4 kV AC voltage; the second one is DC bus 48–400 V [1]. AC buses will supply large power devices such as air conditioner, refrigerator or washing machine. DC bus system may supply lighting system, consumer electronics and provide generating of RS sources circuit of such microgrid is presented in Fig. 3.1.

Two bus microgrid topology in comparison with one bus system is more flexible, optimally uses on site renewable sources and control generation/consumption of various sources of power within microgrid to cover load demands. Other advantages of the suggested arrangement is possibility to use energy of car batteries from parking lot connected to charging outlets of local microgrid to supply DC and AC loads at the time of emergency. This chapter is devoted to designing of structure and modeling of combined AC-DC Microgrid, which consists of two parallel AC and DC microsystems each of them including renewable sources of power, AC loads and DC loads and DC power sources (Fig. 3.2).

3.2 Structure of Combined AC-DC Microgrid

3.2.1 AC and DC Bus Subsystems Microgrid

Generally, AC subsystem microgrid are well known and their structures are studied and understood in detail. There is a good experience in modeling and operation

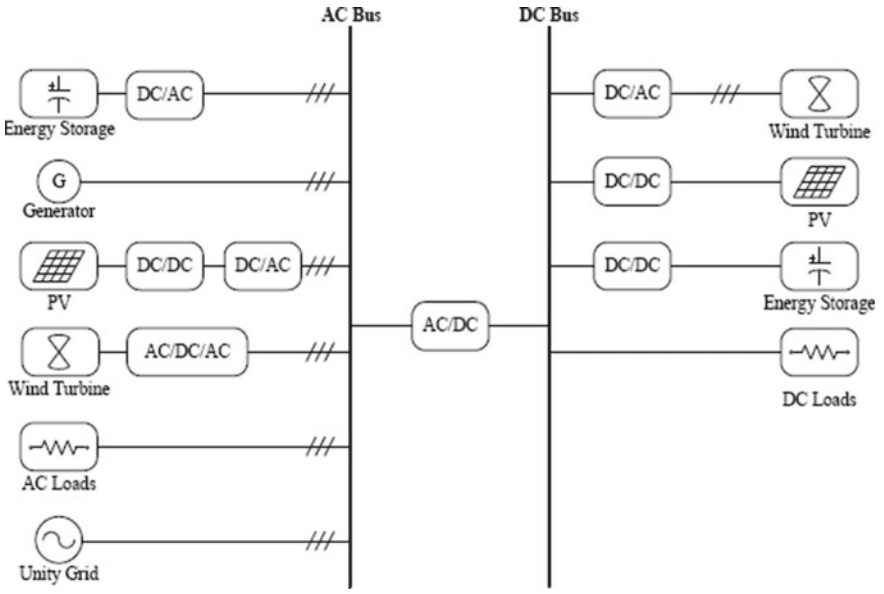

Fig. 3.2 Simplified circuit of two bus AC-DC microgrid system

control for AC systems. For this reason, we are concentrating on microgrid detailed study of DC microgrid systems.

The idea to use dc power supply in distribution network was based on that:

- In our homes and working places most of used electronics and appliances (computer, printer, copier etc.) are operated from dc source of power, using different kind of power supply units being connected to the standard 0.4/0.23 kV AC network. For example, in some countries about 20% of consumed power is used for lighting and some 15% of total energy consumption is used by home electronics including computers. And all these end devices consume dc current [3].
- Distributed generation principle application improves reliability and efficiency of energy supply assuming the creation of microgrid with renewable sources of power (wind turbine, PV-solar unit, fuel cell and some others) which may provide customers with DC power.
- Output power of renewable sources has a random characteristic, so in most cases there are energy storage devices in microgrid—batteries, super-capacitor units, fly wheels and so on. For this reason, a reserve of DC power is always provided for the microgrid.
- DC voltage may be used to charge batteries of electric cars and vice versa if necessary car batteries may provide microgrid by dc power.
- Application of new efficient power conversion devices which can operate in both directions may exclude the use of transformers.

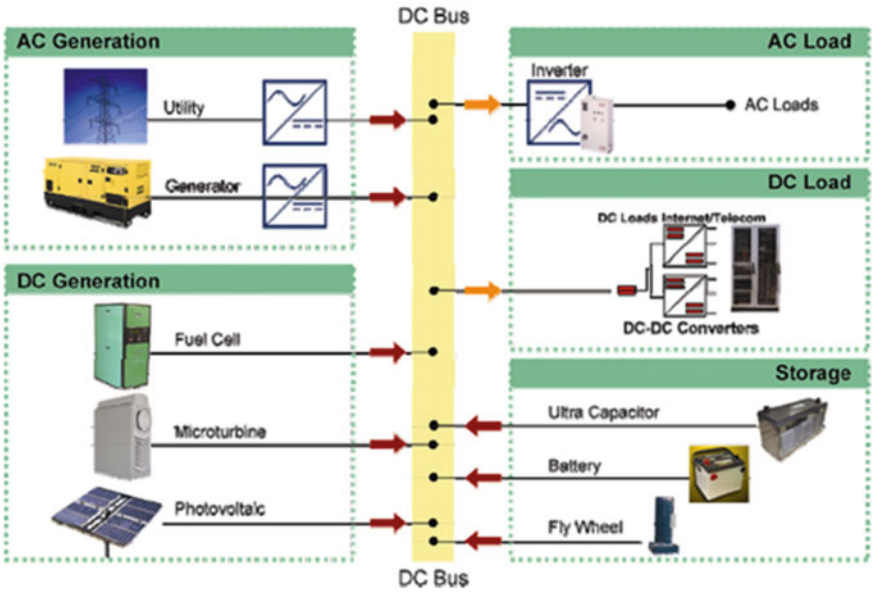

Fig. 3.3 General view of DC microgrid

It is useful to note, that because of existing central energy supply principle deviation of power quality and forced short-term outage of power supply just in the US industrial sector causes the annual loss of 120–190 billions of USD (Fig. 3.3).

3.2.2 Advantages of DC Microgrids Are

- Not necessary the synchronization of DC networks generators.
- Deviation of generated and consumed power may be compensated in Microgrid by installation of energy storage units.
- The loads are not impacted by harmonics, voltage sag or swell, non-symmetry of phase voltages.
- Voltage quality does not change due to current surge (during commutation of inductor containing circuits) or in presence of one phase load or generator.
- DC microgrids are more efficient than AC microgrids [3, 4].

3.2.3 Reluctance to Recognize the Benefits of DC Microgrids

These are including:

- Fear of changing or fear of something new and non-traditional
- Proved case of DC energy delivering still not understood
- Most of the used equipment has no compatible input socket to feed from dc power supply
- There are still no standards on safety and protection
- Standard practice on development, implementation and maintenance of DC microgrid is not mature
- Still no standards in the level of voltages

Induction machines with direct supply from AC terminals—which are the base of most industrial equipment [5].

3.2.4 On the Way to DC Microgrid Transition Stage—A Combined AC-DC Microgrid

On the first stage it is considered to use combined supply of consumers from dc and ac buses.

A combined microgrid was offered because of the development and application of renewable power sources with dc output power and increasing number of end loads, which are using dc currents. Energy management, control and operation of a combined microgrid are rather difficult therefore we would investigate some operating modes of it. Uncertainty and intermittent character of generated energy force the design engineers to develop special control system for hybrid microgrid [6–8]. As it is obvious in design stage *ratModeling* of combined microgrid, results of steady state evaluation and analysis in different operation conditions are presented. Do not focusing on this subject we study different operating modes of a combined microgrid. There are different approaches in building combined microgrid system.

3.2.5 Understanding of Combined Microgrid

There are different approaches in understanding a combined microgrid. Some authors consider combined as a network which has DC and AC power sources. In [9] it is presented a study of a photovoltaic system and a micro turbine operating within a multi-machine network (Fig. 3.4).

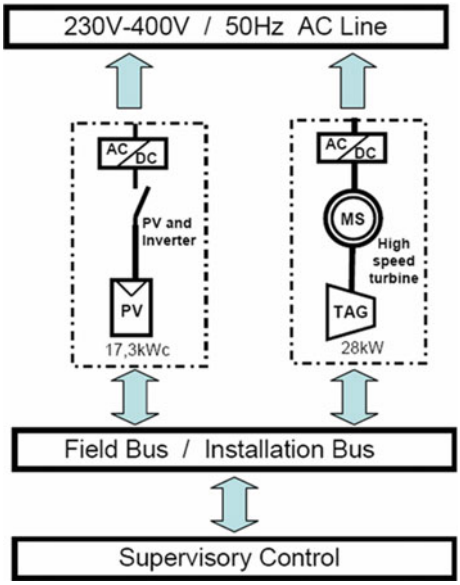

Fig. 3.4 AC Microgrid system with AC and DC sources of power

Figure 3.4 shows the studied hybrid system: a 17.3 kWp photovoltaic system associated to a 28 kW Capstone micro-turbine. This PV-system is installed in the north of France at the L2EP-ENSAM of Lille since December 2004. It can work as a stand-alone system or a grid connected system as it will be a part of a microgrid.

So we can see that this so called hybrid (combined) microgrid system has only one AC bus and both power sources—PV-solar unit and micro turbine are feeding a single AC bus. So it is one understanding of combined microgrid.

Another understanding of combined microgrid is presented below (Fig. 3.5). The microgrid module has AC and DC bus subsystems [10]. The microgrid module can receive power from either AC or DC sources and provide on output either AC or DC power as needed. The microgrid module is comprising transformers and power converters which could modify input AC or DC power sources to provide required characteristics of the output power. The microgrid module also has a control software module. The control software module receives data from sensors installed in the microgrid module and sends commands to controllable elements installed in the microgrid module for power control purpose.

Having in mind a huge number of different energy conversion devices in hybrid microgrid (Fig. 3.5) as AC/DC, DC/AC, DC/AC/DC, AC/DC/AC and DC/DC converters the second approach was updated so that in combined microgrid AC bus was connected to power sources and loads traditionally generating/consuming AC current, for example wind turbine with DFIG (double fed induction generator) machine, loads with induction machines and so on. DC bus get power from PV-solar panels which has DC voltage on their output. There is may be used other sources of DC power as Fuel cell or micro turbine with DC output. Besides, energy storage ele-

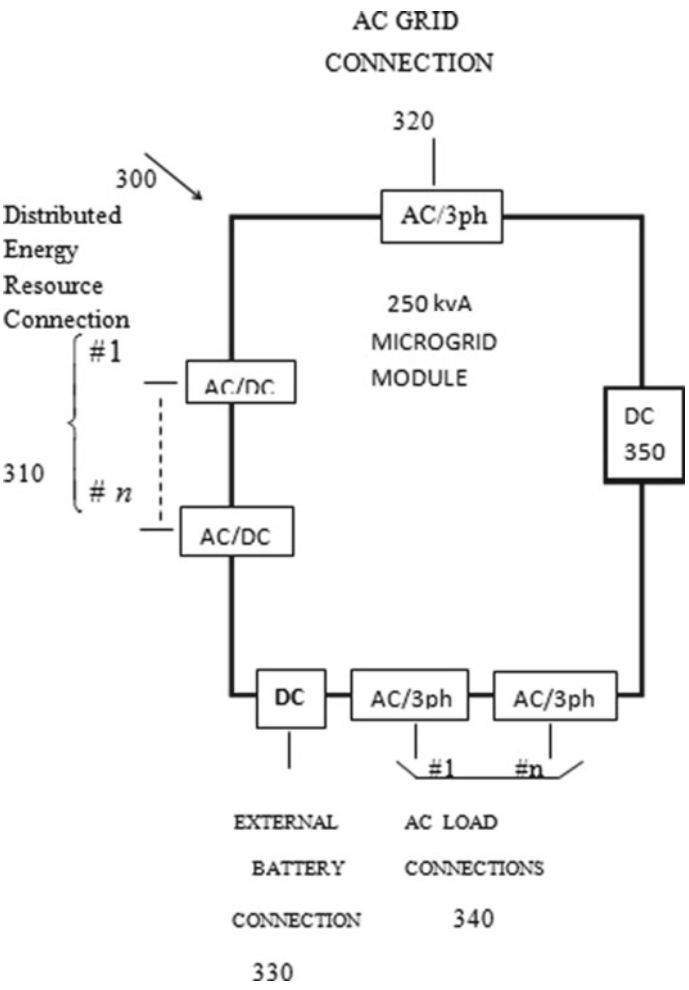

Fig. 3.5 Combined microgrid with AC and DC buses having connections with different sources of power and their loads

ments, batteries and super capacitors also directly coupled to DC bus. Such microgrid network updated buildup (Fig. 3.6) reduces an application of conversion devices, improve reliability and save money. Further we study a combined microgrid which was developed in compliance with above mentioned considerations.

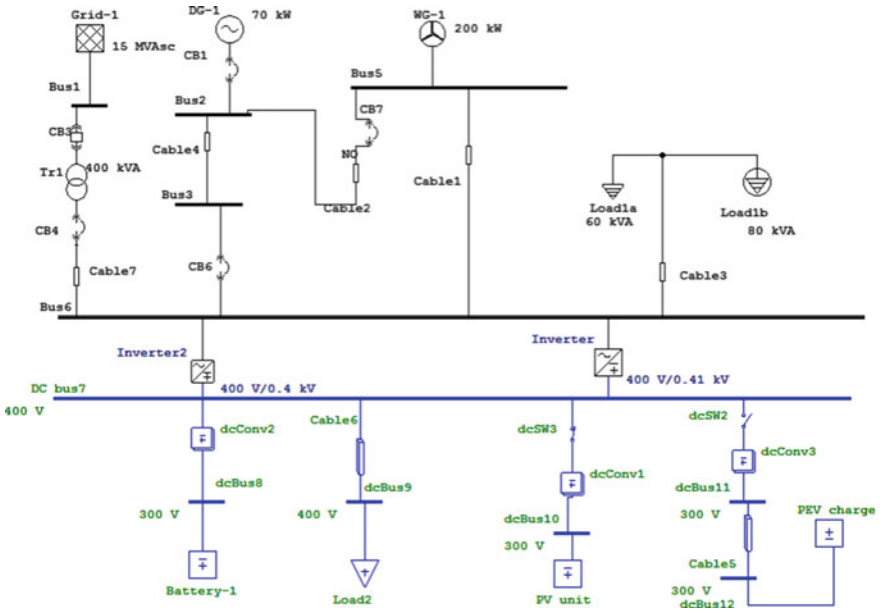

Fig. 3.6 Two bus combined microgrid system

3.2.6 Operation of Combined Microgrid

Definition of conditions for combined AC/DC microgrid functioning generally involve the solution of two tasks: selection the type and number of power sources for each AC and DC subsystems of microgrid; optimal balance of load demands on both subsystems. Type and number of power sources for every microgrid subsystem usually is defined for the day ahead within a week. This problem can be solved applying traditional method of optimization or with help of genetical algorithm technique. The criteria for optimization could be used a minimum of operational expenses as it is successfully used for similar tasks at conventional Grid.

Taking in account that in combined microgrid as conventional power source may be used diesel generator or small gas turbine, which may be activated at time interval with low wind and solar power because of weather conditions and the number of these sources of power being in operation for compensation of stochastic power production of renewable sources.

During the parallel operation of combined microgrid with the main Grid synchronization and control of each AC and DC subsystem microgrid on the base of voltage control at the PCC having been provided. At this point of combined microgrid connection with Grid the voltage variation has an important role on monitoring and operation control at both subsystems and in the whole of combined microgrid. So regime of combined microgrid is supported and coordinated on the base of oper-

ation stability which is provided by controlling of power sources, interconnection inverters.

3.2.6.1 Combined Microgrid Unit Commitment

AC and DC subsystems in combined microgrid have renewable energy sources wind generators and PV-solar units accordingly. The power produced by both sources has intermittent and stochastic character and this create some difficulties in commitment of power sources (definition of their number and type) and operation of whole combined microgrid. Usually in case of intermittence in output power it is recommended to have a hot reserve to compensate those random fluctuations of power. The operation of this reserve even without load does cost a lot. The right definition of unit commitment is an optimization task involving minimization of expenses for start-up and stand-by of conventional sources of power which are part of microgrid subsystem and necessary for island operation of combined microgrid and also expenses for energy consumption from Grid in case of parallel operation of combined microgrid with Grid.

3.2.6.2 Economic Distribution of Power Flow in Combined Microgrid

Power flow in combined microgrid has an aim to cover load demands in AC and DC subsystems mostly at the expense of subsystems on site power sources and then in case of power deficiency in one of subsystem to provide power supply at the expense of power flow between AC and DC subsystems in island as well as in parallel mode of operation. The difference between two mentioned above modes is that in island mode in case of power deficiency in combined microgrid the additional power having been provided from energy storage units.

Optimal power distribution in combined microgrid is a multipurpose optimization task, which can be solved applying various methods.

3.3 Modeling of Combined Microgrid

To provide convenience in comparing results researching various cases of network operation with different combination of renewable and conventional sources and provision of easy connection for DC consumers to the DC collector bus the typical circuit Fig. 3.1 was designed [11]. The studied circuit in Fig. 3.1 has two system buses—AC bus 6 and DC bus 7. AC bus is loaded by 80 kVA lump load1b, 60 kVA static Load1a and DC bus 6 is loaded with static 50 kW Load 2. Static load at DC bus is mostly lighting load. AC buses are supplied from wind unit 200 kW and Diesel generator (DG-1) with rated power 70 kW (Fig. 3.6).

The pilot project for investigated combined network was constructed on the hillside of small town and has a parking lot for charging appliances for PEV (plug-in electrical vehicles).

A studied combined microgrid was modeled using certified software [12]. DC bus 7 is connected with 200 kW PV solar power station, energy storing device (Battery 1) and commercial parking lot with PEV (plug-in electrical vehicles) charging appliances.

Steady-state evaluation in the studied network is made for two cases:

1. Case study 1: microgrid is operating in parallel with Grid.
2. Case study 2: microgrid is in islanded mode.

Simulation models of AC sources—wind turbine (DFIG), and DC sources as PV-unit, batteries are known and described in bibliography [13–15].

Case 1: Parallel Operation

In Fig. 3.7a, b, it is presented the case then DG-1 is switched off (no fuel, for example) and WG-1 does not produce power (wind speed is lower than 3 m/s). PV-unit is producing much power (solar irradiation is high 90%). Both inverters provide AC bus with total 99 kW of power (10 kW are losses in inverters) and AC part of network is using the power generated on DC site plus some 29 kW purchasing from the grid.

In Fig. 3.8a, b it is presented parallel operation of studied microgrid with wind speed 4 m/s. In this case WG-1 does produce 48 kW of power for AC network with wind speed of 4 m/s. Additional power 51 kW are from DC-bus through inverters and the remaining power for AC load is provided by Grid (29 kW). PV unit is capable to produce only 108 kW (solar irradiation low-50%). 52 kW are for local DC load and 56 kW for AC network.

In Fig. 3.9a, b, it is the case then wind speed is 10 m/s. Power delivered into the AC bus is 94 kW and DG-1 is also in operation. Extra power in AC part of the network 30 kW is sold to the Grid. At DC part of microgrid PV-unit is off (night time, for example), but DC load gets power from Batteries through DC converter dcConv2 (Fig. 3.9b). Another case of parallel operation with wind speed 12 m/s and opened DG-1 is presented in Fig. 3.10a, b.

WG-1 is producing 162 kW. 128 kW meets internal AC load demand and 30 kW is sold to the Grid. On DC part of microgrid PV-unit produces only 54 kW to provide energy demand of local DC load.

Case 2: Islanded Operation

If for some reason microgrid lost connection with main Grid this regime is called as islanded operation (Fig. 3.11). Normally lost connection with Grid is not preferable operation for microgrid, but if it happens the microgrid has to activate all internal sources including storage batteries to supply loads on AC and DC buses.

One of the worst cases is to considered with no wind and no PV operation. Power is provided for AC load by diesel generator (60 kW) and partly from DC bus (69 kW) through inverters which is fed by batteries. As it seen in Fig. 3.6, the grid separated by CB3 circuit breaker, WG-1 produces 0 kW because wind velocity is lower than

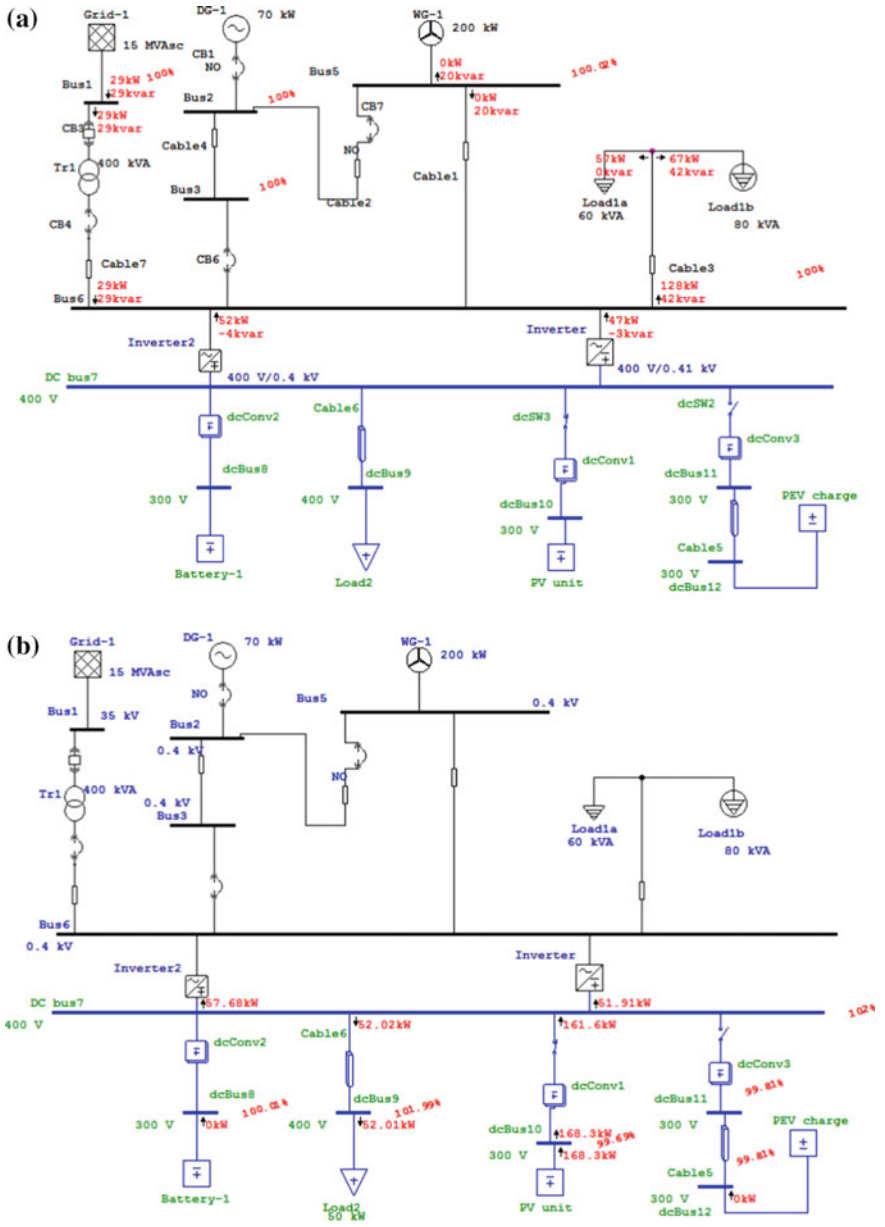

Fig. 3.7 **a** Parallel operation, LF (load flow) on AC part of microgrid, Wind speed <3 m/s. **b** Parallel operation, LF on DC part of the microgrid, Wind speed <3 m/s

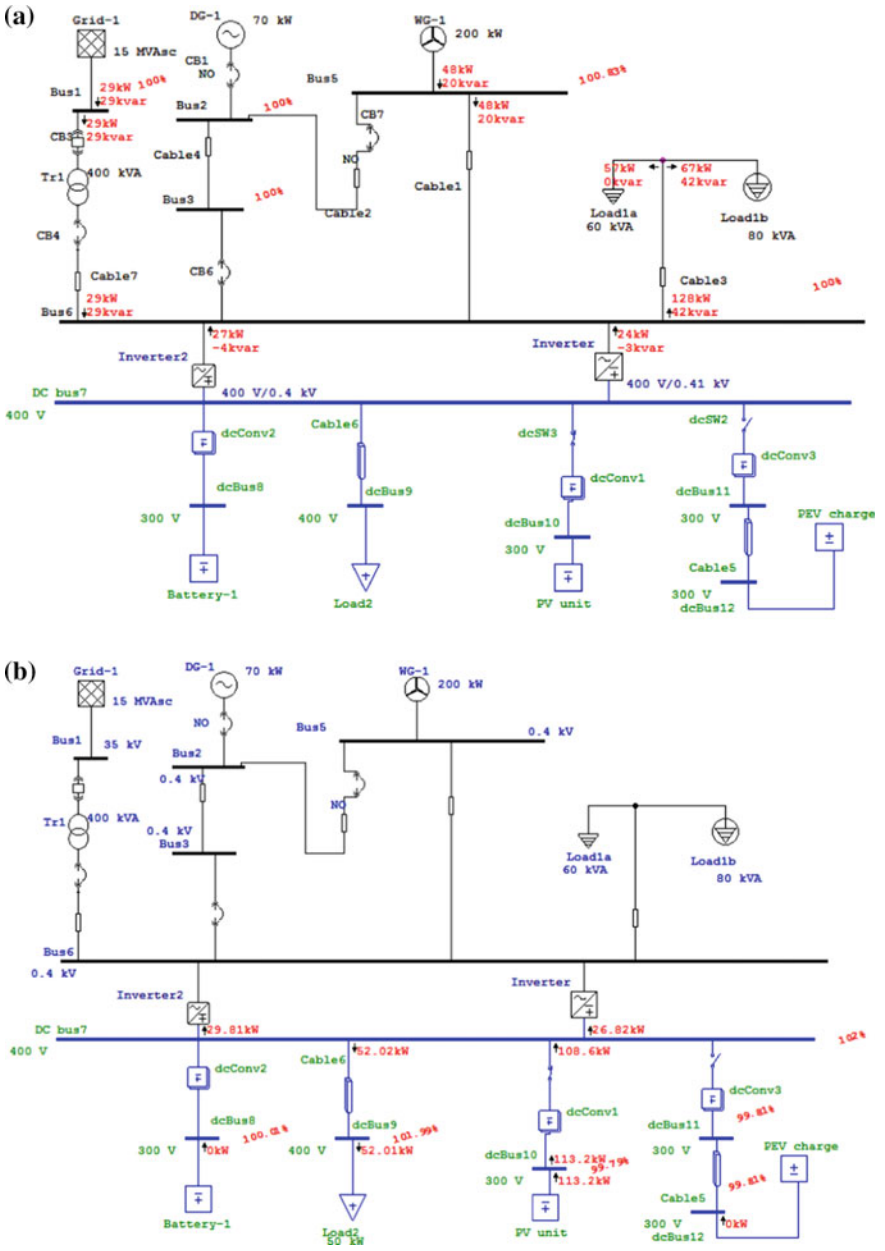

Fig. 3.8 **a** Parallel operation, LF on AC part of microgrid, Wind speed = 4 m/s. **b** Parallel operation, LF on DC network, Wind speed = 4 m/s

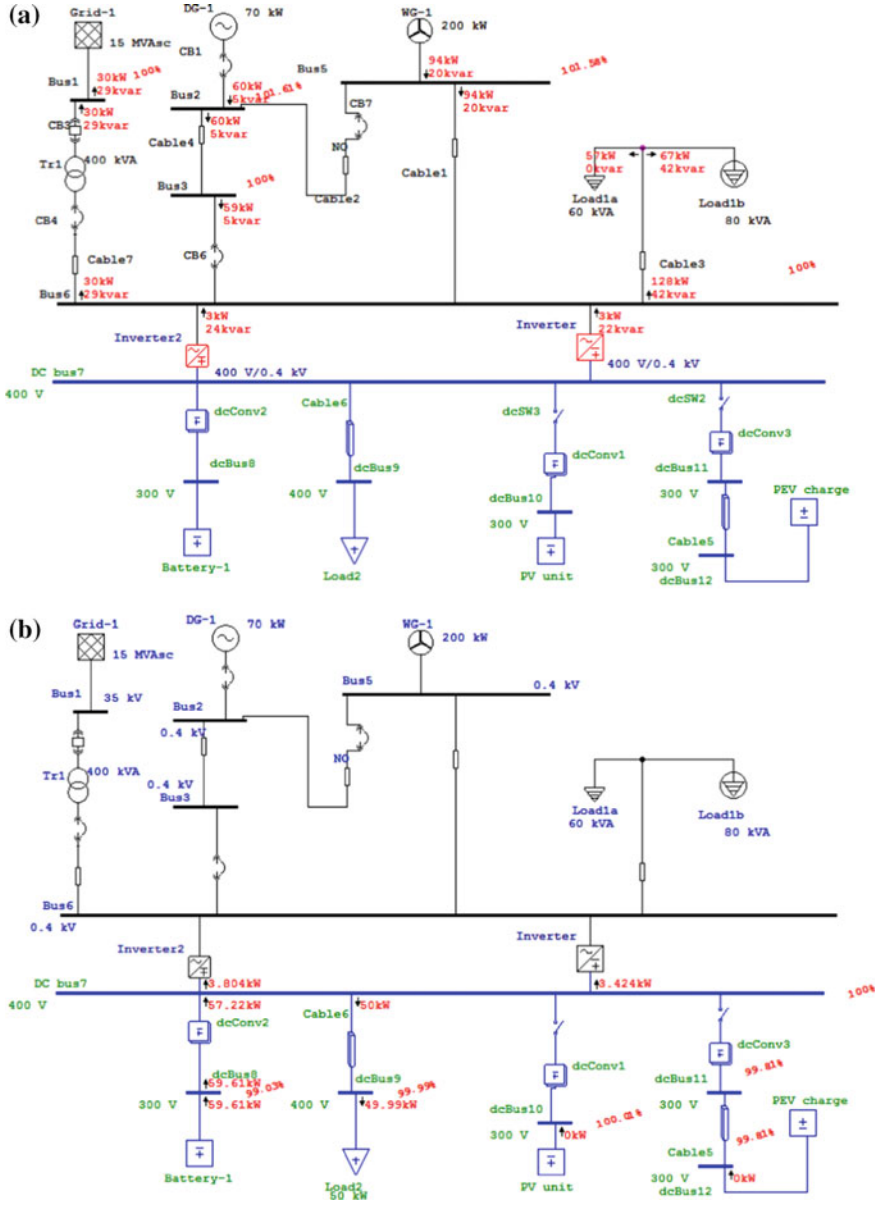

Fig. 3.9 **a** Parallel operation, wind speed = 10 m/s—load flow on AC network. **b** Parallel operation, wind speed = 10 m/s—load flow on DC network

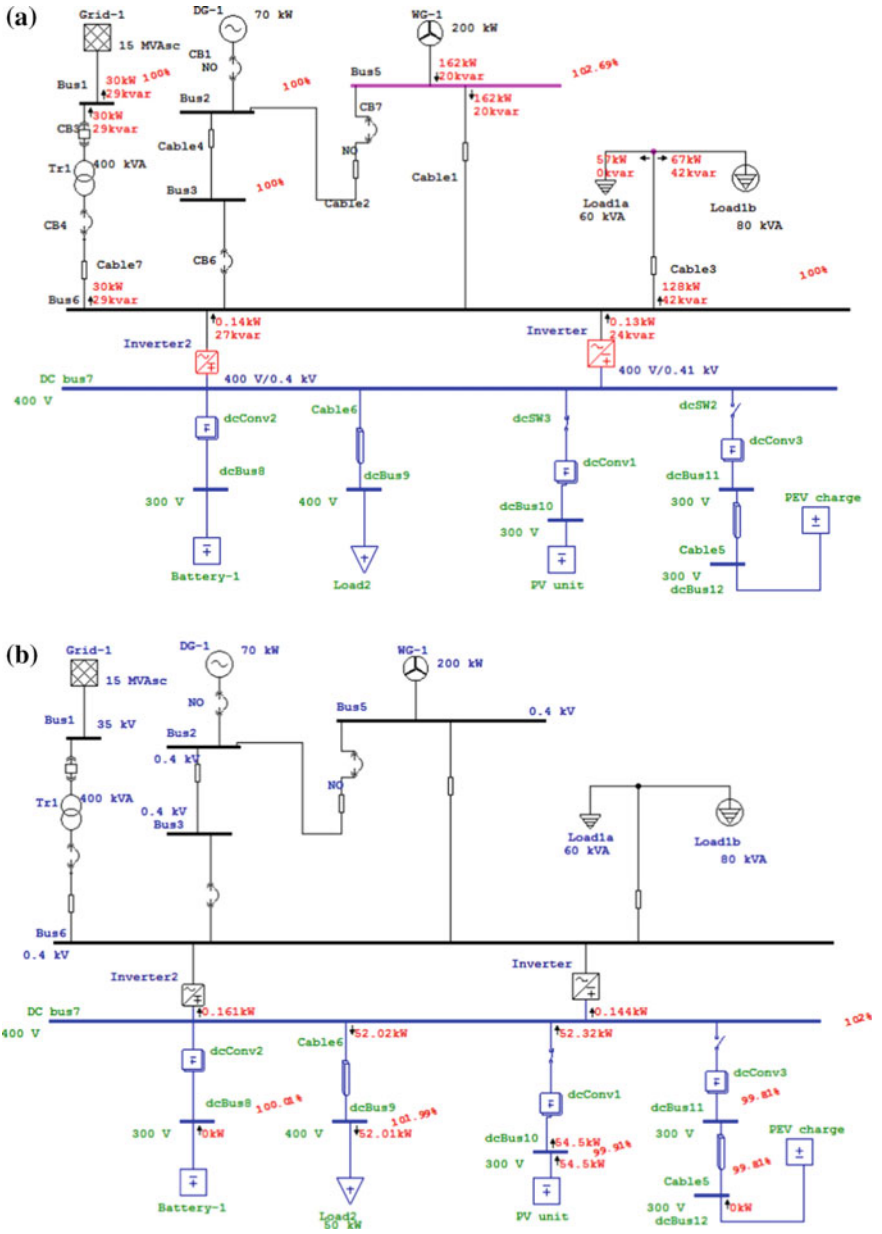

Fig. 3.10 **a** Parallel operation, wind speed = 12 m/s—load flow on AC network. **b** Parallel operation, wind speed = 10 m/s—load flow on DC network

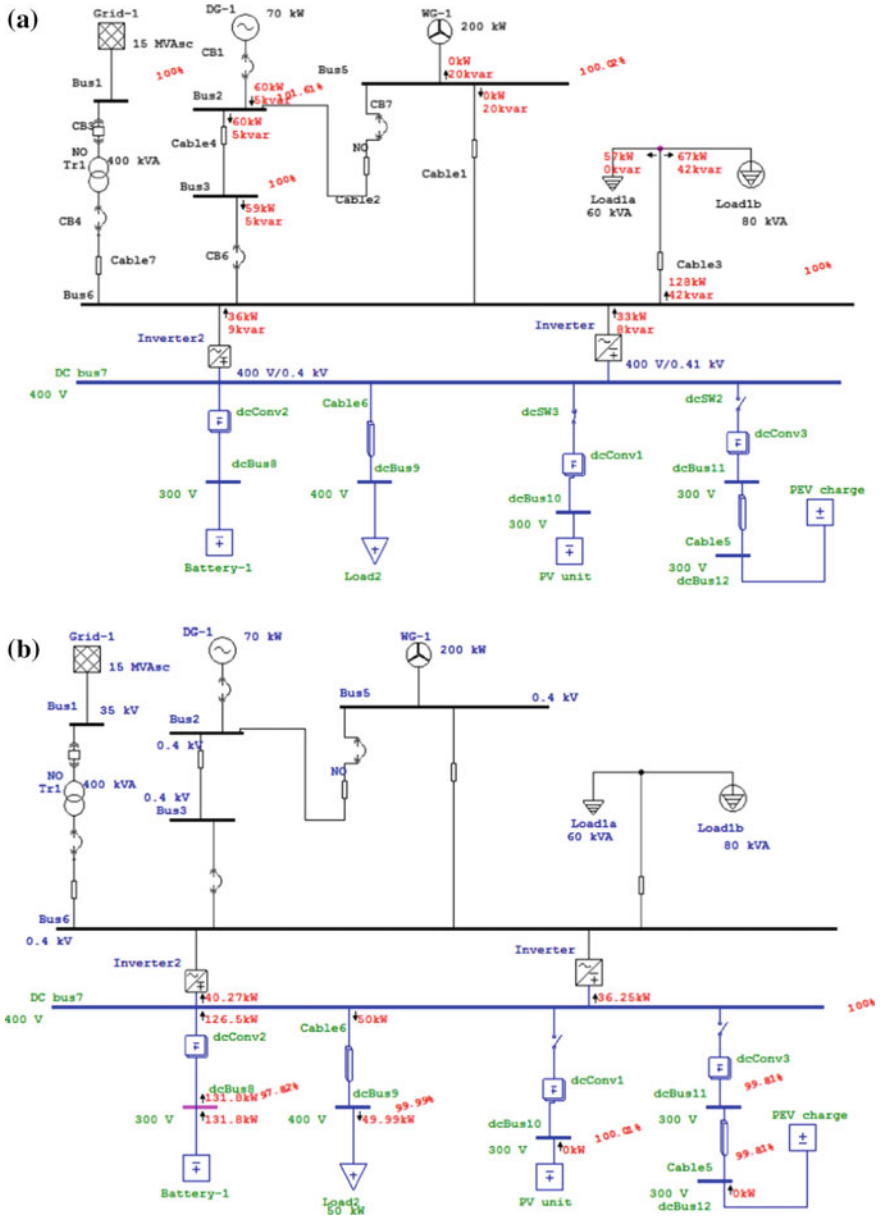

Fig. 3.11 **a** Islanded operation, LF on AC part of the network. **b** Islanded operation, LF on DC part of the network

Table 3.1 Results of steady state regime

Mode of operation	Power flow from the grid or (diesel) kW + kVAr	Power flow to the grid	Power flow from DC to AC bus
Parallel operation, Gen. 1 is off, wind speed 10 m/s	0	$30 + j29$	
Parallel operation, Gen. 1 and PV solar units are off, wind speed 4 m/s	$29 + j29$	0	$51 - j7$
Islanded operation, PV solar units are off, wind speed less than 3 m/s	$60 + j5$		$69 + j17$

3 m/s. In addition to 60 kW generated by DG-1 the remaining 69 kW for AC load is provided by DC bus through inverter. Results of study for steady state regime collected in Table 3.1.

So energy flow and power exchange in studied combined microgrid system depends on working parameters of elements forming the system. The approach considered in this study provides less number of used conversion elements.

3.4 Transient Stability

We study here the reaction of the system on fault in Grid followed by switching off the connection circuit breaker CB3 at the time moment 0.5 s and restoration of the connection 200 ms later. Parallel operation, all units on AC part of microgrid are in operation (Fig. 3.12). Reaction of DG-1 and WG-1 in connection with failure at the Grid pictured at Figs. 3.13 and 3.14.

At the moment of separation from the Grid output power falling down to almost zero and then rising up in the form of spike, then power restores and even some 30% exceeds its normal operation level just before the fault is cleared. After reconnection we can observe low frequency (about 2 Hz) power oscillations within some 8 s. And after that system is in new steady-state operation regime.

Reaction of DG-1 speed on microgrid separation from the regional Grid is very weak. Speed goes down from 1500 to 1488 rev/min, then after reconnection there is some low frequency oscillation (2 Hz) within 5 s and system gets new level of steady state operation condition.

As it follows from the presented pictures: voltage on the output bus of WG-1 reduces during the fault from 407 V till 385 V and then, after reclosing of CB3 (cleared fault in the Grid) voltage level has been restored. There are spikes at the

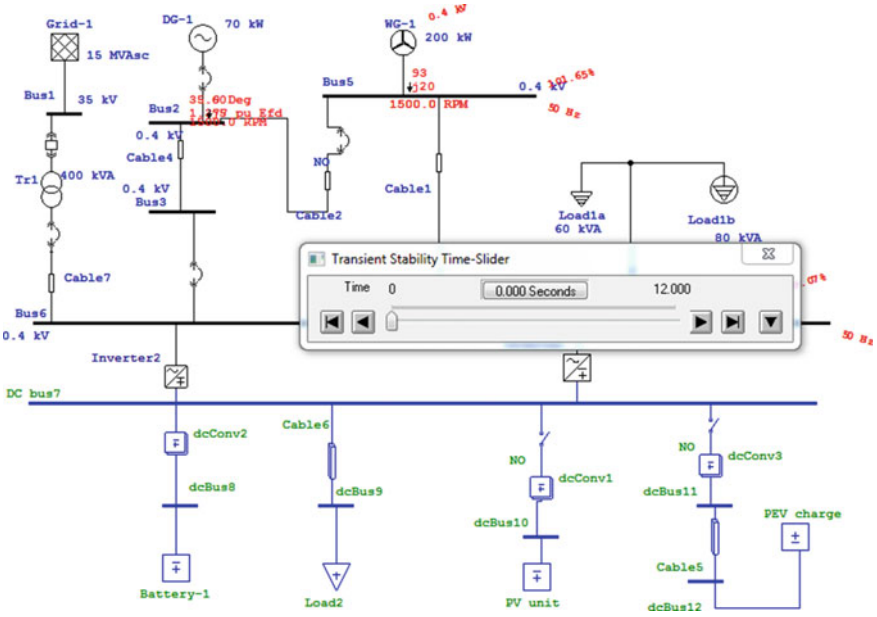

Fig. 3.12 Parallel operation—all units on AC part of microgrid are in operation

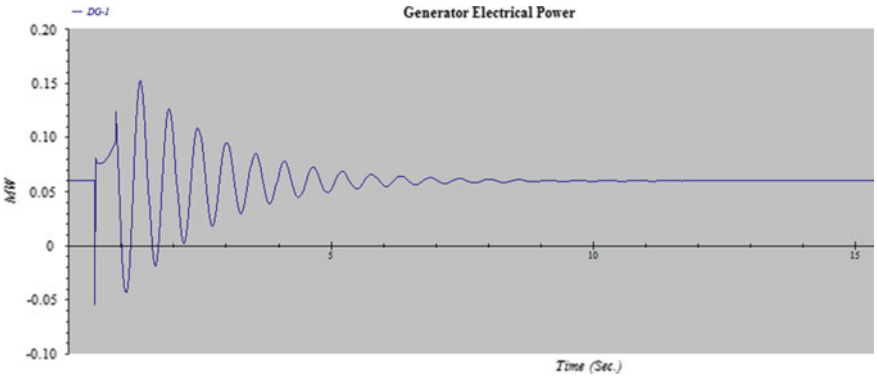

Fig. 3.13 DG-1 output active power

power level on the output of WG-1 at the moment of CB3 contacts separation and at the moment of reconnection.

At the moment of reconnection reactive power goes down to zero and then oscillating 5 s. before getting stable.

Wind generator producing power stably just if you don't take in account two spikes—at the moment of separation from the Grid and reconnection to the Grid again.

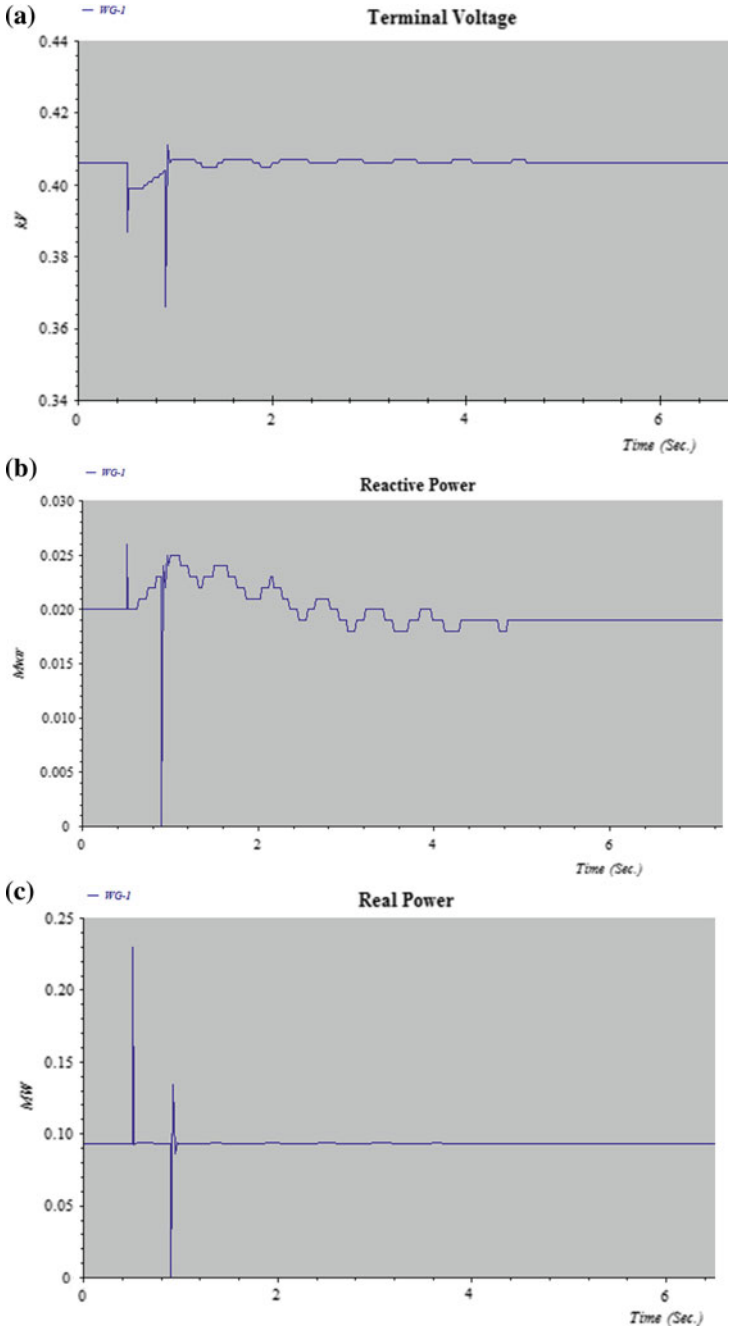

Fig. 3.14 **a** Terminal voltage on the output bus of WG-1. **b** Reactive power produced by wind generator. **c** Real power produced by wind generator

3.5 Energy Storage

The main purpose of using energy storage in microgrid is compensation of random and intermittent power production from renewable energy source such as wind and solar PV units. The type, capacity and allocation of preferred storage system in combined microgrid defined by structures of AC and DC subsystems, lineup of renewable power sources and type of connected loads. At the present time different approaches for choosing storage capacity and their allocation at the microgrid are offered. Usually storage with large capacity is installed at the microgrids there is a need to meet power demand from storage unit within a long time Storages of smaller size can be used to feed microgrid at peak hours. In every specific case for selection of storage type in combined microgrid it is necessary to conduct full study of operation, a possible energy deficiency in both AC and DC subsystems, time of activation and power generation control. Then there is a need to use storage for longer period of time it is suggested to form a structure of storage system with various types of storages as: deep cycle lead acid, zinc air and lithium ion batteries, super capacitors, flywheel, compressed air energy storage and some others. Application of advanced pulse charging technology for batteries developed by John Bedini eliminates sulfating and as a result to get more life cycle for batteries [16].

3.6 Integration

Operation control in combined AC-DC microgrid is easier than control of renewable energy sources which are integrated in main Power Grid. In last case taking in consideration an intermittent character of power produced by wind generators and PV-solar panels for provision of stable operation of Power System it is necessary to have a spinning power capacity. The power of spinning reserve may be almost equal to the level of renewable power sources integrated to the Grid [17].

In combined AC-DC microgrid using state of the art digital system of control and modern energy storage systems it is possible to provide necessary level of frequency at AC system and voltage level on both AC and DC buses with reliable control of reactive power [18, 19].

At voltage dip situation energy storage system acting instantly feeding with energy power deficient subsystem, providing stability in combined AC-DC microgrid.

3.7 Conclusion

The main contribution of this study is development of the hybrid microgrid structure with separation of sources producing alternative current with their loads from sources which traditionally produces direct current together with loads consuming direct current.

Voltage control on appropriate level on the AC and DC buses as well as energy exchange between them is provided by control of AC/DC inverters and DC/DC converters which depends of output production of wind generator and PV-unit.

Parallel and islanded operation of modeled combined microgrid with Grid for some different modes of operation did prove normal steady operation of studied microgrid circuitry with ac and dc elements. Just two conversion elements are enough to provide energy exchange between two energy buses. PV solar panels could contain no built in inverter elements. In used PV solar units it is recommended to apply models without built in inverters so the hybrid microgrid has an advantage to use a minimal number of conversion devices.

Transients caused by separation of microgrid from the main Grid due to fault in Grid or connection line mostly defined by speed oscillation of rotating equipment (diesel generator, wind generator) and in cases of high speed reaction of reconnection equipment do have low impact on operation of microgrid.

- A Combined AC-DC microgrid can reduce the number of AC to DC or DC to AC converters in AC or DC microgrid [6].
- A Combined AC-DC power supply system concept may have implemented on the base of microgrid with further expansion to the cellular microgrid system [2].
- A Combined AC-DC power supply system increase energy efficiency and improve reliability.

References

1. R. Lasseter, Distributed Energy Resources Integration. CERTS Micro-Grid Concept (2003), pp. 1–28
2. N.R. Rahmanov, A.M. Hashimov, O.Z. Kerimov, Effect of Combined Wind and Diesel Generation on Power System Operation, in *Proceedings of the Renewable Energy World Conference*, Milan, Italy (2011)
3. P. Savage, R.R. Nordhaus, S.P. Jamieson, DC Microgrids: Benefits and Barriers (Yale School of Forestry & Environmental Studies, 2010), pp. 51–65
4. A.A. Salam, A. Mohamed, M.A. Hannan, Technical challenges on microgrids. ARPN **3**(6), 64–69 (2008)
5. A. Norkin, *Microgrids: The Future of Worldwide Power System*. FacePla.net (02.04.2012)
6. X. Liu, P. Wang, P. Chiang Loh, A hybrid AC/DC microgrid and its coordination control. IEEE Trans. Smart Grid **2**(2), 278–286 (2011)
7. I. Vechiu, A. Llaria, O. Curea, H. Camblong, Control of power converters for microgrids, in *Ecological Vehicles & Renewable Energies*, Monaco (2009)
8. R. Noroozian, M. Abedi, G. Gharehpetian, Combined operation of AC and DC distribution system with distributed generation units. J. Electr. Eng. **61**(4), 193–204 (2010)
9. P. Degobert, S. Kreuawan, X. Guillaud, Micro-grid powered by photovoltaic and micro turbine. Laboratory of Electrotechnique and Power Electronics of Lille (L2EP) (2006), pp. 188–191
10. L. Miller, D. Barrett, System and Method for a Controlled Interconnected DC and AC Bus Microgrid. US Patent 8 421 270 B1, 2013
11. N.R. Rahmanov, O.Z. Kerimov, S.T. Ahmedova, Simulation of steady state operation for AC/DC microgrid. Int. J. Tech. Phys. Problems Eng. (IJTPE) Issue 21 **6**(4), 22–29 (2014)
12. Operation Technology. ETAP 6.0 Software

13. K. Chao, C. Li, S. Ho, Modeling and fault simulation of photovoltaic generation systems using circuit based mode, in *International Conference Sustainable Energy Technology*, Nov 2008, pp. 290–294
14. D. Zhi, L. Xu, Direct power control of DFIG with constant switching frequency and improved transient performance. IEEE Trans. Energy Conf. **22**(1), 110–118 (2007)
15. L. Bo, M. Shahidehpour, Short term scheduling of battery in a grid connected PV/battery system. IEEE Trans. Power Syst. **20**, 1053–1061 (2005)
16. Bedini's Negative Resistor Process in a Battery. From the book «Energy from the Vacuum», Thomas Bearden (2002)
17. J.M. Guerrero, Connecting renewable energy sources into the smart grid, in *IEEE International Symposium on Industrial Electronics (ISIE)* (IEEE Press, 2011), pp. 2400–2566
18. A. Kamenetz, *Why the Microgrid Could Be the Answer to Our Energy Crisis* (Fast Company, 2009), pp. 1–14
19. F.X. Saury, C. Tomlinson, *Hybrid Microgrids: The Time is Now* (Caterpillar, 2016)

Chapter 4
Distributed Energy Resources and Microgrid Infrastructure

Farid Hamzeh Aghdam and Navid Taghizadegan Kalantari

Abstract Energy has an important part in the modern society. An increment in the amount of energy demand due to progress in different technologies, industrialization, etc. leads to developments in the energy sector. Electrical energy as the most important type, is the subject of so many researches. Environmental issues, deregulation of electrical systems, etc. have caused the arrival of distributed electrical generators better known as Distributed Energy Resources (DERs). However, penetration of DERs is accompanied with some problems. Formation of Microgrids (MGs) could lessen these issues. In this chapter, first different types of DERs alongside their models, would be discussed. Then, substructures for developing MGs would be presented.

Keywords Distributed energy resources (DERs) · Microgrids (MGs)

4.1 Introduction

Reliable and secure energy is one of the main necessities of modern community. However, old parts of the current electrical system and load growth jeopardize the quality, reliability and security of the electrical energy supply. Accordingly, a great amount of money is required to be invested in the electric power industry to alternate the old infrastructures with new ones. For instance, according to the International Energy Agency (IEA) in 2016 more than 1400 billion USD, has been invested in electrical section improvements.

Environmental issues, technology progress, intense increment, electricity market liberalization, in electrical energy demand, which is expected to cross 31 million MWh by the end of the year 2030, economical matters, etc. forces the modern

F. Hamzeh Aghdam · N. Taghizadegan Kalantari (✉)
Electrical Engineering Department, Faculty of Engineering, Azarbaijan Shahid Madani University, Tabriz, Iran
e-mail: taghizadegan@azaruniv.ac.ir

F. Hamzeh Aghdam
e-mail: farid.hamzeh@gmail.com

N. Mahdavi Tabatabaei et al. (eds.), *Microgrid Architectures, Control and Protection Methods*, Power Systems,
https://doi.org/10.1007/978-3-030-23723-3_4

electrical systems to be adjusted to new circumstances. Thus, many issues about the operation and planning of the electrical power systems have emerged. These issues not only limited, but include, expansion of power plants and transmission lines, power system stability, low efficiency and increment in the amount of greenhouse gases in the atmosphere. Besides, due to hazards of nuclear power plants, developed countries are planning on shutting them off [1].

The rapid process of deregulation and privatization of electrical power systems industry, beside the mentioned problems, urges the power system operators to look for substitutions for the conventional methods of producing electrical energy. One possible and logical solution is utilizing distributed generation as distributed energy resources (DERs), especially renewable based DERs. DERs are known as small-scale, grid connected devices, performing electrical generation and storage [2]. There are different standards for accepting a generation unit as a DER. For instance, according to the definition of The Electric Power Research Institute, DERs are known as units with output power from 'a few kilowatts up to 50 MW' [3]. Also, as it can be inferred from its name, the location of DERs is distributed in the operating network. However, a complete definition is brought in [4] as below:

> The distributed generation refers to electrical energy production systems which are located in the distribution network and are connected directly to it.

The DERs include wind turbines, solar generation systems better known as photovoltaic (PV) systems, fuel cells, diesel generators, microturbines, etc. Among the mentioned resources, renewable based DERs such as PV systems and wind turbines are distributed in their nature due to the geographical considerations. But the location of the others, could be determined by the system designer.

In presence of DERs, energy storage devices would be obligatory to cope with the problem of momentary mismatch between power generation and consumption due to stochastic generation of renewable based DERs as their output power is dependent on the environmental conditions [5, 6].

Although DERs have numerous benefits from the consumers and producers' points of view, high penetration of them needs some considerations and alternations in the current electricity system due to emerging of numerous technical and operational problem i.e. protection problems, power quality, reliability decrement, cost management, etc. Such issues, complicate the operation of the electrical energy systems. "Smart grids" are referred to the modern electricity grids which cope with the penetration of DERs and its consecutive problems. Based on the definition of [7–9] a smart grid contains variety of DERs (renewable based and conventional), smart appliances, smart meters, controllers, etc. and with the goal of providing sustainable, economical and secure electrical energy for its consumers.

Thus, the conventional electrical grids as unidirectional ones are transformed to modern smart girds with integration of DERs and bidirectional current flow. In other words, they are changing from passive ones to active ones making active distribution networks. In such system, the end-users change their roles from being an absolute consumer to both producer and consumer and could decide on whether to sell or buy

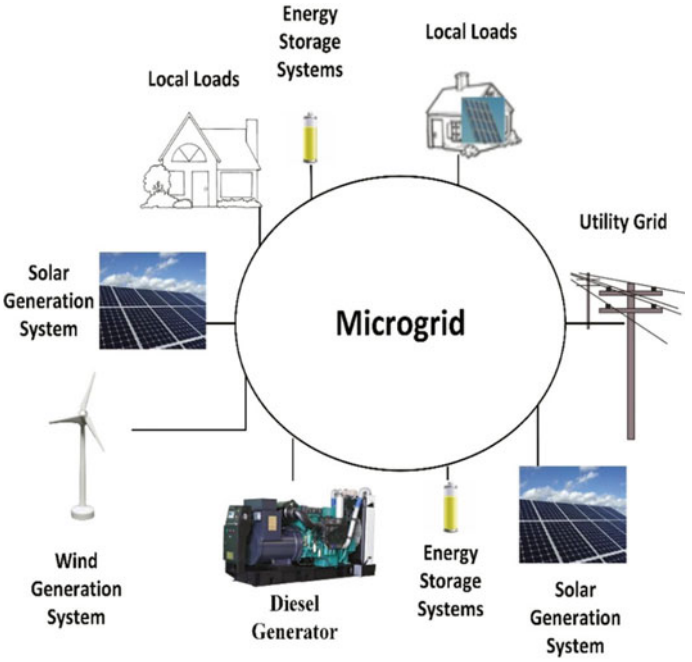

Fig. 4.1 A typical microgrid including different DERs and consumers

electrical energy. However, such a system requires new communication systems, high cost technologies for technical aspects of operation.

Microgrids are the fundamentals of forming smart grids. A microgrid is defined as an integration of DERs, energy storage devices, various types of loads and other equipments such as interfacing converters, local controllers, etc. [10]. Figure 4.1 illustrates a typical microgrid. The main attribute of a microgrid is the controlling capabilities. By means of these control capabilities, microgrids can operate in two operational modes known as islanded and grid-connected modes. The first mode is selected by the operator in case of disasters, faulty conditions or other external disruptions to enhance the reliability level and costumer satisfactions. In the second mode, the aim is to increase the benefit of the microgrid owner [11]. To sum it up, the control capabilities of the microgrid is the main feature that differentiate it from conventional distribution networks which may or may not include DERs.

The following of this chapter is organized as follows. Different types of DERs including PV systems, wind turbines, microturbines, fuel cells and diesel generators with their technical characteristics would be discussed. Also energy storage devices i.e. flywheels, batteries, etc. as other indisputable parts of microgrids would be presented. Then, complete definition of microgrid with its components would be presented.

4.2 Distributed Energy Resources (DERs)

High penetration of DERs would have a significant impact on the electrical energy systems in the future. These DERs include PV system, wind generation units, fuel cells, microturbines and diesel generators. Moreover, batteries, flywheels etc. as energy storage systems could be considered as DERs. In order to avoid high generation cost, the stored energy in these devices could be released onto the grid. All of these DERs require specific considerations and interfacing equipment. Also, operation of these devices, would burden costs for the systems operator. In addition, many constraints should be considered in the operation process to satisfy technical aspects of the system. In this section, different types of DERs and their relative equipment and equations would be discussed.

4.2.1 Photovoltaic (PV) Generation Units

PV units are known as electrical energy producers which performs their tasks by transforming radiance energy of the sun straightly into electrical energy. PV cells, which are built of semiconductors i.e. wafer-based crystalline silicon (c-Si), are bricks for constructing PV modules and they gather together in parallel and series circuits developing a panel (module) with an area of several square centimeters. These panels are developed serially and parallelly to supply sufficient current and voltage (Fig. 4.2).

Usually the combination of PV cells is represented by a simplified equivalent circuit model which contains a current source, diodes, series and parallel resistors which is shown in Fig. 4.3. This figure shows model with one diode and less complexity and a more accurate two diode description of a PV cell. The series resistor,

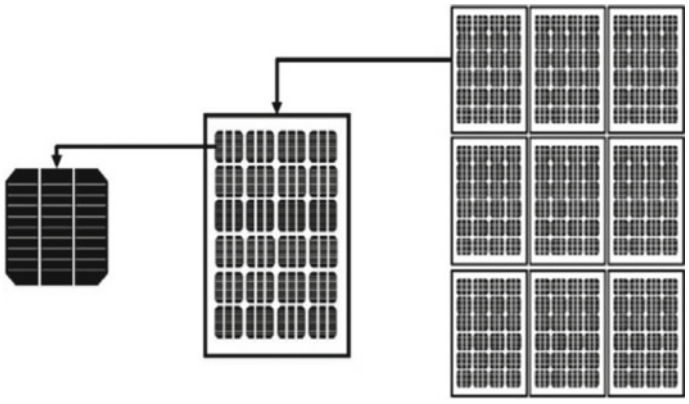

Fig. 4.2 Series and parallel connection of several PV cells, modules and developing arrays

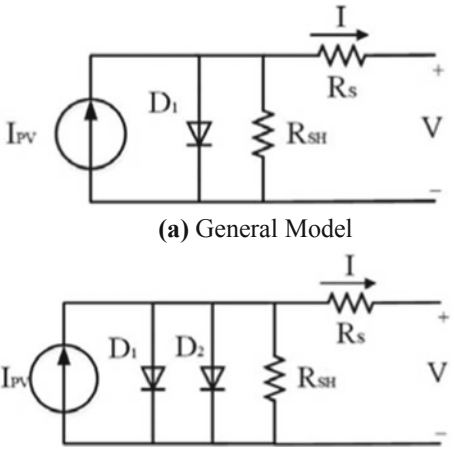

Fig. 4.3 Equivalent circuit models of solar cells

shows the internal resistance of the PV cell and its voltage drop and the parallel one stands for the leakage current.

Equations of this model for its overall current and voltage are as follows [11]:

$$I_{cell} = I_r + \left[\alpha\left(\frac{G}{G_r}\right)(T_c - T_{cr}) + \left(\frac{G}{G_r} - 1\right)I_{sc}\right] \tag{4.1}$$

$$V_{cell} = -\beta \cdot (T_c - T_{cr}) - R_s \cdot \Delta I + V_r \tag{4.2}$$

$$\Delta I = \alpha\left(\frac{G}{G_r}\right)(T_c - T_{cr}) + \left(\frac{G}{G_r} - 1\right)I_{sc} \tag{4.3}$$

In the Eq. (4.1), G and G_r are active and reference values for radiation, T_c and T_{cr} are respective values for the module and reference temperatures of the cell. Mostly, G_r and T_{cr}, are considered as 1000 W/m^2 and 25 °C, respectively which are usually provided by producers as electrical specification of the PV panels at standard conditions. α and β are temperature coefficients of short circuit current and open circuit voltage, respectively. Also, the short circuit current is expressed by I_{sc} and finally, I_r and V_r are reference values calculated from *V-I* characteristic curve of the panel [12, 13].

According to the number of parallel and series modules, the output current and voltage of PV systems could be calculated from Eqs. (4.4) and (4.5) [13]:

$$V_{panel} = N_{series} \times V_{module} \tag{4.4}$$

$$I_{panel} = N_{parallel} \cdot I_{module} \tag{4.5}$$

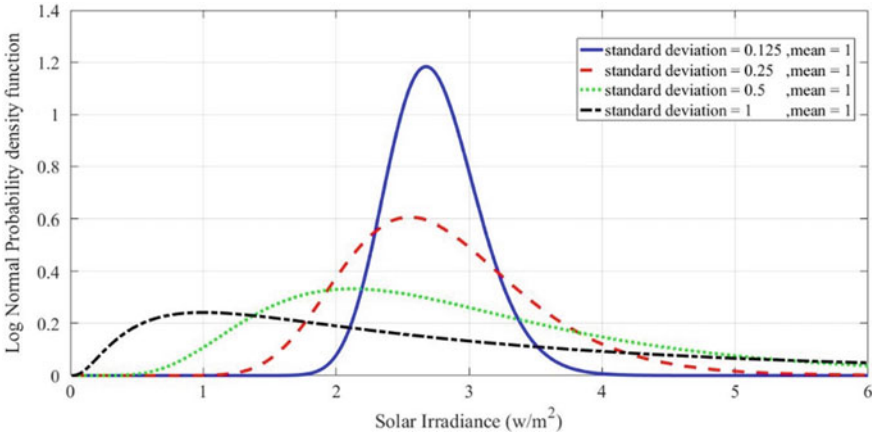

Fig. 4.4 Lognormal distribution function for the solar irradiance with different standard deviations

In above equations, N_{series} and $N_{parallel}$ are respective values for the number of series and parallel PV modules [11]. Environmental conditions such as solar irradiance and the temperature, affects the output power a PV generation system. However, the solar irradiance varies during a day and differs from day to day due to climate changes. In scientific works, the irradiance (Ir) usually is modelled as a random variable and is fitted to a lognormal probability density function (PDF) as bellow [10]:

$$f_{Ir}(Ir) = \frac{1}{Ir \cdot \sigma_{Ir} \cdot \sqrt{2\pi}} e^{\frac{-(\ln Ir - \mu_{Ir})^2}{2\sigma_{Ir}^2}}, \quad Ir \geq 0 \tag{4.6}$$

which σ_{Ir} and μ_{Ir} are the respective standard deviation and mean of the PDF. Figure 4.4 illustrates the lognormal distribution function for the solar irradiance for different standard deviations.

Electrical power generation by a PV system is function of irradiation and the relation between them is presented in Eq. (4.7) [10].

$$P_{PV,Gen} = \begin{cases} P_{rated}\left(\frac{Ir^2}{Ir_{std} Ir_C}\right) & Ir \leq Ir_C \\ P_{rated}\left(\frac{Ir^2}{Ir_{std}}\right) & Ir_C \leq Ir \end{cases} \tag{4.7}$$

In the mentioned equation, Ir_{std} and Ir_C are the respective values for the solar irradiance in standard environment and the certain irradiance point, and finally the rated generated power of the PV system is shown by P_{rated}.

4.2.2 Wind Generation Systems

Release of greenhouse gases i.e. sulfur, nitrogen and carbon oxides and nuclear pollutants into the nature is mainly due to operation of conventional power plants [14]. Thus, inclination to renewable based generation units has been raised.

Wind generation units are renewable based electrical generation systems which is aged backed to 1890. The first grid-connected wind turbines (WTs) with a capacities of 2 and 3 MW were installed in 1979 and 1988 on Howard Knob Mountain and Berger Hill of Scotland, respectively.

Nowadays, WTs are installed, operated with capability of commercially competing with conventional generation units by contaminating so many advantages i.e. clean power production.

Building high strength material for forming the blades of WTs, lower cost of power electronic interfaces in comparison with the past, variable speed generators, etc. could be accounted as the main reasons for the acceleration in the development of the WTs.

WTs transform the kinetic energy of the air into electrical energy. This energy for the air with velocity υ and mass m, is obtained using below equation:

$$E_k = \frac{1}{2} m \upsilon^2 \tag{4.8}$$

The power of the air can be calculated by dividing the kinetic energy of time which changes the mass in the Eq. (4.8) into mass flow over second. The mass flow formula is as follows:

$$Mass\ Flow = \frac{m}{t} = \frac{\rho \cdot v}{t} \tag{4.9}$$

where ρ and v are the density and volume of the swept air. By considering the volume as the multiplication of surface by length, Eq. (4.9) is rewritten as follows:

$$Mass\ Flow = \frac{\rho \cdot v}{t} = \rho \cdot A \cdot \frac{l}{t} = \rho \cdot A \cdot \upsilon \tag{4.10}$$

Using Eqs. (4.8) and (4.10), the power carried by air in a specific site can be calculated as bellows:

$$P_k = \frac{1}{2} \rho \upsilon^3 \tag{4.11}$$

However, the whole power of the air is not harvested by the blades of the WT and only a portion is transferred into a generator shaft. Thus, extracted power by the blades is as follows:

$$P_{blade} = \frac{1}{2} \rho \upsilon^3 \cdot K_p \tag{4.12}$$

K_p is rotor's power coefficient which shows the fraction of the extracted power of the blades of the WT which is dependent on the ratio of the velocity of the wind after and before hitting the WT. In theory the K_p in its highest value is 0.59.

As it can be inferred from the Eq. (4.12), the wind velocity has the most effect on the wind power. The wind velocity is never steady at any place and differs by at different time intervals. It also depends geographical features of the site such as the land shape, the weather system and the altitude. Accordingly, in the studies of wind histories for a site, usually long term data such as over 10-year wind velocity average are considered to ensure the planners for maximum efficiency of the wind generation unit.

Due to high costs of such measurements, usually, short term data such as 1-year data is collected and fit into a probability density function (PDF).

The wind velocity data is best fitted by the Weibull PDF which is expressed by the following equation:

$$f_{\upsilon}(\upsilon) = \left(\frac{\kappa}{\vartheta}\right) \cdot \left(\frac{\upsilon}{\vartheta}\right)^{(\kappa-1)} \cdot e^{-(\frac{\upsilon}{\vartheta})^{\kappa}}, \quad \upsilon \geq 0 \tag{4.13}$$

In above equation, κ and ϑ stand for shape and scale factors, respectively and υ is the velocity of the wind. The plot of is $f_{\upsilon}(\upsilon)$ depicted in Fig. 4.5 for different shape and scale factors. The expected value of the Weibull PDF follows below equation:

$$Ex(f_{\upsilon}(\upsilon)) = \vartheta \cdot \Gamma(1 + \frac{1}{\kappa}) \tag{4.14}$$

where $\Gamma(\chi)$ is the gamma function as below:

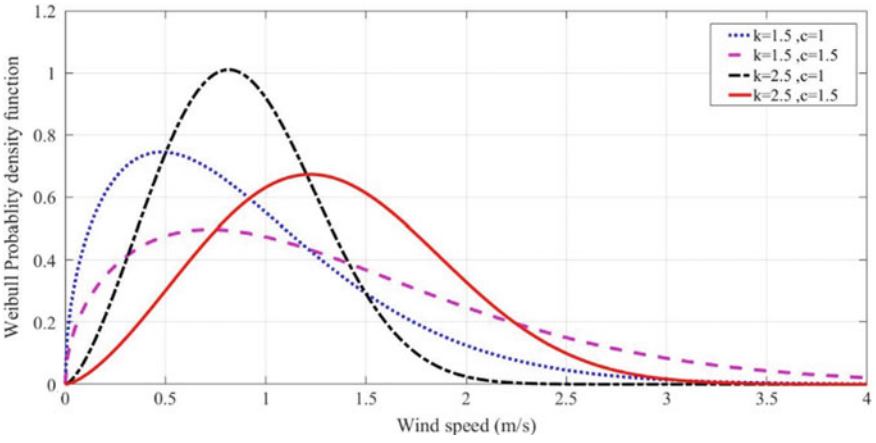

Fig. 4.5 Weibull distribution function with different scale and shape factors

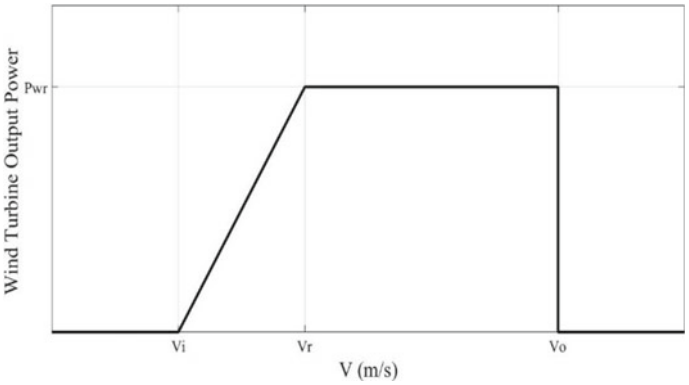

Fig. 4.6 Output power function of a wind turbine

$$\Gamma(\chi) = \int_0^\infty e^{-t} t^{\chi-1} dt \tag{4.15}$$

Using the above equations, the expected values for wind velocity and accordingly WT output power can be derived.

The output power a wind turbine system is a function of the wind velocity and it could be calculated using the equation below:

$$P_{wind} = \begin{cases} 0 & \upsilon \leq \upsilon_i \quad , \upsilon \geq \upsilon_o \\ \frac{\upsilon - \upsilon_i}{\upsilon_r - \upsilon_i} P_{wr} & \upsilon_i \leq \upsilon \leq \upsilon_r \\ P_{wr} & \upsilon_r \leq \upsilon \leq \upsilon_o \end{cases} \tag{4.16}$$

In above equation, υ_i, υ_o and υ_r are cut in, cut out and rated speeds of the WT. Figure 4.6 shows this feature for a WT.

4.2.3 Microturbines

Microturbines are almost new DER technology which were originally designed for aircrafts and helicopters. The microturbines are, in fact, natural gas turbines with size ranges of 25–500 kW.

Microturbines could be used as an absolute electrical DERs or an integration of electrical and thermal energies which are also known as combined heat and power (CHP) systems. In such systems, the exhausted hot gases are used as heat recovery to achieve efficiencies greater than 80%.

Microturbines evolve numerous advantages i.e. lightweight, small size, low emissions, less number of moving parts, great efficiency, low electrical generation costs,

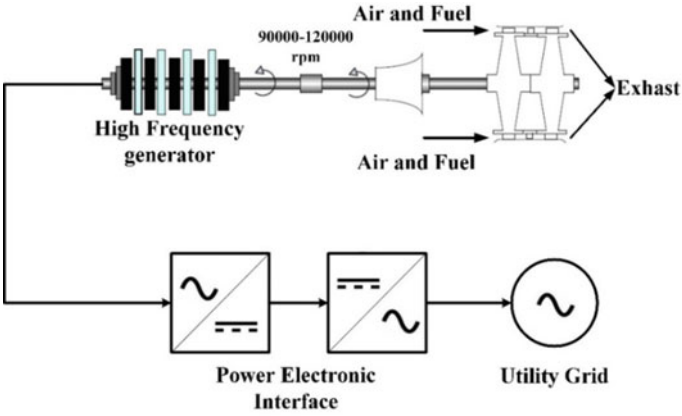

Fig. 4.7 A typical microturbine and its necessary power electronic interface

Table 4.1 Pros and cons of microturbines

Pros	Cons
Tightly packed	Loss of energy in electrical generation mode
Lightweight	Higher ambient temperatures
Less number of moving parts	Low fuel to electricity efficiencies
Less emissions	
Capable of utilizing waste fuels	
Higher efficiency in CHP mode	
Low maintenance necessities	
Low noise	
Low vibration	
Higher energy security	

etc. Also they can bury variety of fuel types such as natural gas, propane, methane, alcohol, diesel, gasoline, naphtha, etc. but the natural gas is most used fuel in the microturbines [15].

In most of microturbines, the jet engine is connected to the turbine shaft which makes it spin at up to 120,000 rpm and it drives a high-frequency generator. For utility grid connections, the output power of the high-frequency generator is rectified to dc power and then inverted to ac power with frequency of the grid. The initial systems could produce electrical energy at almost 30% efficiency; however, the output hot gases could be used in the heating system enhancing the efficiency. Figure 4.7 demonstrates a typical microturbine system.

As mentioned before, microturbines have many potential advantages as DER systems. Table 4.1 illustrates the pros and cons of microturbine technology according to the California Distributed Energy Resources Guide on Microturbines.

4.2.4 Fuel Cell

Fuel cells (FCs) are a kind of DER units which transforms chemical energy straightly into electrical energy and they could provide electricity alongside with heat. Fuel cells could be utilized in stationary applications for energy production, and also instead of the internal combustion engine developing electrical vehicles. High power density, high efficiency and low emission of harmful gases are considered as the main advantages of FCs. For instance, the energy density of a typical FC is almost ten times that of a battery. For an FC working as an electrical generation unit, the efficiency reaches almost 60%. Furthermore, working as a CHP system, the efficiency could be over 80% [16].

There are five classifications for the FCs according to their electrolyte chemistry which are listed as below:

- proton exchange membrane FC (PEMFC)
- molten carbonate FC (MCFC)
- aqueous alkaline FC (AAFC)
- solid oxide FC (SOFC)
- phosphoric acid FC (PAFC).

Table 4.2 illustrates the features and characteristics of each fuel cell type. In above types, PEMFCs are the most used and developed ones due to their features such as working in both vehicles and stationary DGs, low working temperature, high energy density, and simple structure [17]. In PEMFCs, hydrogen and oxygen gases are considered as the fuel and are fed into it. Hydrogen gas with high pressure, is uniformly distributed on the surface of an electrolyte in the anode of the fuel cell making the hydrogen molecules break into atoms and losing their electron, changing into hydrogen positive ions. The cathode is the place that the electrons are carried back to the electrolyte which flow through the external circuit, and the hydrogen ions and oxygen are combined and forming the water. Figure 4.8 describes the operational procedure of PEMFC. The mentioned reactions occur in a single cell which produces an approximate voltage of 0.7 V. Connecting multiple cells in parallel and series increase the DC current and voltage output.

4.2.5 Diesel Generators

Diesel generators are combined of internal combustion engines and electrical generators with the purpose of producing electrical energy. The engine in a diesel generator is usually designed to run on diesel fuel, but some types are redesigned for other kinds of liquid fuel or natural gas as either. Unlike microturbines, these generators could be connected to the utility grid without any interfaces. During the operation, the spinning speed remains low and accordingly the frequency of the output power can be fixed in 50/60 Hz.

Table 4.2 Features and characteristics of each fuel cell type

Electrolyte material	Anticipated applications	Operating temp (time to ready for operation)	Features
PEMFC	Electrical vehicles and stationary DGs	85 °C (short)	Material problem, minimum contamination
MCFC	Stationary DGs	600 °C (long)	Material problems due to high temperature, steam generation working as CHP, high efficiency
AAFC	Space programs	100 °C (short)	Very expensive, susceptible to contamination
SOFC	Stationary DGs	1000 °C (long)	Same as MCFC
PAFC	Stationary DGs	100 °C (medium)	Unsuitable for vehicles due to higher temperature and longer warm up time

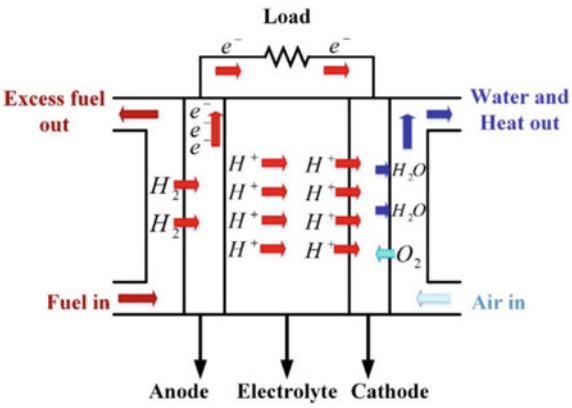

Fig. 4.8 Operation procedure of a typical PEMFC

Proper sizing of diesel generators is an important issue. In size ranges above 50 MWs, the efficiency of a gas turbine is more than of that diesel generator.

Diesel generators, are considered as dispatchable units. They are called dispatchable due to the fact that the output power of them could be easily controlled and they might be committed/uncommitted into the grid intentionally and would produce electrical energy according to a predefined reference value. Equations (4.17)–(4.19) illustrate the constraints of generation for these units [18]:

$$0 \leq P_{diesel} \leq P_{diesel}^{max} \tag{4.17}$$

$$|P_{diesel}(t) - P_{diesel}(t-1)| \leq ramprate \times P_{diesel}^{max} \tag{4.18}$$

$$P_{diesel}^2 + Q_{diesel}^2 \leq S_{rated,diesel}^2 \tag{4.19}$$

Equations (4.17) and (4.18) stand for the active power generation limit and ramp rate constraints and Eq. (4.19) shows the complex power constraint. The cost of producing electrical energy in these types of generators, is usually considered as a quadratic function of output power as below [18]:

$$Cost(P_{diesel}) = \alpha P_{diesel}^2 + \beta P_{diesel} + \gamma \tag{4.20}$$

In the above equation, α, β and γ are the cost coefficients of the diesel generator and depend on its structure and used fuel.

Although the main advantage of the diesel generators is their dispatchability, they release greenhouse gases into the environment. Accordingly, this fact affects their application in the electrical industry.

4.2.6 Batteries

Energy storage units are indisputable parts of the modern electrical power industry. Their presence is obligatory in order to compensate for the energy loss of undispatchable units such as wind and PV energy systems. Also, during a day, customers' electrical energy demand fluctuates. At times of peak-loading, according to Eq. (4.20), the cost of operating utility generators is increased quadratically, causing the total operation cost increment. So energy storage systems harvest excess electrical energy during low loading hours from the most efficient generators. This stored energy in the energy storage device, could be released onto the grid during high-load hours and may help decrease the operational costs. Batteries are the most used energy storage elements in the electrical systems.

The most common batteries in the electrical power systems for grid connection purposes, are lead-acid or flow batteries. Their commercial history goes back over a century, and are used in almost all industries such as emergency power for some critical sites as hospitals, telecommunication industries, etc. due to high availability and their little cost, the default selection for electrical energy storage devices in almost all applications are lead-acid batteries. Despite their advantages, they suffer low ratio of stored energy (known as specific energy (Wh/kg)), low ratio of their power to their weight (known as specific power (W/kg)), need of high maintenance, short life cycle and environmental issues [19].

There are other types but less usual, of batteries such as Nickel Cadmium batteries, Na-S batteries, Zn-Br batteries, V-Redox batteries, Polysulfide Bromide batteries, etc. Table 4.3 describes some characteristics of these batteries [19].

Table 4.3 Different battery types characteristics

Type	Technology	Energy density (Wh/kg)	Specific power (W/kg)	Target markets	Largest unit
Lead-Acid	Using sulfuric acid as the electrolyte and sealed and vented cells with lead oxide and lead electrodes	30–40	180	Vehicles, telecommunications, UPS, utility grid support	20 MW, 20 min (PREPA)
Ni-Cd	Using a caustic electrolyte (usually potassium hydroxide) and sealed and vented cells with cadmium and nickel oxyhydroxide electrodes	30	150–200	Aerospace, aircraft cranking, utility grid support	40 MW, 15 min (GVEA, Alaska)
Na-S	Using beta alumina electrolyte and contain cells with liquid Na and S electrodes	150	200	Stationary power systems with high ratings (almost 100 MW), T&D and renewable applications	6 MW, 48 MWh utility substations
Zn-Br	Using aqueous electrolyte (zinc bromide) and contained cells with Zinc and complexed bromine electrodes	35–54	100	Utility T&D and renewable applications	Detroit Edison 400 kWh system
V-Redox	Two electrolytes (vanadium salts dilute sulfuric acid solutions)	10–20	50	Utility T&D and renewable applications	3 MW for 1.5 s in japan

Table 4.4 Different characteristics of various types of flywheels

Material	M (kg)	σ (Pa)	ρ (kg/m^3)	E_{max} (J)	Energy density (J/kg)
Carbon fiber	450	4.0×10^9	1799	5.0×10^8	1.1×10^6
Titanium	450	8.8×10^8	4506	4.4×10^7	9.8×10^4
Aluminum	450	5.0×10^8	2700	4.2×10^7	9.2×10^4
Steel	450	6.9×10^8	8050	1.9×10^7	4.3×10^4

4.2.7 Flywheels

Flywheel is another type of energy storage system which is very popular due to its simplicity for storing energy. Flywheels work on a simple principle and they store kinetic energy in a spinning mass. Flywheels were used to the main technology for limiting power interruptions in generator/motors [20].

Electromechanical machines i.e. permanent magnet machines, switched reluctance machines and induction machines, have the duty of converting kinetic energy into electrical. The most important issue in designing a flywheel is providing a constant frequency for the electrical system while charging/discharging the flywheel due to its speed variations. Two approaches are proposed for this task: (1) mechanical clutches, (2) power electronic systems. Flywheels are designed to operate at high speeds, usually at speeds more than 10,000 rpm, in order to have the highest energy density. Different characteristics of various types of flywheels are tabulated in Table 4.4.

4.3 Microgrid Concept

In this subsection a thorough definition for the microgrid and its structure would be illustrated. According to the definition of EU research projects [21], a microgrid could be defined as follows:

> Microgrids are considered as low voltage distribution networks which have integrated DERs, energy storage devices and various types of loads. Microgrids, could be operated in two ways as grid connected and autonomous operations. The first one is to increase the benefits of the microgrid and the second one is for enhancing the reliability of the system.

According to the above definition, microgrid could be encountered as a combination of generators, costumers and energy storage systems in small size and low voltage distribution level. All the components are geographically near. The total generation capacity is in the range of few MWs and the voltage level is in few KVs. A microgrid should be capable of operating either in grid-connected (non-autonomous) or islanded modes in emergency events. For long periods of islanded operation, many considerations about the size of energy storage systems and capacity ratings of local

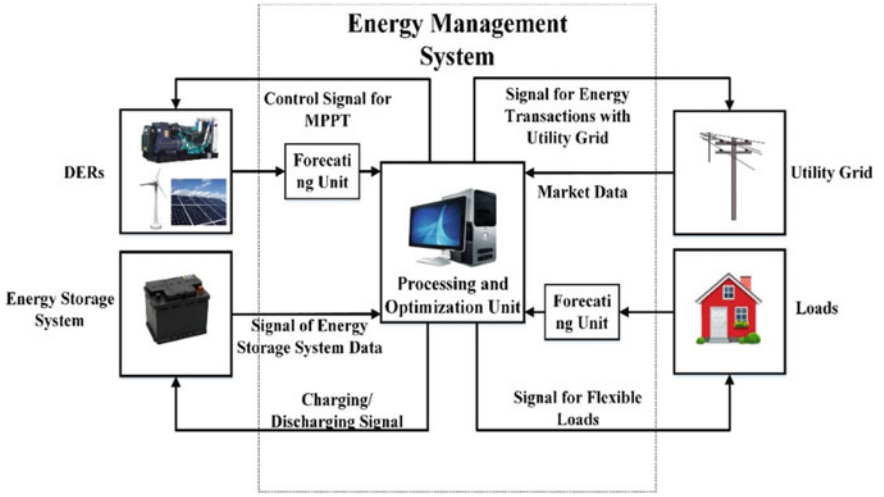

Fig. 4.9 A typical energy management system for the microgrids

generators and also load flexibilities should be made. Any shortcomings in these aspects would cause to load shedding and demand dissatisfactions.

The main factor which can differentiate a microgrid and a distribution network with local DERs is the controllability. Accordingly, appropriate controllers and data acquisition system is mandatory. Also a reliable communication system is another main element in correct operation of microgrids. To perform optimal operation of microgrids, an energy management system seems obligatory.

The energy management system could be accounted as the heart of the microgrid. This system is responsible for collecting data, controlling different components i.e. DERs, energy storage systems and responsive loads, different states of operation and system security. Also, the forecasting of the power generation of renewable energy based DERs, load consumption and network energy planning are considered as other duties of energy management system.

The aim of the energy management system is producing appropriate reference values for all of the distributed sources of energy and energy storage systems, so that the system operates at an optimal economic point to provide the required power of the loads. The use of energy storage devices requires an optimization plan in order to provide energy to the costumers at hours with electrical energy generation shortage in an optimum way. Therefore, the energy management system should plan energy for one or more days. The energy management system determines the optimal energy transactions with the grid for the scheduling period according to the price of electrical power. Figure 4.9 shows a common energy management system for a microgrid.

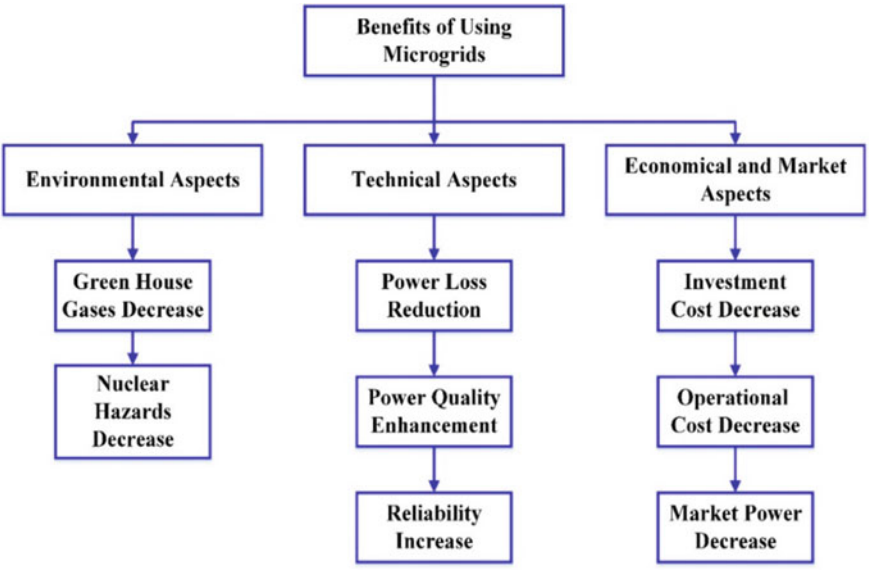

Fig. 4.10 Benefits of developing microgrids

4.4 Conclusion

A bright future stands in the way of microgrids development. There are many reasons for increasing the tendency for development of microgrids in current electrical energy systems, perhaps the most important of which are the economic benefits of using them. Other issues, including environmental reasons, are in the light of economic issues, and economic productivity can be the first objective in the development of microgrids. Figure 4.10 summarizes these benefits.

In this chapter, first different DERs and their characteristics were developed which are the main components of microgrids. These include, PV systems, wind generation units, microturbines, diesel generators and fuel cells. Latter two types of energy storage systems (batteries and flywheels) as indisputable parts of DERs were illustrated. Finally, a complete definition of microgrid alongside its energy management system were defined.

References

1. F.H. Aghdam, M. Abapour, Reliability and cost analysis of multistage boost converters connected to PV panels. IEEE J. Photovolt. **6**(4), 981–989 (2016)
2. *Introduction to Distributed Generation* (Virginia Tech., 2007)
3. Electric Power Research Institute web-page, Jan 1998. http://www.epri.com/gg/newgen/disgen/index.html

4. T. Ackermann, G. Andersson, L. Soder, Distributed generation: a definition. Electr. Power Syst. Res. **57**(3), 195–204 (2001)
5. M.T. Hagh, F.H. Aghdam, Smart hybrid nanogrids using modular multiport power electronic interface, in *IEEE Innovative Smart Grid Technologies-Asia (ISGT-Asia)* (2016), pp. 618–623
6. F.H. Aghdam, M.T. Hagh, M. Abapour, Reliability evaluation of two-stage interleaved boost converter interfacing PV panels based on mode of use, in *7th IEEE Power Electronics and Drive Systems Technologies Conference (PEDSTC)* (2016), pp. 409–414
7. Federal Energy Regulatory Commission, Federal Energy Regulatory Commission Assessment of Demand Response & Advanced Metering. Staff Report and Excel Data (29 Dec 2008)
8. M.S. Saleh, A. Althaibani, Y. Esa, Y. Mhandi, A.A. Mohamed, Impact of clustering microgrids on their stability and resilience during blackouts, in *IEEE International Conference on Smart Grid and Clean Energy Technologies (ICSGCE)* (2015), pp. 195–200
9. Smart Grids, ETP Vision and strategy for Europe's electricity networks of the future. European Commission (2006)
10. F.H. Aghdam, S. Ghaemi, N.T. Kalantari, Evaluation of loss minimization on the energy management of multi-microgrid based smart distribution network in the presence of emission constraints and clean productions. J. Clean. Prod. **196**, 185–201 (2018)
11. F.H. Aghdam, J. Salehi, S. Ghaemi, Assessment of power flow constraints impact on the energy management system of multi-microgrid based distribution network. J. Energy Manage. Technol. **2**(3), 31–41 (2018)
12. C. Keles, B.B. Alagoz, M. Akcin, A. Kaygusuz, A. Karabiber, A photovoltaic system model for Matlab/Simulink simulations, in *IEEE Fourth International Conference on Power Engineering, Energy and Electrical Drives (POWERENG)* (2013), pp. 1643–1647
13. S. Nema, R. Nema, G. Agnihotri, Matlab/simulink based study of photovoltaic cells/modules/array and their experimental verification. Int. J. Energy Environ. **1**(3), 487–500 (2010)
14. F.H. Aghdam, M.T. Hagh, Security Constrained Unit Commitment (SCUC) formulation and its solving with Modified Imperialist Competitive Algorithm (MICA). J. King Saud Univ. Eng. Sci. (2017)
15. F.A. Farret, M.G. Simoes, *Integration of Alternative Sources of Energy* (Wiley, Hoboken, 2006)
16. F. Blaabjerg, Z. Chen, S.B. Kjaer, Power electronics as efficient interface in dispersed power generation systems. IEEE Trans. Power Electron. **19**(5), 1184–1194 (2004)
17. H. Xu, L. Kong, X. Wen, Fuel cell power system and high power DC-DC converter. IEEE Trans. Power Electron. **19**(5), 1250–1255 (2004)
18. F.H. Aghdam, J. Salehi, S. Ghaemi, Contingency based energy management of multi-microgrid based distribution network. Sustain. Cities Soc. **41**, 265–274 (2018)
19. S. Eckroad, I. Gyuk, *EPRI-DOE Handbook of Energy Storage for Transmission & Distribution Applications* (Electric Power Research Institute, Inc., 2003), pp. 3–35
20. J.M. Carrasco et al., Power-electronic systems for the grid integration of renewable energy sources: a survey. IEEE Trans. Industr. Electron. **53**(4), 1002–1016 (2006)
21. Microgrids: Large Scale Integration of Micro-Generation to Low Voltage Grids. ENK5-CT-2002-00610 (2003–2005)

Chapter 5
Virtual Power Plants and Virtual Inertia

Javier Bilbao, Eugenio Bravo, Carolina Rebollar, Concepcion Varela and Olatz Garcia

Abstract In a general way, the electrical network is the set of lines, transformers and infrastructures that carry electricity from generation centers to final consumers. The current networks were designed and are in operation since the mid-twentieth century and were conceived to cover a situation in which the main generation centers were far from the populations. The new energy model is totally different and is transforming the current system into a distributed system, in which any agent that is connected to the network has the possibility of providing energy, enabling the creation of microgenerators, so that there is no such direct dependence as with the current energy generation. Thanks to this type of network, it is possible to drastically reduce losses due to energy transport, facilitate the connection to the network of all types of renewable energies and support energy storage capacities. But this structure requires management systems and integration of the microgenerators in the electrical system and it is in this moment when the concept of Virtual Power Plant (VPP) appears, which arises from the grouping of a series of small generators acting as a unit. Taking value from the energy microgeneration concept and the microgrids, a VPP connects many of these microgenerators to work together as a traditional plant through a centralized control system. A VPP achieves to interlink multiple concentrated sources in one area: wind, solar, storage batteries, biomass plants and conventional generation sources, and coordinate them through remote software. A Virtual Power Plant is one of the main functions of the smart grids. Through it, various distributed generation resources

J. Bilbao (✉) · E. Bravo · C. Rebollar · C. Varela · O. Garcia
Applied Mathematics Department, University of the Basque Country, Bilbao, Spain
e-mail: javier.bilbao@ehu.eus

E. Bravo
e-mail: eugenio.bravo@ehu.eus

C. Rebollar
e-mail: carolina.rebollar@ehu.eus

C. Varela
e-mail: concepcion.varela@ehu.eus

O. Garcia
e-mail: olatz.garcia@ehu.eus

N. Mahdavi Tabatabaei et al. (eds.), *Microgrid Architectures, Control and Protection Methods*, Power Systems,
https://doi.org/10.1007/978-3-030-23723-3_5

are brought together, dispersed throughout the network, with the capacity to respond intelligently to demand control and turn them into positions of active resources that function as a single centralized generating plant. In this way, the capacity of the virtual plant would be the sum of the powers of all the elements that make it up. We can say that VPPs use the Intelligent Network to enter the system and this can represent a reduction in demand and therefore affects the offer. It is called Virtual because it is in the digital world where, through telecommunications and control networks, it can be linked to physical elements through software. For the virtual power plant, sensors are used to collect data that are collected through a secure telecommunications infrastructure to convert them into information and be controlled by the system operator. The VPP is then a technical, operational and economic concept that is located in the digital part of the electrical network and provides facilities that allow greater flexibility of the electrical system. On the other hand, in recent years, within the electrical generation system, wind power has taken on great importance and has significantly increased its share of space in the generation market. This has implied an increasing value in the number of wind turbines connected to the network. This growing penetration of wind generation involves new factors to be taken into account in aspects such as frequency control, where the inertia of the system plays a determining role. The inertia of the system determines how the frequency will vary when a change occurs in the generation or in the power demand. The doubly-fed induction generator wind turbines, the preferred choice for extensive wind farms, can reduce the effective inertia of the system. These variable speed wind turbines can emulate inertia by fast active power control. This virtual inertia can be taken as an important way for the control of the frequency.

Keywords Virtual power plants · Virtual inertia · Electrical network

5.1 Introduction

One of the most important dilemmas facing today's society is how to meet the growing energy demand. Since the early stages of the industrial revolution society has been encouraged to consume and produce. This increases the demand for energy resources, which were initially considered inexhaustible. However, they have been used to such an extent that they become exhausted and this behavior has had negative effects on the planet such as global warming, this being one of the main preoccupations of today's society [1]. Among the main causes of climate change, one is the use of fossil fuels, both for transport and for the production of energy. Despite this, demand is not reduced and there are more and more means of transport circulating and the energy demand increases. This has led to the need for a rethinking of the global energy system and the search for so-called clean technologies that can help significantly reduce the effect of global warming [2]. Figure 5.1 shows data (historic and projection to 2040) that predict the distribution of the world energy consumption by energy source.

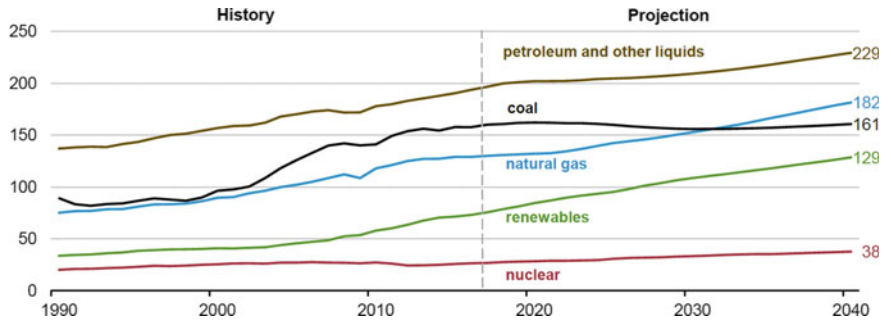

Fig. 5.1 World energy consumption by energy source. *Source* EIA, International Energy Outlook 2018

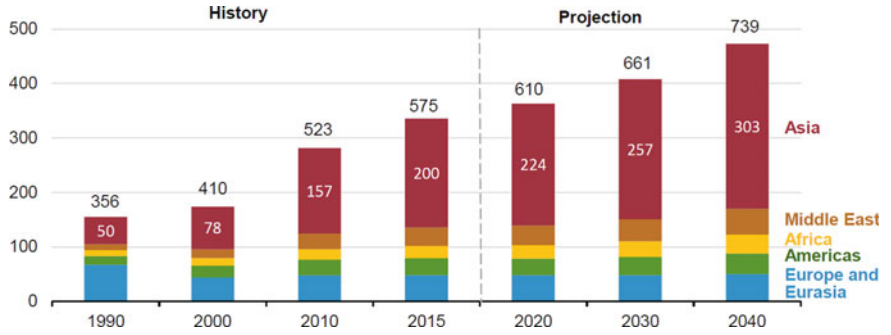

Fig. 5.2 Energy consumption by region. *Source* EIA, International Energy Outlook 2018

This suggests that a change in the use of energy is going to have to take place, electric power being one of the main candidates. However, it does not make sense to continue using fossil fuels to produce this electrical energy and therefore aim to take advantage of renewable resources. The distribution of the energy consumption by region is shown in Fig. 5.2.

As shown in the graphs above, the main resource for producing energy has been, and seems to continue to be, fossil fuels, with a large part of that market for coal. This fossil fuel generates greenhouse gases, which is why, as far as possible, the generation structure must be changed to make more use of renewable resources. The problem is that many of them are difficult to incorporate by themselves in a conventional way to the system, because they are not constant sources and present large oscillations due to their dependence on climatic factors.

In Europe, renewable energies will continue to rise, particularly in the European Union (EU), where its countries agreed in 2014 on a new framework for a renewable energy target of at least 27% of EU's final energy by 2030. This target was part of its energy and climate goals for the year 2030. In 2018, European Union and its countries reached a political agreement which includes a binding renewable energy target for 2030 of 32% of their final energy consumption [3].

In the world, at the end of 2015, the Paris Agreement was adopted to prevent the increase in the global average temperature of the planet exceeding 2 °C, compared to pre-industrial levels, and seeks also to promote additional efforts that make it possible for Global warming does not exceed 1.5 °C [4]. In this way, the Agreement includes the greatest possible ambition to reduce the impacts and risks of climate change around the world and, at the same time, includes all the elements necessary to achieve this objective. Among these elements, we focus on the reduction of fossil fuel consumption and the promotion of renewable energies.

Therefore, we will develop in this chapter the concept of virtual power plant as the next step of the electrical system towards an intelligent electrical network and virtual inertia, specially focused on the Doubly-Fed Induction Generator (DFIG), one of the different technologies of electric generators and the most used for wind energy applications. The structure of the chapter will be the following: in the second section, we will explain why these concepts have arisen with importance in the electrical world. In section three, we will define Virtual Power Plants, to continue in the section four with the different types that exist nowadays, and discussing their possible implementation in the fifth section. The section six is devoted to the world situation of the virtual power plants. Before finishing with some conclusions, in section seven we will develop the concept of virtual inertia and its control for DFIG wind turbines.

5.2 Searching New Ways for the Electrical Network

Currently the electrical system has a very well defined structure with periods of high demand. This occurs because there are defined consumption patterns and therefore there are fairly defined periods of time where these power demand peaks occur. Electric facilities must measure their installed capacity and they have to be able to supply power to the system in order to system will not collapse when these peaks occur, and based on the previous consumption patterns and predictions. This installed capacity refers to the sum of the powers of all the generators that are connected to the network. In the structure of the electrical system, it should be clear two concepts that are power and energy. Power is considered as the amount of energy per unit of time and therefore energy is obtained as the product of power in a given time. Graphically, you could see that the energy is the integral under the curve in a power graph with respect to time. In Fig. 5.3, the demand curve of the Spanish electricity system with its respective distribution of generation is illustrated.

Colors indicate the different generation structure in the different hours of this day. From button to top, dark blue color is the nuclear generation, brown is generation from coal, cream is combined cycle, blue is hydraulic generation, green is wind generation, grey indicates the international power interchanges (France and Africa), dark yellow for photovoltaics, red is for the solar thermal power plants, dark violet for other renewable energies (geothermal, biomass, etc.), and light violet for cogeneration and waste power plants. Under the nuclear generation, especially when there are demand

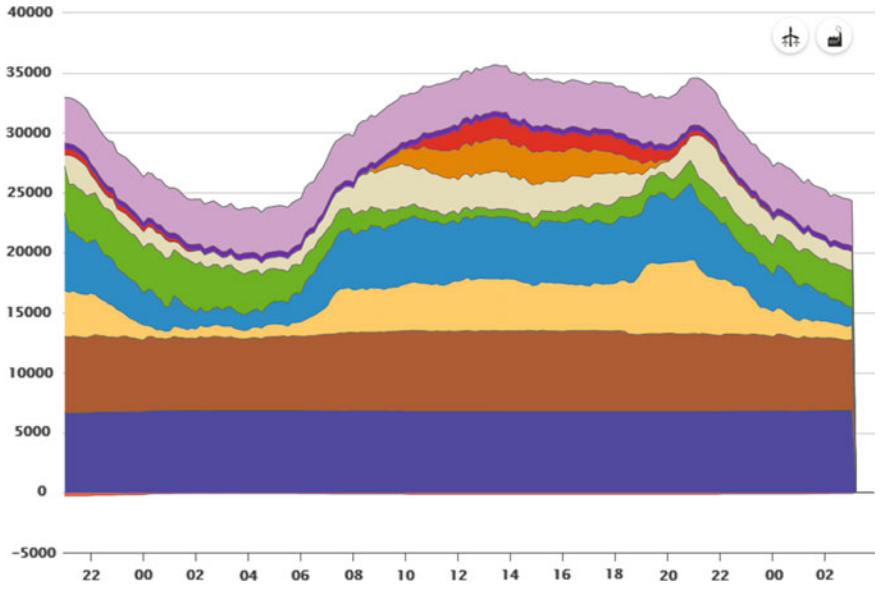

Fig. 5.3 Demand curve of the Spanish electricity on 2018 September 12. *Source* REE, Transmission agent and Operator (TSO) of the Spanish electricity system

peaks, there is a very fine orange band that indicates the link to the Balearic Islands [5] (Fig. 5.4).

However, it is important to analyze if there is any way that the operator can control that demand to redistribute it, and thus be able to save the use of plants whose generation cost is high and make maximum use of plants with low variable costs such as those using renewable resources. To control the system without affecting it, you must have full knowledge of the system at all times. In order to know this, you must have a network monitored and once you know what is happening at each moment, make a redistribution of existing resources in real time; this is where the concept of a Smart Grid comes in [6]. This concept is very broad, but ideally what it seeks is to create a dynamic and self-sufficient electricity network, which by itself can have control of the load and generation looking for the best combination using the resources available on the network. To achieve this, a very important modification must be made in terms of the network infrastructure, installing throughout the power network smart meters that allow a central controller to have information on how energy is being consumed and how much it is being consumed. In this way, the system alone could control its operation based on the energy balance equation controlling both the generation and arranging the load so that an optimal use of resources is had [7]. This broad concept, which is still utopian, is where the network is intended to be. However, from the current network to the Intelligent Network there must be a progressive process with gradual modifications to reach a self-sufficient network. As the intelligent network is a process that seeks control and an optimal use of resources,

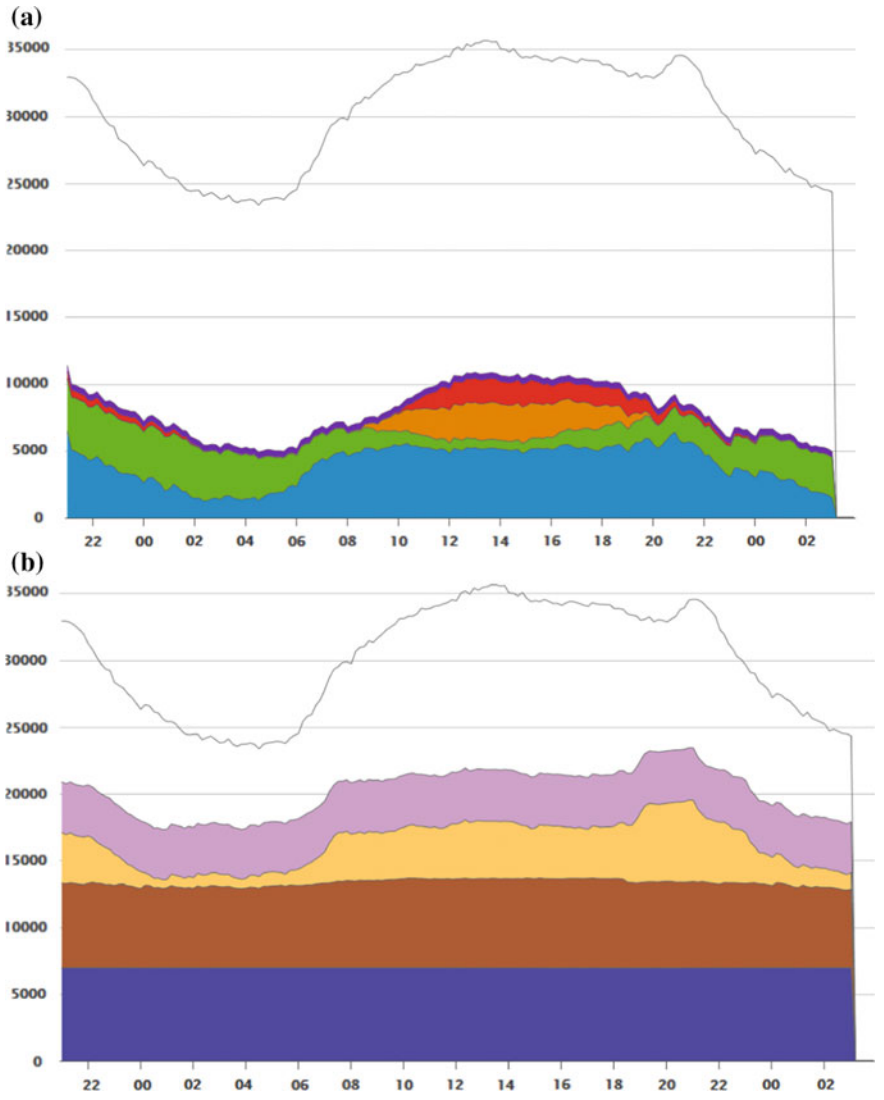

Fig. 5.4 **a** Demand curve of the Spanish electricity on 2018 September 12 supported by renewable energies, **b** supported by non-renewable energies. *Source* REE, Transmission agent and Operator (TSO) of the Spanish electricity system

it is composed of a series of tools that make it possible to control them. One of the main tools, which seems to be the next step to get to have an intelligent network, are the Virtual Power Plants.

5.3 Virtual Power Plants

The Virtual Power Plants (VPP) are the next step of the electrical system towards an intelligent electrical network. There are different definitions of the virtual power plant, and there is still no single definition of them. However, the Pike Research Institute (at present, Navigant Research) states: "The essence of virtual generation plants could be defined as: the ability to take advantage of resources in real time, with enough specificity to control the load profiles of customers, add resources to the network and put them on the operator's desk" [8]. A Virtual Power Plant is one of the main functions of the Smart Grid. Through it, various distributed generation resources are brought together, dispersed throughout the network, with the capacity to respond intelligently to demand control and turn them into positions of active resources that function as a single centralized generating plant. In this way, the capacity of the virtual plant would be the sum of the powers of all the elements that make it up. With the above, we can see how virtual power plants use the Intelligent Network to enter the system, and this can represent a reduction in demand and therefore affects the offer. It is called "virtual" because it is in the digital world where, through telecommunications and control networks, it can be linked to physical elements through software. For the virtual power plant, sensors are used to collect data that are collected through a secure telecommunications infrastructure to convert them into information and be controlled by the system operator. The VPP is then a technical, operational and economic building that is located in the virtual world and provides facilities that allow greater flexibility of the electrical system [9].

Siemens company defined a Virtual Power Plant as a cluster of distributed energy resources (generation, controllable loads and storages such as microCHP, wind-turbines, small hydro, back-up gensets, flexible loads, batteries, etc.), which are collectively run by a central control entity [10].

Jin et al. [11] said that VPP is a technology to efficiently manage different resources related to generation, storage, and demand resources by using software.

According to Mussenbrock, from Altran, a Virtual Power Plant consists of a portfolio of technical and contractual assets, which are able to deliver electrical capacities when needed. The main task of a VPP is to spontaneously deliver positive (production) or negative capacities (consumption) of electric energy (Flexibilities), according to a random call signal from the market [12].

Therefore, we can define a Virtual Power Plant as the set of small power generation systems and storage systems connected telematically in a secure way to be managed remotely and in real time by a system operator.

Most of the definitions of virtual power plants that exist focus on the use of renewable resources; however, it has already been said that there is sufficient speci-

ficity in them to control load profiles, which indicates that by means of the virtual power plant we can control the demand. At the beginning, a virtual power plant was related uniquely to power generation, but it is an entity that comprehends also storage systems and telecommunication systems.

According to Roberta Bigliani, research director of the IDC institute [13], "the contribution of distributed generation in energy policy can be significantly improved with the concept of the Virtual Power Plant". We can see the importance of the virtual power plants for the new energy model to which the current world must migrate, in order to satisfy demand through the use of renewable sources.

This is why VPP is a viable means to flatten the demand curve and improve the country's load factor. Among the most striking advantages of the use of Virtual Power Plants are:

- The use of Virtual Power Plants allows advanced control of energy demand in the system.
- On-site local generation through clean technologies such as cogeneration, solar, wind and small hydroelectric power plants, which, due to their self-consumption, often prevent transmission and distribution losses. In the same way, there is energy saving as well as greenhouse gas emissions are reduced.
- Reduce the demand in peaks with on-site controls by means of load control systems, which saves generation in conventional plants and it is even possible to dispense with the existence of some of them that are only used in peak periods.
- The use of virtual generation plants generates security in the energy of the system due to the flexibility of incorporating different technologies to the system, combined with load control protocols.
- The reduction of global warming through the use of clean energies and their massive incorporation into the system.

5.4 Different Types of VPP

Due to the characteristics of virtual power plants, being an advanced control system, a division has been made into four different groups where they are located according to their operation form. According to the Pike Research Institute they are divided into:

- Virtual Power Plants for load control (Demand Response).
- Alternative Supply Virtual Plants (Supply-Side).
- Virtual Mixed Asset Power Plants (Mixed Asset).
- Wholesale Electric Power Plants (Wholesale Auction).

Load control plants are being implemented mainly in the United States. They search for reducing the demand for power, so that they can vary their energy supply proposals at lower costs. They have smart meters in the sites that allow the bidirectional transfer of information. These smart meters have access to intelligent elements

inside the point to be controlled, being it a residence or an industry. In other cases, terminals with telecommunications ports can be used in which the behavior of the connected element in each receptacle is known, as well as what it is. All this information is sent to a database accessed by an operator. The operator can then, with the prior consent of the user, disconnect a certain amount of load in a certain period of the demand curve to reduce the peaks and thus reduce the power demanded in the system. According to Dan Delurey (President of the Demand Response and Smart Grid Coalition), 10–20% of annual energy costs are concentrated in 100 h per year [14], which could be reduced by means of virtual power plants. These control plants are those that are specified by quantity of load relief. Briefly, load control concept for a system consists of a movement of load from peak periods to valley periods. Normally, from operators, agreements for industrial users are used, with a compensation by the electric facility in the price of the electricity [15].

In the case of traditional plants, when the demand increases, the supply of energy by the distribution company must be increased to the same extent. When virtual power plants are incorporated into the system, demand decreases and the need to incorporate new traditional plants into the system is avoided.

The virtual power plants of alternative supply (Supply-Side) are being developed mainly in the European continent. This is the type of plants that focuses on controlling the elements of distributed generation and use them as a single plant whose capacity is the sum of all its elements. The key to the success of these plants is that, due to the ease of control, the same plant will combine resources and different technologies so that they can be complemented and have the most constant production based on renewable resources. Currently, according to David Brewster (President and Cofounder of EnerNOC), he stated that there is a perception that solar and wind energy require very expensive energy storage networks and technologies, or equivalents in natural gas support plants to have an important weight. However, he said also that, with demand control systems, this need is reduced and in some cases eliminated [16].

The third type of virtual plants is that of mixed assets and consists of the combination among the load control, alternative supply and energy storage plants. This may be the ideal plant model; however, it has not begun to be implemented commercially. In this plant, we could have a control of both generation and demand and the plant alone can find the right balance in an intelligent way to have a self-sufficient intelligent system.

The fourth type is even more elaborate and requires even greater communication protocols and controls. A pilot project is currently being carried out on an island in Denmark [17, 18]. In this case, about 2000 households in Bornholm, Denmark, are connected to the network. The project enables the reduction of power usage in situations of peak loads, with the trade of unused capacity at market prices. Due to a high share of wind power in this island, this project proves to be of major significance. When the market system has peaks in electricity prices and, according to previously set conditions, these clients (houses), equipped with gateway controllers, are automatically turned off their appliances or adjust the thermostat. When this occurs, the non-used power capacity is aggregated and sold to consumers in need, allowing levels of reduction of about 20% in peak loads. The alternative to meet this

demand would be to increase generation, which would have significant economic and environmental costs. This type of free-market virtual power plant pretends that all customers of the system can sell energy in the peak periods, at the time they wish and according to market prices. In these cases, they could contribute by contributing to reduction of the load in the system when disconnecting from the grid or also contributing energy through distributed generation, electric vehicles and other energy storage devices. This would make a technical and economic integration of the entire intelligent network, then operating as a free electric market and making the most of all available resources. In the same way, consumer habits are modified by being able to function as small businesses, thus motivating sectors such as residential savings and making those resources available to the system.

5.5 Possible Implementation of VPP

The implementation of virtual energy systems is currently possible due to a series of technological advances that allow this concept to be a viable solution and a model for future power networks. Next, reference will be made to some of the elements that make this implementation possible.

- Renewable energy conversion plants, particularly the case of wind power plants that use generators with interfaces that allow a better coupling to the electrical system, as well as the reactive power contribution to it with voltage and frequency controls. These technologies make it possible for these plants to be used for energy recovery after faults or blackouts.
- Smart and high efficiency home appliances are available in the market. These elements apart from their low energy consumption can easily be incorporated into the demand control strategies of the intelligent network, which gives them an added value for the network.
- Systems to control so-called “energy vampires” or elements that have phantom consumption in “stand-by” mode. Among them, we can cite the automatic disconnection of the elements when they are in these states.
- The development of new energy storage technologies for short periods of time. These include compressed air, new types of improved lithium batteries and lower cost, ultra-capacitors, among others.
- Other energy storage technologies are also available, such as ice banks and heat pumps that store thermal energy, which is produced by electrical energy at specific times.
- New communication technologies and data collection such as smart meters that provide the network with elements to achieve a large scale control of it and allow demand and supply control processes, thus achieving greater network flexibility. In some cases, a maximum demand is agreed and, also based on that, there is an automatic disconnection of loads.

- In the case of the United States, an aspect that facilitates the implementation of virtual energy systems is the opening of the electricity market, which favors the use of these systems to see the production of energy as a business and have facilities in the field.

For the operators of the network and the companies involved in the energy business, facilities, a series of aspects and requirements must be taken into account that are decisive for the implementation of the virtual power plants.

- The spatial aspect and the topology of the electricity network must be considered in such a way that the costs of transmission and distribution of electricity are minimized. Enabling on-site generation with renewable resources.
- The temporary aspect must consider that the electricity supply must be able to meet the demand at any point of the electrical network and at any time. Therefore, additional security measures must be taken always trying to minimize costs.
- In order to be a profitable business, cooperation strategies must be created between supply and demand among network operators, electricity producers and final consumers.
- In the social aspect, it must be taken into account that in order to develop this system, a cooperation system must be created between the clients and the network administrator. Mainly for the issue of charge control, a new consumption scheme must be created.

The implementation of this system can also bring to the operator a series of benefits, among which we can mention:

- Reduce the costs of measuring and improving systems against electricity theft, fraud and payment evasion, thanks to smart meters.
- Improvements in the sizing and operation of the network infrastructure through real-time measurements and power flows in all parts of the network, including stress profiles.
- The possibility of offering additional services to the client through smart meters, among them telecommunications and information services could be mentioned.
- Optimization of costs in electricity purchases when distributing charges depending on the price of energy in that period.
- Due to the strategies of control of load and generation, companies or facilities have the possibility of modifying their curve in such a way that a producer can concentrate all his resources to generate surpluses in the peak hours and sell it at higher or lower prices to the other companies of network.
- The expansion of the electricity market due to the incentive for the use of electric vehicles and thermal pumps, which would increase the electricity demand and reduce the use of fossil fuels.
- Use the aforementioned resources in the network as elements of distributed generation in the network, as well as loads that can be disconnected and energy storage elements, generating in this way important benefits for facilities and users in the network.

- Learn about customer consumption patterns, as well as their response to variations in price and other incentives.

When the client's consent is needed to implement the virtual power plants, a series of opportunities must be presented for the clients generated due to the development of this new model. Among these can be mentioned:

- The possibility of using energy storage units. Some of them could be cold rooms, ice banks, and thermal pumps in exchange for economic compensation for the change of charges.
- A greater variety of options to optimize the purchase of energy and the business in general.
- A reduction in electricity consumption both through the acquisition of high efficiency electrical appliances and changes in electricity consumption patterns.
- A reduction in consumption due to intelligent lighting control systems.

In 2008, Siemens Power Transmission and Distribution (PTD) and RWE Energy developed a business model for the creation of virtual power plants and the required system management. According to this development, virtual power plants are profitable if a generation of at least 500 kW is integrated [13]. The biggest problem, from the economic point of view, would be in the cost of the communication systems for the correct management of the VPP. The client's consent and participation in certain key aspects must also be available for the plant to function due to the demand control systems. However, the existence in the electricity grid of small (domestic) producers of electricity (photovoltaic and wind, mainly) can be exploited if they form a sufficiently well managed set to become a VPP. This would imply reducing this limit of 500 kW to around 50 kW, taking into account that, in addition, the management systems, via telecommunication, are reducing their costs and increasing their benefits.

In this way, one of the main advantages of the implementation of virtual plants is the security they can provide the system at a lower cost than traditional methods. This security, in the current systems, is usually evidenced with a double cost. In many times, the systems are prepared to cope with a failure, the failure of one of its transformers for example, because it has a backup transformer. However, if a second fault occurs and, during that period, there is a peak demand, the power demanded may exceed the power supplied and, in that case, a collapse of the network may occur. In these cases, if system would have a virtual power plant, during the failure this plant would alert the connected systems to it and an analysis of the situation would be made (including the weather, for the possible entry of solar and/or wind generation) to see the availability of renewable resources [19, 20]. Examples of the elements connected to the network are the following:

- Smart meters and other intelligent control elements that are distributed through the network. They allow the response to the demand that allows the reduction of load or the disconnection of the devices in conditions of shortage.
- Electrical or thermal energy storage elements through the network that store energy outside of peak hours and discharge during peak periods.

Another method is the reduction of voltage as a process to systematically reduce the electrical voltage in the distribution network, which results in a proportional reduction of load. In this case, we must always take into account the lower limit of quality of supply marked by law, which in Spain is 7% over 220 V, although companies such as Iberdrola put their lower limit of supply in only 5%, for reasons of quality of service. Solar technologies and conventional distributed generation are used as an emergency backup for customers, and can also be used as a source.

If the system cannot be restored and a second fault occurs, the intelligent controller automatically reduces the load with a pre-established scheme, so that the transformers are not overloaded. In this way, the fact of having a resource like the virtual power plants in the network can improve the reliability of the system and avoid collapses in a much more profitable way, simply by changing the concept of the network. This is how you can see that the safest and cleanest energy is that energy not consumed or avoided and the elements called "Demand Side Management", such as smart meters and control systems, are a good option for programming investments in an electrical system. Finally, the use of virtual plants is a great opportunity to reorganize the relationship among supply, demand, economic efficiency and environmental issues by creating a new operating model that supports the companies that provide this service.

5.6 World Situation of the Virtual Power Plants

As noted in the 2015 Paris Agreement on Climate Change, due to the multiple challenges of today's society and due to the consumption patterns of society, the planet has suffered and is suffering a significant deterioration from the point of view environmental and resource management. These resources are limited, and even more if the mentality of the current society and the way of generating and consuming energy are not changed in an important way. For this reason and thanks to technological advances, it has been possible to implement a series of tools to form an intelligent electrical network, and among these tools are the Virtual Power Plants.

The first virtual generation plant was created approximately 10 years ago as a research project of the Siemens company, in the Intelligent Networks division. Currently, in various parts of the world, projects with virtual power plants have been implemented both on the European continent and in the United States. In Europe, mainly distributed generation has been promoted and the use of virtual power plants is seen as an opportunity to eliminate the use of nuclear power plants. On the other hand, USA have focused on certain investigations to realize load control plants.

In the United States, the CAISO (California Independent System Operator), the company responsible for operating most of the open electricity market in California, introduced a program called Proxy Demand Response [21]. In this program, companies are given the possibility of being virtual generators by reducing their energy consumption in peak periods in exchange for economic incentives. Among the saving points that are used, we can mention the use of dimmers to regulate the intensity

of lighting; this was used with a chain of grocery stores. Due to the reductions in costs, businesses were able to make a decrease in prices, also benefiting consumers. According to Jon Wellinghoff, president of the Federal Energy Regulatory Commission, if you can reduce the number of plants used to cope with peak demand could save up to 1.2 billion tons of coal per year [22]. This is an important amount, both in the aspect of economic savings and also in the important environmental impact that it has.

In Detroit, there is also a program where a virtual power plant is being created, in this case for distributed generation. This plant intends to have a capacity of 300 MW. According to the integrated resources plan of the operator of the area, Midcontinent Independent System Operator (formerly named Midwest Independent Transmission System Operator) (MISO), it is more profitable to use 250 h a year distributed generation systems against creating a combustion generation plant [23]. Therefore, the modifications have been made to have a dispatchable network of resources generated by customers. In this program, Detroit Edison takes care of the fuel costs, maintenance and repair of the generator of the clients in exchange for 250 annual hours of dispatch for a 10-year contract.

In Germany, on the other hand, virtual power plants are focused on the supply side. One of the main promoters of the initiative of virtual power plants in the country is Siemens company. Siemens started its experience in 2004 together with the energy supply company SaarEnergie, also known as Evonik New Energies, connected several distributed energy resources through a virtual power plant in Saarbrücken, Germany [24]. Another of its projects is to join by means of a VPP nine small hydroelectric plants, which occurred in 2008 in the Saunderland region. Their capacities varied from 150 to 1100 kW, and amounted to a total of 8.6 MW. Siemens company also created a 1450 MW virtual power plant combining the capacity of small generators in hospitals, industries and commercial buildings throughout the country.

Another European company, called RWE Energy, started the initiative, in 2006, to create in Germany a virtual coal plant controlled through the Internet [25, 26]. This plant had units of a minimum of 10 MW and the company offered a generation capacity of 300 MW. On the other hand, the possibility of creating a virtual plant using cogeneration plants was studied in the same European country. However, in the simulations of profitability the price of kilowatt-hour is higher than that obtained by conventional technologies and therefore it is not profitable to replace current basic technologies.

Between 2007 and 2009, a project called FENIX was carried out on the European continent, which consisted of the incorporation of distributed generation resources into the network through virtual power plants. This project was carried out in Spain and the United Kingdom, and they concluded in their cost-benefit analysis that it was an attractive business for investors. This would strongly open the competition which would be an aspect that would affect the traditional generators due to the free energy market [27, 28].

The EPRI (Electric Power Research Institute) in conjunction with the company AEP (American Electric Power) has a similar project in the United States [29]. This project comprises around 10,000 customers, smart meters, communications, end-

use tariffs and controls, automation of distribution and voltage controls. All this on simulation platforms and robust mathematical models. In some parts of the country, as in Ohio, energy storage elements and various intelligent systems are also considered for the network to control them. Currently, the EPRI has another 18 projects in addition to the virtual power plants of the AEP, and it is predicted that the power plants will have an important role due to the growth of distributed generation models.

According to reports from the Pike Research Institute, the global market for virtual power plants doubled its capacity in 2009, where 19.4 GW were installed by 2015, where 41.1 GW were projected. At that point it is expected that the market for clean technologies and virtual plants have returns of $7.4 billion [30]. It is also looking at the possibility of installing distributed energy resources for new residential areas, instead of having to create transmission lines from the central generators, these distributed resources are interconnected through a virtual power plant.

The nuclear disaster in Japan aroused interest in the virtual power plants. There was a fall of almost 4% in capacity due to the crisis in Fukushima Daiichi. This generates blackouts that impact the productive sector of the country. Experts believe that the solution is not to increase the number of centralized generation plants, but to create virtual generation plants that adapt quickly to changes in energy demand. "The most modern virtual generation plant will be the mixed goods … but for now, you can see a combination of projects led by the response to demand", Peter Asmus, Pike Research Institute [31].

The largest VPP in Germany is the called "combined regenerative generation plant" (Kombikraftwerk, in German) [32]. In the first phase (Kombikraftwerk-1), it comprised three wind farms totaling 12.6 MW, 20 photovoltaic solar plants that generated 5.5 MW, 4 of biogas totaling 4 MW, and pumped storage systems equivalent to 8.4 GWh of storage. The projects are combined and monitored through an intelligent control system that allows the operator to quickly adapt to changes in demand. According to the developers of the SolarWorld project, Enercon and Schmack Biogas, this plant proves that 100% of Germany's energy can be provided by renewable resources and load controls. Currently this plant can supply 1:10,000 of Germany's demand. This would correspond to the demand of a small town of around 12,000 households.

In 2013, it was the second phase: Kombikraftwerk-2. It combined several wind farms, biogas and photovoltaic plants with a total capacity of approximately 80 MW to a unique power plant, showing how a combination of different renewable energy systems can already provide "balancing power, making an important contribution to the stability of the power supply" [33]. The results suggested that a secure and stable power supply for Germany on the basis of 100% renewable energy sources was technically possible, and as a result of the aggregation in virtual power plants, renewable energies have the ability to guarantee the safe operation of the grid. The regenerative virtual power plant consists of the following individual installations [33]:

- Wind farm "Altes Lager" of ENERCON GmbH, Juterborg (Brandenburg). 18 turbines with a total of 37.2 MW output

Table 5.1 Some VPP projects in Europe between 2003 and 2015

Projects	Start–end time	Main countries
STADG VPP	2003–2007	Germany
UNNA	2004–2006	Germany
VIRTPLANT	2005–2007	Germany
PM VPP	2005–2007	Netherlands
FENIX	2005–2009	UK, Spain, etc.
GVPP	2006–2012	Denmark
VGPP	2007–2008	Austria
HARZ VPP	2008–2012	Germany
Pro VPP	2008–2012	Germany
EDISON	2009–2012	Denmark
FLEXPOWER	2010–2013	Denmark
WEB2ENERGY	2010–2015	Germany, Poland, etc.
TWENTIES	2012–2015	Belgium, Germany, etc.

- Wind farm "Feldheim" (Brandenburg) of energiequelle GmbH. 19 turbines with a total of 39.2 MW output
- Photovoltaics: 12 photovoltaic plants in Kassel area, among them 9 installations on private residences and 3 photovoltaic large-scale plants with a total output of almost 1 MW
- Biogas plant "Wallerstadten" (Hesse). Output: 1.2 MW
- Biogas plant "Mittelstrimming" (Rhineland-Palatinate). Output: 0.5 MW distributed between 2 CHP with 0.2 and 0.3 MW
- Biogas plant "Zemmer" (Rhineland-Palatinate). Output: approximately 1.4 MW, of this 1 CHP with 889 kW and a satellite-CHP with 536 kW
- Biogas plant "Heilbachhof", Zweibrucken (Rhineland-Palatinate). Output: 0.5 MW distributed among 2 CHP with 250 MW each (Table 5.1).

In August 2018, energy tech company, Limejump from UK, said it received approval from energy regulator, OFGEM, to enter the balancing mechanism market with its Virtual Power Plant, thus allowing both renewable and distributed energy generators to compete with the country's major power players, in what it said is a £ 1 billion a year market, for the first time. Limejump's technology connects distributed storage or generation assets, such as batteries, solar and wind, using big data analytics, trading ability and machine learning, so they "act as if they were one large power station" [34].

In China, and according to the People's Daily newspaper of China, it has been developed the first virtual power plant of this country. The power plant, in order to strike a balance between the output and consumption of power, was put into operation in eastern China's Jiangsu province on 2017, by State Grid Jiangsu Electricity Company. By 2020, the total power reserve of the system is expected to reach 100

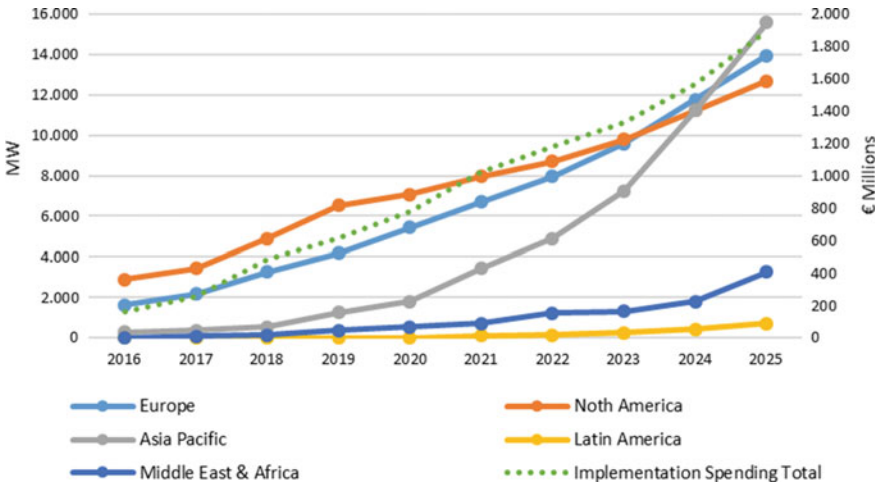

Fig. 5.5 Total annual VPP capacity and implementation spending by region, World Markets: 2016–2025. *Source* Navigant Research, Virtual Power Plant Enabling Technologies Report, 3Q 2016

million kW, replacing 100 million-kW coal-fired units. The system will consume over 100 million kW of clean energy [35].

The South Australian government is embarking on the largest expansion of home battery storage in the world, till now, and has reconfirmed its support for Tesla's virtual power plant of solar and Powerwall home batteries. A 250 MW/650 MWh power plant (which is how big the virtual power plant will be at the end of the 4.5 year schedule for installation of 50,000 systems) can meet around 20% of South Australia's average daily energy requirements (or power approximately 75,000 homes) [36].

Based on the different classifications of virtual power plants, and according to the Pike Research Institute, the projection of their impact on the world over the next few years, both from the aspect of installed capacity and the profitability of them is shown in the Fig. 5.5.

In Fig. 5.5, we can notice how the increases in the capacity of the plants is predicted by 100% in a period of 6 years. This is due to the great importance that the issue of energy saving is taking.

In Fig. 5.5, we can also see the profitability of virtual power plants, which in many cases are manifested as savings points compared to current technologies. Also one of the biggest attractions for investors is the opening of markets, which allows the implementation of this type of plants. Sellers can decide when to do it and this will determine the market prices. Then, we can see how it represents a great attraction for investors due to the ease of incorporating new generation resources into the network. In this way, we can also see how the implementation of virtual power plants worldwide has contributed so much to the improvement of the environment, the opening of new markets and the reduction of energy consumption without harming

producers because they can redistribute and make better use of the resources they have. For these reasons, a boom in the coming years of the use of smart grids is forecast, which would substantially change the current energy model and, in many cases, the energy producers would become service providers, which would generate significant savings, as an increase in infrastructure and an improvement in the quality of the service.

5.7 Inertia

In an electrical system the frequency is established by conventional synchronous electric generators. Each of these generators is provided with a frequency control whose objective is to keep all the them in synchronism and the generation-demand power balance. In addition, the inertia of synchronous machines plays a very important role in the stability of the power system during a transient event [37]. Having a greater rotating mass in the synchronous generators connected to an electrical system implies having smaller variations in the rotor speed during an active power imbalance and, therefore, helps to keep the system stable after a disturbance.

The production of electricity through the use of wind energy has undergone significant progress in the last decade, from a technical and economic point of view. Significantly improved aspects such as: the management and maintenance of wind farms, the integration of electric power in the network, the versatility and adaptation of the design of wind turbines to the specific characteristics of the sites, the regulation and control of the same, the prediction of short-term production and economy of scale with higher power wind turbines with an improvement in the unit costs of investment and electricity production [38].

Of the different technologies of electric generators, the Doubly-Fed Induction Generator (DFIG) is the most used for wind energy applications since 2002 [39, 40].

The control system of a doubly-fed wind turbine regulates the rotational speed of the shaft as a function of the existing wind at the site in order to optimally take advantage of the wind power capture of the turbine; therefore, it maintains an active power level at terminals of the electric generator, very independently of the frequency variations in the network produced by some disturbance. There is then a decoupling between the speed of rotation of the wind turbine and the frequency of the network, which means not contribute inertia to the system, which it would naturally a synchronous generator.

With the increase of the level of penetration of variable speed wind turbines in the electrical systems, and assuming that these will displace part of the conventional generation, the equivalent inertia of the network is decreasing, which supposes the deterioration of the stability.

It is therefore necessary to provide variable speed wind turbines with an adequate response to frequency variations taking into account that, in fact, there are abundant inertial resources in their rotors [41]. A control strategy that makes use of the kinetic

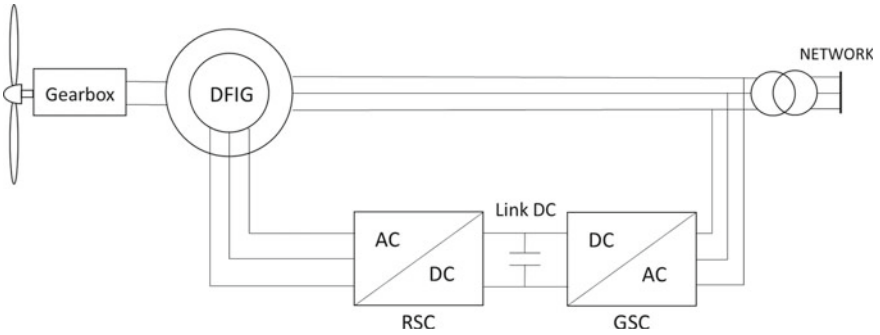

Fig. 5.6 Simple scheme of a DFIG wind turbine

energy stored in the rotating mass of the turbine to provide frequency support to the electrical system is the so-called "virtual inertia".

This wind turbine requires a speed gearbox, to couple the shaft of the wind turbine to the axis of the DFIG electric generator. The generator is asynchronous rotor wound, where the stator is directly connected to the network, while the rotor is connected to it through an electronic power converter (Fig. 5.6).

The operating basic rule of the DFIG is based on injecting in the rotor three-phase currents of variable amplitude and frequency to get to work in different speeds of rotation, while the stator is connected to the constant frequency network (50 or 60 Hz) to dispatch the generated energy.

The use of these electronic converters makes it possible to regulate active and reactive power delivered to the network from the stator, independently of the rotation speed of the rotor axis, which can vary in the order of $\pm 30\%$. It is important to note that the reactive power control provided by the DFIG generator has a lower regulation margin than a synchronous generator. Finally, the power transmitted through the electronic converter corresponds to 25–30% of the nominal power of the machine [38].

There are several strategies for power control for variable speed wind turbines, with vector control being the most widely used [39]. This method provides a decoupled control of active and reactive power by means of the regulation of the quadrature components (d-q) of the rotor current.

In the literature, it is common to find the representation of the rotor current vector referenced to the stator flux (SFRF-Stator Flux Reference Frame) that rotates at the synchronous angular velocity imposed by the network. The major drawback of the SFRF implementation is that the overall performance of the control actions is strongly determined by the accurate detection of the position of the stator flux vector, which can be critical under non-ideal supply voltage conditions. As an alternative modeling and control of DFIG wind turbines, the stator voltage (SVRF-Stator Voltage Reference Frame) is usually used as a reference, which, in contrast to the previous method, allows the stability of the modeled system, independently of the rotor current [39].

According to [42], where, using the stator voltage-oriented control (SVRF), ignoring the stator resistance and assuming the magnetic flux of the stator constant and imposed by the network, the electric torque, the total active power output and the reactive power of the stator can be determined by using the following expressions:

$$T_e = \frac{3pL_m}{2\omega_e L_s} V_s i_{rd} \tag{5.1}$$

$$P_e = \frac{3\omega_r L_m}{2\omega_e L_s} V_s i_{rd} \tag{5.2}$$

$$Q_s = -\frac{3}{2L_s} V_s \left(\frac{V_s}{\omega_e} + L_m i_{rq} \right) \tag{5.3}$$

where p is the number of pole pairs of the DFIG wind turbine, T_e is the electrical torque (N m), P_e is the active power (W), Q_s is the stator output reactive power (VAr), ω_e is the grid synchronous angular speed (rad/s), and ω_r is the rotor angular speed (rad/s), L_m is the mutual inductance (H), L_s is the stator inductance (H), V_s is the stator voltage (V), and I_{rd} and I_{rq} are the rotor current vectors respectively in d-q coordinates (A).

From the above set of equations, the decoupling between the electromagnetic torque/power and the reactive power of the stator is shown, and that its regulation can be carried out by modifying the values of the components in quadrature of the rotor current, d and q, respectively.

Fixed-speed wind turbines, for example, are equipped with squirrel-cage induction generators whose stator is directly connected to the network; therefore, its behavior is equivalent to any conventional electric machine.

Consequently, in the case of a reduction in the frequency of the network, they decelerate at the rate that their inertia constant sets, offering some support for their recovery. On the other hand, it is known that variable-speed wind turbines have electronic converters that allow the speed of the electric generator to be decoupled from the frequency of the network. Thus, a frequency variation does not affect the active power supplied to the network, since this will continue to have a value close to the reference set by the control system, lacking inertial response from the point of view of the electrical system [43].

In other cases, the use of additional schemes that provide regulatory actions complementary to those of speed control systems is proposed, with the aim of modifying the active power generated by a DFIG wind turbine in response to variations in frequency, and achieve a behavior equivalent to that of conventional synchronous generators.

5.8 Definition of Virtual Inertia in a DFIG Wind Turbine

Equation (5.4) expresses the kinetic energy stored in the rotating mass of a synchronous generator, where ω_m is the mechanical angular velocity and J the moment of inertia in the axis.

$$E_c = \frac{1}{2} J \omega_m^2 \tag{5.4}$$

Generally, the inertial constant of a synchronous generator is defined as the quotient between the total energy stored at the nominal speed ω_{mN} and the nominal power P_N (Eq. 5.5).

$$H = \frac{E_c}{P_N} = \frac{J \omega_{mN}^2}{2 P_N} \tag{5.5}$$

In an electrical power system, formed by conventional generation units and wind turbines, the equivalent inertia constant can be determined as in the Eq. (5.6), where E_{GC} and E_{AG} is the kinetic energy stored by the m conventional synchronous generators and by the n wind turbines, respectively. S_N is the nominal capacity of the system.

$$H_{eq} = \frac{\sum_{i=1}^{m} E_{GC,i} + \sum_{j=1}^{n} E_{AG,j}}{S_N} \tag{5.6}$$

Traditionally, in an DFIG wind turbine with MPPT control, it is not possible to take advantage of the kinetic energy stored in its large rotating mass, E_{AG}, so its term is usually zero (Eq. 5.7).

$$\sum_{j=1}^{n} E_{AG,j} = 0 \tag{5.7}$$

This fact implies that the operation of a significant number of DFIG wind turbines instead of conventional generation plants significantly reduces the effective inertia of the power system.

According to Eq. (5.4), when the angular speed of the rotor of a DFIG changes from ω_{r0} to ω_{r1}, the kinetic energy available in the DFIG is given by:

$$\begin{aligned}
\Delta E_{AG} &= \frac{1}{2} J_{AG} \left(\omega_{m1}^2 - \omega_{m0}^2 \right) \\
\Delta E_{AG} &= \frac{1}{2} J_{AG} \frac{\left(\omega_{r1}^2 - \omega_{r0}^2 \right)}{p_{AG}^2} \\
\Delta E_{AG} &= \frac{1}{2} J_{AG} \frac{\left[(\omega_{r0} + \Delta\omega_r)^2 - \omega_{r0}^2 \right]}{p_{AG}^2}
\end{aligned} \tag{5.8}$$

However, if the kinetic energy of this type of wind turbine is expressed as if it were a synchronous generator in which the rotor speed changes from ω_e to ω_{e1}, which has to do with the frequency of the network, we have to:

$$\Delta E_{AG} = \frac{1}{2} J_{vir} \frac{\left(\omega_{e1}^2 - \omega_e^2\right)}{p_{AG}^2}$$
$$\Delta E_{AG} = \frac{1}{2} J_{vir} \frac{\left[(\omega_e + \Delta\omega_e)^2 - \omega_e^2\right]}{p_{AG}^2} \tag{5.9}$$

In Eqs. (5.8) and (5.9), p_{AG} is the number of pole pairs of the DFIG generator, $\Delta\omega_r = \omega_{r1} - \omega_{r0}$, $\Delta\omega_e = \omega_{e1} - \omega_e$, J_{AG} is the natural inertia of the wind turbine, and J_{vir} its virtual inertia. Note that the term "virtual inertia" has been written based on the fact that it is a parameter that allows to relate the accumulated kinetic energy with the change in speed, as if it were a synchronous generator; therefore, it is fictitious from the physical point of view, but could be exploited in the wind turbine operation.

By matching Eqs. (5.8) and (5.9), the virtual inertia of the DFIG can be defined as:

$$J_{vir} = \frac{(2\omega_{r0} + \Delta\omega_r)\Delta\omega_r}{(2\omega_e + \Delta\omega_e)\Delta\omega_e} J_{AG} \tag{5.10}$$

In this analysis, small perturbations are assumed; therefore, considering that typically: $2\omega_{r0} \ll \Delta\omega_r$ and $2\omega_e \ll \Delta\omega_e$, it is possible to obtain Eq. (5.11). In these equations, the ratio $\Delta\omega_r \big/ \Delta\omega_e$ is defined as the virtual inertial coefficient, λ_{vir}.

$$J_{vir} \approx \frac{\omega_{r0}\Delta\omega_r}{\omega_e\Delta\omega_e} J_{AG}$$
$$J_{vir} \approx \lambda_{vir} \frac{\omega_{r0}}{\omega_e} J_{AG} \tag{5.11}$$

From this last expression, it can be seen that the virtual inertia of an DFIG is not only determined by its natural inertia, but also by the rotor speed before the disturbance, ω_{r0}, and the virtual inertial coefficient, λ_{vir}. Unlike synchronous generators, in which the rotational speed of the rotor is rigidly coupled to the frequency of the network, ω_e, the rotor speed variation of the DFIG can be much larger than the frequency variation of the system, normally due to its asynchronous and decoupled operation. Then, the virtual inertia of DFIG can be several times its natural inertia, which according to [42], its value is usually between 6 and 8.

By means of Eq. (5.5), it is possible to define the inertial constant of a doubly fed wind turbine:

$$H_{vir} = \frac{J_{vir}\omega_e^2}{2p_{AG}^2 P_{AG}} \tag{5.12}$$

where P_{AG} is the nominal power of the DFIG. Under this concept, it is possible to take advantage of the kinetic energy stored in the turbine-generator set of the DIFG to contribute with the equivalent inertia of the electrical system. Therefore, it has to be $\sum_{j=1}^{n} E_{AG,j} > 0$.

Although the virtual inertia constant of a DFIG is much higher than the typical values of conventional synchronous generators, it must be taken into account that it corresponds to an instantaneous value, that is, of a transient nature and of relatively short duration. Tests carried out in [44] show that a wind turbine is capable of maintaining an active power increase in its output, making use of its stored kinetic energy, for a time of 20–140 s, depending on factors such as: incident wind speed, speed of rotation of the turbine and the level of load variation required.

5.9 Virtual Inertia Control in a DFIG Wind Turbine

One possible way for the virtual inertia control (VIC) has been proposed by [42, 45] and consists of acting on the reference active power of a DFIG wind turbine before frequency deviations in the electrical system, acting directly on the implemented MPPT characteristic.

One way to regulate the active reference power as a function of frequency deviations is to replace the optimization constant of the MPPT curve, K_{opt}, by the virtual inertia constant, k_{VIC}, which is sensitive to changes in the frequency of the system, Δf. A different value of k_{VIC} will generate a series of maximum power tracking curves, which will be called VIC curves (Fig. 5.7).

To ensure stable operating points under any wind speed regime, an upper and lower limit is assigned to the VIC curves, defined as MPPT_{max} and MPPT_{min}, respectively [42]. In Fig. 5.7, these limits are the green curve and the black curve, respectively.

Referring to Fig. 5.7, when the wind speed is 9.6 m/s and remains at this value, the DFIG operates at point A, under the MPPT control.

During an increment of the demand in the system, the frequency of the network drops. The control system of the DFIG must change its operating characteristic, passing from the MPPT curve to MPPT_{max} (green curve) for example, and place its operating point in O immediately. As a consequence, the rotor decelerates and the kinetic energy stored in the rotating mass is released to support the restoration of the frequency of the network. During this process, the operating point moves from O to B along the MPPT_{max} characteristic (green curve). Once the frequency deviation disappears, it is necessary that the wind turbine returns to its optimum operating point. Therefore, a transition from MPPT_{max} to MPPT will occur to place it again at point A (from B).

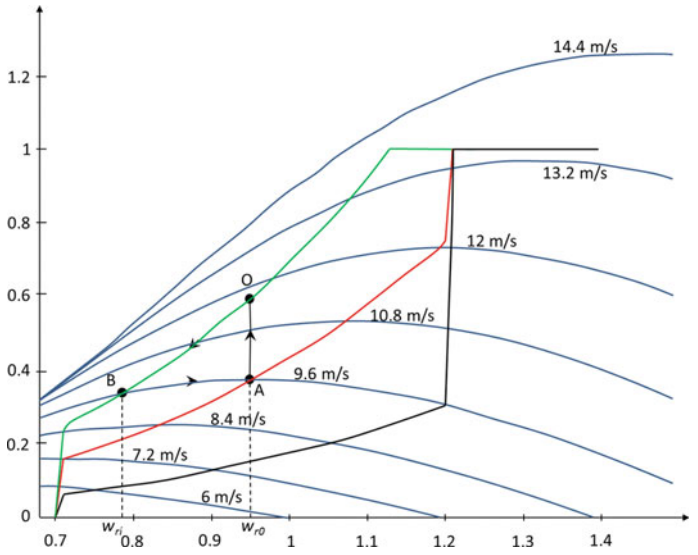

Fig. 5.7 Virtual inertia control based on MPPT characteristics

5.10 Conclusions

The way of consuming energy by citizens and companies is changing. Also, on the one hand, the need to reduce energy transport and distribution losses, and on the other hand, the ecological need to reduce pollution, are making the energy generation centers and consumption centers closer together. The generation of energy is increasingly based on renewable energies, and technology plays a vital role in the management of the energy system, particularly in the electrical system.

In this new framework, Virtual Power Plants have an important role. Virtual Power Plants are the next step of the electrical system towards an intelligent electrical network, very related to the concept of Smart Grids and Intelligent Networks. We can define a Virtual Power Plant as the set of small power generation systems and storage systems connected telematically in a secure way to be managed remotely and in real time by a system operator. Their way of implementation can be different, depending of several factors, but undoubtedly they can be carried out anywhere with the benefit of the users, managers, and system in general. Moreover, to date, there are several projects on VPP and it is expected that their capacity and implementation in the near future of 10 years can be multiplied by 10.

Related to the peak of the energy generation through renewable sources in the last years, and specially related to the wind generation, the concept of virtual inertia has arisen into the electrical system. Due to the importance of the frequency in any electric system, and the role of the inertia of synchronous machines in the stability of the power system, we can help to keep the system stable after a disturbance if

we take into account the virtual inertia. Doubly-Fed Induction Generator (DFIG) is the most used for wind energy applications since 2002, so the control system of a doubly-fed wind turbine regulates the rotational speed of the shaft as a function of the existing wind at the site in order to optimally take advantage of the wind power capture of the turbine. In this way, it maintains an active power level at terminals of the electric generator, very independently of the frequency variations in the network produced by some disturbance.

References

1. J. Bilbao, E. Bravo, O. Garcia, C. Varela, M. Rodriguez, P. Gonzalez, The next future of solar energy generation. Int. J. Tech. Phys. Probl. Eng. (IJTPE) Issue 12, **4**(3), 162–166 (2012)
2. J. Bilbao, E. Bravo, O. Garcia, C. Varela, M. Rodriguez, P. Gonzalez, Some keys for obtaining a secure and solid energy supply in Europe. Int. J. Tech. Phys. Probl. Eng. (IJTPE) Issue 20, **6**(3), 153–157 (2014)
3. European Commission, Renewable energy: moving towards a low carbon economy (2018). https://ec.europa.eu/energy/en/topics/renewable-energy
4. The Paris Agreement. United Nations (2018). https://unfccc.int/process-and-meetings/the-paris-agreement/the-paris-agreement
5. Net Electric from Spain (2018). https://www.ree.es/en
6. S.M. Nosratabadi, R.A. Hooshmand, E. Gholipour, A comprehensive review on microgrid and virtual power plant concepts employed for distributed energy resources scheduling in power systems. Renew. Sustain. Energy Rev. **67**, 341–363 (2017)
7. D. Pudjianto, C. Ramsay, G. Strbac, Virtual power plant and system integration of distributed energy resources. IET Renew. Power Gener. **1**(1), 10–16 (2007)
8. Pike Research Institute, Executive summary: virtual power plants. Retrieved from Smart Grid Platforms for Aggregating Distributed Renewables, Demand Response and Energy Storage Technologies (2001). http://www.pikeresearch.com
9. H. Saboori, M. Mohammadi, R. Taghe, Virtual power plant (VPP), definition, concept, components and types, in *Power and Energy Engineering Conference (APPEEC)*, Asia-Pacific (2011)
10. Siemens, Virtual power plants by Siemens, DEMS-Decentralized Energy Management System (2013)
11. T.H. Jin, H. Park, M. Chung, K.Y. Shin, A. Foley, L. Cipcigan, Review of virtual power plant applications for power system management and vehicle-to-grid market development. Trans Korean Inst. Electr. Eng. **65**(12), 2251 (2016)
12. K. Mussenbrock, Virtual power plant, Altran instrument for dealing with flexibilities in energy markets. European Utility Week, Amsterdam (2014-11-05)
13. C. Webb, Virtual power plants: making the most of distributed generation (01 Aug 2010). http://www.powerengineeringint.com/articles/print/volume-18/issue-7/features/virtual-power-plants-making-the-most-of-distributed-generation.html
14. M. LaMonica, Virtual power plants fill supply gaps in heat wave (13 July 2010). http://news.cnet.com/8301-11128_3-20010317-54.html
15. N. Ruiz, I. Cobelo, J. Oyarzabal, A direct load control model for virtual power plant management. IEEE Trans. Power Syst. **24**(2) (2009)
16. EnerNoc Annual Report 2011. USA, 2011. http://www.annualreports.com/HostedData/AnnualReportArchive/E/NASDAQ_ENOC_2011.pdf
17. S. You, C. Træholt, B. Poulsen, A market-based virtual power plant, in *ICCEP* (2009)
18. J. Kumagai, Virtual power plants. Real power, in *IEEE Spectrum* (Mar 2012)

19. E. Mashhour, S.M. Moghaddas Tafreshi, Bidding strategy of virtual power plant for participating in energy and spinning reserve markets—Part I: problem formulation. IEEE Trans. Power Syst. **26**(2) (2011)
20. E. Mashhour, S.M. Moghaddas Tafreshi, Bidding strategy of virtual power plant for participating in energy and spinning reserve markets—Part II: numerical analysis. IEEE Trans. Power Syst. **26**(2) (2011)
21. R. Madrigal, Overview of reliability demand response resource. California ISO (CAISO), Customer Service Department (May 2014). http://www.caiso.com/Documents/ReliabilityDemandResponseResourceOverview.pdf
22. Energynautics, Bundling decentralized power generation. Retrieved from "Virtual Power Plants" as an Innovative Organizing Principle, http://www.energynautics.com/our_expertise/research/virtual_power_plants/ (n.d.)
23. N. Mahmoudi, T.K. Saha, M. Eghba, Wind offering strategy in the Australian National Electricity Market: a two-step plan considering demand response. Electr. Power Syst. Res. **119**, 187–198 (2015)
24. World Energy Council, Energy for Germany. Facts, outlook and opinions in a global context. Weltenergierat – Deutschland e.V. (2011)
25. European Commission, Virtual power plant at RWE. e-Business Watch report, Germany (2009)
26. P. Duvoor, Virtual power plants in competitive wholesale electricity markets—experience with RWE virtual power plant in Germany. Siemens Smart Grid Division (2012)
27. J.M. Corera, Integrated Project FENIX—what is it all about? FENIX Bulletin 1 (Nov 2007)
28. C. Ramsay, The Virtual Power Plant: enabling integration of distributed generation and demand. FENIX Bulletin 2 (Jan 2008)
29. Electric Power Research Institute, Estimating the costs and benefits of the smart grid (2011). http://ipu.msu.edu/programs/MIGrid2011/presentations/pdfs/Reference%20Material%20-%20Estimating%20the%20Costs%20and%20Benefits%20of%20the%20Smart%20 Grid.pdf
30. C. Ross, Virtual power plants systems of the future (July 2011). http://www.ecmag.com/?fa=article&articleID=12876
31. S. Lacey, Virtual power plants aren't just virtual—they're real (25 Mar 2011), http://www.renewableenergyworld.com/rea/news/podcast/2011/03/virtual-power-plants-arent-just-virtual-theyre-real
32. U. Gerder, Technical summary of the combined power plant. Renewable Energy Campaign Germany (2007). http://www.kombikraftwerk.de/fileadmin/downloads/Technik_Kombikraftwerk_EN.pdf
33. Kombikraftwerk 2. Final report (Aug 2014). http://www.kombikraftwerk.de/fileadmin/ Kombikraftwerk_2/English/Kombikraftwerk2_FinalReport.pdf
34. PV Magazine, August 2018 www.pv-magazine.com
35. L. Yan, China's first virtual power plant put into operation. People's Daily Online (25 May 2017). http://en.people.cn/n3/2017/0525/c90000-9220528.html
36. South Australia's Virtual Power Plant. Government of South Australia (2018). https://virtualpowerplant.sa.gov.au/virtual-power-plant
37. J. Morren, J. Pierik, S.W.H. de Haan, Inertial response of variable speed wind turbines. Electr. Power Syst. Res. **76**(11), 980–987 (2006)
38. M. Villarrubia, in *Wind Energy Engineering* (MARCOMBO, S.A., 2012)
39. M. Mohseni, S. Islam, A space vector-based current controller for doubly fed induction generators, in *35th Annual Conference of IEEE*, Porto, Portugal (2009), pp. 3868–3873
40. M. Liserre, R. Cardenas, M. Molinas, J. Rodriguez, Overview of multi-MW wind turbines and wind parks. IEEE Trans. Industr. Electron. **58**(4), 1081–1095 (2011)
41. J. Ekanayake, L. Holdsworth, N. Jenkins, Control of DFIG wind turbines. Power Eng. **17**(1), 28–32 (2003)
42. X. Zhu, Y. Wang, L. Xu, X. Zhang, H. Li, Virtual inertia control of DFIG-based wind turbines for dynamic grid frequency support, in *Conference on IET. Renewable Power Generation* (2011), pp. 1–6

43. C.M. Deepak, A. Vijayakumari, S.R. Mohanrajan, Virtual inertia control for transient active power support from DFIG based wind electric system, in *The 2nd IEEE International Conference On Recent Trends in Electronics Information & Communication Technology (RTEICT)*, India, May 19–20 (2017)
44. N. Aparicio, New strategies for the contribution of wind farms to the frequency control of electrical systems. Doctoral thesis, Polytechnic University of Valencia (2011)
45. Z. Zhang, Y. Wang, H. Li, X. Su, Comparison of inertia control methods for DFIG based wind turbines, in *IEEE ECCE Asia Downunder (ECCE Asia)* (2013), pp. 960–964

Chapter 6
Power Electronic Converters in DC Microgrid

Ires Iskender and Naci Genc

Abstract There are not many sustainable sources of energy other than renewable energy sources (RES), which are called solar, wind, water and various forms of biomass. The most effective way to increase the use of renewable energy sources is to make use of renewable energy systems in villages, townships or small island-shaped districts where there are significant amounts of energy consumers. For this reason, the microgrid (MG) idea of small power system which is controllable, autonomous and balanced has been developed. Microgrids (MGs) playing a role of carrier for distributed generation resources (DGR), includes different distributed generation (DG) units, storage devices, energy converters, protection devices and load control devices. A MG generally includes renewable small power sources consisting of interconnected distributed energy sources with capacity of providing sufficient and sustained energy for a significant portion of the load. Different architecture types of MGs are presented in the literature. In recent years, the use of MGs being able to operate in two different modes depending on the island and grid-connected, has been expanded for DGR integration. Direct current (DC) microgrid has become an important subject of study in recent years as they have a more reliable and lower losses. A DC MG task distributes the DC power required by loads on a campus. Power generation in DC MG systems can be AC or DC; however, in most cases AC power supplies is converted to DC for distribution. The major advantage of DC microgrids when compared to AC systems is its property of unidirectional power flow. This allows power control to be easily controlled by the power flow direction. In DC MG, the loads must be controllable to keep all loads at the DC range of the voltage in the default range and to regulate the voltage regulation. Besides voltage level and voltage regulation, the voltage ripple ratio should be kept as low as possible in DC microgrids. Therefore, power electronic converters are the most important part of the DC MG systems. There are although many studies published on MGs that control

I. Iskender
Department of Electrical and Electronics Engineering, Cankaya University, Ankara, Turkey
e-mail: ires@cankaya.edu.tr

N. Genc (✉)
Department of Electrical and Electronics Engineering, Van Yuzuncu Yil University, Van, Turkey
e-mail: nacigenc@yyu.edu.tr

N. Mahdavi Tabatabaei et al. (eds.), *Microgrid Architectures, Control and Protection Methods*, Power Systems,
https://doi.org/10.1007/978-3-030-23723-3_6

strategy and power electronic circuits make their important portions. It is obvious that the development of power electronic circuits and control methods has further enhanced the applicability of microgrids. In this study, the types, circuit structures and functions of power electronic converters used in DC microgrid are discussed. Power electronics converters used in DC MGs are grouped and evaluated according to their targets. These power electronic converters have been detailed in terms of AC-DC rectifiers, inverters (for AC loads) and DC-DC converter circuit types. The simulation results of some topologies have been evaluated.

Keywords Microgrid · DC microgrid · Power electronic converters

6.1 Introduction

Considering the changes happening in today's electricity distribution network structure the resources with high quality and continuous power are of great importance for the customers. Due to the limited number of fossil energy sources and related regulations, energy prices are increasing steadily day by day and this increases the importance of the efficiency of the electricity distribution. Parallel to this the use of renewable energy sources (RES) in distributed generation (DG) systems is also increasing. There are not many sustainable sources of energy other than renewable energy sources, which are called solar, wind, water and various forms of biomass. The most effective way to increase the use of renewable energy sources is to make use of renewable energy systems in villages, townships or small island-shaped districts where there are significant amounts of energy consumers. The real question is how to feed these consumers with electricity from renewable energy systems. For this reason, the microgrid (MG) idea of small power system which is controllable, autonomous and balanced has been developed.

A microgrid defined as a combined set of source, load and energy storage devices that exhibit differing behavior, is a power grid composed of different types of Distributed Energy Sources (DER) controlled by the micro-power control center. MGs, which are basically alternating current microgrid (ACMG) and direct current microgrid (DCMG), provide the opportunity to use renewable energy sources for green and clean environment. Furthermore, since the Distributed Energy Sources (DER) forming the microgrids are located near the load, the power transmission losses are lower [1, 2]. A MG which is generally include renewable small power sources consists of interconnected distributed energy sources that can provide sufficient and sustained energy for a significant portion of the load. Different architecture types of MGs are presented in the literature. In recent years, the use of MGs, which can operate in two different modes depending on the island and grid-connected, has been expanded for DGR integration.

Microgrids, which are capable of operating either grid-connected or autonomous generally use three-phase AC power transmission lines [3]. However, in recent years, DC high voltage direct current (HVDC) technology, which has high power density

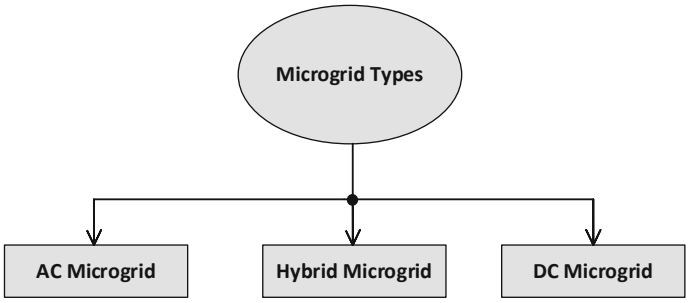

Fig. 6.1 Microgrid configuration diagram according to power structure

and ease of control, has become popular for power transmission [4, 5]. Microgrids can be also classified into three categories as utility microgrids, industrial/commercial microgrids and distant microgrids as part of the architectural application areas. However, there are different microgrid structures for different types customer requirements due to improvements in power electronics and FACTS systems. Different type of classification for microgrid can be made according to the power structure of the microgrid. This classification is carried out as AC microgrids, DC microgrids and hybrid (DC and AC connected) microgrids as given in Fig. 6.1 [6].

In AC microgrid systems, generation systems and loads are connected to an AC bus via power electronics converters according to the type of electrical energy they generate or consume (Fig. 6.2). Storage systems are also connected using AC bus, such as DC loads, that can be adapted to their electrical energy form. The AC bus connects to the power grid from a single point. AC microgrids can be classified considering the operating voltage (high frequency AC (HFAC), line frequency AC (LFAC) microgrids) and phase number of system (single or three phase). There are many studies about the line frequency AC (LFAC) microgrid type used in low voltage. In the structure of AC microgrids containing DC sources such as photovoltaic systems and fuel cells, the overall efficiency of the system is low because of the use of the inverter to connect to the AC bus [7]. In addition, the total cost increases as the number of inverters or inverter power increases in the system [8].

Hybrid microgrid systems consist of a combination of AC microgrid and DC microgrid as shown in Fig. 6.3. In addition, there are power electronics circuits between AC bus and DC bus providing suitable conversion to electrical energy form. In this system, both AC and DC microgrids contain different power systems, storage systems and loads depending on the type of electrical energy they produce or consume. Hybrid microgrids containing all the characteristics of AC and DC microgrids include the advantages and disadvantages of both systems.

It is seen from the above figures; the power electronic converters are the most important part of the microgrid systems. Therefore, the development of power electronic circuits and control methods has further enhanced the applicability of microgrids.

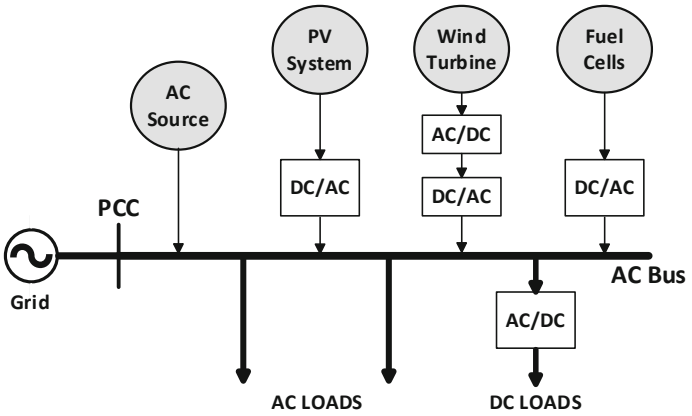

Fig. 6.2 AC microgrid configuration diagram

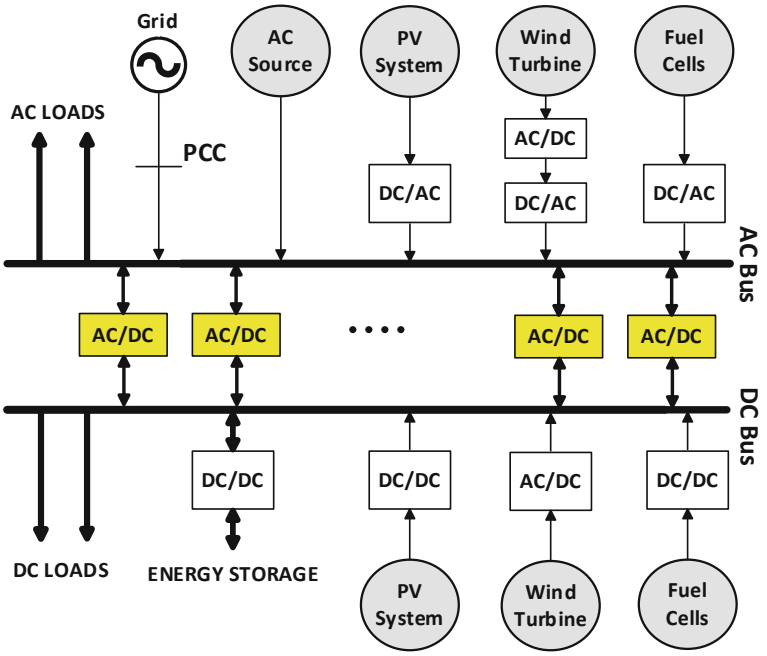

Fig. 6.3 Hybrid microgrid configuration diagram

The circuit structures and power electronic converters used in DC microgrid are the main objectives of this study. In the study, after introducing section, DC microgrid system is introduced in Sect. 6.2. The circuit structures and power electronic converters used in DC microgrid are discussed, grouped and evaluated according to their targets in Sect. 6.3. The conclusion section is given finally.

6.2 DC Microgrid System

The rapid growth of the use of renewable systems such as photovoltaics and fuel cells in recent years and the intensive use of electronic loads have increased the popularity of low voltage DC (LVDC) microgrids. In industrial applications, DC distributed power systems are widely used in telecommunication systems, electric vehicles and ship power systems [9–11]. In addition, there are many studies [12–14] that investigated the operation and control of DC microgrids, including transitions between system voltage controls, different operating scenarios, and DC microgravity protection schemes [15]. A DC Microgrid, containing AC or DC production sources, distributes DC power to a building or campus to supply loads. Power generation in DC MG systems can be AC or DC; however, in most cases AC power supplies is converted to DC for distribution. The major advantage of DC microgrids when compared to AC systems is that the flow direction is unidirectional. This allows power flow to be easily controlled by controlling the power electronics converter included in the system. The power flow is closely related to current and voltage direction. Hence, power control can be based only on current flow. Therefore, DC microgrid has become an important subject of study in recent years as they have a more reliable and lower losses. In most cases, two distribution systems are used in homes and this is due to the fact that the AC distribution line is still used due to the need for plug load. Since there is no common standard for DC lines, there are not many products that use DC plugs as a standard power supply. For this reason, the DC microgrids use a single point of contact with the external service network.

DC microgrid systems, as in AC microgrid systems, are the system in which different production systems, storage systems and loads are connected to a DC bus by means of power electronics converters according to the type of electrical energy they produce or consume (Fig. 6.4). Inverters used in DC microgrids provide sufficient power quality conditions for AC loads. DC microgrids requiring fewer inverters than AC microgrids, increase the efficiency of the system as they will have less conversion losses [16, 17]. In addition, DC microgrids provide ease of control as there is no need for voltage and frequency synchronization [18]. The use of power electronics circuits in DC microgrids enables the ability to use stored energy and even bus capacity to relieve system transitions [19].

The components of a grid-connected DC microgrid are renewable energy systems (PV, wind, fuel cell), load and storage elements. In this system, production units are renewable DERs such as PV, wind and fuel cell. When using a DC-DC circuit to connect PV and fuel cell to DC bus, the wind generator is connected with an AC-DC

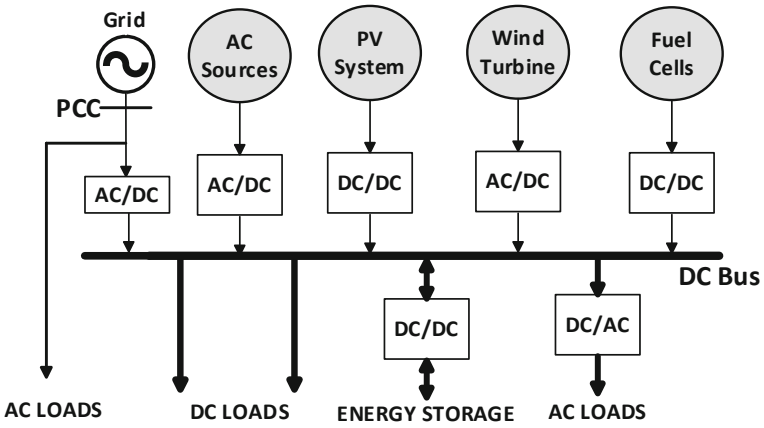

Fig. 6.4 The structure of DC microgrid

converter. These sources usually operate in maximum power point tracking (MPPT) mode to obtain maximum power from the systems. The battery used for energy storage (lead acid, li-ion) is connected to the DC bus using a bi-directional converter. In grid-connected mode, the battery is charged if the requested energy is less than the generated energy. In the absence of mains or in isolated mode, the energy required by the load is supplied by the battery. The DC loads used in the DC microgrid systems are connected to the DC bus via DC-DC converters to operate at the voltage corresponding to the structure. The grid and AC sources are connected to the DC bus via the AC-DC converter, and DC microgrid is supplied from the grid and AC sources as needed. In case of mains connection, transformer and circuit breaker are generally used between the mains and the converter.

A DC microgrid operates in three different modes; uncontrolled grid-connected, controlled grid-connected and isolated mode. In an uncontrolled network-connected mode which is balanced by an AC grid, the battery is charged in more power than the demand. The AC-DC converter connected to the grid regulates the voltage at the DC microgrid. In a controlled grid-connected mode, the converter connected between the DC bus and the grid is not involved in controlling the DC link voltage. This means that the DC link voltage is not regulated by the mains converter. In this case, the battery switches from charge mode to discharge mode to regulate the DC bus voltages. In isolated mode, the AC grid is disconnected and the power required for loads is met by the DERs and the battery. In particular, if less power is supplied by renewable energy sources, the battery switches to discharge mode and regulates the DC bus voltage. If more power is supplied by renewable energy sources, the battery switches to charge mode to regulate DC bus voltage [2].

The summary targets of a DC microgrid can be listed as summary of increasing the use of distributed renewable energy units, to reduce the power plant cost by means of a DC bus that connects distributed renewable source units and storage units by using power electronics converters and to power loads for emergencies. Since renew-

able energy source units are distributed in demand area and power supplies/loads are close to each other, long transmission lines are not required for DC microgrid systems. In the case of DC microgrids, the power demand balance of the loads is an important variable. The compensation system, consisting of storage batteries and a bi-directional power converter, provides a good power balance in the system by absorbing short-term power fluctuations. Consequently, it can be said that a DC microgrid reduces the cost for the stabilization of commercial grids. In addition, a DC microgrid is resistant to harsh climatic conditions. We can have electrical power supplies even when there is no external power supply or sources. A DC microgrid can operate as an independent power supply during the AC mains power failure [20].

Since there are different levels of DC voltage output in renewable energy sources and energy storage systems, power electronic converters are needed to integrate all DERs within the microgrid. Thanks to the development of power electronics technology, it was the preferred solution to integrate these renewable energies into the DC microgrid [1]. In DC microgrids, the sources and loads must be controllable to keep all loads at the DC range of the voltage in the default range and to regulate the voltage regulation. Besides voltage level and voltage regulation, the voltage ripple ratio should be kept as low as possible in DC microgrids. As mentioned before; the power electronic topologies are the main important part of the microgrid systems. It is obvious that the development of power electronic circuits and control methods has further enhanced the applicability of DC microgrids.

6.3 Power Electronic Topologies Used in DC Microgrid System

As mentioned above, DC microgrid systems require AC-DC, DC-DC and DC-AC power electronics converters for both DC bus and loads. The main goal of the microgrids is to feed all consumers with high quality power. This means a constant voltage level in DC microgrids over time. Therefore, all sources and loads require connection via controllable converters. As a result of the development of power electronics, DC microgrids can be operated easily and DC microgrid can be operated effectively. Since the power electronics circuits used in DC microgrids are of high importance, power electronics circuits used in DC microgrids are presented in below sub sections according to their application areas.

6.3.1 AC/DC Converters (Rectifiers)

The grid-connected DC microgrids are required AC-DC power electronics circuits between the grid and the DC bus. If the grid supplying the DC bus is single-phase, the single-phase diode or single-phase thyristor rectifier circuits shown in Fig. 6.5

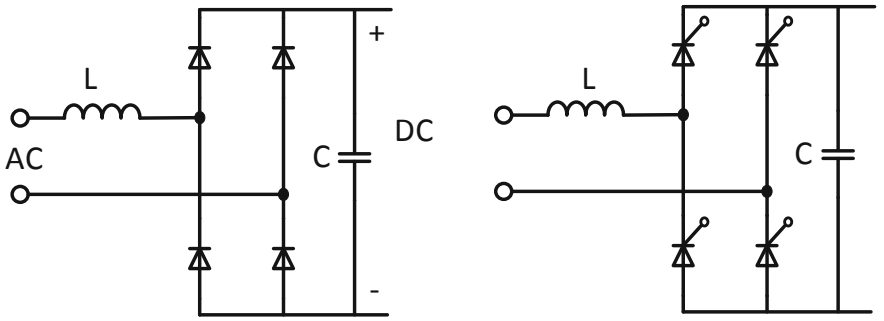

Fig. 6.5 Single-phase diode and single-phase thyristor AC-DC rectifiers

are used. If the grid supplying the DC bus is three-phase, three-phase diode or three-phase thyristor rectifier circuits are used (Fig. 6.6). In the case of a three-phase grid connection, the DC bus can be provided by one-line or two-line AC-DC converter topologies. The 12-pulse half-controlled circuit presented in Fig. 6.6a is the simplest AC-DC topology available in LVDC systems. The DC bus starting current can be limited by the delay angle of the thyristors. With these circuits only one-way power flow is possible. To reduce the output DC voltage ripple ratio by creating a 30° phase shift between the secondary windings, the AC-DC circuit secondary windings are supplied by a three-phase transformer connected to the star and delta.

Two-level and three-level AC-DC line converters (Fig. 6.6b, c) provide bidirectional power flow to DC microgrid. The Vienna AC-DC converter in Fig. 6.6d provides unidirectional power flow. The neutral conductor of this circuit can be connected to the star point of the supply transformer.

It is seen that AC/DC conversion of electric power is widely used in DC microgrid systems. AC-DC conversion use rectifier type of power electronics topologies and these converters have nonlinear characteristics within their architecture. The input stage of these AC-DC power converters consists of a bridge rectifier followed by a large filter capacitor. Pulses of current drawn from the AC grid via these devices as given in Fig. 6.7.

Current is drawn from the line only when the line peak voltage exceeds the voltage on the filter capacitor and this causes the line current to be discontinuous. This produced periodic and discontinuous current includes single harmonic components other than the basic component. These harmonics cause problems for power distribution systems. And also these harmonic components cause additional losses in capacitors and cables, cause dielectric stresses, and cause electromagnetic interference (EMI) [21–24].

Assuming that the input voltage source produces an ideal sinusoidal, the power factor (*pf*) and Total Harmonic Distortion (*THD*) of a power electronics converter is obtained from Eqs. (6.1) and (6.2).

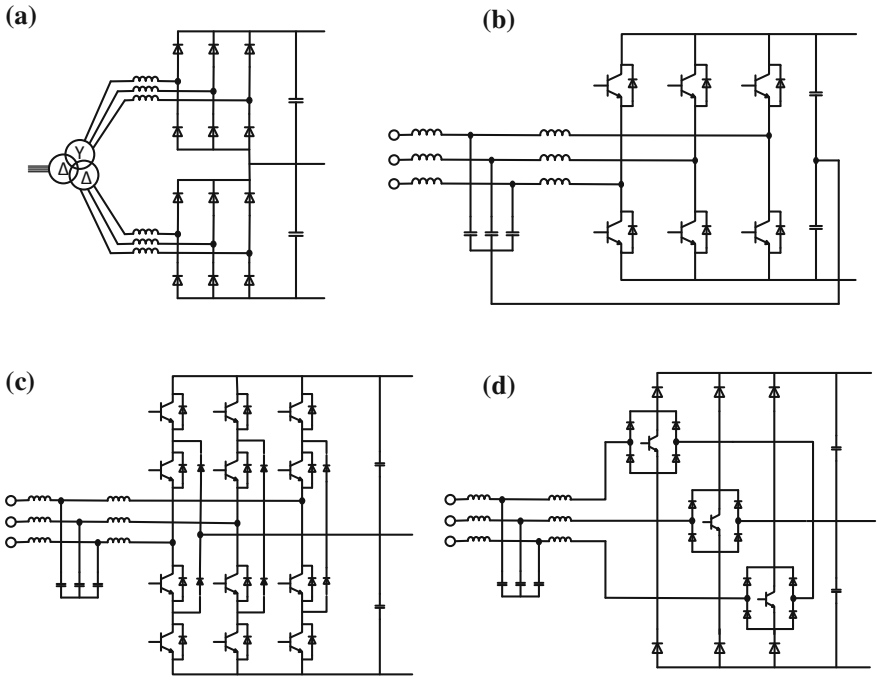

Fig. 6.6 Three-phase AC-DC topologies: **a** 12 pulse half-controlled, **b** two-level line, **c** three-level line, **d** Vienna rectifier

$$I_{rms} = \sqrt{\sum_{n=0}^{\infty} I_{nrms}^2} \tag{6.1}$$

$$THD(\%) = 100\sqrt{\frac{I_{rms}^2 - I_{1rms}^2}{I_{1rms}^2}} = 100\sqrt{\frac{I_h^2}{I_{1rms}^2}} = 100\sqrt{\frac{1}{k_d^2} - 1} \tag{6.2}$$

If the input current is in phase with the voltage ($\cos\theta = 1$), k_θ (displacement factor) will be 1 and therefore the current *THD* value can be given with Eq. (6.3).

$$THD(\%) = 100\sqrt{\frac{1 - pf^2}{pf^2}} \tag{6.3}$$

From Eq. (6.3), it is seen that there is an inverse relationship between *pf* and the current *THD* values. For example, for given *pf* values of 0.995 and 0.95 the corresponding *THD* values are 10 and 32.9% respectively. Though in some applications the *pf* of a converter may be acceptable and higher than a specified value, the *THD* of the corresponding converter may be far from the expected value.

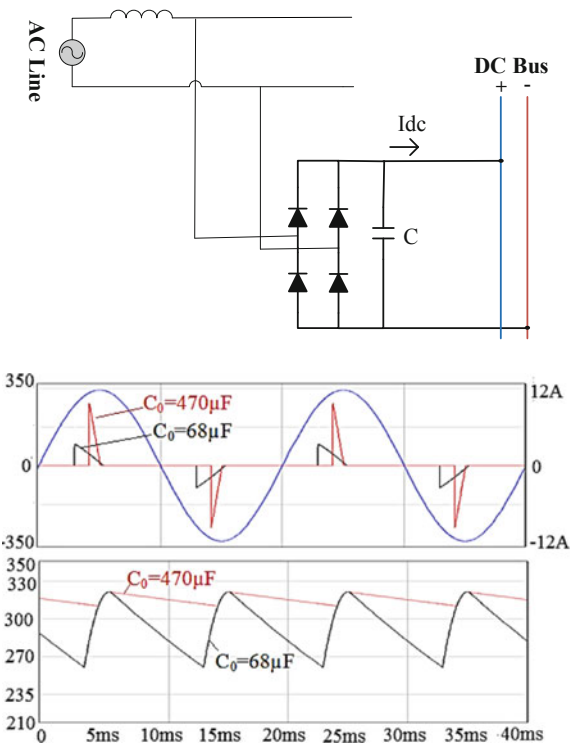

Fig. 6.7 Single-phase rectifier (nonlinear loads) and related waveforms

Thus, the determination of limits for each harmonic component under national or international standards will help to eliminate the contamination of the current content to be drawn into the power system. The process of shaping the input current of the device to be drawn from the power system is called power factor correction. This power factor correction process is the regulation of the harmonic content of the input current drawn by devices under national or international standards. Conventional AC rectification results in the deterioration in the input current waveform drawn from the grid and causes low efficiency. In addition, this process also affects the other users fed from the same grid, causing low power quality with high harmonic current draws. In addition, the utility line cabling, the distribution transformers are affected from these harmonic current values and these harmonic currents resulting in higher electricity costs. Thus, creating harmonics, causing poor power factor, resulting in high losses and reducing the maximum power capability are the main disadvantages of conventional AC rectification [25].

Because many DC-powered electrical loads require low-voltage output voltages, the high-value output capacitor is used before the load. This causes AC/DC converters to draw non-sinusoidal currents from the grid. The AC/DC rectifier diodes have short transmission intervals and the line current consists of pulses with a significant harmonic content. It is necessary to correct the non-sinusoidal currents of these

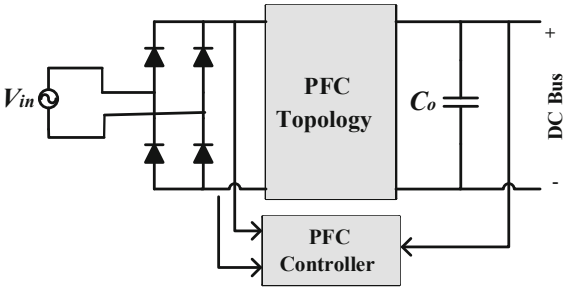

Fig. 6.8 Block diagram of active PFC circuit

rectifiers and to reduce the line current harmonics to comply with the standards. Numerous power factor correction studies are available to correct current harmonics from non-linear loads. Different PFC solution methods are available depending on the content of active semi-conductor switches. These studies available in the literature can be categorized as passive PFC or active PFC methods. In passive PFC method, only passive circuit elements are used in addition to the bridge diode rectifier circuit to correct the shape of the line current drawn from the grid. In this method the output voltage cannot be controlled. In the active PFC method, the active switches correct the line current drawn from the mains and provide a controllable output voltage. The switching frequency of active PFC is considerably higher than the line frequency.

The high frequency active PFC circuit can be realized by using a diode bridge and a DC/DC converter which has a switching frequency much higher than the line frequency. The DC/DC converter operation which has a suitable control method can shape the input current (Fig. 6.8). For all converter topologies, the output voltage ripple is twice the line-frequency and the output DC is usually regulated.

The output voltage of PFC applied non-linear loads may be higher or lower depending on the DC/DC converter structure used. The output voltage is lower when by a buck type AC/DC PFC circuit is applied, while, the output voltage is higher by a boost type AC/DC PFC circuit is applied. However, for DC microgrid systems boost type DC-DC circuits (Fig. 6.9) are used as a PFC circuit which is connected to single-phase or three-phase rectifiers is used to obtain the DC bus voltage level. Therefore, the boost type topologies are the most popular configurations for DC microgrids and PFC applications. Since the conventional boost PFC circuit includes only one switch, this switch can carry the load current and this makes this topology unsuitable at higher power values. Therefore, improved boost type PFC circuits (Fig. 6.9) have been proposed in the literature to meet the requirements of applications and to regulate the power factor at input AC mains and lower value of *THD* with regulated output DC voltage which has lower ripple. The unidirectional boost type configurations which are include diodes have the power flow in one direction. Some other boost topologies include IGBT or MOSFET switches and they eliminate diodes. Interleaved type boost topologies are also introduced in Fig. 6.9. These circuits are used to increase the rated power value of conventional boost converters and to reduce the higher frequency which is a significant advantage of the boost

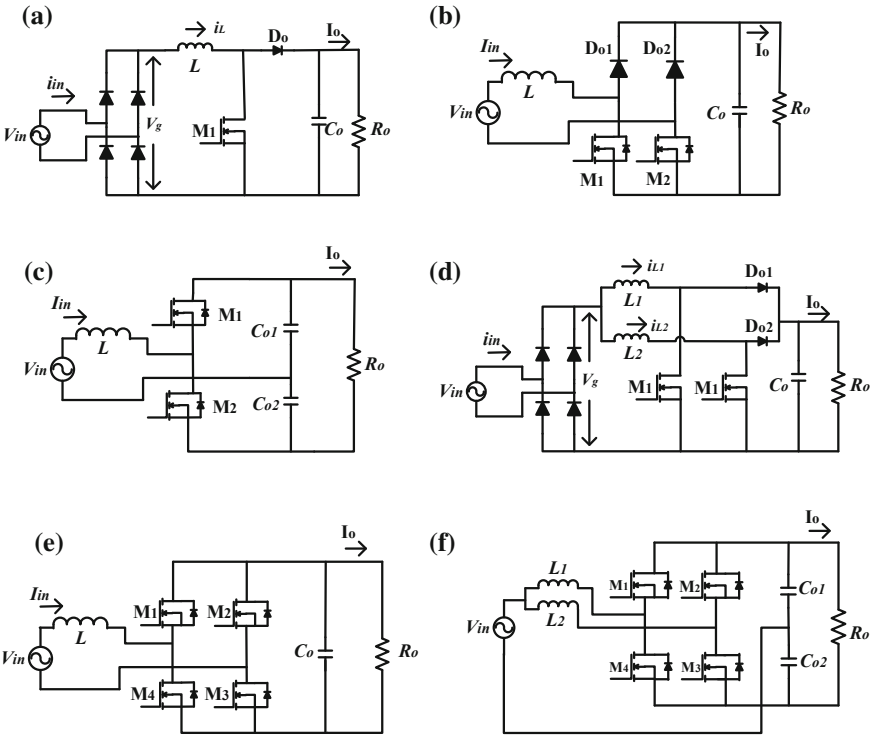

Fig. 6.9 Boost type PFC circuits; **a** single-switch boost, **b** bridgeless, **c** half-bridge, **d** interleaved boost, **e** full-bridge, **f** interleaved full-bridge

type topology ripple ratio of the input current, However, the use of more controllable switches causes the cost to increase and the control circuit becomes more complex than the conventional type boost circuit.

The control strategy of PFC converters is important and determines the inductor current shape which can be either continuous or discontinuous. While the inductor current never reaches the zero point in the circuit operating with the continuous transmission mode (CCM), the inductor current in the circuit operating with the discontinuous transmission mode (DCM) is reduced to zero. The control can force the inductor current to be either continuous or discontinuous related to design parameters. The DCM converter has a switching current mismatches operates at a fixed frequency when compared to CCM or critical transmission mode (CRM) techniques. The DCM converter is rarely used or never used because it causes large peak currents and high EMI problems. On the other hand, the CRM converter typically uses a hysteretic control variation such that the value zero is lower. It is a variable frequency control technique, which naturally has a constant input current control. The power stage equations and the transfer functions of the CRM converter are the same as the CCM converter.

Various control strategies can be implemented to PFC circuits. DCM operation is generally used for low power applications but CCM is suitable for high power applications. The multiplier approach requires a multiplier in its current loop circuit and this makes the control circuit to be more complicated. The commonly control techniques in the literature used for PFC are discussed below and shown in Fig. 6.10 [26, 27]. Discontinuous current mode control method can also be called automatic input current shaper. In this approach, the internal current loop is completely eliminated (Fig. 6.10a) and the converter operates at DCM with fixed switching frequency. The input line current will automatically follow the input voltage. The currents with high peak value increase device stresses and conduction losses. In this strategy, the input current is discontinuous with triangular waveform which requires big value of inductor to decrease the current ripple and distortion factor. In critical boundary current mode control approach (Fig. 6.10b), the switch is turned on when the inductor current falls to zero, so that the converter operates at the boundary between CCM and DCM. The drawbacks of this method are the same as those of discontinuous current mode control method. The frequency in this method is also variable which makes it unsuitable for high-power applications.

Figure 6.10c shows hysteresis current mode control method. In this method two sinusoidal current references are generated which are peak and the other is the valley of the inductor current. Variable frequency is the main important disadvantage of this method. In peak current mode control method (Fig. 6.10d), the switch is turned on at constant frequency by a clock signal, and is turned off when the sum of the positive ramp of the inductor current and the external ramp reaches the sinusoidal current reference. The converter operates in CCM. Average current mode control method is the most used control method, which allows a better input current waveform, is the average current control shown in Fig. 6.10e. Here the inductor current is sensed and filtered by a current error amplifier whose output drives a PWM modulator. In this way the inner current loop tends to minimize the error between the average input current i_L and its reference. Since the converter works in CCM, it has the same advantages that of the peak current control method. Therefore, this method is suitable for medium and high-power applications. The demerit of this technique is the current control system which is more complicated and difficult to analyze and synthesize. In charge control method (Fig. 6.10f), the operating frequency is constant. The input current is detected and integrated with the C_T capacitor. When C_T voltage reaches the sinusoidal reference, the switch is switched off and the C_T capacitor is reset to be ready for the next cycle. Therefore, the average input current is forced to follow the sinusoidal reference even when the converter is operating in the CCM.

In light of the knowledge given above, it can be said that boost types PFC circuits with CCM inductor current wave shape is the most popular circuit used for medium and high-power applications. Also, the average current mode controller has been introduced as the most preferred method in the literature. Therefore, the conventional boost PFC circuit with average current control method (Fig. 6.11) has been simulated to show the related waveforms.

The simulated waveforms of the bridgeless boost PFC circuit are given in Figs. 6.12 and 6.13. These figures show that a PFC circuit can regulate both the

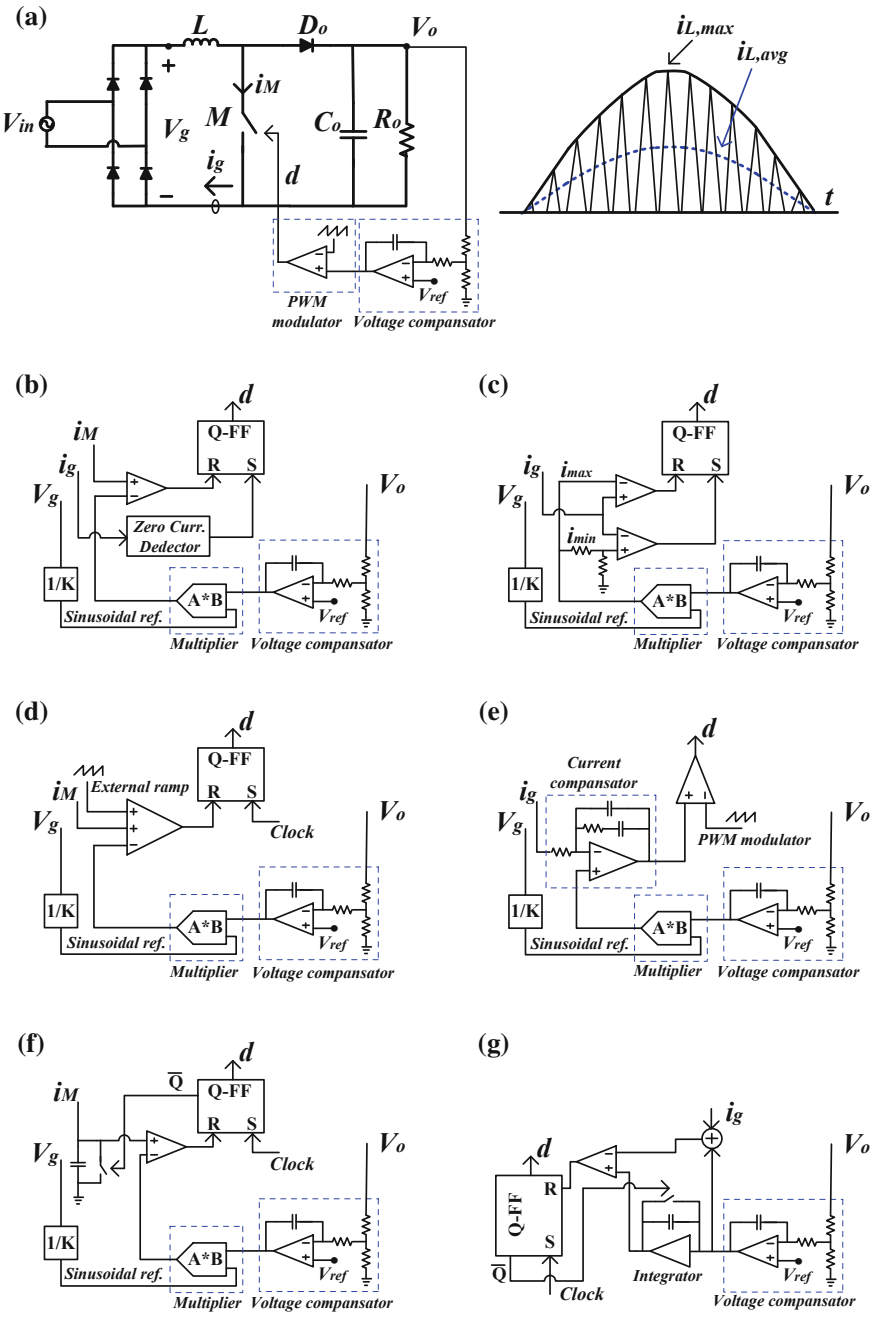

Fig. 6.10 Commonly used control techniques; **a** discontinuous, **b** critical boundary, **c** hysteresis, **d** peak current, **e** average current, **f** charge, **g** one cycle control methods

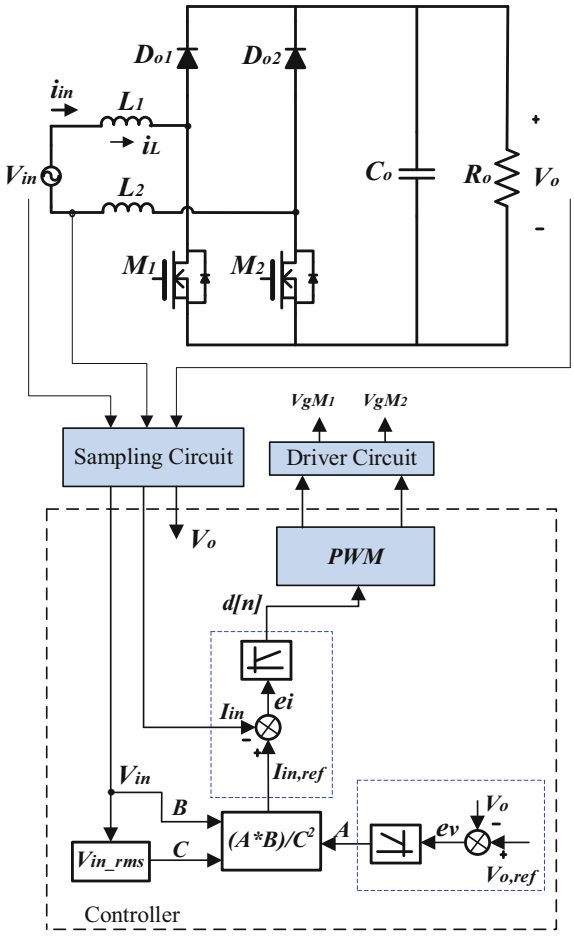

Fig. 6.11 Bridgeless boost type PFC topology with average current control method

output voltage of the topology and the input current drawn from the grid. The shape of the input current is formed according to the shape of the AC grid voltage to obtain high power factor.

6.3.2 DC/DC Converters

Given the DC microgrid structure described above, it is advantageous for most of the loads to use electrical energy in the DC form. Although most of the devices we use in our daily lives work with electrical energy in DC form, we are usually supplied with AC-DC adapters from AC mains. If the mains supply to our devices is DC microgrid,

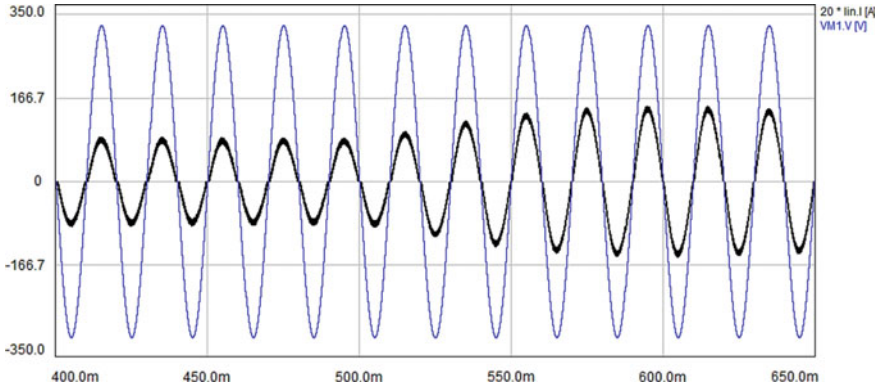

Fig. 6.12 Simulation results of average current controlled bridgeless boost PFC circuit; input voltage and 20* input current

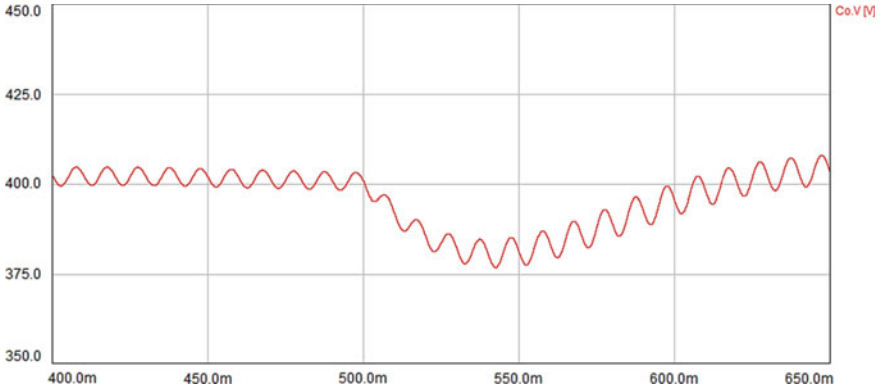

Fig. 6.13 Simulation results of average current controlled bridgeless boost PFC circuit; output voltage waveform

many AC-DC adapters will not be needed. However, the DC voltage level required by most DC-powered devices is not the same. Therefore, even if we use DC microgrids, DC-DC power electronics converters are needed to obtain voltage at different DC levels required by the loads. Generally used DC-DC converters are given in Figs. 6.14 and 6.15. Some of DC-DC converters are used to boost the input voltage level at the output. These type converters are called as boost type converters (Fig. 6.14a, b, e). In addition, the interleaved type of these converters are used in medium and high power loads. Some converters such as buck (Fig. 6.14c), buck-boost (Fig. 6.14d) are used to decrease the input voltage level at the output. Since the buck-boost converter both increases and decreases the voltage level, its application is wide.

Another topology type for DC-DC converters is "isolated type DC-DC converter". The generally used isolated DC-DC converters are flyback (Fig. 6.14f) and isolated full-bridge DC-DC converter (Fig. 6.15). While the flyback converter is used for low

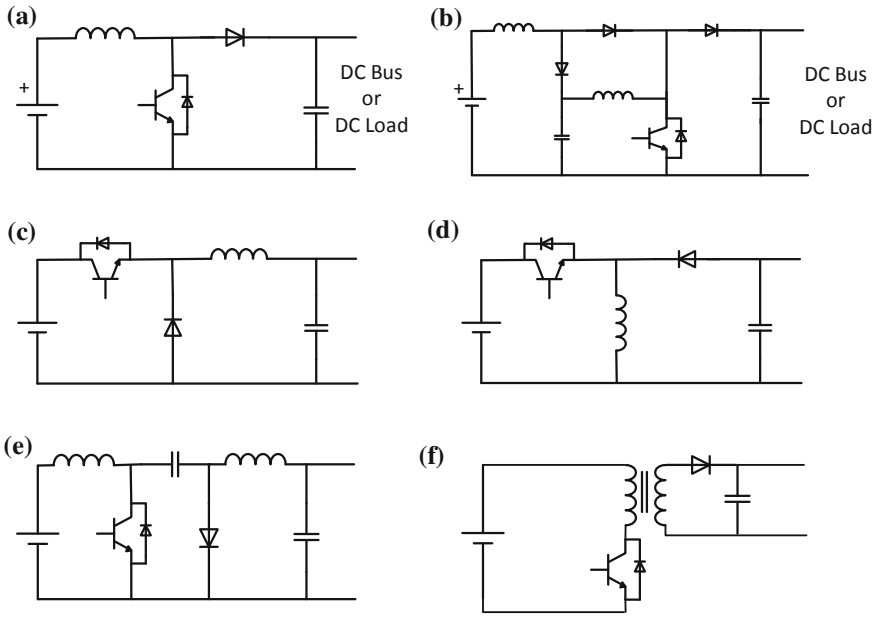

Fig. 6.14 Commonly used DC-DC topologies; **a** conventional boost, **b** cascade boost, **c** buck, **d** buck-boost, **e** sepic, **f** flyback

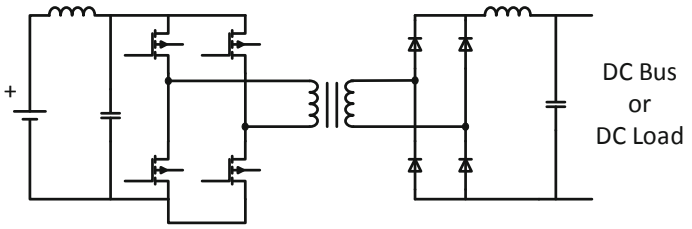

Fig. 6.15 Isolated full-bridge DC-DC converter

power applications, the isolated full-bridge type is used in medium and high power applications. Achieving a stable DC voltage, low current wavelet ratio, small size and low cost are the basic conditions for all type DC-DC converters used in DC microgrids.

In addition, DC-DC converters are generally use to obtain the required DC voltage level from the renewable energy sources to feed the DC bus. The role of DC-DC converters is not only obtaining the regulated voltage but also get the maximum power from the renewable sources. Maximum power point tracking (MPPT) controllers are used to get maximum power from the source. The main aim of MPPT systems to track the maximum power of the renewable source (PV panel or fuel cell). Dealing with many changeable temperature and solar radiation, the MPP is also varies. Thus,

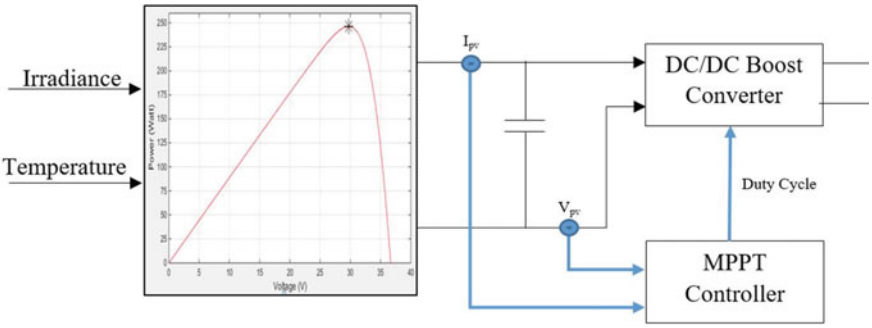

Fig. 6.16 Block diagram of MPPT controller of PV based boost converter

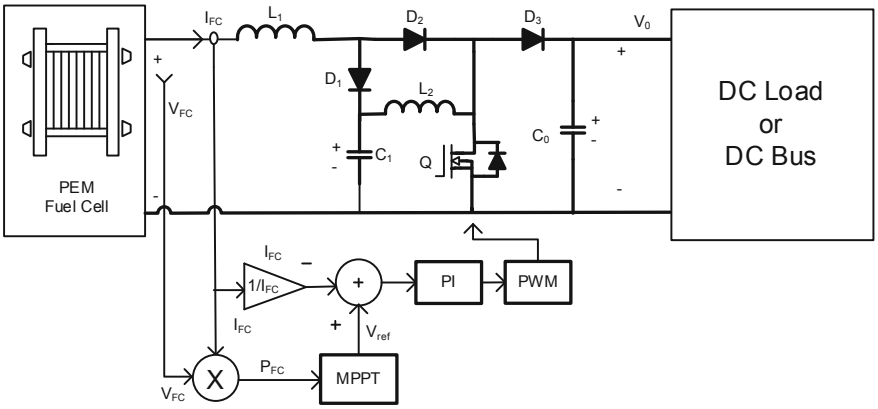

Fig. 6.17 MPPT + PI controller for fuel cell based boost converter

so as to dynamically set the MPP like an operating point for vast range of inputs (solar radiation and temperature), (MPPT) technique is demanded. MPPT application is essentially a DC/DC converter laid in between the load governed by tracking algorithm and the photovoltaic modules as given in Figs. 6.16 and 6.17. Essentially the tracking algorithm will get the inputs which are PV module current and voltage and collaborate with DC/DC converter duty cycles that will set the system operating point of MPP. In some applications a PI controller can be also used to regulate the output of MPPT.

Perturb and Observation method is the widespread MPPT techniques and can be considered as the easiest to use. The flowchart of this technique is shown in Fig. 6.18, running the PV system in the direction where the gained power from the PV system increases is the basic idea of P&O. Depending on the flowchart of the method, in case the alteration of power is positive, the incremental of duty cycle (D) will remain the same to decrease or increase the PV voltage, but if the alteration is negative, the direction of incremental duty cycle command will reverse.

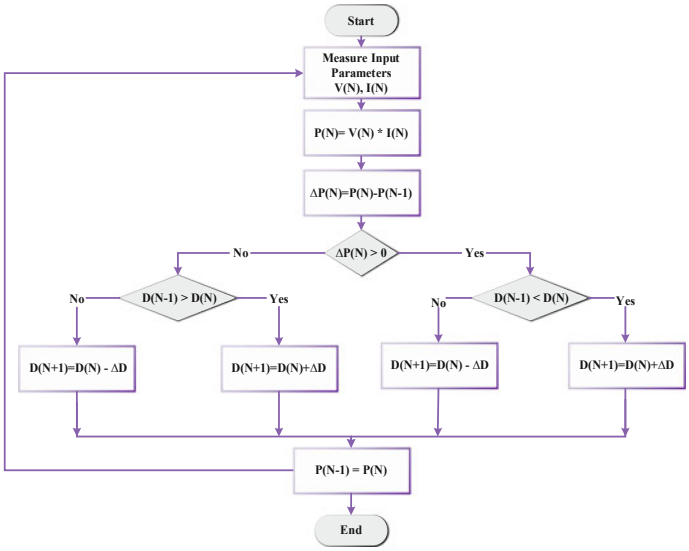

Fig. 6.18 Flowchart of P&O MPPT method

The simulation is performed for variations in irradiance and temperature. Figure 6.19 shows decreasing and increasing in irradiance and temperature in many case, the irradiance starting from 100 W/m^2 and increasing to 1000 W/m^2 in its maximum value, while the temperature is starting from under 20 °C and reaches over 40 °C. This represents many weather conditions to analysis the MPPT controller response. It can be noticed from Fig. 6.20, that using controlling algorithm succeed to track maximum power point under various circumstances. It is also observed that output power can be increased considerably for high irradiance and using MPPT controllers.

6.3.3 DC/AC Inverters

The loads that require the AC form of electrical energy are called AC loads. When AC loads are fed from DC microgrids, they require DC-to-AC power electronics converters that convert the DC voltage form into an AC voltage form. DC-AC power electronics converters are called “inverters” and are three-phase or single-phase. The inverters task is feeding contemporary AC loads from DC microgrid. These inverters can also be half-bridges or full-bridges. Single-phase DC-AC inverters are presented in Fig. 6.21. In most applications, a three-phase supply is not required, and single-phase converters can be used instead. Half bridges are simple, low cost and easy to control. It is important to use DC link capacitors to compensate for voltage fluctuation. The structure of the full-bridge DC-AC circuit is more complex than

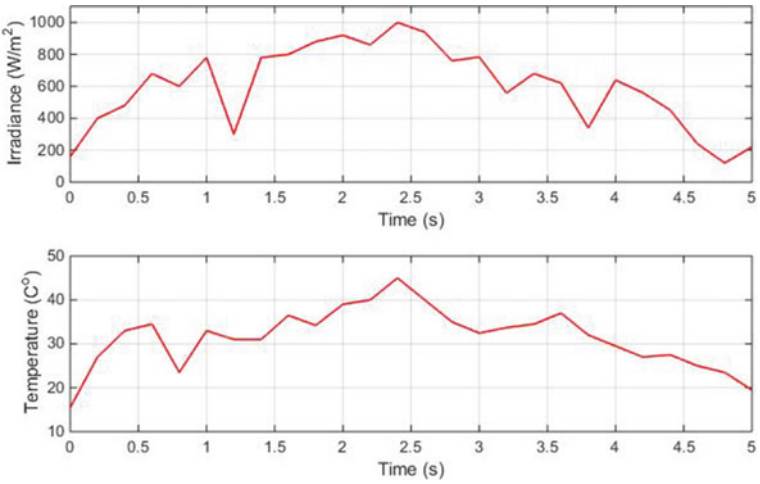

Fig. 6.19 Changing in PV Parameters

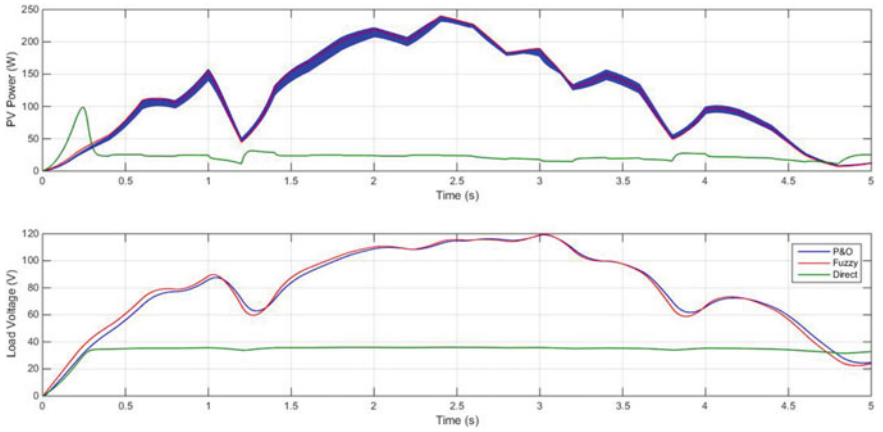

Fig. 6.20 Outputs under various T and G

the half-bridge DC-AC circuit structure, but the passive circuit elements needed on both the DC and the AC side are smaller. The harmonic production at the output is an important problem for all type inverters. Therefore, a lot of methods have been improved to eliminate the harmonics produced by the inverters. In addition to single-phase and three-phase conventional inverter structures, multi-level inverter structures have also been developed for AC loads.

Many different modulation strategies such as PWM, multi-carrier PWM, SPWM and space vector modulation (SVM) have been developed for inverters. The Multicarrier PWM method which is based on the traditional PWM technique uses multiple carriers to control each semiconductor switch of an inverter. The principle of the

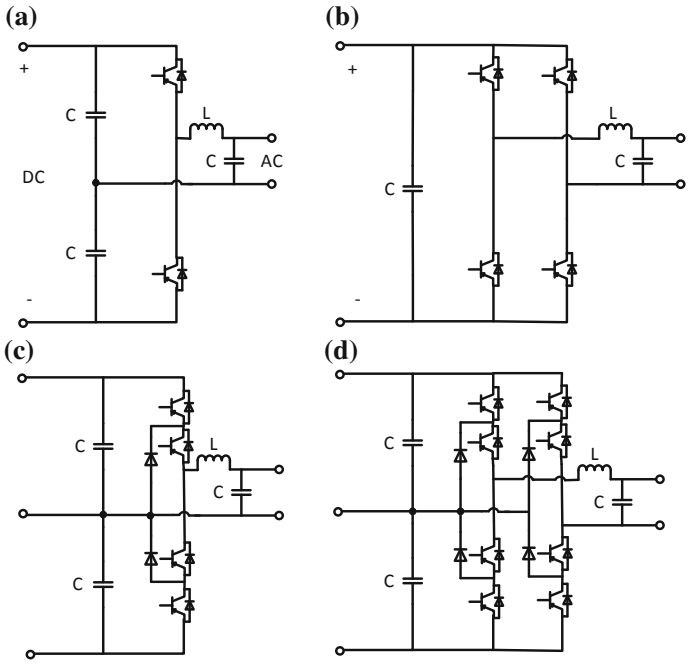

Fig. 6.21 Single-phase half-bridge and full-bridge DC-AC inverter topologies

SVM method is the same as three-level or two-level topologies, but there are more state vectors that make up the switching sequence.

6.4 Conclusion

Today, in addition to AC microgrids, DC microgrids are becoming an important part of the future energy infrastructure. As investment in renewable energy sources increases, the use of DC microgrids is becoming widespread and the value of renewable resources increases. Over time, the use of DC microgrids will increase. DC lines will be constructed in existing buildings and all new buildings will be designed with DC microgrids. These developments will lead to the development of standards for DC power. We can conclude that the use of DC microgrids will continue to increase in the coming years depending on the energy demand increase and energy use awareness in the world. The widespread use of DC microgrids will allow us to use the energy resources more efficiently.

Renewable energy sources (such as wind turbines, PV systems and fuel cells) can be used with DC microgrids. However, power electronics converters are the main important part of DC microgrids. Therefore, the power electronic converters used

in DC microgrid are discussed, grouped and evaluated according to their targets. These power electronic converters have been detailed in terms of AC-DC rectifiers, inverters (for AC loads) and DC-DC converter circuit types. The simulation results of some the given topologies have been evaluated in this study.

References

1. V. Rasouli Disfani, Optimization and control for microgrid and power electronic converters. Ph.D. thesis, College of Engineering University of South Florida (July 2015)
2. M. Lonkar, S. Ponnaluri, An overview of DC microgrid operation and control, in *6th International Renewable Energy Congress (IREC)* (2015)
3. D. Larruskain, I. Zamora, O. Abarrategui, Z. Aginako, Conversion of ac distribution lines into dc lines to upgrade transmission capacity. Electr. Power Syst. Res. **81**(7), 1341–1348 (2011)
4. A. Clerici, L. Paris, P. Danfors, HVDC conversion of HVAC lines to provide substantial power upgrading. IEEE Trans. Power Deliv. **6**(1), 324–333 (1991)
5. T. Ackermann, N. Negra, J. Todorovic, Loss evaluation of HVAC and HVDC transmission solutions for large off shore wind farms. Electr. Power Syst. Res. **76**(11), 916–927 (2006)
6. J. Driesen, F. Katiraei, Design for distributed energy resources. IEEE Power Energy Mag. **6**(3), 30–40 (2008)
7. M. Barnes, J. Kondoh, H. Asano, J. Oyarzabal, G. Ventakaramanan, R. Lasseter, N. Hatziargyriou, T. Green, Real-world microgrids-an overview, in *IEEE International Conference on System of Systems Engineering* (2007), pp. 1–8
8. Y. Ito, Y. Zhongqing, H. Akagi, DC microgrid based distribution power generation system, in *International Power Electronics and Motion Control Conference*, vol. 3 (2004), pp. 1740–1745
9. K. Mizuguchi, S. Muroyama, Y. Kuwata, Y. Ohashi, A new decentralized dc power system for telecommunications systems, in *IEEE INTELEC* (1990), pp. 55–62
10. C.C. Chan, The state of art of electric and hybrid vehicles. Proc. IEEE **90**(2), 247–275 (2002)
11. J. Ciezki, R. Ashton, Selection and stability issues associated with a navy shipboard dc zonal electric distribution system. IEEE Trans. Power Deliv. **15**(2), 665–669 (2000)
12. H. Kakigano, Y. Miura, T. Ise, Low-voltage bipolar-type DC microgrid for super high quality distribution. IEEE Trans. Power Electron. **25**(12), 3066–3075 (2010)
13. A. Kwasinski, C.N. Onwuchekwa, Dynamic behavior and stabilization of DC microgrids with instantaneous constant-power loads. IEEE Trans. Power Electron. **26**(3), 822–834 (2011)
14. D. Salomonsson, L. Soder, A. Sannino, Protection of low-voltage DC microgrids. IEEE Trans. Power Deliv. **24**(3), 1045–1053 (2009)
15. X. Wang, J.M. Guerrero, F. Blaabjerg, Z. Chen, A review of power electronics based microgrids. Int. J. Power Electron. **12**(1), 181–192 (2012)
16. H. Kakigano, M. Nomura, T. Ise, Loss evaluation of dc distribution for residential houses compared with ac system, in *International Power Electronics Conference* (2010), pp. 480–486
17. H. Kakigano, Y. Miura, T. Ise, R. Uchida, DC voltage control of the dc micro-grid for super high quality distribution, in *Power Conversion Conference* (Apr 2007), pp. 518–525
18. H. Kakigano, Y. Miura, T. Ise, Low-voltage bipolar-type dc microgrid for super high quality distribution. IEEE Trans. Power Electron. **25**, 3066–3075 (2010)
19. B. Banerjee, Local digital control of power electronic converters in a DC microgrid based on a priori derivation of switching surfaces. Dissertation, Michigan Technological University (2013)
20. N. Ayai, T. Hisada et al., DC micro grid system, electric wire & cable. Energy **75**, 132–136 (2012)
21. M.H. Rashid, in *Power Electronics: Circuits, Devices and Applications* (Prentice Hall Inc., NJ, USA 2004), pp. 68–120

22. R.W. Ericson, in *Fundamentals of Power Electronics* (Chapman & Hall, New York, 1997), pp. 125–140
23. C. Qiao, K.M. Smedley, A topology survey of single-stage power factor corrector with a boost type input-current-shaper. IEEE Trans. Power Electron. **16**(3), 360–368 (2001)
24. V. Grigore, Topological Issues in Sıngle-Phase Power Factor Correction. Ph.D. Thesis, Helsinki University of Technology, Espoo, Finland, pp. 17–28 (2001)
25. I. Iskender, N. Genc, Chapter 13: power quality improvement using active AC-DC PFC converters, in *Advances in Energy Research: Distributed Generations Systems Integrating Renewable Energy Resources*, ed. by N. Bizon (Nova Publishers, 2011), pp. 515–551
26. L. Rossetto, G. Spiazzi, P. Tenti, Control techniques for power factor correction converters, in *Proceedings of Power Electronics, Motion Control (PEMC)* (September 1994)
27. K.M. Smedley, S. Cuk, One-cycle control of switching converters. IEEE Trans. Power Electron. **10**(6) (1995)

Chapter 7
Power Electronic Converters in AC Microgrid

Marian Gaiceanu, Iulian Nicusor Arama and Iulian Ghenea

Abstract As the major worldwide infrastructure distribution systems are in AC, the chapter intends to review the main power converter types for Energy Sources integration. The requirements imposed by the existing standards are envisaged. An effective solution for injection of electrical power from Renewable Energy Sources (DC and AC power sources) into the grid is presented. Additionally, the efficiency improvement by means of the modulation techniques is implemented and shown in this chapter. Due to the higher power energy in three-phase power systems (PSs), despite of the AC single-phase PSs, the large energy storage systems are not necessary.

Keywords Microgrid · Power converter · Topologies · Wind power · Photovoltaic · Standards

7.1 Introduction

Some convergent factors (power demand, environmental pollution, limited fossil fuel formation, consumers growing) led the world to think seriously about other alternative sources of energy. The main advantages introduced by RES are related both to sustainability developing, and to friendly environment assurance. This chapter underline the worldwide tendency to a clean environment, green energy assurance,

M. Gaiceanu (✉) · I. N. Arama
Department of Automation and Electrical Engineering, Dunarea de Jos University of Galati, Galati, Romania
e-mail: marian.gaiceanu@ugal.ro

I. N. Arama
e-mail: iulian.arama@ugal.ro

I. Ghenea
Doctoral School of Fundamental and Engineering Sciences, Dunarea de Jos University of Galati, Galati, Romania
e-mail: ghenea.iulian@ugal.ro

N. Mahdavi Tabatabaei et al. (eds.), *Microgrid Architectures, Control and Protection Methods*, Power Systems,
https://doi.org/10.1007/978-3-030-23723-3_7

predicting for the long term the evolution of the primary energy. As identified high penetration tendency, RES are the main candidates to providing clean energy. In this chapter the authors have in view the following:—to state the formulation problem of using the alternative energy sources through power converters;—to review the main standards to integrate power converters into distributed systems;—specific requirements of static power converters used in AC microgrids;—classification of power converters (DC-DC and DC-AC);—to put in evidence the modern power structures for both the future wind, and photovoltaic power systems;—to present the experimental results of the implemented modulation strategies on the AC Power Converters used in microgrids. The chapter provides the technical aspects of network to meet the utilities connection rules, including harmonics improvements, power factor control, the assurance of the required performances and stability. This chapter begins with an overview of the current state of power converters topologies into the microgrids. The requirements defined by the actual microgrid power converters standards are mentioned in this chapter. The specific case study, based on the hybrid system integration (wind and fuel cells primary energy sources) is provided. Through the adequate modulation strategies, the overall efficiency of the PS has been increased. The chapter ends with the Reference Section.

7.2 Overview

The challenges of development of power converters technology are [1]:

- The increased electricity demand obtained by controlled energy conversion from primary sources (Fig. 7.1);
- Off-shore power distribution for long distance;
- The requirements of the systems components (materials, and devices) to handle normally high power in extreme conditions.

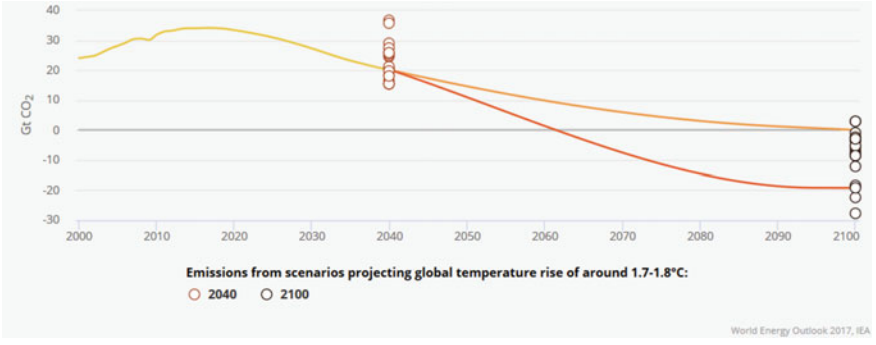

Fig. 7.1 The sustainable development scenario [3]

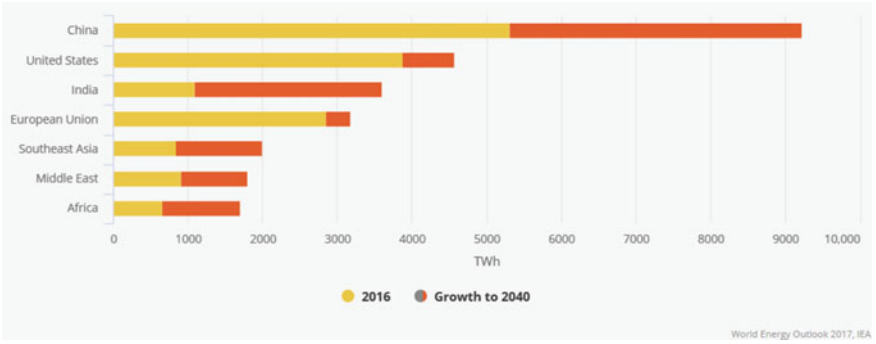

Fig. 7.2 The electricity demand by specific region [3]

To face-up to the above-mentioned challenges, the future power converters should includes

- Increased high-performance cost-ratio for power converters;
- Capability of self-healing power converters and materials; dynamic reconfigurations of the distributed power converters [2];
- The fast development of the material properties (insulators, conductors, magnetics, so on).

Due to the progress of new technology in order to increase the comfort and fast development of the industry, smart cities, fast spreading of the Internet of Things concept, penetration of the autonomous vehicles, the electricity demand is an ascendant way; it depends on the specific region (Fig. 7.2). Global average annual net capacity additions of primary energy sources are shown in Fig. 7.3. From the Fig. 7.3 can be concluded that the development of the electrifying sector would rise yearly. In the near future (up to 2030) the electrifying sector will be developed mainly by introducing Renewable Energy Sources and by increasing the shares of gas energy primary source (Figs. 7.4 and 7.5) [4]. Therefore, the technology development of the power converters in RES area is a priority.

Currently the power systems are based on fossil fuels (coal, gas, oil) energy conversion systems. The fossil fuels are exhausted and no environment friendly. The energy security is more vulnerable in bulk power systems as it is nowadays in many worldwide countries. Therefore, the global energy strategy is oriented through diminishing the energy obtained based on fossil fuels. International Energy Agency (IEA) makes a realistic scenario regarding the fossil fuel decreasing trend (Fig. 7.3) [5]. The no pollutant energy resources [6] combined with the renewable energy conversion power systems will replace gradually the conventional electricity generation (Fig. 7.5).

The Renewable Energy Sources (wind, biomass, solar, hydro)—RES—are inexhaustible, no costs, and without greenhouse gas emissions being considered as green energy. Therefore, the conventional energy systems based on the synchronous generators will be completed with new generation of power conversion systems. The

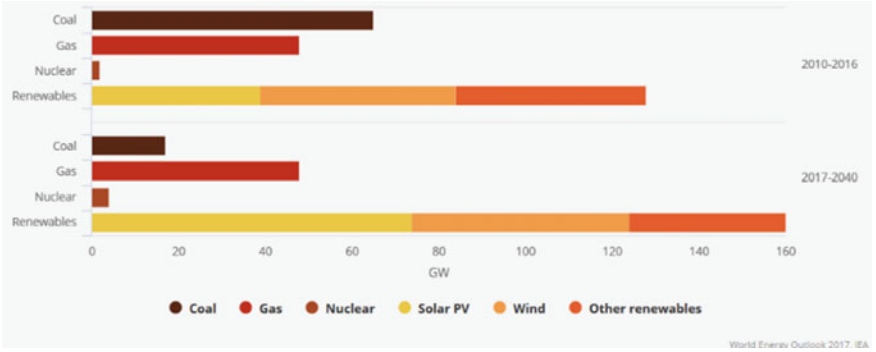

Fig. 7.3 Global average annual net capacity additions by type [3]

Fig. 7.4 World commercial energy use [4]

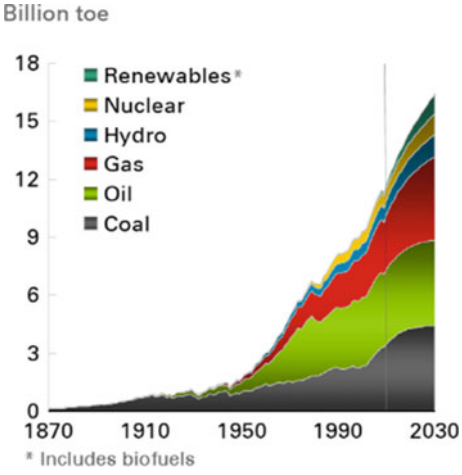

Fig. 7.5 Shares of world primary energy by type [4]

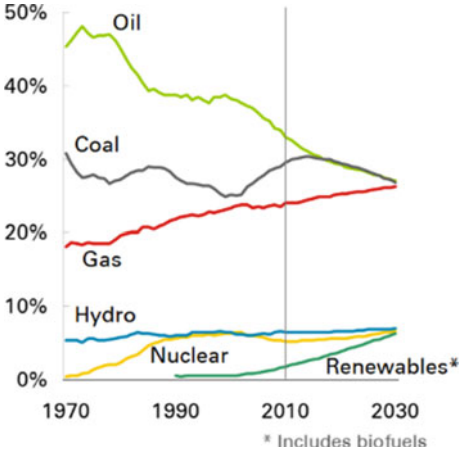

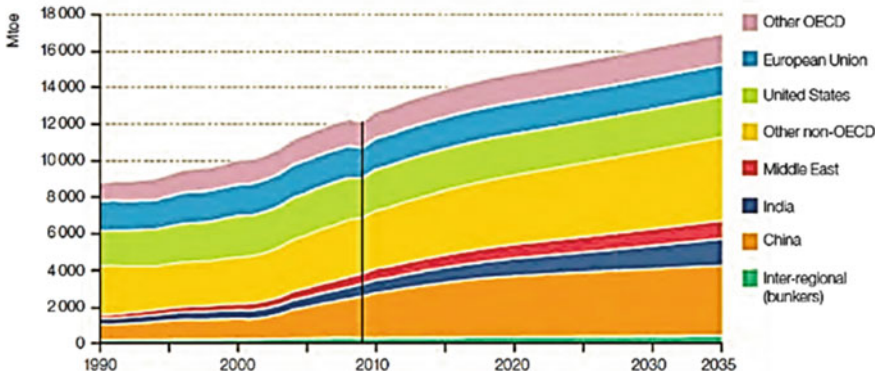

Fig. 7.6 The demand of the electricity by region in IEA policies scenario [5]

electrical parameters of the utility network the modern energy conversion systems can be controlled based on the static power converters.

The main factors (stability, flexibility and expandability) of developing the utility network through the *distributed energy* (*DE*) systems are taken into consideration. The DE power systems include the RES, microturbine, fuel cells, and internal combustion engines.

The future worldwide demand of primary energy is envisaged by IEA making a Policy Energy Scenario provided in the Fig. 7.6 (*OECD*) [5].

From the energy security point of view the DER power systems are more appropriate than the utility network.

7.3 Problem Formulation

The alternative energy by definition includes any other source energy different from fossil fuel combustion (e.g. wave and tidal power, solar and wind power, biomass or biogas, hydrogen power, gas micro turbines and small hydropower farms).

On the one hand, the large *distributed generation* (*DG*) PS includes RES units (photovoltaic panels, generators for wind turbines, wave, hydro and tidal, generators), and on the other hand the generators based on fuel cells or *combined heat and power stations—CHP*—using the steam or natural gas as primary fuel [7, 8].

There are many low consumption isolated sites (rural communities), and extending power grids to meet the end-users necessary energy which requires high-costly investments to assure the upgrades in transmission and distribution PSs. Therefore, the locally alternative energy sources are more attractive and economic solutions, which require renewable energy technologies. From the other point of view the use of RES clean the environment and helps to regenerate it.

During the last years, the small power resources up to 1 MVA (wind turbines, fuel-cells, microCHP plants, and microturbines) connected to the utility network has been increased.

The main tasks of the power converters operating in the grid-connected mode are related to direct and quadrature current control, DC-link voltage control, and the frequency control which has to be synchronized with the utility grid. Additional power quality features are required. In the grid connected operation mode the power converters can deliver the adequate grid frequency through the phase-locked loop.

In islanded power operation, the power converters have to take the additionally tasks: to deliver the appropriate voltage level with the same frequency as PS has.

In the Fig. 7.7 the generic microgrid architecture is shown (C-converter, EV-electric vehicle, T-power transformer). Into the autonomous microgrid the sensitivity to the load variations is high [8]. The continuity, stability, and the resiliency can be

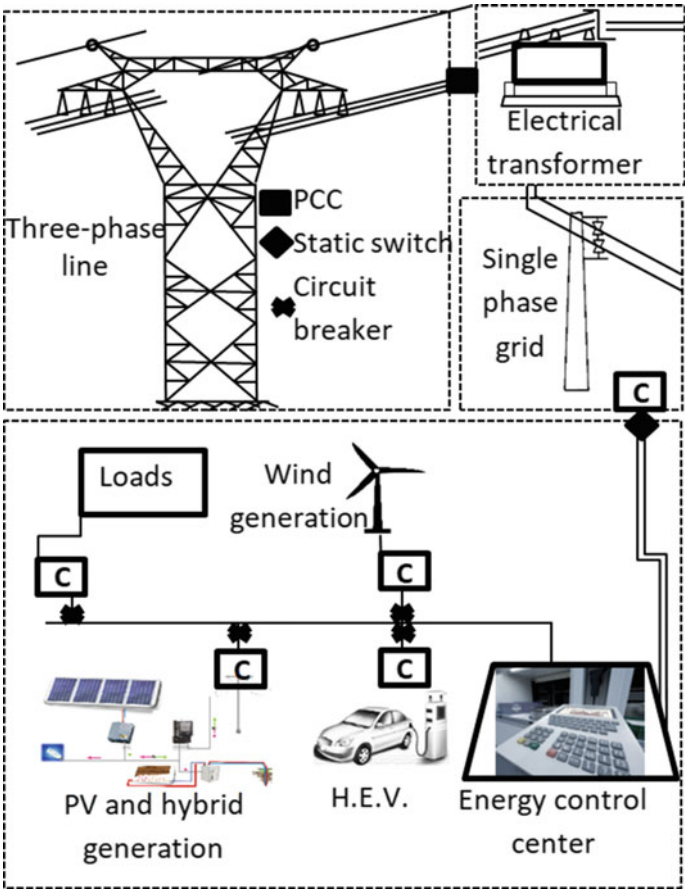

Fig. 7.7 The power structure of the microgrid

assured by cooperative control among all power converter interfaces, taken into account the optimization of the energy prices, reliability, efficiency, primary fuel costs.

7.4 Standards for Power Converters as Interfaces Into the Distributed Energy Resources

The specific standards for distributed energy resources (DER) are still under the development. However, the standards can be grouped as:

1. The *IEEE 1547–2018 Interconnection Standard*, in which the requirements of the equipment for power system connection (this includes default activation for anti-islanding, fault response, and automatic reconnection) are specified. The standard for Photovoltaic (PV) systems, *IEC61727*, named as *Characteristics of the utility interface*—2004. This standard specific the rules related to parameters of the power quality feature: power factor, harmonics, voltage range, frequency range, flicker, waveform distortion, and the allowable DC injection component. *IEC 62116* Edition 1, 2005: this standard specify the measures for photovoltaic inverter which interacts with the utility (the tests for the IEC 61727 standard) for the testing procedure of islanding prevention (approved in 2007);—the standard *VDE0126-1-1* (*2006*) for specifying the requirements of an automatic disconnection device placed between the public low-voltage grid and the generator;—the Italian standard, *CEI 0–21* regarding the Safety issues- applied on Italy market, respectively E-On, for German utility.

Voltage Quality—*EN50160* standard is dedicated to three phase inverters, and specifies the voltage unbalance. The unbalance allowable limit voltage is 3%; the maximum amplitude variations of the voltage: +/−10%; the maximum frequency variations is +/−1%; the deep <60% specification for the voltage dips with duration <1 s; the 8% maximum voltage THD harmonic levels.

2. The *IEEE 2030.5* (SEP2), IEEE 1815 (DNP3), SunSpec Modbus *Interoperability Standards*, which defines the DER communications
3. The *IEEE 1547.1 Certification Test Standard*, compatibilized with UL 1741, *IEC 62109* (Safety of Static Inverters), defines the procedure for equipment validation for the interconnection or interoperability standards. Inverter Testing *IEEE* 1547.1, Efficiency Testing *CEC-300*; testing procedure of Islanding Prevention and Methods for Utility-Interactive Photovoltaic Inverters have been addressed in the *IEC 62116* standard.

Regarding the available standards, for the wind power plant systems there are important requirements regarding the:

(1) Voltage and frequency admissible domain for uninterruptible operation;

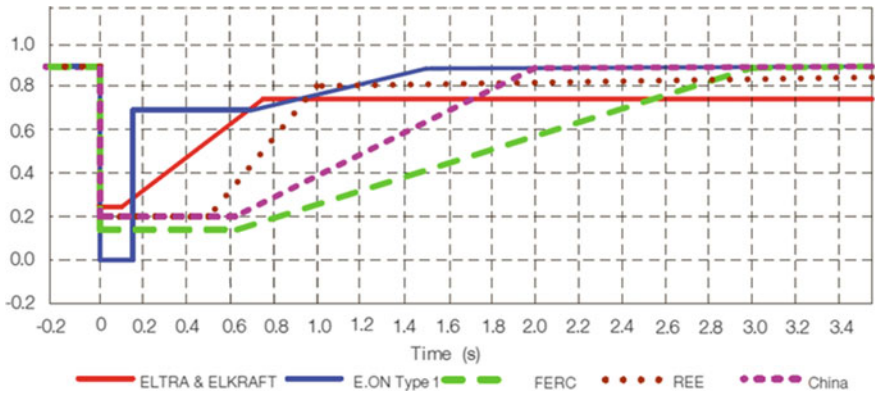

Fig. 7.8 The different requirements for important grid companies (E.ON Netz—Germany) or countries [9]

(2) the control of the active and reactive power for power quality and voltage regulation;
(3) Low-voltage ride-through requirement (LVRT): Fig. 7.8 shows the different requirements for important grid companies (E.ON Netz—Germany) or countries [9]. In order to maintain the voltage stabilization during fault period (voltage recovery) the reactive power requirement is necessary.

7.5 Specific Requirements of Power Converters in AC Microgrids

In order to ensure the frequency and voltage stabilization in disturbed conditions, the operators should inject the appropriate active or reactive into the grid.

In order to configure and design the appropriate power converters topology into the microgrid, the basic control requirements in the conventional power systems should be revised:

- Frequency control (should reacts on a seconds-to-minutes time scale). The *automatic generation control* (*AGC*) regulates the generators;
- Power control: a quick response time (within 10 min of disturbed utility grid the adequate power should be available from the generators) and a slower response time (used generators in case of failure of other generators).
- Voltage support: the reactive power should be injected by the synchronous generators. In this manner, the voltage raises.
- Black-start capacity: this feature is necessary to assure the power system restarting when a cascading black-out occurs.

Another important feature of one robust power system is to follow the loads demand. In the traditionally power system this function is assured through the "fast energy market". When a peak power occurs (in the morning or evening) into the microgrids, the required surplus of energy could be obtained through the utility grid or by introducing a battery system.

Taking into account the intervention of the operators, the solar and wind power generation could be integrated into the grid. For low penetration of RES, the problems appear into the local grid and more on the primarily device (i.e. the subsynchronous resonance due to the wind turbine or the harmonics due to the power converters). Therefore, by assuring an appropriate topology with the associated power converter control the problems are locally solved.

For high penetrations of RES the power balance at grid level is necessary. The Energy Management System (EMS) block should be inserted in the overall topology of the utility network.

The generated power could operate adequately if the decision time is taken into consideration (Fig. 7.9) [10].

Figure 7.9 shows the places into the power systems where the action is done [10]. As component, the EMS includes the SCADA system and the support functions in order to assure normal operation of the utility network.

The EMS system takes part of the smart power grid. On the one hand, in order to take the data from the RES and of the real prices from the power market and on the

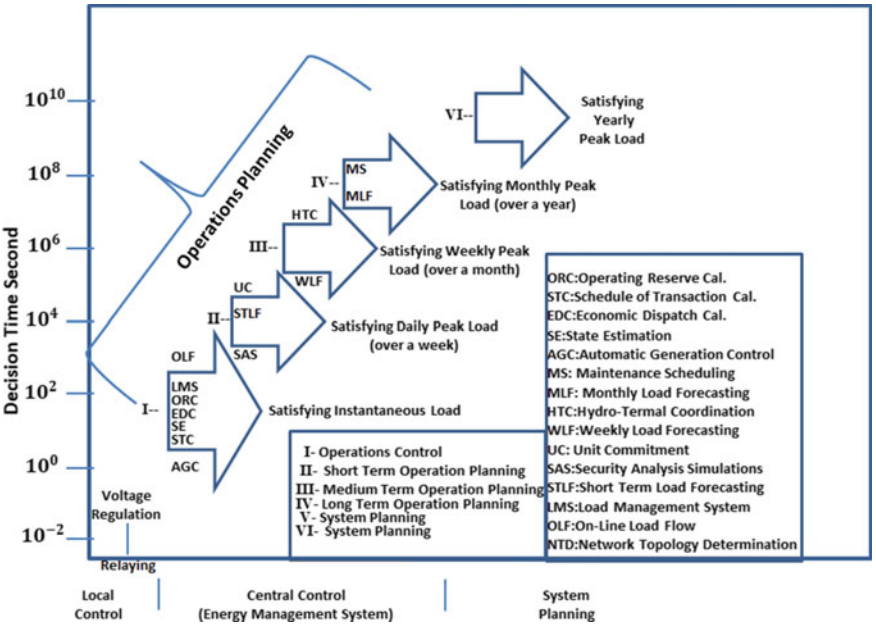

Fig. 7.9 Energy Management System and its functions versus decision time

other hand, to manage the stability operation the communication channel should be inserted into the smart grid power architecture.

The power converters technologies are developed function on the renewable energy generation technology.

In the energy production area different types of green power sources should agree with the grid requirements. The dc power sources, like fuel cells or photovoltaic arrays should deliver the maximum power at fixed voltage level. The ac green power sources delivers variable frequency different from the grid one (wind turbines or micro gas-turbines). The induction generators connected to wind turbines can be directly connected to the grid, but in most cases, the green power sources require the power converters as interfaces with the power grid. The AC power sources, in most cases, require two stages of power conversion: from AC to DC and from DC to AC grid. The controlled power semiconductor devices, as IGBTs, MCTs, GTOs or more recently devices based on *Silicon carbide* (*SiC*), and *Galium ARsenide* (*GAAS*) technologies can manipulate large power at high switching frequency [11]. Therefore, the use of power converters instead of the conventional synchronous machine conducts to increased control opportunities. During power outages a grid connected inverter-based solution can be used (*uninterruptible power supply- UPS*). Moreover, in order to improve the power quality, the UPS can be used also in normal operation conditions [12]. In this manner, the UPS can add the other functions than as main generator function like mitigating swell/voltage sag or the waveform distortion. The most cases include the use of the three-phase power inverters. Due to the component availability, reliability and cost only low power inverter applications have been developed.

Power quality problem implies control of the two variables (the line current and the voltage) such that the power factor can be controlled. Due to the standard restriction [12]: at the point of common coupling the power, inverter does not control the voltage (PCC). Therefore, in [13] the authors underline that the power quality problem is solved by acting on the current. The presence of the zero sequence or the DC components in the generated voltage in distributed system should be avoided. This task is performed through a grid connected isolating transformer.

The control architectures of the power distribution systems imply the phase-locked loop, DC link voltage, current and power control loops.

The utility network is slow to evolve; different technical issues (voltage and frequency regulations, protection, low voltage ride through, so on) are the challenges for the new generation of the power inverters.

7.6 Classification of Power Converters for RES

A global power conversion block diagram for RES penetration is presented in Fig. 7.10. Generally, the Power Conversion System for RES integration supposes three power conversion stages: AC to DC, DC to DC, and DC to AC [14, 15]. Figure 7.10 presents a classical energy converter incorporating power factor correc-

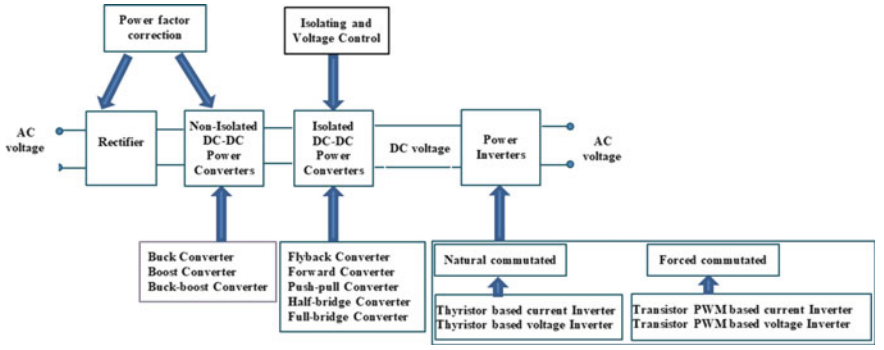

Fig. 7.10 Classification of AC-AC power converters, with changes of voltage type, integrated into a power factor correction regulated scheme

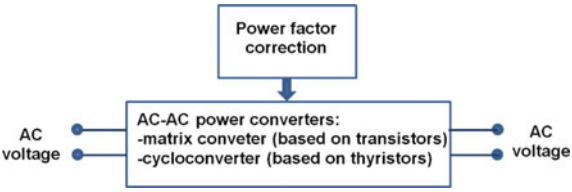

Fig. 7.11 Classification of power converters based on direct AC-AC power conversion

tion feature. It presents the types of converters that can be fitted to such a system, which involves changing the type of power two times (AC to DC, and DC to AC). Because of nonlinear loads and switching the static power converters, the power electronic devices can interact with other sensitive electronic equipment, disturbing the smooth functioning of the latter.

For this reason, both at the conversion AC into DC, and vice versa, circuit able to improve the power factor (Fig. 7.10) are provided. In Fig. 7.11, classification of the power converters based on direct AC-AC power conversion (without changes of voltage type) integrated into a power factor correction regulated scheme is represented.

In the Fig. 7.12, the corresponding power converters for AC-DC power conversion stage are depicted.

In Fig. 7.13, the topology of the voltage grid or source power converter (VSC) is shown. The power flow circulates from AC side to DC side. From topology point of view, taken into consideration the four quadrants operation, the VSC is similar with Voltage Source Inverter (VSI). In this case, the power flows from the DC to AC side. This basic principle is used to develop the specific control into a microgrid.

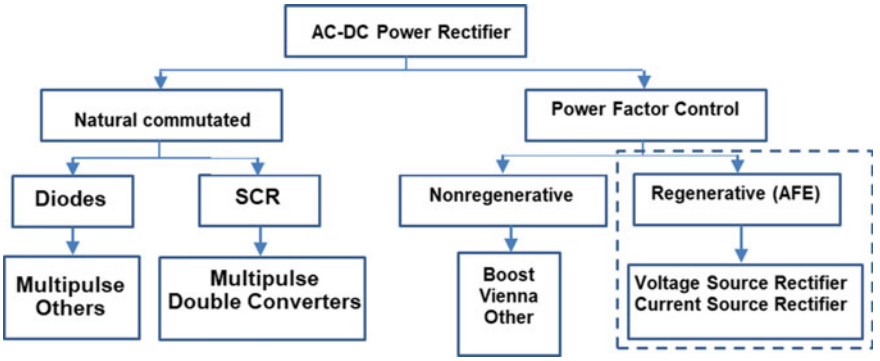

Fig. 7.12 Rectifiers classification

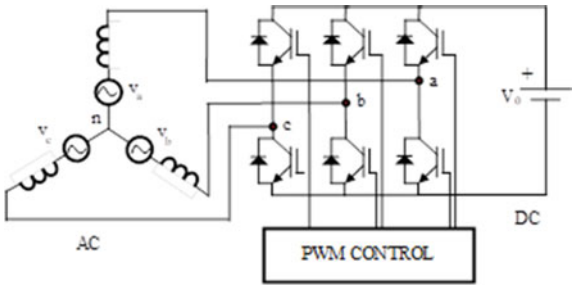

Fig. 7.13 Voltage source converter

7.6.1 Topologies of the Power Inverters (DC-AC Power Conversion)

The inverters can be classified in VSI (voltage source inverter) and CSI (current source inverter). The VSI produces switched voltage in order to supply the electrical machine, and the CSI delivers a switched current waveform. In the case of a VSI, the voltage in the DC link is maintained at a constant value by using a capacitor. Instead of the DC link voltage, the current delivered by the VSI depends on the load and the electrical machine speed.

The power switching devices in the VSI and CSI can be controlled by using different modulation strategies: square or quasi-square modulation; pulse amplitude modulation or pulse width modulation, PWM. The most implemented modulation technique into a commercial power inverter is sinusoidal modulation. The improving modulation techniques increase the DC link voltage utilization: third harmonic insertion, space vector modulation strategy, harmonic elimination.

According to the voltage type (number of power stages converted), there are two categories of power inverters:

1. Direct Conversion;
2. Indirect Conversion.

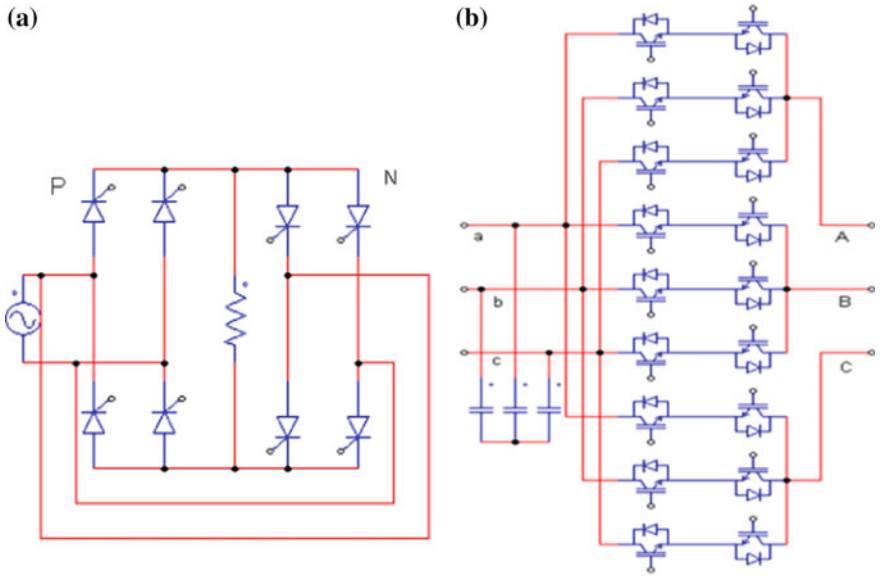

Fig. 7.14 **a** Single-phase cycloconverter, **b** Three-phase matrix converter

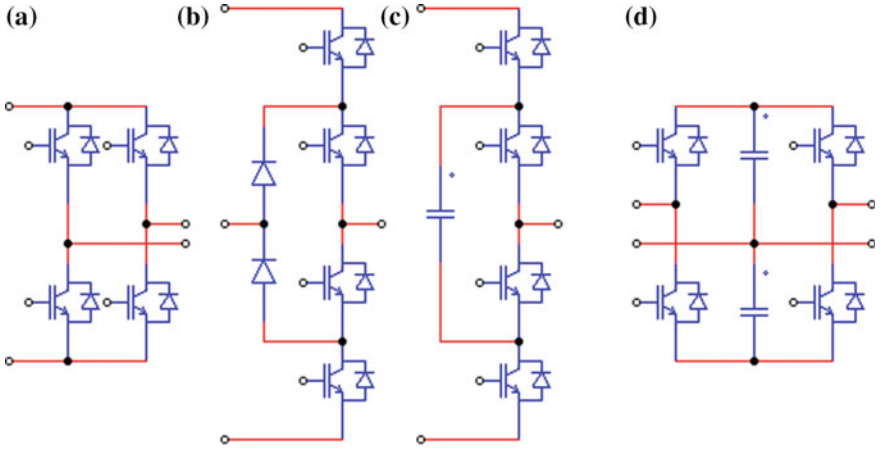

Fig. 7.15 Neutral Point Diode Clamped (NPC) three-level legs: **a** H-bridge inverter, **b** NPC, and **c** flying capacitor multilevel legs, **d** ac-dc-ac power stage conversion with two dc-link midpoint connections (single-phase to single-phase power converter)

The VSI and CSI are part of the Indirect Conversion Topology. The Cycloconverter (Fig. 7.14a) and matrix converter (Fig. 7.14b) takes part of the Direct Conversion Topology (Fig. 7.11). The VSI are divided in multilevel VSI and 2-level VSI [16, 17]. The multilevel inverter (MLI) topologies are based on Neutral Point Diode Clamped, Cascaded H-Bridge, and Flying Capacitor [16] (Fig. 7.15).

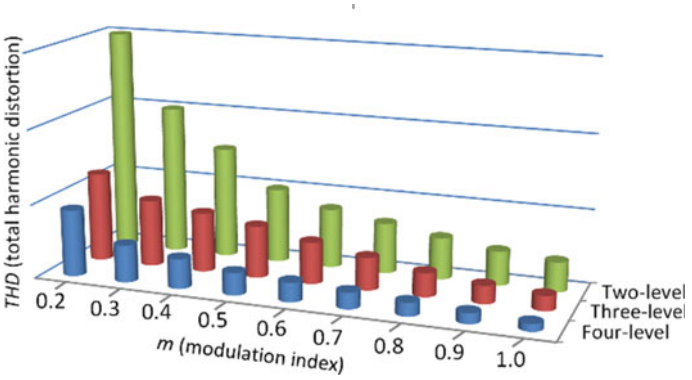

Fig. 7.16 *THD* comparison of the conventional power converter (2 level) and MLI (3, 4 levels) function on the modulation index

The cascade H-bridge inverter has the minimum components for a given number of levels. By connecting in series several H-bridge inverters (Fig. 7.15a), the cascade multilevel H-bridge inverter is obtained. Due to the high number of clamped diodes (Fig. 7.15b) of the NPC, this type of inverter is limited to three-level.

The flying capacitors—MLIs (Fig. 7.15c) contain the capacitors instead of diodes and are balancing on phase buses. The challenge is to balance the DC-link. These MLIs are used in order to obtain a sinusoidal output voltage from different DC sources like *PV*, *fuel cells* or *battery*. The CSI are divided in Load Commutated Inverter and PWM-CSI [16, 17].

In the Fig. 7.16, related to power quality issue, a comparison of the total harmonic distortion (*THD*) function on the amplitude-modulation ratio (modulation index, $m_a = V_m/V_t$ the ratio between the sinusoidal amplitude or the control signal and the carrier voltage as triangular waveform) for two-level and MLI (three, and four-level) waveforms is shown.

From the Fig. 7.16 it could be noted that with number of levels increasing the *THD* decreases. For each level, the *THD* decrease as the modulation index reaches 1 (one) value [8]. The explanation consists of output voltage waveform improving as the number of level increases. These applications are appropriate for *wind energy conversion* due to the high voltage (6.6 kV) and power ratings (1–40 MW) at low switching frequency (below 1 kHz).

7.6.2 Topologies of the DC-DC Static Power Converters

In the Fig. 7.17, the basic configuration of the boost DC-DC power converter is shown. The main disadvantage is that it cannot provide galvanic isolation. In addition, the wide variation in amplitude between input and output puts a strain on the static

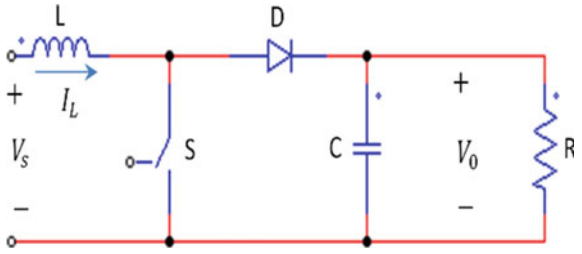

Fig. 7.17 Step-up DC-DC power converter without isolation

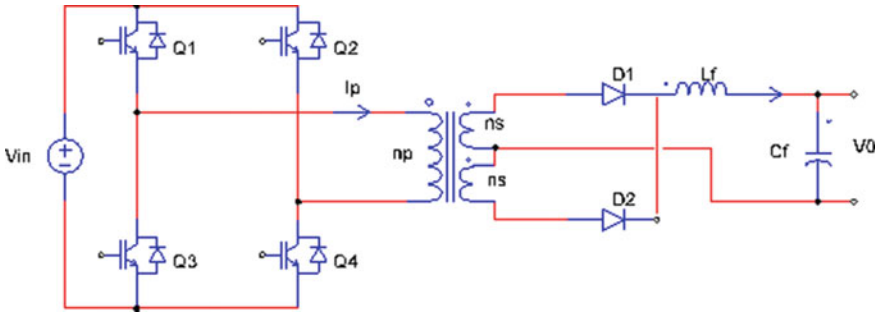

Fig. 7.18 Boost full bridge DC-DC converter with isolation

power device. If galvanic isolation is required, the boost full bridge converter is often employed (Fig. 7.18). For galvanic isolation and a high gain factor, several solutions could be used: full bridge, push-pull, forward power converter or half-bridge power converter.

From the above mentioned isolated power converter the full bridge is preferred for ability to transmit high power By using this type of power converter, the voltage applied to power transistors and the flow current through it are not very high compared with the other isolated power converter. The push-pull and forward power converters are used in high power applications. Compared with the DC-DC half-bridge power converter, the rated current across the devices and the ratio of the transformer are reduced to half. The full bridge power converter assures the low input-output currents and no voltage variation. The full bridge converter topology is preferred in the techniques of pulse width modulation with zero-voltage switch (ZVS).

7.6.3 DC-DC Full Bridge Converter with Multiple Secondary Windings [5]

This topology uses a transformer with multiple secondary devices connected in series (Fig. 7.19). This topology is able to obtain zero voltage switching, leading to a high

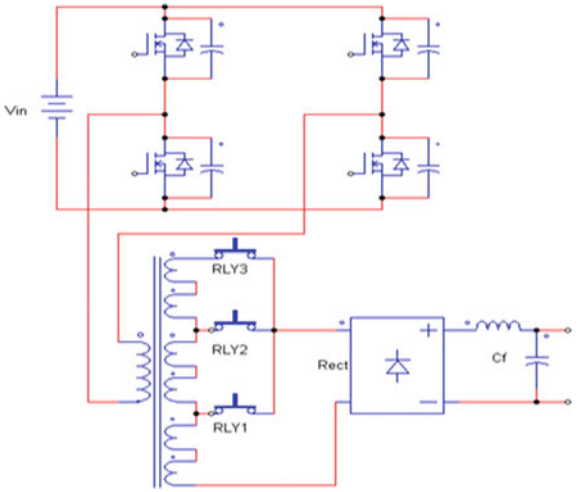

Fig. 7.19 Full bridge DC-DC converter with multiple secondary windings

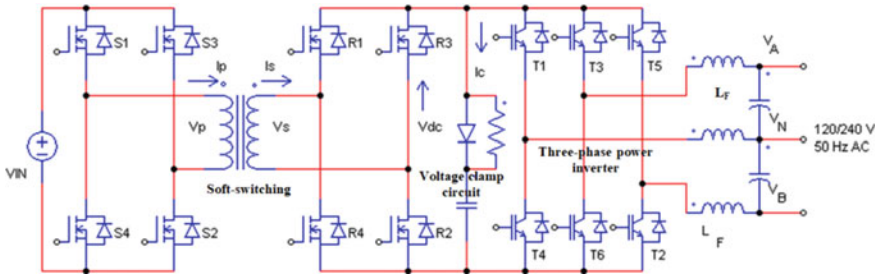

Fig. 7.20 DC-DC soft switching without DC-link

efficiency. This converter allows operation either at constant current or constant voltage; therefore, high flexibility is obtained. The electromechanical relays are used in the secondary transformer windings to control the voltage amplification, allowing appropriate adjustment to the conversion ratio (Figs. 7.20, 7.21, 7.22 7.23, 7.24, 7.25 and Table 7.1).

Remarks in order to provide galvanic isolation or to use the soft-switching techniques the number of components would increase; therefore, the efficiency of the power conversion decreases) [19]; the adequate topology can be chosen only by the designer of the power converters with strong skills. In order to assure a high output voltage despite of low input one, the DC-DC high boost converter is chosen if galvanic isolation is not required.

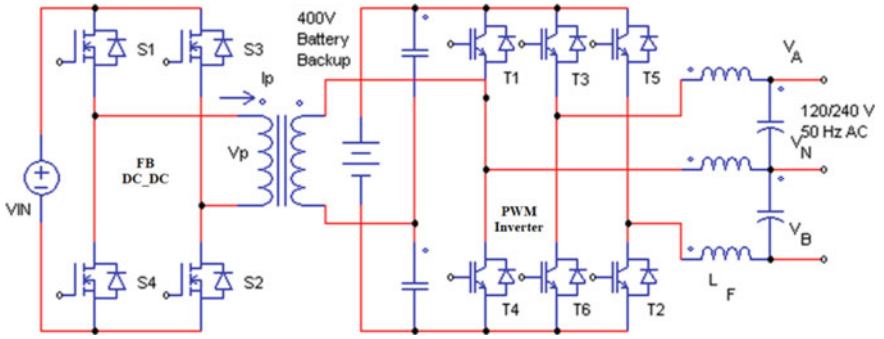

Fig. 7.21 DC-DC voltage doubler

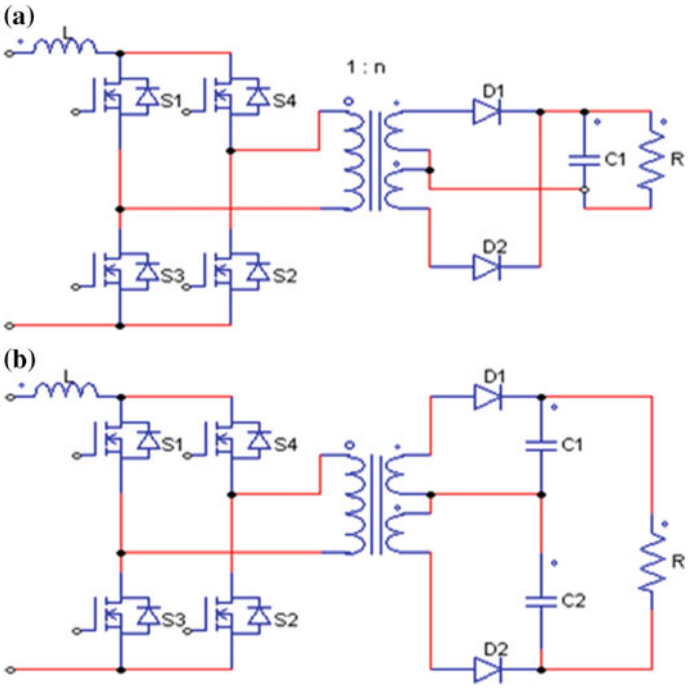

Fig. 7.22 Current injection DC-DC converter, **a** conventional, **b** with voltage doubler

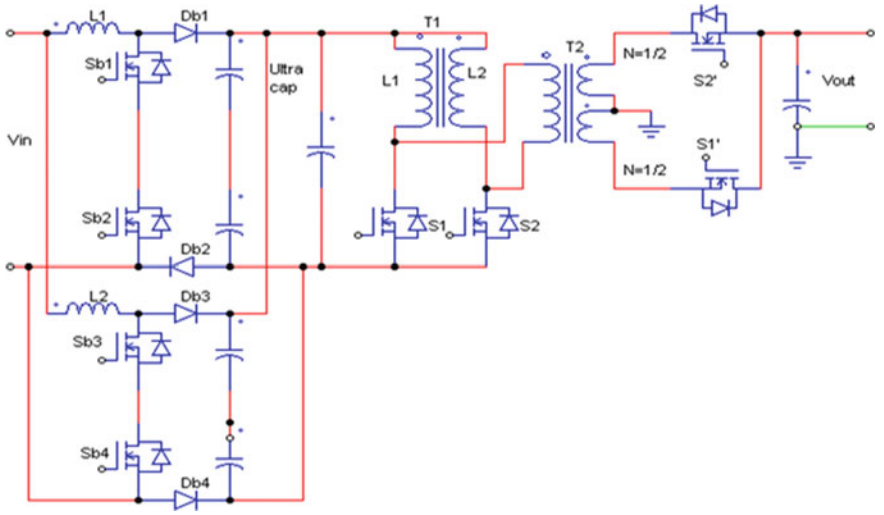

Fig. 7.23 Converter with wide input range

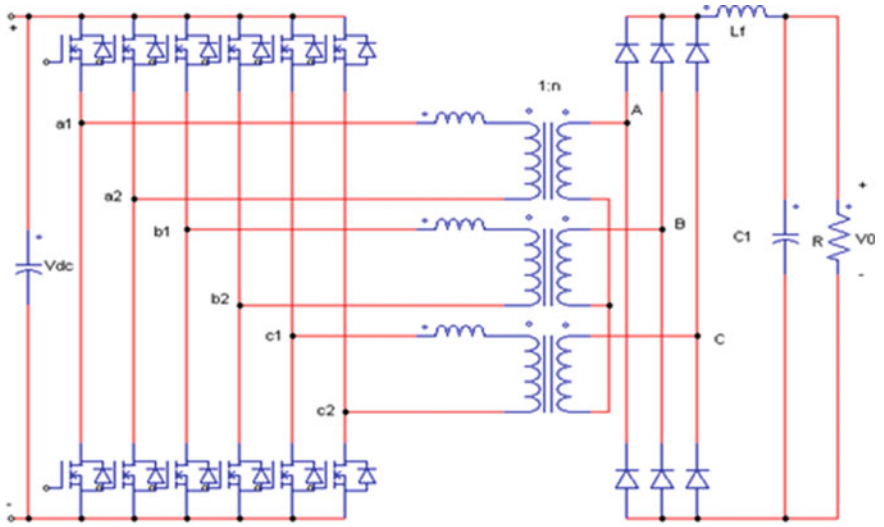

Fig. 7.24 Converter with multiple phases

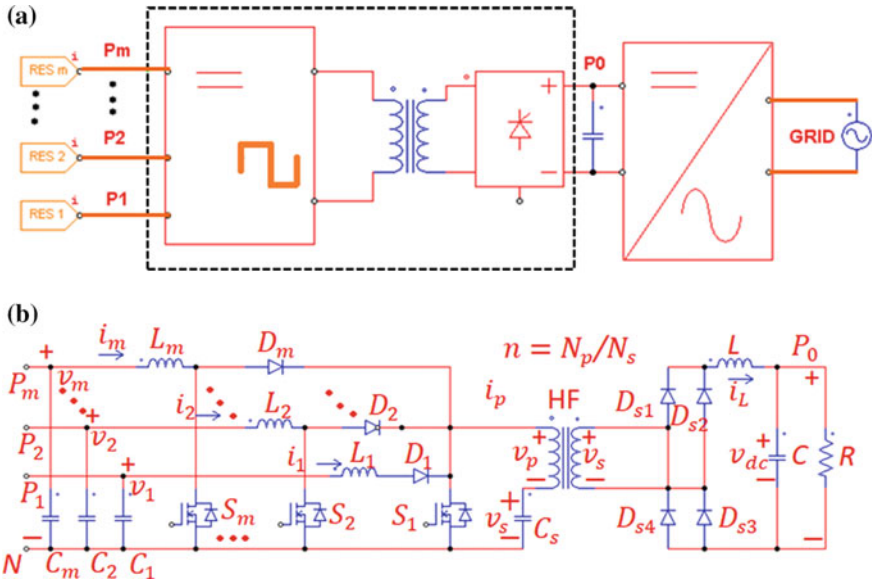

Fig. 7.25 Multiple RES integration into the utility grid: **a** principle, **b** DC-DC converter [16]

Table 7.1 Comparison between different DC-DC converter topologies [18]

Topologies	Advantages	Disadvantages
Boost	Low components, elementary design and control	The inexistence of electrical isolation feature
Full-bridge (FB)	Galvanic isolation; implementation of soft-switching methods (high efficiency); high power	
FB with secondary winding	Electrical isolation; implementation of soft-switching methods (low switching stress); fitted to adjustable transformer-ratio (reduced leakage inductance)	
Soft-switching	Electrical isolation; soft-switching; without DC link capacitor	DC link capacitor is missing (necessary clamp circuit, slow dynamical response)
Voltage doubler	Isolation; implementation of soft-switching methods; due to the reduced leakage inductance the transformer size is reduced; the output current has low ripple	Complex control

(continued)

Table 7.1 (continued)

Topologies	Advantages	Disadvantages
Isolated three-phase transformer	Electrical isolation; based on the soft-switching; use of delta—star connection (additional boost, reduced leakage inductance); high frequency current ripple; modularity	Very complex
Current injection	Electrical isolation; contains a voltage doubler (reduced leakage inductance);	Large inductors required
Converter with wide input range	Electrical isolation; reduced current ripple; independent constant output voltage while input voltage may vary; sizing of the semiconductor devices for low current rating	Very complex
Converter with multiple phases	Galvanic isolation; transformer's secondary star connection allows high output voltage; interleaved connection allows the converter to be controlled so that symmetrical output waveforms are obtained; high efficiency (zero voltage and current switching for a wide variation range), low transformer ratio, high modularity, high frequency of the output signal ripple (the switching frequency is 6 times higher than of the single-phase power inverter). Therefore, the significant reduction of the output filter take place	Complexity of designing a control for 12 static soft-switching devices
Multiport DC-DC RES integration	Electrical isolation, low-cost, simple, minimum components, simultaneous power management of multiple RES, high efficiency	

7.7 Wind Power Conversion Systems

The well-known purpose of the wind power turbines is to extract from the wind kinetic energy the corresponding power. The used generators are synchronous or asynchronous induction. Therefore, the three-phase voltage system can be generated. In order to connect to the grid, the power grid converter should be inserted.

The considered power converter interfaces are as follows:

- The first power interface between the electrical generator and the DC link with variable voltage can be realized through an *active power rectifier*.
- The second power interface between the variable DC voltage provided by the electric generator and the DC link with constant voltage requirement. This task can be performed by using a *unidirectional DC-DC power converter*. Usually, to assure the required voltage level of the power inverter *a step-up (boost) converter* is necessary.

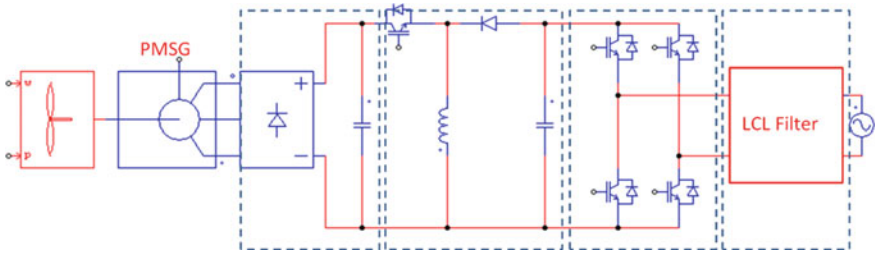

Fig. 7.26 Diode rectifier based wind power converter [20]

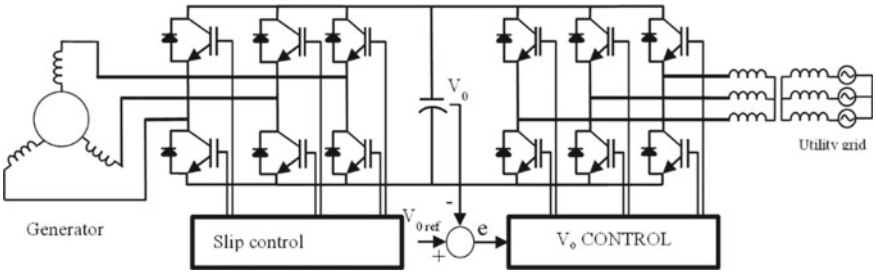

Fig. 7.27 Wind generator with variable speed and constant frequency

– The third power interface is located between battery and DC-link with constant voltage. In order to assure charging and discharging states of the battery a *bidirectional buck-boost* power converter topology is necessary;
– The fourth power interface between the constant voltage DC-link and the AC grid is provided by a three-phase power inverter.

This view provides a basis for different wind power systems design studies.

In the first stage, the wind power conversion is performed through AC generator (Induction generator or permanent magnet synchronous generator) and the appropriate AC-DC power converter (rectifier).

The main types of the AC-DC power converters are: diode rectifier based converter (Fig. 7.26), back to back (Fig. 7.27), back to back converter for connecting wind turbine based on DFIG generator to the three-phase grid (Fig. 7.28), matrix converter (Fig. 7.14b), cycloconverter (Fig. 7.14a), multilevel converters (Fig. 7.15), and Z-source converter (Fig. 7.29).

The power plant in Fig. 7.27 shows a wind generator based on induction machine and frequency inverter. The DC link voltage control of the voltage source converter will maintain the DC link voltage at a constant value. The inverter connected to the generator controls the slip of the generator and adjusts it according to the wind speed or power requirement. The back to back power converter maintain the machine's cos φ power factor independent of the power supply. The same configuration can also be used with synchronous machines.

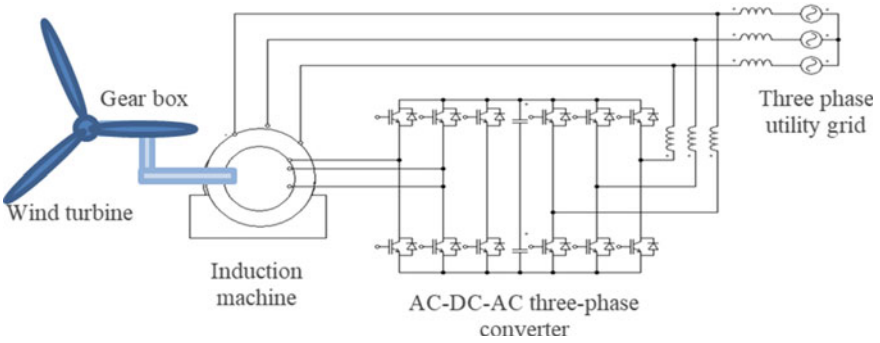

Fig. 7.28 Double-fed induction generation system based on back-to-back converter

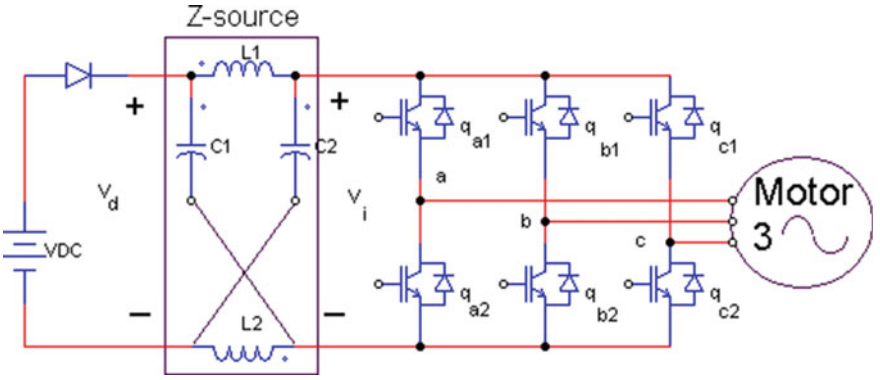

Fig. 7.29 Z-source power converter

The Z-source power converter is an impedance fed power converter. The DFIG cannot be used due to the unidirectional feature of the Z-source power converter. The Z-source power inverter operates both buck voltage mode (by decresing the modulation index) and boost mode (by increasing the modulation index). The low cost Z-source power inverter has high efficiency, it is simple and reliable with wide voltage output range [21].

Neutral-Point-Clamped *multilevel inverter* (*MLI*) has low harmonic content due to delivered three-phase voltages (Fig. 7.30) [22]. The switching losses are low (switching frequency is lower than 500 Hz. Due to the operation at fundamental frequency the reactive power flow is not necessary for switching devices.

Figure 7.31 illustrates the direct network connection of rotating generators without additional power electronics or compensation elements. This configuration can only be considered for high power systems that already include a relatively large fossil fuel generator or a battery system capable of controlling and stabilizing the utility network and providing the necessary reactive power.

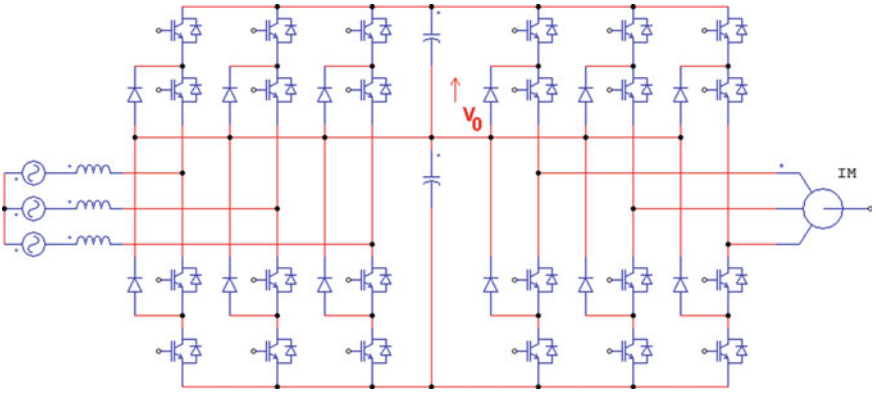

Fig. 7.30 Three-levels MLI: diode clamped

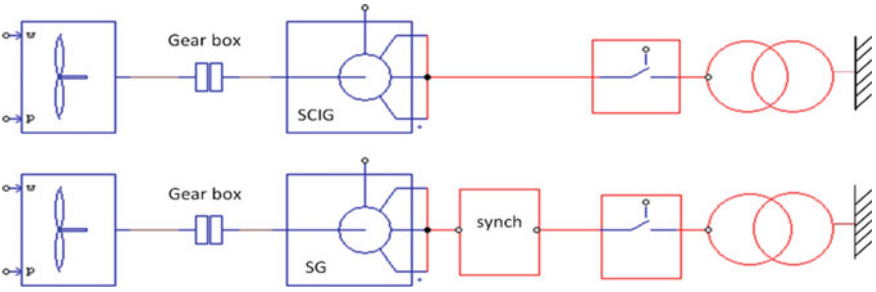

Fig. 7.31 Direct connection to the utility network of asynchronous/synchronous generators

The types of wind power systems can be classified according to: (1) *fixed or constant* including the asynchronous (squirrel cage) generator (SCIG) or synchronous generator (Fig. 7.31). The asynchronous machine absorbs reactive power for magnetization purposes and produces the active power. Therefore, the reactive power should be inserted through the adequate compensator (Fig. 7.32) [23]; (2) variable speed induction generator, based on the *wound rotor induction generator* (*WRIG*). The active pitch control and reactive power components are added to this type (Fig. 7.33) [23]; (3) *Doubly fed induction generator system* (*DFIG*): the rotor side is grid-connected by means of the AC-DC-AC power converter. The advantage of using DFIG system is the size decreasing of the power converter to 40% of power. The rest of 60% goes directly to the utility network. No additional reactive power compensation is necessary (Fig. 7.33). The pitch control, voltage ride-through and fast voltage recovery are included; (4) *Full power conversion*. The induction generator is connected through *back-to-back* power converter designed at full power (Fig. 7.27). Figure 7.32 illustrates the various possibilities for applied power electronics and compensation devices together with rotary generators. They allow modern systems to function in the following ways:

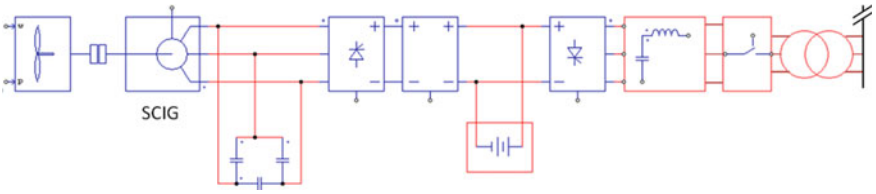

Fig. 7.32 Grid connection with frequency converter and DC link power converter

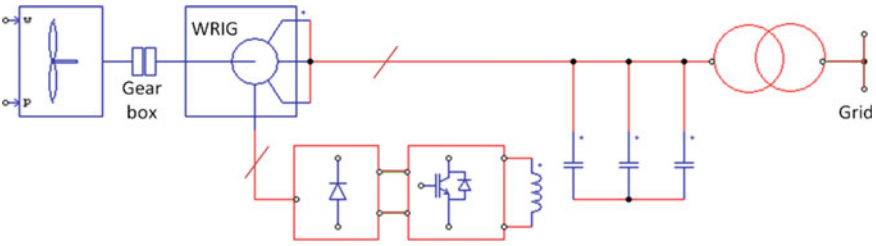

Fig. 7.33 Grid connection with WRIG

(1) grid control or grid forming;
(2) grid connected or grid feeding;
(3) grid supporting.

The *grid forming* (microgrid can be in island operation mode) power system control both the active and reactive power according to the loads such that the voltage and frequecny of the utlity grid are assured adequately. In the case of an asynchronous generator, capacitor batteries may be used to meet the demand for excitation of the reactive power generator required by its own system. The grid will therefore be exempted from the reactive power demand and in principle such a system will be able to control and work alone in the grid.

In order to stabilize the fluctuating voltage generated by the variable speed generator at a continuous and constant voltage value the DC-DC power converter is used. The first advantage is the simple connection of the rectifier and the inverter. The second advantage is the possibility of using a battery in the DC-link circuit.

Grid-feeding power converter delivers the appropriate active and reactive power to fulfill the requirements of the power dispatch [24]. Moreover, the power converter compensates power flow fluctuations and the load variations in the feeder.

Grid-supporting power converter is used to extract maximum active power from the power source, and to improve the power quality [10, 24].

If the inverter can operate in *grid control mode*, the battery can be used as a safety supply for short network interruptions, but also for balancing the energy fluctuations produced, for example from a wind turbine.

In order to generate sinusoidal voltage, even with low quality inverters, LC or LCL filters can be used at the inverter output.

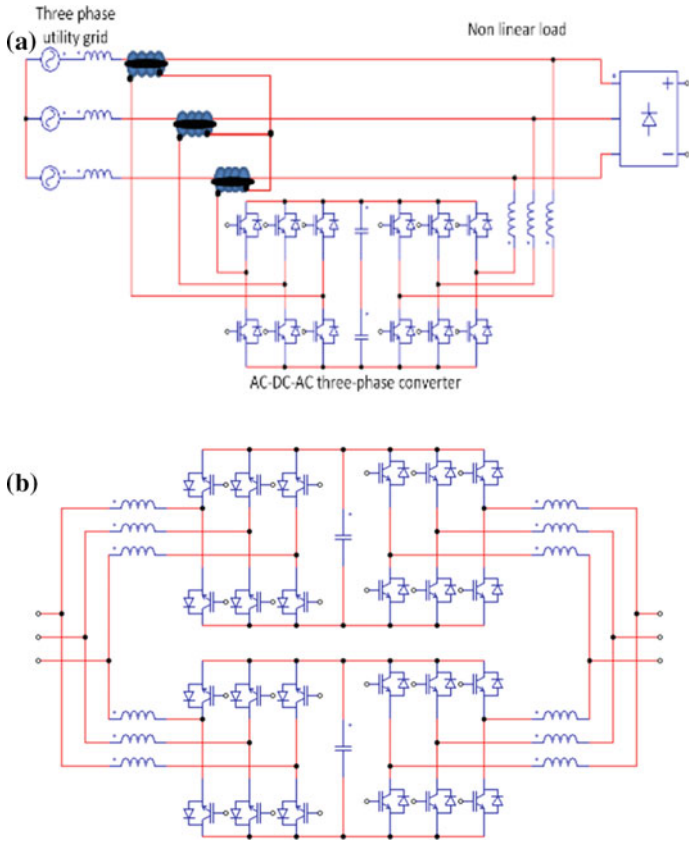

Fig. 7.34 BB power converter as **a** active power filter, **b** parallel connection

In wind power conversion systems the *back-to-back* (*BB*) power converter can be connected in series or parallel as active filters (Fig. 7.34a). The nonlinear three-phase load is supplied by means of the BB power converter from the main grid.

The parallel connection of the BB power converters is the used as the solution for high power manipulation (Fig. 7.34b). Moreover, the quality of the output and input signals are improved [10]. Depending on the power inverter characteristics, such a system can deliver the requested reactive power in the control-grid mode or to succesfully perform the reactive power balance in the grid support mode.

Using an asynchronous generator without a battery system, but along with a frequency converter, the bidirectional power converters are necessary. In this situation, the reactive power across the utility network to the generator and the active power from the generator to the network must be transferred simultaneously. The cost of the power electronic converters increases as the power increases.

7.8 Photovoltaic Power Conversion System

The photovoltaic panels are considered as power source by converting energy from sunlight to electrical power. The photovoltaic panels consist of photo cells connected in modules or arrays. Advanced Power Converter Systems should include solutions to power system challenges being a right pathway for increasing in depth and fast penetration of the RES (Renewable Energy Sources) into power system. They actively support the utility network parameters: voltage and frequency, are more robust tor grid disturbances, and actively monitor and control the microgrid via communications.

The existing installed *photovoltaic* (*PV*) power systems, the near future capacity development planning of the PV power systems and the necessity of growing of the power distribution systems conduct to finding the emergent solution of adapting the electrical parameters of the PV power systems to the utility network [12]. The photovoltaic modules delivers the DC voltage. Therefore, the power conversion system consists mainly of the series connected MPPT (maximum power point tracking) controlled step-up DC-DC power converter with grid-connected power inverter. The PV systems with backup power (battery) will add a vidirectional dc-dc power converter for charging/discharging the battery bank.

The low efficiency of the solar energy conversion (11–18%) through the PV module or array is compensated by introducing high efficiency power inverter.

7.8.1 Transformerless Inverters

The topolgies are classified as it follows: full bridge totpology, half-bridge topology (**NPC Based Inverter Structures**), DC side decoupling and AC side decoupling [25, 26].

7.8.2 Full Bridge Topology

The *High Efficiency Reliable Inverter Concept* (*HERIC*) concept is used by Sunways (2.7–5 kW commercialized power inverter). The topology of the power inverter consists of a bipolar PWM H-bridge (or FB-full bridge) and a bypass branch formed by two IGBTs connected back to back. The HERIC invertor is presented in Fig. 7.35 [25]. The lower switches S4 (S2) are force commutated at high frequency. Instead, there is a grid frequency commutation of the upper switches S1 (S3). On the AC side, the purpose of the bypass switching is to improve the current mode voltage changes. By switching ON the S+ (S−) switches the zero output voltage states are obtained (the H bridge state is switched OFF).

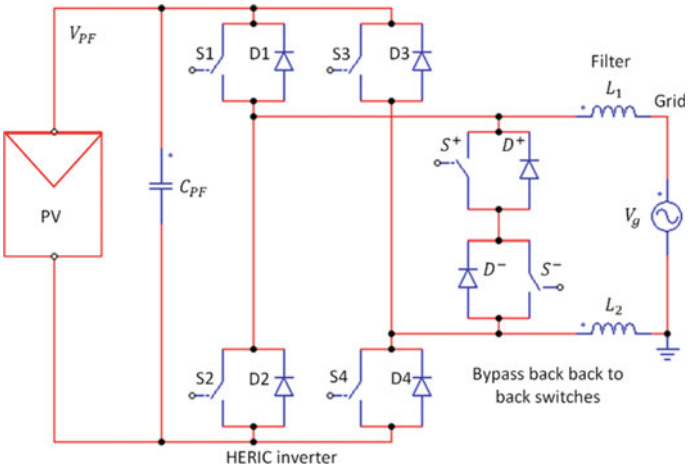

Fig. 7.35 HERIC topology of the power inverter (Sunways) [19]

Different FB HERIC inverter topologies have been developed: REFU Solar Inverter (11/15 kW) [27], FB-DCBP (Ingeteam) Inverter (2.5/3.6/6 kW) introduces of DC bypass in FB power inverter topology, *Full-Bridge Zero Voltage Rectifier-Inverter,* FB-ZVR.

For the several kilowatts, the photovoltaic generators are connected to the DC-module converter. The DC-module converters are series or parallel connected to one phase or three-phase power inverter. Up to 10 kW the string inverters collect the energy from the PV strings. For the [10, 27] kW range, the multiple PV strings connected to the common DC link through DC-DC converters supply the energy to the multi-string inverter. For the delivered power more than 30 kW the three-phase central inverter converts the power from the PV strings into the AC grid. Therefore, the power inverters for PV energy conversion are module level (AC and DC), string, multi-string, and central. String, multistring, and modular concept power inverters are the used types in the single-phase PV power systems [27]. In the three-phase topology of the PV systems the central inverter is used.

Half bridge topology (NPC Based Inverter Structures) classification: NPC Half Bridge Inverter (made by Danfoss Solar Inverter) with series TripleLynx (three-phase in power range of [10, 15] kW, *Conergy NPC Inverter* (patented by Conergy in string inverter IPG in power range of [2–5] kW), *oH5*—there is an optimized technology of the H5 power inverter, multilevel power inverter connected to the grid, *HRE*—high reliable and efficient power inverter, *HR-ZVR*—hybrid zero voltage rectifier configuration.

A DC fault current in the transformerless power inverter topology can take place; therefore, diminishing the personal safety (Fig. 7.36). Taking into account the above mentioned remark, the DC Residual Current Monitoring Unit (RCMU) is necessary. The classical RCDs are sensitive only to AC fault currents. The German safety

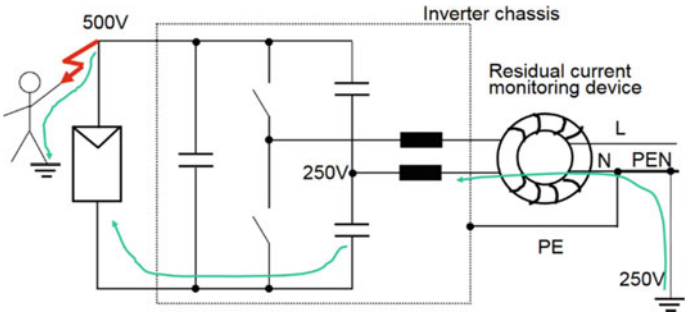

Fig. 7.36 Transformerless power inverter topology [28]

Standard DIN VDE 0126, requires an automatic AC disconnect interface, redundancy and one-fault tolerance; anti-islanding (the test is specified in UL 1741), DC current injection. The standard specify the RCMU test.

7.9 Case Study: AC Microgrid

In order to achieve the above mentioned objectives, a generic block diagram of the grid power inverter delivering the energy from RES, with local load connected at Point of Common Coupling (PCC) is proposed in Fig. 7.37. Microgrids are island systems for local utility or energy distribution systems and contain at least one distributed power source and a corresponding load.

The energy sources of a microgrid can be disconnected and reconnected to utility grid. For the *grid-connected mode*, the hybrid topology of the RES integration is shown in Fig. 7.38 [29].

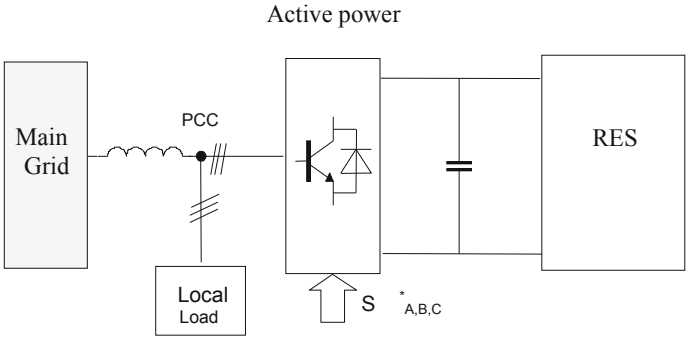

Fig. 7.37 RES integration into the main grid through the power inverter

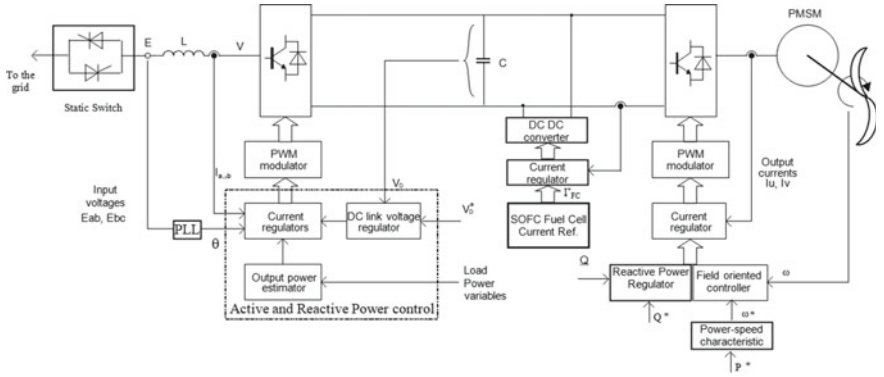

Fig. 7.38 Hybrid topology for RES integration [29]

The RES consists of the wind turbine and solide oxide fuel-cell generation system (Fig. 7.38). The proposed power conversion system derives from the all ready past research of the author [29]. The improvements consists of power loop integration in the inverter utillity grid, only one DC voltage converter is involved, and robust grid synchronization algorithm has been involved.

The control scheme is in cascaded manner [29], as depicted in Fig. 7.38. Another contribution is the transformation of the hybrid topology into a microgrid by adding a voltage controller.

Distributed generation (DG) concept is embedded in the proposed block diagram, the RES is closely exploited to the PCC in which the loads (consummers) are connected. This topology allows to avoid the expansion of the power transmission system [30]. Recently, in order to increase the reliability and to avoid the blackouts the intentional islanding concept has been introduced [30–32].

The features of the Microgrid should include two operation modes (island mode of operation and grid connected) and smooth transfer between them [30].

Intentional islanding is very helpful during disturbances on the power grid. In this manner, the local consummers can be supplied locally by the existing RES [29]. The control techniques used in distributed generation are as follows: voltage control for island operation mode and current control for grid-connected operation mode.

For the grid-connected mode the control task is to deliver current references for the system by using the measured inverter voltages and desired power levels. By using the power balance concept, the grid power inverter provides the currents into the main grid, and controlling the DC link voltage.

In the islanding mode of operation the system is disconnected from the utility; therefore the voltage is no longer regulated by it. The control needs to actively regulate the voltage of the Local Load. The control can work by using the voltage regulation through current compensation.

The inverter controllers have been generally inspired by control techniques of motor drives that are typically balanced loads. However, a distributed generation

inverter needs to operate in an ambient with a broader degree of variability [26]: steady state and transient imbalances in the utility grid voltage [26, 27] and, in case of stand-alone mode, persistent imbalance in loads due to single-phase distribution circuits. Under such conditions the system requires implementation of more complicated controllers [29].

In conclusion, the main requirements on the utility network converter can be summarized as follows:

1. Adjustable power factor operation
2. Low input current harmonics
3. Optimization of the system's reactive components
4. Energy optimization (maximize the use of the available power)
5. Maintain a continuous supply with voltage and frequency within required limits
6. The system with full-scale converter must be easily adapted to different grid requirements.

7.9.1 Pulse Width Modulation Strategies

Fourth types of pulse width modulation techniques have been simulated and numerically implemented on DS1104 platform:

(1) sinusoidal PWM;
(2) third harmonic insertion;
(3) space vector-PWM;
(4) optimized modulation.

By using Matlab Simulink programming environment, the simulation results are provided [33]. In order to reduce the total harmonic distortion factor and to increase the power converter efficiency various pulse width modulation techniques were studied: sinusoidal PWM (Fig. 7.39a), space vector PWM (Fig. 7.39b), third harmonic insertion (Fig. 7.39b), optimized modulation (Fig. 7.39c), and the zero sequence signal generation by the adequate Simulink modulator and the generated signal by simulation (Fig. 7.40a,b).

The experimental results obtained through the dSpace platform are presented as follows (Figs. 7.41, 7.42, 7.43, 7.44, 7.45).

7.9.1.1 Sinusoidal PWM

See Figs. 7.41 and 7.42.

7.9.1.2 Third Harmonic Insertion

See Figs. 7.43 and 7.44.

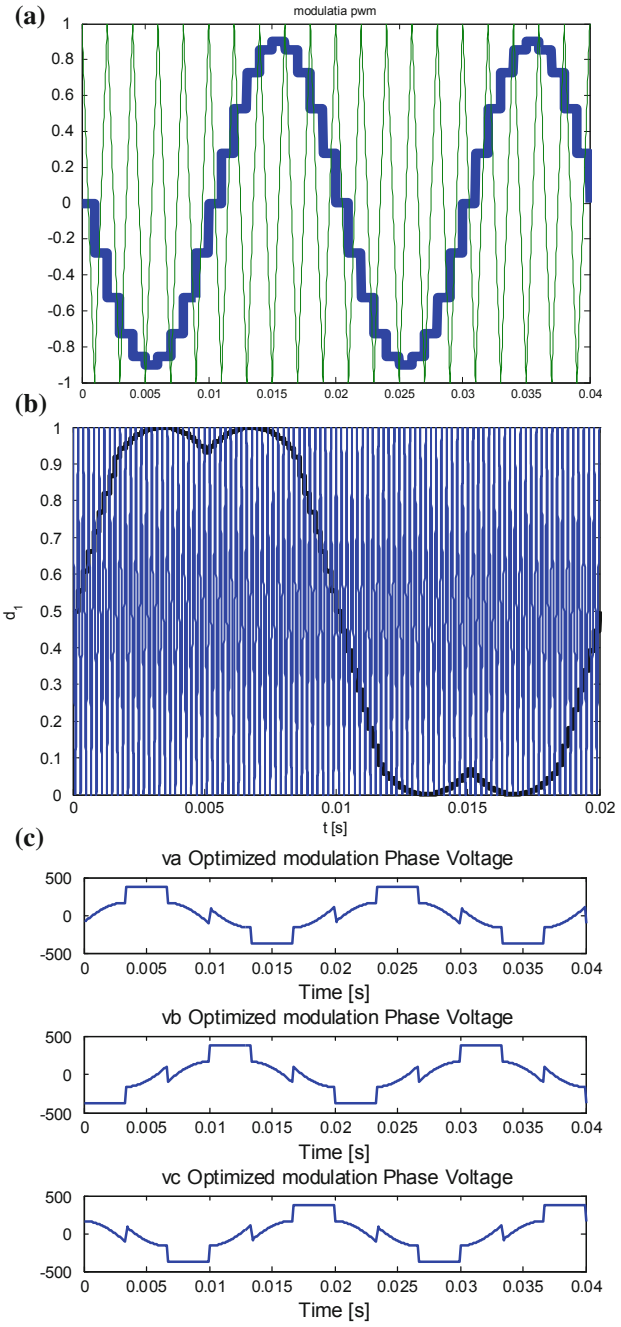

Fig. 7.39 **a** Simulation results: sinusoidal PWM, **b** SV-PWM, **c** optimized modulation

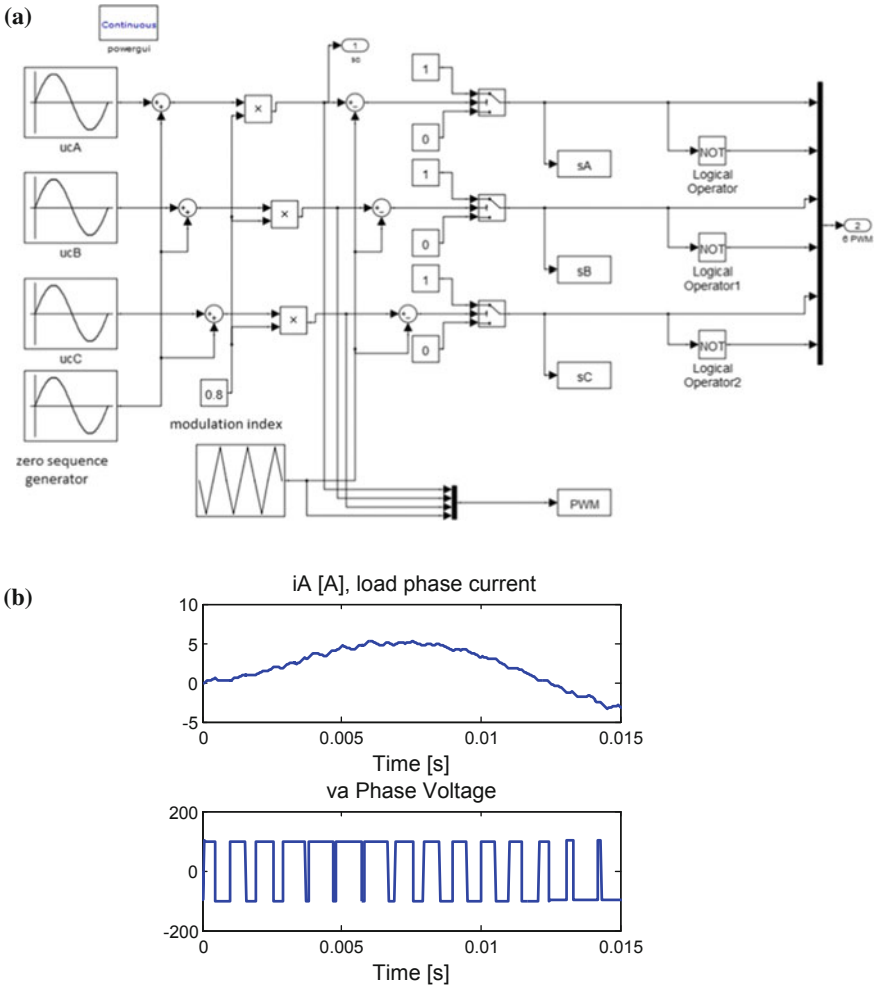

Fig. 7.40 **a** Zero sequence signal generation by the adequate Simulink modulator, **b** and the generated signal by simulation on RL load

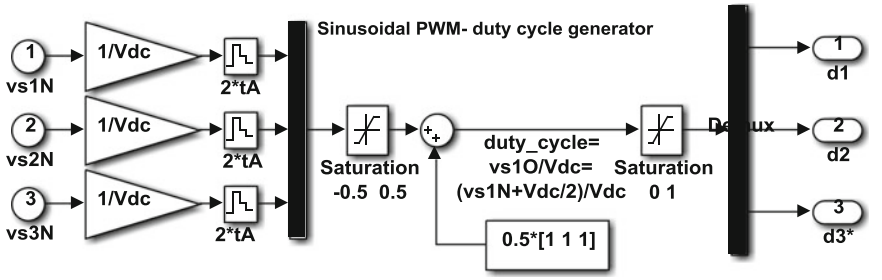

Fig. 7.41 Sinusoidal PWM modulator

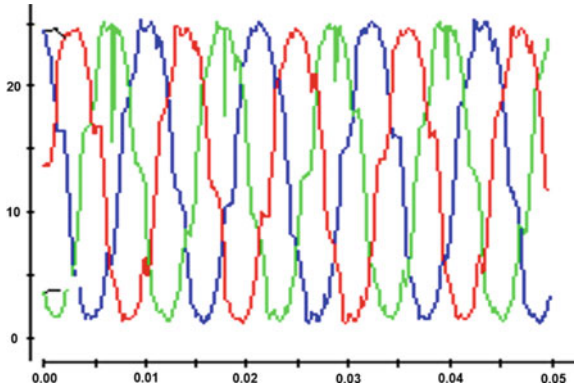

Fig. 7.42 The experimental modulated voltages

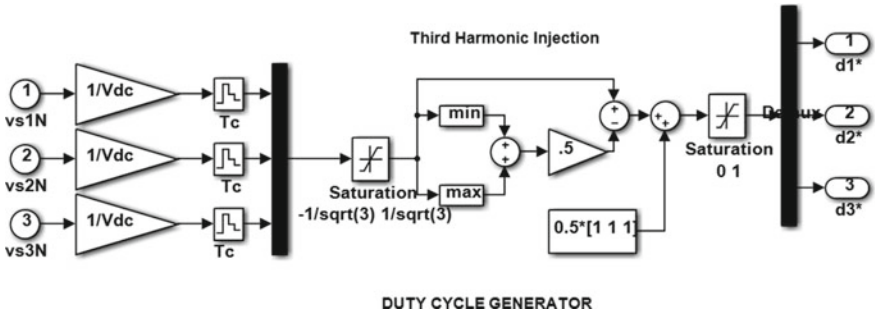

Fig. 7.43 Third harmonic injection modulator

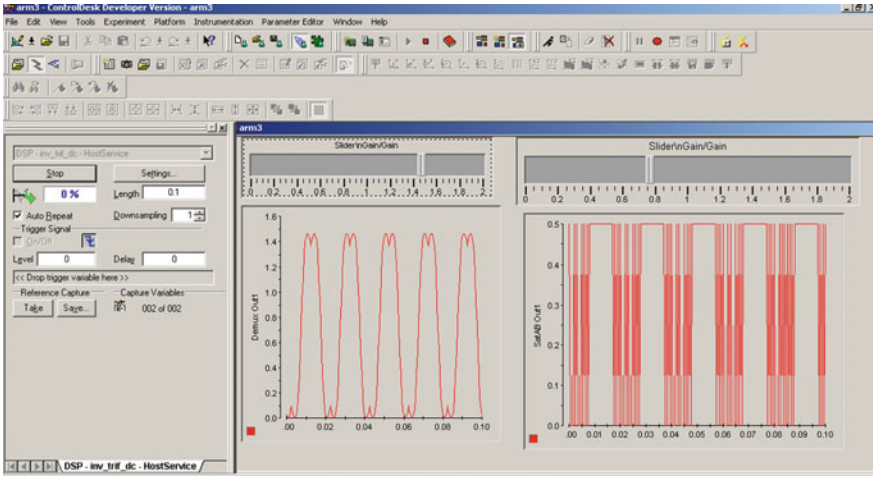

Fig. 7.44 The generated duty cycles by using dSpace platform

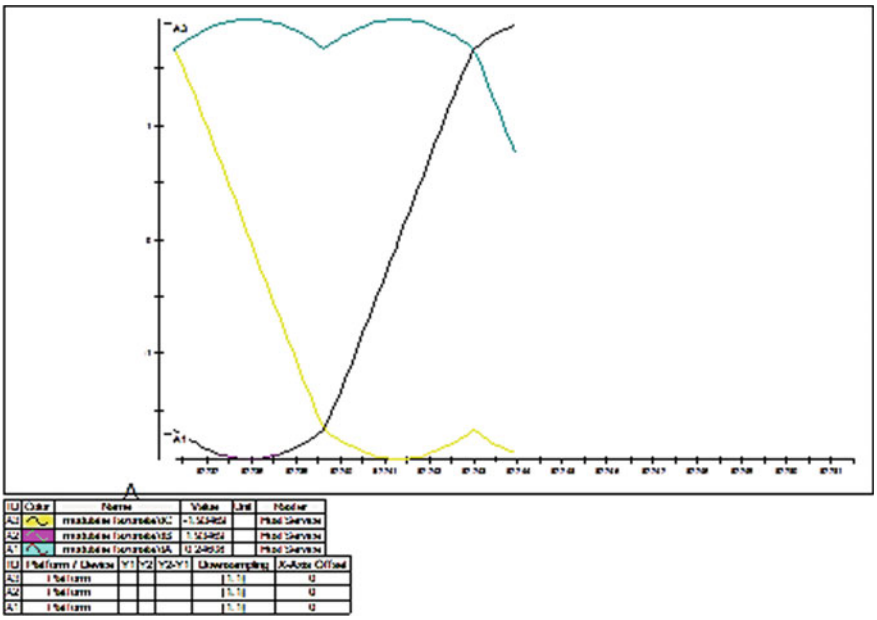

Fig. 7.45 The generated duty cycles for SVM-PWM, transient behaviour

7.9.2 Space Vector PWM

See Fig. 7.45.

7.9.3 Simulation Results on the Proposed Topology

From the simulation results, both the active current and reactive current regulators can be concluded that are correct tuned. The DC-link voltage controller assures the voltage regulation on the DC link capacitor and fast rejection of the perturbation. Unity power factor operation and bidirectional power flow are demonstrated in the Figs. 7.46, 7.47.

7.10 Conclusions

The chapter presents an overview of the power converters used in AC microgrids. The specific power topologies for both wind power and sunlight power integration are presented. The requirements imposed by the adequate standards are discussed.

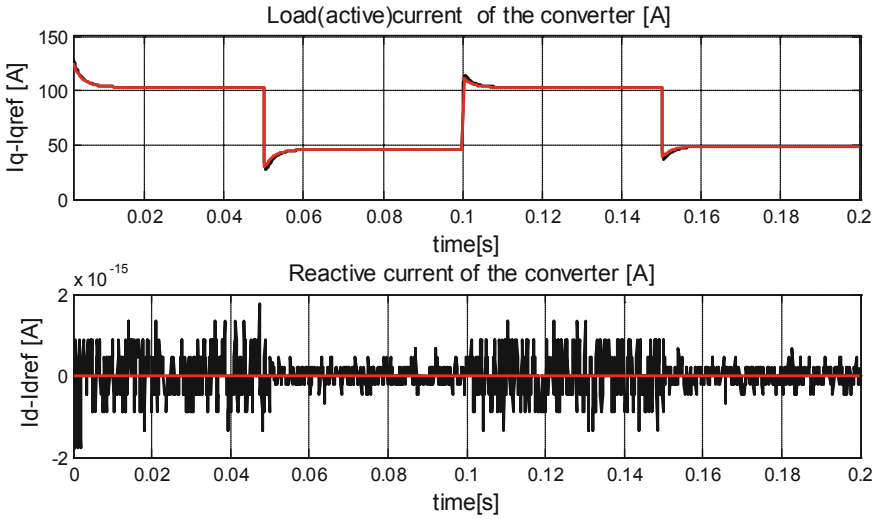

Fig. 7.46 Test on current regulators: active currents, and reactive currents (reference and the feedback current)

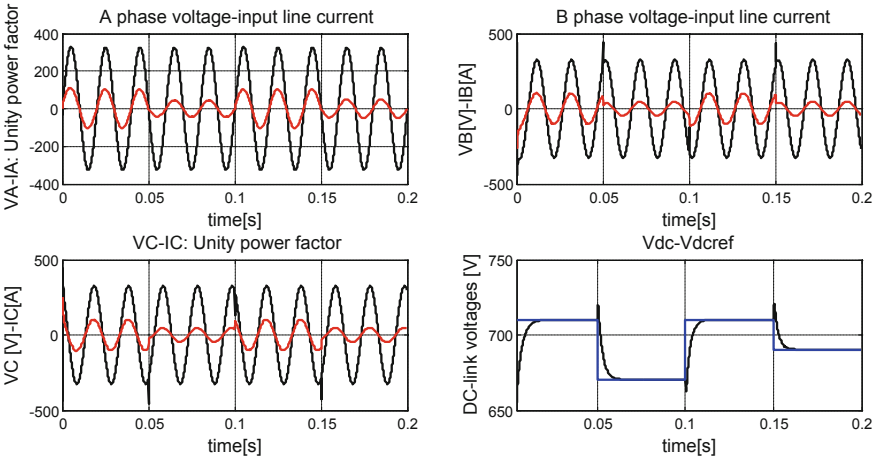

Fig. 7.47 Unity power factor operation and the DC link voltage controller

One solution as AC microgrid has been proposed. The main modulation techniques have been simulated and practical implemented by means of dSpace platform.

The chapter addresses the technical challenges of network interconnection to meet the requirements of utilities, including power quality, system stability and dynamic performances.

Acknowledgements This work was supported by a grant of the Romanian National Authority for Scientific Research, CNDI–UEFISCDI, project number PN-II-PT-PCCA-2011-3.2-1680.

References

1. L. Azar, G. Bindewald, Ch. Clark, J. Davenport, J. Downes Angus, I. Gyuk, M. Johnson, S. Landsberg, K. Lynn, D. Meyer, W. Parks, R. Ram, Visioning the 21st Century Electricity Industry: Outcomes and Strategies for America (U.S. Department of Energy, Draft Vision of a Future Electric Grid, National Electricity Forum) (February 8–9, 2012)
2. Ch. Wang, Zh. Li, D.L.K. Murphy, Z. Li, A.V. Peterchev, S.M. Goetz, Photovoltaic multilevel inverter with distributed maximum power point tracking and dynamic circuit reconfiguration, in *IEEE 3rd International Future Energy Electronics Conference and ECCE Asia (IFEEC 2017—ECCE Asia)*, Kaohsiung, China Taiwan (June 2017)
3. https://www.iea.org/weo2017/. Accessed 2018
4. B. Dudley, BP Energy Outlook 2030. https://www.bp.com/content/dam/bp/en/corporate/pdf/energy-economics/energy-outlook/bp-energy-outlook-2011.pdf. Accessed 2018
5. IEA, Grid Integration of Large-Capacity Renewable Energy Sources and Use of Large-Capacity. Electrical Energy Storage, White Paper (2012)
6. http://mpaenvironment.ei.columbia.edu. Accessed 2018
7. G. Dehnavi, Coordinated Control of Power Electronic Converters in an Autonomous Microgrid. Doctoral dissertation, 2013, http://scholarcommons.sc.edu/etd/2175. Accessed 2018
8. E. Cipriano Dos Santos, E.R. Cabral Da Silva, *Advanced Power Electronics Converters PWM Converters Processing AC Voltages* (Wiley, The Institute of Electrical and Electronics Engineers, 2015)
9. IEC, Grid integration of large-capacity renewable energy sources and use of large-capacity electrical energy storage. White paper (2012)
10. A. Keyhani, *Design of Smart Power Grid Renewable Energy Systems* (Wiley, Publication, 2011)
11. S. Pendharkar, GaN and SiC enable increased energy efficiency in power supplies. Texas Instrument (March 2018)
12. L.B.G. Campanhol, S.A. Oliveira da Silva, A. Albano Oliveira, V.D. Bacon, Power flow and stability analyses of a multifunctional distributed generation system integrating a photovoltaic system with unified power quality conditioner. IEEE Trans. Power Electron. 1–16 (2018)
13. T.D. Trung, Stability, voltage performance and power sharing issues of inverter-based microgrids via LMI optimization. M.Sc. Thesis (2018)
14. O.A. Ahmed, J.A.M. Bleijs, An overview of DC-DC converter topologies for fuel cell-ultracapacitor hybrid distribution system. Renew. Sustain. Energy Rev. (2015)
15. I. Batarseh, A. Harb, *Power Electronics* (Springer Nature, 2018)
16. S. Tahir, J. Wang, M.H. Baloch, Gh.S. Kaloi, Digital control techniques based on voltage source inverters in renewable energy applications: a review. Electronics, **7**(18) (2018)
17. R. Lizana, S. Rivera, Zh. Li, J. Luo, A.V. Peterchev, S. Goetz, Modular multilevel series/parallel converter with switched-inductor energy transfer between modules. IEEE Trans. Power Electron. (2018)
18. X. Yu, M.R. Starke, L.M. Tolbert, B. Ozpineci, Fuel cell power conditioning for electric power applications: a summary. IET Electr. Power Appl. **1**(5), 643–656 (2007)
19. M. Xu, L. Zhang, Y. Xing, L. Feng, A novel H6-type transformerless inverter for gridconnected photovoltaic application, in *7th IEEE Conference on Industrial Electronics and Applications (ICIEA)* (2012)
20. H.G. Jeong, R.H. Seung, K.B. Lee, An improved maximum power point tracking method for wind power systems. Energies **5**(5), 1339–1354 (2012)
21. U. Supatti, Low cost z-source converter/inverter system for wind power generation. Ph.D. Thesis, Michigan State University (2011)

22. R. Palanisamy, K. Selvakumar, P. Kumar Sinha, D. Sen, A. Kumar, 3-Phase 3-Level transformerless neutral point clamped inverter for wind energy system. Int. J. Control Theor. Appl. **10**(16) (2017)
23. Stadtwerke Karlsruhe GmbH, Karlsruhe, Germania; Solarpraxis AG, Berlin, Germany
24. X. Wang, J.M. Guerrero, F. Blaabjerg, Zh. Chen, A review of power electronics based microgrids. J. Power Electron. (2012)
25. R. Aparnathi, V.V. Dwivedi, Design and simulation low voltage single-phase transformerless photovoltaic inverter. TELKOMNIKA Indonesian J. Electr. Eng. **12**(7), 5163–5173 (2014)
26. T. Orlowska Kowalska, F. Blaabjerg, J. Rodriguez, *Advanced and Intelligent Control in Power Electronics and Drives* (Springer, 2014), The H5 topology, patented by SMA manufacturing company on Sunny Boy converter, Assures up to 98% efficiency
27. K. Zeb, I. Khan, W. Uddin, M. Adil Khan, P. Sathishkumar, T.D. Curi Busarello, I. Ahmad, H.J. Kim, A review on recent advances and future trends of transformerless inverter structures for single-phase grid-connected photovoltaic systems. Energies (2018)
28. https://www1.eere.energy.gov/solar/pdfs/16_panhuber.pdf. Accessed 2018
29. M. Gaiceanu, G. Fetecau, Grid connected wind turbine-fuel cell power system having power quality issues, EPQU'07 Barcelona (2007), pp. 7–13
30. S. Bolognani, M. Zigliotto, A space-vector approach to the analysis and design of three-phase current controllers. Conf. Rec ISIE **2002**(2), 645–650 (2002)
31. A. von Juanne, B.B. Banerjee, Assessment of voltage unbalance. IEEE Trans. on Power Deliv. **16**(4), 782–790 (2001)
32. M.H.J. Bollen, Fast assessment methods for voltage sags in distribution systems. IEEE Trans. Ind. Appl. **32**(6), 1414–1423 (Nov/Dec 1996)
33. A. Tounsi, H. Abid, M. Kharrat, Kh. Elleuch, MPPT algorithm for wind energy conversion system based on PMSG, in *18th International Conference on Sciences and Techniques of Automatic Control and Computer Engineering (STA)*, 2017

Chapter 8
Energy Storage Systems in Microgrid

Horia Andrei, Marian Gaiceanu, Marilena Stanculescu, Paul Cristian Andrei, Razvan Buhosu and Cristian Andrei Badea

Abstract The microgrid represents a controllable electric entity that contains different loads into distributed energy resources. All typical microgrids use two or more sources by which electricity is generated, at least one of which is a renewable source. In this respect the main issues of the energy storage systems (ESS) are the enhancing of the stability of microgrid and power balance. Also the insertion of the energy storage systems is beneficial for both operation modes of microgrids, grid connected and islanded. This chapter begins with an overview of the current state of microgrids and ESS. The island operation mode of microgrids is based on the energy storage system. At the first level the control tasks during this mode of operation are to regulate the voltage and to maintain the frequency at the constant value. The power in each unit is shared among the storage units by secondary control of the energy storage system taking into account the energy level of each of them. Further, the authors present storage technologies of the electrical energy, i.e. converting it into mechanical, chemical, electrochemical, electromagnetic and thermal energy. The widespread mechanical energy storage technology is the pumped hydro

H. Andrei (✉)
Doctoral School of Engineering Sciences, University Valahia of Targoviste, Targoviste, Romania
e-mail: hr_andrei@yahoo.com

M. Gaiceanu · R. Buhosu
Department of Automation and Electrical Engineering, Dunarea de Jos University of Galati, Galati, Romania
e-mail: marian.gaiceanu@ugal.ro

R. Buhosu
e-mail: razvan.buhosu@ugal.ro

M. Stanculescu · P. C. Andrei
Department of Electrical Engineering, Polytechnic University of Bucharest, Bucharest, Romania
e-mail: marilena.stanculescu@upb.ro

P. C. Andrei
e-mail: paul.andrei@upb.ro

C. A. Badea
Interface Engineering, Bucharest, Romania
e-mail: bcristianandrei@yahoo.com

N. Mahdavi Tabatabaei et al. (eds.), *Microgrid Architectures, Control and Protection Methods*, Power Systems,
https://doi.org/10.1007/978-3-030-23723-3_8

(99% of the world total storage capacity) followed by the compressed air energy and flywheel. Afterwards, the fuel cell, biomass and fossil fuel compose the chemical storage domain. Batteries constitute the electrochemical storage technology. Electromagnetic and thermal energy storage technologies are represented by the super capacitors respectively the heat pumps. Both the features of the energy Storage technologies and the main properties will be presented. A comparison of the discharge time of the storage technologies by application is taken into account. The advantages and disadvantages of the storage technologies will be highlighted. The lack of the appropriate standards of interconnecting different kinds of energy sources and ESS to the microgrid is a disadvantage in technology developing. Thereby the IEC/ISO 62264 standards refers to wind turbine technology, while the IEEE 2000 standard refers to photovoltaic interconnection power systems. In order to reduce air pollution and mitigate climate change, in recent years the need to use renewable energy sources in microgrids has become important. In fact, technological development, public and political policies, availability of different renewable energy resources to be used in microgrids, are elements that create real perspectives in widespread development of renewable energies and their required ESS. The environmental impact and the costs of renewable energy resources have been estimated through the life cycle assessment (LCA) methodology, which determines whether the use of renewable sources and ESS is sustainable. A case study regarding a PV system with and without batteries used into a microgrid that supply a wastewater treatment plant situated in Romania will be presented. Life cycle assessment was used to quantify ecological sustainability and costs in both cases compared to a conventional supply of electricity from the grid. Conclusions and measures are drawn in order to increase the utilization of renewable sources and ESS in microgrids. Also the technically, economic and environmental benefits of inserting microgrids are discussed. The bibliographic references will be presented at the end of the chapter.

Keywords Microgrid · Energy storage systems · Storage technology · Standards

8.1 Introduction

Generally speaking, a controllable electric entity that contains different loads into distributed energy resources form a microgrid. All typical microgrids use two or more sources by which electricity is generated, at least one of which is a renewable source. In this respect the main issues of the energy storage systems (ESS) are the enhancing of the stability of microgrid and power balance. Also the insertion of the energy storage systems is beneficial for both operation modes of microgrids, grid connected and islanded.

This chapter starts by presenting an overview of the current state of microgrids and ESS. The island operation mode of microgrids is based on the energy storage system. At the first level the control tasks during this mode of operation are to regulate the voltage and to maintain the frequency at the constant value. The power in each unit

is shared among the storage units by secondary control of the energy storage system taking into account the energy level of each of them.

Further, the authors present storage technologies of the electrical energy, i.e. converting it into mechanical, chemical, electrochemical, electromagnetic and thermal energy. The widespread mechanical energy storage technology is the pumped hydro (99% of the world total storage capacity) followed by the compressed air energy and flywheel. Afterwards, the fuel cell, biomass and fossil fuel compose the chemical storage domain. Batteries constitute the electrochemical storage technology. Electromagnetic and thermal energy storage technologies are represented by the supercapacitors respectively the heat pumps. Both the features of the energy storage technologies and the main properties will be presented. A comparison of the discharge time of the storage technologies by application is taken into account. The advantages and disadvantages of the storage technologies will be highlighted.

The lack of the appropriate standards of interconnecting different kinds of energy sources and ESS to the microgrid is a disadvantage in technology developing. Thereby the IEC/ISO 62264 standard refers to wind turbine technology, while the IEEE 2000 standard refers to photovoltaic interconnection power systems.

In order to reduce air pollution and mitigate climate change, in recent years the need of using renewable energy sources (RES) in microgrids has become important. In fact, technological development, public and political policies, availability of different renewable energy resources to be used in microgrids, are elements that create real perspectives in widespread development of RES and their required ESS. The environmental impact and the costs of RES have been determined through a methodology called life cycle assessment (LCA), which determines whether the use of renewable sources and ESS is sustainable. An example of a Photovoltaic (PV) system (without and with batteries) used into a microgrid that supply a wastewater treatment plant situated in Romania, will be presented. Life cycle assessment was used to quantify ecological sustainability and costs in both cases compared to a conventional supply of electricity from the grid.

The chapter is organized as follows: Sect. 8.2 presents an overview of the energy storage systems. The technologies of energy storage systems and standards are described in Sect. 8.3. In Sect. 8.4 is analyzed an application of energy storage in electrochemical batteries, for waste water treatment plants. The conclusions are drawn in Sect. 8.5. At the end of the chapter the list of bibliographic references is presented.

8.2 Overview

Conventional electricity production has a negative impact on the environment, through emissions of pollutant and greenhouse gases [1–3]. This is one of the reasons, along with decreasing natural resources and increasing energy security, for which the clean energy technologies are being developed and widely deployed worldwide [4].

Clean energy technologies can provide the necessary heat and energy in an environmentally friendly manner [5, 6].

Because RES possess an irregular nature, the complexity of the national power system is increasing. The insertion of RES into national power systems is limited by the energy storage capacity.

For example, Fig. 8.1 presents the potential of major energy primary sources in Romania. It is also possible to identify the wind potential or the solar potential at any point on the surface of Romania, but also the corresponding pollution level.

Figure 8.2 shows the situation of Romania during the period 1990–2015 in the context of highlighting the dynamics of reducing the primary polluting energy sources, together with the increase of clean energy technologies [8].

Evolution of RES penetration in Romania, for a period of 25 years (1990–2015) is illustrated in Fig. 8.3 [9].

In Fig. 8.4 is detailed at the European level the RES components, according to Special Report No. 5/2018 [10].

According to Fig. 8.4 it can be said that the renewable source of primary energy for the EU is biomass (63% of the total energy produced from RES).

It is mentioned that biomass includes: wood, solid biofuels other than wood, biogas, liquid biofuels, renewable waste (biodegradable).

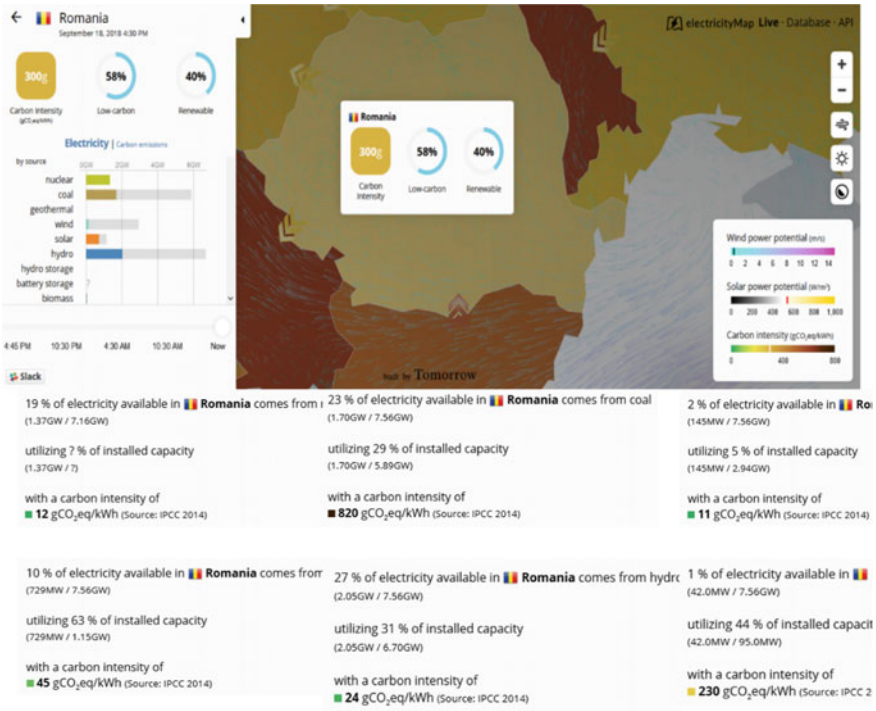

Fig. 8.1 Total RES in Romania and primary energy components [7]

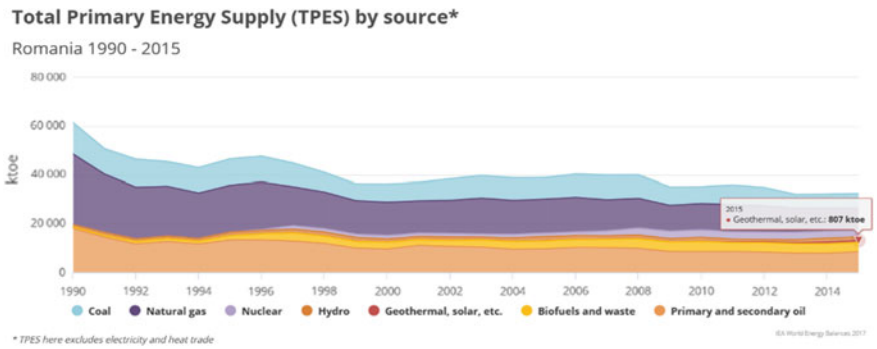

Fig. 8.2 The dynamics of the reduction of primary polluting energy sources, along with the growth of clean energy technologies [8]

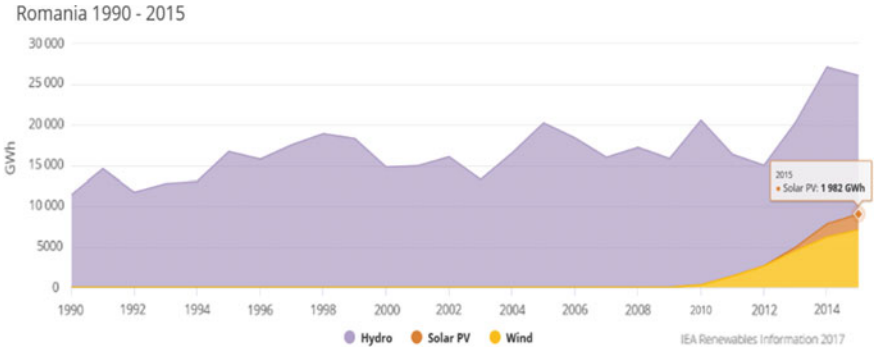

Fig. 8.3 The penetration of renewable energy sources in Romania in the period 1990–2015 [9]

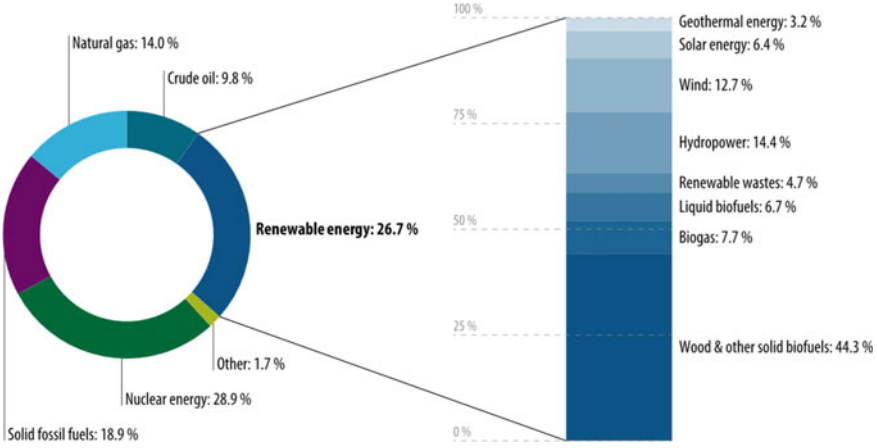

Fig. 8.4 Primary energy production in EU-28 in 2015 (% of total, tons of oil equivalent) [10]

Energy storage systems (ESS) can be considered as backup sources when integrating into island or autonomous energy systems. Traditional national energy systems are easily adapting to changing demand on the energy market, leading to increased consumer safety. Under other conditions, the massive increase in the integration of RES leads to instability of the energy supply without adequate equilibrium provided by suitably sized ESS's. Thus, with the introduction of RES, it is necessary to introduce ESS's as well.

ESS, besides the role of energy conservation, ensures continuity, increased reliability and quality of energy supply to consumers. In the next section, storage technologies used in power supply systems will be presented.

8.3 Energy Storage Technologies and Standards

Energy storage has applications in:

- *power supply*: the most mature technologies used to ensure the scale continuity of power supply are pumping and storage of compressed air. For large systems, energy could be stored function of the corresponding system (e.g. for hydraulic systems as gravitational energy; for thermal systems as thermal energy; also as compressed air or energy in batteries);
- *auxiliary services*: accumulators batteries are used; these lead to an increased quality and reliability;
- *power supply support* (transmission and distribution congestion improvement during peak demand);
- *renewable energy integration*: the use of pumped storage hydropower (PSH) and compressed air energy storage (CAES), but also accumulator batteries or hydrogen storage;
- *end-user applications*: residential and commercial consumers.

Batteries systems are the most used in the case of servers powering, but to smooth the power, one uses flywheels. For example, for the case of small systems, energy could be stored using different storage technologies and by taking different types which vary from kinetic, chemical to superconductors and supercapacitors, as is presented in Table 8.1 [11].

Storage system parameters are defined as:

1. *Storage capacity*: represents the quantity of available energy in the storage device after the loading cycle is completed.
2. *Available energy*: depends on the size of the motor-generator system used in the conversion process of the stored energy. The available power had average value. The maximum value of the power, P_{max}, represents the maximum power corresponding to the loading and unloading cycles.
3. *Loading time*, τ [s] is the ratio between the total stored energy [Wh] and the maximum or the peak value [W]. From this point of view, the unloading can be:

Table 8.1 Energy storage technologies in small systems

Kinetic energy			Potential energy		
Thermal technologies	Electrical technologies	Mechanical technologies		Electrochemical technologies	Chemical technologies
Hot water	Supercapacitors	Flywheels	Pumped hydro	Lithium ion	Hydrogen
Molten salt	Super-conducting magnetic energy		Compressed air energy	Lead acid	Synthetic natural gas
Phase change material				Redox flow	
				Sodium sulphur	

3.1. $\tau < 1$ (order of seconds to minutes). In ESS's could be: flywheel, superconducting, or double layer capacitors energy storage systems and they are used for frequency regulation;
3.2. $\tau \in [1, 10]$, from minutes to hours. The ESS's systems include the batteries packs with Pb (LA), Li Ion, NaS, FES. These systems are used to maintain the energy quality and energy balance. These storage systems store energy out of their peak load hours and can supply power during the peak hours;
3.3. $\tau \in [5, 30]$, from hours to days. ESS's include: the pumping and air compressed storage type systems, REDOX flow batteries. These systems work on load gaps, providing the maximum power.

4. The s*torage system efficiency* represents the ratio between the useful supplied energy and the stored energy.
5. *Durability*: is provided by the number of times the storage device can release energy. It is expressed as a maximum number of cycles—*N*. A cycle corresponds to a loading and unloading process.
6. *Autonomy* [s]: is the maximum amount of time in which energy can be released continuously by a system. The autonomy is the ratio between the useful energy (in Wh) and maximum power unloading (in W) (Fig. 8.5).

ESSs, for applications of distributed power generation, can be classifies as [12]:

– mechanical systems: low-speed and high-speed flywheel energy storage (LSF, HSF);
– pneumatic systems;
– thermal systems;
– electrical systems;
– magnetic systems;
– electrochemical systems: internal storage: batteries (Pb, NiCd, Li-ion) or external storage which may be in their turn: (i) external regeneration primary batteries (ex. Zn-air); (ii) gas storage (electrolyser, fuel cells); and (iii) liquid electrolyser storage (ex. redox with vanadium).

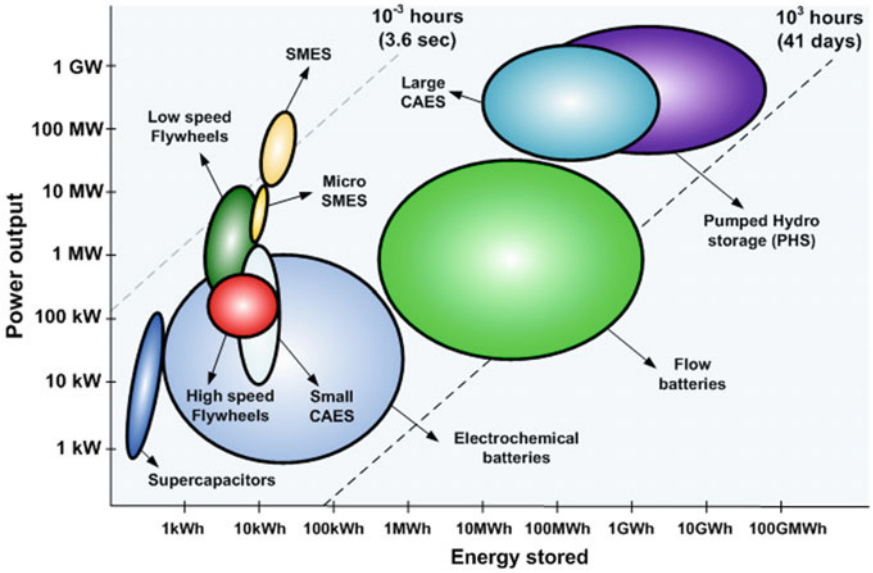

Fig. 8.5 Applications of energy storage systems [12]

For large power systems, the pumped heat electrical storage (PHES) systems are used. On short term, the battery technologies prove to be able to offer the most rapid improvements in these domains. Nowadays, lead-acid or lithium-ion batteries are gaining popularity among residential users, while advanced lead-acid or sodium lead batteries are widely used in big buildings.

8.3.1 Batteries Types

In order to properly select the batteries, in autonomous systems, it is important that the system designers know the performance characteristics and the operating requirements [13].

In the following, the battery operating characteristics in autonomous systems will be presented.

Since energy produced by the Stirling motor does not always cover the consumer's energy demand, accumulators are used in autonomous systems.

The main functions of the batteries in an autonomous system are:

1. *storage capacity and autonomy*: stores the produced energy by Stirling motor and provides electricity to consumers.

2. *stabilization of current and voltage*: this function is useful to ensure a stabilized voltage when the current requirement changes, an important function during the transient regime to eliminate potential disturbances;
3. *leakage currents*: for proper feeding when load peaks occur.

8.3.2 Classification [14]

First generation batteries or primary batteries have the function of energy supply, but they cannot be recharged. These types of batteries are used in autonomous systems. The most common form of primary battery is Leclanche cell (dry cell), invented by the French scientist with the same name in the 1860. The electrolyte consists of a solution of ammonium chloride. The anode is made of zinc, being the cell's case and the positive electrode (cathode) has a carbon tube surrounded by manganese and carbon mixture tis improve absorption and conductivity. Leclanche battery produces appreciatively 1.5 V.

Second generation batteries or secondary batteries are presented in Table 8.2.

The accumulator or the secondary battery can be recharged by reversibility of the base chemical reaction. Plante cell (1859, Gaston Plante) is a battery consisting of lead-acid cell, which is also used today. It consists of three or six cells placed in series and are used in cars, trucks, planes and other vehicles. It has the advantage that it can distribute a lot of current when the engine starts. However, it is consumed quickly.

The electrolyte is solution of sulphuric acid; the positive one made of lead dioxide while the negative one is made of lead. In operation, the negative one is dissociated in electrons and lead positive ions. Furthermore, the electrons circulate along the external circuit and the positive lead ions combine with the sulphate ions from the

Table 8.2 Second generation batteries

Battery	Price	Efficiency	Sustenance
IP-A batteries (Immersed plumb-acid)			
Lead-antimony	Low (L)	Good (G)	High(H)
Flooded lead-calcium, open vent	L	L	Medium (M)
Flooded lead-calcium, sealed vent	L	Very low (VL)	L
Lead-antimony/lead-calcium hybrid	M	G	M
CEL-A batteries (Captive electrolyte lead-acid)			
Gelled batteries	M	L	L
Absorbed Glass Mat (AGM) batteries	M	L	L
Ni-Cd			
Sintered plate Ni-Cads	High (H)	G	None
Pocket plate Ni-Cads	H	G	M

electrolyte to form the lead sulphate. The lead dioxide combines with the hydrogen ions in electrolyte and with the returned electrons forming the water and by releasing the lead ions in the electrolyte in order to form the supplementary lead sulphate.

An acid lead accumulator is consumed while sulphuric acid is converted into water; at the same time the electrodes are converted into lead sulphate. When the recharging process of the battery takes place, the previous chemical reactions are reversed until the battery is brought to its initial state. Such a battery can be used for about four years and produces about 2 V on cell. Recently, the battery life of such a cell has been extended to up to 50–70 years and it can be used for special applications.

Another secondary battery which is widely used is the alkaline cell (Thomas Edison). The using principle is similar to one corresponding to the lead battery, except the composition of the electrodes (positive electrode: nickel oxide; negative electrode: iron; electrolyte: potassium hydroxide). This battery has the disadvantage of releasing the hydrogen during charging. It is used especially in heavy industry, lasts about ten years and produces 1.15 V.

In order to choose a battery, sizing is done according to the load (from 1/3 up to 1/4 from the peak load). In Table 8.3 [15], we present the standard battery selection values.

If one chooses a battery which has a capacity larger than the required one, then the loading/unloading cycles can be reduced, increasing the life of the battery. If there is a high energy demand for a period longer than 2 h, then a larger capacity battery will be chosen.

In the following Table 8.4 will be presented the standard values corresponding to periods up to the subsequent recharge (charge level < nominal value) and the viable times corresponding to the power supply for different battery sizes (with acid) function of average consumption [15].

Table 8.3 Choosing the size of a battery—standard values

Average consumption [kW]/day	Up to 15 kWh	Up to 20 kWh	Up to 30 kWh	Up to 50 kWh	Up to 70 kWh	Up to 90 kWh	Over 90 kWh
Minimum battery size (Ah) for voltage of 48 V (Ah)	420	490	600	800	1000	1200	Over 1500

Table 8.4 battery sizing—standard values

Voltage (V)	Capacity (Ah)	Average consumption [kW]	Time Estimated (up to recharging) [h]	Energy supply possibility [h] considering the fully charged battery
48	420	0.5	6.5	24
		1	3.5	13
		2	2	6.5
		4	1	2.5
		6	0.5	1
48	600	0.5	9.5	35
		1	5.5	19
		2	3	10
		4	1.5	4
		6	1	2
48	800	0.5	13	48
		1	7	26
		2	4	14
		4	2	6
		6	1.2	3.5
48	1000	0.5	16	57
		1	9	29
		2	5	16
		4	2.5	8
		6	1.5	4.5

8.3.3 Technologies with Low Environmental Impact

The increased interest in fuel cells is justified in view of the near-zero emission of zero emission vehicles. Unfortunately, the development of such systems is closely linked to the development of the pure hydrogen market and the cost of electrolytes used [16, 17].

The use of hydrogen for power fuel engines minimizes the generation of reaction by-products, such as carbon monoxide and carbon dioxide, and further reduces the complexity of the whole system, providing more space inside the machine. Instead, the cost of use today is very high due to the high cost of hydrogen production and distribution.

8.3.4 Fuel (Combustion) Cell

The fuel cell is an equipment used to convert directly the reactants' chemical energy (fuel—usually hydrogen, and an oxidant—usually oxygen or air) into electricity, in the form of Direct Current (DC). The fuel cell performs this conversion through electrochemical reactions. Unlike ordinary batteries, they do not use substances that are integral or contained by the battery, leading to a very long lifetime, as long as the substances used (fuel and oxidant) are fed from the outside and the reaction products are removed.

Sir William Grove, in 1839, builds the first prototype of the fuel, based on water electrolysis. This process consists of dividing water molecules into constituents (hydrogen and oxygen) when the cell is traversed by electricity. Recombination of the two elements leads to the occurrence of a small current in the opposite direction to the one described above. This experiment laid the foundations for fuel cells, but the current produced by this method is very small. The reasons why this current is low can be the following:

– small contact area between gas, electrode and electrolyte;
– considerable distance between the electrodes, and, as a consequence, a considerable resistance that opposes to the electrons circulation through the electrolyte.

Therefore, the fuel cells have found no practical application till 1959, when two American research groups build a prototype for an electric vehicle whose engine worked with the energy produced by this type of converter.

8.3.5 Electric Energy Production

Among all hydrogen production systems, water electrolysis is currently the most solid solution, being used on the industrial scale for more than 80 years, using alkaline electrolysers. More, this procedure allows obtaining completely pure hydrogen.

However, the produced hydrogen is "indirectly" generated by using electrical energy; therefore, this product becomes economically viable only if electrical energy is generated at an extremely low cost. On short term, this can be done only in the presence of large power plant or where there is a significant energy excess given by the nuclear power plants. Another solution is to use the electrical energy produced by photovoltaic panels.

8.3.6 Storage Systems

The minimum autonomy, to be expected in the design phase of a vehicle, may range from 80 to 90 km, which is sufficiently for urban use and from 300 to 500 km, for

the general use. This autonomy condition defines the dimensional requirements for a minimum energy storage system on board of a vehicle which should be fulfilled with respect to the distance traveled per unit of volume or weight: the conventional internal fuel reference vehicle (average dimension) travels on average between 7.8 and 9.3 km per liter of tank and about 7.7 km per unit of mass [18].

The Department of Energy, established a program having as a specific objective the development of hydrogen storage (volume density 2.7 kWh/l, respectively 3 kWh/kg).

Choosing the hydrogen storage system is a process that involves compromises of different criteria. The external parameters (infrastructure, vehicle and fuel cell interface) and internal (compactness, fast dynamic response, high efficiency, life cycle, cost, safety and environmental impact) are carefully assessed with regard to the development of storage technologies.

The main proposed or investigated methods for hydrogen direct storage (without going through the reforming process), are the following:

- high pressure compressed gaseous hydrogen;
- liquid hydrogen in very low temperature containers;
- solid hydrogen, more used in chemistry, metal hydrides;
- absorbed hydrogen (active carbon adsorption on carbon nanostructures or encapsulation in glass microspheres).

A particular attention is given to the possibility of using methanol (CH_3OH), in a direct form (fuel cells with direct methanol) or in an indirect from ("on-board" production systems), which reduces the production costs, but, in contrast, do not eliminate the oil and its by-products dependence, which generate more carbon dioxide in acceptable amounts.

8.3.7 Available Types

The study and the researches in the fuel cell field have led to the introduction of several types of fuel cells, trying to optimize performance and costs, depending on their field of use. Extending the knowledge of the physical and chemical processes that govern the operation of the fuel cell allows for the study of new materials that can lead to an increased efficiency and performance of the entire system using these ERS. There are several types of fuel cells, which differ function of the used electrolyte, working temperature, etc.

As follows, there are presented the fuel cell types which are widely used by the market [19]:

– *Alkaline Fuel Cell* (AFC); the electrolyte solution is usually an aqueous solution of KOH (potassium hydroxide). Most often, they have nickel-based porous electrodes. This structure allows them to operate at working temperature between 60 and 100 °C. The fuel is hydrogen, but in some cases, hydrazine is also used.

Efficiency is high and can reach more than 70%. Alkaline cell technology can be considered mature, but the characteristics of these cells make them suitable only when hydrogen and pure oxygen are available. The high cost of the building materials prevents the mass distribution. They were tested especially in space applications (Apollo) and military applications.

- *Proton Exchange (PE) Membrane* (PEM), called also Solid Polymer Fuel Cell (SPFC), is equipped with a PE membrane placed between the electrodes (the average working temperature is 60–120 °C). The only allowed fuel is hydrogen (hydrocarbons can also be used but their reformation must be done perfectly). A cooling system becomes necessary. In fact, the fuel cell, should operate under conditions such that the water produced does not evaporate too quickly, otherwise the polymer membrane is not sufficiently hydrated. The maximum efficiency is about 50%, but due to high power density and to lack of corrosion problems it is used in electrical traction applications. Also, there are steady applications with polymeric membrane batteries for power generation.
- *Phosphoric Acid (PA) Fuel Cell* (PAFC): uses a PA solution as electrolyte, in a silicon carbide situated between two graphite electrodes treated accordingly (average temperature interval: 180–200 °C). There are severe corrosion problems that reduce the choice of electrodes and catalyst. The necessary hydrogen is derived from the methane reforming process. These are fuel cells used in commercial applications, small and medium installations (100 kW–1 MW). They can be also used to produce hot water for heating the homes.
- *Solid Oxide Fuel Cell* (SOFC): with an oxide zirconium stabilized with yttrium oxide the electrolyte; the cathode is suitably treated with manganese lanthanum; the anode is a ceramic based on nickel-zirconium oxide (average temperature range: 800–1000 °C). These cells are the most used ones among the cells that use hydrocarbon-based fuel. In fact, they are simple, extremely effective (60%), tolerant of impurities and can do cell reforming. The high temperature in which they operate allows the non-use of a catalyst to feed the reaction. Moreover, the power density is high and therefore, compact systems can be obtained. Because the start time is long enough, this allows the use of such systems, especially for devices that operate continuously. Indeed, applications for this type of cell are medium and large power cogeneration applications.
- *Molten Carbonate Fuel Cell* (MCFC): the use of a carbonates mixture as electrolyte (lithium and potassium); the two electrodes are nickel-based: cathode treated with lithium, nickel oxide, the anode uses nickel with small percent of (average temperature: 600–700 °C). All oil products can be used as fuel. Molten carbon cell, while they require technological and material improvements (efficiency abut 60%), can be very close to the market as a result of the demonstration already made for large-scale cogeneration power plants (up to MW).

The main characteristics of the fuel cell types are listed in the following Table 8.5 [20].

Table 8.5 Synoptic table of fuel cell types

	AFC	PEM	PAFC	SOFC	MCFC
Cathode	Porous nickel	Nickel	Gold, titanium, coal	Lanthanum manganate	Nickel oxide
Anode	Porous nickel	Nickel	Gold, titanium, coal	Nickel + zirconium oxide	Nickel
Catalyst	Nickel	Platinum	Platinum	NO	Nickel
Electrolyte	Alkaline	Polymer	Phosphoric acid	Zirconium oxide	Potassium and lithium carbonate
Cooling	NO	YES	NO	NO	NO
Reformer for CH_4	NO	YES	YES	YES	YES
Temperature (°C)	60–100	60–120	180–200	800–1000	600–700
Efficiency (%)	70	50	40–45	50–60	50–60
Applications	Air-space	Traction	Cogeneration (kW)	Cogeneration (kW-MW)	Cogeneration (MW)

For the consideration made so far, PEM cells are therefore more adaptable for automotive applications for the following reasons:

(1) They have a satisfactory start time due to reduced operating temperatures. In fact, they reach maximum efficiency at temperatures below 100 °C.
(2) Because of the high power density and specific power, high-power small cells can be made; this allows the occupation of a smaller space in the vehicle and, therefore, to achieve substantial improvements in comfort and weight.
(3) They provide a satisfactory dynamic response to changes in energy demand.
(4) The simple structure of the system, compared to the other fuel cell structures, implies great maintenance advantages.
(5) They are very compact, allowing easy absorption of vibrations and strokes caused by road conditions.

An important issue related to using PEM fuel cells is that they cannot accumulate large amounts of carbon monoxide, which, in any case, is a reaction product. An accumulation of this substance, which exceeds 10 ppm, causes great losses in terms of efficiency and performance. This means that the cell, despite, the structure is simple and easy to maintain, it requires a carbon monoxide disposal system. Another problem with the choice of PEM is that they require very expensive reaction catalysts to optimize system dynamics. This requires CO capture, or even requires CO conversion $\rightarrow CO_2$.

8.3.8 Standards

Standards represent general rules (norms) that: (i) can be imposed as mandatory, or (ii) can provide guidance by including milestone and best practices to be used. As follows are briefly presented the main organization engaged in energy production and development [21–24]:

- IEC means International Electrotechnical Commission;
- UL means Underwriter Laboratories Inc.;
- IEEE means The Institute of Electrical and Electronics Engineers;
- CEN means European Committee for Standardization.

The following storage standards are required (Table 8.6):

8.4 Energy Storage Applications

In this Section is presented an application of energy storage in electrochemical batteries, for waste water treatment plants (WWTPs).

WWTPs are indispensable infrastructures for the modern urban communities. The energy consumed by them represents about 30–40% of the total energy consumed by the community's public services. At the same time, the WWTPs have important areas on the technological objects, which can be covered with photovoltaic panels to produce electricity. Consequently, the conversion of waste water treatment plants from passive energy consumers to "prosumers" (both producer and consumer, simultaneously) can have a positive impact on the entire community and on the power distribution network.

In the literature, a parameter called "matching index" was defined to measure the impact of a "prosumer" on the network. This index measures the ratio between the electricity produced and the electricity consumed at that production-consumption point. Therefore, if this index has a value of 1, then the electricity production fully covers the energy requirement, minimizing the impact on the energy distribution network. The closer the value of this index is to 0, the greater the impact on the network.

Installing a battery bank at a WWTP that produces electricity using a photovoltaic plant can minimize the impact on the network, measured by the "matching index".

In Fig. 8.6, the power supply of the WWTP block chart is shown.

8.4.1 Sizing the Photovoltaic System

For the calculation of the photovoltaic system, the available space on the buildings and technological objects within the treatment plant was estimated. Following this

Table 8.6 Storage systems' standards

IEC 60095	IEC 60086	IEC 60119	IEC 60254	IEC 60622	IEC 60623	IEC TS
Lead-acid starter batteries	Primary batteries	Polycrystalline Semiconductor Rectifier Stacks and Equipments	Lead-acid traction batteries	SCBAoNAE—Sealed NCdPRSC	SCBAoNAE—NCdPRSC	SCB—Test methods for checking the performance of devices designed for reducing explosion hazards—Lead-acid starter batteries
IEC 62196	IEC/TR 62914					
Plugs, socket-outlets, vehicle couplers and vehicle inlets—CCEE	SCBAoNAE—Experimental procedure for the forced internal short-circuit test of IEC 62133:2012					

SCBAoNA Secondary cells and batteries containing alkaline or other non-acid electrolytes
NCdPRSC Nickel-cadmium prismatic rechargeable single cells
CCEE Conductive charging of electric vehicles

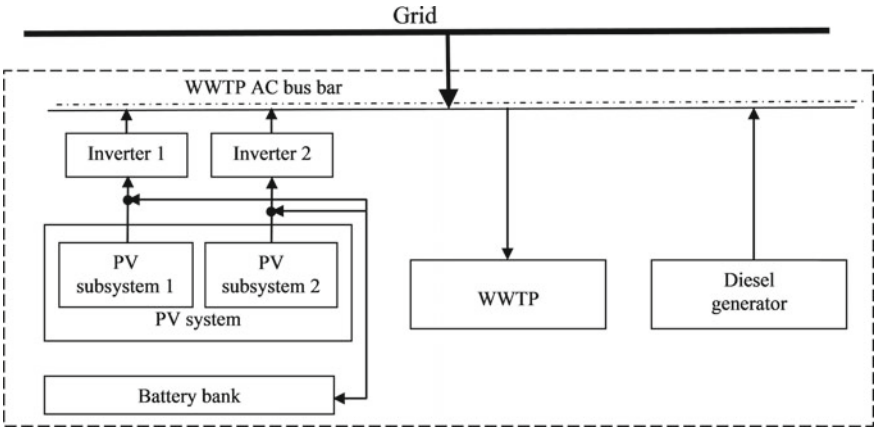

Fig. 8.6 Block chart of the power supply for a typical WWTP

analysis, for a WWTP, it was found that 1248 PV modules could be installed on this space. 250 kWp modules were chosen for this application, therefore the capacity of the plant was 312 kWp [25, 26].

Starting from these data, in the following is presented the calculation for the PV system.

For this application was chosen an ABB PVS800-57-0500 kW-A inverter having the following electrical characteristics, according to the datasheet:

- Recommended power: 600 kWp
- $I_{\max} = 1145$ A
- $V_{\max\, cc} = 900$ Vcc
- $V_{MPP} = 450$–750 V
- Minimum temperature: -15 °C
- Number of MPP blocks: 4.

The chosen photovoltaic modules are Altius 250 Wp having the following electrical characteristics, according to the datasheet:

- $P = 250$ Wp
- $V_{OC} = 37.1$ V
- $I_{SC} = 8.92$ A
- $V_{MPP} = 29.9$ V
- $I_{MPP} = 8.35$ A
- Temperature coefficient: -0.32%/°C
- Efficiency: 15.7%.

To calculate the maximum number of modules that we can connect to the inverter in a string, we will take into account the opening voltage (V_{oc}) at the minimum temperature the module can reach at the respective installation location, because it

produces an increase of module voltage compared to the voltage produced at the normal temperature (25 °C):

$$\begin{aligned} V_{oc}(-15\,^{\circ}\mathrm{C}) &= V_{oc}(25\,^{\circ}\mathrm{C}) \\ &\quad - \left[-0.32\% \cdot (25\,^{\circ}\mathrm{C} - (-15\,^{\circ}\mathrm{C})) \cdot V_{oc}(25\,^{\circ}\mathrm{C})\right] \\ &= 41.85\ \mathrm{V} \end{aligned} \tag{6.1}$$

Therefore, the maximum number of modules that can be connected is:

$$N_{\max} = \frac{V_{\max}(inverter)}{V_{oc}(-15\,^{\circ}\mathrm{C})} = 21\ \text{modules} \tag{6.2}$$

In order to calculate the minimum number of modules that we can connect to the inverter in a string, we must take into account the voltage at maximum power point (V_{MPP}) at the maximum temperature the module can attain at the respective installation location:

$$\begin{aligned} V_{MPP}(80\,^{\circ}\mathrm{C}) &= V_{MPP}(25\,^{\circ}\mathrm{C}) \\ &\quad + \left[-0.32\% \cdot (25\,^{\circ}\mathrm{C} - 80\,^{\circ}\mathrm{C}) \cdot V_{MPP}(25\,^{\circ}\mathrm{C})\right] \\ &= 24.64\ \mathrm{V} \end{aligned} \tag{6.3}$$

Also, from the inverter datasheet we read that the recommended maximum voltage V_{DC}, max is 900 V, which would allow us to connect 36 V_{MPP} modules at a maximum temperature of 80 °C.

But taking into account that there is a limit given by the minimum temperature, we choose to make rows of 21 modules.

Then, a string of 21 modules of 250 Wp will supply 5.250 Wp/string. Consequently, we will need 59 strings to get a power of 309.7 kW.

To connect parallel junctions to junction boxes, one must take into account the number of MPP blocks that the inverter has.

With 4 MPP blocks, we distribute the strings on each MPP block, as follows: on the first 3 blocks we distribute 15 strings linked to a parallel junction box, and on the fourth MPP block we divide 14 strings linked to a junction box in parallel.

For this configuration, one must check the maximum current corresponding to the inverter DC input.

From the datasheet we read that the maximum current ($I_{\max}$) is 1.145 A, the short circuit current (I_{SC}) of the photovoltaic modules is 8.92 A. Therefore, the inverter can support 128 rows connected in parallel.

Taking into account the previously established configuration, we find that at each MPP block, 15 strings are connected in parallel, with a short-circuit current (I_{SC}) of 8.92 A, i.e. 133.8 A for each MPP block. Therefore, the total short-circuit current is 526.28 A, which is lower than the maximum current admitted by the inverter. In conclusion, the configuration was checked both in voltage and current.

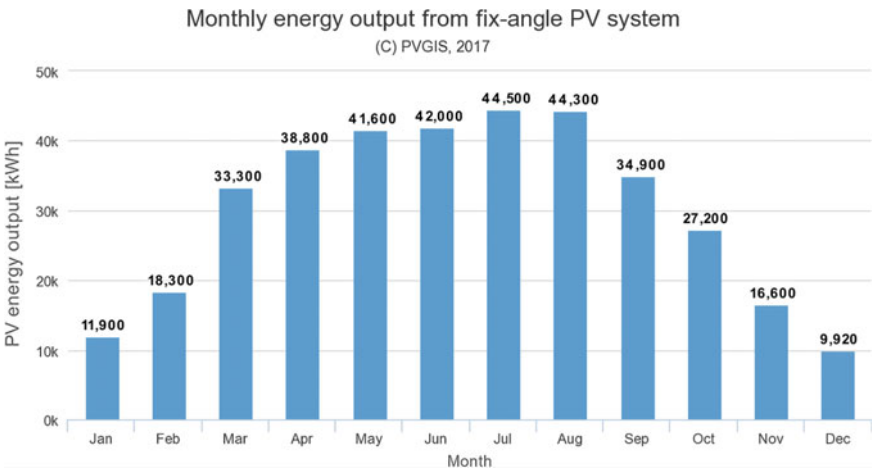

Fig. 8.7 Energy output for 1 kWh simulated by using PVGIS5

8.4.2 System Simulation Using PVGIS

The system previously calculated was simulated for the location at the geographical coordinates (46.495 °C; 24.096 °C).

The PVGIS application, developed by the *European Commission—Joint Research Center*, has been used to simulate on-grid and off-grid photovoltaic systems, taking into account meteorological data [27].

Monthly simulation results are shown in Fig. 8.7.

Figure 8.7 shows that the highest energy output is recorded in July. Therefore, we will dimension a battery bank for this month for impact minimization of PV system on the distribution network.

8.4.3 Sizing the Battery Bank

For the sizing of the battery bank it is necessary to evaluate the consumption profile of the treatment plant [28, 29]. This profile is shown in Fig. 8.8 for an average day in July. It is noted that during the day the energy consumption is quasi-instant, about 58 kW.

The PV system energy output is compared with the energy profile of the consumer, as shown in Fig. 8.9.

In Fig. 8.9, it can be seen that between 6:00 and 15:00 the power flow provided by the PVPV system is higher than the one required by the installation. Therefore, this energy difference must be stored in batteries. This energy can be used by consumers outside of the mentioned time period when energy production is below demand, as it

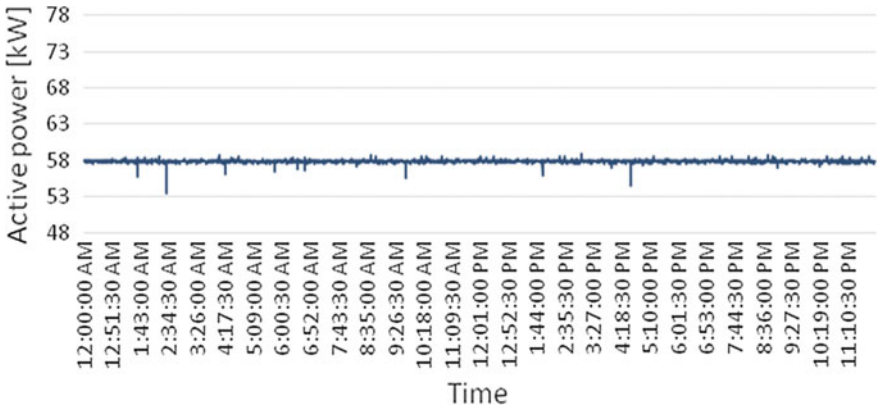

Fig. 8.8 Typical energy consumption for a day in July

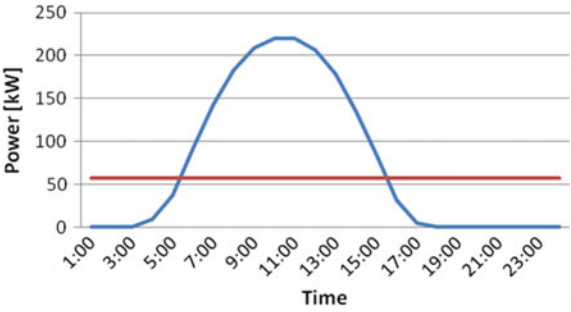

Fig. 8.9 Supplied power for PV system (in blue) and consumed power for WWTP for a typical day in July (in red)

can be seen from the Fig. 8.9. In this way, the entire amount of energy produced by the photovoltaic system is consumed locally, minimizing the impact on the distribution network. The data represented in Fig. 8.8 are shown below in Table 8.7.

The first column in Table 8.7 represents the hours of the day. The second column is the energy output of the 312 kW PV system installed at the site of consumption. The data in this column resulted from the simulation with the PVGIS 5 application. The third column shows the consumption profile of the WWTP. In the fourth column is presented the difference between absorbed power (by the consumers) and the discharged power (by the PV system).

Negative values in the fourth column represent the surplus of power produced that can not be consumed instantly. The sum of these average hourly values results in battery capacity: 1.1 MWh. If 48 V batteries are used, then the battery capacity is 22.8 kAh.

Deep cycle lead-acid batteries of 482 Ah were chosen. As the batteries will be discharged with only 60% of the capacity, the useful capacity is 289 Ah. Therefore, 78 batteries are required, connected in series.

Positive values in the fourth column represent the power absorbed by consumers, which can not be covered by the instant production of the photovoltaic system. The

Table 8.7 PV system supplied power, WWTP consumed power, power to be stored in batteries

Time	Supplied power (PV system) [kW]	Consumed (WWTP) [kW]	Power difference [kW]
01:00	0	58	58
02:00	0	58	58
03:00	0	58	58
04:00	9	58	49
05:00	37	58	20
06:00	92	58	−35
07:00	143	58	−85
08:00	183	58	−126
09:00	209	58	−151
10:00	220	58	−162
11:00	220	58	−163
12:00	206	58	−149
13:00	178	58	−121
14:00	136	58	−78
15:00	85	58	−27
16:00	32	58	26
17:00	5	58	53
18:00	1	58	57
19:00	0	58	58
20:00	0	58	58
21:00	0	58	58
22:00	0	58	58
23:00	0	58	58
00:00	0	58	58

sum of these hourly values is 725 kW. Therefore, we find that the energy stored in batteries covers this energy requirement.

The photovoltaic battery system was simulated using PVGIS to evaluate battery charging status during the year. The input data are as follows:

- Installed PV power: 312 kW
- Battery capacity: 1096 kW
- Daily consumption: 1388 kW
- Discharge limit: 40%.

The result of the simulation is shown in Fig. 8.10. It is found that in only 10% of the year the battery is fully charged, and in 58% of the year the battery is charged 40%.

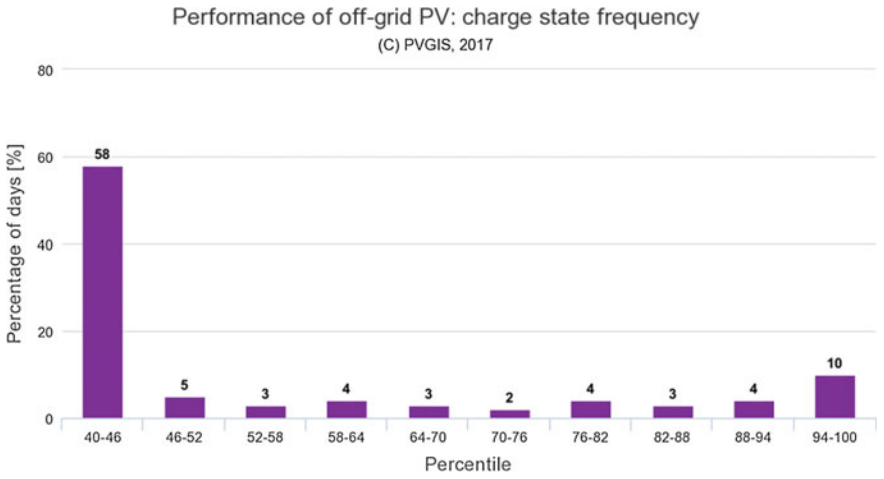

Fig. 8.10 Simulation of PV system with battery bank

From economical point of view, if the battery bank is used only to store the energy produced by the PV system, then this way of using it is uneconomical. However, surplus storage capacity can be used to store energy if there is a differentiated pricing plan (for example, if the energy tariff is lower at certain times of the night when demand is low on the market).

From technical point of view, this way of dimensioning the battery bank has the advantage of minimizing the impact on the distribution network, as outlined in the next paragraph.

8.4.4 The Impact of the Photovoltaic System on the Energy Distribution Network

To characterize the autonomy of a consumption and production power system point, the terms of self-sufficiency and self-supply have been introduced in the literature. The "matching index" introduced in [30, 31] characterizes a production-consumption point taking into account both aspects.

The "matching index" is defined by as follows:

$$\varphi = \frac{M^2}{L \times P} \tag{6.4}$$

where M represents the PV system produced energy inside the treatment plant, L represents WWTP consumption and P represents the total annual energy supplied by the photovoltaic system.

Table 8.8 Value of the "matching index"—PV system without/with storage (one day time window)

	PV system without storage	PV system with storage
L [kWh]	1389	1389
P [kWh]	1759	1759
M [kWh]	869	1759
φ	0.3	1.26

Table 8.9 Value of the "matching index"—PV system without/with storage (one year)

	PV system without storage	PV system with storage
L [kWh]	537,188	537,188
P [kWh]	368,345	368,345
M [kWh]	205,476	368,345
φ	0.21	0.68

Maximizing the matching index ensures maximizing the local energy used, minimizing both the energy required by the wastewater treatment plant from the grid and the impact on the grid.

The time window chosen for computing the matching index plays a major role in interpreting its relevance. In Table 8.7, the time window is one day, corresponding to one day in the month of July.

The values of the matching index for a PV system without/with storage system are 0.3, respectively 1.26. The value greater than 1 indicates that the photovoltaic system covers the consumer's energy demand but also produces an excess of energy that accumulates from day to day in its storage system. These situations are illustrated in Table 8.8.

The time window selected for the next calculation was one year, because the power and economy impact of the WWTP is calculated by the operator for one year. In this respect, Table 8.9 illustrates the "matching index" calculated over a one-year period.

Ideally the "matching index" has a value of one, which means that all site energy is used on site and that the entire site's energy is produced locally.

In this study, the second condition mentioned above can not be fully satisfied as the energy produced on site can not cover the needs of the wastewater treatment plant due to surface limitations, which are reflected in the energy purchased from the public energy grid.

8.4.5 Life Cycle Assessment

Life cycle assessment (LCA) is a method used for assessing the environmental effects related to all the steps of a life of a given product. These steps include the chain from

extraction of the raw material till the processing and up to recycling. LCA is widely used by designers to find, from the very beginning, the weak points of their products [32, 33].

LCA is also used for comparisons between various effects upon environment given by the products and therefore they can be quantified. The environmental impacts of the energy mix used by the WWTP were compared in two cases:

- When the WWTP uses energy only from the national grid
- When the WWTP uses energy from the national grid and in-house PV generator.

The ecological impact was assessed using the software SimaPro 7 [34, 35]. SimaPro is a software tool for professional LCA studies. Among others, SimaPro uses the Ecoinvent database, which contains inventory data of life cycle of: energy, waste management, transports, agriculture, electronics, metals processing and building ventilation.

The energy used by the WWTP was modelled as a product in SimaPro.

For the WWTP supplied exclusively by the power grid case the authors used the Romanian energy mix defined in the Ecoinvent database under Processes\Energy\Low voltage.

For the mixed energy case, the energy product for the WWTP was defined as an energy mix between the national grid and photovoltaic generation (included in the Ecoinvent database under Processes\Electricity by fuel\Photovoltaic\Infrastructure). For this case the proportions between grid energy and PV energy were: 68% PV energy and 32% national grid energy.

The two products were compared using the EDIP 2003 method included in SimaPro [36].

This method is used to assess certain environmental impact categories. Given that one of the main reasons WWTPs are built is to avoid eutrophication, the following parameters are of major interest for our study: terrestrial eutrophication, aquatic eutrophication, used resources. More generally, global warming and ozone depletion are also of interest for the environmental impacts of any industrial installation. The eutrophication is defined as the enrichment of an ecosystem with nutrients in excess of a certain optimum point. The excess of certain nutrients favors some species in detriment of others, which leads to disequilibrium of the ecosystem. The eutrophication can take place both in water and land. The WWTP avoids the eutrophication of waters by eliminating the compounds of nitrogen, phosphorous and carbon from the water before discharging into a natural effluent.

Global warming refers to the increase of global average temperatures due to man-made activities, leading to the accumulation of green-house effect gases in the atmosphere.

The depletion of the ozone refers to ozone content decrease in the Earth's stratosphere due to halocarbons emissions [37–40].

The ozone layer thinning effect is represented by the increased quantities of ultraviolet radiation reaching the surface of the Earth with consequences including skin cancer in humans, damage to the plants and hence to the ecosystems. The including of a PV system into the considered WWTP is expected to have a beneficial impact

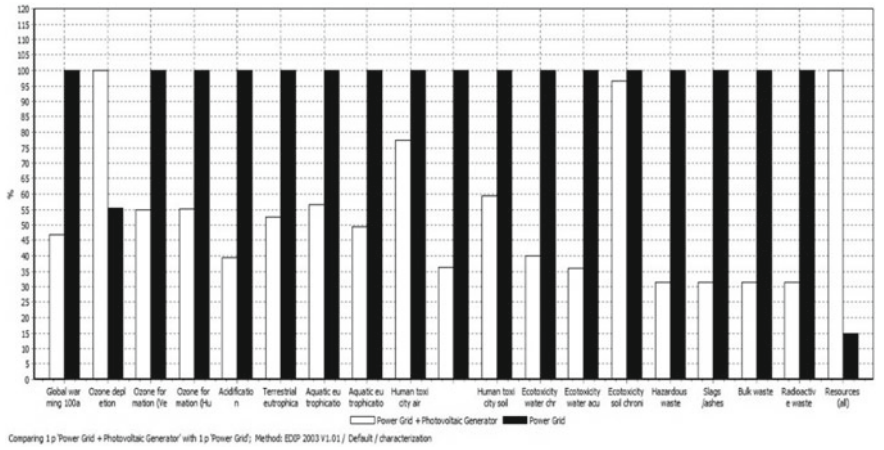

Fig. 8.11 LCA of energy mix

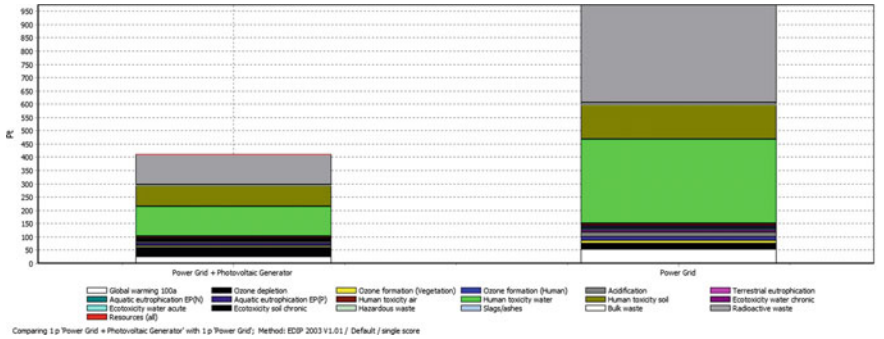

Fig. 8.12 Life cycle assessment of the energy mix, single score

on the above-mentioned parameters (a decrease of these parameters) at the expense of natural resources (an increase of this parameter).

By analyzing Figs. 8.11 and 8.12, which show the results of the LCA, one can observe that by installing a PV system for supplying the technological processes of WWTP has a beneficial impact on most indicators of environmental interest.

The eutrophication indicators and the global warming are decreased when the WWTP uses the mixed power system. From this point of view, the mounting of a photovoltaic generator to the WWTP increases its capacity of mitigating detrimental effects to the environment.

Ozone depletion is increased when the PV system is used and the reason can be attributed to the fabrication process of the PV system components.

It is also shown that the resources use is increased in the case of the mixed power system, as a result of the expenditure to build the PV system.

8.5 Conclusion

A typical and modern microgrid uses two or more sources by which electricity is generated, at least one of which is renewable. Due to the intermittent and unpredictable nature of the most used renewable sources such as solar and wind systems, then are absolutely necessary energy storage systems that provide the possibility of using energy produced in excess in other periods when power generation is low, or lacking or the power demand is high. The installation of different types of energy storage systems together with renewable sources requires a careful analysis of the financial and environmental, respectively on the power grid effects that these conjugate systems introduce. In this regard the application presented shows the improvement of indicators that measure the eco-financial and on power grid effects of installing a PV system with storage batteries in a WWTP.

References

1. S. Suh, E. Hertwich, S. Hellweg, A. Kendall, *Life-Cycle Environmental and Natural Resource Implications of Energy Efficiency Technologies, Environmental and Economic Impacts of Decarbonization: Input-Output Studies on the Consequences of the 2015 Paris Climate Agreements* (Routledge, London, 2017)
2. R. Crume, *Environmental Health in the 21st Century 2 volumes.: From Air Pollution to Zoonotic Diseases* (Greenwood Publishing Group, Incorporated, 2018)
3. A. Mazza, E. Bompard, G. Chicco, Applications of power to gas technologies in emerging electrical systems. Renew. Sustain. Energy Rev. **92**, 794–806 (2018)
4. International Energy Agency, Tracking Clean Energy Progress 2017, Energy Technology Perspectives 2017 Except Informing Energy Sector Transformations, https://www.iea.org/publications/freepublications/publication/TrackingCleanEnergyProgress2017.pdf. Accessed 2018
5. P. Asantewaa Owusu, S. Asumadu-Sarkodie, S. Dubey, A review of renewable energy sources, sustainability issues and climate change mitigation. Cogent Eng. **3**(1), 1–14 (2016)
6. IRENA, IEA and REN21, Renewable Energy Policies in a Time of Transition. IRENA, OECD/IEA and REN21 (2018)
7. https://www.electricitymap.org/?page=country&solar=false&remote=true&wind=false&country. Accessed 2018
8. IEA Renewables Information 2017. Accessed 2018
9. Eurostat nrg_100a, nrg_107a (http://ec.europa.eu/eurostat/statistics-explained/index.php/Energy_production_and_imports and http://ec.europa.eu/eurostat/statistics-explained/index.php/Renewable_energy_statistics)
10. http://publications.europa.ru/webpub/eca/special-reports/renewable-energy-5–2018/ro/. Accessed 2018
11. R. Manghani, R. McCarthy, Global Energy Storage: 2017 Year in Review and 2018–2022 Outlook. GTM Research (2018)
12. J.I. San Martín, I. Zamora, J.J. San Martín, V. Aperribay, P. Eguia, Energy storage technologies for electric applications, in *International Conference on Renewable Energies and Power Quality (ICREPQ'11)* (2011)
13. http://www.sc.ehu.es/sbweb/energias-renovables/temas/almacenamiento/almacenamiento.html
14. IEC: International Electrotechnical Commission, http://www.iec.ch/

15. D. Frankel, A. Wagner, Battery Storage: The Next Disruptive Technology in the Power Sector. (McKinsey & Company, 2017)
16. D. Gladman, The Clean Energy Council's Director of Smart Energy. Explained the Significance of AS IEC 62619:2017 (2018)
17. H. Abe, NAS Battery Storage System, in *Transmission, Distribution & Metering Conference* (2013)
18. ARE (Alliance for Rural Electrification), Using Batteries to Ensure Clean, Reliable, and Affordable Universal Electricity Access, Brussels (2013)
19. IRENA—International Renewable Energy Agency. Battery Storage for Renewable: Market Status and Technology Outlook (2015)
20. N. Bigdeli, Optimal management of hybrid PV/fuel cell/battery power system: A comparison of optimal hybrid approaches. Renew. Sustain. Energy Rev. **42**, 377–393 (2015)
21. C. Chen, S. Duan, T. Cai, B. Liu, G. Hu, Optimal allocation and economic analysis of energy storage system in microgrids. IEEE Trans. Power Electron. **26**, 2762–2773 (2011)
22. M.R. Aghamohammadi, H. Abdolahinia, A new approach for optimal sizing of battery energy storage system for primary frequency control of islanded Microgrid. Int. J. Electr. Power Energy Syst. **54**, 325–333 (2014)
23. A.E. Sarasua, M.G. Molina, D.H. Pontoriero, P.E. Mercado, Modelling of NAS energy storage system for power system applications, in *IEEE/PES Transmission and Distribution Conference and Exposition: Latin America (T&D-LA)* (2010)
24. L. Balza, PbC Battery Overview Potential for Energy Storage (2014), www.axionpower.com/PbC_Battery_Overview
25. C.A. Badea, H. Andrei, E. Rus, Power analysis of PV system used in wastewater treatment plant based on technological analysis. Sci. Bull. Electr. Eng. Fac. (SBEEF) **6**(2), 25–34 (2016)
26. R. Kadri, H. Andrei, J.P. Gaubert, T. Ivanovici, G. Champenoise, P.C. Andrei, Modelling of the photovoltaic cell circuit parameters for optimum connection model and real-time emulator with partial shadow conditions. Energy **42**(1), 57–67 (2012)
27. PV-GISphotovoltaic-software.com/pv-softwares-calculators/online-free-photovoltaic-software/pvgis
28. E. Diaconu, H. Andrei, G. Predusca, P. Pencioiu, V. Ursu, M. Hanek, P.C. Andrei, L, Constantinescu, modelling the charging characteristics of storage batteries for PV power systems, in *IEEE—International Conference Electronics, Computers and Artificial Intelligence—ECAI* (2013)
29. C.A. Badea, H. Andrei, Optimization of energy consumption of a wastewater treatment plant by using technological forecasts and green energy, in *IEEE-International Conference on Environment and Electrical Engineering—EEEIC* (2016)
30. R. Luthander, J. Widen, D. Nilsson, J. Palm, Photovoltaic self-consumption in buildings: a review. Appl. Energy **142**, 80–94 (2015)
31. Ecoinvent Centre. Ecoinvent Data v2.2 (2007), http://www.ecoinvent.org/
32. EPA 2006. Life Cycle Assessment: Principles and Practice. EPA, Cincinnati, 68CO2-067
33. V.M. Fthenakis, E.A. Alsema, M.J. Wild-Scholten, Life cycle assessment of photovoltaics: perceptions, needs, and challenges, in *31st IEEE Photovoltaic Specialists Conference* (2005)
34. R. Battisti, R.A. Corrado, Evaluation of technical improvements of photovoltaic systems through life cycle assessment methodology. Energy **30**, 952–967 (2005)
35. P.C. Andrei, Simulation results of life-cycle assessment of 30 kWp PV system installed at Polytechnic University of Bucharest, Romania. Sci. Bull. Electr. Eng. Fac. (SBEEF) **1**(3), 45–50 (2011)
36. Spatial Differentiation in Life Cycle Impact Assessment—The EDIP 2003 Methodology. Danish Ministry of the Environment, Environmental Protection Agency (2005)
37. H.M. Ramos, F. Vieira, D.I.C. Covas, Energy efficiency in a water supply system: energy consumption and CO_2 emission. Water Sci. Eng. **3**, 331–340 (2010)

38. C.A. Badea, H. Andrei, Optimization of energy consumption of a wastewater treatment plant by using technological forecasts and green energy, in *IEEE-International Conference on Environment and Electrical Engineering—EEEIC* (2016)
39. C.A. Badea, H. Andrei, Case studies of energy efficiency in wastewater treatment plant, in *IEEE Conference Electronics, Computers and Artificial Intelligence—ECAI* (2017)
40. S. Ould Ambrouche, D. Rekioua, A. Hamidat, Modeling photovoltaic water pumping systems and evaluation of CO_2 emissions mitigation potential. Appl. Energy **87**(11), 3451–3459 (2010)

Chapter 9
Design and Experimental Investigations of an Energy Storage System in Microgrids

Mircea Raceanu, Nicu Bizon, Adriana Marinoiu and Mihai Varlam

Abstract The continuous increasing in distributed renewable generation mainly based on wind and solar has complicated recently the normal grid operations. An accurate development in proper energy storage systems with high ability to store and supply energy on demand should effectively eliminate the potentially adverse negative impacts of actual grid operation technologies, such as severe power fluctuation provided by intermittent power generations and photovoltaic arrays. Therefore, the hydrogen economy is regarded as continuous research that can be understood as a significant effort to modify the actual energy system into a system that combines the hydrogen advantage of as energy carrier with high efficiency of proton exchange fuel cells (PEMFC) as electrochemical processes that converts energy power into electricity and heat. In this chapter an experimental investigation on the performance of an integrated microgrid, installed at the National Centre for Hydrogen and Fuel Cell, is presented. This system is equipped with specific components such as photovoltaic generator, solid polymer electrolyzer producing 1 m^3 h^{-1}, 4.2 kW PEMFC and power conditioning system to develop different topologies. Experimental investigations of an energy storage system in microgrids were analysed under realistic scenarios in different environmental conditions. The water electrolyzer stack is powered mainly by the solar PV energy source, then the produced hydrogen is stored

M. Raceanu (✉) · A. Marinoiu · M. Varlam
National Center for Hydrogen and Fuel Cell, National Research and Development Institute for Cryogenics and Isotopic Technologies, Râmnicu Vâlcea, Romania
e-mail: mircea.raceanu@icsi.ro; mircearaceanu@yahoo.com

A. Marinoiu
e-mail: adriana.marinoiu@icsi.ro

M. Varlam
e-mail: mihai.varlam@icsi.ro

N. Bizon
Department of Electronics, Computers and Electrical Engineering, Faculty of Electronics, Communications and Computers, University of Pitesti, Pitesti, Romania
e-mail: nicu.bizon@upit.ro

M. Raceanu · N. Bizon
Polytechnic University of Bucharest, Bucharest, Romania

N. Mahdavi Tabatabaei et al. (eds.), *Microgrid Architectures, Control and Protection Methods*, Power Systems,
https://doi.org/10.1007/978-3-030-23723-3_9

in the hydrogen tank. The role of water electrolyzer is to generate hydrogen when the generated power by solar PV is greater than the power demand, and the role of PEMFC is to consume the generated hydrogen from water electrolyzer and to transform in electrical power energy. The target of the present work has been to assess the dynamic model of both systems to investigate the effect of these elements into the microgrid using measurements of the real systems. Modelling of the described system has been achieved using the MATLAB/*Simulink*. The model parameters have been acquired from manufacturer's performance data-sheets. Based on above information, the proposed concept combining the PEMFC and water electrolyzer hybrid sources could offer an important improvement for real time power imbalances. Therefore, this chapter take into account the control system based power conditioning and energy management of a controllable electrolyzer in order to investigate the real time fluctuations of microgrid's real power balance.

Keywords Microgrids · Energy storage systems · PEM fuel cell · Alkaline water electrolyzers · Control strategy · Hydrogen

9.1 Introduction

The lately increasing in energy consumption, as well as the cost, the nature of fossil fuel, have indicated a great interest in renewable energy sources. In comparison to the conventional centralized power plants, mentioned systems are more sustainable, due to a low size and to the fact that could be installed closer to load locations. Due to a constant progress in power deregulation and utility restructuring, the distributed generation applications are expected to increase [1, 2].

Wind and solar power generation are recognized as promising renewable power generation systems. Among them, Fuel cells (FC) demonstrated a great potential as green power sources because of several advantages such as efficiency, low pollutant emissions, flexible modular structure, low temperature) [3, 4]. However, wind and solar power are connected to climate while FC need hydrogen fuel. Moreover, to date the FC cost is still very high. In this context different renewable energy sources (RES) could be taken into consideration, namely multi-source hybrid alternative energy systems [5, 6].

The green energy could be used to minimise the greenhouse gas, by introducing of energy systems based on microgrids (MG). The primary role of MGs to distribute power to a backup power supply while a detected disaster. An unstable green energy in a small-scale electric MGs have to demand laborious studies to offer the quality and stability of the power. For this reason, many researches of MG technologies with the operation, design and optimization and control, have been proposed [7–9]. The unbalance between generation and load cause the frequency fluctuation. This situation is detrimental in MG because of the poor inertia of the system. Moreover, the different forms of small-scale generations require many power electronic interfaces. For example, to alleviate the unstable green energy provided by MG, the hydrogen

and oxygen are used by FC. It's are produced by an electrolyzer and a gas storage unit tank [10, 11].

A complex system of photovoltaics and water electrolysers is involved [12–14]. In the grid connected mode, MGs has the capability to forward the power with the main grid, which is very useful in keeping of frequency. However, the high investment of the power transmission system, MGs are usually designed as off grid systems [15–17]. There are many investigations regarding various energy storage systems (ESS) for the challenge of RES. Simulation versus experimental results established by applying the algorithm for the charging/discharging of battery storage were also investigated [18–20]. There are known only several works focused on the optimum usage of a hybrid power sources and energy system management [21–23]. Moreover, the scaling of storage technologies and capacity calculations, used in MG, are also important subjects.

Grid-connected solar photovoltaic (PV) system is the most used solar energy application up to now. To date, the large-scale grid connected PVs are considered as the most important routes to decrease the costs, by reducing the energy consumption and developing of a reliable and flexible PV systems coupled with ESSs are broadly used as energy supplies in faraway areas or emerging MG. ESSs offer an opportune energy buffer in respect to the fluctuant PV generation in order to provide an adequate and sustainable energy supply [24, 25].

Fuel cell generation systems have been recognized as new-energy technology to reduce environment pollution and also with big contribution in solving the petrol energy crisis [26]. Among these, proton exchange membrane (PEM) fuel cells seem to be the best alternative due to its simple structure, high power density, quick start, no moving parts and superior reliability and durability, low operating temperature and environmental aspects [27]. Taking into account the more and more increasing interest in PEM fuel cell research and development, its operational performances are focused on various mathematical models, expressing both the dynamic and steady-state conditions. Thus, the PEM fuel cell system behaviour can be analysed starting even with the design step by different pathways with respect to computer simulations in different operational conditions [4, 28].

PEMFCs are used in industry for both stationary and automotive power generation [29] because they have high energy density and operate at low temperatures [30]. However, it is not practical to estimate the real experimental results of actual fuel cell performance directly by measuring the current phenomena and operating conditions, such as electrochemical reactions, flow rates of the reactants, operating temperature, or humidity. Therefore, parametric models and numerical models play a significant role in investigating various operating parameters of a fuel cell system [6].

The main advantages of modelling are the reduction of the number of performed experiments, the finding of optimal algorithms for minimizing the consumption of hydrogen [31], the investigation of the water flooding and air starvation for the sudden load without any risk, which causes the deterioration of the platinum catalyst. Recently, many models have been developed in order to understand the electrochemical reactions in fuel cell, thus PEMFC modelling can be categorized into three different approaches: theoretical, empirical and neural models.

It is known that the dynamic performance of PEM fuel cells strongly depends by operating conditions such as pressure, humidity, temperature, stoichiometric ratios and load changes. Moreover, the dynamic operation of FC should be understood as a complex phenomenon manly due to involved mechanisms, based on characteristic of each process such as water flooding, air starvation, water/heat and gases management. The most models developed in the literature put a burden in the simulation using too many parameters of operation [32], so this approach for real situations is often not justified. In most real application scenarios, the main parameters should be treated as fixed values or slightly changed. For example, some of main conditions such as the temperature, the stoichiometric ratios of reactants fed to the fuel cell, humidity, pressure are considerate to be fixed, as effect of adjustment with an automatic controllable device. This means that is very useful to take into consideration the most valuable output performance, namely voltage of PEMFC as result of current changes during developed sudden load.

There are several well-known possibilities of alternative energy sources and storage sources for building of a hybrid power sources, such as PEMFC/battery/SC system [33], PV/battery [34] and Wind/PV/FC/Electrolyzer/Battery system [35]. Generally, a MG system includes various devices such as DC or AC distribution system, power converters, storage devices, active power filters and programmable automation controller. These components could be connected in different types of MG topologies [36, 37]. Most investigations focused on MG include the optimization using maximum power point tracking (MPPT) techniques, as well as technical-economic feasibility by using mathematical models in MATLAB and Simulink, and/or energy management strategies in real time [38, 39].

Some papers are dealing with hybrid systems containing storage system [40, 41]. For example, the alternative of a hybrid plant which uses a variable consumption, by taking into account an adaptive controller, fuzzy controller was studied. Moreover, a power source fed by RES (wind and photovoltaic) and PEMFC, with an energy storage sources (battery/ultracapacitors) was considered.

Integration of various alternative energy power sources to compose a hybrid power system is still a hot topic. The methods can be classified into two routes: DC coupling and AC coupling. In a DC coupling configuration, different alternative energy systems are coupled to a DC bus by power electronic devices. Then the DC energy is converted into 50/60 Hz AC through a DC/AC converter/inverter which can be bidirectional [42, 43].

The chapter includes following sections. Section 9.1 presents a short introduction of distributed renewable generation with focus on identifying the advantages of hydrogen as energy carrier with high efficiency of PEMFC to convert energy into electricity and heat. Section 9.3 presents: (a) modelling and experimental tests of PEMFC and (b) modelling and experimental tests alkaline electrolyzer. Section 9.4 presents a strategy control to ensure the energy required by the AC load and meantime the maintaining the state of charge (SoC) of the battery level and the hydrogen tank level, all these to demonstrate the microgrid system's ability to solve power quality solutions. Section 9.5 analyses the experimental results of developed Energy Storage

System based on the real time oscillations of real MG power system. Section 9.6 presents the conclusions.

9.2 Microgrid System Description

The microgrid system used to obtain the field data was a standalone system installed at National Centre for Hydrogen and Fuel Cell (NCHFC), Rm. Valcea, Romania (latitude 45°6′17″, longitude 24°22′32″). The system laboratory microgrid is illustrated in Fig. 9.1. The test bench, including a 2.2 kW alkaline electrolyzer, a 2.0 kW PEM fuel cell and a 24 V/200 Ah lead-acid battery bank, a 4.5 Nm^3 hydrogen storage tank, as main components are presented. The renewable energy source (PV) is emulated using the programmable 10 kW DC electronic power supply. Similarly, a 5 kW AC electronic load emulates the demand profiles (electric vehicles, household, industry, etc.). The components are connected to a DC/AC current bus with the compatible power electronic devices. The NCHFC laboratory test-facility has a modular structure in order to obtain a high degree of flexibility in respect to various types of individual components/system to be investigated.

To enhance the understanding of the microgrid topology, a schematic representation of the microgrid system, including the whole control system is presented in Fig. 9.2. In this figure, the components forming grid power system are clearly seen. Beside them, we have to mention the brake resistor (not seen), with role of to dissipate the energy surplus.

The electrolyzer and fuel cell are controlled analogically using the power converters, having their own local controllers, which work with signals received from the converters. In contrast, the battery bank is directly plugged to the DC bus. Bus voltage is maintained by the battery bank, which simplify the topology. This method is a common option in DC microgrids in order to reduce costs and to increase the reliability, as well as the unbalance in the microgrid system is absorbed in the batteries [13]. In this way, a compromise between fully centralized and fully decentralized control architectures could be obtained by taking into account the hierarchical control architecture.

The main components are described briefly as follows:

9.2.1 Alkaline Water Electrolyzer

The most appropriate from economically point of view for an ESS are the Alkaline Water Electrolyzer. The electrolyte is usually the aqueous potassium hydroxide (KOH) with concentrations between 20 and 30 wt%. The typical operating temperatures and pressures are 30–60 °C and 1–30 bar respectively. The included electrolyser in developed system is a 4.2 kW (1.0 Nm^3/h) water alkaline Electrolyser, composed

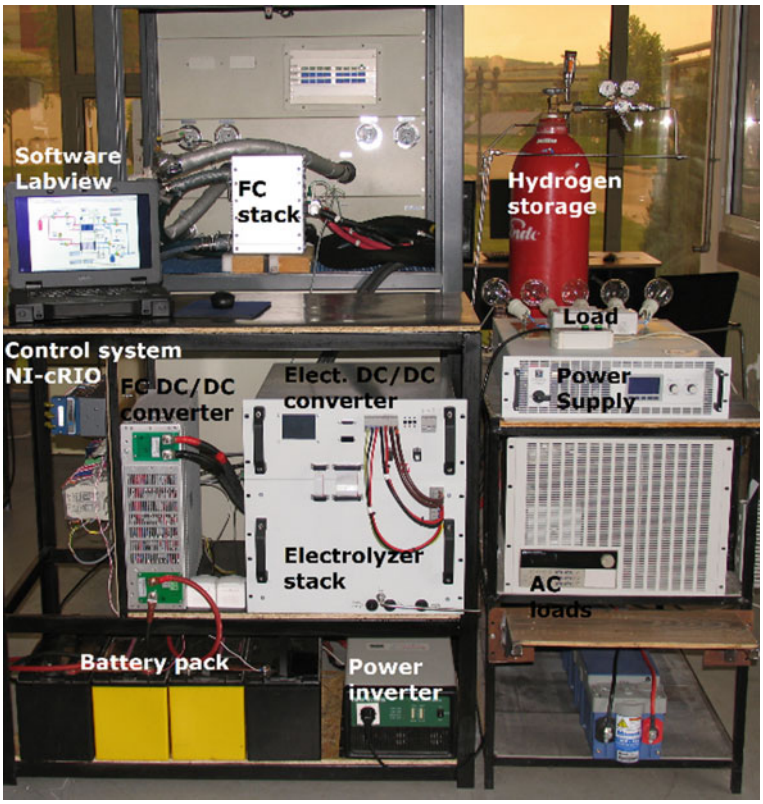

Fig. 9.1 Laboratory-scale microgrid comprising: fuel cell stack, electrolyzer, hydrogen tank, battery pack, converter/inverter and load

of 76 cells each with an active area of 120 cm^2. The deionized water supplied to electrolyser should have a maximum electric conductivity of < 10 μS/cm.

The normal operating parameters are: approximately 35 A at a stack voltage of 120 V, electrolyser pressure (<30 bars) regulated by opening and closing a solenoid valve; stack temperature (<70 °C) cooled with air exchanger controlled by a PI regulator; and deionized water level controlled by upper and lower level sensors.

The main reasons for choosing this electrolyser type are presented:

(i) it was our intention to use it in order to connect to a fluctuating renewable energy source;
(ii) electrolyser produces hydrogen at a pressure of 30 bars, thus eliminates the need for supplementary pressurization using a compressor.

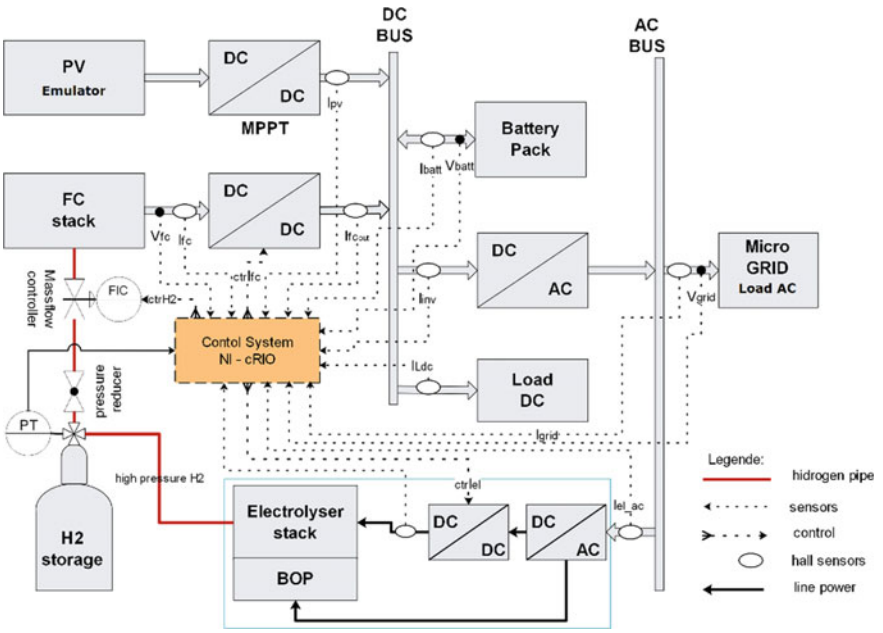

Fig. 9.2 Schematic of the microgrid topology

9.2.2 PEM Fuel Cell

Their distinguishing features are based on low temperatures (50–80 °C) low pressures ranges (0–2 bar) and a special polymer electrolyte membrane. PEM fuel cells are developed mainly for transport applications, as well as for stationary and portable FC applications. The structure of PEM fuel cells includes several parts, namely: (i) membrane electrode assemblies (MEA) consisting in electrodes, solid membrane electrolyte, catalyst, and gas diffusion layers; (ii) bipolar and electrical plates. The reactants are hydrogen (H_2) supplied at anode and oxygen (O_2) supplied at cathode. The chemical mechanism reaction assumes the dissociation of hydrogen molecules into electrons and ionized atoms in form H^+. The oxygen picks up the electrons and completes the external circuit. The electrons go through this circuit thus providing the electrical current. The oxygen then combines with the H+ hydrogen, and water (H_2O) is formed as the waste product leaving the fuel cell. The electrolyte allows the appropriate ions to pass between the electrodes [44]. The most important feature in a single fuel cell is that it typically produces about 0.5–1 V, depending on operational conditions. Therefore, fuel cells are usually connected in series in order to form a fuel cell assembled system. The stack is the system used in cars, generators, or other electrochemical devices that produce power.

The main reason for including the FC in described system that it supplies the energy power on demand. The PEM fuel cell (model name: 2 K Nedstack) is a flow

through-humidified of 16 individual cells. The PEM fuel cell stack consists of cells with an active area of 230 cm^2 each. The PEMFC stack is connected to an Arbin Instruments Fuel Cell Test Stand (FCTS) that meets all the real operating conditions of the PEMFC stack. FCTS communicates through an Ethernet interface with a computer running a dedicated MITS Pro.

FC system is composed of five major subsystems: (1) a fuel and oxidant subsystem, with role in supplying of reactants (oxygen and hydrogen) at the required flow and pressure for chemical reaction; (2) a humidifier subsystem, leading the reactant gases to the appropriate temperature and level of humidity; (3) a cooling water subsystem, removing the heat produced in electrochemical reaction and maintains the proper temperature; (4) an electrical power subsystem, connecting the stack to electric load with different load profiles; (5) an instrumentation and control subsystem, implementing an adequate strategy in order to control the system operation parameters, e.g. flow rates, stoichiometric ratio, temperature, pressure, and so on.

Initially, in the experimental PEMFC test protocol, the stack conditioning procedure should be performed in order to ensure an optimum humidification. Humidified nitrogen is introduced at a flow rate of 5 NL/min, humidified air at a flow rate of 20 NL/min, respectively. Both gases are humidified at 100% RH at 60 °C to clean the anode and cathode sides of the PEMFC stack. When the temperature and humidity conditions are met, for at least 10 min, humidified nitrogen from the anode is replaced with humidified hydrogen. During the experiments the reactant gases are introduced in excess. The open circuit voltage (zero current) should be between 0.8 and 1 V and should be maintained between 0.80 and 0.5 V during operation. During the studied experiments, the fuel gas with 99.998% purity was supplied at the anode and the air was supplied at cathode, several parameters had fixed values being adjusted through an automated control system. The only input-controlled parameter is the stack current that implicitly modifies the hydrogen and air flow rates. The output parameter is the stack voltage.

9.2.3 Power Supply

The fluctuating characteristics of PV are emulated using a programmable power supply (EA-PSI 8240-170). The power supply offers a peak power of 15 kW at 170 V voltage and 200 A current, respectively.

9.2.4 DC Electronic Load

A programmable electronic load, IT 8518C from ITECH was included to emulate different consumption patterns, at maximum 5000 W.

9.2.5 Lead Acid Battery

For short time energy storage, lead acid batteries battery comprises of 2 parallel strings of 12 cells with a nominal voltage of 24 V and a capacity of 200 Ah bus bar in the MG.

9.3 Modelling of Energy Storage System for Microgrid

9.3.1 Modelling of Alkaline Water Electrolyzer

The electrolyzer model approached is based on electrochemical equilibrium operation, which can be assumed to be the opposite of that of a fuel cell when the reactants are hydrogen and oxygen. Specifically, the reactions involved in the electrolyzer cell are:

Anode: $2OH^- \rightarrow \frac{1}{2}O_2 + H_2O + 2e^-$

Cathode: $2H_2O + 2e^- \rightarrow H_2 + 2OH^-$

Total: $H_2O \rightarrow H_2 + \frac{1}{2}O_2$

The Alkaline Electrolysis System consists of a stack consisting of 38 cells connected in series with an active surface of 113 cm^2, an AC/DC converter, a heat exchanger, a water pump and several sensors and actuators for controlling the temperature and current absorbed by the electrolyzer and data measurement. To control the temperature of the electrolyzer, a PID controller is used which regulates the speed of an air fan cooling/heating the electrolyzer. Our chosen model for the alkaline electrolyzer is based on a semi-empirical and stationary electrochemical model connected with a pressure, temperature and load dynamic model. The MATLAB/Simulink model of the water alkaline electrolyzer is presented in Fig. 9.3.

The operating cell voltage of a cell E_{cell} is calculated as the sum of the open circuit voltage E_{ocv}, the activation overvoltage E_{act}, the ohmic overvoltage E_{ohm} and the concentration overvoltage E_{conc}, [Eq. (9.1)].

$$E_{cell} = E_{ocv} + E_{act} + E_{ohm} + E_{conc} \tag{9.1}$$

The open circuit voltage E_{ocv} is the reversible voltage required to start hydrogen production and is defined by the electromotive force (emf) of cell voltage and also referred to by the Nernst equation as shown in Eq. (9.2).

In Eq. (9.2), partial pressures are expressed in Nm^{-2} units, where, T is the stack temperature, R is the gas constant, F is faraday constant, ΔG is Gibbs free energy, P_{H_2} and P_{O_2} are the hydrogen and oxygen partial pressures, and P_{H_2O} is the water partial pressure.

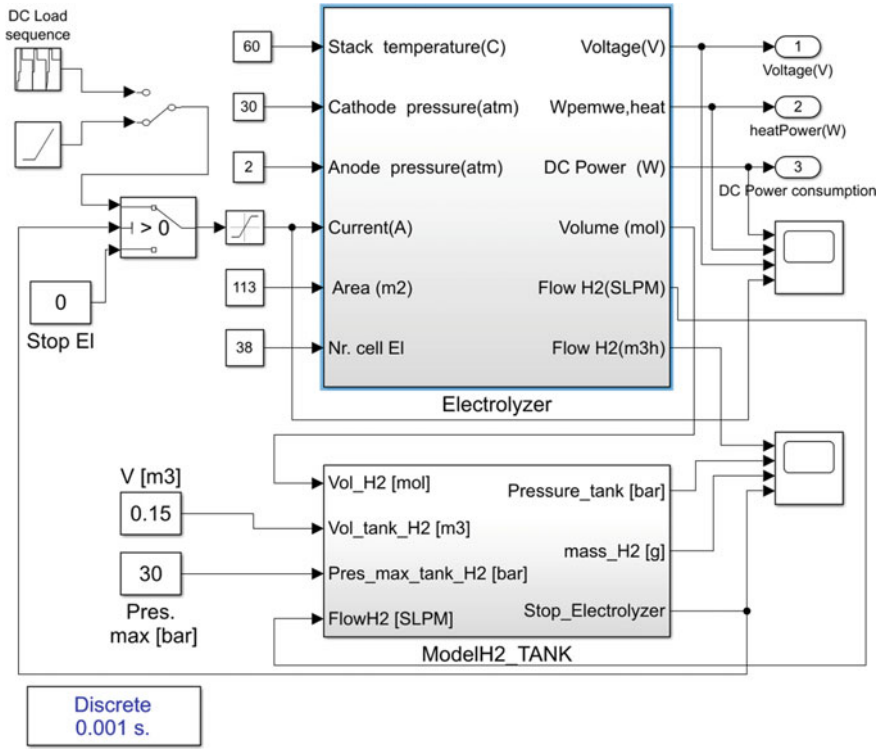

Fig. 9.3 The simulation diagram of the water electrolyzer model

In order to determine the partial pressure at the anode, it is assumed that there is only oxygen and water vapor, as the cathode, only hydrogen and water vapor. In both cases the pressure is very low, so Dalton's law can be applied. Partial hydrogen/oxygen pressures are calculated based on the total pressure at the cathode/anode. In this modelling, the cathode and anode pressures during the experimentation were 1×10^6 and 1×10^5 Nm^{-2}, respectively.

$$E_{ocv} = \frac{\Delta G}{2F} + \frac{RT}{2F}\left[\ln\left(\frac{P_{H_2} P_{O_2}^{0.5}}{P_{H_2O}}\right)\right] \tag{9.2}$$

$$P_{H_2O} = \frac{610}{10^5}\exp\left[\frac{t}{t + 238.3} \cdot 17.2694\right] \tag{9.3}$$

$$P_{O_2} = P_{anode} - P_{H_2O} \tag{9.4}$$

$$P_{H_2} = P_{cathode} - P_{H_2O} \tag{9.5}$$

The activation potential is an overpotential to be exceeded by an electrochemical reaction before the reactants are transformed into products. This electrochemical process is modelled by the Tafel equation. The activation polarization is calculated as the sum of the energy required to start the electrochemical reaction at both anode and cathode. The Tafel equation for the non-zero polarization electrochemical process for each semi-cell is described by Eqs. (9.6) and (9.7). Both overpotentials depend on current density i and exchange current density $i_{0,an}$ and $i_{0,ca}$ with the charge transfer coefficients α_{an} and α_{ca} at the respective electrode.

$$E_{act} = E_{act,an} + E_{act,ca} \tag{9.6}$$

$$E_{act} = \frac{R \cdot T}{2\alpha_{an} \cdot F} a \cdot \sinh\left(\frac{i}{2 \cdot i_{0,an}}\right) + \frac{R \cdot T}{2\alpha_{ca} \cdot F} a \cdot \sinh\left(\frac{i}{2 \cdot i_{0,ca}}\right) \tag{9.7}$$

The value of the charge transfer coefficient depends on the applied potential of the electrode interface with the electrolyte and has an effect on the electrochemical reaction rate. The value of these coefficients can vary from 0.1 to 0.9. The magnitude of the $E_{act,ca}$ is much smaller than the $E_{act,an}$, because kinetics of the hydrogen evolution reaction at the cathode is much faster than kinetic of the oxygen reaction evolution of the anode. For this reason, the $E_{act,ca}$ can be neglected, and Eq. (9.7) is simplified in Eq. (9.8).

$$E_{act} = \frac{R \cdot T}{2\alpha_{an} \cdot F} a \cdot \sinh\left(\frac{i}{2 \cdot i_{0,an}}\right) \tag{9.8}$$

The literature suggests that the exchange current density is in the range of 10^{-12} and 10^{-7} A cm^{-2}. However, the exchange current density can be calculated with Arrhenius equation according to temperature and presented in Eq. (9.9), E_{exc} is the activation energy required for the transport of electrons to the anode.

$$i_{0,an} = i_{0,an,st} \cdot \exp\left(-\frac{E_{exc}}{R} \cdot \left(\frac{1}{T} - \frac{1}{T_{std}}\right)\right) \tag{9.9}$$

The ohmic overvoltage is associated with the cell voltage loss due to the resistance of components to the electron flow. The magnitude of ohmic loss depends on the nature of the interface materials between the electrode and the electrolyte. This overvoltage is modelled by the Eq. (9.10), where, δ_{mem} is membrane thickness (cm), δ_{mem} is cell conductivity (S/cm), and i is current density.

$$E_{ohm} = \frac{\delta_{mem}}{\sigma_{mem}} \cdot i \tag{9.10}$$

Similarly, to the definition of anode exchange current density, the temperature dependence of membrane conductivity can also be defined using the Arrhenius law

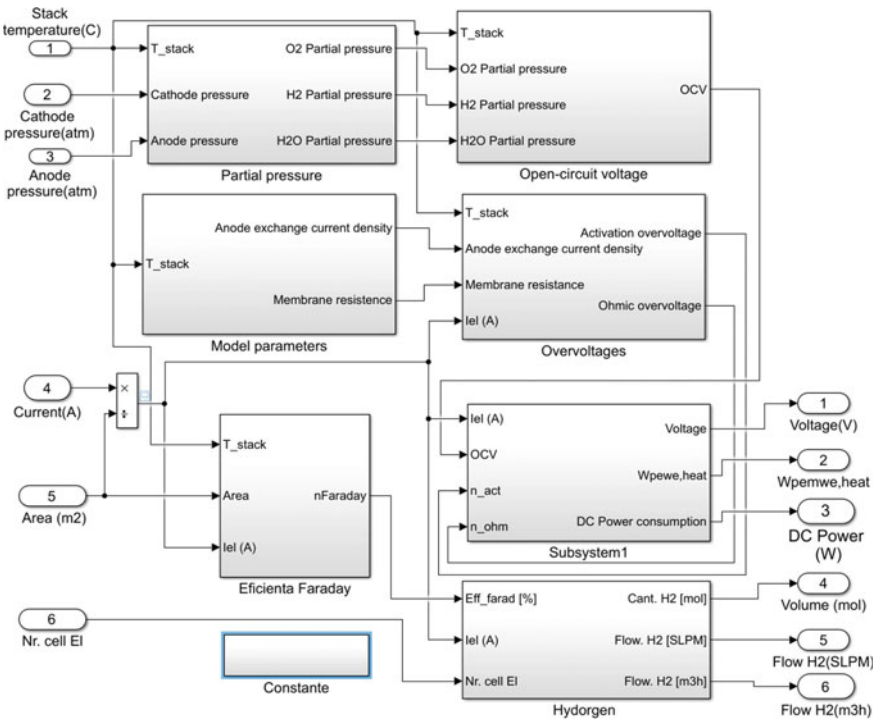

Fig. 9.4 The simulation diagram of the electrochemical submodel

as shown in Eq. (9.11). Where, the value $\sigma_{mem,st}$ and E_{pro} will be determined experimentally and compared to the values reported in the literature.

$$\sigma_{mem} = \sigma_{mem,st} \cdot \exp\left(-\frac{E_{pro}}{R} \cdot \left(\frac{1}{T} - \frac{1}{T_{std}}\right)\right) \tag{9.11}$$

The concentration overvoltage occurs at very high currents, where the gas bubbles are not rapidly removed from the surface of electrodes, which involves lowering the performance of the electrolyzer. This phenomenon is usually not observed because the current density is never high enough to observe these losses.

The electrochemical submodule block which includes all the submodules discussed above is presented in Figs. 9.4 and 9.5 show the values of the constants used in the simulation.

Figure 9.6 shows the polarization curves for simulated and experimental electrolysis model for three different temperatures. The polarization curves were performed at an anode pressure of 30 and 1 bar pressure at the cathodic side. It is noticed that the energy efficiency increases with increasing the electrolyser temperature. The simulated data of the electrolyzer model shows good accuracy with the experimental data for all the currents, pressures and temperatures values in which the electrolyzer

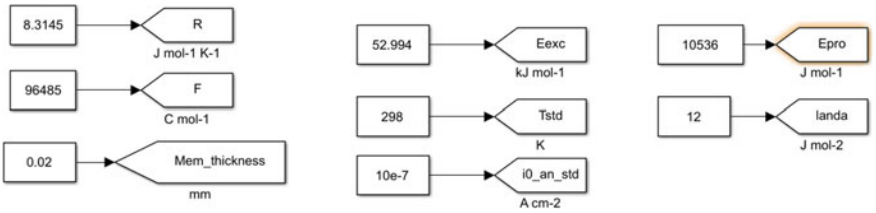

Fig. 9.5 Constants used in the simulation of electrolyzer

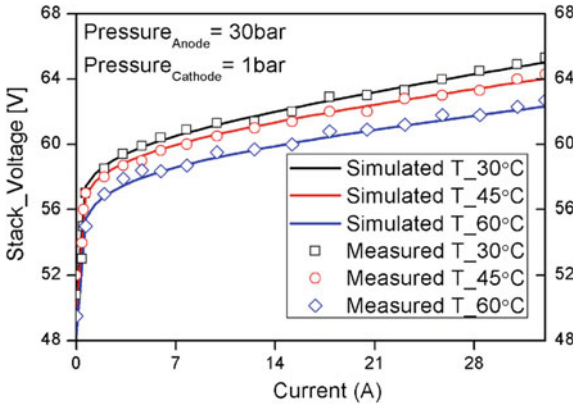

Fig. 9.6 *I-V* curves for an electrolyzer stack at different operating temperatures

usually works. The mean absolute percentage error (MAPE) between the measured and simulated data was calculated and it is observed that the value of 1.39% is at temperature of 60 °C.

Figure 9.7 shows the electrolyzer response at a constant current of 33 A. The temperature was set to the optimum working temperature of 45 °C, reached in about 800 s. Under these conditions, the maximum product hydrogen output is 16.6 slpm. Major error values have been reported between measured and simulated temperatures, mainly due to the lack of precision of the temperature regulator that regulates the thermal gradients between the electrolyzer stack and the heat exchanger system. These experimental data are useful in calculating operating ramp of the electrolyser into the microgrid.

Figure 9.8 shows the start-up ramp of the electrolyzer, then operating at a constant current of 33 A where it is maximum efficiency, and then stopping the electrolyzer in the ramp. Another phenomenon not envisaged by the proposed model is seen in Fig. 9.8. When the electrolyzer is off, the stack load distribution occurs as a consequence of the intrinsic capacitive properties of the stack components. For this reason, a voltage potential can be measured even when the electrolyzer does not produce gas. During operation, the effect of this phenomenon is minor and can be neglected in comparison with the important effect of temperature and pressure on the dynamic modelling of the electrolyzer.

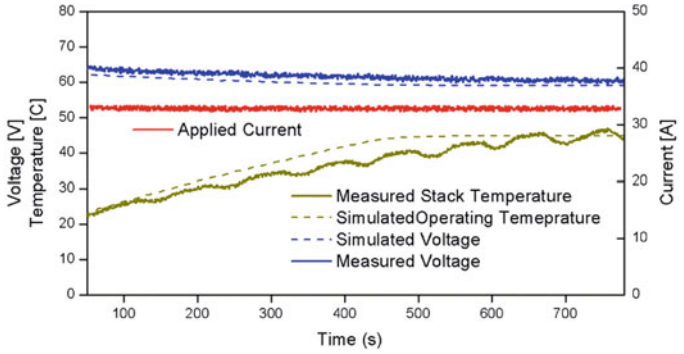

Fig. 9.7 Experimental tests of the electrolyzer to reach the temperature of 45 °C

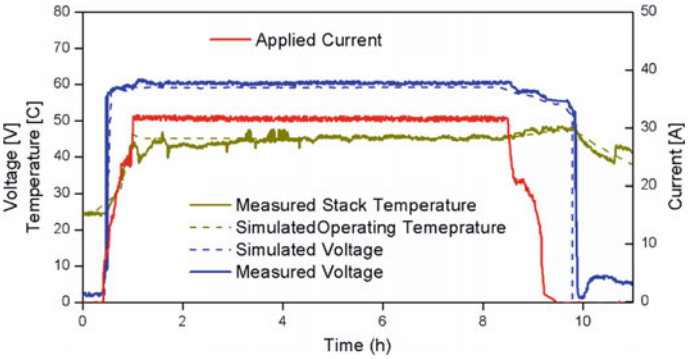

Fig. 9.8 Experimental tests of the electrolyzer for a current constant of 33 A

9.3.2 Modelling of PEM Fuel Cell

The model used to simulate a 2 kW PEM fuel cell is shown in Fig. 9.9. Using the PEM fuel cell derived equations, a simulation model is developed using the SimPowerSystems toolkit of MATLAB/Simulink. The reactants flow rates were calculated using the Faraday's law [Eqs. (9.12) and (9.13)] taking into consideration mainly the expected drawn current and also several parameters such as stack temperature, reactants pressure and reaction stoichiometry.

$$Q_{v,H_2} = \frac{6000 \cdot R \cdot T_{stack} \cdot n \cdot I_{fc} \cdot \lambda_{H_2}}{2 \cdot F \cdot P_{anode} \cdot x_{H_2}}; \; Q_{v,H_2} > 5 \tag{9.12}$$

$$Q_{v,Air} = \frac{6000 \cdot R \cdot T_{stack} \cdot n \cdot I_{fc} \cdot \lambda_{air}}{4 \cdot F \cdot P_{cathode} \cdot y_{Air}}; \; Q_{v,Air} > 10 \tag{9.13}$$

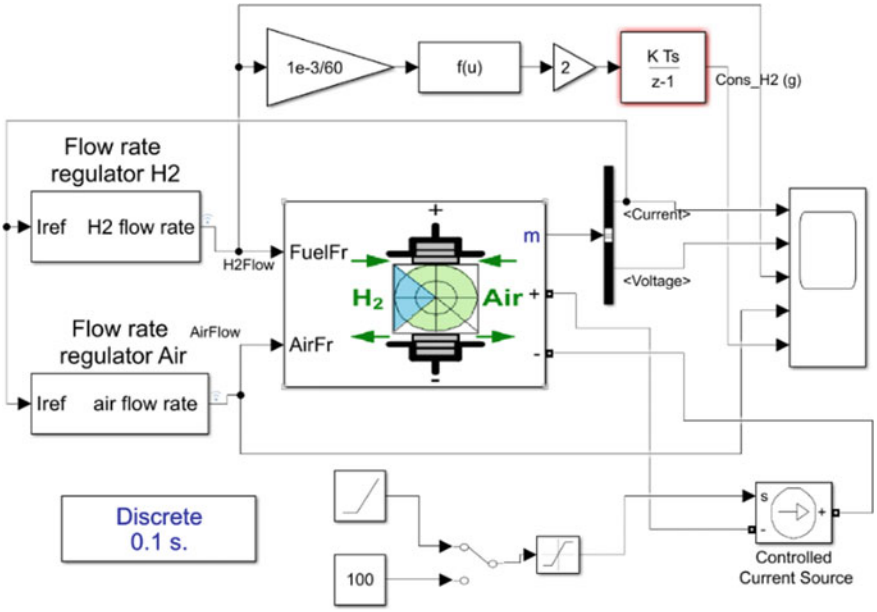

Fig. 9.9 The simulation diagram of PEM fuel cell model

where:
n = is the number of cells in series of the stack (16);
R = universal gas constant [8.3145 j/(mol K)];
F = Faraday's constant (96,485 As/mol).

The I/V curves allow the DC voltage to be monitored when operating in a steady state mode at a given pressure and temperature. The results obtained can be seen in Fig. 9.10, representing the I/V polarization curves for a 65 °C temperature and an anode pressure of 1.5 bar, and the cathode having atmospheric pressure.

The PEMFC stack is connected to an Arbin Instruments Fuel Cell Test Stand (FCTS) that meets all the real operating conditions of the PEMFC stack. FCTS communicates through an Ethernet interface with a computer running a dedicated MITS Pro. The FCTS is located at the National Centre for Hydrogen and Fuel Cell Romania and has been operated taking into account the expertise of our group in dynamic and steady-state conditions of different loading cycles. FCTS is composed of five major subsystems: (1) a fuel and oxidant subsystem, with role in supplying of reactants (oxygen and hydrogen) at the required flow and pressure for chemical reaction; (2) a humidifier subsystem, leading the reactant gases to the appropriate temperature and level of humidity; (3) a cooling water subsystem, removing the heat produced in electrochemical reaction and maintains the proper temperature; (4) an electrical power subsystem, connecting the stack to electric load with different load profiles; (5) an instrumentation and control subsystem, implementing an adequate strategy

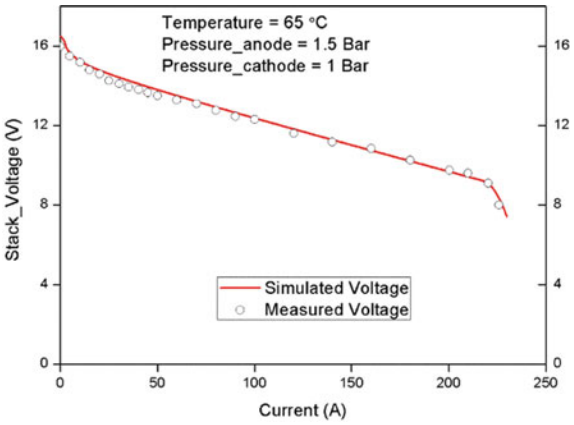

Fig. 9.10 Experimental validation and simulated polarization curves of PEM fuel cell stack

in order to control the system operation parameters, e.g. flow rates, stoichiometric ratio, temperature, pressure, and so on.

Due to the activation losses in the first area of the I/V curve, a non-linear relation is observed for currents lower than 40 A. In the area of the ohmic losses, from 40 to 220 A there is a linear relation, in this area the activation losses remain constant. In the third area there is a strong nonlinearity due to concentration losses. These polarization curves are performed to see the fuel cell response across the operating range. As a rule, the fuel cell is operated in the second zone and, as far as possible, to operate in a constant current mode. The polarization curve is made at a current variation of 4 A/s. Figure 9.10 shows that the experimental results of the fuel cell are very similar to the simulated ones, this allows the Simulink model to be used in different power source architectures.

Further, the proposed model was validated for a dynamic operating regime by means of the test shown in Fig. 9.11. In this test the current was controlled on different current stages, from 20 to 120 A over a duration of 1100 s, so as shown in Fig. 9.11. It can be noticed that, as the current extracted from fuel cell increases, the DC voltage decreases and the operating temperature FC slow increases. It can be seen that the simulated voltage follows precisely the experimental voltage. The experimental test was performed for 20, 40, 60, 90 and 120 A current, achieving operating temperatures of 60.8, 61.6, 63.2, 66.5 and 69.8 °C, respectively. The implemented methodology did it is possible to obtain a more complex PEM fuel cell characterization than that provided by the manufacturer. The results of the modelling obtained in the experiment shown in Fig. 9.11 were quantified for voltage through the mean absolute percentage error (MAPE) is 1.26% and the root mean square error (RMSE) is 0.28 V, and for temperature the MAPE is 2.83% and the RMSE 1.71 °C.

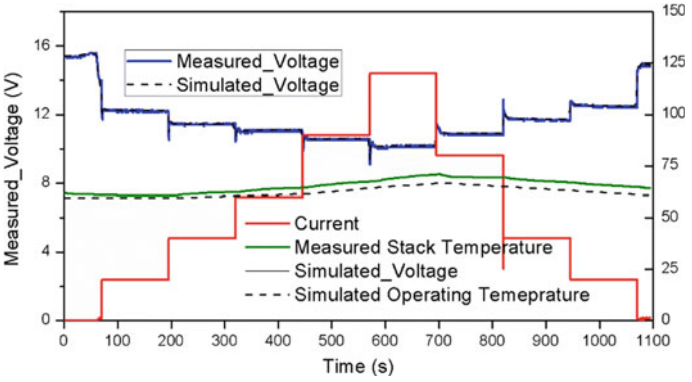

Fig. 9.11 Experimental validation of the PEMFC stack, drawing a stepped current from 20 to 120 A

9.4 Control System

The proposed control system is based on solar power system as input and it is designed to supply a load varying between 0 and 3700 W to power a small power grid. It is known that PV surplus energy could be stored as hydrogen by the electrolyser and deficit energy can be provided by fuel cell generator. The battery system plays the role of power buffer, it also powers the components of the microgrid system. The control system under study is designed to optimize the energy utilization from the different components of the microgrid system.

It is known that if we have an excess of power in the photovoltaic panels, we must be careful not to exceed the maximum current of the battery system and maintain battery state of charge under the level required by the manufacturer (SoC < 90%). The excess power is converted to hydrogen gas by an electrolysis system. Similarly, during the night when the battery charge state drops below the limit value (SoC > 40%), a fuel cell generator is switched on to compensate for the lack of electrical power.

The electrolyzer system and the fuel cell generator are controlled by digital signals of the relay type (on/off), depending on the battery state of charge, and the hydrogen pressure in the storage tank. The battery system is used to compensate the current variations from the photovoltaic panel during the day and during the night of feeding the load. The battery state of charge is calculated by integrating charging/discharging current.

The aim of the control system is to manage the power flow in the microgrid so as to ensure the power of the consumer and protect the battery system from power variations.

Supervisory control and data Acquisition (SCADA) uses a computer connected via Ethernet to a c-RIO NI controller with distributed I/O modules, mass flow controllers, solenoid valves for automatic operation of the complete system/individual components. The control and data acquisition uses a soft designed in LabVIEW. The

main system control is focused on the on/off control of the alkaline electrolyser and the PEM fuel cell, on one hand and on the battery stat of charge (SoC), on the other hand.

The fuel cell stack is connected to the DC bus via a DC/DC convertor. The converter is controlled by an analog signal 0–5 V by c-RIO. In this application, the PEM fuel cell is designed to operate in a stationary mode depending on the condition of the battery charge. The fuel cell stack is connected to a test station that has the role of humidifying hydrogen and air. The control of these gases is made according to the current produced by the fuel cell, this control is carried out by an analogue output module of the c-RIO component. The control algorithm determines when and how much power must produce the fuel cell. All starts and stops of fuel cell are done with a control ramp to ensure the necessary operating conditions (temperature, humidity, pressure).

The alkaline electrolysis system consists of two independent stacks producing 0.5 m^3/h (on each stack). The electrolyzer is connected to the AC bus and has a maximum consumption of 4.2 kW with an efficiency of 98%. The stacks are powered by two DC/DC converters in the 40–70 V voltage range. These are provided with 0–5 V analogue control. The start/stop ramp is used as well as the fuel cell generator. The electrolyzer produces hydrogen up to a maximum pressure of 30 bar, then goes into the standby procedure.

Another parameter monitored by the control system is the hydrogen pressure in the storage vessel. Depending on the minimum set pressure (3 barg), c-RIO sends the stop command to the fuel cell system. Also, for the maximum set pressure (30 barg), c-RIO sends the stop command to the electrolyzer.

The inverter must maintain the output frequency and voltage stable; it is connected to the DC bus and must be able to cover the entire AC load. The AC current and voltage are measured by cRIO through specific modules.

The flow diagram of the control strategy for long-term steady state operation is presented in Fig. 9.10 The parameters are mentions as follows: *P_load* defines the load power; *Ppv* means the solar power; *Pmin* and *Pmax* represent the hydrogen values of pressure stored in tank; *SoC_batt* is state of charge of battery; *P_fc* means fuel cell power at output of the converter; *P_batt* means the battery power; *P_electr* means the electrolyzer power; *Flag* is a boolean variable and has the role of avoiding the on/off switches of the electrolyzer.

In our application, Control strategy treats the following five cases:

1. If $P\_load \geq Ppv$; $Pres\_H_2 < 30$ bar; $SoC\_Batt \geq 85\%$ or $Flag =$ true; and $SoC\_batt > 70\%$. This means that the power of photovoltaic panels is large enough to feed the AC load, and excess power is consumed by the electrolyzer to produce hydrogen with both stacks $P\_electr = 4.2$ kW (case 5);
2. If $P\_load \geq Ppv$; $Pres\_H_2 < 30$ bar; $SoC\_Batt \geq 60\%$ or $Flag =$ true; and $SoC\_batt > 70\%$. This means that the power of photovoltaic panels is large enough to feed the AC load, and excess power is consumed by the electrolyzer to produce hydrogen with a single stack $P\_electr = 2.1$ kW (case 4);

3. If $SoC\_Batt \in [60–80\%]$ and $Flag$ = true; This means that the AC load is fed only from photovoltaic panels and battery, it acts as a power buffer to take power transitions (case 3);
4. If $P\_load < Ppv$; $Pres\_H_2 > 3$ bar and $SoC\_Batt \in (50–60\%]$; This means there is a power deficiency from the solar panels, the AC load power is covered by the battery system and the fuel cell generator with a power of $P\_fc = 1$ kW (case 2);
5. If $P\_load < Ppv$; $Pres\_H_2 > 3$ barg and $SoC\_Batt < 50\%$; This means that the PV panels do not supply power, the AC load is fed by the fuel cell generator, which maintains the SoC to an acceptable level, the fuel cell is set to maximum, $P\_fc = 2$ kW (case 1).

As can be seen from Fig. 9.12, the control strategy implemented in c-RIO makes a balance of power depending on the zone in which it is found. The role of this strategy is to ensure a stable functioning of the microgrid in order to obtain the most energy efficient, with minimal wear on the individual components.

9.5 Experimental Results of Developed Energy Storage System

In this study we used the emulated PV array with power supply connected to a common DC bus, this interconnecting PEM fuel cell, electrolyser, battery and the load. The PEM fuel cell and electrolyser are connected to the DC bus bar using the boost/buck converters.

The power generated by the power sources (PV, FC) is presented as positive values, while the power consumed by the electrolyser is indicated as negative values. Also, the negative/positive values for the battery system mean that it is discharge/charge.

The power balance for the microgrid system is given by:

$$P_{load} = P_{PV} + P_{electr} + P_{FC} + P_{Batt} \tag{9.14}$$

Figure 9.13 shows different operating cases to experimentally test the energy flows between different types of energy components, microgrid and load; taking into account the battery SOC, the hydrogen pressure in the storage tank, the available photovoltaic power and the demand for energy from consumers in the microgrid. The experimental system considered for our microgrid system consists of photovoltaic modules with nominal power of 6 kW, fuel cell PEM system of 1.9 kW, lead acid battery system (200 Ah and 24 V) and an electrolyzer system that produces 1 m^3/h of hydrogen (4.2 kW maximum power) to meet the power load variations of Fig. 9.13a.

The experimental results of the energy storage system developed for the operation of the microgrid system are described as follows:

– In case 3, the fuel cell and the electrolyser are in the off mode, the battery state of charge is between 60 and 80%, this guarantees that the load power can be supported

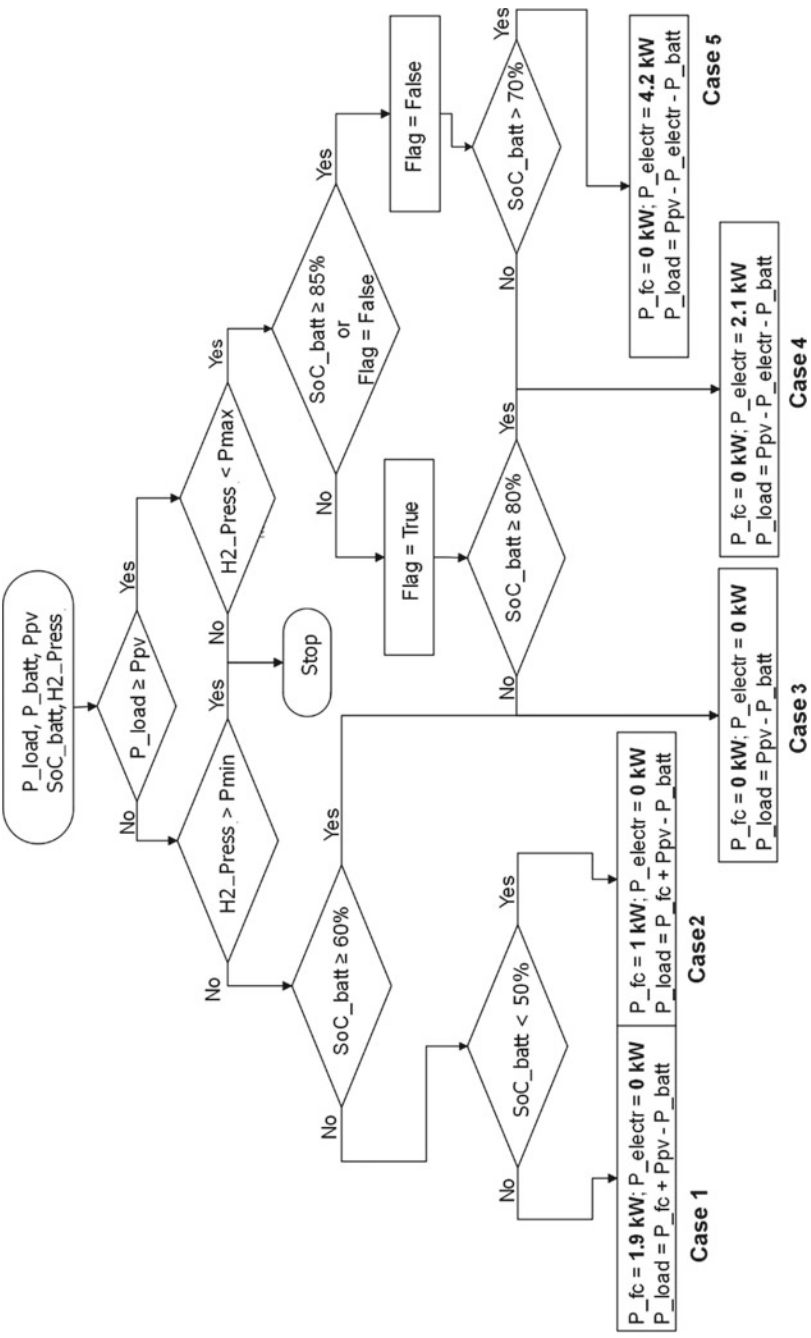

Fig. 9.12 Control strategy of the microgrid

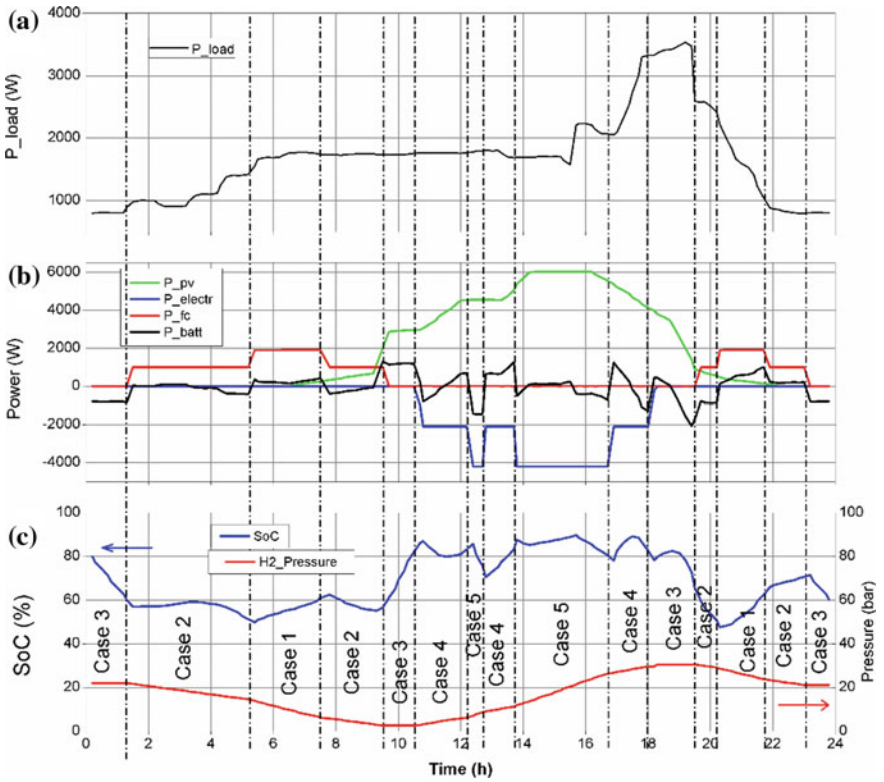

Fig. 9.13 The microgrid power profile, battery SoC and pressure of hydrogen over 24 h

by the battery system and the photovoltaic panels. At night when photovoltaic panels do not produce energy, the load is fully supported by the battery system. In this case the power balance of the microgrid is presented in Eq. (9.15).

$$P_{load} = P_{PV} - P_{Batt};\ P_{FC} = 0;\ P_{electr} = 0 \tag{9.15}$$

– In case 2, the state of the battery charge is between 50 and 60%, the battery cannot fully charge the load and the controller decides to start the fuel cell, on the first power stage (1 kW), the electrolyzer is in the off mode. Starting the fuel cell is done in the ramp to meet the required temperature (60 °C), pressure (0.6 bar) and avoiding the starvation phenomenon. The hydrogen consumed by the fuel cell is about 12.5–13 slpm. In this case, the fuel cell works with maximum efficiency. The controller must check the minimum pressure level in the tank (3 barg) to ensure the operation of the PEM fuel cell. In this case the power balance of the microgrid is presented in Eq. (9.16).

$$P_{load} = P_{PV} + P_{FC} - P_{Batt};\ P_{FC} = 1\,\text{kW};\ P_{electr} = 0 \tag{9.16}$$

– In case 1, the SoC value of the battery is very low, below 50%, the controller decides to start the fuel cell on the second power stage (1.9 kW), the hydrogen consumption is around 27 slpm. The electrolyzer is in the off mode. The controller checks all the operating conditions explained in case 2. The power balance of the microgrid is presented in Eq. (9.17).

$$P_{load} = P_{PV} + P_{FC} - P_{Batt};\ P_{FC} = 1.9\,\text{kW};\ P_{electr} = 0 \tag{9.17}$$

– When the SoC value is between 80 and 85% (case 4), the controller decides that the excess energy is converted to hydrogen, starting the electrolyzer with the first stage of 2.1 kW power. Starting the electrolyzer is done in the ramp to protect the battery system. The controller always checks the pressure in the tank, at the maximum pressure of 30 bar the electrolyzer will stop. The microgrid system is equipped with electrical resistors that consume excess power. The power balance of the microgrid is presented in Eq. (9.18).

$$P_{load} = P_{PV} - P_{electr} - P_{Batt};\ P_{FC} = 0;\ P_{electr} = 2.1\,\text{kW} \tag{9.18}$$

– In case 5, the state of charge of the battery is more than 85%, in order not to destroy the battery, the controller modifies the Flag value in false to avoid transition switching the electrolyzer, this will work on the second stage (4.2 kW) until SoC will reach 70%. The electrolyzer produces hydrogen at a 16–17 slpm flow rate. The fuel cell is in the off mode. The electrolyzer as well as the fuel cell will work in the ramp, both uphill and downhill. The power balance of the microgrid is presented in Eq. (9.19).

$$P_{load} = P_{PV} - P_{electr} - P_{Batt};\ P_{FC} = 0;\ P_{electr} = 4.2\,\text{kW} \tag{9.19}$$

The experimental results obtained confirm that the performance of the proposed microgrid system are satisfactory under both dynamic and stationary loading cases. The results of the experimental test check the efficiency and robustness of the proposed microgrid. Figure 9.13 shows the power profiles of the microgrid. The fuel cell operated on the first level for about 7.3 h where its energy efficiency is high and on the second level about 3.8 h, the total power of the fuel cell over 24 h is 14.52 kW. The electrolyzer operated at the first level for about 3.9 h, and on the second level about 3.1 h, consuming a power of 21.2 kW.

Since fuel cell and electrolyzer degradation mechanisms are strongly dependent on the number of start-stop events [45], such a cost is defined as a key performance indicator. The start-stop number for the fuel cell is 6 on the first level and 2 on the second level respectively for the electrolyzer is 3 on the first level and 2 on the second level.

In Fig. 9.13b it is observed that fluctuations of the solar panels are taken over by the battery system only, the fuel cell and electrolyzer having an operation quasi-stationary mode which increases their lifetime. In the future, the battery system will be replaced with li-ion batteries that have a longer life.

The microgrid efficiency was evaluated in accordance with [46]. The microgrid efficiency can be defined by the ratio between the load energy and the sum of the energy from the renewable energy source, as it is written in Eq. (9.20):

$$\eta_{sys} = 100 \cdot \frac{E_{load}}{E_{PV} + E_{FC} + E_{elctr} + E_{batt}} = 46.2\% \tag{9.20}$$

The purpose of the MG system was to confirm that it is an autonomous energy supply system that stores the excess energy in hydrogen and converts it into energy when needed. Power sources were connected to a DC bus, a DC/AC inverter was used to cover an AC load. The power conditioners devices used were matched appropriately between the components. The control system developed have been successfully tested for autonomous operation.

9.6 Conclusions

In this chapter, a microgrid system consisting of distributed generation sources, energy storage device, a load and a solid polymer electrolyzer have been investigated experimentally. The purpose of the microgrid system was to validate that an independent electricity energy system can be achieved with the storage of hydrogen energy and that the operation of such a system is efficient and robust. The microgrid efficiency was evaluated at 46.2%.

The microgrid system was equipped with photovoltaic modules with a nominal power of 6 kW, a fuel cell system of 1.9 kW, a lead acid battery system (200 Ah and 24 V) and an electrolyzer system that produces 1 m^3/h of hydrogen. Power flow management was achieved by a control algorithm implemented in an automat programmable, the role of this strategy was to ensure a stable functioning of the microgrid in order to obtain the most energy efficient, with minimal wear on the individual components. Experimental investigations of an energy storage system in microgrids were analysed under realistic scenarios in different environmental conditions. Experimental investigations of an energy storage system in microgrid were analysed under realistic scenarios in different environmental conditions to supply a load varying between 0 and 3700 W.

The control algorithm treats five cases depending on the battery state of charge and hydrogen pressure in the tank and determines when the fuel cell or electrolyzer is switched on/off.

The fuel cell and electrolyzer mathematical models were implemented in MATLAB-Simulink to demonstrate these models in the different of steady state and dynamic operating environments. The simulation and experimental validation are

considered acceptable as model simulations accurately reproduce the performance of thermal and electrical modules.

The fuel cell and electrolyzer mathematical models were implemented in MATLAB-Simulink to demonstrate these models in the different of steady state and dynamic operating environments. The simulation and experimental validation are considered acceptable as model simulations accurately reproduce the performance of thermal and electrical modules. More specifically, a root mean square error was less than 0.28 V for the prediction of fuel cell voltage and a root mean square root error of less than 1.71 °C for predicting the fuel cell operating temperature.

Acknowledgements This work has been funded by the National Agency of Scientific Research from Romania by the National Plan of R&D, Project PN 19 11 02 02, PN-III-P-1.2-PCCDI-2017-0194/25 PCCDI and contract 117/2016.

References

1. A. Navaeefard, S.M.M. Tafreshi, M. Barzegari, A.J. Shahrood, Optimal sizing of distributed energy resources in microgrid considering wind energy uncertainty with respect to reliability, in *IEEE International Energy Conference Exhibition Energy Conference* (2010), pp. 820–825
2. X. Li, Y.J. Song, S.B. Han, Study on power quality control in multiple renewable energy hybrid MicroGrid system, in *IEEE Lausanne Power Tech* (2007), pp. 2000–2005
3. P. Pei, H. Chen, Main factors affecting the lifetime of proton exchange membrane fuel cells in vehicle applications: a review. Appl. Energy **125**, 60–75 (2014)
4. W.R.W. Daud, R.E. Rosli, E.H. Majlan, S.A.A. Hamid, R. Mohamed, T. Husaini, PEM fuel cell system control: a review. Renew Energy **113**, 620–638 (2017)
5. N. Bizon, Load-following mode control of a standalone renewable/fuel cell hybrid power source. Energy Convers. Manag. **77**, 763–772 (2014)
6. N. Bizon, M. Oproescu, M. Raceanu, Efficient energy control strategies for a standalone renewable/fuel cell hybrid power source. Energy Convers. Manag. **90**, 93–110 (2015)
7. J. Zhao, F. Dorfler, Distributed control and optimization in DC microgrids. Automatica **61**, 18–26 (2015)
8. R. Zhou, Z. Wang, A. Mcreynolds, C.E. Bash, W. Thomas, R. Shih, *Optimization and Control of Cooling Microgrids for Data Centers*. Experiment, Method Results n.d. HP Laboratories (2012), pp. 1–14
9. Z. Luo, Z. Wu, Z. Li, H.Y. Cai, B.J. Li, W. Gu, A two-stage optimization and control for CCHP microgrid energy management. Appl. Therm. Eng. **125**, 513–522 (2017)
10. F. Alavi, E. Park Lee, N. van de Wouw, B. de Schutter, Z. Lukszo, Fuel cell cars in a microgrid for synergies between hydrogen and electricity networks. Appl. Energy **192**, 296–304 (2017)
11. T. Chaiyatham, I. Ngamroo, Alleviation of power fluctuation in a microgrid by electrolyzer based on optimal fuzzy gain scheduling PID control. IEEJ Trans. Electr. Electron Eng. **9**, 158–164 (2014)
12. W. Gao, V. Zheglov, G. Wang, S.M. Mahajan, *PV—wind—fuel cell—electrolyzer micro-grid modeling and control in real time digital simulator* (Int. Conf. Clean Electr. Power, ICCEP, 2009)
13. R.E. Clarke, S. Giddey, F.T. Ciacchi, S.P.S. Badwal, B. Paul, J. Andrews, Direct coupling of an electrolyser to a solar PV system for generating hydrogen. Int. J. Hydrogen Energy **34**, 2531–2542 (2009)
14. E. Akyuz, C. Coskun, Z. Oktay, I. Dincer, Hydrogen production probability distributions for a PV-electrolyser system. Int. J. Hydrogen Energy **36**, 11292–11299 (2011)

15. J. Li, R. Xiong, Q. Yang, F. Liang, M. Zhang, W. Yuan, Design/test of a hybrid energy storage system for primary frequency control using a dynamic droop method in an isolated microgrid power system. Appl. Energy **201**, 257–269 (2017)
16. P. Ji, X.X. Zhou, S.Y. Wu, Review on sustainable development of island microgrid, in *International Conference on Advanced Power System Automation and Protection (APAP 2011)*, vol. 3 (2011), pp. 1806–1813
17. H. Liang, Y. Dong, Y. Huang, C. Zheng, P. Li, Modeling of multiple master-slave control under island microgrid and stability analysis based on control parameter configuration. Energies **11**, 2223 (2018)
18. E. Sortomme, M.A. El-Sharkawi, Optimal power flow for a system of microgrids with controllable loads and battery storage BT, in *IEEE/PES Power Systems Conference and Exposition (PSCE 2009)* (March 15–18, 2009), pp. 1–5
19. E.R. Sanseverino, M.L. Di Silvestre, R. Badalamenti, N.Q. Nguyen, J.M. Guerrero, L. Meng, Optimal power flow in islanded microgrids using a simple distributed algorithm. Energies **8**, 11493–11514 (2015)
20. M. Raceanu, M. Iliescu, M. Culcer, A. Marinoiu, M. Varlam, N. Bizon, Fuelling Mode Effect On A Pem Fuel Cell Stack Efficiency. Prog Cryog Isot Sep 18, 15–24 (2015)
21. P. Thounthong, V. Chunkag, P. Sethakul, S. Sikkabut, S. Pierfederici, B. Davat, Energy management of fuel cell/solar cell/supercapacitor hybrid power source. J. Power Sources **196**, 313–324 (2011)
22. N. Bizon, M. Raceanu, Energy Efficiency of PEM Fuel Cell Hybrid Power Source, in *Energy Harvesting, Energy Efficiency. Technology Methods, Applications*, vol. 37, ed. by N. Bizon, N. Mahdavi Tabatabaei, F. Blaabjerg, E. Kurt (Springer International Publishing, Cham, 2017), pp. 371–391
23. S. Sikkabut, P. Mungporn, C. Ekkaravarodome, N. Bizon, P. Tricoli, B. Nahid Mobarakeh, et al., Control of high-energy high-power densities storage devices by Li-ion battery and supercapacitor for fuel cell/photovoltaic hybrid power plant for autonomous system applications. IEEE Trans. Ind. Appl. **52**, 4395–4407 (2016)
24. A. Hirsch, Y. Parag, J. Guerrero, Microgrids: a review of technologies, key drivers, and outstanding issues. Renew. Sustain. Energy Rev. **90**, 402–411 (2018)
25. A. Etxeberria, I. Vechiu, J.M. Vinassa, H. Camblong, Hybrid energy storage systems for renewable energy sources integration in microgrids: a review, in *Conference Proceeding IPEC* (2010), pp. 532–537
26. A. Ahmed, A.Q. Al-Amin, A.F. Ambrose, R. Saidur, Hydrogen fuel and transport system: a sustainable and environmental future. Int. J. Hydrogen Energy **41**, 1369–1380 (2016)
27. A. Biyikoglu, Review of proton exchange membrane fuel cell models. Int. J. Hydrogen Energy **30**, 1181–1212 (2005)
28. N. Bizon, Nonlinear control of fuel cell hybrid power sources: Part II—current control. Appl. Energy (2011)
29. I. Aschilean, M. Varlam, M. Culcer, M. Iliescu, M. Raceanu, A. Enache et al., Hybrid electric powertrain with fuel cells for a series vehicle. Energies **11**, 1294 (2018)
30. M. Raceanu, A. Marinoiu, M. Culcer, M. Varlam, N. Bizon, Preventing reactant starvation of a 5 kW PEM fuel cell stack during sudden load change, in *6th International Conference Electron Computer Artificial Intelligence* (2015), pp. 55–60
31. N. Bizon, Improving the PEMFC energy efficiency by optimizing the fueling rates based on extremum seeking algorithm. Int. J. Hydrogen Energy **39**, 10641–10654 (2014)
32. M. Grotsch, Nonlinear Analysis and Control of PEM Fuel Cells. Ph.D. Thesis, Otto-von-Guericke University of Magdeburg, Germany (2010)
33. P. Garcia, J.P. Torreglosa, L.M. Fernandez, F. Jurado, Viability study of a FC-battery-SC tramway controlled by equivalent consumption minimization strategy. Int. J. Hydrogen Energy **37**, 9368–9382 (2012)
34. G. Angenendt, S. Zurmuhlen, H. Axelsen, D.U. Sauer, Comparison of different operation strategies for PV battery home storage systems including forecast-based operation strategies. Appl. Energy **229**, 884–899 (2018)

35. P. Garcia, J.P. Torreglosa, L.M. Fernandez, F. Jurado, Optimal energy management system for stand-alone wind turbine/photovoltaic/hydrogen/battery hybrid system with supervisory control based on fuzzy logic. Int. J. Hydrogen Energy **38**, 14146–14158 (2013)
36. E. Bullich Massague, F. Diaz Gonzalez, M. Aragues Penalba, F. Girbau Llistuella, P. Olivella Rosell, A. Sumper, Microgrid clustering architectures. Appl. Energy **212**, 340–361 (2018)
37. P. Wu, W. Huang, N. Tai, S. Liang, A novel design of architecture and control for multiple microgrids with hybrid AC/DC connection. Appl. Energy **210**, 1002–1016 (2018)
38. M. Garcia Plaza, J. Eloy Garcia Carrasco, J. Alonso Martinez, A. Pena Asensio, Peak shaving algorithm with dynamic minimum voltage tracking for battery storage systems in microgrid applications. J. Energy Storage **20**, 41–48 (2018)
39. A. Guichi, A. Talha, E.M. Berkouk, S. Mekhilef, S. Gassab, A new method for intermediate power point tracking for PV generator under partially shaded conditions in hybrid system. Sol. Energy **170**, 974–987 (2018)
40. M. Jayachandran, G. Ravi, Design and optimization of hybrid micro-grid system. Energy Procedia **117**, 95–103 (2017)
41. S.H.I. Jing, G. Kang, L.I.U. Yang, W. Shu, Application of Hybrid Energy Storage System in Microgrid, vol. 2, 2980–2985 (2015)
42. J.J. Justo, F. Mwasilu, J. Lee, J.W. Jung, AC-microgrids versus DC-microgrids with distributed energy resources: a review. Renew. Sustain. Energy Rev. **24**, 387–405 (2013)
43. H.R. Atia, A. Shakya, P. Tandukar, U. Tamrakar, T.M. Hansen, R. Tonkoski, Efficiency analysis of AC coupled and DC coupled microgrids considering load profile variations, in *IEEE International Conference on Electro Information Technology* (August 2016), pp. 695–699
44. A. Jayakumar, S.P. Sethu, M. Ramos, J. Robertson, A. Al-Jumaily, A technical review on gas diffusion, mechanism and medium of PEM fuel cell. Ionics (Kiel) **21**, 1–18 (2015)
45. E. Zakrisson, The Effect of Start/Stop Strategy on PEM Fuel Cell Degradation Characteristics. Master of Science Thesis in the Master Degree Prog (2011)
46. G. Bruni, S. Cordiner, V. Mulone, Domestic distributed power generation: effect of sizing and energy management strategy on the environmental efficiency of a photovoltaic-battery-fuel cell system. Energy **77**, 133–143 (2014)

Chapter 10
Energy Management Requirements for Microgrids

Farid Hamzeh Aghdam and Navid Taghizadegan Kalantari

Abstract Load growth as a result of progress in technology, industrialization, environmental issues, etc. have caused the arrival of distributed energy resources and consequently formation of microgrids. Proper strategy for the operation of microgrid, could provide various economical, technical, social benefits and environmental benefits. One of the main units in the formation of a microgrid is its energy management center. It is responsible for right decisions about energy generations, consumptions and transactions. The bi-directional energy and data flows in microgrids, cause new challenges for energy management in microgrids. In this chapter, first the energy management system of a microgrid would be introduced. Then, its different parts would be illustrated. Finally, modelling and simulations for the energy management of a typical microgrid will be presented.

Keywords Energy management · Microgrids · Modellings

10.1 Introduction

Distribution networks are facing many different challenges as economic, technical and environmental issues due to demand growth, nowadays. In order to overcome these issues, distributed generation, and consequently microgrids, were developed. The arrival of microgrids have lessen so many issues about the operation of the power systems [1–3].

The main feature of the microgrids is the notion of their controllability which makes them different with active distribution networks. One layer of controlling the microgrids is the energy management process. Energy management is a system-

F. H. Aghdam · N. T. Kalantari (✉)
Electrical Engineering Department, Faculty of Engineering, Azarbaijan Shahid Madani University, Tabriz, Iran
e-mail: taghizadegan@azaruniv.ac.ir

F. H. Aghdam
e-mail: farid.hamzeh@gmail.com

N. Mahdavi Tabatabaei et al. (eds.), *Microgrid Architectures, Control and Protection Methods*, Power Systems,
https://doi.org/10.1007/978-3-030-23723-3_10

atic procedure of managing the energy within the microgrid and transactions with the upper grid network in order to satisfy technical, environmental, economic constraints [4]. In the energy management process inside of a microgrid, by optimizing the production and consumption of different types of energy carriers i.e. electricity, etc. the benefits of the owner would be maximized. Accordingly, a unit known as energy management system is required in order to perform this task. The energy management system is the main and most important part of a microgrid. It has the duties of gathering information, controlling various entities such as distributed energy resources (DERs), energy storage devices, performing demand response programs, choosing the best strategies for operation of microgrid according to different circumstances, the forecasting of the generation for renewable energy resources and load consumption. Some of the main responsibilities of the energy management system is as follows:

- Determining the amount of produced/consumed energy by the generation units/consumers.
- Ensuring the generation and consumption balance.
- Ensure compliance and implementation of the rules for connecting the microgrid to the upper distribution system.
- Optimal utilization of its existing resources.
- Minimizing the overall operational costs.
- Separating the microgrid from the upper grid in case of emergencies.
- Providing convenient control strategy for re-connecting to the upper network after the islanded operation.

Microgrids can be operated in two modes known as islanded and grid-connected operations. In the first mode, the purpose of the energy management procedure, is enhancement of the reliability and in the second mode, it tries to maximize the benefit.

The energy management procedure, can be done as a short term or long term tasks which are called in fact power balancing or energy management, respectively.

In power balancing task, the following goals are pursued:

- Load control capability.
- Voltage regulation.
- Frequency control.
- Avoiding mismatch between production and consumption.
- Acceptable dynamic response for the microgrid, voltage recovery and frequency during and after transients.
- Providing high power quality for the consumers.
- Resynchronization after transient states in order to retrieve the main network requirements for connecting to the upper grid.

Long-term energy management, follows the below purposes:

- Scheduling generation and storage units in order to control the power exchange with the network, reducing losses, increasing the production of renewable resources and minimizing the cost of production.

- Considering the constraints of DERs and environmental impacts.
- Performing demand response programs and recovering the interrupted loads in executing these programs.

According to the modelling of the energy management problem, it could be solved using deterministic or stochastic approaches. Also according to the modelling of the problem, it can be divided into four subcategories as linear programming (LP), nonlinear programming (NLP), and mixed integer linear or non-linear programming (MILP-MINLP).

It is noteworthy to mention that the energy management process is the most important procedure in the operation of microgrids. The scope of this chapter is to represent an overview of requirements for the energy management system. First different types of energy management approaches would be presented. After that a literature review of the scientific works which have focused on the energy management problem will be reported. Next, the main necessary parts of the energy management system, including communication systems, smart meters, etc. would be introduced. Then a modelling for a centralized energy management problem of a typical grid-connected microgrid would be illustrated. Finally, simulations on a test system would be presented.

10.2 Centralized and Decentralized Energy Management

In order to coordinately control the DERs, within a microgrid, various approaches, as centralized and decentralized approaches, are presented in the literature review.

In centralized approaches, a central controller better known as microgrid central controller (MGCC) has the main responsibility for the optimization procedure for the microgrid energy management. According to the energy price and energy demands from local consumers and upstream networks, the MGCC determines the reference values for power generation in local generators, and the amount of power that the microgrid should buy/sell from/to the utility grid. In this procedure, flexible and noncritical loads might be shed or shifted to increase the profit.

In decentralized approaches, local controllers (LCs) have the main responsibilities to optimize their operation, in a competitive environment. Decentralized approaches are appropriate in systems with a variety of owners of the utilities of the microgrid. In such systems local controllers should take various decisions, thus, centralized energy managements intensifies the process. Also, in this approach, the privacy of the owners is one of the priorities [5].

Table 10.1 shows the pros and cons about centralized and decentralized energy management approaches [6]. Also, Figs. 10.1 and 10.2 demonstrates these approaches.

Clearly, for the entities of the microgrid with the same purpose and cooperative operations, centralized energy management would be appropriate. For instance, in microgrids with a single owner, the MGCC would perform the scheduling of all its units such as energy sources and loads, as a central controller aiming on the

Table 10.1 Advantages and disadvantages of centralized and decentralized approaches

Centralized		Decentralized	
Pros	Cons	Pros	Cons
Easy implementation	Powerful MGCC	Less amount of information	Expensive initial setup
Standardized procedure	Large amount of real-time data	Distributing the computational burden on the local controllers	Vulnerable to cyber and physical attacks
Secure against physical and cyber attacks	Requiring reliable two-way communication infrastructure	Reduction of the computational need	Difficult implementation
Simplicity	High expansion cost	Releasing the stress on the communication network	Complexity
	Low privacy for the entities	Easier expansion	
		High privacy for the Entities	

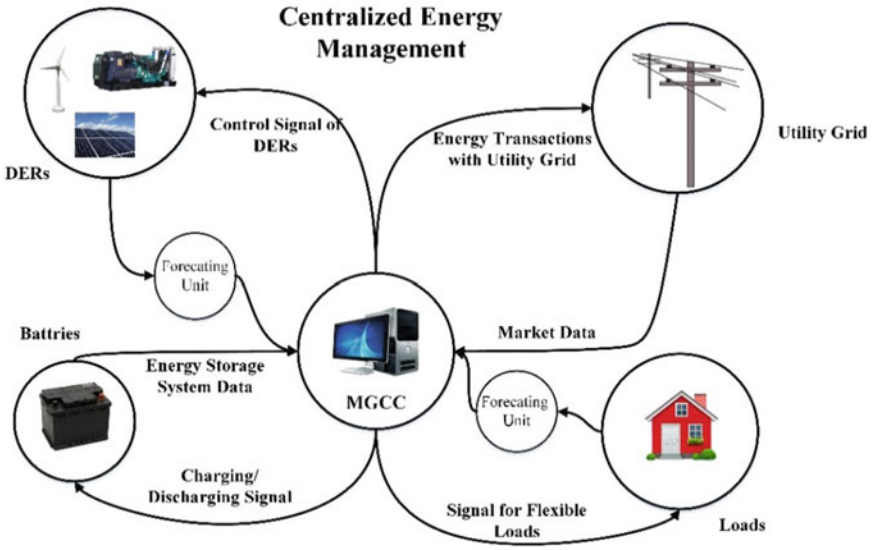

Fig. 10.1 Centralized energy management system

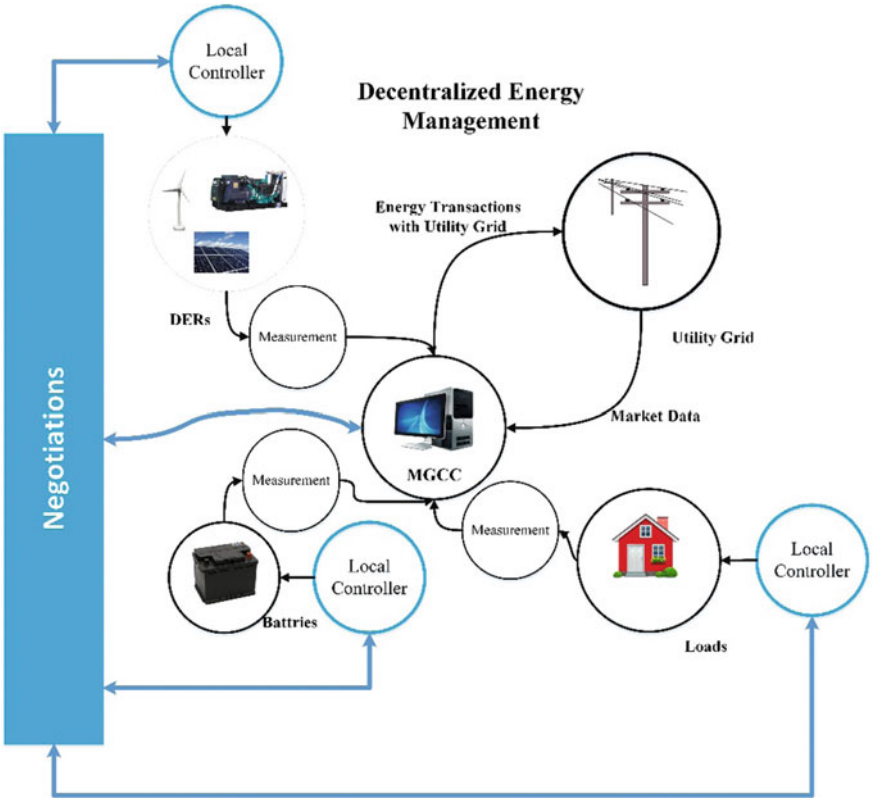

Fig. 10.2 Decentralized energy management system

maximizing the operational benefit. So the energy management system, faces an optimization problem with numerous operational and even environmental constraints where the costs should be minimized in order to maximize the benefit [7].

A competitive and market environment obliges the microgrids to choose decentralized approaches for the energy management process. In such system, local controller of each entity could independently be responsible for its own actions. However, the MGCC would have the duties of monitoring for system security and upper grid transactions. In such procedure, each entity tries to minimize its own energy cost minimization, even though it might be in conflict with actions of other entities [8].

To sum it up, the centralized energy management system seems convenient for the microgrids with one common purpose and the decentralized energy management systems is suitable for the systems with a variety of goals.

10.3 Literature Review

As mentioned earlier, energy management system is one of the most essential parts of a microgrid. Various studies have been done by introducing novel and efficient algorithms and optimization models for the energy management process. Authors in [9], have presented an analysis of energy management system of a microgrid using a robust optimization taking the uncertainties of wind power and solar power generations and energy consumption into consideration. The studied structure has been modelled using an agent-based modelling.

Prodan and Zio, have proposed a reliable energy management approach for microgrids. Energy storage scheduling have been performed in order to minimize the operational costs. The proposed algorithm is constructed based on a predictive control framework taking cost values, energy consumption and generation constraints into consideration. Besides, sources of uncertainties such as generation and consumption have been considered [10].

A novel method for energy management in a microgrid containing energy storage devices and renewable energy based DERs in grid-connected microgrids, has been proposed in [11]. The neighboring microgirds in the presented approach, could share the capacity of their DERs and energy storage devices aiming at reducing the operational costs. The energy management process is done by solving a multi-objective optimization problem as lexicographic program.

Authors in [12], have modelled the equivalent CO_2 emissions for the fossil-fuel-based DERs. Furthermore, fuel consumption and accordingly, individual emission characteristics of these units have been developed. The proposed models, have been applied within the energy management process of a microgrid. Also, demand response programs as shiftable loads are taken into consideration to evaluate the effect on total system emissions and operational costs of the microgrid.

Authors in [13], have assessed the effect of congestion in the lines of a microgrid on its operational cost. Congestion is a common issue due to load growth in distribution networks. A security constrained energy management process have been proposed for a network of microgrids as a centralized approach. Besides, in the energy management procedure, the influence of the load flow constraints of the network on the scheduling problem has been evaluated. Taking extra limits in an optimization problem increases the operational costs. Thus, the authors have suggested using independent tie lines between microgrids and consequently the microgrids would decide whether trading energy with the upper grid or other microgrids in the vicinity. Moreover, sharing a common goal between the microgrids, leads to more profit than operating as individual enitities.

Marzband et al. [14], have presented an algorithm for energy management system of a microgrid using multi-layer ant colony approach aiming on determining the optimum point of operation for local DERs with least electricity production cost. The presented algorithm has the capability of analyzing the constraints related to technical and economic aspects of the problem. The ant colony based optimization problem, showed much better performance in comparison with particle swarm optimization

based energy management. Besides, the authors have investigated the plug and play capability of the algorithm for different scenarios.

Load uncertainty causes power systems to face overwhelming challenges may lead to cause damage for the power systems. Accordingly, authors in [15], have proposed a novel approach for energy management of microgrids considering uncertainties in the amount of demand. The proposed model is nonlinear optimization problem and in order to decrease the computational burden and enhance the customers' privacy they have applied a distributed approach for solving the problem. A simplification has been assumed on the neglecting power network and its constraints and the problem is decomposed into two subproblems performed by MGCC and LCs.

In [16], a robust energy management procedure for the microgrids has been proposed which may make its economic operation easier. Also, a precise forecasting of renewable based DERs has been suggested in order to make the energy management process more accurate.

Unexpected failure in the branches of a power system as a result of load growth, failures of different entities and also high penetration of DERs (conventional or renewable based), are other issues that system operators are facing with. These outages in the microgrid systems, could have an influence on their optimum energy management and may increase the operational costs. Accordingly, the system operator should confront such problems also better known as contingencies in their energy management process. Authors in [17], have proposed a novel method for energy management known as contingency based energy management for system of microgrids. In this method, the system operator takes the probability of the contingency in the lines of the network into consideration for the energy management procedure. A stochastic optimization has been proposed according to various scenarios of the contingencies. One possible solution to overcome this issue is making the structure of the microgrids, changeable recolonized as reconfiguration. This capability and optimal scheduling of the microgrids are utilized as the tools for handling the contingency issue. It has been shown that the proposed method could effectively prevent the network operator from economic loss.

A fuzzy energy management approach has been proposed in [18] to flatten the power profile of a microgrid containing combined heat and power unit. The mentioned structure of the microgrid, contains electrical and thermal generation units, energy storage systems, loads. The energy management system aims on using the extra electrical power of the microgrid to for storing in electrical energy storage systems and keeping the water temperature of the thermal storage system in a desirable range in order to supply residential houses.

Shi et al. [19], have suggested a distributed energy management approach for the microgrids taking the network and power flow constraints into consideration. The energy management problem has been modelled as an optimal power flow problem, and the local controllers and the MGCC cooperatively perform the energy management process.

In [20], a stochastic multi-layer energy management for grid of microgrids has been presented. In order to make the procedure more realistic, the network constraints such as power flow and voltage limitations have been considered. Furthermore, due

to the high ratio of resistance to inductance in distribution networks, the effect of the active power loss on the energy management problem has been assessed. Demand response programs as one of tools to lessen the operational costs have been contemplated in the energy management strategy. Also, emission constraints have been taken into account to consider the environmental issues. In the proposed algorithm, a priority list based approach has been selected which leads to dominance of renewable based generators over conventional generators such as diesel generators.

The performance of the microgrids and supplying a reliable power, strictly is dependent to the interactions between the generators and the loads. Authors in [21], have applied an energy management system based on model predictive approach for a microgrid containing fuel cells, photovoltaic (PV) systems, and an energy storage systems. A bi-level controlling strategy has been selected in order to cope with both low level and high level component management.

10.4 Energy Management Requirements

In this section, the main requirements of proper application of energy management system would be introduced. The information technologies as one of main infrastructures of energy management system, which could improve the operation of microgrids will be discussed. These technologies could facilitate the monitoring, metering and control capabilities in the microgrid. Data of the microgrid is processed by means of information technologies. These applications include data storage, data analysis, data acquisition, data forecasting, data compression, data optimization, etc. [22].

Another main part of the energy management system, is a communication system. The communication system helps the connection of different entities in both centralized and decentralized energy managements. It transfers the data of metering, monitoring, and management signals and accordingly the energy management process is executed. Figure 10.3, depicts an example of a communication system application in a microgrid, with wired and wireless communication lines. A brief introduction of the communication technologies applied in microgrids, including wireless or wireline communications would be discussed in this subsection.

10.4.1 Smart Metering

One of the main tools for the data acquisition from the energy consumers, is the smart metering which is based on advanced metering infrastructure (AMI) [23]. Smart meters log the data for energy consumption of the costumers and transfer the data to the controllers. They have a bidirectional communication with the central controller which and not only send the logged data to the center, but also receive data form the center. This feature of smart meters, could enable the customer-side

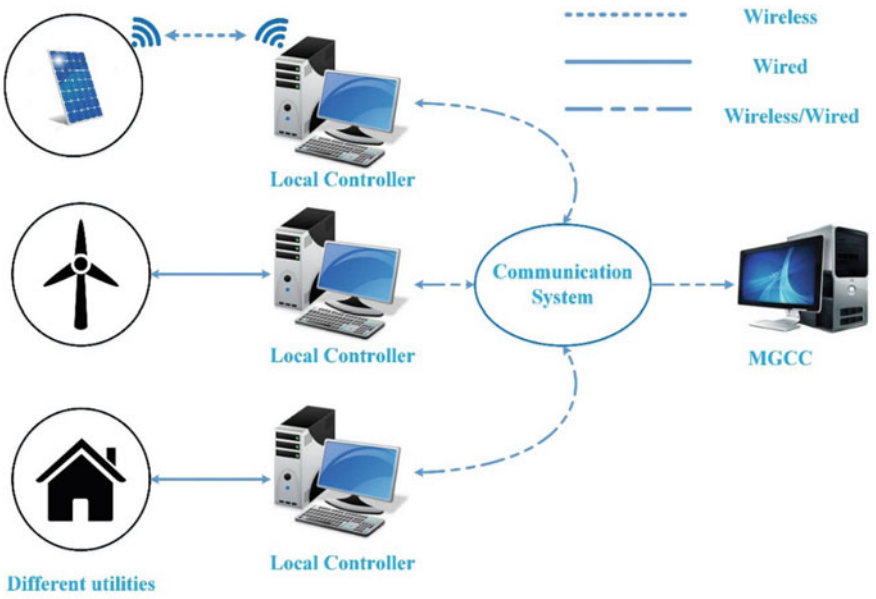

Fig. 10.3 A typical communication system with both wired and wireless connections

services such as adjusting the schedule of utilizing electrical appliances based on the electrical energy price and executing demand response programs [22].

10.4.2 Sensors

Sensors are the first blocks of a measurement system. They transform physical and chemical signals of units into electrical signals. This transformation, must also mirror as closely as possible the involved variables. Sometime, because of noise signals, usage conditions, interference, etc. sensors may generate false signals. In microgrids, sensors are usually used for detecting faults, component failures, malfunctions, sensing environmental conditions, temperature, wind direction, solar irradiance, humidity, etc. A group of sensors which could communicate with wireless technology, is called wireless sensor network (WSN) which have low operational and implementation cost, is widely used in electrical power systems [24].

10.4.3 Phasor Measurement Units (PMUs)

PMUs are units applied for estimating and measuring phase angles and magnitudes of electrical waves which could be usually encountered as phasors in mathematical form such as voltage, current and apparent power in electrical power systems grid using a common time source for synchronization. A common source is used for synchronization which is done by means of global positioning system (GPS). They could also measure the frequency of the power network. PMUs log the measured data measurements with a very frequency as 30–60 measurement samples in a second which facilitate analyzing dynamic characteristics of the network. The microgrid operators could decide on the site of the installation of the PMUs and the output data of the PMUs are used for determining the status of correct operation of the microgrid. Thus, proper usage of these devices, would enhance the reliability and security of the microgrid.

10.4.4 Wired Communication

Power line communications (PLC) and fiber-optic communications are widely used and the most important wired communication systems. Power line communication refers to a technology in which the data signals of different parts and the electrical energy are transferred simultaneously sharing the lines of the network. It could cover all the area that the network is supplying. It is economical due to the fact that they do not need installing new lines and wires particularly for the communication purposes. But this economic benefit comes along with many disadvantages i.e. including large noise with the main signal, low capacity, security issues, etc. Figure 10.4 shows the application of PLC in a microgrid.

Fiber-optic communications are one of the most usual communication systems which have numerous advantages. The technology relies on sending data as pulses of light by means of optical fiber instead of wires. The process of optical fiber communications follows a few steps as creating an optical signal which carries data and is obtained by means of appropriate transmitters, then the signal is relayed along the fiber to avoid its weakening. After that the receiver at the destination receives the optical signal and transforms it into an electrical signal. Due to its optical nature, the transferring data is immune of electromagnetic interference and noises and it can be used for sending signals to the distant places without power loss [25]. Figure 10.5 depicts the operation of fiber-optic communication system.

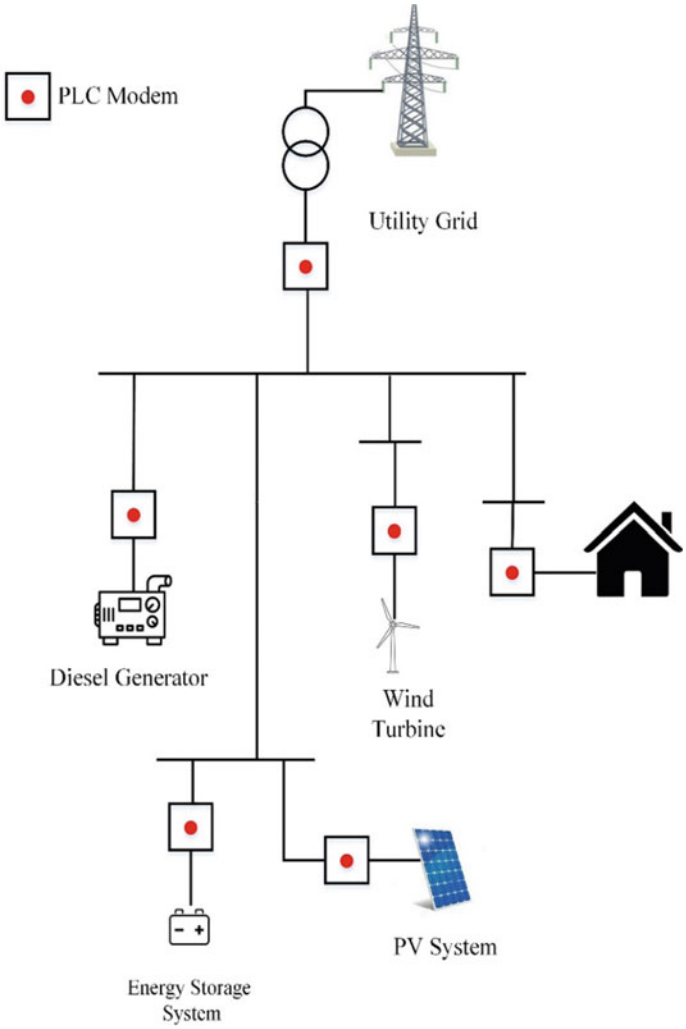

Fig. 10.4 Application of PLCs in a microgrid

10.5 Energy Management Problem Formulation for a Typical Microgrid

In this section energy management problem formulation for a typical grid-connected microgrid in detailed form for different units and its objective function will be presented. Related constraints to each individual would be introduced. The objective function is minimizing the overall operational cost and the output of the energy man-

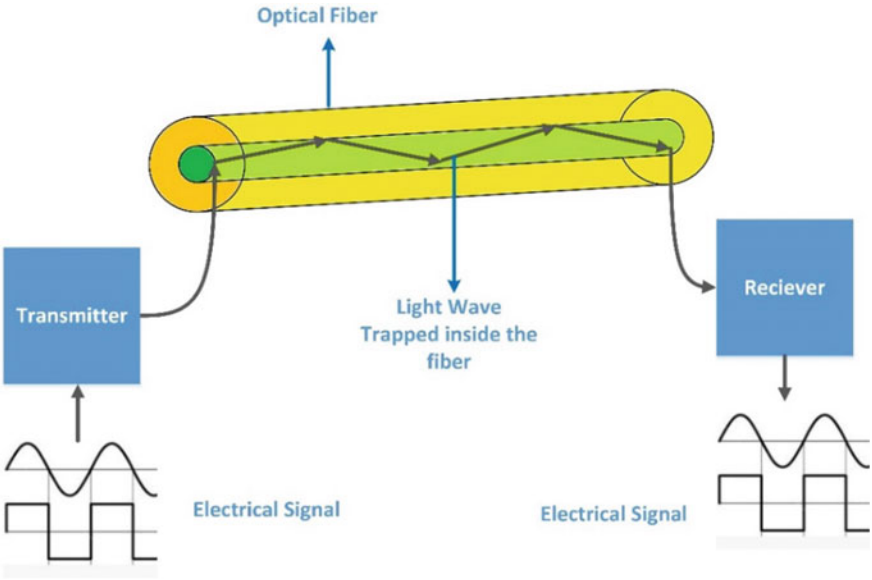

Fig. 10.5 Fiber optic communication system

agement is the schedule of each entity for the upcoming 24 h. It would be modelled as a deterministic MINLP problem.

10.5.1 Structure of a Typical Microgrid

Microgrids are usually accounted as parts of distribution networks. Distribution networks and microgrids are mostly operated in a radial form. In this chapter it is assumed that the microgrid has a radial topology and contains different DERs as diesel generators, PV systems, wind turbines, energy storage systems as batteries, flexible loads and fixed loads. The flexible loads could help the system operator to perform demand response programs. Also, the system structure would be taken into consideration to contemplate the constraints of the network.

10.5.2 Renewable Based DERs

Wind turbines and PV systems are renewable based DERs. The output of these units is stochastic and involved with uncertainty. Forecasting is an essential tool for the systems with the integration of renewable based DERs. This is due to the fact that the system operator in deregulated markets, needs to participate in day ahead markets

and thus it should take decisions beforehand. Also, all the scheduling of the units in the energy management process is done for the next 24-h. In this chapter in order to avoid stochastic modelling of the energy management, we assume that the generated power of these units are forecasted with efficient forecasting tools [26, 27].

10.5.3 Dispatchable DERs

Generation systems such as microturbines, fuel cells, diesel generators, etc. are considered as dispatchable generation systems. It is due to the fact that these systems have controllable output power and could be dispatched. In this chapter it is assumed that the microgrid contains a diesel generator as a dispatchable unit. The following equations illustrates the related equations of a diesel generator [20, 28].

$$0 \leq P_g(t) \leq Y_g(t) \cdot P_g^{\max}, \quad Y_g(t) \in \{0, 1\} \tag{10.1}$$

$$\left|P_g(t) - P_g(t-1)\right| \leq \text{ramp}_g \times P_g^{\max} \tag{10.2}$$

$$C(P_g, t) = \alpha P_g^2(t) + \beta P_g(t) + \gamma \tag{10.3}$$

$$Cst_{start}(t) = X(t) \times C^{S.U.} \tag{10.4}$$

$$X(t) = \max\{Y_g(t) - Y_g(t-1), 0\} \tag{10.5}$$

Equation (10.1) shows the generation capacity of the diesel generator and Eq. (10.2) stands for the ramp-up rate constraint. Equations (10.3)–(10.5) illustrates the operation and startup costs of the generator relations. In the above equations, $P_g^{\max}$, P_g, C and $C^{S.U.}$ are respective symbols for defining maximum power capacity, value of generation, operational cost and startup cost of the generator. Y_g and X are ancillary binary variables which indicate on-off status of and starting moment of the generator. α, β, γ and ramp_g are the coefficients of operational cost and ramp-up rate of the generator which relies on the characteristics of the diesel generator.

10.5.4 Energy Storage System

Energy storage systems are indisputable parts of microgrids. They can compensate energy shortage and collect excess energy during operation. They seem to be vital in presence of renewable based DERs due to their stochastic output power. In this chapter it is assumed that the microgrid contains batteries as the energy storage system. Following equations shows the constraints of a battery for its operation [17].

$$0 \leq P_{bat,ch}(t) \leq Y_{ch}(t) \cdot P_{bat,cap} \cdot (1 - SoC(t-1)) \tag{10.6}$$

$$0 \leq P_{bat,disch}(t) \leq Y_{bat,disch}(t) \cdot P_{bat,cap} \cdot SoC(t-1) \tag{10.7}$$

$$Y_{bat,ch}(t) + Y_{bat,disch}(t) \leq 1\,, \quad Y_{bat,ch}(t), Y_{bat,disch}(t) \in \{0, 1\} \tag{10.8}$$

$$SoC(t) = SoC(t-1) - \frac{1}{P_{bat,cap}} \cdot (P_{bat,disch}(t) - P_{bat,ch}(t)) \tag{10.9}$$

$$0 \leq SoC(t) \leq 1 \tag{10.10}$$

$$SoC(t_0) = SoC_{initial} \tag{10.11}$$

$$SoC(t_{end}) = SoC_{final} \tag{10.12}$$

Equations (10.6) and (10.7) stand for the power capacity constraints of the battery for charging and discharging status. Equation (10.8) keeps the simultaneous occurrence of charging and discharging of the battery. Finally, Eqs. (10.9)–(10.12) are related to the state of charge (SoC) or the level of the stored energy in the battery. In the above equations, $P_{bat,ch}$, $P_{bat,disch}$ and $P_{bat,cap}$ stand in the charging power, discharging power and the maximum available power from the battery, respectively. Also, $Y_{bat,ch}$ and $Y_{bat,disch}$ are ancillary binary variables indicating the charging or discharging status of the battery.

10.5.5 Loads

Two types of loads are assumed in this chapter: (1) critical fixed loads, (2) flexible loads. The latter is capable of participating in the demand response programs. Flexible loads are divided into two subcategories. The first type is sheddable loads and the second one is called shiftable loads. Sheddable loads are cut in some hours by paying a penalty cost to these loads. The energy for shiftable loads should be provided, however the time of this providing could alter during the scheduling horizon. Below equations demonstrate the constraints and costs of providing flexible loads. Equations (10.13) and (10.14) demonstrate the constraints of shiftable loads. Also Eqs. (10.15) and (10.16) represent the cost of performing demand response programs on shiftable and sheddable loads, respectively.

$$P_{shift}^{\min} \leq P_{shift,l}(t) \leq P_{shift}^{\max} \tag{10.13}$$

$$E_{shift}^{\min} \leq \sum_{t=1}^{24} P_{shift,l}(t) \leq E_{shift}^{\max} \tag{10.14}$$

$$C_{shift,l}(t) = \vartheta \cdot \left[E_{shift}^{\max} - \sum_{t=1}^{24} P_{shift,l}(t) \right] \tag{10.15}$$

$$C_{shed,l} = \nu \cdot \left[\sum_{t=1}^{24} P_{shed,l}(t) \right] \tag{10.16}$$

In the above equations, $P_{shift}^{\min}$, $P_{shift}^{\max}$ and $P_{shift,l}$ are the respective symbols for maximum and minimum of shiftable loads and the amount of shifted loads. Also, $E_{shift}^{\min}$ and $E_{shift}^{\max}$ are minimum and maximum energy which is required to supply shiftable loads. ϑ, $C_{shift,l}$, ν and $C_{shed,l}$ are representing shifting price, shifting cost, shedding price and shedding cost, respectively.

10.5.6 Network Constraints

The network of a microgrid could be modeled as a radial network. Bus number 1 is the reference bus that is connected to the upstream network and has a variable power exchange rate and a voltage magnitude of 1 at per unit system.

Each line between the bus bars i and j has the respective resistance and reactance of R_{ij} and X_{ij}. The voltage of the bus i and the current passing through the line are shown with V_i and I_{ij}, respectively. The net output power of each bus follows the bellow relationships:

$$S_i(t) = S_i^{battery}(t) + S_i^{load}(t) - S_i^{gen}(t) \tag{10.17}$$

$$S_i(t) = P_i(t) + jQ_i(t) \tag{10.18}$$

In the above relations, S_i, $S_i^{battery}$, S_i^{load} and S_i^{gen} are the respective representatives of pure power injected power, battery power, load power, and generator power in the ith bus. Also $P_i(t)$ and $Q_i(t)$ are respective symbols for active and reactive powers of the ith bus.

Load flow equations are expressed in the form of the following relations for a radial network:

$$P_j^{net}(t) = P_{ij}(t) - R_{ij} \cdot I_{ij}^2 - \sum P_{jq}(t) \tag{10.19}$$

$$Q_j^{net}(t) = Q_{ij}(t) - X_{ij} \cdot I_{ij}^2 - \sum Q_{jq}(t) \tag{10.20}$$

$$V_j^2(t) = V_i^2(t) - 2(R_{ij} \cdot P_{ij}(t) + X_{ij} \cdot Q_{ij}(t)) + (R_{ij}^2 + X_{ij}^2) \cdot I_{ij}^2(t) \tag{10.21}$$

$$I_{ij}^2(t) = \frac{S_{ij}^2(t)}{V_i^2(t)} \tag{10.22}$$

$$V_{\min} \leq V_i(t) \leq V_{\max} \tag{10.23}$$

$$I_{\min} \leq I_{ij}(t) \leq I_{\max} \tag{10.24}$$

The microgrid operator, can sell its excess power to the upstream network to gain benefit. Also, it can buy power from the utility grid to compensate its shortage or reduce its operational costs. The power transactions with upper grid, $P_{trans}(t)$, depends on the price of electricity, $\rho(t)$.

10.5.7 Objective Function

The objective function of the microgrid operator, maximizing its benefit which is obtained by minimizing the operational costs. Also, it should provide high quality and reliable energy to the consumers. In other words, the main objective is minimizing operational costs of the dispatchable DERs and power transactions with the upstream grid and the cost of executing demand response programs. Furthermore, the operational constraints of different entities should be taken into account. Thus, the optimization problem for the energy management of a microgrid can be formulated as below:

$$\text{O.F.} \sum_t \left[\rho(t) \cdot P_{trans}(t) + \sum_l C(P_g, t) + \sum_l C_{shift,l}(t) + \sum_l C_{shed,l}(t) \right] \tag{10.25}$$

Subject to: Eqs. (10.1)–(10.24)

The above problem is an MINLP problem which is solved by the MGCC to obtain the schedules of the entities for the energy management horizon.

10.6 Simulations

In this section, simulations for the energy management of a test system would be presented. Solver KNITRO in General Algebraic Modeling System (GAMS) software under windows operation system is utilized to solve the energy management problem. The microgrid consists of PV systems, wind turbines, diesel generator, batteries residential loads. Figure 10.6 shows the detailed microgrid structure. It is assumed that the load at bus 5, is a shiftable load and the rest of the loads are sheddable. The maximum capacity of power transactions with upstream network grid is 3 MW and the maximum capacity of the lines are 1 MW. Also, 30% of the load of each bus, is the maximum sheddable power. Penalty factor for cutting off the loads is assumed to be 700 $/MWh. Tables 10.2 and 10.3 demonstrate the characteristics of the entities of the microgrid. Also, Fig. 10.7 shows the energy prices for selling

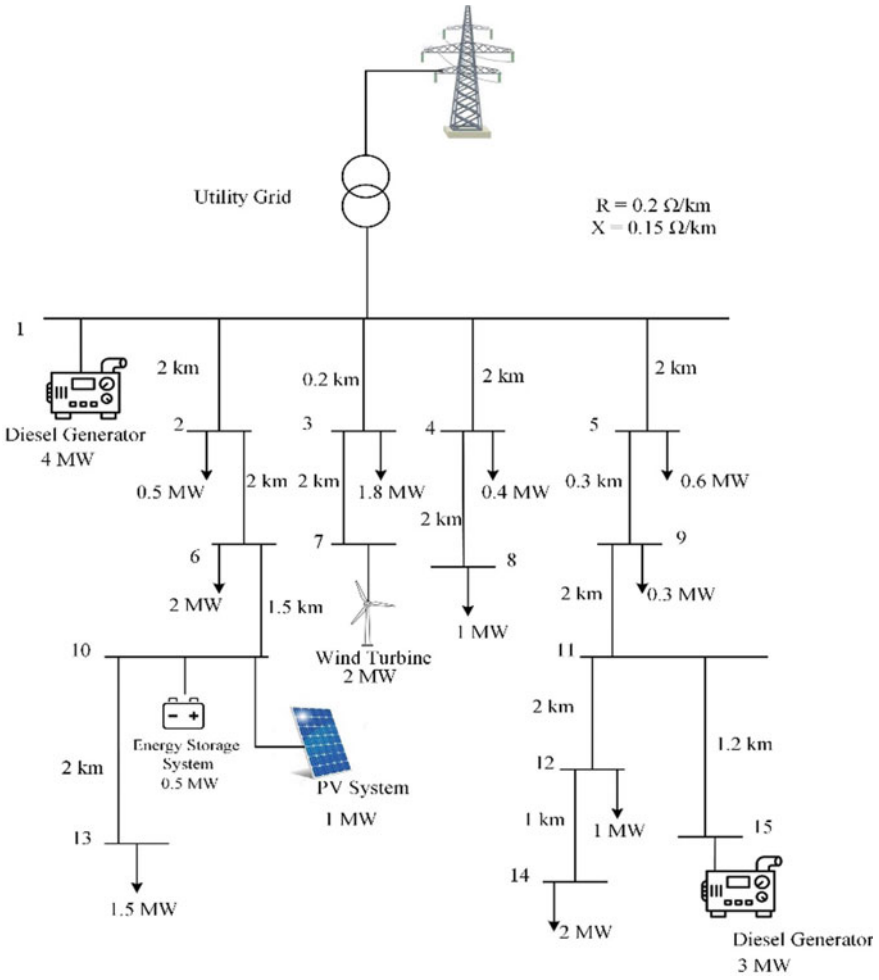

Fig. 10.6 Structure of the test microgrid system

and buying electricity in various hours of the day. The energy management is done for 24-h horizon and the day ahead scheduling of the units would be presented.

The results of the energy management process are shown in Fig. 10.8. This figure illustrates the output schedules of the diesel generators, load curve, forecasted output powers of wind system and solar system, battery power exchanges and transactions with the upper grid. Obviously, in times with lower energy price, the system operator tries to buy energy from the utility grid and sell its excess energy to the upstream network in hours with higher price. The loads are cut in expensive hours or shifted to the hours with lower price. The battery, absorbs energy in cheap hours and release

Table 10.2 Parameters of diesel generators of the microgrid

Diesel generator #	Capacity (MW)	α ($/MW^2)	β ($/MW)	γ ($)	ramp$_g$ (MW/h)	$C^{S.U.}$ ($)
1	4	15	80	0	0.3	15
2	3	20	85	0	0.2	13

Table 10.3 Battery characteristics

Capacity (MWh)	Initial energy (MWh)	Final energy (MWh)
5	1	1

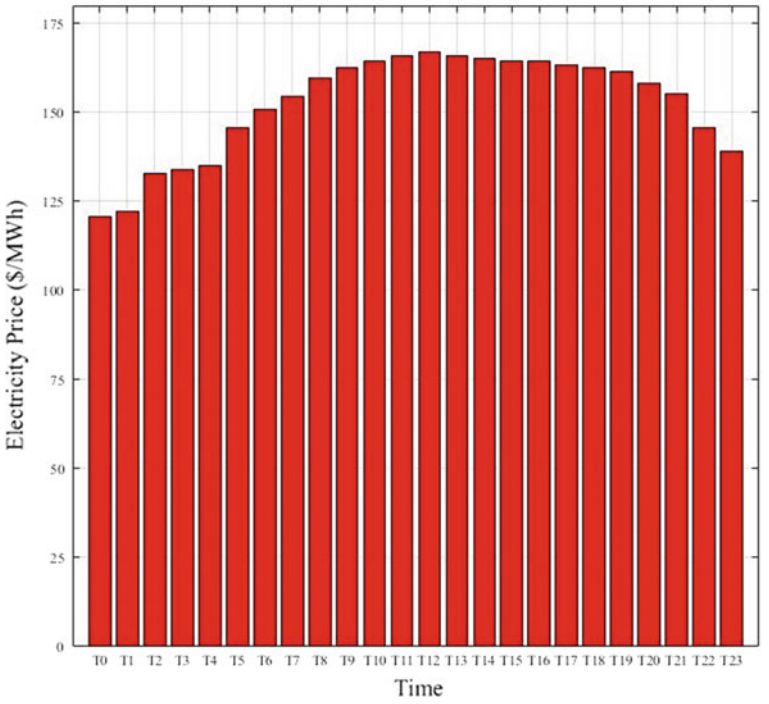

Fig. 10.7 Electricity price during the scheduling horizon

its energy to the grid in hours with high price of electricity. The operational cost for the microgrid during 24 h becomes 8302.28 $. Also the energy loss in the lines of the microgrid is 1.2 MWh.

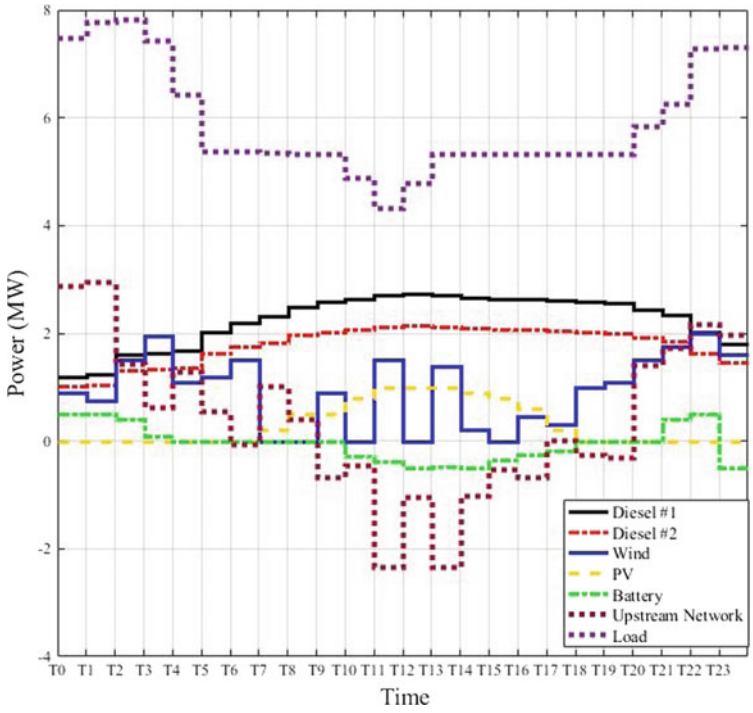

Fig. 10.8 Energy management result of the test system

10.7 Conclusion

In this chapter, energy management system of a microgrid was introduced. The energy management system is the main part of controlling a microgrid. It is responsible for executing many tasks i.e. determining the schedule of power generation of its dispatchable DERs, performing demand response programs, ensuring the generation and demand power balance, complying technical constraints, etc. Then required parts for the energy management procedure were represented. Different parts as information technology and communication systems participate in the energy management process. After that, formulation of energy management for a typical microgrid was presented. Detailed relations for different units were introduced. Finally, simulations in a test system as a typical microgrid were done and the output of the energy management process, has been declared. The energy management system, tries to reduce the operational costs by functioning its units in hours with higher price and selling its excess power to the upper grid. For example, around noon, which has the most expensive prices for electricity, energy sold to the utility grid is maximized. Optimal scheduling of the test microgrid system, showed an operational cost of 8302 $ for 24 h of operation. This is the least possible cost which can be obtained from the proper scheduling of the units.

References

1. M.T. Hagh, F.H. Aghdam, Smart hybrid nanogrids using modular multiport power electronic interface, in *IEEE Innovative Smart Grid Technologies-Asia (ISGT-Asia)*, pp. 618–623 (2016)
2. F.H. Aghdam, M.T. Hagh, M. Abapour, Reliability evaluation of two-stage interleaved boost converter interfacing PV panels based on mode of use, in *7th IEEE Power Electronics and Drive Systems Technologies Conference (PEDSTC)*, pp. 409–414 (2016)
3. F.H. Aghdam, M. Abapour, Reliability and cost analysis of multistage boost converters connected to PV panels. IEEE J. Photovolt. **6**(4), 981–989 (2016)
4. F. Katiraei, R. Iravani, N. Hatziargyriou, A. Dimeas, Microgrids management. IEEE Power Energy Mag. **6**(3), 2008
5. N. Hatziargyriou, *Microgrids: Architectures and Control* (Wiley, 2014)
6. W. Su, J. Wang, Energy management systems in microgrid operations. The Electr. J. **25**(8), 45–60 (2012)
7. D.E. Olivares, C.A. Canizares, M. Kazerani, A centralized energy management system for isolated microgrids. IEEE Trans. Smart Grid **5**(4), 1864–1875 (2014)
8. Z. Wang, B. Chen, J. Wang, Decentralized energy management system for networked microgrids in grid-connected and islanded modes. IEEE Trans. Smart Grid **7**(2), 1097–1105 (2016)
9. E. Kuznetsova, C. Ruiz, Y.F. Li, E. Zio, Analysis of robust optimization for decentralized microgrid energy management under uncertainty. Int. J. Electr. Power Energy Syst. **64**, 815–832 (2015)
10. I. Prodan, E. Zio, A model predictive control framework for reliable microgrid energy management. Int. J. Electr. Power Energy Syst. **61**, 399–409 (2014)
11. M.R. Sandgani, S. Sirouspour, Priority-based microgrid energy management in a network environment. IEEE Trans. Sustain. Energy **9**(2), 980–990 (2018)
12. B.V. Solanki, K. Bhattacharya, C.A. Canizares, A sustainable energy management system for isolated microgrids. IEEE Trans. Sustain. Energy **8**(4), 1507–1517 (2017)
13. F.H. Aghdam, J. Salehi, S. Ghaemi, Assessment of power flow constraints impact on the energy management system of multi-microgrid based distribution network. J. Energy Manag. Technol. **2**(3), 31–41 (2018)
14. M. Marzband, E. Yousefnejad, A. Sumper, J.L. Dominguez Garcia, Real time experimental implementation of optimum energy management system in standalone microgrid by using multi-layer ant colony optimization. Int. J. Electr. Power Energy Syst. **75**, 265–274 (2016)
15. A. Silani, M.J. Yazdanpanah, Distributed optimal microgrid energy management with considering stochastic load. IEEE Trans. Sustain. Energy (2018)
16. S. Ganesan, S. Padmanaban, R. Varadarajan, U. Subramaniam, L. Mihet Popa, Study and analysis of an intelligent microgrid energy management solution with distributed energy sources. Energies **10**(9), 1419 (2017)
17. F.H. Aghdam, J. Salehi, S. Ghaemi, Contingency based energy management of multi-microgrid based distribution network. Sustain. Cities Soc. **41**, 265–274 (2018)
18. D. Arcos Aviles et al., Fuzzy energy management strategy based on microgrid energy rate-of-change applied to an electro-thermal residential microgrid, in *IEEE 26th International Symposium on Industrial Electronics (ISIE)*, pp. 99–105 (2017)
19. W. Shi, X. Xie, C.C.P. Chu, R. Gadh, Distributed optimal energy management in microgrids. IEEE Trans. Smart Grid **6**(3), 1137–1146 (2015)
20. F.H. Aghdam, S. Ghaemi, N.T. Kalantari, Evaluation of loss minimization on the energy management of multi-microgrid based smart distribution network in the presence of emission constraints and clean productions. J. Clean. Prod. **196**, 185–201 (2018)
21. S. Bifaretti et al., Domestic microgrid energy management: model predictive control strategies experimental validation, in *IEEE 15th International Conference on Environment and Electrical Engineering (EEEIC)*, pp. 2221–2225 (2015)
22. Y. Wang, S. Mao, R.M. Nelms, *Online Algorithms for Optimal Energy Distribution in Microgrids* (Springer, 2015)

23. D.G. Hart, Using AMI to realize the smart grid, in *IEEE Power and Energy Society General Meeting-Conversion and Delivery of Electrical Energy in the 21st Century*, pp. 1–2 (2008)
24. V.C. Gungor, B. Lu, G.P. Hancke, Opportunities and challenges of wireless sensor networks in smart grid. IEEE Trans. Industr. Electron. **57**(10), 3557–3564 (2010)
25. V.C. Gungor, F.C. Lambert, A survey on communication networks for electric system automation. Comput. Netw. **50**(7), 877–897 (2006)
26. S.S. Soman, H. Zareipour, O. Malik, P. Mandal, A review of wind power and wind speed forecasting methods with different time horizons, in *North American Power Symposium (NAPS)*, pp. 1–8 (2010)
27. C. Monteiro, L.A. Fernandez Jimenez, I.J. Ramirez Rosado, A. Munoz Jimenez, P.M. Lara Santillan, Short-term forecasting models for photovoltaic plants: analytical versus soft-computing techniques. Math. Prob. Eng. (2013)
28. F.H. Aghdam, M.T. Hagh, Security constrained unit commitment (SCUC) formulation and its solving with modified imperialist competitive algorithm (MICA). J. King Saud Univ.-Eng. Sci. (2017)

Chapter 11
Energy Management of the Grid-Connected PV Array

Florentina Magda Enescu, Nicu Bizon and Ioan Cristian Hoarca

Abstract Solar energy has an important place in the global energy context, this leading to an intense concern in the unconventional energies field. Even if the earth receives only a small fraction of the solar radiation emitted by the Sun (because the radiation suffers the phenomena of absorption and diffusion in the atmosphere) the solar energy has become one of the most important renewable sources. Solar energy can be captured and converted into electrical energy by using the photovoltaic technologies and/or thermal energy, through the use of various types of solar panels heat shields. In this context, the field of producing electricity with photovoltaic panels is approached in this chapter. The photovoltaic panels are devices that convert the solar energy into electrical energy. Depending on weather conditions, the generated renewable energy oscillates, being required an energy storage system to store the excess energy or to discharge energy during the lack of energy. The best solution applied for short-term storage of energy is the battery. On the other hand, the photovoltaic systems only use a portion of the solar radiation and of certain wavelengths, in order to produce electrical energy. The rest of the energy received at the surface is converted into heat, leading to a rise in temperature of the cells components and reduction in yield. In conclusion, increasing productivity and energy efficiency of these facilities involves both the efficiency of their operation in the electric field and the study of the thermal phenomena that take place. In order to ensure a high degree of felicity of the electrical energy management at the level of a microgrid type user, it is necessary to know the energy flows, the structure of the distribution network, and identification of the technical solutions depending on the field. In this chapter, the

F. M. Enescu (✉) · N. Bizon
Department of Electronics, Computers and Electrical Engineering, Faculty of Electronics, Communications and Computers, University of Pitesti, Pitesti, Romania
e-mail: florentina.enescu@upit.ro

N. Bizon
e-mail: nicu.bizon@upit.ro

I. C. Hoarca
National Research and Development Institute for Cryogenics and Isotopic Technologies, Râmnicu Vâlcea, Romania
e-mail: cristi.hoarca@icsi.ro

N. Mahdavi Tabatabaei et al. (eds.), *Microgrid Architectures, Control and Protection Methods*, Power Systems,
https://doi.org/10.1007/978-3-030-23723-3_11

main functional parameters of the system considered will be analyzed, the quality parameters at the level of the electricity system of the user will be estimated, and the operating parameters of the system considered will be also analyzed. The objective of the chapter is to propose a technical solution to improve the efficiency of a photovoltaic power plant within an area of seventy hectares through control, surveillance, metering and monitoring of the system from distance based on Supervisory Control and Data Acquisition (SCADA) system. The photovoltaic power plant used to carry out the experiments is located in Romania. The location of the photovoltaic park is in a plain area where solar radiation is higher (over 1450 kWh/m^2 year, in particular in the summer). With the help of the SCADA system, the energy management of the photovoltaic park can be achieved for: a short period (one day) or for a longer period (a week). The SCADA system offers information about: total energy delivered (kWh), day energy delivered (kWh), active inverter power (kW), percent of availability for photovoltaic power plant, weather info (ambient temperature, plane radiation etc.), hourly graphs about plant production, alarms, current strings, energy meter (exported active-reactive power, imported active-reactive power), data about the weather station, inverter graphs, state of power transformers, breaker state, earthing state, month radiation, month exported active energy, currents variation (I_a, I_b, I_c), leakage current variation (I_g), and voltage variation (V_a, V_b, V_c). The data stored by the system will allow the user to receive current information, but also these data can be compared with the data stored in the same period of the past years, in order to establish the productive efficiency of the photovoltaic power plant.

Keywords Alarms · Control · Energy management · Energy meter · Metering · Monitoring · Photovoltaic power plant · SCADA · Surveillance

11.1 Introduction

The sun is the most important source of energy for all natural processes on Earth. It is a source of energy vital for the survival of all species of plants and animals and supplies power for many critical processes such as photosynthesis.

The production of energy using solar radiation can be made using direct or indirect methods. The indirect form of solar energy is biological material from the past which has been converted into fossil fuels (oil or coal), and the wind energy, hydro and bioenergy. The photovoltaic installations generate a form of direct solar energy.

11.2 SCADA Microgrid Architecture for Photovoltaic Power Plant Studied

Key parts of a photovoltaic system for the generation of electricity are:

– The photovoltaic cells and modules for capturing solar energy;
– An inverter to convert the direct current (DC) in alternating current (AC);

– A set of batteries and charging controller for autonomous systems;
– The other components of the system.

All the components of the system, with the exception of the photovoltaic modules, are called components of the Balance-of-System (BOS).

Measurements have been carried out in a photovoltaic park situated in the southern part of Romania.

Modules are connected in series (called string) to obtain necessary voltage. Enumerated strings are connected in parallel to obtain required current of the system (Fig. 11.1).

The PV modules can generate power between 25 Wp up to 350 Wp depending on the size of PV panel. The small power modules are usually used in standalone applications, where usually required power is not so big. Modules can be dimensioned for quick installation in any location (Fig. 11.2). The module manufacturers usually provide an output power of 70% from the nominal power and after 25 years of use [1–3].

11.2.1 SCADA System-Presentation

Supervisory Control and Data Acquisition (SCADA) are the management and supervisory components system [4–7].

This system is composed of:

– The center of computing equipment which is considered as a Master User Terminal (MUT);
– Units located in the field (remote terminal) for acquisition and adjustment (RTU);
– Software for monitoring, control, remote control and adjustment of the equipment.

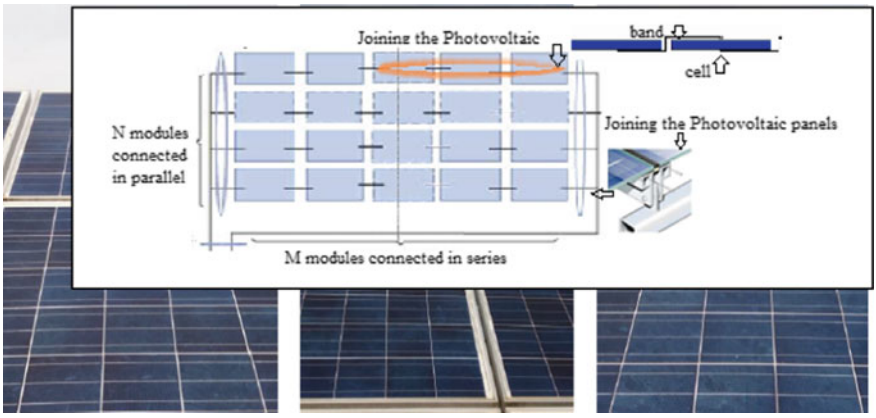

Fig. 11.1 Modules checks in the park of the PV analyzed

Fig. 11.2 Cables arranged on the structure

Fig. 11.3 IBM compatible PC computer

The calculation is intended to allow the process and the execution of the application program which will allow monitoring and implementation of the energy balance sheets.

In this respect, an IBM compatible PC computer (Fig. 11.3) is used, which must to have the following minimal features:

– Intel Core 2 Duo Processor: 2.13 GHz;
– Hard disk—1 × 160 GB SATA drives;
– RAM—1 GB;
– 2 free slots on the standard PCI bus;
– DVD—R/W;
– 10/100 Fast Ethernet network interface;

– Audio—on board;
– Power management;
– Graphical User Interface—least 256 MB RAM;
– TFT color Monitor—22″;
– Mouse, Keyboard;
– A Windows Operating System;
– Uninterruptible Power Supply 220 V/50 Hz;
– Putter: 1000 VA.

11.2.1.1 The Switch Cabinet with Programmable Automation Automatically

The cabinet of automation is structured on the programmable resources of the automatics Simatic S Series 7 200 [4].

The process automatically interfaces with Siemens programmable is composed of:

1. Uch block CPU 224 XP AC/DC/Relay (component 6ES7 224-2BD23-0XB0):
   – The maximum expansion modules: 7;
   – Number of communication interfaces RS 485: 2;
   – Numeric inputs: 14 galvanic isolations by optocoupler;
   – Numeric outputs: 10 with relay;
   – The maximum number of I/O Extension numeric controlled: 256 256 entries and exits numerics;
   – The maximum number of analog I/O:16-16 analog inputs and outputs;
   – The maximum number of central unit on RS 485 Serial Bus: 32;
   – Power: 220 V/50 Hz through the filter.
2. The Profibus communication protocol (Code 6ES7 277-022-0 said AA0)
   – Industry Standard serial port RS 485;
   – The Profibus communication protocols: DP (slave); MPI (slave);
   – The Communication Speed: 12 Mbit/s with automatic detection of the transmission speed;
   – The address of the programmable station: 0–99; (Fig. 11.4).
3. Block Extension analog EM231 you 4 × 12 Bit (Code 6ES7 231-0HC20-0XA0):
   – Number of analogue channels: 8;
   – Type entry: Current unipolar/unified selectable voltage.
4. A display device type Touch Panel TP 177A:
   – The touch control panel;
   – 16 shades of gray, the protocol dialog: PPI, MPI, Profibus.

Fig. 11.4 Communication from PV ST1

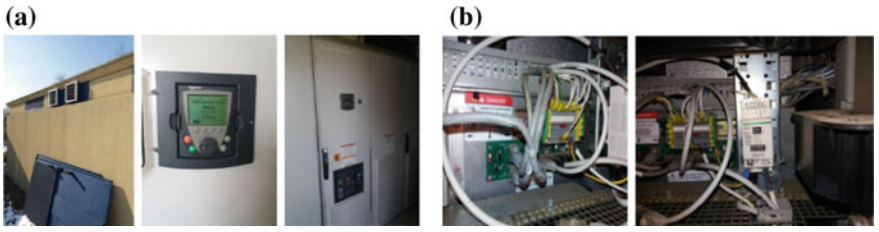

Fig. 11.5 **a** Inverter checks, **b** the inverter communication system

5. The control block/pump drive:

   – The safety switch (breaker) Code 3CC10 11-1JA1;
   – Soft starter type 3RW 30-16/380 VAC—3RW30 16-1CB14;
   – Fuses 3NA 3807-0; support fuse 3NP 40-10.

11.2.1.2 The Closet of the Electronic Regulators

In the closet are installed:

– The regulator TriStar is an all-in-one;
– Sources photovoltaic regulators;
– Accumulator battery;
– Inverter type XTH 6000-48 system: (Fig. 11.5a);

– The task of unloading (diversion);
– Connecting Block photovoltaic sources (Fig. 11.5b).

11.2.2 The SCADA System Functions

The system drop is implemented for the purpose of monitoring the main parameters of the energy sector, the establishment of arrangements for operation, the acquisition of data and storing them in the database, processing on the data bases for the drawing up of energy balances and the determination of the efficiency of the generation [3, 4, 7].

The main functions are:

- Achievement of the console operator—dispatcher man—machine interface (HMI);
- Tracking System layout of detail at each point of monitoring and other equipment integrated into the fall;
- Sending commands to the equipment performance;
- Measurement of analogue and numerical magnitudes continuously and storage in the data bases of measurements;
- View analog and numerical data from each measuring point on the general or his own screen automation cabinet;
- Demonstration in real time the occurrence of critical events of alarm or hazard warning lights and visual and audible alert the operator to operator interfaces;
- Configuration of the generating equipment; set the parameters for the transducers; the allocation of signals; defining the damage, filtering information and generate a report of events;
- Saving data acquired and the specific information events in relational database;
- Tracking status for the operation of the energy sources and protections in real time;
- Perform the correlation between parameters and processing on the quantities purchased;
- Display of reports and tables relating to the operation of the system and equipment for the generation technology.

11.2.2.1 The Structure of the SCADA Informatics Systems

The computer system uses the standard procedures by defining a rigorous task for the used and developed documents and detailed rules for the testing and validation stages. Application software packages are developed under development environments as appropriate for the type of application by using the facilities given by the specific functions developed in the language of high level, the modules provided by the libraries environment for development, the possibilities for the generation, and the management of databases.

It will ensure that the computer after the implementation of the Decision Support System (DSS) components system must comply with the following essential requirements of the application [3, 8]:

- Compliance with the response times, required by technological processes;
- The concomitance use (facilities for multiple users at the same time, the execution of several independent tasks for the same user);
- The efficiency of the system in the optimum use of the resources;
- Sharing and protection, prevent unauthorized access and accidental or intentional alteration of information;
- Reliability and availability of the system;
- Commonality, flexibility, and expandability;
- Modularity horizontally and vertically;
- The transparency and visibility for the purposes of the efficient use and performance;
- Flexible structure, so as to permit the integration into the system of databases used for storing the historical data [6, 7].

11.2.2.2 Decision Support System (DSS)

Decision support system, being integrated into the main system of supervision and control at the level of the human operator, is one liabilities for a single human decident (does not have effective role in the process control; see F.G. Filip in presentation about decision support systems, 2004).

Its construction consists of a series of activities which have as their purpose the obtaining of stable, usable variants of the decision support system.

Further improvement is provided by its capacity of supervised learning [4, 5, 9–14]. The decision system support is detailed by stages of development in Fig. 11.6.

11.2.2.3 The Analysis of the System

It involves the collection and processing of data. It includes:

- The inventory and the in-depth study of the decision-making statements for which it is intended to provide a computer;
- The identification of each operator who will become a user of the system;
- Registry of items of context that the restrictions placed at the top level in the development of the transmission infrastructure/decisions, the computerized existence;
- The assessment of the results of initiatives prior to the introduction of the decision support system.

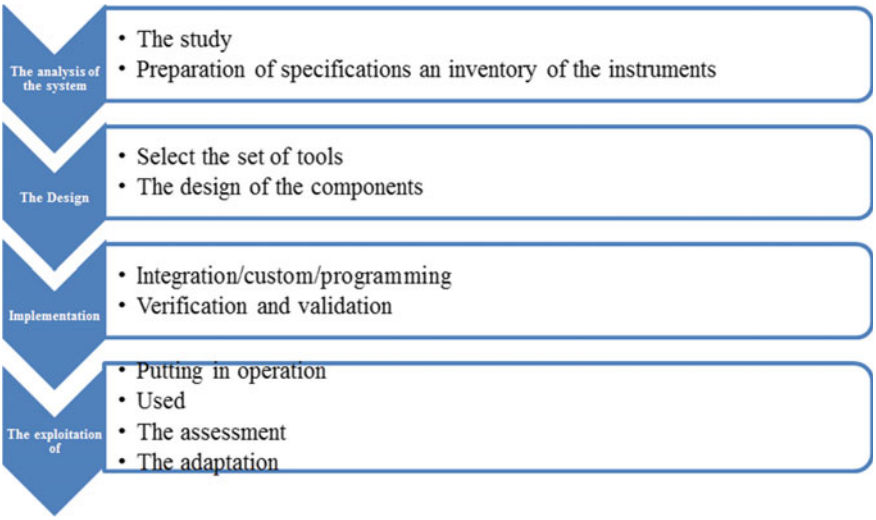

Fig. 11.6 The stages of development of the decisional system support

11.2.2.4 Technical Design

At this stage, the system and its components is actually designed as a whole from the point of view of information technology, the content of the specification being already transposed into a project of execution. The modern design is based on modern and modular information tools, which provides high flexibility in designing of the system. The design process consists in activities to establish of the structure of the DSS, define the technology of each component of the system, and set ways of integration with other parts of the main information system (note that the DSS is a software module embedded in the system of supervision and control at the level of the dispatcher).

11.2.2.5 Implementation

It is the stage at which will be carried out of the DSS software module in accordance with the technical project. It is the implementation and testing of the model of the original DDS. The test involves checking the solutions generated by the DSS with an indication that the system has the ability to learn while supervised. The activities of the verification and validation are intended to determine the extent to which the implementation has led to the achievement of an efficient system. Checking the aims to the appreciation of the correctness of the transposition of the systems of the project Validation is intended to determine the extent to which they are satisfied with the detailed specifications regarding the functions carried out by the DSS.

11.2.2.6 The Exploitation and Development

Operation consists in the putting into service of the system validated and constant analysis by dispatcher performance decisions generated by the DSS. Supervised learning capability (storage of corrections introduced by the dispatcher) allows the decision support system to evolve [4, 6].

11.2.2.7 The Implementation of an Embedded System for Decision Support at the Level of the SCADA Application

Decision support system will be implemented at the level of the operator who will supervise the system energy efficiency through SCADA platform.

The practical implementation of the DSS will consists in adding additional functions of specific SCADA functions.

The operating strategy must help the human operator of the system to decide how many and which generators must be running, which controllable tasks to be connected and storage control energy. Selecting the best combination of operation for each application depends on several parameters: the load characteristics; the system configuration; requirements regarding the quality of energy.

The control strategy adopted should determine the best operating mode of the system.

It is influenced by multiple factors:

- Change in energy demand in time; the variation of power;
- The number of renewable energy generators;
- The uncertainty of power products from specific sources;
- The quality of the energy supplied (of the required quality—variation in frequency and voltage around the nominal value).

The quality of the power represents a main concern in electrical networks, especially in our days when the power converters producing harmonicas are most often encountered in all branches of industry and in the residential sector.

Improvement of the quality of the power will consist of the following:

- Compensation and voltage voids;
- Frequency Control;
- The control voltage;
- The phase unbalance compensation;
- Compensation harmonics.

Of these adjusting voltage and frequency are the most important aspects in the framework of the control system of a Micro MN (Network Micro).

In addition to these another very important aspect is to ensure continuity in the energy supply of consumers [5, 7, 15, 16].

11.3 Management Processes Through SCADA

Since 1980, the supervisory Control and data acquisition (SCADA) has been used as a computerized system for the collection and analysis of data in real time of the supply system [5, 6, 17, 18].

11.3.1 The Correlation Energy Resources on the Basis of Geographic Area

Choosing the location of a photovoltaic park is of great importance from the point of view of the effectiveness of the investment and the acceptability for the population.

Also, the cost of connection to the main power supply will be influenced by the position of the site in relation to the connection point.

On completion of the site the following general aspects:

- The characteristics of the solar radiation in the area (evaluate the solar potential);
- Graph of the temperatures in the area;
- Atmospheric moisture;
- The air density;
- Solar irradiation;
- Important weather phenomena;
- The presence of the chemical active substances;
- The presence of active mechanical particles;
- The possibility of the employment land (environmental impact).

11.3.2 Location of the Photovoltaic Panels

For the location of the solar sources knowledge of solar potential is required (the quantity of solar irradiation in that area).

The photovoltaic panels will be placed on a flat surface, free of mechanical shock. The surface occupied by a photovoltaic panel is proportional to its power.

Thus, photovoltaic panel of 80 W will occupy an area of 0.75456 m^2 less than the area of 1,773 m^2 needed for a 150 W photovoltaic panel.

For these reasons, the calculation of the available surface used to place the panels in relation to the energy production desired by the solar source needs to be analyzed during the farm design phase.

The photovoltaic panels must be placed in such a way as to be oriented toward the sun. As a rule, when it is necessary to power in the winter months when solar radiation is low, the tilt angle of the panel should be located toward the vertical position (approximately equal to the latitude plus 15°) to maximize exposure to sunlight.

The photovoltaic systems (PV) contain cells which convert the sun's energy into electricity. The light intensity determines the amount of electrical power generated by PV module.

11.3.3 Corrective Maintenance

For the photovoltaic park analyzed based on the results stored by SCADA, maintenance adjustments can be made as shown in the Table 11.1.

In Table 11.1 equipments used for corrective maintenance is described: inverter, SCADA, Diesel generator, air oven.

The following data are presented for equipment: failure of the equipments, repair explanation, failure data, response data, fixed data for repair, total time reparation, spares uses. Based on these technical dates, corrective maintenance is made [6, 8, 18–25].

Based on these data, the proposals for the pursuit of preventive maintenance are made in Table 11.2.

In Table 11.2 (preventive maintenance) the dates are fixed to verify the equipments, task description are set for every equipment, results and observation are also made.

11.3.3.1 Preventive Maintenance Works

1. Meteorological Stations—Cleaning of pyranometers and etalon PV sensor/weekly;
2. String and Combiner Boxes/monthly:

   – Visual inspections of string and combiner boxes,
   – External enclosure (No broken or scratched envelope),
   – Electrical boxes wear the proof integrity,
   – Checking doors properly opening and closing,
   – No rust on metallic parts,
   – Checking switchgears fuse bases, fuses, circuit-breakers and surge arrestors integrity and operating condition and calibration,
   – No dust, moisture, corrosion, etc.,
   – Checking correct switch opening and closing,
   – Checking correct execution and state of terminal screws,
   – Checking correct box labeling,
   – Verify electrical testing (open circuit voltage, ground continuity, switches, disconnects),
   – Checking tightening torques,
   – Visual inspections for every inside of combiner boxes and check the functionality of electronic modules (string monitoring);

Table 11.1 PV plant corrective maintenance—2017

PV plant corrective maintenance log									
No.	Equipment	Failure	Repair explanation	Failure data (data hour)	Response data (data hour)	Fixed data (data hour)	Repair total time	Spares uses	Obs.
1	Inverter	AC Switch Response. Service Mode	Check the cables, power suply, AC switch	06.12.2017 11:21:00	06.12.2017 23:22:00	06.12.2017 12:58:00	1.62 h		The reinforcing mechanism was blocked
2	SCADA	Problems with the EDPR server	Verification of communication equipment. Reset server	13.12.2017 08:30:00	13.12.2017 09:00:00	13.12.2017 22:00:00	1 h		
3	Diesel generator	Failure to start the Diesel Generator	Checking automatic switching between AASS transformer and Auxiliary Diesel Generator	14.12.2017 10:30:00	14.12.2017 14:00:00 PM	14.12.2017 14:30:00 PM	0.5 h	Diesel fuel pump	
4	Air oven	Switch burn	Replace the switch from the air oven	15.12.2017 09:00:00	15.12.2017 21:05:00	15.12.2017 21:35:00	0.5 h		
5	SCADA	Problems with the EDPR server	Verification of communication equipment. Reset server	27.12.2017 11:30:00	27.12.2017 11:35:00	27.12.2017 12:15:00	0.67 h		

Table 11.2 PV plant preventive maintenance—2017

Ingeteam			PV plant preventive maintenance log		
No.	Date	Equipment	Task description	Status	Observations
1	04.12.2017	Transformation centers	Transformer isolation measurements. Operation checking of transformer protections. Checking tightness of connection at transformer	OK	TRAFO, MV Cubicles to PVST8, PVST9 and PVST10
2	05.12.2017	Transformation centers	Transformer isolation measurements. Operation checking of transformer protections. Checking tightness of connection at transformer	OK	TRAFO, MV Cubicles to PVST1, PVST3 and PVST5
3	06.12.2017	Transformation centers	Transformer isolation measurements. Operation checking of transformer protections. Checking tightness of connection at transformer	OK	TRAFO, MV Cubicles to PVST6 and PVST7
4	07.12.2017	Transformation centers	Transformer isolation measurements. Operation checking of transformer protections. Checking tightness of connection at transformer	OK	TRAFO, MV Cubicles to PVST2 and PVST4
5	07.12.2017	Inverters, meteorogical stations	Checking for general condition of the inverters. Checking the fans working. Cleaning pyranometers and calibrated cells	OK	

(continued)

Table 11.2 (continued)

Ingeteam			PV plant preventive maintenance log		
No.	Date	Equipment	Task description	Status	Observations
6	12.12.2017	PV modules	Check the modules in fields number 1, 2 and 3	OK	I don't found any broken modules
7	12.12.2017	Security systems	Check all the cams and the perimetral alarm	OK	The cams work ok, without the cam D5: has image but when in move up, down, left or right don't work, don't made any move
8	14.12.2017	PV modules	Check the modules in fields number 4 and 5;	OK	I don't found any broken modules
9	15.12.2017	PV modules	Check the modules in fields number 6 and 7	OK	I don't found any broken modules
10	15.12.2017	Inverters, meteorogical stations	Checking for general condition of the inverters. Checking the fans working. Cleaning pyranometers and calibrated cells	OK	
11	19.12.2017	Buildings (connection point, SCADA, control room, inverters)	Visual inspection of the electrical/lightning installation of the building. Checking there is no signs of animals (rodents). Inspection of door lock	OK	The electrical installation from the inverters building are ok
12	19.12.2017	Buildings (connection point, control room, inverters)	Checking there is no abnormal humidity conditions or signs of water accumulation	OK	
13	19.12.2017	Inverters, String and Combiner Boxes	Checking for general condition of the inverters. Checking the fans working. Visual inspection of string and combiner boxes. The connection boxes verified to inverters PVST1 and PVST2	OK	

(continued)

Table 11.2 (continued)

Ingeteam			PV plant preventive maintenance log		
No.	Date	Equipment	Task description	Status	Observations
20	29.12.2017	Inverters, meteorogical stations	Checking for general condition of the inverters. Checking the fans working. Cleaning pyranometers and calibrated cells	OK	

3. Inverters General and other Conditions/daily and monthly:

   – Checking for general condition of the inverters (physical appearance),
   – Checking the heating working,
   – Checking proper condition of inverts building/enclosure,
   – Visual inspections of general condition and cleanliness,
   – Checking for adequate temperature,
   – Checking for adequate ventilation,
   – Visual inspection of the electrical/lightning installation of the building,
   – Checking there is no signs of animals (rodents) and installation of traps for rodents,
   – Checking general cleanliness and filters;

4. DC & AC Cabling—biannually:

   – Checking physical integrity of cabling. General appearance of grounding cables/connectors,
   – Checking physical integrity/tightness of cable connections, Checking state of the splices,
   – AC and DC cabling properly traced inside trays or buried corrugated conducts,
   – All cabling fastened to structural elements to ensure its stability and no sharp edges which may damage the cabling;

5. Civil Infrastructure—monthly, biannually and annually:

   – Terrain condition: Fence and Road;

6. Security Systems—Visual inspection/monthly [2, 24, 25];
7. Diesel Generator—Visual inspection/monthly;
8. Cleaning Building PUNCT CONNECTING PBL and PVST/daily and monthly.

11.3.4 Estimation of Energy Production for the Photovoltaic Park

For the year 2017, the amount of energy produced by the photovoltaic park is presented in Table 11.3. These estimates of the annual production energy for each month are made in accordance with the capacity of the photovoltaic park and estimated solar radiation for each month of the year.

Table 11.3 shows the energy values to be realized each month, but also the cumulative values from the beginning of the year to the current month [8, 26, 27].

11.4 Data Collection and Processing System

11.4.1 Analyzed Solar Park Configuration

The analyzed solar park, as site location, has the following configuration (Fig. 11.7).

The characteristics of the photovoltaic park analyzed:

- Solar potential—7.5 MWh;
- 30646 Modules/14 Inverters—7.5 MW;
- SUNTECH STP 245—20Wd/Schneider XC540.

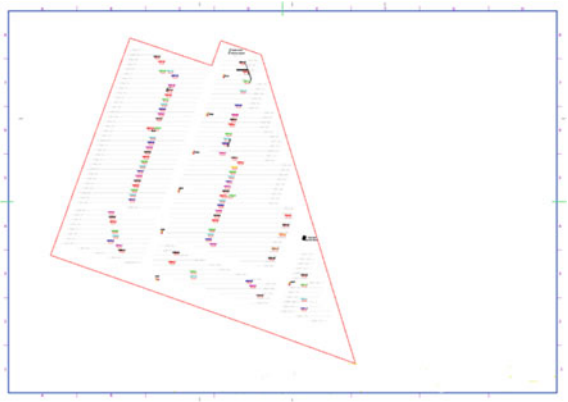

Fig. 11.7 The solar park—general plan connecting panels

Table 11.3 2017 proposal budget PV energy park

Production budget	*Monthly*											
	January	February	March	April	May	June	July	August	September	October	November	December
	386,81	520,76	882,30	943,31	1102,99	1086,91	1204,52	1141,43	1017,09	776,11	463,85	407,93
	Cumulative											
	386,81	907,57	1789,88	2733,18	3836,17	4923,08	6127,59	7269,02	8286,11	9062,22	9526,07	9934,00

11.4.2 The SCADA System Functions

Functions available to the operator in the control room of the Fire Emblem Heroes (FEH) [5]:

(1) Control Functions—allowing operation through a friendly man-machine graphical interface:

- View functions of the system setup, carried out by:
  - The Base Station/workstation operator;
  - Additional Equipment in the control room;
  - The Network Connections.

The organization of the view through the graphical interface man—machine is based on a hierarchical structure, containing information with different degrees of abstraction and detailing, which will allow the operator to request a comprehensive or detailed analysis of the processes:

- Level 1: screens with overview of installations and equipment in field (at the level of technological installations)—Fig. 11.8;
- Level 2: screens with overview of the main functions of the facilities and equipment;
- Level 3: displays images detail regarding the operation of installations, with surveillance information (Figs. 11.9 and 11.10), and allow corrective actions (Table 11.4) and provide diagnoses (Figs. 11.11, 11.12 and 11.13).

In Fig. 11.9 is presented the man machine interface, which provides information about energy production (total energy delivered, day energy delivered), ambient temperature, active inverter power, plane irradiation, and total availability [24, 28].
In Fig. 11.10 the power, currents for a certain string (array box 1.1.2); and the diagram of current versus voltage on the same graph are presented.

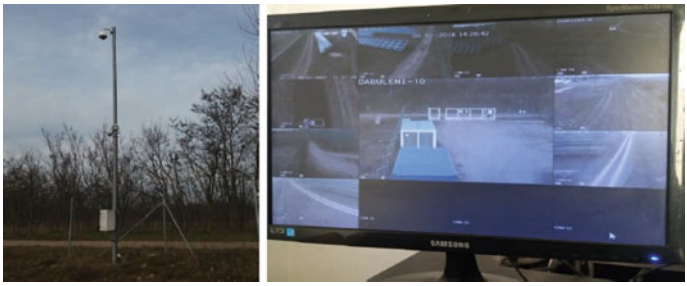

Fig. 11.8 CCTV checks

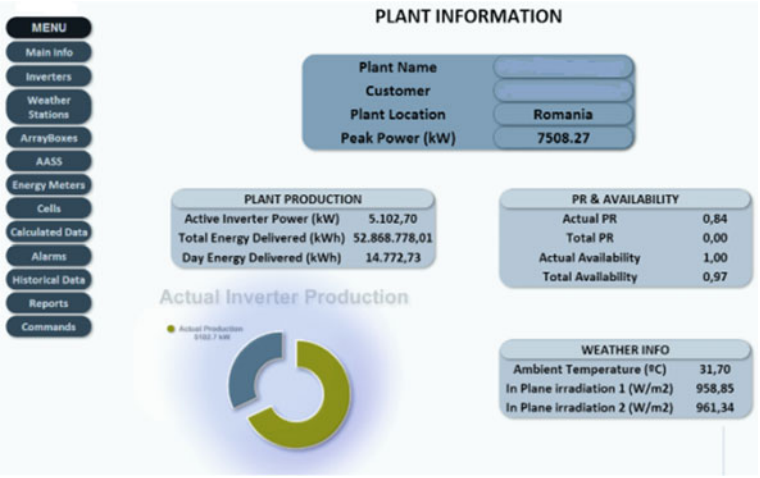

Fig. 11.9 The surveillance information

Fig. 11.10 Example of the string selection and obtaining information

Table 11.4 Work order table—March 2017

Date stop	Hour stop	Date start	Hour start	Total down-time	Code alarm	Alarm	Part descrip-tion	Comments	State	Intersor
08.03.2017	10:20	08.03.2017	10:26	0:06	Main Cell/PBL/SIM UNDERf REQ1 STATUS			CEZ dis-tribution	o.k	Total
16.03.2017	11:02	16.03.2017	11:03	0:06	Main Cell/PBl/27P Phase STATUS			CEZ dis-tribution	o.k	Total
16.03.2017	14:00	16.03.2017	14:11	00:11	Wain Cell/PBl/27P Phase STATUS			CEZ dis-tribution	O.k	Total
17.03.2017	10:44	17.03.2017	10:55	00:11	Wain Cell/PBl/27P Phase STATUS			CEZ dis-tribution	o.k	Total
17.03.2017	14:11	17.03.2017	14:17	00:06	Wain Cell/RBL/Z7P Phase STATUS			CEZ dis-tribution	o.k	Total

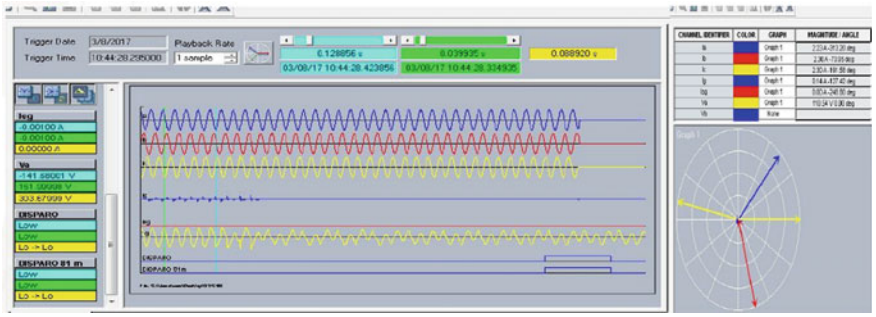

Fig. 11.11 Diagram and oscillogram from 08.03.2017/10:44

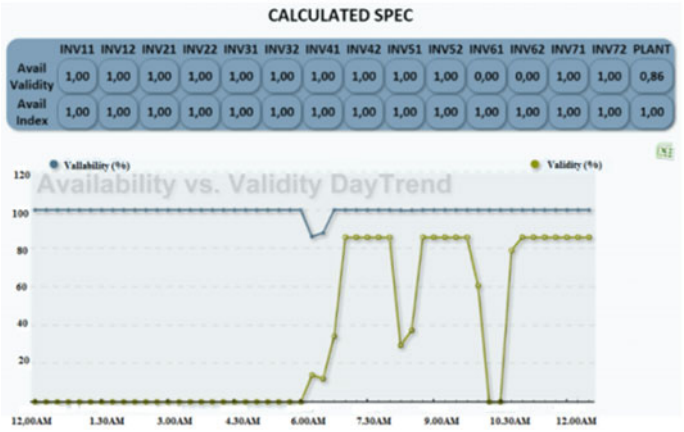

Fig. 11.12 The variation of yield daily

Table 11.4 presents information obtained when the alarm is triggered. The information is related to: date of the incident, time for stop alarm, periods of stagnation, causes of the alarm, and comments and conditions [20, 29–32].
Diagram and oscillation of currents on the three phases (I_a, I_b, I_c), leakage current (I_g) and voltage variation (V_a, V_b, V_c) are presented in Fig. 11.11. Also the yield daily variation and current variation for the sting number one are presented in Figs. 11.12 and 11.13 [6, 27].

- Alarm Functions: informs the operator in good time of any abnormal operation or fault in the technological processes.

The organization screens for viewing the alarms will be made taking into account the features:

– The screen with the overview of all alarms from process;
– The screen with the latest Alarms Window;

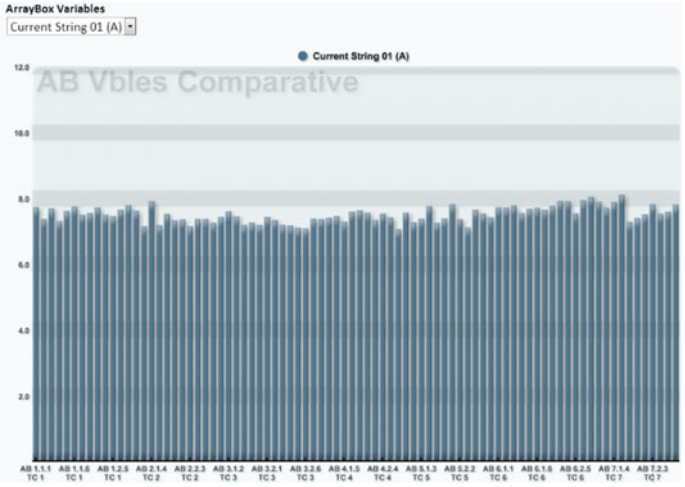

Fig. 11.13 Current of string

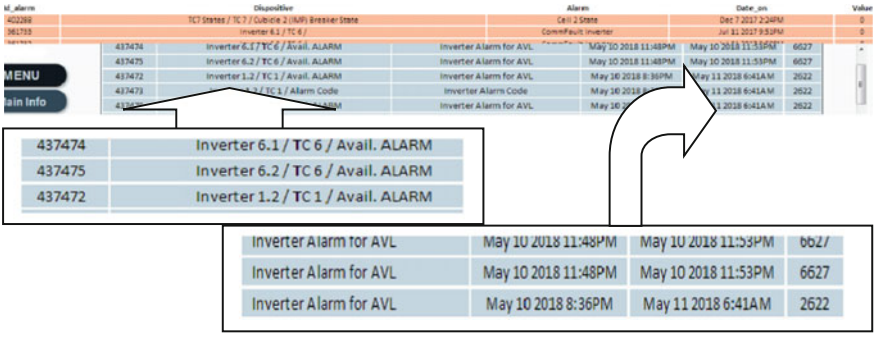

Fig. 11.14 Alarms

– The window with the other lists of alarms, sorted by various criteria (pre-program) Fig. 11.14.

An example of alarm functions is presented in Fig. 11.14. It describes the cod of the alarm (example: 437474), the breaker state (TC6/avail.alarm), time and hours (May 10 2018, 11:48 PM).
Monitoring Functions of the variables in the technological processes: display on the screen of the graphs of evolution in time of the magnitudes of the importance of the measured from the process allowing highlighting deviations from the normal values (differentiated colors) Fig. 11.15 [5, 6, 24, 26, 28, 30, 33–36].

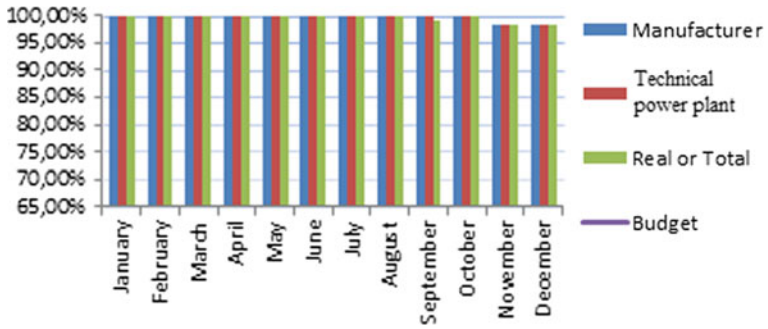

Fig. 11.15 Availabilities

(2) Advanced Functions:

- Historical data storage features (database—date, year, hour) is presented in Table 11.5, showing the cumulative values for the requested period;
- Successfully archiving of the regular data with the ability to view at any time, the form of graphical trend;
- Successfully archiving of the events accompanied by the date of the occurrence, with the possibility to view in the form of lists with the chronological Table 11.6;
- Functions for the preparation of the various reports (historical records for a specified period of time of the main variables from process; reports on the maintenance of technological developments; reports on the events, incidents, etc.) Table 11.7 [25, 27, 31, 36].

11.5 Computer Simulations

Data storage and simulation was performed using the SCADA system, used to track and process on-line data [28, 30, 33, 35, 37].

All problems that occur are automatically signaled by the system to be repaired in a timely manner so that the capture of solar energy is achieved near maximum capacity.

For example, we chose three months of the year—January, February and March—months with a small solar radiation, precisely to show the performance of the photovoltaic park, at a time of year when the solar radiation is low.

Tables 11.5, 11.6 and 11.7 shows differences that occur within the same time frame but in two different years 2017 and 2018. Graphical expression of these dates is made in Tables 11.5, 11.6 and 11.7 [24, 27, 31, 32, 36].

Table 11.5 Historical data storage features

	Meteo						
Date	Isol. A1 (Wh/m^2)	Isol. A2 (Wh/m^2)	Isol. HZ (Wh/m^2)	Avg. Calib. cell isol. (Wh/m^2)	Avg. Mod. temp. (°C)	Air temp. (°C)	Filtered avg. isol. (Wh/m^2)
May 1, 2018 1:00 AM	0	0	0	0,05	13,94	19,83	0
May 1, 2018 1:15 AM	0	0	0	0,07	14,7	20,28	0
May 1, 2018 3:45 PM	199,54	196,1	178,59	1451,10	53,48	34,64	197,82
May 1 2018 4:00 PM	193,09	190,83	174,1	1397,23	52,65	35,11	191,96
May 1, 2018 4:15 PM	168,68	167,4	153,03	1242,64	50,59	34,89	168,04
Total	7294,66	7257,09	6958,28	54287,08	29,93	25,51	7234,5

(continued)

Table 11.5 (continued)

	DC	AC	AC MV					Switchgear
Date	Total DC prod. (kWh)	Total AC prod. (kWh)	Exp. meter act energy (kWh)	Exp. meter react energy (kWh)	PR (%)	ETA AC (%)	Avail. (%)	Status
May 1, 2018 1:00 AM	0	0	0	0	0	0	0	0
May 1, 2018 1:15 AM	0	0	0	0	0	0	0	0
May 1, 2018 3:45 PM	1056,43	921	1200,00	0	0,81	1,14	1	0
May 1, 2018 4:00 PM	1035,66	1309,30	1227,27	0	0,85	1,19	1	0
May 1, 2018 4:15 PM	930,27	640,6	954,55	0	0,76	1,03	1	0
Total	39212,04	37953,90	44154,55	990,91	0,81	1,13	1	0

Table 11.6 Summary list of the dates of occurrence in chronological order—report for PV plant, February 2018

Day	Hours with working condition for inverter to produce (radiation > 10 W/mp)	Total string hours	Total radiation (Wh/mp)	Exported active energy end Landis (MWh)	PR (%) calculated in SCADA	Real availability (%)	Expr. availability (%)	Real IT availability (%)	Availability in SCADA (%)	Events and disturbance in energy production
27.02.18	9,50	13233,50	5035,99	16,34	56,00	100,00	100,00	100,00	97,00	The panels are covered by snow
28.02.18	10,50	14626,50	4780,52	7,78	28,00	100,00	100,00	100,00	94,00	The panels are covered by snow
Total	265,25	369493,25	64713,65	331,56	84,21	98,55	100,00	98,55	96,79	
Panels	30646,00									
Strings	1393,00									

Table 11.7 Summary of data for the year 2017

Production (MWh)	Monthly											
Source	January	February	March	April	May	June	July	August	September	October	November	December
SCADA	384,31	667,49	963,83	1094,28	1114,32	1202,27	1211,54	1174,46	973,31	676,93	309,00	437,49
Meter	385,49	669,67	967,25	1098,55	1118,93	1207,43	1216,85	1179,71	977,24	916,36	341,30	505,45
Cumulative												
SCADA	384,31	1051,80	2015,63	3109,91	4224,23	5426,50	6638,04	7812,50	8785,81	9462,74	9771,74	10209,2
Meter	385,49	1055,16	2022,41	3120,96	4239,89	5447,32	6664,17	7843,88	8821,12	9737,48	10078,78	10584,23
Performance Ratio	Monthly											
Source	January	February	March	April	May	June	July	August	September	October	November	December
SCADA	74,84	91,40	87,87	86,90	84,65	81,30	80,39	79,90	83,63	84,23	92,57	90,23
Cumulative												
SCADA	74,84	83,12	84,70	85,25	85,13	84,49	83,91	83,41	83,43	83,51	84,33	84,83
Radiation	Monthly											
Source	January	February	March	April	May	June	July	August	September	October	November	December
SCADA	77585,00	92286,00	150633,00	171454,00	178868,00	199665,00	204351,00	199136,00	163509,00	128759,00	51786,00	77767,00
Cumulative												

(continued)

Table 11.7 (continued)

Production (MWh)	Monthly											
Source	January	February	March	April	May	June	July	August	September	October	November	December
SCADA	77585,00	169871,00	320504,00	491958,00	670826,00	870491,00	1074842,00	1273978,00	1437487,00	1566246,00	1618032,00	1695799,00
Theoretical Performance Ratio	Monthly											
Source	January	February	March	April	May	June	July	August	September	October	November	December
SCADA	66,05	96,44	85,31	85,10	83,06	80,29	79,05	78,64	79,37	70,10	79,56	75,01
Meter	66,25	96,75	85,62	85,43	83,41	80,63	79,40	78,99	79,69	94,89	87,87	86,66
Cumulative												
SCADA	66,05	81,24	82,60	83,22	83,19	82,71	82,19	81,74	81,48	80,34	80,27	79,83
Meter	66,25	81,50	82,87	83,51	83,49	83,01	82,50	82,06	81,80	83,11	83,54	83,80

Operation and Maintenance Report

– PV 30646 modules/14 inverters—7.5 MW

A. Operational data—March 2017

Production (MWh)	Monthly		
Source	January	February	March
SCADA	384,31	667,49	963,83
Meter	385,49	669,67	967,25

Production Budget	Monthly		
	January	February	March
	386,81	520,76	882,30

3

3	Production (MWh)	
Source	March	Cumulative
SCADA	963,83	2.015,63
Meter	967,25	2.022,41
*Diff. (*Meter- SCADA*)*	3,42	6,78
Dev. SCADA Meter (%)	0,35%	0,34%

3, 42/967, 25/100

Production Status Real vs Budget		
	4 March	5Cumulative
	882,30	1.789,88
Diff. Meter	84,95	232,53
Dev. Meter (%)	9,63%	12,99%

967,25-882,30 2.022,41-1.789,88

84, 95/882, 30/100

	Availability (%)	
	6March	7Cumulative
Contractor	97,10%	99,01%
EDPR or Technical	97,10%	98,52%
Total or Real	97,10%	98,52%

	Normal Load Factor		Equivalents Hours	
Source	March	Cumulative	March	Cumulative
SCADA	17,27	12.47	128,51	268,75
Meter	17,33	12.51	128,97	269,65

((963, 83/1)*1000*100) / (744*7500)

((967, 25/1)*1000*100) / (744*7500)

963, 83/7, 5

967, 25/7, 5

2	Performance Ratio	
Source	March	Cumulative
SCADA	87,87	84,70

1	Radiation (Wh/sm)	
Source	March	Cumulative
SCADA	150.633,00	320.504,00

Theorical Performance Ratio**		
	SCADA	85,31
	Meter	85,62

(**without temperature corrections, etc.)

(963, 83*100) / ((150.633, 00 /1000)*7, 5)

(967, 25*100) / ((150.633, 00 /1000)*7, 5)

$$PR_T = \frac{\text{Energy produced during a certain period } T\,(\text{kWh})}{\frac{\text{Average incident solar radiation during } T}{1000\ \text{W/m}^2} \times \text{Peak plant wattage} \times T\,(h)}$$

B. Operational data—March 2018

3

Source	Production (MWh) March	Production (MWh) Cumulative
SCADA	743,37	1.624,15
Meter	743,37	1.627,33
Diff.	0,00	3,18
Dev. SCADA Meter (%)	0,00%	0,20%

Production Status Real vs Budget	4March	5Cumulative
	882,30	1.789,88
Diff. Meter	-138,93	-162,55
Dev. Meter (%)	-15,75%	-9,08%

	Availability (%) 6March	7Cumulative
Contractor	97,10%	99,01%
EDPR or Technical	97,10%	98,52%
Total or Real	97,10%	98,52%

Source	Normal Load Factor March	Normal Load Factor Cumulative	Equivalents Hours March	Equivalents Hours Cumulative
SCADA	13,32	9,95	99,12	216,55
Meter	13,32	9,97	99,12	216,98

2

Source	Performance Ratio March	Performance Ratio Cumulative
SCADA	84,84	85,13

Theorical Performance Ratio**		
	SCADA	78,63
	Meter	78,63

(**without temperature corrections, etc.)

1

Source	Radiation (Wh/sm) March	Radiation (Wh/sm) Cumulative
SCADA	126.056,00	266.219,00

Graphical expression of these dates is made in Table 11.8. Comparatively, we can observe the differences that occur during the same period of time from year to year [24, 25, 27, 30, 31, 33, 36].

The legend:

1Radiation (Wh/mp)
2Performance Ratio
3SCADA vs Meter
4 Meter vs Budget
5Meter vs Budget
6Availabilities
7Cum. Availabilities

Table 11.8 Operational data

2017	2018
1Radiation (Wh/mp)	
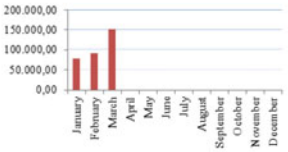	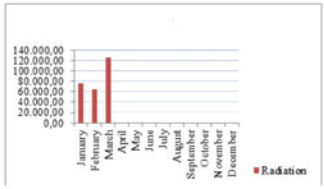
2Performance Ratio	
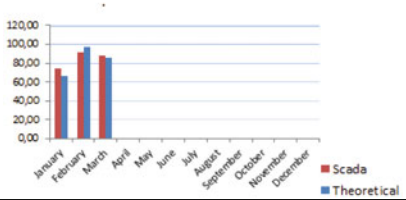	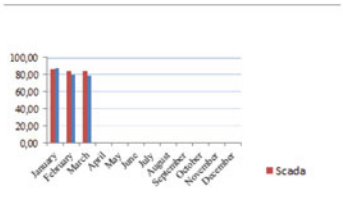
Production	
3SCADA vs Meter	
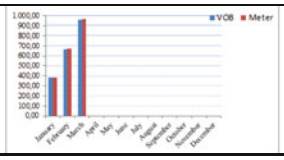	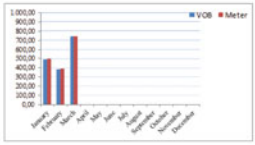
4 Meter vs Budget	
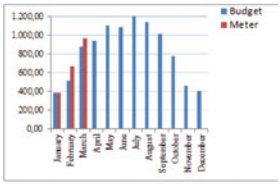	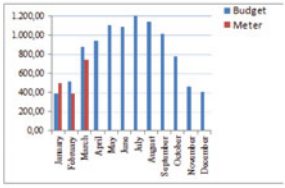
Cumulative	
5Meter vs Budget	
	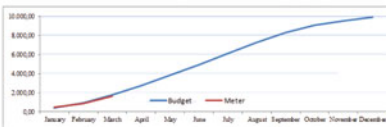

(continued)

Table 11.8 (continued)

Availability
6Availabilities
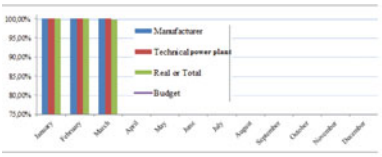 
7Cumulate availabilities
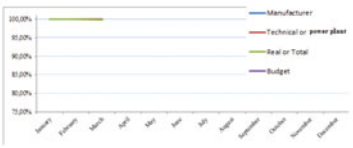 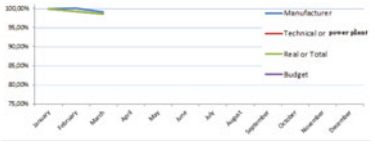

11.6 Conclusion

In this chapter, the main functional parametres of a photovoltaic power plant are presented using Supervisory Control and Data Acquisition (SCADA) and these parameters are used to obtained information about energy management of PV system.

The dates presented are obtained from a photovoltaic power plant within an area of seventy hecters, located in the south part of Romania, where the solar radiation is over 1450 kWh/m^2 year.

With the help of SCADA system, the control, the surveillance, the metering and monitoring of the photovoltaic power plant can be made from distance. Also the energy management can be achieved starting white one day and finishing with one year.

Total energy delivered (kWh), daily energy delivered (kWh), active inverter power (kW), percent of availability for photovoltaic power plant, weather info (ambient temperature, plane radiation etc.), hourly graphs about plant production, alarms, current strings, energy meter (exported active-reactive power, imported active-reactive power), data about weather station, inverters graphs, state of power transformers, breaker state, earthling state, month radiation, and month exported active energy can be achieved using SCADA.

Also, the dates obtained from a certain months of the year are compared with the dates obtained from the same months but for different years in order to establish the efficiency of the photovoltaic power plant.

Based on the resulting dates stored by SCADA, the corrective maintenance can be done.

References

1. N. Nafi, K. Ahmed, M. Gregory, M. Datta, A survey of smart grid architectures, applications, benefits and standardization. J. Netw. Comput. Appl. **76**, 23–36 (2016)
2. E. Zio, Challenges in the vulnerability and risk analysis of critical infrastructures. Reliab. Eng. Syst. Saf. **152**, 137–150 (2016)
3. A. Nicholson, S. Webber, S. Dyer, T. Patel, H. Janicke, SCADA security in the light of cyber-warfare. Elsevier, Comput. Secur. **31**, 418–436 (2012)
4. B. Genge, C. Siaterlis, Physical process resilience-aware network design for SCADA systems. Comput. Electr. Eng. **40**, 142–157 (2014)
5. F.M. Enescu, N. Bizon, C.M. Moraru, *Issues in Securing Critical Infrastructure Networks for Smart Grid Based on SCADA, Other Industrial Control and Communication Systems*. pp. 289–324 (Springer, London, 2018)
6. F.M. Enescu, C.N. Marinescu, V. Ionescu, C. Stirbu, System for monitoring and controlling renewable energy sources, in *9th International Conference on Electronics, Computers and Artificial Intelligence (ECAI 2017)*, Targoviste, Romania, 29 June–01 July, 2017
7. F.M. Enescu, N. Bizon, SCADA applications for Electric Power System. in: N. Mahdavi Tabatabaei, A. Jafari Aghbolaghi, N. Bizon, F. Blaabjerg (Editors), *Reactive Power Control in AC Power Systems, Fundamentals and Current Issues* (Springer, 2017)
8. R. Billinton, Distribution system reliability performance and evaluation. Electr. Power Energy Syst. **10**(3), 190–200 (1998)
9. K. Pipyros, C. Thraskias, L. Mitrou, D. Gritzalis, T. Apostolopoulus, A new strategy for improving cyber-attacks evaluation in the context of Tallinn manual. Comput. Secur. (2017)
10. N. Nezamoddini, S. Mousavian, M. Erol Kantarci, A risk optimization model for enhanced power grid resilience against physical attacks. Electr. Power Syst. Res. **143**, 329–338 (2017)
11. L. Hughes, M. de Jong, X.Q. Wang, A generic method for analyzing the risks to energy systems. Appl. Energy **180**, 895–908 (2016)
12. B. Karabacak, S.O. Yildirim, N. Baykal, Regulatory approaches for cyber security of critical infrastructures: the case of Turkey. Comput. Law Secur. Rev. **32**, 526–539 (2016)
13. NIST 2 The Smart Grid Interoperability Panel—Cyber Security Working Group, Guidelines for smart grid cyber security. NISTIR 7628, pp. 1–597 (2010)
14. T. Liu, Y. Sun, Y. Liu, Y. Gui, Y. Zhao, D. Wang, C. Shen, Abnormal traffic-indexed state estimation: a cyber-physical fusion approach for Smart Grid attack detection. Future Gener. Comput. Syst. **49**, 94–103 (2015)
15. H. Suleiman, I. Alqassem, A. Diabat, E. Arnautovic, D. Svetinovic, Integrated smart grid systems security threat model. Inf. Syst. **53**, 147–160 (2015)
16. C. Pursiainen, Critical infrastructure resilience: a Nordic model in the making? Int. J. Disaster Risk Reduct. (2017)
17. D.A. Visan, M. Jurian, A.I. Lita, Virtual instrumentation based acquisition and synthesis module for communication signals, in *9th International Conference on Electronics, Computers and Artificial Intelligence (ECAI 2017)*, Targoviste, Romania, 29, June–01 July, 2017, pp. 1–4
18. N. Mahdavi Tabatabaei, A. Jafari Aghbolaghi, N. Bizon, F. Blaabjerg (eds.), *Fundamentals and Contemporary Issues of Reactive Power Control in AC Power Systems* (Springer, London, 2017)
19. L. Langer, F. Skopik, P. Smith, M. Kammerstetter, From old to new: assessing cybersecurity risks for an evolving smart grid. Comput. Secur. **62** (2016)
20. K.M. Muttaqi, J. Aghaei, V. Ganapathy, A. Esmaeel Nezhad, Technical challenges for electric power industries with implementation of distribution system automation in smart grids. Renew. Sustain. Energy 129–142 (2015)
21. N. Moreira, E. Molina, J. Lazaro, E. Jacob, A. Astarloa, Cyber-security in substation automation systems. Renew. Sustain. Energy Rev. **54**, 1552–1562 (2016)
22. Y. Xiang, L. Wang, N. Liu, Coordinated attacks on electric power systems in a cyber-physical environment. Electr. Power Syst. Res. **149**, 156–168 (2017)

23. V.M. Ionescu, The analysis of the performance of RabbitMQ and ActiveMQ, in *IEEE 14th RoEduNet International Conference-Networking in Education and Research (RoEduNet NER)*, Sep 24, 2015, pp. 132–137
24. M. Emmanuel, R. Rayudu, Communication technologies for smart grid applications: a survey. J. Netw. Comput. Appl. **74**, 133–148 (2016)
25. I.C. Hoarca, F.M. Enescu, N. Bizon, Energy efficiency for renewable energy application. Renewable Energy Sources and Clean Technologies, in *17th International Multidisciplinary Scientific Geo Conference (SGEM 2018)*, Albena, Bulgaria, Scopus (2018)
26. A. Baggini, *Handbook of Power Quality* (Wiley, UK, 2008)
27. N. Bizon, N. Mahdavi Tabatabaei, H. Shayeghi (eds.), *Analysis, Control and Optimal Operations in Hybrid Power Systems—Advanced Techniques and Applications for Linear and Nonlinear Systems* (Springer, London, UK, 2013)
28. S. Massoud Amin, Smart Grid: overview, issues and opportunities—advances and challenges in sensing, modeling, simulation, optimization and control. Eur. J. Control (5–6), 547–567 (2011)
29. A.V. Gheorghe, M. Masera, M. Wiejnen, L. De Vries, *Critical Infrastructures at Risk* (Springer, 2006)
30. C. Alcaraz, S. Zeadally, Critical infrastructure protection: requirements and challenges for the 21st century. Int. J. Crit. Infrastruct. Prot. **8**, 53–66 (2015)
31. N. Bizon, N. Mahdavi Tabatabaei, F. Blaabjerg, E. Kurt (Ed.), *Energy Harvesting and Energy Efficiency: Technology, Methods and Applications* (Springer, 2017)
32. R. Billinton, P. Wang, Teaching distribution system reliability evaluation using Monte Carlo simulation. IEEE Trans. Power Syst. **14**(2), May 1999
33. D.P. Varodayan, G.X. Gao, Redundant metering for integrity with information-theoretic confidentiality, in *IEEE International Conference on Smart Grid Communications*, pp. 345–349 (2010)
34. F. Birleanu, N. Bizon, Reconfigurable computing in hardware security—a brief review and application. J. Electr. Eng., Electr., Control Comput. Sci. (JEEECCS) **2**(1), 1–12 (2016)
35. M. Ficco, M. Chora, R. Kozik, Simulation platform for cyber-security and vulnerability analysis of critical infrastructures. J. Comput. Sci. (2017)
36. A.K. Siposs, C. Stirbu, F.M. Enescu, Software application for exploring a virtual solar system. Bull.—Ser.: Electr. Comput. Sci., Pitesti, Romania **16**(1), 25–28 (2016)
37. N. Mahdavi Tabatabaei, S. Najafi Ravadanegh, N. Bizon, *Power Systems Resiliency: Modeling, Analysis and Practice* (Springer, London, 2018)

Chapter 12
PV Microgrids Efficiency: From Nanomaterials and Semiconductor Polymer Technologies for PV Cells to Global MPPT Control for PV Arrays

Cristian Ravariu, Nicu Bizon, Elena Manea, Florin Babarada, Catalin Parvulescu, Dan Eduard Mihaiescu and Maria Stanca

Abstract The chapter has to contribute to the part of electronic devices related to solar cells development, aided by new innovation technologies and new photovoltaic (PV) cells made by organic compounds and nanomaterials. Also, advances on the part of control techniques by presenting the results for Extremum Seeking Control (ESC)-based Global Maximum Power Point Tracking (GMPPT) applied to PV microgrids in partially shaded regimes are considered. The influence of the photovoltaic arrays topologies to multimodal characteristic of the PV power is also highlighted. Alternative new materials like ferrite Nano-Core-Shell (NCS) multilayer can be used to

C. Ravariu (✉) · F. Babarada
Department of Electronic Devices, Circuits and Architectures, Faculty of Electronics, Telecommunications and Information Technology, Polytechnic University of Bucharest, Bucharest, Romania
e-mail: cristian.ravariu@upb.ro

F. Babarada
e-mail: florin.babarada@upb.ro

N. Bizon
Department of Electronics, Computers and Electrical Engineering, Faculty of Electronics, Communications and Computers, University of Pitesti, Pitesti, Romania
e-mail: nicu.bizon@upit.ro

E. Manea · C. Parvulescu
National Institute for Research and Development in Microtechnologies—IMT Bucharest, Bucharest, Romania
e-mail: elena.manea@imt.ro

C. Parvulescu
e-mail: catalin.pirvulescu@imt.ro

D. E. Mihaiescu · M. Stanca
Department of Organic Chemistry "Costin Nenitescu", Faculty of Applied Chemistry and Material Science, Polytechnic University of Bucharest, Bucharest, Romania
e-mail: dan.mihaiescu@upb.ro

M. Stanca
e-mail: maria.stanca@upb.ro

N. Mahdavi Tabatabaei et al. (eds.), *Microgrid Architectures, Control and Protection Methods*, Power Systems,
https://doi.org/10.1007/978-3-030-23723-3_12

construct Thin Film Transistors (TFT) or can be applied for photovoltaic (PV) cells. Hence, the chapter firstly presents how the NCS technology generates nanomaterial layers. The ferrite core is self-assembled by an intermediary first shell to an organic shell represented by para-aminobenzoic acid (PABA). The fabricated nano-layers are investigated by Scanning Electron Microscopy technique (SEM) and also by Dynamic Lighting Scattering (DLS). These techniques find a hydrodynamic width for the ferrite NCS of 70.9 nm, besides to a zeta potential for these nanoparticles of 51.6 mV, proving an appropriate stability of the fabricated nanoparticles. Organic semiconductors are recently introduced for the transistor and Organic Solar Cell (OSC) manufacturing. Some Athena/Atlas simulations capture the better feature for the static characteristics for different electronic structures working as transistor or texturized solar cells. Either Nano-Core-Shell, Amorphous-Silicon or Polymers are suitable materials for PV microgrids. The demonstration of current vectors traces and experimental static characteristics of the proposed electronic devices sustain these materials future use to enhance the PV arrays. Furthermore, the energy generated by the PV arrays can be fully harvested using GMPPT algorithm based on advanced ESC scheme.

Keywords PV microgrids · Thin film transistors · Energy efficiency · Organic electronics · Simulation · Nano-material synthesis · PV cells technologies · Global MPPT control

12.1 Introduction

One of the most accessed green energy sources seems to come from Photovoltaic (PV) microgrids [1]. The purpose of this chapter is to emphasize the potential resources of the thin film transistors made by new materials, organic devices, nano-transistors, processed solar cells, which are currently used in PV microgrids. The consumers must be correlated with these green sources of energy. If additionally, the power consumption of the integrated electronics will tend to zero, the photovoltaic panels can be integrated on a large products spectrum, including automotive, [2]. On the other hand, domestic applications require non-breakable PV systems, ideally integrated on flexible substrate, [3], ultra-thin films that are transparent, generating the branch of the transparent electronics, [4], or nano-materials that are by excellence ultra-thin, generating the nanoscale shaped devices [5]. Starting from these demands, an entire electronic device classes were developed in the last ten years. The industry pays attention mainly to the Thin Film Transistors (TFT), including their organic variant, few electron devices and alternative devices with nano-materials [6–11].

The thin film transistors usually work with poly-crystalline silicon as the semiconductor film, [8]. These transistors allow a much simpler technology, without any source or drain diffusions, as in the MOSFET case. Electrical conduction inside the TFT transistors is not reduced only to inversion. The accumulation regime of the semiconductor film represents the most efficient conduction work regime, [8].

Because the carrier transport occurs through a disordered Silicon lattice, the conduction performances are inferior to a MOSFET, but this fact is a matter of time and will be automatically solved for next stages of the nano-printing and atomic layers deposition, [9].

From the material point of view, a large palette of alternative materials to Silicon, are continuously searched for electronic devices fabrication: Carbon Nano-Tubes (CNT) [12], organic semiconductors, [13], nano-core Si-Ge materials [7], besides to Ge-core-shell used in field effect transistors with nanowires, [6]. The organic compounds are frequently used as semiconductor layers or insulators in organic active devices, including Organic Thin Film Transistors (OTFT) [14] or Organic Solar Cells (OSC), [15]. The OSC have improved the power conversion efficiency (PCE) to more than 13%, when C-related materials or proper polymers are used, [16]. The main OSC advantage consists in low-cost at a low-temperature technology, outside of the expensive white rooms. The OSC also allows the color tuning, making available the deposition on a large spectrum of wafers. Last studies propose PBDB-T-SF new polymer as donor photovoltaic material and acceptor made from small fluorinated molecules for fullerene-free organic solar cells, [14–16].

In this chapter, some Nano-Core-Shell materials with ferrite core [17] are considered as alternative candidates for nano-scale thin film transistors. The ferrite NCS with graphene shells nano-materials are still used for the Schottky diode applications, [18]. As a reference transistor, a traditional thin film transistor with amorphous silicon and adapted sizes are considered from experimental and simulation point of view. A particular attention is focused to the nanostructured composites synthesis having a nano-core of ferrite and to NCS-TFT simulation.

The PV arrays under Partial Shading Conditions (PSCs) are analyzed to design the PV power patterns. These PV power patterns are studied for the Global Maximum Power Point Tracking (GMPPT) control of the photovoltaic array under PSCs. The general and specific performance indicators used for MPPT and GMPPT control are presented. The results for GMPP control based on Extremum Seeking (ES) schemes are presented in this chapter as well. It is worth to mention that the energy efficiency could increase with more than 30% if the GMPPT control is used instead of the MPPT control.

The conclusion will integrate all the results from device simulations, nanomaterials preparation and solar cell demands to global MPPT control of PV microgrids.

12.2 PV Technologies and Characteristics

12.2.1 Novel Nano-structured Materials Synthesis for PV

All the technologies to minimize the power consumption, including nano-scaling, thin and ultra-thin film transistors and alternative materials with lower conductivity

draw attention both for consumers and PV cells designers, but also for PV microgrids implementers.

In this section, some Nano-Core-Shell materials with ferrite core are considered as alternative candidates for PV devices instead amorphous silicon.

The ferrite NCS material can be fabricated by chemical synthesis successive steps to provide assembled nanoparticles of sub-100 nm width. The primary shell consists in np's Fe_3O_4 shell of the NCS ions, sub-10 nm width, [19]. The main synthesis technology is based on the co-precipitation technique. It is structured from ionic precursors of the Fe_3O_4 core skeleton. Then the secondary shell binds to an organic acid abbreviated by PABA, by the self-assembling technique, [11]. The PABA acid reacts and binds to metallic ions like Fe^{+2} or its oxides to create NCS nano-aggregates, Fig. 12.1.

In a first preliminary simulation step, the electrical interactions of the ferrite NCS molecular structure in the synthesis solution are emphasized by the Hyperchem and Gamess modeling software, Fig. 12.1a, b. The PABA molecule is highly charged in the head of the organic acid molecule that is responsible for the secondary shell binding, Fig. 12.1a.

The evolution of the synthesized nano-aggregate inside a liquid volume, show a global size after first and secondary shells binding. The nanoparticle modeling is tri-dimensional performed by Tomviz software, Fig. 12.1b.

The PABA acid is chosen for the secondary shell assembling, due to its feature to interact with metal ions of Fe^{+2} or Fe^{+3} by the carboxylate group. The final material Fe_3O_4/PABA is carried out by co-precipitation of the Fe ions in NaOH solution, under the molar ratio of Fe_3O_4:PABA = 1:7.

A first characterization method that is applied to the fabricated NCS nano-particles consists in Dynamic Light Scattering. The DLS measured curve and a SEM cropped image of the NCS-Fe_3O_4/PABA material is presented in Fig. 12.2a and respectively b. DLS method measures a medium hydrodynamic diameter of

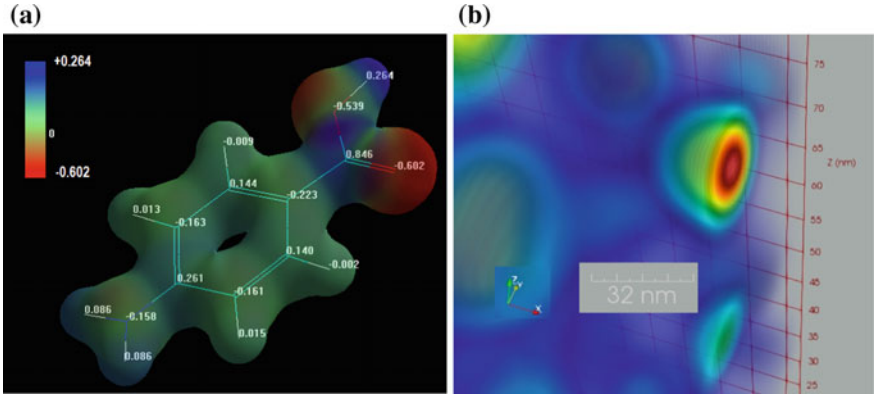

Fig. 12.1 The software results for, **a** the electrical charge at atomic level for a PABA molecule [11], **b** a global solvatation shell [11]

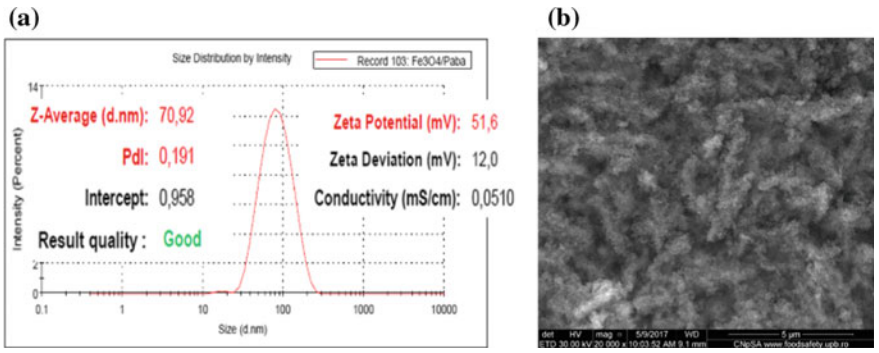

Fig. 12.2 **a** DLS characteristics result for the synthesized Fe_3O_4/PABA nano-material [11], **b** a SEM image [20]

70.9 nm for Fe_3O_4/PABA nanoparticles. Also, a reasonable zeta potential is measured ($v = 51.6$ mV), which proves an elevate technology stability.

Other researchers already applied the nano-core-shell NiS:Co/MnS films as n-type semiconductor with a band gap of 2.34 eV, a carrier density of 3.99×10^{16} cm^{-3}, for organic solar cells, [15]. The advantage of NCS nanocomposite consists in high surface-volume aspect ratio that allows the induced charges segregation, as the previous theory in silicon was emphasized for photovoltaic cells.

12.2.2 Electronic Structure Simulations and Characterization

The experimental application of the previous NCS synthesized materials for future electron devices is in progress. Therefore, only the simulations of NCS-TFT transistors are approached in this chapter. For comparison, a reference thin film transistor, fabricated by polysilicon and also simulated after the Atlas standard techniques, is presented [21]. So, the NCS-TFT simulations start from an entire list of parameters and models in a good agreement with polysilicon experiments.

The Atlas simulations of the TFT variants allow the main current vectors finding, at different bias points. The simulated characteristics of the NCS-TFT transistors have to be compared with traditional simulated TFT curves and with experimental picked points from literature.

For the simulation of the TFT with amorphous silicon, a reference TFT transistor with typical sizes is picked from literature. This TFT has: 100 nm n-type amorphous silicon film that is doped with phosphorus 7×10^{14} cm^{-3} in the middle of film, and also phosphorus of 3×10^{18} cm^{-3} near to the drain and source contacts, accordingly to the reference TFT structure from Silvaco, [21]. The silicon is placed over 200 nm oxide on 200 nm nitride. The proper wafer is represented by a SiO_2 layer, which gets

in simulations only 200 nm, Fig. 12.3. The Atlas simulator gets a material statement, where any new materials as our novel NCS material, can be depicted.

Sake of the simulation accuracy, the following material parameters are defined in Atlas: electrons and holes mobility of $\mu_n = 20$ cm^2/Vs, $\mu_p = 1.5$ cm^2/Vs, density of energetic levels in the conduction band and valence band of 5×10^{20} cm^{-3}, defects density in conduction band and valence band of 10^{20} cm^{-3}, silicon-oxide charge of 3×10^{10} e/cm^2, [8]. The device models include the Fermi carrier distributions, Lombardi mobility model, Shockley–Read–Hall recombination rate and defect statement. For the simulation of the TFT with NCS materials in Atlas, some new simulation strategies are performed for these NCS-TFT transistors. The layer sizes, doping and geometry are re-considered: (i) channel length is decreased to 4 μm; (ii) the source and drain electrodes get 100 nm Tungsten/100 nm Al; (iii) oxide thickness is decreased to 0.1 μm to offer a better gate modulation; (iv) the doping concentration in Silicon is modified to three distinct regions: n$^-$ with 10^{12} cm^{-3}, n with 10^{15} cm^{-3}, n^{++} with 10^{20} cm^{-3}, closer to the NCS material facilities, Fig. 12.4a.

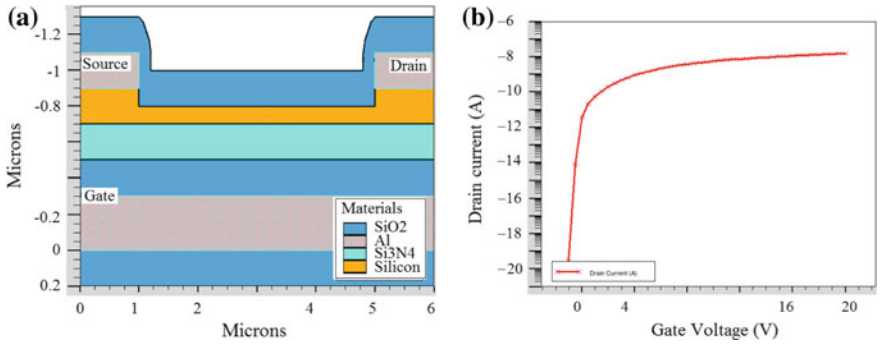

Fig. 12.3 **a** The simulated TFT reference transistor [11], **b** the static characteristics at logarithmic scale [11]

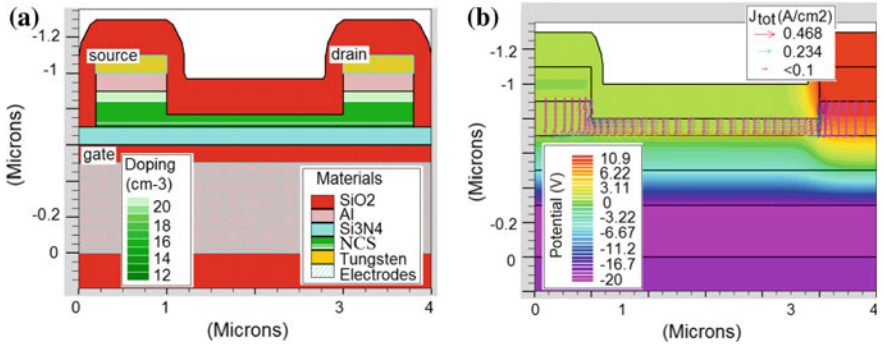

Fig. 12.4 The simulations of NCS-TFT transistor, **a** doping and materials map [11], **b** vectors of the current density at $V_{DS} = +10.9$ V, $V_{GS} = -20$ V [11]

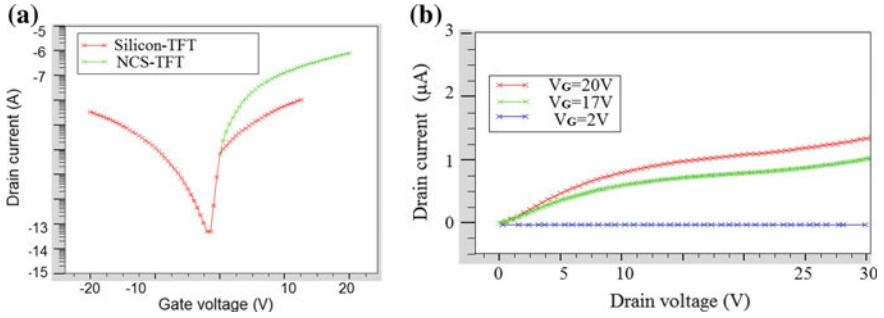

Fig. 12.5 The simulated characteristics for the NCS-TFT transistors, a the transfer caracteristics I_D–V_{GS} plus the comparison with traditional silicon-TFT [11], b the output characteristics I_D–V_{DS}, only for NCS-TFT [11]

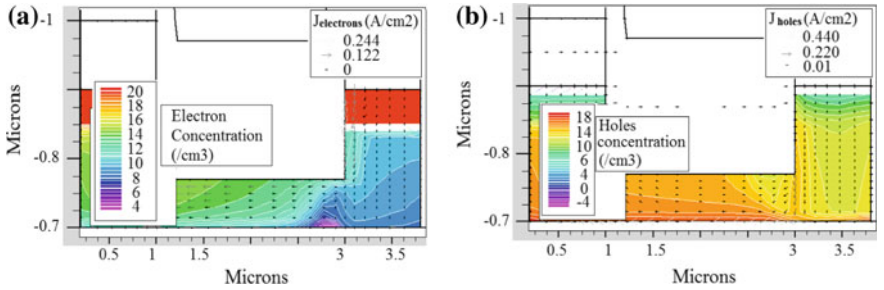

Fig. 12.6 Details inside the simulated NCS-TFT transistor when $V_{DS} = 10$ V and $V_{GS} = -20$ V, **a** the contours of the electrons concentration, besides to the vectors of pure electrons current density [11], **b** the contours of the holes concentration, besides to the vectors of pure holes current density [11]

Figure 12.4b explores the total current density flow, mapping the current vectors at $V_S = 0$ V, $V_D = +10.9$ V, $V_G = -20$ V. A comparison of the static characteristics for NCS-TFT and traditional TFT [21] are presented in Fig. 12.5.

One obvious reason for the augmented current in NCS-TFT device comes from its lower size in respect to the traditional variant, Fig. 12.5a. The total current density, J_{tot}, of the NCS-TFT device adds both electron and hole current components. A negative gate voltage rejects the electrons from the bottom of the film, Fig. 12.6.a. But the holes act as minority carriers and are attracted to the bottom. They basically increase the total current density to $J_{tot} = 0.44$ A/cm^2, Fig. 12.6b. The electron current component is only drafted to the Si-surface. At $V_{DS} = +10$ V, the drain voltage is high enough to admit a saturation domain that decreases the holes concentration at the drain region. Figure 12.6b proves a lower holes concentration next to drain—10^{12} cm^{-3}, as next to source—10^{17} cm^{-3}.

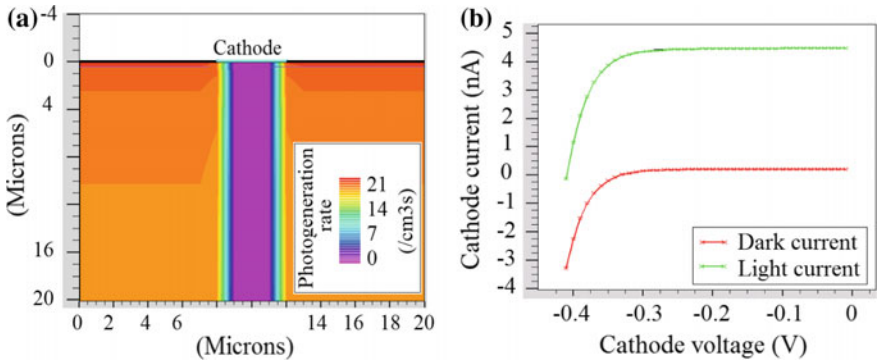

Fig. 12.7 Simulation results from Atlas of a typical solar cell, **a** the structure, **b** Illuminated and un-illuminated *I*–*V* characteristics

For the solar cells investigation, the optimization techniques of a simple amorphous silicon solar cell are analyzed in respect to the presence or absence of the mid-band gap defect states. The Density of States (DOS) at the silicon interface is considered by donor (HD) and acceptor (HA) states with Gaussian profile and exponential tail redistributions. The next Atlas tests simulate the reply of this PV cell to illumination from solar spectrum. The specific material parameters for the structure (e.g. doping, HA, HD, etc.) are implemented by an input in-type file. The light from the solar spectrum is defined in Atlas within the Beam statement, specifying the angle of 90° and the power from an internal file, Fig. 12.7b. The cathode current suffers an increasing under solar light, in agreement to the photogeneration rate, Fig. 12.7a.

12.2.3 Organic Active Devices Toward OSC

In the usual solar cells, as in thin film transistors, the active layers are the amorphous or poly-crystalline silicon. Recently, these devices are produced by organic semiconductors, generating Organic Thin Film Transistors (OTFT) and respectively Organic Solar Cells (OSC). The OSC have improved the power conversion efficiency (PCE) to more than 13%, when C-related materials or proper polymers are used, [22]. The main OSC advantage consists in low-cost at a low-temperature technology, outside of the expensive white rooms. The OSC also allow the color tuning and the deposition availability on a large spectrum of wafers. Last studies propose PBDB-T-SF new polymer as donor photovoltaic material for fullerene-free OSC [23]. Besides the PV cells technologies, the influence of PV microgrid architecture to power characteristic of multimodal type is also analyzed and then modeled in order to define appropriate PV power patterns.

Firstly, a preliminary study of an OTFT transistor with similar features as a fabricated Pentacene-OTFT, in the configuration Bottom-Contacts Bottom Gate (BCBG)

is performed: Pentacene film of 30 nm thickness doped p-type of 7×10^{17} cm^{-3}, channel length of 5 μm, the same mobility parameters—$\mu_p = 0.45$ cm^2/Vs and Poole-Frenkel parameters as beta.pfmob $= 7.7 \times 10^{-5}$ (V/cm)$^{0.5}$, deltae.pfmob $= 0.018$ eV, [24], Fig. 12.8a. Most accessed models of the organic devices are used in order to activate the Poole-Frenkel mobility model and the Langevin recombination models, [25]. The gold source/drain contacts with well aligned work function of 4.9 eV to the highest occupied molecular orbital level of Pentacene 4.8 eV. Figure 12.8b explains the functionality. The OTFT bias point is visible as black and white contours on electrodes: $V_S = 0$ V, $V_D = -5$ V, $V_G = 3$ V. Along the entire channel, the holes concentration is decreased up to 10^{-4} cm^{-3} and lower, under $V_G > 0$, so that only leakage drain-source current vectors are captured, Fig. 12.8b.

Because the density of states are not clear explicated in [24], the output characteristics are simulated from comparable DOS values as the doping, $HA = HD = 7 \times 10^{17}$ cm^{-3} Fig. 12.9. In this case, the I_D–V_D curve is far away from the experimental picked points at $V_{GS} = -3$ V, [24]. To match the simulated curve over the experimental points, the Acceptor/Donor-like trap density must be increased to 3×10^{20} cm^{-3}. For higher DOS density of 10^{21} cm^{-3}, the current is alleviated, Fig. 12.9.

The organic solar cells work principle is based on the exciton dissociation in connection with the bulk heterojunction concept. An exact location of the heterointerface

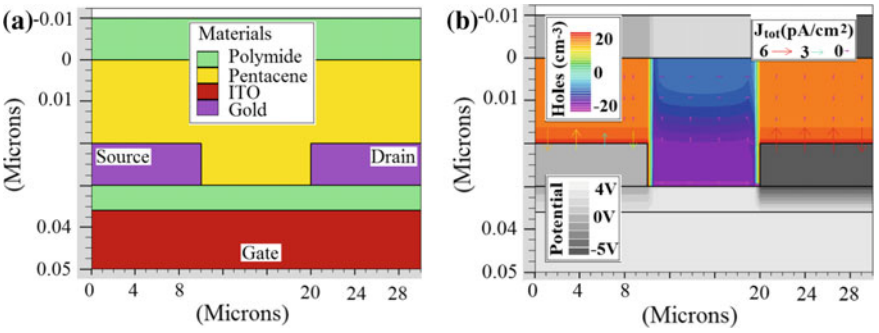

Fig. 12.8 **a** The OTFT conceptual structure [20], **b** a cross-section through OTFT biased to $V_G = +4$ V [20]

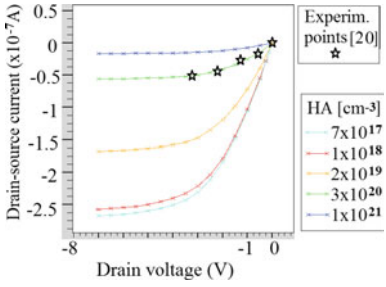

Fig. 12.9 The simulated output characteristics of OTFT at $V_{GS} = -3$ V and experimental I_D–V_D picked points [20]

is not defined, but it is modeled by a random interpenetrating mixture of touching multidomains.

The exciton dissociation is taken into account by three main parameters into Atlas MODEL statement: (i) singlet exciton continuity equation inclusion, (ii) Langevin recombination rate inclusion and (iii) singlet dissociation model inclusion, considered respectively by the parameters SINGLET, LANGEVIN and S.DISSOC. Another feature to organic photodetection is modeled by the QE.EXCITON parameter that characterizes the number of singlet excitons generated for each absorbed photon. The other absorbed photons that do not generate singlets, but have to generate electron-hole pairs. For instance, a standard OSC simulation [21], in agreement with a fabricated polymer/fullerene bulk heterojunction solar cell [26], sets up the organic semiconductor parameters as: dielectric permittivity of 3.4, electrons affinity of 1 eV, band gap as the difference between LUMO and HOMO levels of 1.34 eV and the density of states in the valence and conduction band of 2.5×10^{19} cm^{-3}. An energy distribution arises in organic semiconductors, too, due to the analogous edge of the valence band as the highest occupied molecular orbital (HOMO) level and the analogous edge of the conduction band as lowest unoccupied molecular orbital (LUMO).

12.2.4 Technological Hints for Optimized Solar Cells

This paragraph presents the fabrication of the solar cells developed in the silicon technology, based on the textured surface process that is able to offer the optimum reflectance. The main step of the texturization process is based on the KOH etching. The fabricated structures are studied by optical techniques, including SEM. The general technology flow possesses maximum 7 steps. The start structure is a multi-crystalline Silicon wafer; the top surface of the solar cell is texturized since to minimize the light reflectivity. Additionally, the wafer is p+ diffused onto the back-side to allow low series contact resistance, [27]. In the active area of PV cell, the silicon surface is texturized using an acidic solution of HNO_3:HF:CH_3COOH in the ratio 25:1:10, close to the room temperature and a basic solution KOH of 25% concentration at a temperature of 80 °C, Fig. 12.10a. The roughness effect by an increased texturization at the wafer surface allows a longer optical way for the light interaction with the surface material, enhancing the light absorption and improving the PV cell efficiency, [28]. A next technological step is the phosphor diffusion at 975 °C for 10 min, simultaneously with a non-reflexive oxide layer growing, having 120 nm thickness. The texturized silicon cell characteristics are measured with a characterograph and are presented in Fig. 12.10b.

Then, the texturing technology was varied in order to capture an optimum flow. The filing factor FF, where $FF = P_{\max}/(I_{sc} \cdot V_{oc})$ is extracted by the static characteristics measurement. For these PV cells, texturized in 25%—KOH solution, the filing factor is highest, while for the texturized cells in acids this factor is medium and for untexturized cells this filing factor is lowest.

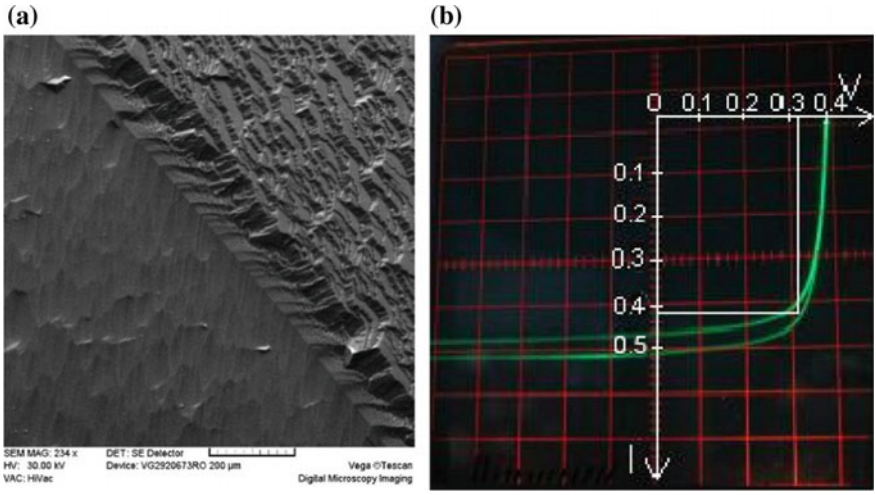

Fig. 12.10 **a** PV cell texturization obtained by KOH solution and boron back diffusion [27], **b** the electrical *I*–*V* measured characteristics of the texturized PV cells with boron enhanced metal back-side contact [27]

Novel efforts are dedicated on the conversion efficiency increasing, absorption optimization, decreasing of the light reflectivity and reducing of the series resistance. For PV cells with boron enhanced metal back-side contact, a consistent short-circuit current increasing occurs after the boron doping. The effect is a low-series resistance contact, based on the aluminium film sputtered on the wafer substrate.

After the texturized structure was fabricated, the Atlas simulation was run, in the same conditions as in the previous structure from Fig. 12.7, resulting in a slightly different *I*–*V* characteristic. Whereas the *I*–*V* characteristic shape is approximately conserved, an increase of the output current can be detected. The previous result indicated a maximum current of 4.5 nA, whereas the textured solar cell has an output higher current of 4.8 nA. The current gain is not much, but it can be further optimised by etching processes, modifying the whole surface or etching type. So, another method of improving the efficiency consists in deposition of pyramids on top of the PV silicon solar cell. Different results can be obtained depending on the height and length of the pyramids. Using the Athena simulator, this method was implemented with pyramids, defining 10 μm length and 5 μm height, Fig. 12.11a, b.

By introducing pyramids, the efficiency increases from 19.35 to 24%, which is a global optimization of 4.65%. For additional parameters, see the section of performance indicators.

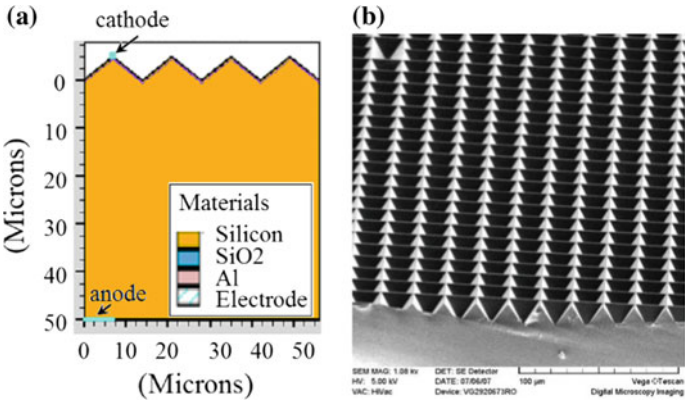

Fig. 12.11 **a** Solar cells simulated surface with pyramids—technology simulation result, **b** pyramid implementation [28]

12.3 PV Arrays Under Partially Shaded Conditions

The PV array operates in real environment under Partially Shaded Conditions (PSCs) due to shading by the clouds, neighboring buildings, or dust of the PV panels installed on rooftop or as facades and eaves of buildings [29, 30]. Thus, the power characteristics of the PV array could have multiple Local Maximum Power Points (LMPPs), besides the Global Maximum Power Point (GMMP) [30, 31]. The MPP tracking (MPPT) algorithm can remain stuck in a LMPP if this has no Global MPPT (GMPPT) feature integrated. In this case, a power gap appears between the PV power generated and the GMPP power will appear, reducing the potential energy generates with up to 40% [32, 33]. To solve this issue, hundreds of the GMPPT algorithms are proposed in the last decade [34, 35].

Because the power characteristics of the PV array under PSCs were presented and discussed in different papers [29–36], this subject will be briefly approached in next section only to justify the shape of the PV patterns chosen.

12.3.1 PV Power Characteristics

The PV panel used in simulation is built with solar cells that are modeled with one-diode model operating at $T = T_R = 298$ K. The errors in modeling due to temperature variation will not affect the conclusion of this work because the GMPPT algorithm used is of adaptive type, being based on Extremum Seeking Control (ESC) scheme proposed in [32].

Table 12.1 Parameters of the solar cell model [37]

Parameter	Description	Value [unit]
G_R	Reference irradiation	1000 [W/m^2]
T_R	Reference temperature	298 [K]
q	Electron charge	1.6e^{-19} [C]
k_B	Boltzmann's constant	1.38e^{-23} [JK^{-1}]
n	Diode ideality factor	1.3 [−]
V_G	Silicon band-gap energy	1.12 [eV]
$V_T = k_B T_R/q$	Thermic voltage	26 [mV]
I_{OR}	Reverse saturation current at $T = T_R$	2e^{-9} [A]
α	Short-circuit current temperature coefficient	0.0025 [AK^{-1}]
R_s	Cell series resistor	3 [mΩ]
R_p	Cell shunt resistor	10 [Ω]
$V_{oc(cell)}$	Cell open-circuit voltage	0.61 [V]
$I_{sc(cell)}$	Cell short-circuit current	3.8 [A]

12.3.1.1 Solar Cell Model

The one-diode solar cell model neglecting the parallel resistance, R_p, is given by Eq. (12.1):

$$I_{PV(cell)} = K_{IG(cell)} \cdot G - I_{0R} \cdot \left[\exp\left(\frac{V_{PV(cell)} + R_s I_{PV(cell)}}{n V_T} \right) - 1 \right] \tag{12.1}$$

where,

$V_{PV(cell)}$ is the solar cell voltage;
$I_{PV(cell)}$ is the solar cell current;
R_s is the series resistance of the solar cell;
$K_{IG(cell)} = I_{sc(cell)}/G_R$ is the irradiation to short-circuit current gain;
$I_{L(cell)} = I_{sc(cell)} \times G/G_R$ is the light-generated current;
G is the irradiance's level.

Other parameters that will be used in simulation are mentioned in Table 12.1.

12.3.1.2 PV Panel Model

The SX60 PV module has 34 cells in series, ensuring under the standard test conditions the open-circuit voltage, V_{oc}, and the short-circuit current, I_{sc}, of 21 V and 7.8

A (Table 12.2). The MPP values (V_{MPP}, I_{MPP}, and P_{MPP}) under constant irradiance of 500 W/m^2 are given in Table 12.3.

The PV panels are integrated in series and parallel into an array to increase the power generated. The PV pattern may have multiple LMPPs due to the PSCs, which depends on shading pattern used and PV array construction.

Different profiles for the irradiance will be used in next section to obtain the PV power characteristics of a PV array using n_p strings in parallel, and each string has n_s PV panels in series (named below as n_pP$x n_s$S PV array).

12.3.1.3 The PV Power Characteristics Under Partially Shaded Conditions

The shading pattern is set for the n_pP$x n_s$S PV array by the irradiance profile used for each PV panel of SX60 type. The power characteristics of the 1Px3S, 1Px5S, and 1Px7S PV arrays are shown in Figs. 12.12, 12.13, and 12.14 [32, 37, 38].

For example, the profiles for the irradiance (G_k: [time sequence in seconds], [irradiance sequence in W/m^2], $k = 1$–5) used for 1Px5S PV array (Fig. 12.13) are given by the following vectors:

G_1 [0 1 2 4] [500 1500 1500 500];
G_2 [0 4], [500 500];
G_3 [0 3 4], [500 1000 1000];
G_4 [0 2 3 4], [500 1500 1000 1500];
G_5 [1 4], [500 750].

The PV power characteristics represented in Fig. 12.13 considering the time samples of 0, 1, 2, 3, and 4 s.

Also, the irradiance for each panel could be set different, but constant, by the vector (G_1, G_2, G_3, G_4, G_5, G_6, G_7), resulting multiple LMPPs (Fig. 12.14) as follows:

(1500, 1000, 875, 750, 675, 565, 500) ⇒ 6 LMPPs
(1500, 1065, 1000, 875, 750, 600, 500) ⇒ 5 LMPPs

Table 12.2 Electrical specifications for the SX60 PV module [37]

Electrical specifications		
N_S	Number of cells in series	34
N_P	Number of strings in parallel	1
I_{sc}	Short-circuit current	3.8 A
V_{oc}	Open-circuit voltage	21 V

Table 12.3 MPP values under 500 W/m^2 irradiance [32]

I_{MPP}	MPP current	3.5 A
V_{MPP}	MPP voltage	14.63 V
P_{MPP}	MPP power	51.2 W

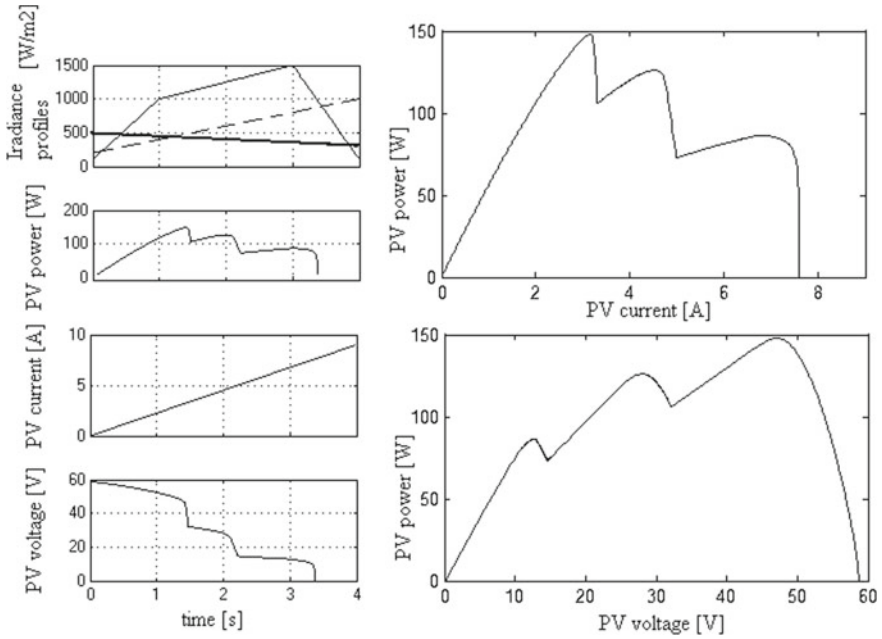

Fig. 12.12 PV power characteristics of the 1Px3S PV array [37]

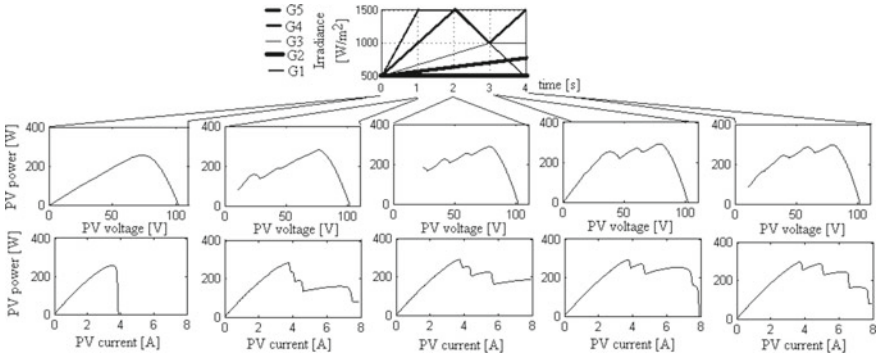

Fig. 12.13 PV power characteristics of the 1Px5S PV array [32]

(1500, 1250, 1000, 1000, 835, 625, 500) ⇒ 4 LMPPs
(1000, 1000, 1000, 1000, 1000, 690, 500) ⇒ 3 LMPPs.

Note that the PV power characteristic of a 1Pxn_sS PV array under PSCs could have up to n_s LMPPs (Fig. 12.12, where the 1Px3S PV array has 3 LMPPs) and only a maximum if all panels will operate under the same irradiance [39]. Also, it can be

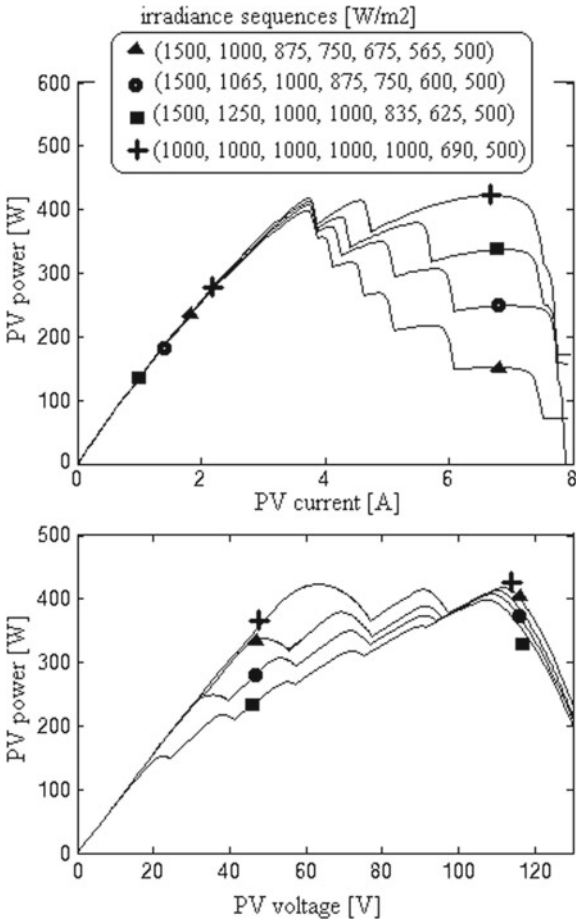

Fig. 12.14 PV power characteristics of the 1Px7S PV array [38]

observed that the GMPP could be located on left, middle, and right of the PV power characteristics. Thus, the PV power patterns will be designed as follows.

12.3.2 PV Power Patterns

The PV patterns $y = h(p)$ given by Eq. (12.2) [38]:

$$y = \text{sat}\left(M_l - (p-l)^2\right) + \text{sat}\left(M_m - (p-m)^2\right) + \text{sat}\left(M_r - (p-r)^2\right) \qquad (12.2)$$

where, the (l, m, r) triplet was designed to be (20, 50, 80) considering the PV power characteristics of the 1Px7S PV array. The (M_l, M_m, M_r) triplet defines the amplitude

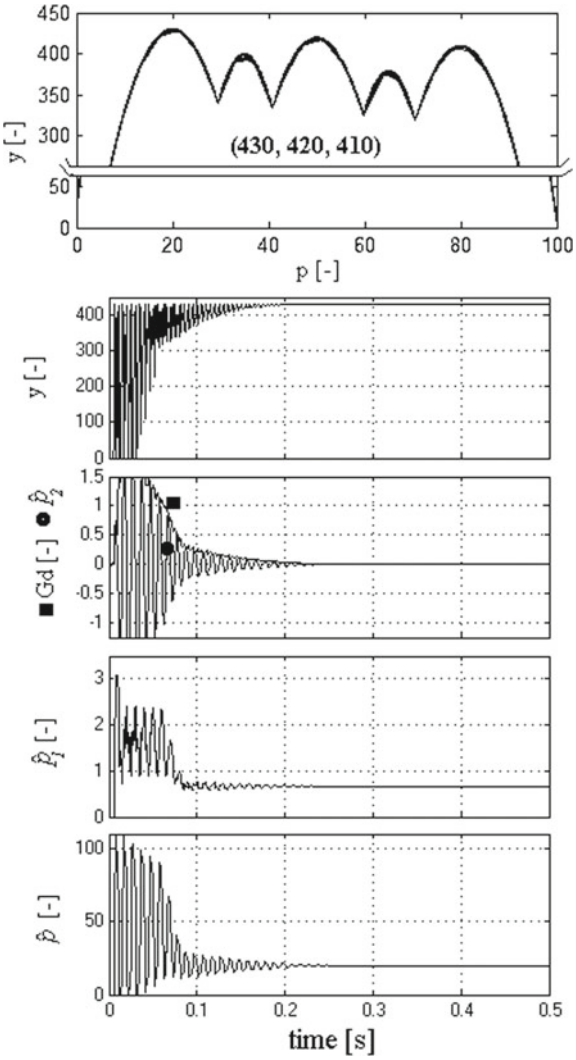

Fig. 12.15 Searching of the GMPP on the PV pattern (430, 420, 410) [38]

and position of the GMPP on PV power pattern. The saturation function (sat) has the lower limit zero and the upper limit is infinite. For example, the GMPP is located in the left (Fig. 12.15), middle (Fig. 12.16), and right side (Fig. 12.17) if the (M_l, M_m, M_r) triplet is (430, 420, 410), (410, 430, 420), and (410, 420, 430), respectively.

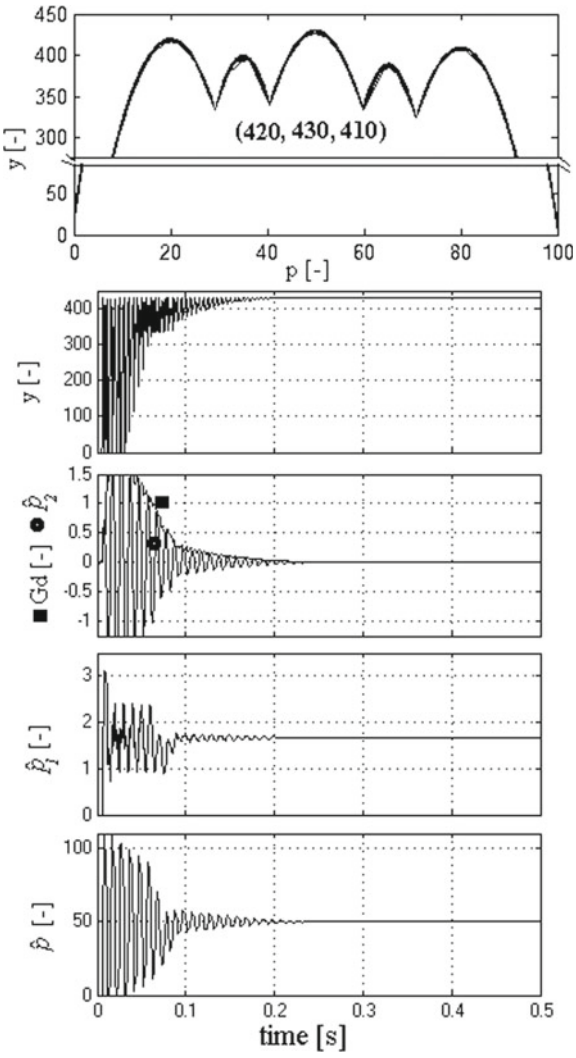

Fig. 12.16 Searching of the GMPP on the PV pattern (420, 430, 410) [38]

But also a generic PV pattern Eq. (12.3) could be used in simulations [32]:

$$y = \text{sat}\left(l - (p-2)^2\right) + \text{sat}\left(m - (p-5)^2\right) + \text{sat}\left(r - (p-8)^2\right) \tag{12.3}$$

where, the (l, m, r) triplet define the position of the GMMP on the PV power pattern. For example, the GMPP is located in the left (left side of the Fig. 12.18), middle (middle side of the Fig. 12.18), and right (right side of the Fig. 12.18) if the (l, m, r) triplet is (5,4,4), (4,5,4) and (4,4,5), respectively.

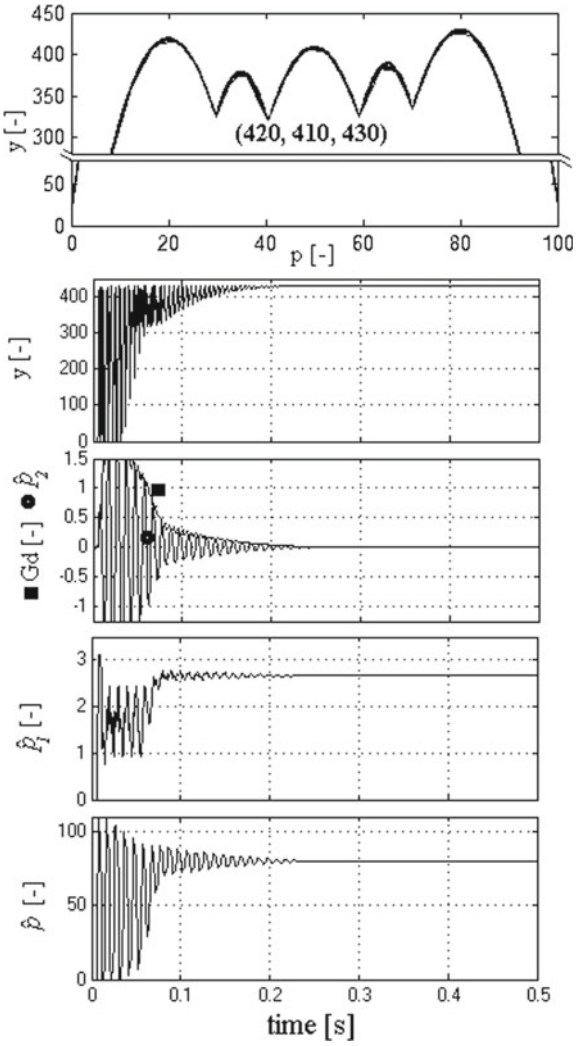

Fig. 12.17 Searching of the GMPP on the PV pattern (420, 410, 430) [38]

The structure of the plots of Figures show in this section will be explained and commented in section of Results, being related to the GMPPT control schemes based on the ESC methods that will be presented in next section.

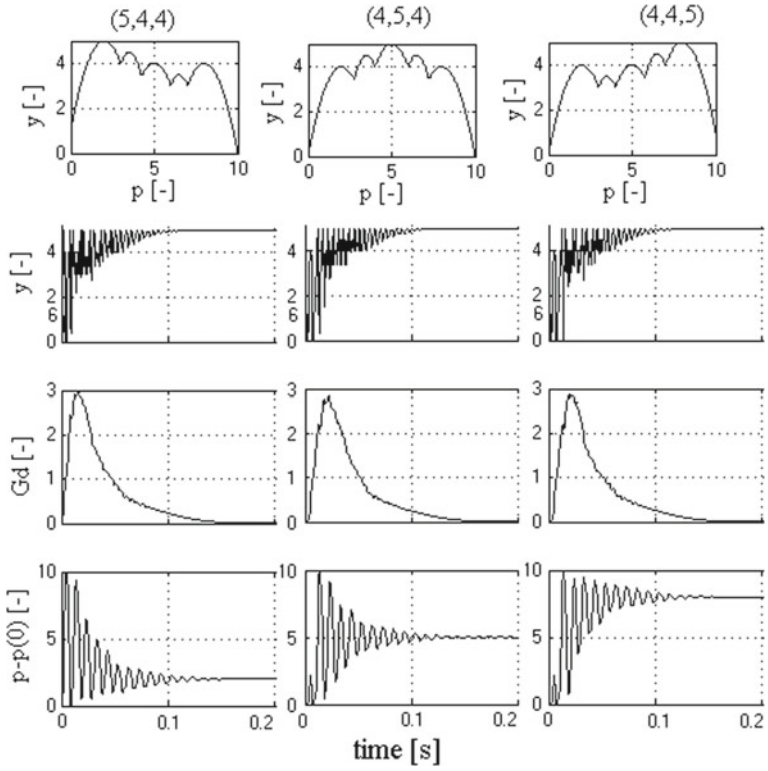

Fig. 12.18 Searching of the GMPP on the generic PV pattern [32]

12.4 Global MPPT Control Schemes

Different MPPT algorithms and their improved variants as performance related to the search speed and the tracking accuracy have been proposed in the last years such as Perturb and Observe (P&O) [40, 41], Incremental Conductance (IC) [42, 43], and the Hill Climbing (HC) [44, 45], Ripple Correlation Control (RCC) [46, 47], sweep current or voltage methods [48], load current and load voltage minimization [49, 50], Fractional Short Circuit Current [51], Fractional Open Circuit Voltage [52], *dP*/*dV* or *dP*/*dI* feedback control [53], model predictive control [54], and so on, being identified more than fifty MPPT algorithms in recent reviews [34, 35, 55–61].

From these reviews, the reviews [34, 35, 60, 61] approach the issue of the GMPP searching on PV array under PSCs considering the firmware-based and hardware architecture-based algorithms.

The hardware-based algorithms are dependent to topology of the power converter [30, 62–65]. The PV array can be of centralized, hybrid, or decentralized type, using a central inverter [65], an inverter for each string of PV panels [64], or a micro-inverter for each panel [63].

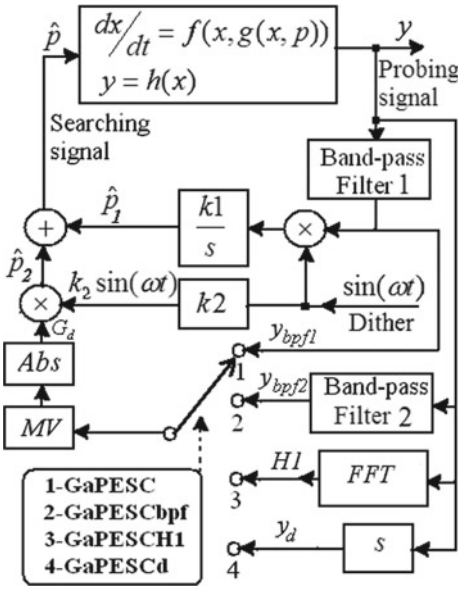

Fig. 12.19 The aPESC schemes [38]

Due to its natural adaptability to multimodal functions such as represented by the PV patterns, the soft computing techniques search the GMPP based on the chaotic search [66], Fuzzy Logic Controller (FLC) [67, 68], Artificial Neural Network (ANN) [69] and Evolutionary Algorithms (EAs), where EAs include genetic algorithms (GAs) [70], differential evolution (DE) [71], particle swarm optimization (PSO) [72], ant colony systems (ACSs) [73].

The review [34] highlights that the advantages of GMPP search based on perturbation-based and model-based ESC methods [74–77]. The perturbed ESC (PESC) schemes will use a dither gain which can decrease exponentially [78] or asymptotically [79] to zero, so these schemes are called as asymptotic PESC (aPESC) schemes.

12.4.1 Asymptotic Perturbed Extremum Seeking Schemes

The aPESC schemes are presented in Fig. 12.19.

All schemes include the searching loop and the locating loop with tuning parameters k_1 and k_2. The aPESCH1 scheme uses the magnitude of first harmonic ($H1$) as modulation signal of the dither (G_d) [33]. The $H1$ magnitude can be approximated by a using an additional Band-Pass Filter (BPF2) centered on the first harmonic (GaPESCbpf scheme), a derivative operator (GaPESCd scheme), or only the BPF1 (GaPESC scheme) which must be designed to ensure the appropriate dither persistence in the searching loop [80, 81]. The performance between these aPESC schemes

are minor, so only GaPESC scheme will be discussed in next section and used in simulation.

12.4.2 Modeling the GaPESC Scheme

The signal processing using the GaPESC scheme is based on the following relationships [38]:

$$y = h(p), \quad y_N = k_{Ny} \cdot y \tag{12.4a}$$

$$\begin{cases} \dot{y}_f = -\omega_h \cdot y_f + \omega_h \cdot y_N \\ y_{HPF} = y_N - y_f \\ \dot{y}_{BPF1} = -\omega_l \cdot y_{BPF} + \omega_l \cdot y_{HPF} \end{cases} \tag{12.4b}$$

$$y_{DM} = y_{BPF1} \cdot s_d, \quad s_d = \sin(\omega t) \tag{12.4c}$$

$$\dot{y}_{Int} = y_{DM} \tag{12.4d}$$

$$G_d = |y_{MV}|, \; y_{MV} = \frac{1}{T_d} \cdot \int y_{BPF1} dt \tag{12.4e}$$

$$p_1 = k_1 \cdot y_{Int}, \quad k_1 = \gamma_{sd} \cdot \omega \tag{12.4f}$$

$$p_2 = k_2 \cdot G_d \cdot s_d \tag{12.4g}$$

$$p_3 = A_m \cdot s_d \tag{12.4h}$$

$$p = k_{Np} \cdot (p_1 + p_2 + p_3) + p_0 \tag{12.4i}$$

where Eqs. (12.4a)–(12.4i) represent the static map, normalization, BPF filtering, demodulation, integration, computing of the dither gain (G_d), and the components p_1, p_2 and p_3 of the searching signal (p). The component p_3 is used to start the searching on static PV patterns. Signal y_f is an intermediate variable related to High-Pass Filter (HPF) operating, and the Mean Value (MV) block is used to further smooth the signal y_{bpf1} (the output of the BPF1).

12.4.3 The Searching Gradient and Harmonics' Persistence on the Searching Loop

As it was mentioned, the amplitude of the dither gain G_d signal is similar to that obtained with the GaPESCd scheme. So, the searching gradient and harmonics'

persistence on the searching loop will be evaluated for this scheme, considering the first three harmonics of the initial searching signal (p_{init}):

$$p_{init} = \sum_{j=1}^{3} a_j \sin(j\omega t) + k_2 \left|\frac{dy}{dx}\right| \cdot \sin(\omega t) \tag{12.5}$$

Around the GMPP, the PV pattern $y = h(x)$ can be approximated by Eq. (12.6):

$$y \cong h(x_{GMPP}) + (x - x_{GMPP}) \cdot \left.\frac{dh}{dx}\right|_{x_{GMPP}} + (x - x_{GMPP})^2 \cdot \frac{1}{2} \cdot \left.\frac{d^2h}{dx^2}\right|_{x_{GMPP}} + (x - x_{GMPP})^3 \cdot \frac{1}{6} \cdot \left.\frac{d^3h}{dx^3}\right|_{x_{GMPP}} \tag{12.6}$$

If $\tilde{x} = x - x_{GMPP}$, then the nonlinear map $\tilde{y} = y - h(x_{GMPP})$ can be rewritten as:

$$\tilde{y} \cong \dot{h} \cdot \tilde{x} + \frac{1}{2}\ddot{h} \cdot \tilde{x}^2 + \frac{1}{6}\dddot{h} \cdot \tilde{x}^3 \tag{12.7}$$

where,

$$\dot{h} \triangleq \frac{dy}{dx},\ \ddot{h} \triangleq \frac{d^2y}{dx^2},\ \dddot{h} \triangleq \frac{d^3y}{dx^3} \tag{12.8}$$

Thus, the initial probing signal is:

$$\tilde{y}_{init} \cong \dot{h} \cdot p_{init} + \frac{1}{2}\ddot{h} \cdot p_{init}^2 + \frac{1}{6}\dddot{h} \cdot p_{init}^3 \cong \cong \sum_{j=1}^{4} \left(\dot{h} \cdot p_{init(j)} + \frac{1}{2}\ddot{h} \cdot p_{init(j)}^2 + \frac{1}{6}\dddot{h} \cdot p_{init(j)}^3 \right) \tag{12.9}$$

where,

$$p_{init(j)} = a_j \sin(j\omega t),\ j = 1, 2, 3, \quad p_{init(4)} = k_2 \left|\dot{h}\right| \cdot \sin(\omega t) \tag{12.10}$$

So, considering an ideal BPF, the y_{BPF} components are:

$$y_{BPF} = \sum_{j=1}^{4} y_{BPF(j)} \tag{12.11}$$

where,

$$y_{BPF(j)} = \dot{h}a_j \sin(j\omega t) + \frac{1}{2}\ddot{h}a_j^2 \sin^2(j\omega t) + \frac{1}{6}\dddot{h}a_j^3 \sin^3(j\omega t)\ , \ j = 1, 2, 3$$

$$y_{BPF(4)} = \dot{h}k_2|\dot{h}| \sin(\omega t) + \frac{1}{2}\ddot{h}\left(k_2|\dot{h}|\right)^2 \sin^2(\omega t) + \frac{1}{6}\dddot{h}\left(k_2|\dot{h}|\right)^3 \sin^3(\omega t) \quad (12.12)$$

The signal after demodulation is given by Eq. (12.13):

$$p_{DM} = \sum_{j=1}^{4} \sin(\omega t) \cdot y_{BPF(j)} \quad (12.13)$$

After trigonometric manipulations, the searching signal will be given by Eq. (12.14):

$$p = g_S \cdot t + p_{1LF} + k_2|\dot{h}| \cdot \sin(\omega t) + A_m \cdot \sin(\omega t) \quad (12.14)$$

where the g_S searching gradient and signal p_{1LF} (the low frequency components of the p_1 signal) are given by Eqs. (12.15) and (12.16):

$$g_S \cong \frac{\dot{h}}{2} \cdot k_1\left(a_1 + k_2|\dot{h}|\right) + \frac{\dddot{h}}{16} \cdot k_1\left(a_1^3 + \left(k_2|\dot{h}|\right)^3\right) \quad (12.15)$$

$$p_{1LF} = \sum_{j=1}^{3} \left(s_j \cdot \sin(j\omega t) + c_j \cdot \cos(j\omega t)\right) \quad (12.16)$$

Thus, the low frequency harmonics of the p_1 signal are:

$$p_{1LF} = \sum_{j=1}^{3} b_j \cdot \sin(k\omega t + \varphi_j) \quad (12.17)$$

$$b_j = \sqrt{s_j^2 + c_j^2}, \quad tg\varphi_j = \frac{c_j}{s_j} \quad (12.18)$$

The searching gradient Eq. (12.19) has more components in addition of the gradient of classical ESC scheme [76], components which ensure GMPP searching and then its tracking. The amplitude of first harmonic (a_1) is high during the searching of the GMPP, so

$$g_{S1} \cong k_1 \cdot \left(\frac{\dot{h}}{2} \cdot a_1 + \frac{\dddot{h}}{16} \cdot a_1^3\right) \quad (12.19a)$$

The a_1 amplitude is small close to a Local MPP (LMPP), so

$$g_{S2} \cong k_1 \cdot \left[\frac{\dot{h}}{2} \cdot k_2|\dot{h}| + \frac{\dddot{h}}{16} \cdot \left(k_2|\dot{h}|\right)^3\right] \quad (12.19b)$$

The g_{S2} component sets the sweeping range. The searching process will not be blocked in a LMPP if the parameter k_2 is appropriately designed [80, 81].

12.5 Performance Indicators

12.5.1 Performance Indicators for PV Cells

One of the main performance indicators of the analysed PV cells is the energetic efficiency. The external collection efficiency is described as a global photocurrent intensity of a specific wavelength divided to area and to the number of the incident photons, multiplied by the elementary electric charge. The simulations prove similar shapes for the collection efficiency curve, as for the short-circuit current. But the last one includes small peaks, due to the transmittance effect. To increase the light capture inside the cell, a rear-surface processing is concerned to allow the unabsorbed light reflection or front-surface texturization to reduce as much as possible the reflection at the wafer surface.

Another performance indicator is the filing factor *FF*, which is depending on the maximum power dissipation and the shortcut current at an output voltage of the cell. The filing factor is extracted from the measured static characteristics.

The fabricated cells with texturized surface are characterized by spectrophotometric tests. So, another investigated parameter is the spectral reflectance of the textured PV cells. Using different patterning geometries and different etching solutions of the silicon wafers, the wavelength range was measured from 350 to 900 nm by a spectrophotometer, SPECORD—M42 with double beam. The spectral reflectance was extracted for different textured surfaces of silicon multi-crystalline wafers and is presented in Fig. 12.20a, b.

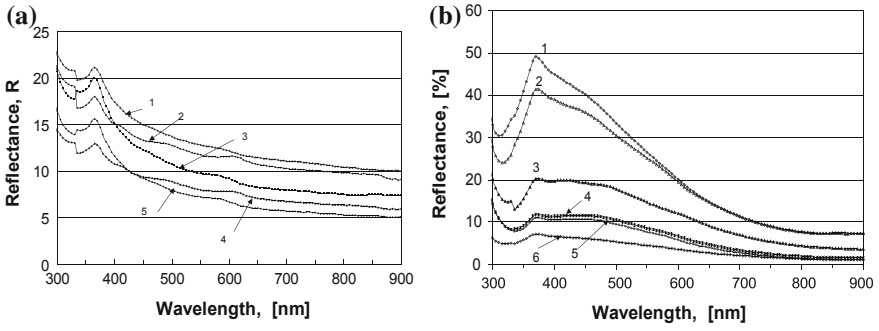

Fig. 12.20 Measured spectral reflectance traces of the texturized silicon surface, **a** without anti-reflection film [28], **b** with anti-reflection film [28]

In Fig. 12.20a, b, the traces 1÷6 are achieved by different chemical treatments, with different widths (z): trace 1—untexturized surface and $z = 6$ μm; traces 2, 3, 6—simple texturized shell, achieved by isotropic etch (trace 2 for $z = 6$ μm in HNO_3:HF:CH_3COOH (25:1:10); trace 3 for $z = 20$ μm in HNO_3:H_2O:NH_4F:HF-(280:140:6:3); trace 6 for $z = 10$ μm in HNO_3:H_2O:NH_4F:HF-(280:140:6:3); trace 4, 5—pyramidal texturized shell, at KOH 40% (trace 4 for $z = 4$ μm; trace 5 for $z = 10$ μm).

Figure 12.20a describes the spectra of the textured PV cells without anti-reflection surface and a simple silicon wafer mechanical thinned, frequently exploited in the PV cells made by mono-crystalline Silicon. The analysis proves a reflectance decreasing sub-30% when texturization is applied, indifferently of the geometry or etching technology. As a performance indicator for PV cells, the reflectance evolves in a range of 5–50%. The traces from Fig. 12.20a reveal an increasing consequence of the geometry selection in respect to the etching technology. Hence, in the case of the Si-100 type, processed by anisotropic etching to achieve the pyramidal shape under similar technological conditions (40% KOH etching at 80 °C), a lower reflectance is observed. This corresponds to a shape with smaller size ($z = 20$ μm), see trace 3, compared to the case $z = 10$ μm, trace 5 from Fig. 12.20. Similar dependence on the selected geometry is also accomplished in the simple structures, by the acidic treatment in HNO_3:HF:NH_4F:H_2O, see trace 1 and 4 for the defined windows width of 6 μm and 4 μm. The reflectance variation was poorer for the trace 2 with texturized surfaces, for the same geometry and different etching solution. The conclusion concerns the efficiency of the HNO_3:HF:NH_4F:H_2O solution that possesses a lower etch rate. To keep a reflectance sub-10%, the texture must use small pyramidal geometries, as for traces 4 or 5. Figure 12.20b presents the reflectance of the processed samples by the same technologies as previously, when an anti-reflecting SiO_2 film of 154 nm thickness covers the structures. In this last case, the reflectance is lower than the previous case, observing a decreasing sub-5% for $\lambda > 0.750$ nm.

12.5.2 Performance Indicators for GMMP Searching

The performance indicators related to GMPP searching on PV patterns are as follows:

(i) The searching resolution (R_S):

$$R_S = \frac{\min_i |y_{GMPP} - y_{LMPPi}|}{y_{GMPP}} \cdot 100[\%] \tag{12.20}$$

(ii) The tracking accuracy (T_{acc}):

$$T_{acc} = \frac{y_{PV}}{y_{GMPP}} \cdot 100[\%] \tag{12.21}$$

(iii) The tracking efficiency (T_{eff}):

$$T_{eff} = \frac{\int_0^t y_{PV}\,dt}{\int_0^t y_{GMPP}\,dt} \cdot 100[\%] \tag{12.22}$$

where, y_{PV}, y_{GMPP} and y_{LMPPi} are the available PV power, the effective power harvested using the GaPESC scheme, and the power of a LMPP.

The tracking efficiency depends to PV pattern shape and dynamics, so the value of the tracking time to steps in irradiance profile must be shorter as possible. The performance in tracking time for GaPESC scheme is given by number of dither's periods. The GMPP is not always found, so this performance is given by the percent of the hit count (PHC):

$$PHC = \frac{\text{number of positive results in finding the GMPP}}{\text{number of tests performed}} \cdot 100[\%] \tag{12.23}$$

The PHC value is 100% and close to 100% using the GaPESC scheme [38] and PSO-based GMPPT algorithm [82] for PV patterns with $R_S > 5\%$. The PHC value remains 100% even for PV patterns with $R_S > 0.25\%$ if the GaPESC scheme is used, but the PHC value decreases considerably for PSO-based GMPPT.

12.6 Results

12.6.1 The Solar-Cell Efficiency

The nano-core-shell NCS resulted films can be alternatively used to polycrystalline Si, amorphous silicon, as to any multi-domains materials. The theory of multi-crystalline silicon structures is based on several small crystals or micro-domains, separated by multiple frontiers. These edges produce a gap-stated distribution and prevent the electron current flow. Rather they stimulate the electrons-holes recombination, reducing the output power of the solar cell. Additionally, multi-crystalline silicon is cheaper than the mono-crystalline silicon. However, the usual methods to augment the solar-cell efficiency consist in doping profile optimization, the lighting window location, profile of the gap-state and design of the back side contact. The illumination window can be optimized by an appropriate oxide thickness, as antireflective layer and a film that ensure the light trapping by the frontal surface. The transmittance and the short-circuit current recommend an oxide film of 0.12 μm thickness, as an optimum (Fig. 12.21a, b).

For thicker silicon oxides, the transmittance gets a maximum if the incident wavelength increases. For thinner silicon oxide, the transmittance gets a maximum if the incident wavelength decreases. The optimum oxide thickness is 0.12 μm because

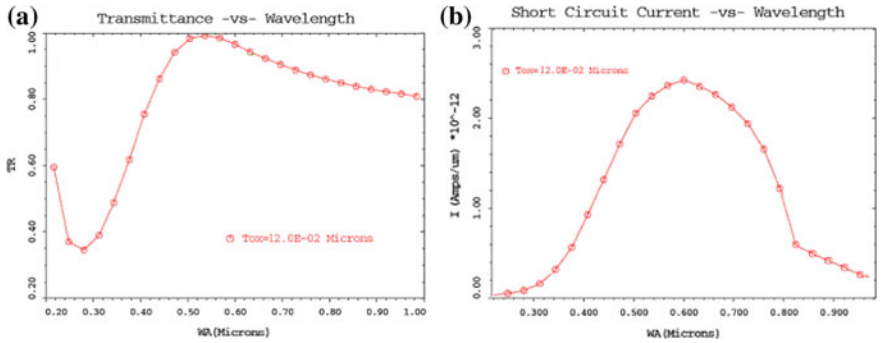

Fig. 12.21 The PV, **a** transmittance [27], **b** short-circuit current - through the PV cell with 0.12 μm oxide thickness versus wavelength [27]

Table 12.4 The measured parameters of the PV cells

Wafer no. (—texturization by)	Light intensity (mW/cm^2)	I_{SC} (mA)	V_{OC} (mV)	FF (%)	Eff (%)
1—KOH + B^+	10	5.1	390	75.3	15
2—KOH	10	3.7	460	74.7	12.7
3—Acid + B^+	10	4.8	360	67.6	11.7
4—Acid	10	3.5	470	67.1	11
5—No texturization	10	3.8	350	56	7.5

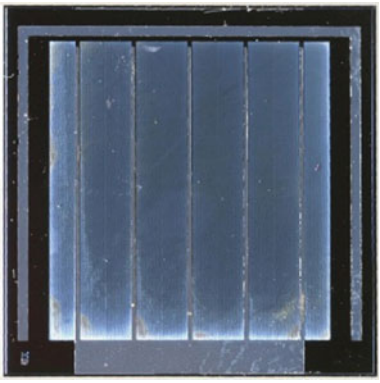

Fig. 12.22 The finalized solar cell made in KOH solution [27]

the transmittance maximum occurs in the range 0.4–0.7 μm wavelength, which corresponds to the solar energy in practice.

An optimization technology based on the surface texturization was presented in Sect. 12.2.4. Here it was demonstrated that the efficiency increased from 10% at classical PV cells, to 13% for special organic materials OSC, or to 15% for texturization in KOH solution of the poly-silicon surface, Table 12.4.

Table 12.5 PV solar cells with/without pyramids

Wafer type	Light intensity (mW/cm^2)	V_{OC} (mV)	*FF* (%)	*Eff* (%)
Without pyramids	34	670	84	19.35
With pyramids	40	700	84	24.01

The filing factor FF of the PV cell was 75% if the processed surface occurred in KOH solution, 67% in HNO3:HF:CH3COOH solution and the minimum of 56% for untexturized cells. A similar ladder is also fulfilled for efficiency, Table 12.4.

After the last technological step that consists on the PV cell structures separation, the obtained solar cell is presented in Fig. 12.22.

The maximum efficiency of 24% occurs for surface texturing with multiple pyramids, Table 12.5. Also, the impact of the surface texturizing by micro-pyramid surface processing consists in an increased supply voltage, Table 12.5.

12.6.2 Discussion

PV solar cells based on silicon technology contribute with 94% from the international green energy market. They are produced either from mono-crystalline or multi-crystalline silicon. Due to the high electronic properties of mono- or multi-crystalline silicon, as the diffusion lengths that is expected to be hundreds of micrometer, the high efficient photovoltaic cells between 10 and 24%, can be made from this nowadays material. However, multi-crystalline silicon is much less expensive as mono-crystalline silicon and frequently applied.

Keeping these silicon related materials, an optimized solar-cell structure that was fabricated by the front-surface texturization of a multi-crystalline silicon wafer, was investigated. The structure adds further antireflection coating, silicon active layer and front and back wafer improved contacts.

Alternatively, as materials and technologies, the nano-structured materials based on NCS grafted on organic compounds and its application in the photovoltaic cells, biosensors and devices is in progress, [83–85]. Very recent, promising performances were highlighted for similar nano-transistors with Si-Ge nano-core-shell, by other researcher groups, too [6, 11]. A technological advantage of the presented technology of NCS synthesis comes from ferrite core that facilitates the purification by magnetic separation.

Besides to a high efficiency for PV cells in order to have as much power generated by PV array under different environmental conditions, it is necessary to harvest all available PV power using advanced GMPP-based algorithms. The performance of GaPESC scheme has been analyzed and the results were presented in next section.

12.6.3 GMPP Search on the PV Pattern

The values of the parameters of the GaPESC scheme used in simulation are as follows: 100 Hz dither frequency ($f_d = \omega/2\pi$), the cut-off frequency of the BPF1 to better approximate the H1 magnitude are $f_{h1} = \beta_{h1} \cdot f_d = 10$ Hz and $f_{l1} = \beta_{l1} \cdot f_d = 190$ Hz, $A_m = 0.001$, $\gamma_{sd} = 20$, $k_1 = \gamma_{sd}\omega$, $k_2 = 10$, and starting point is $p_0 = p(0) = 0$. The normalization gains, $k_{Ny} \cong 1/y_N$ and $k_{Np} \cong \Delta p$ are set to 0.5 and 5 for generic PV pattern (12.3), because y_N value must be between estimated values for $y = h(p)$ and $\Delta p = |p_{GMPP} - p_0|$ [81]. But for generic PV pattern (12.2) the normalization gains k_{Ny} and k_{Np} are set to 1/200 and 20. The other parameters are the same because not depend to shape of the PV pattern.

12.6.3.1 The Behavior of GMPP Search

The sweeping of the LMPPs until the GMPP is located is shown in Figs. 12.15, 12.16, and 12.17 for the PV pattern (12.2) having the GMPP located in left, middle, and right side, and in Fig. 12.15 for the PV pattern (12.3) that also represent the cases of the GMPP located in left, middle, and right side. The structure of Figs. 12.15, 12.16, and 12.17 is as follows: the first plot presents the PV pattern; the second plot presents the output (y); the searching signal (p) and its components are presented in next plots. The GMPP is found in all cases starting from $p(0) = 0$, being located after 10 periods of the dither.

The tracking time is of 0.1 s for 100 Hz dither. The dither gain G_d decay asymptotically to zero after the tracking time. The GMPP is accurately found even if this is located in the opposite side to starting point.

The performance remains the same for the PV pattern Eq. (12.3).

12.6.3.2 The Performance of GMPP Search

The results presented in Fig. 12.23 prove the performance of the GaPESC scheme on the PV pattern Eq. (12.3). The highest LMPP differs to GMPP by 0.001, so the tracking accuracy and searching resolution are 99.9988% and 0.0238% (=0.001/4.2) (see Fig. 12.23). The tracking accuracy reported in [82] is of 99.96%. The PV pattern is swept until the GMPP is located using the localization loop and the tuning parameter k_2. After the tracking time, only the GMPP peak (where GMMP was located) is swept until the GMPP is accurately found using the searching loop and the tuning parameter k_1.

The searching resolution is of 0.25% (≅1/402) for the PV pattern Eq. (12.2) shown in Fig. 12.24, but can be decreased by appropriate design of the tuning parameters [81]. The tracking accuracy and the tracking time are less dependent to PV pattern's shape is the same tuning parameters are used.

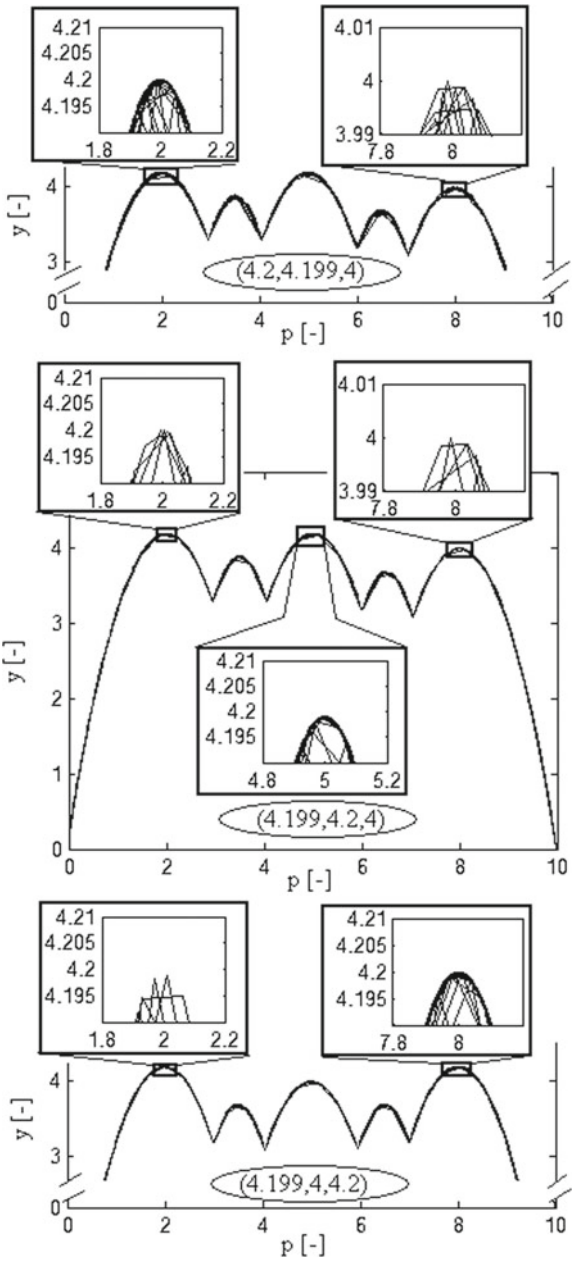

Fig. 12.23 The searching of the GMPP on the pattern Eq. (12.3) [32]

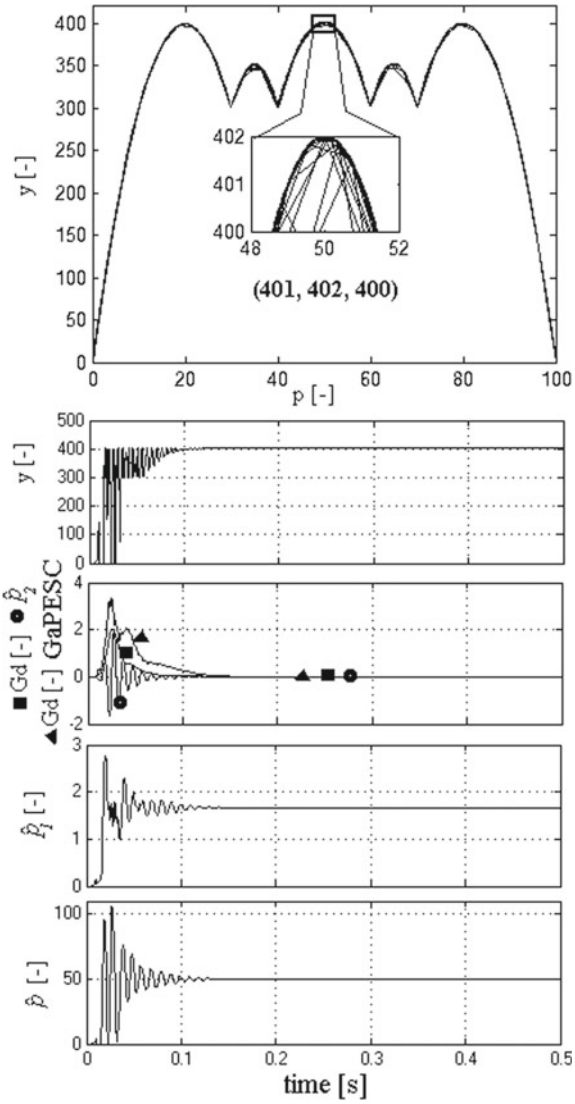

Fig. 12.24 The searching of the GMPP on the pattern Eq. (12.2) [38]

12.7 Conclusion

A nano-core-shell ferrite nano-particles technology able to be used in thin film transistors with low power dissipation, as a suitable consumer for microgrids network, were depicted. Their self-assembling was achieved with external shell of PABA and proved a good stability. The simulated thin film transistors with NCS-PABA nanomaterial show superior electrical characteristics then silicon-TFT.

Another target concerned the PV cell in Si-compounds, keeping the usual costs, but aiming an improvement within the PV cell performances. In this scope, the technology flow is reduced to maximum 7 steps. If a multi-crystalline silicon wafer was started-up, the doping profile was improved, the front-surface of the solar cell was texturized by different etching techniques to minimize the light reflectivity. Also, the wafer was doped by Boron on the back-side to ensure optimum series resistance toward anode. The experimental tests were in fine agreement with the Atlas simulations and proved better performance parameters than the older literature [22, 23, 29].

Also, some simulations have been presented for the GaPESC scheme analyzed in this chapter to improve the energy harvested from the PV array. The performance of the GaPESC scheme is as follows [32, 37, 38]: (1) 99.99% stationary tracking accuracy and 99.96% transitory tracking accuracy; (2) the searching process based on GaPESC scheme is robust even for high noisy PV patterns; (3) 0.1 s searching time for 100 Hz dither; (4) the searching resolution is lower than 0.1%; (5) the design of tuning parameters and normalization gains is not restrictive due to adaptive feature of the ESC loops; (6) the starting point can be anywhere in the searching range; (7) the power ripple around GMPP is very small due to asymptotic decrease of the dither.

The performance is better than those obtained with the PSO algorithm, and also much better compared to well-known P&O and IC algorithms, where 98.4% tracking accuracy was obtained for both algorithms using the European Efficiency Test, EN 50530 [86].

Acknowledgements This work was produced under a grant of Ministry of Research and Innovation, CNCS-UEFISCDI, project number PN-III-P4-ID-PCE-2016-0480 within PNCDI III project number 4/2017 (TFTNANOEL), project 53PED (ID: PN-III P2-2.1-PED-2016-1223. Hy-DeMo), and project PN-III P1-1.2-PCCDI2017-0332, and within RDI Program for Space Technology and Advanced Research—STAR, project number 167/2017 (SMESinSpace).

References

1. L. Mariam, M. Basu, M.F. Conlon, A review of existing microgrid architectures. Hindawi J. Eng. **937614**, 1–8 (2013)
2. N. Bizon, M. Oproescu, M. Raducu, Applications in control of the hybrid power systems. Chapter in book: *Analysis, Control and Optimal Operations in Hybrid Power Systems* (Springer Press, London, Heidelberg New York, 2013), pp. 227–290
3. Z. Tehrani, D.J. Thomas, T. Korochkina, C.O. Phillips, D. Lupo, S. Lehtimaki, J. O'Mahony, D.T. Gethin, Large-area printed supercapacitor technology for low-cost domestic green energy storage. Energy Elsevier **118**(1), 1313–1321 (2017)
4. G.A. Salvatore, N. Munzenrieder, T. Kinkeldei, L. Petti, C. Zysset, I. Strebel, L. Buthe, G. Troster, Wafer-scale design of lightweight and transparent electronics that wraps around hairs. Nat. Commun. **5**(1), 2982, 1–8 (2014)
5. C. Ravariu, Gate swing improving for the nothing on insulator transistor in weak tunneling. IEEE Trans. Nanotechnol. **16**(6), 1115–1121 (2017)

6. S. Barraud, J.M. Hartmann, V. Maffini Alvaro, L. Tosti, V. Delaye, D. Lafond, Top-down fabrication of epitaxial SiGe/Si multi-(core/shell) p-FET nanowire transistors. IEEE Trans. Electr. Devices **61**(4), 953–956 (2014)
7. D. Yang, L. Zhang, H. Wang, Y. Wang, Z. Li, T. Song, Pentacene-based photodetector in visible region with vertical field-effect transistor configuration. IEEE Photonics Tech. Lett. **27**(3), 233–236 (2015)
8. H.C. Lin, C.I. Lin, T.Y. Huang, Characteristics of n-type junctionless poly-Si thin-film transistors with an ultrathin channel. IEEE Electron Device Lett. **33**(1), 53–55 (2012)
9. R.W. Johnson, A. Hultqvist, S.F. Bent, A brief review of atomic layer deposition: from fundamentals to applications. Mater. Today **17**(5), 236–246 (2014)
10. D. Dragomirescu, A. Takacs, M.M. Jatlaoui, S. Charlot, A. Rumeau, A.D. Fotache, D.E. Mihaiescu, A.E. Poting, C. Ravariu, Low cost flexible assembly technique applied in wireless sensors and organic transistors. Adv. Nano-Bio-Mater. Devices **2**(2), 262–268 (2018)
11. C. Ravariu, D.E. Mihaiescu, D. Istrati, B. Purcareanu, Nano-core-shell technologies suitable for thin film transistors implementation, in *XX-th International Symposium on Electrical Apparatus and Technologies SIELA*, Bourgas, Bulgaria, 2–6 June 2018, pp. 221–223
12. A.D. Franklin, Electronics: the road to carbon nanotube transistors. Nature **498**(6), 443–445 (2013)
13. H. Klauk, Organic thin-film transistors. Chem. Soc. Rew. **38**, 2643–2666 (2010)
14. N. Wrachien, N. Lago, A. Rizzo, R. D'Alpaos, A. Stefani, G. Turatti, M. Muccini, G. Meneghesso, A. Cester, Effects of thermal and electrical stress on DH4T-based organic thin-film-transistors with PMMA gate dielectrics. Microelectron. Reliab. **55**(10), 1790–1794 (2015)
15. T.R. Heera, L. Cindrella, Synthesis and characterization of NiS/MnS core-shell embedded conducting polyaniline composite for photovoltaic application. Int. J. Polym. Mater. Polym. Biomater. **59**(8), 607–621 (2010)
16. B. Kumar, B.K. Kaushik, Y.S. Negi, V. Goswami, Single and dual gate OTFT based robust organic digital design. Microelectron. Reliab. **54**(2), 100–109 (2014)
17. D.E. Mihaiescu, R. Cristescu, G. Dorcioman, C.E. Popescu, C. Nita, G. Socol, I.N. Mihailescu, A.M. Grumezescu, D. Tamas, M. Enculescu, R.F. Negrea, C. Ghica, C. Chifiriuc, C. Bleotu, D.B. Chrisey, Functionalized magnetite silica thin films fabricated by MAPLE with antibiofilm properties. Biofabrication **5**(1), 1–6 (2013)
18. O. Metin, S. Aydogan, K. Meral, A new route for the synthesis of graphene oxide-Fe_3O_4 (GO-Fe_3O_4) nanocomposites and their Schottky diode applications. J. Alloy. Compd. **585**(2), 681–688 (2014)
19. D.E. Mihaiescu, A.S. Buteica, J. Neamtu, D. Istrati, I. Mindrila, Fe_3O_4/salicylic acid nanoparticles behavior on chick CAM vasculature. J. Nanopart. Res. **15**(8), 1–5 (2013)
20. C. Ravariu, D.E. Mihaiescu, D. Istrati, M. Stanca, From pentacene thin film transistor to nanostructured materials synthesis for green organic-TFT, in *IEEE International Conference of Semiconductors*, Sinaia, Romania, 10–13 Oct 2018, pp. 181–184
21. ATLAS user's manual & Examples: Device Simulation Software (SILVACO International, Santa Clara, 2016) www.silvaco.com
22. W. Zhao, S. Li, H. Yao, S. Zhang, Y. Zhang, B. Yang, J. Hou, Molecular optimization enables over 13% efficiency in organic solar cells. Journ. Amer. Chem. Soc. **139**(21), 7148–7151 (2017)
23. C. Dyer Smith, J. Nelson, Y. Li, Chapter I-5-B—Organic Solar Cells, in book: McEvoy's Handbook of Photovoltaics (Third Edition), Fundamentals and Applications, Edited by: Soteris Kalogirou (Academic Press, 2018), pp. 567–597
24. P. Mittal, B. Kumar, Y.S. Negi, B.K. Kaushik, R.K. Singh, Channel length variation effect on performance parameters of organic field effect transistors. Microelectron. J. **43**(12), 985–994 (2012)
25. C. Ravariu, D. Dragomirescu, Different work regimes of an organic thin film transistor OTFT and possible applications in bioelectronics. Am. J. of Biosci. Bioeng. **3**(3), 7–13 (2015)
26. L.J.A. Korster, E.C.P. Smits, V.D. Mihailetchi, P.W.M. Blom, Device model for the operation of olymer/ fullerene bulk heterojunction solar cell. Phys. Rev. B **72**(085205), 1–9 (2005)

27. S. Burtescu, C. Parvulescu, F. Babarada, E. Manea, The low cost multicrystalline silicon solar cells. J. Mater. Sci. Eng. B: Adv. Funct. Solid-State Mater. **165**(3), 190–193 (2009)
28. E. Manea, E. Budianu, M. Purica, C. Podaru, A. Popescu, C. Parvulescu, A. Dinescu, A. Coraci, I. Cernica, F. Babarada, Front surface texturing processes for silicon solar cells, in *Proceedings of the IEEE International Conference of Semiconductors*, CAS'2007, Sinaia, Romania, pp. 191–194 (2007)
29. S. Silvestre, A. Chouder, Effects of shadowing on photovoltaic module performance. Prog. Photovoltaics Res. Appl. **16**(2), 141–149 (2008)
30. M. Garcia, J.M. Maruri, L. Marroyo, E. Lorenzo, M. Perez, Partial shadowing, MPPT performance and inverter configurations: observations at tracking PV plants. Prog. Photovoltaics Res. Appl. **16**(6), 529–536 (2008)
31. E. Duran, J.M. Andhjar, J. Galan, M. Sidrach de Cardona, Methodology and experimental system for measuring and displaying I-V characteristic curves of PV facilities. Prog. Photovoltaics Res. Appl. **17**(8), 574–586 (2009)
32. N. Bizon, Global maximum power point tracking based on new extremum seeking control scheme. Prog. Photovoltaics Res. Appl. **24**(5), 600–622 (2016)
33. N. Bizon, Energy harvesting from the PV hybrid power source. Energy **52**, 297–307 (2013)
34. Z.H. Liu, J.H. Chen, J.W. Huang, A review of maximum power point tracking techniques for use in partially shaded conditions. Renew. Sustain. Energy Rev. **41**, 436–453 (2015)
35. K. Ishaque, Z. Salam, A review of maximum power point tracking techniques of PV system for uniform insolation and partial shading condition. Renew. Sustain. Energy Rev. **19**, 475–488 (2013)
36. P. Sanchis, J. Lopez, A. Ursua, E. Gubia, L. Marroyo, On the testing, characterization, and evaluation of PV inverters and dynamic MPPT performance under real varying operating conditions. Prog. Photovoltaics Res. Appl. **15**(6), 541–556 (2007)
37. N. Bizon, Global maximum power point tracking (GMPPT) of photovoltaic array using the extremum seeking control (ESC): a review and a new GMPPT ESC scheme. Renew. Sustain. Energy Rev. **57**, 524–539 (2016)
38. N. Bizon, Global extremum seeking control of the power generated by a photovoltaic array under partially shaded conditions. Energy Convers. Manag. **109**, 71–85 (2016)
39. M.M. Rahman, M. Hasanuzzaman, N.A. Rahim, Effects of various parameters on PV-module power and efficiency. Energy Convers. Manage. **103**, 348–358 (2015)
40. M. Fortunato, A. Giustiniani, G. Petrone, G. Spagnuolo, M. Vitelli, Maximum power point tracking in a one-cycle-controlled single-stage photovoltaic inverter. IEEE Trans. Ind. Electron. **55**, 2684–2693 (2008)
41. H. Patel, V. Agarwal, MPPT scheme for a PV-fed single-phase single-stage grid-connected inverter operating in CCM with only one current sensor. IEEE Trans. Energy Convers. **24**, 256–263 (2009)
42. K. Harada, G. Zhao, Controlled power interface between solar cells and AC source. IEEE Trans. Power Electron. **8**, 654–662 (1993)
43. M. Qiang, S. Mingwei, L. Liying, J.M. Guerrero, A. Novel improved variable step- size incremental-resistance MPPT method for PV systems. IEEE Trans. Ind. Electron. **58**, 2427–2434 (2011)
44. E. Koutroulis, K. Kalaitzakis, N.C. Voulgaris, Development of a microcontroller-based, photovoltaic maximum power point tracking control system. IEEE Trans. Power Electron. **16**, 46–54 (2001)
45. A. Safari, S. Mekhilef, Simulation and hardware implementation of incremental conductance MPPT with direct control method using Cuk converter. IEEE Trans. Ind. Electron **58**, 1154–1161 (2011)
46. J.W. Kimball, P.T. Krein, Discrete-time ripple correlation control for maximum power point tracking. IEEE Trans. Power Electron. **23**, 2353–2362 (2008)
47. L. Yan Hong, D.C. Hamill, Simple maximum power point tracker for photo-voltaic arrays. Electron. Lett. **36**, 997–999 (2000)

48. M. Bodur, M. Ermis. Maximum power point tracking for low power photo-voltaic solar panels, in *7th Mediterranean Electrotechnical Conference,* vol. 752, pp. 758–761 (1994)
49. D. Shmilovitz, On the control of photovoltaic maximum power point tracker via output parameters. IEE Proc. Electr. Power Appl. **152**, 239–248 (2005)
50. G.W. Hart, H.M. Branz, C.H. Cox Iii, Experimental tests of open-loop maximum-power-point tracking techniques for photovoltaic arrays. Solar Cells **13**, 185–195 (1984)
51. N. Hyeong Ju, L. Dong Yun, H. Dong-Seok, An improved MPPT converter with current compensation method for small scaled PV-applications. Proc. IECON Conf. **1112**, 1113–1118 (2002)
52. S.J. Chiang, K.T. Chang, C.Y. Yen, Residential photovoltaic energy storage system. IEEE Trans. Ind. Electron. **45**, 385–394 (1998)
53. J.A.M. Bleijs, A. Gow, Fast maximum power point control of current-fed DC-DC converter for photovoltaic arrays. Electron. Lett. **37**, 5–6 (2001)
54. N. Bizon, N. Mahdavi Tabatabaei, F. Blaabjerg, E. Kurt (Ed.), *Energy Harvesting and Energy Efficiency: Technology, Methods and Applications* (Springer, London, 2017)
55. V. Salas, E. Olias, A. Barrado, A. Lazaro, Review of the maximum power point tracking algorithms for stand-alone photovoltaic systems. Sol. Energ Mat. Sol. C **90**(11), 1555–1578 (2006)
56. T. Esram, P.L. Chapman, Comparison of photovoltaic array maximum power point tracking techniques. IEEE Trans. Energy Convers. **22**, 439–449 (2007)
57. A.R. Reisi, H.M. Moradi, S. Jamas, Classification and comparison of maximum power point tracking techniques for photovoltaic system: a review. Renew. Sustain. Energy Rev. **19**, 433–443 (2013)
58. B. Subudhi, R. Pradhan, A comparative study on maximum power point tracking techniques for photovoltaic power systems. IEEE Trans. Sustain. Energy **4**, 89–98 (2013)
59. M.A.G. de Brito, L. Galotto Jr., L.P. Sampaio, G. de Azevedo e Melo, C.A. Canesin, Evaluation of the main MPPT techniques for photovoltaic applications. IEEE Trans. Ind. Electron. **60**, 1156–1167 (2013)
60. P. Bhatnagar, R.K. Nema, Maximum power point tracking control techniques: state-of-the-art in photovoltaic applications. Renew. Sustain. Energy Rev. **23**, 224–2241 (2013)
61. M.A. Eltawil, Z. Zhao, MPPT techniques for photovoltaic applications. Renew. Sustain. Energy Rev. **25**, 793–813 (2013)
62. A. Bidram, A. Davoudi, R.S. Balog, Control and circuit techniques to mitigate partial shading effects in photovoltaic arrays. IEEE J. Photovolt **2**, 532–546 (2012)
63. H.A. Sher, K.E. Addoweesh, Micro-inverters—promising solutions in solar photovoltaics. Energy. Sustain. Dev. **16**, 389–400 (2012)
64. L. Hassaine, E. Olias, J. Quintero, V. Salas, Overview of power inverter topologies and control structures for grid connected photovoltaic systems. Renew. Sustain. Energy Rev. **30**, 796–807 (2014)
65. E. Syafaruddin, T. Karatepe, Hiyama, Performance enhancement of photovoltaic array through string and central based MPPT system under non-uniform irradiance conditions. Energy Convers. Manag. **62**, 131–140 (2012)
66. L. Zhou, Y. Chen, K. Guo, F. Jia, New approach for MPPT control of photovoltaic system with mutative-scale dual-carrier chaotics search. IEEE Trans. Power Electron. **26**, 1038–1048 (2011)
67. E. Syafaruddin, T. Karatepe, Hiyama, polar coordinated fuzzy controller based real-time maximum power point control of photovoltaic system. Renew. Energy **34**(12), 2597–2606 (2009)
68. A.D. Karlis, T.L. Kottas, Y.S. Boutalis, A novel maximum power point tracking method for PV systems using fuzzy cognitive networks (FCN). Electr. Pow. Syst. Res. **77**(3–4), 315–327 (2007)
69. C.C. Liao, Genetic k-means algorithm based RBF network for photovoltaic MPP prediction. Energy **35**(2), 529–536 (2010)
70. Y. Shaiek, M.B. Smida, A. Sakly, M.F. Mimouni, Comparison between conventional methods and GA approach for maximum power point tracking of shaded solar PV generators. Sol. Energy **90**, 107–122 (2013)

71. M.F.N. Tajuddin, S.M. Ayob, Z. Salam, Tracking of maximum power point in partial shading condition using differential evolution (DE), in *IEEE International Conference on Power and Energy (PECon)*, p. 384 (2012)
72. K. Ishaque, Z. Salam, A deterministic particle swarm optimization maximum power point tracker for photovoltaic system under partial shading condition. IEEE Trans. Ind. Electron. **60**(8), 3195–3206 (2013)
73. L.L. Jianga, D.L. Maskell, J.C. Patra, A novel ant colony optimization-based maximum power point tracking for photovoltaic systems under partially shaded conditions. Energy Build. **58**, 227–236 (2013)
74. R. Leyva, C. Alonso, I. Queinnec, A. Cid Pastor, D. Lagrange, L. Martinez Salamero, MPPT of photovoltaic systems using extremum-seeking control. IEEE Trans. Aerosp. Electron. Syst. **42**(1), 249–258 (2006)
75. C. Zhang, R. Ordonez, *Extremum-Seeking Control and Applications: A Numerical Optimization-Based Approach* (Springer, London, 2012)
76. K.B. Ariyur, M. Krstic, *Real-time Optimization by Extremum-seeking Control* (Wiley-Interscience, Hoboken, 2003)
77. D. Dochain, M. Perrier, M. Guay, Extremum seeking control and its application to process and reaction systems: a survey. Math. Comput. Simulat. **82**, 369–380 (2011)
78. Y. Tan, D. Nesic, I. Mareels, A. Astolfi, On global extremum seeking in the presence of local extrema. Automatica **45**(1), 245–251 (2009)
79. N. Bizon, Searching of the extreme points on photovoltaic patterns using a new asymptotic perturbed extremum seeking control scheme. Energy Convers. Manag. **144**, 286–302 (2017)
80. N. Bizon, E. Kurt, Performance analysis of tracking of the global extreme on multimodal patterns using the asymptotic perturbed extremum seeking control scheme. Int. J. Hydrogen Energy **42**(28), 17645–17654 (2017)
81. N. Bizon, P. Thounthong, M. Raducu, L.M. Constantinescu, Designing and modelling of the asymptotic perturbed extremum seeking control scheme for tracking the global extreme. Int. J. Hydrogen Energy **42**(28), 17632–17644 (2017)
82. Y.H. Liu, S.C. Huang, J.W. Huang, W.C. Liang, A particles warm optimization-based maximum power point tracking algorithm for PV systems operating under partially shaded conditions. IEEE Trans. Energy Convers. **27**, 1027–1035 (2012)
83. C. Ravariu, Vacuum nano-triode in nothing-on-insulator configuration working in Terahertz domain. IEEE J. Electr. Devices Soc. **6**(1), 1115–1123 (2018)
84. C. Ravariu, E. Manea, F. Babarada, Masks and metallic electrodes compounds for silicon biosensor integration. J. Alloys Compd. Elsevier **697**(3), 72–79 (2017)
85. C. Ravariu, Deeper insights of the conduction mechanisms in a vacuum SOI nanotransistor. IEEE Trans. Electron Devices **63**(8), 3278–3283 (2016)
86. K. Ishaque, Z. Salam, G. Lauss, The performance of perturb and observe and incremental conductance maximum power point tracking method under dynamic weather conditions. Appl. Energy **119**, 228–236 (2014)

Part II
Microgrid Control Systems

Chapter 13
Control of Power Electronic Converters in AC Microgrid

Rajendrasinh Jadeja, Amit Ved, Tapankumar Trivedi and Gagandipsinh Khanduja

Abstract The main advantage of AC microgrid is it has the compatibility with existing ac grid. The book chapter emphasizes on the current controlling strategies of power converters operating in different modes with AC microgrid system simplified structure. The challenging part to meet the defined output parameters for Distributed Energy Resources (DERs) with increased penetration of the same is also jagged with controlling strategies of power converters. DER and ESS are integral part of microgrid and for AC microgrid they require converter interface. Various converter topologies and their control is included. Microgrid requires extensive control strategy to meet with grid requirements and load requirements under verity of conditions. Control strategies of multilevel is used. Control methods related to primary control, secondary and tertiary control is discussed. The crucial parameter for selection of power converters control, selection of L, LC and LCL filters, according to application is included. Moreover, depending on the operating modes i.e. Grid Connection Mode and Stand-Alone Mode the respective control strategies are compared for the better understanding along with requirement of synchronization to estimate several grid parameters to achieve accurate control of the active and reactive power delivered to the grid.

Keywords Current control · Filters · Phase locked loop (PLL) · Frequency locked loop (FLL) voltage oriented control (VOC) · Direct power control (DPC)

R. Jadeja (✉) · A. Ved · T. Trivedi · G. Khanduja
Marwadi University, Rajkot, India
e-mail: rajendrasinh.jadeja@marwadieducation.edu.in

A. Ved
e-mail: amit.ved@marwadieducation.edu.in

T. Trivedi
e-mail: tapankumar.trivedi@marwadieducation.edu.in

G. Khanduja
e-mail: luckykhanduja@gmail.com

N. Mahdavi Tabatabaei et al. (eds.), *Microgrid Architectures, Control and Protection Methods*, Power Systems,
https://doi.org/10.1007/978-3-030-23723-3_13

13.1 Introduction

AC microgrid has prime advantage of its compatibility with existing ac grid. Wind, small hydro power, biomass etc. and existing load are connected with existing grid without changing waveform. Over and above existing structure, knowledge of protection, control and standards majorly in the same way is applied to ac microgrid. Different types of power converters are required in microgrids for power flow control. DC sources like fuel cell, battery storage systems, solar PV and AC sources like wind and marine turbine use them for grid connection at given frequency or in grid isolated mode to supply local load. The control of a grid connected system depends on the different operating modes [1, 2]. Microgrid converters controlled with PWM [3] are used to connect Distributed Generation (DG) system to function in Grid Connection Mode, Stand-Alone Mode etc. [4].

From control point of view, converters are classified as grid forming, grid supporting and grid feeding converter. Simplified structure and detailed control schemes are discussed during the detailed discussion. Purpose of the inverter with dc source, is to export controllable power with establishment of voltage during grid connected mode while it ensures reference rated supply conditions while in grid isolated mode. Depending upon the operating mode of the microgrid, the control techniques like v-f control and *p-q* control is employed for standalone system and grid connected mode respectively. A precise synchronization algorithm is also required to estimate various grid parameters in context to achieve accurate control of the true power and reactive power supplied to the grid. Synchronization algorithm also influences the overall performance of the grid connected power converters [5–9]. An inner loop control of a converter uses different reference frames such as synchronous reference frame, stationary reference frame and natural transformation frame (with dq axis, αβ axis and abc axis respectively) [10]. The different control techniques for the AC microgrid is broadly categorized into communication based and non-communication-based techniques. The former ensures the closeness of frequency and magnitude of converter output voltage without additional control level while non-communication-based methods also known as droop control ensures voltage regulation and power sharing with absence of communication medium. The communication-based control further classified into (a) concentrated control, (b) master/slave control (c) distributed control, while droop-based control is classified as traditional droop control, virtual framework structure-based control and hybrid droop/signal injection control. Due to interconnection of different systems, hierarchical control becomes necessary to attain the optimum output from microgrid. The three main layers of hierarchical control are primary control, Microgrid supervisory control and grid supervisory control. Another control level is used at internal loop to achieve the source operating control.

DC-AC inverter or matrix converter requires filters for grid interface, in order to meet the grid code. The selection of filters that is L, LC, and LCL filter depends on application i.e. complication in design of control system to avoid the filter resonance, as the size and cost of the filter becomes very significant. Two popular topologies of the filter namely LC and LCL filters are elaborated [11, 12]. To synthesize the

commanded power by a converter, VOC and DPC methods are in use. VOC comprises of method of control with PI control, PR control, RC control and Predictive control, utilizes control loops in form of an external dc bus voltage loop and an internal current loop to accomplish quick unique reaction. Methods of DPC are Lookup table, Virtual flux, space vector modulation, Predictive control. Both methods are presented for the readers.

The sequence followed in chapter is: The Operating modes used for the microgrid are discussed in Sect. 13.2. To achieve precise inverter voltage control different reference frames control strategies including Synchronizing of power inverter by using PLL and FLL is elaborated in Sect. 13.3. The different control techniques useful to microgrids and its comparative analysis are included in Sect. 13.4. The choice of filters like L, LC and LCL is outlined in Sect. 13.5 VOC and DPC control strategies are discussed in Sects. 13.6 and 13.7 with additional reference [13–19].

13.2 Converter Configurations

Inverters are key component in AC microgrid, they control power flow from DER and Energy storage systems in grid connected and grid isolated modes. Microgenerators in AC Microgrid are non-dispatchable (PV, wind turbines whose output varies with time due to variation in atmospheric conditions) and dispatchable (Fuel cell and Diesel generator whose output is available at all time) [20–26]. Energy Management system controls Inverters in order to meet with demands by optimal operation of sources to reduce the cost and achieve desired power quality. Inverters in AC Microgrid regulates both (P & Q) power transferred to AC bus and also controls the connection of source to AC bus. Inverters in AC Microgrid is categorized into, (i) Grid following (Grid feeding) (ii) Grid forming and (iii) Grid supporting as per the function. Operating modes of converter configuration in AC Microgrid is given in Fig. 13.1 and Table 13.1.

13.2.1 Grid Following (Grid Feeding) Inverters

Converters are associated with non-dispatchable sources and they inject generated power into grid at unity power factor ($Q_{ref} = 0$). Such inverters inject power in ac bus by measuring grid voltage and injecting sinusoidal current at unity power factor. Such inverter is represented in form of constant current source in parallel with large impedance. The inverter behavior is same for grid connected and grid isolated mode and requires common control strategy. Current control methods are presented in literature for grid following inverters. Power control strategies like VOC represents converter as synchronous machine. Direct power control (DPC) methods are also

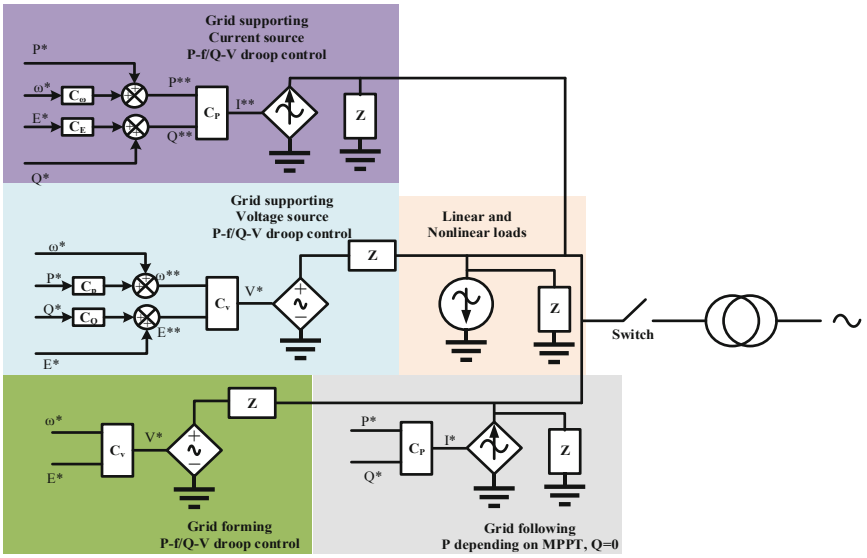

Fig. 13.1 Operating modes of converter configuration in AC microgrid

Table 13.1 Different operating conditions for converters in AC microgrids

Operating conditions	Functions	Control methods
Grid-feeding inverters	Power dispatch	Current control, voltage control, VOC, DPC
	Active/reactive power support	UPF control, +ve sequence control, constant P and Q power control
Grid-forming inverters	Voltage and frequency control	Hybrid AC V and I control, indirect I control, AC V control
	Load sharing	V and f droop-based control, active current sharing
Grid-supporting inverters	Maximum active power output	MPPT
	Q support	AC V control

suggested. Fault condition in utility grid or microgrid can cause ride through short grid disturbances or high voltage transients respectively.

13.2.2 Grid Forming Inverters

Various Energy storage devices (ESD) are chemical, Electrical and Mechanical based. Chemical based sources are batteries, hydrogen storage etc. Electrical

storage sources are in form of BESS and Ultra capacitors and Mechanical storage sources includes flywheels and system based on pneumatics and hydraulics. These energy storage sources use converters with objective to regulate P and Q injected to ac bus as well as improvement in power quality in grid connected mode while they generate or form the sinusoidal voltage for the bus in grid isolated mode. Grid forming converters are represented in form of controlled voltage source with low impedance in series. Inverters for ESD use droop control named as power-frequency/reactive power—voltage control in grid connected mode.

In islanded mode, f and V references are constant, droop controls active and reactive power to achieved desired parameters in magnitude and quality to maintain balance between supply and demand. Voltage controlled mode is used in grid isolated mode. When grid connected, active and reactive power is exchanged as per microgrid control, inverter acts as grid feeding inverter and in current control mode. Along with droop control active current sharing techniques are also essential for such inverters. In either mode ESD are charged and discharged making a bidirectional DC/DC converter necessary to be connected between ESD and inverter.

13.2.3 Grid Supporting Inverters

ESD has limited amount of energy, which may not be sufficient to maintain f and V of AC bus within desired limits in islanded mode. This requires additional dispatchable generators (Diesel or FC) or additional ESD along with grid forming inverters. These additional inverters connecting dispatchable source or additional ESD are termed as Grid supporting inverters. Grid supporting inverters have droop controls to serve purpose of maintaining power quality and are operated as controlled voltage source. In grid connected mode, grid supporting inverters are not used or may be added to system to improve power quality.

13.3 Synchronization of Power Converters in AC Microgrid Using PLL, FLL

RES/ESS connected to AC microgrid through converter interface needs precise synchronization algorithm to control output voltage waveform and parameters like voltage amplitude, frequency and phase angle so as to synchronize it with grid voltage in stable operation as well as when grid is under disturbances or under fault or under distorted voltage conditions. Grid faults in particular can cause high V_{dc} at dc link, over current and loss of synchronization [1]. Method used for synchronization should meet with grid codes (IEEE1547, IEEE 1588-2008, IEC1727, IEEE 929-2000). A synchronization approach should track and detect phase angle and frequency, should respond to grid changes and estimation of harmonics.

To meet with grid standard for synchronization, current injected should be pure sinusoidal and needs to be in phase with grid voltage. Transient minimization is necessary to avoid tripping of inverter. Distributed Generation systems of higher power have also requirements in terms of voltage support or reactive power injection capability and of frequency support or active power droop. Microgrid distributed generation systems have wider range of voltage and frequency and the estimated grid voltage parameters are often involved in control loops.

Various grid synchronization methods viz. Zero crossing detector (ZCD), Kalman filter, discrete Fourier transform (DFT), PLL (estimates phase angle), FLL (estimates frequency) etc. are presented in literature. PLL and FLL are widely used methods and are discussed in detail.

13.3.1 Phase Locked Loop

Phase locked loop (PLL) is oldest and widely used method for grid synchronization. Due to simplicity, accuracy speed, insensitivity to harmonics and disturbances, robustness etc., PLL is used for verity of applications including control of motors and heating applications, communication, instrumentation, power supplies etc. Basic PLL is shown in Fig. 13.2. Phase detector generates a voltage which is proportional to the phase difference in between input signal and a reference signal received from output. Loop filter which is eventually a 1st order low pass filter removes high frequency signal, output of loop filter is supplied to VCO, VCO generates a signal whose frequency is dependent of input voltage. Actual angle is tracked with reference till error angle is 0.

For tuning of PLL, assuming K_o and $K_m = 1$, then,

$$H_\varphi(s) = \frac{\varphi_{out}(s)}{\varphi_{in}(s)} = \frac{k_p s + \frac{k_p}{T_i}}{s^2 + k_p s + \frac{k_p}{T_i}} \tag{13.1}$$

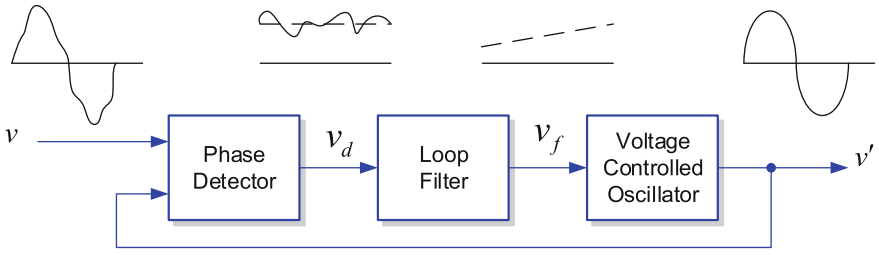

Fig. 13.2 Basic structure of PLL

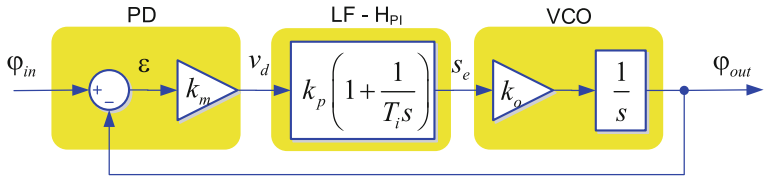

Fig. 13.3 Mathematical model of PLL

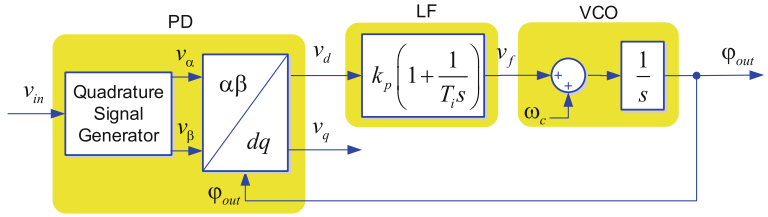

Fig. 13.4 SRF PLL

$$H_{\varphi}(s) = \frac{\varphi_{out}(s)}{\varphi_{in}(s)} = \frac{2\zeta\omega_n s + \omega_n^2}{s^2 + 2\zeta\omega_n s + \omega_n^2}$$
$$\omega_n = \sqrt{\frac{k_p}{T_i}}; \quad \xi = \frac{\sqrt{k_p T_i}}{2} \tag{13.2}$$

PLL is tuned as function of the damping and settling time (Fig. 13.3)

$$k_p = \frac{9.2}{t_s}; \quad T_i = \frac{t_s \xi^2}{2.3} \tag{13.3}$$

Various modifications in basic PLL is suggested in [7]. In suggested methods major difference is in application of PD block.

For 3-phase GCI, SRF-PLL is very popular due to its speed, simple structure and accurate estimation of phase or frequency. Here abc phase of Vin which is in abc frame is converted to dq frame. However, it performs poorly when there is unbalanced grid voltage or in presence of harmonics (Fig. 13.4).

A digital synchronizing PLL based on instantaneous real and imaginary power theory (PQ-PLL) maintains synchronization in presence of subharmonics, harmonics and negative phase sequence unbalance. DSF-PLL transforms both positive and negative sequence components into double synchronous frame and removes the detection error. This PLL has decoupling network to cancel out the double frequency oscillation. The PLL is also has its application for the grid condition having severe frequency and unbalanced conditions. SSI-PLL tracks utility voltage by extracting fundamental positive sequence, enabling it to wok under voltage distortion and unbalanced conditions.

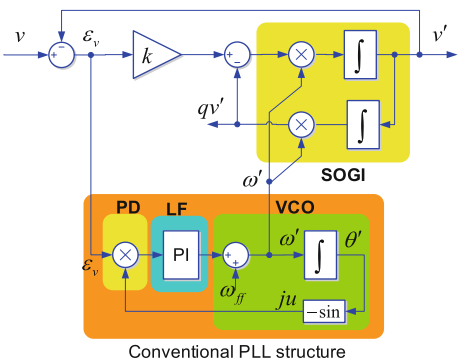

Fig. 13.5 SOGI-PLL

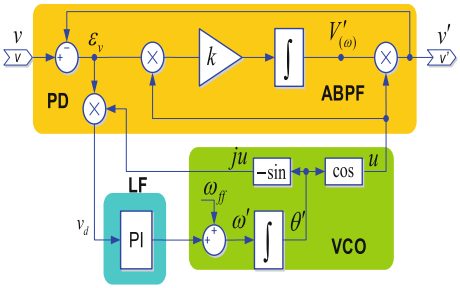

Fig. 13.6 Enhanced PLL

Second order generalized inverter (SOGI) PLL extracts fundamental positive sequence and uses SOGI to make quadrature signal generator to provide accurate positive sequence information for grid synchronization even under faulty condition (Fig. 13.5).

Enhanced PLL (Fig. 13.6) is frequency adaptive nonlinear synchronization approach. PD block allow higher flexibility and generates additional details such as amplitude and phase angle. The PLL provides higher degree of immunity and insensitivity to noise, harmonics and unbalance of input signal. It is very suitable for GCI in polluted and variable frequency environment.

13.3.2 Frequency Locked Loop (FLL)

PLL techniques are widely used for grid synchronization under balanced condition. However, under unbalanced grid voltage and in presence of nonlinear load where waveform is distorted, the response of PLL is poor. Frequency Locked Loop estimates frequency of input signal unlike phase angle determine by PLL. FLL are very less affected by transient conditions as frequency remains same but phase angle changes. PLL and FLL in structure are closely related but are not same. A PLL tracks phase angle only when frequency is same, hence it reduces frequency and phase angle

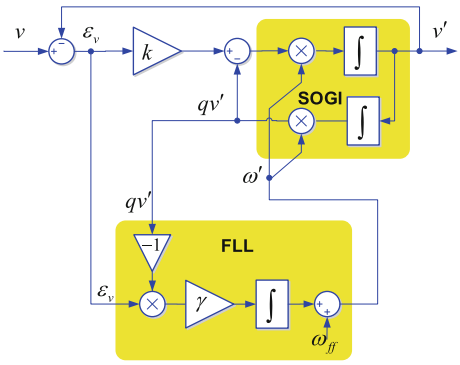

Fig. 13.7 SOGI based FLL

error to zero. An FLL tracks frequency and hence reduces phase angle error to zero. SOGI based FLL is shown in Fig. 13.7. SOGI acts as adaptive band pass filter having bandwidth dependent on gain k but independent of resonant frequency. SOGI generates two signals v' and qv' at phase difference of 90°. Output of comparator block in FLL is zero for frequency determined by SOGI resonant frequency, which keeps on shifting frequency values until locking occurs.

Other variations of FLL are reported in literature. DSOGI-FLL utilizes double adaptive filter even in presence of voltage sags. DSOGI-FLL is also used to control disconnection, reconnection and resynchronization in microgrid. MSOGI-FLL utilizes harmonic decoupling network, useful with nonlinear load,

13.4 Different Control Technique in Microgrid

A microgrid is envisaged to control power flow in between local generation, local load and grid through power electronic interface. Control system should act in either modes: grid connected and in grid isolated mode, also should act for seamless transfer from one mode of operation to the other. The principal objectives for microgrid control structure are aiming at:

i. Maintaining voltage and frequency parameters as desired under grid connected and grid isolated mode.
ii. Appropriate load management and efficient utilization of DG.
iii. Reconnection of MG with the main grid in synchronized condition.
iv. Accurate control of power between the MG and the grid.
v. Optimization for MG operating cost.
vi. Parameters optimization during switching between two modes.

A microgrid control system has multi-level control termed as hierarchical control includes tasks for control of power, grid parameter control, power quality improve-

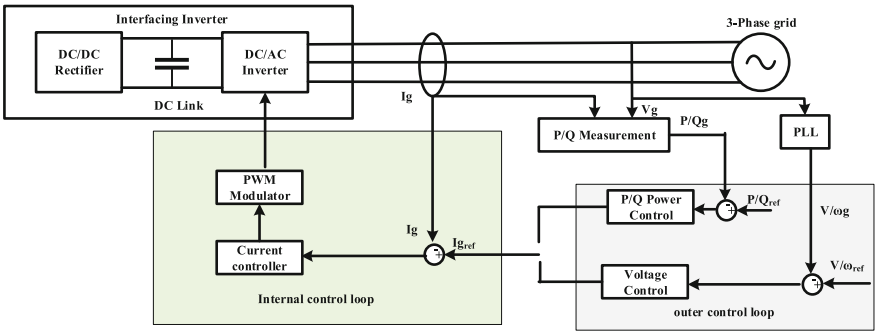

Fig. 13.8 Converter output control

ment, power balance, voltage and frequency control under fault or abnormal conditions.

Microgrid control levels are categorized as,

1. The converter output control: controls V_{out}, frequency and power.
2. The power sharing control: controls power management among DER and ESS.
3. The MG supervisory (Secondary) control: Control and regulates grid parameters.
4. The grid supervisory (Tertiary) control: Power/Energy management between main grid and the microgrid.

13.4.1 Converter Output Control

Converter in form of VSI are popular for RES/ESS. Typical converter control is given in Fig. 13.8. Internal loop generates current as required by grid and DER input, while outer loop control P/Q or regulates f/v depending on the grid connected or grid isolated mode. The brief information for inner loop control strategies are discussed in the subsequent section. Fuzzy, Neural network-based methods and other advanced control strategies are given in literature as part of internal loop control [17].

13.4.1.1 Proportional Integral (PI) Control

A Proportional Integral (PI) controller is many times used, along with synchronous reference frame transformation, by implementation of the transfer function as;

$$C_{PI}(s) = K_p + \frac{K_I}{s} \tag{13.4}$$

$$v_q^* = v_q + \omega L i_q + K_p * di_q + K_i \int di_q dt$$

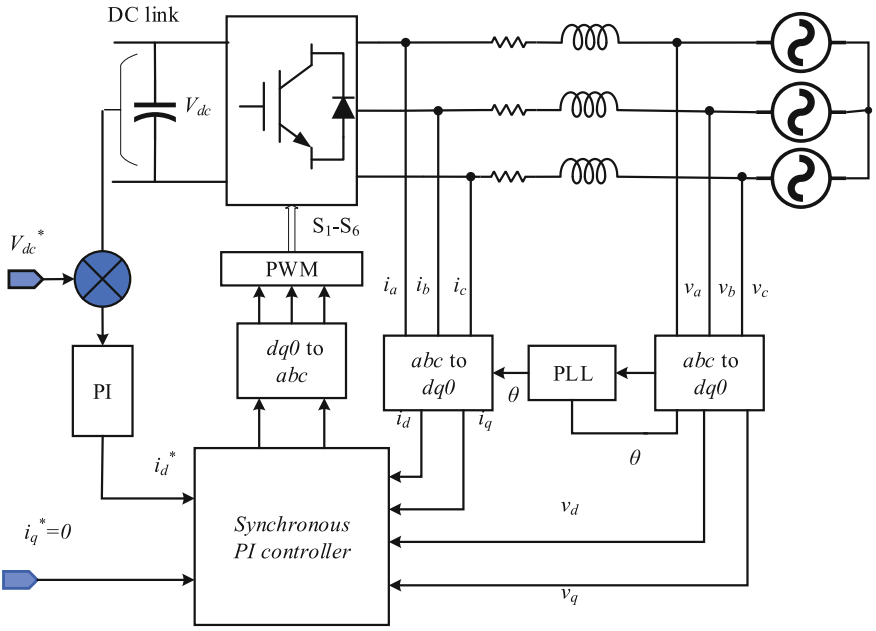

Fig. 13.9 PI control technique for grid connected converter

$$v_d^* = v_d - \omega L i_q + K_p * di_d + K_i \int di_d dt \tag{13.5}$$

where, $di_d = \left(i_d^* - i_d\right)$, $di_q = \left(i_q^* - i_q\right)$.

where K_p, K_i be proportional and integral gain for the transfer function and i_d^* is calculated by external voltage control loop. Since reactive power control is not possible i_q^* is taken zero. v_d^* and v_q^* are calculated from Eq. (13.5). Figure 13.9 shows block diagram representation and Fig. 13.10 shows dynamic response when I_d was changed in hardware.

PI controller has advantage of zero steady state error. The d-q frame supports in obtaining P & Q power flows in a network by direct controlling of I_d and I_q current components. The PI control approach with d-q transformation is not suitable for distorted conditions. Moreover, the implementation of PI controller in the d-q axis is comparatively difficult compared to Proportionate Resonant control in the stationary frame, as acquaintance of the synchronous frequency and phase are crucial for implementation.

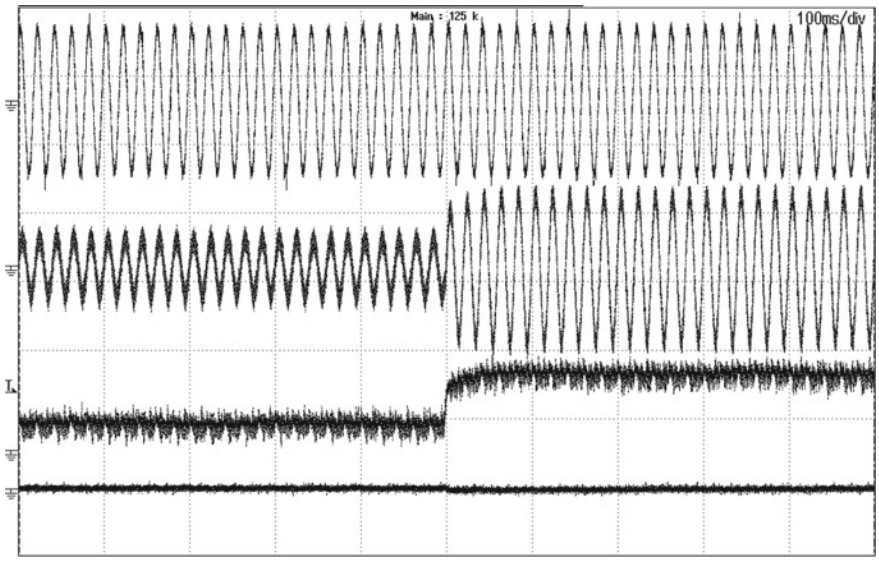

Fig. 13.10 Dynamic performance of PI controller (CH1—Voltage 100 V/div, CH2—Current 5 A/div, Ch-3 I_d 5 A/div, Ch-4 I_q 5 A/div)

13.4.1.2 Proportional Resonant (PR) Control

The principal advantage of a Proportionate Resonant controller is that it can be implemented in αβ reference frames (Fig. 13.11).

The controller helps at great extent to abolish the steady state error as it provides increased gain around the resonant frequency. The mathematical expression for PR controller is;

$$C_{PR}(s) = K_p + K_I \frac{s}{s^2 + \omega^2} \tag{13.6}$$

where, ω represents the resonant frequency. The performance of controller is achieved by adjusting the resonant frequency same as the network frequency. The relationship can be adjusted (attenuated) according to variation in grid parameters and subsequently to variation in grid frequency. The precise tuning of frequency and sensitivity of frequency variation is the major challenges for PR control method.

13.4.1.3 Repetitive Controller (RC)

The Repetitive Controller (RC) (Fig. 13.12) algorithm is a modest self-tuning control that removes the error in a dynamic system by using repetitive controller. The RC on the basis of error equation provides the series of pole pairs at multiple frequen-

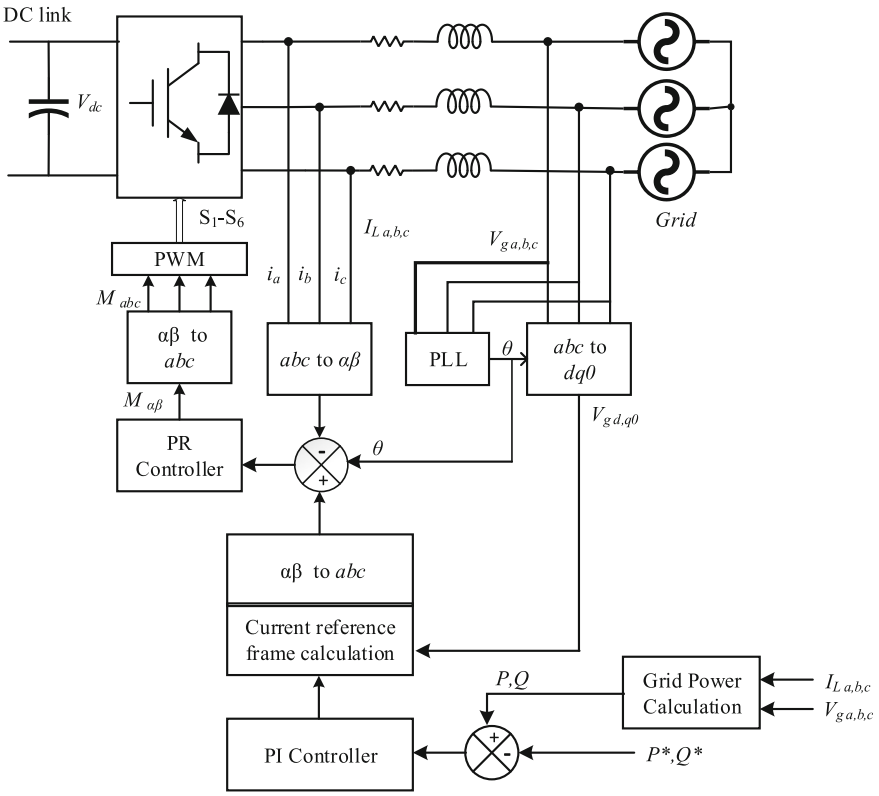

Fig. 13.11 PR control

cies. Moreover, the parallel grouping of an integral controller, PR and proportional controller are mathematically modelled to form repetitive controller. The Repetitive Controller has advantage of low *THD* in voltage and current due to presence of a low pass filter which attenuates higher harmonic peaks. The robustness of the controller remains the same in case of system having the large non-linear loads also. The narrated internal models can be controlled via either feed-forward or feedback control . Above three controllers are compared in Table 13.2.

13.4.1.4 Hysteresis Control (HC)

Hysteresis control methodology (Fig. 13.13) is one of the simplest method among the existing technique with the fast response. The control technique generates switching signal for each leg of an inverter when error between reference and measured value crosses certain band. Though the hysteresis control approach is easy to implement and having simple construction, has fast dynamic response and inbuilt current protection,

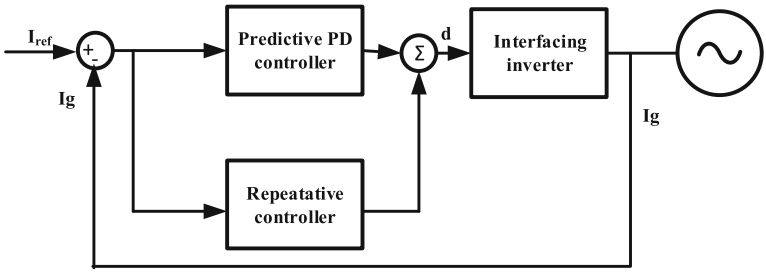

Fig. 13.12 Repetitive controller

Table 13.2 Comparison between PI, PR and RC controller

Parameter	Proportionate integral	Proportionate resonant	Repetitive controller
High gain	For lower frequencies	Near resonant frequencies	$X*f_1, f_1$ is fundamental frequency and X is integer
Steady state error elimination	High	High	High
Dynamic response	Good	Very good	Poor
Harmonic compensation	Bad	Bad	Better

the issue of controlling the current ripple in the output side and subsequently to reduce the total harmonic distortion (*THD*) is not satisfactory. At the same time variation in switching frequency makes design of output filter relatively complex.

13.4.1.5 H-Infinity (H∞) Control

The H-Infinity (H∞) control as shown in Fig. 13.14 is a robust control method. It has superior response under parameter variations and worst-case disturbances, as it looks at the control problem not based on control domain but as a mathematical optimization problem. The action of the controller is to reduce the disturbance effect on the output. The first step in this methodology is to express the problem in an optimization process, afterwards the controller is applied to resolve the problem. The advantages of the control technique include robust behavior under unbalance load condition, reduction in *THD* even in presence of non-linear load, easy execution in practice and reduction in tracking error. The need of perfect mathematics (complexity) and comparatively slow dynamic response and poor response to non-linear constraints like saturation are the major drawbacks of the H∞ controller. Though many methods are available for designing H∞ control, loop shaping method with mixed weighing applied to various signals is generally used.

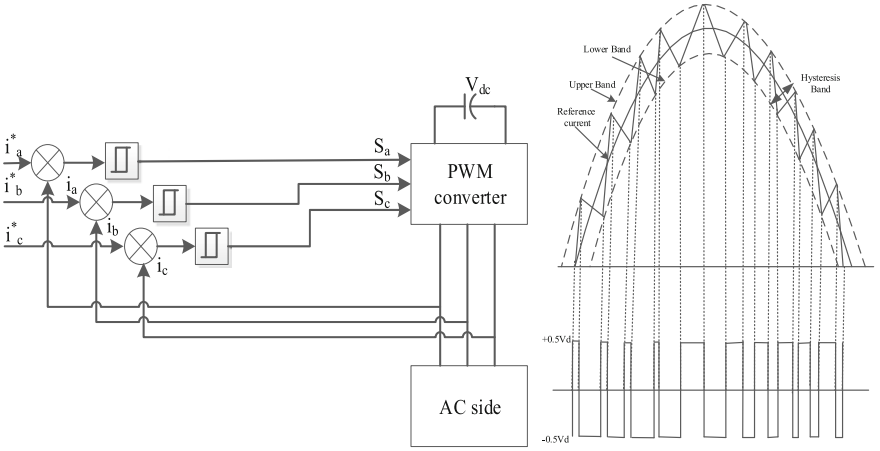

Fig. 13.13 Hysteresis current control and Hysteresis band

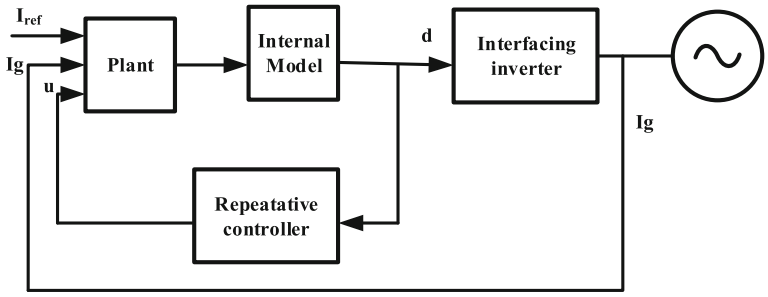

Fig. 13.14 H∞ control

13.4.2 Control Scheme for Power Converter in AC Microgrid for Power Sharing

The crucial characteristics of operation during the islanding mode of operation for ac microgrid (MG) includes load sharing among the inverters connected on common bus in proportionality and to maintain the stability in the context of voltage and frequency. The power electronics converters (PECs) play active role as interfacing device to synchronize the device with the network, as the generated power and frequency from the renewable energy sources are different than the parameters of the conventional power system. In power electronics converters, the voltage source inverters (VSIs) is the prime concluding contact point for the conversion process to yield ac voltage with tailoring grid requirements i.e. power output, frequency and voltage regulation. The DG units of a MG can be categorized in different categories as grid-forming i.e. voltage-controlled units, grid-following i.e. current controlled units and the grid-connected mode, which frequently controlled as grid-following inverters.

In grid connected mode, voltage and frequency of MG is adjusted to be grid synchronized. But, in grid isolated mode synchronizing signal is not available and hence operating point is decided by parallel VSI (prior to grid isolation, they were operated for current control which now will work in voltage control mode). A small difference of voltage or frequency produces high circulating current to flow in MG.

This necessitates accurate power sharing control enabling desired voltage and frequency setpoints for each inverter to be set according to power contribution made. Depending upon the communication links, the power sharing methods are classified as:

A. Communication based methods.
B. Non-communication-based methods.

13.4.2.1 Communication-Based Methods

The communication-based power sharing methods have separate communication system made up of controller, line etc. that controls grid voltage and frequency very accurately. The method is classified as concentrated control, Master-Slave method and distributed sharing method.

Concentrated control has centralized synchronizing signal and average current sharing reference. Since there is same phase angle and frequency, current error between output current and reference current acts as compensation of V_{ref}. The method provides good current sharing under all control conditions. The disadvantage is higher cost, high bandwidth requirement and reduced reliability.

One of another method, known as the master-slave methods where one inverter referred as the master and is responsible for voltage regulation and controls parallel operation by providing current reference whereas remaining are termed as slaves. No PLL required by slaves. The major drawback is slave and whole system can not work in the event of failure in master unit unless there is provision to switch master unit. The other issue is the poor transient response as master current is not taken care by control.

To overcome the deficiency of master-slave control, and to adaptively switch master inverter a distributed sharing method with distributor controller introduced. The distributed sharing method helps in achieving instantaneous current sharing for every inverter. Each inverter has its own control circuit avoiding central inverter. A current sharing bus provides same average reference current. As information in this method is shared locally, limited bandwidth is required.

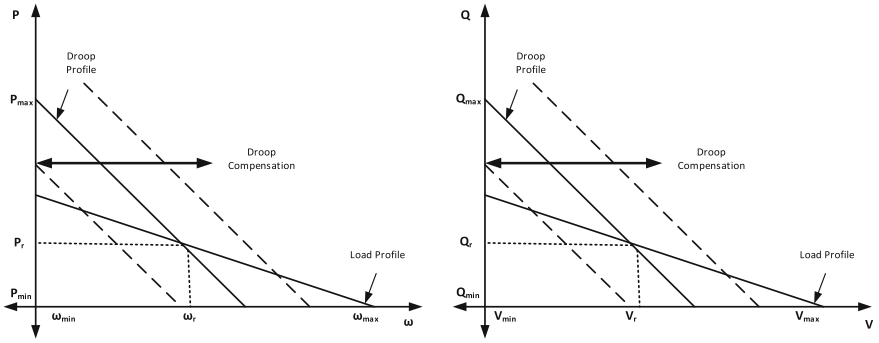

Fig. 13.15 Conventional P–ω and Q–V droop

13.4.2.2 Non-communication-Based Control

A. Droop Characteristics Based Techniques

The non-communication-based methods control power sharing between parallel inverters are based on droop control. These methods i.e. non-communication-based power sharing methods are often essential to connect the isolated inverter. The major advantage of power sharing without usage of communication leads to higher reliability, cost reduction and easier scalability. Moreover, expansion of system is provided by adjustable configuration feature that allows the substituting one unit (due to fault or for expansion) without interrupting the whole system. This is one of the reasons to avoid communication lines particularly for long distance, which involves higher cost.

Conventional Droop Technique:

Droop control is provided from the fact that increase in P will reduce δ, which will reduce f. Same way, increased Q reduces V. So, active power is function of $\delta_2 - \delta_1$ and reactive power is function of $(V_2 - V_1)$. The method considers impedance of inverter to be 0 lagging. Decoupled P/Q is expressed in terms of inverter output parameters

$$\begin{aligned} \omega_i &= \omega_r - M_p(P - \mathrm{P}_r) \\ V_i &= V_r - M_q(Q - Q_r) \\ M_p = \frac{\Delta\omega}{P - P_{\max}}, M_q &= \frac{\Delta V}{Q - Q_{\max}} \end{aligned} \tag{13.7}$$

where, ω_r, V_r, P_r and Q_r are reference values, and ω_i, V, P and Q are inverter output parameters.

Equation (13.7) represents the concept of P-ω and Q-V droop controllers depicted in Fig. 13.15, droop slopes M_P and M_Q is calculated in reference to stipulated MG V/f

changes, and the actual active/VAR power capacity of each DER. Though having the several advantages, droop-based techniques suffers from some disadvantages like; effect of variation in reactance to resistance ratio in inverter output, poor sharing of power under unbalance load, non-linear loads etc.

To overcome drawbacks mentioned, improved droop methods are suggested as.

1. conventional and variants of droop control,
2. virtual structure-based methods,
3. construct and compensate-based methods,
4. hybrid droop/signal-injection-based methods,

VPD/FQB Method:

Conventional droop method is best suited for inductive feeder. LV feeders are considered as resistive one. The voltage active power droop and frequency reactive power boost (VPD/FQB) method overcome the problem of convention droop method while implementation on MG, for feeders that have unity power factor impedance in nature. The control technique highly depends on the system parameter providing restriction to application. The increment in active power along with the voltage variation ($E - V_{com}$) can be expressed as:

$$\begin{aligned} P &\approx \frac{V_{com}E - V_{com}^2}{z} \\ Q &\approx -\frac{V_{com}E}{Z}\varphi \end{aligned} \tag{13.8}$$

VPD/QFB characteristics are taken as

$$\begin{aligned} \omega_i &= \omega_{rated} + m_Q \cdot Q_i \\ E_i &= E_{rated} + n_P \cdot P_i \end{aligned} \tag{13.9}$$

Dependency on system parameters and impaired sharing of active load current makes the method applicable only for limited situations.

Complex Line Impedance-Based Droop Method:

The method removes Z_{line} dependency and slow transient response by simplifying coupling relationship of active and reactive power majorly when the Z_{line} with $X \approx R$ in Mid Voltage microgrids. A P–Q–V droop method allows simultaneous control of active and reactive power and also controls voltage at PCC. A look up table adjusts droop coefficient.

For the said condition the droop function with slope S_P, S_Q can be obtained as:

$$\begin{aligned} \omega_i &= \omega_0 - S_P \cdot (P - Q) \\ E_i &= E_0 + S_Q \cdot (P + Q) \end{aligned} \tag{13.10}$$

Angle Droop Control

Phase of DER Source voltage in relation to common timing reference maintained throughout system is set, resulting into distribution of power requirement among DG. The same mathematically can be expressed as:

$$\begin{aligned} \delta_i &= \delta_r - m_P \cdot (P_i - P_{i,r}) \\ E_i &= E_r - m_Q \cdot (Q_i - Q_{i,r}) \end{aligned} \tag{13.11}$$

where, δ_r and E_r are the angle and voltage magnitude of DG at their power level $Q_{i,r}$ and $P_{i,r}$ respectively. The active and reactive power droop gains are indicated by m_P and m_Q respectively, chosen in such a way that their load sharing is in proportion to the rating. To apply this control method, it becomes essential to synchronize local boards, failing to which system stability is at risk.

Voltage-Based Droop Control:

Issues with DER is they do not have inertia, have resistive line and large no of DG which are not controllable in compare to central generating system. The control method works with all above constraints on constant power band control strategy for islanding MG without intercommunication. The data of MG characteristics controlled by two droop controllers V_g/V_{dc} and P/V_g droops and both are part of P/V droop controller.

In-case of unbalance between generation and the demand, the V_{dc} deviate that will work as an indicator for to change in ac power in accordance for V_g/V_{dc} droop. The same can be expressed as:

$$V_g^* = V_{ac,\,nominal} + m \cdot (V_{dc} - V_{dc,\,nominal}) \tag{13.12}$$

A minor change in V_g will lead to change of power delivery. To bound ac side voltage within limits, P_{dc}/V_g droop is used. The mathematical expression for the same is:

$$P_{dc} = \begin{cases} P_{dc,nominal} - K_P \cdot (V_g - (1+w) \cdot V_{g,nominal} \\ for,\, V_g \rangle (1+w) V_{g,nominal} \\ P_{dc,nominal} \\ \text{for,} (1-w) V_{g,nominal} \langle V_g \langle (1+w) V_{g,nominal} \\ P_{dc,nominal} - K_P \cdot (V_g - (1+w) \cdot V_{g,nominal} \\ \text{for,}\, V \langle (1+w) V_{g,nominal} \end{cases} \tag{13.13}$$

where, w is width of band, V_g/V_{dc} droop control used along with P/V_g droops in order to take advantage of both methods. Here we get an advantage of controlling MG voltage by detecting variation in V_{dc} without affecting P_{dc}. Method is most suitable for DER as it allows maximum variation in voltage by MPPT tracking. Multistage controllers are required which may affect efficiency of system.

B. Virtual Structure Based Techniques

Virtual Output Impedance Loop

Coupling between active and reactive power is avoided by implementation of fast loop control using droop control in the virtual output impedance method. The reference voltage is given in terms of virtual output impedance ($Z_D(s)$) as:

$$V_{ref} = V^* - Z_D(s) \cdot i_0 \tag{13.14}$$

By controlling $Z_D(s)$, current spikes are avoided when DER is connected to MG. the method also provide soft starting, improvement of system stability and harmonic current sharing.

Enhanced Virtual Impedance Loop

Due to nonlinear loads, the major problem with islanding mode of operation is pertaining to power quality. A method similar to above, but producing virtual impedance at fundamental and selected harmonic frequency is used. Method provides superior reactive power and harmonic sharing, reducing harmonic impedance at PCC, at reduced computing for local DER controller.

Virtual Frame Transformation Method

Virtual frame transformation method, utilizes virtual frequency/voltage (ω'/E') frame for power sharing control. Advantage being decoupling of active and reactive power flow and improved stability. The bus power is articulated as:

$$\begin{cases} P_i \cong \dfrac{V}{Z}[(E_i - V)\cos\theta + E_i\varphi\sin\theta] \\ Q_i \cong \dfrac{V}{Z}[(E_i - V)\sin\theta + E_i\varphi\cos\theta] \end{cases} \tag{13.15}$$

Impedance is given as $Z\angle\theta$ and The φ is the phase angle between E and V. Power terms are modified by orthogonal linear rotational transformation matrix T

$$\begin{bmatrix} P' \\ Q' \end{bmatrix} = T_{PQ} \cdot \begin{bmatrix} P \\ Q \end{bmatrix} = \begin{bmatrix} \sin\theta & -\cos\theta \\ \cos\theta & \sin\theta \end{bmatrix} \cdot \begin{bmatrix} P \\ Q \end{bmatrix} \tag{13.16}$$

Similarly, the virtual voltage and frequency frame transformation ($\omega' - E'$) depicted as

$$\begin{bmatrix} \omega' \\ E' \end{bmatrix} = T_{\omega E} \cdot \begin{bmatrix} \omega \\ E \end{bmatrix} = \begin{bmatrix} \sin\varphi & -\cos\varphi \\ \cos\varphi & -\sin\varphi \end{bmatrix} \cdot \begin{bmatrix} \omega \\ E \end{bmatrix} \tag{13.17}$$

In the above equation ω and E are calculated from conventional droop method.

C. **Construction and Compensation Based Techniques**

Adaptive Voltage Droop Control

Construction and compensation-based techniques are proposed to facilitate parallel operation among DER in grid isolated mode. Conventional control helps to construct the voltage drop among line to be compensated and construct for improving system stability and improved reactive power sharing in the presence of extreme load. Let two DER connected by individual line to share a load. Voltage of one DER is given as

$$V_i = E_i^* - D_{Qi}Q_i - \frac{r_i P_i}{E_i^*} - \frac{x_i Q_i}{E_i^*} \tag{13.18}$$

The above equation that be considered under any condition by considering the method that uses D_{Qi}, m_{Qi}, and m_{Pi} are droop coefficients. The same can be represented as:

$$\begin{cases} E_i = E_i^* - D_i(P_i Q_i) \cdot Q_i + \left(\dfrac{r_i P_i}{E_i^*} + \dfrac{x_i Q_i}{E_i^*} \right) \\ D_i(P_i Q_i) = DQ_i + m_{Qi} Q_i^2 + m_{Pi} P_i^2 \end{cases} \tag{13.19}$$

Limitation of method is by knowhow of power line parameters. Errors may produce positive feedback making system unstable.

Synchronized Reactive Power Compensation Method (SRPCM)

SRPCM aims to improve accuracy of reactive power sharing. A central converter activates low bandwidth sync signal. This activates injection of active power disturbance and estimation of Q error. Control strategy uses conventional droop method in step-1 and Q error is compensated in step-2 Limitation being requirement of central converter for providing sync signal.

Droop Control-Based Synchronized Operation

The robust power sharing method employs Operations related to error reduction and voltage recovery. If sharing error is reduced, sharing accuracy be improved. A low bandwidth sync signal is used. A voltage recovery operation is needed to compensate the output voltage decrement caused by error reduction operation. This also results in plug and play operation with simple communication requirement. The improved droop control in mathematical terms is represented in form of

$$E_i(t) = E^* - n_i Q_i(t) - \sum_{n=1}^{ts-1} K_i Q_i^n + \sum_{n=1}^{ts} G^n \Delta E \tag{13.20}$$

where, t_s times of synchronization even up to t.

D. **Hybrid Droop/Signal-Injection-Based Technique**

Conventional droop control cannot ensure a constant voltage and frequency, neither an exact power sharing. But an advantage of the control can avoid communication among the DGs. Communication-based control is a simple and stable strategy providing a good current sharing, yet a low reliability and redundancy. Therefore, to take advantage of their individual advantages, a hybrid scheme combining two control methods is vital. The sharing of real and reactive powers between the DGs is easily implemented by two independent control variables: (1) power angle and (2) voltage amplitude. Signal injection method appropriately controls the reactive power sharing and is not sensitive to variations in the line impedances. This method is also adequate for linear and nonlinear loads but at the same time the assurance for the voltage regulation is discourage part for the method.

Common Variable Based Control Method

True and reactive power sharing considers common variable as key. As output interface inductor is different in MG, Q sharing is not exactly possible. The strategy adopted regulates common bus voltage by an I controller. If Common bus voltage and reference voltage for each DER is set to same value, Reactive power will be same for all DER. The method requires load voltage information, which is tough for far distant DER from common bus. Common Bus availability is impaired in complex MG configuration or in system having dispersed load.

Q–V Dot Droop

The method relates reactive power Q with rate of change of voltage to improve reactive power sharing. The method is found to compensate for inverter parameter variation and Z_{line} disturbances. A Q–V dot droop technique is used to share harmonic load and reactive power. Issues of poor voltage regulation, complexity, poor power quality and impaired stability are the challenges with the method.

AC microgrid control methods are abridged in Table 13.3.

13.4.3 Supervisory Control

Task of ensuring reliability and economic Supervisory control of Microgrid operation is taken care by supervisory control.

13.4.3.1 MG Supervisory Control (MG SC) Level (Secondary Level)

The MG SC controllers have following types:

1. Decentralized controllers realized using local parameters
2. Centralized controllers with communication links.

Table 13.3 Comparison of control methods for AC MG

Control level	Sharing method	Transient sharing	Steady-state sharing	Reliability	Expandability	Parameter sensitivity	Regulation capability
Active and reactive power sharing	Centralized	3	3	1	1	1	3
	Master/slave	1	3	2	1	2	2
	Distributed network	2	3	1	1	1	3
	Conventional droop	1	2	3	3	2	1
	P–V, Q–ω droop	1	3	3	3	3	1
	Virtual; output impedance droop	2	3	2	2	1	2
	Adaptive droop	3	3	3	2	3	3
	Enhanced voltage droop	3	3	2	2	1	3

1—Poor/low; 2—medium; 3—good/high

The simultaneous power sharing and regulation of parameter cannot be achieved in conventional droop control because of internal conflicts. The same leads to deviation in voltage and frequency regulation achievement during the load changing. The robust droop controller is one of the controls strategies to achieve the transient characteristics of droop controller to resolve the haring issue and also taking care of regulation parameters. One another method is distributed network control implement distributed secondary controllers to reestablish regulation parameters in absence of centralized system.

The centralized controller requires a main controller and high bandwidth communication to collect and record the data, that control signals for converter controllers. The signals ensure the reliable functioning of MG with considered the economic consideration. A central controller provides the reliability as part of hierarchical control system.

13.4.3.2 Grid Supervisory Control Level (Tertiary Level)

Tertiary control or grid supervisory control provides frequency and voltage setpoints for microgrid control (Secondary control) as desired by grid. It interacts with grid operators and other Microgrid tertiary controller to achieve desired settings of voltage/frequency and active/reactive power.

13.5 Control of Grid Connected Converter with L, LC and LCL Filters

High frequency switching PWM of converters produces significant harmonics in output. To reduce harmonics and to get desired voltage and current waveform, a grid filter is used (Fig. 13.16). However, care is required to be taken to avoid oscillations in the system.

L filter is 1st order filter with inductor in series with grid. It has simple design and also avoids resonance. The size of inductor for current harmonic attenuation is very high. It has attenuation of 20 dB/decade and is suitable for high frequency PWM.

$$f_r = \frac{1}{2\pi\sqrt{LC}}\,,\; P_a = \frac{3V_g}{X_L}\sqrt{V_I^2 - V_g^2} \tag{13.21}$$

Output power increases as L decreases. If L cannot reduce harmonics, higher switching frequency is to be used.

LC filter has second order. It has gain of −12 dB/octave. When grid connected, LC filter is prone to have issue of resonance. LCL filter, a 3rd order control system, provides an attenuation of 60 dB/decade and gives better decoupling and lower current ripple. Dynamic control is obviously more complicated. As additional poles and zeros can lead to instability in control, active and passive damping is employed. Active damping utilizes an independent control mechanism based on real time measurement or estimated value wile passive damping requires additional components.

13.6 Voltage Oriented Control (VOC) of Grid Connected Converter

The method is derived from field-oriented control applied for IM control. Voltage Oriented Control(VOC) is based on rotating frame where true power P and reactive power Q are controlled by a current controller. VOC has d-axis directed to grid space. VOC provides high steady state and dynamic performance based on current control loop. VFVOC has d-axis towards virtual flux calculated by integrating grid voltage component in time.

Advantage of VOC with respect to DPC is low resolution ADC required due to reduced sampling frequency and fixed switching frequency makes filter design

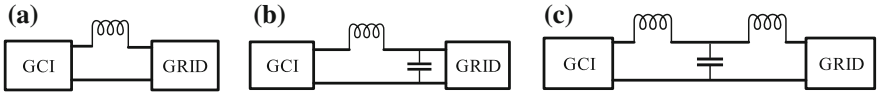

Fig. 13.16 Configuration of filters, **a** L type, **b** LC type, **c** LCL type

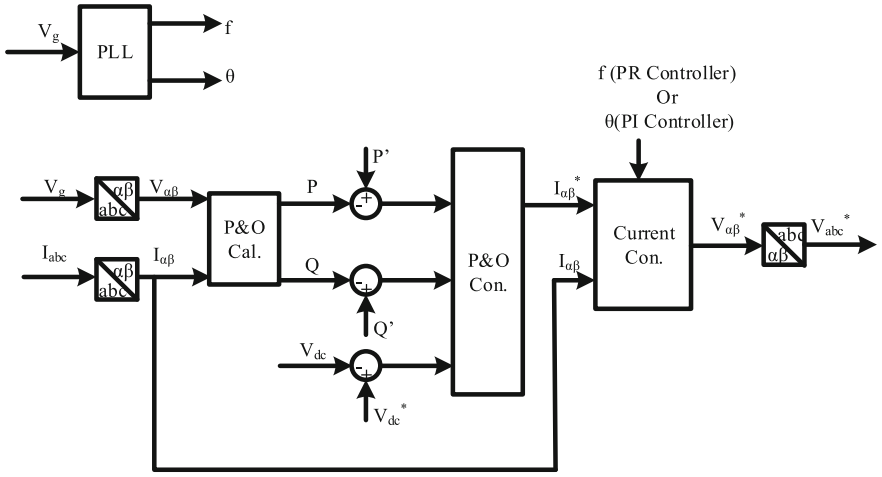

Fig. 13.17 A general scheme for VOC system

simple. However, αβ to dq conversion and PI controller is must. A typical block diagram representation is shown in Fig. 13.17.

13.7 Direct Power Control (DPC) of Grid Connected Converter

Direct Power Control (DPC) is widely used because of its faster-dynamic performance and easy control implementation for control of power flow from an inverter to grid. DPC provides total control over active and reactive power without employing PWM or internal current control. Basic DPC block diagram is given in Fig. 13.18. *P–I* and sectors are calculated from I_{ac} and U_{ac} phasors, from switching table firing pulses are calculated.

DPC in basic structure utilizes L on grid side $L_{gi.}$ which is sufficient for high frequency applications. For large power applications, low switching frequency is used and hence LCL filter is employed to reduce level of harmonics. The LCL filter has disadvantage of causing distortion under both conditions in current in the event of resonance. In DPC switching harmonic spectrum is wide due to variable switching frequency. Switching states should be selected through switching table in such a way that damping of harmonics can be done. DPC algorithm should select correct switching state and quickly estimate active and reactive powers. Improvements in DPC includes application of switching table, estimation of *P* and *Q* by using virtual flux estimation etc.

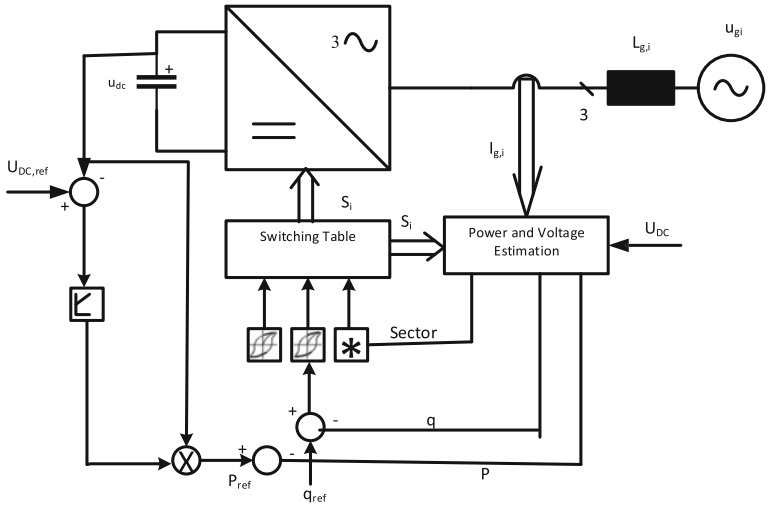

Fig. 13.18 DPC block diagram

13.8 Conclusion

AC microgrid has direct relevance to existing grid and type of load. However Renewable energy sources and energy storage systems which generates dc or even ac requires an converter interface for difference in waveform, magnitude and frequency. So, controlling converter is a tedious task. PLL and FLL provides synchronization signal for grid connection. Many methods are available for controlling different level of microgrid. Chapter has given outline for converter output control, power sharing control, supervisory control and tertiary control. Selection of filter and its parameters adds to complexity. Power control methods are introduced at the end of chapter for reader to get an overview of control methods for AC Microgrid.

References

1. N. Jaalam, N. Rahim, A. Bakar, C. Tan, A.M. Haidar, A comprehensive review of synchronization methods for grid-connected converters of renewable energy source. Renew. Sustain. Energy Rev. **59**, 1471–1481 (2016)
2. P. Borazjani, N.I.A. Wahab, H.B. Hizam, A.B.C. Soh, A review on microgrid control techniques, in *IEEE Innovative Smart Grid Technologies-Asia (ISGT Asia)* (2014)
3. R. Jadeja, A. Ved, S. Chauhan, An investigation on the performance of random PWM controlled converters. Eng. Technol. Appl. Sci. Res. **5**(6), 876–884 (2015)
4. A. Bidram, V. Nasirian, A. Davoudi, F.L. Lewis, Control and modeling of microgrids, in *Cooperative synchronization in distributed microgrid control* (Springer, 2017)
5. E. Papaioannou, E. Bassi, P.G.P. Incremona, Comparison between several control methods, for connecting distributed generation units to the electrical grid. Master Thesis, Aristotle University

of Thessaloniki, Greece (2017)
6. S.M. Kaviri, M. Pahlevani, P. Jain, A. Bakhshai, A review of AC microgrid control methods, in *IEEE 8th International Symposium on Power Electronics for Distributed Generation Systems (PEDG)* (2017)
7. X.Q. Guo, W.Y. Wu, H.R. Gu, Phase locked loop and synchronization methods for grid-interfaced converters: a review. Electrotechn. Rev. **87**(4), 182–187 (2011)
8. E. Kabalci, Design and analysis of a hybrid renewable energy plant with solar and wind power. Energy Convers. Manag. **72**, 51–59 (2013)
9. Y. Zhou, C.N.M. Ho, A review on microgrid architectures and control methods, in *IEEE 8th International Power Electronics and Motion Control Conference (IPEMC-ECCE Asia)*, 2016
10. X. Wang, J.M. Guerrero, Z. Chen, Control of grid interactive AC microgrids, in *IEEE International Symposium on Industrial Electronics (ISIE)*, 2010
11. X. Wang, J.M. Guerrero, F. Blaabjerg, Z. Chen, A review of power electronics based microgrids. J. Power Electron. **12**(1), 181–192 (2012)
12. T.A. Trivedi, R. Jadeja, P. Bhatt, A review on direct power control for applications to grid connected PWM converters. Eng. Technol. Appl. Sci. Res. **5**(4), 841–849 (2015)
13. N. Mahdavi Tabatabaei, A. Jafari Aghbolaghi, N. Bizon, F. Blaabjerg, in *Reactive power control in AC power systems: fundamentals and current issues* (Springer, 2017)
14. K. Rajesh, S. Dash, R. Rajagopal, R. Sridhar, A review on control of AC microgrid. Renew. Sustain. Energy Rev. **71**, 814–819 (2017)
15. M. Malinowski, M.P. Kazmierkowski, A.M. Trzynadlowski, A comparative study of control techniques for PWM rectifiers in AC adjustable speed drives. IEEE Trans. Power Electron. **18**(6), 1390–1396 (2003)
16. H. Li, J. Zhao, X. Yang, Mathematical model of grid-connected inverter system in weak grid. Electron. Lett. **51**(23), 1922–1924 (2015)
17. M. Jamil, B. Hussain, M. Abu Sara, R. Boltryk, S. Sharkh, Microgrid power electronic converters: state of the art and future challenges. in *IEEE the 44th International Universities Power Engineering Conference (UPEC)* (2009)
18. M.A. Hossain, H.R. Pota, W. Issa, M.J. Hossain, Overview of AC microgrid controls with inverter-interfaced generations. Energies **10**(9), 1300 (2017)
19. H. Han, X. Hou, J. Yang, J. Wu, M. Su, J.M. Guerrero, Review of power sharing control strategies for islanding operation of AC microgrids. IEEE Trans. Smart Grid **7**(1), 200–215 (2016)
20. J.M. Guerrero, P.C. Loh, T.L. Lee, M. Chandorkar, Advanced control architectures for intelligent microgrids—part II: power quality, energy storage, and AC/DC microgrids. IEEE Trans. Industr. Electron. **60**(4), 1263–1270 (2013)
21. J.M. Guerrero, M. Chandorkar, T.L. Lee, P.C. Loh, Advanced control architectures for intelligent microgrids—part I: decentralized and hierarchical control. IEEE Trans. Industr. Electron. **60**(4), 1254–1262 (2013)
22. S. Eren, M. Pahlevaninezhad, A. Bakhshai, P.K. Jain, Composite nonlinear feedback control and stability analysis of a grid-connected voltage source inverter with LCL filter. IEEE Trans. Industr. Electron. **60**(11), 5059–5074 (2013)
23. S. Eren, M. Pahlevani, A. Bakhshai, P. Jain, A digital current control technique for grid-connected AC/DC converters used for energy storage systems. IEEE Trans. Power Electron. **32**(5), 3970–3988 (2017)
24. I. Colak, E. Kabalci, G. Fulli, S. Lazarou, A survey on the contributions of power electronics to smart grid systems. Renew. Sustain. Energy Rev. **47**, 562–579 (2015)
25. N. Bizon, N. Mahdavi Tabatabaei, H. Shayeghi, in *Analysis, control and optimal operations in hybrid power systems: advanced techniques and applications for linear and nonlinear systems* (Springer, 2013)
26. N. Bizon, M. Oproescu, M. Raceanu, Efficient energy control strategies for a standalone renewable/fuel cell hybrid power source. s **90**, 93–110 (2015)

Chapter 14
DC Microgrid Control

Marian Gaiceanu, Iulian Nicusor Arama and Iulian Ghenea

Abstract The current challenges of the current power system are to face-up with the integration of the increased renewable energy sources, energy storage systems, access to the energy market in an optimal manner, reconfiguration under faults using microgrid concept, being capable to assure more flexibility, and stability, through advanced control. The chapter makes a modern introduction into the DC microgrid architectures and their control. As the most used control into the DC microgrids, the hierarchical control is presented. In order to guide the readers, the most used standards related to DC microgrids are presented. As case study, the advanced control of the utility converter has been developed and simulated in Matlab/Simulink. Nowadays, the security protection of the energy network is a concern. An introduction to cyber-physical system (CPS) related to the power system field is presented.

Keywords Microgrid · Control · Cyber-physical system · Standards · Distributed · Security protection

14.1 Introduction

The evolution of the power delivery networks supposes the transition from the centralised control to the microgrids control. The introducing of the microgrids offers the flexibility, the autonomy of power supply, increased dynamical response due

M. Gaiceanu (✉) · I. N. Arama
Department of Automation and Electrical Engineering, Dunarea de Jos University of Galati, Galati, Romania
e-mail: marian.gaiceanu@ugal.ro

I. N. Arama
e-mail: iulian.arama@ugal.ro

I. Ghenea
Doctoral School of Fundamental and Engineering Sciences, Dunarea de Jos University of Galati, Galati, Romania
e-mail: gheneaiulian@yahoo.com

N. Mahdavi Tabatabaei et al. (eds.), *Microgrid Architectures, Control and Protection Methods*, Power Systems,
https://doi.org/10.1007/978-3-030-23723-3_14

to the power electronics interfaces. For the transmission and distribution systems, depending on the nature of the load, and to the choose energy way the types of the microgrids are as following: DC, AC and hybrid DC and AC-coupled.

The distributed energy system (DES) is the main component of the microgrid architecture. Besides DES, the microgrid contains the energy storage system (ESS), and loads (linear or/and nonlinear). Distributed energy systems are based on photovoltaic panels, wind turbines, hydro turbine, fuel cell, micro-CHP, biomass, Stirling engines so on. Thus, the microgrid architecture enables the integration of renewable sources, fossil fuels and biofuels. The storage system has the role of balancing (stability) power fluctuations from renewable energy sources. The storage system is sized so that it can feed most of its loads autonomously for a certain amount of time. The main storage systems are batteries, super capacitors, flywheels, compressed air, thermal, pumped hydro.

The structure of this chapter is as follows: overview Section, followed by the current state of microgrids control architectures Section; the hierarchical control is very specific to the microgrid; the specific standards are mentioned in the dedicated Section; as case study, the robust state-feedback (SF) control of the DC microgrid has been employed. For the modern microgrids, the Cyber-Physical System is presented. The chapter ends with the Reference Section.

14.2 Overview

The microgrids include the important environmental, technical and economic benefits through increased energy efficiency and reduced CO_2 emissions, being considered as safe power source.

The load into a microgrid is variable. Therefore, the microgrid will have to distribute energy in a balanced way (without overload), ensuring the stability and continuity of the energy supply (increasing the quality of services).

The main types of the DC microgrids control architectures are classified as follows: centralized, decentralized and distributed [1]. All DC Power Systems (PSs) are not facing problems such in AC PSs. Therefore, the reactive power control, frequency issues as stability and synchronization are disappeared in DC PSs [2]. Taken into consideration the above mentioned advantages, the DC PSs are very attractive. The PSs are vulnerable to natural disasters, being exposed to the blackouts. The microgrids are the solutions to reduce the risk of blackouts, are friendly environment, increase the energy efficiency, and integrate the renewable energy sources.

14.3 Architectures of the DC Microgrids

In an energy system, generator control and economic energy delivery can be achieved through a centralized method (Fig. 14.1) [3]. Through this method, in order to process the data, the central controller receives all the information from the entire system. The Supervisory, control and data acquisition system (SCADA) will send the control signals from each agent. This advanced automation control system manages the control, acquisition and monitoring of the operation of the power supply system [4]. Each agent will use a bidirectional communication channel to transfer data to the central computer system. This control architecture is disadvantageous for systems with high number of agents. The centralized structure is not reliable, economical, and inflexible. The simplicity of control and the economic delivery of energy are the main advantages. To make a decision on the entire centralized system, the system uses global information.

As mentioned above, the decentralized method is a control way of the microgrid. In this control type a particular agent or sub-system self-regulates, which means that in order to gain more market profit and more stability, the individual agent decides the actions based on data (voltage, frequency) taken locally [5].

The decentralized method has no communication links; it does not send information to agents. The method consists in controlling the sources from the data obtained on the basis of local measurements (voltage, frequency). However, it is based on some agents, called leader agents, who receive and send information. The method does not ensure global stability and optimization, but only local (even if the link with some leading agents is lost, stable microgrid remains). Advantages include the protection of agents' data, ensuring system stability. Instantaneous power can be balanced between sources connected in parallel in both DC and alternating currents (AC) with this control strategy. In DC power microgrids, the power balance of parallel connected, decentralized output sources is implemented using voltage drop control [6–8]. With regard to power management within microgrids with energy stor-

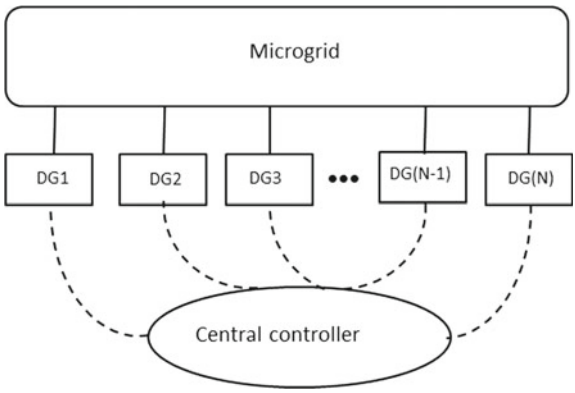

Fig. 14.1 Centralized control

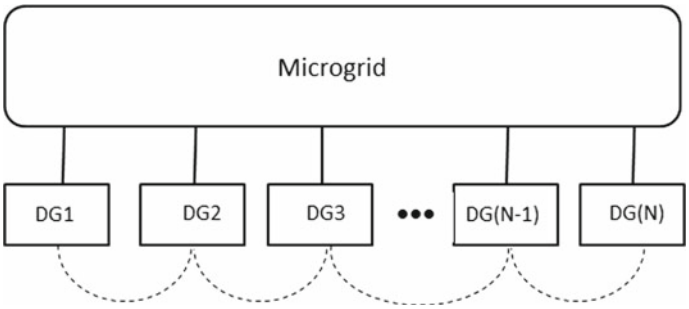

Fig. 14.2 Decentralized control

age elements, if the loads exceed the maximum system power, the storage system is discharged. The storage system is charged when there is extra energy from sources.

As agent a generator, a consumer, or a microgrid could be taken into account.

On the decentralized method (Fig. 14.2), to perform the objectives (increased market profit, system stability assurance) the individual agents decide the actions based on the locally data [3]. The centralized method collects the global information in order to control the entire system. The decentralized method does not require the data exchange (locally or globally) between the agents or with the central room control. There are only special agents (leaders) which may exchange the data through the center.

One disadvantage of the decentralized method is that the entire stability or optimization is not assured, but only locally. The reason is simple: no data communication exchanges exist. More deeply, each method has its own advantages and disadvantages the decentralized method has to be taken into account. From point of view of security data, the decentralized systems protect the confidentiality of the agents by acquiring privileged data [9–11]. In addition, the stability of the decentralized system (DS) is higher than the similar centralized system (CS); the reason is very simple, if there are leaders without connection with any agents, the distribution system is being capable to maintain the stability due to the local stability assures by the other agents. Figure 14.2 shows the decentralized method principle [3].

One other reason to implement distributed control is its expandability feature (plug-and-play feature). By using this concept into the conventional power system (PS), more flexibility is assured. Moreover, new alternative energy can be introduced in the PS or to the local consumers. One agent is considered one bidirectional energy port (i.e. the energy entrance from the generators or energy delivery to the users). In the distributed control method, also known as the consensus control, the necessary local information transmitted to the agents can be obtained from the local parameter measurement (e.g. voltage and frequency) or from the neighbours. In Fig. 14.3 one example of the distributed control system (DCS) using the local information through the communication links is shown [3, 9].

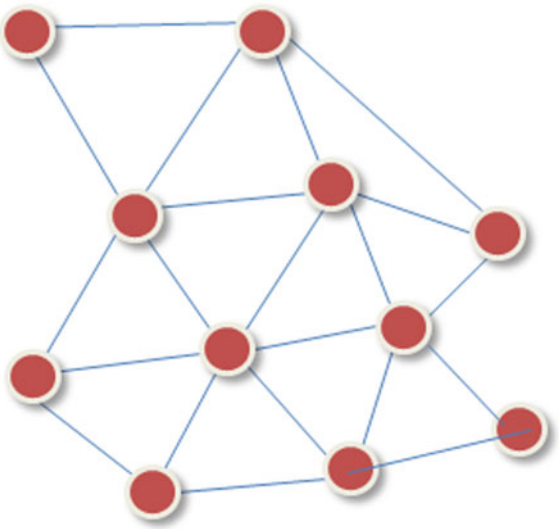

Fig. 14.3 Distributed control system

In the DCS, the information shared by the local agents to the others is bidirectional. In the decentralized systems there is no communication between the agents, each agent can use only the local measurements. In turn, in the distributed systems the users can share the information. In this manner, the global optimization methods could be applied in the distributed systems. This qualitative task is allowable also in the centralized method. The expandability of the distributed system architectures through plug and play feature will not influence the operation of the smart grid thanks to existing local information. Therefore, the smart grid could be extended easily through the new agents that can be connected to the grid. Figure 14.3 shows how a simple microgrid with the distributed method can be equipped [3, 9].

The advantage of using distributed control is to ensure the micro-relay function even when the node's controller no longer performs its functions. As a disadvantage, control is dependent on the distributed communications system.

14.4 Hierarchical Control

The coordinated control is classified according to the specified objectives: decentralized, centralized and distributed type. Taking into consideration the fluctuation and discontinues of the energy provided from renewable energy sources (RES) the energy storage system is necessary. The delivered electrical energy by the RES can be included in the utility network through the static power converters. In order to deliver the maximum extracted energy different maximum power point tracking (MPPT) methods are involved. From control point of view the main power sources

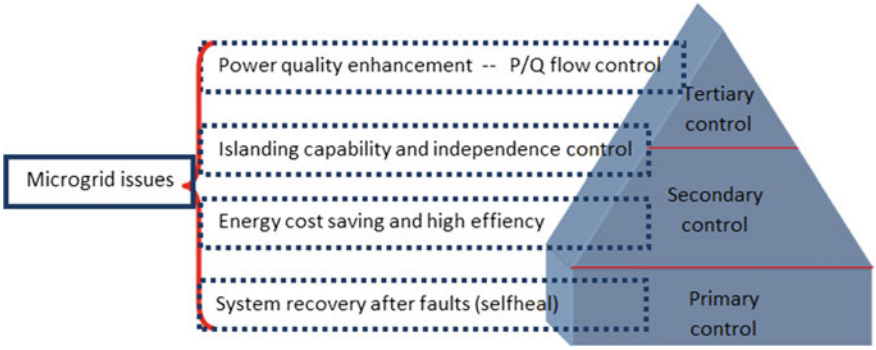

Fig. 14.4 The hierarchical control: main concerns

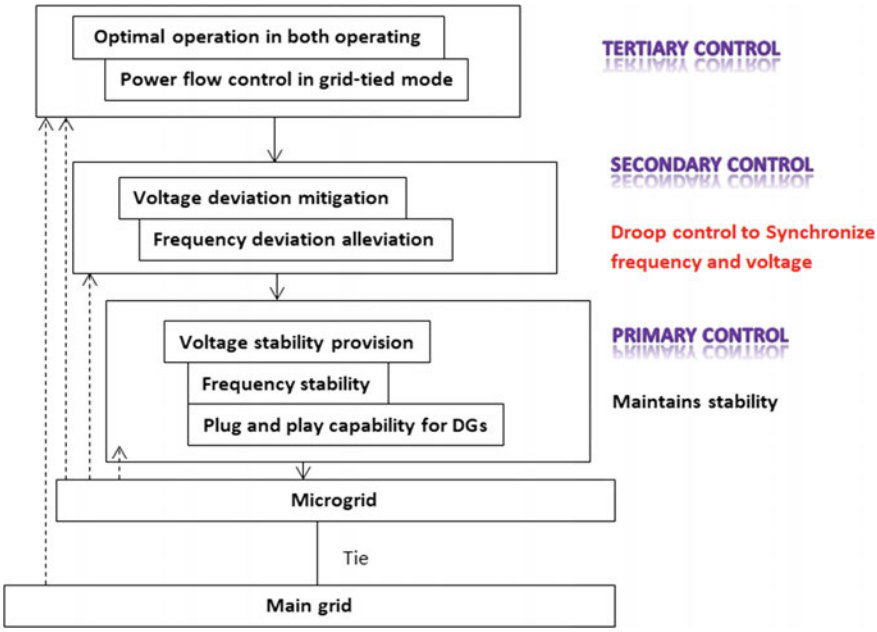

Fig. 14.5 The hierarchical control: main features

of the PS are controlled by the primary control. The photovoltaic panels, the batteries and the fuel cells provide DC power and can insert in the DC microgrid by using one or two-stage power conversion. Depending on the size of the microgrid, the small size microgrid are controlled by using master-slave control [4].

Hierarchical control is often used in DC power microgrids. This method uses 3 control types [12]: primary control, secondary control, and tertiary control (Fig. 14.4). Figure 14.4 contains the main concerns of the microgrids [13]. The Fig. 14.5 comprises the features of each level from the hierarchical control [13].

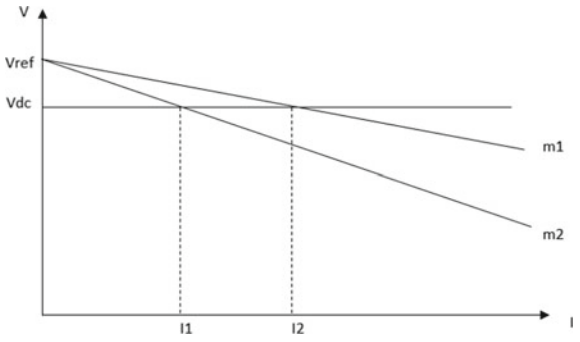

Fig. 14.6 The load distribution function on the droop constants

This hierarchical control (Fig. 14.5) can be implemented in both centralized architecture and distributed architecture. Centralized architecture faces uncertainty about the availability of renewable energy sources, load demands. This type of architecture has the deafness of a delayed response to problems [10]. The distributed control approach does not need a central controller and needs less information (communication) than in the centralized case. For stabilization purposes, the primary control (PC) as part of the hierarchical architecture is almost similar with the decentralized one. In the hierarchical control architecture, PC (for stabilization purposes) is almost similar with the decentralized control. As primary control, the voltage droop control (VDC) is used [8, 11]. By using the VDC, by using different droop constants (m_1 or m_2, Fig. 14.6) the load distribution can be performed.

In order to ensure both local operation and interconnection between distributed sources parallel connected, the proposed control block diagram [7, 14] has in view the balanced distribution of power or load between the connected parallel converters (Fig. 14.7) [7]. The control system contains local control loops and an external voltage loop (Fig. 14.7) [7]. However, this method cannot achieve a balanced distribution of loads, especially in systems with different values of line resistances. Many improvements have been made to this method [15], including an adaptive power balance control [15, 16].

In any case, almost the same with the AC power supply, the PC in the DC system cannot assure the zero steady state error. Therefore, the stationary regime the voltage error is obtained. In order to obtain the zero steady state voltage error, the secondary distributed control (voltage and frequency synchronization) is introduced. The most commonly used method is the consensus control [9, 10]. In this type of control there is a global control objective (e.g., the global voltage deviation), and one agent works with his local estimate. In the DC PS, one agent can be a distributed source, user or microgrid. Through this method, the control variable value will be the same for all agents thanks to available information from the neighbors [17, 18]. For this control type, the global voltage averages is necessary. This value can be estimated from the exchangeable information between the neighbors and from the local data. The necessary data between the microgrids is obtained through a dynamic consensus-based protocol [19]. By introducing Proportional Integral (PI) controller, the cancellation

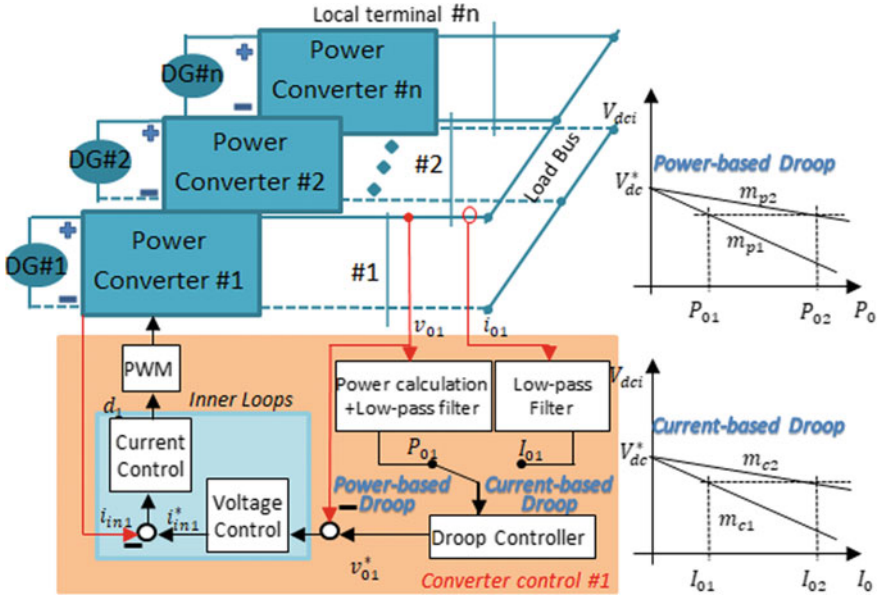

Fig. 14.7 The droop control method (power or current—based droop) applied in DC microgrid

of the voltage error (obtained by subtracting the estimated voltage from the reference value) takes place. In order to restore the average tension by respecting the load sharing, the discrete consensus method is used [20]. The optimal task is performed by the tertiary control. The tertiary control delivers a reference for the system by using power flow control (between the microgrids or between the distributed sources within a microgrid) [21–23].

14.5 Standards

Microgrids are island systems for local utility or energy distribution systems and contain at least one distributed power source and a corresponding load.

By performing the connection or disconnection of the power sources from a microgrid with minimum interruption from the PS, the reliability of the microgrid is increased [24, 25].

Network interconnection standards (IEEE 1547) are the optimum way for engineers, to perform fast the tasks of custom engineering, to prepare and obtain the specific approval processes, with minimal costs.

The planning and operation of the microgrids are included in IEEE 1547.4 standard. The IEEE 21 Standards Coordination Committee (SCC21) develops a guide

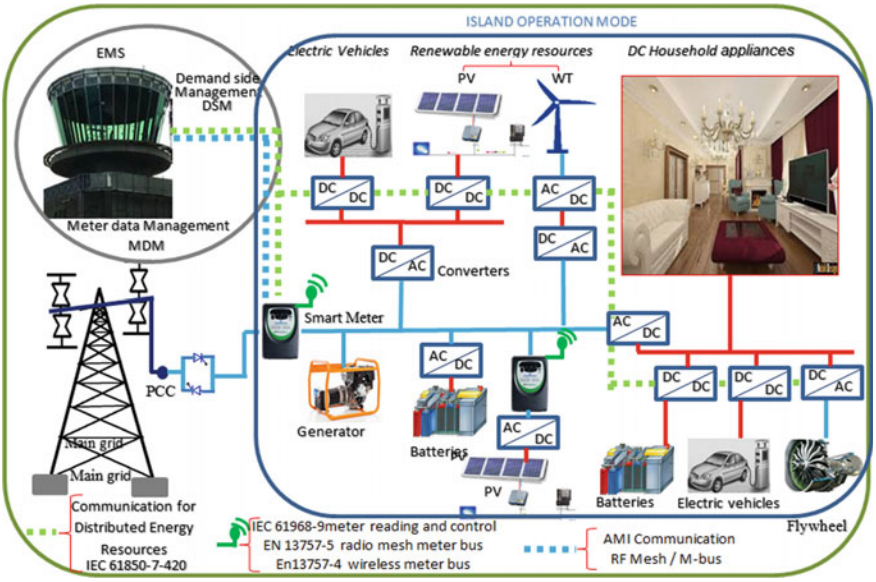

Fig. 14.8 Topology of the Intelligent microgrid

to help the operators of the PS, the specialists, and the manufacturers to use the technical aspects of the microgrid operation and implementation.

The communications standards at the microgrid level are mentioned and represented the associated flux in the Fig. 14.8:

- IEC 61850-7-420 Communications for Distributed energy Resources,
- IEC61968-9 m reading control,
- EN13757-5 radio mesh meter bus,
- EN13757-4 wireless meter bus.

14.6 Three-Phase Grid Active Power Converter: Case Study

In this Section the authors consider the DC microgrid, operating in both modes: grid-connected and standalone (island mode). The microgrid components are the Three-Phase Grid Active Power Converter (TP-GAPC), the back-up PS and the active load. The power flow continuity through the system is assured by introducing a back-up PS. The photovoltaic panels, and battery bank have been considered for back-up PS.

14.6.1 The TP-GAPC Mathematical Model Description

The modern vector control theory is employed. The synchronous reference frame and decoupled loop techniques are envisaged.

Firstly, the TP-GAPC mathematical description is based on the synchronous reference frame, the coupled dynamical Eq. (14.1) are as follows:

$$\begin{aligned} \frac{dI_d}{dt} &= -\omega \cdot I_q - \frac{1}{L} \cdot V_d + \frac{1}{L} \cdot E_d \\ \frac{dI_q}{dt} &= \omega \cdot I_d - \frac{1}{L} \cdot V_q + \frac{1}{L} \cdot E_q \end{aligned} \tag{14.1}$$

The above mentioned differential form can be expressed as state-space mathematical model:

$$\begin{aligned} \begin{bmatrix} \dot{I}_d \\ \dot{I}_q \end{bmatrix} &= \begin{bmatrix} 0 & -\omega \\ \omega & 0 \end{bmatrix} \cdot \begin{bmatrix} I_d \\ I_q \end{bmatrix} + \begin{bmatrix} -\frac{1}{L} & 0 \\ 0 & -\frac{1}{L} \end{bmatrix} \cdot \begin{bmatrix} V_d^* \\ V_q^* \end{bmatrix} + \begin{bmatrix} \frac{1}{L} & 0 \\ 0 & \frac{1}{L} \end{bmatrix} \cdot \begin{bmatrix} E_d \\ E_q \end{bmatrix} \\ y &= \begin{bmatrix} 1 & 0 \\ 0 & 1 \end{bmatrix} \cdot \begin{bmatrix} I_d \\ I_q \end{bmatrix} \end{aligned} \tag{14.2}$$

where, V is the converter voltage, E is the source voltage, I is the line current and ω is the grid pulsation.

The Eq. (14.2) contains both the state variable and the output of the grid active power converter (GAPC). Therefore, the standard state-space form representation of the dynamical system can be written as:

$$\begin{aligned} \dot{x}(t) &= A \cdot x(t) + B \cdot u(t) + F \cdot e(t) \\ y(t) &= C \cdot x(t) + D \cdot u(t) \end{aligned} \tag{14.3}$$

in which the components of the control vector are the dq converter voltages:

$$u = \begin{bmatrix} V_d^* \\ V_q^* \end{bmatrix} \tag{14.4}$$

the components of the disturbance vector are the dq grid voltages:

$$e = \begin{bmatrix} E_d \\ E_q \end{bmatrix} \tag{14.5}$$

and, obviously, the output vector, y, of dynamical system consists of the dq current components solution. The control vector does not affect the output; therefore, $D = 0$.

Based on the knowing dq current and voltage components, the AC grid power can be deducted:

$$P_{AC} = \frac{3V_d \cdot I_d + 3V_q \cdot I_q}{2} \tag{14.6}$$

The DC-link power is the product of the known DC-link voltage and of the output DC:

$$P_{DC} = V_{DC} \cdot I_{OUTDC} \tag{14.7}$$

By neglecting the power loss in the GAPC, the ac grid power (input) equals the DC link power (output). Therefore, by inserting the Eq. (14.7) into Eq. (14.6), the unknown variable (output DC current, I_{OUTC}) is obtained:

$$I_{OUTDC} = \frac{3}{2V_{DC}} \cdot \left(V_d \cdot I_d + V_q \cdot I_q\right) \tag{14.8}$$

In order to obtain a decoupled system, some additional terms are required (voltage decoupling terms). In this manner, the decoupled synchronous reference frame current loops are attained:

$$\begin{bmatrix} \dot{I}_q \\ \dot{I}_d \end{bmatrix} = \begin{bmatrix} \frac{1}{L} & 0 \\ 0 & \frac{1}{L} \end{bmatrix} \cdot \begin{bmatrix} E_q \\ E_d \end{bmatrix} - \begin{bmatrix} \frac{1}{L} & 0 \\ 0 & \frac{1}{L} \end{bmatrix} \cdot \begin{bmatrix} V_q \\ V_d \end{bmatrix} \tag{14.9}$$

By analyzing the DC-link circuit node, the relation between the currents can be obtained:

$$C \cdot \frac{dV_{dc}}{dt} = I_{INDC} - I_{OUTDC} \tag{14.10}$$

The voltage across the DC-link capacitor (14.7) is obtained from the applied power balance [11]:

$$\frac{dV_{dc}}{dt} = \frac{1}{C} I_{RES} - \frac{3V_d \cdot I_d + 3V_q \cdot I_q}{2C \cdot V_{dc}} \tag{14.11}$$

in which I_{RES} [A] is the instantaneous current from Renewable Energy Source (RES).

The utility voltage components are calculated taking into consideration the fulfilled mission of the PLL (phase-locked loop) [11]:

$$E_q = E, \quad E_d = 0, \tag{14.12}$$

active component of the source voltage vector has the RMS value (E) of the source voltage.

14.6.2 Robust Control of the Active Three-Phase Power Converter Supplying the Active Load

The authors proposed a robust solution to disturbances effect. It derives from the conventional linear control of the three-phase power converter [26–28] connected to the grid. Based on the input error, an integral term has been added.

$$\dot{\mathbf{z}}(t) = y^*(t) - y(t) \tag{14.13}$$

By considering the output equation of the GAPS (14.2), one more state vector has been added to the dynamical system:

$$\dot{z}(t) = y^* - C \cdot x(t) \tag{14.14}$$

Therefore, the new dynamical model in standard state space is obtained:

$$\begin{cases} \begin{bmatrix} \dot{x}(t) \\ \dot{z}(t) \end{bmatrix} = \begin{bmatrix} A & 0 \\ -C & 0 \end{bmatrix} \cdot \begin{bmatrix} x(t) \\ z(t) \end{bmatrix} + \begin{bmatrix} B \\ 0 \end{bmatrix} \cdot u(t) + \begin{bmatrix} F \\ 0 \end{bmatrix} \cdot e(t) + \begin{bmatrix} 0 \\ I \end{bmatrix} \cdot y*(t) \\ y(t) = \begin{bmatrix} C & 0 \end{bmatrix} \cdot \begin{bmatrix} x(t) \\ z(t) \end{bmatrix} \end{cases} \tag{14.15}$$

In this condition, the new state feedback control, namely integral state space control, is derived:

$$u(t) = \sum_{i=1}^{3} u_i(t) \tag{14.16}$$

The new control contains three components, each of them having a certain role. The classical state feedback control is nominated by u_1, being placed on the state feedback:

$$u_1(t) = G \cdot x(t) \tag{14.17}$$

The task of the u_2 control component has in view the reference tracking and it is inserted on the reference,

$$u_2(t) = K \cdot y^*(t) \tag{14.18}$$

The last control component, u_3, is placed on the disturbance vector, in order to compensate it [26–28]

$$u_3(t) = R \cdot e(t) \tag{14.19}$$

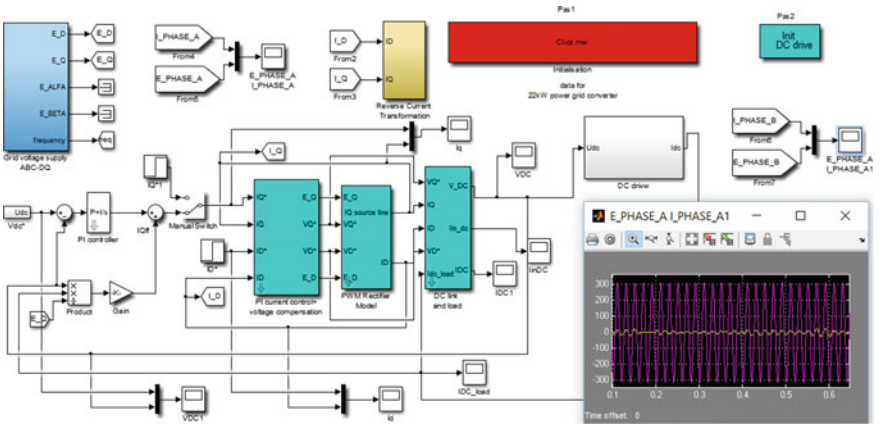

Fig. 14.9 The microgrid Simulink implementation: AC–DC power converter, PV back-up PS supplying the active load

By using an appropriate design, the matrix gain R can be deducted. The main role of it is to compensate the perturbation effect [27] (Fig. 14.9).

$$R = -B^{-1} \cdot F \tag{14.20}$$

By introducing the Eqs. (14.17)–(14.19) into Eq. (14.16), the grid power converter control is obtained [28, 29]:

$$u(t) = Gx(t) + Kz(t) + Re(t) = \tilde{G}\tilde{x}(t) + Re(t) \tag{14.21}$$

where, the matrices G, K, R are obtained as in [26–29], the augmented state $\tilde{x}(t) = \begin{bmatrix} x(t) \\ z(t) \end{bmatrix}$, and the obtained robust control matrix $\tilde{G} = \begin{bmatrix} G & K \end{bmatrix}$.

This type of control is known as integral SF. Figure 14.10 depicts very clear the action of the integral SF control on the dynamical system [26–29].

14.6.3 Design of the Gain Matrices

The first control component, the SF, assures the stability and dynamic performances of the utility converter. The SF control is based on the desired pole placement. Based on the imposed performances (time response T_R, and damping factor d) the desired poles are deducted:

$$\lambda_{1,2} = -d \cdot \omega_0 \pm \omega_0 \cdot \sqrt{1 - d^2} \tag{14.22}$$

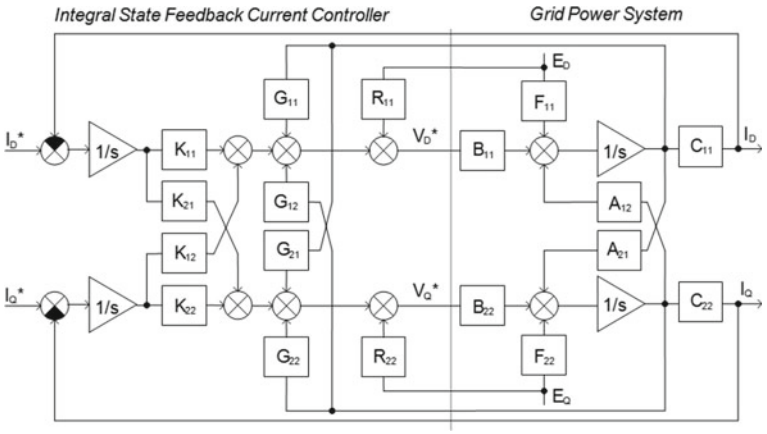

Fig. 14.10 Robust SF current loop control of the utility grid converter

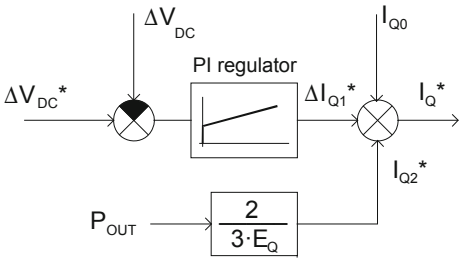

Fig. 14.11 The PI voltage controller with the power feedforward component

with

$$\omega_0 = \frac{1}{d \cdot T_R} \cdot \left[3 - \frac{1}{2} \ln\left(1 - d^2\right) \right] \tag{14.23}$$

The second control component has in view the cancelation of the steady-state error (i.e. the output of the current loop will be equal with the imposed reference). This task is performing by adequate design of the K gain matrix:

$$K = -B^{-1} \cdot (A + B \cdot G) \cdot C^{-1} \tag{14.24}$$

The third control component has in view the disturbance rejection and uses the Eqs. (14.19) and (14.20).

Additionally, one load current component is inserted in order to obtain a fast dynamic response to load variations. This component, feedforward, is obtained from power balance concept and it is added to the reference (Fig. 14.11). In this manner, all the time, power of the utility converter meets the requirements of the power load. The feedforward current component is:

$$I_{q2}^{*} = \frac{2}{3E} \cdot P_{out} \tag{14.25}$$

The Eq. (14.25) shows that the feedforward current component controls indirectly the active power. At the same time, the output power, P_{out} (see the Fig. 14.11), can be calculated, measured or estimated.

By imposing a zero *d*-axis current reference value the power quality requirement is fulfilled by the utility converter:

$$I_{d}^{*} = 0 \tag{14.26}$$

The Eq. (14.26) will conduct to unity power factor operation.

14.6.4 The Voltage Control

The main task of the DC link voltage loop is to control the DC link voltage. The second task is to eliminate the disturbances. Therefore, technical specifications should contain the imposed undervoltage and overvoltage limits during the load transitory regimes.

14.6.5 The Proportional-Integral (PI) Voltage Controller with Power Feedforward

The added component into the voltage loop, the load power feedforward component, P_{out}, has in view the fast compensation of the load variations. Therefore, the fast time response is obtained to load variations. The PI voltage controller with power feedforward is represented in Fig. 14.11 [26, 27].

The output feedforward signal results as follow:

$$I_{Q2}^{*} = \frac{2}{3 \cdot E_{Q}} \cdot P_{OUT} \tag{14.27}$$

$$P_{OUT} = I_{outdc} \cdot V_{dc} \tag{14.28}$$

The expression of the PI controller is as follows:

$$\frac{\Delta I_{Q}^{*}}{\Delta e_{V_{dc}}} = C_{PIv}(s) = K_{pv}(1 + \frac{1}{T_{iv}s}) \tag{14.29}$$

where, $e_{V_{dc}}$ is voltage error V_{dc}, that is $e_{V_{dc}} = V_{dc}^{*} - V_{dc}$. Therefore, the outline to blocks of the controlled complete system is that one shown in Fig. 14.12 [26, 27].

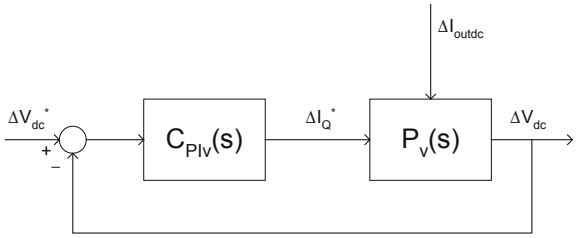

Fig. 14.12 Outline to the controlled system blocks (voltage and current loops)

The DC link voltage controller is based on PI control. In order to find the controller parameters (proportional gain K_{pv}, and integral time, T_{iv}), the adequate performances should be imposed:

1. The phase magnitude φ_{mv} (in radian)
2. The bandwidth ω_{cv} (in radian per second).

Based on the Refs. [26–29], the controller parameters K_{pv}, and integral time, T_{iv} are obtained:

$$T_{iv} = \frac{1}{\omega_{cv} \cdot \tan(\varphi_c - \varphi_{mv})} \tag{14.30}$$

$$K_{pv} = \frac{T_{iv} \cdot \omega_{cv}}{M \cdot \sqrt{1 + (T_{iv} \cdot \omega_{cv})^2}} \tag{14.31}$$

where M and φ_c are the module and phase (in radian) of the PS, $P_v(s)$, under control.

The DC-link voltage loop is a nonlinear system. Therefore, the linearization method (small perturbation method around equilibrium point) should be applied.

The basic initial values are the imposed response time $T_r = 0.55\text{e}{-3}$, and the desired damping coefficient $d = \sqrt{2}/2$. Based on the desired performances, the imposed closed loop poles are deducted $P = [\text{l1 l2 l3 l4}]$. The input inductance is a key design factor. Based on its value, the integral SF controller has been designed. Thus, the necessary matrices (G, K, and R) are obtained.

14.7 Simulation Results

The proposed control of the three-phase utility power converter has been developed and tested in Matlab program environment (Fig. 14.9). The 22 kVA apparent power (S_n) of the TP-GAPC has been taken into account. The $C = 1565$ μF, DC-link capacitor value is considered. The parameters of the real line inductance are $R_{in} = 0.001$ Ω, $L_{in} = 2.1$ mH. The load is driven by a $P_n = 1$ [kW] DC machine, rated power. The TP-GAPC has a battery bank PS as backup power. Considering around 300 min load autonomy in case of grid failure, 4 series batteries have been chosen (MK 8A27DT-DEKA 12 V 92Ah AGM). By taken into account a grid failure

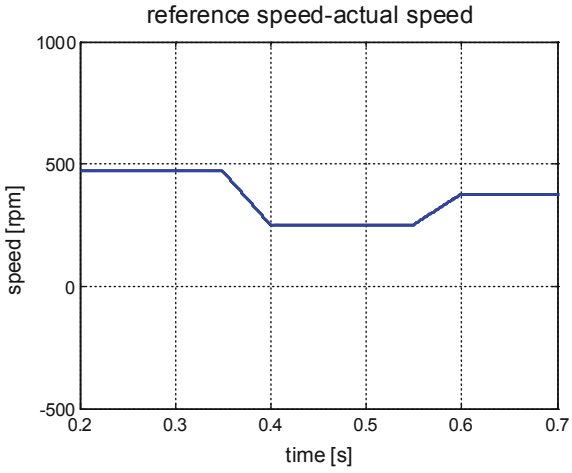

Fig. 14.13 Comparison between speed reference and the feedback speed

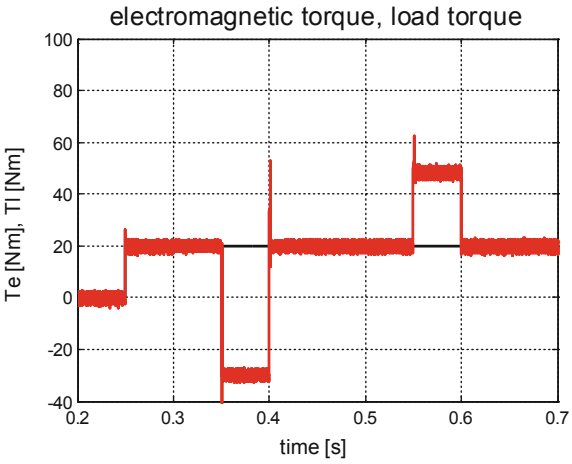

Fig. 14.14 Electromagnetic torque and load torque comparison

the entire microgrid PS has been numerical simulated (based on Matlab-Simulink software) [29]. In Figs. 14.13, 14.14, 14.15, 14.16, 14.17 and 14.18 the obtained simulation results are presented.

Taken into account the speed reference of the DC machine, the speed control loop assures the fast reference tracking in both dynamic and steady-state regimes (Fig. 14.13). The numerical validation of the mechanical motion equation is shown in the Fig. 14.14. During the steady state regime, the load torque is the same as the electromagnetic torque. The unity power factor operation of the utility converter is demonstrated in Fig. 14.15. The performances of the DC link voltage controller are shown in the Fig. 14.16. In Fig. 14.17 the bidirectional energy transfer is demonstrated. The performances of the active current controller for the utility grid are shown in Fig. 14.18. Voltage outage has been simulated at the moment

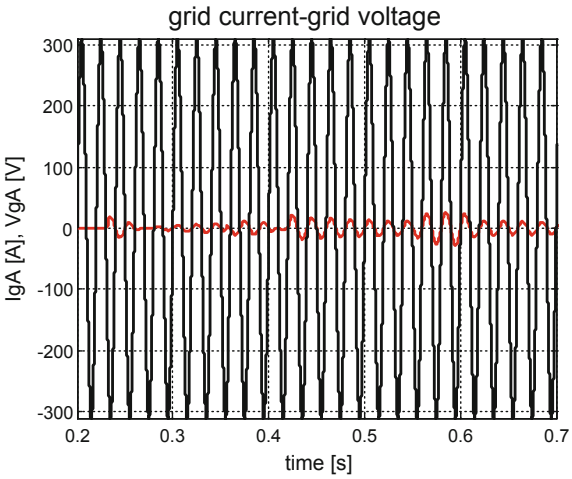

Fig. 14.15 Unity power factor in any operating conditions

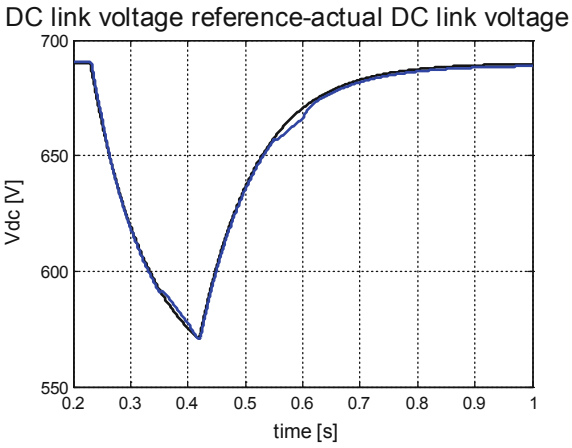

Fig. 14.16 DC link voltage, VDC [V]

$t = 0.22$ s (Fig. 14.16). The obtained numerical results prove the well design of the back-up system.

14.8 Cyber-Physical System

The future requirements for the smart grid design are well identified by Department of Energy (DOE) of the US [30, 31]. Nowadays, the most important future is the resistance to attack. One functional requirement is to restore the normal operation through self-healing feature. The other features are as in PS: power quality assurance

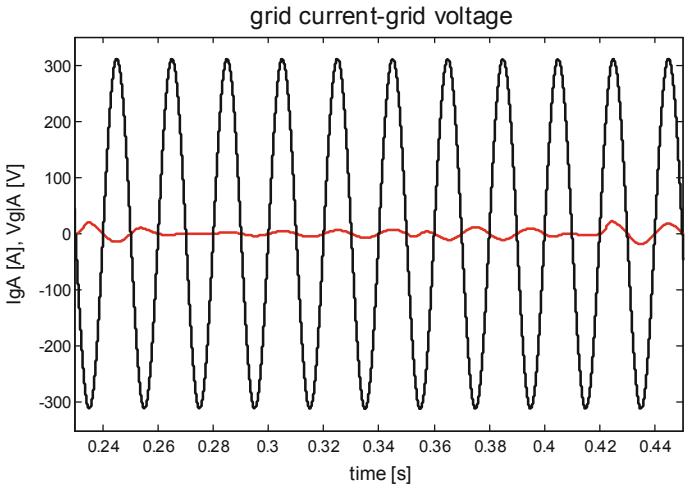

Fig. 14.17 The unity power factor (magnified area): bidirectional power flow

Fig. 14.18 Active current controller: the reference and the feedback

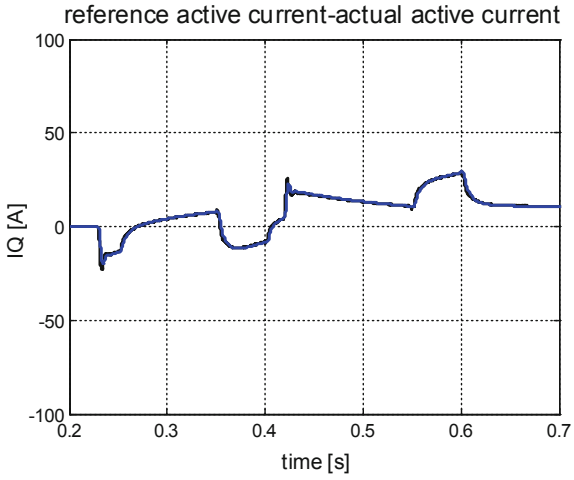

of PS, win-to-win strategy related to consumers, generation resources and backup capability through the storage system, access to energy markets in an optimal way.

In order to satisfy the above mentioned requirements advanced metering infrastructures (AMIs), Phase Measurement Units (PMUs), wide-area measurement systems (WAMS) are used. At the same time, the introduction of AMIs will get the PS more vulnerable to attack [32]. The PMUs are used both for real time measurements in order to estimate the state of the PS, and for increasing of the PS safety by avoiding cyber-attacks. The WMS will allow collecting the parameters of the transmission line in dynamic regimes.

A holistic approach within an energy grid, regarding the security of it, needs to study cyber-physical system (CPS) interactions to properly quantify the impact of attacks [33] and evaluate the effectiveness of countermeasures.

An analysis of system vulnerability should begin by identifying cyber resources (software protocols, hardware and communications protocols). Potential environmental security issues can be investigated by testing penetration and vulnerability scanning. In order to identify the additional vulnerabilities of the PS, a rigorous and continuously analysis of the information about the security of the providers, the system logs and the implemented intrusion detection systems are necessary.

A PS consists of three parts: generation, transmission and distribution.

The power supply system contains several control loops connected to different communication signals and protocols. It can be said that cyber-attacks directed to these control loops have a major influence on the stability of the electrical system throughout the system.

The data received by the central controllers comes from the installed sensors into PS. By using the adequate algorithms, the central controllers delivers the appropriate decisions to the field equipment. In Fig. 14.19, one representative control loop which includes both the physical system and the central controller (CC) is shown [34]. In Fig. 14.19, there are the sizes of command and exit of the physical system (substations, transmission lines and other physical machines). With the data acquisition system, system voltage and power are transmitted to the central control system via dedicated communication protocols.

In the CC, based on the measurements made, the data are processed by means of numerical algorithms. In this way, adequate control is given to the physical elements of the system. These algorithms are integrated into the Energy Management System (EMS). An opponent could exploit vulnerabilities along communications links by creating attacks (integrity attacks to compromise the content or denial or delayed communication with the equipment field, like denial of service—DoS). The DoS attack will compromise the synchronization between the measurement and control signals [35].

The impact of the attacks on the PS should be analysed for further security strategy approach. The results of the analyses conduct to the adequate defend countermeasures

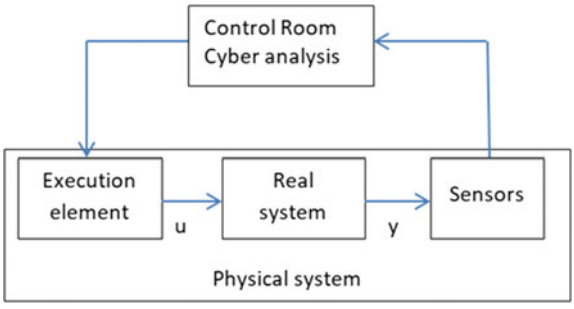

Fig. 14.19 The cyber-physical system

of the PS. The improper data detection methods can be used as a countermeasure. Therefore, for control purposes the new attack-resistant algorithms will be used.

The energy distribution system provides energy to the customer. In an intelligent network, there are common con loops of the end-user task.

To ensure the security of the network, at the level of communication protocols and parameters, some specific keywords are included.

(1) *Load shedding*. This expression is used in the distribution system in order to avoid the collapse of the energy system. To do this, emergency load charging circuits are used. These circuits are classified proactively, reactively, and manually. The proactive emergency line uses the automatic relay to maintain the normal operation of the distributed system. If the generation power sources are less than the connected load, an adequate frequency relay will disconnect the user distribution feeder in order to restore the normal frequency value. CPS use modern networks (they work on well-established Internet communications protocols (IP) such as IEC 61850).
In Fig. 14.19 present the interaction between Cybernetics and the Physical Part in a Cyber-Physical System [33].

(2) *Advanced metering infrastructures* and *demand management*: The use of AMIs assures the increased security of the distributed energy systems, penetration of the RES, and real time data consumption monitoring (by using smart meters—SMs—placed at the user locations). SMs are capable to switch off the users when there is no-load. Cyber-metering infrastructure is linked to consumer energy through a cyber-physical connection according to demand management [32]. The meter data management system (MDMS) controls the configuration of the meters. MDMS is network controlled. MDMS distributes the operational commands to SMs and processes the received data from the meters placed into the infrastructure. The technologies used by AMI can be: WiMax, mesh RF network, WiFi and power line. In order to transmit both power usage operations and meter-to-MDMS operation application layer protocols will be used (C12.22 or IEC 61850).

An intelligent smart grid requires a concept of layer protection, which consists of a cyber-infrastructure that limits opponent's access and increases resilience to power applications that are capable of functioning properly during an attack.

Sandia National Laboratories (SNL) owns the proprietary Energy Surety Microgrid technology™ (ESM) for managing a microgrid (connected to a grid or island operating modes) [35]. This technology uses a load connectivity hierarchy as well as a backup generation system. Developed microgrids through ESM methodology have high efficiency, increased reliability and strong cyber security.

A secure microgrid must be: simple, segmented, monitor operation, independent and reconfigurable.

14.9 Conclusions

The DC microgrid main architectures have been discussed. The specific control applied in DC microgrids has been presented. The requirements of the DC microgrids are presented in the Standards Section. One case study has been approached by the authors. It consists by robust SF control of the utility converter. The simulated power back-up system takes into account an active load [29]. During considered power supply outage the proposed microgrid maintain the performances in both sides: input and output of the PS. At the input, the necessary ac voltages are assured through the back-up PS (PV panels and battery power bank interfaced by the adequate power converters), by maintaining the adequate voltage amplitude and appropriate frequency. Moreover, the power quality constraints are maintained, the microgrid delivering the ac power at unity power factor.

Therefore, by introducing autonomous DC power sources (PV panels, and battery bank) an adequate autonomy of the active load has been assured. The above mentioned theory has been implemented in the Matlab-Simulink programming environment. The security of the microgrid is the most important task. A CPS has been presented related to the power system.

Acknowledgements This work was supported by a grant of the Romanian National Authority for Scientific Research, CNDI–UEFISCDI, project number PN-II-PT-PCCA-2011-3.2-1680.

References

1. A. Werth, A. Andre, D. Kawamoto, T. Morita, S. Tajima, M. Tokoro, D. Yanagidaira, K. Tanaka, Peer-to-peer control system for DC microgrids. IEEE Trans. Smart Grid **9**(4), 3667–3675 (2018)
2. Z. Wang, F. Liu, Y. Chen, S. Low, S. Mei, Breaking diversity restriction: distributed optimal control of stand-alone DC microgrids (2017), https://arxiv.org/abs/1706.02695. Accessed 2018
3. D. Wu, F. Tang, J.C. Vasquez, J.M. Guerrero, Control and analysis of droop and reverse droop controllers for distributed generations, in *IEEE 11th International Multiconference on Systems, Signals & Devices, SDD* (2014)
4. F. Valenciaga, P.F. Puleston, Supervisor control for a stand-alone hybrid generation system using wind and photovoltaic energy. IEEE Trans. Energy Convers. **20**(2), 398–405 (2005)
5. H. Pourbabak, T. Chen, B. Zhang, W. Su, Control and energy management system in microgrids. Institution of Engineering and Technology (IET) (2017), http://digital-library.theiet.org/content/books/10.1049/pbpo090e_ch3. Accessed 2018
6. R. Hidalgo Leon, C. Sanchez Zurita, P. Jacome Ruiz, J. Wu, Y. Munoz Jadan, Roles, challenges, and approaches of droop control methods for microgrids, in *IEEE PES Innovative Smart Grid Technologies Conference—Latin America (ISGT Latin America)*, Quito, Ecuador (2017)
7. T. Dragicevic, X. Lu, J.C.V. Quintero, J.M. Guerrero, DC microgrids—Part I: A review of control strategies and stabilization techniques. IEEE Trans. Power Electron. **31**(7), 4876–4891 (2016)
8. Q. Shafiee, T. Dragicevic, F. Andrade, J.C. Vasquez, J.M. Guerrero, Distributed consensus-based control of multiple DC-microgrids clusters, in *Annual Conference of the IEEE Industrial Electronics Society* (2014), pp. 2056–2062

9. L. Meng, T. Dragicevic, J.M. Guerrero, J.C. Vasquez, Dynamic consensus algorithm based distributed global efficiency optimization of a droop controlled DC microgrid, in *IEEE International Energy Conference* (2014)
10. X. Lu, K. Sun, J.M. Guerrero, J.C. Vasquez, L. Huang, Double-quadrant state-of-charge-based droop control method for distributed energy storage systems in autonomous DC microgrids. IEEE Trans. Smart Grid **6**(1), 147–157 (2015)
11. https://blog.482.solutions/distributed-ledger-technology-and-its-types-ad76565ae76. Accessed 2018
12. T.L. Vandoorn, J.C. Vasquez, D.M. de Kooning, J.M. Guerrero, L. Vandevelde, Microgrids: hierarchical control and an overview of the control and reserve management strategies. IEEE Ind. Electron. Mag. **7**(4), 42–55 (2013)
13. Z. Wang, F. Liu, Y. Chen, S.H. Low, S. Mei, Unified distributed control of standalone DC microgrids. IEEE Trans Smart Grid (2017)
14. J.M. Guerrero, J.C. Vasquez, J. Matas, L.G. de Vicuna, M. Castilla, Hierarchical control of droop-controlled AC and DC microgrids—a general approach toward standardization. IEEE Trans. Ind. Electron. **58**(1), 158–172 (2011)
15. Q.C. Zhong, Robust droop controller for accurate proportional load sharing among inverters operated in parallel. IEEE Trans. Ind. Electron. **60**(4), 1281–1290 (2013)
16. H. Kakigano, Y. Miura, T. Ise, Distribution voltage control for DC microgrids using fuzzy control and gain-scheduling technique. IEEE Trans. Power Electron. **28**(5), 246–2258 (2013)
17. R.S. Balog, P.T. Krein, Bus selection in multibus DC microgrids. IEEE Trans. Power Electron. **26**(3), 860–867 (2011)
18. M. Majid Gulzar, S. Tahir Hussain Rizvi, M. Yaqoob Javed, U. Munir, H. Asif, Multi-agent cooperative control consensus: a comparative review. Electronics **7**(22) (2018)
19. K. de Brabandere, B. Bolsens, J. den Keybus, A. Woyte, J. Driesen, R. Belmans, A voltage and frequency droop control method for parallel inverters. IEEE Trans. Power Electron. **22**(4), 1107–1115 (2007)
20. Z. Yan, D. Wu, Y. Liu, Consensus of discrete multiagent system with various time delays and environmental disturbances. Entropy **16**, 6524–6538 (2014)
21. S.G. Anand, B. Fernandes, J.M. Guerrero, Distributed control to ensure proportional load sharing and improve voltage regulation in low-voltage DC microgrids. IEEE Trans. Power Electron. **28**(4), 1900–1913 (2013)
22. S. Moayedi, A. Davoudi, Distributed tertiary control of DC microgrid clusters. IEEE Trans. Power Electron. **31**(2), 1–10 (2015)
23. G. Chen, E. Feng, Distributed secondary control and optimal power sharing in microgrids. IEEE/CAA J. Autom Sin **2**(3) (2015)
24. B. Kroposki, T.S. Basso, R. Deblasio, Microgrid standards and technologies, in *IEEE Power and Energy Society General Meeting—Conversion and Delivery of Electrical Energy in the 21st Century* (2008)
25. P2030 TM Smart Grid Interoperability Series of Standards. https://www.nrel.gov/docs/fy12osti/53028.pdf
26. M. Gaiceanu, Integral state feedback control of grid power inverter. Buletinul AGIR (3/2012)
27. F. Profumo, R.Uhrin, Complete state feedback control of quasi direct AC/AC converter, in *IEEE Industry Applications Conference, Thirty-First IAS Annual Meeting (IAS-96)* (1996)
28. M. Gaiceanu, Advanced State Feedback Control of Grid- Power Inverter. Energy Procedia **14**, 1464–1470 (2012)
29. M. Gaiceanu, C. Nichita, S. Statescu, Photovoltaic power conversion system as a reserve power source to a modern elevator, in *3rd International Congress on Energy Efficiency and Energy Related Materials (ENEFM2015)*. Springer Proceedings in Energy, Springer
30. S. Sridhar et al., Security of cyber-physical systems for the power grid. IEEE Process. **100**(1) (2012)
31. A modern network view system. National Energy Technology Laboratory (NETL), US Department of Energy (DOE) (2007)

32. NISTIR 7628, Guidelines for Intelligent Network Security. National Institute for Standards and Technology, August (2010)
33. GAO-11-117, Upgrading the Electricity Network: Progress has been made on the IT security guidelines, but key challenges remain to be addressed. US Government Accountability Office (GAO), January (2011)
34. D. Callaway, I. Hiskens, B who performs controllability of electrical loads. Proc. IEEE **99**(1), 184–199 (2011)
35. https://energy.sandia.gov/energy/ssrei/gridmod/integrated-research-and-development/esdm/. Accessed 2018

Chapter 15
Hierarchical Control in Microgrid

Ersan Kabalci

Abstract It is required to utilize several control loops together to increase reliability and performance of microgrids. The current and voltage magnitudes, frequency and angle information, active and reactive power data provide the involved feedback for normal and island mode operations of microgrid. The hierarchical control structure of microgrid is responsible for microgrid synchronization, optimizing the management costs, control of power share with neighbor grids and utility grid in normal mode while it is responsible for load sharing, distributed generation, and voltage/frequency regulation in both normal and islanding operation modes. The load control of microgrid is performed by using more sophisticated electronic devices as well as regular circuit breakers. This regulation capacity could be improved since the ESS decreases the dependency to primary power sources. Although several improvements have been experienced in microgrid control strategies, the most intensive research areas are listed as decreasing the structural instability, improving the system performance to increase reliability, monitoring the harmonic contents, scaling the control infrastructure, enhancing the operation characteristics in error states, and implementing new control algorithms for normal and islanding operation. The microgrid system has hierarchical control infrastructure in different levels similar to conventional grids. The microgrid requires enhanced control techniques to manage any level of system. Safe operation of microgrid in both operation modes and connection and disconnection between microgrid and utility grid are depended to microgrid control techniques. The controllers should ensure to operate the system regarding to predefined circumstances and efficiency requirements. The hierarchical control methods and applications of microgrid infrastructure are presented in the proposed chapter.

Keywords Microgrid · Hierarchical control · Central controller · Microgrid hierarchy · Information and communication technologies · Distributed control

E. Kabalci (✉)
Department of Electrical and Electronics Engineering, Faculty of Engineering and Architecture, Nevsehir Haci Bektas Veli University, Nevsehir, Turkey
e-mail: kabalci@nevsehir.edu.tr

N. Mahdavi Tabatabaei et al. (eds.), *Microgrid Architectures, Control and Protection Methods*, Power Systems,
https://doi.org/10.1007/978-3-030-23723-3_15

15.1 Introduction

The power network has gained more effective, flexible, and tended to distributed generation (DG) regarding to achieved technical and economic improvements. It is not possible to ignore contributions of communication technologies to these achievements. It is expected that the improved power electronics and equipments will play important role on development of power infrastructure in a few decades. This new grid trend enables the power network to be more distributed and interactive to integrate generation and consumption as two main components of grid infrastructure. In this regard, the increased use of distributed energy resources (DERs) have leveraged integration of energy storage systems (ESSs) to the same power plants. This new grid scenario that is also known as smart grid (SG) will enable to deliver generated electricity from plants to consumer by using digital communication and control technologies, and will allow consumers to control their consumption rates, to improve reliability and monitoring opportunities. The improved power network is much more interactive, smart, and distributed by comparing to conventional utility grid. The ESSs will facilitate to achieve energy balance among DERs and existing power network.

The microgrid infrastructure is one of the most important concepts of DG system and it cooperates with ESSs. Although the microgrid concept is improved to cope with integration of renewable energy sources (RESs) to power network, it is meaningful with participation of consumers to generation, energy storage, control, and management sections of power network. This improvement transforms consumers to prosumers by their active participation to generation cycle. There are extensive researches for DC and AC microgrids where hybrid microgrid applications have been developed [1–3].

The widespread use of RESs and penetration to utility grid over microgrids have caused several challenges and problems on reliability, resiliency, and control issues of both utility grid and microgrids. These challenges and control methods improved to cope with these challenges are presented in this chapter. There is an increasing interest on microgrid control and protection topics among reliability, security, and economical operating issues that are widely researched since a few decades. The achieved improvements in microgrid control have leveraged to improve grid potential and enabled high-scale microgrid integrations to utility grid. these improvements have not only enabled the individual or joint operation of microgrids with connection, interconnection, and disconnection cycles but also have provided to eliminate challenges met in the general operation of distribution networks.

This chapter deals with basic principles of microgrid control where local control, central control, emergency control, and general control principles are presented as initial control requirements. The control methods except general control are related to internal control requirements of microgrid while the general control method performs operating conditions of microgrid for interacting with neighbor microgrids and utility grid. On the other hand, hierarchical control functions and requirements are presented in the next section where internal control loops, primary, secondary, and tertiary control methods are introduced with application areas. The technical details

and control requirements are presented in a comprehensive hierarchical structure regarding to central and distributed control operations in microgrid infrastructure.

15.2 Basic Principles of Control and Management in Microgrid

Control is one of the key components providing improvement of microgrid systems. The microgrid networks require similar control structures at different layers and in hierarchical orders. The reliability and sustainability of microgrid infrastructure depends to enhanced control methods that are effectively operated at each layer. The healthy operation of microgrid in normal and islanded operations modes, and successful integration or disconnection with utility grid is also depended to microgrid control techniques. The controllers should ensure smooth operation of entire system in the context of predefined operation conditions. It is known that microgrid does not only operate in autonomous islanded mode but also in normal mode. In the normal operation mode, voltage and frequency of microgrid should comply with amplitudes of utility grid. In this sense, microgrid should have appropriate control loops for ensuring active power/frequency (P/f) regulation, reactive power/voltage (Q/V) regulation and to react instant grid disturbances that are caused by ever-shifting load conditions. Moreover, detection algorithms of island mode are required to prevent sequential problems occurring during island mode and normal mode shifts.

A general schematic presentation of control methods used in microgrid operations is illustrated in Fig. 15.1. The whole microgrid model is controlled by a microsource control system (MCS) in this presentation. The load controllers (LCs) are used to manage controllable loads located in load models as its name implies. A central controller (CC) is located between microgrid and distribution management system (DMS) or distribution system operator (DSO) for each microgrid infrastructure. These controllers are responsible to perform medium voltage (MV) and low voltage (LV) controls in systems where more than single microgrid exists. Several control loops and layers as in conventional utility grids also comprise the microgrids. This hierarchical control scheme meets fundamental infrastructure and dynamic interface requirements in addition to providing integrity through central and distributed control systems [4].

The local control includes primary control systems such as voltage and current control loops that are used in DG and RES integration. The secondary control is essential to regulate frequency and average voltage fluctuations caused load or source variations. The secondary control is also responsible for local auxiliary services. Central and emergency control layer operates featured protection and emergency control protocols against unexpected events in the context of microgrid reliability. The emergency control techniques perform fault estimations by realizing protective and regulative measurements. The general control ensures economical operating conditions of microgrids by arranging the organization between microgrids and dis-

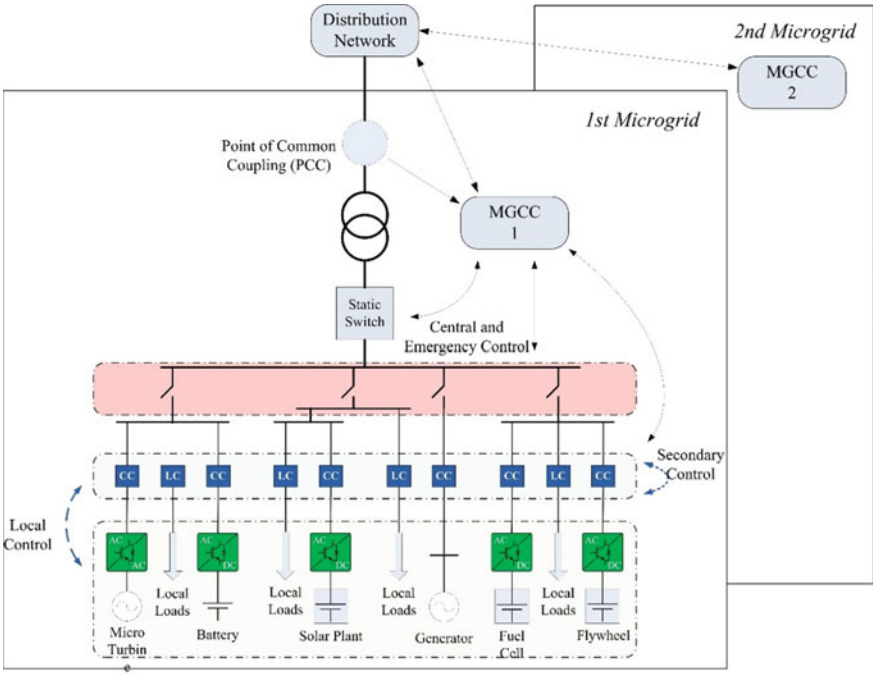

Fig. 15.1 A general view of microgrid control structure

tribution networks. The general control infrastructure seen in Fig. 15.1 operates as a distribution network interface for microgrid central controller (MGCC) and manages the power flow control. This control interface provides power distribution at predicted values by controlling the microgrid infrastructure. In spite of local control, the secondary, general and emergency control infrastructures require communication channel [5–7].

The local controllers used in microgrid are defined as distributed controllers while secondary and emergency controllers operate as CCs. The processes of general control level take from a few minutes to an hour and general controller transmits control signal to controllers at central level and to interconnected distribution systems. On the other hand, CC is capable to coordinate secondary controllers and local controllers in the microgrid in a few minutes. The secondary control mechanism can react to system disturbances or control commands in a few seconds to a minute. Eventually, local controller systems are designed to operate in an independent way and according to predefined event schedules. The detailed introduction of LCs, secondary controllers, general controllers, central and emergency controllers are presented in the following sections.

15.2.1 Local Control

The local control is known as primary or internal control and comprises the primary level of hierarchical control. This control method that has the most rapid response time can vary regarding to microgrid type and is used in asynchronous and synchronous generators, power electronic inverters and converters. The power electronic devices provide flexible operating conditions comparing to those in synchronous and asynchronous generators. The local controllers are mostly operated with internal control loops that do not require communication, with low cost and simple device structures. The local controllers are the most basic category of microgrid control that targets to manage DG under normal operating conditions.

A DG local controller of power electronic inverter that is operated regarding to reference voltage inherited from conventional droop controller is shown in Fig. 15.2. The droop controllers calculate virtual inertia of each parallel-connected inverter by determining average P and Q power depending to frequency and voltage values of inverters. These control loops that are also known as P–f and Q–V enable inverters to be connected in parallel as uninterruptible power supplies (UPSs) and load sharing operations. Although these methods provide reliability and flexibility, it is known that there are some drawbacks exist in conventional droop control. For instance, droop control method does not properly operate in non-linear load sharing requirements of parallel-connected systems since it needs to consider harmonic currents and active-reactive power balance. Therefore, a novel method called harmonic current sharing is improved to eliminate circulating distortions occurred in non-linear load sharing conditions. The developed control methods cause to voltage distortions while sharing harmonic currents, and thus it is required to acquire an average value among two situations [1, 5, 7–9].

The voltage and frequency control loops of a local controller is illustrated in Fig. 15.2 where the controller uses current measurement that is inherited from transfer function of virtual impedance as the feedforward signal. The proportional-integral

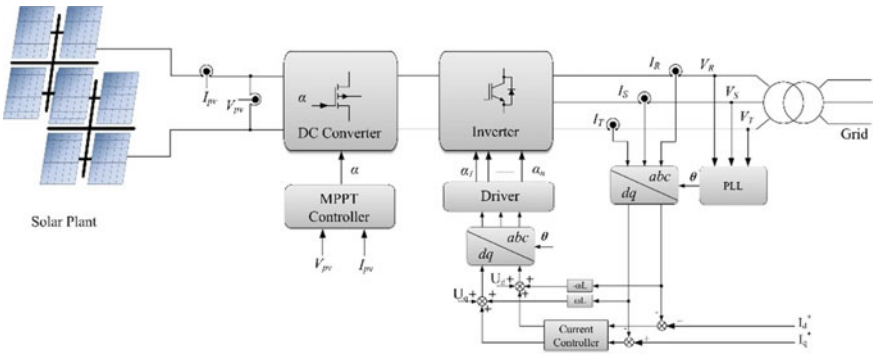

Fig. 15.2 A general view of local controller used in DG

(PI) observer is widely used in droop controllers that are located at local control level. The PI observers are used either individually in open control loops or with feedforward compensator in a closed loop to improve system performance.

These kinds of controllers are essential for managing operation conditions of DERs and power electronic interface as seen in the above example. In addition to primary V and f controls, it is required to control P and Q power in DG processes. The droop based active and reactive power controls are the most widely used methods in this context. Moreover, the control among sources is also handled in this context similarly to DG output control. To this end, inner control loop is used for current and outer control loop is used for voltage control in output control of DG system. The power sharing control provides active and reactive power control regarding to frequency and voltage fluctuations that are inherited from local measurements without any communication requirement.

The local controller designs are based on detailed dynamic models of distribution network parameters and resistive, inductive, and capacitive load profiles of DERs. This model requires to response immediately to internal dynamics and transient-state fluctuations of controller system. There are three basic reference frames as natural (abc), rotating (αβ) and synchronous (dq) exist for modelling, stability analyses, and synthesis of local control in inverter-based DG system. The natural reference frame is controlled with fundamental observers such as PI, and DG provides essential results for time axis response analyses of microgrid in time-domain. The rotating reference frame is mostly related with sinusoidal variables and synchronous reference frame operates with DC components and controllers [4].

15.2.2 Secondary Control

The secondary control is comprised by second level control loops that are used to enhance system performance by eliminating reliability problems and to increase power quality of microgrid network. The secondary control closely works with LC and CC groups. In normal operation mode, the inverters through the microgrid inherit reference electrical signals from voltage and frequency data of utility grid. On the other hand, inverters lose the reference signals provided by utility grid in the island mode operation. It is required to coordinate the cooperation of synchronized operation by using single or multiple operation methods. The secondary controllers include various control mechanisms to improve parallel operation performances of inverters or DGs. There have been several studies reported in literature on control of DGs, master and slave operation of inverters, current and power sharing, and generalized frequency and droop control [10–14].

The secondary control of microgrid operates similar to that of conventional power systems to prevent frequency fluctuations occurred in load shifts, to ensure stable and reliable voltage, and to operate local controllers in island mode operations; i.e., the voltage and frequency reference signals (E^* and ω^*) depicted in Fig. 15.3 are provided by secondary control loops. The secondary control loops represent rela-

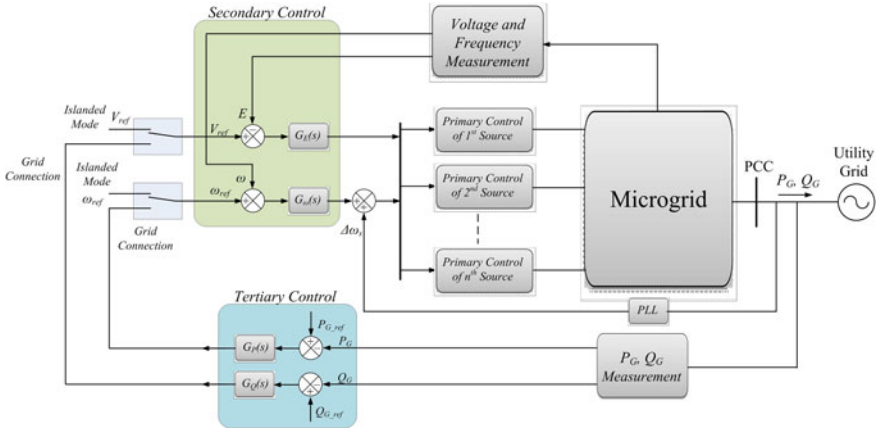

Fig. 15.3 The secondary and tertiary controllers in distributed generation

tively slower response times comparing to primary controllers, and thus they require low bandwidth communication. The improvement of power quality of DG sources connected at a common power line is also accomplished by secondary control. The integration of a secondary control system to central controller has been illustrated in Fig. 15.3 where the frequency and voltage of microgrid is compared to parameters of DG system that are used as reference values, ω_{ref} and V_{ref}. Afterwards, the generated error signals are evaluated by independent controllers to compensate frequency and voltage fluctuations [10, 15].

15.2.3 Central and Emergency Control

The central and emergency control concepts imply the central energy management system (CEMS) that is responsible for secure, reliable, and economic operation of microgrid in islanded and normal operation modes. The fundamental duties of this control level are active and reactive power control, voltage and frequency control, regulation, system restoration, and control of existing DG system for load shedding and featured protection procedures. The central and emergency control that has significant roles in islanded operation of microgrid is the control mechanism located on top of hierarchical control. Moreover, central control is used for synchronization of microgrid during shifting from island mode to normal mode. This operation is accomplished by coordinating the central controller and management system. The block diagram illustrating the coordinations of local, secondary, and central controller in voltage and frequency regulation is shown in Fig. 15.4 where the common role is also denoted.

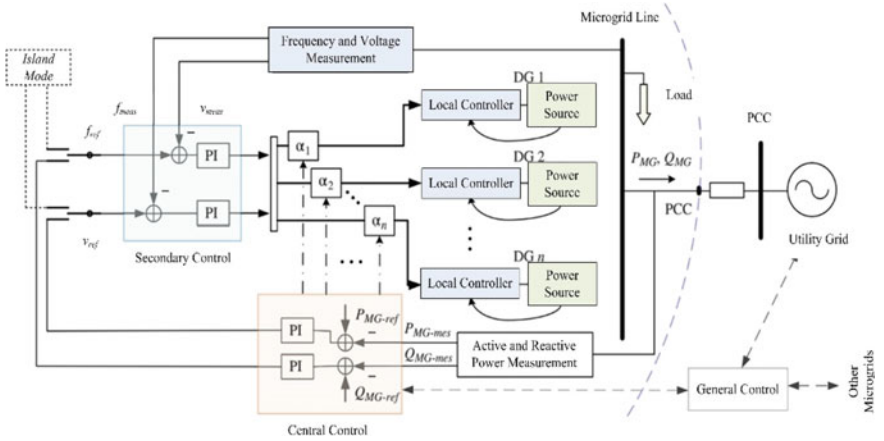

Fig. 15.4 The secondary, local, central and general control structure

While the utility grid is supported by auxiliary services of microgrid, the general control is also integrated to system under these operation conditions. The power flow between utility grid and microgrid is adjusted by using voltage and frequency of DG sources in normal operation mode as seen in Fig. 15.4. The active and reactive output power of microgrid are measured at the first step and then these amplitudes are compared to reference values (P_{ref}, Q_{ref}) to generate voltage and frequency references (f_{ref}, V_{ref}).

The inherited references are then used as the input parameters of secondary control. The α values denote contribution rate to voltage and frequency regulation for each DG sources located in the microgrid. A secondary control signal is generated and is distributed to each DG sources along the microgrid for detecting the load distortion and thus, each DG source is expected to compensate its generation-load imbalance by providing appropriate contribution.

The coordinating microgrids are much more essential against intermittency, outages and emergencies comparing to single microgrid structures. Besides, the collaborating microgrid connections improve the reliability of entire grid system by benefiting advantages of coordinated operation. The output power control of microgrid is adjusted to regulate power mode and frequency-voltage controls in emergency conditions. The island mode planning is assumed as the most significant emergency control systems for microgrid systems. Once a microgrid shifts to island mode, the voltage and frequency magnitudes can excess power quality limits. Therefore; DG sources, ESSs, load shedding at local loads, and particular protection schemes are required for ensuring to sustain islanded mode operation of microgrid. The load shedding procedure is an emergency control method that is operated when a significant loss is experienced in voltage or frequency magnitudes. Central controller of microgrid operates the emergency control. The improved communication and network technologies play crucial role in microgrid operation and control processes.

Therefore, information and communication technology (ICT) is an indispensable component of central and emergency control mechanisms in microgrid [2, 4, 12, 15].

15.2.4 General Control

The general or global control is also known as tertiary control that provides cooperation of microgrids with utility grid by using communication infrastructure. The general control ensures power control between utility and microgrids. On the other hand, microgrid can be dispatched in terms of distribution grid and can be controlled as a continuous inductance load if it is analyzed in the view of control perspective. Moreover, the general controller acts as a central controller to manage optimum power flow at point of common coupling (PCC) in addition to its duties on sustaining reliability and security of distribution feeders, generation planning, and active and reactive power flow controls.

The general controller is converted to central controller that manages demand side management (DSM), security controls, economic planning, and load estimation functions. Eventually, the general control level is responsible for facilitating the operation conditions of microgrid and improving the operation of distribution buses by controlling active and reactive power rates of DG sources. These improvements are usually related to economic conditions and target to ensure demand and generation balance [4, 6]. The detailed presentation of general control is conducted in tertiary control section of hierarchical control.

15.3 Hierarchical Control

Microgrid control standards are expected to find widespread use in near future. In this regard, ISA95 is the most widely used standard to improve an automatic interface between operation and control systems. The fundamental task of ISA95 is to provide a convenient terminology defining how the data will be used between service provider and producer communication. The hierarchical control that is defined in the context of this standard includes multilevel control structure:

5th Level: This level includes the highest management principles throughout a commercial enterprise. The operation, improvement responsibilities, transmission lines, and plants are controlled at this level.
4th Level: The plant level is directly related with economic and financial operations that are required for management strategies.
3rd Level: This level accommodates situations of generation systems and their behaviours for management requirements.

2nd Level: This is the level where management and control strategies are defined on a particular area or generation line behaviours.
1st Level: This level includes predefined management procedures for automation and generation systems.
0th Level: The device level is comprised by physical connections and equipments to detect changes occurred in peripheral and generation systems.

Each level includes a command section and performs managed control on low ordered systems. It should be noted that a control and reference signal transferred from higher level to lower one has little effect on system reliability and performance. Therefore, it is required to decrease the bandwidth as the control level increases. The integration of ISA95 standard to any microgrid infrastructure requires following control levels from 0th level to 3rd level [1]:

0th Level Control (*Internal Control Loops*): The regulation of each module is performed at this level. It is provided to obtain reliable output voltage and current by using current, voltage, feed-forward, feedback, linear and nonlinear control loops.
1st Level Control (*Primary Control*): The droop control method is widely used in this level and the physical operations are virtually performed to increase system stability. This level is also used for modeling the physical output impedance of system by using virtual impedance control layer.
2nd Level Control (*Secondary Control*): This control layer ensures to obtain output voltage and currents of microgrid at the desired values. Moreover, it operates synchronization control loop to enable appropriate connection and disconnection with utility grid.
3rd Level Control (*Tertiary Control*): This control level controls power generation and power flow between microgrid and utility grid.

Nowadays, these control methods have been extensively used in penetration of solar plants and wind turbine systems to microgrid and utility grid. In addition to this, microgrid infrastructures that can be operated in islanded and grid-connected modes increased the hierarchical control and energy management requirements. There are numerous studies have been published on hierarchical control, coordinated control, frequency control, and tertiary level control in the recent literature [5, 9, 16–18]. The main problem to be solved seems as frequency control according to majority of literature surveys. However, voltage reliability and synchronization are also researched in order to provide reliability and flexibility to both operation modes of microgrids. The primary control is based on internal control loops such as voltage, frequency, and droop control while secondary control is related with synchronization and coordination regarding to load shedding, grid monitoring, active and reactive power control. The tertiary control provides microgrid management controls such as ICT based measurements, remote monitoring and remote-control procedures.

15.3.1 Internal Control Loops

It is mandatory to comprise an interface by using intelligent electronic systems between DG sources and microgrid. These interfaces are provided either by current source inverters (CSIs) that include phase locked loop (PLL) for grid synchronization and internal current loop or by voltage source inverters (VSIs) including an internal current loop and an outer voltage control loop. CSIs are used to provide stable current or VSIs are used to provide stable voltage to grid in island mode or autonomous operations. VSIs present an interesting operation since they do not need any external reference to sustain grid synchronization in microgrid applications. Moreover, VSIs provide significant contribution to DG power systems by improving power quality and sustaining the operation under fault conditions. These inverters can be converted to CSIs on demand in normal operation modes. Although the CSIs may operate as VSIs on demand, they are mostly connected to solar or small wind turbines that are operated by maximum power point tracking (MPPT) algorithms. Thus, a string comprised by CSI and VSIs or just VSIs are connected in parallel to comprise power electronics interface of microgrid [4, 16].

15.3.2 Primary Control

When two or more VSI are connected in parallel, the active and reactive power circulation occurs as seen in Fig. 15.5. This control level adjusts the reference voltage and frequency values that are provided to internal current and voltage control loops. The fundamental idea of this control level is to mimic behaviors of a synchronous generator that decreases frequency while active power is increasing. This process is the use of widely known P–Q droop control in VSI control where the analytical presentation is as follows:

$$\omega = \omega^* - T_P(s)(P - P^*) \tag{15.1}$$

$$V = V^* - T_Q(s)(Q - Q^*) \tag{15.2}$$

where, ω and V denote frequency and voltage of output reference voltage while ω^* and V^* are reference of them, P and Q are active and reactive power, P^* and Q^* are references of active and reactive power, and $T_P(s)$ and $T_Q(s)$ are related transfer functions.

The general representation of proportional droop control that is illustrated in Fig. 15.6 is defined as $T_P(s) = m$ and $T_Q(s) = n$ transfer functions where DC components m and n are calculated as presented below:

$$m = \Delta\omega / P_{\max} \tag{15.3}$$

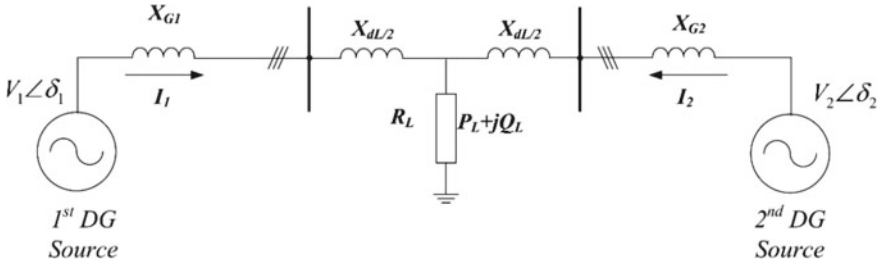

Fig. 15.5 Electrical equivalent circuit of parallel connected two inverters

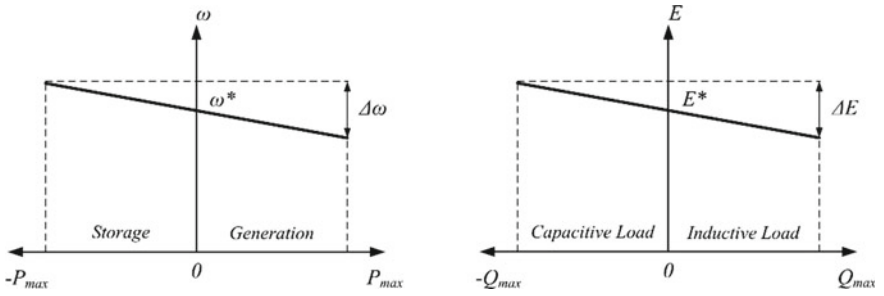

Fig. 15.6 *P–Q* droop control functions

$$n = \Delta V / 2Q_{\max} \tag{15.4}$$

Since the transferred power will not be equal to total load in islanded mode operation of microgrid, it is not allowed to design a controller that is based on just a pure integrator. Although it may be essential for detecting the accurate rates of P and Q power that are transferred to grid during normal operation mode, the most accurate rates are detected at tertiary level control. The compensators of $T_P(s)$ and $T_Q(s)$ can be designed by using various control synthesis techniques. Moreover, the DC gain of these compensators m and n control the $\Delta P/\Delta\omega$ and $\Delta Q/\Delta V$ fluctuations that ensure system synchronization and voltage limits [1, 10].

The output impedance of synchronous generators is mostly assumed inductive as transmission lines in classical droop control of large power systems. In addition to this, the output impedance of those systems using power electronics may vary depending to internal control loops at fundamental level. On the other hand, it draws almost resistive characteristics in low voltage applications. Therefore, the Eqs. (15.1) and (15.2) can be rearranged as follows regarding to Park transformation using impedance angle θ:

$$\omega = \omega^* - T_P(s)[(P - P^*)\sin\theta - (Q - Q^*)\cos\theta] \tag{15.5}$$

$$V = V^* - T_Q(s)[(P - P^*)\cos\theta + (Q - Q^*)\sin\theta] \tag{15.6}$$

The primary control should meet fundamental requirements such as stabilizing voltage and frequency, plug-and-play operation capability for DG sources, active and reactive power sharing without communication, and decreasing the circulating currents. The reference current and voltage control loops of DG sources are generated by primary control using fundamental level or zeroth level controls that are operating in P–Q or voltage control modes. The voltage and current control loops of this system is shown in Fig. 15.7 where the controller uses current signal as a feedback transfer function in virtual impedance operation. An appropriate control is performed by using one of proportional-integral-derivative (PID), adaptive or proportional resonance (PR) controllers as voltage controllers. The power quality of small scale and islanded microgrids are particularly important since the microgrid has low inertia and characteristics of single-phase loads are not linear [10, 11].

Therefore, the power quality can be increased by parallel connecting a number of strings as shown Fig. 15.8. The $H_{LPF}(s)$ depicts the transfer function of a low pass filter in the figure where each converter has an independent current control loop and a central voltage controller distributes fundamental component of active and reactive power between different sources.

Primary controller determines the reference point of voltage control loop and independent current controllers enhance the power quality of entire system by controlling the harmonic components in the current that is provided to utility grid. The DG source operation mode is accomplished by using active load sharing or droop characteristic control methods. The active load sharing is a kind of control procedure that is used in parallel-connected inverters and is based on communication capability. The current or active-reactive power references are determined according to central, master-slave, average load sharing or circular chain control methods. In the central control method, all the load currents are controlled regarding to reference current that is determined for a single inverter. On the other hand, a master converter operates as VSI and other converters tending as slaves operates as CSIs that are tracking the current reference value defined by master VSI in master-slave control method. In average load sharing control, the required current reference is determined considering weighted average value of all independent converters. The circular chain control method considers converters as chains that are connected to each other, and the current reference is determined regarding to previous converter. The active load sharing

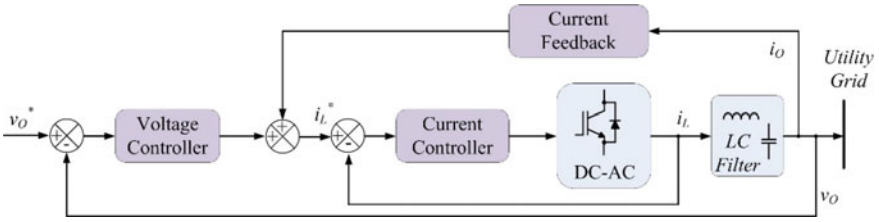

Fig. 15.7 Voltage and current control loops in voltage control mode

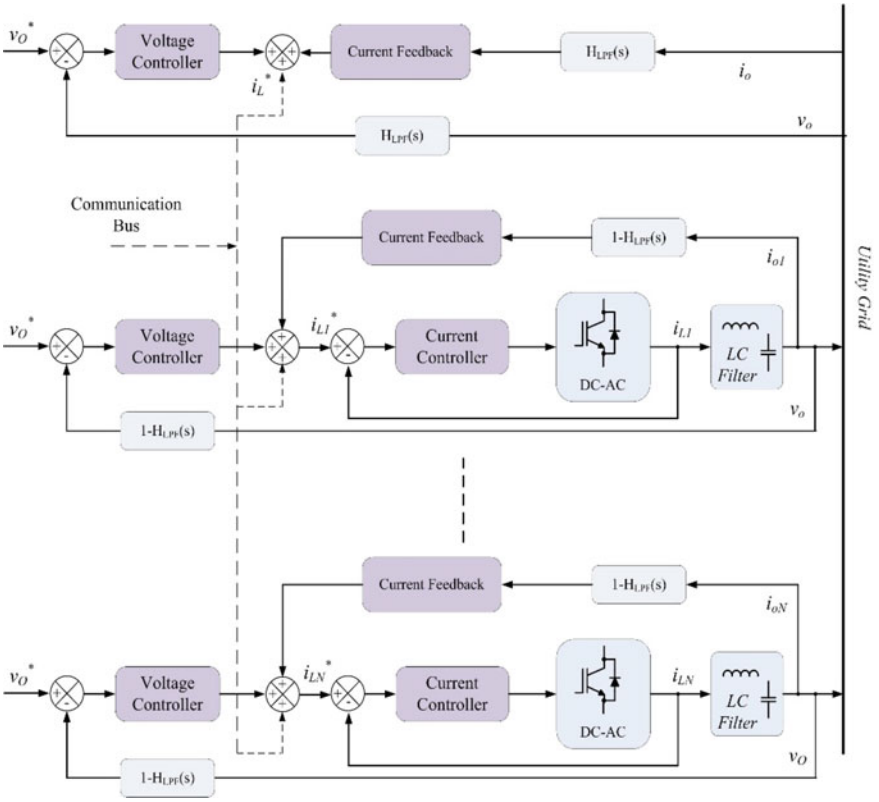

Fig. 15.8 Zero level control of parallel-connected DG sources

method requires communication buses and high bandwidth control loops. However, it provides highly accurate current sharing and power quality among others [19].

The droop control is known as independent, autonomous and wireless control method since it eliminates communication requirement through converters. The operation principle of classical droop control can be explained considering electrical equivalent circuit of a VSI that is connected to AC line. If the switching fluctuations and high frequency harmonics are neglected, the VSI can be modelled as an AC source with $E\angle\theta$ voltage. Also, common AC line voltage, output impedances of converter and line impedances can be accepted as a single-circuit line model with $V_{com}\angle 0$ impedance [19]. The power transferred to AC line is then calculated as:

$$S = V_{com}I^* = \frac{V_{com}E\angle\theta - \delta}{Z} - \frac{V_{com}^2\angle\theta}{Z} \tag{15.7}$$

The active and reactive power can be dispatched as follows by using Eq. (15.7) and obtained as:

$$\left.\begin{aligned} P &= \frac{V_{com}E}{Z}\cos(\theta-\delta) - \frac{V_{com}^2}{Z}\cos(\theta) \\ Q &= \frac{V_{com}E}{Z}\sin(\theta-\delta) - \frac{V_{com}^2}{Z}\sin(\theta) \end{aligned}\right\} \tag{15.8}$$

and they are rearranged as seen in Eq. (15.9) by assuming the line impedance is pure inductive $Z\angle\theta$:

$$\left.\begin{aligned} P &= \frac{V_{com}E}{Z}\sin\delta \\ Q &= \frac{V_{com}E\cos\delta - V_{com}^2}{Z} \end{aligned}\right\} \tag{15.9}$$

15.3.3 Secondary Control

The secondary control level is improved to compensate voltage and frequency fluctuations in microgrids. The secondary control manages regulation process to eliminate the fluctuations in case of any load or generation changes. The voltage and frequency levels of the microgrid V_{MG} and ω_{MG} are immediately detected anc compared to reference values, V_{MG}^* and ω_{MG}^*. The error signals (δV and $\delta\omega$) that are processed in compensator block are transmitted to each section of the system and output frequency and voltage are get regulated. It is known that the allowed maximum frequency fluctuations are ± 0.1 Hz in North Europe while it is ± 0.2 Hz in central Europe. This situation is denoted with

$$\delta P = -\beta G - \frac{1}{T_k}\int G dt \tag{15.10}$$

where output reference of secondary controller is depicted by δP, proportional controller parameter is given by β gain parameter, and T_k is time constant of secondary controller while G denotes field control error. The block diagram of primary and secondary control loops is shown in Fig. 15.9. The primary control is based on local measurements of output voltage and currents, virtual impedance control loops, and droop control of P–Q values. On the other hand, the secondary controller operates as a central controller that is improved to regulate frequency and voltage fluctuations presented in Eqs. (15.11) and (15.12) [1]:

$$\delta\omega = k_{p\omega}(\omega_M^* - \omega_M) + k_{i\omega}\int(\omega_M^* - \omega_M)dt + \Delta\omega_s \tag{15.11}$$

$$\delta V = k_{pV}(V_M^* - V_M) + k_{iV}\int(V_M^* - V_M)dt \tag{15.12}$$

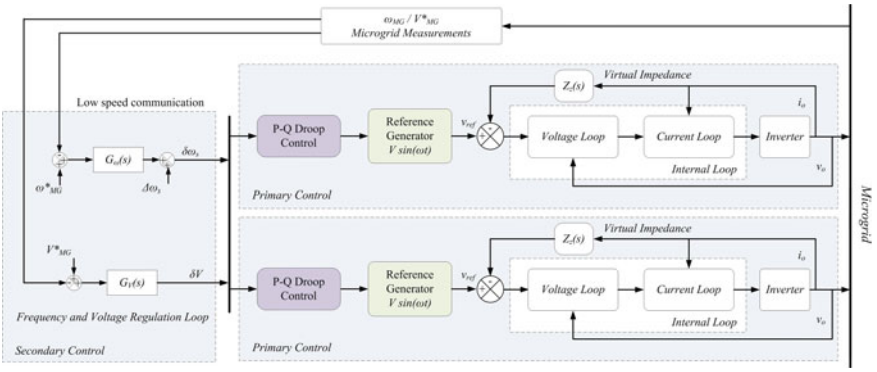

Fig. 15.9 Primary and secondary control in AC microgrid

The microgrid connection to utility grid is depended to voltage and frequency measurements of main grid and usage as references in secondary control. The phase differences are regulated and synchronization is performed by PLL algorithm acting as synchronization control loop. The output signal $\Delta\omega_S$ is transmitted by secondary controller through the entire system for synchronization that is completed within a few cycles and microgrid is connected to utility grid. The dynamic response of secondary control is relatively lower than primary control systems [1, 10, 15, 20].

15.3.4 Tertiary Control

The tertiary control is the highest level in hierarchical control structure, and has the lowest operation speed among others. This control level is related with economic and optimum operation of microgrid and manages power transmission through utility grid. The power transmission is controlled by adjusting voltage and frequency of DG sources in normal operation mode as presented earlier in Fig. 15.3. The control system initially detects output powers P_G, Q_G of microgrid and then compares these measurements with reference values P_{REF}, Q_{REF}. After the comparison process, the voltage and frequency references V_{REF} and ω_{REF} are obtained as presented below:

$$\omega_{REF} = k_{PP}(P_G^{REF} - P_G) + k_{iP}\int (P_G^{REF} - P_G)dt \tag{15.13}$$

$$V_{REF} = k_{PQ}(Q_G^{REF} - Q_G) + k_{iQ}\int (Q_G^{REF} - Q_G)dt \tag{15.14}$$

The parameters K_{PP}, K_{iP}, K_{PQ}, and K_{iQ} denotes control coefficients, and V_{REF} and ω_{REF} are used as reference values for secondary control procedure. The tertiary control ensures that all the DG sources are operated at equal marginal costs

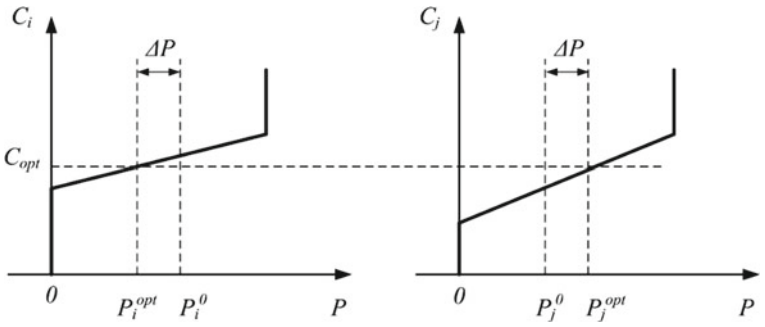

Fig. 15.10 Marginal cost detection of two separate DG source along microgrid

to provide optimum economic operation of entire microgrid. This control process is accomplished by using an algorithm that defines an optimum cost coefficient C_{opt}. The predefined coefficient selects arbitrary initial starting power values with i and j for DG sources as P_{oi} and P_{oj}. Thus, the algorithm operates iterations until the starting values are reached to optimum values and calculations are repeated to detect required output power of DG sources. Once the required power value has been calculated, the control commands are generated to force DG sources to generate desired output power. The operation principle of search algorithm is illustrated in Fig. 15.10 for i and j DG sources [10].

The searching procedure is performed for each pair of DG sources along microgrid and all the sources are forced to operate in optimum conditions. Several algorithms based on game theory and other metaheuristic algorithms have been improved to facilitate communication requirement. Thus, it is researched to easily obtain the local measurement results [1, 10, 13].

15.4 Central and Distributed Control in Microgrid

It became mandatory to use intelligent power electronics between microgrid and generation sources. These infrastructures have output stages based on CSI or VSI interfaces as discussed earlier. A microgrid control infrastructure is composed of a number of central and distributed controllers. The central controllers are connected to MGCC to improve and enhance operation features of microgrid. The MGCC determines demand power, enhancement conditions and load capacities considering the auxiliary services of distribution system. The defined enhancement and operating scenarios are performed by transmitting control signals to controllable field loads and microgrid controllers. The non-critical and flexible loads can be shaded from grid if it is required. Moreover, active and reactive power measurements should be performed instantly. In the complete distributed control approach, microgrid controllers cooperate with other controllers to transfer the available maximum power to

grid by considering market conditions. This approach is improved to tackle MGCC problems met in the systems where many DG sources exist and decisions are made locally.

Regardless the controlled microgrid characteristics and main tasks, the decision on use of central or distributed control is made considering current equipment and staff situations. The block diagrams of central and distributed control systems are shown in Figs. 15.11 and 15.12 respectively. Both systems include local functions such as local generation, demand estimation and security monitoring. The significant criteria of each system are based on calculation period, scalability, and accuracy that all are related with complexity of algorithm [6].

Several micro sources and controllable loads that may cause complexity and latencies due to numbers of DG source comprise a microgrid. The sources and loads are mostly distributed along the microgrid and they operate with low bandwidth communication system in low voltage level. The low bandwidth may cause message transmission problems when high ordered control hierarchy is used. Therefore, the complexity of control system should be considered to prevent missing of control commands and communication messages. The decision on microgrid control that are defined by different system operators can increase the node number in addition to technical complexities. Another important issue to be considered is data communication level that can be defined by different system operators to decide which parameters will be used and whether there will be any prevention policy.

The reliability is also an important issue for microgrid control system. The outcomes of any algorithm should be accurate and reliable to control the microgrid. The selection of central or distributed control approach is performed considering the requirements of microgrid and particular needs where the conditions are listed in Table 15.1 [6]. In case users have common targets and common operation conditions, the central controller will be the most appropriate for this type of microgrid. When an industrial microgrid considered, a generation provider may control all the

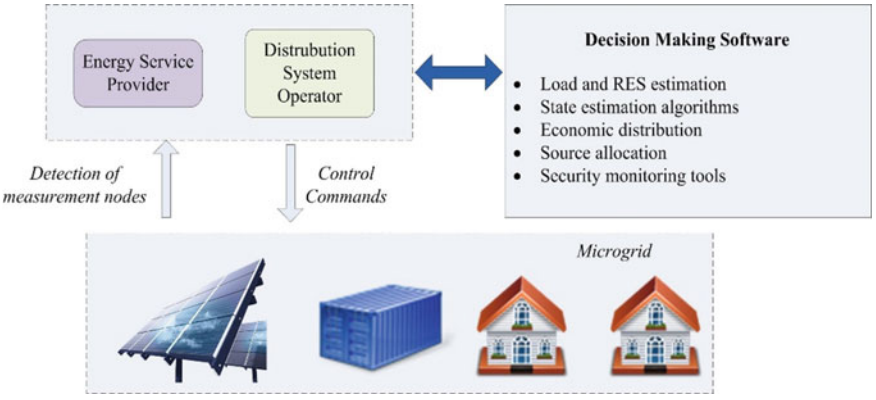

Fig. 15.11 Central controller system

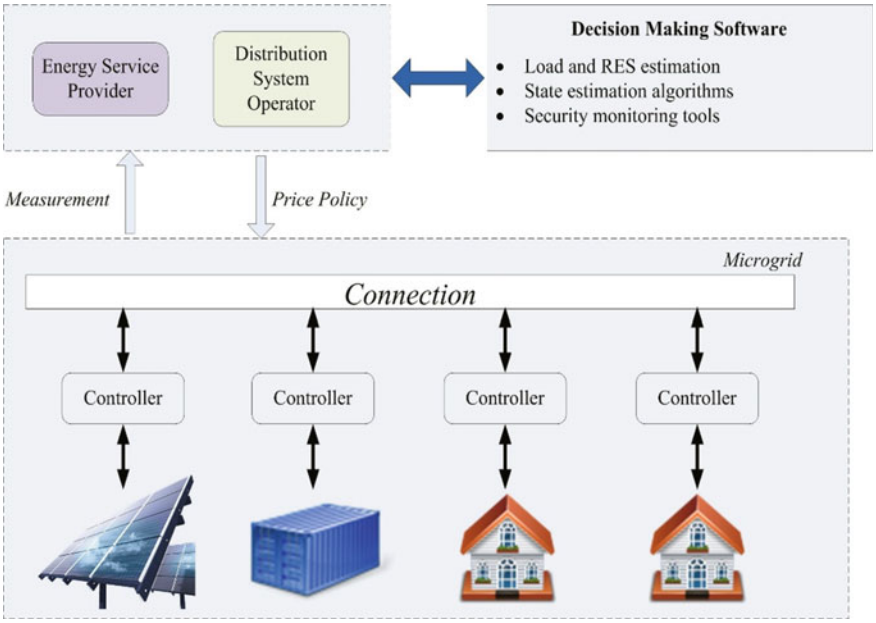

Fig. 15.12 Distributed control system

Table 15.1 Features and differences of central and distributed control systems

Feature	Central control	Distributed control
DG source ownership type	Single ownership	Joint ownership
Targets	Single and main task (i.e. cost decrement)	Each owner may have different target
Staff and source requirement	Exists	Does not exist
Market participation	Complex algorithms	Simple algorithms
New equipment installation	Requires qualified staff	Plug-and-play
Communication requirement	High	Medium
Critical system connection	Possible	Not possible

DG sources and loads, may monitor the situations of generation and consumption or may perform arrangements for economic operation.

It is possible to install faster communication infrastructure and sensor nodes by limiting the measurement and transmission node numbers as discussed earlier. Moreover, specific researches are done to decrease facilitation and cost decrement problems. A microgrid operating under market conditions and requiring competitive precautions need to be controlled by mostly independent and intelligent systems. The local DG source owners may also have different expectations such as cooling, protecting the critical loads and backups in addition to power transfer to utility grid.

A DG platform may include dozens of such neighboring small microgrids with their subgrid infrastructures. The classification of data transmission requirements and management decreases the costs and allows owners to control their microgrid in efficient ways. On the other hand, the distributed calculation technology enables plug-and-play operation of DG sources and accelerates integration to microgrid that provides flexible and secure monitoring infrastructures.

15.5 Conclusion

This chapter presents fundamental and improved control structures of microgrids. The basic control principles are presented in classification of local control, secondary control, central and emergency control, and general control methods that are related with hierarchical control concept. The local control is known as primary level control that is responsible for operating internal control loops to improve stability of microgrid. It is based on device level where physical and power electronics controls are performed. The hierarchical control is performed by using primary, secondary and tertiary level controllers along the microgrid structure to ensure maximum power transmission to utility grid in normal operation mode. Therefore, power quality of microgrid should be improved by using secondary control in addition to voltage and current improvement in primary control. The secure, reliable and sustainable control of microgrid is depended to healthy operation of hierarchical control. General or global controllers that ensure to obtain optimum power level at PCC manage the tertiary control structure. Although the basic control principles seem similar to hierarchical control infrastructure, they differ in organization scheme where hierarchical control system includes three control levels in a single microgrid to cooperate with neighbor microgrids and utility grid.

The tertiary control is required to ensure economic operation of microgrid in both operation modes. Moreover, central or distributed control strategies are considered to determine the appropriate control scheme for any microgrid. The features and selection criteria of central and distributed control schemes are tabularized in the last section. The presented researches have outlined that intelligent control systems are much more efficient on power sharing and decreasing the voltage and frequency fluctuations. The improved control methods are widely researched to enhance power quality and operation conditions of microgrids interacting neighbor microgrids and utility grid.

References

1. J.M. Guerrero, J.C. Vasquez, J. Matas, L.G. de Vicuna, M. Castilla, Hierarchical control of droop-controlled AC and DC microgrids—a general approach toward standardization. IEEE Trans. Ind. Electron. **58**(1), 158–172 (2011)

2. L. Fan, *Control and Dynamics in Power Systems and Microgrids* (Boca Raton, CRC Press Taylor & Francis Group, 2017)
3. E. Kabalci, Y. Kabalci, *Smart Grids and Their Communication Systems* (Springer, New York, 2018)
4. H. Bevrani, B. Francois, T. Ise, *Microgrid Dynamics and Control* (Wiley, Hoboken, 2017)
5. A. Kaur, J. Kaushal, P. Basak, A review on microgrid central controller. Renew. Sustain. Energy Rev. **55**, 338–345 (2016)
6. N. Hatziargyriou, *Microgrid: Architectures and Control* (Wiley, India, 2014)
7. A. Kwasinski, W. Weaver, R.S. Balog, *Microgrids and Other Local Area Power and Energy Systems* (Cambridge University Press, Cambridge, 2016)
8. I.J. Balaguer, Q. Lei, S. Yang, U. Supatti, F.Z. Peng, Control for grid-connected and intentional islanding operations of distributed power generation. IEEE Trans. Ind. Electron. **58**(1), 147–157 (2011)
9. X. Sun, Y. Hao, Q. Wu, X. Guo, B. Wang, A multifunctional and wireless droop control for distributed energy storage units in islanded AC microgrid applications. IEEE Trans. Power Electron. **32**(1), 736–751 (2017)
10. A. Bidram, V. Nasirian, A. Davoudi, F.L. Lewis, Control and modeling of microgrids, in *Cooperative Synchronization in Distributed Microgrid Control* (Springer International Publishing, Cham, 2017)
11. Q. Shafiee, J.M. Guerrero, J.C. Vasquez, Distributed secondary control for islanded microgrids—a novel approach. IEEE Trans. Power Electron. **29**(2), 1018–1031 (2014)
12. X. Ma, P. Yang, H. Dong, J. Yang, Y. Zhao, Secondary control strategy of islanded micro-grid based on multi-agent consistency. (2017), pp. 1–6
13. E.A.A. Coelho et al., Small-signal analysis of the microgrid secondary control considering a communication time delay. IEEE Trans. Ind. Electron. **63**(10), 6257–6269 (2016)
14. N. Moreira, J. Lazaro, U. Bidarte, J. Jimenez, A. Astarloa, On the utilization of system-on-chip platforms to achieve nanosecond synchronization accuracies in substation automation systems. IEEE Trans. Smart Grid **8**(4), 1932–1942 (2017)
15. A. Bidram, A. Davoudi, F.L. Lewis, J.M. Guerrero, Distributed cooperative secondary control of microgrids using feedback linearization. IEEE Trans. Power Syst. **28**(3), 3462–3470 (2013)
16. M.H. Moradi, M. Eskandari, S.M. Hosseinian, Cooperative control strategy of energy storage systems and micro sources for stabilizing microgrids in different operation modes. Int. J. Electr. Power Energy Syst. **78**, 390–400 (2016)
17. L.I. Minchala Avila, L.E. Garza Castanon, A. Vargas Martinez, Y. Zhang, A review of optimal control techniques applied to the energy management and control of microgrids. Procedia Comput. Sci. **52**, 780–787 (2015)
18. Z. Yu, Q. Ai, J. Gong, L. Piao, A novel secondary control for microgrid based on synergetic control of multi-agent system. Energies **9**(4), 243 (2016)
19. A. Bidram, A. Davoudi, Hierarchical structure of microgrids control system. IEEE Trans. Smart Grid **3**(4), 1963–1976 (2012)
20. O. Palizban, K. Kauhaniemi, Hierarchical control structure in microgrids with distributed generation: island and grid-connected mode. Renew. Sustain. Energy Rev. **44**, 797–813 (2015)

Chapter 16
Distributed Control of Microgrids

Ahmet Karaarslan and M. Emrah Seker

Abstract The aim of this chapter discusses the relationship between hierarchical control and review of distributed control systems that is used in microgrids. The microgrids are differs from the conventional power systems. Because of the widespread use of advanced control technologies with features such as power electronics devices, detection/measurement applications, and communication infrastructures. These features of microgrids make it easier for renewable energy sources that are included in the power systems. Therefore, distributed control methods are applied in addition to centralized and de-centralized controls for reliable operation of the system in microgrids and between different microgrids. This section discusses the features of these methods.

Keywords Distributed control · Microgrids · Renewable energy systems

16.1 Introduction

In this study, distributed control methods of microgrids are discussed and compared with other methods. Renewable energy sources are available free of charge and they do not have any fuel transportation costs. However, it is not reliable because of its dependence on weather, season and time of day. With renewable energy resources becoming more efficient and smarter every day, their reliable control has become inevitable. When these renewable energy sources are connected or connected to an existing power distribution system, these sources of energy named 'Distributed Energy Resources' (DERs) or 'Distributed Generations' (DGs). These distributed

A. Karaarslan (✉) · M. E. Seker
Department of Electrical and Electronics Engineering, Yildirim Beyazit University, Ankara, Turkey
e-mail: akaraarslan@ybu.edu.tr

M. E. Seker
e-mail: emrah-seker@hotmail.com

N. Mahdavi Tabatabaei et al. (eds.), *Microgrid Architectures, Control and Protection Methods*, Power Systems,
https://doi.org/10.1007/978-3-030-23723-3_16

generators that form small electrical networks called 'Microgrids' (MGs), are smaller in terms of installed power, but they are very effective in their performance.

Since centralized control of the reactive and active power distribution of distribution system is costly and difficult with the addition of distributed generators, it is convenient to distribute power distribution between distributed generators with distributed control. For this purpose, it is the common method of performing conventional droop control for both frequency and voltage between generators distributed in the same way as synchronous generator control. This method usually works well for active power sharing and frequency control, but it causes an unstable network because the grid voltage and reactive power support mechanism are poor.

Some of the control strategies are used for reactive power compensation based on Lyapunov functions; result in damping system voltages using only local measured parameters.

Conventional droop-based algorithms are still considered to be the most effective in terms of the stability of network voltage and reactive power sharing. The basis of this acceptance lies in the fact that the structures of the pendant controllers are simpler, do not require additional communication infrastructure, are not centralized and their performance is similar to synchronous generators [1–5]. In order to further improve the Droop Controller and bring its performance closer to that of a synchronous generator, it has been proposed to include the droop inverters and the virtual inertial load. These inverters make the oscillation equation a system to behave like conventional generators.

Power sharing between distributed generators on the algorithms studied; centralized, decentralized and distributed control algorithms [6]. In studies conducted with central control systems, particle swarm algorithms, mixed integer linear algorithms and genetic algorithms are used. However, as the number of distributed generators increased, the performance of these control systems started to decrease [7]. In the studies conducted with decentralized control systems, the principle of adding virtual impedance in the output of distributed generators is studied.

Therefore, the most appropriate method for power sharing and control between distributed generators is distributed control systems. They require simple communication and control equipment; they do not lose operational functionality even when the number of distributed generators is increased by a large number [6]. However, traditional droop control does not work efficiently with distributed generators. As more microgrids are introduced in the future, this problem will become even more severe.

Control of microgrid is currently developed in a 3-level hierarchical control [8]. The primary control of the microgrid provides a general setpoint of the distributed generators to keep the microgrid constant in the tolerance band at the required nominal frequency and voltage. The secondary control reacts more slowly than the primary control and brings the minor deviations of the primary controller to the true value. Tertiary control is slower than primary and secondary control and specifies the reactive and active power flow between main grids and the microgrids or other microgrids [9, 10].

Therefore, central control units may not be able to operate under large numbers of DG units. The reasons are listed below:

(1) The absence of a special central control unit;
(2) When the number of units to be controlled is high, the calculation load increases;
(3) Communication is needed due to geographical area width;
(4) Redesign demands for modification is made only on one unit;
(5) Data sharing complexity;
(6) The undefended of the central controller.

16.2 Control Structure Overview

16.2.1 Control Needs

Difficulties and requirements of microgrid control are listed below.

16.2.1.1 Contact Based

Distributed control techniques depend on the existence of communication between hierarchical units in a microgrid. However, not all units in microgrid need to intercommunicate with other units.

16.2.1.2 Topological and Time Variance Changes

In a communication network in microgrid, a time variant can be used depending on reasons such as weakening of wireless signals. However, topological changes in the network, such as separation of DG units and the addition of new units, may also disturb the system performance.

16.2.1.3 Stability and Low Inertia Problems for New Components

Power electronic devices with fast switching enable most DG units to be connected to the grid. While these features can improve the performance of the system, it is difficult to balance the voltage and frequency if there are no suitable control elements in the island mode operation. This is the reverse of conventional networks with high inertia synchronous generators limiting the deflection rate of the system frequency (Table 16.1).

Table 16.1 Summary of the mainly microgrid functions [11]

Control functions	Descriptions
Islanding/grid-connected management	The Microgrid Management System (MGMS) can smoothly changeover between grid and island mode
Black start	Electrical restoration occur especially in island mode after the microgrid is disconnected from the main grid
Electricity market participation	MGMS has an interface for energy, ancillary services and capacity in the electricity market
Fault detection and protection	MGMS communicates with local protection devices such as relays, circuit breakers and sensors to detect and isolate errors
Operation cost optimization	The MGMS optimally adjusts the production cost and the load according to market information by estimating the load and weather information
Voltage/VAr control	The MGMS adjusts the participation rates of the DG units to the reactive power control for voltage regulation
Frequency control	The MGMS watches and adjusts the active output power of the DG units to keep the frequency at the setpoint

16.2.2 Control Hierarchy

The control hierarchy is closely related to the distributed control, it is difficult to evaluate separately. In the network containing many DG units, hierarchical control is generally used as shown in Figs. 16.1 and 16.2 [12]. A hierarchical control structure has three levels as explained below.

16.2.2.1 Primary Control

The primary control gives the fastest response because it is the first control level. It ensures the system frequency and voltage are at setpoints. The primary control works according to locally measured data and does not require communication. At this control level, output control power sharing, island mode operation detection and controller modes are changed [8, 12, 16, 17]. Energy storage units can help control this by providing strengthening while power fluctuations. Natural relationship between power sharing and voltage regulation makes this approach disadvantageous. This disadvantage can be overcome by secondary control.

Besides, some studies consider communication-based approaches such as average load sharing, active load sharing [9] and master-slave system [18]. It is understood that high-bandwidth communications connections are required for better voltage regulation, rapid response in transient situations, and improved load sharing [9].

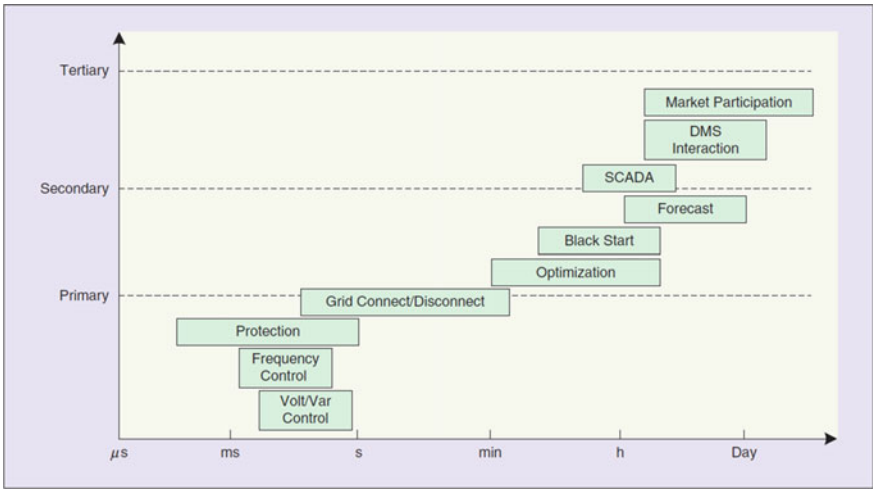

Fig. 16.1 The time rule of hierarchical control functions [8, 10, 13, 14]

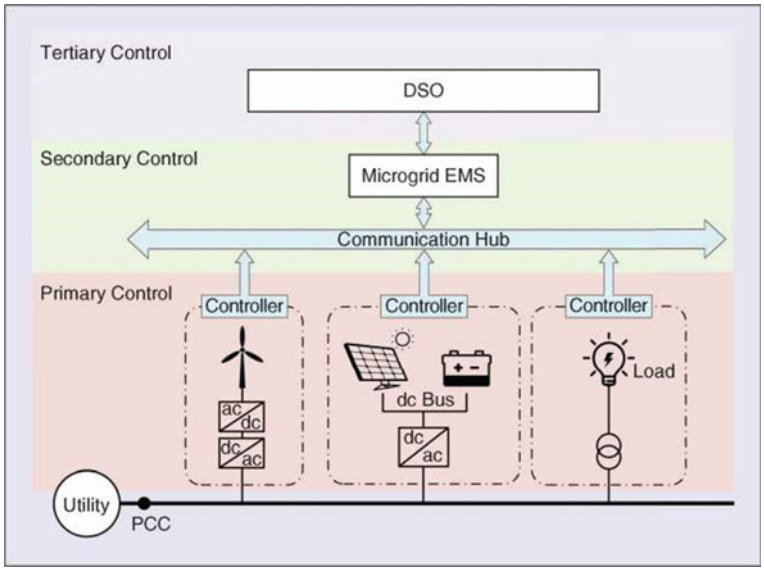

Fig. 16.2 The hierarchies of microgrid control [10, 13, 14, 15]

16.2.2.2 Secondary Control

It is used for the optimum operation of individual DG units that known as centralized control. The Energy Management System (EMS) ensures power quality, regulates voltage, compensates for frequency deviations, enables power sharing and primary control to return to setpoints [19–22]. In addition, EMS is directly connected to the distribution management system (DMS) via the communication link. In addition, it may have different effects, such as secondary control, reactive power sharing and loss reduction.

One of the factors facilitating the synchronization of the microgrid with the home network is the secondary control. In [23], a central secondary controller was developed to maintain the main busbar voltage at the desired level. In Ref. [11] a function-based method suggests for secondary control. A potential function defined by the central controller specifies that for each DG units that use the measured values from the other DG units as inputs for this function in this method.

The secondary control must be set to take part after the primary control. Separation of this first control and double control requires less bandwidth for communication [24]. A central controller must ensure that the main system operates as smoothly as possible during main faults or when switching to island mode [22]. With this approach, the secondary control makes the main control device the most important part necessary for the safe operation of the microgrid.

16.2.2.3 Tertiary Control

The slowest control level is Tertiary control that is activated after the primary and secondary control and enables the system to operate at setpoints based on other system requirements to ensure system stability over the long term. It is part of the main controller to manage multiple microgrids.

16.2.3 Distributed Control in Control Hierarchy

The primary control generally does not require communication and is locally effective. Secondary and tertiary control can be centralized or distributed. Secondary and tertiary control is based on central controls requiring communication system. Although the application of secondary control to central control has gained value in recent years, these methods are expensive and slow due to the need for a communication system.

16.3 Distributed Control Methods

The common problem of distributed control is to solve the problem of optimization of distributed system with the existing communication infrastructure. For this reason, the separation between distributed control techniques is not clear. The main separation consists of using alternative way for the problem.

16.3.1 Model Prediction Control (MPC)—Based Method

The Model Prediction Control (MPC) is an advanced process control method used to control a process where there are restrictions. Firstly, it is used in the control of processes in industrial plants such as petrochemical plants, and in recent years it has been used in the control of power electronic devices. Model prediction controllers are based on dynamic models of the process; often, empirical models obtained by system identification. The main advantage of the MPC is that it allows real-time work to take into account as well as to optimize its future work. This is achieved by repeating a limited time horizon over time so that the current time zone differs from the linear quadratic regulator (LQR). By optimizing the LQR, the MPC is capable of performing control actions by estimating the future operating state. It is not capable of predicting the future operating status of conventional PID controllers. Although it continues to work with an analog circuit specially designed to achieve faster response times with MPC, it generally implemented as a digital control [25].

MPC is an actually using standard in industry for controlling big plants [26, 27]. MPC offers plenty of alluring properties, such as it deals with the multivariate control problems, easy to set up, open to assessing constraints.

MPC is a discrete-time control method that minimizes cost function. The cost function includes variables related to the cost of the system. Each step of the MPC involves calculating the control sequence of N, if it is assumed that N is the prediction horizon. Nevertheless, initial input is applied and the others are reconditioned in the next step. The same operation repeats at every cycle.

The study in [28] presents the application of an MPC-based algorithm in unstable microgrids for reactive power control. In this method, using a linear model and an MPC scheme, estimates the voltage profile at the next time steps. It makes reactive power and voltage control by determining setpoints to obtain an appropriate voltage profile.

A MPC-based algorithm is recommended for controlling microgrid DG units in reference [29]. This algorithm decomposes the optimization problem as a temporary sub-problem and a fixed-state sub-problem. This distinction reduces the time to solve the steady-state problem and the calculation tasks.

16.3.2 Consensus-Based Method

Distributed control optimization is focused by distributed computing, where every unit of microgrid exactly knows of the common goal and examining it under the term compromise. A promising consensus approach about expandability and scalability for the solution of distributed optimization problems are given in [30, 31]. The purpose of the consensus is that various DG units approach only one value. A consensus-based approach obtains universal optimal solution without the need for a specific unit using restricted, time-varying communication among DG units. Etemadi et al. [30] and Olfati Saber et al. [4] and a new distributed multicenter based load restoration algorithm [32] are presented in a distributed environment. This algorithm relies on each unit to communicate with neighboring units to explore global information to provide consensus.

16.3.3 Multi Agent-Based Method

Multi-agent based system (MAS) is another distributed control method. Multi-agent based system works through agents that can move and communicate on the environment. They are autonomous in accordance with their purpose and have restricted information about the environment [33]. A smart agent response to alteration in the environment, looks for initiatives, and is open to communication. The situation estimation in Microgrid can use to address limited information [34, 35]. Although agents can communicate according to their autonomy, most of the control is carried out not globally.

Agents can classify as central, de-centralized and hierarchical. Central Agent Architecture (CAA) consists of a single agent. De-centralized Agent Architecture (DAA) consists of several non-communicating agents. Hierarchical Agent Architecture (HAA) consists of different agent layers.

In the HAA, information flow occurs between layers. Demand transmits from upper layer to the lower layer. In addition to the information flow in the layers, different agents on the same layer can communicate one another [36]. Figure 16.3 shows an example of HAA.

MAS is applicable for tough complex power systems with many different types of agents.

This method is open to interaction and most of the information required used locally. MAS used for control and management as microgrids must work in island mode.

MAS applied in the areas of control, monitoring, protection and modeling of power systems [37]. A comprehensive overview of the challenges and technologies in MAS applications: A comprehensive overview of suitable study and practices in MGs are given in [37, 38]. Simulation of agent-based MGs conjecture the connection of MG and the communication infrastructure to the same simulator.

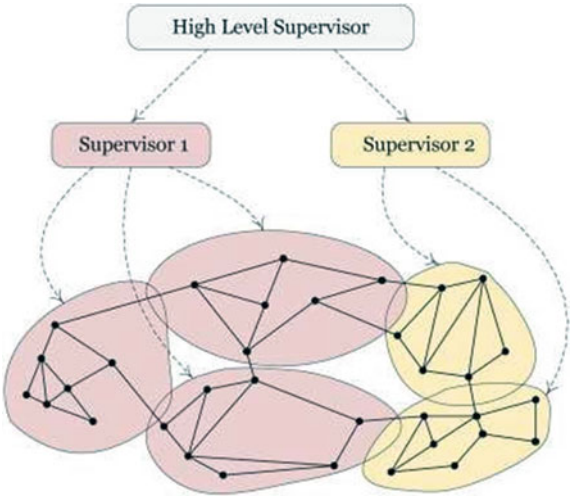

Fig. 16.3 Example of hierarchical agent architecture flow diagram [16]

Reference [39] applies the neighbor-to-neighbor three-step communication layout to apply the microgrid MAS control architecture. The purpose of the control is to maintain power balancing and to keep system voltage within limits. The hierarchical hybrid control proposed in Reference [40, 41] takes over the task of control for the dynamic response of MG. This ensures that the system voltage is within the limits and increases the efficiency of the microgrid.

16.3.4 Decomposition-Based Method

There are various decomposition methods in power systems control, including Auxiliary Problem Principle (APP), Alternating Direction Method (ADM) and Predictor-Corrective Proximal Multiplier method (PCPM) [42, 43, 13, 44, 45, 46, 47, 48, 48]. These techniques established on the solving the original optimization problem by iterative method. Although there are different methods for identifying the sub-problems in these methods, there are different applications based on different sensitivity factors and controllability.

16.3.5 Droop-Based Method

In synchronous generators, there is a power balance between the input power and the output power. An imbalance in this power balance causes a deviation in the frequency. Similarly, the reactive power variation at the output causes the voltage value to deviate. This deviation is eliminated by adjusting the excitation current

of the synchronous generator. This can be generated electronically for DG Units. The Droop control method is a widely used method due to the power balance of synchronous generators.

Although Droop control does not have the advantages of many modern control methods, the most important advantage is that there is no need for communication because the measurements are local. Its main effect is that it cannot keep the frequency constant and is not suitable for non-linear loads. Recently, different methods have been studied to improve the steady-state performance of droop control (Table 16.2).

16.4 Distributed Control Methods Applications

16.4.1 Primary Control

Central controller allows the units to operate at setpoints and ignore small fluctuations in frequency. The task of local controllers is to eliminate large frequency components in the system. A multi-module inverter system using on distributed control explore to enhance the stability of the renewable energy resources [49]. The drop control is another method for primary control.

16.4.2 Voltage Regulation Coordination

The purpose of voltage regulation is to get a suitable voltage profile. Voltage regulation can perform locally or centrally. Differences between bus-bar voltages can occur due to the impedance of high current carrying lines. A distributed or centralized controller updates the reagent setpoints of each DGs for voltage regulation. However, due to high line resistance in low and medium voltage networks, it is necessary to control the active power in addition to the reactive power.

16.4.3 Economic Power Dispatch Coordination

The interdepartmental coordination of the power system and the economic operation of the system are significant matters. O ptimal power flow (OPF) generally focuses on the solution of this problem. OPF has been studied in the power system since the 60s [50]. However, the OPF does not guarantee the closest approximation to the absolute best. Also, generally distributed optimization methods ignore time delays caused by communication links. Some methods take into account the time delays of the communication connections, but the limit sets of each generator must be the same. Reference [51] formulates distributed OPF with discrete variables and [48]

Table 16.2 Primary and secondary control advantages and disadvantages

Level	Control technique	Advantages	Disadvantages
Primary control level	Conventional Droop Control	Simple control architectures to install	Imprecise reactive power distribution
	Q–V dot droop	Stability is maintained	Applicable for highly inductive transmission lines
			Insufficient control ability for non-linear load
	VPD/FQB based Droop	Sufficient control ability in highly resistive line	Dependent on system parameter variation
		Easy to install	Insufficient control ability for nonlinear load
	Multi-variable Based	Maintaining Sufficient voltage and frequency regulation with accurate power sharing with different output impedance	Installation difficulty in large system
	Universal Droop		
	Pining Droop		
	Adaptive Voltage Droop	Sufficient voltage regulation and power sharing even with heavy load	System variables must be defined before
	Voltage-current droop	Applicable for high resistive network of microgird	Complex architecture for practical installation
		Accurate power balancing	
	Virtual Output Impedance with Droop Control	Improves the control ability of power sharing	Stable operation is the most important issue

(continued)

Table 16.2 (continued)

Level	Control technique	Advantages	Disadvantages
	Virtual Flux Drooping	Sufficient frequency regulation	Slow dynamic control ability
			Not applicable for wide system
	Angle Droop	Sufficient frequency regulation	Insufficient power sharing
	Hybrid/Signal Injection based droop	Independent of system parameter variation	Complex system architecture to install
		Suitable for non-liner and linear loads	Insufficient voltage regulation due to harmonic issues
	Non-linear load sharing based droop	Exactly removes the voltage harmonics and shares the current harmonics	Insufficient voltage regulation
			Dependent on system parameters
	Predictive control based algorithm	Sufficient for non-linear system, less switching frequency	Requires complex computing
	Predictive power control	Proper current control with relatively lesser THD Total Harmonic Distortion (THD) and harmonics	Complex control architecture
			Dependent of system parameter variations
	GPS -based primary control	Using GPS timing technology and removing the transformation errors resulting from Park/ inverse Park Transformations	Need to incorporate the GPS timing into grid connected control applications
		Independent of system parameters	

(continued)

Table 16.2 (continued)

Level	Control technique	Advantages	Disadvantages
	Consensus-Control	Increase flexibility, supports plug- and play, uses low bandwidth communication networks	Voltage convergence is the most important issue
	Consensus-based p–f droop Control		Need to choose cluster parameters correctly to establish stability condition
Secondary Control Level	Consensus-based distributed voltage control	Advanced backup and easy installation functionality increase flexibility	Convergence rate is a great concern
	Consensus-based distributed frequency control	Providing low-bandwidth communications	System stability affected by the system parameters
	MAS Control	Capable of handling decentralized data updating and uncertain disturbances, causing a faster decision making method and action	The coordination and synchronization method necessitates the exchange of data among agents based on particular communication protocols
		Increase computational and flexibility efficiency	
	Distributed finite time control	Parametric uncertainties, non-modelable dynamics and stability against disturbances that disrupt system reliability	Cannot ensure robust stability
			Cannot restore voltage/frequency in a finite time separately

(continued)

Table 16.2 (continued)

Level	Control technique	Advantages	Disadvantages
	Distributed Average Proportional Integral based on Consensus	Provides easy-to-install architecture with voltage and frequency regulation combined with precise reactive and active power sharing	Synchronization problem of frequency and voltage restoration
	Model Predictive Control	It can maintain a regular agreement as well as a consistent study of uncertainties such as time-varying communication methods, parameter perturbations and load disturbances	Complex configuration, reactive power sharing and restraining circulating currents require further analysis
	Feedback Linearization	More reliable	Frequency restoration depends on system parameters
		Feedback linearization converts secondary voltage and frequency controls to the first test synchronization problem	
	Fuzzy Logic based secondary control	Independent for parameter changing	Slow control process
		Suitable for non-linear system	
	GPS based secondary control	The time constant at the secondary level is too big to work with a low bandwidth communication network	Need to incorporate the GPS timing into grid connected control applications
		Independent of system parameter variation	

suggests a coarse-grained OPF. A comparison of three separation-based methods [52] is provided.

In the literature; the coordination of solar and wind systems with the distributed MPC [53], the most appropriate way of carrying electric vehicles [54], Field Correction Error (ACE), the setting of each generator to the set-point by consensus-based algorithm [55], the center of autonomous and identical agents In the case of non-microgrids, the economic operation of DG units [56], recommendations for solving the distributed central economic dispatch problem (EDP) using the incremental cost consensus (ICC) algorithm are included.

16.4.4 Frequency Stabilization Coordination

Frequency control performed when the frequency is independent and the DG units connect electronically with each other. A common frequency of different units provides by frequency control. The presence of an independent frequency setpoint for each unit is essential for frequency control. It can also operate in a certain range for each unit, power and bus voltage.

There is a connection between the mechanical rotational speed and electric frequency, which results from the structures of synchronous generators. In contrast, most of the renewable energy sources do not have this connection. This puts renewable energy resources at a disadvantage in terms of frequency regulation.

In the literature, there are attempts to contribute to the frequency control by providing virtual inertia by simulating the operation of synchronous generators for renewable energy sources. Operation of the power control loop by adding a term related to frequency time derivative is an example of making frequency controls for the generation of virtual inertia [17].

Although the drop control has some disadvantages, it makes it advantageous to implement the distributed MPC for consensus-based frequency control for the optimal coordination of the frequency in multilink HVDC systems [40] and for the multi-terminal HVDC [57].

In addition to frequency regulation, secondary control apply to return the microgrid frequency to normal operating conditions. In the common power system, the automatic generation controller (AGC) and the load frequency controller (LFC) work to bring the system frequency to.

16.5 Differences Between Centralized and Decentralized Control

As the distributed microgrid control technologies progress, both academia and industry are increasingly benefiting. Here are some benefits of distributed control methods compared to those that are centrally controlled.

16.5.1 Communications

Generally, energy programming on secondary control performs 15 min periods [58]. So that the primary control time interval control action must be smaller than that in the secondary control. Many centralized primary control techniques require real-time monitoring of system voltage and current signals [59]. Therefore, the performance of the central control is highly responsive to communication delay and packet loss [14]. Furthermore, central control is based on a star network topology to communicate with field devices; this is not possible in a large MGs due to geographical and communication limitations. For distributed control, the droop-based primary control application eliminates the need for communication between Voltage Source Inverters (VSIs) [14]. The drop-controlled VSIs can operate to relieve load and voltage changes because they work based on local measurements. This eliminates the communication constraint for distributed control. Furthermore, implementation of different algorithms makes global system information reachable to area tools under several topologies such as collector, ring, tree and knitting topologies.

16.5.2 Scalability

Central control techniques need for online observing and computation for power assignment in the primary control layer. System size is limited by communication topology and bandwidth. For dispersed Microgrid, however, pendant-based control techniques allow autonomous operation of DG units. For the secondary control, as the number of controllable devices increases, the optimization problem will be complicated by the nature of the MILP, and the convergence time will increase in logarithmic manner [60, 61]. For a centrally controlled Microgrid, more computing infrastructure is required to meet system growth. System growth will result in an overload of the Microgrid central control system. In one study, the scalability of scattered energy programming algorithms has been investigated [62]. Here, It shows a linear correlation between the convergence time and the number of devices that can be controlled and scaled better.

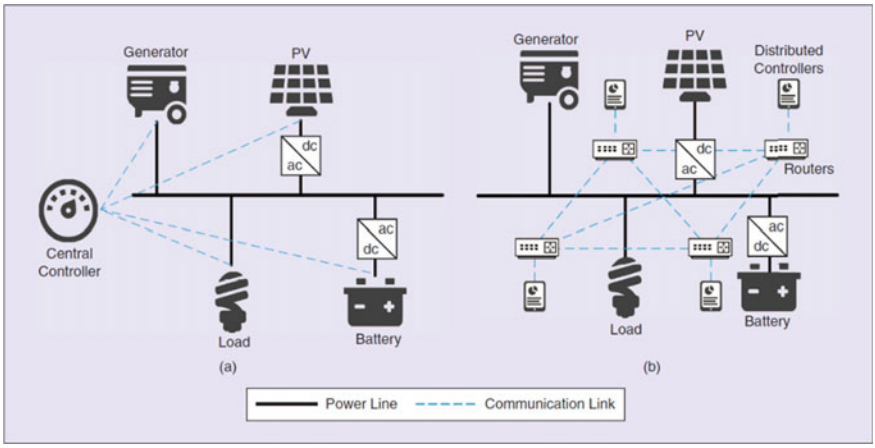

Fig. 16.4 **a** A centralized control framework, **b** A distributed control framework [31, 4, 15, 63, 64]

16.5.3 Reliability and Resiliency

The supremacy of distributed control is mainly due to reliable, flexible, controllable and smart control algorithms (Fig. 16.4).

16.6 Conclusion

In recent years, an increasing number of microgrids have been engaged and DG units and small renewable energy sources have accelerated the entry into the system. These resources can be spread over a wide area due to the distance between them. This is not easy to control the distributed system and shows some differences between traditional control systems. Distributed control is preferred in order to overcome this difficulty in microgrids and to reduce calculation loads. Microgrids use the data and communication infrastructure necessary for control to ensure the optimal operation of the system. In this chapter, distributed control techniques and basic architecture used in microgrids are discussed together with hierarchical control methods. The advantages and disadvantages of the existing techniques were compared with hierarchical control methods in the table. In addition to the difficulties encountered in microgrid applications of distributed control, it will continue to be developed and used thanks to its contribution to system operation.

References

1. C. Sao, P. Lehn, Autonomous load sharing of voltage source converters. IEEE Trans. Power Del. **20**(2), 1009–1016 (2005)
2. M.C. Chandorkar, D.M. Divan, R. Adapa, Control of parallel connected inverters in standalone AC supply systems. IEEE Trans. Ind. Appl. **29**(1), 136–143 (1993)
3. C.L. DeMarco, C.A. Baone, Y. Han, B. Lesieutre, Primary and secondary control for high penetration renewables. Future Grid Initiative White Paper (2012)
4. Y.A.R.I. Mohamed, E. El Saadany, Adaptive decentralized droop controller to preserve power sharing stability of paralleled inverters in distributed generation microgrids. IEEE Trans. Power Electron. **23**(6), 2806–2816 (2008)
5. K. Tan, P. So, Y. Chu, M. Chen, Coordinated control and energy management of distributed generation inverters in a microgrid. IEEE Trans. Power Del. **28**(2), 704–713 (2013)
6. J. Guerrero, L. Garcia de Vicuna, J. Matas, M. Castilla, J. Miret, Output impedance design of parallel-connected ups inverters with wireless load-sharing control. IEEE Trans. Ind. Electron. **52**(4), 1126–1135 (2005)
7. N. Hatziargyriou, H. Asona, R. Iravani, C. Marnay, Microgrids. IEEE Power Energy Mag. **5**(4), 78–94 (2007)
8. H. Karimi, H. Nikkhajoei, M.R. Iravani, Control of an electronically-coupled distributed resource unit subsequent to an islanding event. IEEE Trans. Power Del. **23**(1), 493–501 (2008)
9. X. Sun, L.K. Wong, Y.S. Lee, D. Xu, Design and analysis of an optimal controller for parallel multi-inverter systems. IEEE Trans. Circuits Syst. II, Exp. Briefs **53**(1), 56–61 (2006)
10. J.M. Guerrero, J.C. Vasquez, J. Matas, L.G. de Vicuna, M. Castilla, Hierarchical control of droop-controlled AC and DC microgrids—a general approach towards standardization. IEEE Trans. Ind. Electron. **58**(1), 158–172 (2011)
11. W. Bower, D. Ton, R. Guttromson, S. Glover, J. Stamp, D. Bhatnagar, J. Reilly, The advanced microgrid integration and interoperability. Sandia National Laboratories, Albuquerque, NM, Report SAND2014–1535 (2014)
12. M. Begum, M. Abuhilaleh, L. Li, J. Zhu, Distributed secondary voltage regulation for autonomous microgrid. in *20th International Conference on Electrical Machines and Systems (ICEMS)*, Sydney, Australia, pp. 1–6, 11–14 August 2017
13. C.X. Dou, B. Liu, Multi-agent based hierarchical hybrid control for smart microgrid. IEEE Trans. Smart Grid **4**(2), 771–778 (2013)
14. Y. Han, H. Li, P. Shen, E.A.A. Coelho, J.M. Guerrero, Review of active and reactive power sharing strategies in hierarchical controlled microgrids. IEEE Trans. Power Electron. **32**(3), 2427–2451 (2017)
15. N. Rahbari Asr, Y. Zhang, M.Y. Chow, Cooperative distributed scheduling for storage devices in microgrids using dynamic KKT multipliers and consensus networks. in *Proceedings of IEEE Power and Energy Society General Meeting* 9 (2015), pp. 1–5
16. A. Mehrizi Sani, M. Yazdanian, Distributed Control Techniques in Microgrids. IEEE Trans. Smart Grid. **5**(6), 2901–2909 (2014)
17. F. Katiraei, M.R. Iravani, P.W. Lehn, Micro-grid autonomous operation during and subsequent to islanding process. IEEE Trans. Power Del. **20**(1), 248–257 (2005)
18. J.A.P. Lopes, C.L. Moreira, A.G. Madureira, Defining control strategies for microgrids islanded operation. IEEE Trans. Power Syst. **21**(2), 916–924 (2006)
19. F. Gao, M.R. Iravani, A control strategy for a distributed generation unit in grid-connected and autonomous modes of operation. IEEE Trans. Power Del. **23**(2), 850–859 (2008)
20. Y.J. Cheng, E. Sng, A novel communication strategy for decentralized control of paralleled multi-inverter systems. IEEE Trans. Power Electron. **21**(1), 148–156 (2006)
21. M. Prodanovic, T.C. Green, High-quality power generation through distributed control of a power park microgrid. IEEE Trans. Ind. Electron. **53**(5), 1471–1482 (2006)
22. L. Dimeas, N.D. Hatziargyriou, Operation of a multiagent system for microgrid control. IEEE Trans. Power Syst. **20**(3), 1447–1455 (2005)

23. A. Mehrizi Sani, R. Iravani, Secondary control of microgrids: Application of potential functions. in *Proceedings of CIGRE Session*, Paris, France (2010), pp. 1–8
24. Angela Chuang, Mark McGranaghan, Mack Grady, Master controller requirements specification for perfect power systems (as outlined in the Galvin electricity initiative). 3rd Edition, EPRI, Chicago, IL, USA, 45-83 (2007)
25. M. Savaghebi, A. Jalilian, J. Vasquez, J. Guerrero, Secondary control scheme for voltage unbalance compensation in an islanded droop-controlled microgrid. IEEE Trans. Smart Grid **3**(2), 797–807 (2012)
26. B. Marinescu, H. Bourles, Robust predictive control for the flexible coordinated secondary voltage control of large-scale power systems. IEEE Trans. Power Syst. **14**(4), 1262–1268 (1999)
27. Final report on the August 14, 2003 blackout in the United States and Canada: Causes and recommendations. U.S.-Canada Power System Outage Task Force, Tech. Rep. https://www.energy.gov/sites/prod/files/oeprod/DocumentsandMedia/BlackoutFinal-Web.pdf
28. P.M. Namara, R.R. Negenborn, B.D. Schutter, G. Lightbody, Optimal coordination of a multiple HVDC link system using centralized and distributed control. IEEE Trans. Control Syst. Technol. **21**(2), 302–314 (2013)
29. M. Moradzadeh, R. Boel, L. Vandevelde, Voltage coordination in multi-area power systems via distributed model predictive control. IEEE Trans. Power Syst. **28**(1), 513–521 (2013)
30. M. Ilic-Spong, J. Christensen, K.L. Eichorn, Secondary voltage control using pilot point information. IEEE Trans. Power Syst. **3**(2), 660–668 (1988)
31. A. Etemadi, E. Davison, R. Iravani, A decentralized robust control strategy for multi-der microgrids—Part I: Fundamental concepts. IEEE Trans. Power Del. **27**(4), 1843–1853 (2012)
32. R. Olfati Saber, A.A. Fax, R.M. Murray, Consensus and cooperation in networked multi-agent systems. Proc. IEEE **95**(1), 215–233 (2007)
33. R.P. Agaev, P.Y. Chebotarev, The matrix of maximum out forests of a digraph and its applications. Autom. Remote Control **61**(9), 1424–1450 (2000)
34. T. Keviczky, F. Borrelli, K. Fregene, D. Godbole, G.J. Balas, Decentralized receding horizon control and coordination of autonomous vehicle formations. IEEE Trans. Control Syst. Technol. **16**(1), 19–33 (2008)
35. Y. Xu, W. Liu, Novel multiagent based load restoration algorithm for microgrids. IEEE Trans. Smart Grid **2**(1), 152–161 (2011)
36. S. Russell, P. Norvig, *Artificial Intelligence: A Modern Approach*, 2nd edn. (Prentice Hall, Upper Saddle River, NJ, USA, 2003)
37. F.C. Scheweppe, J. Wildes, Power system static-state estimation, part I: Exact model. IEEE Trans. Power App. Syst. **89**(1), 120–125 (1970)
38. J.J. Grainger, W.D. Stevenson, *Power System Analysis* (McGraw-Hill, New York, NY, USA, 1994)
39. R. Negenborn, B. De Schutter, J. Hellendoorn, Multi-agent model predictive control: A survey. Delft Center for Systems and Control , Delft University of Technology, Delft, The Netherlands, Tech. Rep. 04–010 (2004)
40. S. McArthur et al., Multi-agent systems for power engineering applications—Part I: Concepts, approaches, and technical challenges. IEEE Trans. Power Syst. **22**(4), 1743–1752 (2007)
41. M. Falahi, K. Butler Purry, M. Ehsani, Dynamic reactive power control of islanded microgrids. IEEE Trans. Power Syst. **28**(4), 3649–3657 (2013)
42. S.D.J. McArthur et al., Multi-agent systems for power engineering applications—Part II: Technologies, standards, and tools for building multi-agent systems. IEEE Trans. Power Syst. **22**(4), 1753–1759 (2007)
43. N. Cai, J. Mitra, A decentralized control architecture for a micro- grid with power electronic interfaces. in *Proceedings North America Power Symposium (NAPS)*, Arlington, TX, USA (2010), pp. 1–8
44. A. Nedic, A. Ozdaglar, Distributed subgradient methods for multi-agent optimization. IEEE Trans. Autom. Control **54**(1), 48–60 (2009)

45. A. Nedic, A. Ozdaglar, P.A. Parrilo, Constrained consensus and optimization in multi-agent networks. IEEE Trans. Autom. Control **55**(4), 922–938 (2010)
46. G. Beccuti, T. Demiray, G. Andersson, M. Morari, A Lagrangian decomposition algorithm for optimal emergency voltage control. IEEE Trans. Power Syst. **23**(4), 1769–1779 (2010)
47. A. Ravindran, K. Ragsdell, G. Reklaitis, *Engineering Optimization: Methods and Applications*, 2nd edn. (Wiley, Hoboken, NJ, USA, 2006)
48. J. Conejo, E. Castillo, R. Mmguez, R. Garaa-Bertrand, *Decomposition Techniques in Mathematical Programming: Engineering and Science Applications* (Springer, New York, NY, USA, 2006)
49. G. Hug Glanzmann, G. Andersson, Decentralized optimal power flow control for overlapping areas in power systems. IEEE Trans. Power Syst. **24**(1), 327–336 (2009)
50. H. Kim, R. Baldick, A comparison of distributed optimal power flow algorithms. IEEE Trans. Power Syst. **15**(3), 599–604 (2000)
51. R. Baldick, B.H. Kim, C. Chase, Y. Luo, A fast distributed implementation of optimal power flow. IEEE Trans. Power Syst. **14**(3), 858–864 (1999)
52. M. Parker, L. Ran, S. Finney, Distributed control of a fault-tolerant modular multilevel inverter for direct-drive wind turbine grid interfacing. IEEE Trans. Ind. Electron. **60**(2), 509–522 (2013)
53. H.W. Dommel, W.F. Tinney, Optimal power flow solutions. IEEE Trans. PowerApp. Syst. **87**(10), 1866–1874 (1968)
54. C.H. Lin, S.Y. Lin, Distributed optimal power flow with discrete control variables of large distributed power systems. IEEE Trans. Power Syst. **23**(2), 1383–1392 (2008)
55. B.H. Kim, R. Baldick, A comparison of distributed optimal power flow algorithms. IEEE Trans. Power Syst. **15**(2), 599–604 (2000)
56. W. Qi, J. Liu, P.D. Christodes, Distributed supervisory predictive control of distributed wind and solar energy systems. IEEE Trans. Control Syst. Technol. **21**(2), 504–512 (2013)
57. L. Gan, U. Topcu, S.H. Low, Optimal decentralized protocol for electric vehicle charging. IEEE Trans. Power Syst. **28**(2), 940–951 (2013)
58. R. Mudumbai, S. Dasgupta, B. Cho, Distributed control for optimal economic dispatch of a network of heterogeneous power generators. IEEE Trans. Power Syst. **27**(4), 1750–1760 (2012)
59. D. McLarty, C. Civit Sabate, J. Brouwer, F. Jabbari, Micro-grid energy dispatch optimization and predictive control algorithms; A UC Irvine case study. Int. J. Electr. Power Energy Syst. **65**, 179–190 (2015)
60. E. Olivares, A. Mehrizi Sani, A.H. Etemadi, C.A. Canizares, R. Iravani, M. Kazerani, A.H. Hajimiragha, O. Gomis Bellmunt, M. Saeedifard, R. Palma Behnke, G.A. Jimenez Estevez, N.D. Hatziargyriou, Trends in microgrid control. IEEE Trans. Smart Grid **5**(4), 1905–1919 (2014)
61. S. Butenko, R. Murphey, P.M. Pardalos, *Recent Developments in Cooperative Control and Optimization* (Springer-Verlag, Boston, 2013)
62. L.A. Wolsey, G.L. Nemhauser, *Integer and Combinatorial Optimization* (Wiley, Hoboken, NJ, 2014)
63. NETL modern grid strategy—Powering our 21st-century economy: A compendium of smart grid technologies. White Paper, National Energy Technology Laboratory (NETL) for the U.S. Department of Energy Office of Electricity Delivery and Energy Reliability (2009)
64. Z. Cheng, J. Duan, M. Chow, Reliability assessment and comparison between centralized and distributed energy management system in islanding microgrid. in *Proceedings North American Power Symposium (NAPS)* (2017), pp. 1–6

Chapter 17
Intelligent and Adaptive Control

Mehmet Zile

Abstract Intelligent and adaptive control is defined as a feedback control system that can adjust the character to the change in the environment in order to carry out the system optimally according to some specific criteria. An adaptive control system that overcomes the change in the environment over time is different from the optimal control system or feedback control systems. Feedback or optimal systems occur in the specified environment. If the changes in the environment are very sensitive, these systems cannot be designed in the manner requested by the designer. On the other hand, the adaptive system evaluates the environment. More accurately evaluates the performance of the system. It makes the necessary changes to the control characteristic to improve. Adaptive control includes the following three functions: identification, decision and change. In any adaptive control system, it is difficult to separate the system into its components. Conversely, these three functions must be present in the system for adaptation to occur. In this section, different intelligent and adaptive control systems are described.

Keywords Artificial intelligence (AI) · Intelligent control · Adaptive control

17.1 Introduction

Intelligent and adaptive control is a control method in which the control parameters are automatically adjusted by feedback in the direction of the measured process variables to achieve near optimum performance. This feedback ensures that the system is aware of the current situation and takes the necessary precautions to remove any imbalances that may arise. Adaptive control can be used at every stage of production; sensor-based feedback to robots and computer numerically controlled machine tools, feedback from inspection stations to production units or feedback from a factory database to a process planning system [1].

M. Zile (✉)
Mersin University, Mersin, Turkey
e-mail: mehmetzile@mersin.edu.tr

N. Mahdavi Tabatabaei et al. (eds.), *Microgrid Architectures, Control and Protection Methods*, Power Systems,
https://doi.org/10.1007/978-3-030-23723-3_17

The aim of this chapter is to provide new designs, at the cutting edge of true intelligent control, as well as opportunities for future research to improve on these designs and real-world applications. The intelligent control field emerged as a response to the difficulty of controlling highly complex and indeterminate nonlinear systems [2].

This chapter represents a step in this direction. A number of original neural network based adaptive control designs have been introduced to deal with plants characterized by unknown functions, nonlinearity, multimodal behavior, randomness and disturbances. The proposed schemes achieve high performance levels by enhancing the controller's adaptability, stabilization, uncertainty management and learning capabilities. Both deterministic and stochastic plants are considered. Compared to other schemes, the presented methods lead to more efficient use in combined time systems and better global fit for continuous-time systems, and to greater global stability with less prior knowledge in discrete-time systems [3].

Artificial intelligence, in particular expert system techniques have been developing rapidly in control engineering. Expert-system techniques in control engineering are control-system design, fault diagnosis, simulation, modeling and identification, on-line performance monitoring, adaptation and auto-tuning and supervisory control. A computing system capable of representing and reasoning about some knowledge rich domain usually requires a human expert, with a view toward solving problems and/or giving advice. Such systems are capable of explaining their reasoning. Does not have a psychological model of how the expert thinks, but a model of the expert's model of the domain. This chapter is to provide a quick overview of neural networks and to explain how they can be used in control systems. We introduce the Multilayer Perception (MP) neural network and describe how it can be used for function approximation [4].

In addition, there are some rational behaviors that do not result from inference. Artificial intelligence can be grouped under the following groups.

- Knowledge-based artificial intelligence
- Artificial neural networks (ANN)
- Fuzzy logic (FL)
- Expert systems (ES)
- Natural Languages that communicate directly with the computer
- Visualization, speech, hearing, sniffing, simulation of perception
- Robotics.

The knowledge-based Artificial Intelligence System works based on a knowledge base consisting of practical solutions or routing information for a particular field of application.

17.2 Artificial Intelligence

Artificial Intelligence is a field of computer science. Feedback; The science of psychology, knowledge and understanding is closely linked to various other disciplines such as computational linguistics, data processing, decision support systems and

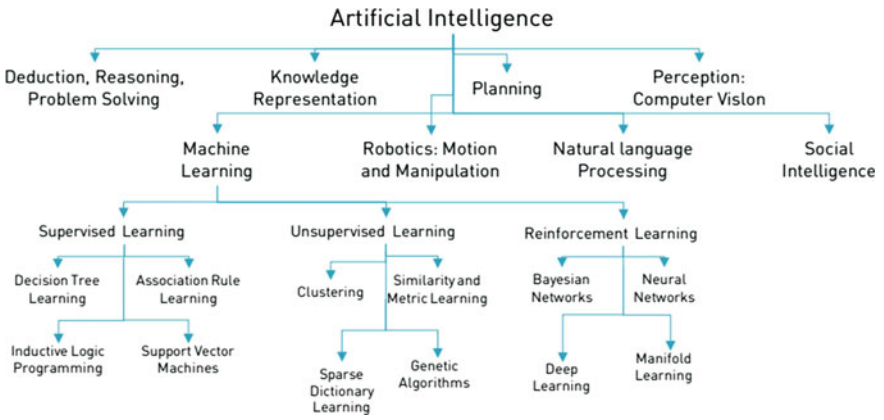

Fig. 17.1 Classification of stream under artificial intelligence [7]

computational modeling. Use all these disciplines as sources. Computer Science with Artificial Intelligenceis designed to have computer systems that are intelligent, language capable, learning, reasoning and problem solving [5].

Artificial intelligence can be defined as trying to understand the thinking structure of the human and to develop the computer processes that will reveal the similarity of this. So it is an attempt to think of a programmed computer. According to a wider definition, artificial intelligence, knowledge, perception, vision, thinking and decision-making, such as computers are equipped with capabilities specific to human intelligence. The idea of using programs equipped with knowledge in a particular area of expertise instead of a general purpose program to solve each problem led to a revival in the field of artificial intelligence [6].

In a short time a methodology called "Expert Systems" developed. Classification of stream under Artificial Intelligence is shown in Fig. 17.1.

At the end of all these studies, artificial intelligence researchers is divided into two groups. One group tries to make systems that think like human. While the other group aimed to produce systems that could make rational decisions. It is necessary to determine how people think to produce a human-like program. This can be done by psychological experiments. After a sufficient number of experiments, a theory can be created with the information obtained. The computer program can then be produced based on this theory. If the program's input/output and timing behavior is the same as in humans, it can be said that some of the mechanisms of the program may be present in the human brain. To produce systems that think like human beings is within the research area of cognitive science. The main goal in these studies is to use computer models as a tool for analyzing human thinking processes. Artificial intelligence researchers want to reach from the beginning, ideal to produce systems that behave like human [3].

The process that produces intelligent behavior in the computer can be obtained by modeling the processes in the human brain. But it is possible to produce it by acting

completely from other principles. Rational thinking systems are based on logic. The aim here is to find the solution by using the inference rules after depicting the problem with a logical representation. Logic tradition, which holds a very important place in artificial intelligence, aims to produce such programs to produce intelligent systems.

In Rational Behavioral Systems, artificial intelligence is defined as the examination and creation of rational behaviors. One of the conditions required to act rationally is to make correct inferences and act according to the results of these inferences. In some cases, it may be necessary to do something, even though it is not a proven solution. The ability of people to solve certain problems using "if-then" rules in their own knowledgebase system has inspired this type of artificial intelligence.

The most advanced example of knowledge based systems are expert systems. The expert knowledge of a particular problem is placed in the knowledge base of an expert system. A communication between the user and the computer based expert system will occur until the problem is solved. It is also possible to use information-based systems in military field. For example, the decision-making situation is complex, however in the areas of expertise where decision-making logic can be transformed into a certain rule hierarchy. Such systems can be created depending on need if it is economical to use the knowledge based system [5].

17.3 Artificial Neural Networks (ANN)

Artificial Neural Networks are information processing models created by using the physiology of the brain. There are many artificial neural network models in the literature. Some scientists have tried to transfer the powerful thinking, recall and problem solving abilities of our brain to the computer [4]. Some researchers have tried to create many models that partially fulfill the functions of the brain. Artificial Neural Networks is one of the most important characteristics that attracts the attention of researchers. Because the relationship between the inputs and outputs of any event, whether linear or not, by learning from the existing examples, never seen before. The previous examples of the ability to produce solutions to the event by associating to the phenomenon constitutes the basis of intelligent behavior in the Artificial Neural Networks [2].

Artificial Neural Networks have been tried to be developed by taking the working principle of human brain as an example. Single or bidirectional activation functions may also be used in accordance with the use of Artificial Neural Networks. The basic unit of an Artificial Neural Networks model is shown in Fig. 17.2.

It can be said that the Artificial Neural Networks have computational features, parallel scattered structure and ability to learn and generalize. Generalization is defined as Artificial Neural Networks to produce appropriate responses for inputs that are not used during training or learning. Neural Networks with these features are capable of solving complex and difficult to solve problems.

Artificial Neural Networks have been successful in many engineering fields such as object recognition, signal processing, system identification and control. Artificial

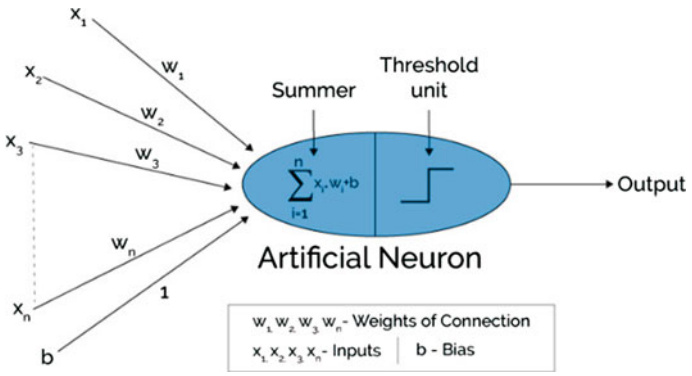

Fig. 17.2 Artificial neural networks [8]

Neural Networks cell which is the basic processing element is not linear. Therefore, Neural Networks which are formed by the incorporation of cells are not linear. This feature is scattered across the entire network. Neural Networks with this feature provide solutions to nonlinear complex problems. In Artificial Neural Networks, it tries to learn the problems related to the problem by using the samples taken from the problem and provides a different solution.

Artificial Neural Networks have the ability to produce the reaction indicated for the test samples that they did not encounter during the training after learning the problem. For example, an Artificial Neural Network trained for character recognition, provides the correct character in bad character entries. Memory is combined in the neural calculation. That is, even if only a part of the input to the trained network is given the network accepts the memory as if it were receiving the full input data by selecting the closest to this input and generating a corresponding output value. Even if the data is given to Artificial Neural Networks as missing, corrupt, or never before encountered, the network will produce the most acceptable output. This feature is the generalization feature of the network.

Artificial Neural Networks weights are changed according to the applied problem. That is, it can be re-educated according to the changes in the problem of Artificial Neural Networks trained to solve a specific problem. If changes are continuous, education can continue in real time. Artificial Neural Networks with this feature are used effectively in areas such as adaptive sample recognition, signal processing, system identification and control.

One of the most important features of Artificial Neural Networks is that they store information. The information is distributed on the weights in the neural calculations. The weights of the connections are the memory unit of the neural network. These weights give information about the current knowledge of the network or the behavior of the samples. This information is distributed to many memory units in the network. If a different input is applied to the educated network no used in the training, the network will be able to produce an output according to the expected output according

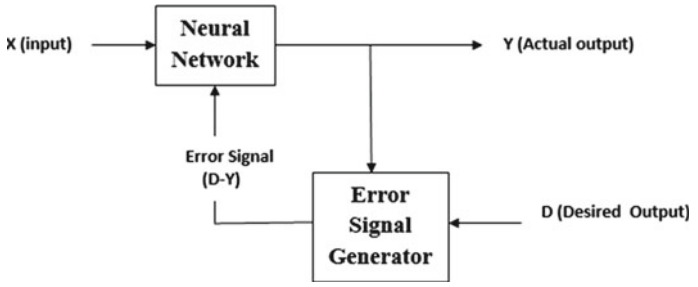

Fig. 17.3 Block diagram for feedback network [9]

to the behavior learned from the previous inputs. Even if the data applied to Artificial Neural Networks are missing, noisy or never before, the network will produce the most acceptable output. This property is called the globalization feature.

Artificial Neural Networks have a parallel structure with the connection of a large number of processor elements. The information the network has is scattered throughout the network. Noise can be tolerated as any noise that may be present in the input data distributed over all the weights. According to traditional methods, the ability to tolerate the error is higher. Due to its parallel structure, Artificial Neural Networks can be implemented with large-scale integrated circuit technology. This feature enhances its ability to process information quickly and its use in real-time applications such as sample recognition, signal processing, system identification and control.

Artificial Neural Networks are generally composed of interconnected processor units or processor elements. The structure of the connections between each nerve cell determines the structure of the network. How to change the connections to reach the desired target is determined by the learning algorithm. According to a learning rule used, the weights of the network are changed to reduce the error to zero. Block diagram for feedback network is shown in Fig. 17.3.

Artificial Neural Networks are classified according to their structures and learning algorithms. Artificial neural networks are classified according to their structure intwo ways: feed forward and feed back networks. In a forward-feed network, the processor elements are usually divided into layers. Signs are transmitted from the input layer to the output layer by one-way links. While they link from one layer to another, they don't have links in the same layer. Examples of feed-through networks are Multi Layer Perseptron and Learning Vector Quantization Networks [4].

A feedback network is a network structure in the outputs. The output and intermediate floors are fed back to the input units or the preceding intermediate layers. Thus, the inputs are transmitted in both forward and reverse directions. These kinds of neural networks have dynamic memories. The current output reflects both the current and previous entries. Therefore, they are particularly suitable for prediction applications. These networks have been very successful in estimating time-series of various types. The structure of the mentored learning is shown in Fig. 17.4.

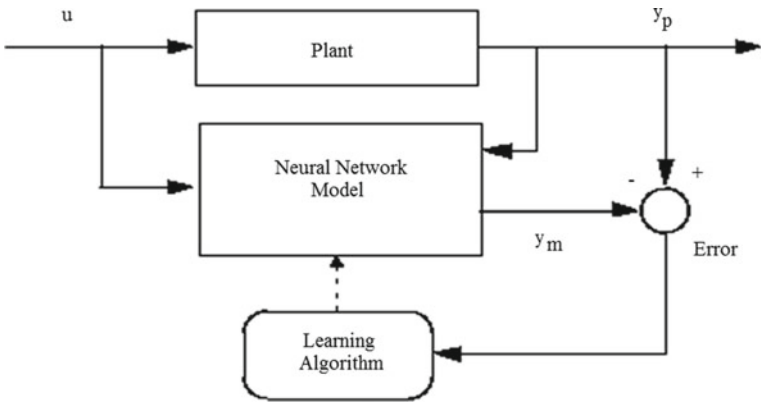

Fig. 17.4 Structured learning structure [10]

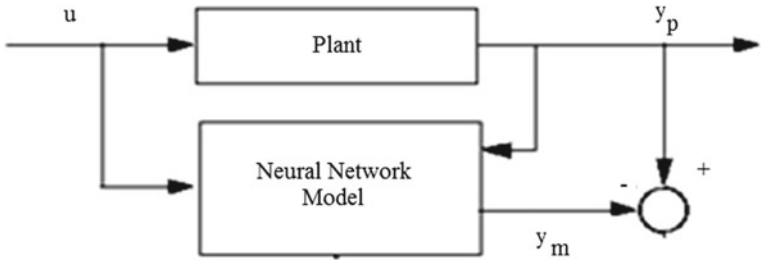

Fig. 17.5 Unsupervised learning structure

Learning observation, education and behavior are defined as behavioral changes in the natural structure. Therefore, it should be ensured that the weights in the network are changed according to some methods and rules, observation and training. For this, in general, three learning methods and different learning rules can be mentioned. In Supervised Learning, an accurate output is given as an example of Artificial Neural Networks. Depending on the error between the desired and actual output, the weight of the interconnections can be subsequently edited to obtain the most suitable output. For this reason, the consultant learning algorithm needs a teacher algorit or a consultant.

Unsupervised Learning also develops the network classification rules according to the output information obtained from the sample given to the entrance. In these learning algorithms, it is not necessary to know the desired output value. Only the entry information is provided during the learning period. The network then sets the connection weights to create patterns that show the same properties. A non-consultative learning structure is shown in Fig. 17.5.

The Rule of Reinforcement Learning is close to counseling. The unsupervised learning algorithm does not need to know the desired output. A criterion that evaluates

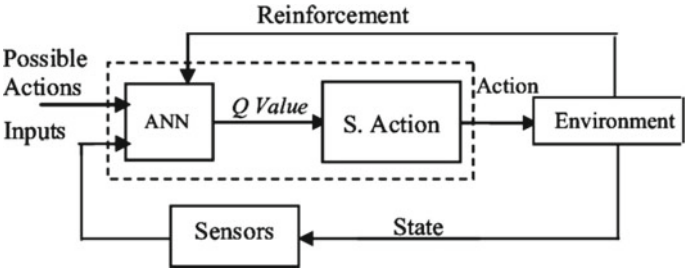

Fig. 17.6 Reinforced learning structure [11]

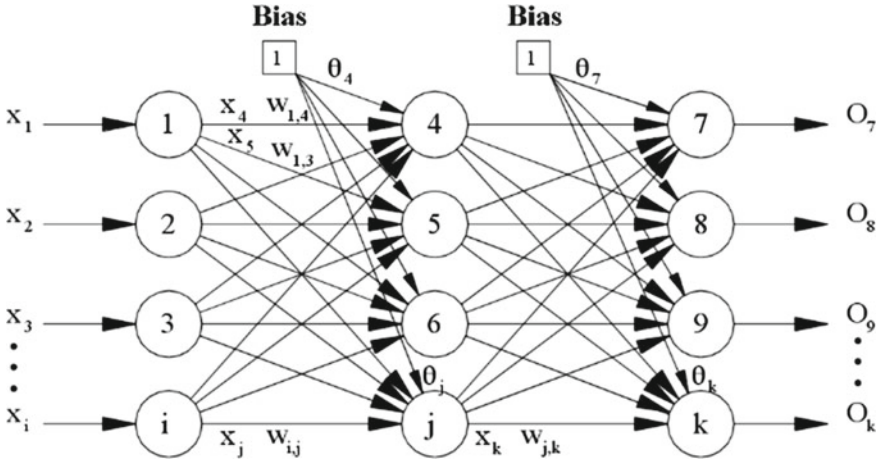

Fig. 17.7 Back-propagation Multilayer perceptron structure [12]

the output versus the given input is used. The reinforced learning structure is shown in Fig. 17.6. Many layered perseptron neural network models are shown in Fig. 17.7.

This network model is the most widely used model of neural networks in engineering applications. The flow chart of this algorithm is given in Fig. 17.8.

Many teaching algorithms can be used to train this network is the reason why this model is widely used. A multi-layered perseptron model consists of one input, one or more intermediate and an output layer. All processing elements in a layer are connected to all processing elements in a top layer. The information flow is forward and there is no feedback. This is referred to as a feed-forward neural network model. No information is processed in the input layer. The number of processing elements in this case depends entirely on the number of problems applied. The number of intermediate layers and the number of processing elements in the intermediate layers are found by trial and error. The number of elements in the output layer is again determined based on the applied problem. In many layered perseptron networks, an example is shown to the network and the result of the example is also reported.

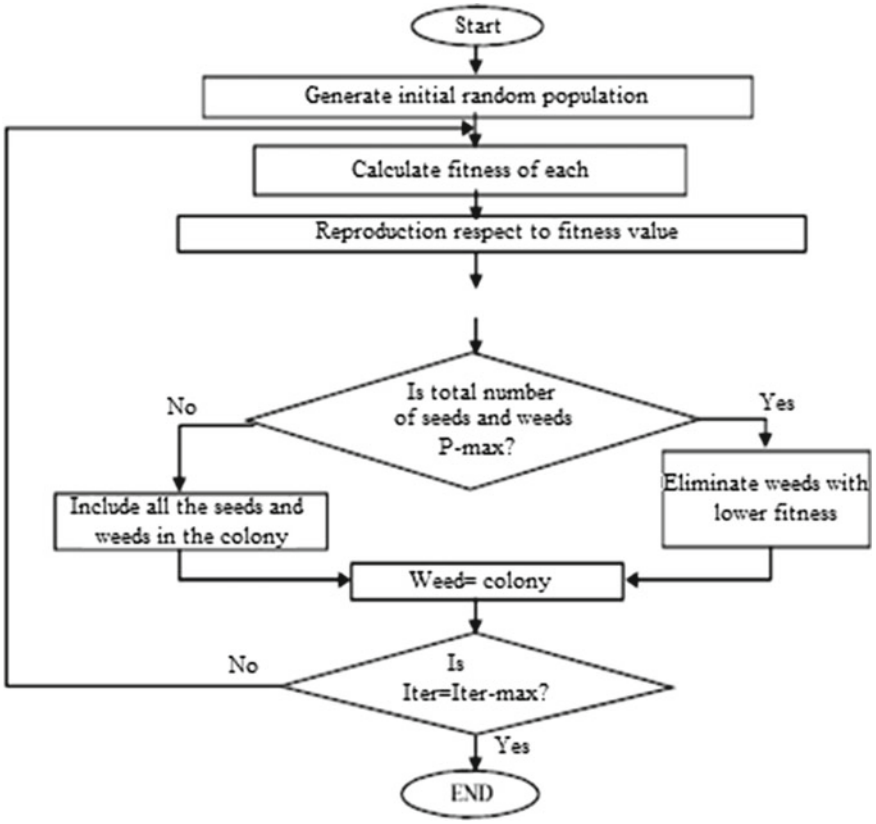

Fig. 17.8 Multi-layered perseptron backflow flow chart [13]

Samples are applied to the input layer, processed in the inter layers and outputs are output from the output layer [1].

According to the training algorithm used, the error between the output of the network and the desired output is shifted backwards and the weights of the network are changed until the error is minimized. The most common teaching algorithm used in many applications is the back propagation algorithm. It is the most preferred teaching algorithm because it is easy to understand and can be proved mathematically. This algorithm is called back propagation because it tries to reduce errors from backward to output. Forward-feed networks, in the most general sense, make static mapping between the input space and the output space. The current output is only a function of the current input. The typical multi-layered back-spread network has always an inlet layer, an outlet layer and at least one hidden layer. There is no theoretical limitation in the number of hidden layers.

Feed-forward Artificial Neural Network structures are often complex. It may be quite time-consuming to determine the most appropriate set of learning coefficients

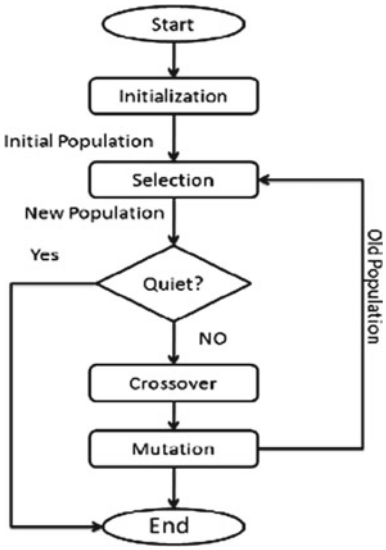

Fig. 17.9 Flow chart of the genetic algorithm [14]

for each link in the network. Using the past values of the slope, intuition can be applied to remove the curvature of the local fault surface. When the sign of weight changes for a link changes a few consecutive time steps in order, the learning rate for the link should be reduced. The connection weight dimension has a large curvature associated with the error surface. Heuristic methods can be simplified for the decision-making mechanism. The heuristic method can be used for learning as part of any complete method. It is not always easy to establish a mathematical formulation for real world problems. The error caused by this simplification may be greater than the error of the optimal solution provided by an intuitive method.

Genetic algorithms are research and optimization algorithms and based on the natural development principle of living things. One of the most important advantages is that they have important features such as probabilistic characters and multiple possible solutions research. They do not need to know the gradient of the objective function. Information about potential solutions in a Genetic algorithm is expressed in string-shaped numbers. The flow chart of the genetic algorithm is shown in Fig. 17.9.

As can be seen from Fig. 17.9, at the beginning of the optimization, a number of solutions are generated randomly by a number generator. Another advantage of the genetic algorithm is that, for a good approximate solution at the beginning, no information is needed. Following the generation of the initial density, the suitability or goodness of each solution is evaluated using a selected conformity function. Genetic operators, such as selection, crossing and mutation are used to produce tried-and-tested new solutions. This improvement is continued until a number of generation has been determined or a satisfactory result reached. The crossover operator produces two new untested solutions by displacing the extensions of the two existing solutions from a certain point.

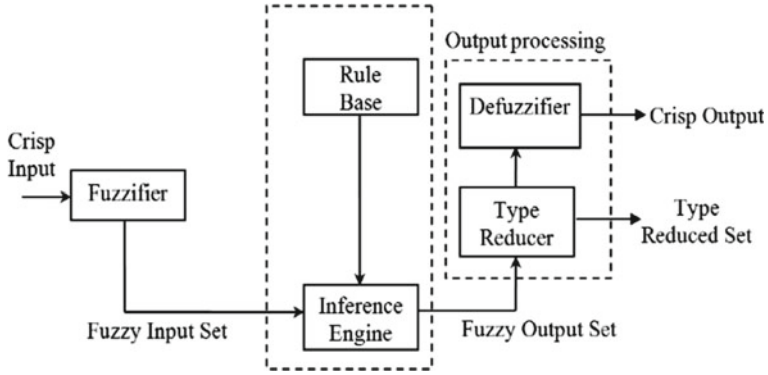

Fig. 17.10 Fuzzy logic system block diagram [15]

17.4 Fuzzy Logic

In recent years, fuzzy logic and fuzzy logic-based applications have become a topic that has been followed with interest by both the university and the manufacturers. Many terms that we use in our daily life are generally fuzzy. When defining something, verbal or numerical expressions that we use when explaining an event. When commanding and in many cases are blurred. For example, too much, little, little, much, too little, too much, hot, cold, elderly, young, long, short, warm, cloudy, partly cloudy, sunny, fast, slow, such as more than a very verbal term can be shown. We use terms that do not express such certainty when people tell an event and make a decision about a situation. All this is an example of how the human brain behaves in uncertain, non-precise situations and how it evaluates, defines and commands events.

Fuzzy logic applications can be found in almost all areas. Fuzzy logic is used in robotic, automation, intelligent control, monitoring systems, commercial electronic products, information storage and recall, expert systems, information processing in information based systems, machine imaging, function optimization, filtering and curve fitting methods. Unlike conventional control systems, without the mathematical model of the systems, only the signal applied to the input is set to give the desired output [1–5]. The handling of fuzzy control is similar to a master person controlling that system. Fuzzy logic system block diagram is shown in Fig. 17.10.

Using fuzzy logic and fuzzy set operations, machines can make decisions like people. Fuzzy logic has taken its place as an alternative approach to the control of linear and nonlinear systems. Almost none of the real-life systems are linear. Conventional design methods use different methods for linearizing. By using linear, segmented linear and sub-table tables, the factors affecting the complexity, cost and system performance are tried to be eliminated. Fuzzy inference system is shown in Fig. 17.11.

Linear approximation techniques are actually simple, but have a negative impact on the performance of the control system. The fractional linearization technique

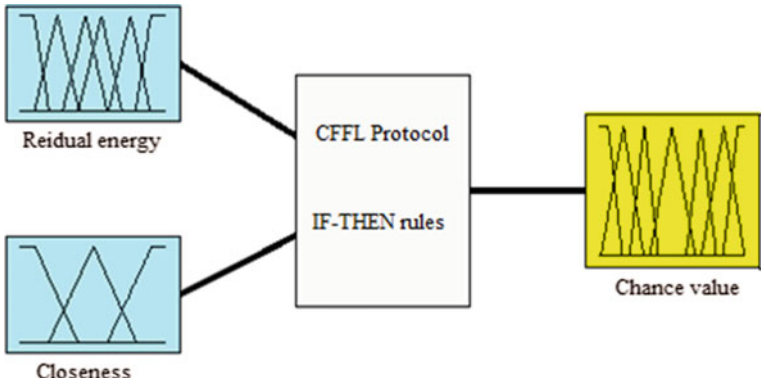

Fig. 17.11 Fuzzy inference system [16]

works better, but is more difficult to implement. Usually requires several linear controller design. As it is closer to the real world, fuzzy logic is an alternative approach to nonlinear control. The non-linear characteristics of the systems are represented by rules, membership functions and conclusion. Using fuzzy logic approach increases system performance, simplifies implementation, and reduces financial expenses.

The control, which is closer to the real system and which is not linear by using a more natural rule base can be performed better than conventional methods. In this case, system performance can be improved perfectly and a more effective and sensitive control can be achieved. Most control applications are multi-input and require many parameters to be designed and configured. This makes the application difficult and time-consuming. The rules of a fuzzy logic-based controller simplify implementation by combining multiple inputs with 'if … then …' expressions taking into account nonlinear properties. Using fuzzy logic, the output size can be expressed as a function of two or more inputs connected by logic processors. This relationship between the inputs and the output can also be shown by a table of rules.

The fuzzy approach requires significantly less input. The rules can be more easily developed, more easily integrated into the program and more easily adjusted. Dimensions with complexity and uncertainty are defined by membership functions, which can also be called fuzzy numbers and characterize fuzzy sets. Fuzzy numbers, again in a fuzzy environment similar to human thought and decision-making mechanism 'if … then … else' in the form of the rule subjected to a fuzzy conclusion is reached. A system operating on fuzzy logic principles uses the information previously taught to reach a conclusion about the new situation. Fuzzy modeling design and software are implemented using fuzzy set operations. Fuzzy set theory or the application of fuzzy logic for a specific system in itself is not much different from actually implementing boolean logic or probability logic. Fuzzy set theory makes fuzzy logic or fuzzy processor theory more general.

Fuzzy set theory and fuzzy set operations make it easy to perform blurry operations. This provides the necessary structuring to create fuzzy processors. The main

element of fuzzy logic is the fuzzy set. Fuzzy sets are characterized by membership functions. In fact, these membership functions are nothing more than a fuzzy number. The most basic element of fuzzy systems is the fuzzy cluster. A fuzzy set is a type of cluster with elements that have degrees of belonging different memberships. Such a cluster may be characterized by a membership function that can assign 0 to 1 membership values to each of its elements. The membership values of the elements are not included in the cluster assigned as 0. The membership values of the ones included in the set are assigned as 1. If there are uncertainties in the group, the values are assigned values between 0 and 1 depending on the uncertainty. In the definitive set theory, there is no such thing as an indefinite element. An element is either included in the cluster or is completely outside the cluster. The value of an element in the definitive sets can be either 0 or 1. Membership functions that characterize fuzzy sets have different forms.

The most commonly used fuzzy set functions as a membership function are triangular, trapezoidal, gaussian and bell-shaped functions. In addition to these membership function types sigmoid, sinusoid and cauchy type functions are used. Sigmoid functions either look to the right or to the left, and are usually located at the lower and upper boundary of the precise general set. In order to facilitate their use, membership functions that represent fuzzy sets are formulated based on their parameters. The ease with which parameters can be set makes it easy to set up membership functions [2–6].

17.5 Expert Systems

Computers are capable of tremendous processing, but unfortunately they do not have learning skills. Knowledge based systems and a branch of artificial intelligence research are trying to change this phenomenon. Artificial intelligence researchers aim to provide knowledge based systems with the ability to simulate and learn the human reasoning system. Expert systems and knowledge based systems are terms used in the same sense. The expert system is the most advanced form of an information-based system. An expert system is a system open to dialogue that answers questions, asks questions, makes recommendations and helps in decision-making. Less advanced knowledge based systems are called auxiliary systems. The helper system is a system that helps the user to make relatively simple decisions. Ancillary systems aim to reduce the likelihood of an error that the end user can do in the process of reasoning rather than solving a particular problem.

The technology needed to develop expert systems, auxiliary systems and any system between them is the same technology. Expert systems try to imitate the human thought process. Expert systems can reason, inference and judgment. It is used effectively in medical diagnosis, petroleum research, financial planning, tax calculation, chemical analysis, surgery, locomotive repair, weather forecasting, computer repair, satellite repair, computer system design, nuclear power plants operation, interpreting state laws and many other areas. The expert system is an advanced computer program

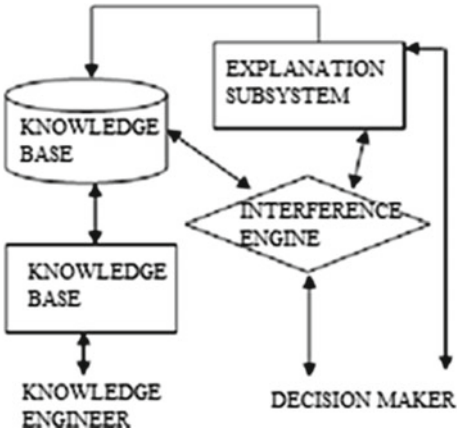

Fig. 17.12 The structure of an expert system [17]

that requires extensive use of expertise and experience. The structure of an expert system is shown in Fig. 17.12.

The expert system can only solve difficult problems at a high level of competence, with a broad-based knowledge of only a specific area. Technical knowledge is accomplished using knowledge, heuristic methods and problem-solving processes used by experts to solve such problems. Expert systems enable human knowledge, expertise, and experience to be stored on computers. The expert system has four basic features. These are important performance capability, reasonable response time, interchangeability and active user interface.

For successful implementation and use of expert systems, at least the performance of the expert should be performed. Otherwise, it is unnecessary to create the system. In fact, the system will be asked to perform better by the expert. The system is not used if it spends unreasonable time in providing answers with questions, and end users return to consulting the expert itself for expert advice. When a standard computer system is designed, the criteria for response times must be met. New facts, techniques and methods are discovered; new facts and rules come to light. An expert system must provide the users with the same flexibility as they can change their knowledge. It has a very good knowledge base; however, a system with a weak user interface will not be used. The system consisting of a small knowledge base and a good interface can be very useful.

Expert systems have various capabilities and features that distinguish themselves from traditional computer programs. The main objective of an expert system is to have the experts' intuitive expertise and disseminate it. The goal of a traditional program is to complete an algorithm set. Expert systems can be used in situations where it is thought to be difficult or impossible to handle with traditional approaches. Expert systems are able to address situations where the information needed is incomplete or the information available is inconsistent. Techniques in expert system technology analyze ambiguous situations and uncertain data, and some expert systems can change their judgment when new information is reached. Often, an expert system

may explain why it takes decisions or why it performs a particular operation or asks for specific information.

Expert systems are primarily based on symbolic reasoning about concepts rather than numerical calculations. These systems are often programmed using explanatory approaches rather than approaches to processing and programming techniques allow the program control to be widely separated from the field information. The use of descriptive information removed from program control often makes it easier for expert systems to be more flexible, revised and updated than traditional programs. If the information of the expert is stored in a file, it is possible to distribute this information widely within the organization. Each section that you need can get a copy of this file and this copy which is always available. Unlike human experts, computer programs do not get angry, get tired, go on vacation, become sick and do not die. The information is always ready for use. Even the best expert can make mistakes or forget an important point. Flaws will occur less well with a good expert system.

A computer program is consistent. If programmed correctly, it will always give correct results. It is very difficult to get the common opinion of more than one expert. It is almost impossible to put together a group of experts to discuss and agree on a topic. An expert can only use his/her own knowledge and experience. With a computer system, an expert system may contain information from multiple specialists. Thus, the decision given by the expert system will be at least as good as the decision of the other participants. In addition, expert systems can exchange views with each other and offer a variety of options. Some of the expert system applications work well while others do not work. The decision to use or not to use a particular technology in a particular area is important in computer-based systems. Some problems may be too complex for expert systems. If the experts do not agree or if the specialist in that field is not available, the field is not suitable. Similarly, problems that take a long time to dissolve, many interactions or problems with too much dependence on spatial relationships and procedures are not suitable for specialist systems.

Testing expert systems is a critical need, especially in systems used to help make decisions rather than simply giving advice. There are many problems in testing an expert system. The developers of the program are not always sure how the system should behave and therefore cannot fully test the system. It is not easy to define the path that the expert system program will follow. This is a serious problem in applications involving too much risk. As the size of the system increases, the difficulty of inspection and maintenance increases. The user has to make sure that the recommendation recommended by the system which is the most appropriate advice and take into account all possible side effects. The accuracy and completeness of the system is very difficult to test.

In the real world we are not only interested in true and false truths. Usually we only make sure of a certain degree. Ideally, an expert system should be able to overcome uncertainty. Finding valid statistical rules for the use of logical reasoning offered by the expert system is a major theoretical problem. Knows the limits of the expert; a computer-based system cannot know if it is not specifically programmed. Expert systems do not do so well. They are always intended to produce an answer. This

may be a problem and it should be emphasized that it would be more appropriate for expert systems to be used as an aid rather than substituting for experts. Introduction to expert system technology has important implications for the company's organizational structure. Not may everyone want to rely on a computer or use it.

Some people resist computer use and prefer to work with experts. Even the experts are sometimes skeptical about expert systems. Even systems do not trust expert systems because they think they work well and do not use the same type of reasoning method even when they agree with the experts. These factors should be considered when considering the use of expert systems. The process of storing and revealing the expert's knowledge is often a long and slow process. The areas where the information changes frequently are not suitable for the development of expert systems. The expert system must constantly update the knowledge base in order not to lose expertise. Necessary, conditions should be established to update the database [1–6]. Although, the aim of expert systems is to imitate human professionals, there are very few systems that can do so.

Dialogues between the system and the user are usually guided by the program and are often difficult to understand. Expert systems should only be used when necessary. The conditions in which some businesses are located may not justify the use of the expert system because of the cost and the invalidity of the benefit. An expert system analyzes a situation, takes a decision, and then acts directly or directly controls a human activity. There is no human participation in all these stages. Reacts to rare or unusual situations. The expert system acts as an autonomous expert, but presents its decisions to a specialist who will ignore or change these decisions. In this role, an expert system can formulate a complex design which will be reviewed by a designer before application. An expert system provides expert level advice for the person performing the task, as advised by expert consultants, especially for difficult or unusual situations. The expert system makes recommendations to people at their site. Although he cannot have a higher level of mastery than man, he can make analyzes that man cannot find time to do. While trying to obtain the most probable option of human activity, the expert system can investigate a number of complex alternatives. For example, an expert system that detects and resolves malfunctions can examine the possible causes of errors.

The expert system is like a clever assistant of the practitioner. When a particular situation occurs, he/she may make a number of reasonable suggestions or may specify a number of items that should be considered. He/she can observe the data by investigating certain combinations of variables as the practitioner is concerned. The expert system performs relatively low and time-consuming tasks in order to allow the practitioner to separate the time of the work into the more difficult parts of the work. As the interest in technology expands, the number of problem types in which expert systems are applied constantly increasing. Expert systems are used for diagnosis, scheduling, planning, monitoring, process control, design, forecasting, signal interpretation, configuration and training purposes. Expert system technology; it can be considered in cases where it is valuable to protect the expertise or to extend the range of access to expertise and expertise. Thus, expert systems; They provide expert knowledge to improve performance and quality, to improve efficiency,

to ensure stability, to protect important information, to ensure better utilization of human resources and to enable the marketing of new or better products.

In any field, it is not possible for these systems to solve the problems that the experts cannot solve, because a specialist system has the full expertise and experience of a leading expert and is based on human knowledge. Developing an expert system is only possible in narrow and confined spaces. Existing expert systems often perform poorly on their borders, and many of these systems have difficulty in determining whether a situation is within their area of activity. Existing commercial expert systems do not have significant learning abilities, and only a few allow the use of the basic principles of the field of activity when heuristic methods do not work.

There are no fixed rules in expert system development, there are many situations where more than one approach can be used, and there are several standard techniques that work in every situation. The primary objective of the expert system development is to obtain information from an expert in the chosen field, from a task experience in the field, and then to use that information in an expert system program. Expert system development; It consists of the basic steps of field selection, selection of experts, acquisition of knowledge and program development. One or more specialists are selected for the selected field. When designing expert systems, the planner must focus on specialist knowledge derived from the deep experience and repeated observations of experts.

There are many factors that need to be considered when determining a field expert for an expert system development project. The key point here is to find an expert with the right type of knowledge for the identified objectives and problems. When building a large information system with a large number of defined subproblems, it is appropriate to collect frequent information at every stage of the organization, from the bottom to the top management [1–6].

The idea is to analyze how the problem grows, how it affects the organization and who should be involved in the solution. During the expert system development, the process of acquiring knowledge of facts, rules, heuristic methods, procedures obtained from experts, is called knowledge. In developing an expert system, knowledge engineers try to identify the way experts solve the problem the expert system is trying to solve, based on documents and directly from experts. The result of obtaining the information is to define the knowledge of the expert system in detail. The acquisition of knowledge is often achieved through meetings between knowledge engineers and field experts, where knowledge engineers try to provide the knowledge of experts. A general approach to contacting a field expert for information engineers is to ask questions about how the expert performs the task of the chosen area in order to determine the procedures and heuristic methods used by the expert.

Information engineers provide the specialist with specific situations and try to provide heuristic methods for making decisions in that case. This is a typical cycle. Information engineers and experts use test problems to compare the field information with the expert's performance. There are weaknesses in the knowledge of the system, it is changed and resubmitted to the expert evaluation. This cycle continues until the information of the expert system is reached to the desired point. Obtaining information is often difficult. Most experts cannot easily identify their expertise

or decision-making. Many of them are not talkative persons who can express their thoughts comfortably, as desired. Furthermore, experts often perform their tasks without fully becoming aware of the processes they use, their heuristic methods and how they make use of their expertise.

When they make a decision, they may not be aware of the stages they actually consider. Due to factors such as these, knowledge engineers should interact with field experts over a long period of time in order to determine the most complete and accurate heuristic expert methods possible in the process of obtaining information. It is the design of a computer program that combines the techniques, knowledge and heuristic methods. In the development of an expert system program to regulate expert knowledge provided during the process of obtaining information. There are basic elements such as selection of hardware, testing of information, transformation of information and testing and reevaluation of the program. Most expert systems are developed using a software tool or shell. The software tool or shell is a software package that allows the development of an expert system. They should also determine which computer equipment will be developed by the expert system.

The representation of information is the process of obtaining the field information provided in the process of obtaining information and describing the approach to be used to represent this information in the expert system program. Expertise information can be represented on the computer using a programming language. The production rules are represented by making one or more Artificial Intelligence Paradigms, such as roofs or object-oriented programming. With these paradigms, expert system developers define a representation plan for expert knowledge.

It is the process of converting information into an operational expert system program, using structures and paradigms, including information transformation, information retrieval and information representation. The expert system program must be tested and reevaluated during the development process and also before the final transfer or dissemination. An expert system consists of information acquisition unit, knowledge base, inference system and user and communication unit. The knowledge base is created by an information engineer as a result of the coordinated work of a specialist in one or more subjects.

The information engineer tries to convey a set of rules and rules related to the subject to the expert system as a knowledge base. Information in the knowledge base is given as “if-then” rules. Knowledge base is a different concept from the database. The subject of the classical database is the data about the static relations between the elements. The inference mechanism is the core of an expert system. It is the tool that makes the determination and rules in the knowledge base apply to a certain problem. In this system, the expert system is given the ability to reason. This reasoning power is provided to the user by providing a logic sequence, so that the solution is reached.

The reasoning of an inference system is based on the use of the forward or backward chain extraction time alone. In the forward chain, the expert system receives information from the end user and follows the rules in accordance with the situation from the knowledge base respectively until it reaches the solution. During this process, there is always communication between the user and the expert system. This communication is carried out according to the logic sequence created by the set of

pre-set rules. In the process of back-chain extraction, an exact opposite approach is used. The system asks the end user for the desired target or result, and then returns to "if-then" logic sequence to determine whether the desired target or result is correct. In the knowledge base matches the target or result, the target or result determined by the user is the solution of the problem. The procedure is not formal.

So, there is no written algorithm to solve a problem. If a specialist system is a strategy, it continues to use the process it creates. The option to return to a new strategy in the system is always available. This procedure therefore always requires communication with the user. Through communication with the user, the end user specifies the problem or target to the expert system. Management must determine the need for an expert system. So, it must assume that the benefits of the organization derive from the system.

The information engineer should make the information in the knowledge base appropriate and organize the information intuitively. The user prepares how the system will be used, what kind of problems will be solved and what kind of programs will communicate with the human operator. The system requires specialists or specialist groups to provide information for any subject in the factual information form and with analytical methods used to solve problems within the field.

In the machine direction, there are software tools of the knowledge base in which the facts are represented symbolically. In all expert systems; connection between the knowledge base, the user interface and the inference is determined by the intuitive rules. Each rule has 'if' suggestion and 'then' result. Events that are the result of the previous and next coincidence are defined. The degree of certainty of real claims is not always absolute. Factors of quantification accuracy increase the accuracy of the results of expert systems. The reliability of these relevant statements is based on statistics, probability, or purely personal opinions. The inference mechanism establishes a logical relationship between the result drawings and the rules of the results test. The user interface examines the system and communicates with the administrator [2–6].

17.6 Natural Languages that Communicate Directly with the Computer

Natural languages is the name used for software that enables the end-user to communicate with the computer through their natural language. The natural language works is shown in Fig. 17.13. The ultimate goal in natural language software is to eliminate the need for commands used in traditional program languages. The point reached in practice is not satisfactory.

Most of the natural languages used in the market do not function more than to provide communication with an expert system or database. In some areas where information processing is limited, it is observed that natural language practice is quite successful. For example, in the research and report preparation activities related

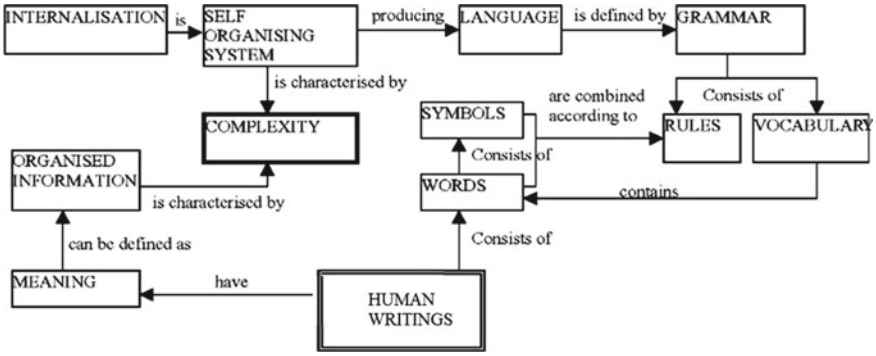

Fig. 17.13 The natural language generation process [18]

to human resources and procurement, the natural language application is highly developed. The user can communicate with the computer as he/she speaks normal English. Natural language software analyzes the above question sentence as we do in our grammar study. The sentence word is divided into pieces. The above sentence is converted into the application commands that the computer will understand.

In the semantic analysis phase, the elements of the sentence are generally compared with the keywords in the application dictionary starting with predicate. The words in the application dictionary are words used in the daily language. In this example, the system will compare with the words used for question purposes. The word will be converted to "display" which is the application command by using natural language software. Other words are also interpreted in natural language software and converted into application commands. If the user's request cannot be understood by the system, natural language software continues to try to understand the request by asking points that are ambiguous. For example, if the system does not understand "what is it?". We cannot understand "what is it?" and then asks "what the meaning of this" is in the same meaning as "what is it?". The process continues according to the response [1–6].

17.7 Visualization, Speech, Hearing, Sniffing, Simulation of Perceptions

This type of artificial intelligence is related to the simulation of human abilities and it is trying to equip the computer systems with the abilities of seeing, hearing, speaking and feeling. It seems possible to realize these artificial intelligence capabilities to a certain extent by using today's technology. Computers with human sensing capabilities may have the ability to communicate with the environment, just like people. The user selects output from prerecorded words, sentences, music and alarm.

In these voice response units, the actual analog size of the sound is converted to digital data and loaded into a memory chip continuously. When output is output, the selected sound is converted back to analog. These types of chips are manufactured with serial production technology for certain applications. Speech Synthesizers convert raw data into electronically generated conversations. For this purpose, these devices try to use sounds similar to the basic sound that make up the speech. With today's technology, it is possible to do this for a limited number of sentences, but this technology is increasingly in use.

Another application is the system developed for children with speech impairment. By means of this device, these children have the opportunity to talk with their environment. Computers are great speakers, but they are not good listeners. It's common for computers to misunderstand very natural sounds. However, there are also a number of applications of voice recognition. When the person speaks into the microphone, each sound is decomposed and has frequencies. The sound at each frequency is digitized to compare the format in the electronic dictionary of the computer.

Digital format is a format that the computer interprets and stores as 1 and 0. Invoice recognition, the process of creating the database is called training. Most voice recognition systems are speaker dependent. The voice of certain speakers can be recognized by the system. Therefore, a separate word database must be created for each person using the system. In the process of creating this database, the system user must repeat each word in order to ensure that the system is able to understand each word correctly. In a sense, it is necessary to train the computer. This training is indeed compulsory.

Therefore, the computer needs to be accustomed to these different expressions. Vision is the most difficult human perception ability to simulate. It is impossible for a computer to see and interpret an object like a human. A camera is used to gain visibility to the computer. The inputs required to create the data base through the camera are obtained. A visual system digitizes the standardized state of the object to be interpreted by camera support and the image of these digitized objects is loaded into the database. Then, when the digital system is running, the camera sends the image to the digital converter. This digitized image is compared to pre-recorded digital images in the computer's database. The system recognizes the object as a result of this comparison. It is possible to use visual systems only for special cases where several images can take place.

17.8 Robotics

Robots are a harmonious integration of computers and industrial robots. It is possible to teach industrial robots how to do any routine movement with the helpof computers. For example; car painting, screw tightening, material handling, and even defective parts such as detecting more complex behavior of robots today is possible to see. The area where artificial intelligence achieves the greatest commercial success is the robotic field. Robots are quite different in terms of appearance and function

from robots seen in science fiction films. Industrial robots, the most used today is a computer-controlled mechanical arm. This arm, also called the manipulator. It has the ability to do most of the movements that a human arm can do.

Industrial robots are more suitable for uniform work. For example, it is possible to use industrial robots to carry heavy loads and carry out dangerous work. Such dangerous and heavy monotonous works are available in almost every business area. The automotive sector is the sector that makes the most use of robots. In this sector, robots are mostly used in painting and assembly processes. Robots are used in the testing of electronic circuits and the placement of chips. Robots can even be used in surgery. Robots can perform a biopsy with a great accuracy, thus making the operation faster, more accurate and safer. The robots are taught by the computer how to do the work. It is possible to control the robots with a computer program. This program is a program that gives command to the robot about the time, direction and distance of the movement. Once programmed, there is little need to control the movements of the robots.

A robot will continue to do its job with great care without demanding anything. Another development in robots is the ability to detect some human perception of robots. Previously produced robots have the ability to do uniform work. Because they do not have human perception skills. Such robots are called pick and place robots. If these robots can gain human perception skills such as vision, hearing and speech, it would be possible for these robots to behave like human beings and thus to call them robots. With today's technology, a robot can be equipped with a visual sub-system. So that the robot can differentiate objects from a certain standard object.

Naturally, as improvements in visual system technology continue, it will be possible for robots to circulate in the workplace just like a human being. The developments in robot technology seem to make some scenes we see in science fiction films real. With the development of robot technology, new business areas were born. Manpower needed to design, manufacture, sell, assemble, program, repair and maintain robots. In addition, the robots have reduced costs and some businesses have been saved from bankruptcy. As a result, robot technology will continue to be used as long as it increases productivity. This increase in productivity will bring about a welfare increase throughout the society.

17.9 Conclusion

Intelligence and adaptive control are the most important approaches of information technology today. Now, the studies are not only at the laboratory level but also in industrial and social life. In recent years, it has been possible to see the intense use of intelligence and adaptive control techniques in manufacturing systems. The success of the studies depends on the use of the right technique in the right place for the right job. Thanks to the systematic approach, both costs will decrease and efficiency will be increased.

Many systems developed today show the accuracy of this. Intelligence and adaptive control systems are often used in jobs that require the use of people's intelligence, such as decision-making, problem-solving, interpretation, planning and control. They process symbolic information instead of numerical information. Instead of solving problems by using certain algorithms, they solve problems with intuitive approaches. They are capable of processing incomplete and uncertain information. They deal with the problems that cannot be built with known techniques and mathematical models. They have the ability to learn. Also, they can make mistakes. These programs are not developed to make mistakes. The fact that the error is not considered as an error in terms of the developers. Because their intuitive approaches require this. Therefore, information and its processing resulted in intelligent behaviors.

Intelligence and adaptive control deals with information organization, learning, problem solving, proofing theorem, modeling of scientific discoveries, sound and shape recognition, games, information representation, commenting, perception, natural language comprehension, and designing intelligent computer systems. Intelligence and adaptive control a computer-controlled machine has the ability to perform tasks related to high mental processes, such as reasoning, generalization and learning from past experiences, which are often considered to be human-specific attributes. Human-like robots will be manufactured in the future with the development of intelligence and adaptive control.

References

1. B. Kosko, *Fuzzy Engineering* (Prentince Hall, 1997), pp. 25–59
2. I. Satoru, B. Kosko, Fuzzy logic. Sci. Am. **269**(1), 76–81 (1993)
3. D. Driankov, H. Hellendoorn, *An Introduction to Fuzzy Control* (Springer-Verlag, Berlin Heidelberg Publisher, 1993)
4. G. Klir, B. Yuan, *Fuzzy Sets and Fuzzy Logic* (Prentince Hall, 1995)
5. S. Hayki, *Neural Networks* (Macmillan, New York, 1994)
6. A. Carrie, *Simulation of Manufacturing Systems* (Wiley, New York, 1988)
7. A. Nazre, R. Garg, A deep dive in the venture landscape of artificial intelligence and machine learning (2018), https://www.linkedin.com/pulse/deep-dive-venture-landscape-ai-ajit-nazre-rahul-garg-nazre. Accessed 25 August 2018
8. N.S. Gill, Artificial neural networks, neural networks applications and algorithms (2018), https://www.xenonstack.com/blog/data-science/artificial-neural-networks-applications-algorithms. Accessed 25 August 2018
9. F. Rosenblatt, Artificial neural networks tutorial (2018), https://www.tutorialspoint.com/artificial_neural_network/artificial_neural_network_building_blocks.htm. Accessed 25 August 2018
10. Mathworks. Design neural network predictive controller in Simulink (2018), https://www.mathworks.com/help/deeplearning/ug/design.htm. Accessed 25 August 2018
11. M. Hatem, F. Abdessemed, Simulation of the navigation of a mobile robot by the qlearning using artificial neuron networks. in *Proceedings of the 2nd International Conference on Computing and its Applications (CIIA'09)*, Saida, Algeria (2009)
12. C. Sammut, Reinforced learning structure (2016), https://www.cse.unsw.edu.au. Accessed 25 August 2018

13. P. Moallem, N. Razmjooy, A multi layer perceptron neural network trained by invasive weed optimization for potato color image segmentation. Trends Appl. Sci. Res. **7**, 445–455 (2012)
14. U. Ravale, N. Marathe, P. Padiya, Feature selection based on genetic algorithm and support vector machine for intrusion detection system. Procedia Comput. Sci. **45**, 428–435 (2015)
15. A. Al Khazraji, J. Zaytoon, Observer-based indirect adaptive sliding mode control design and implementation for a class of nonlinear systems, in Book: *Nonlinear Estimation and Applications to Industrial Systems Control*, Chapter 8, pp. 225–246 (2012)
16. H. El Alami, A. Najid, *Cluster Formation Using Fuzzy Logic for Wireless Sensor Networks, IEEE/ACS 12th International Conference of Computer Systems and Applications* (Marrakech, Morocco, 2015)
17. A.K. Aderonke, S.A. Babajide, A.A. Kayode, An integrated knowledge base system architecture for histopathological diagnosis of breast diseases. I. J. Info. Technol. Ccomput. Sci. **1**, 74–84 (2012)
18. P. Kokol, V. Podgorelec, T. Njivar, Computer and natural language texts—a comparison based on long-range correlations. J. Am. Soc. Info. Sci. **50**, 1295–1301 (1999)

Chapter 18
Load Shedding, Emergency and Local Control

Amin Mokari Bolhasan, Navid Taghizadegan Kalantari and Sajad Najafi Ravadanegh

Abstract Nowadays, control of smart grids is of great importance in power networks. Considering loads and generations uncertainties is a paramount idea amongst researchers to illustrate real conditions of smart networks. Furthermore, special methods are being required to prevent cascading failures in emergency conditions whenever an islanded Microgrids (MGs) tends to work independently. The first important factor is that loads demand are supposed to be completely catered in islanded MGs. Sometimes, shedding some unnecessary predetermined loads to attain systems previous balanced condition is common in electrical networks. In this chapter, we want to present an array of methods to control MGs in emergency conditions considering uncertainties. In this chapter, we focus our effort on developing a coordination control algorithm using Emergency Demand Response (EDR) resources and Under Frequency Load Shedding (UFLS) methods considering various probabilistic scenarios. It is of supreme importance to design an optimal load shedding strategy in which customers and distribution companies' rights are guaranteed.

Keywords Microgrid · Microgrid control · Microgrid states · Emergency control · Under frequency · Load shedding

A. M. Bolhasan · N. T. Kalantari (✉) · S. N. Ravadanegh
Electrical Engineering Department, Faculty of Engineering, Azarbaijan Shahid Madani University, Tabriz, Iran
e-mail: taghizadegan@azaruniv.ac.ir

A. M. Bolhasan
e-mail: amin.mokari67@gmail.com

S. N. Ravadanegh
e-mail: s.najafi@azaruniv.ac.ir

N. Mahdavi Tabatabaei et al. (eds.), *Microgrid Architectures, Control and Protection Methods*, Power Systems,
https://doi.org/10.1007/978-3-030-23723-3_18

18.1 Introduction

The economic growth for each region is directly related to producing energy of it. Usually, most of the country's energy consumption is obtained from fossil fuels. Widespread use of fossil fuels contributes to environmental pollution, resulting in climate change and environmental degradation. On the other hand, these fuels are not renewable sources, and would be depleted in the future. Each country is trying to decrease carbon emissions with using renewable resources instead of fossil fuels. These types of Distributed Generations (DGs) have little environmental effects due to their less amount of toxic emissions. The problem is that DG units like wind and solar Photo-Voltaic (PV) power are non-dispatchable [1].

In addition, because of the probabilistic status of the load usage in electric power networks, it is needed to analyze the demand uncertainty nature in operation and planning stages of power network [2]. MGs are able to provide various financial and environmental benefits but their independent implementation has a myriad of protection, control and energy managing [3]. In this chapter, we discuss about the control management of MGs in presence of emergency conditions. Facilities used to prevent MGs instability in the preventive control schemes include: Load Shedding (LS), re-dispatch of active and reactive powers of generators, and Demand Response (DR) [4].

Load shedding is one of the most important and costly countermeasures against MGs instability. UFLS has become an important control scheme to keep the frequency of MGs exposed of power deficit. In this chapter, an optimal adaptive UFLS method with the advent of two main modules is proposed. Two main modules presented in this chapter are Pre-determined Load Shedding Calculator (PLSC) and Determined Load Shedding Calculator (DLSC). These two main modules provide an accurate load shedding procedure. This chapter also illustrates the effect of DR programs in an islanded MGs. EDR program provides consumers the lower electricity price since they are supposed to decrease their consumption when the system faces an unbalance. Distribution Network Operator (DNO) confronts fewer shedding loads and cost function reduction when DR programs are implemented. DR programs also impose an excessive unintentional delay time which can cause a limitation boundary to use these methods in MGs. For the big power unbalances, the system frequency experiences an unallowable minimum frequency threshold which causes cascading failure [5].

In this chapter, an optimal load shedding procedure is used to minimize shedding cost function. In addition, comparative simulations based on various probabilistic scenarios are also analyzed to find the best technique for the beneficial control of islanded MGs. This chapter is organized as follows: In Sect. 18.2, MGs are described in detailed. In Sect. 18.3, MG control is explained. In Sect. 18.4, MG load shedding procedures are presented. In Sects. 18.5 and 18.6, uncertainty and probabilistic frequency regulation in MGs are illustrated separately. Finally, conclusions are presented in the last session.

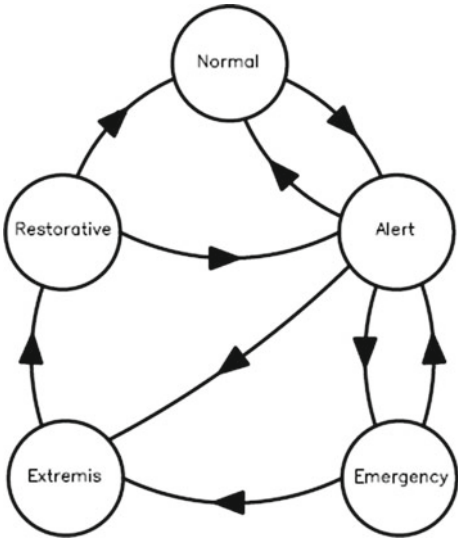

Fig. 18.1 Microgrid operational states

18.2 Microgrids

MGs are composed of Distributed Energy Resources (DER) and controllable loads. MGs are able to work controllably in both isolated and connected forms [6]. MGs can improve the reliability and security of network. Furthermore, they provide extra power and help voltage support to the network during interconnected state of operation. The DG have a great impact on distribution protection system causing loss of protection coordination, and unnecessary tripping. The DER and the type of that can considerably affect microgrid protection system. On the other hand, islanded operating mode [7] can endanger the sensitivity of the network caused by drop of fault current contribution from the utility and malfunction of relays. So, the novel method in designing the control system is mandatory. In [8], IEC 61850 and IEC 60870-5-104 communication standards are used in the microgrid substation centralized controller.

Microgrid Operation States (MGOS) of power system can be classified into various major states containing: normal, alert, emergency, restorative and last but not least extremis [9]. In the normal sate, the entire system correctly functions and the variables are in the expected range. In this state, the network is able to tolerate disturbances, which may cause deviation of variables from their steady state value. The system can be in normal state without losing stability whether it can withstand potential contingencies such as generator trip. A network configuration or loading state is called N-1 secure, when it can withstand an element outage without loss of supply to any load. However, we can call the system insecure in the alert state. In Fig. 18.1, the transition flow chart between aforementioned states considering system security degree is portrayed.

The network state goes to an alert state provided that the level of system security decreases to a lower level because of the higher probability of disturbance occurrence. The network in an alert state is not strong enough as before and it is on the verge of passing to other states. In this state, all of the variables are still inside the satisfactory limits. Preventive control actions are required in this state to change the network to the normal state whether the network operator understands from the measured data that the system is in the alert state. Conversely, the network operator may not react in time before a contingency actually occurs.

Two reasons may cause system to operate in an alert state. 1. High cost preventative control 2. Inadequate reserve margin. Being in an alert state is not acceptable and it may lead to emergency condition if emergency control actions fail. Great economic loss will occur when the system faces blackouts. If we want to classify system state as an alert or normal, we need to simulate some disturbances using power system software's. The system may face three different states after it experiences an alert state. These states can be normal, emergency, and extremis. In the normal state, the security indices are returned to the normal values. In an emergency state, some parts of the network may be overloaded or the level of voltages of some buses dropped to an unacceptable values. System state would be distinguished as extremis when the disturbance is very severe.

If the system cannot overcome extremis state, the whole system would experience cascading events, outages and perhaps shutting down of power system and blackouts. In some cases, proper countermeasures have been used early enough to restore an unbalance system from extremis state and pass the state to either normal or alert state.

18.3 Microgrid Control

Microgrid is an independent power system, which operates autonomously. Microgrid considers customers rights in providing reliable and high-quality power. To access this aim we need an acceptable microgrid control methodology.

The aims of this methodology are as follows [10]:

1. Novel micro sources are added to the network without any revision.
2. Operation points can be chosen automatically.
3. In a quick way, the microgrid can isolate or connect to the upstream network.
4. Reactive and active power can be independently controlled.
5. Voltage sag and system imbalances can be corrected.

Microgrids control strategies may face some challenges as low inertia and uncertainty [11].

Microgrid's reliability and economical operation should be guaranteed by the control system while addressing the aforementioned issues. In the control system, output power, power balance, Demand Side Management (DSM), economic dispatch, and transition between modes of operation should be considered.

To begin with, oscillations of currents and voltages of the different DERs should be monitored and damped in the control system. Frequency and voltage values should be maintained within the acceptable ranges by DER units when the microgrid is facing sudden active power imbalance. DSM methods can be used to control a portion of the load to overcome system frequency unbalance. The active participation of the distant units with many renewable units might be valuable in designing profitable DSM methods which will improve load-frequency controlling [12, 13]. Reducing the operation costs, and increasing the profit can be accessible by using an appropriate dispatch of DER units. Furthermore, working in connected and separate states of operation is the desirable feature of microgrid which will impose some challenges. To overcome these issues, for each state of operation, various control methodologies should be considered [14].

18.3.1 Microgrid Emergency Control

The system can transit from a supposed alert state to an emergency state if no preventive control actions are implemented, while a contingency occurs, or may directly transfer to an emergency state from a perceived normal state provided that an unanticipated sequence of several contingencies occur. Some equipment limits are exceeded, if the system enters into an emergency state, which may cause tripping of further equipment, so may lead to blackout. Emergency control system is required to overcome the issues. Because most of equipment can resist a short-time thermal overload, there is a short window of time where some manual emergency measures can be used. For instability or other urgent situations, too short reaction time and automatic emergency measures will be required. However, in most cases, a quickly respond is needed which relies on automatic controls.

Microgrid Emergency Control (MEC) actions are the last solutions to prevent blackouts in an emergency state. In MEC actions, voltage and frequency indices play a paramount factor in decision-making. DGs, especially Renewable Energy Sources (RESs), are of great importance in MEC actions. Network voltage and frequency are significantly influenced with the integration of wind power in various disturbances. In microgrids with high penetration of Wind Turbine Generations (WTGs), MEC action requires a revision to address problems properly. In addition, severity of the events should be considered as various disturbances may occur in the power system, but only few of them may cause system blackout. Severity of the events can be measured in an online basis, which can help Distribution System Operators (DSOs) to properly tune emergency control factors.

Power unbalance in microgrids may change the state of the system to the emergency state. To overcome this issue, spinning reserves have been used. In some cases, the severity of the disturbance is high and they are not fast enough to overcome serious active power deficit and prevent system blackout. So, spinning reserves cannot address this problem accurately in severe events.

In severe events, load shedding can be the last and fastest MEC action to prevent system blackout and generator outages. Under frequency and under voltage load shedding controller shed loads that cannot be supplied within permissible range of frequency and voltage.

The penetration level of WTGs considering their capacity, technology, and location should be considered from a protection point of view according to numerous papers. For investigating the penetration limit, various tests should be implemented to evaluate mitigation strategies regarding system protection. The presence of WTGs in microgrid feeders can change the behavior of the feeder as a load, which may generate blind zone of detection to protection relays or cause problems in protection coordination zones.

18.4 Load Shedding

System will face emergency conditions when it experiences the deviations of the system frequency. The imbalance between generation and demand can be caused by a sudden rise of the system demand or electric power supply failures. If there is no way to compensate this imbalance, finally, the network will face an imbalance. In small imbalances, governors and spinning reserves can control the output power and solve the problem individually [15].

On the other hand, whenever we face a big imbalance, the response time of governors and spinning reserves are not appropriate and the system cannot compensate an imbalance and may result in blackout. In these emergency conditions, we need to use UFLS schemes to return the system back to the normal state. UFLS methods are categorized as traditional, adaptive and semi-adaptive techniques [16]. The simple traditional UFLS method is often used among the others, due to its simplicity in manufacturing of the frequency relays. When the frequency declines below a predetermined threshold, the traditional method curtails a specific amount of load. The frequency will become stable due to load-frequency control capability of generators if this amount of shedding loads are appropriate. The next load shedding stage is executed provided that the frequency crosses the next threshold value.

The semi-adaptive load shedding procedure utilizes the Rate of Change of Frequency (ROCOF) as a pointer of the active power deviation. The amount of predetermined shedding loads are proportional to ROCOF whenever the frequency arrives to the specific threshold value. By and large, the ROCOF amount is employed only once at the first frequency threshold. The ROCOF thresholds and the amount of shedding loads at each stage are determined off-line based on simulation and test. The scheme is dependent on the severity of the disturbance because of proportionality of the amount of shedding loads to the ROCOF value. Using ROCOF and utilizing the power swing equation provide an estimation of power deficit in an adaptive UFLS method. Adaptive UFLS methodology has been presented to enhance the act of traditional load shedding procedures.

18.4.1 Adaptive UFLS Methods

Adaptive UFLS procedures can be modified with the advent of centralized UFLS schemes to curtail appropriate amounts of loads [17–19]. If the frequency of the system has been decreased to a specified amount, UFLS method will be activated. Using a calculated primary ROCOF, the amounts of shedding loads are determined [20, 21]. In [22], System Frequency Response (SFR) flowchart and proposed reduced models are put forward which can ease the procedure of the power deficit calculation. Power system load is influenced by the variations of voltage magnitude. Therefore, the major drawback of using the SFR model is that loads voltage dependency is not considered. There are some literatures considering loads voltage dependency in calculation of an unbalanced power [23–25]. An adaptive SFR model incorporating system inertia, response of governors and considering load's frequency and voltage dependence is presented in [26]. According to [27], calculated primary ROCOF is multiplied with a specified amount to consider loads voltage dependency. The major drawback of distant adaptive UFLS methods in determining power deficit is the presence of uncertainty.

In [28], the author has proposed a Centralized Adaptive UFLS controller (CAULSC) that makes use of the frequency, ROCOF, and a Distribution State Estimator (DSE) for estimating load demand to maintain system frequency response. In contrast to majority of adaptive schemes, the author in [29] solves the problem of power deficit estimation in which system voltage variation during an islanding mode is considered. In this method, future minimum frequency value determined by implementing the frequency versus Frequency First Time Derivative (FTD) phase-plane is predictable for various scenarios.

The priority and locality of the loads to be curtailed is of great importance in load shedding procedure. ROCOFL indices presented in [30] provides a correct comparison and selection of loads to shed sufficiently. An optimal load shedding method using an optimization solution to build loads priority look-up table is presented in [31]. The cost of curtailed loads has been considered in [32] to have an economical load shedding process. Three stages are proposed in [32] that can be divided into the following categories:

- Requirement Analysis (RA)
- Pre-disturbance Preparation (PP)
- Real-Time (RT).

Using CPLEXs solution pool feature provides an optimal cost effective solution to solve load shedding problem [32]. Reddy et al. [33] implement the study of sensitivity in Phasor Measurement Unit (PMU) to determine the position and size of loads to be curtailed. In [34], representative Operating and Contingency (OC) schemes have been selected. The UFLS methodology can be efficient by implementing an optimization scheme for example Simulated Annealing (SA) to regulate the UFLS parameters in [34]. The size of shedding steps is not supposed as decision variables. Frequency, ROCOF thresholds and internal time delays are optimized in the proposed method.

Through finding the optimal amount of shedding loads while satisfying load flow equation and static power system limitations such as line flows, voltages, angular constraints and curtailing limitations are proposed in [35]. A hybrid technique, namely the mixture of Genetic Algorithm (GA) and Artificial Neural Network (ANN), is implemented in [35] to minimize load shedding and voltage deviation. Smart grid approaches for UFLS procedures are fully explained in [36, 37].

18.4.2 Demand Response and UFLS Programs

Nowadays, DR programs are used to control frequency of the system using economic incentives for the sake of maintaining frequency responses. Many frequency control strategies by DR are presented in which disturbance magnitude estimation based methods, hill climbing control methods and methods based on Linear Quadratic Regulator (LQR) for controlling frequency of singular areas are considered. In [38], the author presented a DR control methodology which considers tie-line power swing as a conventional feedback control signal in multi area system. This method makes use of a multi-objective optimization problem to determine parameters of DR and AGC control optimally. Furthermore, Loads can be divided into controllable and non-controllable ones. Loads used in DR programs are usually considered non-essential loads. For instance, these loads are heaters of water, Heating, Ventilation and Air Conditioning (HVAC) systems, refrigerators and so forth. Increasing or decreasing amounts of these residential loads would not affect their convenience. According to [39], DR appliances consists of electrical appliances and controllers. Controllers can manage electrical appliances by changing convenient set point.

In [40], the author applies DR program to the area after calculating the magnitude of unbalance and determining the area in which a disturbance is occurred. A regional DR to use in controlling of multi-area power system frequency is also presented in [41]. This method uses the second derivative of power of tie line to determine disturbance size and the location during events.

18.4.3 UFLS Methods in Microgrids

Modern microgrids will be equipped with Information and Communication Technology (ICT) [42]. In [43], an online control methodology is illustrated. Load curtailments are assumed as a part of DR programs to maintain the distribution's feeder's voltage within the specified range. In this methodology, EDR programs are used. In this paper, Supervisory Control and Data Acquisition (SCADA) solution bring comprehensive merits for monitoring and control tasks in Distribution Automation (DA) and Distribution Management System (DMS).

In [44], the new optimal UFLS scheme for islanded distribution system integrated with DGs is proposed. Here, the estimation of power deficit by reduced SFR pattern

is not needed. Moreover, the proposed procedure offers ROCOF based method that assumes dependence of loads voltage and network frequency. Regardless of the previous methods, this paper considers dependence of loads voltage and frequency during the ROCOFL determination. Revised $ROCOFL^{*}_{pv}$ is presented in this paper to consider voltage dependence of loads for the sake of shedding fewer and accurate amounts of loads. Here, an optimal centralized adaptive UFLS method with the advent of two main modules is proposed.

18.5 Uncertainty

Nowadays, small DGs regularly based on renewable resources are near the consumers. These sources has presented MGs a promising answer for environmental economic issues. Micro gas turbines, diesel generators, energy storage systems, and demand side management systems make Microgrid. Dispatchable units can address the problem of unpredictability of renewable energy resources such as wind micro turbines [45]. On the other hand, the optimal operation of microgrids can be complex matter by using the controllable units and the uncertainty in renewable sources. Furthermore, in the grid-connected mode, the microgrids can do power exchange with day-ahead and real-time markets. To decrease overall costs, cover uncertainties and maintain power balance microgrids can participate in the real-time markets cleared each hour [46]. However, market price can also impose an uncertainty in power exchange. To deal with this problem, it is better to develop proposed day-ahead optimization model which considers real-time operation, uncertainty of market price and renewable sources.

18.5.1 Load Uncertainty

Modeling of load uncertainty in both operation and planning stages of power system is of great importance. By and large, load uncertainty been modeled using Gaussian PDF [47]. In Eqs. (18.1) and (18.2), it is supposed that standard deviation and the mean of the load PDF, i.e. δ and μ_D are identified values. π_d identifies the possibility of d-th load scenario. It is important to notify that $P_{Dd\min}$ and $P_{Dd\max}$, as shown in Fig. 18.2, are the minimum and maximum values of real power demand at d-th load scenario.

$$\pi_d = \int_{P_{D_d}^{\min}}^{P_{D_d}^{\max}} \frac{1}{\sqrt{2\pi\delta^2}} \exp\left[-\frac{(P_D - \mu_D)^2}{2\delta^2}\right] \tag{18.1}$$

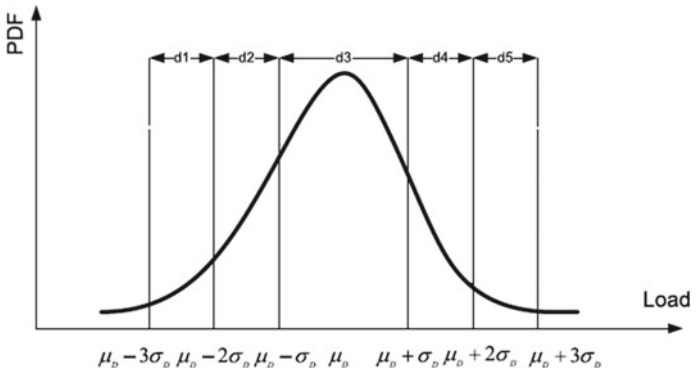

Fig. 18.2 The load PDF

$$P_{D_d} = \frac{1}{\pi_D} \int_{P_{D_d}^{\min}}^{P_{D_d}^{\max}} \left(P_D \frac{1}{\sqrt{2\pi\delta^2}} \exp\left[-\frac{(P_D - \mu_D)^2}{2\delta^2} \right] \right) dP_D \tag{18.2}$$

18.5.2 Wind Power Uncertainty Evaluation

Furthermore, to model the wind speed uncertainty the Rayleigh or Weibul *PDF* is used [48]. The generalized form of the Rayleigh *PDF* is the Weibull distribution. To model the wind speed with Rayleigh *PDF*, we can use the Eq. (18.3).

$$PDF(v) = \left(\frac{v}{c^2} \right) \exp\left[-\left(\frac{v}{\sqrt{2}c} \right)^2 \right] \tag{18.3}$$

Considering the wind speed range, we can generate scenarios. Using the Eqs. (18.4) and (18.5), we can determine the probability of scenarios separately. The corresponding wind speed v and the occurrence probability of scenario s are calculated as follows:

$$\pi_w = \int_{v_{i,w}}^{v_{f,w}} \left(\frac{v}{c^2} \right) \exp\left[-\left(\frac{v}{\sqrt{2}c} \right)^2 \right] dv \tag{18.4}$$

$$v_w = \frac{1}{\pi_w} \times \int_{v_{i,w}}^{v_{f,w}} \left(v \times \left(\frac{v}{c^2} \right) \exp\left[-\left(\frac{v}{\sqrt{2}c} \right)^2 \right] \right) dv \tag{18.5}$$

The wth scenarios starting and ending points of wind speed are identified as $v_{i,w}$, $v_{f,w}$ separately. In addition, v_w is the wind speed at wth wind scenario. Using historical

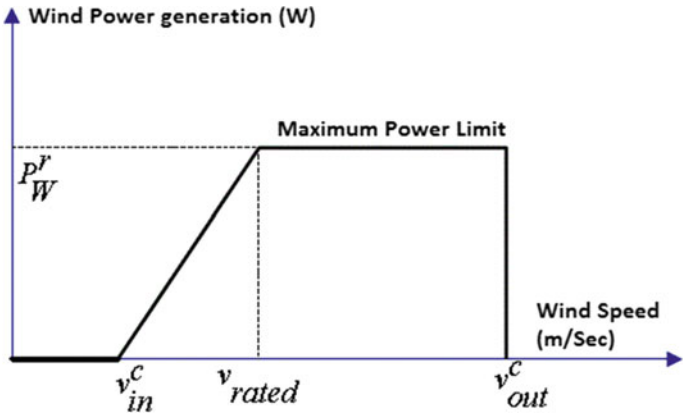

Fig. 18.3 A linearized characteristics curve of a wind turbine

data, we can obtain the c parameter. Furthermore, the relation between both wind speed and generated power can be obtained using wind turbine characteristic curve.

The linearized characteristics curve is portraying in Fig. 18.3. Using the Eq. (18.6) and characteristics curve, wind turbine forecasted output power for various speeds could be determined [49].

$$P_w^{avl} = \begin{cases} 0 & v_w \leq v_{in}^c \; or \; v_w \geq v_{out}^c \\ \frac{v_w - v_{in}^c}{v_{rated} - v_{in}^c} P_r^w & v_{in}^c \leq v_w \leq v_{rated} \\ P_r^w & v_{rated} \leq v_w \leq v_{out}^c \end{cases} \tag{18.6}$$

The number of load and wind scenarios can be multiplied to determine the number of scenarios for wind power and load demand (wind-load scenarios). The probability of scenario s, which is obtained considering wth scenario of wind and d-th scenario of load demand, can be obtained as Eq. (18.7).

$$\pi_s = \pi_w \times \pi_d \tag{18.7}$$

18.6 Probabilistic Frequency Regulation in Microgrids

Nowadays, microgrid deployment is an answer for electricity consumers who are not be able to be dependent on the main grid power or are keen on the financial profits from local generated power. However, microgrid implementation poses an array of technical issues in control section, protection system design, and management of power system. DERs, local loads, ancillary services, Energy Storage Systems (ESSs) , and power system control center (PSCC) form microgrids while connected or isolated from the main grid [50]. One of the most popular items in technical challenges of

the microgrid belongs to the power management, which is highly likely affected by DERs uncertainty [51]. In addition, any unbalance between demand and generated power in the microgrid should be compensated and maintained by the emergency reserves, which is called emergency Frequency Control Ancillary Services (FCAS) requirement.

18.6.1 Energy Storage System

ESS is widely implemented in power network applications. ESSs are able to offer spinning reserve and consumption power to maintain the frequency in MGs (called Frequency Ancillary Reserves (FAR)). Several types of ESSs are available and amongst them, Battery Energy Storage Systems (BESSs) are mostly used compared to others since their faster response time [52]. If we look at recent papers, they propose using Hybrid Energy Storage System (HESS), which has higher power density and longer lifetime compared to BESSs [53, 54]. The HESS uses the different effects of BESSs and Ultra-Capacitor (UC) to provide the fast dynamic response.

We can also find various specific ESS technologies such as Li-ion batteries, vanadium redox batteries, flywheels, or lead-acid batteries, etc. Recently, Electrical Vehicles (EVs) connected to the networks are similarly exploited to act as energy storage system. Using Vehicle-to-Grid (V2G) technology, frequency control can be accessible in the networks with Plug-in Electric Vehicles (PEVs) [55]. Today, BESSs are providing several services e.g., energy management, frequency and voltage regulation, and peak shaving in microgrids. The total daily use of battery capacity varies because stochastic resources play a paramount role in providing power in microgrids. According to recent literature, if a portion of the ESSs capacity remains unexploited of its main service, the system operator can use it for the secondary service for the sake of safety and income [56].

Several works propose variety of methods to couple multiple services in using ESSs to address the problem of uncertainty in power systems. According to [57], three distinct services can be proposed for the BESSs are Energy Arbitrage (EA), Ancillary Services (AS), and achievement of control objectives such as self-consumption. Although providing various services increases BESS's economic income, operation scheduling problems would arise. The FR providers are paid for providing a frequency regulation through ancillary services market. FR plays an important role in maintaining network stability by addressing the problem of power imbalance between generated and consumed power. Three levels of FR are Primary, Secondary, and Tertiary [58]. The Primary Frequency Regulating (PFR) needs high-speed actions whenever the system frequency fells outside the zone of non-critical frequency [54].

18.6.2 Ancillary Service Market

Prices in the wholesale electricity would be changed are based on the new market clearing price set every half hour by Energy Market Operator. ISO undertakes the responsibility for power management in electrical grids. The Regulation Service (RS) provider delivers its regulation bids (price, power and time of operation) to the ISO to participate in the ancillary service market. The electricity price follows the pattern of high price during on peak and low price during off-peak hours. RS provider can benefit from the electricity price discrepancy, which refers to as energy arbitrage. In some projects, the capacity of BESSs should have a fix amount to have a significant impact in frequency control.

In these cases, the aggregation of multiple small-scale BESSs into a large-scale entity is introduced. Here, BESS aggregation center would submit regulation capacities to the ISO for the sake of participating in FR services. ISO will send a regulation signal to the RS provider or BESS aggregation center after accepting the offer. Charging and discharging signals are sent to each BESS units by the BESS aggregation center controllers considering the participation factor and State-of-Charge (SOC) [53]. In [59], authors proposed the methodology to maintain the ESS SOC near to the favorable limit considering Automatic Generation Control (AGC) operation state, in which a continues frequency support is guaranteed.

18.7 Conclusion

In emergency conditions, the microgrid can be changed to the robust operation such as islanded state, to provide power to the local loads. In this case, prevailing uncertainties imposed by non-dispatchable renewable sources, local load's power consumption, ESS energy and power control, and the market price make the problem very challenging. To providing resiliency, the microgrid control system should be designed before, in the preventive stage. Furthermore, load shedding is exploited in cases of high consumption since FR services should operate instantaneously to protect the system's security. Some emergency conditions, such as generation loss, would affect the generation capacity of the power system. Islanded microgrids usually face imbalances between generation and load demand, which leads to disturbing the system frequency.

In particular, for small microgrids in which loads are small, frequency stability is a major concern during an islanded condition. Furthermore, wind power penetration increases in microgrids recently, which leads to small system inertia because of the existing power electronic devices used to decouple wind turbines from the ac grid. To address this issue, an optimal frequency control scheme should be considered to restore the security of the system. In the normal mode, the microgrid is connected to the upstream distribution grid. Therefore, it is sensible that microgrid would schedule

local generators and ESS power to transfer energy to upstream grid for the sake of reducing the microgrid operational costs.

References

1. M. Sedighizadeh, M. Esmaili, A. Jamshidi, M.H. Ghaderi, Stochastic multi-objective economic-environmental energy and reserve scheduling of microgrids considering battery energy storage system. Int. J. Electr. Power Energy Syst. **106**, 1–16 (2019)
2. A. Conejo, J. Antonio, L. Baringo, Power systems, in *Power System Operations* (Springer, Cham, 2018), pp. 1–15
3. M. Bello, A. Maitra, R. Dugan, M. McGrail, A. Reid, R. Rodrigo, Protection coordination considerations for a highly meshed urban microgrid. in *2018 IEEE Power & Energy Society Innovative Smart Grid Technologies Conference (ISGT)* (2018), pp. 1–5
4. M.N. Alam, S. Chakrabarti, A. Ghosh, Networked microgrids: State-of-the-art and future prospectives. IEEE Trans. Ind. Info (2018)
5. N.M. Sapari et al., Application of load shedding schemes for distribution network connected with distributed generation: A review. Renew. Sustain. Energy Rev. **82**, 858–867 (2018)
6. Smartgrids European Technology Platform—Vision and strategy for Europe's electricity networks of the future. Office for Official Publications of the European Communities, Luxembourg (2006), http://www.smartgrids.eu/documents/vision.pdf
7. H. Nikkhajoei, R. Lasseter, Microgrid protection. in *Proceedings of IEEE PES General Meeting*, Tampa, FL, USA (2007)
8. D. Ishchenko, A. Oudalov, J. Stoupis, Protection coordination in active distribution grids with IEC 61850. in *Proceedings of IEEE T&D Conference*, Orlando, FL, USA (2012)
9. P. Kundur, Power system stability and control. Tata McGraw-Hill Education (1994)
10. W. Huang, M. Lu, L. Zhang, Survey on microgrid control strategies. Energy Procedia **12**, 206–212 (2011)
11. D.E. Olivares, A. Mehrizi Sani, A.H. Etemadi, C.A. Canizares, R. Iravani, M. Kazerani, A.H. Hajimiragha, et al., Trends in microgrid control. IEEE Trans. Smart Grid **5**(4), 1905–1919 (2014)
12. C. Wang, M. Nehrir, Power management of a stand-alone wind photovoltaic/fuel cell energy system. IEEE Trans. Energy Convers. **23**(3), 957–967 (2008)
13. C. Alvial Palavicino, N. Garrido Echeverria, G. Jimenez Estevez, L. Reyes, R. Palma Behnke, A methodology for community engagement in the introduction of renewable based smart microgrid. Energy Sustain. Dev. **15**(3), 314–323 (2011)
14. H. Karimi, Islanding Detection and Control of an Islanded Electronically-Coupled Distributed Generation Unit. Ph.D., University of Toronto, Department of Electrical & Computer Engineering (2007)
15. W.A. Elmore, *Protective Relaying, Theory and Applications* 2nd edn. (Marcel Dekker, 2004)
16. B. Delfino, S. Massucco, A. Morini, P. Scalera, F. Silvestro, Implementation and comparison of different under frequency load-shedding schemes. Power Eng. Soc. Summer Meet. **1**, 307–312 (2001)
17. D. Xu, A.A. Girgis, Optimal load shedding strategy in power systems with distributed generation. in *Proceeding IEEE Power Engineering Society Winter Meeting* (2001), pp. 788–793
18. D. Hazarika, A. Sinha, Method for optimal load shedding in case of generation deficiency in a power system. Int. J. Electr. Power Energy Syst. **20**(6), 411–420 (1998)
19. P. Wang, R. Billinton, Optimum load-shedding technique to reduce the total customer interruption cost in a distribution system. Proc. Inst. Elect. Eng. Gen. Trans. Distrib. **147**(1), 51–56 (2000)
20. H. Seyedi, M. Sanaye-Pasand, Design of new load shedding special protection schemes for a double area power system. Am. J. App. Sci. **6**(2), 317–327 (2009)

21. V.V. Terzija, Adaptive under-frequency load shedding based on the magnitude of the disturbance estimation. IEEE Trans. Power Syst. **21**(3), 1260–1266 (2006)
22. P.M. Anderson, M. Mirheydar, A low order system frequency response model. IEEE Trans. Power Syst. **5**(3), 720–729 (1990)
23. U. Rudez, R. Mihalic, Analysis of underfrequency load shedding using a frequency gradient. IEEE Trans. Power Delivery **26**(2), 265–275 (2011)
24. A. Li, Z. Cai, A method for frequency dynamics analysis and load shedding assessment based on the trajectory of power system simulation. in *Proceedings of 3rd International Conference on Electric Utility Deregulation and Restructuring and Power Technology (DRPT)*, April 6–9 (2008), pp. 1335–1339
25. D. Prasetijio, W.R. Lachs, D. Sutanto, A new load shedding scheme for limiting underfrequency. IEEE Trans. Power Syst. **9**(3), 1371–1378 (1994)
26. T. Shekari, F. Aminifar, M. Sanaye Pasand, An analytical adaptive load shedding scheme against severe combinational disturbances. IEEE Tran. Power Syst. **31**(5), 4135–4143 (2016)
27. A. Mokari, H. Seyedi, B. Mohammadi Ivatloo, S. Ghasemzadeh, An improved under-frequency load shedding scheme in distribution networks with distributed generation. J. Oper. Autom. Power Eng. **2**(1), 22–31 (2014)
28. M. Karimi, P. Wall, H. Mokhlis, V. Terzija, A new centralized adaptive under frequency load shedding controller for microgrids based on a distribution state estimator. IEEE Trans. Power Delivery **32**(1), 370–380 (2017)
29. U. Rudez, R. Mihalic, Predictive under frequency load shedding scheme for islanded power systems with renewable generation. Electr. Power Syst. Res. **126**, 21–28 (2015)
30. P. Mahat, Z. Chen, B. Bak Jensen, Under frequency Load Shedding for an Islanded Distributed System with Distributed Generation. IEEE Trans. Power Delivery **25**(2), 911–918 (2010)
31. A. Mokari Bolhasan, H. Seyedi, B. Mohammadi Ivatloo, S. Abapour, S. Ghasemzadeh, Modified centralized ROCOF based load shedding scheme in an islanded distribution network. Int. J. Electr. Power Energy Syst. **62**(1), 806–815 (2014)
32. A. Gholami, T. Shekari, F. Aminifar, M. Shahidehpour, Microgrid scheduling with uncertainty: The quest for resilience. Smart Grid IEEE Trans. **7**(6), 2849–2858 (2016)
33. C. Reddy, S. Chakrabarti, S. Srivastava, A sensitivity-based method for under-frequency load-shedding. IEEE Trans. Power Syst. **29**(2), 984–985 (2014)
34. L. Sigrist, I. Egido, L. Rouco, A method for the design of UFLS schemes of small isolated power systems. IEEE Trans. Power Syst. **27**(2), 951–958 (2012)
35. V. Tamilselvan, T. Jayabarathi, A hybrid method for optimal load shedding and improving voltage stability. Ain Shams Eng. J. **7**(1), 223–232 (2016)
36. S. Mullen, G. Onsongo, Decentralized agent-based under frequency load shedding. Integr. Comput.-Aided Eng. **14**(2), 321–329 (2010)
37. V. Chuvychin, R. Petrichenko, Development of smart under frequency load shedding system. J. Electr. Eng. **64**(2), 123–127 (2013)
38. B. Yu Qing, L. Yang, W. Beibei, H. Minqiang, C. Peipei, Demand response for frequency control of multi-area power system. J. Modern Power Syst. Clean Energy **5**(1), 20–29 (2017)
39. Y. Bao, Y. Li, FPGA-based design of grid friendly appliance controller. IEEE Trans. Smart Grid **5**(2), 924–931 (2014)
40. P. Babahajiani, Q.Shafiee, H. Bevrani, Intelligent demand response contribution in frequency control of multi-area power systems. IEEE Trans. Smart Grid PP (99), 1–10 (2016)
41. P. Babahajiani, H. Bevrani, Q. Shafiee, Intelligent coordination of demand response and secondary frequency control in multi-area power systems (2016)
42. L. Nikonowicz, J. Milewski, Virtual power plants—general review: Structure, application and optimization. J. Power Technol. **92**(3), 135–149 (2012)
43. A. Zakariazadeh, O. Homaee, S. Jadid, P. Siano, A new approach for real time voltage control using demand response in an automated distribution system. Appl. Energy **117**, 157–166 (2014)
44. A. Mokari Bolhasan, N. Taghizadegan Kalantari, The new adaptive under frequency load shedding technique in an automated distribution network considering demand response programs. J. Power Technol. **98**(1), 127–138 (2018)

45. S. Chowdhury, P. Crossley, *Microgrids and active distribution networks* (Inst. Eng, Technol, 2009)
46. A.J. Conejo, M. Carrion, J.M. Morales, *Decision Making Under Uncertainty in Electricity Markets* (Springer, 2010)
47. A. Rabiee, A. Soroudi, B. Mohammadi-ivatloo, M. Parniani, Corrective voltage control scheme considering demand response and stochastic wind power. Power Syst. IEEE Trans. **29**, 2965e2973 (2014)
48. A. Soroudi, B. Mohammadi-Ivatloo, A. Rabiee, *Energy Hub Management with Intermittent Wind Power. Large Scale Renewable Power Generation* (Springer, Singapore, 2014), pp. 413–438
49. A. Soroudi, A. Rabiee, A. Keane, Stochastic real-time scheduling of wind thermal generation units in an electric utility. IEEE Syst. J. (2014)
50. S. Kakran, S. Chanana, Smart operations of smart grids integrated with distributed generation: A review. Renew. Sustain. Energy Rev. **81**(1), 524–535 (2018)
51. A. Gholami, T. Shekari, F. Aminifar, M. Shahidepour, Microgrid scheduling with uncertainty: The quest for resilience. IEEE Trans. on Smart Grid **7**(6), 2849–2858 (2016)
52. S. Chen, T. Zhang, H.B. Gooi, R.D. Masiello, W. Katzenstein, Penetration rate and effectiveness studies of aggregated BESS for frequency regulation. IEEE Trans. Smart Grid **7**(1), 167–177 (2016)
53. U. Akram, M. Khalid, A coordinated frequency regulation framework based on hybrid battery-ultracapacitor energy storage technologies. IEEE Access **6**(99), 7310–7320 (2018)
54. X. Zhou, C. Dong, J. Fang, Y. Tang, Enhancement of load frequency control by using a hybrid energy storage system. in *Proceeding of 2017 Asian Conference on Energy, Power and Transportation Electrification (ACEPT)*, Singapore (2017), pp. 1–6
55. H. Fa, L. Jiang, C. Zhang, C. Mao, Frequency regulation of multi-area power systems with plug-in electric vehicles considering communication delays. IET Gener. Trans. Distrib. **10**(14), 3481–3491 (2016)
56. J. Engels, B. Claessens, G. Deconinck, Combined stochastic optimization of frequency control and self-consumption with a battery. IEEE Trans. Smart Grid PP (99), 1–1 (2017)
57. E. Namor, F. Sossan, R. Cherkaoui, M. Paolone, Control of battery storage systems for the simultaneous provision of multiple services. IEEE Trans. Smart Grid PP (99), 1–1 (2018)
58. P. Kundur, N.J. Balu, M.G. Lauby, *Power System Stability and Control* (McGraw-Hill, New York, NY, USA, 1994)
59. J.W. Shim, G. Verbic, N. Zhang, K. Hur, Harmonious integration of faster-acting energy storage systems into frequency control reserves in power grid with high renewable generation. IEEE Trans. Power Syst. PP (99), 1–1 (2018)

Chapter 19
Smart Metering Based Strategies for Improving Energy Efficiency in Microgrids

Gheorghe Grigoras, Ovidiu Ivanov, Bogdan Constantin Neagu and Pragma Kar

Abstract In the last years, in the operation of electric distribution grids (EDGs), the optimization process is reduced to small size grids (namely microgrids) for which the number of variables is much lower, and finding the optimal solution is not a problem. To better supervise and control each microgrid, the emergence of smart metering system (SMS) can be interpreted as a transformation in progress encountered at the level of majority of distribution grid operators (DGOs). In these conditions, distribution grid operators (DOGs) have possibility to obtain online data about the electricity consumption of customers, respectively the electricity amounts product by the renewable sources, which allows them to take some technical measures which enable the microgrids to operate more energy efficient and better plan their investments. A critical assessment of microgrids referring to improving the energy efficiency brings out a series of problems partially unresolved due to the particularities of microgrids where they have been implemented. These problems are studied in this chapter and SMS-based new solutions are proposed for load modelling, phase load balancing and voltage control. All approaches are tested using real microgrids, and the obtained results highlight the performances on the energy efficiency measures.

Keywords Smart metering · Energy efficiency · Microgrids · Load modelling · Phase load balancing · Voltage control

G. Grigoras (✉) · O. Ivanov · B. C. Neagu
Power System Department, Electrical Engineering Faculty, "Gheorghe Asachi" Technical University of Iasi, Iasi, Romania
e-mail: ggrigor@tuiasi.ro

O. Ivanov
e-mail: ovidiuivanov@tuiasi.ro

B. C. Neagu
e-mail: bogdan.neagu@tuiasi.ro

P. Kar
Department of Information Technology, Jadavpur University, Kolkata, India
e-mail: pragyakar11@gmail.com

N. Mahdavi Tabatabaei et al. (eds.), *Microgrid Architectures, Control and Protection Methods*, Power Systems,
https://doi.org/10.1007/978-3-030-23723-3_19

19.1 Introduction

Due to the high complexity of electricity distribution grids (EDGs) and interconnection of various equipment and installations that operate on large geographic areas, the DGOs should supervise and control the EDGs with very large sizes. The decomposition into smaller grids from the technic and economic perspectives would bring many advantages, because it simplifies the solving of operation and planning problems and also the implementation of energy efficiency solutions. Thus, in many cases, the optimization of a large EDG is reduced at the level of some small grids (namely microgrids) for which the number of variables is much lower, and the optimal solution can be easily obtained. To better supervise and control each microgrid, the DSOs from many countries around the world have implemented in the last ten years SMSs.

Until recently, the EDGs were generally characterized by the lack of technical possibilities represented by smart devices that can help DGOs in the supervisory, control and decision making processes. Although the distribution feeders belonging to low voltage grids—LVGs (grids with small sizes, hereinafter referred to as microgrids) supply a high number of consumers, few information were gathered from inside (from the consumers and producers), with a delayed response time. In order to obtain as much data as possible from these microgrids, it was necessary to install smart meters which would allow the storage of supervised data (energy consumptions, active and reactive powers, voltage, power factors, harmonics etc.) and their transmission to DGO level.

The Smart Metering technology is essential for achieving the targets regarding the energy efficiency and renewable energy set for 2020, as well as the delineation of future smart grids. The implementation of smart metering systems at the European Union level is finished in some countries and is in different stages in others [1–5]. In this chapter, a special attention is paid to the management of databases built with the help of information provided by smart meters from consumers and producers for improving energy efficiency in microgrids. The benefits of smart meters consist in the fact that, in addition to the metering function, they also provide a whole range of applications, such as the following [6, 7]:

- secure transmission of data to the consumer or a third party (for example Metering Operator), respectively to the DGO;
- bidirectional communication between the smart meters installed at consumer/prosumer sites and the concentrators (information management points) belonging to the DGO;
- remotely controlled connection/disconnection from the grid or demand limitation at consumer sites;
- implementing of differentiated time-of-use tariffs.

In these circumstances, the DGOs can get accurate online information regarding electricity consumptions and productions from renewable sources, which allows them to take some measures which will enable the microgrids to operate more energy efficient and better plan their investments.

A critical assessment of the current approaches found in the literature referring to improving the energy efficiency brings out a series of problems partially unresolved due to the particularities of microgrids where they have been implemented. These problems are mainly referring at the following technical aspects: load modelling, phase load balancing, and voltage control.

Load modelling. Smart metering is an indispensable component of a smart grid. Using data received from smart meters, the operation of a microgrid can be improved, especially when renewable energy sources are present. On the other hand, the overwhelming amount of acquired information requires efficient and easy to use data management tools. The information provided by the smart meters can be used for load modelling, taking advantage of the advent of smart microgrids. In this context, profiling and forecasting models should be developed to work with large databases.

Phase load balancing. The existing theoretical and practical approaches regarding the phase load unbalances are targeted mainly on passive microgrids which do not contain distributed generation sources, and do not envision creating new customer services such as electric vehicle charging stations. But, the integration of distributed generation (DG) sources, high efficiency technologies, and new consumption behaviours of consumers/prosumers lead to power flow changes in the system, with negative effects on keeping electrical parameters in the ranges prescribed by regulations. The phase load balancing measure is applied with the purpose increasing the transmission capacity of electric distribution lines, having economic and technical benefits on the microgrid planning referring at the possibility to supply new consumers and to improve the voltage quality because the voltage drops are smaller for the balanced loadings of phases. In this context, new approaches will be presented to balance the phase loads. These approaches are based on the data recorded using the smart metering system, thus as the phase load balancing to be made at the microgrid level or connection points level of the consumers/producers.

Voltage control. In microgrids, the voltage control strategies were developed until recently on the assumption of unidirectional power flow. But, in certain extreme circumstances, due to the intermittent and sometime unpredictable behaviour of loads and distributed energy sources, their generation excess could lead to a reversed power flow, from the consumers, through the microgrids, into the supply grid. This problem necessitates the development and implementation of effective voltage control strategies so as to reliably serve the loads, particularly under islanded operation mode, to obtain the best solutions, with positive effects on the minimization of energy losses, also improving the energy efficiency of microgrids.

These problems will be discussed in the following, and new solutions will be proposed based on information provided by the smart metering system.

The structure of the chapter is based on the following sections: Sect. 19.2 includes the proposed solutions in the load modelling and testing using real microgrids; Sect. 19.3 discusses the phase load balancing problem and the new approaches to solve it with the evaluation of their impact on energy efficiency improvement in microgrids; Sect. 19.4 details the theoretical and practical aspects of proposed solutions in voltage control.

19.2 Smart Metering Based Load Modelling

19.2.1 Load Profiling Solutions

19.2.1.1 Solution Description

The SM system can help DGOs in the energy efficiency improvement, also emphasizing the trends of some factors (technic, economic or environmental) which influence the optimal operation of microgrids [8, 9].

Various real-time monitoring systems (for real-time electricity consumption, load or voltage profiles) or offline monitoring systems (using recordings from smart meters with structures adapted to the particular configuration of microgrids) can be developed [10].

The proposed monitoring system is based on a load profiling algorithm which uses database of the smart metering system from microgrids and extrapolation of data regarding the typical load profiles (TLPs) assigning them those customers from microgrids without a SM system.

The main stages of solution offered by algorithm are presented below. Also, these are indicated in Fig. 19.1.

Stage 1. Customers' Analyse: Identification of consumers from the microgrids based on the smart meter code and the most relevant attributes which will be recorded in the database.

Stage 2. Getting the electricity consumption macro-categories: Partitioning of the consumers into macro-categories (identified by electricity consumptions) considering the framing in the following economic domains: residential, commercial and industrial.

Stage 3. Getting the processed database: In practical applications, between the smart meters' consumers and data concentrators can occur the following problems: the communication line is faulty, the equipment are unavailable due to failure of a component, and also some consumers can have irregular atypical behaviours. Due to these possible problems, recordings with missing values and outliers could be detected in the databases. To process the data, these recordings will be cleaned or reconstituted (using Missing Data techniques).

Stage 4. Classification: Using the energy consumption from each day from the database, respectively average and maximum values of daily load as characteristic variables, a clustering based classification into more classes (clusters) inside each electricity consumption category is made. For each class, the characteristic load profiles will be achieved by calculation the average values inside the cluster in function by the used sampling (quarter hour, half hour and hour: 96, 48 or 24 values).

Stage 5. Assignation: A load profile will be assigned to each class based on the characteristic variables used at the Stage 4.

Stage 6. Total load estimation for the microgrid. A statistical method is used to estimate the hourly values using the following relations:

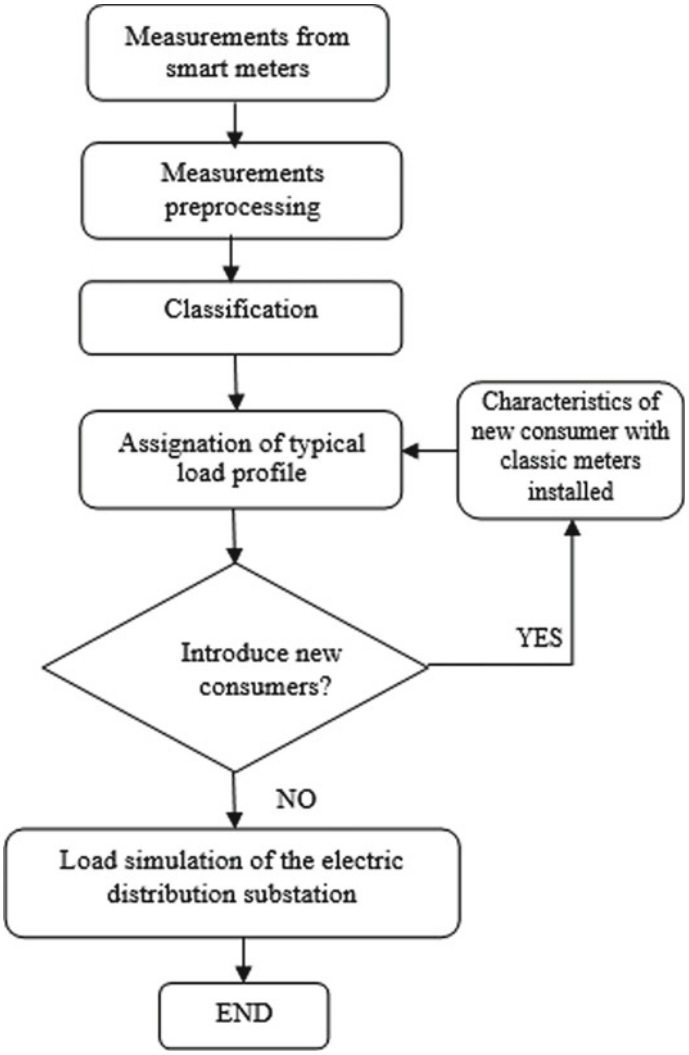

Fig. 19.1 The flow-chart of the proposed method

$$P^h_{microgrid} = \sum_{k=1}^{N_{ECC}} P^h_k, \quad h = 1, \ldots, T \tag{19.1}$$

$$P^h_k = \sum_{i=1}^{N^k_C} n^{(k)}_i W^{(k)}_{avg\,i} p^{h(k)}_i + \sqrt{\sum\nolimits_{i=1}^{N^k_C} n^{(k)}_i \left(W^{(k)}_{avg\,i} \sigma^{h(k)}_i \right)^2} \tag{19.2}$$

where, $P^h_{microgrid}$ is the load of the microgrid at hour h, $h = 1, \ldots, T$, T is the analysed time period (for a day $T = 24$), [kW]; CC is the consumption category ($ECC \in$ {residential, commercial and industrial}), N_{ECC} is the number of consumption categories identified in the microgrids (the maximum value can be 3); P^h_k is the load of consumption category k, $k = 1, \ldots, N_{ECC}$; $n_i^{(k)}$ is the customers from cluster i of consumption category k; $W^{(k)}_{avg\,i}$ is the average value of daily energy for all customers belonging the consumption group (cluster) i from the category k, [kWh]; $p_i^{h(k)}$ is the average hourly value of normalized active power belonging the consumption group (cluster) i from the category k [kW/kWh]; $\sigma_i^{h(k)}$ is the hourly standard deviation of normalized active power belonging the consumption group (cluster) i from the category k [kW/kWh]; $N_C^{(k)}$ is the number of consumption groups (clusters) belonging the category k of customers.

19.2.1.2 Testing the Solution

The database is described by 87 hourly load profiles transmitted by the smart meters of consumers belonging the residential category from a real microgrid. After recording the profiles, the data cleaning and pre-processing processes were initialized and 15 load profiles with lost, exceptional or equal with zero values were excluded. In the following stage, from the processing of eligible load profiles (74 load profiles) the following characteristic variables were extracted: the energy consumption from each day, respectively the average and maximum values of daily load. Using these variables, the classification process based on the Ward clustering method [11] was initialized and the customers were clustered in classes (groups).

The membership of each consumer to one from the obtained classes can be observed in Fig. 19.2.

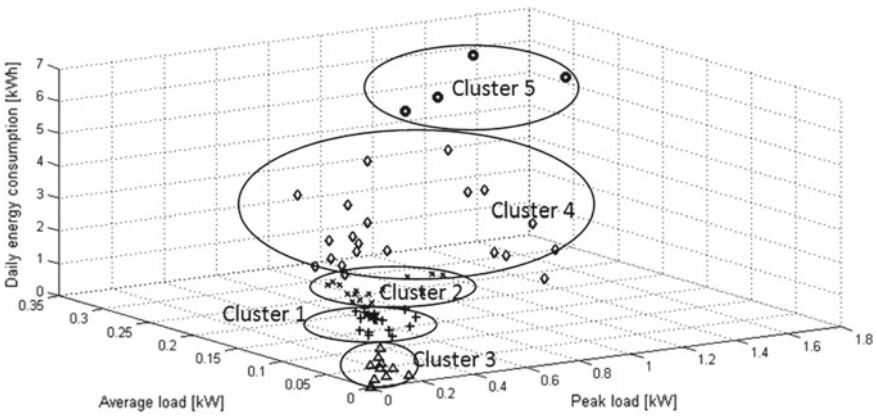

Fig. 19.2 The representation of the classes

The values from Table 19.1 were obtained through averaging inside each cluster the characteristic variables belonging to the consumers assigned in the classification process. The TLPs of residential consumers' category, for each class, are presented in Figs. 19.3, 19.4, 19.5, 19.6 and 19.7.

In these figures it can observed a different variation of load for the customers belonging the classes obtained in the clustering process. This variation influences the total load forecast from the microgrid which is used in electricity production schedule from the renewable sources. It is very important to know what the weight of each consumption class is in the total load to obtain a minimum cost of the kWh produced.

The testing of the approach was made for 60 consumers belonging to the same consumption category (residential) from another microgrid. Thus, based on the variables which characterize the electricity consumption (daily energy consumption, average

Table 19.1 The characteristic variables of classes

Class	No. consumers	Peak load (kW)	Average load (kW)	Daily energy consumption (kWh)
Cluster 1	20	0.233	0.060	1.35
Cluster 2	15	0.313	0.089	2.05
Cluster 3	14	0.072	0.011	0.25
Cluster 4	21	0.605	0.138	3.08
Cluster 5	4	1.273	0.262	5.87

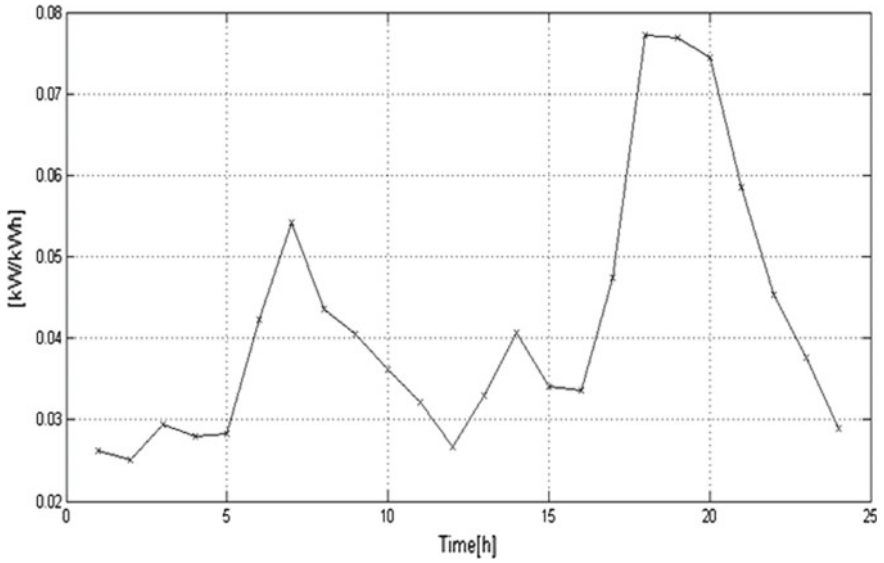

Fig. 19.3 TLP of class C1

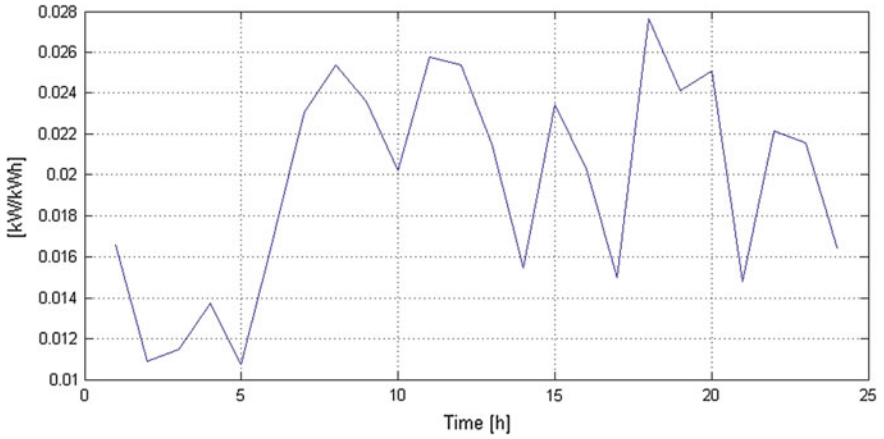

Fig. 19.4 TLP of class C2

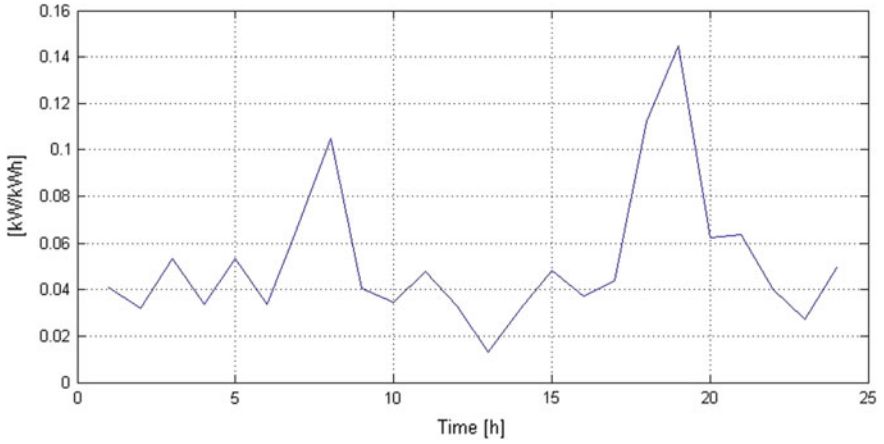

Fig. 19.5 TLP of class C3

load and peak load), the consumers were assigned to one of the classes obtained in the previous stage (Fig. 19.8).

Finally, the hourly load of the microgrid can be estimated using the values from Table 19.1 and Eq. (19.2). The graphical representation of the real and estimated hourly loads is shown in Fig. 19.9. The estimation process led at percentage errors between 1.5 and 5%, with the mean absolute percentage error having the value 3.8%.

Following the obtained results, the proposed approach should represent a technical solution which could be implemented in the planning process of microgrids where the energy efficiency strategies become priority for the DGOs.

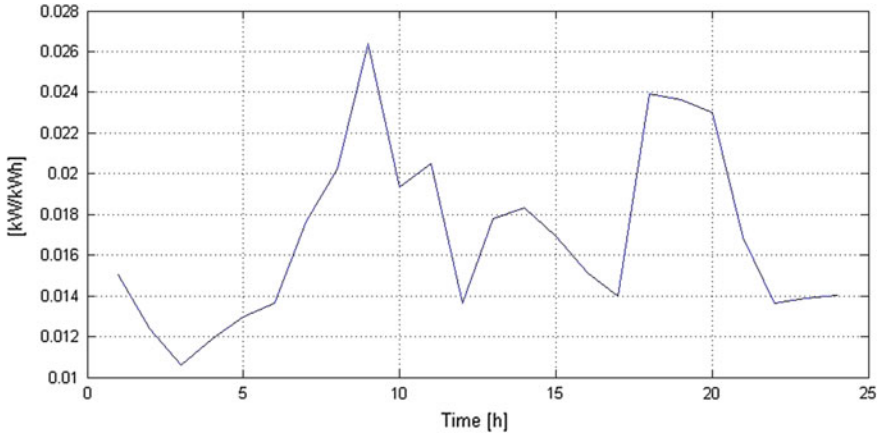

Fig. 19.6 TLP of class C4

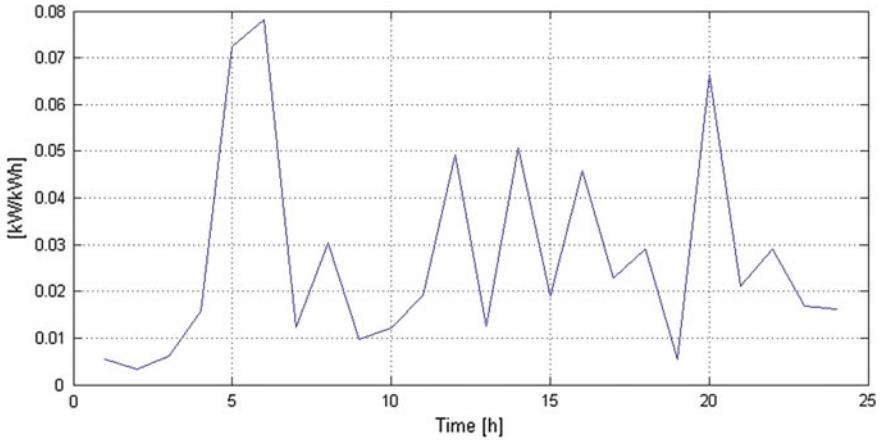

Fig. 19.7 TLP of class C5

19.2.2 Demand Response Solutions

19.2.2.1 Solution Description

Demand Response (DR) programs are used by DGOs for managing the loads from a microgrid at peak hours. Customers enrolled in DR initiatives are asked to reduce their consumption in exchange for some benefits received in return. Based on the used approach, DR types are classified into two categories: Incentive-Based (IB) and Price-Based (PB) [12, 13]. IB programs can be classical or market-based. Classical programs give incentives such as invoice credit or discounts and they can be Direct Load Control (DLC), which give the utility permission to automatically disconnect

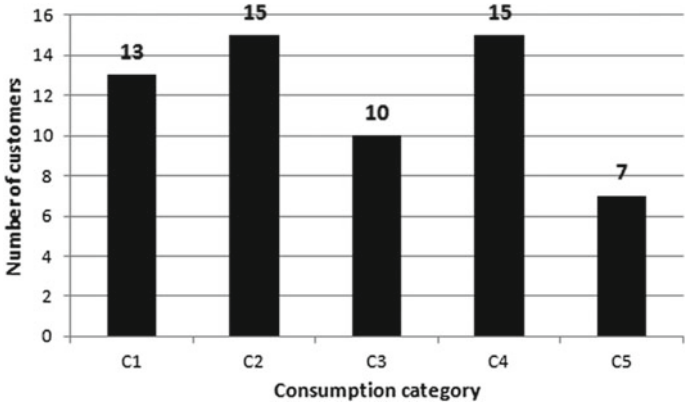

Fig. 19.8 The assignation process of the consumers in the testing stage

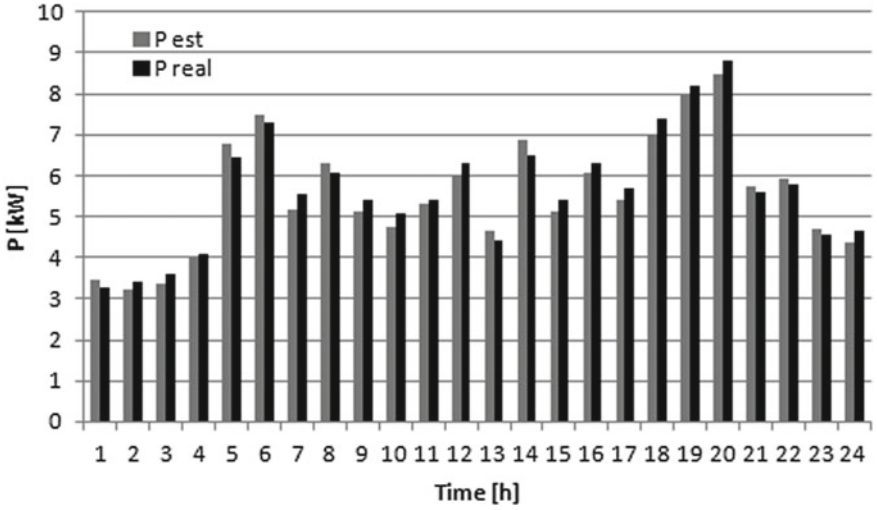

Fig. 19.9 The real and estimated load of the microgrid

loads, and Curtailable Load, which allow the user itself to limit its consumption down to a requested level. IB programs, which include Ancillary Services Market, Capacity Market, Demand Bidding and Emergency DR, give rewards according to the demand reduction achieved by the user. PB programs employ differentiated tariffs in order to stimulate load reduction at peak hours. Time-of-Use tariffs (ToU), where the electricity cost is lower in off-peak intervals, Critical Peak Pricing (CPP), Critical Day Pricing and Real-Time Pricing (RTP) can be used for this purpose.

DR algorithms have also been developed for microgrids. They take into account the possibility to build an optimal schedule for the interruptible and controllable loads considering CPP, ToU or RTP constraints, incorporating DG and RES at the level of a

microgrid [14]. Such an algorithm could try a day-ahead multi-objective scheduling optimization to match the consumer load profile with the utility load profile both ways, from the consumer to the utility and from the utility side to the consumer. Here, appliances are controlled using signals sent though the SM infrastructure. The consumers can be from different consumption categories (residential, industrial or commercial) [15].

To obtain the optimal solution, a wide array of solving methods were used until now in the literature: Mixed Integer Linear Programming [14] or Genetic Algorithm [15], the branch-and-bound algorithm [16], and Particle Swarm Optimization and a fuzzy model [17].

This paragraph describes a PSO based efficient DR optimization algorithm having strong links with SMS, which can be used at the level of a microgrid. The task of the optimization algorithm is to manage the DR signals sent by the DGO to the DR-enabled consumers, according to several individual criteria. Using as reference the present-day load patterns of the microgrid, DR-enabled consumers are selected, for which it is considered that Home Energy Management Systems (HEM) infrastructures exist, that can automatically provide to the utility data regarding the home appliances available for DLC. For these appliances, the individual users can define priority levels for automatic disconnection. The minimization of the number of affected users, comfort disturbance and of power loss, and load balancing on the three phases are considered as objectives.

The Particle Swarm Optimization (PSO) based proposed solution can be used in microgrids with bidirectional communication and DLC capabilities between the DGO and consumers. In these microgrids, it is also assumed that only a fraction of the consumers is available for DR, and these consumers have individual HEM systems, which provide to the DGO the following data: the instantaneous load drawn from the microgrid and the power available for DR, given as a list of maximum 4 priority or comfort levels, each with its own instantaneous active power value, that can be automatically disconnected by the algorithm in the event of a DR request. For privacy reasons, the operator is unaware of the actual appliances disconnected. For each customer, regardless of its DR availability, the algorithm receives the information given in Fig. 19.10 and Table 19.2.

In Table 19.2, the variables denote: $dist_i$ is the distance between the substation and the consumer, in [m], ph_i is the phase on which consumer i is connected, (ph_i can have the value 1, 2 or 3 for single phase consumers or 0 for three phase consumers), TP_i is the total measured power draw for consumer i, in [kW], and $DP_{i,j}$—the power

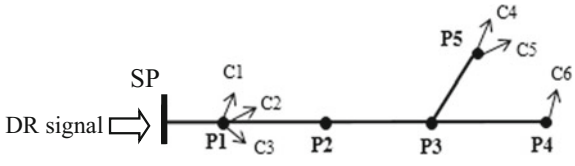

Fig. 19.10 A section of a microgrid

Table 19.2 Consumer data

1	2	3	4	5	6
ph_1	ph_2	ph_3	ph_4	ph_5	ph_6
$dist_1$	$dist_2$	$dist_3$	$dist_4$	$dist_5$	$dist_6$
TP_1	TP_2	TP_3	TP_4	TP_5	TP_6
$DRP_{1,1}$	$DRP_{2,1}$	$DRP_{3,1}$	$DRP_{4,1}$	$DRP_{5,1}$	$DRP_{6,1}$
$DRP_{1,2}$	$DRP_{2,2}$	$DRP_{3,2}$	$DRP_{4,2}$	$DRP_{5,2}$	$DRP_{6,2}$
$DRP_{1,3}$	$DRP_{2,3}$	$DRP_{3,3}$	$DRP_{4,3}$	$DRP_{5,3}$	$DRP_{6,3}$
$DRP_{1,4}$	$DRP_{2,4}$	$DRP_{3,4}$	$DRP_{4,4}$	$DRP_{5,4}$	$DRP_{6,4}$

available to be disconnected during Demand Response for consumer i at priority level j, in [kW].

The priority levels $DRP_{i,j}$ define the comfort settings defined by users, who decide the number and order in which some appliances (given as their instantaneous power draw) can be disconnected via DLC when the maximum power draw of the house is limited with a DR signal.

Consumers which are not available for DR have all $DRP_{i,j}$ values equal to 0. Also, in order to consider for the possibility that some appliances, while generally available for DR, are momentarily not accessible, because they will not be turned on during the DR interval or they cannot be switched off, any level of a DR-enabled consumer can be set to 0.

The task of the algorithm is to distribute the amount of active power requested as DR signal at a given moment by the utility at Supply Point (SP) level, between the DR-enabled customers, considering one of the four considered criteria, individually:

- $C1$. The minimization of the number of users affected by the DR signal:

$$\min(count(C_i)), \quad i = 1 \ldots NC_{DR} \tag{19.3}$$

- $C2$. The minimization of the overall number of comfort levels affected across the microgrid:

$$\min\left(\frac{1}{NC_{DR}} \sum_{i=1}^{NC_{DR}} \sum_{j=1}^{NL_i} CL_j^2\right) \tag{19.4}$$

- C3. Load balancing at SP level, on all three phases (where TP_i, TP_j and TP_k are given in kW):

$$\min\left(\sigma^2\left(\sum_{i=1}^{NC_a} TP_i, \sum_{j=1}^{NC_b} TP_j, \sum_{k=1}^{NC_c} TP_k\right)\right) \tag{19.5}$$

- $C4$. Active power loss minimization.

The last objective uses a simple alternative approach, which avoids the computation of unbalanced three phase estimation or load flow, thus decreasing the complexity of the algorithm and improving its speed. Instead, the distance between the consumer and SP, and the load value, are considered for computing a disconnection priority level. A reference distance mark is chosen, measured from SP, based on which the microgrid is split in two sides, lower (closer to SP) and upper. The initial disconnection priorities (DP) are assigned in ascending order, in both microgrid sides, lower and upper, based on the distance (higher distance means higher priority). For each solution generated by the algorithm, a lower side priority *lp* and upper side priority *up* is computed by summing the priorities of the customers chosen from each side. In this process, if a customer from the lower side has a load at least 50% greater than another customer with higher priority, their priorities are switched. The objective of this criterion is to maximize the sum of priorities, minimizing *lp* and maximizing *up*.

$$\max\left(\sum DP_i\right) \quad i = 1 \ldots NC_{DR} \tag{19.6}$$

For all criteria, C1–C4, the following constraint must be observed: the value of the total disconnected load must match as closely as possible the DR target given at the SP level:

$$\min\left|\sum DRP_{i,j} - T_{DR}\right|, \quad i = 1 \ldots NC_{DR}, \quad j = 1 \ldots 4 \tag{19.7}$$

Also, the load available for DLC from a client cannot exceed its total instantaneous load.

$$\sum_{j=1}^{NL_i} DRP_{i,j} < TP_j, \quad i = 1 \ldots NC_{DR} \tag{19.8}$$

In Eqs. (19.3)–(19.8), the variables denote: C_i is customer i; NC is the total number of customers in the microgrid; NC_{DR} is the number of clients available for DR; NL_i is the number of comfort levels used by customer i, CL_j is the j-th comfort level of customer i, NC_a, NC_b, NC_c is the number of customers connected in the microgrid on phase a, b, and c respectively; DP_i is the disconnection priority of customer i; T_{DR} is the target Demand Response level for *SP*, in [kW]. All other notations are the same as in Table 19.2.

For all these criteria, the possible solutions can be encoded using number vectors. The length of the vector is equal to the number of customers available for DR in the microgrid. The value of each vector element is equal to the comfort level up to which appliances are disconnected as DR requested limitation, for that user (from 0 to 4).

It is generally expected that in residential microgrids, the number of customers willing to participate in DR programs will be lesser than the total number of consumers. Reasons include low daily consumption, which makes the user ineffective for DR, or personal choice. For optimizing the speed and performance of the algo-

rithm, those consumers are not included in the solution. However, as presented in Table 19.2, they are included in the data set and used in computing criterion C3, which must consider for phase balancing all consumers from the microgrids, regardless of their DR availability status.

19.2.2.2 Testing the Solution

The PSO based DR algorithm proposed above was tested on a real microgrid with 178 residential consumers. Out of these, 5 are three-phase consumers, while the rest are single phase consumers. The phase distribution of the consumers belonging to each feeder of the microgrid, is given in Table 19.3. Using as reference a set of daily energy consumption profiles provided by the SM system, only selected consumers were considered for DR, out of the total of 178 consumers present in the microgrid.

The consumers having evening peak hour demand between 0.3 and 0.5 kWh were considered to have 1 DLC level, the consumers having 0.5–0.7 kWh were considered with up to 2 DLC levels, while the consumers exceeding 0.7 kWh were considered with 3 or 4 levels.

By choosing two peak hours from the daily load profiles of the consumers, a scenario was simulated, for which the initial data (load of microgrid, DR-enabled consumers and their phase distribution) is given in Table 19.4.

In Table 19.5 are given the comfort levels available for DLC for the DR-enabled consumers. The power values for individual comfort levels were chosen using the technical data of common household appliances, which can range from hundreds of watts to 2–3 kW. The actual placement of the DR-enabled consumers in the microgrid is presented in Fig. 19.11. In the figure, lines are sections from microgrid and dots

Table 19.3 Consumer feeder and phase allocation

Feeder 1	Feeder 1	Feeder 2	Feeder 3	Total
3-phase: 2	3-phase: 0	3-phase: 1	3-phase: 2	3-phase: 5
Phase a: 0	Phase a: 26	Phase a: 17	Phase a: 20	Phase a: 63
Phase b: 0	Phase b: 19	Phase b: 29	Phase b: 15	Phase b: 63
Phase c: 0	Phase c: 19	Phase c: 17	Phase c: 11	Phase c: 47

Table 19.4 Consumer feeder and phase allocation

Total no. of DR-enabled consumers		Total power demand (kW)		Number of customers and available DLC levels	
Total	32	Total	232.08	Up to 1 level only	18
Phase a	15	Phase a	79.66	Up to 2 levels	7
Phase b	9	Phase b	92.26	Up to 3 levels	3
Phase c	7	Phase c	60.16	Up to 4 levels	4
Three-phase	1	–		–	–

Table 19.5 Consumer feeder and phase allocation

	Cons. no.															
	1	2	3	4	5	6	7	8	9	10	11	12	13	14	15	16
Ph_i	1	2	1	2	3	3	1	2	1	2	1	1	3	3	1	1
$dist_i$ (m)	80	80	80	120	160	160	200	200	120	160	160	240	240	240	280	280
TP_i (kW)	1.8	2	1	6.3	1.5	7.4	1.7	6.4	1.9	2.8	1.2	6.7	1.3	2.9	1.8	1.3
$DRP_{i,1}$ (kW)	0.4	0.5	0.2	1.2	0.1	2.6	0.4	1.4	0.4	0.6	0.3	2.3	0.4	0.6	0.4	0.2
$DRP_{i,2}$ (kW)	0	0	0	1.1	0	1	0	1.1	1	1.6	0	1	0	1	0	0
$DRP_{i,3}$ (kW)	0	0	0	0.1	0	1.4	0	1.9	0	0	0	1.4	0	0	0	0
$DRP_{i,4}$ (kW)	0	0	0	2.8	0	1.1	0	1.4	0	0	0	1.5	0	0	0	0
	Cons. no.															
	17	18	19	20	21	22	23	24	25	26	27	28	29	30	31	32
Ph_i	2	3	1	0	3	1	1	1	2	2	1	3	1	2	1	2
$dist_i$ (m)	280	40	40	120	200	160	160	160	200	40	40	80	160	200	120	120
TP_i (kW)	6.1	1.4	2.4	1.6	1.7	1	1.2	1.1	3.8	7.1	5	1.8	2.6	1.3	1.5	2.4
$DRP_{i,1}$ (kW)	2.8	0.3	0.4	0.6	0.3	0.1	0.2	0.5	0.6	2.1	0.4	0.6	0.6	0.6	0.2	0.5
$DRP_{i,2}$ (kW)	1	0	1.4	0	0	0	0	0	1.7	1.9	0.8	0	1.1	0	0	1
$DRP_{i,3}$ (kW)	1	0	0	0	0	0	0	0	0	2.4	2.9	0	0	0	0	0
$DRP_{i,4}$ (kW)	0	0	0	0	0	0	0	0	0	0	0	0	0	0	0	0

are poles. For poles where consumers are connected, the total number of consumers is specified. If one or more of these consumers are DR-enabled, the pole is marked with red, and, above the number of consumers, the position of that consumer or those consumers in the solution particles is given. As specified in Table 19.4, there are 32 DR-enabled customers.

The PSO algorithm was run 10 times for each scenario, with a DR target of 15% of the total load from microgrid. Table 19.6 give the best obtained results for each of the four considered criteria.

Regarding to DR programs for residential consumers, these are expected to become more widespread in the future, together with the expansion of smart grids, capable of automatic two-way communication between utilities and their clients. From the point of view of optimal DR allocation scheme, investigating several optimization criteria: minimization of the number of affected users, the minimization

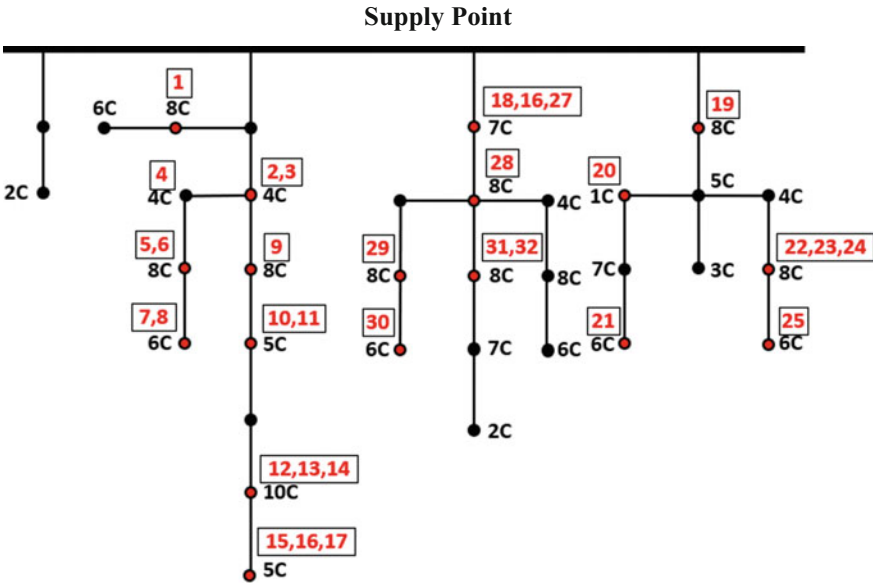

Fig. 19.11 The DR-enabled consumers

Table 19.6 Consumer feeder and phase allocation

Criterion	Fitness function for all criteria				DR achieved (kW)
	C1	C2	C3	C4	
C1—minimum users affected	11	5.28	130.99	0.0911	36
C2—minimum discomfort	14	2.31	22.56	0.0161	36.8
C3—phase balancing	21	6.16	19.20	0.0502	36.5
C4—minimum losses	23	5.22	134.84	0.0152	36.4

of user discomfort, phase load balancing at substation level and indirect power loss reduction, by favouring remote and high load consumers.

19.3 Smart Metering Based Phase Load Balancing

19.3.1 Solution Description

From the energy efficiency perspective, the "power savings" concept has become a key challenge in the microgrids. The unequal distribution of the consumers amongst the three phases along with variations in their individual demand, leads to unequal phase loads in the LV grid, through the so-called "current unbalance" [18].

Power/energy losses reduction can be achieved upgrading the existing equipment and installations from the microgrid. Recent researches showed that the minimization of active power losses represents the cheapest resource of EDG efficiency [19, 20]. Consequently, phase balancing minimizes the losses in the microgrids because each load peak reduction affects the losses for the phases directly proportional with the square of the current magnitude [21]. One of the cheapest measures that a DGO can take to increase the efficiency in the microgrids is a better load balancing on the three phases, by changing the phase connection of some consumers.

In this paragraph, a phase load balancing solution based on a heuristic algorithm applied in each consumer connection point which employs a dynamic reallocation process on phases is presented. The proposed solution uses as input data the configuration of the microgrid (structure, number of poles (connection points) and consumer allocation on each pole and phase) and load data for each consumer and finds the optimal phase connection for all consumers using as optimization criterion the minimization of a current unbalance factor (CUF) value closer to 1.

This factor can be evaluated using the following equation [22, 23], and the value should be under 1.10 p.u:

$$CUF = \frac{1}{3}\left[\left(\frac{I_a^p}{I_{abc}^{average}}\right)^2 + \left(\frac{I_b^p}{I_{abc}^{average}}\right)^2 + \left(\frac{I_c^p}{I_{abc}^{average}}\right)^2\right] \tag{19.9}$$

where, a, b, and c are the notations for the three phases of network; $I_{abc}^{average}$ represents the average phase currents; I_a^p, I_b^p, I_c^p are the total currents of phases a, b and c at pole p.

The Heuristic Phase Load Balancing (H-PLB) algorithm considers all available possibilities for the load balancing at the level of each pole p from the total N_p poles from the microgrid ($p = 1, \ldots, N_p$, where N_p is the number of poles). The process is based on a dynamic process inside which some consumers are switched (for example, from phase a to phases b or c), such that to obtain at each connection pole a minimum CUF.

Initially, CUF should have values between 1 and 2, where 1 corresponds to the ideal case (perfectly balanced), when values of phase currents are identical, and the value 2 corresponds to the maximum unbalancing when only one phase is loaded while the other two phases are unloaded (the currents have the value 0 or close to 0). The algorithm begins the balancing from the final poles and stops at the SP with the external grid, where CUF must have the minimum value (close to 1.0). Finally, at each pole, the load should be balanced using different combinations of the phase interchange based on the shifting of loads from a phase to another. In Table 19.7, different combinations are presented.

The minimization of the deviation between phase currents, at the level of each connection pole p ($p = 1, \ldots, N_p$) at each hour h, represents the objective of the balancing problem:

$$\min(\varepsilon) = \min\left(\max\left(\Delta_a^p, \Delta_b^p, \Delta_c^p\right)\right), \quad p = 1, \ldots, N_p \tag{19.10}$$

Table 19.7 Different combinations of phases to obtain a minimum value of the unbalance factor

Phases	Initial connection	Final connection
Three phases	[a/b/c]	[c/a/b] [b/c/a]
Two phases	[a/b/*]	[b/*/a] [*/a/b]
	[*/b/c]	[c/*/b] [*/b/c]
	[c/a/*]	[a/*/c] [*/c/a]
One phase	[a/*/*]	[*/a/*] [*/*/a]
	[b/*/*]	[*/b/*] [*/*/b]
	[c/*/*]	[*/c/*] [*/*/c]

where,

$$\Delta_a^p = \frac{I_a^p}{I_{abc}^{average}} - 1 \tag{19.11}$$

$$\Delta_b^p = \frac{I_b^p}{I_{abc}^{average}} - 1 \tag{19.12}$$

$$\Delta_c^p = \frac{I_c^p}{I_{abc}^{average}} - 1 \tag{19.13}$$

$$I_{abc}^{average} = \frac{1}{3}\left(I_a^p + I_b^p + I_c^p\right) \tag{19.14}$$

$$I_a^p = \sum_{k=1}^{n_a^p} i_a^{p(k)} \tag{19.15}$$

$$I_b^p = \sum_{k=1}^{n_b^p} i_b^{p(k)} \tag{19.16}$$

$$I_c^p = \sum_{k=1}^{n_c^p} i_c^{p(k)} \tag{19.17}$$

$$n^p = n_a^p + n_b^p + n_c^p \tag{19.18}$$

The variables from equations Δ_a, Δ_b and Δ_c are the phase current deviations on each phase; I_a^p, I_b^p, I_c^p are values of the total currents of each phase (a, b) and at pole p; N_p is the number of poles in the microgrid; where, n_a^p, n_b^p, n_c^p are the number of loads connected at pole p, on each phase (a/b/c); n^p is the number of loads connected at pole p.

All combinations between loads connected at each pole will be considered by the algorithm. The flow chart of the H-PLB algorithm is given in Fig. 19.12.

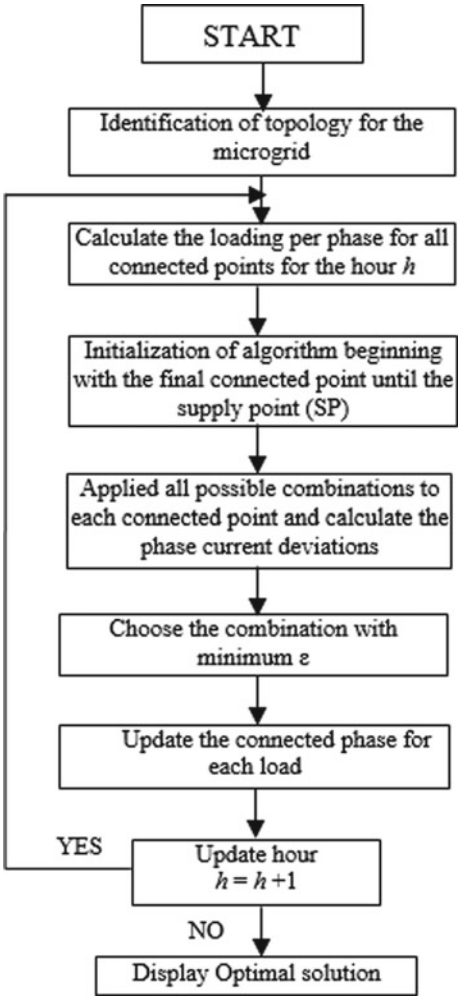

Fig. 19.12 The flow-chart of the heuristic algorithm

19.3.2 Testing the Solution

A real test microgrid was used to test the H-PLB algorithm. The topology of the microgrid can be seen in Fig. 19.13. The poles represent points where the consumers are connected via the single-phase or three-phase branching, and these are identified using circles. The primary characteristics (number of poles, total length, cable type, cable size, length of sections using given cable types, and number of consumers) are shown in Table 19.8. Also, consumers' characteristics can be identified in Table 19.9. The connection phase of each consumer reflects the real situation, and this aspect helped to establish a true-to-reality unbalanced model.

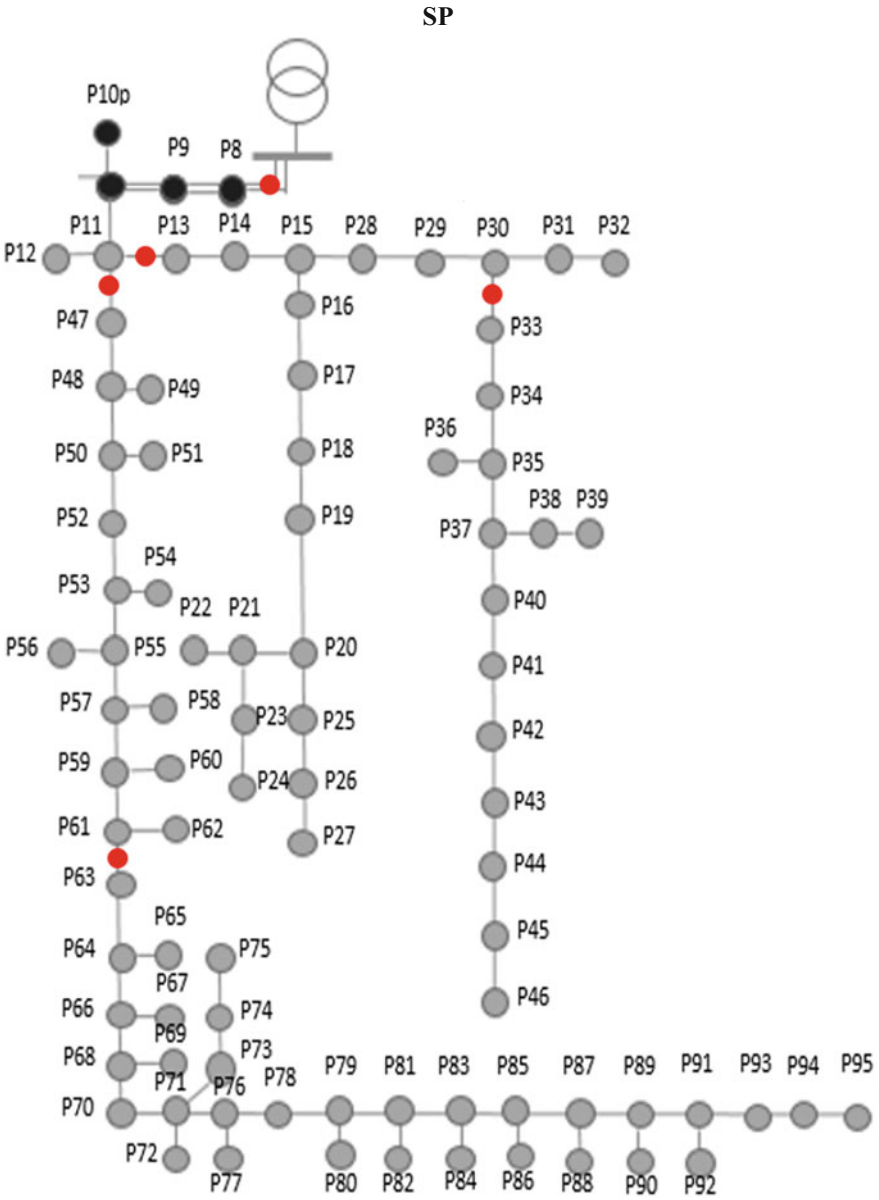

Fig. 19.13 The test microgrid

Table 19.8 The primary characteristics of the grid

Number of poles	Total length (m)	Number of consumers	Cable type	Cable size (mm^2)	Length (m)
88	3520	163	Stranded	$3 \times 35 + 35$	120
			Classical	$3 \times 50 + 50$	3760

Table 19.9 The consumers' characteristics

Consumer type	No.	Phase			Consumption category (kWh/year)				
		a	b	c	0–400	400–1000	1000–2500	2500–3500	>3500
1-phase	161	25	81	55	69	64	26	1	3
3- phase	2	–	–	–	1	1	0	0	0

The hourly load recordings for each consumer integrated in the Smart Metering system were imported for the day when the analysis was made. Based on these profiles, the loading per phase at the SP level with the external grid was calculated. The current flows on the three phases for the analysed 24 h time interval is presented in Fig. 19.14. It can be observed that there is a high unbalance between the three phases. This was evaluated using CUF calculated with Eq. (19.9). The average calculated value was 1.38, above the maximum allowed value (1.10).

Using the H-PLB algorithm, the unbalance factor was reduced until the value 1.008 was obtained. This translates into sensibly equal current flows on the three phases, as evidenced in Fig. 19.15.

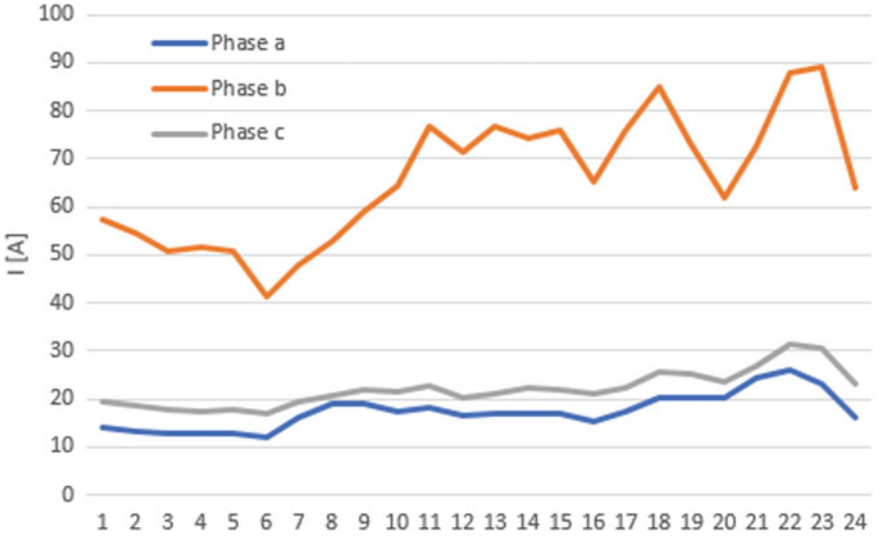

Fig. 19.14 The phase loading on the first section of the microgrid, the reference unbalanced scenario

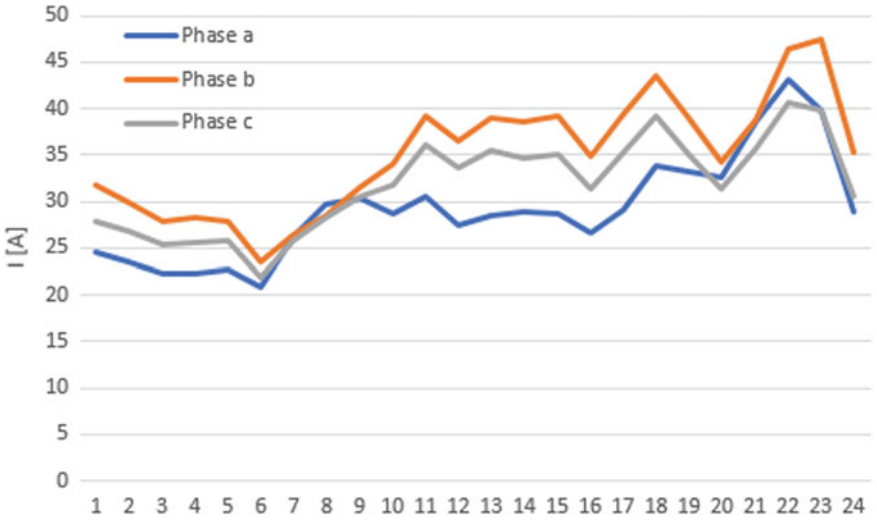

Fig. 19.15 The phase loading on the first section of the microgrid, the balanced scenario obtained with the H-PLB algorithm

Table 19.10 Energy losses in the analysed day

Case	Energy consumed (kWh)	ΔW_{loss} (kWh)	ΔW_{loss} (%)	Energy infeed (kWh)
Unbalanced (reference)	442.47	78.95	15.14	521.42
Balanced (H-PLB)	442.47	27.64	5.88	470.11

Based on the input data (structure, technical parameters and consumer load profiles), the hourly regime calculations were performed. The obtained output data are presented in Table 19.10. The analysis of data lead to the conclusion of a decreasing for the energy losses (approximately 9%), from 15.14 to 5.88% in the microgrid.

19.4 Voltage Control

19.4.1 Solution Description

Voltage level control is essential in ensuring the secure and efficient operation of microgrids [24]. Many EDG were built one century ago to respond to changes of end-user needs. Electricity is produced in classical grids by central power plants, and then is transmitted and delivered through EDG to the end-user in a one-way direction [25]. Microgrids supply a large number of one-phase consumers, connected in a three-

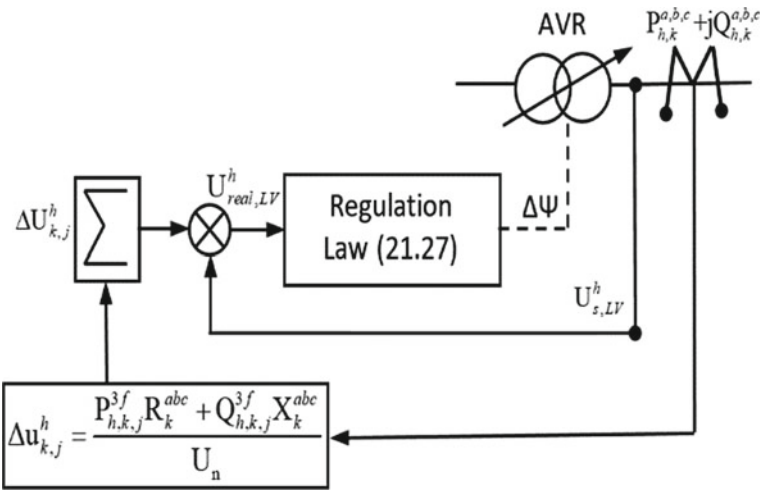

Fig. 19.16 The voltage control strategies using the LDC method

phase grid. Because the number of consumers and their load behaviour is dynamic, the load pattern of the three phases of the grid is different. One of the cheapest measures that a DGO can take is to optimize the steady state through voltage control and power losses and voltage drop minimization. Thereby, the real operation state of an EDG is unbalanced, and in this type of grid, the voltage control represents a relevant index, especially for microgrids, which are frequently built using overhead lines mounted on poles, supplying paths more than 1–2 km long.

The voltage control strategies are sometimes a key performance indicator in active microgrids. In the literature, this problem is solved using pseudo-measurements [26, 27]. Due to the intermittent and unpredictable behaviour of consumptions and distributed energy sources, the generation excess could lead to a reversed power flow, from the consumers, through the microgrids to the supply external point. This drawback requires a real-time effective voltage control strategy, particularly under islanded operation modes, to obtain the best solutions, with reliable effects on the minimization of energy losses, and energy efficiency improvement in microgrids [24].

In the following, the influence of a hybrid energy system which uses automatic voltage regulators (AVR) on the active power losses and bus voltage levels in a microgrid is presented.

The voltage control strategy based on SM loads, described in Fig. 19.16, applies AVR to control the voltage levels based on an optimal control strategy that uses the voltage drop compensation method. Theoretically, the voltage control follows a regulation law [28], because the power flows over an inductive electrical line with a specific voltage drop [29].

The objective of the optimization procedure is to assess the influence of renewable sources (i.e. wind turbines) into a microgrid in order to improve the voltage at the

end-users and also to minimize the active power losses, considering the technical constraints. The proposed approach was formulated as:

$$\min F([U],[\Psi]) = \min\left(\Delta U_{\mu G}^{h}\right) + \min\left(\Delta P_{\mu G}^{h}\right) \tag{19.19}$$

where, min F is the objective function; $[U]$ is the voltage magnitude vector; $[\Psi]$ is the transformers tap changing matrix; ΔU is the voltage drop; $h = 1 \ldots T$, the hourly measurement interval for the steady state; μG is microgrid; ΔP is the active power losses.

The equality constraints coincide with the bus power balance in the microgrid. For a given bus $k = 1, \ldots, N$, a time sample h, and an operating states j, the equations are the following:

$$P_{h,k,j}^{3ph} + jQ_{h,k,j}^{3ph} = \overline{U}_{h,k,j} \cdot \overline{I}_{h,k,j}^{*} \tag{19.20}$$

where the active and reactive power (Fig. 19.16) are considered as sum of the three phases of the microgrid, respectively:

$$P_{h,k,j}^{3ph} = P_{h,k,j}^{a} + P_{h,k,j}^{b} + P_{h,k,j}^{c} \tag{19.21}$$

$$Q_{h,k,j}^{3ph} = Q_{h,k,j}^{a} + Q_{h,k,j}^{b} + Q_{h,k,j}^{c} \tag{19.22}$$

The mathematical model has the following inequality constraints:

1. Voltage allowable limits:

$$U_{h,k,j}^{\min} \leq U_{h,k,j} \leq U_{h,k,j}^{\max} \tag{19.23}$$

2. Thermal limits of the branch loadings:

$$S_{h,k,j} \leq S_{h,k,j}^{\max} \quad or \quad I_{h,k,j} \leq I_{h,k,j}^{\max} \tag{19.24}$$

3. The allowable reactive power of distributed generation sources must be constrained as:

$$Q_{h,\min}^{wind} \leq Q_{h}^{wind} \leq Q_{h,\max}^{wind} \tag{19.25}$$

4. The constraints for the transformer tap changer must be in accordance with the proposed strategy (Fig. 19.16), and are the following:

$$\Psi_{\min}^{h} \leq \Psi_{k,j}^{h} \leq \Psi_{\max}^{h} \tag{19.26}$$

where, $U^{\min}$, $U^{\max}$ are the inferior and superior voltage limit; $I_{h,k,j}$ is the branch current value; $I^{\max}$ is the branch ampacity value; $S_{h,k,j}$ is the branch apparent

power; $S^{\max}$ is the maximum apparent power on branch; Q^{wind} is the injected reactive power from the DG source; $Q_{\min}$, $Q_{\max}$ the allowable reactive power limits; Ψ is the tap position of the transformer.

The voltage control law changes the tap position up and down, as follows:

$$\Delta\Psi = \begin{cases} +1 & if\ \Delta U_{k,j}^{h} < -\varepsilon \quad and \quad \Psi(h) \neq \Psi_{\max} \\ 0, & if\ -\varepsilon \leq \Delta U_{k,j}^{h} \leq +\varepsilon \\ -1, & if\ \Delta U_{k,j}^{h} > -\varepsilon \quad and \quad \Psi(h) \neq \Psi_{\min} \end{cases} \tag{19.27}$$

and

$$\Psi(h+1) = \Psi(h) + \Delta\Psi \tag{19.28}$$

where, ε is the dead zone of the AVR (e.g. 2.5% for MV/LV transformers).

19.4.2 Testing the Solution

The smart voltage control approach proposed above was tested on a real microgrid with 163 residential consumers, presented in Fig. 19.13. The phase distribution of the consumers is given in Table 19.3. It must be highlighted that the unbalanced microgrid includes already two connected wind turbines.

To demonstrate the capabilities of the proposed voltage control strategy, three scenarios for simulation were considered. First, the base case (Case I) without wind generators and AVR control (with the initial tap position). The second case (Case II) considers the two real wind generators (2 × 5 kW) connected into the microgrid, while the last case (Case III) uses the voltage control strategy Eqs. (19.19)–(19.28). Case II is proposed for assessing the influence of the DG sources on the voltage and power losses magnitude in a real microgrid. In addition, Case III follows the improvement of voltage magnitude based on a coordination between the generation of the distributed sources and the automation distribution devices.

The results regarding the voltage magnitude in the three considered cases, are given in Table 19.11, only for two representative connected points of DGs: pole no. 78 and the last microgrid bus, pole no. 95. The daily energy losses are presented in Table 19.12.

It can be observed in Table 19.12 a reduction of energy losses, with over 3%, from 15.14 to 12.13% with energy savings of about 17.82 kWh for the entire microgrid.

Table 19.11 Voltage magnitude for the two representative buses (kV)

Hour/cases	Pole no. 78			Pole no. 95		
	I	II	III	I	II	III
1	0.3684	0.3924	0.3925	0.3673	0.3913	0.3915
2	0.3701	0.3928	0.3929	0.3691	0.3919	0.3919
3	0.3721	0.3933	0.3933	0.3712	0.3924	0.3925
4	0.3718	0.3932	0.3932	0.3708	0.3923	0.3923
5	0.3719	0.3933	0.3933	0.3710	0.3924	0.3924
6	0.3764	0.3947	0.3947	0.3755	0.3939	0.3939
7	0.3715	0.3936	0.3935	0.3705	0.3926	0.3925
8	0.3681	0.3927	0.3927	0.3670	0.3916	0.3916
9	0.3653	0.3918	0.3920	0.3641	0.3907	0.3909
10	0.3640	0.3913	0.3916	0.3628	0.3901	0.3905
11	0.3584	0.3896	0.3897	0.3571	0.3883	0.3884
12	0.3617	0.3902	0.3907	0.3605	0.3890	0.3896
13	0.3591	0.3894	0.3902	0.3579	0.3882	0.3891
14	0.3600	0.3900	0.3907	0.3587	0.3887	0.3895
15	0.3593	0.3897	0.3905	0.3580	0.3884	0.3893
16	0.3646	0.3914	0.3917	0.3634	0.3902	0.3906
17	0.3591	0.3897	0.3905	0.3578	0.3884	0.3892
18	0.3534	0.3883	0.3885	0.3519	0.3868	0.3869
19	0.3583	0.3900	0.3901	0.3568	0.3886	0.3887
20	0.3628	0.3914	0.3917	0.3615	0.3901	0.3904
21	0.3561	0.3906	0.3898	0.3545	0.3892	0.3882
22	0.3482	0.3895	0.3880	0.3462	0.3879	0.3861
23	0.3493	0.3880	0.3882	0.3474	0.3861	0.3863
24	0.3642	0.3917	0.3920	0.3629	0.3905	0.3908

Table 19.12 Comparison between the simulation cases

Case	Energy consumed (kWh)	ΔW_{loss} (kWh)	ΔW_{loss} (%)	Energy infeed (kWh)
Case I (base)	442.47	78.95	15.14	521.42
Case II (DG connected)	442.47	62.36	12.35	504.83
Case III (DG + AVR)	442.47	61.13	12.13	503.60

References

1. G. Grigoras, Impact of smart meter implementation on saving electricity in distribution networks in Romania, in *Application of Smart Grid Technologies. Case Studies in Saving Electricity in Different Parts of the World* (Academic Press, 2018), pp. 313–346
2. R. Hierzinger, M. Albu, H. Van Elburg, A. Scott, A. Lazicki, L. Penttinen, F. Puente, H. Saele, European smart metering landscape report (IEE), 2013, https://ec.europa.eu/energy/intelligent/projects/sites/iee-projects/files/projects/documents/smartregions_landscape_report_2012_update_may_2013.pdf
3. J. Zadnik, Cost benefit studies (CBA) for smart metering roll-out in the EU. Overview and way forward, Smart Grids in Practice, 29 Sept 2015
4. Institute of Communication & Computer Systems of the National Technical University of Athens ICCS—NTUA for European Commission; Study on cost benefit analysis of in EU Member States Smart Metering Systems, Final Report, 25 June 2015
5. European Commission, Smart Metering deployment in the European Union. http://ses.jrc.ec.europa.eu/smart-metering-deployment-european-union
6. European Commission, Directorate-General for Energy, Standardization Mandate to CEN, CENELEC, and ETSI in the field of measuring instruments for the developing of an open architecture for utility meters involving communication protocols enabling interoperability. M 441/EN (2009), https://ec.europa.eu/energy/sites/ener/files/documents/2011_03_01_mandate_m490_en.pdf
7. European Commission, Directorate-General for Energy, Standardization Mandate to European Standardisation Organisations (ESOs) to support European Smart Grid deployment. M/490 EN (2016), https://ec.europa.eu/energy/sites/ener/files/documents/2011_03_01_mandate_m490_en.pdf
8. B.C. Neagu, G. Grigoras, F. Scarlatache, Load management in distribution systems with smart metering. Energetica **63**(4), 150–156 (2015)
9. G. Grigoras, F. Scarlatache, Use of data from smart meters in optimal operation of distribution systems, in *OPTIM*, Brasov, Romania (2014), pp. 179–184
10. G. Grigoras, F. Scarlatache, Knowledge extraction from Smart Meters for consumer classification, in *EPE*, Iasi, Romania (2014), pp. 978–982
11. G. Grigoras, F. Scarlatache, B.C. Neagu, *Clustering in Power Systems/Applications* (Lambert Academic Publishing, Saarbrucken, 2016)
12. M.H. Albadi, E.F. El Saadany, Demand response in electricity markets: an overview, in *IEEE PES General Meeting*, Tampa, Florida (2007)
13. B.P. Bhattarai, B. Bak Jensen, P. Mahat, J.R. Pillai, M. Maier, Hierarchical control architecture for demand response in smart grids, in *IEEE PES Asia-Pacific Power and Energy Engineering Conference*, Kowloon, China (2013)
14. S. Nan, M. Zhou, G. Li, Optimal residential community demand response scheduling in smart grid. Appl. Energy **210**, 1280–1289 (2018)
15. N. Kinhekar, N.P. Padhy, H.O. Gupta, Multiobjective demand side management solutions for utilities with peak demand deficit. Int. J. Electr. Power Energy Syst. **55**, 612–619 (2014)
16. Y. Ozturk, P. Jha, S. Kumar, G. Lee, Personalized home energy management system for residential demand response, in *POWERENG*, Istanbul, Turkey (2013), pp. 1241–1246
17. L. Wang, Z. Wang, R. Yang, Intelligent multiagent control system for energy and comfort management in smart and sustainable buildings. IEEE Trans. Smart Grid **3**(2), 605–617 (2012)
18. S. Beharrysingh, Phase unbalance on low-voltage electricity networks and its mitigation using static balancers. Doctoral Thesis, Loughborough University, UK (2014)
19. T.T. Son, T.A. Tung, Current unbalance reduction in low voltage distribution networks using automatic phase balancing device. Vietnam J. Sci. Technol. **55**(1) (2017). 2525-2518
20. G. Grigoras, B.C. Neagu, F. Scarlatache, Smart metering-based approach for phase balancing in low voltage distribution systems, in *ATEE*, Bucharest, Romania (2017), pp. 551–554
21. C.G. Fei, R. Wang, Using phase swapping to solve load phase balancing by ADSCHNN in LV distribution network. Int. J. Control Autom. **7**(7), 1–14 (2014)

22. H. Albert, A. Mihailescu, *Power Losses in Electric Networks* (Technical Publishing, Bucharest, 1994). (in Romanian)
23. G. Grigoras, M. Gavrilas, Phase swapping of lateral branches from low-voltage distribution networks for load balancing, in *EPE*, Iasi, Romania (2016), pp. 715–718
24. F. Scarlatache, G. Grigoras, B.C. Neagu, C. Schreiner, R.C. Ciobanu, Influence of hybrid energy systems on micro-grids control, in *CPE-POWERENG*, Cadiz, Spain (2017), pp. 313–317
25. B.C. Neagu, G. Grigoras, An efficient metaheuristic algorithm for optimal capacitor allocation in electric distribution networks, in *SMCE*, Shanghai, China (2017), pp. 327–328
26. D. Ranamuka, A.P. Agalgaonkar, K.M. Muttaqi, Online voltage control in distribution systems with multiple voltage regulating devices. IEEE Trans. Sustain. Energy **5**(2), 617–628 (2014)
27. F. Capitanescu, I. Bilibin, E. Romero Ramos, A comprehensive centralized approach for voltage constraints management in active distribution grid. IEEE Trans. Power Syst. **29**(2), 933–942 (2013)
28. G.G. Matei, B.C. Neagu, M. Gavrilas, Optimal voltage control using a modified line drop compensation method in real distribution systems, in *EEEIC*, Palermo, Italy (2018), pp. 1–6
29. B.C. Neagu, G. Georgescu, The optimization of reactive power sources placement in public repartition and distribution systems for power quality improvement, in *OPTIM*, Brasov, Romania (2012), pp. 200–207

Chapter 20
Optimal Microgrid Operational Planning Considering Distributed Energy Resources

Mehrdad Setayesh Nazar, Ainollah Rahimi Sadegh and Alireza Heidari

Abstract This chapter introduces an approach for Optimal Microgrid Operational Planning (OMOP) considering wind and photovoltaic power generations, combined heat and power generation units, electrical energy storages and interruptible loads. The problem explores the optimal maintenance scheduling and operational planning of a microgrid. A framework for OMOP is presented based on a two-level optimization procedure taking into account the system uncertainties. The formulated problem is modelled as a Mixed Integer Nonlinear Programming (MINLP) problem and a heuristic optimization method is utilized for the first level problem; meanwhile, a MINLP solver is used for the second level problem. This model is applied to the 9-bus and 33-bus test systems and the numerical results assess the effectiveness of the introduced method.

Keywords Microgrid · Maintenance scheduling · Optimal operational planning · Heuristic optimization

Nomenclature

C_{MC}	Maintenance cost
C_{OP}	Operation cost
X	Decision variable of maintenance
Nsub	Number of substations

M. Setayesh Nazar (✉) · A. Rahimi Sadegh
Faculty of Electrical Engineering, Shahid Beheshti University, A.C., Tehran, Iran
e-mail: m_setayesh@sbu.ac.ir

A. Rahimi Sadegh
e-mail: a.rahimisadegh@gmail.com

A. Heidari
School of Electrical Engineering and Telecommunication, University of New South Wales, Sydney, Australia
e-mail: alireza.heidari@unsw.edu.au

N. Mahdavi Tabatabaei et al. (eds.), *Microgrid Architectures, Control and Protection Methods*, Power Systems,
https://doi.org/10.1007/978-3-030-23723-3_20

Fr	Number of feeders
$DERM$	Number of DERs
MWI	Maintenance time window
$NDASC$	Number of DA market scenarios
λ	Probability of scenario
ρ^{DA}	Energy price purchased from DA market
NH	Number of DA market hours
E^{DA}	Energy purchased from upward network in DA market
ρ'^{DA}	Energy price sold to DA market
E'^{DA}	Energy purchased to upward network in DA market
NDG	Number of DGs
φ^{DG}	Decision variable for DG commitment
C^{DG}	Operational cost of DG
$NESS$	Number of ESSs
φ^{ESS}	Decision variable for ESS commitment
C^{ESS}	Operational cost of ESS
NIL	Number of ILs
φ^{IL}	Decision variable for IL commitment
C^{IL}	Operational cost of IL
$NCHP$	Number of CHPs
φ^{CHP}	Decision variable for CHP commitment
C^{CHP}	Operational cost of CHP
$NCONT$	Number of contingencies
$ENSC$	Energy not supplied costs
P	Active power generation
Q	Reactive power generation
$S_{\max}$	Maximum apparent power generation
RU	Ramp up power generation
RD	Ramp down power generation
P^{IL}	Active power interrupted in IL
$\cos\varphi^{IL}$	Power factor of IL
P^{ESS}	Active power of ESS

Sets

I	Index of substation set
J	Index of under maintenance substation set
K	Index of feeder set
l	Index of under maintenance feeder set
m	Index of DER set
n	Index of under maintenance DER set
i'	Index of DA scenarios set
j'	Index of hour-ahead scenarios set

k' Index of DG set
I'' Index of ESS set
m' Index of IL set
n' Index of CHP set
l' Index of contingencies set

20.1 Introduction

Distributed Energy Resources (DERs) are widely integrated into power system operational planning paradigms and the DER-based systems are mainly Microgrids (MGs) [1].

As shown in Fig. 20.1, a microgrid can be introduced as a system, which includes DERs such as solar Photo Voltaic (PV) system, Combined Heat and Power (CHP) unit, small Wind Turbine (WT) , Electrical Storage System (ESS) and Interruptible Loads (ILs) ; in a way that it has it has at least one controllable energy source [1].

The Microgrid Operator (MGO) performs the optimal scheduling of its dispatchable resources by considering the uncertainties of upward electricity market price, intermittent energy resources and ILs [2].

Over recent years, different aspects of optimal scheduling of the microgrid problem have been studied. Ref. [3] presents an optimal stochastic meta-heuristic scheduling algorithm for the networked microgrids considering uncertainties of DERs and Demand Response Programs (DRPs). Reference [4] explores the day-ahead scheduling of CHP systems considering DERs and boilers and considers different scenarios of demand and electricity price.

Reference [5] introduces an optimal day-ahead operational planning algorithm that minimizes pollutant emission and operating cost. The model is solved using a Species-based Quantum Particle Swarm Optimization (SQGA) evolutionary method. Reference [6] proposes a robust optimization algorithm for scheduling of microgrid resources that uses an information gap method to model the wholesale electricity market uncertainties.

Reference [7] presents a bi-level algorithm to optimize interactions between parking lot agent and distribution system operator. The upper-level problem minimizes the cost of DSO; meanwhile, the lower-level problem schedules the parking lot owner resources.

Reference [8] introduces a risk-based optimal scheduling of reconfigurable system that maximizes profit the system operator. The uncertainties of upward network prices, intermittent electricity generation facilities are considered. The optimal combination of system switches is explored using a meta-heuristic optimization method.

Reference [9] introduces a two-stage stochastic algorithm to minimize the reserve cost that is used for compensating the intermittent DER power generation forecast errors.

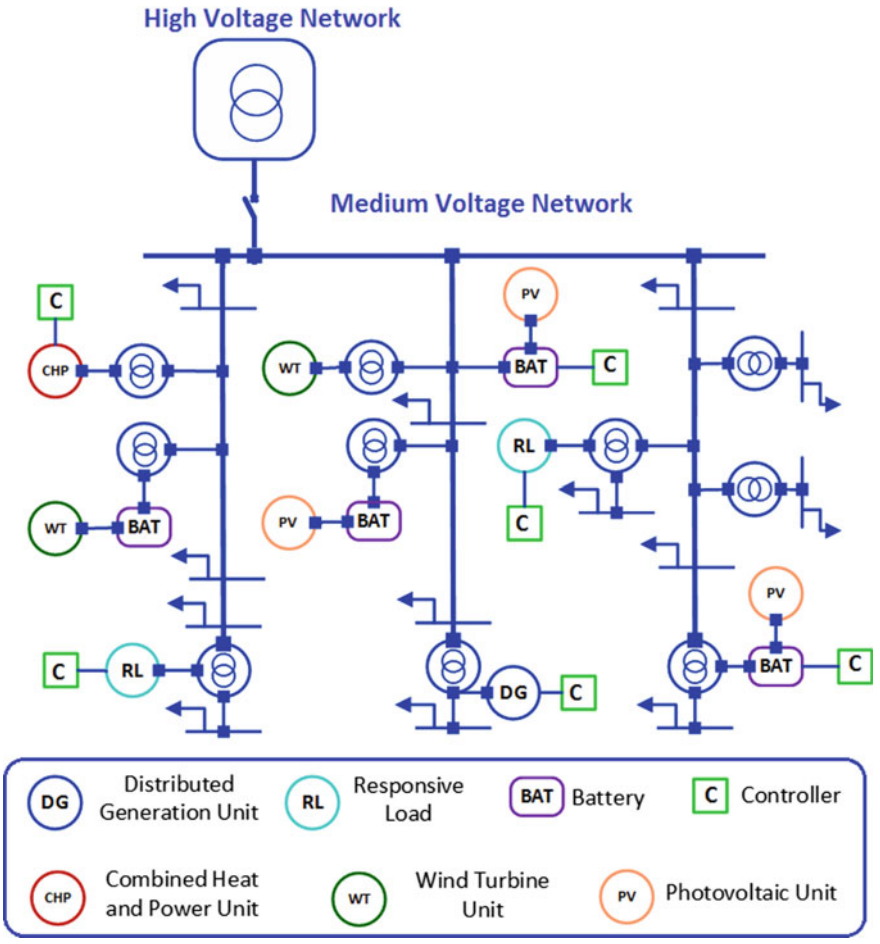

Fig. 20.1 Schematic diagram of a microgrid

Reference [10] presents an algorithm for maximizing of MGO profit considering WT power generation and wholesale market uncertainties. The algorithm uses a stochastic optimization method to model uncertainties.

Reference [11] uses a stochastic optimization algorithm to minimize the operation cost. The uncertainties of the DERs and DRPs are modelled by scenarios and interruptible load bids, respectively. Reference [12] introduces a stochastic scheduling algorithm that the uncertainties of intermittent DERs are modelled by the probability density functions. The results show that the DRP can reduce operating costs. These references do not consider the security constraints and thermal loads.

This book chapter is about the OMOP algorithm that considers the intermittent power generation uncertainties and contingencies scenarios.

20.2 Problem Modelling

The MGO maximizes its profit in the Day-Ahead (DA) market; meanwhile, it minimizes its system's operational costs. In addition, the DA market price is assumed to depend on unpredictable market conditions, which makes it extremely difficult to investigate the problem by considering the stochastic parameters. Therefore, in this book chapter, the uncertainty of the intermittent energy resource outputs, MG contingencies and the DA market price are modelled with the scenario.

Figure 20.2 shows the MGO interactions with upward network and its DERs.

The MGO must determine the optimal values of problem decision variables. Thus, the OMOP decision variables can be categorized as:

(1) Maintenance scheduling of MG's resources,
(2) Energy generation of MG's dispatchable energy resources,
(3) The volume of energy purchased from the upward network.

The system costs can be presented as:

(1) Operation and maintenance costs of system resources,
(2) Energy purchased costs,
(3) The expected profit of energy sold to upward network in the DA market.

The Energy Not Supplied Cost (ENSC) is considered in OMOP as reliability criteria [13].

20.2.1 First Level Problem Formulation

The MGO optimizes its monthly maintenance scheduling and it encounters the uncertainties of power exchanges with the upward network, intermittent power generation,

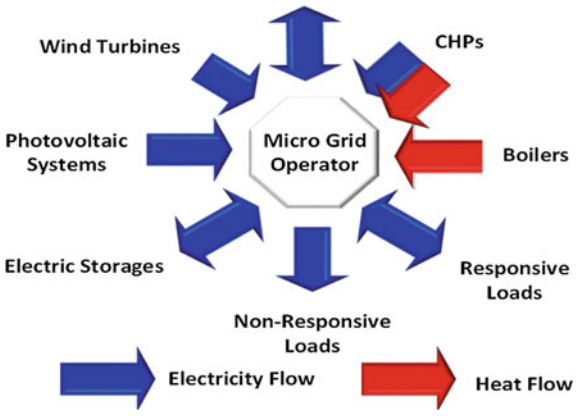

Fig. 20.2 The MGO interactions

and system contingencies. The first level optimization problem considers the maintenance starting periods, forecasted peak load, and system costs.

The first level problem objective function is proposed as:

$$\begin{aligned}\min C_1 = & \sum_{i\in Nsub}\sum_{j\in MWsub} C_{MC\_Sub\,ij}\times(1-X_{Sub\,ij})+X_{Sub\,ij}\times C_{OP\_Sub\,ij}\\ & +\sum_{k\in Fr}\sum_{l\in MWFr} C_{MC\_Feed\,kl}\times(1-X_{Feed\,kl})+X_{Feed\,kl}\times C_{OP\_Feed\,kl}\\ & +\sum_{m\in DER}\sum_{n\in MWDER} C_{MC\_DER\,mn}\times(1-X_{DER\,mn})+X_{DER\,mn}\\ & \times C_{OP\_DER\,mn}\end{aligned} \tag{20.1}$$

The objective function is decomposed into transformers, feeders and DERs maintenance costs. The first level optimization problem is subjected to maintenance constraints and load flow constraint.

The second level problem deals with optimal MGO estimated costs in DA market for the different scenarios.

20.2.2 Second Level Problem Formulation

At the second level optimization problem, the MGO maximizes its expected profit; meanwhile, it minimizes the system operation costs. The MGO determines the optimal schedule of dispatchable DERs and the energy transacted in the DA market.

$$\begin{aligned}\min & \sum_{i'=1}^{NDASC}\lambda_i\left(\sum_{j'=1}^{NH}\rho_{i'j'}^{DA}*E_{i'j'}^{DA}-\sum_{j'=1}^{NH}\rho_{i'j'}^{\prime DA}*E_{i'j'}^{\prime DA}\right.\\ & +\sum_{k'=1}^{NDG}\varphi_{i'k'}^{DG}\times C_{i'k'}^{DG}+\sum_{k''=1}^{NESS}\varphi_{i'k''}^{ESS}\times C_{i'k''}^{ESS}\\ & \left.+\sum_{m'=1}^{NIL}\varphi_{i'm'}^{IL}\times C_{i'm'}^{IL}+\sum_{n'=1}^{NCHP}\varphi_{i'n'}^{CHP}\times C_{i'n'}^{CHP}+\sum_{l'=1}^{NCONT}ENSC_{i'l'}\right)\end{aligned} \tag{20.2}$$

The objective function consists of the following groups: (1) the costs of energy purchased from the upward wholesale market; (2) the profits of energy sold to the upward network; (3) the commitment of DGs; (4) the commitment of ESSs; (5) the commitment of ILs; (6) the commitment of CHPs; (7) ENSCs.

The objective function is restricted to these constraints:

The maximum and minimum power generations of microgrid energy resources, ramp constraints, minimum up-time and down-time, AC power flow, state of charge and the limits of ESSs that can be written as:

$$P_{Min}^{DG}.\varphi^{DG} \leq P^{DG} \leq P_{Max}^{DG}.\varphi^{DG} \tag{20.3}$$

$$Q_{Min}^{DG}.\varphi^{DG} \leq Q^{DG} \leq Q_{Max}^{DG}.\varphi^{DG} \tag{20.4}$$

$$P_{Min}^{CHP}.\varphi^{CHP} \leq P^{CHP} \leq P_{Max}^{CHP}.\varphi^{CHP} \tag{20.5}$$

$$Q_{Min}^{CHP}.\varphi^{CHP} \leq Q^{CHP} \leq Q_{Max}^{CHP}.\varphi^{CHP} \tag{20.6}$$

$$\sqrt{\left(Q^{DG}\right)^2 + \left(P^{DG}\right)^2} \leq S_{Max}^{DG} \tag{20.7}$$

$$\left(P_{(t+1)}^{DG}\right) - \left(P_{(t)}^{DG}\right) \geq RU^{DG} \tag{20.8}$$

$$\left(P_{(t)}^{DG}\right) - \left(P_{(t+1)}^{DG}\right) \geq RD^{DG} \tag{20.9}$$

$$\sqrt{\left(Q^{CHP}\right)^2 + \left(P^{CHP}\right)^2} \leq S_{Max}^{CHP} \tag{20.10}$$

$$\left(P_{(t+1)}^{CHP}\right) - \left(P_{(t)}^{CHP}\right) \geq RU^{CHP} \tag{20.11}$$

$$\left(P_{(t)}^{CHP}\right) - \left(P_{(t+1)}^{CHP}\right) \geq RD^{CHP} \tag{20.12}$$

$$P_{Min}^{IL} \times \varphi^{IL} \leq P^{IL} \leq P_{Max}^{IL} \times \varphi^{IL} \tag{20.13}$$

$$Q^{IL} = \left(P^{IL}\right)\sqrt{\frac{1}{\cos\varphi^{IL}} - 1} \tag{20.14}$$

$$\sum_{k=1}^{t} P_k^{ESS} \leq P_{\max}^{ESS} \tag{20.15}$$

20.3 Solution Algorithm

For the first level optimization problem, the Genetic Algorithm (GA) ALGORITHM is used. Figure 20.3 depicts the flowchart of the introduced algorithm. The upper-level problem implements the GA for finding the best solutions of the estimated scenarios; meanwhile, the second level problem uses a mixed-integer nonlinear optimization procedure [13, 14].

The MATLAB software is used to generate random numbers. Then, by connecting the MATLAB to GAMS, the generated scenarios are inserted into GAMS, and scenario reduction is implemented by a forward method. Next, for each of the scenarios, the introduced decomposition method is applied. The scenario generation and reduction procedure are shown in Fig. 20.4.

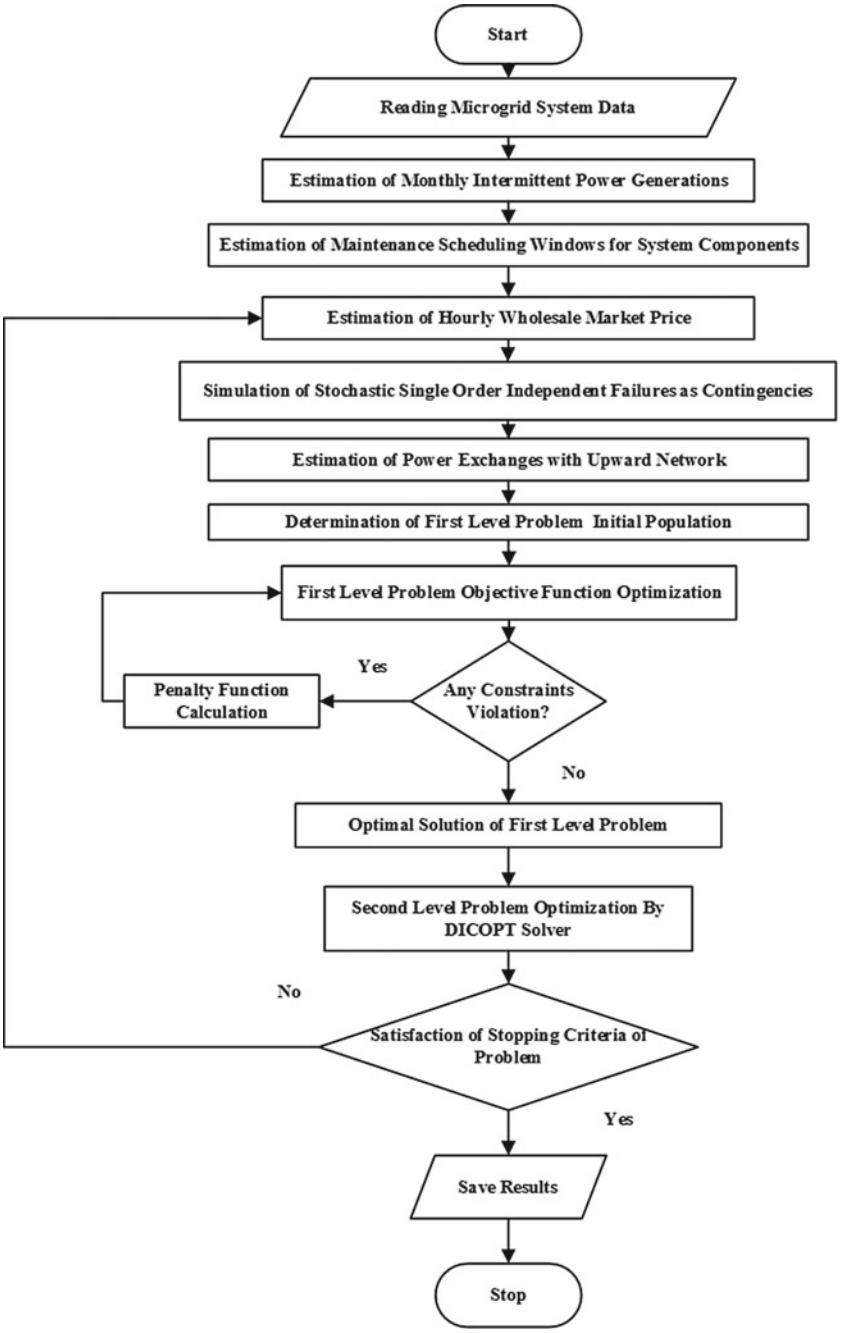

Fig. 20.3 The flowchart of the two-level optimization introduced algorithm

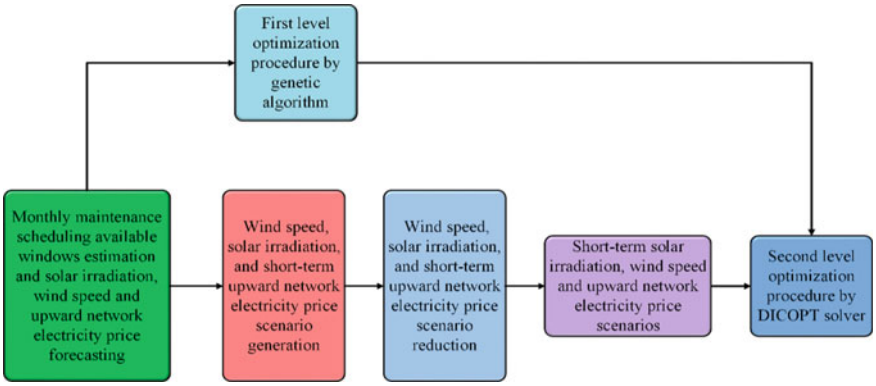

Fig. 20.4 The scenario generation and reduction procedure

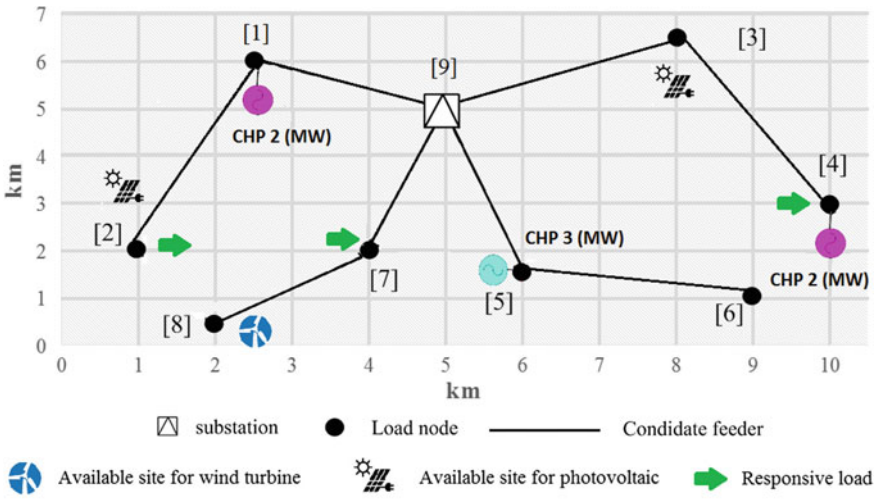

Fig. 20.5 The 9-bus microgrid

20.4 Numerical Results

The introduced model is implemented on the 9-bus and 33-bus test systems. Figures 20.5 and 20.6 depict the 9-bus and 33-bus system, respectively. The 9-bus and 33-bus test system data are presented at [15–18], respectively. The wind turbine and solar panel data are available at [18].

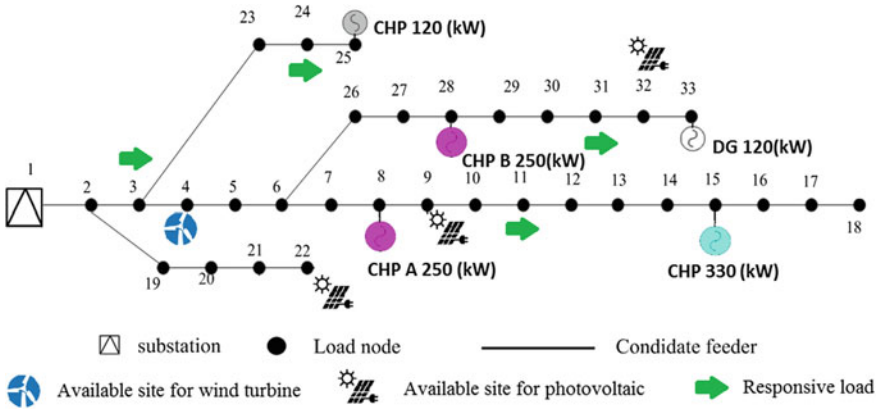

Fig. 20.6 The 33-bus microgrid

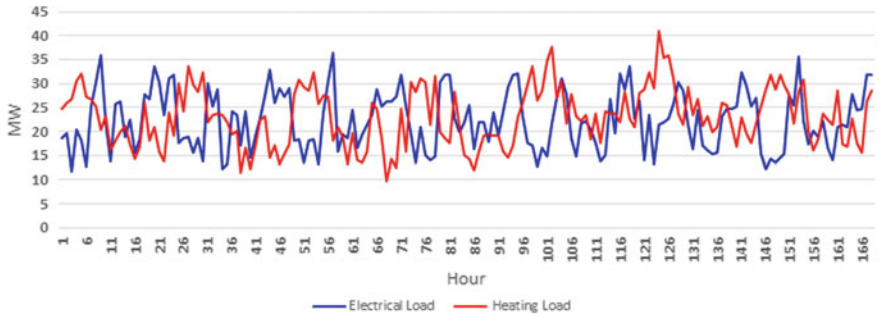

Fig. 20.7 The base load of the 9-bus system

20.4.1 The 9-Bus Test System

Figures 20.7 and 20.8 depict the base load and upward network electricity price of the 9-bus microgrid, respectively.

Table 20.1 presents the optimization input data for the 9-bus system.

Figures 20.9 and 20.10 show the electricity generation of solar photovoltaic panels and wind turbines, respectively.

Figure 20.11 shows the stacked column of the estimated electricity generation of CHPs. As shown in Fig. 20.11, the CHPs are at full load when they are committed. The first CHP is supplying the base electrical load of the MG and the third CHP is supplying the peak electrical load.

Figure 20.12 depicts the heating generation of CHPs and boilers. As shown in Fig. 20.12, the CHPs are at full load when they are committed and the boiler is tracking the heating load.

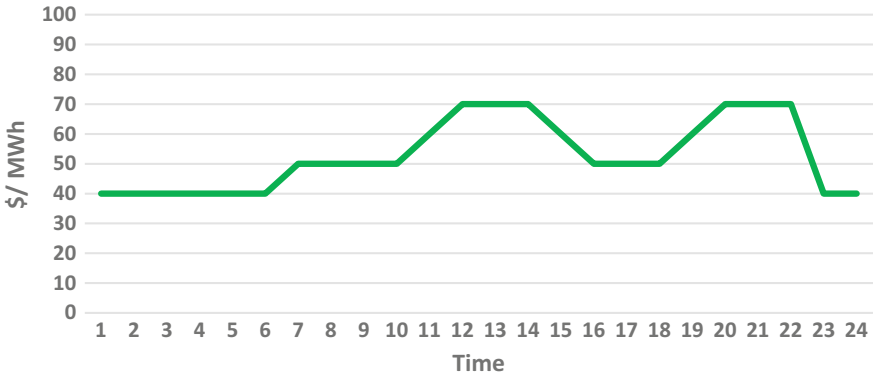

Fig. 20.8 The base electricity price of upward network of the 9-bus system

Table 20.1 The optimization input data for the 9-bus system

Parameter	Value
Discount rate (%)	13
Load power factor	0.90
Load growth rate of (%)	5
Number of solar irradiation scenarios	5000
Number of wind turbine power generation scenarios	6000
Number of upward market price scenarios	500
Number of solar irradiation reduced scenarios	400
Number of wind turbine power generation reduced scenarios	45
Number of upward market price reduced scenarios	15

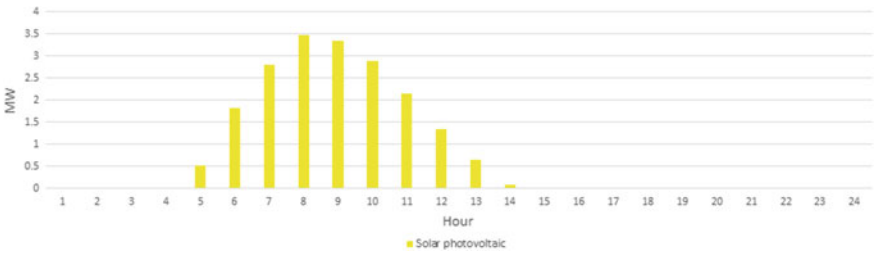

Fig. 20.9 The electricity generation of solar photovoltaic of 9-bus system

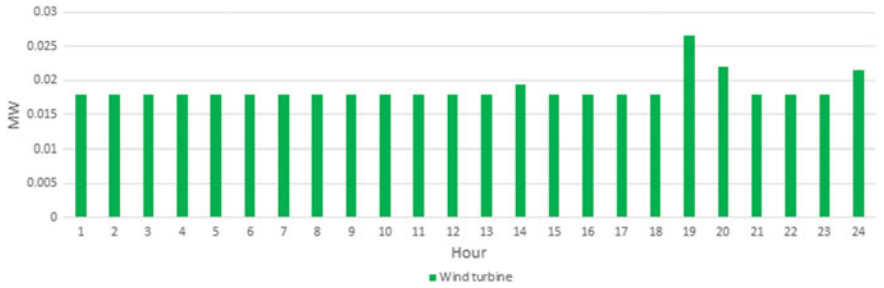

Fig. 20.10 The electricity generation of wind turbines of 9-bus system

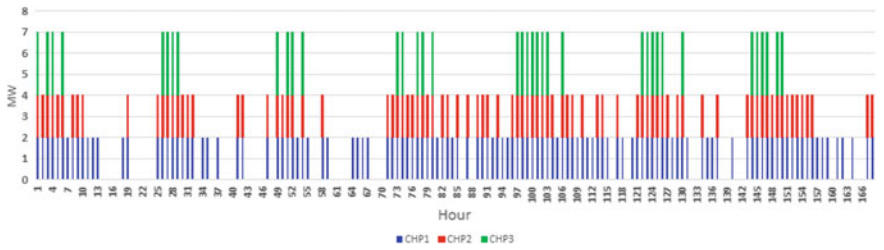

Fig. 20.11 The stacked column of the estimated electricity generation of CHPs of 9-bus system

Fig. 20.12 The stacked column of the estimated heating generation of CHPs and boilers of 9-bus system

Figure 20.13 displays the optimal maintenance scheduling of system for the first half of the year. The optimal maintenance scheduling for the second half of the year is the same as the first one. The OMOP ensures the maintenance workload of the system is evenly distributed across the year. Table 20.2 depicts the optimal operational and maintenance costs of the system.

20.4.2 The 33-Bus Test System

Figure 20.14 depicts the base load of the 33-bus microgrid.

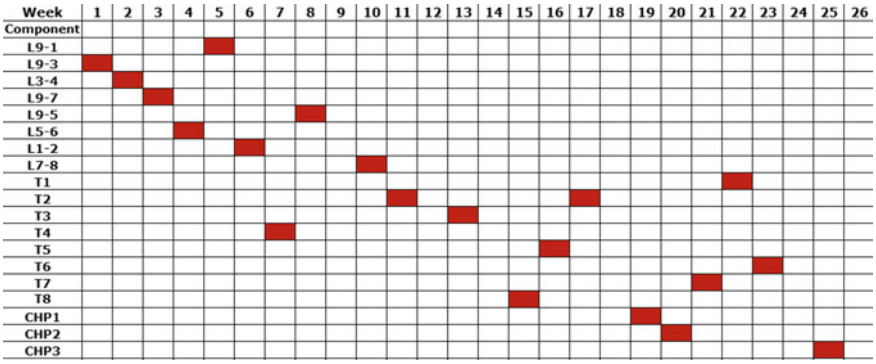

Fig. 20.13 The optimal maintenance scheduling of 9-bus system for the first half of the year

Table 20.2 The optimal aggregated operational and maintenance costs of the 9-bus system

Costs (MMUs)			
CHP operation and maintenance costs (MMUs)	3.9812	Transformers operation and maintenance costs (MMUs)	0.5871
ENSCs	0.36541	IL costs (MMUs)	0.7982
Energy loss costs (MMUs)	0.13815	Energy purchased from upward network costs (MMUs)	0.1974

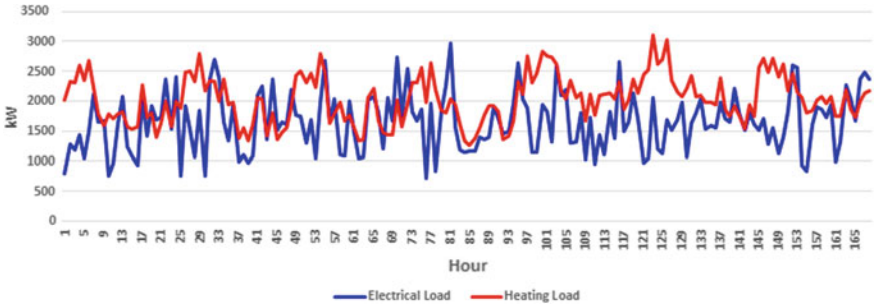

Fig. 20.14 The base load of the 33-bus test system

Figure 20.15 shows the electricity generation of solar photovoltaic panels and wind turbines.

Figure 20.16 presents the stacked column of the estimated electricity generation of CHPs and DGs. As shown in Fig. 20.16, the CHPs and DGs are at full load when they are committed. The CHP250A and CHP330 are fully committed to supplying the base electrical load of the system.

Figure 20.17 depicts the stacked column of the estimated heating generation of CHPs and boilers of the system. The boiler is tracking the heating load.

Figure 20.18 displays the optimal maintenance scheduling for the first half of the year. The optimal maintenance scheduling for the second half of the year is the same

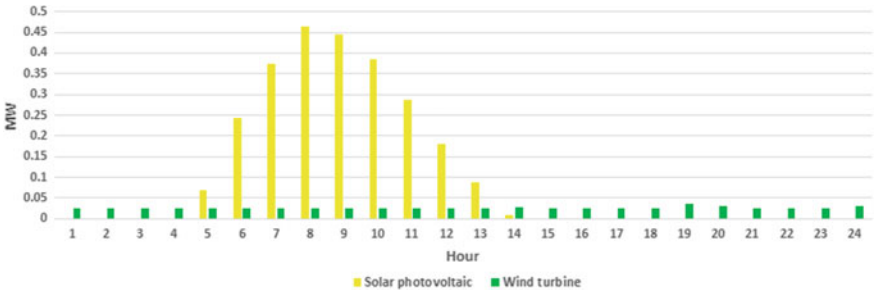

Fig. 20.15 The electricity generation of solar photovoltaic panels and wind turbines of 33-bus system

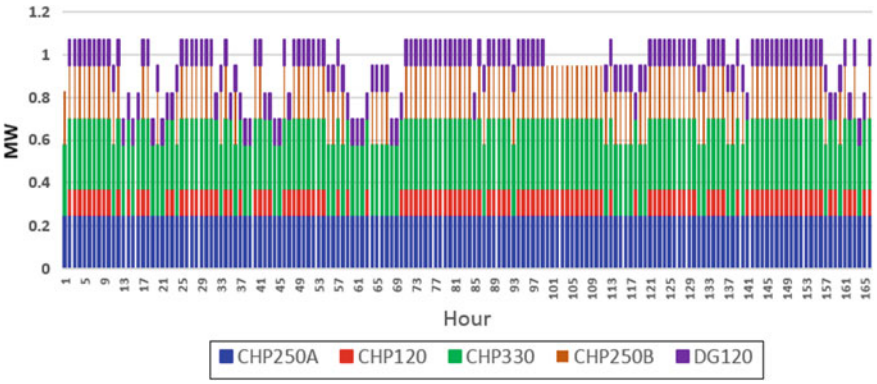

Fig. 20.16 Stacked column of estimated electricity generation of CHPs and DGs of 33-bus system

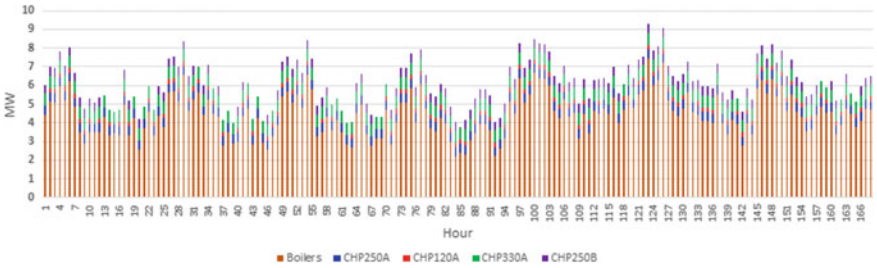

Fig. 20.17 Stacked column of estimated heating generation of CHPs and boilers of 33-bus system

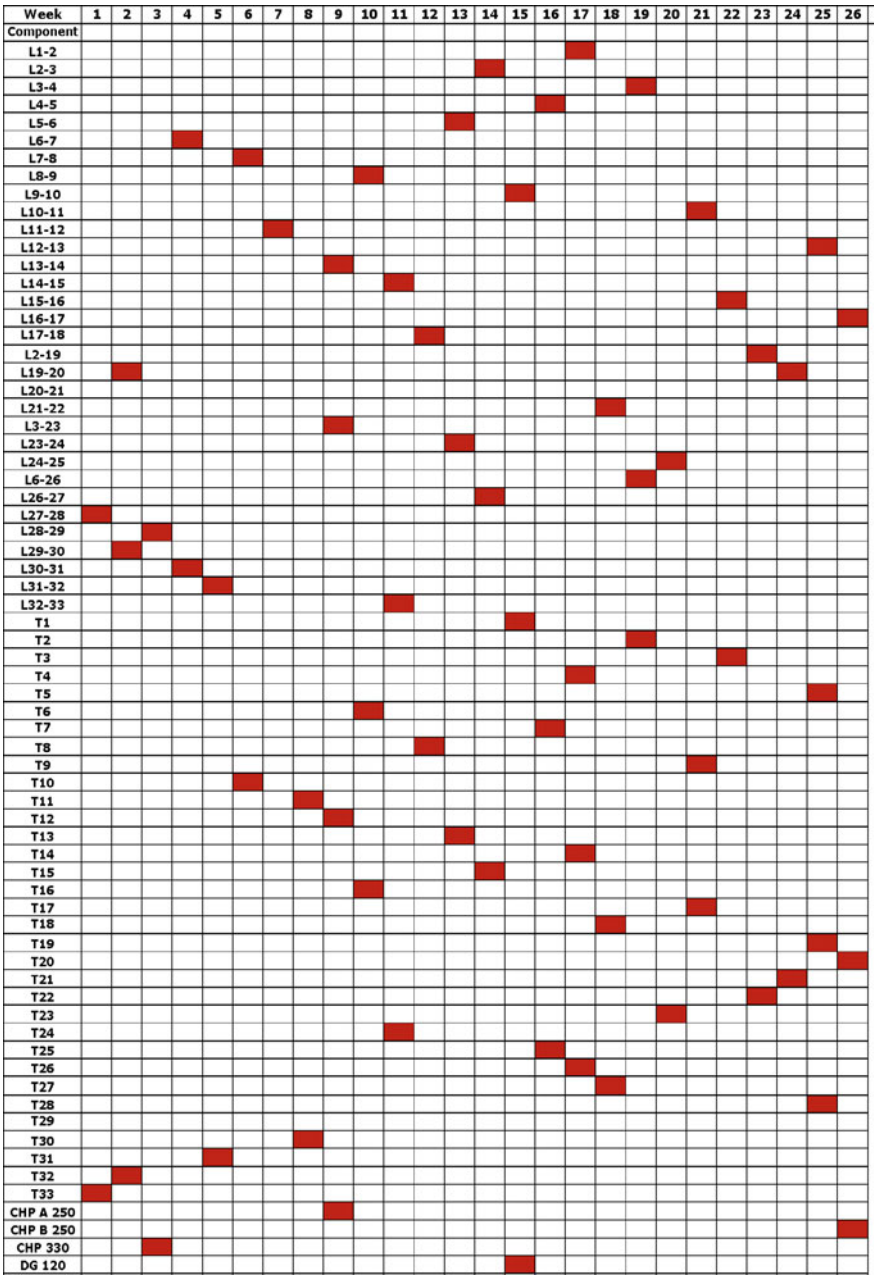

Fig. 20.18 The optimal maintenance scheduling of 33-bus system for the first half of the year

Table 20.3 The optimal aggregated operational and maintenance costs of the 33-bus system

Costs (MMUs)			
CHP and DG operation and maintenance costs (MMUs)	12.3918	Transformers operation and maintenance costs (MMUs)	2.6918
ENSCs	0.3487	IL costs (MMUs)	4.1287
Energy loss costs (MMUs)	0.3915	Energy purchased from upward network costs (MMUs)	0.3621

as the first one. The optimization algorithm distributes the maintenance workload across the year.

Table 20.3 depicts the optimal operational and maintenance costs of the 33-bus system for the operational planning horizon.

20.5 Conclusions

A microgrid optimal operational planning framework was reviewed in the present chapter. The introduced method used a two-level optimization model to investigate the intermittent power generations and ILs impacts on the OMOP problem. The proposed framework for OMOP considered the system uncertainties and the problem explores the optimal maintenance scheduling and operation. The OMOP procedure had a great non-convex discrete state space and the proposed solution algorithm had the ability to model the nonlinearity and non-convexity of the system's state space and the dynamic coupling constraints of the electric and heating systems.

The model of OMOP was a MINLP problem, and the GA algorithm was used for the first level problem. The second level problem utilized the DICOPT solver. The algorithm was assessed for the 9-bus and the 33-bus test systems with quite acceptable results.

In conclusion, the adoption of the proposed OMOP includes maintenance scheduling allows increasing significantly the microgrid benefits and reliability.

References

1. S. Chowdhury, S.P. Chowdhury, P. Crossley, Microgrids and active distribution networks. IET Renewable Energy Series (2009)
2. N.I. Nwulu, X. Xia, Optimal dispatch for a microgrid incorporating renewables and demand response. Renew. Energy **101**, 16–28 (2017)
3. N. Nikmehr, S. Najafi Ravadanegh, A. Khodaei, Probabilistic optimal scheduling of networked microgrids considering time-based demand response programs under uncertainty. Appl. Energy **198**, 267–279 (2017)

4. M. Alipour, B. Mohammadi Ivatloo, K. Zare, Stochastic risk-constrained short-term scheduling of industrial cogeneration systems in the presence of demand response programs. Appl. Energy **136**, 393–404 (2014)
5. V. Hosseinnezhad, M. Rafiee, M. Ahmadian, P. Siano, Optimal day-ahead operational planning of microgrids. Energy Convers. Manag. **126**, 142–157 (2016)
6. J. Aghaei, V.G. Agelidis, M. Charwand, F. Raeisi, A. Ahmadi, A. Esmaeel Nezhad, A. Heidari, Optimal robust unit commitment of CHP plants in electricity markets using information gap decision theory. IEEE Trans. Smart Grid **8**, 2296–304 (2017)
7. S. Aghajani, M. Kalantar, Operational scheduling of electric vehicles parking lot integrated with renewable generation based on bilevel programming approach. Energy **39**, 422–432 (2017)
8. M. Hemmatia, B. Mohammadi Ivatlooa, S. Ghasemzadeha, E. Reihanib, Risk-based optimal scheduling of reconfigurable smart renewable energy based microgrids. Int. J. Electr. Power Energy Syst. **101**, 415–428 (2018)
9. M. Mazidi, A. Zakariazadeh, Sh Jadid, P. Siano, Integrated scheduling of renewable generation and demand response programs in a microgrid. Energy Convers. Manag. **86**, 1118–1127 (2014)
10. M. Alipour, B. Mohammadi Ivatloo, K. Zare, Stochastic scheduling of renewable and CHP—based microgrids. IEEE Trans. Ind. Inform. **11**, 1049–58 (2015)
11. M.H. Shams, M. Shahabi, M.E. Khodayar, Stochastic day-ahead scheduling of multiple energy carrier microgrids with demand response. Energy **155**, 326–338 (2018)
12. A. Zakariazadeh, S. Jadid, P. Siano, Smart microgrid energy and reserve scheduling with demand response using stochastic optimization. Elect. Power Energy Syst. **63**, 523–533 (2014)
13. M. Setayesh Nazar, M.R. Haghifam, M. Nazar, A scenario driven multiobjective Primary–Secondary microgrid Expansion Planning algorithm in the presence of wholesale–retail market. Int. J. Electr. Power Energy Syst. **40**, 29–45 (2012)
14. F. Shahnia, A. Arefi, G. Ledwich, in *Electric Distribution Network Planning* (Springer, 2018)
15. W. El Khattam, K. Bhattacharya, Y. Hegazy, M.M.A. Salama, Optimal investment planning for distributed generation in a competitive electricity market. IEEE Trans. Power Syst. **19**(3), 1674–1684 (2004)
16. W. El Khattam, Y.G. Hegazy, M.M.A. Salama, An integrated distributed generation optimization model for distributed system planning. IEEE Trans. Power Syst. **20**(2), 1158–1165 (2005)
17. H. Falaghi, M.R. Haghifam, ACO based algorithm for distributed generation sources allocation and sizing in distribution systems, in *Power Tech, IEEE Transactions on Power Systems* (2007), pp. 555–560
18. S.Y. Derakhshandeh, A.S. Masoum, S. Deilami, M.A.S. Masoum, M.E.H. Golshan, Coordination of generation scheduling with PEVs charging in industrial microgrids. IEEE Trans. Power Syst. **28**(3), 3451–3461 (2013)

Chapter 21
Self-healing: Definition, Requirements, Challenges and Methods

Ali Zangeneh and Mohammad Moradzadeh

Abstract One of the most important issues in power grids is the outage problem that occurs due to weaknesses of the power system infrastructure or the occurrence of human or natural faults in the power system. The issue of complete deletion of power outages is unlikely due to unpredictable nature of major faults. After a fault, it is necessary to isolate the fault location as soon as possible. Thus, the energy path may be interrupted to some of the loads. However, new technologies or advanced methods can be used to reduce the interruptions duration. By appearance of smart grids and developing its level of intelligence, it is possible to automatically detect a fault in the shortest time, isolate it from the system and feed healthy parts of the system on a different path. The set of automatic activities that occur after a fault occurrence to achieve previous goals is called self-healing. In other words, Self-healing of the distribution system means changing the distribution network structure after fault in order to feed disconnected loads while maintaining the network's electrical constraints. Undoubtedly, self-healing is one of the main abilities of the smart grids with respect to traditional systems to automatically retrieve system after fault occurrence or keep away system from critical conditions. Self-healing usually consists of three steps: fault location, isolation and system restoration (FLISR). The large number of lines, branches, and equipment of the distribution network can complicate this process. In this chapter, definition, requirements and challenges of self-healing are introduced and various approaches which have been recently proposed by researchers are assessed. Also some tools and methods like demand response, load shedding, distributed energy resources and autonomous microgrids which can facilitate self-healing process are assessed.

Keywords Self-healing · Microgrid · Centralized and decentralized · Graph theory · Multi agent system

A. Zangeneh · M. Moradzadeh (✉)
Electrical Engineering Department, Shahid Rajaee Teacher Training University, Tehran, Iran
e-mail: m.moradzadeh@sru.ac.ir

A. Zangeneh
e-mail: a.zangeneh@sru.ac.ir

N. Mahdavi Tabatabaei et al. (eds.), *Microgrid Architectures, Control and Protection Methods*, Power Systems,
https://doi.org/10.1007/978-3-030-23723-3_21

21.1 Introduction

It is predictable that the total consumption of electric energy will be twice of other energy sources in the next decay, thus it is important to use electric power more efficient and reliable [1]. We never think about turning on a light or charging cell phone as so many other activities, which have far greater importance in our lives. These daily activities rely on the expectation of people to have high reliable electrical grid with smooth running. Nowadays our social welfare and vital needs are highly dependent to electrical services. Just imagine conditions that power goes wrong and there is no electricity for hospitals, internet and communication, electronic baking, water station, stock markets, government buildings, transportation and traffic. These examples confirm that to what extent our new lives rely on electric power and an outage may cause significant damages.

Nowadays, so many problems such as voltage instability, blackouts and slow control responses have spread due to increased inter-area power transfers, aging infrastructure, and old technologies. These problems have formed a crucial demand to move from the current electric power system to a highly measurable, controllable, efficient, and self-healing electric power system, which has been termed "smart grid" [2]. Smart grid (SG) have been recently introduced and developed to increase the efficiency, reliability and security of electric power systems. The US Department of Energy (DOE) defines SG as "A grid that is intelligent, efficient, accommodating, motivating, opportunistic, quality-focused, resilient and green" [3]. Among these features, reducing of energy not served and time outage are very important. Some experts believe that it is possible to increase the reliability from 99.9% (approximately 8 h of power loss per year) to 99.99999999% (roughly 32 s of power loss per year) through recent technologic developments [4]. Self-healing is, in general, control actions that helps the power system operator to have a more secure and reliable operating state. According to the electric power system research institute (EPRI), self-healing is introduced as a key function of smart grid to keep away electric grid from the critical conditions in the normal operation as well as to automatically fault diagnosis, clearance and system restoration after fault occurrence [5].

In the current state of electric grid, slow response to the fault occurrence in the conventional distribution system was one of the main reason to increase outage duration. It is possible to see the approximate location of fault but it takes hours to send crew to actually find out the faulted area, sectionalize it and restore power to customers. It should be noted that several factors such as location and complexity of grid might increase blackout hours. Self-healing, as one of the valuable capabilities of the smart technologies, helps distribution system to heal itself automatically after fault occurrence. It uses digital and real time devices to measure and communicate the characteristics of electric grid at all times. In other words, self-healing is a series of measures to manage power disturbances. In the self-healing process, besides corrective measurements after disturbance occurrence, the securing and hardening of the system against disturbance spread is also crucial. To this aim, following functions are considered in the self-healing process [6]:

- Quick and appropriate detection and insulation of disturbances.
- Rescheduling of grid resources to avoid critical influences.
- Preserving the service continuity of the electric grid under any conditions.
- Minimizing the restoration time after outage.

For a grid to be self-healing, it must dynamically optimize its own performance and robustness, react quickly to potential problems in order to avoid disturbances, and, if a disturbance does occur, restore the system quickly and effectively to stability area. For this purpose, after fault occurrence, fault location isolation service restoration (FLISR) control system directly communicates with automatic feeder and line switching to isolate fault and determine the optimal reconfiguration and capability of the new circuits to supply customers. FLISR is becoming one of the most popular modules in distribution automation (DA). FLISR module can significantly decrease the fault detection/isolation/restoration time, significantly enhancing reliability indices.

An interesting feature of FLISR module is that, if more than one options are available for restoration (e.g. in N-2 secure systems) of un-faulted area, then FLISR module provides all the possible options for restoration, giving the operator the flexibility to choose the best restoration path, significantly improving power quality in post-restoration scenario. In traditional methods, the efficiency and quality of isolation/restoration process considerably depends on the experience of the operator in the control room. The automated actions issued by FLISR module eliminates this reliance on the expert experience.

21.2 Fault Location and Diagnosis

Electric utilities have traditionally performed the fault diagnosis activities based on the customers' outage calls. Upon receiving the trouble calls from the customers, a repair crew is sent to patrol the outage area. The crew performs a set of additional switchings nearby already-opened circuit breaker (opened by the protection system as a reaction to the fault) based on trial-and-error in order to identify the exact faulty section. The diagnosis of the fault in this manually-operated manner can be an unsafe, rigorous and time-consuming task, which finally results in the poor quality and reliability of electric power delivered to the customers. In order to overcome these issues, various schemes have been developed to automate the fault diagnosis activities.

Development of fault diagnosis schemes aiming at accurate detecting and locating of the deteriorated components for power systems are major steps in realizing their self-healing capability. In [7], the impacts of corrective (reactive) and preventive (proactive) diagnosis schemes on distribution system reliability are compared.

Figure 21.1 shows the failure modes of a component in electric power system and their corresponding maintenance activities. Unlike normal operating state in which no maintenance is required, passively failed components in degradation state

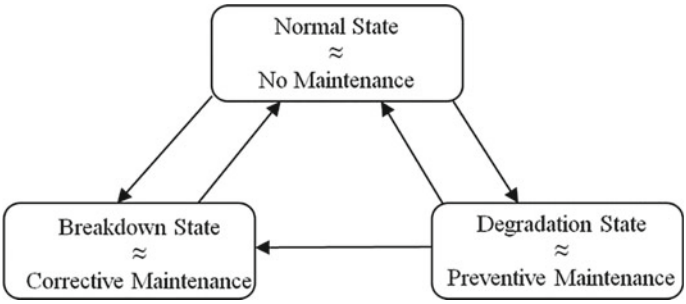

Fig. 21.1 Failure modes of a component in an electric power system

requires preventive maintenance activities in order to avoid complete breakdown of the component. If proper preventive maintenance activities is not carried out here, the degraded component will eventually move into breakdown state, in which actively failed components will require costly and time-consuming repair or replacement for returning to their normal operating status.

21.2.1 Phasor Measurement Unit (PMU)

The phasor measurement units (PMUs) provide synchronized measurements accurately capturing real-time wide-area dynamics of the smart power grid within a microsecond. This has been made possible by the availability of Global Positioning System (GPS) and the sampled data processing techniques developed for computer relaying applications. IEEE Std. C37.118.2-2011 (IEEE Standard for Synchrophasor Data Transfer for Power Systems) developed in the Power System Relaying Committee of IEEE allows the interoperability of PMUs from different manufacturers.

PMU technology and its dedicated high-speed communications can provide high speed, real-time, synchronized system-wide data across an entire system. In this way, it will enhance the system operator's situational awareness creating wide-area visibility across the bulk power system. Minimal number of PMUs are expected to be placed in strategic locations to increase the observability of power systems, and allow grid operators to identify the emerging grid problems in real-time, and better diagnose, implement and evaluate remedial actions for system protection purposes [8].

21.2.2 *Wide-Area Monitoring, Protection and Control (WAMPAC)*

The smart grid brings opportunities and challenges to the power system monitoring, protection and control [9]. Wide Area Monitoring, Protection and Control systems (WAMPAC), utilizes PMUs to gain real-time awareness of current grid operations in order to provide real-time protection and control functions. WAMPAC can be subdivided further into its constituent components namely, Wide-Area Monitoring Systems (WAMS), Wide-Area Protection Systems (WAPS), and Wide-Area Control Systems (WACS).

PMUs, as the heart of WAMS, utilize high sampling rates and accurate GPS-based timing to provide very accurate, synchronized grid readings. The full potential of PMUs will not be realized unless these measurement data can be shared among other utilities and regulators.

The development of advanced control schemes in WACS, as well as ability of WAPS to perform fast switching actions for counteracting the propagation of large disturbances, will depend on WAMS that can effectively distribute information collected over a wide geographic area in a secure and reliable manner [10].

Unlike the traditional power system protection and control schemes which were only based on local measurements, WAPS and WACS provide a system-wide protection and control, complementary to the conventional local strategies. By employment of WAMPAC, early recognition of large- and small- scale instabilities, well-coordinated control actions, flexible relaying schemes, and fewer load shedding events can be accomplished. The advent of PMU has transformed protection from a local concept into a system-level wide-area concept of WAPS to handle disturbances. WAPS facilitates detection and localization of transmission line faults in a shorter time span with enhanced accuracy.

The major drawback of the conventional protection schemes is the uncoordinated and non-optimized local actions taken by different nearby decentralized protective devices which results from lack of a wide-area system view.

The main requirements of WAPS are then as below [11]:

- Dynamic measurement and representation of events
- Wide-area system view
- Coordinated and optimized stabilizing actions
- Adaptive relaying in coordination with local protective devices
- Handling of cascaded outages.

21.3 Centralized Self-healing Algorithms

There are several different techniques used in the centralized self-healing algorithms. In the centralized-based approaches, it is necessary to have a communication system between all measurement and switching equipment with central control system.

21.3.1 Network Reconfiguration

After fault diagnosis and clearance, a part of distribution system, which is downstream of the fault location isolated from the main grid. In this state, loads in the isolated area lose their electricity supply until the reconnecting after repair. Network reconfiguration as one of the traditional self-healing techniques tries to find the new path for feeding unsupplied loads by closing and opening some switches. In other words, loads in the isolated area are transferred to the healthy feeders. It is obvious that this process has to be performed by taking into account the technical constraints of the distribution system such as radial configuration, overload and voltage violation. There are usually more than one feasible switching scheme and therefore it is necessary to define appropriate objective and constraints to find the best switching scheme.

21.3.1.1 Objective Functions

Various objective functions are defined in the literature [12]. The most usual objective functions are maximizing number of customers under service and energy restored (f_1), reliability improvement as minimizing the weighted sum of three reliability indices (f_2) including system average interruption duration index (SAIDI), system average interruption frequency index (SAIFI) and energy not supplied (ENS), minimizing number of switching (f_3) and energy losses (f_4). These functions, which are explained as follow can be used as individual or composite objective functions in the self-healing strategy through single/multi objective optimization.

$$\max f_1 = w_1 \sum_{i \in \Omega} N_i + w_2 \sum_{i \in \Omega} L_i \,, \quad w_1 + w_2 = 1 \tag{21.1}$$

where, N_i and L_i are number of the restored customers and load at ith bus in the outage area respectively, w_1 and w_2 are respectively the weighting factor represents the importance of each term and Ω is the set of buses in the outage area.

$$\min f_2 = w_1 \cdot SAIDI + w_2 \cdot SAIFI + w_3 \cdot ENS, \quad w_1 + w_2 + w_3 = 1 \tag{21.2}$$

where, w_1, w_2 and w_3 are weighting factors.

$$\min f = \sum_{j=1}^{ns} \left(I_{0,j} - I_{1,j}\right)^2 \tag{21.3}$$

where, $I_{0,j}$ and $I_{1,j}$ are respectively the status of jth switch before and after applying the switching scheme and ns is the number of total switch.

$$\min f_4 = \sum_{k=1}^{nbr} R_k I_k^2 \tag{21.4}$$

where, R_k and I_k are respectively resistance and flowing current of kth branch and nbr is the total number of branches. Also minimizing of energy losses are usually considered in the objective functions it is not so crucial in the restoration process during emergency conditions.

21.3.1.2 Constraints

The set of constraint equations in an optimization problem determines the search space, which includes feasible solutions. The usual constraints in the self-healing problem are introduced as follow:

- Maintaining radial configuration of distribution network
  This constraint can be satisfied using the graph theory based approaches such as spanning tree.
- Allowable feeder power flow

$$P_k \leq P_k^{\max}, \quad k = 1, \ldots, nbr \tag{21.5}$$

  where, P_k and $P_k^{\max}$ are respectively the flowing power and maximum power at kth branch.
- Allowable voltage range

$$V_{\min} \leq V_i \leq V_{\max}, \quad i = 1, \ldots, n_{bus} \tag{21.6}$$

  where, V_i is the voltage magnitude at ith bus and $V_{\min}$ and $V_{\max}$ are respectively the maximum and minimum permissible voltage in distribution system.

21.3.2 Network Partitioning Based on Intentional Islanding

The increased penetration of distributed generation creates two challenges during faults: increase rate of the fault current as well as decrease in the fault ride through capability of DGs [6]. In the conventional operation of distribution system, there is just one feed point to supply customers and power flows from upstream substation to the downstream customers throughout the system. By occurring a fault and its clearance, all customers downstream of the fault point are went wrong. In this case, microgrid, as a reliable source, can supply customers in the outage area and help the system to restore in a proper and quick manner. Hence, local reliability and continuous supply will be increased by intentionally partitioning of the system and

feeding loads in each islanded area. However, the customers in the islanded microgrid will still be able to send/receive information with the power grid. It is expected that by removing the disturbance, the microgrid is able to reconnect to the power grid [13]. To this aim, it is important to measure the status of power grid and microgrid during the processing period.

Although it is supposed that reconfiguration can increase reliability of the system by reconnecting an outage zone to the main grid or to unfaulted area with surplus power, it may also increase number of interruptions due to the frequent switching [14]. In addition, it could be possible that the adjacent feeders are not able to feed all loads in the outage area due to the feeder overloading and load shedding is not also a good choice. In this case, then network partitioning are applied to build intentional islands, that are able to supply their demands individually. Intentional islanding finds a feasible solution to enhance the reliability of active distribution system by supplying critical loads through the local distributed generation (DG) when a fault occurs [15]. Recently, the intentional partitioning of distribution system equipped with DG units, has attracted much attention as a self-healing strategy in comparison with conventional ones such as reconfiguration and load shedding. IEEE Standard 1547.4 states that distribution system partitioning can improve the operation and reliability of the distribution system [16]. Partitioning has some expected benefits such as easier control and energy management approaches, the possibility of applying distributed control in the partitions, load routing and transfer among partitions to decrease the energy not served and therefore and minimize load shedding and increase the efficiency of DG utilization [17].

Although network partitioning can be done either centralized or decentralized based, it is assumed that there is a central controller to make final decisions about partitioning and DG rescheduling. In some self-healing algorithms, the network partitioning is executed after reconfiguration. If the reconfiguration process are not able to completely reconnect the isolated area to the main grid, the partitioning strategy sectionalizes the isolated area and makes intentional islands, which are called self-adequate islands. It means they are able to supply their local power demands based on their local generations. This strategy is performed using an adaptive mapping strategy to match and allocate generation units to high-priority demands in each area. The key point of partitioning is to find the boundaries of island so that balance of active and reactive power is maintained. In addition to power loss, key technical requirements such as bus voltages, power balance, and load controllability should be considered in the island partitioning solution. In the case of grid connected, the shortage of active and reactive power is compensated using main grid and thus maintaining the characteristics of the system is simple. While in the islanded mode, maintaining the voltage and frequency in the allowable range is difficult and challenging due to the inequality of generation and demand. To deal with such challenges, each island must have at least one dispatchable distributed generation unit to control voltage and frequency in its island.

Due to the similarity of a graph and distribution system configuration, graph theory has appropriate and compatible features to be used in the self-healing strategies either in reconfiguration or in partitioning algorithms. A distribution system can be modeled

by a graph including a set of vertices (buses) and a set of edges (branches). A graph theory-based algorithm such as the transportation problem can be used to create appropriate islands by optimally assigning the loads to DGs. In this problem, the cost of transporting one type of merchandise from some certain origins to other certain destination is minimized [18]. The distribution system partitioning can be adapted to the transportation problem by assuming DGs as origins (root vertices), loads as destinations (end vertices) and power losses as transportation cost are representative of branch resistances. To minimize the power losses, the shortest path is selected using the weighted sum of shortest path between DGs and load buses to assign the proper DGs to the proper loads. The allocation of power to each load achieved by solving the following Eqs. (21.7)–(21.10) [17]. Equation (21.7) represent the total transportation cost that must be minimized. Equation (21.8) states that total active power transferred from DGs to dth load bus must be equal to demand at this bus. Also the active power supplied by each DG must not violate from its maximum capacity (21.9) and finally the negative values of power transfer in (21.10) is defined meaningless.

$$\min f = \sum_{d} \sum_{i \in G} c_{di} x_{di} \tag{21.7}$$

$$\text{s.t.} \quad \sum_{i \in G} x_{di} = D_d, \quad \forall d \tag{21.8}$$

$$\sum_{d} x_{di} \leq P_i, \quad \forall i \in G \tag{21.9}$$

$$x_{di} \geq 0, \quad \forall i \in G, \forall d \tag{21.10}$$

where, G is the set of all available and dispatchable DGs, d is the index for load buses, D_d is the active power of dth load bus, c_{di} and x_{di} is the transferring cost and active power from ith DG to dth load bus respectively.

The obtained solution allocates each load to a specific DG and thus the set of assigned loads are defined as the individual island of that DG. In this case, all branches have a common load will be emerged together and build the final island.

In the lack of power generation in the isolated area from the main grid, it is necessary to execute load shedding before partitioning the isolated area. This process can be performed by selecting the high priority loads in accordance to maximum generation capacity of the isolated area. This goal can be achieved using graph-related algorithms such as the knapsack problem presented in Eqs. (21.11) and (21.12) [14]. In this algorithm, the specified capacity of total available generation resources H is assigned to the most valuable loads.

$$\max f = \sum_{d} \sigma_d \left(\sum_{\alpha} D_\alpha I_\alpha + \sum_{\mu} D_\mu I_\mu \right) \tag{21.11}$$

$$\text{s.t.} \quad \sum_{d} \left(\sum_{\alpha} D_{\alpha} I_{\alpha} + \sum_{\mu} D_{\mu} I_{\mu} \right) \leq H \tag{21.12}$$

where, α and μ are controllable and non-controllable loads respectively. I is the binary value that shows the commitment state of loads, 0 for shed load and 1 for the supplied load and σ is the value of each load bus.

Wang et al. [19] proposed a similar approach shown in Fig. 21.2 to manage both grid connected and isolated area after fault occurrence. In the grid-connected area, due to the variation of supply and demand balance, a rescheduling of dispatchable generation and storage units are performed based on the minimization of distribution system operation cost and technical constraints. However, the voltage and frequency control are still managed using the main grid. On the other hand, the most important part of the self-healing strategy is applied in the isolated area to reduce not supplied load as well as outage duration. To this end, partitioning strategies can be applied to build self-adequate microgrid, which are able to meet their demand and keep voltage and frequency in the permissible range. Unlike the cost function applied in the grid-connected area, the first priority of defining objective function in an isolated area is to reliably supply affected customers. Thus, Eq. (21.13) and its constraints (21.14)–(21.25) is defined to simultaneously create optimal boundaries of the island and minimize the voltage deviations and the amount of load shedding according to the load priorities in the created islands.

$$\min f = \sum_{t}^{t+T_p} \left(\sum_{k} \left(\left| V_{k,t} - V_n \right| + \sum_{j} x_{kj} + \omega_k p_{k,t}^{D} \left(1 - y_{k,t} \right) \right) \right) \tag{21.13}$$

$$\text{s.t.} \quad 1 - \varepsilon \leq V_{k,t} \leq 1 + \varepsilon \tag{21.14}$$

$$p_{k,t}^{G} - y_{k,t} p_{k,t}^{D} + \sum_{n \in N} p_{k,n,t}^{R} = \sum_{j} P_{k,j,t} \tag{21.15}$$

$$q_{k,t}^{G} - y_{k,t} q_{k,t}^{D} + \sum_{n \in N} q_{k,n,t}^{R} = \sum_{j} Q_{k,j,t} \tag{21.16}$$

$$P_{kj,t} = x_{kj} V_{k,t} V_{j,t} \left(G_{kj} \cos \theta_{kj,t} + B_{kj} \sin \theta_{kj,t} \right), \quad \forall k, t \tag{21.17}$$

$$Q_{kj,t} = x_{kj} V_{k,t} V_{j,t} \left(G_{kj} \sin \theta_{kj,t} - B_{kj} \cos \theta_{kj,t} \right), \quad \forall k, t \tag{21.18}$$

$$\left(p_{k,t}^{G} \right)^2 + \left(q_{k,t}^{G} \right)^2 \leq S_k^{G}, \quad \forall k, t \tag{21.19}$$

$$-P_k^{ch,\max} \lambda_{k,t} \leq p_{k,t}^{E} \leq P_k^{dch,\max} \varphi_{k,t}, \quad \forall k, t \tag{21.20}$$

$$\lambda_{k,t} + \varphi_{k,t} \leq 1, \quad \forall k, t \tag{21.21}$$

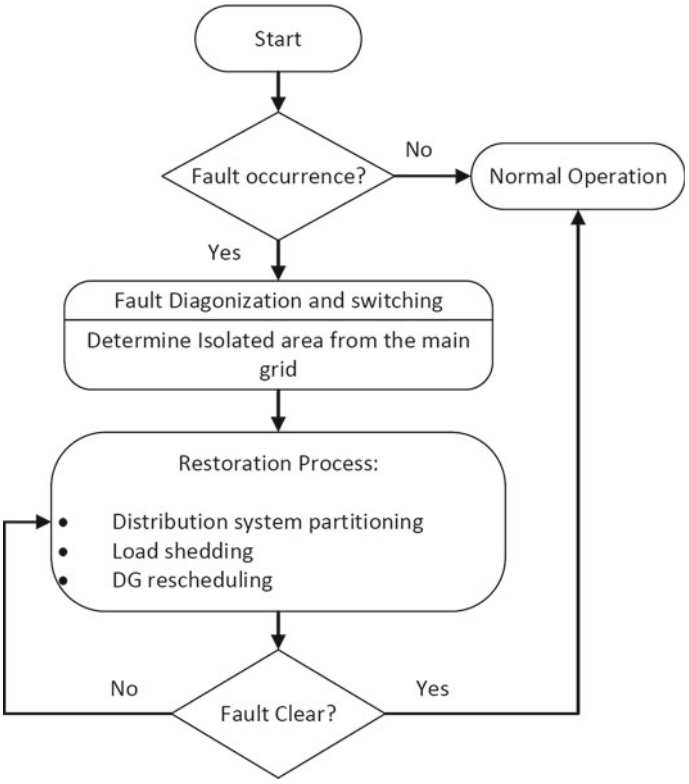

Fig. 21.2 Self-healing strategy

$$SOC_{k,t} = SOC_{k,t-1} - \frac{T}{EC}\left(\varphi_{k,t} p^{E}_{k,t} \pi_d^{-1} + \lambda_{k,t} p^{E}_{k,t} \pi_c\right), \quad \forall k, t \tag{21.22}$$

$$0 \le SOC_{k,t} \le SOC_k^{\max}, \quad \forall k, t \tag{21.23}$$

$$\sum_k \left(p^{G}_{k,t} + p^{E}_{k,t} + \sum_n p^{R}_{k,n,t}\right) \ge \sum_k p^{D}_{k,t}, \quad \forall k, t \tag{21.24}$$

$$\sum_k \left(q^{G}_{k,t} + \sum_n q^{R}_{k,n,t}\right) \ge \sum_k q^{D}_{k,t}, \quad \forall k, t \tag{21.25}$$

The first term in the objective function (21.13) is the voltage deviation from nominal voltage (where, V_n and $V_{k,t}$ are respectively nominal voltage and voltage magnitude at node k and time t), the second term represents the boundary lines of the islands [where x_{kj} represents if the line between node k and j is in use ($x_{kj} = 1$) or not ($x_{kj} = 1$)]. The last term is the penalty of load shedding (where ω_k is the load priority index at node k, $y_{k,t}$ is the load shedding index, 0 for load shed and 1

for connect). Voltage magnitude at each node is maintained in permissible range by (21.14) where ε is the maximum permissible voltage deviation.

Constraints (21.15)–(21.18) are power flow equations and active and reactive balance. In these equations, G_{kj} and B_{kj} are respectively conductance and susceptance of line between node k and j, $\theta_{kj,t}$ is the difference of voltage phase between node k and j, $p^D_{k,t}$ and $q^D_{k,t}$ denote active and reactive demand at node k, $p^G_{k,t}$ and $q^G_{k,t}$ are active and reactive generation at node k, $p^R_{k,n,t}$ and $q^R_{k,n,t}$ are active and reactive generation of renewable energy type n at node k. Constraint (21.19) restricts the active and reactive power generation with respect to its maximum capacity. The relation between charge, discharge, efficiency and state of charge (SOC) in energy storages are defined in Eqs. (21.20)–(21.23). In Eqs. (21.24) and (21.25), the total active and reactive generation should be equal or greater than total active and reactive load.

In [20], a graph theory based spanning algorithm is presented to find the best islands using existing DG and microgrids. The normal operation of a distribution system, which has radial and connective path, can be considered as a spanning tree graph. The problem of distribution system restoration is defined as finding a spanning tree after fault clearance so that it meets various constraints. To simple the distribution system graph, the nodes of DGs and upstream substation are represented as root node. A pair of switching operation are usually applied in the self-healing process. It means that for each normally closed switch which is opened and remove a line/branch of the distribution system, another normally open switch will be closed and add a line/branch into the graph of the distribution system. This strategy keeps the connectivity as well as the radially of the spanning tree.

By occurring a fault and its clearance, one or more lines are opened to isolate the faulted area. The strategy of the graph-based self-healing is to find the fundamental cut-set for each opened (removed) branch and replace that with another branch (edge) in its fundamental cut-set so as a new spanning tree is built. After a fault occurrence, usually one pair of switching is sufficient to isolate the faulted branch and connect another branch to build a new spanning tree. However, sometimes more pair of switching are needed to open and close another branches due to the overloading of some branches in the new configuration or lack of enough generation in the constructed microgrids.

21.4 Decentralized Self-healing Algorithms

Although centralized control strategy has the best performance in any situation either disturbance or unusually high demands, it requires complete measurements, two-way communication links, and a powerful computing center to collect data, process among big data and make proper decisions. Thus, it may not be practical due to the fact that a failure in the centralized controller or one its equipment such as communication and measurement may cause to lose all control process. Therefore, the centralized control cannot be completely reliable. An alternative strategy is to find a mechanism

to distribute making decisions throughout the network and to intervene locally by originating the disturbance [4].

Multi agent system (MAS) is a new emerging technology to employ distributed intelligence in various parts of power systems. Todays, by gradually improving system models from simple structures to more realistic, designers try to adapt each component to an adaptive agent. By defining the adaptive agents, the whole system can be controlled and managed using multilevel distributed control. Each agent receives continuously measuring messages from other agents through communication links. In the case of abnormal conditions, adjacent agents can sense and work together to reschedule the controller set points or essentially reconfigure the system for resolving the problem locally. Thus, the agents could prevent losing the central controller of the system and the cascading effect, which is the main source of vulnerability in power systems [4].

A Multi Agent System (MAS) consists of various intelligent agents, which are either hardware or computer programs. These agents can autonomously sense, act, communicate and collaborate with each other across open and distributed environments [21]. Different type of agents are used in smart grid to collect data, make decision, control and keep the optimal operation of system during normal and emergency conditions. Capabilities of collecting information and knowledge as well as decision-making are key challenges for each agent. In MAS, decisions are made based on various techniques such as fuzzy logic, statistical hypothesis testing, Bayesian belief networks, constraint satisfaction, and distributed optimization [21]. Heterogeneous and cooperative are two main feature of agents in the smart grid. They are heterogeneous because they do various actions and are not similar in their responsibility. They are cooperative due to the fact that they all contribute with each other to follow an overall objective, even if they have their own localized objectives to achieve.

21.4.1 The MAS Control Model [22]

In this section a cooperative model of MAS control is illustrated for self-healing problem. Figure 21.3 shows a distribution system with three feeders each of that has a feeder agent as well as some partitioned zones. The zones are built by two or more switches in its boundary area (shown with letter B in Fig. 21.3). All zones have agents, which are able to measure, make decision, send open/close command and communicate with each other. On the other hand, the responsibility of a feeder agent is to negotiate with adjacent feeders, which are connected to them by tie switches (normally open switches). Thus, the MAS control model has two layers: zone and feeder.

When a fault occurs in a distribution feeder, first the feeder control agent detects the fault and opens its circuit breaker at the beginning of the feeder. Then the fault diagnosis algorithm are applied to determine and isolate the faulted area from both directions. After that, the feeder circuit breaker is closed and the upstream out of service loads are restored again. Now the key action is to actuate the restoration

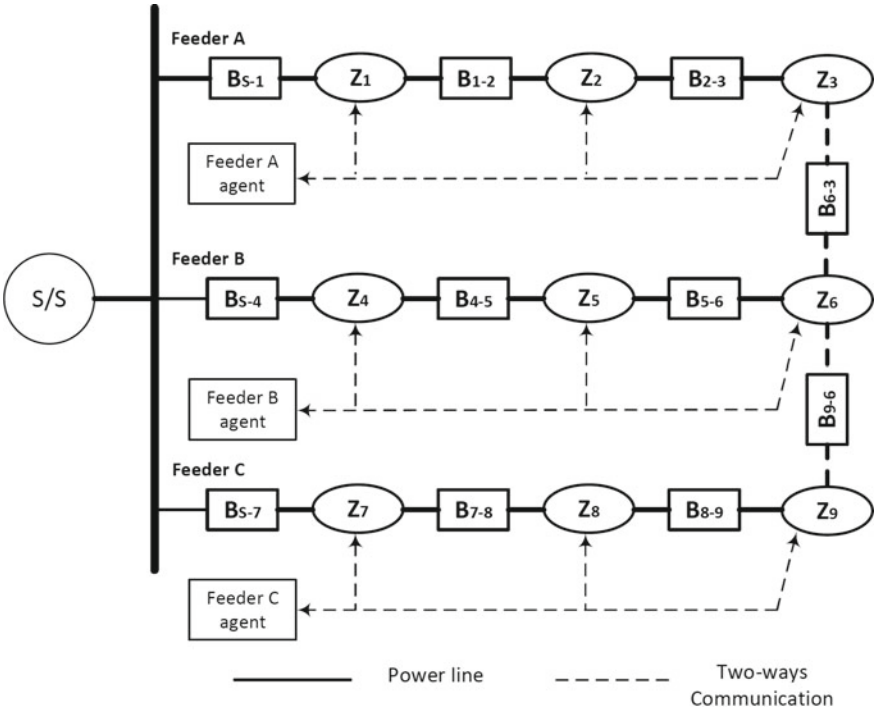

Fig. 21.3 A MAS control schematic of a typical distribution system [22]

process to feed out of service loads. Figure 21.4 shows a distribution system with a fault on the middle feeder. The different role of feeders in the hierarchical control are shown in this figure during restoration process. The pink color shows the outage area after fault isolation.

The first option is to check if the adjacent feeders (level-1 backup feeder) specified with blue color are able to restore whole out of service loads as a single group. The advantage of this option is that the restoration achieved with minimum number of switching and thus least time duration. If the first backup feeders (BF) do not have enough capacity to feed all out of service loads, the second option is to partition the outage area into different zones and connect them with level-1 BF. In the case that the second option is not possible too, some loads from level-1 BF are transferred to the level-2 BF so as the first BF has enough capacity to supply individual zones in the outage area. If not all the previous options are successful, the only and last option is to shed low priority loads to make free capacity in backup feeders. This process is managed by multi agent system shown in Fig. 21.5. In this figure, objectives of agents as well as two-way communication between them are depicted. Initiator feeder is the feeder that a fault has been occurred on one of its components. The responder feeder is the adjacent feeder in level-1 BF and subcontractor feeder is the level-2 BF.

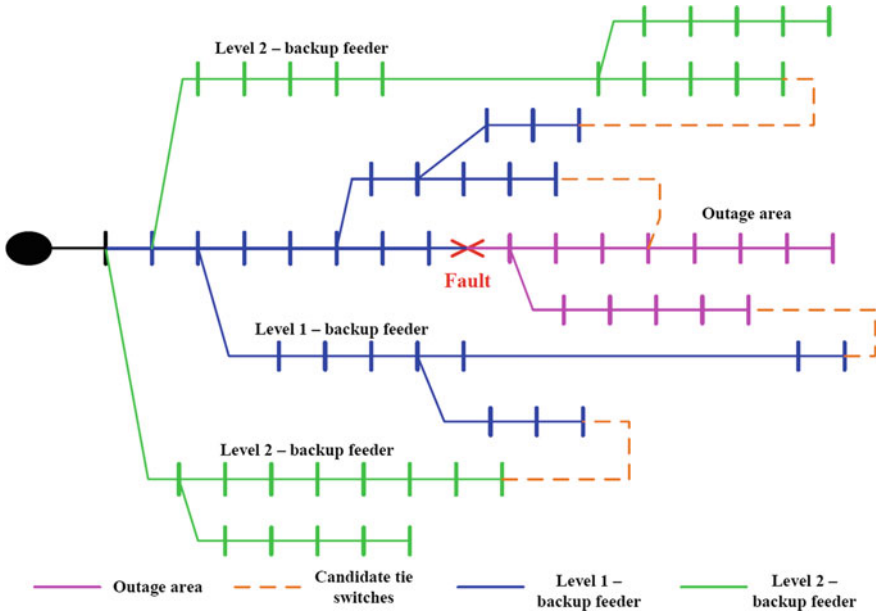

Fig. 21.4 Different level of controls in the restoration process [22]

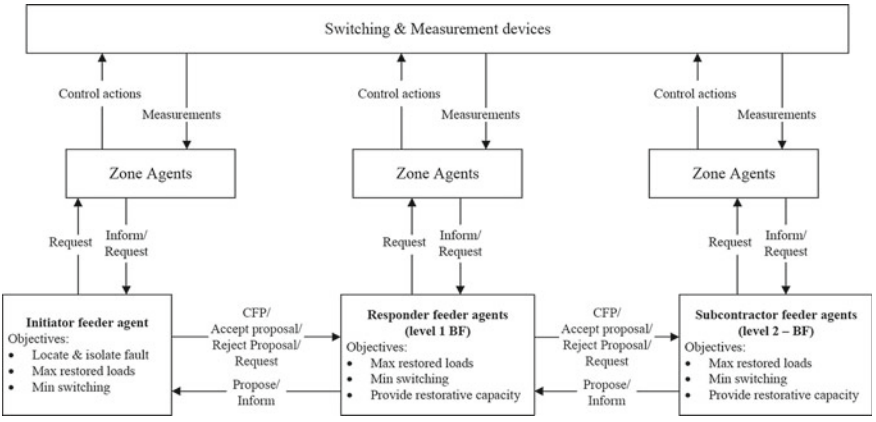

Fig. 21.5 Objectives and communication between agents [22]

21.5 Conclusion

In this chapter self-healing strategy, a modern feature of smart grids, are introduced as an automatic control action that detect a fault in the shortest time, isolate it from the system and feed healthy parts of the system on a different path. In other words, self-healing is a set of activities, preventive or corrective, which is try to operate smart grid in a safe operation condition either before or after fault occurrence. These activities can be divided into three groups: fault detection, isolation and restoration, which were assessed in two sections: fault location and diagnosis, centralized and decentralized self-healing algorithms. Various algorithms of restorative solutions such as network reconfiguration, network partitioning and load shedding were presented in centralized or decentralized viewpoint.

References

1. J. Popovic Gerber, J. Oliver, N. Cordero, T. Harder, J. Cobos, M. Hayes, S. O'Mathuna, E. Prem, Power electronics enabling efficient energy usage: energy savings potential and technological challenges. IEEE Trans. Power Electron. **27**(5), 2338–2353 (2012)
2. C.P. Nguyen, *Power System Voltage Stability and Agent Based Distribution Automation in Smart Grid*. Illinois Institute of Technology (2011)
3. ERGEG, Position paper on smart grids. An ERGEG public consultation paper. Ref: E10-EQS-38-05 (2009)
4. M. Amin, Toward self-healing energy infrastructure systems. IEEE Comput. Appl. Power **14**(1), 20–28 (2001)
5. U.S. EPRI, Methodological approach for estimating the benefits and costs of smart grid demonstration projects (2010)
6. M.A. Elgenedy, A.M. Masoud, S. Ahmed, Smart grid self-healing: functions, applications, and developments, in *SGRE Conference*, Qatar (2015)
7. S. Kazemi, M. Lehtonen, M. Fotuhi Firuzabad, Impacts of fault diagnosis schemes on distribution system reliability. IEEE Trans. Smart Grid **3**(2), 720–727 (2012)
8. C. Sutar, K.S. Verma, A.S. Pandey, S.P Singh, Wide area measurement and control using phasor measurement unit in smart grid, in *The 2nd IEEE International Conference on Power, Control and Embedded Systems* (*ICPCES*), pp. 1–5 (2012)
9. L. Luo, N. Tai, G. Yang, Wide-area protection research in the smart grid. Energy Procedia **16**, 1601–1606 (2012)
10. A. Ashok, A. Hahn, M. Govindarasu, Cyber-physical security of wide-area monitoring, protection and control in a smart grid environment. J. Adv. Res. **5**(4), 481–489 (2014)
11. K.S.N. Singh Seethalekshmi, S.C. Srivastava, Wide-area protection and control: present status and key challenges, in *The 15th National Power Systems Conference*, Bombay, India, pp. 169–175 (2008)
12. M. Zarei, A. Zangeneh, Multi-objective optimization model for distribution network reconfiguration in the presence of distributed generations. Int. Trans. Electr. Energ. Syst. **27**(12) (2017)
13. T. Caldognetto, P. Tenti, Microgrids operation based on master-slave cooperative control. IEEE J. Emerging Select. Top. Power Electron. **2**(4), 1081–1088 (2014)
14. V. Hosseinnezhada, M. Rafieea, M. Ahmadiana, P. Sianob, A comprehensive framework for optimal day-ahead operational planning of self-healing smart distribution systems. Electr. Power Energy Syst. **99**, 28–44 (2018)

15. M.H. Oboudi, R.A. Hooshmand, F. Faramarzi, M.J.A. Boushehri, Framework of intentional islanding operation of active distribution network based on selfhealing perspective. IET Renew. Power Gener. **12**(2), 219–226 (2018)
16. S.A. Arefifar, Y.A. Mohamed, T.H. El Fouly, Comprehensive operational planning framework for self-healing control actions in smart distribution grids. IEEE Trans. Power Syst. **28**(4), 4192–4200 (2013)
17. S.A. Arefifar, Y.A. Mohamed, T.H. El Fouly, Supply-adequacy-based optimal construction of microgrids in smart distribution systems. IEEE Trans. Smart Grid **3**(3), 1491–1502 (2012)
18. S.S. Rao, *Engineering Optimization: Theory and Practice* (Wiley, Hoboken, 2009)
19. Z. Wang, J. Wang, Self-healing resilient distribution systems based on sectionalization into microgrids. IEEE Trans. Power Syst. **30**(6), 3139–3149 (2015)
20. J. Li, X.Y. Ma, C.C. Liu, K.P. Schneider, Distribution system restoration with microgrids using spanning tree search. IEEE Trans. Power Syst. **29**(6), 3021–3029 (2014)
21. S.B. Ghosn, P. Ranganathan, S. Salem, J. Tang, D. Loegering, K.E. Nygard, Agent-oriented designs for a self-healing smart grid, in *First IEEE International Conference on Smart Grid Communications*, pp. 461–466 (2010)
22. A. Zidan, E.F. El Saadany, A Cooperative multiagent framework self-healing mechanisms in distribution systems. IEEE Trans. Smart Grid **3**(3), 1525–1539 (2012)

Chapter 22
Various Droop Control Strategies in Microgrids

Pegah Zafari, Ali Zangeneh, Mohammad Moradzadeh, Alireza Ghafouri and Moein Aldin Parazdeh

Abstract Droop control is a well-known strategy to control active power in power systems without internal communication. It is usually implemented on the conventional power plants to control the injected power of synchronous generators to the grid. As this strategy is local, there is no need to communication systems. Thus, it reduces the complexity and cost of the system operation and improves the reliability indices. Also, droop control has been used to control the active and reactive power of distributed generations in microgrids. Frequency and voltage control of microgrid and proper power sharing between DGs are the most important goals of droop control in the islanded mode of operation. The conventional droop control has some disadvantages that limits their application in the modern microgrids. Slow transient dynamics, load dependency of voltage and frequency, low accuracy on power sharing, low power quality for non-linear or unbalanced loads and circulating current between DGs are some of the main disadvantageous. Different methods have been proposed by researchers to overcome the problems, which are still an attractive subject for them. This chapter discusses different improved droop controllers, which have been used to overcome some of the problems.

Keywords Droop control · Microgrid · DG · Active/reactive power control

P. Zafari · A. Zangeneh · M. Moradzadeh (✉) · M. A. Parazdeh
Electrical Engineering Department, Shahid Rajaee Teacher Training University, Tehran, Iran
e-mail: m.moradzadeh@sru.ac.ir

P. Zafari
e-mail: p.zafari@sru.ac.ir

A. Zangeneh
e-mail: a.zangeneh@sru.ac.ir

M. A. Parazdeh
e-mail: parazdeh@sru.ac.ir

A. Ghafouri
Electrical Engineering Department, Sari Branch, Islamic Azad University (IAU), Sari, Iran
e-mail: ghafuriar@gmail.com

N. Mahdavi Tabatabaei et al. (eds.), *Microgrid Architectures, Control and Protection Methods*, Power Systems,
https://doi.org/10.1007/978-3-030-23723-3_22

22.1 Introduction

As a power plant, the droop characteristic can be implemented for DGs with appropriate control system. It is required that each DG has a control system to implement the droop characteristic [1–3]. Local implementation, no need to communication systems, easy expansion, acceptable reliability and low investment cost are some important benefits of droop controllers. Despite of the benefits, some of their shortcomings are:

a. Frequency and voltage deviations: In the islanded mode, the frequency and voltage of microgrid are highly sensitive to load changes. Increasing the slope of the droop characteristic improves the response of microgrid to the load changes but destroys the frequency and voltage regulation, as well as the stability of microgrid [4].
b. Harmonic loads: traditional droop control is appropriate for the basic load dispatch and it does not perform harmonic load dispatch among nonlinear loads. Low power quality and slow dynamic response are two important shortcomings of this control [5, 6].
c. Unknown and different line impedances: line impedances between parallel converters affects the power flow. Different impedances between inverters and point of common coupling leads to a large circulating current between inverters and decreases the accuracy of power dispatch [7, 8].
d. Output power oscillations of DGs: As the primary energy resources of renewable DGs are variable, the conventional droop cannot provide a smooth power for the microgrid [9].

In recent years, new studies have been performed to overcome the previous illustrated problems. In [10], a transformation matrix, which consider the line impedance in the calculation of droop parameters are presented to overcome the strong coupling between active and reactive power. To assess the stability of the microgrid with high penetration of renewable systems, a special droop control called virtual multi-slack has been introduced [11]. Peyghami et al. [12] propose a new droop control scheme for low voltage DC microgrid to avoid active power sharing errors by merging secondary voltage regulation and primary power sharing. In [13], an optimization method is introduced to find optimal droop parameters in the control mechanism. The information considered in [13] is not sufficient and determination of the optimal droop parameters are also dependent to microgrid stability [14].

In this chapter, we introduce various droop strategies and simulate some the prevalent ones to assess the strength and weakness of each approach.

22.2 Conventional Droop Control

This method is based on the conventional droop control of synchronous generators. The active and reactive power of each DG is determined regarding its nominal capacity and the droop coefficient. The droop coefficient plays the role of a virtual resistance regarding the grid side of DG inverters. Adjusting the droop coefficient changes the output resistance of DG inverters and controls the injected power of each DG to the grid. So the local controller of each DG should control the output characteristics of its inverter and it can be used for the frequency and voltage control of microgrid. Some controllers add a virtual series reactance to the power line in series with DGs. The output voltage and frequency of the inverter is controlled based on the reference active and reactive power of DGs, so the Q-V and P-f droop controllers are usually good candidates [15–17]. The typical equivalent circuit of a DG connected to the grid through its inverter has been shown in Fig. 22.1.

The injected active and reactive powers are derived by Eqs. (22.1)–(22.3).

$$S = P + jQ \tag{22.1}$$

$$P = \left(\frac{EV}{Z}\cos\varphi - \frac{V^2}{Z}\right)\cos\theta + \frac{EV}{Z}\sin\varphi\ \sin\theta \tag{22.2}$$

$$Q = \left(\frac{EV}{Z}\cos\varphi - \frac{V^2}{Z}\right)\sin\theta + \frac{EV}{Z}\sin\varphi\ \cos\theta \tag{22.3}$$

Considering Z as an imaginary reactance, Eqs. (22.2) and (22.3) can be simplified as:

$$P = \frac{EV}{X}\sin\varphi \tag{22.4}$$

$$Q = \frac{EV\cos\varphi - V^2}{X} \tag{22.5}$$

where, X, φ, E and V are the output reactance of inverter, the phase angle difference between the voltages of the inverter output and the PCC, the voltage magnitude of inverter bus and the voltage of PCC, respectively. The active power can be adjusted directly by φ and the reactive power by E. so the droop controller can be designed based on this relationship by Eqs. (22.6) and (22.7).

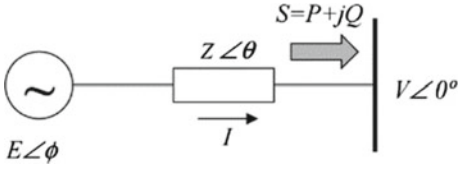

Fig. 22.1 Connection of DG to the AC bus [18]

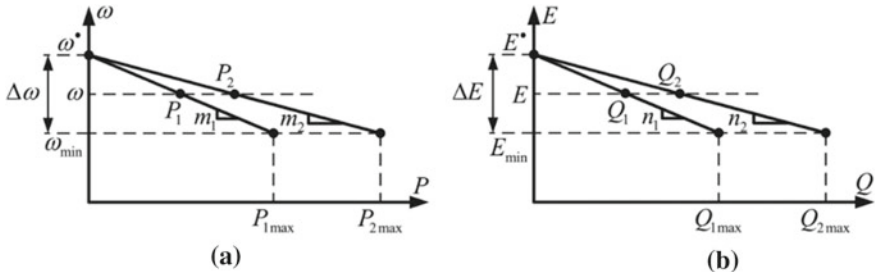

Fig. 22.2 Conventional droop characteristics [21]

$$\omega = \omega^* - mP \tag{22.6}$$

$$E = E^* - nQ \tag{22.7}$$

where, E^* and ω^* are the voltage and frequency references and E and ω are the output voltage and frequency of the inverter. n and m are the frequency and voltage droop coefficients defined by Eqs. (22.8) and (22.9) [19, 20].

$$m = \frac{f_i - f_{i\min}}{P_i - P_{i\max}} \tag{22.8}$$

$$n = \frac{E_{i\max} - E_{i\min}}{Q_{i\min} - Q_{i\max}} \tag{22.9}$$

Frequency and voltage droops have been shown in Fig. 22.2.

The conventional droop control has some disadvantages that limit their application in the modern microgrids. Some of the weaknesses are the slow transient dynamics, load dependency of voltage and frequency, low accuracy on reactive power sharing, low power quality for non-linear or unbalanced loads and circulating current between DGs [22].

In the conventional droop, reactive power sharing is not accurate due to highly dependency between line impedance and local load as well as the coupling between active and reactive power. Kosari and Hosseinian [23] proposed a reactive power compensation process (RCP) to resolve this problem. In this method, the error of reactive power sharing among DGs is compensated by simultaneously forming a transient coupling between active and reactive power and applying following droop equations in Eqs. (22.10) and (22.11) instead Eqs. (22.6) and (22.7). The reactive power term in Eq. (22.10) consider the reactive power sharing error in the P-f control and the third term in Eq. (22.11) consider the error in V-Q droop control by integrating during the transient coupling conditions.

$$\omega_i = \omega_0 - m_i P_i + G k_q (n_i Q_i) \tag{22.10}$$

$$E_i = E_0 - n_i Q_i + \frac{k_I}{s} G\left(P_{i,avg} - P_i\right) \tag{22.11}$$

where, k_q and k_I are respectively reactive power coefficient and integral gain, G is soft compensation gain which increases as a ramp at the beginning and decreases similarly at the end of compensation, $P_{i,avg}$ is the average active power in the steady state before load change.

22.3 Reverse Droop Control (*V-P* and *Q-F* Boost)

The conventional droop control of the previous section is appropriate for the high voltage transmission systems because of small line resistance respect to the line reactance. Unfortunately, it does not work for the low voltage microgrids with high resistive lines. The typical equivalent circuit of a DG connected with its inverter to the grid has been shown in Fig. 22.3 [24, 25].

The injected active and reactive powers are derived by Eqs. (22.1)–(22.3) [24].

$$P = \left(\frac{EV}{Z}\cos\varphi - \frac{V^2}{Z}\right)\cos\theta + \frac{EV}{Z}\sin\varphi\ \sin\theta \tag{22.12}$$

$$Q = \left(\frac{EV}{Z}\cos\varphi - \frac{V^2}{Z}\right)\sin\theta + \frac{EV}{Z}\sin\varphi\ \cos\theta \tag{22.13}$$

where, Z, θ, φ, E and V are respectively the magnitude of output impedance, impedance phase angle, the phase angle difference between the voltages of the inverter output and the PCC, the voltage magnitude of inverter bus and the voltage of PCC, respectively.

Considering Z as a resistive impedance, Eqs. (22.12) and (22.13) can be simplified as:

$$P = \frac{EV}{R}\cos\varphi - \frac{V^2}{R} \tag{22.14}$$

$$Q = -\frac{EV}{R}\sin\varphi \tag{22.15}$$

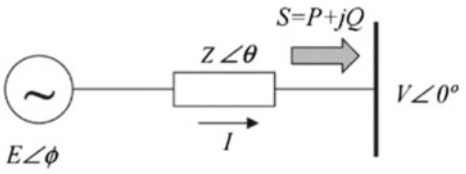

Fig. 22.3 Connection of DG to the AC bus [24]

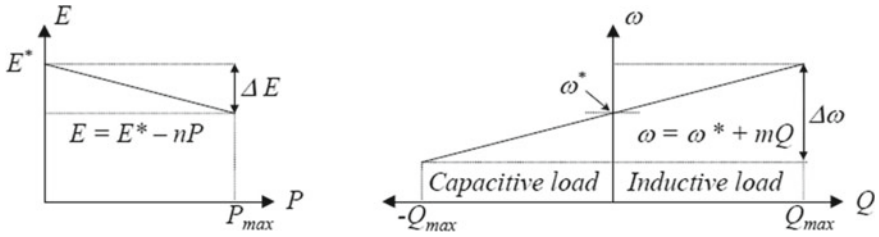

Fig. 22.4 Reverse droop control [25]

In a typical power system φ is approximately zero ($\cos\varphi \approx 1$, $\sin\varphi \approx \varphi$) and Eqs. (22.14) and (22.15) can be approximated as:

$$P \approx \frac{V}{R}(E - V) \tag{22.16}$$

$$Q \approx -\frac{EV}{R}\varphi \tag{22.17}$$

From Eqs. (22.16) and (22.17), it can be seen that the active power is proportional to the voltage of inverter bus and the reactive power decreases by increasing the phase angle. So droop characteristics should be defined by the curves in Fig. 22.4 and Eqs. (22.18) and (22.19) [25].

$$E_i = E^* - n \cdot P_i \tag{22.18}$$

$$\omega_i = \omega^* + m \cdot Q_i \tag{22.19}$$

where, m is the boost coefficient of the reactive power (Q) and n is the droop coefficient of the active power (P). Although this method improves the power sharing of low voltage microgrids including high resistive lines, its performance is highly dependent to the system parameters and has a weak response to the reactive power control [25].

22.4 Complex Line Impedance-Based Droop

The conventional droop control has a weak performance for the microgrids including complex impedance lines. To improve the dynamic response and exact power control of microgrid, some modified droop controllers should be utilized. The typical equivalent circuit of a DG connected with its inverter to the grid has been shown in Fig. 22.5 [18].

The injected current by DG to the grid can be derived from Eqs. (22.20) and (22.21).

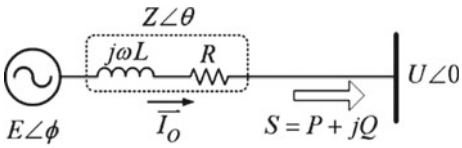

Fig. 22.5 Connection of DG to the AC bus [18]

Table 22.1 Active and reactive power with different types of system impedance [18]

System impedance	Pure inductive $\theta = 90,\ \bar{Z} = jX$	Pure resistive $\theta = 0°,\ \bar{Z} = R$	Complex impedance $\theta,\ \bar{Z} = R + jX$
Active power	$P \cong \frac{UE\varphi}{Z}$	$P \cong \frac{U(E-U)}{Z}$	$P \cong \frac{U}{Z}[(E-U)\cos\theta + E\varphi\sin\theta]$
Reactive power	$Q \cong \frac{U(E-U)}{Z}$	$Q \cong -\frac{UE\varphi}{Z}$	$P \cong \frac{U}{Z}[(E-U)\sin\theta - E\varphi\cos\theta]$

$$\overline{I_o} = \frac{E\angle\varphi - U\angle 0}{Z\angle\theta} = \frac{E}{Z}\angle(\varphi-\theta) - \frac{U}{Z}(-\theta) \tag{22.20}$$

$$\bar{Z} = R + jX \tag{22.21}$$

Also, active and reactive powers can be deriving from Eqs. (22.22) and (22.23).

$$P = \frac{U}{Z}[(E\cos\varphi - U)\cos\theta + E\sin\theta\sin\varphi] \tag{22.22}$$

$$Q = \frac{U}{Z}[(E\cos\varphi - U)\sin\theta - E\cos\theta\sin\varphi] \tag{22.23}$$

As the phase angle between the inverter bus voltage and PCC is negligible, Eqs. (22.22) and (22.23) can be simplified in the form of Eqs. (22.24) and (22.25) and Table 22.1.

$$P \cong \frac{U}{Z}[(E-U)\cos\theta + E\varphi\sin\theta] \tag{22.24}$$

$$Q \cong \frac{U}{Z}[(E-U)\sin\theta - E\varphi\cos\theta] \tag{22.25}$$

The relation between system impedance and the output active and reactive power of DG, the polar diagram of Figs. 22.6, 22.7 and 22.8 has been derived. The polar radius stands for active and reactive power and the radius is the power angle. It should be noted that only the shaded area is the acceptable in the real power system.

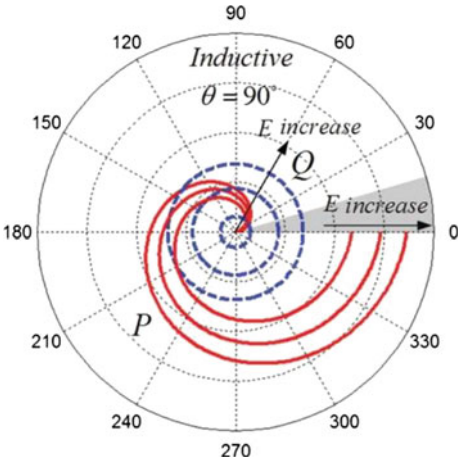

Fig. 22.6 Polar locus of active and reactive power—pure inductive case [18]

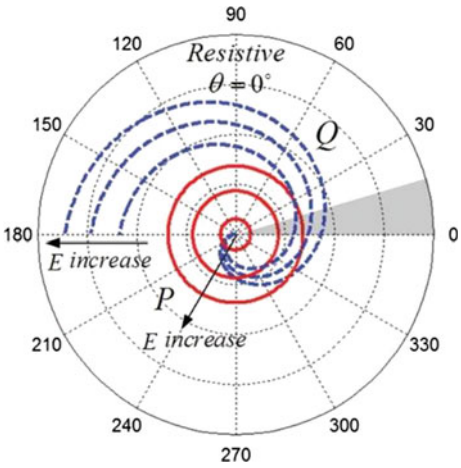

Fig. 22.7 Polar locus of active and reactive power—pure resistive case [18]

22.4.1 Pure Inductive Impedance

The active and reactive power curves have been shown in Fig. 22.6 for the pure inductive impedance. Both of them increase by increasing the inverter bus voltage. The active power is independent of phase angle but the reactive power increases by increasing the power phase angle.

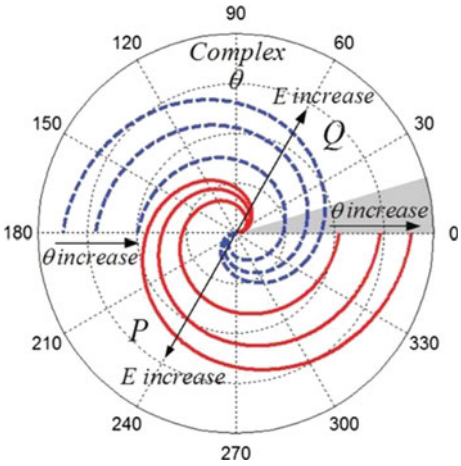

Fig. 22.8 Polar locus of active and reactive power—complex impedance case [18]

22.4.2 Pure Resistive Impedance

As shown in Fig. 22.7, the behavior of active and reactive power is opposite to the pure inductive case. Both active and reactive power increase by increasing the inverter bus voltage. The reactive power is independent of phase angle but the active power increases by increasing the power phase angle.

22.4.3 Complex Impedance

For the complex impedance, both the active and reactive powers increase by increasing the power phase angle. They move in the counter clockwise direction by increasing the power phase angle (Fig. 22.8). The behavior of powers in this case is more complicated than inductive or resistive cases. So designing the controller will be more complicated in this case.

In the case of equal resistance and reactance ($X = R$), the droop controllers can be defined by Eqs. (22.26) and (22.27).

$$\omega = \omega_0 - m_p \cdot (P - Q) \tag{22.26}$$

$$E = E_0 - n_Q \cdot (P + Q) \tag{22.27}$$

In [7], a PQV control method has been proposed to facilitate the simultaneous control of active and reactive power by voltage controlling the voltage of PCC. The proposed controller is presented in (22.28).

$$V = V_{ref} + (n_d \cdot P) + (m_d \cdot Q) \tag{22.28}$$

where, V_{ref} is the reference voltage of PCC, n_d and m_d are the droop coefficients of the active and reactive power. These coefficients are adaptively adjusted by a lookup table based on the PCC voltage.

To improve the dynamic behavior of the system, an advanced droop controller has been proposed in [26] as presented in Eqs. (22.29) and (22.30).

$$\varphi = -m \int_{-\infty}^{t} P d\tau - m_p P - m_d \frac{dP}{dt} \tag{22.29}$$

$$E = E^* - nQ - n_d \frac{dQ}{dt} \tag{22.30}$$

where, n_d is the coefficient of reactive power derivation. m, m_p and m_d are the coefficients of integrator, proportional and derivation of active power, respectively. These coefficients are dynamic and are derived for the small signal studies. Derivative part of the controller is added to the droop control to improve the controller speed. Also, it can reduce the circulating and startup currents in low voltage microgrids [27, 28]. Droop controllers are derived by Eqs. (22.31) and (22.32).

$$\omega = \omega^* + K_p\left(P_i - P_{i,ref}\right) + K_{pd}\frac{dP_i}{dt} \tag{22.31}$$

$$V_i = V_{ref} + K_Q\left(Q_i - Q_{i,ref}\right) + K_{qd}\frac{dQ_i}{dt} \tag{22.32}$$

where, K_{pd} and K_{qd} are adjusted by pole placement method to improve the performance of overall system.

22.5 Angle Droop Control

Power flow of a microgrid can be controlled by adjusting the phase angle of DG bus voltages [29]. Schematic diagram of a DG connected to the microgrid is shown in Fig. 22.9. The injected active and reactive power of DG to the grid has been derived by Eqs. (22.33) and (22.34).

$$p = \frac{V \times V_t \sin(\delta - \delta_t)}{X_f} \tag{22.33}$$

$$q = \frac{V^2 - V \times V_t \cos(\delta - \delta_t)}{X_f} \tag{22.34}$$

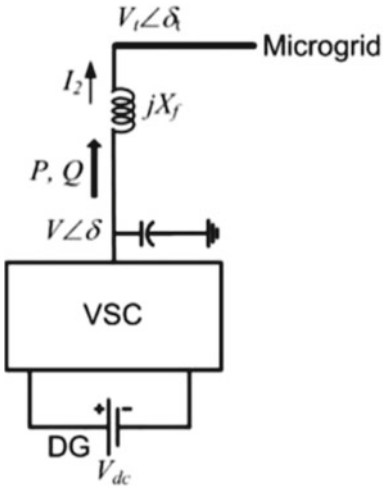

Fig. 22.9 DG connected to a microgrid by VSC [29]

As the phase angle between the output voltage of VSC and the PCC voltage is small, the active power is proportional to the phase angle. So similar to the frequency droop the following controllers can be derived.

$$\delta_i = \delta_{rated} - m_p \cdot P_i \tag{22.35}$$

$$E_i = E_{rated} - n_Q \cdot Q_i \tag{22.36}$$

where, E_{rated} and δ_{rated} are the nominal voltage and phase angle of DG, respectively. n_Q and m_p are the gains of active and reactive power gains, respectively. Phase droop can improve the power flow control of DGs and frequency stability considerably.

22.6 Droop Control Based on Virtual Impedance

The power quality of islanded microgids is highly damaged by nonlinear loads. Adjusting the virtual impedance by the droop controller can improve the impedance matching between DGs and the microgrid [25]. This leads to better dynamic performance of microgrid and reduces the circulating currents between DGs. Moreover, it is useful for harmonic reduction and appropriate power flow [24, 30].

The circuit diagram of two parallel DGs has been shown in Fig. 22.10. Phasor of voltages and impedances are defined as Eqs. (22.37)–(22.40).

$$|VO_1| = |VO_1|e^{j\theta 01} \tag{22.37}$$

$$|VO_2| = |VO_2|e^{j\theta 02} \tag{22.38}$$

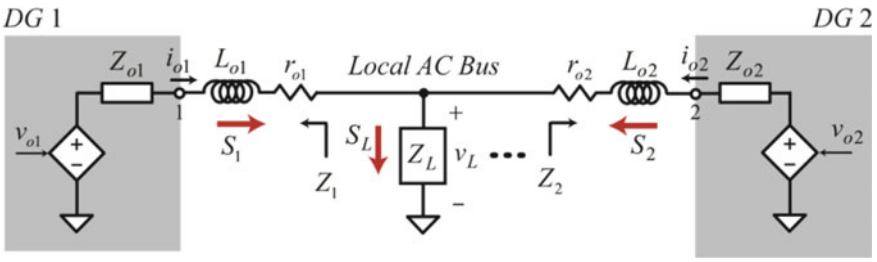

Fig. 22.10 Circuit diagram of connected DGs [30]

$$v_L = |v_L| e^{j\theta_L} \tag{22.39}$$

$$Z_1 = |Z_1| e^{(j<Z_1)} \tag{22.40}$$

Injected power from DG_1 to the AC bus can be derived by Eq. (22.41).

$$S_1 = V_{O1} I_O^* = \frac{|V_{O1}|^2}{Z_1} e^{(j<Z_1)} - \left(\frac{|V_{O1}||V_L|}{|Z_1|}\right) e^{(j<Z_1+\theta_{1L})} \tag{22.41}$$

where,

$$\theta_{1L} = \theta_{o1} - \theta_L \tag{22.42}$$

$$Z_1 = Z_{o1} + \omega_L + L_{01} e^{\frac{\pi}{2}} + r_{o1} \tag{22.43}$$

So, active and reactive powers are derived by Eqs. (22.44) and (22.45).

$$P_1 = \mathrm{Re}\{S_1\} = \left(\frac{|VO_1|^2}{|Z_1|} - \frac{|VO_1||vL|}{|Z_1|}\cos\theta_{1L}\right)\cos < Z_1 + \frac{|VO_1||V_L|}{|Z_1|}\sin\theta_{1L}\sin < Z_1 \tag{22.44}$$

$$Q_1 = \mathrm{Im}\{S_1\} = \left(\frac{|VO_1|^2}{|Z_1|} - \frac{|VO_1||vL|}{|Z_1|}\cos\theta_{1L}\right)\sin < Z_1 + \frac{|VO_1||V_L|}{|Z_1|}\sin\theta_{1L}\cos < Z_1 \tag{22.45}$$

The power transfer from DG1 to DG2 can be derived by Eqs. (22.46) and (22.47).

$$P_{12} = \left(\frac{|VO_1|^2}{|Z_{12}|} - \frac{|VO_1||VO_2|}{|Z_{12}|}\cos\theta_{12}\right)\cos < Z_{12}$$

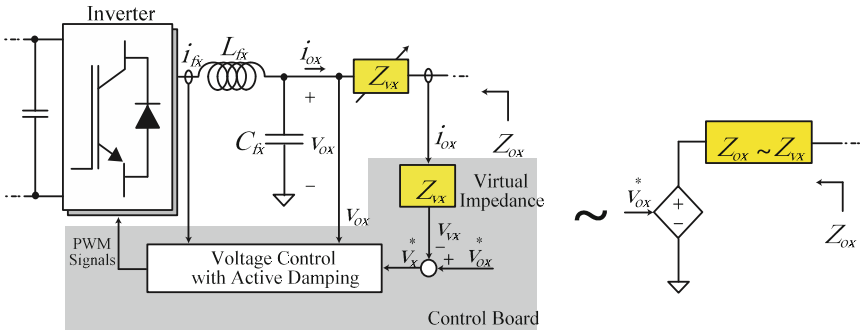

Fig. 22.11 Virtual impedance of DG [30]

$$+ \frac{|VO_1||VO_2|}{|Z_{12}|} \sin\theta_{12} \sin < Z_{12} \tag{22.46}$$

$$Q_{12} = \left(\frac{|VO_1|^2}{|Z_{12}|} - \frac{|VO_1||VO_2|}{|Z_{12}|} \cos\theta_{12} \right) \sin < Z_{12}$$
$$+ \frac{|VO_1||VO_2|}{|Z_{12}|} \sin\theta_{12} \cos < Z_{12} \tag{22.47}$$

Power transfer between DGs is not acceptable, because it leads to power oscillations and power losses. The internal impedance values of DG1 and DG2, Z_{o1} and Z_{o2} in Fig. 22.10, can be adjusted by control mechanism called virtual impedance.

It can be reduced by adjusting the virtual impedances of DGs. virtual impedance is the internal impedance of DGs that can be adjusted by the switching control of their inverter, as shown in Fig. 22.11.

The virtual impedance (Z_{vx}) can be derived by Eq. (22.48).

$$V_x^* = V_{ox}^* - V_{vx} = V_{ox}^* - Z_{vx} i_{ox} \tag{22.48}$$

As Z_{vx} is approximately equal to Z_{ox}, it can be presented in the form of Eq. (22.49) in the Laplace domain.

$$Z_{vx}(S) = SL_{vx} \tag{22.49}$$

where, S is the Laplace operator and L_{vx} is the inductance of the virtual impedance. So the voltage droop is defined by Eq. (22.50).

$$V_{vx}(S) = SL_{vx} i_{ox} \tag{22.50}$$

For the real implementation of Eq. (22.50), a real pole should be added to the differentiator as a low-pass filter, as shown in Eq. (22.51).

$$V_{vx}(S) = L_{vx}\frac{\omega_v s}{s+\omega_v} i_{ox} \tag{22.51}$$

where, ω_v is the cut-off frequency of the low-pass filter [30].

22.7 Droop Control Based on Virtual Frame

This control method is based on the definition of a virtual reference frame for voltage and frequency to decouple the active and reactive control in microgrid. In the pure inductive microgrids, active power can be controlled by the frequency (or phase angle) of DG inverter and the reactive power can be controlled by the output voltage of the inverter. These relations have been derived by Eqs. (22.52)–(22.59) based on the circuit diagram of Fig. 22.12 [31].

$$\begin{aligned} S &= P + jQU_1 \\ I^* &= U_1\left(\frac{U_1 - U_2}{Z}\right)^* \\ &= U_1\left(\frac{U_1 - U_2 e^{j\delta}}{Z e^{-j\theta}}\right)^* \\ &= \frac{U_1^2}{Z}e^{j\theta} - \frac{U_1 U_2}{Z}e^{j(\theta+\delta)} \end{aligned} \tag{22.52}$$

$$P = \frac{U_1^2}{Z}\cos\theta - \frac{U_1 U_2}{Z}\cos(\theta+\delta) \tag{22.53}$$

$$Q = \frac{U_1^2}{Z}\sin\theta - \frac{U_1 U_2}{Z}\sin(\theta+\delta) \tag{22.54}$$

where,

$$Ze^{j\theta} = R + jX \tag{22.55}$$

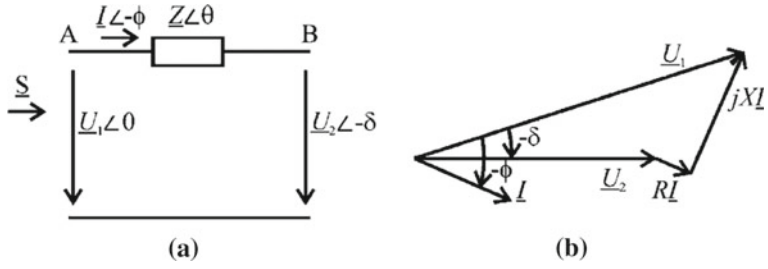

Fig. 22.12 Circuit and phasor diagram to calculate power transfer [31]

Substituting Z in the previous equations leads to Eqs. (22.56)–(22.59).

$$P = \frac{U_1^2}{R^2 + X^2}[R(U_1 - U_2\cos\delta) + XU_2\sin(\delta)] \tag{22.56}$$

$$P = \frac{U_1^2}{R^2 + X^2}[R(U_1 - U_2\cos\delta) + XU_2\sin(\delta)] \tag{22.57}$$

$$U_2\sin(\delta) = \frac{XP - RQ}{U_1} \tag{22.58}$$

$$U_1 - U_2\cos\delta = \frac{RP + XQ}{U_1} \tag{22.59}$$

For the transmission lines with $X \gg R$, R can be neglected and if δ is considerably small (near zero), then, $\sin(\delta) = \delta$ and $\cos(\delta) = 1$. With these assumptions, Eqs. (22.58) and (22.59) can be rewritten as follows.

$$\delta \cong \frac{XP}{U_1U_2} \tag{22.60}$$

$$U_1 - U_2 \cong \frac{XQ}{U_1} \tag{22.61}$$

It can be seen that phase angle is proportional to the active power and the voltage difference is dependent to the reactive power. It means that phase angle and inverter voltage can be controlled by active and reactive power, respectively. It should be noted that the proposed droop control is appropriate when the line resistance is considerably smaller than the line inductance. The linear transformation matrix of Eq. (22.62) can be used to overcome this shortcoming of droop control.

$$\begin{bmatrix} P' \\ Q' \end{bmatrix} = T\begin{bmatrix} P \\ Q \end{bmatrix} = \begin{bmatrix} \sin\theta & -\cos\theta \\ \cos\theta & \sin\theta \end{bmatrix}\begin{bmatrix} P \\ Q \end{bmatrix} \tag{22.62}$$

Applying this transformation to Eqs. (22.56) and (22.57) results in:

$$\sin\delta = \frac{ZP'}{U_1U_2} \tag{22.63}$$

$$U_1 - U_2\cos\delta = \frac{ZQ'}{U_1} \tag{22.64}$$

For the small phase angle (δ), it is proportional to the transformed active power (P') and the voltage difference is dependent to the transformed reactive power (Q'). So, these equations can be used to define the frequency and voltage droops, as shown in Fig. 22.13.

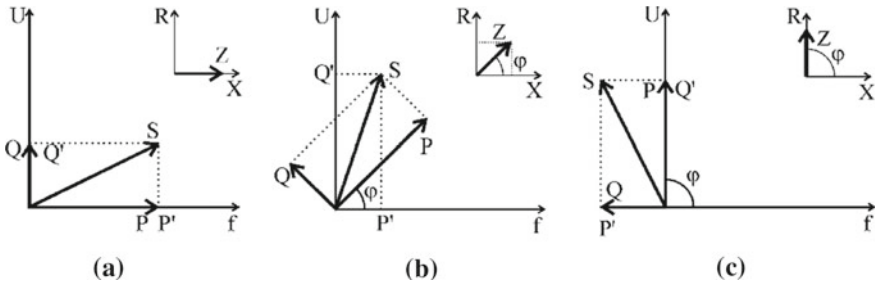

Fig. 22.13 Effect of transformed powers on frequency and voltage for different *R*/*X* [31]

For the pure inductive lines:

$$P' \approx P \tag{22.65}$$

$$Q' \approx Q \tag{22.66}$$

For the pure resistive lines, Eqs. (22.67) and (22.68) can be used.

$$P' \approx -Q \tag{22.67}$$

$$Q' \approx P \tag{22.68}$$

So the droop controller can be derived by Eqs. (22.69) and (22.70).

$$f - f_0 = -k_p\left(P' - P'_0\right) = -k_p\frac{X}{Z}(P - P_0) + k_p\frac{R}{Z}(Q - Q_0) \tag{22.69}$$

$$U_1 - U_0 = -k_q\left(Q' - Q'_0\right) = -k_q\frac{R}{Z}(P - P_0) - q\frac{R}{Z}(Q - Q_0) \tag{22.70}$$

22.8 Adaptive Voltage Droop Control

VSCs with the conventional voltage droop controller allocate reactive power between DGs of the microgrid. The accuracy of power flow depends on the parameters of the system and controllers [32]. To study the dependency, a simple microgrid is considered in Fig. 22.14 [32].

The relation between bus voltage and DG voltage is derived by Eq. (22.71).

$$V_i\angle\alpha_i = E_i\angle\delta_i - Z_iI_i\angle - \theta_i, \quad i = 1, 2 \tag{22.71}$$

As stated before, the conventional droop defines by Eqs. (22.72) and (22.73).

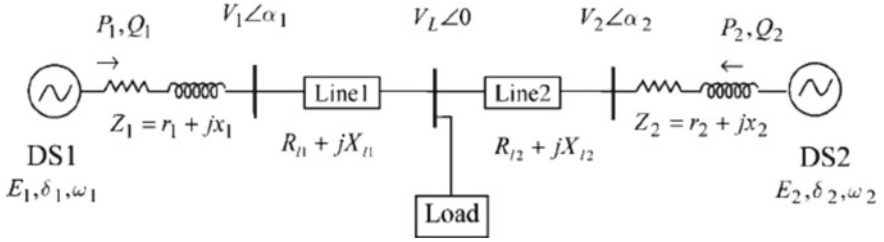

Fig. 22.14 Circuit diagram of a simple microgrid [32]

$$\omega = \omega_0 - m_p P \tag{22.72}$$

$$E = E_0 - n_q Q \tag{22.73}$$

Substituting Eqs. (22.72) and (22.73) by Eq. (22.71) leads to the following equation [33].

$$V_i\angle\alpha_i = \left(E_0 - n_{qi}Q_i\right)\angle\delta_i - Z_i I_i\angle\theta - \theta_i \tag{22.74}$$

By defining $Z_i = r_i + jX_i$, $\gamma_i = \alpha_i + \theta_i$ and assuming $\delta_i - \alpha_i \cong 0$, V_i can be derived by Eq. (22.75).

$$V_i = E_0 - n_{qi}Q_i - r_i I_i \cos\gamma_i - x_i I_i \sin\gamma_i \tag{22.75}$$

Based on the active and reactive powers, V_i can be written by Eq. (22.76) [33].

$$V_i = E_0 - n_{qi}Q_i - \frac{r_i P_i}{E_i} - \frac{x_i Q_i}{E_i} \tag{22.76}$$

The voltage magnitude of ith bus depends on the control parameters n_{qi} and E_o, active and reactive power of VSC and the connection impedance. To reduce the effect of these parameters, the voltage drop on the connection impedance is added to the voltage reference of the VSC. So the conventional E-Q droop modifies by Eqs. (22.77) and (22.78).

$$E_i = E_0 + \left(\frac{r_i P_i + x_i Q_i}{E_0}\right) - n_{q_i} Q_i \tag{22.77}$$

$$D_i(P_i \cdot Q_i) = D_{Qi} + m_{Qi}Q_i^2 + m_{pi}P_i^2 \tag{22.78}$$

where, D_i, m_{Qi} and m_{Pi} are droop coefficients. Although this method reduces the effect of active control, high loading and different parameters of microgrid, the need to know some parameters of the system is its weakness.

The reference of VSC voltage can be adaptively adjusted based on the active and reactive powers by the droop control of Eq. (22.79).

$$E_i = \left(E_0 + \frac{r_i P_i}{E_{0i}}\right) - \left(n_{qi} - \frac{X_i}{E_0}\right) Q_i \tag{22.79}$$

The first part of E_i varies from E_o (no load condition) to $E_0 + r_i P_i / E_0$ and the second part (voltage droop coefficient) varies from n_{qi} to $n_{qi} - x_i / E_0$. It means that the slope of droop controller varies in different operating conditions. This controller removes the effect of the connection impedance between VSC and PCC [32].

22.9 Simulation Results

Figure 22.15 shows a typical microgrid including two distributed generations (DG1 and DG2) to assess the conventional droop, virtual impedance and coupling in a medium voltage distribution network. The microgrid is a three-wire distribution network, operated in the islanded mode. It is assumed that the load 1 is fixed and load 2 is connected to the microgrid at $t = 2.5$ s. The general information of the microgrid and its components are depicted in Table 22.2. The active and reactive sharing of DGs are illustrated in Figs. 22.16, 22.17, 22.18, 22.19, 22.20 and 22.21.

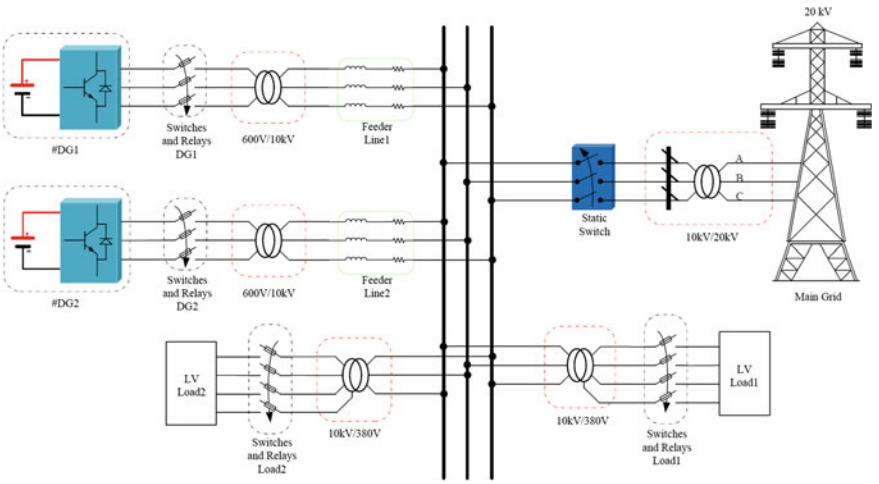

Fig. 22.15 Configuration of a typical MV microgrid

Table 22.2 General information of the MV microgrid

General information			
Parameter		Value	
Nominal voltage (rms, L-L)		10 kV	
Allowable voltage range (%)		±5	
Frequency		60 Hz	
Allowable frequency range (%)		±1	
Feeder and branches			
Voltage level	*R* (Ω/km)	*X* (Ω/km)	*R*/*X* (p.u.)
MV (10 kV)	0.161	0.19	0.85
Feeder DG1: 2 km, Feeder DG2: 6 km			
DG units			
DG No.	Technology		Capacity
DG1	Fuel cell		1.5 MW
DG2	Photovoltaic with battery		1.5 MW
Load			
Load No.	Type	Nominal active power	Power factor (cosφ)
Load 1	3×ϕ	100 kW	0.85 lag
Load 2	3×ϕ	100 kW	0.85 lag

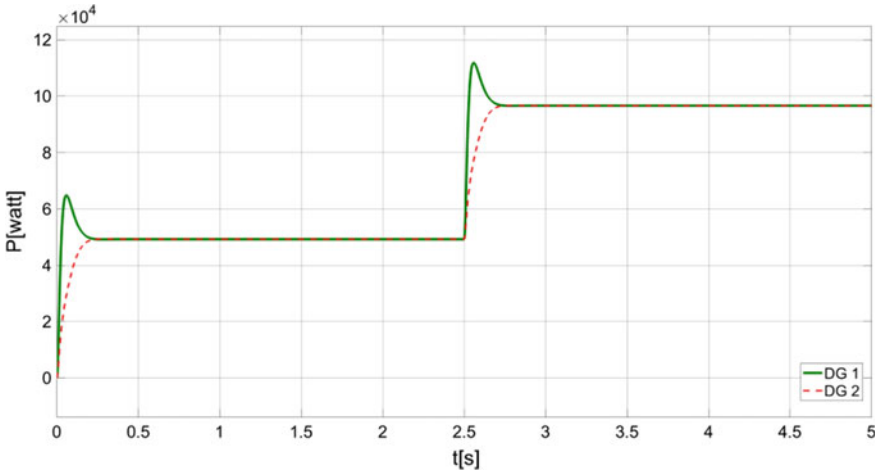

Fig. 22.16 Active power sharing with conventional droop method

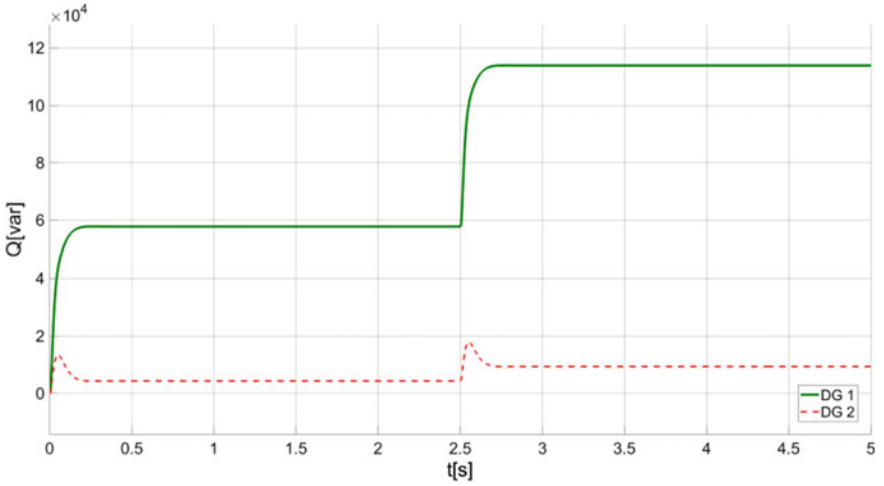

Fig. 22.17 Reactive power sharing with conventional droop method

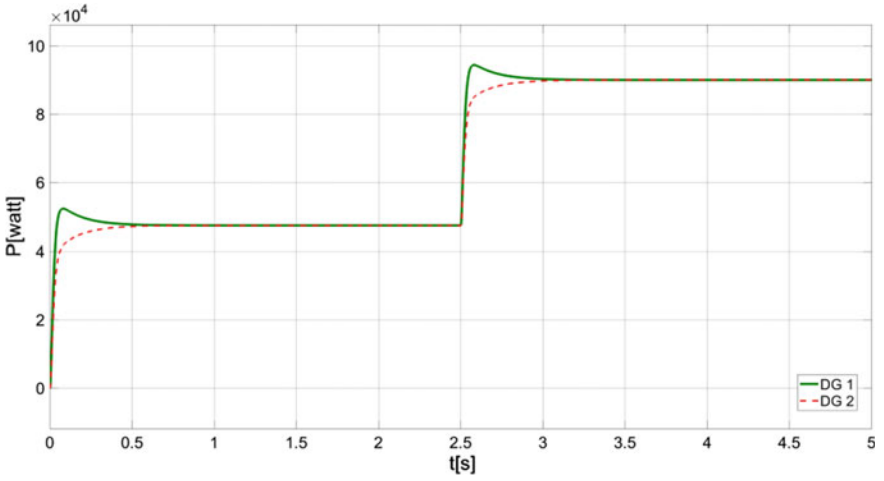

Fig. 22.18 Active power sharing among DG units by applying virtual impedance in the conventional droop

22.9.1 Conventional Droop

Figure 22.16 shows that due to the interdependency between active power and frequency in the conventional droop, DG units with equal capacity have to inject same active power. As expected, the sharing of reactive power through conventional droop

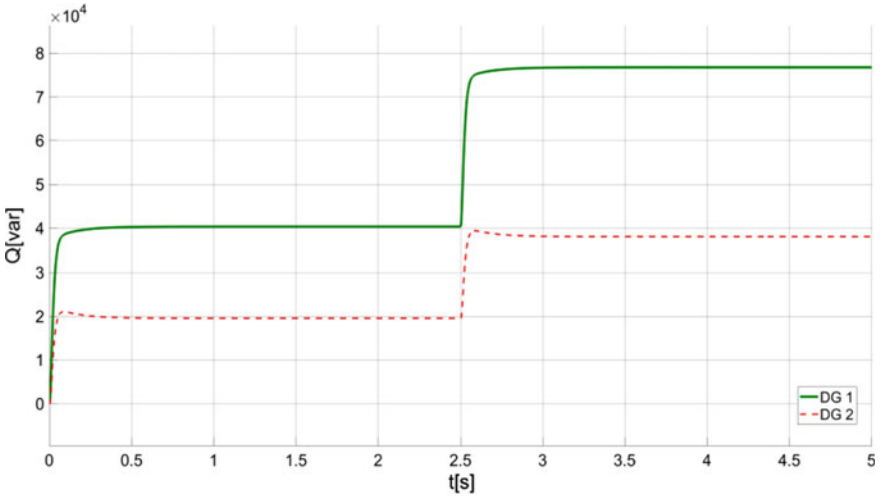

Fig. 22.19 Reactive power sharing among DG units by applying virtual impedance in the conventional droop

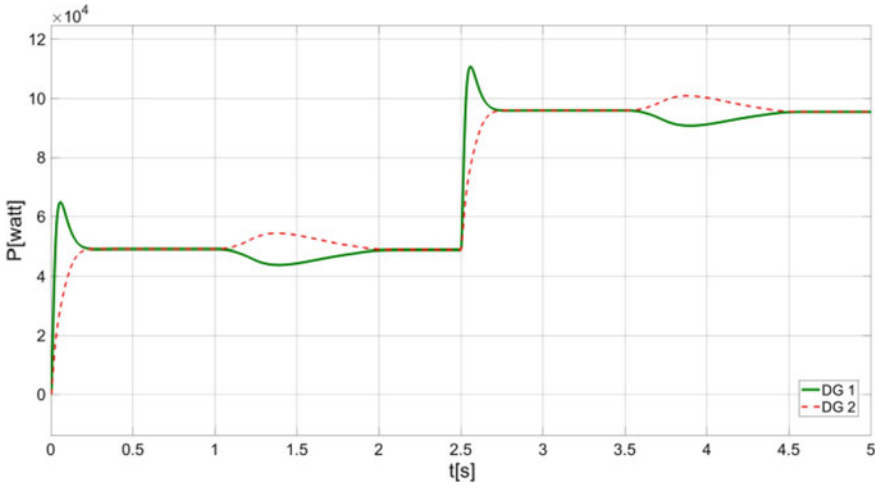

Fig. 22.20 The effect of decentralized reactive power sharing on conventional active power sharing

is dependent on the feeder impedance DG and local load. Thus, as shown in Fig. 22.17, the higher load current, the higher feeder voltage drops and the greater lack of reactive power sharing among DG units.

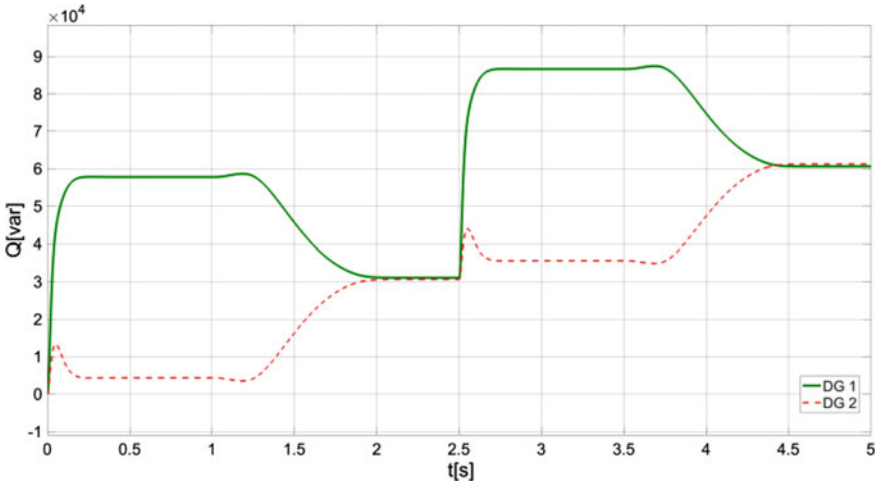

Fig. 22.21 The effect of decentralized reactive power sharing on conventional reactive power sharing

22.9.2 Effects of the Virtual Impedance on the Conventional Droop

By applying appropriate virtual impedance, it is possible to get better results in comparison with the conventional droop. Figures 22.18 and 22.19 shows the result of active and reactive power sharing among DG units respectively. It is observed that difference between the reactive power sharing in Fig. 22.17 has been reduced in Fig. 22.19.

22.9.3 Effects of the Reactive Power Compensation on the Conventional Droop

This approach has an appropriate active and reactive power sharing for the conventional droop. Figures 22.20 and 22.21 show the result of active and reactive power sharing between DG1 and DG2 respectively. It is observed that after applying the decentralized reactive power sharing, the active and reactive power of both DGs follow the same value and an equal power sharing obtain.

22.9.4 *Reverse Droop—LV Microgrid*

Figure 22.22 shows a typical microgrid including five (DGs) to analysis the reverse droop in low voltage (LV) distribution network (380 V). The microgrid is a four-wire distribution network, which is operated in the islanded mode. The wiring is based on underground cables and it is assumed that all loads are balanced three-phase. DG units are dispatchable and power electronic interface based with total capacity equal to 140 kW. Each DG has an inverter and a local controller consists of reverse droop, inner voltage and current loop. A LC filter has been set in the output of the inverter to eliminate switching harmonics. Table 22.3 presents the general information of the microgrid shown in Fig. 22.22. It is assumed that load 1 is fixed and connected to the microgrid, load 2 is disconnected from the microgrid at $t = 0.5$ s, while load 3 is connected at $t = 1$ s.

In the reverse droop, the reactive power and frequency has interdependency and therefore the reactive power of DG units with equal capacity follow a same value after any change. Figure 22.23 shows the reactive power sharing among DG units

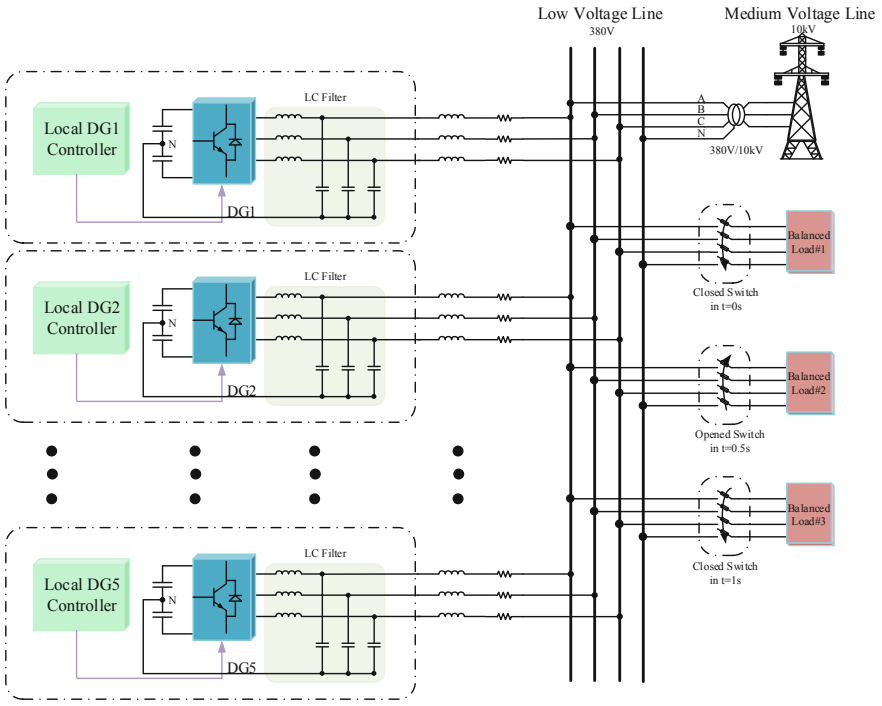

Fig. 22.22 Configuration of a typical MV microgrid

Table 22.3 General information of LV microgrid

General information			
Parameter		Value	
Nominal voltage (rms, L-L)		380 V	
Allowable voltage range (%)		±5	
Frequency		60 Hz	
Allowable frequency range (%)		±1	
Feeder and branches			
Voltage level	*R* (Ω/km)	*X* (Ω/km)	*R*/*X* (p.u.)
LV (380 V)	0.642	0.083	7.7
Feeder DG1: 2 km, Feeder DG2: 6 km, Feeder DG3: 3 km, Feeder DG 4: 9 km, Feeder DG5: 2.5 km			
DG units			
DG No.	Technology		Capacity
DG1	Fuel cell		35 kW
DG2	Photovoltaic with battery		35 kW
DG3	Photovoltaic with battery		35 kW
DG4	Photovoltaic with battery		17.5 kW
DG5	Fuel cell		17.5 kW
Load			
Load No.	Type	Nominal active power	Power factor (cosφ)
Load 1	3×ϕ	10 kW	0.85 lag
Load 2	3×ϕ	10 kW	0.85 lag
Load 3	3×ϕ	20 kW	0.85 lag

through reverse droop. It is observed that DG 1, 2 and 3 with equal capacity has the same reactive power generation. Similarly, DG 4 and 5 with half capacity of the others proportionally participate in reactive power sharing. Reactive power sharing is performed appropriately after any change in the microgrid at 0.5 and 1 s. None of DG units injects equal active power into the microgrid due to the different impedance between DGs and loads. Figure 22.24 shows the difference between values of active power generation which increases by increasing the load current. The effects of load change on the frequency of the microgrid are shown in Fig. 22.25.

22.10 Conclusion

Each of the mentioned droop controllers has some benefits and shortcomings. The common benefits of droop controllers are Local implementation, no need to communication systems, easy expansion, acceptable reliability and low investment cost. Fre-

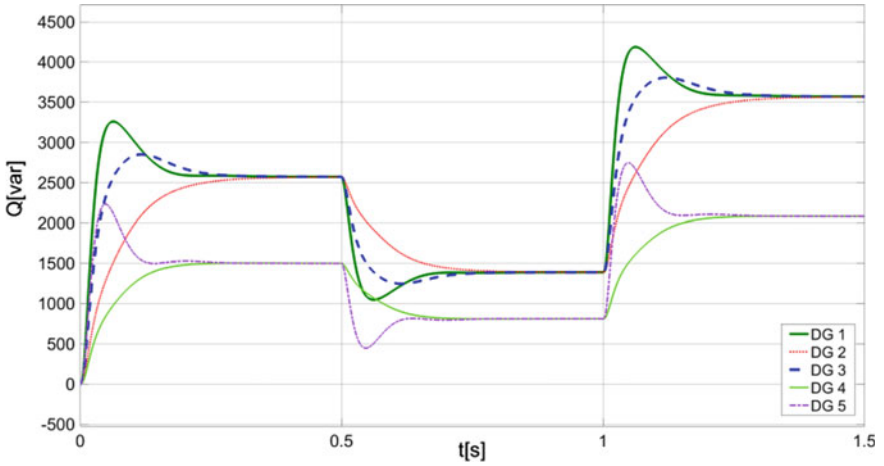

Fig. 22.23 Reactive power sharing among DG units based on reverse droop

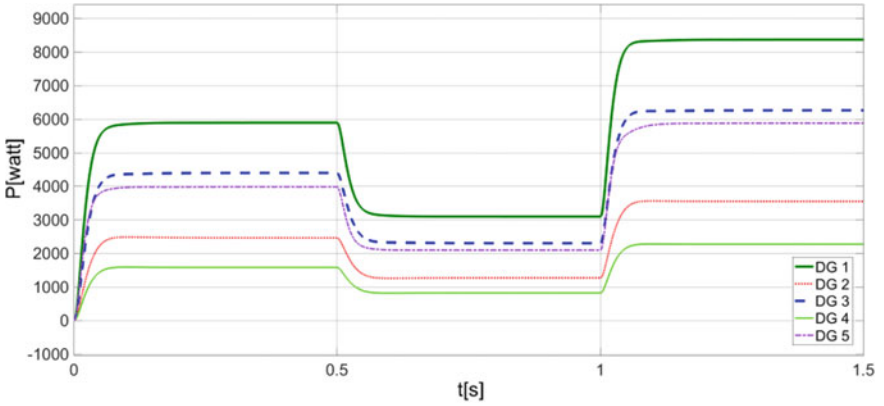

Fig. 22.24 Active power sharing among DG units based on reverse droop

quency deviation, slow dynamic response and circulating current are some shortcomings of droop controllers. Improving the performance of droop controllers, improves the performance of the microgrids considerably. Some advanced methods like multi agent systems and fractional order controllers are good candidates to modify droop controllers.

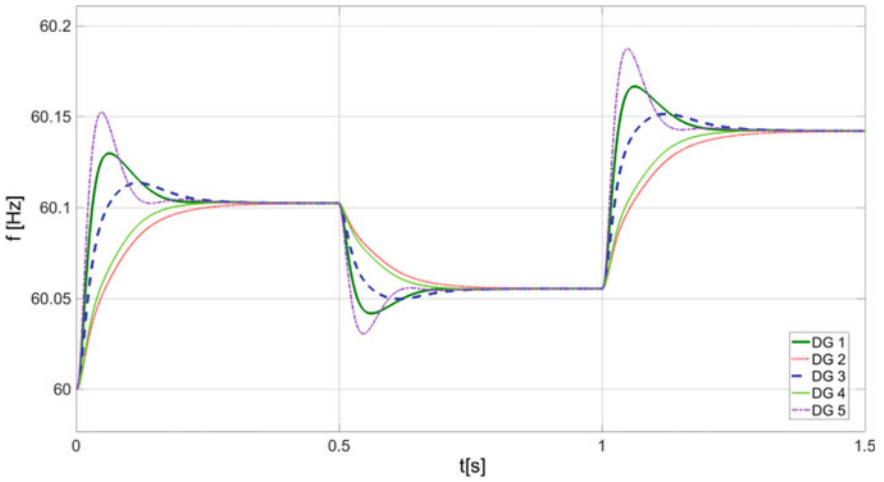

Fig. 22.25 Load change effects on the frequency of the microgrid

References

1. M.C. Chandrokar, D.M. Divan, B. Banerjee, Control of distributed UPS systems, in *Proceedings of 1994 Power Electronics Specialist Conference—PESC'94*, Taipei, Taiwan, vol. 1, pp. 197–204 (1994)
2. M.C. Chandorkar, D.M. Divan, R. Adapa, Control of parallel connected inverters in standalone AC supply systems. IEEE Trans. Ind. Appl. **29**(1), 136–143 (1993)
3. L. Lu, C. Chu, Consensus-based droop control synthesis for multiple DICs in isolated microgrids, in *IEEE Power & Energy Society General Meeting*, Denver, CO, pp. 1–10 (2015)
4. J. He, Y.W. Li, An enhanced microgrid load demand sharing strategy. IEEE Trans. Power Electron. **27**(9), 3984–3995 (2012)
5. A. Tuladhar, H. Jin, T. Unger, K. Mauch, Parallel operation of single phase inverter modules with no control interconnections, in *Proceedings of APEC 97—Applied Power Electronics Conference*, Atlanta, GA, USA, vol. 1, pp. 94–100 (1997)
6. A. Tuladhar, H. Jin, T. Unger, K. Mauch, Control of parallel inverters in distributed AC power systems with consideration of line impedance effect. IEEE Trans. Ind. Appl. **36**(1), 131–138 (2000)
7. J.C. Vasquez, J.M. Guerrero, A. Luna, P. Rodriguez, R. Teodorescu, Adaptive droop control applied to voltage-source inverters operating in grid-connected and islanded modes. IEEE Trans. Industr. Electron. **56**(10), 4088–4096 (2009)
8. Y.W. Li, C. Kao, An accurate power control strategy for power-electronics-interfaced distributed generation units operating in a low-voltage multibus microgrid. IEEE Trans. Power Electron. **24**(12), 2977–2988 (2009)
9. M.A. Mahmud, M.J. Hossain, H.R. Pota, A.M.T. Oo, Robust nonlinear distributed controller design for active and reactive power sharing in islanded microgrids. IEEE Trans. Energy Convers. **29**(4), 893–903 (2014)
10. B. John, A. Ghosh, F. Zare, Load sharing in medium voltage islanded microgrids with advanced angle droop control. IEEE Trans. Smart Grid **9**(6), 6461–6469 (2018)
11. D. Choi, J. Park, S.H. Lee, Virtual multi-slack droop control of stand-alone microgrid with high renewable penetration based on power sensitivity analysis. IEEE Trans. Power Syst. **33**(3), 3408–3417 (2018)

12. S. Peyghami, H. Mokhtari, P.C. Loh, P. Davari, F. Blaabjerg, Distributed primary and secondary power sharing in a droop-controlled LVDC microgrid with merged AC and DC characteristics. IEEE Trans. Smart Grid **9**(3), 2284–2294 (2018)
13. F. Cingoz, A. Elrayyah, Y. Sozer, Optimized settings of droop parameters using stochastic load modeling for effective DC microgrids operation. IEEE Trans. Ind. Appl. **53**(2), 1358–1371 (2017)
14. Q. Peng, T. Liu, S. Wang, Y. Qiu, X. Li, B. Li, Determination of droop control coefficient of multi-terminal VSC-HVDC with system stability consideration. IET Renew. Power Gener. **12**(13), 1508–1515 (2018)
15. D. Shanxu, M. Yu, X. Jian, K. Yong, C. Jian, Parallel operation control technique of voltage source inverters in UPS, in *IEEE International Conference on Power Electronics and Drive Systems. PEDS'99*, Hong Kong, vol. 2, pp. 883–887 (1992)
16. K. Siri, C.Q. Lee, T. Wu, Current distribution control for parallel connected converters, II. IEEE Trans. Aerosp. Electron. Syst. **28**(3), 841–851 (1992)
17. J.F. Chen, C.L. Chu, Combination voltage-controlled and current-controlled PWM inverters for UPS parallel operation. IEEE Trans. Power Electron. **10**(5), 547–558 (1995)
18. W. Yao, M. Chen, J. Matas, J.M. Guerrero, Z. Qian, Design and analysis of the droop control method for parallel inverters considering the impact of the complex impedance on the power sharing. IEEE Trans. Industr. Electron. **58**(2), 576–588 (2011)
19. Y. Pei, G. Jiang, X. Yang, Z. Wang, Auto-master-slave control technique of parallel inverters in distributed AC power systems and UPS, in *IEEE 35th Annual Power Electronics Specialists Conference*, Aachen, Germany, vol. 3, pp. 2050–2053 (2004)
20. J. Tan, H. Lin, J. Zhang, J. Ying, A novel load sharing control technique for paralleled inverters, in *IEEE 34th Annual Conference on Power Electronics Specialist (PESC '03)*, Acapulco, Mexico, vol. 3, pp. 1432–1437 (2003)
21. U.B. Tayab, M.A.B. Roslan, L.J. Hwai, M. Kashif, A review of droop control techniques for microgrid. Renew. Sustain. Energy Rev. **76**, 717–727 (2017)
22. X. Hou, Y. Sun, W. Yuan, H. Han, C. Zhong, J.M. Guerrero, Conventional P-ω/QV droop control in highly resistive line of low-voltage converter-based ac microgrid. Energies **9**(11), 943 (2016)
23. M. Kosari, S.H. Hosseinian, Decentralized reactive power sharing and frequency restoration in islanded microgrid. IEEE Trans. Power Syst. **32**(4), 2901–2912 (2017)
24. J.M. Guerrero, L. Garcia de Vicuna, J. Matas, M. Castilla, J. Miret, Output impedance design of parallel-connected UPS inverters with wireless load-sharing control. IEEE Trans. Industr. Electron. **52**(4), 1126–1135 (2005)
25. H. Han, X. Hou, J. Yang, J. Wu, M. Su, J.M. Guerrero, Review of power sharing control strategies for islanding operation of AC microgrids. IEEE Trans. Smart Grid **7**(1), 200–215 (2016)
26. J.M. Guerrero, L.G. de Vicuna, J. Matas, M. Castilla, J. Miret, A wireless controller to enhance dynamic performance of parallel inverters in distributed generation systems. IEEE Trans. Power Electron. **19**(5), 1205–1213 (2004)
27. G. Yajuan, W. Weiyang, G. Xiaoqiang, G. Herong, An improved droop controller for grid-connected voltage source inverter in microgrid, in *The 2nd International Symposium on Power Electronics for Distributed Generation Systems*, Hefei, pp. 823–828 (2010)
28. Y.A.I. Mohamed, E.F. El Saadany, Adaptive decentralized droop controller to preserve power sharing stability of paralleled inverters in distributed generation microgrids. IEEE Trans. Power Electron. **23**(6), 2806–2816 (2008)
29. R. Majumder, A. Ghosh, G. Ledwich, F. Zare, Angle droop versus frequency droop in a voltage source converter based autonomous microgrid, in *IEEE Power & Energy Society General Meeting*, Calgary, AB, pp. 1–8 (2009)
30. Y.O. Choi, J. Kim, Output impedance control method of inverter-based distributed generators for autonomous microgrid. Energies **10**(7), 904 (2017)
31. K. de Brabandere, B. Bolsens, J. Van den Keybus, A. Woyte, J. Driesen, R. Belmans, A voltage and frequency droop control method for parallel inverters. IEEE Trans. Power Electron. **22**(4), 1107–1115 (2007)

32. E. Rokrok, M.E.H. Golshan, Adaptive voltage droop scheme for voltage source converters in an islanded multibus microgrid. IET Gener. Transm. Distrib. **4**(5), 562–578 (2010)
33. A. Bidram, A. Davoudi, Hierarchical structure of microgrids control system. IEEE Trans. Smart Grid **3**(4), 1963–1976 (2012)

Chapter 23
Fuzzy PID Control of Microgrids

Hossein Shayeghi and Abdollah Younesi

Abstract The purpose of this chapter is design and application of intelligent methods based on the fuzzy logic (FL) type PID controller for adaptive controlling of the microgrids. The traditional structure of the power systems is being changed continuously due to environmental limitations and depreciated infrastructures. The creation of distinct electrical boundaries between different areas of the power system with the ability to connect/disconnect and locating distributed generation (DG) resources near the load points has transformed the face of power systems. In this situation, power systems can be considered as a set of multiple microgrids that work in conjunction with each other in a coordinated manner. Although, in this case, the power system's efficiency is increased, but its control is faced with bigger challenges. Coordination between microgrids, resource scheduling in the islanding and main utility-connected modes, exchanging power between different microgrids, and etc., are the reasons that necessitate the use of adaptive control methods for controlling such power systems. In this chapter, adaptive controlling mechanisms based on FL based PID control will be discussed in detail. FL based controllers are expanding due to their simple structure, easy implementation and adaptive behavior. This kind of controllers has a superb performance in controlling large-scale complex systems with high degree of nonlinearities by using their membership functions and fuzzy rules. Here, different control strategies based on Fuzzy PID type controller will be described and discussed for controlling microgrids.

Keywords Microgrid · Fuzzy logic controller · Microgrid frequency control · Microgrid voltage control

H. Shayeghi (✉) · A. Younesi
Department of Electrical Engineering, University of Mohaghegh Ardabili, Ardabil, Iran
e-mail: hshayeghi@gmail.com

A. Younesi
e-mail: younesi.abdollah@gmail.com

N. Mahdavi Tabatabaei et al. (eds.), *Microgrid Architectures, Control and Protection Methods*, Power Systems,
https://doi.org/10.1007/978-3-030-23723-3_23

23.1 Introduction

Integration of distributed generation resources in a synergy manner makes the μGs an effective solution to improve reliability and resilience of the distribution systems [1]. However, the increasing development of RER with uncertain outputs and increasing the number of μGs makes the operation and control of them a major challenge [2]. The adjustment of the μG voltage and frequency with the use of classical controllers in such situation, is a challenging work and requires new and appropriate control strategies [3].

In recent decades, FL based controllers have been markedly developed and their ability to be used in various industrial applications has been proven [4]. The performance of these controllers is influenced by fuzzy rules and control coefficients that determine their degree of controllability [5]. Compared to other adaptive control methods such as neural networks, FL controllers have a special place in the industry and have been used in a variety of applications such as electric machine ripple minimization [5], energy management system in μG [6], automatic voltage regulator system [7], load frequency control [8] and a major area of the industry.

In this chapter, an adaptive control mechanism based on the FL is considered for simultaneous stabilizing the oscillations of frequency and voltage in an islanded μG. The proposed FL controller is a parallel fuzzy type PID controller which is called FP + FI + FD [9]. The FP + FI + FD controller integrated the characteristics of FL based controllers like robustness and adaptive behavior along with PID controller characteristics such as high speed and an acceptable precision. Thanks to this property, the FP + FI + FD is a controller with an adequate dynamic performance for controlling different kind of industrial processes even with a high degree of nonlinearities and parameters uncertainty. On the other hand, optimal tuning of the FP + FI + FD controller parameters is a challenging effort which may be impossible with traditional methods like Zigler-Nichols and needs more efficient and fast mechanisms. Thus, Salp swarm algorithm (SSA) [10] is used for the optimal configuration of FP + FI + FD controller in order to obtain it's best performance. The SSA is a particle-based optimization algorithm which models the motion of the Salp individuals mathematically into their target point which is food location. A part of the electric distribution system of Denmark is used for evaluating the performance of the proposed control methods. The test system is an islanded μG which is consist of 14 buses, nine line with six generation units (one combined heat and power (CHP) with three gas turbines and three wind turbine power stations), and ten loads. The considered μG will be modelled using MATLAB/Simulink software. Then the structure and the optimal designing procedure of the FL based voltage and frequency controllers will be described in detail. Simulation results prove that the proposed FP + FI + FD control method has a superb dynamic performance compared to other control mechanisms.

23.2 Different Control Strategies

The main purpose of this chapter is to evaluate the dynamic efficiency of the FL based controllers compared to classical PID controller. Thus, three control methods are considered for voltage and frequency control of an islanded μG, i.e. PID, fuzzy PID, and FP + FI + FD controllers.

23.2.1 Conventional PID Controller

The proportional integral derivative controller is a well-known controller with a simple structure and acceptable dynamic performance for controlling a major number of industrial processes [11]. The block diagram of a PID controller is shown in Fig. 23.1 which is consist of three links, proportional with K_p control gain, integral with K_i control gain, and derivative with K_d control gain. In order to reach the best control performance of the PID controller, three K_p, K_i, and K_d gains must be tuned optimally.

23.2.2 Fuzzy Logic Controller

In line with the main purpose of this chapter, which is to confirm the ability of FL in the μG control, two type of FL controllers are considered to be used for stabilizing voltage and frequency oscillations in a μG, which are described in more detail in following.

23.2.2.1 Fuzzy PID Controller

The structure of fuzzy PID (FPID) is shown in Fig. 23.2. This controller has a simple structure including an integrator, a derivative, five control gains and fuzzy interface [7]. The relationship between the input and output signals of fuzzy system is defined based on the fuzzy membership function and rules. The membership function and fuzzy rules of the FPID controller are shown in Fig. 23.3 and Table 23.1, respectively.

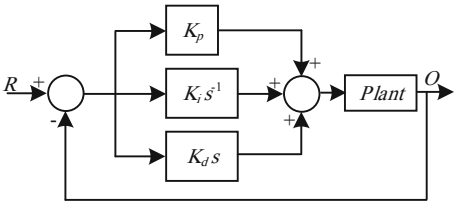

Fig. 23.1 Block diagram of PID controller

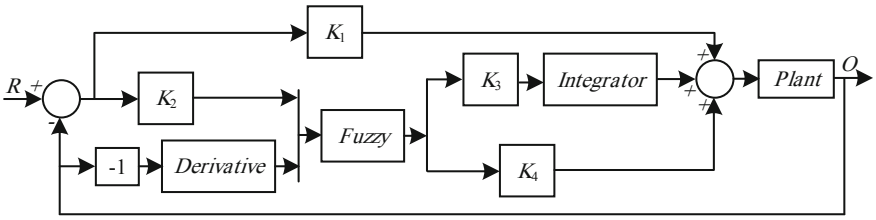

Fig. 23.2 Structure of FPID controller

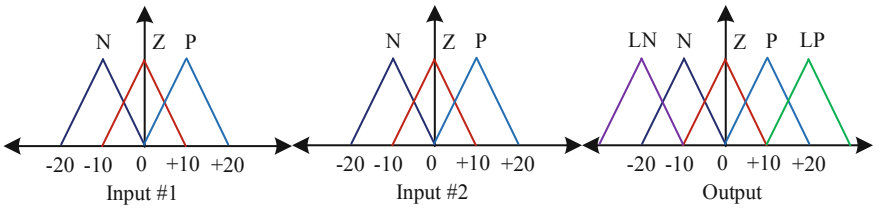

Fig. 23.3 The FPID controller's input/output MFs

Table 23.1 Fuzzy rules of the fuzzy interface system of FPID controller

		Input #2		
		N	Z	P
Input #1	N	LN	N	Z
	Z	N	Z	P
	P	Z	P	LP

Each input has three membership functions of trimf type and the output has five membership functions of type trimf that are linked by nine fuzzy rules which are obtained based on the engineering knowledge and the system behavior [7, 12].

It should be noted that to obtain the best dynamic property of the FPID controller, it's four control gains, i.e. K_1 to K_4 must be determined carefully.

23.2.2.2 Parallel FuzzyP + FuzzyI + FuzzyD Controller

Discrete FP + FI + FD controller is a parallel fuzzy PID controller which its main idea is based on fuzzification of each PID links independently [9]. Structure of this controller which is shown in Fig. 23.4 is relatively complex but the combination of three independent fuzzy systems along with nine control parameters improved the controllability and dynamic performance of FP + FI + FD controller compared to classical and even other adaptive controllers. Each of three links of FP + FI + FD controller has their own duty. for example, FP is used to speed up the system, the FD part is used for improving transients of dynamic response, and the FI section removes the steady-state error properly [13]. Finally, the output control signal of

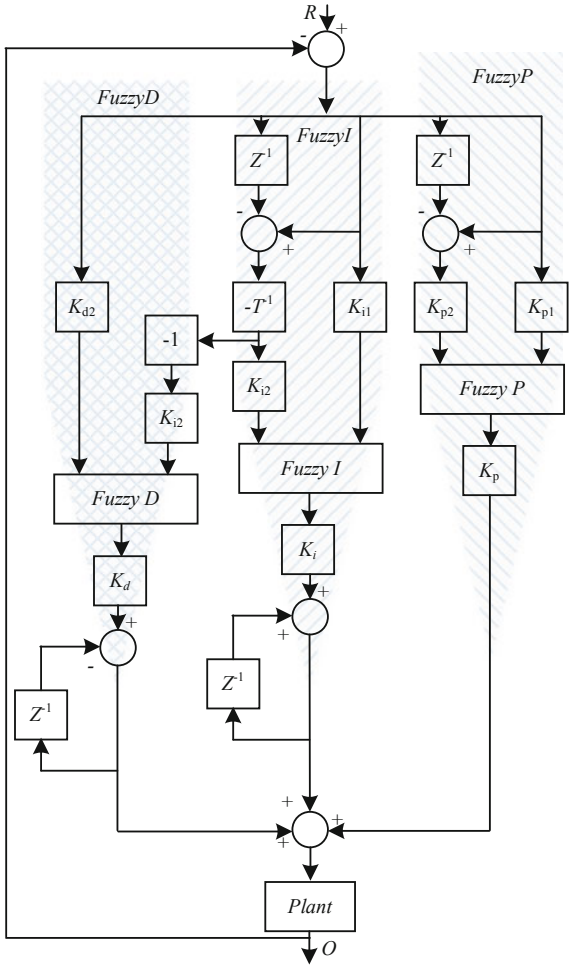

Fig. 23.4 Structure of FP + FI + FD controller

FP + FI + FD is obtained by the algebraic sum of FP, FI, and FD control actions as described in Eq. (23.1).

$$U_{FP+FI+FD} = u_{FP} + u_{FI} + u_{FD} \tag{23.1}$$

Each fuzzy interface system has two inputs and one output signals with three singleton membership functions in the output and two triangular membership functions in the inputs. Figure 23.5 shows the membership functions of input and output signal of fuzzy interface systems. Also, four fuzzy rules, max-min interface mechanism and center of mass for the defuzzification method are considered. Tables 23.2, 23.3 and 23.4 show the fuzzy rules for FP, FI, and FD fuzzy systems, respectively. In order

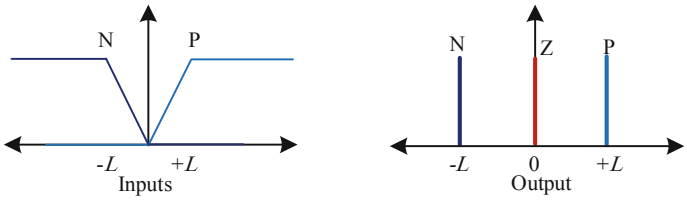

Fig. 23.5 The FP + FI + FD controller's input/output MFs. *Note L* is an adjustable parameter which has to be determined for each specific control process

Table 23.2 Fuzzy rules of the fuzzy P system

		Input #2	
		N	P
Input #1	N	Z	P
	P	N	Z

Table 23.3 Fuzzy rules of the fuzzy I system

		Input #2	
		N	P
Input #1	N	N	Z
	P	Z	P

Table 23.4 Fuzzy rules of the fuzzy D system

		Input #2	
		N	P
Input #1	N	Z	P
	P	N	Z

to further study on FP + FI + FD Controller, refer to [7, 9, 13, 14]. It should be noted that the fuzzy rules of the FP + FP + FD controller have been obtained based on the engineering knowledge [9]. In addition, to achieve its best performance, it is necessary to optimally determine its nine control parameter (K_{p1}, K_{p2}, K_p, K_{i1}, K_{i2}, K_i, K_{d1}, K_{d2}, and K_d) along with the range of the input and output membership functions (L), simultaneously [7]. In this way, Salp swarm algorithm (SSA) is used in this chapter. Salp is similar to jelly fishes and the water is pumped through the body as propulsion to move forward. Similar to other particle-based optimization methods, the position of the particles is defined in an n-dimensional space, where n is the number of variables to be optimized. The target of the Salp particles to move towards it (the optimal solution of the optimization problem) is a hypothetical source of food.

23.3 Salp Swarm Algorithm (SSA)

Salp swarm algorithm is a particle-based optimization method which mathematically models the movement of Salp particles toward the food location that is considered as the best solution. In order to cope with multi parameter optimization problems an n-dimensional space is suggested, where n is the number of variables to be optimized [10]. In each iteration, the particle with the best position (nearest to the food location) is selected as the leader of the other particles and its position is updated by Eq. (23.2).

$$X_j^1 = \begin{cases} F_j + c_1((ub_j - lb_j)c_2 + lb_j) & c_3 \geq 0 \\ F_j - c_1((ub_j - lb_j)c_2 + lb_j) & c_3 < 0 \end{cases} \tag{23.2}$$

where, X_j^1 is the first leader, F_j is food location, ub_j and lb_j are the upper and lower bonds of the parameters all in jth dimension. c_1, c_2, and c_3 are random numbers. Parameter c_1 which is important because it balances the exploration and exploitation phases, is calculated by Eq. (23.3).

$$c_1 = 2\mathrm{e}^{-(\frac{4l}{L})^2} \tag{23.3}$$

where, l is the current iteration and L is the maximum number of iterations. c_2 and c_3 parameters are determined using normal distribution in the range [0 1].

According to Newton's displacement law, the position of the imitative Salp individuals is derived by Eq. (23.4).

$$X_j^i = \frac{1}{2}at^2 + v_0 t \tag{23.4}$$

where, $i > 2$, X_j^i is the position of ith Salp particle in jth dimension, t refers to time, v_0 is the initial speed, $a = v_{final}/v_0$ which $v = (x - x_0) \times t^{-1}$. In the concept of optimization, time is equivalent with iteration and the space between the iterations is 1. With this in mind and proposing 0 for the initial speed of all individuals, (23.4) can be rewritten as Eq. (23.5).

$$X_j^i = \frac{1}{2}(X_j^i + X_j^{i-1}) \tag{23.5}$$

More detail about the SSA can be found in [10]. Figure 23.6 shows the flowchart of the SSA.

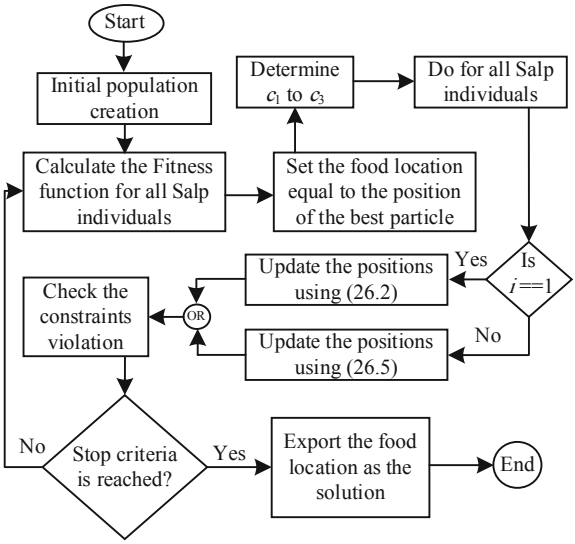

Fig. 23.6 The flowchart of the SSA

23.4 Model of the μG Under Study

A typical European distribution power system owned by Himmerlands Elforsyning located in Aalborg, Denmark with high penetration of DG units is considered in this chapter. It consists of 3 fixed-speed stall-regulated wind turbine generators, a combined heat and power plant (CHP) with three gas turbine generators (GTG) namely CHP1, CHP2, and CHP3, and 10 loads. It is assumed the WTG units have the capacitor banks for necessary compensation and they operate close to unity power factor. A test case situation is used to assess the dynamic performance of the FP + FI + FD, FPID and classical PID controllers to damp the frequency and voltage fluctuations with productions of 2.5, 2.8, and 2.8 MW from CHP1, CHP2, and CHP3 respectively, and 0.08 MW from each WTGs. Figure 23.7 shows the single line diagram of the proposed μG and locations of load and power plants [15]. The Simulink model of Figs. 23.8 and 23.9 are used for the induction and synchronous generators, respectively. Load, WTG, and exciter system data are given in Tables 23.5, 23.6 and 23.7 [15]. In order to simulate the proposed μG in Simulink, the reduced Y_{bus} method is used. In this way, firstly, the Y_{bus} of the power system will be calculated. Then by eliminating the load buses the reduced Y_{bus} will be formed. The voltage of the generation units multiplied by the reduced Y_{bus} and the input current of generation units will be determined. Figure 23.10 shows this process.

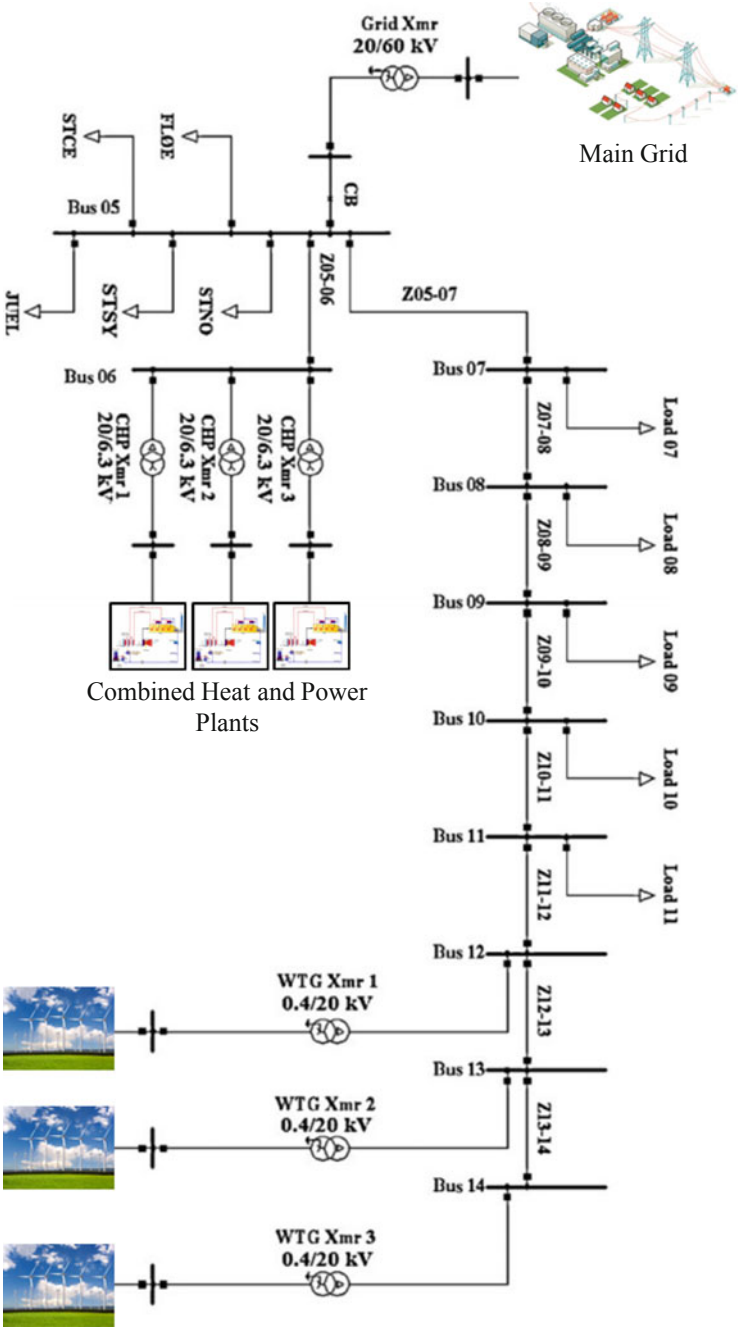

Fig. 23.7 Single line diagram of the proposed μG [15]

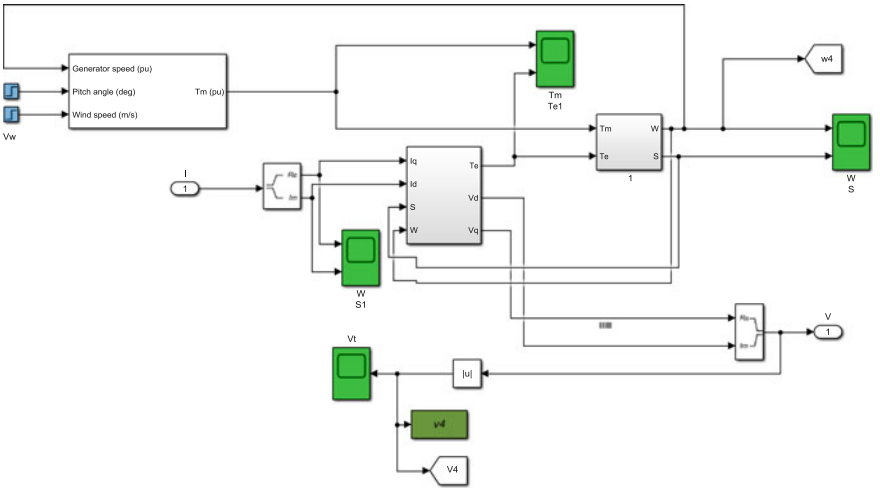

Fig. 23.8 Simulink model of the induction generator (WTG1 to WTG3 in Fig. 23.9)

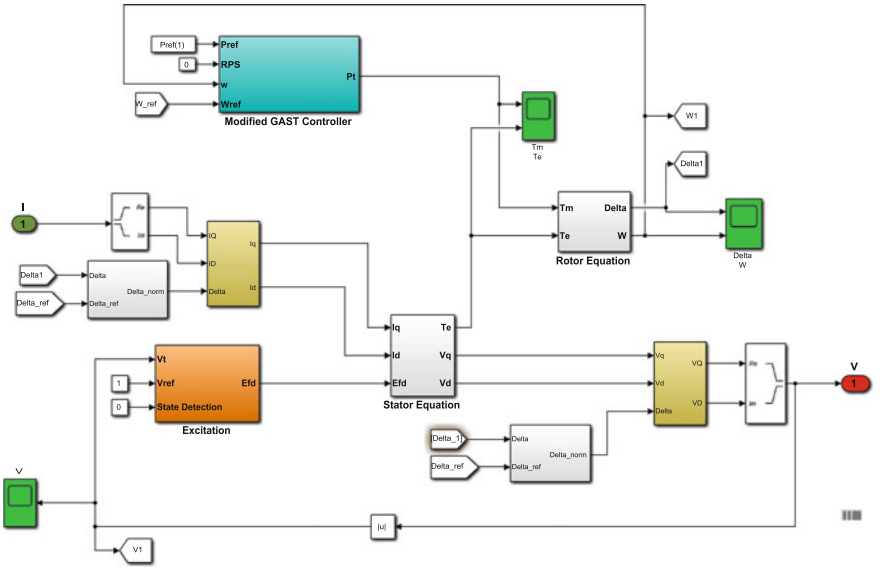

Fig. 23.9 Simulink model of the synchronous generator (CHP1 to CHP3 in Fig. 23.9)

Table 23.5 Load data

Load name	Active power (MW)	Reactive power (MVar)
FLOE	0.787	0.265
JUEL	2.442	0.789
STCE	1.212	0.16
STNO	2.109	0.286
STSY	0.4055	0.0735
Load 07	0.4523	0.2003
Load 08	0.7124	0.3155
Load 09	0.1131	0.0501
Load 10	0.1131	0.0501
Load 11	0.1131	0.0501

Table 23.6 Excitation system data

Parameter		Value
T_r	Measurement delay (s)	0.0
K_a	AVR dc gain	500
T_a	AVR time constant (s)	0.02
K_e	Exciter constant (p.u.)	1.0
T_e	Exciter time constant (s)	0.9
K_f	Stabilization path gain (p.u.)	0.03
Tf_1	1st stabilization path time constant (s)	0.6
Tf_2	2nd stabilization path time constant (s)	0.38
Tf_3	3rd stabilization path time constant (s)	0.058
E_1	Saturation factor 1 (p.u.)	5.6
Se_1	Saturation factor 2 (p.u.)	0.86
E_2	Saturation factor 3 (p.u.)	4.2
Se_2	Saturation factor 4 (p.u.)	0.5
$V_{\min}$	Controller minimum out (p.u.)	−7.3
$V_{\max}$	Controller maximum output (p.u.)	7.3

Table 23.7 WTG system data

Parameter	Value
Rotor inertia (kg.mm)	4×10^6
Drive train stiffness (N.m/rad)	8000
Drive train damping (N.m/rad)	0
Rotor (m)	34

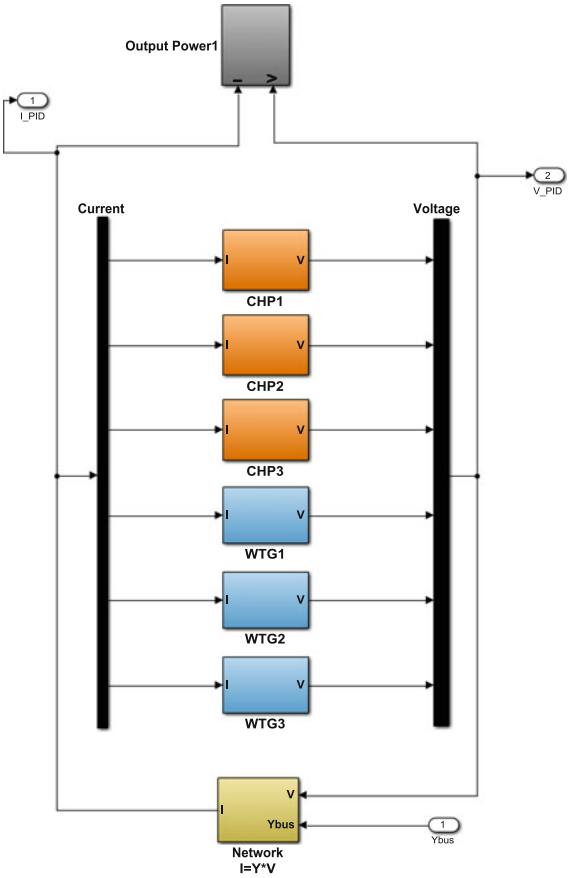

Fig. 23.10 Simulink model of the simulation process

23.5 Optimization Problem Formulation

Obviously, the design of the voltage and frequency controller for all power plants simultaneously is complex and uneconomic. For this reason, some simplistic assumptions are considered. (1) Designing controller for WTG units is neglected because the capacity of WTGs is very small compared to CHP units. (2) The same voltage and frequency controllers are designed for all units, because they are completely identical. According to the above assumptions, two independent controllers are designed for the μG. An identical frequency controller and an identical voltage controller for all the CHP units. As Eq. (23.6) describes a time-domain objective function is considering for evaluation of the dynamic response of the proposed controllers which is based on the integral of time multiplied by absolute error criteria. Both frequency and voltage deviations in CHP buses are used for calculation of objective function.

$$J = ITAE_{freq\,\&\,voltage} = \int_0^{40} t \times [(\Delta\omega_{CHP1} + \Delta\omega_{CHP2} + \Delta\omega_{CHP3}) \cdots + \beta \times (\Delta V_{CHP1} + \Delta V_{CHP2} + \Delta V_{CHP3})]dt \quad (23.6)$$

In Eq. (23.6), β is a weight factor that places the values of the voltage and frequency errors in the same range. Here, β is considered equal to 3.

23.5.1 Classical PID Controller

The optimization problem for optimally tuning two PID controllers can be mathematically described by Eq. (23.7).

$$\begin{aligned} &\text{minimize } J \\ &\text{subject to:} \\ &\qquad 0 < K_{p,\,PID}^{f\,\&v} < 1 \\ &\qquad 0 < K_{i,\,PID}^{f\,\&v} < 1 \\ &\qquad 0 < K_{d,\,PID}^{f\,\&v} < 1 \end{aligned} \quad (23.7)$$

In (23.7), f and v indices refer to frequency and voltage controllers, respectively.

23.5.2 Fuzzy PID (FPID) Controller

The considered FPID controller has four control gains. The optimization problem of tuning two FPID controllers given by Eq. (23.8).

$$\begin{aligned} &\text{minimize } J \\ &\text{subject to:} \\ &\qquad 0 < K_1^{f\,\&v} < 1 \\ &\qquad 0 < K_2^{f\,\&v} < 1 \\ &\qquad 0 < K_3^{f\,\&v} < 1 \\ &\qquad 0 < K_4^{f\,\&v} < 1 \end{aligned} \quad (23.8)$$

23.5.3 FP + FI + FD Controller

Equation (23.9) mathematically models the optimization problem of tuning FP + FI + FD controller considering parameter constraints.

$$\begin{aligned} &\text{minimize } J \\ &\text{subject to:} \\ &\quad 0 < K_{p1}^{f\&v}, K_{p2}^{f\&v}, K_{p}^{f\&v} < 1 \\ &\quad 0 < K_{i1}^{f\&v}, K_{i2}^{f\&v}, K_{i}^{f\&v} < 1 \\ &\quad 0 < K_{d1}^{f\&v}, K_{d2}^{f\&v}, K_{d}^{f\&v} < 1 \\ &\quad 0.1 < L < 1000 \end{aligned} \tag{23.9}$$

23.6 Optimization Results

In order to solve the optimization problems of Eqs. (23.7), (23.8), and (23.9), SSA is used considering 50 initial population size and 50 iterations. The convergence of cost function (J) during optimization process of different control strategies is illustrated in Fig. 23.11.

It is evident from Fig. 23.10 that FP + FI + FD controller well minimizes the cost function compared to FPID and classical PID controllers. Optimization results are shown in Table 23.8.

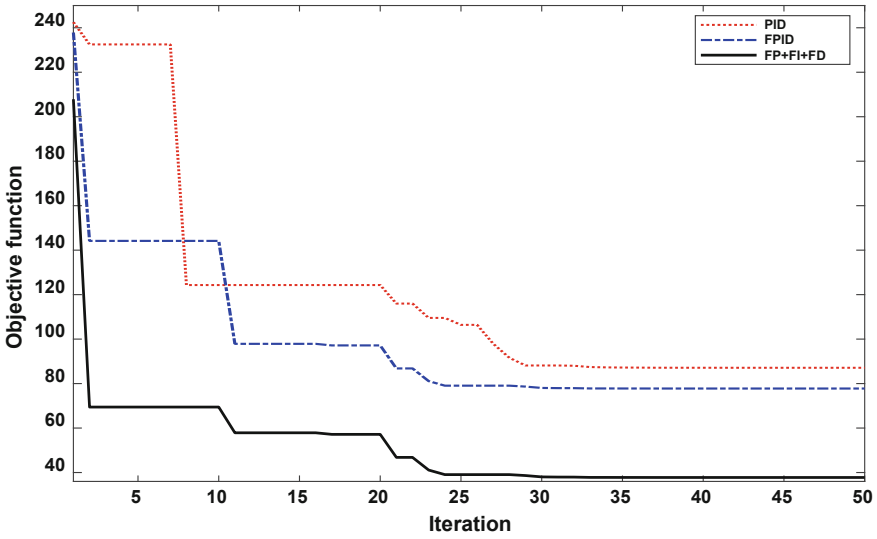

Fig. 23.11 Convergence of the objective function for different control mechanisms

Table 23.8 Optimal parameter of different control mechanisms obtained by SSA

$FP + FI + FD$										
K_p	K_{p1}	K_{p2}	K_i	K_{i1}	K_{i2}	K_d	K_{d1}	K_{d2}	L	Controller type
0.9562	0.5624	0.6251	0.1524	0.2514	0.3012	0.0895	0.1259	0.0954	680	Frequency
0.2491	0.4621	0.3674	0.0985	0.1237	0.0753	0.0146	0.0089	0.0149	730	Voltage
FPID										
K_1			K_2		K_3		K_4			
0.8974			0.6249		0.0967		0.7658			Frequency
0.8219			0.4251		0.0901		0.6490			Voltage
PID										
K_p			K_i				K_d			
0.4978			0.1408				0.00117			Frequency
0.0704			0.0383				0.0012			Voltage

23.7 Simulation Results and Discussion

In order to evaluation of the dynamic performance of the proposed FL controllers compared to classical PID controller, μG of Fig. 23.7 is simulated with MATLAB/Simulink. A Three phase fault at bus 7 is considered as a challenging condition of the system. The angular velocity of the generators is plotted in Figs. 23.12 and 23.13. According to Figs. 23.12 and 23.13, all three control strategies have the ability to eliminate the oscillations of angular velocity (frequency) of the generation units. However, it's clear that the FP + FI + FD controller has a tremendous dynamic efficiency compared to FPID and classical PID controllers. FP + FI + FD controller has an excellent dynamic performance thanks to its flexible structure, which integrates the fuzzy logic adaptive property with the speed and precision of the PID controller.

In order to more highlight the capabilities of the FL-based controllers, the oscillations of the voltage of the generation buses are shown in Figs. 23.14 and 23.15. Under the conditions of the same fault, the amplitude of the voltage fluctuations is much smaller than the frequency fluctuations. In these circumstances, the superiority of the FP + FI + FD controller is inferred from simulation results compared to the other control methods.

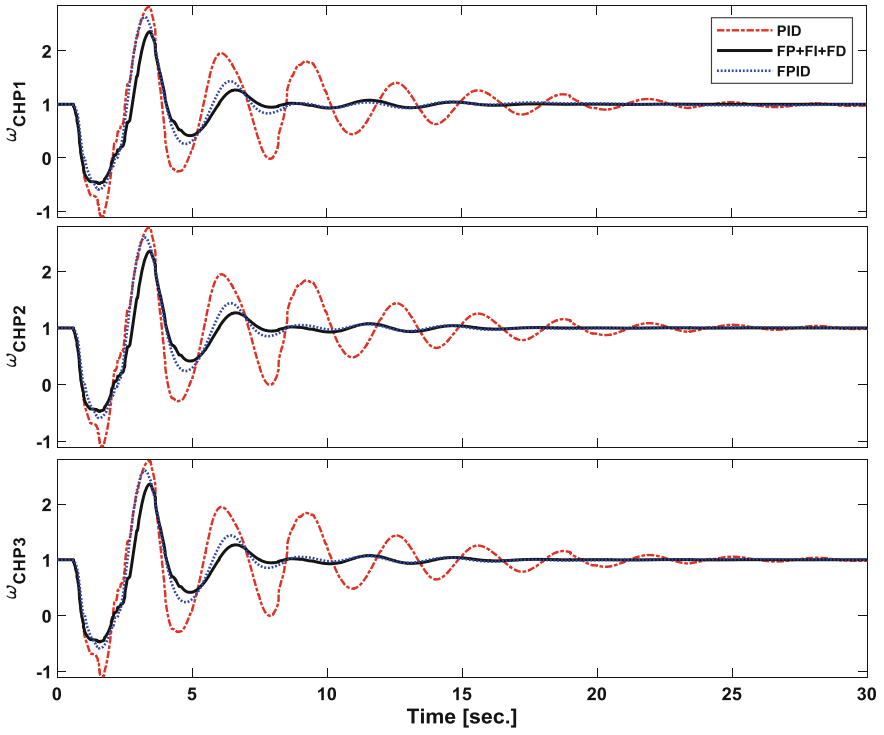

Fig. 23.12 The angular velocity of the CHP units

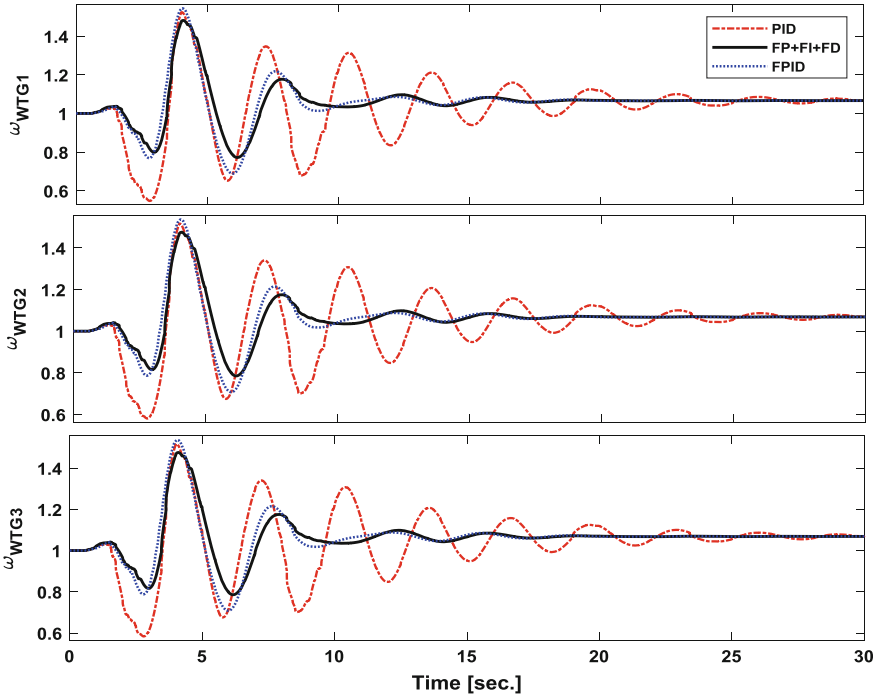

Fig. 23.13 The angular velocity of the WTG units

Results show that the optimal tuning of the FP + FI + FD controller parameters makes the different parts of it consistent together, and each of them perform their tasks correctly. So, dynamics will be improved in terms of overshoot/undershoot, increasing the speed of the oscillation damping, and the complete removal of the steady-state error.

Total production of active and reactive powers of μG during fault occurrence is shown in Fig. 23.16. The active power remains constant after some oscillations. Wherever it is evident that the FL based controllers and especially FP + FI + FD controller are superb in damping the oscillations compared to traditional PID controller.

Figure 23.17 shows that how the μG power factor changes during the fault. Since the reactive power is decreased and active power remains constant, the power factor is increased. It can be revealed through Fig. 23.17 that the dynamic performance of the FL-based controllers is much better than the classical PID controller.

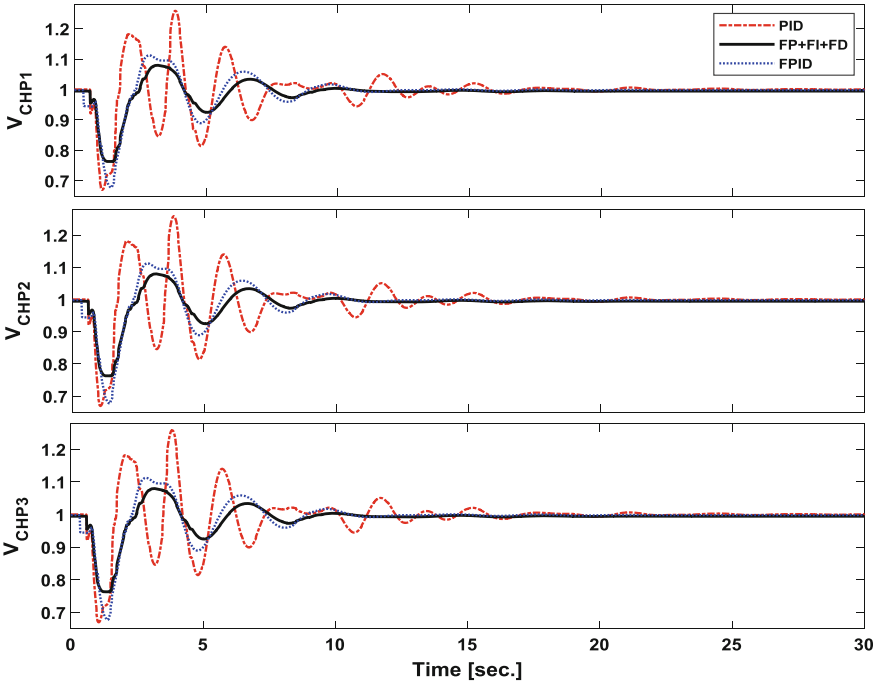

Fig. 23.14 The variations of voltage at the CHP unit buses

23.8 Conclusion

In this chapter, adaptive controlling mechanisms based on fuzzy logic was discussed. Fuzzy logic based controllers are expanding due to their simple structure, easy implementation and adaptive behavior. This kind of controllers has a superb performance in controlling large-scale complex systems with high degree of nonlinearities by using their membership functions and fuzzy rules. The FuzzyP + FuzzyI + FuzzyD controller is a discrete parallel type fuzzy PID controller which is used in this chapter to controlling the frequency and voltage of a Microgrid with high penetration of distributed generations. This controller integrates the characteristics of traditional PID controller such as speed and precision along with adaptive and robustness behavior of fuzzy logic. In order to evaluate the performance of the proposed control methods, a part of the Denmark distribution network was considered which is consists of large combined heat and power plants and wind turbine generators. Simulation results prove that the fuzzy logic controllers can overcome the challenging conditions in a large-scale Microgrid with a high degree of nonlinearities.

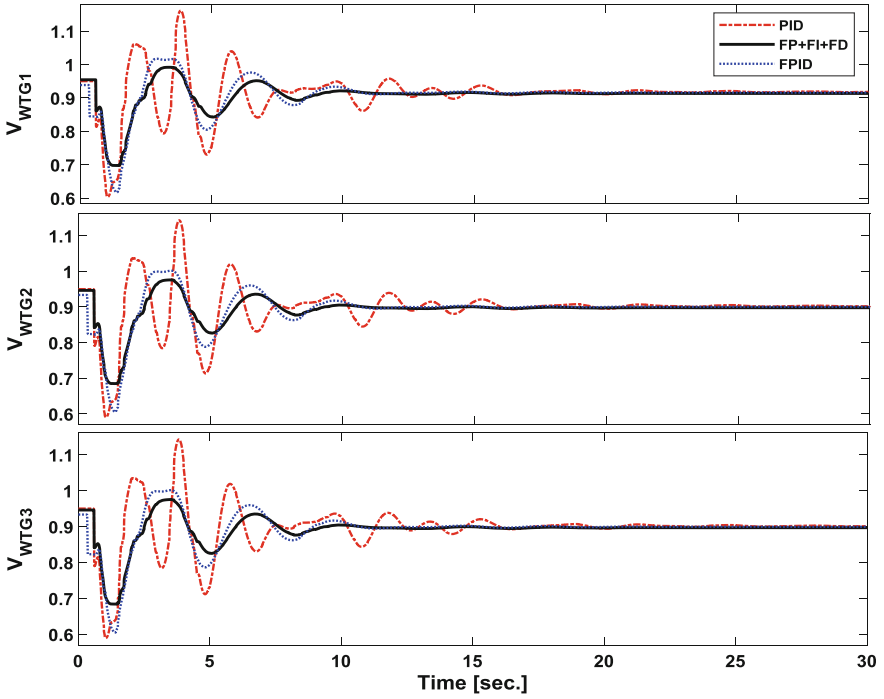

Fig. 23.15 The variations of voltage at the WTG unit buses

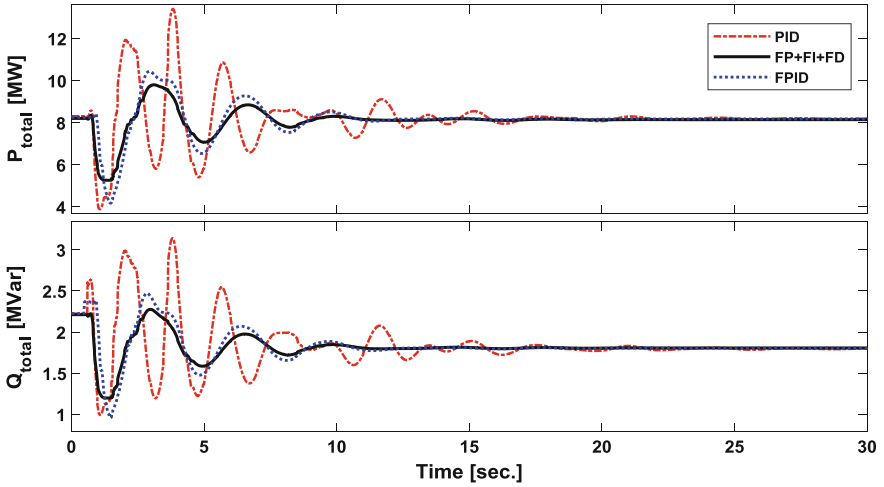

Fig. 23.16 Total production of the active and reactive power of μG

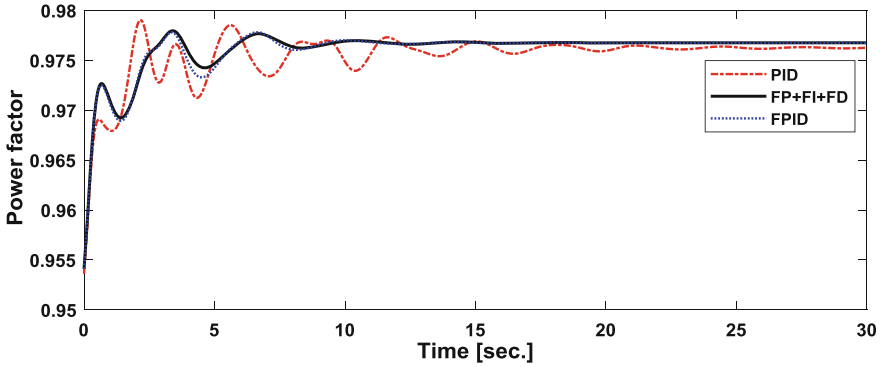

Fig. 23.17 Variations of μG power factor

References

1. S. Teimourzadeh, F. Aminifar, M. Davarpanah, M. Shahidehpour, Adaptive control of microgrid security. IEEE Trans. Smart Grid **9**, 3909–3910 (2018)
2. M.S. Sadabadi, Q. Shafiee, A. Karimi, Plug-and-play voltage stabilization in inverter-interfaced microgrids via a robust control strategy. IEEE Trans. Control Syst. Technol. **25**, 781–791 (2017)
3. D.O. Amoateng, M.A. Hosani, M.S. Elmoursi, K. Turitsyn, J.L. Kirtley, Adaptive voltage and frequency control of islanded multi-microgrids. IEEE Trans. Power Syst. **33**, 4454–4465 (2018)
4. X. Xiang, C. Yu, L. Lapierre, J. Zhang, Q. Zhang, Survey on fuzzy-logic-based guidance and control of marine surface vehicles and underwater vehicles. Int. J. Fuzzy Syst. **20**, 572–586 (2018)
5. G. Feng, C. Lai, N.C. Kar, A closed-loop fuzzy-logic-based current controller for PMSM torque ripple minimization using the magnitude of speed harmonic as the feedback control signal. IEEE Trans. Ind. Electron. **64**, 2642–2653 (2017)
6. D. Arcos Aviles, J. Pascual, L. Marroyo, P. Sanchis, F. Guinjoan, Fuzzy logic-based energy management system design for residential grid-connected microgrids. IEEE Trans. Smart Grid **9**, 530–543 (2018)
7. H. Shayeghi, A. Younesi, Y. Hashemi, Optimal design of a robust discrete parallel FP + FI + FD controller for the automatic voltage regulator system. Int. J. Electr. Power Energy Syst. **67**, 66–75 (2015)
8. H. Shayeghi, A. Younesi, A robust discrete FuzzyP + FuzzyI + FuzzyD load frequency controller for multi-source power system in restructuring environment. J. Oper. Autom. Power Eng. **5**, 61–74 (2017)
9. V. Kumar, A.P. Mittal, Parallel FuzzyP + FuzzyI + FuzzyD controller: design and performance evaluation. Int. J. Autom. Comput. **7**, 463–471 (2010)
10. S. Mirjalili, A.H. Gandomi, S.Z. Mirjalili, S. Saremi, H. Faris, S.M. Mirjalili, Salp swarm algorithm: a bio-inspired optimizer for engineering design problems. Adv. Eng. Softw. **114**, 163–191 (2017)
11. J.J. Castillo Zamora, K.A. Camarillo Gomez, G.I. Perez Soto, J. Rodriguez Resendiz, Comparison of PD, PID and sliding-mode position controllers for V–tail quadcopter stability. IEEE Access **6**, 38086–38096 (2018)
12. J.X. Xu, C.C. Hang, C. Liu, Parallel structure and tuning of a fuzzy PID controller. Automatica **36**, 673–684 (2000)
13. V. Kumar, B.C. Nakra, A.P. Mittal, Some investigations on FuzzyP + FuzzyI + FuzzyD controller for non-stationary process. Int. J. Autom. Comput. **9**, 449–458 (2012)

14. V. Kumar, A.P. Mittal, R. Singh, Stability analysis of parallel FuzzyP + FuzzyI + FuzzyD control systems. Int. J. Autom. Comput. **10**, 91–98 (2014)
15. P. Mahat, Z. Chen, B. Bak Jensen, Control and operation of distributed generation in distribution systems. Electr. Power Syst. Res. **81**, 495–502 (2011)

Chapter 24
Adaptive and Online Control of Microgrids Using Multi-agent Reinforcement Learning

Hossein Shayeghi and Abdollah Younesi

Abstract The primary aim of this chapter is the design and application of intelligent methods based on reinforcement learning (RL) for adaptive and online controlling the hybrid microgrids (HMGs). The traditional structure of the power systems is being changed continuously due to environmental limitations and depreciated infrastructures. The creation of distinct electrical boundaries between different areas of the power system with the ability to connect/disconnect and locating distributed generation (DG) resources near the load points has transformed the face of power systems. However, in this case, the power system's efficiency increases, but its control is faced with bigger challenges. Coordination between HMGs, resource scheduling in the island and main utility-connected modes, exchanging power between different microgrids, and etc., are the reasons that necessitate the use of adaptive control methods in controlling such power systems. Reinforcement Learning is an adaptive control structure that is considered in this chapter. RL is a branch of multi-agent systems in the field of machine learning which is the main solution method for Markov decision process (MDP). In this chapter, based on RL features like an unpretentious structure, robust versus severe disturbances, and online behavior a novel method will be suggested for controlling different aspects of HMGs. The proposed control method uses the features of the RL and capabilities of the classical controllers to give an effective online controller with plain anatomy which is robust versus uncertainties and operating condition changes.

Keywords Hybrid microgrid · Reinforcement learning · Q-learning · Multi-agent systems · Microgrid frequency control

H. Shayeghi (✉) · A. Younesi
Department of Electrical Engineering, University of Mohaghegh Ardabili, Ardabil, Iran
e-mail: hshayeghi@gmail.com

A. Younesi
e-mail: younesi.abdollah@gmail.com

N. Mahdavi Tabatabaei et al. (eds.), *Microgrid Architectures, Control and Protection Methods*, Power Systems,
https://doi.org/10.1007/978-3-030-23723-3_24

Parameters

A	Action set
a	Selected action
c_1, c_2 and c_3	Random numbers
F_j	Food location
K_{AE}	DC gain of AE
K_{BESS}	DC gain of BESS
K_{FC}	DC gain of FC
K_{FESS}	DC gain of FESS
K_T and K_s	DC gains of STPS
K_{UC}	DC gain of UC
K_{WTG}	DC gain of WTG
l	The current iteration
L	The maximum number of iterations
P_{AE}	Power produced by AE
P_{BESS}	Power produced by BESS
P_{FC}	Power produced by FC
P_{FESS}	Power produced by FESS
P_{STPS}	Power produced by STPS
P_{UC}	Power produced by UC
P_{Wind}	Power produced by WTG
r	Received reward
$\Re_t$	Reward at instant t
s	Current state
S_t	System state at instant t
t	Time instant
T_{AE}	Time constant of AE
T_{BESS}	Time constant of BESS
T_{FC}	Time constant of FC
T_{FESS}	Time constant of FESS
T_T and T_s	Time constants of STPS
T_{UC}	Time constant of UC
T_{WTG}	Time constant of WTG
ub_j/lb_j	Upper and lower bounds of the parameters in jth dimension
v_0	The initial speed of Salp individuals
X_j^i	The position of ith Salp particle in jth dimension
X_j^1	The first leader of Salp swarm
A	Attenuation coefficient
γ	Discount factor
Δf	Deviation in frequency
Π	Control policy
Υ	A function for determining system states

24.1 Introduction

Undoubtedly, one of the most natural learnings is defined as intercommunication with an environment. Looking at history reveals that humans were acquired most of their applied science from interplay with their environs. Whenever they speak, do anything or play a game, they are heavily aware of their impact on their environs and they analysis these affect to improve their demeanor [1].

In this Chapter, we try to show how a computational approach can be used to learn the optimal control policy from interaction with the environment of the system to be applied for controlling the frequency of an islanded hybrid Microgrid (HMG). The computational mechanism used is called reinforcement learning (RL). Reinforcement learning is learning from intercommunication how to select the best action in each state in the orientation of maximizing a numerical reward signal. In this framework, the intelligent agent is not told explicitly which actions to be selected to take but instead must discover himself which actions yield the highest rewards by trying out various possible actions and by observing their consequences [2]. At least two types of applications can be considered. The first one is to use this RL based mechanism in an offline mode o find the optimal control policy they have learned to control the real power system. The other application consists of using these agents directly on the real power system in online mode [3].

In recent years, RL has obtained a special position in controlling power systems and has been successfully applied to small signal stability [2, 4, 5], voltage stability [6], transient stability and power market issues [7]. Authors in [8] represent an RL-fuzzy-PID frequency controller for a microgrid. The structure of the suggested controller is relatively complex and its impact on the dynamic performance of the original fuzzy-PID controller is low. Must be noticed, an important point in using RL is the time it takes to learn the optimal control policy [9]. In Ref. [8], there are twenty-seven actions for each state of the system, which means it needs much more time to learn the optimal control policy in the nonlinear complex power systems. Maybe, that's why the proposed strategy does not have much effect on the performance of the fuzzy-PID controller, according to the simulations results.

In this Chapter, an innovative control structure based on the RL integrated with a classical PID controller is proposed to enhance the frequency fluctuations of an HMG with a high penetration of renewable energy resources. The suggested controller consists of two distinct parts. The first part is a traditional PID controller whose parameters are optimized using the new optimizer called Salp swarm algorithm (SSA) [10]. This section of the controller is fixed and will be tuned once. The second part is a consistent control mechanism that is robust against changes in the parameters and system operating points, based on the learning of intelligent agents in the context of multi-agent systems. The suggested strategy learns the optimal control policy (which is the recognition of the correct state of the system and applying the best control signal) with a trial and error method in offline simulations. Eventually, in addition to applying the optimal control signal to the system under different conditions, it also updates its knowledge about the system. Another key point of the proposed

controller is that operates independently from the system dynamics and the type and location of the disturbance. In other words, when a disruptive event occurs, the frequency of the HMG begins to oscillate. The intelligent agent understands the frequency oscillation after a while (based on the sampling time in simulation) and damps the deviations immediately. To clarify the effectiveness of the suggested control mechanism, first, a microgrid including renewable energy resources such as wind turbines and solar-thermal system along with diesel generator, integrated with energy storages, like batteries, flywheel and ultra-capacitor, are simulated in MATLAB environment considering system uncertainties and nonlinearities. After that, in different realistic scenarios, the dynamic response of the proposed controller is compared to a traditional PID controller, which is optimized using SSA. In the final analysis, the superb performance of the proposed control strategy in damping frequency oscillations is clearly verifiable compared to PID control method.

24.2 General Reinforcement Learning

This Chapter describes a computational approach for solving discontinues control problems in the condition of lacking of the system dynamic. In order to cope with the challenge of the absence of knowledge about the system under control, it is assumed the system is a block box with some possible output and inputs. In each step time, t, it is possible to calculate the state of the system s_t and reward value r_t based on the output signals of the system. The main capability of RL is to solve such kind of problems. In each state s_t, the intelligent agent applies the appropriate action through the inputs of the system and receives reward r_t from the system. The generic framework of RL is shown in Fig. 24.1.

24.3 The Proposed RL-PID Controller

The supposed supervisory controller is made of two independent parts. The first part is a traditional PID controller whose parameters are fixed and will be tuned once. The second part is a consistent control mechanism that is robust against changes in the parameters and system operating points, based on the learning of intelligent agents in the context of multi-agent systems. In following, each part of the suggested controller will be described in detail.

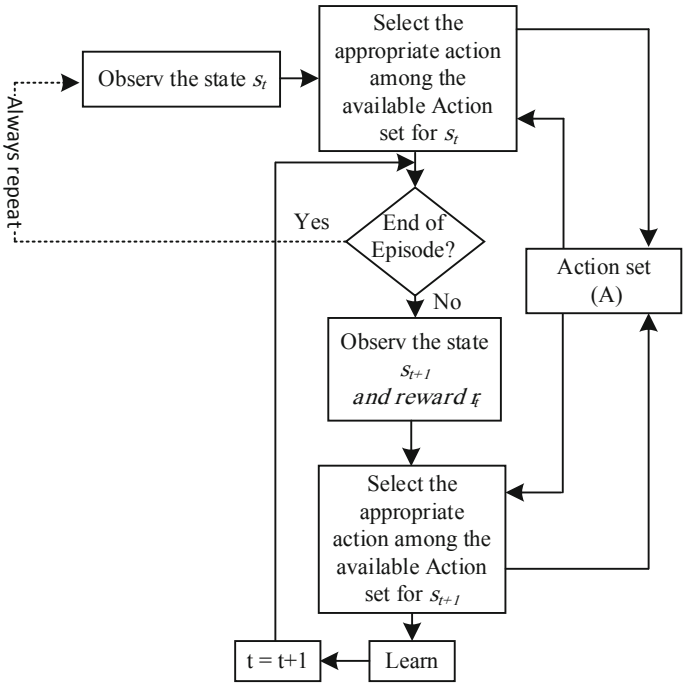

Fig. 24.1 Generic framework of RL

24.3.1 Conventional PID

The proportional integral derivative controller is a well-known controller with a simple structure and acceptable dynamic performance for controlling a major number of industrial processes [11]. The schematic of a PID controller is shown in Fig. 24.2 which is consist of three links, proportional with K_p control gain, integral with K_i control gain, and derivative with K_d control gain. In order to reach the best control performance of the PID controller, three K_p, K_i, and K_d gains must be tuned optimally.

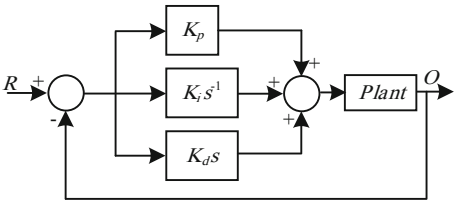

Fig. 24.2 General structure of PID controller

24.3.2 RL-Based Strategy for Supervising PID

Reinforcement learning is an algorithmic method based on trial and error, in which several agents learn an desirable control policy by interact with their environment (system under control) [12]. In other words, the environment is divided into several discrete states, in each state; there are a definite number of actions to be implemented. The intelligent agent learns to determine the optimal action that has to be applied to the system in each state [4]. In general, there are several methods for solving RL problems like adaptive heuristic critic (AHC), Q-learning, average reward (AR), and etc. [13]. In this Chapter, Q-learning is used to solve the proposed RL based frequency controller.

24.3.2.1 Q-Learning

The main properties of Q-learning based controllers are a simple structure, model-free, robustness versus changes in the system uncertainties and adaptive behaviour [4, 14]. The proposed Q-learning takes the system under control as a fragmentary area with a limited number of states which are shown with set S. Agent forms a matrix Q with a value of '0' for each set of action-state pairs. In each time step, at the preprocessing stage the agent calculates its state s_t, and selects the action a among available actions for stat s_t. Instantly, the agent calculates the reward r and next state s_{t+1} using feedback signal of system. Then the values of the Q matrix will be updated [15, 16]. The discounted long-term reward of the system is given by Eq. (24.1).

$$R_t = \sum_{k=0}^{\infty} \gamma^k r_{t+k+1} \tag{24.1}$$

where, r and γ are reward and a number, respectively. γ is called discount factor and is at the range 0–1. Q matrix is defined as [16]:

$$Q^{\pi}(s, a) = E_{\pi}\left\{\sum_{k=0}^{\infty} \gamma^k r_{t+k+1} | s_t = s,\ a_t = a\right\} \tag{24.2}$$

where, π is control policy, s refers to current state, a, and r indicate the selected action, and the received reward, respectively. In each step, Eq. (24.2) is updated using the optimal Bellman equation, which is given by Eq. (24.3).

$$\Delta Q = \alpha\left[r_{t+1} + \gamma \max_{a} Q(s_{t+1}, a_{t+1}) - Q(s_t, a_t)\right] \tag{24.3}$$

where, α is attenuation coefficient and is in range of 0–1. The flowchart of the proposed Q-learning method is summarized in Fig. 24.3. It is evident from Fig. 24.3 that after completing the learning phase (offline simulation), the system will be

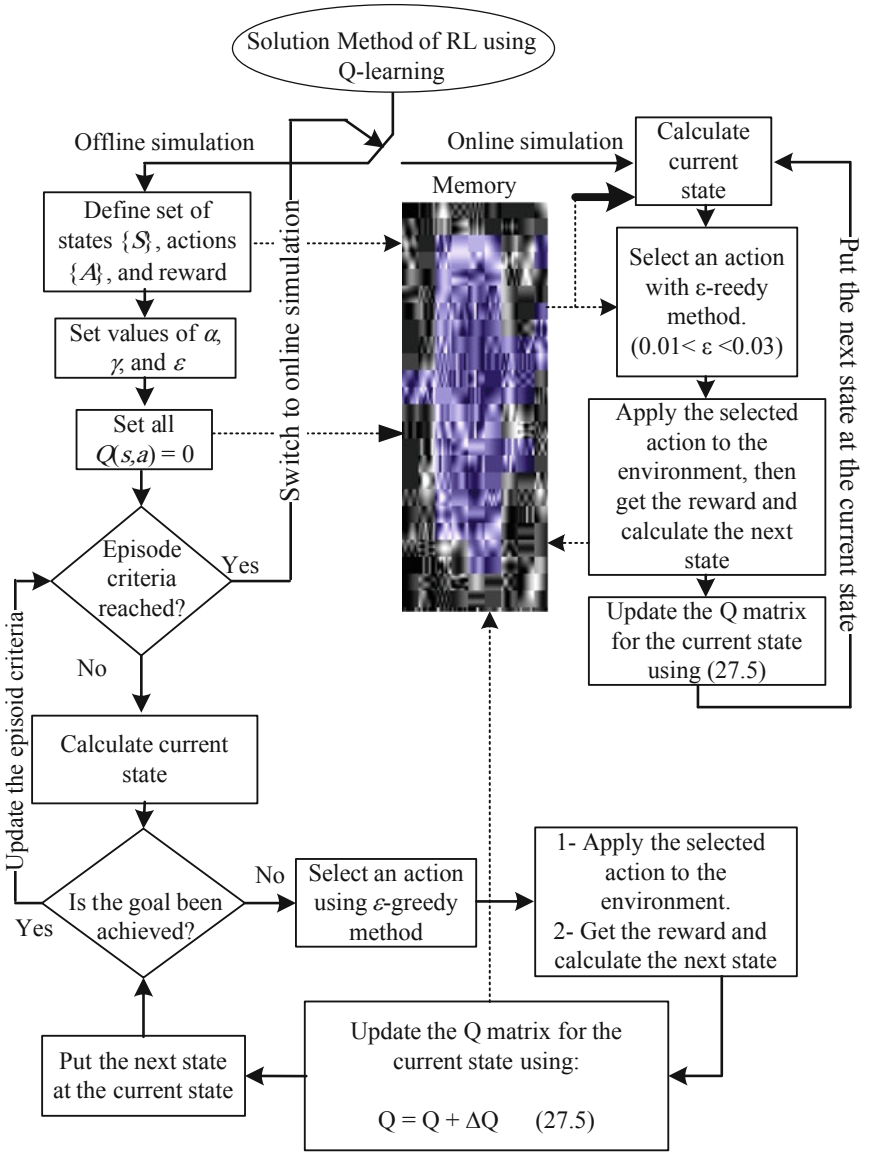

Fig. 24.3 Steps of the Q-learning solution method for RL [16]. *ε-greedy method is expressed in [9]

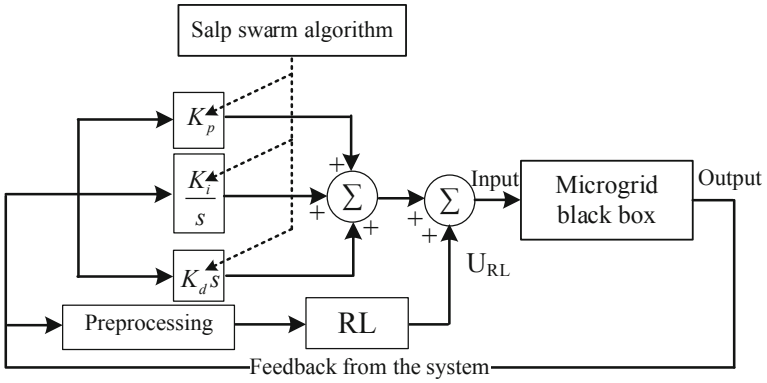

Fig. 24.4 Descriptive model of the proposed adaptive RL-PID controller

switched to online simulation. Figure 24.4 shows the block diagram of the RL-PID controller. As can be seen, the RL-PID controller consists of two parts. The first part is a traditional PID controller that its coefficients are optimized using SSA [10] in this Chapter. It must be noticed that this section is fixed and is adjusted only once. The second part, which is a compatible controller, has two stages. In the preprocessing section, the system state after the previous action is determined by using the received signal discretization. In the other part, the RL control mechanism, in a supervisory manner, corrects the output of the PID controller utilizing information obtained in the preprocessing stage. This part is variable and updated at any time step. As its name implies, reinforcement learning, this controller after applying an action to the system, receives the impact of it in a reward/penalty form and gives it a score in the corresponding state. Certainly, in each state of the system, an action with a higher score is best suited to be implemented to the system.

24.3.2.2 Determination of the States

As mentioned before, the primary aim of this chapter is to damp the oscillations of frequency, thus, deviation in frequency (Δf) is used for determining the states of the system. In this Chapter, Δf with its derivative are be used for this purpose.

The speed of the generator oscillates when a disturbance occurs in the HMG. Amplitude and frequency of the oscillations depend on the disturbance severity [16, 17]. Assume that the controller diagnoses the disturbance after a step time (50 ms in this chapter) and determines the state of the system using Υ as Eq. (24.4):

$$S_t = \Upsilon\left(\Delta f_t, \frac{d\,\Delta f_t}{dt}\right) \tag{24.4}$$

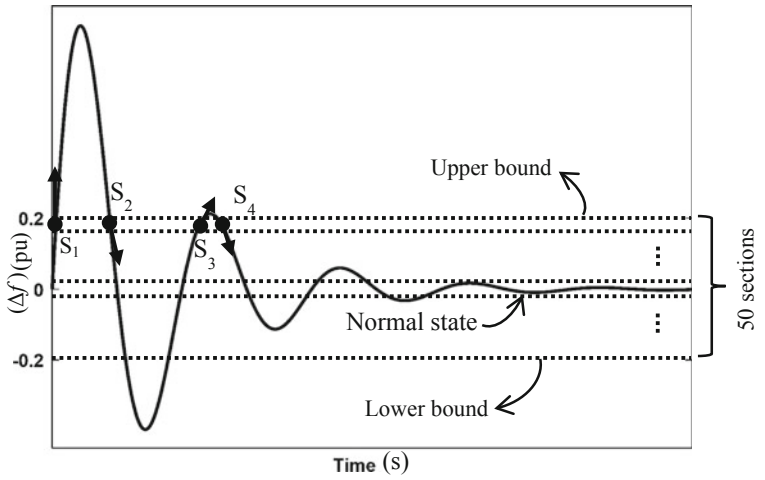

Fig. 24.5 The proposed idea behind the state definition for RL [16]

The first term of Υ shows the value of the variations in Δf. In order to avoiding mistakes in finding the real state of the power system, a derivative term is also added to Eq. (24.4). This procedure depicted in Fig. 24.5.

In Fig. 24.5, a limit of 0.2 p.u. is considered for upper/lower bound, respectively. When $|\Delta f| > 0.2$, the system is in the worst state, ignoring the sign of derivative term of Δf [16]. The agent must avoid going to this state of the system [18]. Fifteen equal segments are proposed for the area between upper and lower bounds. An illustrative example is used in order to better understand the procedure of state determination. Consider states S_1–S_4 in Fig. 24.5. The value of Δf term is equal in all four states, the derivative term is however different. The first difference is in the sign of the derivative. When Δf is not negative, if the sign of the derivative term is positive (states S_1 and S_3 in Fig. 24.5) the state of the system is moving away from the normal state. Otherwise, if derivative term is negative (states S_2 and S_4 in Fig. 24.5), the state of the system is getting closer to the normal state. These conditions are vice versa when Δf is not positive. It is clear that when the system oscillations are damped, the magnitude value of the derivative term will be reduced in the same sample time. This is a key feature which is used for making difference between states S_1 with S_3 and S_2 with S_4. In other words, the magnitude of the term derivative term in S_1 is greater than S_3. Thus, the agent can understand that in the state S_3 the system is closer to full damping in comparison to the state S_1. Moreover, ± 0.004 is considered for normal state margins (2% of 0.2). The normal state is defined as the goal for the agent [16].

24.3.2.3 Action Definition

Although, there are no particular laws for defining of actions for RL based controllers, and this makes it a complex matter [5]. But it may be determined by inspiring from the output limits of the usual controllers that used for the same purpose [9]. Must be noticed, various actions can be defined for different states of the system and they can even be increased. These efforts have two positive and negative aspects. On the positive side, it can enhance the dynamic efficiency of the controller by increasing the degree of freedom (the controller has more choices to perform). On the negative side, it increases the learning time extremely and makes it challenging (or even impossible) to find the optimal control policy. With this in mind, in this Chapter, the same actions are suggested for all states and expressed by Eq. (24.5).

$$A = \{-0.02, -0.01, 0, 0.01, 0.02\} \tag{24.5}$$

24.3.2.4 Reward/Penalty Function Determination

It is evident that the satisfaction from the last done action is obtained throughout the reward/penalty function. In the concept of frequency control in HMGs, the primary objective is to damp the frequency oscillations [5]. The reward is calculated by Eq. (24.6).

$$\Re_t = \begin{cases} +1 & \text{If } s_{t+1} \text{ is normal state} \\ -1 & \text{If } s_t \text{ is normal state and } s_{t+1} \text{ is not normal state} \\ \frac{1}{\left(1+\sum_{k=t-1}^{t} \Delta f(k)\right)} & \text{Otherwise} \end{cases} \tag{24.6}$$

In the current work, the agent performs the best action to the system for 50 ms; after then the simulation is paused and the reward and the next state are determined in preprocessing stage. In this Chapter, the simulation step time considered constant and equal to one ms. The primary objective of the proposed controller is to minimize the area under Δf signal that is shown in Fig. 24.6, throughout the reward signal. In order to clarify the proposed mechanism, assume the system is in the time t in Fig. 24.6, after performing the action (for 50 ms) the new situation of the system will be in the time $t + \Delta t$. Based on the (24.6) the area under the Δf signal in the period of Δt is considered for calculating the reward. When the next state is the normal state, the agent receives the reward $+1$ (the highest reward) from the environment. This reward will be -1 if the next state is the worst state (the lowest reward). Otherwise, the reward function is calculated based on the area under the Δf signal [16].

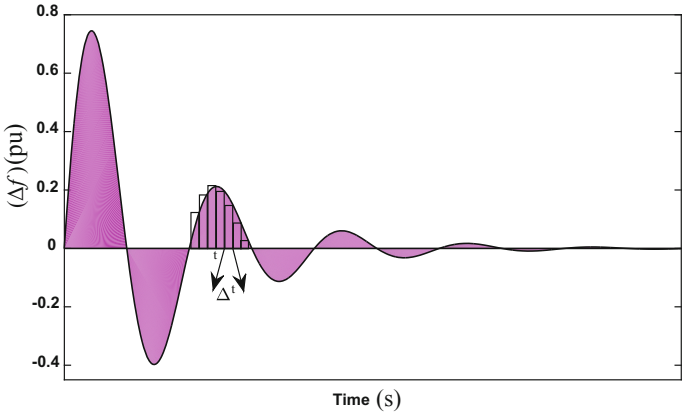

Fig. 24.6 The area under Δf will be minimized through reward signal [16]

24.4 Salp Swarm Algorithm (SSA)

Salp swarm algorithm is a particle-based optimization method, which mathematically models the movement of Salp particles toward the food location that is considered as the best solution. In order to cope with multi-parameter optimization problems an n-dimensional space is suggested, where n is the number of variables to be optimized [10]. In each iteration, the particle with the best position (nearest to the food location) is selected as the leader of the other particles and Eq. (24.7) update its position.

$$X_j^1 = \begin{cases} F_j + c_1((ub_j - lb_j)c_2 + lb_j) \ c_3 \geq 0 \\ F_j - c_1((ub_j - lb_j)c_2 + lb_j) \ c_3 < 0 \end{cases} \tag{24.7}$$

where, X_j^1 is the first leader, F_j is food location, ub_j and lb_j are the upper and lower bounds of the parameters all in jth dimension. c_1, c_2, and c_3 are random numbers. Parameter c_1, which is important because it balances the exploration and exploitation phases, is calculated by Eq. (24.8).

$$c_1 = 2\mathrm{e}^{-(\frac{4l}{L})^2} \tag{24.8}$$

where, l is the current iteration and L is the maximum number of iterations. c_2 and c_3 parameters are determined using normal distribution in the range [0 1]. According to Newton's displacement law, the position of the imitative Salp individuals is derived by Eq. (24.9).

$$X_j^i = \frac{1}{2}at^2 + v_0 t \tag{24.9}$$

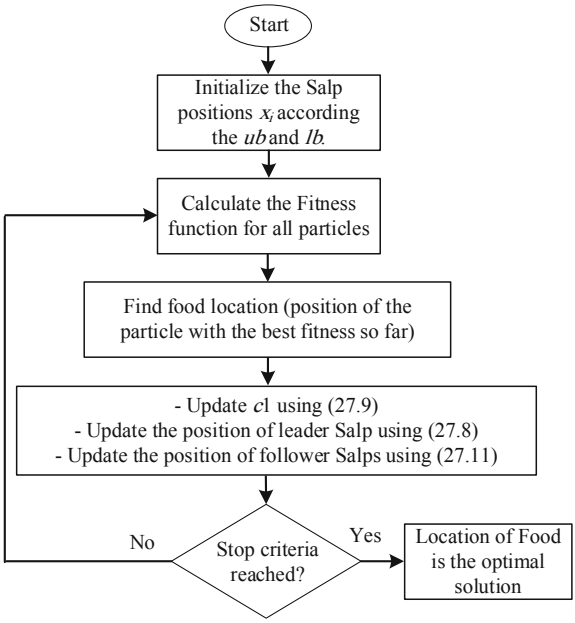

Fig. 24.7 The simplified flowchart of SSA

where, $i > 2$, X_j^i is the position of ith Salp particle in jth dimension, t refers to time, v_0 is the initial speed, $a = v_{final}/v_0$ which $v = (x - x_0) \times t^{-1}$. In the concept of optimization, time is equivalent with iteration and the space between the iterations is 1. With this in mind and proposing 0 for the initial speed of all individuals, (24.9) can be rewritten as Eq. (24.10). More detail about the SSA can be found in [10]. Figure 24.7 shows the flowchart of the SSA.

$$X_j^i = \frac{1}{2}\left(X_j^i + X_j^{i-1}\right) \tag{24.10}$$

24.5 Formulation of the Components of the HMG

In order to evaluate the dynamic performance of the supposed RL-PID controller, a standard HMG considered which integrates a different kind of energy resource and storages systems. The proposed HMG in this Chapter is consists of wind turbine generator (WTG), solar thermal power station (STPS), aqua-electrolyzer (AE), fuel cell (FC), diesel engine generator (DEG), ultra-capacitor (UC), battery energy storage system (BESS), and flywheel energy storage system (FESS) which are formulated at the following in detail.

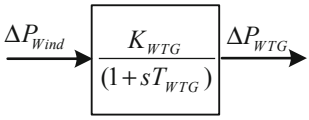

Fig. 24.8 WTG transfer function model

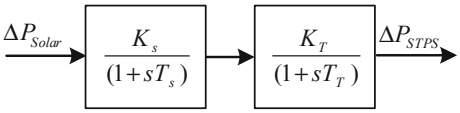

Fig. 24.9 STPS transfer function model

24.5.1 Wind Turbine Generator

The commonly used first-order model of WTG [19] is described by (24.11) which is used in this chapter and shown in Fig. 24.8.

$$\frac{\Delta P_{WTG}}{\Delta P_{Wind}} = \frac{K_{WTG}}{(1 + sT_{WTG})} \tag{24.11}$$

where, T_{WTG} is time constant, K_{WTG} is gain of WTG and P_{Wind} is the power of wind.

24.5.2 Solar Thermal Power Station

The STPS is modelled with a second-order transfer function given by (24.12) [3].

$$\frac{\Delta P_{STPS}}{\Delta P_{Solar}} = \frac{K_s K_T}{(1 + sT_s)(1 + sT_T)} \tag{24.12}$$

where T_T and T_s are time constants, K_T and K_s are DC gains. The transfer function model of STPS is shown in Fig. 24.9.

24.5.3 Aqua-Electrolyzer

Aqua-electrolyzer is used to provide the requested hydrogen for fuel-cell based on a portion $(1 - K_n)$ of renewable power. As a result, fuel-cell can improve the uncertainties of renewable power [3].

$$\frac{\Delta P_{AE}}{\Delta P_{WTG} + \Delta P_{STPS}} = \frac{K_{AE}}{(1 + sT_{AE})}(1 - K_n) \tag{24.13}$$

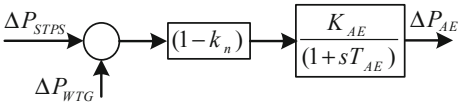

Fig. 24.10 Block diagram model of AE

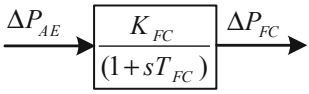

Fig. 24.11 FC transfer function model

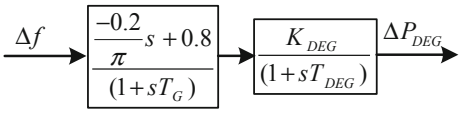

Fig. 24.12 DEG transfer function model with GDB

In Eq. (24.13), T_{AE} is time constants and K_{AE} is DC gain of aqua-electrolyzer. Figure 24.10 shows the block diagram model of AE.

24.5.4 Fuel Cell

The fuel cell can be described using a first-order transfer function, which is given by Eq. (24.14) [3].

$$\frac{\Delta P_{FC}}{\Delta P_{AE}} = \frac{K_{FC}}{(1 + sT_{FC})} \tag{24.14}$$

where, T_{FC} and K_{FC} are time constant and DC gain of FC, respectively. Figure 24.11 shows the block diagram of FC.

24.5.5 Diesel Engine Generator

Diesel engine generator has a first-order transfer function with a DC gain and a time constant along with generation rate constraint (GRC) integrated with governor dead band (GDB). Equation (24.15) and Fig. 24.12 show the relation of the output power and frequency deviation in DEG [3].

$$\frac{\Delta P_{DEG}}{\Delta f} = \frac{\frac{-0.2}{\pi}s + 0.8}{(1 + sT_G)} \cdot \frac{K_{DEG}}{(1 + sT_{DEG})} \tag{24.15}$$

where, T_G is governor time constant.

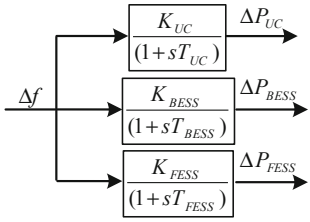

Fig. 24.13 Energy storage systems transfer function model

24.5.6 UC, BESS and FESS

Ultra-capacitor, batteries energy storage system, and flywheel energy storage system have a similar first-order transfer function with a DC gain and a time constant along with generation rate constraint (GRC) [3]. Consequently, the mathematical model of this parts can be expressed by Eqs. (24.16)–(24.18). Figure 24.13 shows the block diagram model of energy storage systems.

$$\frac{\Delta P_{UC}}{\Delta f} = \frac{K_{UC}}{(1 + sT_{UC})} \tag{24.16}$$

$$\frac{\Delta P_{BESS}}{\Delta f} = \frac{K_{BESS}}{(1 + sT_{BESS})} \tag{24.17}$$

$$\frac{\Delta P_{FESS}}{\Delta f} = \frac{K_{FESS}}{(1 + sT_{FESS})} \tag{24.18}$$

Finally, the block diagram of the considered HMG along with renewable and storage energy devices and system physical nonlinearities is shown in Fig. 24.14.

24.6 Optimization of PID

In order to obtain the best dynamic efficiency of the PID controller, it's control coefficients optimized using the SSA. For optimizing this controller, an objective function defined based on the integral of time multiplied by absolute error (ITAE) criterion. In accordance with Eq. (24.19), in the simulation time interval and under microgrid disturbances along with the uncertain output of renewable resources, the area under the frequency deviation curve is considered as the controller optimal criterion.

$$J = \int_0^{120} t \times |\Delta f| \, dt \tag{24.19}$$

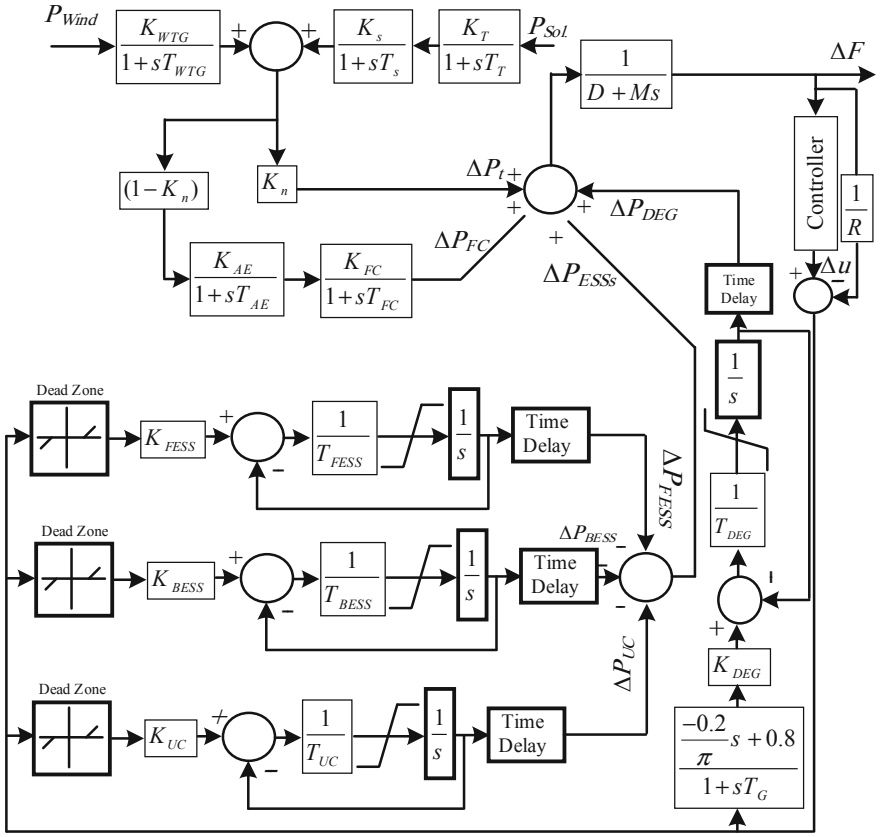

Fig. 24.14 The block diagram of the considered HMG

Table 24.1 SSA based control parameters of PID controller

Parameter	K_p	K_i	K_d
Value	4.9834	4.6713	3.6949

The optimization of PID controller, which has three control parameters, namely K_p, K_i, and K_d, can be formulated as the constrained optimization problem of Eq. (24.20).

$$\begin{aligned} &\text{minimize} \quad J \\ &\text{subject to:} \quad 0 < K_p, K_i, K_d < 5 \end{aligned} \tag{24.20}$$

The optimization problem of Eq. (24.20) is solved by SSA with 50 initial populations and 50 iterations. The optimization result and the convergence process of the objective function are shown in Table 24.1 and Fig. 24.15, respectively.

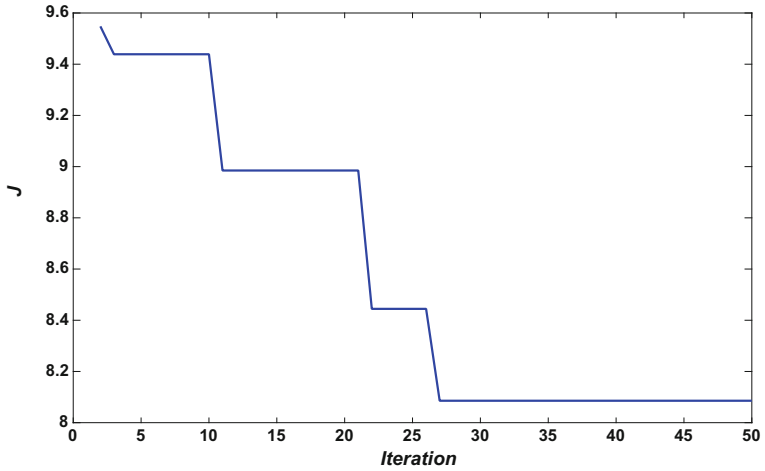

Fig. 24.15 The convergence curve of the objective function

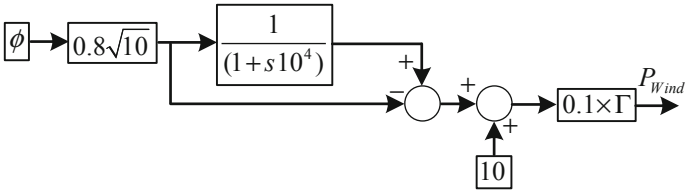

Fig. 24.16 The Simulink block diagram for uncertain wind speed generation

24.7 Results and Discussion

Finally, in order to assess the RL controller's ability for mitigation of the frequency deviations, first, the dynamic equations of the microgrid of Fig. 24.14 are simulated in MATLAB R2015b environment. Then the superiority of the proposed controller is proved in realistic scenarios compared to the traditional PID controller. It should be noted that the simulation time step and sampling time are considered equal to 1 and 50 ms, respectively. Moreover, in computer simulations, physical constraints on energy storage devices and DEG, including dead band and generation rate constraints, are considered. For this reason, the dead band is considered equal to 20 ms and located at the input of the devices and GRC is considered as 0.02, 0.005, 1.2, and 0.001 for FESS, BESS, UC, and DEG, respectively. In addition, variable wind speed and solar radiation have been created using Eqs. (24.21) and (24.22), respectively. Figures 24.16 and 24.17 show the Simulink diagram who generates the wind and solar powers, respectively. More details are given in [20].

$$P_{wind} = (((0.8\sqrt{10} \times \phi \times (1 - \frac{1}{10^4 s + 1})) + 10) \times \frac{1}{10}) \times \Gamma \tag{24.21}$$

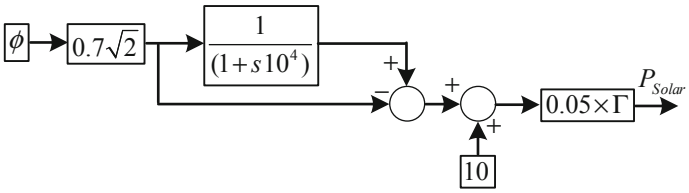

Fig. 24.17 The Simulink block diagram for uncertain solar radiation generation

where, $\phi \equiv U(-1, 1)$, and Γ is a function of Heaviside step function.

$$P_{sol.} = (((0.7\sqrt{2} \times \phi \times (1 - \frac{1}{10^4 s + 1})) + 10) \times \frac{1}{20}) \times \Gamma \tag{24.22}$$

where, $\phi \equiv U(-1, 1)$.

24.7.1 Analysis Case #1: Performance of the Controllers in Nominal Conditions of the HMG

In this Case, it is assumed that all the elements exist in the HMG are in their nominal conditions. The renewable resources don't have production from the beginning, and they start production at time 25 s according to the pattern shown in Fig. 24.18. Moreover, the sudden load changes of 10 and 20% occur at seconds 5 and 65, respectively.

Under those circumstances, the dynamic frequency response of the proposed control strategy is shown in Fig. 24.19 compared to traditional PID controller.

As shown in Fig. 24.19, it is obvious that in the first overshoot/undershoot after disturbance, the performance of the RL has a mild superiority over the PID control

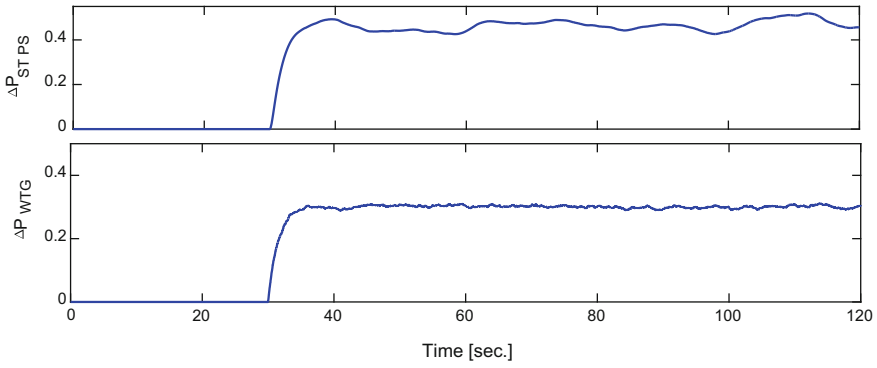

Fig. 24.18 The renewable resources production in analysis case #1

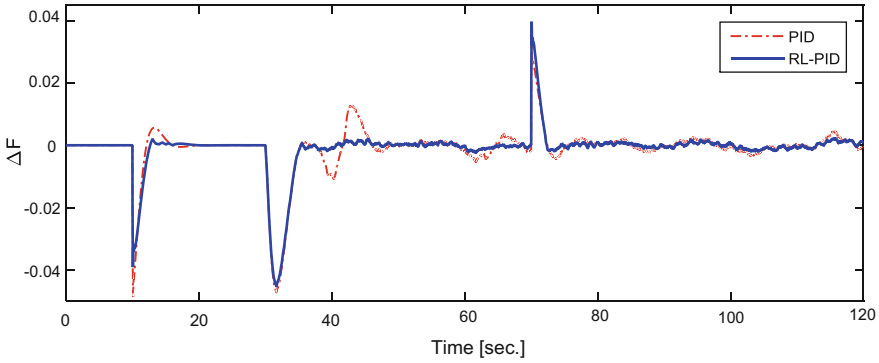

Fig. 24.19 The dynamic response of the proposed control strategy compared to the PID controller in analysis case #1

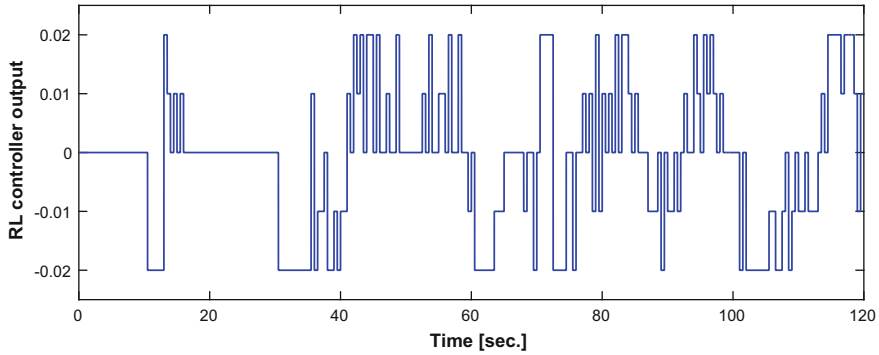

Fig. 24.20 The optimal control signal generated by the RL controller during simulation time in analysis case #1

method. This is due to the delay in detecting the turmoil by the intelligent agent. From Fig. 24.19, after few sampling steps, Δf is going out of the normal range and the controller recognizes the disturbance, then the intelligent agent immediately begins to apply a supplementary control signal to improves the dynamics of the system. Figure 24.20 shows the output signal of the RL controller during simulation time.

Comparing Figs. 24.19 and 24.20, it is evident that the controller is inactive and when the frequency oscillations start, it will be activated. In the time interval of 0–5 s, which disturbance has not yet occurred, the RL controller is inactive (its output is zero). Once turbulence is triggered, it will be activated and performs the optimal control policy. The output power of various ES devices along with DEG is shown in Fig. 24.21.

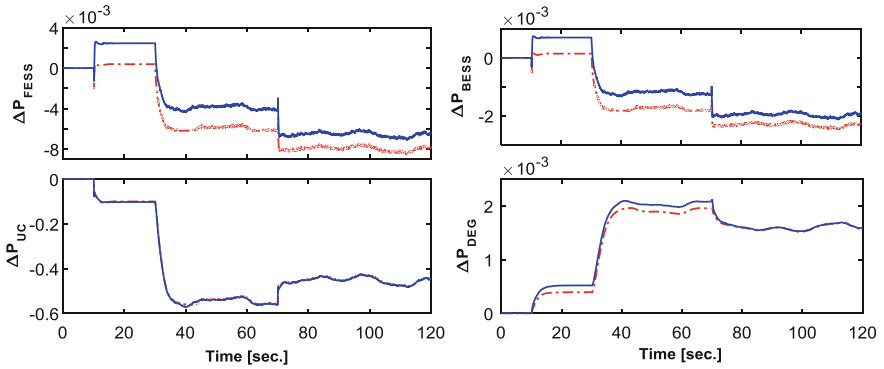

Fig. 24.21 The power absorbed/supplied by ES devices and DEG in analysis case #1; solid: RL and dashed-dotted: PID

24.7.2 Analysis Case #2: Performance of the Controllers in Presence of Changing in HMG Components

As can be seen from Fig. 24.21, the output power of UC is much more than the other ES devices. Thus, UC parameter changing can be considered as the worst test case for robustness of the controllers against system parameter changes. Therefore, in this Case, 2% increase in the gain along with a 2% decrease in the time constant of UC energy storage device are assumed. All the other conditions are as same as the conditions of Case #1. Figure 24.22 shows the frequency deviation of the HMG with two control methods.

Figure 24.22 shows that the changes in the UC parameters have caused the frequency oscillations to be continued more in comparison with Case #1 after disturbance. Under those circumstances, it is evident from Fig. 24.22 that the

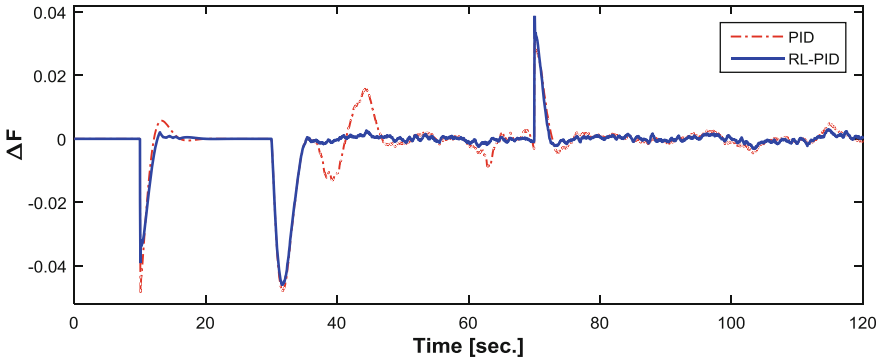

Fig. 24.22 The dynamic response of the proposed control strategy compared to the PID controller in analysis case #2

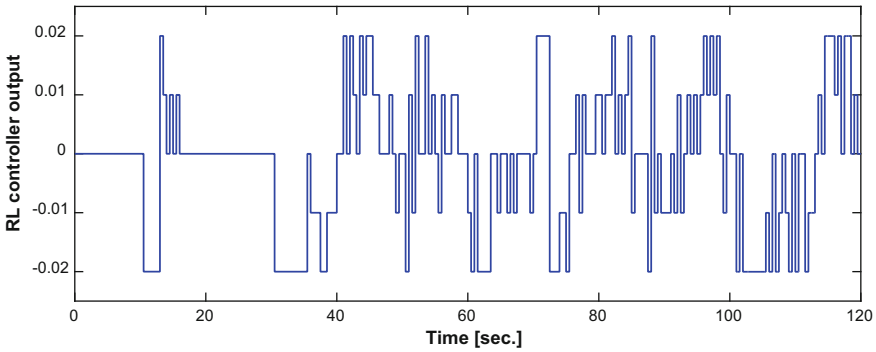

Fig. 24.23 The optimal control signal generated by the RL controller during simulation time in analysis case #2

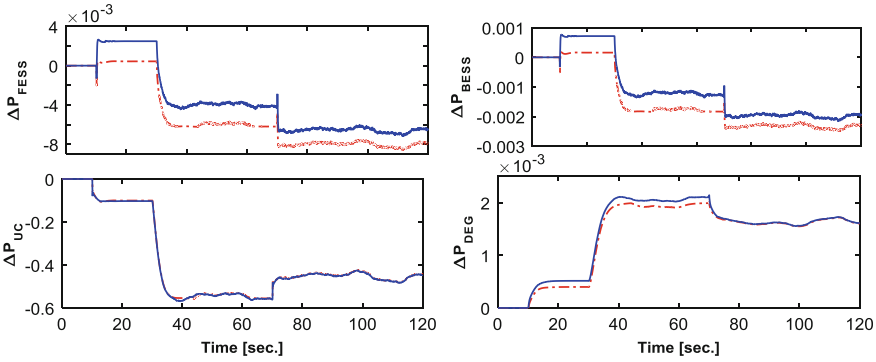

Fig. 24.24 The power absorbed/supplied by ES devices and DEG in Scenario 2; solid: RL and dashed-dotted: PID

dynamic performance of the proposed control mechanism is superb compared to the PID control method. Further, the optimal control signal of the RL and the power absorbed/supplied by ES devices and DEG are shown in Figs. 24.23 and 24.24, respectively.

24.7.3 Analysis Case #3: Performance of the Controllers with Large Variations in the Output Power of the Renewable Resources Along with the Pattern Load Changes

In this Case, in order to demonstrate the excellent performance of the proposed controller compared to the classical PID controller, a challenging condition is produced

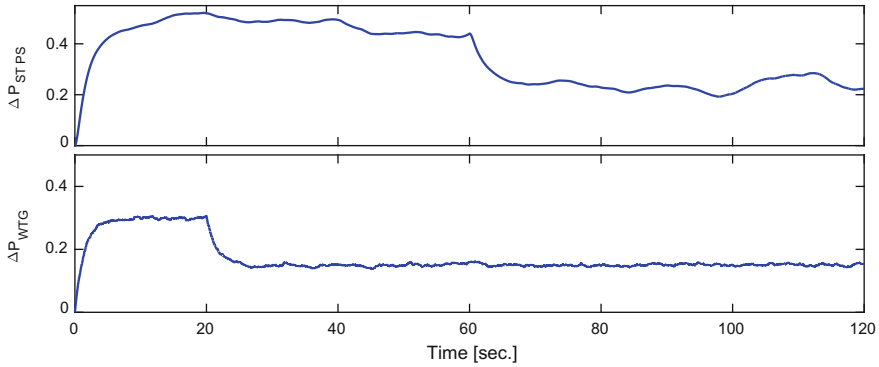

Fig. 24.25 The renewable resources production in analysis case #3

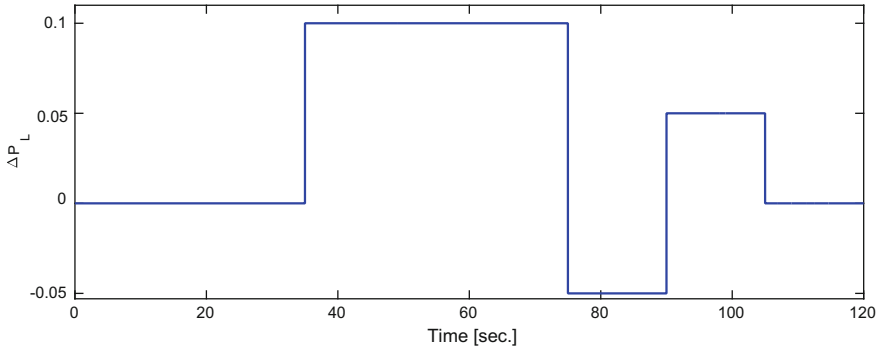

Fig. 24.26 The load variation pattern in analysis case #3

by sudden decreasing the output power of WTG and STPS by 13 and 15% in seconds 20 and 60, respectively. Figure 24.25 shows the power generated by renewable resources in Case #3. Additionally, to make a more realistic scenario a pattern load change in accordance with Fig. 24.26 is considered. The performance of the two control strategies is shown in Fig. 24.27.

24.7.4 Discussion

As can be seen in some cases of simulations, the proposed RL control method has a mild superiority over the other PID controller. For this reason, in order to demonstrate the superiority of the RL control structure compared to the PID controller, four appropriate numerical criteria are chosen and computed for all scenarios.

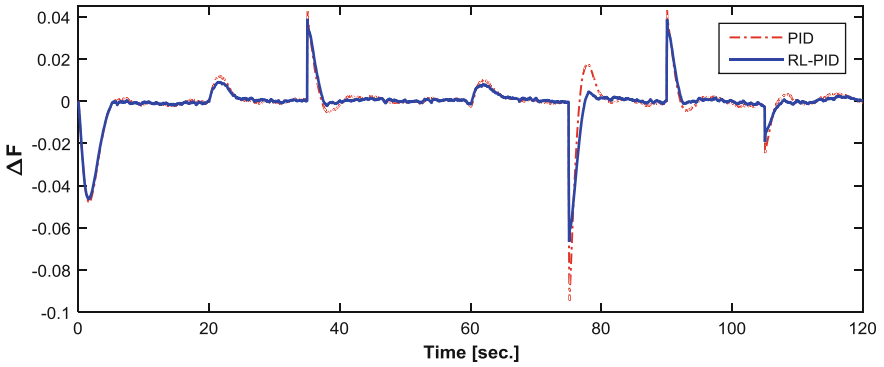

Fig. 24.27 The dynamic response of the proposed control strategy compared to the PID controller in analysis case #3

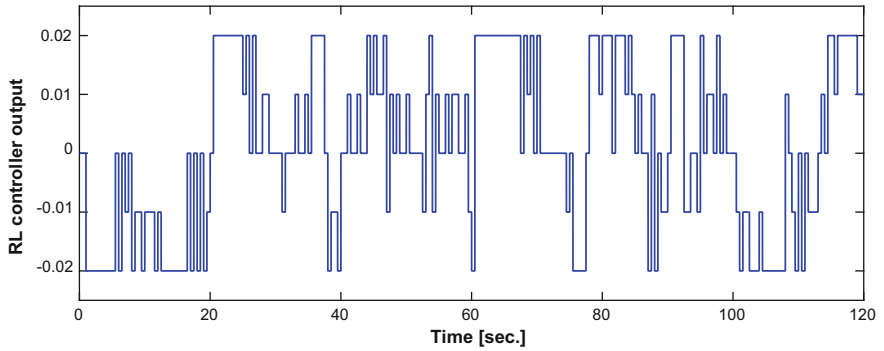

Fig. 24.28 The optimal control signal generated by the RL controller during simulation time in analysis case #3

The optimal control signal generated by the RL controller and the powers absorbed/supplied by ES devices and DEG are shown in Figs. 24.28 and 24.29, respectively.

Integral of squared error (ISE), ITAE, overshoot (OS) and undershoot (US) are the criteria which are computed according to Eqs. (24.23)–(24.26), respectively. Table 24.2 shows the numerical time domain analysis of the dynamic performance of the proposed RL controller compared to PID in damping of hybrid microgrid frequency deviations.

$$ISE = 1000 \times \int_0^{t_{sim}} (\Delta f)^2 dt \tag{24.23}$$

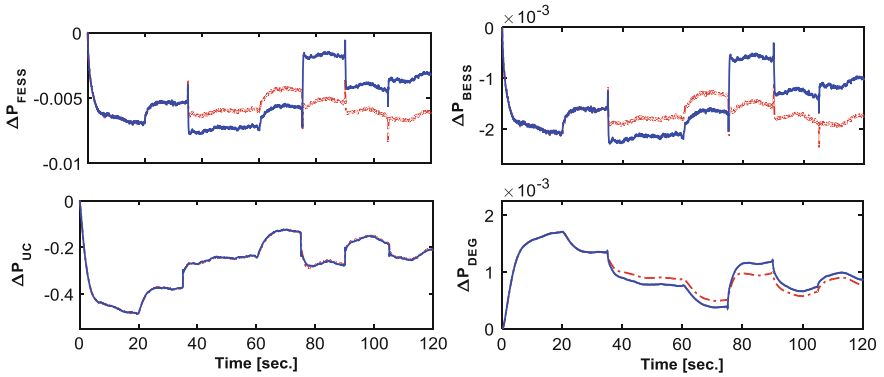

Fig. 24.29 The powers absorbed/supplied by ES devices and DEG in analysis case #3; solid: RL and dashed-dotted: PID

Table 24.2 Time domain performance indices for RL controller compared to PID

	Control method	Scenario 1	Scenario 2	Scenario 3
ISE	PID	14.959	15.038	17.271
	RL	5.888	5.607	4.985
ITAE	PID	9.96407	10.32941	31.8615
	RL	5.23144	5.36027	15.92594
OS	PID	9.23	9.11	4.26
	RL	9.00	8.95	4.00
US	PID	5.00	5.24	7.08
	RL	3.8	3.9	6.68

$$ITAE = \int_0^{t_{sim}} t \cdot |\Delta f| dt \tag{24.24}$$

$$OS = \max(\Delta f) \times 100 \tag{24.25}$$

$$US = |\min(\Delta f)| \times 100 \tag{24.26}$$

where, t_{sim} is equal to 120 in all Analysis cases.

As can be seen in Table 24.2, the dynamic response of the RL controller has a remarkable superiority over the PID control method. In the final analysis, in order to emphasize the superiority of the proposed controller compared to the PID controller, the results shown in Table 24.2 are statistically analyzed. In this regard, it can be seen that the RL controller has improved the index ISE 60, 62, and 71% in Analysis cases 1, 2, and 3, respectively. In the view of ITAE index, frequency deviations have been improved by approximately 50% in all three scenarios. It must be noted that the US and OS were calculated in the worst case of each controller. As can be seen,

the OS index has been decreased by approximately 2–6% in all Cases. Similarly, the RL controller has enhanced the US of the frequency deviations by 24, 25, and 5% in Cases 1, 2, and 3, respectively. In conclusion, as shown above, the proposed consistent mechanism based on RL can optimally control the frequency deviations of a hybrid microgrid with high penetrations of renewable and storage energy devices.

Another Key point is that this simple and portable controller can be applied to the classical existent controllers to make them robust and adaptive with an excellent dynamic performance.

24.8 Conclusion

The precise coordination of the mechanisms for controlling renewable resources and energy storages for suppressing the oscillation of frequency in the hybrid microgrids is always considered as a challenge due to uncertainties in the wind and solar power. This challenge needs the advanced and intelligent control methods for damping the grid frequency deviations. For this reason, this Chapter is suggested an RL based control mechanism for controlling the frequency of hybrid microgrids. The suggested control strategy integrates the RL features with the traditional PID controller and provides a simple, model-free, adaptive, and robust control method against system parameter changes and operating conditions. In this paper, the RL controller is added to a traditional PID controller as a complementary controller. Because the PID controller has a satisfactory performance in addition to its simple structure and extensive use in the industry. Eventually, in order to evaluate the effectiveness of the proposed controller, a hybrid microgrid with high penetration of renewable and energy storage devices and physical limits such as GRC, GDB and time delay was modelled. Then several realistic scenarios and challenging conditions were considered to demonstrate the excellent dynamic performance of the proposed RL based controller compared to classical PID controller that was optimized using SSA. Simulation results expressively demonstrate the superiority of the proposed control mechanism compared to PID control method under different operating conditions and uncertainties of the system parameters. In the final analysis, suitable numerical time domain criteria such ISE, ITAE, OS, and US were calculated for the two control methods. Clearly, the results confirm the superiority of the proposed control method. As can be seen, the proposed controller has improved the ITAE and ISE more than 50% in different operating conditions. In addition, OS is enhanced 2–6% in all Cases. Also, US, the other considered performance index has been decreased by more than 20% in all conditions. Thanks to its simple and portable structure, the RL controller can be applied as a supervisory controller to any other control system to improve its performance.

For future works, our focus will be on the other solution methods of reinforcement learning and application of multi-agent learning in controlling microgrids.

References

1. D. Ernst, Near Optimal Closed-Loop Control Application to Electric Power Systems. Ph.D., Department of Electrical and Electronic Engineering, Informatique Institut Montefiore, Liege, Belgium (2003)
2. D. Ernst, M. Glavic, L. Wehenkel, Power systems stability control: reinforcement learning framework. IEEE Trans. Power Syst. **19**, 427–435 (2004)
3. A. Younesi, H. Shayeghi, Q-learning based supervisory PID controller for damping frequency oscillations in a hybrid mini/micro-grid. Iran. J. Electr. Electron. Eng. **01**, 126–141 (2018)
4. A. Younesi, H. Shayeghi, M. Moradzadeh, Application of reinforcement learning for generating optimal control signal to the IPFC for damping of low-frequency oscillations. Int. Trans. Electr. Energy Syst., e2488-n/a (2017)
5. R. Hadidi, B. Jeyasurya, Reinforcement learning based real-time wide-area stabilizing control agents to enhance power system stability. IEEE Trans. Smart Grid **4**, 489–497 (2013)
6. J.G. Vlachogiannis, N.D. Hatziargyriou, Reinforcement learning for reactive power control. IEEE Trans. Power Syst. **19**, 1317–1325 (2004)
7. V. Nanduri, T.K. Das, A Reinforcement learning model to assess market power under auction-based energy pricing. IEEE Trans. Power Syst. **22**, 85–95 (2007)
8. M. Esmaeili, H. Shayeghi, H. Mohammad Nejad, A. Younesi, Reinforcement learning based PID controller design for LFC in a microgrid. COMPEL Int. J. Comput. Math. Electr. Electron. Eng. **36**, 1287–1297 (2017)
9. H. Shayeghi, A. Younesi, An online Q-learning based multi-agent LFC for a multi-area multi-source power system including distributed energy resources. Iran. J. Electr. Electron. Eng. (Iran University of Science and Technology) **13**, 385–398 (2017)
10. S. Mirjalili, A.H. Gandomi, S.Z. Mirjalili, S. Saremi, H. Faris, S.M. Mirjalili, Salp swarm algorithm: a bio-inspired optimizer for engineering design problems. Adv. Eng. Softw. **114**, 163–191 (2017)
11. J.J. Castillo Zamora, K.A. Camarillo Gomez, G.I. Perez Soto, J. Rodriguez Resendiz, Comparison of PD, PID and sliding-mode position controllers for V-Tail quadcopter stability. IEEE Access **6**, 38086–38096 (2018)
12. C. Weber, M. Elshaw, N.M. Mayer, *Reinforcement Learning, Theory and Applications* (I-TECH Education and Publishing, 2008)
13. L.P. Kaelbling, M.L. Littman, A.W. Moore, Reinforcement learning: a survey. J. Artif. Intell. Res. **4**, 237–285 (1996)
14. R.S. Sutton, A.G. Barto, *Reinforcement Learning: An Introduction* (MIT Press, 2005)
15. C.J.C.H. Watkins, P. Dayan, Technical note: Q-learning. Mach. Learn. **8**, 279–292 (1992)
16. A. Younesi, H. Shayeghi, M. Moradzadeh, Application of reinforcement learning for generating optimal control signal to the IPFC for damping of low-frequency oscillations. Int. Trans. Electr. Energy Syst. **28**, e2488 (2018)
17. A.M. Parimi, Modeling and Control of Interline Power Flow Controller for Power System Stability Enhancement. Ph.D. Thesis, University Teknologi Petronas (2011)
18. J.M. Vidal, *Fundamentals of Multiagent Systems* (2010), http://jmvidal.cse.sc.edu/papers/mas.pdf
19. I. Pan, S. Das, Fractional order fuzzy control of hybrid power system with renewable generation using chaotic PSO. ISA Trans. **62**, 19–29 (2016)
20. D.C. Das, A.K. Roy, N. Sinha, GA based frequency controller for solar thermal–diesel–wind hybrid energy generation/energy storage system. Int. J. Electr. Power Energy Syst. **43**, 262–279 (2012)

Part III
Microgrid Protection Systems

Chapter 25
Microgrid Protection

Horia Andrei, Marian Gaiceanu, Marilena Stanculescu, Ioan Marinescu and Paul Cristian Andrei

Abstract The power system remained far beyond in adopting new technologies in key domains such as: automation, information technology and telecommunications. Globally, energy demand is constantly increasing and nowadays the power system has developed according to past and present needs. But, this has to be changed in order to adapt to the future rapid evolutions: today's digitized society need efficient, scalable and resilient power systems, because, without it, our life style will reduce to an almost medieval existence. The difficulty and complexity of the power system transition from the traditional to the intelligent system consists in the fact that this must be done in order to solve the present problems and to prevent those which the system might face in the future by allowing the new technological innovations. All of this must take place while the system is in operation, without affecting the consumers. Among the risks associated with the traditional power system, based on a small number of large power stations, we mention the need to implement some power plants to take over the over-consumption (peaks), with major disadvantages. Some of the disadvantages can be summarized as follows: they only work temporarily; they do not easily depreciate their costs; low resiliency (e.g. collapse of the system, for natural reasons, or a malfunction in the production or transport chain. Microgrids come with added value through protection, resilience and low cost due to the avoidance of power

H. Andrei (✉) · I. Marinescu
Doctoral School of Engineering Sciences, University Valahia of Targoviste, Targoviste, Romania
e-mail: hr_andrei@yahoo.com

I. Marinescu
e-mail: ioan.marinescu@yahoo.com

M. Gaiceanu
Department of Automation and Electrical Engineering, Dunarea de Jos University of Galati, Galati, Romania
e-mail: marian.gaiceanu@ugal.ro

M. Stanculescu · P. C. Andrei
Department of Electrical Engineering, Polytechnic University of Bucharest, Bucharest, Romania
e-mail: marilena.stanculescu@upb.ro

P. C. Andrei
e-mail: paul.andrei@upb.ro

N. Mahdavi Tabatabaei et al. (eds.), *Microgrid Architectures, Control and Protection Methods*, Power Systems,
https://doi.org/10.1007/978-3-030-23723-3_25

cuts which, with respect to each sector of activity, generate significant financial losses in case of occurrence. About these challenges and the link between the connectivity of microgrids and the risks they are exposed to, the authors refer in the second paragraph of this chapter. Taking into account the technical requirements of the microgrids, protection solutions for both DC and AC currents will be presented. The level of pollution which our planet is facing imposes certain standards that change the approach of some industries. For example, in the transport sector, the authorities prohibit or impose extra-charges for cars with diesel engines and provide aid for the purchase of electric cars. Such a car raises the electricity needs of a home a few times, the colder winters and hotter summers put pressure on the system again, increasing the likelihood that the power system will crash. Therefore, reference will be made to the appropriate standards to which these protections should be aligned. At the end of the chapter, development trends in this area will be mentioned. The microgrids solve many problems of the classic power system because a power system made up of a microgrids array acts as a whole and, in the event of a problem, it disconnects from the system without propagating up. The probability of the occurrence of a power cut is much diminished because, for example, as in the case of Denmark, the system is decentralized and a problem can be propagated at most on the local level, not nationally, and the energy storage component in the microgrids ensures good functioning during peak periods as well as in the event of a public network failure. Besides certain advantages of implementing microgrids, they come also with new threats from the cyber spectrum, with increased complexity, threats which other sectors have already faced and found solutions. Such examples are given in the fourth paragraph. The chapter ends with conclusions and a large number of references in the field of microgrids protection.

Keywords Microgrid · Connectivity · Protection · Standards

25.1 Introduction

The introduction will highlight the close connection between the Internet of Things (IoT) and the development of the smart grids and present the methods for increasing the robustness (resiliency) of power system (PS) to extreme disruptions and shocks posed by natural, manmade, or random events, problems solved by this kind of approach and the protection against the new ones.

The PS remained far beyond in adopting new technologies in key domains such as: automation, information technology and telecommunications. Globally, energy demand is constantly increasing and nowadays the PS has developed according to past and present needs. But, this has to be changed in order to adapt to the future rapid evolutions: today's digitized society need efficient, scalable and resilient PS, because, without it, our life style will reduce to an almost medieval existence.

The difficulty and complexity of the PS transition from the traditional to the intelligent system consists in the fact that this must be done in order to solve the present problems and to prevent those which the system might face in the future by allowing the new technological innovations. All of this must take place while the system is in operation, without affecting the consumers. Among the risks associated with the traditional PS, based on a small number of large power stations, we mention the need to implement some power plants to take over the over-consumption (peaks), with major disadvantages. Some of the disadvantages can be summarized as follows: they only work temporarily; they do not easily depreciate their costs; low resiliency (e.g. collapse of the system, for natural reasons, or a malfunction in the production or transport chain). Microgrids come with added value through protection, resilience and low cost due to the avoidance of power cuts which, with respect to each sector of activity, generate significant financial losses in case of occurrence. About these challenges and the link between the connectivity of microgrids and the risks they are exposed to, the authors refer to the following Section as the first objective of this chapter.

The next objective is to present protection solutions closely with international standards for both Direct current (DC) and Alternating current (AC) network, considering the technical requirements of the microgrids and by using different topology. The level of pollution which our planet is facing imposes certain standards that change the approach of some industries. For example, in the transport sector, the authorities prohibit or impose extra-charges for cars with diesel engines and provide aid for the purchase of electric cars. Such a car raises the electricity needs of a home a few times, the colder winters and hotter summers put pressure on the system again, increasing the likelihood that the PS will crash. Therefore, reference will be made to the appropriate standards to which these protections should be aligned. At the end of the Sect. 25.3 of this Chapter, development trends in this area will be mentioned.

The microgrids solve many of the problems of the classic PS because a PS made up of a microgrids array acts as a whole and, in the event of a problem, it disconnects from the system without propagating up. These aspects represent the third objective of this chapter which is presented in Sect. 25.4. The probability of the occurrence of a power cut is much diminished because for example in several national grid the PS is decentralized and a problem can be propagated at most on the local level, not nationally, and the energy storage component in the microgrids ensures good functioning during peak periods and for PS failure. Besides certain advantages of implementing microgrids, they come also with new threats from the cyber spectrum, with increased complexity, threats which other sectors have already faced and found solutions. Such examples are given in this Section.

Conclusions are drawn in Sect. 25.5. The chapter ends with a large number of references in the field of microgrids protection.

25.2 Connectivity and Risks of Microgrids

The role of safety and resiliency of the PS under the conditions of transition from the classic grid to intelligent microgrids is a concept which is already applied in other sectors but which makes its way harder in the PS sector. In this respect, the connectivity and risks of the microgrids are tightly bound, together with the definition of IoT new concept in the progress of smart grids, the exposure of the growth methods of the PS resiliency, as well as the approach of the evolution towards the smart grid in a globalized word, are the problems which must be addressed [1].

The PS has lagged behind in what concerns the adoption of new technologies from the domains of automation, information technology and telecommunications. At a global level, the energy demand is in a continuous increase and until now the PS developed depending on the past and present necessities, but it must adapt to the rapid evolutions from the future; the contemporary digitized society, in a continuous evolution, needs an efficient PS, scalable and resilient, because without this, the lifestyle we have become accustomed to might reduce to an almost medieval existence.

The pollution level which the planet is confronted with imposes certain standards which modify the approach of some industries. For example, in the transportation domain, the authorities forbid or put supplementary fees to Diesel automobiles and offer grants for acquiring electric vehicles. Such a vehicle raises the electrical energy demands of a residence a couple of times. Colder winters and hotter summers also put pressure on the system, increasing its probability to fail in the peak loads.

In the traditional PS, electrical energy must be used when it is produced, because until recently there were no solutions to store this energy at an industrial lever at an acceptable price. Among the associated risks of the traditional PS, based on a limited number of large plants, we remind the necessity of starting up some plants built as back-ups for taking over the peaks, which operate only temporary and don't cushion their costs easily, as well as the system collapse (low resiliency level) when, because of natural or anthropic reasons, a malfunction is produced on the production or transport chain. The PS based on microgrids add value through protection, resiliency and low cost due to the avoiding of power failures, which, referred to every sector of activity produce significant financial losses in case of occurrence [2].

The difficulty and complexity of the PS transition from the traditional state to smart system consists in the fact that it must be done in order to solve the current problems but also to prevent problems which the system might face in the future, allowing the implementation over the course of new technological innovations, all these while the system is operating and the consumers are not affected.

The microgrids solve by themselves a lot of such issues because PS composed of a microgrid matrix operates as a whole in usual utilization and, in the case a problem occurs, it disconnects from the system without the power failure propagation. The probability of a failure occurrence is much diminished, because, like the case of Denmark, the system is decentralized (as is shown in Fig. 25.1) and a problem might propagate at most locally, not nationally, and the energy storage component in

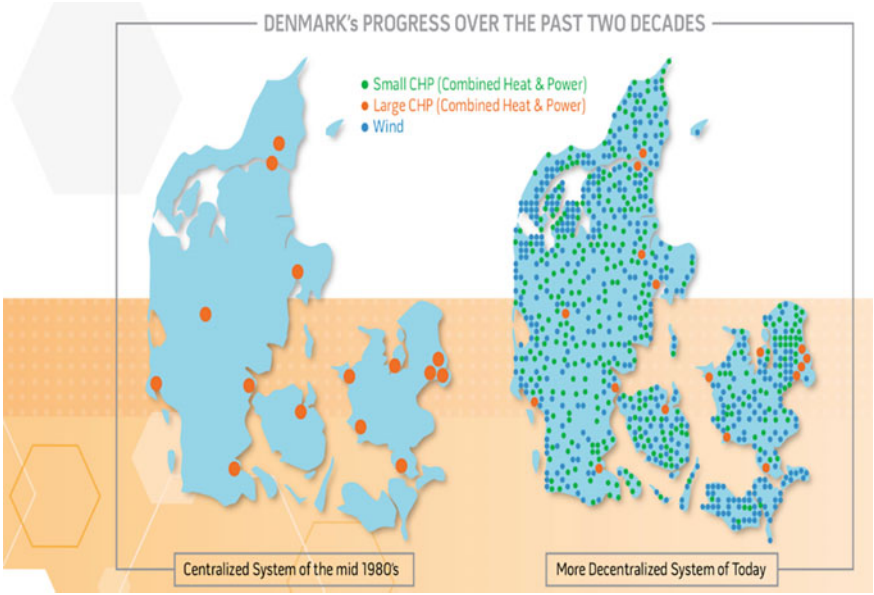

Fig. 25.1 Decentralization of PS in Denmark [26]

microgrids assures the good functioning in the peak periods as well as in the event of a out of order to the public grid [3, 4].

Besides the clear advantages regarding microgrid implementations, these also bring new threats from the cybernetic spectrum, with increased complexity, but with which other sectors already confronted and to which solutions exist.

The companies involved in the national PS as well as the commercial and industrial users search for new modern methods through which they produce, distribute and consume energy, preparing the transition from traditional technologies to innovative ones which increase the reliability and network efficiency. Such an advanced system offers safety in functioning, resiliency and cost economies, being represented by microgrids.

These can be built for functioning in two states: the network connected mode (most of the time) and island mode (when a malfunction is propagated through the system, affecting the electrical energy quality parameters of if the national system collapses).

Regardless of the operating mode of a network in which a microgrid works, the energy storage has an essential role in the system's success [5].

A microgrid is composed of the following parts:

- distribution automation;
- a control system;
- alternative generation;
- energy storage.

While all these individual components are important, the dynamic energy storage system represents the innovative part which serves as the backbone of the microgrid because it comes into operation at:

- the cease of generation from alternative sources (for example bad meteorological conditions which halt or diminish the wind turbines or photovoltaic panels generating capacity);
- during nighttime;
- during daytime, for taking over the peak loads;
- in case of a failure propagation in the national PS.

DC microgrids offer numerous advantages in the contemporary digitized world; however, DC is facing challenges in what concerns the integration in a market in which AC is prevailing.

Although the national PS had been designed and built in AC, DC is widely used in high power industrial electrical machines, equipment and engines from the transport sector (railway, underground or surface) all over the world are built for operating in DC. The use of local energetic resources and DC microgrids reduce the losses during remote transport as well as those from step-up and step-down transformers, therefore being more efficient.

25.3 Microgrid Protection Solutions: Standards

In classical power distribution systems (passive energy grids), electrical energy is supplied from high voltage levels to loads connected to medium/low voltage grids. These systems are not able to connect the power sources. The topology of classical distribution systems is configured based on economic considerations and reliability required by the consumers. In energy systems, the most widely used energy distribution topology is the radial one [6].

System protection using the radial topology shown in Fig. 25.2.

The radial system is characterized by one-way energy circulation: from the power source to the load. This topology has the disadvantage of interrupting the power supply when a fault occurs. As a consequence, the functioning of the relays should

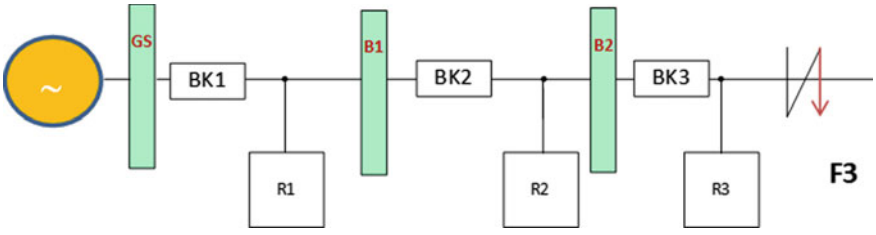

Fig. 25.2 Radial topology

be correctly hierarchized over time. The minimum amount of time that can be allowed for two consecutive switches depends on their own release time, plus a safety margin. When the failure occurs at bar B2, the overcurrent relay R3 should function first, without the action of the other relays. Therefore, the time necessary for the R3 relay to operate must be less than the time required by R2 relay and so on. This indicates that the time required by the operation of these relays must be correctly classified.

In microgrids there are also the parallel and ring topologies, as are presented in Fig. 25.3 respectively in Fig. 25.4 [7].

25.3.1 System Protection Using the Parallel Topology

The connection in parallel of the power supply is mainly used to ensure the power continuity and load distribution. At the moment of the fault occurrence at the protection feeder, the protection circuit will select and isolate the fault at the appropriate feeder. As a consequence, the remaining feeder will immediately assume an increased loading. One of the simplest protection methods using relays is the overload relay (R) with time function. The characteristic of the R is inverse time at the end of the power transmission. The directional relays are placed at the receiving end, as shown

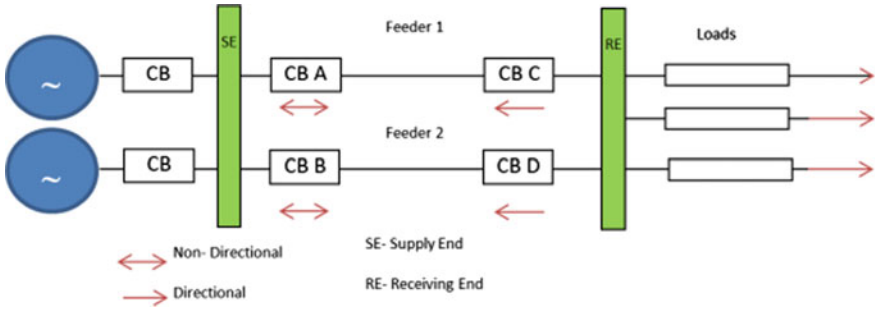

Fig. 25.3 Parallel topology

Fig. 25.4 Ring topology

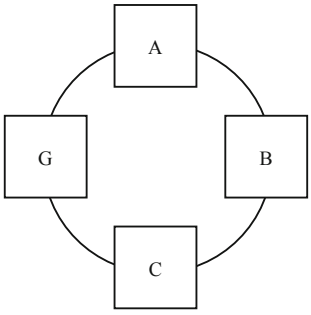

in Fig. 25.3. By supposing that a major fault F appears on one of the lines, the energy is fed into the fault both: from the transmitting and from the receiving ends of the line. The direction of the power flux will be reversed through relay D, which will be open. The excess current is then limited to B until the overload relay is operating and triggers the circuit breaker (CB), completing isolating the faulty feeder ensuring the power supply through the healthy feeder. This method is satisfactory only when the fault is strong and changes the direction of the circulation of the power *D*. Therefore, at both ends of the feeders, a differential protection is added together with the overload protection.

25.3.2 System Protection Using the Ring Topology

The ring topology consists of a series interconnection between power plants through another route. In the main system of the ring, the direction of the power can be change at discretion, especially when interconnection is being used. The elementary diagram of such a system is shown in Fig. 25.4, where *G* is the *generation station* and *A*, *B* and *C* are *substations*. At the generation station, the power flow has only one direction, and therefore, no overload relays with time delays are used. The overload relay, from the time point of view is placed at the end o the station and will only start when the overload arises at the station it protects. Circulating around the ring following the direction *GABCD*, the relay placed on the lateral side of each station is set with decreasing time offsets. At the generation station: 1.5 s, at stations *A*, *B*, *C*: 1, 0.5 s and, respectively instantaneously. Similarly, around the ring in the opposite direction if a fault appears in point *F*, the power *F* is supplied in the fault via two paths: *BFC* and *CFB* respectively. The relay which functions is the one between station *B* and the fault point *F* and station *C* and fault point *F*. Thus, the failure of any section will determine the functioning of the relay from that section, the rest of the sections will operate uninterruptedly.

The operations modes of the microgrids are: grid-connected and isolated. In the case of fault condition into the grid, the island operation mode will be selected. The switching between the above-mentioned operations modes will assure the continuity of the power supply for the emergency loads, but the traditional system cannot be efficient in both modes of energy circulation [6]. If the microgrid operates in the islanding mode, the values of the short-circuit currents are smaller than the case of the grid connected operation mode [8]. Considering this aspect, the protection system cannot detect all malfunctions.

In addition, in most cases, the energy fluxes in microgrids are bidirectional. Relocation strategies used in the conventional distribution systems cannot be applied to protect the microgrids. The high complexity of the protection system derives from the fact that depends on the changes into the grid: topology, equipment interruptions, fault events, charging, and PS stability. For this reason, different protection principles are applied to design and implement of the protection system. The grid voltage levels (low-LV, medium-MV, and high-HV) affect the cost of the protection system.

As a consequence of the increased costs for the HV equipment the corresponding protection system is more expensive than in the LV equipment. Nowadays, the digital systems are incorporated into the protection relays. Therefore, one relay may have many embedded functions. From the cost point of view the use of the modern digital relay into the LV grid is not an acceptable solution.

The protection of the systems can assure locally the protection of the unit, and globally the protection of the system [6]. The protection of the unit is necessary to protect an equipment or an area in a system, but there is no need to establish the hierarchy time with other protection relays, for example the differential relay. Examples include protection of: power supply transformer, energy transport line, generator or collector bars.

The system protection is made up of hierarchized time relays in order to protect a number of connected pieces of equipment; overload and distance relays are examples of system protection.

The system's protection schemes are not precisely delimited. One basically protection system incorporates the current measurement and includes into the protection process an inverse time characteristic. In this manner, the operation of that protection which is closest to the fault is allowed.

The protection scheme includes the following:

(a) The overcurrent time-hierarchized protection.
(b) The overcurrent time-hierarchized protection by its level.
(c) Distance or impedance protection.

25.3.3 Microgrids Specific Problems

Local and global protections may assure the integrity of the protected equipment: the transformers and the generators. Both of them are normally protected by overcurrent and differential relays. At the LV distribution grid level, the equipment is protected downstream by fuses and upstream by overcurrent relays [8].

In the *distribution system* the grid is mainly in radial configuration. Depending on the operating trend the topology of the grid is changeable. But the operating trend depends on the *distributed generations* (DGs). For the conventional protection systems there are very big differences between radial systems and *distribution generators*. In the *distribution system* the overcurrent protection is assured by the fuse or relay. This type of protection depends on the current sensitivity.

In the *radial system*, there is a gradual difference between the values of the upstream and downstream fault current. This difference facilitates the classification of the overcurrent devices. In order to protect the radial system, the different algorithms of the overcurrent relays may be used. By introducing multiple algorithms increased protection flexibility is obtained. Therefore, the engineers in the field may use more degree of freedom in the designing process of the protection system.

DG grids, on the other hand, are complex configurations which determine the traditional protecting system not to be used. In case of failure, each DG will contribute to the defect according to its size and characteristics. In power electronics systems, the current value cannot exceed twice the nominal value.

The distribution of the DGs over the grid conducts to the current reversibility. Therefore, the complexity of the protection system through the overcurrent detection devices increases significantly.

Moreover, any moment, DG sources can be connected and disconnected on the grid. This causes considerable changes a short-circuit currents level.

25.3.4 Considerations Regarding Microgrid Protection

The protection system for a microgrid must consider the requirements for the design and regulation of the protection relays: simplicity, reliability, selectivity, redundancy, operating speed, sensitivity, and consistency.

Example 1 Maximum directional protection of bi-directional power lines.

The coordination of the overcurrent in case of the PS with two or more power sources placed in different locations becomes very difficult or impossible [9]. For example, one PS with two sources is considered, as depicted in Fig. 25.5, where B1, B2, B3 denotes the grid ramification nodes. It is assumed there is a defect at F1. It is desirable that the circuit breakers (BK) BK23 and BK32 flxeliminate the malfunction, such that the continuity of all three loads operation is assured. By using the time delayed overload relays, the BK23 trigger faster than BK21 (as it was previously set).

If a defect is considered at F2, the breaker BK23 works firstly (comparing with BK21) and the consumer C2 will be isolated (out of the PS). In case of feeding the fault from both ways (left, right) the overload relays cannot be a solution. By using the DORs, one solution can be provided. Thus, to each overload protection, a directional relay is added, relay which senses the power circulation direction and acts only if the power transfer takes place according to the admitted direction, exciting the corresponding time relay [10].

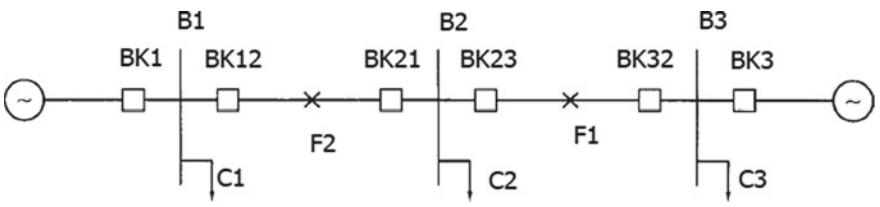

Fig. 25.5 Maximum directional protection of bi-directional power lines

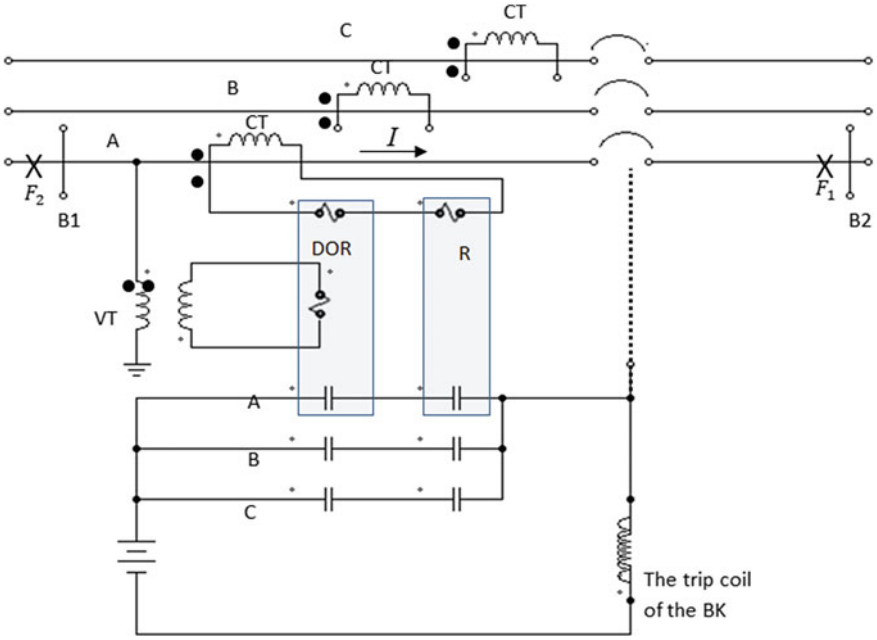

Fig. 25.6 Single phase (A) connection of the DOR

Example 2 In this example it will be studied the protection of the two-ways system with directional relay (D) and overload relay (R) with time characteristic.

It will be explained the way in which the directional and time delay relays can be used overtime to ensure the protection of the system depicted in Fig. 25.5. Also, there will be argued the relays which will be coordinated for a specific fault:

(a) F1;
(b) F2;
(c) Study of the protection system against failures at collecting bars;
(d) If the imminent faults appear to the "line" parts or in the "forward" direction of the breakers BK12, BK21, BK23 and BK32 they should respond adequately. For the above-mentioned breakers, the *directional overload relays* (DOR) can be used in the secondary of the current transformer (CT) (Fig. 25.6 [9]).

The DOR is connected in series with overcurrent relay (R) as it is presented in Fig. 25.6, such that the triggering coil of the breaker is powered if the current from the secondary of the CT satisfies simultaneously the below mentioned conditions: (I) exceeds the maximum value of the relay R, and (II) is in the forward triggering position.

For BK1 and BK3 the use of the overcurrent relays (R) is necessary for the protection task; therefore, the directional relays (DOR) are not used anymore.

(a) Considering the fault at F1 (Fig. 25.5), the relay BK21 does not operate; BK23 coordinates BK12, such that BK23 trigger firstly, i.e. before BK12 and BK1. At the same time, BK32 coordinates BK3.
(b) Considering the fault at F2 (Fig. 25.5), the relay BK23 does not work; BK21 coordinates BK32 with such that BK21 trigger firstly, i.e. before BK32 and BK3. At the same time, BK12 coordinates BK1.
(c) The other task of the DORs is to protect the PS from defects on the bars (B1, B2, B3). By supposing the defect appears on the collector bar B2, the BK21 and BK23 relays do not works. By contrast, the bar B1 is protected by both BK12 and BK32 by eliminating the supposed defect. At the same time, in order to eliminate the defect at B3, both BK3 and BK23 will work.

25.3.5 Protection Methods for AC Systems with Distributed Generations (DGs)

25.3.5.1 Protection Based on Voltage

The protection based on the voltage technique is delivered in [11]. For this method the Root Mean Square (RMS) voltage value from the DG terminals is measured all the time. The normal state is for the values greater than 88% of the RMS rated voltage value (the fault is outside of the considered area). If this value is greater than 88% of the rated voltage, it is considered a normal state; otherwise, it is considered as a fault near to DG. The control system of the DG will limit the output current. The performances of the protection methods based on the voltage measurement are independently from the direction or the value of the DGs current. Therefore, the grid voltage can be affected by transient cases (i.e. energizing of the dynamic load or the load commutation), not by the faults. The conclusion is that the protection methods based on the voltage measurement are sensitive to the transient incidents. The disadvantage is that the selective protection does not work.

25.3.5.2 Impedance or Distance Protection

This type of protection, the impedance one, takes part from the conventional protection systems in order to transport the energy through the transmission lines [12, 13]. The DGs can be introduced into the distribution systems in the same manner as in the transport networks (the energy can circulate in both ways). The distance relays can be used in applications where the DG's location determines the protection areas, for the active distribution systems. However, this method has the main disadvantage the effect introduced by the fault resistance into the impedance.

25.3.5.3 Differential Relays

Differential protection is used to detect the defects in a short period of time and it is independent of the size or location of the DGs [14]. As a conclusion, the differential relays are used to solve the protection limitations due to the existence of the DGs in the system.

25.3.5.4 Directional Protection Based on Overcurrent Relays R

As it is well-known, in the active distribution systems the current error can be powered from many sources and from different directions [15]. As a consequence, in the cases when each power supply incorporates more DGs the directional overcurrent relays have been used to determine the fault to the power supply.

25.3.6 DC Systems: Protection Techniques

The DC distribution grids cannot be efficiently protected by traditional protection techniques used in AC systems. Therefore, for these systems there are necessary methods for detecting/breaking the modified faults or to fully replace them.

25.3.6.1 Faults Breaking (Switching) Schemes

The main issue for protecting the DC systems is to choose the adequate scheme from the economical and rapid fault breaking point of views [16].

25.3.6.2 Static Power Converter Breaking (Switching) Schemes

The conventional, respectively the renewable energy sources are interfaced with DC systems through static power conversion systems. Consequently, in order to protect the main grid, the adequate control of the power converters can block the switching devices when the fault appears [17]. For the multi-port distribution systems, this method is not reliable because does not provide the adequate selectivity [18].

25.3.6.3 Blocking the Conversion Blocks Using AC Type Circuit Breakers (BK)

BKs' operation from the AC part (which has been introduced together with the converter blocking scheme) can offer an economical protection technique for the DC grids by using the voltage source converter (VSC). In this method, after fault's

apparition and VSC's blocking, the CBs situate on AC's side of the VCSs work to prevent the fault's supply through free circulation diodes. Although this method can interrupt the supply of the fault current from the AC side, this is not sufficiently rapid to prevent the deterioration of the free circulation diodes of the VSCs; this is because the working time of the MV BK is about several tens of milliseconds. The BK terminals from the AC side cannot interrupt the discharging current from the DC link capacitors.

Also, the selectivity problems represent the main weakness of this method.

25.3.6.4 Blocking the Converter Using BK's and DC Isolation Breakers

In order to deliver a selective protection, the fast DC isolation switches are used. The disadvantage is that the DC isolation switches cannot clear the fault current. The main purpose of using these is to deactivate the LV. The other purpose is to deactivate the no-load DC feeders.

25.3.7 Standards

IEC61850 represents a standard protocol used in order to be a reference for station automation applications and for development of the PS. The IEC61850 it is a protocol based on Ethernet and can be translated for future communication networks [19]. In this protocol, the represented data in this protocol is treated as an object-oriented. In order to ensure the data reception, the information is transmitted several times. More, the IEC61850 protocol is very useful in the application where the time of intervention is a critical factor, assuring a rapid protection. In order to communicate in distribution systems between intelligent electronic devices (IED) for the data format a standard format is used. As an application, the reference [20] provides one illustrative example in which the different IED data from the grid is translated to a centralized controller through IEC61850 standard. For this application the settings of the microprocessor relays are multiple and are choose according to the grid functioning conditions. IEC 61850 has been also proposed to localize the faults based on voltage and positive sequence of the current phasors at the ends of the feeder.

As following, will be listed the ANSI standards specific for energy system protection together with the associated functions [21, 22].

25.3.8 ANSI Standards

The used ANSI standards for protection purposes are briefly named in Tables 25.1, 25.2, 25.3, 25.4, 25.5 and 25.6 [21].

Table 25.1 Current protection functions

50/51	50N/51N 50G/51G	50BF—DRRI	46	49RMS
Phase overcurrent	Earth fault or sensitive earth fault	Breaker failure	Reverse-phase or phase balance current relay or stator current unbalance	Thermal overload for transformers

Table 25.2 Energy protection directional functions

32P	32Q/40
Directional active overpower	Directional reactive overpower

Table 25.3 Voltage protection functions

27D	27R	27	59
Positive sequence undervoltage	Remanent undervoltage	Phase-to-phase undervoltage and minimum undervoltage protection	Phase-to-phase overvoltage
59N	47		59
Neutral voltage displacement	Phase-sequence or phase balance voltage relay		Overvoltage protection

Table 25.4 Directional current protection

27D	67N/67NC	67N/67NC	67N/67NC	67N/67NC
AC directional phase overcurrent	Directional earth fault	Type 1	Type 2	Type 3

Table 25.5 Machine protection functions

37	48/51LR/14	66	50V/51V	
Phase undercurrent	Locked rotor/excessive starting time	Starts per hour	Voltage-restrained overcurrent	
26/63	38/49T	50, 50N, 51, 51N	49	38/49T
Thermostat, Buchholz, gas, pressure, temperature detection	Temperature monitoring by RTD	Earth fault protection based on measured or calculated residual current values	Overload protection	Temperature monitoring by RTD

Table 25.6 Frequency protection functions

81H	81L	81R	81
Over frequency	Under frequency	Rate of change of frequency (ROCOF)	Frequency protection

To coordinate the numerical protections with the electromechanical ones, there are applied recovering characteristics according to ANSI C37.112 and CEI 60255-3/BS 142 standards; big impedance homopolar differential protection (ANSI 87N).

25.4 Case Studies

Applying the notion of "smart" to a PS means it integrates the technological development from nowadays from fields like electronics, Information Technology IT and telecom in the traditional power grid (PG). An example of Smart Grid architecture in Romania as seen by the country's Transport and System Operator "Transelectrica" is presented in Fig. 25.7. Bidirectional energy flow, command and control capacities will allow new applications and functionalities, beyond smart metering for household and industrial appliances [23].

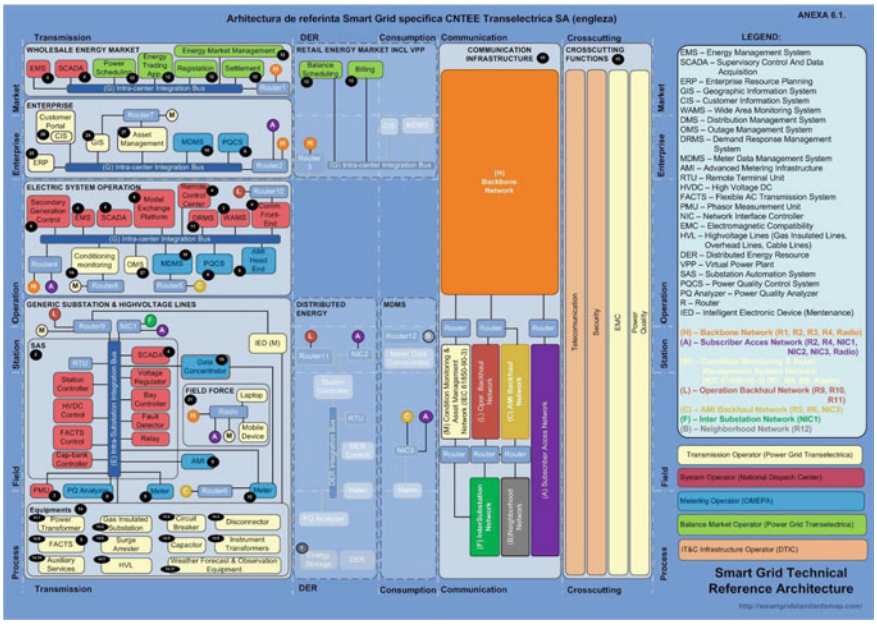

Fig. 25.7 Romania's smart grid approach (Transelectrica)

Another example is the United States of America's law (the Energy Independence and Security Act from 2007) which proclaimed the evolution of the PG to a smart grid as a national interest policy for the USA, under coordination from the National Institute of Standards and Technology [24].

To assess the progress, USA Department of Energy monitors the following features of the smart grid as is shown in Fig. 25.8:

- Allows wittingly customer contribution;
- Hosts heterogeneous devices as brands and generations;
- Hosts storage facilities;
- Admits new products, services and markets;
- Provides energy in quality parameters for a wide range of customer needs;

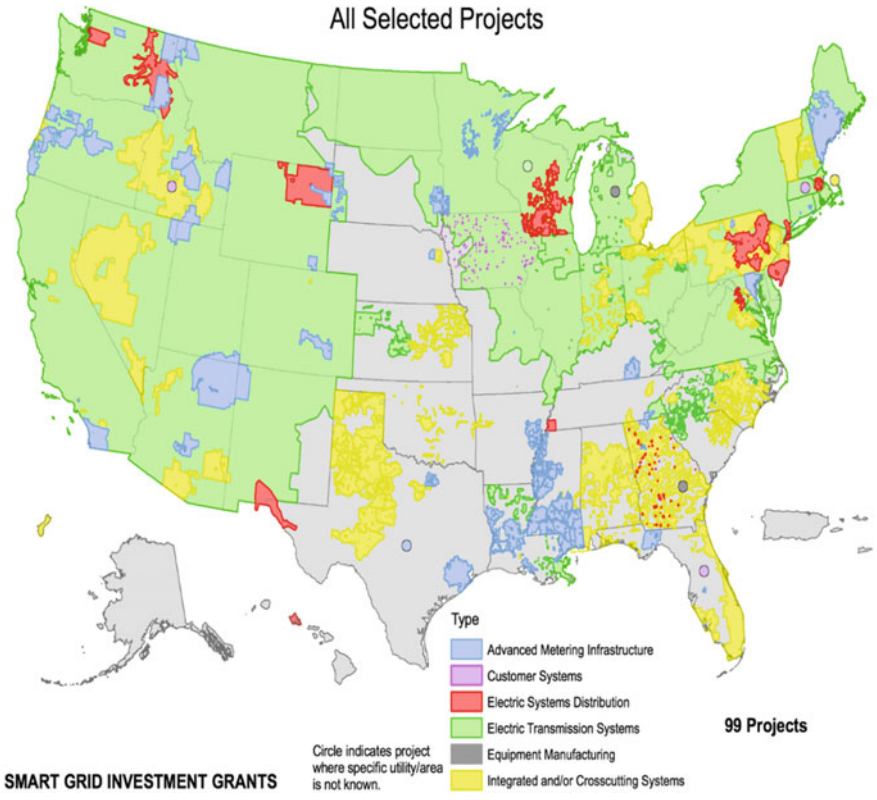

Fig. 25.8 Department of Energy Smart Grid Investment Grants 2009 (Office of electricity)

- Optimizes the use and operation of assets;
- Provides resiliency (disturbances, natural disasters, attacks).

The American Recovery and Reinvestment Act from 2009 targeted USA's economy growth and energy independence improvement through PG telecommunications upgrades. The Department of Energy provided 4.5 bn$ for transition to smart grid while more than 200 electricity companies and other interested private investors/organizations invested 3.5 bn$ in 99 projects which aim to improve cross-platform operability, cyber security, supervisory control and data acquisition (SCADA) regarding benefits of the evolving smart grid [25].

Energy companies and state regulators became aware of this evolution after large black-outs like the one who severely affected North America in 2003 while domestic users realised that the prices are growing and so are their energy needs, the environmental regulations accelerated the evolution from Otto/diesel engines to electric or plug-in hybrid vehicles.

Brown-outs or black-outs influence the electric energy quality so the final users became more responsible and preoccupied to have access to stable, reasonably-priced and eco-friendly energy. Also, as the request for equipment which allows users to save upon the bill or even go of the grid (e.g. Tesla's Solar Roof and Powerwall), went up, the prices became more affordable and will continue like this as more producers become interested and decide to invest in these technologies.

Industrial, commercial, financial, governmental institutions (e.g. fine or electronic mechanics, cold stores, data centres, stock exchanges, hospitals, research facilities, etc.) require quantitative and qualitative electricity, because each alteration of these parameters have the potential to cause loss of life (e.g. medical services), material damage (by disrupting/delaying the technological processes), impossibility of access of the population or users to certain services (e.g. telecommunications, data centres, etc.), loss or erroneous results in the research activity.

The reliability of traditional PG is decreasing as the population of the planet is on the rise, those in rural areas migrate to cities where lifestyle is based on a growing demand for uninterrupted, quality energy; global energy demand follows an upward trajectory and disproportionate loading from the above-mentioned traditional grid reveals the need of starting a revolutionary upgrade as well as establishing the means to follow; as more consumers decide to upgrade to smart grid technologies, we hope that this trend will grow from a niche mainstream and we are entitled to believe so, as important steps have already been made in this direction.

Siemens view of microgrid represents a separate energy system consisting of distinct energy sources like renewable, conventional, storage, etc. and tasks capable of running connected to or independent from the national PG.

The main purposes of a microgrid is to ensure energy security, reliability and affordability for consumers with benefits like less greenhouse gas emissions and reduced PG load during peak consumption.

A microgrid can also be designed for permanent disconnection from the national PG in case of isolated targets or communities, but generally a microgrid is a local solution that reduces costs and emissions of pollutant gases and increases resilience

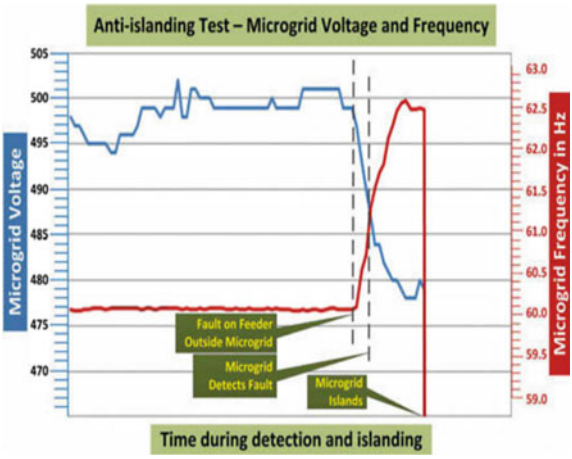

Fig. 25.9 Microgrid protection in case of PG failure [28]

for that area as the storage (part of the microgrid) automatically counterbalances the national PG load during peak consumption. Also, a microgrid automatically disconnects from the national PG in the event of a black-out, providing power to at least the critical systems in that community, and after the problem is detected, fixed and the national PG is back on-line, the microgrid automatically reconnects.

An essential feature of a microgrid is the independent, disconnected operation from the national PG represented in Fig. 25.9 where the microgrid protection is presented in the event of a black-out [26, 27].

Usually, the core of a microgrid consists of one or more conventional generators with a power of maximum 50 MW powered by LNG or biomass. When connected to the national PG, a microgrid will rely on a combination of power generation sources depending on the operating state and the PG loading which needs optimization. Specialized hardware and software systems control the integration and management of microgrid components and connection to public services as presented in Fig. 25.10 [28].

Generally speaking, a microgrid contains:

- Power generating facilities (one or more small turbines or other traditional ways of power generation);
- A distribution system;
- Energy storage (to reduce system load during daylight peaks, to distribute night-time energy produced by photovoltaic panels during the day to fill the periods when wind turbines do not work, and the examples may continue);
- Consumers (loads).

The above-mentioned components are managed by advanced monitoring, control and automation. By installing a microgrid, the following goals are achieved:

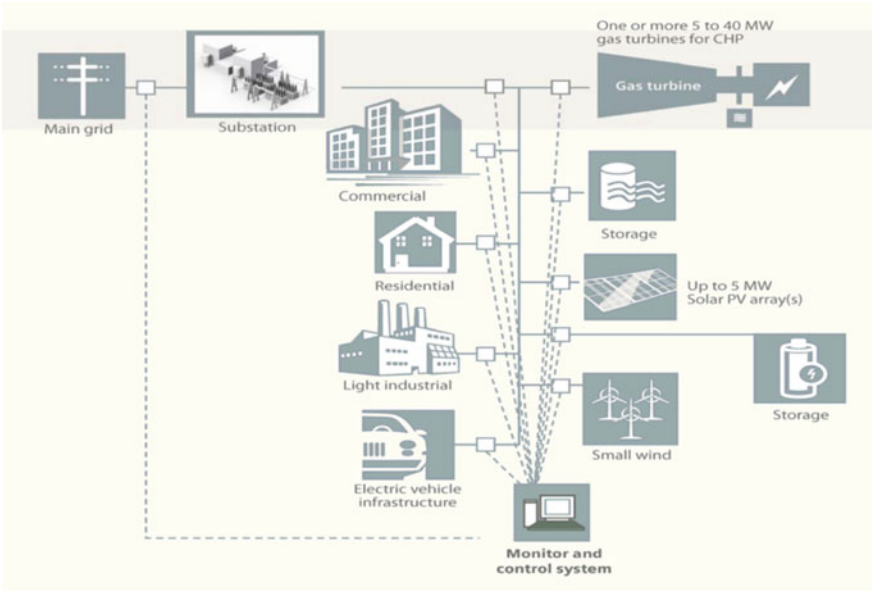

Fig. 25.10 Microgrid structure

- Lower energy consumption (visible and quantifiable measure with immediate economic impact);
- The impossibility of cascading black-outs (advantages: (a) if the failure is produced inside the microgrid, it will not be propagated; (b) if the failure is produced in the national PG, the microgrid will disconnect and will function in island-mode);
- Reduced consequences to a power outage in the national PG as the microgrid automatically disconnects from it and provides energy based on its own generation and energy stored for predefined critical areas, thus:
  - Necessary for public services (healthcare, fire & rescue, law enforcement, drinking and firefighting water supply, sewage services, warehouses and stores managing fresh or perishable products, street lightning and other critical services;
  - Preferably for low power home lightning (LED lighting solutions have low power consumption) and another electric outlet to power the fridge.

When the national PG goes back online the microgrid is supposed to automatically reconnect, distribute energy to all its users and recharge the storage systems. A microgrid solution decreases the load during consumption peaks by renewable energy produced on-site and/or energy storage, dynamically offsetting the PG load. Modular designed systems are suitable for microgrids in areas where rapid development is expected.

The installation of a microgrid for both household and industrial consumers reduces costs straight away by savings on invoices, but also includes better qual-

ity of life in households and continuation of production/services activity for business where even a short duration black-out in the national PG may induce interruption of activity with associated capital losses. At the same time, users pay less or even get paid for system services, if the microgrid participates in maintaining the electricity quality parameters in the national PG (frequency regulation, restarting the national electricity system following a black-out, etc.) another reason for the investment to be cost-effective [29].

If Allies would have destroyed a few critical power plants in Germany the Second World War would have ended significantly faster as the industry supporting the Nazi army would have collapsed. Nowadays, even if Romania does not face an imminent threat, the country still relies upon a centralized PG and a physical attack (terrorist, sabotage, etc.) or cyber-attack targeting such vulnerable points could cause significant damage. Implementing more microgrids solutions would enhance the country's energy security and resilience, a much-needed passive improvement to counter hybrid war strategies and emerging threats.

In order to function efficiently and achieve its goal, a microgrid is based on [29, 30]:

- user awareness of how it works in order to efficiently use resources;
- generate its own power and use predominantly renewable energy;
- traditional power generating facilities with enhanced efficiency (better than the national PG);
- energy storage solutions;
- monitoring, control and automation systems coordinated by IT and telecommunication solutions to provide the best performance of the micro-network in real time;
- solutions chosen being customized for each microgrid.

Thus, the microgrid gains the adeptness to operate independently from the PG and does so at the lowest cost to consumers, with the smallest emissions and highest reliability.

The implementation of microgrids in the national PG should also be approached at a strategic level because each area according to reality and perspectives requires a personalized solution for the best yield, the costs are high but they are amortized over an average time while offering benefits for decentralization, energy security, resilience and environmental protection. The solution for implementing microgrids is suitable for many but not any situation; nevertheless, a microgrid is an excellent mean of protection against risks for critical infrastructures.

From an economic point of view, the microgrid market has grown eightfold since 2010 in 2015, with expected revenues for 2020 estimated at $20 billion. Their strong implementation is due to increasingly competitive prices for renewable energy (offshore wind energy is expected to decrease with 71% by 2040), from 12% in 2017, it is estimated to reach 50% by 2040 [31, 32].

Energy storage systems based on Li-ion technology will maintain a growing trend, Bloomberg's projection suggesting a ten times larger market in 2040 reported to 2017,

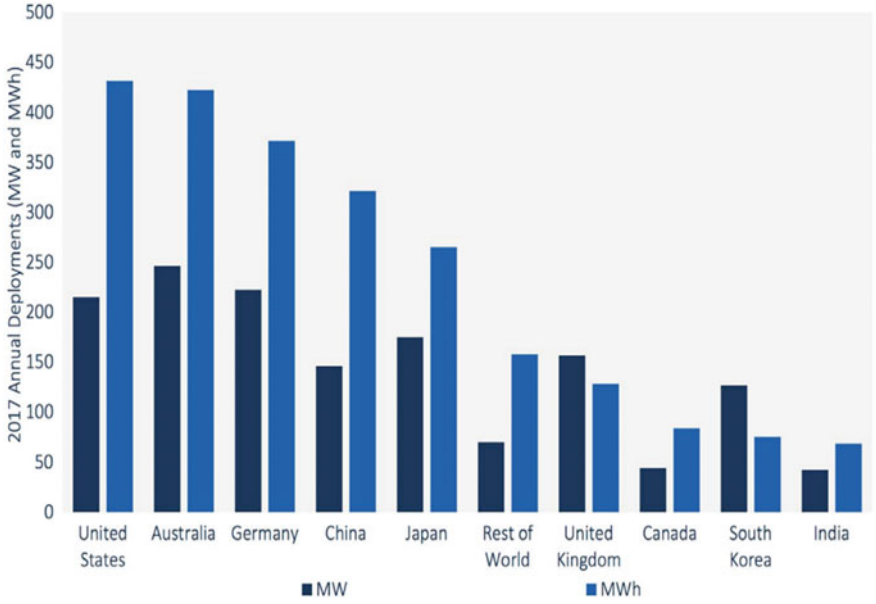

Fig. 25.11 Statistics of battery usage for household appliances [34]

reaching an estimated $20 billion while the estimated world's energy storage capacity is growing even more, the forecast indicating a fifteen times growth from 2015 to 2024. Overall, according to Fig. 25.11, global energy storage projects of 1.4 GW and 2.3 GWh were implemented in 2017 with Australia and the United States leading the chart with 246 MW and 431 MWh respectively [33, 34].

Household energy storage in batteries such as Tesla Powerwall, industrial energy storage installations or national PG upgrades, backed-up by photovoltaic systems, have the potential to reach 57% of world-wide storage capacity by 2040.

Cheaper and more efficient storage systems make installing microgrids a solution that is economically viable over an increasingly short period of time, while energy storage inside the microgrids reduces or cancels distribution-related charges.

Forwards several microgrid examples are presented [35, 36]:

1. Fort Bragg, North Carolina, United States of America. In order to increase energy efficiency and reduce costs, the United States Army has implemented one of the largest microgrids at Fort Bragg military base. Bearing over 260 km^2, the facility has its own power distribution network that works in conjunction with the existing utility infrastructure and can monitor various systems from a central energy management centre. The large surface of the base could have been an impediment but the different generation technologies were successfully integrated with the IT and telecommunications in the microgrid, with the purposes of increasing energy reliability and reducing total energy costs.

2. Illinois Institute of Technology, Chicago, United States of America. The university's microgrid was installed with governmental grants and industrial funding totalling $14 million and features roof-top solar panels, wind generation units, flow batteries, charging stations for electric vehicles, LED lightning, smart building automation technology for energy efficiency and demand response, the buildings being colour coded according to energy needs and the time of the day when consumption reaches peaks. The microgrid's goal and objectives are intelligent features that identify and isolate defects, redirect power according to generation capability and load changes, and adapt to market price, weather forecasts, and interruptions in the national PS, having the capability to function islanded if a black-out propagates in the national PG.

In the early 20th century, the centralized development of the PG and standardization of energy parameters made possible one of the largest leaps in mankind evolution [37–39]. This started with a series of microgrids, merged and standardised to form the national PG and later on, cross-border grids like ENTSO-E. We can observe this evolution in Fig. 25.12 together with the necessary upgrade through decentralization as in present we face severe weather phenomena, hybrid wars, terrorism, etc. [40, 41]. The decentralization through smart, bidirectional, connected microgrids would tackle the energy challenges we are facing today, adding reliability, resilience reducing the cost with a more environmentally friendly approach [42–44].

25.5 Conclusion

The vulnerabilities of microgrids related to the level of connectivity are defined and analyzed from the point of view of the consequences for the normal operating of the system. In order to reduce the consequences different protection solutions closely with international standards for both DC and AC network are presented. Considering the technical requirements of the microgrids ring, parallel and radial topologies are used to ensure the power continuity and load distribution. International standards to which these protections should be aligned are presented.

The capacity of microgrids to solve many problems toward classic PS is described in the case of several national grids where the PS is decentralized and a problem can be propagated at most on the local level, not nationally, and the energy storage component in the microgrids ensures good functioning during peak periods and for PS failure. Besides certain advantages of implementing microgrids, they come also with new threats from the cyber spectrum, with increased complexity, threats which other sectors have already faced and found solutions.

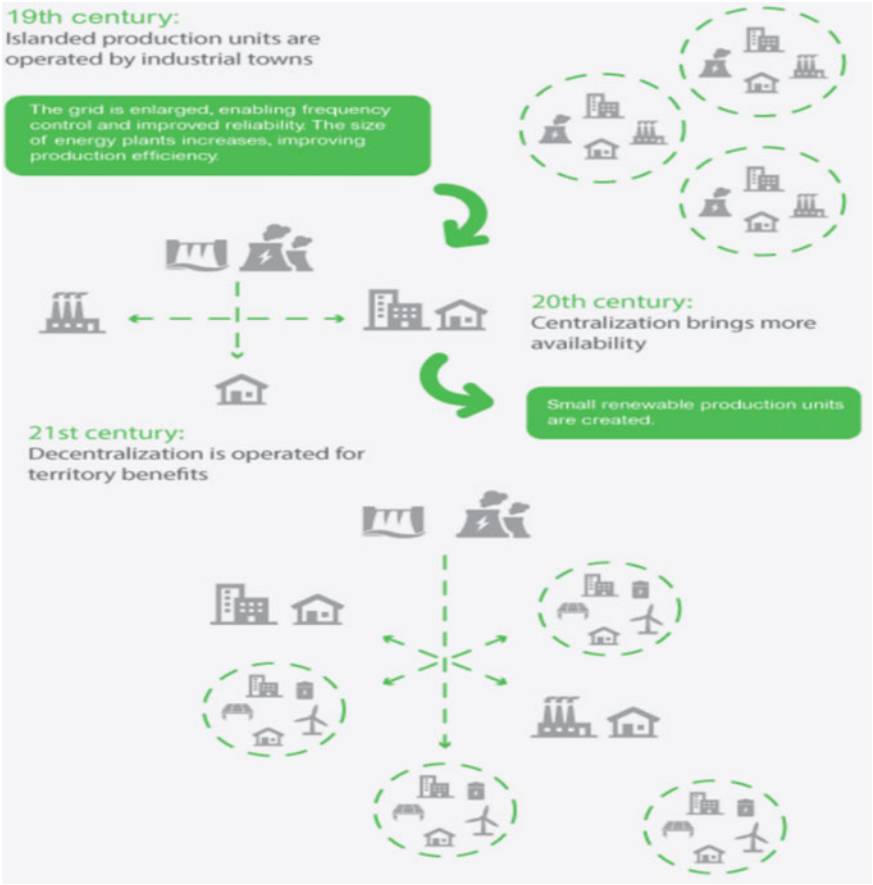

Fig. 25.12 The evolution of PG [37]

References

1. X. Feng, L.T. Yang, L. Wang, A. Vinel, Internet of Things. Int. J. Commun. Syst. **25**(9), 1101–1115 (2012)
2. W.E. Feero, P.A. Reedsvill, D.C. Dawson, J. Stevens, Consortium for electric reliability technology solutions white paper on protection issues of the microgrid concept. Transmission Reliability Program Office of Power Technologies. Assistant Secretary for Energy Efficiency and Renewable Energy, U.S. Department of Energy (March 2002)
3. The Danish Government, Energy Strategy 2050—From Coal, Oil and Gas to Green Energy (February 2011), http://dfcgreenfellows.net/Documents/EnergyStrategy2050_Summary.pdf
4. Danish Energy Agency, Security of Electricity Supply in Denmark (2015), https://ens.dk/sites/ens.dk/files/Globalcooperation/security_of_electricity_supply_in_denmark.pdf
5. X. Tan, Q. Li, H. Wang, Advances and trends of energy storage technology in microgrid. Int. J. Electr. Power Energy Syst. **44**, 179–191 (2013)

6. M. Monadia, M.A. Zamanic, J.I. Candela, A. Luna, P. Rodriguez, Protection of AC and DC distribution systems embedding distributed energy resources: a comparative review and analysis. Renew. Sustain. Energy Rev. **51**, 1578–1593 (2015)
7. M. Soshinskaya, W. Graus, J.M. Guerrero, J.C. Vasquez, Microgrids: experiences, barriers and success factors. Renew. Sustain. Energy Rev. **40**, 659–672 (2014)
8. J.D. Park, J. Candelaria, Fault detection and isolation in low-voltage DC-bus microgrid system. IEEE Trans. Power Delivery **28**, 779–787 (2013)
9. J.D. Glover, M.S. Sarma, T.J. Overbye, *Power System Analysis and Design*, Fifth edn. (Cengage Learning, 2012)
10. http://schemaelectrica.blogspot.com/2015/04/protectia-retelelor-electrice.html
11. H. Yazdanpanahi, Y.W. Li, W. Xu, A new control strategy to mitigate the impact of inverter-based DGs on protection system. IEEE Trans. Smart Grid **3**, 1427–1436 (2012)
12. J. Ma, J. Li, Z. Wang, An adaptive distance protection scheme for distribution system with distributed generation, in *IEEE 5th International Conference on Critical Infrastructure (CRIS)* (2010), pp. 1–4
13. T.S. Ustun, C. Ozansoy, A. Ustun, Fault current coefficient and time delay assignment for microgrid protection system with central protection unit. IEEE Trans. Power Syst. **28**, 598–606 (2013)
14. E. Sortomme, S. Venkata, J. Mitra, Microgrid protection using communication-assisted digital relays. IEEE Trans. Power Delivery **25**, 2789–2796 (2010)
15. D. Jones, J. Kumm, Future distribution feeder protection using directional overcurrent elements, in *IEEE Rural Electric Power Conference (REPC)* (2013), pp. B4-1–B4-7
16. R. Mackiewicz, Overview of IEC 61850 and benefits, in *IEEE-PES Power Systems Conference and Exposition* (2006), pp. 623–630
17. D. Ishchenko, A. Oudalov, J. Stoupis, Protection coordination in active distribution grids with IEC 61850, in *IEEE PES Transmission and Distribution Conference and Exposition (T&D)* (2012), pp. 1–6
18. M. Baran, N.R. Mahajan, PEBB based DC system protection: opportunities and challenges, in *IEEE PES Transmission and Distribution Conference and Exhibition* (2006), pp. 705–707
19. J. Peralta, H. Saad, S. Dennetiere, J. Mahseredjian, S. Nguefeu, Detailed and averaged models for a 401-level MMC-HVDC system. IEEE Trans. Power Delivery **27**, 1501–1508 (2012)
20. J.D. Park, J. Candelaria, Fault detection and isolation in low-voltage DC-bus microgrid system. IEEE Trans. Power Delivery **28**, 779–787 (2013)
21. E. Csanyi, Protection Relay—ANSI Standards (22 February 2011), https://electrical-engineering-portal.com/protection-relay-ansi
22. T.S. Ustun, C. Ozansoy, A. Zayegh, Modeling of a centralized microgrid protection system and distributed energy resources according to IEC 61850-7-420. IEEE Trans. Power Syst. **27**, 1560–1567 (2012)
23. http://www.transelectrica.ro/web/tel/sistemul-energetic-national. Accessed 2018
24. Energy Independence and Security Act of 2007, USA, Public Law No: 110-140, Title XIII, Sec. 1301 (2007)
25. U.S. Department of Energy, Smart Grid System Report (July 2009)
26. The Smart Grid: An introduction. Litos Strategic Communication for U.S. Department of Energy (2008)
27. U.S. Department of Energy, Smart Grid System Report (July 2009)
28. G. Turner, I. Stamenkovic, V. Bhavaraju, J. Dankowski, Microgrid solutions sustain power—even when the grid is off. Nema Electroindustry (2015)
29. F. Aloula, A.R. Al Alia, R. Al Dalkya, M. Al Mardinia, W. El Hajjb, Smart grid security: threats, vulnerabilities and solutions. Int. J. Smart Grid Clean Energy **1**, 1–6 (2012)
30. S. Seidi, *The Role of Microgrids in Grid Modernization Initiatives* (Tetra Tech, 2017)
31. R.L. Dohn, *The Business Case for Microgrids: The New Face of Energy Modernization* (Siemens AG, 2011)
32. Federal Energy Regulatory Commission, Smart Grid Policy. 128 FERC 61,060, Docket No. PL09-4-000, 16 July 2009

33. New Energy Outlook 2017, Bloomberg New Energy Finance (2017)
34. C. Porteous, B. Godfrey, A. Finkel, Taking charge: the energy storage opportunity for Australia. Office of the Chief Scientist, Occasional Paper (July 2018), pp. 1–10
35. NIST Framework and Roadmap for Smart Grid Interoperability Standards, Release 1.0. Office of the National Coordinator for Smart Grid Interoperability, NIST Special Publication 1108 (2010)
36. https://building-microgrid.lbl.gov/illinois-institute-technology
37. V. Boutin, M. Feasel, K. Cunic, J. Wild, *How Microgrids Contribute to the Energy Transition* (Schneider Electric, 2016)
38. Economic Forecast on the World's Power Sector (Bloomberg New Energy Finance, July 2018)
39. R. Manghani, R. McCarthy, Global Energy Storage: 2017 Year in Review and 2018–2022 Outlook, in *Energy Storage* (April 2018)
40. I. Marinescu, B. Botea, H. Andrei, Critical infrastructure risk assessment of romanian power systems, in *IEEE-International Symposium on Electrical and Electronics Engineering (ISEEE)*, (October 2017)
41. I.D. Deaconu, Marilena Stanculescu, A.I. Chirila, V. Navrapescu, H. Andrei, On automatic transfer switch system security, in *IEEE-International Conference on Applied and Theoretical Electricity (ICATE)* (2018), pp. 1–6
42. http://galvinpower.org/resources/microgrid-hub/smart-microgrids-faq/examples
43. https://chicagotonight.wttw.com/2017/11/20/exploring-technology-behind-iit-s-microgrid
44. G. Chicco, A. Mazza, A. Russo, An overview of the probability-based methods for optimal electrical distribution system reconfiguration. Int. J. Electr. Power Energy Syst. **54**, 255–267 (2014)

Chapter 26
Microgrid Protection and Automations

Omer Usta

Abstract After the decision on devolution of electric power generation, a great number of dispersed storage and generation (DSG) units, which is mainly driven by renewable energy sources, has been connected to the power distribution networks. Existing of DSG units in the distribution network has converted the traditional distribution systems into active distribution networks, which are also called microgrids, and has created several technical difficulties from the operation points of view. Therefore, the conventional protection and control systems need to be improved to overcome these difficulties, and provide a reliable protection and control for microgrids operating in both grid connected and islanded modes. Today it is realized that partially developments in protection and control systems will not provide an ideal solution for the todays and future microgrids. Therefore, a full automated distribution network is certainly required for a proper protection and control of microgrids. This chapter will be deal with the protection and automation requirements of the microgrids, protection schemes and developments in the related fields.

Keywords Microgrid protection · Microgrid automation · Intelligent electronic devices · Multi-Source islanding · Islanding protection

26.1 Introduction-Devolution of Power Generation

Electricity was locally generated and distributed at a variety of voltages and frequencies in the early beginning of commercially use of electricity. In a later stage, the authorities promoted to standardize the generation and distribution of electricity. Then the local power systems were combined together to introduce the national interconnected power networks to overcome economical and technical problems due to the need of huge amount of power transmission to the long distances. It took nearly 100 years to enjoy the advantages of interconnected power network and centralized

O. Usta (✉)
Istanbul Technical University and Entes Electronics, Istanbul, Turkey
e-mail: ustao@itu.edu.tr

N. Mahdavi Tabatabaei et al. (eds.), *Microgrid Architectures, Control and Protection Methods*, Power Systems,
https://doi.org/10.1007/978-3-030-23723-3_26

power generation. Insufficiency of present grid, liberation of electricity, lack of the energy sources and environmental considerations have forced the authorities to convert the present power network into a smart grid. This includes the devolution of electric power generation.

Devolution of power generation is the most important part of smart grid considerations. There has been increasing numbers of local power generation units using renewable energy sources throughout the world. Unlike the early use of electricity, these local generations are connected to the utility power system at both medium and low voltage distribution networks [1]. They are also called embedded generation units and usually operating with grid-connected mode. However, when there is a disconnection from the utility power system, they can be operated in a power island mode without the main power supply.

Benefits obtained from the devolution of the power generation are:

- Using renewable energy sources for power generation,
- Decreasing power losses and hence increasing efficiency,
- Reducing the voltage drop,
- Reducing the peak demand on the main network,
- Improving the supply security.

On the other hand, connection of embedded generation units into the traditional distribution networks has converted the distribution systems into microgrids, and created several difficulties from the technical and operation points of view. These difficulties are resulted from:

- Intermittent characteristics of renewable energy sources,
- Resulting in bi-directional power flow,
- Contributing to the fault current,
- Low level of fault current and inertia in islanding mode,
- Possibility of a portion of main grid left connected to the power island,
- Possibility of multiple islands or sub-microgrids due to different switching operation,
- Varied levels of fault current due to occurrence of different type of islanding and microgrid configuration.

Because of these, the conventional protection and control systems need to be improved to provide a proper protection and control for microgrids operating both in parallel with grid and isolated modes. A full-automated microgrid may be the ideal solution to protect, control and manage the future microgrids. IEC 61850 is an international communications standard for Ethernet-based distribution automation, and hence for microgrid automation. This enables to integrate metering, monitoring, protection and control functions within an electric substation. Centralized or decentralized protection and control schemes can be implemented using IEC 61850 protocol for microgrids. IEC 61850 also provides a reliable platform for implementing an adaptive and integrated protection scheme for microgrid. In an adaptive protection scheme, the setting values of over current relays can easily be updated according to the network configuration created by any switching operation. However,

an integrated protection scheme based on any unit protection concept provides the most reliable and selective protection for the microgrids.

The objective of this chapter can be stated as follows.

- Microgrid operation, integration and automation,
- Protection requirements of microgrids,
- Grounding of microgrids,
- Protection of passive and active distribution networks,
- Protection of multi-source microgrids,
- Integrated protection of microgrids,
- Managing a microgrid and a multi-source power island.

Section 26.1 provides a brief introduction about benefits obtained from the devolution of the power generation, the technical and operation difficulties resulted from the devolution power generation, and protection and automation requirements of microgrids. Section 26.2 includes basics of IEC 61850 based microgrid automation. A brief discussion about the neutral grounding of microgrid is given in Sect. 26.3. Section 26.4 contains a comprehensive analysis about protection of microgrids. This includes passive and active distribution network protection, centralized and decentralized protection, adaptive protection, integrated protection, under/over voltage protection, under/over frequency protection, islanding protection and multi-source microgrid operation and management. The summary of the chapter is given in Sect. 26.5.

26.2 Basics of Distribution Automation

As stated above, the complex structure and different operating configuration of microgrid requires a means of automation in order to have a reliable and economic operation of today's microgrid. The sub-station to which the microgrid connected should be a base of the microgrid automation. Figure 26.1 shows an example of sub-station automation.

It mainly consists of three different sections [16], which are named as lower, middle and upper layers. Each layer has different structure and different functions as explained below.

26.2.1 Lower Layer

The lower layer provides an interface between the harsh power environment and the intelligent electronic devices (IEDs), and contains voltage transformers (VTs) and current transducers (CTs), surge protective devices, switching equipment and related cabling. This interface system provides the switching states of information, low level of voltage and current signals from the power network to each IED. IEDs use these to monitor the power system, to detect a fault and have a trip decision, and

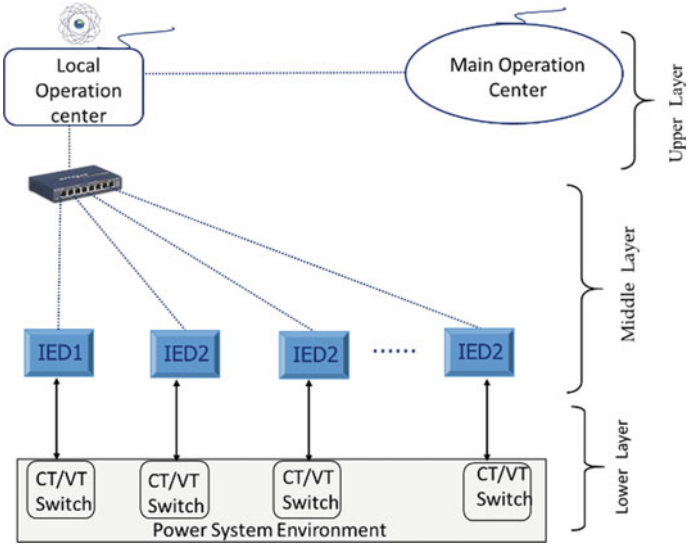

Fig. 26.1 Basic configuration of sub-station automation

to initiate a control action. All these actions are conveyed to the power network over the interface unit. Interfacing between the harsh power network and the IEDs may be implemented in two different ways. The first one of them is the conventional way as indicated in Fig. 26.2.

In the traditional approach, analogue signals received from the secondary windings of current and voltage transformers are connected to the relay IEDs via cable. They are firstly digitized via an analogue to digital converter. Then, they are used by the application software of the IEDs to evaluate the power system conditions. Digital signals representing the state of the switch are directly cabled to the IED using digital inputs. The cabling work in the traditional approach requires several kilometers of wiring. This results in a lack of flexibility and dramatically increase in the installation cost. It is also not suitable for a full-automated power network structure.

The modern approach do not need this type of massive cabling. They require Ethernet based IEC61850 communications to convey the sampled values from the measuring point to the subscribers. Figure 26.3 shows the configuration of interface between the power network and IEDs in a modern substation. Each power line has an interface unit connected to its end in a sub-station. The interface unit contains a merging unit (MU) and control unit (CU). MU digitalizes the analogue signals received from power network and then pass them into the local IEDs. MU also sends the digitalized data to the remote IED using the communication channel. The IED continuously evaluates the power system conditions using digitalized signals. Whenever a trip decision is taken, the IED sends the decision to the related switch over the control unit CU. The trip decision can also be conveyed to a remote switch via communications interface unit (CIU) as a transfer trip.

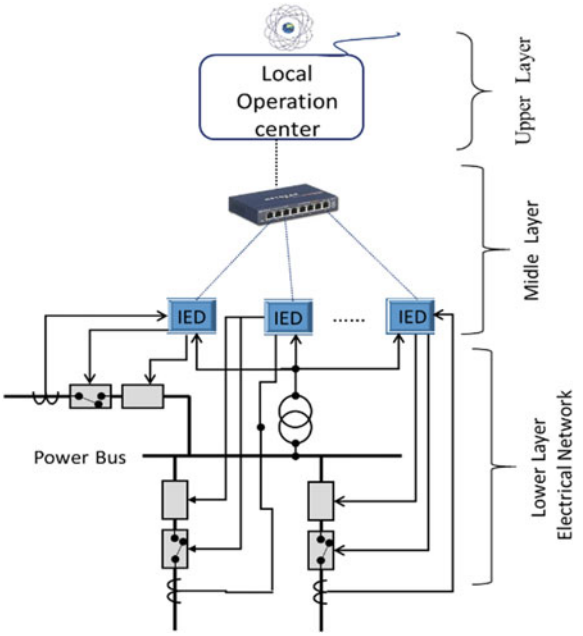

Fig. 26.2 The layout of conventional interface unit

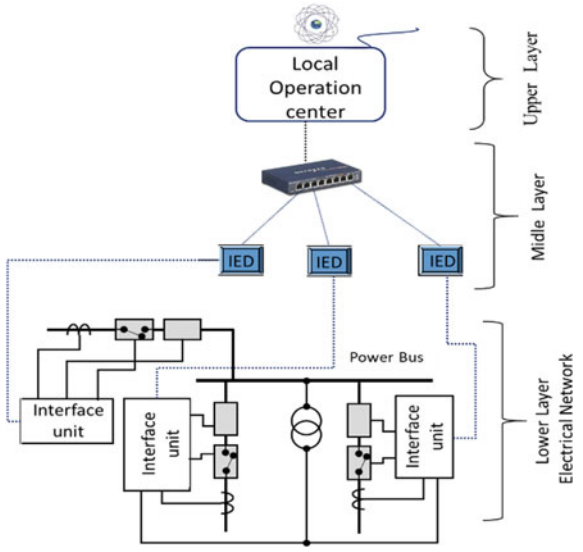

Fig. 26.3 The layout of modern interface unit

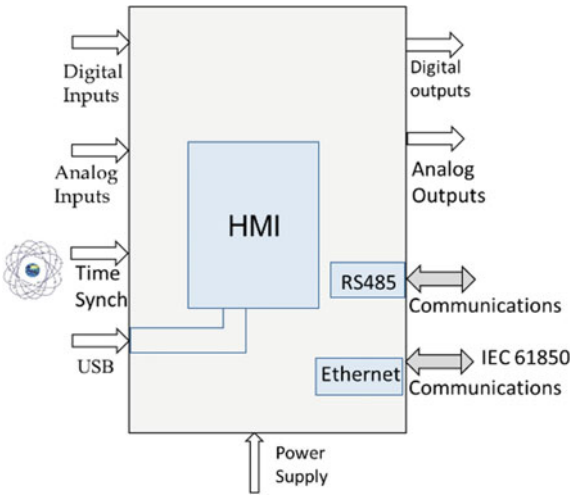

Fig. 26.4 Basic components of an Intelligent Electronic Device

26.2.2 Middle Layer

The middle layer is composed of Intelligent Electronic Devices-IEDs and data bus (an Ethernet switch). The functions of IEDs can be classified as metering, monitoring, recording, protection, control, managing and communications. Some of IEDs could be more advanced than the other. Some of them may emphasize certain functional aspects over the others. They could be protective relays, bay controllers, network analyzers, disturbance recorders, RTUs, PMUs etc. As stated above, IEDs gather information of voltages, currents and states of components from electrical power networks via interface unit. They use this information and evaluate the operating conditions of power network according to its application program. They can also conveys these signals to other locally and remotely located IEDs. Figure 26.4 show the layout of an intelligent electronic device.

An IED contains following sub-units.

Digital inputs: are used to monitors the states of the power system elements.
Digital outputs: are used to change the states of the power system elements.
Analog inputs: are need to receive voltage and current signal from the power network.
Analog outputs: are need to convey an analogue signal to a display.
RS485 port: is required for communication with Modbus protocol.
Ethernet port: is need to communicate with IEC 61850 protocol.
USB port: is required to connect a computer to the IED.
Time synch: is need to synchronize the clock of the IED.
HMI: Contains the human machine communication facilities such as operation keys, LEDs etc.

Communication port: is used to communicate with the master computer within the local operation center, other local and remote IEDs.
Time synch: is the time synchronizer.

26.2.3 The Upper Layer

The upper layer consists of the local and main operation centers. A host computer located at the local operation center is the master for local area network related to the sub-station. The IED Relays are connected to the local operation center with a local communication switch known as station bus. The master computer timely polls any information from the IEDs. Following an immediate relay action, the IED may also inform the master computer about what action it has taken. The program logics are application, data access, data storage and presentation logics, which are distributed between the master computer and IEDs. The application logic needs to be run within the IEDs, since the application logic is related to time critical events.

The main central controller communicates with all local operation centers located throughout the power network, and form a master-slave computer network with local operation centers. The main central controller polls any information from the local operation centers.

The above automation infrastructure or a modified version of it can be used to implement advanced monitoring, protection and control system for managing the present and future microgrids.

26.3 Grounding Microgrid

Network grounding can be considered an integrated part of a protection system. The level of earth fault current, which is vital for the earth fault detection and isolation, is determined by the type of system grounding. While a direct grounding system results in a very high level of earth fault current which may damage the connected equipment, an ungrounded system will produce no fault current for a ground fault to be detected by an over current protection. Grounding over an impedance is mainly preferred to produce suitable level of earth fault current to be detected by an over current protection.

Microgrids are generally connected to the main source of supply over a distribution transformer. This is usually a Δ–Y connected transformer and Y-side is directly grounded or grounded over an impedance. This grounding installation is also used for microgrid provided that microgrid is operating in grid connected mode. TT or TN type of system grounding can be chosen. Since TN system produces more earth fault current, it is usually preferred.

Islanding is initiated by any one of CBs connecting the embedded source of supply to the utility supply. Location of this CB defines the configuration of the power

island created. When a microgrid is left without the grounding system following an islanding, a local grounding system is required to have a path for the flow of earth fault current. Whenever an islanding condition is detected, the local grounding will be switched on. Thus in both operation modes a level of earth fault current is flow to be detected by an over current protection.

On the other hand, firstly as stated above use of IT system grounding will not produce any earth fault current. Secondly, TT and TN types of grounding requires a direct earthing, however the grounding resistance is not exactly zero and changes from 2 and to 5 Ω. Because of this, an earth fault may not produce enough current to be detected by an over current element. For both cases under/over voltage protection is required to detect the earth fault, since the voltage of un-faulted phase will increase at the instant of a ground fault. Under/over voltage protection is also need against low voltage condition. Therefore, under/over voltage protection is strongly recommended to provide protection for the microgrid, which is connected to MV or LV distribution networks. Setting of the U/O voltage relay is chosen such that the protection system let the microgrid to operate as long as the system voltage stays within allowable limits.

26.4 Microgrid Protection

26.4.1 Overcurrent Protection

Over current protection is a very simple and effective relaying principle, which monitors the current magnitude as an indicator of a fault. Whenever the current going through the protected element is greater than a pre-defined value it initiates a trip signal to clear the fault after a time delay. Therefore, over current relays can be used to protect practically any power system element such as feeders, generators, motors, transformers etc. The relay settings must be provided in such a way that the relay will operate for the fault within the protected zone only. There are two types of settings for overcurrent relays. These are the pickup current and the time delay. The pickup current must be between the minimum fault current and maximum load current. The way of setting time delay depends on the type of overcurrent protection. The time delay setting is predefined or automatically calculated by the relay according to the pre-selected curve at the instant of a fault.

There are three types of overcurrent protection [1, 2]. These are; inverse time overcurrent (ITOC), definite-time and instantaneous overcurrent protection. Figure 26.5a shows the time-current characteristics of overcurrent relaying. The operating time of the ITOC relay is inversely proportional to the measured current. This provides fast tripping for high fault current and slow tripping for low fault currents. IEEE and IEC defined several types of standard inverse time overcurrent characteristics. Every type of characteristic has its own curve family defined by time multiplier settings. Choosing one of these standardized characteristics depends on the thermal charac-

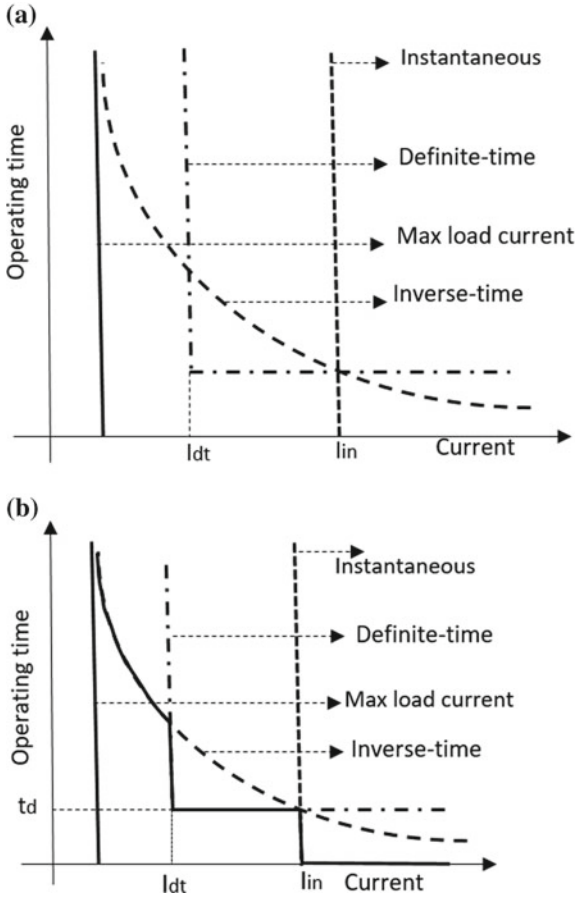

Fig. 26.5 **a** Overcurrent relaying characteristics. **b** Three stage Overcurrent protection

teristic of protected element. In case of a fault, the relay automatically calculates the tripping time using the pickup current level and the curve selected in advance.

In case of the definite time protection, a time delay is predefined. This time delay will be the tripping time of the relay and is selected according the fault current level. Instantaneous overcurrent protection is in fact a type of definite time relaying, but it has no time delay. It is used to provide protection against severe fault conditions producing large amount of fault current. Whenever the fault current gets greater than a pre-defined trip level, it will initiates an instant trip to clear the fault.

Any one of these characteristics is chosen for the protection of any component of microgrid networks. In some cases, a combination of two or three characteristics may be used to produce an advance characteristic for a proper protection of a special condition. An example of this is illustrated in Fig. 26.5b, and known as stage protection.

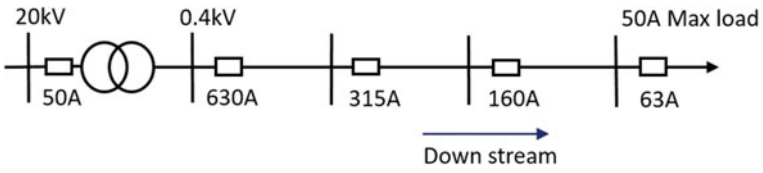

Fig. 26.6 Radial feeder protection using fuses

For instance, in a three stage protection, if the fault current is higher than the maximum load current and less than the definite time pickup current (I_{dt}), inverse time relay will operate. When the fault current greater than definite time pickup current (I_{dt}) and less than instantaneous pickup current level (I_{in}), definite time relay will operate just after the pre-set time delay (t_d).

Whenever the fault current becomes greater than the instantaneous pickup current level (I_{in}), instantaneous overcurrent relay will operate without any time delay.

26.4.2 Protection of Radial Distribution Lines Using Fuses

The oldest of the protective devices is the fuse. The fuse is also perceived to be the simplest protection element used in power supply networks. When the current entering into the protected zone exceeds a pre-defined value, the fuse melts and thus breaks the supply circuit. It interrupts the circuit by melting the fuse link in response to the over current flow. Thus, the fuse both detects the fault condition and directly isolates the faulted plant from the network. In addition to the breaking the supply circuit, a fuse is also able to limit the magnitude of the fault current by interrupting the current flow before taking its maximum value. The melting time of a fuse is inversely proportional to the magnitude of the current going through it. The current-limiting ability of the fuse is a very important characteristic for many industrial installations.

The fuses are direct acting, cheap, fail to safe, very fast at high fault current, and their operating characteristic can be graded. However, they require replacement after operation, provide poor protection against low fault current, are non-directional, and have limited voltage-breaking capacity.

The fuses are extensively used in the low voltage systems, with rating 2 to 1600 Amps. High voltage fuses are also available for 33 and 66 kV with ratings 5 to 60 amperes. The MV and LV radial distribution lines can be protected by using the fuse. An example of this can be seen in Fig. 26.6. The rating currents of the fuses may approximately be defined as follows. The fuse nominal current, which is the closest to the load, is chosen as 1.10 or 1.20 times greater than the maximum load current. The ratings of the other fuses should not be less than twice the rating of the downstream fuse current.

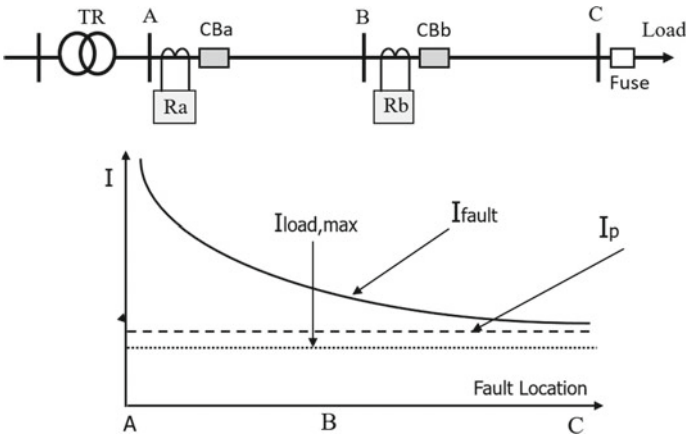

Fig. 26.7 Fault current deviation according to the fault location

26.4.3 Protection of Radial Feeders Using Over-Current Relays

When there is a phase-to-ground fault in three-phase networks, it will cause only one of the fuses to blow up. This operation brakes one phase of the three-phase system, and allows the protected element left connected to the remaining two phases. This results in subsequent excessive heating and network unbalance. In order to solve these problems, over current relaying principle is preferred to protect the radial distribution lines.

For the radial distribution lines, the current pickup and time delay settings are need to provide a proper protection, and coordination among the relays, since the power flow is from the source to the load only. Both phase and earth faults are detected and cleared using different over current relaying characteristics. The pickup level of over current relaying must be chosen such a value, which will be greater than *the maximum load current* and less than *the minimum fault current* occurring at the relaying point. However, as it is expected, the fault current is exponentially decreases as the distance increases from the source location. There might be an uncertainty about selection of a pickup level through the end of distribution line, since the maximum load current and minimum fault current get closer to each other through the end of the line as seen in Fig. 26.7. In this case, an over current relay can not guarantee to provide protection through the end of the line.

Figure 26.8 shows an example of the protection of radial distribution line. The load is protected by a fuse. Since the fuse is the closest to load, it must be the fastest to operate. Lines *b*-*c* and *a*-*b* are protected by inverse time overcurrent relays. Relay *b* needs to be coordinated with the fuse in such a way that it provides backup protection for the load and primary protection for the line *b*-*c*. Relay *a* should provide primary protection for line *a*-*b* and backup protection for line *b*-*c*. Therefore, a protection

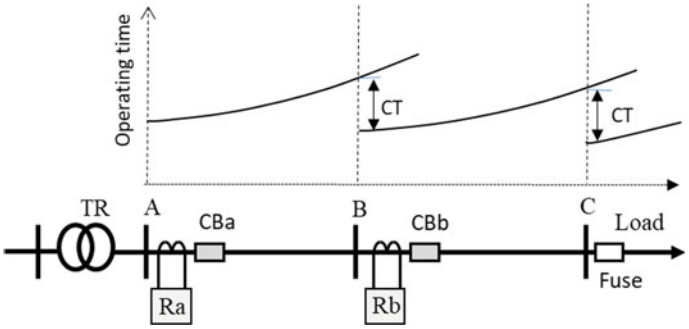

Fig. 26.8 Time-distance characteristic and protection coordination

Fig. 26.9 Operating characteristics of fuse and relays

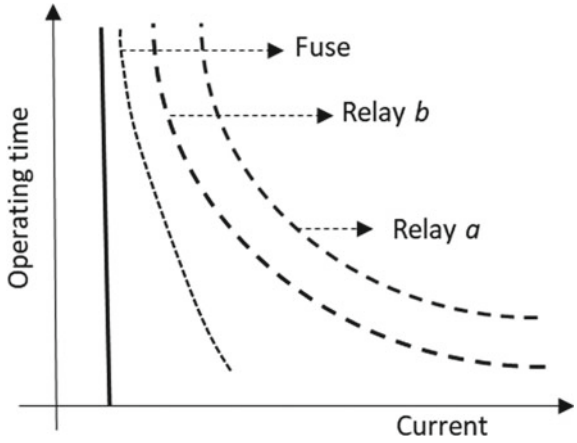

coordination needed between primary and back up protection as seen in the figure. This coordination time (CT) can be chosen as (0.3–0.4) s practically. In other words, relay *b* will operate with a time delay of (0.3–0.4) s after the fuse operation for a fault at the load side.

Figure 26.9 shows time-operation characteristic of the fuse, relay *a* and relay *b*, and the protection coordination.

26.4.4 Protection of Distribution Lines Having Bi-Directional Power Flow

Whenever the power flow becomes bi-directional in the distribution systems, the lines need to have protective relays at each end for directional over current protection [2, 3]. Otherwise, protection reliability cannot be provided, since more than one relay will response the same fault. Hence, in addition to the current pickup and time

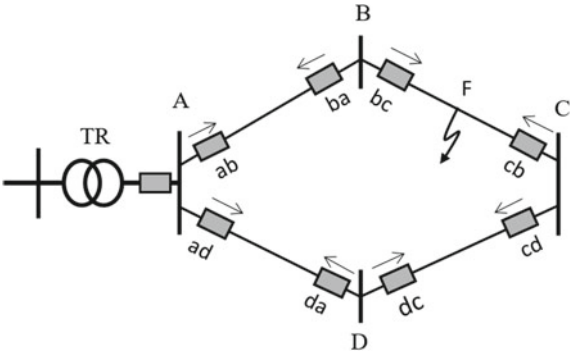

Fig. 26.10 Overcurrent protection of ring distribution feeders

delay settings, the direction of fault current is also necessary for protection and relay coordination.

Figure 26.10 shows a typical example of directional protection for a ring feeder. The relays having downstream direction (*ab, bc, cd, da*) are coordinated together, the relays having upstream direction (*ad, dc, cb, ba*) need to be coordinated together with a proper coordination time. Thus, the protection reliability is maintained at a proper level.

If there is a fault at *F* relay *bc* and relay *cb* see the fault current in the forward direction and will operate to clear the fault. Although relay *cd* and relay *ba* detect the same fault and will not operate, since they see the fault current in the reverse direction. Relay *ab* and relay *dc* will provide backup protection for relay relay *bc* and relay *cb* respectively. They will operate, if relay *bc* and relay *cb* do not clear the fault.

26.4.5 Adaptive Protection of Active Distribution Networks

The connection of increasing number of DSG units, which are also known as distributed generation (DG) units to the distribution networks [1, 4–9], has changed the structure and operating conditions of the power distribution networks. Since they have DSG units, they have become active networks and are called microgrid anymore. Microgrids operate in both grid connected or disconnected modes. As stated in Sect. 26.1, existing of DSGs in distribution networks creates some technical difficulties from the protection and operation points of view.

The electricity generated from renewable sources directly depends on weather conditions and causes highly variable power flow in the active distribution systems. The switching off any DSG will also create a different operation condition and produces different level of current flow. Microgrid moves to the islanding operation mode following a switching operation, which disconnects the microgrid from the main source of supply, when there is a fault or abnormal condition in the main

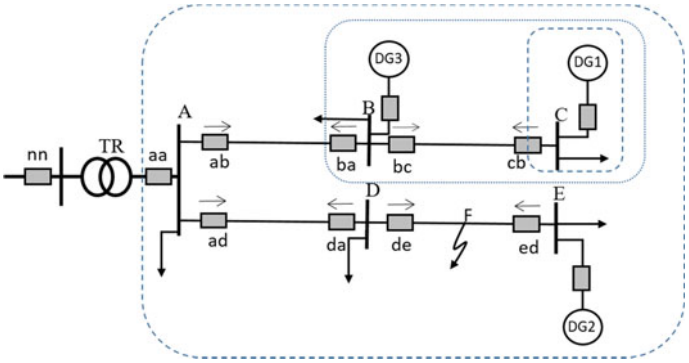

Fig. 26.11 An example of multi-source active distribution network

network. The islanding configuration depends on the switching operation creating the islanding. Different switching events result in different types of islanding, and hence different operating configurations of a microgrid in island mode.

Figure 26.11 shows the normal operation of DSGs with grid connected mode. Opening of circuit breaker *cb* leads an islanding only with a DSG, whereas opening of circuit breaker *ba* creates an islanding with two DSGs. Opening of circuit breaker *aa* or *nn* will result in a larger power island. Hence, operation of each circuit breaker will result in a different microgrid configuration. Every microgrid configuration needs to be analyzed separately, since each microgrid configuration will have different operating conditions such as load current, minimum and maximum fault currents, direction of current flow. Hence, each configuration requires different protection settings of overcurrent relays.

Therefore, over current relays require a dynamic setting procedure according to the microgrid configuration. Whenever the microgrid moves from an operating configuration to another operating configuration due to any switching event, settings of every overcurrent protective relay may be required to cope with the system conditions. This can only be done using adaptive relaying principles [4–9], which is required communicated information, and hence a communication facility.

Adaptive protection is actually an on-line facility to convey the new setting values to the relays in response to a change in the system conditions. A master-slave or a peer to peer communication system is required to implement a centralized or decentralized adaptive protection respectively. IEC61850 communication platform is a power system automation frame and used for installation of peep to peer and mater-slave computer network for adaptive relaying.

26.4.5.1 Decentralized Adaptive Protection

Figure 26.12 shows an example of a decentralized adaptive protection scheme for a microgrid. In this scheme every bus need to have an advanced protective relay known

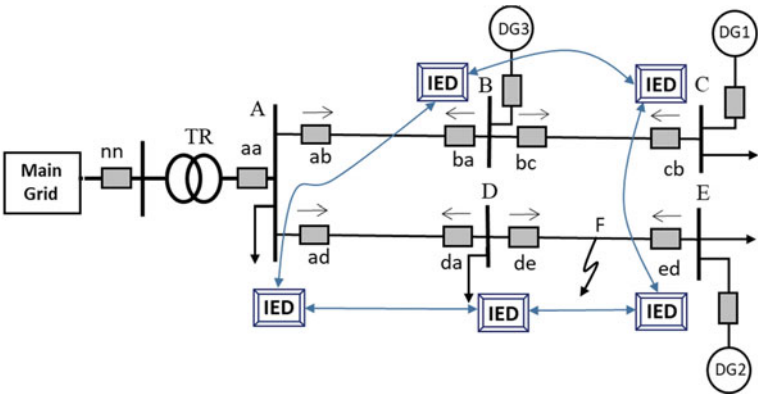

Fig. 26.12 Decentralized adaptive protection for a type of microgrid

as intelligent electronic device (IED). Each IED is equipped with the necessary intelligence and information to detect and isolate the fault. Since there is no a local protection center, each IED runs all programs itself including a type of data storage, data access, presentation and application logics. A peer to peer communications also requires between IEDs. Each local IED may communicate with its adjacent local IED to exchange the protection information such as the direction of fault current, maximum fault current and operating time of the relay. A combination of these information is required to detect a fault and isolate the faulted component from the rest of the system. Each IED has its own action independently following a contingency.

When a microgrid runs in parallel with the utility network, a decentralized adaptive scheme provide a reliable protection and coordination performance. However, it may not provide adequate performance following any switching operation, since every switching operation will create a different network configuration.

26.4.5.2 Centralized Adaptive Protection

Figure 26.13 illustrates an example of a centralized adaptive protection scheme for a microgrid. A central adaptive relaying requires a protection and central controller known as operation center, an IED for each bus and a communication platform. The operation center acts as a host computer and each IED behaves as an intelligent terminal. All logics may be shared between master unit and IEDs, but the application logic must be run in each IED. Every IED sends its status information of the related circuit breaker to the operating center for informing about the occurrence of any contingency within its region. Since any switching event results in a different configuration of microgrid as stated above, the operation center will estimate the new settings for all IED and conveys the related settings to each IED. Whenever it needs, the master computer in the local operation center also scan IEDs to collect states and other types of information.

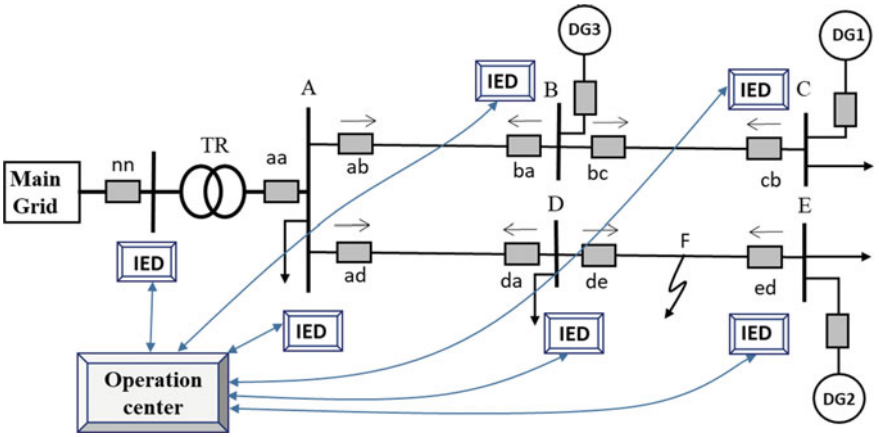

Fig. 26.13 Centralized adaptive protection for a type of microgrid

Overcurrent protection is a non-unit protection scheme, and has only measurement from one end of the protection zone and produces trip decision for the same end only. The current pickup setting of the relay must be greater than the maximum load current and less than the minimum fault current. This is required to detect the fault producing minimum fault current and not to operate under load change conditions. The margin between the minimum fault current and maximum load current may not be enough to have a reliable pickup value through the other end of the line. Therefore, non-unit over current protection of the lines has always an uncertainty about the discrimination between the maximum load current and minimum fault current. Adaptive overcurrent protection will not overcome this uncertainty.

The unit protection schemes having measurements from both ends of the line do not have this type of uncertainty. Therefore, it provides a very reliable protection for networks as long as communication facility available. Although unit protection scheme has been used to provide protection for high voltage transmission lines, IEC 61850 communications protocol and microgrid automation enable us to use the unit type of protection for the lines of a microgrid.

Overcurrent protection and unit protection can be implemented in the frame of integrated protection of active distribution networks using IEC 61850 protocol.

26.4.6 Integrated Bus-Bar and Line Protection of Microgrids

IEC61850 was introduced as a standard for communications within a sub-station [10, 11]. This can be used as a protection frame to implement an integrated sub-station protection scheme. Figure 26.14 shows a platform for sub-station protection scheme integrated into an advanced relay (IED) using IEC61850 protocol frame [12–17].

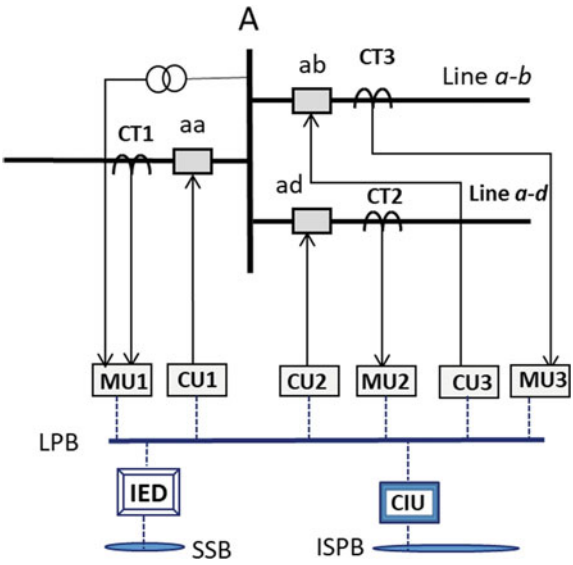

Fig. 26.14 Bus protection integrated into a computer relay

Voltage and current measurements taken from the sub-station bus using VTs and CTs are converted into digital form via merging units (MUs). A MU communicates with IED over sub-station (local) process bus (LPB). IED evaluates the network conditions and produces relaying decision. The relaying trip decision is then conveyed to the control unit (CU) to issue an opening operation for CB. Unlike the conventional system, after data acquisition a MU conveys the digitalized measurements to the local IEDs over local process bus (LPB) and remote IEDs located in a different substation over communication interface unit (CIU). In addition, an IED can conveys a trip command to a remote CU to have a remote CB opened.

By considering Fig. 26.15, the IED related to bus *A* received the samples values of local bus voltage and the currents of all line connected to bus *A* via local process bus and calculates the voltage and current phasors. These phasor values consist of amplitudes and phase angles of all currents and voltage related to bus A. Since the direction and amplitude of each line current can be extracted from the phasor values, this information is used to provide protection for the bus using any one of bus protection schemes such as overcurrent (non-unit) or differential (unit) protection based schemes. As long as the summation of currents entering to the bus are equal to that of currents leaving the bus, there is no fault within the bus. Any difference between them indicates a fault within the bus.

As stated above, an IED related to bus *A* has phasor values of all currents and voltages related to local bus. It also has capability of receiving sampled values of currents and voltages related to the neighboring bus (say Bus *D*) via a communication facility and can calculate the related phasor values. Hence, IEDs related to Bus *A* and *D* have both local and remote measurement of line *a-b*. Therefore, a unit protection scheme such as directional comparison, phase comparison, differential relaying etc.,

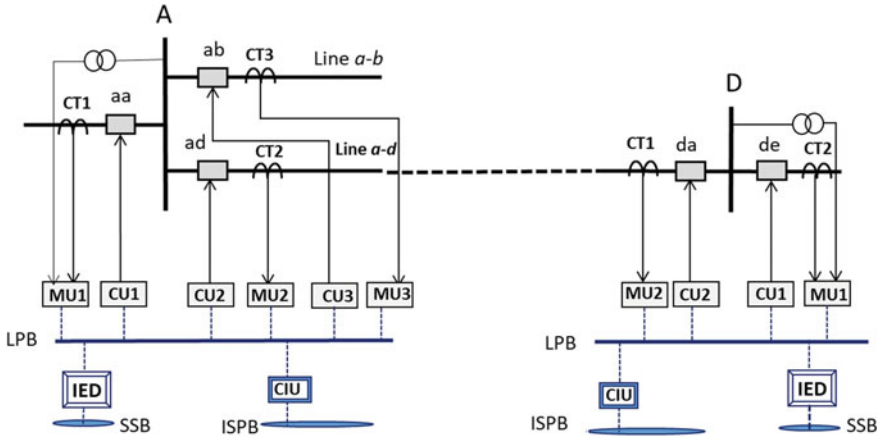

Fig. 26.15 Integrated network protection of a line of a microgrid

can be utilized to protect line *a-b*. Under normal operation condition, the currents at the each end of line *a-b* have the same magnitude, direction and the phase angle. When there is a fault within the line, the current at each end of the line will have different magnitudes, an opposite direction and an 180° phase difference. This information is used to detect and isolate the fault within the line in a very short period of time.

Also the direction and amplitude of the negative sequence reactive powers related to each line measured at the local bus are a good indicator to detect and discriminate an unbalanced fault. If there is a fault within the bus *A,* the negative sequence reactive power of each line connected to it will be exist and its direction will be from the bus through the line, since the source of unbalance is the unbalanced fault itself [20]. A fast tripping is initiated immediately after occurring a fault. This can be done for an integrated protection of each bus in the microgrid.

The same scheme can also be used to protect each line of the microgrid [15], since a local IED is able to have the local measurement related one end of the line and remote measurements related to the far end of the line. When there is an unbalanced fault within the line, the direction of the negative sequence reactive power at each end of the line will be from the line into the bus. They are opposite direction. Any unbalanced fault within the line will be detected and discriminated using this information. When the fault is within any one of buses, currents at each end of the line has the same direction of the negative sequence reactive power.

Therefore, this protection scheme can be used to provide a combination of bus and line protection of a microgrid against unbalanced fault and over unbalanced conditions.

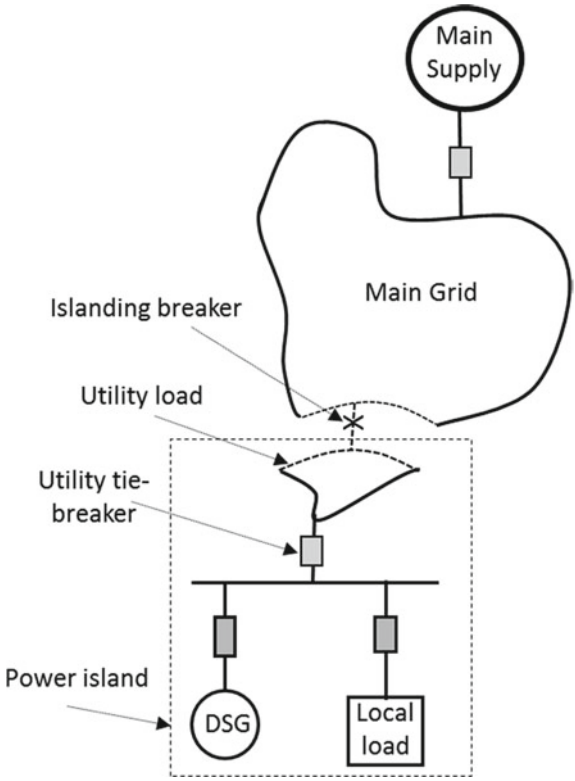

Fig. 26.16 Schematic representation of a power island

26.4.7 Islanding Protection of Microgrid

Figure 26.16 shows a schematic representation of a single source of microgrid and a power island. The DSG unit, which is also known as embedded generation unit, is a synchronized with the main source of supply over the generator tie-breaker or utility tie-breaker. If the local generation exceeds the local demand, the DGS exports the exceed power into utility network, whereas when the local load is greater than the local generation, the required additional power is imported from the main network. When the local generation is not available, the local load is fed by the utility source of supply. Whenever the utility supply is lost, the local load is supplied by the local generation, as long as the local load is within the capacity of local generation. Otherwise, a load shedding process may be required.

During the operation of grid-connected mode, the system frequency and voltage are kept nearly constant by the utility supply, since the network inertia and capacity are much greater than those of the DSG. The local control function will regulate the active and reactive power. Following islanding detection, the utility part is disconnected from the power island. Then the DSG feeds the load connected to the local bus only. The local control system requires to control the system frequency and voltage in

the power island. This will continuous until an orderly restoration of main source of supply.

Islanding [18, 19], which is also known as loss of grid supply is used to describe the case where a part of utility remains connected to the DSG unit without the main power supply following a random opening of one of the utility circuit breakers as seen in Fig. 26.16. Loss of grid could be resulted either from a fault on the network or from a non-fault tripping. Loss of grid results in an independent power island. The local generation unit may continue to supply the power island provided that the system voltage and frequency remain within the required standard limits. However, back feeding a portion of the utility load without the main power supply may result in a safety hazard to the utility personnel and the public, since the utility part of the island would be assumed to be de-energized. An islanding operation may complicate the restoration of utility supply. There are also serious concerns about the quality of service being provided to the customers left connected power island.

The utility part of the power island is required to disconnect from the power island immediately after islanding. This is known as islanding or loss of grid protection. The objectives of islanding protection are to detect the loss of grid and initiate a trip command for the inter-tie circuit breaker. The circuit breaker can then be reclosed under the control of the local control system following the restoration of the main supply. The islanding protection scheme must operate before the response of the local control system, otherwise the control system operates and may bring the system voltage and frequency within the standard limits.

When the DSG is not permitted to export power to the utility network, islanding will cause a power flow from the local source of supply to the utility part. In such a condition, a reverse power protection can detect loss of main supply by solely monitors the power flow in the inter-tie circuit.

Small DSGs can be operated to export power to the main network, and a loss of grid will certainly result in an overloading of the DSG unit. This will certainly cause voltage and frequency drop in the power island. Then under voltage and frequency relay will operate to trip the inter-tie breaker.

In case of large DSGs fitted with a high speed local control, there is always a possibility that the local power generation unit will be able to keep the system voltage and frequency within required limits without the utility source of supply. Therefore, the protection scheme monitoring the system voltage and frequency may not response to islanding. In this case advanced relaying is need to detect islanding and produce a trip command for the inter-tie breaker. This action will let the local generation system to feed the load only connected to the local bus.

Several protection algorithms have been introduced to detect loss of main supply using local measurements taken on the DSG site. Without considering communications, loss of main detection methods can be separated into two main groups. The first group is known as active techniques since each directly interact with the on-going operation of the power system. They include monitoring the system short circuit level and forced reactive power flow. The second group includes under/over frequency, under/over voltage, rate of change of power, phase shifting and can be

considered passive techniques, since they detect islanding by monitoring the power system operating conditions only.

The most practically used relay to detect islanding is the rate of change of frequency relay (ROCOF) based on the system dynamics. This passive method monitors the system voltage to measure the network frequency. Whenever the rate of change of system frequency exceeds a pre-setting for longer than a predefined time delay, ROCOF relay produces a trip signal for the inter tie-breaker. ROCOF relay will response to any condition where frequency changes associated with islanding. A trip level of 0.3 Hz/s is found to be ideal choice with an operating time of half a second. As long as an islanding produces enough disturbance resulting in frequency change more than trip level, islanding can be detected by the frequency relay. Otherwise, a possible failure to detect islanding may occur. An advance protection scheme is required to detect the power island in such a condition.

26.4.8 Multi-source Islanding Detection and Managing Inter-connected Microgrid

Section 26.4.7 has discussed the protection and operation of a single source microgrid. The islanding detection and managing the power island is relatively easy, since the microgrid resulted from islanding is not very complicated as seen in Fig. 26.16. However, microgrid may consist of several number and types of DSG units, which are connected to different point of distribution network as seen in Fig. 26.11. There are several possibilities of switching operations each of which will create different network configuration and related operation conditions. Opening operation of any switch will almost certainly create an interconnected power island (multi-source power island) resulting in power flow among the microgrids. In such a complex structure, islanding detection and managing islanded microgrid require communicated information and possibly a type of microgrid automation. Microgrid automation is needed not only for islanding protection, but also microgrid operation and control. IEC 61850 communication standard provides an effective automation platform for managing of such a complex microgrid.

Figure 26.17 shows flowchart for managing of multi-source microgrid. During the parallel operation, voltage and frequency are kept constant by the utility source of supply. Any switching operation will be sensed by the protection and central controller. If the switching is related to generation and load, the control system controls the active and reactive power locally generated.

Whenever a switching operation results in an islanding, the local operation center identifies the power island configuration. Following the identification of power island, the operation center checks the total generation capacity of the islanded microgrid. If the generation capacity is enough to supply the connected load, then the control function will response to regulate system frequency and voltage by adjusting local active and reactive power. When the generation capacity is not enough, a load shed-

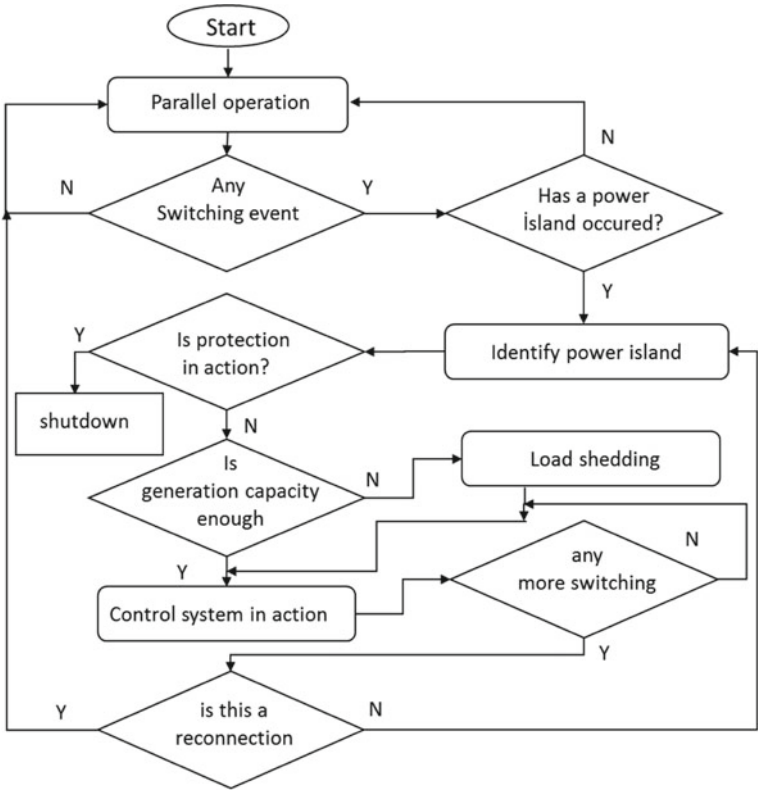

Fig. 26.17 Flowchart of managing a microgrid and an interconnected power island

ding occurs firstly, then the control system will be in action to regulate the system frequency and voltage.

During or after above stage if a new switching operation happens, the operating center identifies this switching operation whether it is a reconnection with the utility source of supply or a new switching in the power island. If it is a switching in the current island the configuration of the new island will be identified by the center, and a new action will be started. If it is a reconnection related switching, the system moves a new stage with grid connected. A new control and protection setting will be required for the parallel operation.

26.5 Under/Over Voltage Protection

An under/over voltage relay continuously monitor the system voltage. When the system voltage is out of allowable limits, the relay responses after a predefined time

delay to protect both local generation units and loads. Pre-set time delay is usually inversely proportional to the change in the system voltage. Instead of using definite time voltage protection, an inverse time characteristic voltage curve may also be used. In this case, the operating time of the voltage relay is automatically calculated by the voltage relay logic.

Under normal operating conditions, while the microgrid is operating in parallel with the utility grid, the voltage is nearly kept constant by the utility source of supply. Any load and generation switching will not seriously affect the system voltage. When there is a fault related switching, the system voltage will be seriously affected and may dramatically decreases. Although other protection techniques will detect and isolate the fault as stated in the introduction, in some conditions such as a high impedance fault, the fault may not be able to be detected using the overcurrent protection principles. In this case, under/over voltage relay will operate to provide protection.

On the other hand, during the islanded operation mode the system voltage will dramatically effected by any load and generation switching. Therefore, under or over voltage conditions may occurs at any time. If the switching creates a controllable situation within the island, the control system will control the case without any difficulties. When a switching creates an uncontrollable case, protection system responses very fast before any control action to isolate the fault.

26.6 Under/Over Frequency Protection

An under/over frequency relay continuously monitor the system frequency. When the system frequency is within the predefined limits, the frequency relay will not response. Whenever the system frequency is out of allowable limits, the relay operate after a predefined time delay to provide protection against under/over frequency conditions.

As long as there is a balance between real power generation and the total load, the system frequency will be stable around the nominal frequency. When there is a difference between the real power generation and the system load, the frequency starts deviate from its normal value. During the parallel operation of microgrid with the power network, the frequency is dominated by the utility source of supply. Any change in the frequency is governed by the power network. In this case, the local control system may regulate active power generation only.

The system frequency may be affected by the load changes, whenever the microgrid is disconnected from the utility source of supply, since the system capacity and inertia will drop immediately after loss of grid. The local control system may not regulate the system frequency in the island. Therefore, microgrid needs an under/over frequency relay to protect the generation units and local loads against under/over frequency conditions.

26.7 Conclusion

This chapter has focused on protection and automation of microgrids in the frame of smart grid. It firstly concentrates on devolution of power generation and the conversion of the radial distribution network into a microgrid. A basic of automation of microgrid is also given. Then, the protection and control requirements of a microgrid are discussed. A further discussion is made on islanding detection and a possible management scheme for single source and multi-source islanded microgrids.

This study indicates that the conventional protection and control systems need to be improved to provide a proper protection and control for the microgrids. A full-automated microgrid infrastructure based on IEC 61850 would be the ideal solution to protect, control and manage the future microgrids.

References

1. G. Fielding, J. Bradley, Local generation-the devolution of power. IER Review (1990)
2. Alstom, *Network Protection and Automation Guide-Protective Relays* (Alstom, 2011)
3. S.H. Horowitz, A.G. Phadke, *Power System Relaying* (Wiley, Oxford, 2013)
4. F. Coffele, C. Booth, A. Dysko, An adaptive overcurrent protection scheme for distribution networks. IEEE Trans. Power Delivery **30**(2), 561–568 (2015)
5. A simple adaptive overcurrent protection of distribution systems with distributed generation. IEEE Trans. SG **2**(3), 428–437 (2011)
6. M.J. Daryani, A.E. Karkevandi, O. Usta, Multi-Agent Approach to Wide-Area Integrated Adaptive Protection System of Microgrid for Pre- and Post-Contingency Conditions. in *IEEE PES ISGT Europe Conference*, Sarajevo (2018)
7. A. Hussain, H.M. Kim, A Hybrid framework for adaptive protection of microgrids based on IEC 61850. Int. J. Smart Home **10**(5), 285–296 (2016)
8. A. Oudalova, Advanced architectures and control concepts for more microgrids (2011), www.microgrids.eu/documents/654.pdf
9. J.B. Brearley, R. Raja Prabu, A review on issues and approaches for microgrid protection. Renew. Sustain. Energy Rev. **67**, 988–997 (2017)
10. IEC standard for communications network and systems in substation, 61850 (2003–2004)
11. Use of IEC 61850 for communications between substations. IEC Standard 61850-90-1 (2010)
12. J. Miao, D. Dastanow, M.A. Redfern, Using IEC 61850 data transfer beyond the substation for enhanced protection for distribution networks. in *48th Power Engineering Conference* (2013)
13. Z.Q. Bo, J.H. He, X.Z. Dong, B.R.J. Caunce, A. Klimek, Integrated protection of power systems. *IEEE PES General Meeting* (2006)
14. Z. Bo, B. Caunce, et al., An integrated protection scheme for distribution systems based on overcurrent relay principle. *CIRED* (2007)
15. O. Usta, F. Ozveren, B. Kara, C. Gocer, H.M. Ozgur, A new directional relaying scheme for the protection of active distribution networks against asymmetric faults. *IEEE PES ISGT Europe* (2018)
16. J. Ekanayake, K. Liyanage, J. Wu, A Yokoyama, N Jenkins, *SG Technology and Applications* (Willey, 2012)
17. I. Ali, S. Hussain, A. Tak, T.S. Ustun, Communication Modeling for Differential Protection in IEC 61850 Based Substations. IEEE Trans. IA (2017)
18. M.A. Redfern, O. Usta, G. Fielding, Protection against loss of utility grid supply for a dispersed storage and generation unit. IEEE Trans. Power Delivery **8**(3), 948–954 (1993)

19. O. Usta, A power based digital algorithm for the protection of embedded generators. Ph.D. Dissertation, the University of Bath (1993)
20. O. Usta, M. Bayrak, M.A. Redfern, A new digital relay for generator protection against asymmetrical faults. IEEE Trans. Power Delivery **17**(1) (2002)

Chapter 27
Protective Systems in DC Microgrids

Ersan Kabalci

Abstract The aging power system causes to several grid problems such as intermittency, power quality issues, and blackouts since a few decades. Therefore, the power infrastructure requires serious troubleshooting studies in a wide manner. The distributed generation and integration of large photovoltaic (PV) plants to the existing utility have led to intensive interest on DC power grid infrastructure. The widespread use of DC based microgrids decreases significant power losses and facilitates operation and maintenance of microgrids. Besides, DC loads are easily supplied by DC microgrids that eliminate the requirement for power inverters. It is noted that elimination of DC-AC power conversion can prevent power losses of entire system between 7 and 15% that is remarkable ratio for a microgrid. In one hand, the DC microgrids provide increased interest due to their advantages such as power density and distribution efficiency comparing to AC power systems. On the other hand, short-circuit current capabilities of DC microgrids lead to significant hazards for users and properties. Moreover, it is not possible to overcome arc faults occurred in a DC microgrid by using regular circuit breakers since DC current do not draw a natural zero crossing waveform. The cost and bulky structure of DC circuit breakers is another important issue in this regard. The actual fault protection systems are based on over current detection for power electronic devices and improved circuit breakers, distributed generation source controllers, and several types of relays. This chapter deals with fault detection methods and protection devices in low voltage DC (LVDC), medium voltage DC (MVDC), and high voltage DC (HVDC) networks. Protection schemes and improved devices with circuit topologies are presented regarding to DC microgrids.

Keywords Microgrid · Protection devices · Grounding · Circuit breakers · Mechanical circuit breakers (MCB) · Multi modular converters (MMCs) · Solid-State circuit breaker (SSCB)

E. Kabalci (✉)
Department of Electrical and Electronics Engineering, Faculty of Engineering and Architecture, Nevsehir Haci Bektas Veli University, Nevsehir, Turkey
e-mail: kabalci@nevsehir.edu.tr

N. Mahdavi Tabatabaei et al. (eds.), *Microgrid Architectures, Control and Protection Methods*, Power Systems,
https://doi.org/10.1007/978-3-030-23723-3_27

27.1 Introduction

The reliability and power quality researches have been gradually increased due to widespread integration of renewable energy sources (RESs) to utility grid, increased demand on distributed generation (DG) on distribution line level, decrements on fossil-based fuels and transmission line efficiencies. It is well known that utility grid benefits from small scale and more flexible DG sources while the behavior has been changed by the penetration of these sources. Therefore, these improvements have leveraged microgrid installations and increased use of DG sources integrated to utility grid. The microgrids are assumed as active distribution grid that is comprised by numerous DG sources, intelligent loads, and energy storage systems (ESSs) such as batteries or fuel cells [1]. When the microgrid infrastructure is handled on grid side, it provides several advantages due to it has been comprised by controlled units and intelligent load profiles. The microgrid infrastructure improves local reliability, decreases the feeder losses, and increases the efficiency and power quality on the consumer side.

On the other hand, it allows decreasing carbon emission and global warming due to its contribution to environment protection by decreasing use of fossil-fuels. However, the technical challenges on planning and efficient operation of microgrid still require laboratory researches to tackle the drawbacks on microgrid management. The most widely met technical challenges are about protection, power quality, islanded and normal operation modes, plug-and-play operation, energy management and system reliability. It is hard to improve an appropriate protection system in terms of two main aspects that one is related with dynamic structure of microgrids while the other one is operation modes of microgrid. Any DG source or load can connect or disconnect from microgrid while microgrid is operating in islanded or normal modes. Therefore, a featured protection system should handle with connection and disconnection in both operation modes [1–3].

The power infrastructure of conventional grid represents a top to down structure starting from transmission to consumption. Since this architecture causes different losses in many distribution systems, it presents limited reliability against faults. This situation has forced to improve a dynamic and active distribution system called microgrid against its conventional and passive grid model. The microgrid sustains its operation even under faulty conditions of utility grid since it generates the power at very close nodes to loads. On the other hand, microgrid supports utility grid by using its ESSs as a feedback system and decreases demand of grid. These features of microgrid allow increasing the reliability and flexibility of utility grid against faults and grid problems. However, the reliability of microgrid can be a problem for utility grid under short circuit conditions if the microgrid protection is not assured. Although the microgrid are installed at distribution level, the common protection devices such as fuses, reclosers and circuit breakers do not provide appropriate protection for microgrid. The short circuit capacity of utility grid is much greater than capacity of microgrid or any DG source in microgrid. This capacity difference causes significant problems on arranging protection devices and coordination of them.

There is an increasing interest on microgrid protection researches and a set of new approaches have been improved [4–6]. The microgrid should be tested and be verified by several protection recommendations in order to ensure their commercial and industrial usage. The researches surveyed in the literature have shown that the current research and developments studies are not at the desired level at this stage. The existing directional over current, distance and differential relays used in current sub-transmission and transmission systems are unique solutions since there are not special relays improved for microgrids. These relays provide more sensitive protection infrastructures against challenging short current levels of microgrids. Although there are significant differences between fault characteristics and topologies of microgrids and utility grids, it is expected that the aforementioned relays will be main protection devices in microgrids. It is assumed that these relays will present same successful operation for microgrids as performed in main grid infrastructures.

This chapter presents main protection challenges, fault detection methods, and protection schemes of DC microgrids in LV, MV, and HV. The fault detection methods are surveyed considering voltage prediction, disturbance detection, and fault classification and locating methods.

27.2 Challenges in DC Microgrid Protection

The HVDC technologies have been used for long years, but MVDC and LVDC microgrid systems and their protection technologies are recently being improved. In spite of the widespread AC microgrids, the DC microgrids are designed and applicated for specific applications. These application areas include LVDC microgrids for data centers up to 1500 V, MVDC microgrids for electric ships up to 35 kV, and medium voltage connection centers for offshore wind energy plants. The recent technical developments have facilitated residential and building microgrids for LVDC systems. The protection is one of the challenging issues in DC microgrid improvements.

International Council on Large Electric Systems (Conseil International des Grands Reseaux Electriques, CIGRE) has proposed a test system for MV distribution line with DG sources. The reference test system is based on a number of features such as short circuit ratio exceeding 20, current imbalance factors up to 20%, and voltage source converters with load supply over than 50% of entire loads. A microgrid represents features of transmission and distribution systems together with bidirectional fault currents and low-cost relay requirements. Therefore, the faulty state behaviors of DG sources in transmission and distribution systems enlighten the DG source faults in a microgrid regardless of source characteristics or types. In this regard, operation of DG sources and power factor fluctuations under fault conditions are researched to improve appropriate protection schemes.

A general architecture of a microgrid comprised by AC and DC sources and loads is shown in Fig. 27.1. The DC microgrid infrastructure is installed by using DC sources, ESSs, and DC loads in general approach, but AC microsources can also be

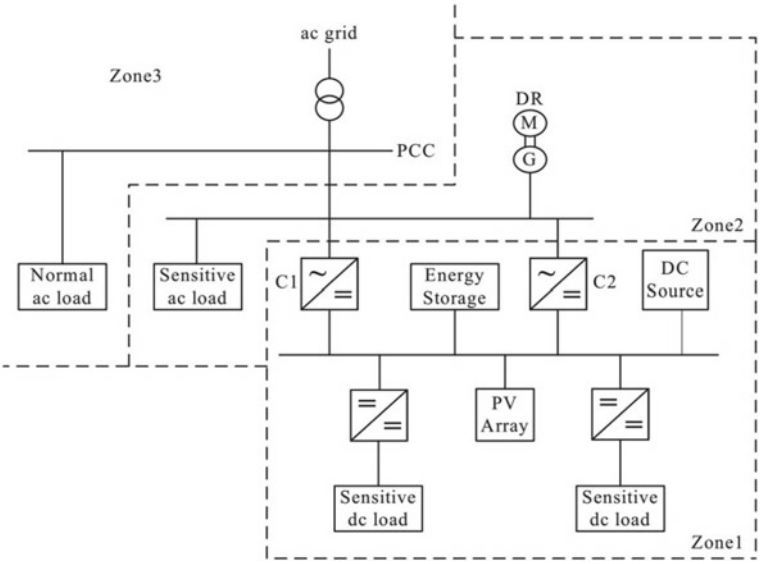

Fig. 27.1 A general architecture of AC and DC microgrid [1]

integrated to DC microgrid by rectifier interfaces. On the other hand, RESs used in a DC microgrid are mostly preferred with DC output voltages such as photovoltaic (PV) arrays, fuel cells, and batteries. The Zone 1 represents a DC microgrid infrastructure while Zone 2 and Zone 3 are AC microgrids. The integration of DC microgrid to AC microgrids require intelligent power converters to condition output power quality and efficiency of Zone 1 to connected neighbor microgrids [1].

The DG sources existing in distribution grid and their contribution to fault currents in both operation modes have caused to several problems for conventional protection devices used in distribution grid. Besides the protection systems, regular control and grid interaction controls also cause to several challenging situations in microgrid protection. The microgrid is expected to overcome following situations considering these conditions;

- Generation systems comprising the bidirectional power flow in LV and MV,
- Islanded and normal mode operation,
- The topological changes occurred with connection of generators, ESSs, and load to LV grid,
- Intermittent operations of various micro sources connected to microgrid,
- Excessive fault currents caused by increment of rotationary machine type microsources in microgrid,
- Inadequate short circuit current levels due to DG sources in islanded operation mode,
- Decreased reclosing time to sustain reliability of LV and MV grids,
- Faulty closing of protection devices due to faults occurred in sequential feeders.

The most significant problems and their reasons are summarized in the following section [1, 5, 7, 8].

The faults occurred in microgrids are classified into threefolds as low impedance faults (LIFs), high impedance faults (HIFs) and voltage sags. The LIFs can be detected by using simple measurement methods while the HIFs are the fault types that fault current is equal to load current. Therefore, voltage sags and fault currents caused by HIFs are not enough to trigger protection devices. In some systems, grounding fault relays also cannot detect HIFs since many groundings exists in the system and ground circulation currents complete their return from different paths. There are special and featured protection devices have been improved since it is quite hard to detect faults in such systems. Some of the HIF detection methods are based on differential current measurement while others focus on detecting the negative component of current. The featured microgrid protection relays include three operational modules for detection of islanded mode, normal mode and impedance faults. Although the HIF detection module operates slower than others, it prevents to become a problem since HIF currents are at small values.

The voltage sag that is the third type of faults seen in microgrids is detected by tracking voltage phasor of point of common coupling (PCC) and comparing to its nominal value. Moreover, the voltage phasor tracking and comparing to nominal value method is effectively used for critical loads by detecting load voltage phasor. A high voltage difference is seen between output voltage of inverter and distribution line during voltage sag faults, and this situation induces high current flow on low impedance lines.

The two different operation modes of microgrid is one of the challenges on improving an appropriate protection plan since the short circuit levels of islanded and normal modes are quite different. In the normal operation mode, the microgrid is connected to MV grid and thus fault current level of grid and DG sources are gradually increased. If the contribution of DG sources to fault current cause short circuit level to exceed rated values of systems, it is required to replace circuit breakers or reclosers with high capacity ones. On the other hand, microgrid is disconnected from MV grid in islanded operation mode and the fault current of DG sources becomes equal to the rated limits of microgrid. Since the fault currents that are generated in this operation mode are limited, the fault current of microgrid will be very low comparing to normal operation mode. The low current level is not enough to be detected by protection devices of utility grid since they are designed for higher current levels. Hence, a protection method that can detect fault currents in both operation modes is required to be improved for microgrid protection [5, 7].

The false tripping that is known as faulty circuit breaking is caused by the increment of a fault current of a DG sources in substation that is fed by another fault current. The protection devices of neighboring feeders disconnect the connection between microgrids and false tripping or unnecessary breaking of feeders is prevented in such conditions. Another protection error is known as “blindness of protection” that is related with pick up current level. The operating region of over current relays are determined by pick up current that is depended to feeder impedance. The pick-up current is selected higher than feeder current and lower than minimum short circuit

current of the protected region. Once a DG source is connected to grid, the feeder impedance increases and the fault current rate that is detected by over current relay decreases. This situation reduces operation range of relay and the relay cannot handle the protection line that causes blindness of protection. The distribution grid without any DG source is installed in radial type, and recloser can manage the disconnection process on demand. However, DG source participation to MV distribution grid changes operation conditions of recloser since DG source sustains to supply fault current even though recloser had disconnected the MV grid from microgrid. Under these circumstances, DG source continues to supply fault current until recloser is broken down and this operation causes transformation of transient fault to a permanent fault [1].

These kinds of faults and challenges should be carefully handled in microgrid protection system design. The fault detection methods and protection system improvements play crucial role on microgrid reliability and security. The solutions of aforementioned fault types rely on adaptive and intelligent protection schemes that are presented in the following sections.

27.3 Fault Detection Methods in DC Microgrid

One of the most important barriers for improving an appropriate protection scheme is related with dc fault of voltage source inverters (VSIs). On the other hand, the accurate and instant detection of faults are other significant challenges in microgrid protection. Lack of efficient dc circuit breakers, fast and accurate relays, and sensitive reclosers mostly cause the challenges [1, 5]. The fault current flows from MV network to distribution grid and microgrid in a conventional grid structure where microgrid is connected to MV network. Therefore, fault detection is accomplished by using simple methods such as comparing the value of measured current with the threshold value. However, the DG sources located in conventional or recent microgrid infrastructure increase the complexity of fault direction and magnitude detection processes. This section presents most important fault detection methods that are used in dc microgrids. These include regular analysis inherited from conventional microgrid protection, voltage prediction, disturbance detection, and fault detection and location methods.

The voltage prediction is inherited by enhancing conventional analysis methods. It relies on monitoring output voltages of VSIs, DG sources and other sources, and the measured value are converted from rotationary plane to d-q stationary plane. The stationary plane generates DC equivalent of any three-phase power system, and thus the dc calculations are obtained. The voltage prediction and analysis method are used by comparing obtained dc values with reference value to detect fault situation of distorted signal. The distortion measurement is essential to determine error rate between reference values where it is zero if there is not any fault occurs in the microgrid. In any faulty condition, the measured distortion signal fluctuated from zero to maximum to represent phase voltage error. In case of bus faults, the error signal

exceeds its maximum value. Total harmonic distortion (THD) analysis is another significant method in fault monitoring and detection researches. The output voltage of DG sources and VSIs are monitored to detect phase faults that causes low impedance voltage at sources [1].

The widely seen fault types in DC microgrid infrastructures are pole-pole and pole-ground faults. Positive and negative lines mostly cause the pole-pole faults while pole-ground faults occur between terminals and ground nodes. The pole-pole faults can be easily detected since they cause protection damages while poe-ground faults cannot be determined by basic methods. The DC ark faults are seen in highly resistive ground applications such as PV plant connections where UL 1699B ark mitigation standards should be followed for protection. The existence of power converters causes several drawbacks and latencies on fault detection of DC microgrids [9]. The arc sources cause power dissipation in microgrid infrastructure. Lee et al. proposed a resistance model for DC microgrid to detect arc faults in series and parallel circuits [10]. The modelled arc fault types are presented in Fig. 27.2 where series arc fault is illustrated in Fig. 27.2a and series arc fault model is shown in Fig. 27.2b while parallel arc fault is shown in Fig. 27.2c and parallel arc fault model is designed as seen in Fig. 27.2d. The arc types and arc detection methods are analyzed according to these models. The power meters are located between positive terminal of utility source and negative terminal of DG source or load side. A microprocessor-based measurement board monitors the power exchange and current or voltage changes in faulty series and parallel branches are rapidly detected [10].

The disturbance detection methods rely on transient analysis by extracting measured grid distortion signals. The measured wavelet transforms dispatch transients into wavelet series for obtaining time domain signals to detect researched information on a certain frequency domain in AC microgrids. The DC microgrid integrations are also protected by using impedance relays and travelling wave analyses [11]. The fault locating is performed by using several methods such as fundamental phasor information, phasor measurement unit (PMU), and phasor voltage sag in AC microgrids. The travelling wave analysis is an essential detection method for locating grid faults. However, there is a serious limitation for detecting the fault location in dc microgrids since it does not have frequency and phasor data for analysis. Current fault locating methods are based on measurement of current rise ratio, detection of current oscillation pattern, continuous wavelet transform, iterative estimations and artificial neural network detections [12].

27.4 Protection Schemes in LVDC Microgrids

The improvements in power electronics devices have promoted development of LVDC microgrids. The LVDC microgrid architectures decrease losses of AC microgrids in LV. The LVDC infrastructure is mostly comprised by PV plants and ESSs, and connected to AC grid at MV level or can be integrated to an AC microgrid architecture. The most widely seen protection requirement is short-circuit (SC) cur-

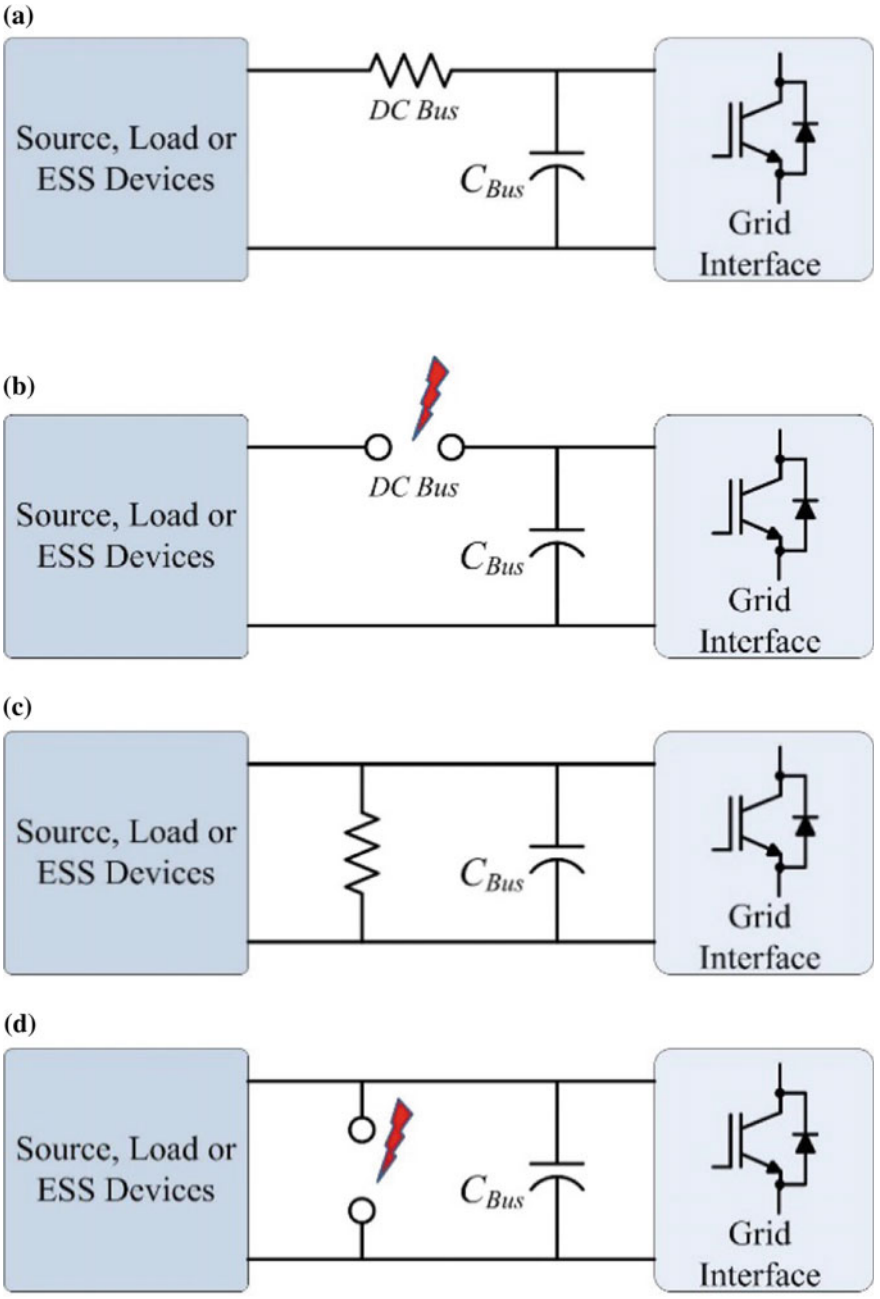

Fig. 27.2 Arc fault models and types in a DC grid, **a** series arc fault model system, **b** series arc fault, **c** parallel arc fault model system, **d** parallel arc fault

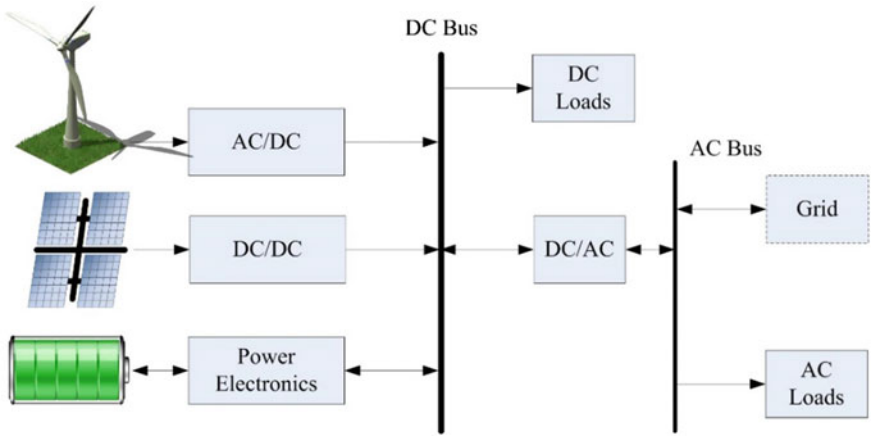

Fig. 27.3 Block diagram of a single bus DC microgrid

rent protection in LVDC networks. In case of any fault occurred in LVDC, the PV and ESSs contribute to this SC level. Power converters limit the SC current levels and power electronic devices prevent increment of SC. The output capacitors of dc converters cause to higher SC current levels comparing to LVAC microgrids [13]. The fault types of LVDC have been presented in [14] as short circuit fault, ground fault, disconnection faults. The DC SC fault protection systems should be designed considering IEC 61660-1 that is the most widely used international standard for DC SC characterization. Any power converter, ESSs, output capacitors, and DC motors with external excitation can supply the LVDC SC currents [13].

The DC microgrids are classified into three categories according to bus topologies as single-bus, multibus, and reconfigurable bus. The single bus topology that is shown in Fig. 27.3 is comprised by most common dc sources as DG equipments and even AC sources are integrated by using a rectifier while the multi bus configuration is illustrated in Fig. 27.4. The single bus topology is mostly preferred in industrial applications and sometimes in residential applications. In this topology, a single dc bus is installed and sources are connected to this bus with ESS integration for comprising the backup of system. The most widely known usage area of single bus dc topology was improved for telecommunication applications at −48 V supply. This topology is now widely researched for LVDC microgrid networks in literature.

In spite of its advantages, several technical challenges and problems are related with LVDC systems. The direct connection of ESS to DC bus decreases equivalent bus capacitance and it should be considered while designing dc bus and control system. On the other hand, single bus supplying all consumers can be a problem itself. Therefore, the positive and negative single bus sharing has been analyzed and Kakigano et al. [15] have proposed a new method called bipolar single bus where positive and negative voltage levels are generated. In the proposed LVDC line, the 340 V Japanese standard dc voltage level is shared to +170 V at positive line and

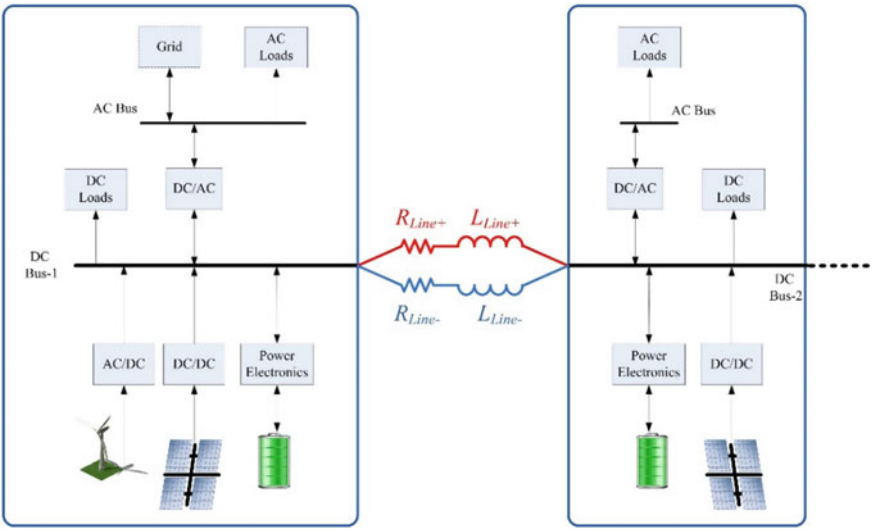

Fig. 27.4 General architecture of multi bus DC microgrid

−170 V at negative line while an additional neutral line is also installed. This approach increases prevention rate of one line fault and two different lines are supplied by different converters [16].

The multi bus DC microgrids are configured to increase power rates and reliability by integration of several single bus DC microgrids as seen in Fig. 27.4. The bus configuration and automated connection between buses are widely researched and several approaches have been presented in [16, 17]. Regardless of bus architecture, the reliability and secure operation of any LVDC network is depended to a tailored protection system that is comprised by protection and current control devices, protection relays, monitoring tools, and grounding solutions.

If we recall AC and DC microgrid architecture shown in Fig. 27.1, the LV protection scheme can be performed for DC system existing in Zone 1, and AC protection for the system located in Zone 2 that includes grid and consumer interconnection bus and generation system. The LVDC protection system includes grounding, power electronics protection devices, circuit breakers (CBs), fuses, and monitoring devices.

Grounding is a detailed issue since there are many topologies and design approaches exist. It is required to ensure device and user safety besides increasing the performance of microgrid. A LVDC microgrid can be ungrounded or grounded with high resistance or low resistance. Furthermore, the grounding can be done between positive and negative terminals or at the common node of converter and ESSs. The main grounding alternatives are shown in Fig. 27.5a and b regarding to TN-S and IT grounding approaches [18]. The T in TN-S system denotes terra term where earth connection is directly done and it supplies neutral node. There is a spare protective earth (PE) connection and a neutral (N) connection seen in TN-S grounding as

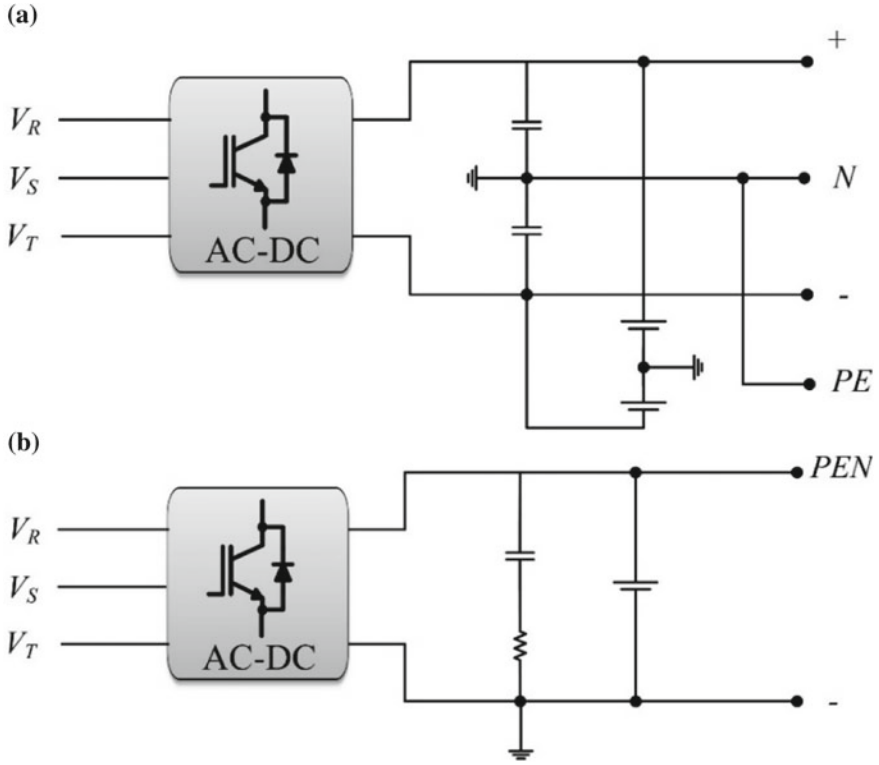

Fig. 27.5 Grounding methods in LVDC microgrid, **a** TN-S grounding, **b** IT grounding

depicted in Fig. 27.5a. The common node of converter output is connected to N node of microgrid. In the IT network shown in Fig. 27.5b, positive terminal is connected to neutral that is depicted as PEN and power network is not connected to earth but has high impedance due to ground connection.

The TN-S system provides a high ground current and high dc transient voltage if a low-resistance ground fault occurs. The high transient voltage can cause damages on loads that are connected to faulty terminal, but the other loads are not affected from this transient voltage. In this regard, the fault is rapidly detected and can be cleared in a short while. On the other hand, the IT dc networks represent small current and voltage transients during fault conditions. Thus, reliable operation of loads will be ensured during single ground faults, but pol-ground voltage can be changed by any ground in the system and critical or sensitive loads can be affected from this change. The high impedance results small ground fault currents that are not easily detected and causes power losses in the network [18].

The protection devices that can be used in LVDC networks are fuses, LV CBs, molded case CBs (MCCBs), and isolated case CBs (ICCBs). Although some of these are specifically improved, high majority can be found commercially and used

Table 27.1 Comparison of most widely used LVDC protection methods

Protection method	Advantages	Disadvantages
Under voltage protection	Independent from fault current level	Hard to detect HIFs, and difficult to coordinate
Impedance based protection	Most appropriate method for islanded microgrids	Sensitive to DG source contributions
Differential protection	Insensitive to fault current level, DG source type and location	Communication and synchronization requirements
Symmetrical component-based protection	Efficient on asymmetrical fault detection	Unable to detect all fault types
Adaptive protection	Can be configured according to microgrid operating conditions	Reliable communication line is required
Fault current limiter usage	Existing DC protection devices can be used	Only appropriate for grid connected operation
Fault current source	Existing protection devices can be used	High cost comparing to other methods

in LVDC and AC microgrids. The fuses are designed regarding to their current-time and voltage ratings relying on fuse link and heat absorbing material structure. The copper or silver materials are mostly used as fuse link and silica sand is used for heat-absorbing material. The current-time constant of a fuse determines its breaking time since a minor constant allows rapid increment of current and fast melting of metal section.

On the other hand, the current increment will be slow if time constant is high. The main operation of a LVDC protection system is to find and isolate faults in a fast and accurate way. The faults can be seen on pole-pole and pole-ground as discussed earlier. The pole-pole faults are occurred in LIF characteristics while pole-ground faults can be LIFs or HIFs. On the other hand, faults can occur on buses or feeders. The critical faults are short circuits between poles and positive pole to ground that affect converter and battery systems. The feeder faults are important to determine faulted loads and planning to improve a backup protection system. The source faults are generally occurred on bus while load faults are seen on feeders. The bus faults affect all the DG sources connected to the common DC bus. The proposed protection methods have been compared regarding to their advantage and disadvantages in Table 27.1 [2].

The under voltage based protection scheme is efficient since it is independent from fault current value and direction. However, it is vulnerable to transient voltages, load switchings, connection and disconnection surges, and it is hard to coordinate protection scheme. Although the voltage-based protection schemes are not efficient in HIFs, they provide better success on detecting the low fault currents and provide improved fault detection comparing to regular over current relays. Another protection type is developed for impedance measurements alternatively to voltage or current

based protection schemes. They provide appropriate solutions in islanded microgrid operations since the impedance is stable and detection is performed by using an easy and accurate calculation. The differential protection provides insensitivity to fault current levels to facilitate detection and it is not affected by any type, size, profile or location of DG sources along the microgrid. However, differential protection method is not an appropriate solution for backup systems and it requires communication and synchronization mechanisms that increase the overall cost of system.

The symmetrical component-based protection scheme requires additional protection devices to be used together, and it is efficient on asymmetrical fault detection. However, it cannot be used to detect all fault types along the microgrid [2].

27.5 Protection Schemes in MVDC and HVDC Microgrids

The improvements of power electronics and semiconductors have facilitated to install DC distribution networks in MV and HV. Although the HVDC systems are known as a mature technology, the MVDC distribution and transmission networks are proposed as experimental and industrial applications at present. One of the widest use areas of MVDC is marine sector where hybrid or all electric ships (AESs) are being implemented. The MVDC distribution network provides the following advantages comparing to MVAC alternative,

- Synchronization and phase measurement are not required and connection and disconnection of different type and power rated sourced to microgrid is facilitated,
- The elimination of line frequency transformer decreases cost, weight, and volume of power systems,
- The fault current elimination increases efficiency on system configuration and power flow control,
- The removal of frequency and components improve design and operation flexibility.

However, MVDC system is posed to several technical challenges on system protection, reliability, and stability. The reliability of an MVDC network is ensured by using reliable and efficient power sources, high power DC-DC converters and protection systems for SC currents. In an MV network of AES sample of MVDC microgrid, the power electronics devices are required for rectifying the output voltage of AC generator, transferring the rectified power to MVDC microgrid, supplying the MV loads such as propulsion drives, connecting LV service units to MVDC microgrid, and operating high efficient and accurate CBs [19]. The MVDC networks are connected to AC grids and AC RESs over VSIs where the conventional protection schemes are affected on reliability. The low fault tolerant structure of VSIs requires rapid protection methods and CBs. Therefore, MVDC systems require fast detection and location methods to ensure protection. The protection systems should be designed by complying with strict recommendations for rapid detection in MV and

HVDC systems. The traditional distribution system is comprised in a radial topology and over current relays are the most widely used protection devices since the power flow is not bidirectional in this network type. The improvement of microgrid and DG integration to distribution network has changed this situation to consider bidirectional power flow. Thus, the over current relays lack on reliability and fault detection since over current rates of feeders rapidly change during islanded and normal operation modes of DG sources. On the other hand, the fault current rapidly increases in VSI-based DC networks and it prevents over current relays to operate in their main protection zone. Although there have been numerous studies proposed in literature [20], the grounding is one of the most important topic affecting transient SC currents and overvoltage (OV) rates that complicate fault detection and protection [21–23]. The MVDC and HVDC systems are classified into three categories such as ungrounded, resistively grounded, and solidly grounded systems [21].

The ungrounded system that is known as floating system provides better reliability of power supply under single-pole ground faults comparing to grounded systems. Although the ungrounded system is preferred due to installation simplicity and low-cost features, it is not easy to rapid detection of faults except single-pole ground types. In case of second ground connection is realized at the next pole of system, it causes pole-pole fault and accelerates serious damages. Another significant drawback of ungrounded system is related with leakage current detection. It is not possible to detect small leakage currents in ungrounded system configuration and it results to determine an exact DC reference for offset requirements. The DC voltage fluctuations increase the inductor cross-sections and costs in high voltage applications.

The resistively grounded system is installed by connecting resistors between poles and ground as its name implies. The resistive connection can be done between pole-ground or in the middle point of shunt connected two series resistance. In the second configuration, two series resistors are shunt-connected between positive and negative poles of power converter and a virtual ground is comprised at the middle point of resistors that is mostly preferred for HVDC systems. The major advantage of resistively grounded system is that it limits transient voltage and currents to small values during ground faults and the system sustains reliable operation even during single-pole ground faults. This configuration prevents high voltage transients occurred single-pole ground faults.

The solidly grounded systems are mostly used in bipolar DC (BPDC) power networks where dual power converters are series connected to generate positive and negative poles, and ground point is located in the middle point of converters. The neutral point of this system causes higher ground current and dc link voltage transients comparing to other grounding systems. However, solidly grounded systems are convenient to rapid detection and clearance of faults due to appropriate designs with protective relays, CBs, and switches. The comparison of grounding systems in unipolar DC (UPDC) and BPDC configurations are presented in Table 27.2 considering several factors [21].

As expressed earlier, the efficient and robust protection scheme is based on use of reliable CBs for rapid detection and isolation of fault current. The protection devices are as important as design and implementation methods in DC microgrids. There

Table 27.2 Comparison of grounding methods and DC converter configurations [21]

	Ungrounded		Resistively ground		Solidly grounded	
	UPDC	BPDC	UPDC	BPDC	UPDC	BPDC
SC current	Very low	Very low	Low	Medium	Low	High
Transient OV	High	High	Medium	Medium	Low	Low
Leakage current	Very low	Very low	Medium	Medium	Low	Medium
Insulation	Nominal	Nominal	Nominal	Nominal	Nominal	Half
Power loss	No	No	Yes	No	No	No
Safety	Low	Low	High	High	High	High

are several challenges may be met in DC microgrids while designing a protection system since there is not any zero-crossing available in current or voltage waveforms. Furthermore, the low inductance of DC power networks causes rapid rise of fault currents and limits fast response capability of CBs. The rapid detection and reacting to fault current are main motivation of CB development researches. The fundamental requirement of protection devices is control simplicity, low-cost installation, rapid operation, low response time, and power losses.

The fuses are essential protection devices for MVDC and HVDC networks as they are used in LVDC systems. The self-triggered fuses provide SC and OV protection for DC systems up to 36 kV voltage ratings. They can be securely used in DC networks due to their high *di/dt* ratios that cope with low inductance of DC grid. However, fuses are designed for single use and should be replaced with fixed one after any fault has been cleared. The most important advantage provided by SSCBs is their operating speed and reliability supplied by semiconductor switches. The SSCBs can react to faults in microseconds and can isolate faulty systems rapidly. They ensure rapid fault detection and increases fault current or voltage ratings due to use of several power switches in series or parallel connections. The power losses of SSCB can be reasonable in steady state but some decrement on switching frequency is required at high voltage applications to decrease losses [21, 22].

Mechanical circuit breakers (MCB) are legacy technologies that have been improved for DC power systems. The fundamental idea behind MCB is its resonance circuit that has been improved for AC CBs as mechanical AC circuit breakers (MACCB) shown in Fig. 27.6. The resonance network that is directly connected to main CB or through a switch is used to generate a zero crossing for fault current. The basic circuit diagram of a passive MCB seen in Fig. 27.6 is based on opened and closed situation of MACCB that causes resonance fluctuation of circuit. The resonance circuit produces a negative increasing oscillation current when MACCB is opened. Since the produced current is higher than fault current, MACCB recognizes the zero-crossing current and fault current is cleared. On the other hand, active MCB is operated according to recharge of capacitor in resonance network and the resonance network is connected to grid when MACCB is opened. The obtained maximum resonance value triggers the operation of MCB and thus, increased frequency of

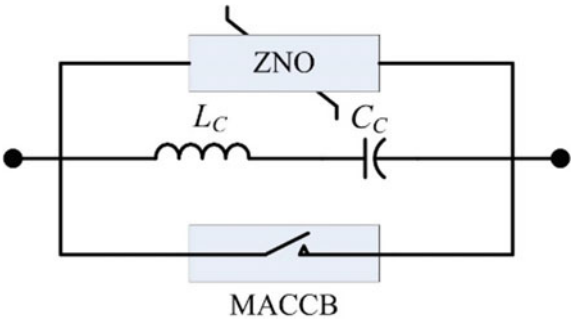

Fig. 27.6 Circuit diagram of a passive MCB

resonance network copes with high rise fault currents. The fault current clearance of a MCB is completed in 30–100 ms according to its response time that is appropriate for line commutated converter and low speed protection systems in a transmission network [21]. When the higher speeds are required, the solution is brought by solid-state circuit breakers (SSCB) that are based on semiconductor switching devices such as insulated-gate bipolar thyristors (IGBT).

The device topology of a SSCB can be designed either in unidirectional or in bidirectional configuration that are shown in Fig. 27.7a and b, respectively. The unidirectional configuration, the surge arrester and a series freewheeling diode is located in shunt to output DC bus. The IGBT switch is operated at on-state during normal operations and allows to flow of load current. In case of any fault, the IGBT is shifted to off-state and fault current forces freewheeling diode to suppress the surge voltage. The series connection of surge arrester limits the operating rates and facilitates surge arrest. The bidirectional SSCB seen in Fig. 27.7b is comprised by back-to-back connection of IGBTs and pair of surge arrester and freewheeling diode are located at the input and output of SSCB. The operating voltage and current ratings of SSCBs are depended to switching devices where series connection of IGBTs increases operating voltage while shunt connection is required to increase fault current rates [21].

The hybrid HV circuit breaker (HHVCB) is another protection device that is improved for decreasing switching losses of SSCB devices. A SSCB and an additional bypass branch as shown in Fig. 27.8 comprise the HHVCB for HVDC protection applications [21]. The bus current flows over bypass branch during normal operation conditions and the bus current of main switch line is zero. In any fault situation, the mechanical contactor of bypass branch immediately opens and load communication is provided by switching SSCB semiconductors on main bus.

The main SSCB bus and semiconductors should be able to operate at fault current and peak DC voltage levels in order to ensure appropriate operation of HHVCB. The mechanical contactor should neglect to open at zero current due to low voltage drop. The load communication switches are required to be rated at current and voltage levels of transmission line.

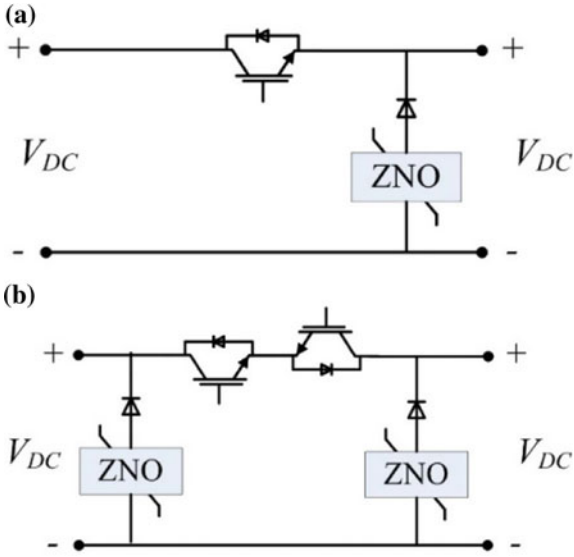

Fig. 27.7 Circuit diagrams of SSCB systems, **a** unidirectional, **b** bidirectional

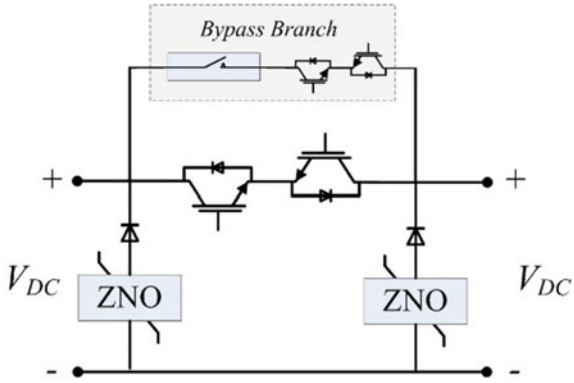

Fig. 27.8 Circuit diagrams of hybrid HVCB

Although the SSCB and HHVCB are appropriate protection devices to be used in MVDC and HVDC systems, the absence of galvanic isolation causes some drawbacks for these devices. Both devices require galvanic isolators to clear leakage current that is occurred after fault current and SSCB operation in addition to increase the safety and security of entire system. The galvanic isolator connection that provides physical isolation is performed to SSCB or HHVCB devices as seen in Fig. 27.9. The high fault current protection is accomplished by galvanic isolator switches in addition to semiconductor devices in CB topologies. The mechanical galvanic isolators are located two poles of HVDC system to ensure rapid protection of entire system. The controllers of isolators are triggered by leakage current that is produced after activation of HHVCB to clear fault current.

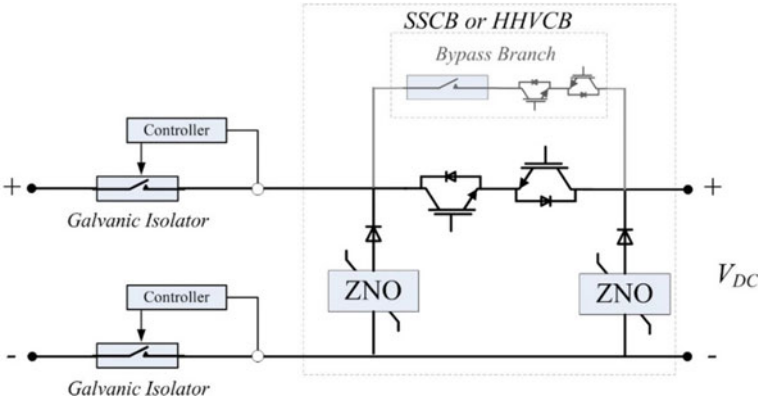

Fig. 27.9 Circuit diagrams of CBs with galvanic isolator

As discussed earlier, the isolation is required to ensure safety and security of entire system. The isolation provides different grounding applications on the input and output systems of an isolated HVDC system. The semiconductor-based DC-DC converters are essential on isolating any faulty section through a DC network. The fundamental topologies are based on regular half-bridge or full bridge choppers, and line-commutated converters [21, 24]. In addition to conventional topologies, dual active bridge (DAB) and flyback based converter topologies are utilized to meet isolation requirement of CBs.

While the two-level DABs are comprised by fundamental two-level voltage source converters (VSCs), cascaded multi-level and multi modular converters (MMCs) allows to have some advantages such as lower dv/dt on switches, decreased electromagnetic interference (EMI), and increased power density comparing to two-level DABs. The cascaded multi-level converters are comprised by series connection of two-level DABs as their name implies, and the galvanic isolation is provided by transformers located between each converter stages [24].

Another important protection device that is used in MVDC and HVDC systems is superconductive fault current limiter (SFCL). It is based on zero-resistance superconductors that are comprised as resistive SFCL (RSFCL) and inductive SFCL (ISFCL) to be used in DC systems. Although these superconductive devices are being researched for a long time, they are still accepted as immature technologies for industrial use. The comparisons of aforementioned CBs are listed in Table 27.3 [21].

Table 27.3 Comparison of CB devices

	MCB	SSCB	HHVCB	Converters	SFCL
Response time	Up to 100 ms	100–200 μs	500 μs–1 ms	100–200 μs	A few ns
Power loss	10^{-3} p.u.	<0.02 p.u.	10^{-3} p.u.	0.05 p.u.	10^{-3} p.u.
Cost	Low	Low	Medium	High	N/A
High-speed protection	No	Yes	Yes	No	No
Galvanic isolation	Yes	No	No	No	No

27.6 Conclusion

This chapter presents protection schemes and devices that are used in DC microgrids. The DC microgrids are being extensively researched since a few decades. The main reason behind this is brought by large integration of DC based renewable and distributed energy sources to utility grid. The wide use of PV plants, batteries, fuel cells, and ESSs have increased interest on DC microgrid infrastructures at LV, MV, and HV ranges. The LVDC systems that were used in telecommunication applications for long years have been integrated to residential and industrial uses. On the other hand, electric vehicles and electric transportation including ships, trams, and trains promoted researches on DC microgrid applications as an alternative to legacy HVDC systems.

Although the researches on DC microgrid have been extensively performed, the protection systems of DC grids are still based on conventional circuit breakers and isolators that are widely used in AC grids. One of the most important barriers for improving an appropriate protection scheme is related with dc fault of voltage source inverters (VSIs). On the other hand, the accurate and instant detection of faults are other significant challenges in microgrid protection. Lack of efficient dc circuit breakers, fast and accurate relays, and sensitive reclosers mostly cause several challenges for DC protection. The fault detection and clearing approaches cause these challenging issues due to lack of dedicated DC protection devices. However, surveyed studies have shown that featured protection devices and protection schemes are being researched for DC microgrids. Moreover, power electronics is widely used to tackle drawbacks of conventional electromechanical circuit breakers, fuses, and isolators. The specific protection schemes and improved protection devices are presented in detail for DC microgrid applications.

References

1. S.A. Hosseini, H.A. Abyaneh, S.H.H. Sadeghi, F. Razavi, A. Nasiri, An overview of microgrid protection methods and the factors involved. Renew. Sustain. Energy Rev. **64**, 174–186 (2016)
2. J. Shiles et al., *Microgrid protection: An overview of protection strategies in North American microgrid projects* (IEEE Power & Energy Society General Meeting, Chicago, IL, 2017), pp. 1–5
3. L. Che, M.E. Khodayar, M. Shahidehpour, Adaptive protection system for microgrids: Protection practices of a functional microgrid system. IEEE Electrification Mag. **2**(1), 66–80 (2014)
4. K.Y. Lien et al., A novel fault protection system using communication-assisted digital relays for AC microgrids having a multiple grounding system. Int. J. Electr. Power Energy Syst. **78**, 600–625 (2016)
5. A. Hooshyar. R. Iravani, Microgrid protection. Proc. IEEE **105**(7), 1332–1353 (2017)
6. H.M. Sharaf, H.H. Zeineldin, E. El Saadany, Protection coordination for microgrids with grid-connected and islanded capabilities using communication assisted dual setting directional overcurrent relays. IEEE Trans. Smart Grid **9**(1), 143–151 (2018)
7. G. Buigues, A. Dysko, V. Valverde, I. Zamora, E. Fernandez, Microgrid protection: Technical challenges and existing techniques. Renew. Energy Power Qual. J. 222–227 (2013)
8. O. Nunez Mata, R. Palma Behnke, F. Valencia, P. Mendoza Araya, G. Jimenez Estevez, Adaptive protection system for microgrids based on a robust optimization strategy. Energies **11**(2), 308 (2018(
9. S. Dhar, R.K. Patnaik, P.K. Dash, Fault detection and location of photovoltaic based DC microgrid using differential protection strategy. IEEE Trans. Smart Grid **9**(5(, 4303–4312 (2018(
10. K.J. Lee, G.S. Seo, B.H. Cho, DC arc fault Detection method for DC microgrid using branch monitoring. in *9th International Conference on Power Electronics and ECCE Asia (ICPE-ECCE Asia)*, Seoul, South Korea (2015), pp. 2079–2084
11. C. Aguilera, E. Orduna, G. Ratta, Adaptive Noncommunication Protection Based on Traveling Waves and Impedance Relay. IEEE Trans. Power Deliv. **21**(3), 1154–1162 (2006)
12. J.D. Park, J. Candelaria, L. Ma, K. Dunn, DC Ring-bus microgrid fault protection and identification of fault location. IEEE Trans. Power Deliv. **28**(4), 2574–2584 (2013)
13. A. Virdag, T. Hager, R.W. De Doncker, Estimation of short-circuit currents in future LVDC microgrids. CIRED—Open Access Proc. J. **1**, 1098–1101 (2017)
14. M. Yu, Y. Wang, L. Zhang, Z. Zhang, DC short circuit fault analysis and protection of ring type DC microgrid. in *IEEE 8th International Power Electronics and Motion Control Conference (IPEMC-ECCE Asia)*, Hefei, China (2016), pp. 1694–1700
15. H. Kakigano, Y. Miura, T. Ise, Low-voltage bipolar-type DC microgrid for super high quality distribution. IEEE Trans. Power Electron. **25**(12), 3066–3075 (2010)
16. T. Dragicevic, X. Lu, J.C. Vasquez, J.M. Guerrero, D.C. Microgrids-Part II, A Review of power architectures, applications, and standardization issues. IEEE Trans. Power Electron. **31**(5), 3528–3549 (2016)
17. T. Dragicevic, J.C. Vasquez, J.M. Guerrero, D. Skrlec, Advanced LVDC electrical power architectures and microgrids: A step toward a new generation of power distribution networks. IEEE Electrification Mag. **2**(1), 54–65 (2014)
18. D. Salomonsson, L. Soder, A. Sannino, Protection of low-voltage DC microgrids. IEEE Trans. Power Deliv. **24**(3), 1045–1053 (2009)
19. S. Castellan, R. Menis, A. Tessarolo, F. Luise, T. Mazzuca, A review of power electronics equipment for all-electric ship MVDC power systems. Int. J. Electr. Power Energy Syst. **96**, 306–323 (2018)
20. M. Monadi, M.A. Zamani, C. Koch-Ciobotaru, J.I. Candela, P. Rodriguez, A communication-assisted protection scheme for direct-current distribution networks. Energy **109**, 578–591 (2016)
21. M. Farhadi, O.A. Mohammed, Protection of multi-terminal and distributed DC systems: Design challenges and techniques. Electr. Power Syst. Res. **143**, 715–727 (2017)

22. A.E.B. Abu Elanien, A.A. Elserougi, A.S. Abdel Khalik, A.M. Massoud, S. Ahmed, A differential protection technique for multi-terminal HVDC. Electr. Power Syst. Res. **130**, 78–88 (2016)
23. Q. Yang, S. Le Blond, R. Aggarwal, Y. Wang, J. Li, New ANN method for multi-terminal HVDC protection relaying. Electr. Power Syst. Res. **148**, 192–201 (2017)
24. J.D. Paez, D. Frey, J. Maneiro, S. Bacha, P. Dworakowski, Overview of DC-DC Converters dedicated to HVDC Grids. IEEE Trans. Power Deliv. 119–128 (2018)

Chapter 28
Adaptive Protection Systems

Marian Gaiceanu and Iulian Nicusor Arama

Abstract Sustainable resources would replace traditional energy production solutions in the near future. There are determinant factors that force to adopt the changes in actual power system: environmental protection, and the increasing price of natural gas, coal and oil. The chapter provides a short overview of protection functions in adaptive systems. Nowadays, the alternative energy sources forced the power system to support major transformations. The energy producers or medium voltage (MV) electricity market operators through remote controllable line disconnectors achieve new technology in distribution power systems. The remote-controlled recloser is one of the most important equipment used in MV distribution systems. The chapter contains the most features of the remote-controlled recloser. The adaptive protection of a distributed system is based on the Loop Automation Scheme, described largely by the authors. The main advantage is the restoration of energy supply to consumers in minimum time. The chapter includes a case study in the Galati distribution operator activity area (Romania).

Keywords IEC 61850 · Adaptive protection · Smart grid · Loop automation

28.1 Introduction

Traditional methods of energy production are considered to be replaced by sustainable resources in the near future. The main factors contributing to these changes are the environmental protection, continuous increases price of the fossil sources (coal, oil and natural gas).

M. Gaiceanu (✉) · I. N. Arama
Department of Automation and Electrical Engineering, Dunarea de Jos University of Galati, Galati, Romania
e-mail: marian.gaiceanu@ugal.ro

I. N. Arama
e-mail: iulian.arama@ugal.ro

N. Mahdavi Tabatabaei et al. (eds.), *Microgrid Architectures, Control and Protection Methods*, Power Systems,
https://doi.org/10.1007/978-3-030-23723-3_28

In this context, the energy generation from the renewable energy sources (RES), based on distributed generations (DG) has been encouraged in recent years by a number of environmental, political and economic factors.

To implement such a system based on these DGs, arises new necessities in terms of investing in energy distribution. The use of the DGs is the foundation of the Smart Grid System (SGS) concept implementation.

Integration of the DG to the electrical distribution system (EDS) increases the complexity of the operation, control, and protection in the medium (MV) and low voltage (LV) networks. The impact of the DG introduction into the EDS of electricity on the main grid protection has been the subject of many research studies.

The power flows are unidirectional in the EDS without DGs. By introducing the DSs into the EDS in many areas of the electrical network, the power flows become bidirectional and as a result, conventional protections thought for unidirectional power flow are insufficiently.

The connection of DGs to the network contributes decisively to the occurrence of additional short-circuit currents. In addition, the connection/disconnection of DGs to the network have a short but strong impact on current variations. This case can be seen especially in DG equipped with wind turbine based on the asynchronous generators.

Another aspect is the fact that most renewable energy sources (wind turbines, solar panels) depends on whether factors such as wind speed, solar radiation. For these reasons, there are frequent connections/disconnections that would cause the above-mentioned problems.

In case of operation with DGs in the main network, two modes of operations are available: in Smart Grid System or Island Mode. These two operation modes can be used to overhaul the protection because it is especially important to protect the installations in both operating modes.

Current solution suitable for protecting Smart Grids is to implement the protocol IEC 61850 by a series of Intelligent Equipment Device (IED), installed in the network as an architecture that takes into account the fact that the tasks in all of these nodes, containing the installed IEDs, are constantly communicated bidirectional to IED central.

Within this chapter, a case study in the Galati distribution operator activity area (Romania) is provided. The IED equips in this case a remote-line sectionalizer (Tie Device). It should be noted that this solution determines the direction of the current flow through a real-time analysis of phase difference between current and voltage.

This breaker is installed on a medium voltage line between a wind turbine and the rest of the electrical distribution in the area network. In this chapter, the sectionalizer operation function is enabled in order to show the feasibility of the depicted solution. The screenshots of the monitoring system is shown.

The chapter ends with the Reference Section.

28.2 Overview of Protection Functions in Adaptive Systems

The main role of automation and relay protection used in Overhead Power Line (*OPL*) MV (medium voltage) networks is to limit the effects of the damage and to ensure the power supply without interruption of electricity to consumers [1]. Relay protection, which is itself the automation, generally has two main functions [2]:

- Separating the damaged element from the rest of the electrical installations and thus ensuring their continued operation under normal conditions;
- Refer to the abnormal (not permitted) operation of electrical installations and their signalling to prevent damage occurring.

In order to fulfil these two fundamental functions, the protective devices, regardless of the type or the constructive principle on which they are based, must satisfy the following general conditions [3]:

- *Selectivity*, i.e. disconnecting only the damaged element and allowing the continued operation of the unattended installations;
- *Sensitivity*, i.e. sensing all defects and abnormal operating modes, even when they differ only slightly from the normal operation of the installations;
- The *rapidity*, which is necessary because only a rapid disconnection of the damaged elements can remain without any effect on the functioning of the unattended installations;
- *Safety*, which consists in the fact that relay protection devices, which act very rarely, need to be prepared, even after a long period of rest, in order to operate properly.

Taking into consideration the classification of defects in electrical installations by their nature, it is necessary to mention firstly those that consist of *insulation damage*. Most defects are some form of damage to the insulation, whether it is made of insulating materials specially provided, be represented by the natural insulation (air), damage consisting in this case the cancellation of air insulating qualities. The various forms underlying this general defect are mono, two or three-phase short-circuits and grounding are simple or double, each of these types of defects having distinctive characters and manifestations, depending on the nature of the electrical network in which they occur.

The *short circuit* is the worst defect; it can occur between three phases, between two phases or between one phase and the earth (in networks with neutral point grounded).

Stripping or *overturning* the insulation creates for the current a generally small resistance pathway, much smaller than the consumer, which produces a great increase of the current, which thus becomes a “short circuit current”.

The high-current short-circuit current causes an increase in the voltage drop across the generators and all the impedances they travel, resulting in a general drop in network voltage with harmful effects on the consumers and on parallel operation of the power plants. At the short-circuit point the voltage may become zero and the consumers in the vicinity or downstream remain unpowered.

Besides these shortcomings in the functioning of the consumers, the short circuit current causes damage to the installations, which can be very serious due to its dynamic and thermal action. Electrodynamics stresses caused by short-circuit currents can cause bending and breaking of the bars, pulling of the coils, detachment of the parts, untimely opening of the sectionalizers. Very high heat developed by the short-circuit current can cause melting and even vaporising of materials, expansion and detachment of parts.

The *adaptive protective functions* required in a medium voltage (20 kV) electrical network are as follows:

(a) Maximum current protection (ANSI 50) [4]—allows protection against fault currents whose value is particularly high (the threshold selected for this protection is in the order of hundreds and thousands of amps). It is called fast because the timing associated with its operation is small (usually 0.1–0.3 s);
(b) Maximum current protection (ANSI 51) [5]—similar to the maximum fast current protection, but the fault currents it operates on have lower values in the order of tens or hundreds of amps and the associated timing is usually in the 0.6–2 s range;
(c) Maximum timed current protection (ANSI 67) [6]—similar to the ANSI 51 protection function, except that two sets of adjustments (fault current threshold and tripping threshold) for each direction are required (upstream or downstream of the network connection point);
(d) Timed current homopolar protection (ANSI 51N) [7];
(e) Maximum Voltage Protection (ANSI 59) [8];
(f) Minimum voltage protection (ANSI 27) [9, 10]—This function protects against dangerous voltage drops. The result consists in the isolation of wind power plants from the power grid to which it is connected, to prevent unwanted crashes and to maintain the power grid stability. Safe operating conditions are best evaluated with the help of the direct sequence component. The protection function becomes effective in the large frequency range [45–55 Hz];
(g) Maximum frequency protection (ANSI 81H) [11];
(h) Minimum frequency protection (ANSI 81L) [12, 13];
(i) Rate of change of frequency protection (ANSI 81R) [14]—Through this protection function, the rate of frequency variation in the unit of time is monitored (in NT 51/2009, a velocity variation of maximum 0.5 Hz/s is required).

28.3 General Features of the Remote-Controlled Recloser

Primary equipment used in MV electrical distribution networks is the remote-controlled recloser, which is mounted on poles of the medium-voltage (20 kV) poles, on the branches or even on the main line axis.

The recloser is used to protect medium voltage lines, wind and photovoltaic power plants, transformers, switches and other distribution equipment from exposure to harmful current levels, also detecting fallen lines (conductors) and reducing the risk of electrocution.

The numerical relay for the remote-controlled recloser, installed in the medium voltage (20 kV) power lines, presents a number of facilities such as:

- Performing manoeuvres for connecting/disconnecting the circuit breaker from the remote control (from the point of dispatch control) and locally (via the relay control panel);
- Knowledge (tele signalling) status monitoring equipment;
- Possibility for putting into operation/cancelling the activated protection functions, both locally and remotely by remote control;
- Activating/cancelling, locally or remotely, the security group;
- Triggering of active protections; there is also a high-speed rapid auto-reclosure which can be activated or cancelled, both locally and by remote control;
- Ensures the availability of a complex set of protection functions such as: maximum current protection, maximum current timed, maximum timed current homopolar protection, inverse sequence protection, directional protection (by activating two control groups simultaneously, the first group for protection). forward and downstream direction, reverse and upward direction protection, minimum and maximum voltage protections, minimum and maximum frequency protections, frequency variation protection (frequency derivative), the possibility of implementing the mechanism anti-insularity by monitoring the presence of tension;
- Since the relay has a complex set of analogue sizes such as voltages (for both directions), currents (for each phase), powers (active, reactive, apparent), power factor, phase-to-phase angles and voltage-to-current, sizes that can be activated for logging and archiving, it can be deduced that the reactor also presents the function of a quality analyser of electric power;
- Remote parameters can be monitored at a distance to indicate the proper operation of the reactor, such as: SF6 pressure, cc voltage value for the rechargeable batteries and the GPRS modem, contact status, circuit breaker status etc.;
- It presents various communication and integration protocols in the SCADA system, such as: IEC 810510-104, MODBUS TCP/IP, DNP 3.0;
- The digital relay shows multiple types of communication ports such as:
  - RS232 serial communication ports that can be used for local configuration via a laptop or a modem GSM/GPRS tele signalling and remote control;
  - TCP/IP communication ports used both for local configuration as well as for tele signalling and remote control;

  – USB port used only for local configuration.

- Introduce recording function by parameterisation registration oscilo-perturbograme to burst through the various functions of active protection;
- Checking the state of the radio communication;
- Reduced operating costs due to rapid isolation of defects;
- Reducing the demand for the distribution network by reducing the duration of the transitory fault regimes;
- Reduces the number of short-circuit trips of switches in electrical distribution stations, and implicitly the number of technical revisions of medium voltage switches to meet the number of triggers by various faults (single, two phase- and three-phase short-circuits, grounding);
- Reducing expenses by lowering the number of accidental overhaul at medium voltage switches in power stations.

28.4 The Used Adaptive Protection System to Implement the Automation Based on the LOOP AUTOMATION Scheme

The simplified synoptic scheme of Fig. 28.1 is considerate, in which is represented the looping of MV electric lines, *OPL* 20 kV Tecuci—Ciorasti with 20 kV *OPL* Tecuci—Repumping, through the remote loop sectionalizer *STC Bucla 71*. It can be noticed that on the *OPL* 20 kV Tecuci—Ciorasti is mounted a remote control *STC* 27 (in axle at the pole 219) and on the 20 kV *OPL* Tecuci—Repump is mounted a remote control sectionalizer (Tie) *STC* 102 (in axle at the pole 304).

At the occurrence of a permanent short-circuit or homopolar defect on the electrical gird portion represented in Fig. 28.2, between the circuit breaker in the 20 kV Ciorasti cell and the *STC* 27 remote control sectionalizer, there is the starting and functioning of the type of fault protection (protection implemented by a numerical relay) which leads to the trigger of the 20 kV Ciorasti cell breaker.

Remark: The portion of the electrical network affected by the defect is represented in *yellow*. In the case of the MV network, the color used describes its energizing status (*red*—for a energized network, *green* grid for disenergized grid).

In the case of switching equipment (sectionalizers, circuit breakers, remote splitters, remote re-actuators), the red color is used to represent the state of the connected or closed state, respectively, the green color is used to represent the state disconnected or open.

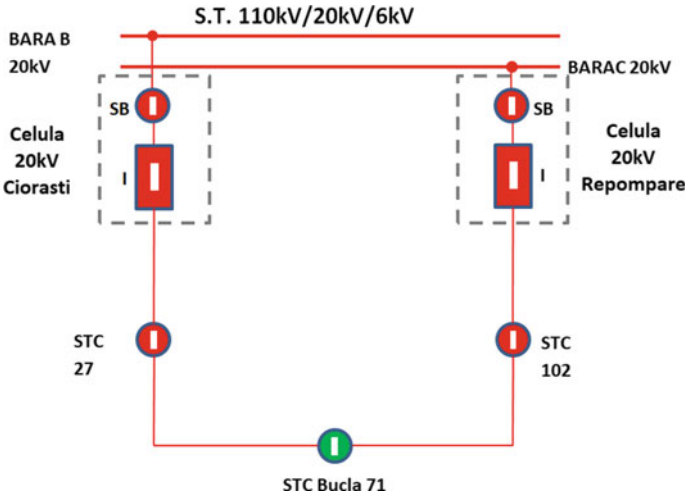

Fig. 28.1 Simplified synoptic scheme for the representation of *OPL* 20 kV Tecuci—Ciorasti loop with 20 kV Tecuci *OPL—Repump I*

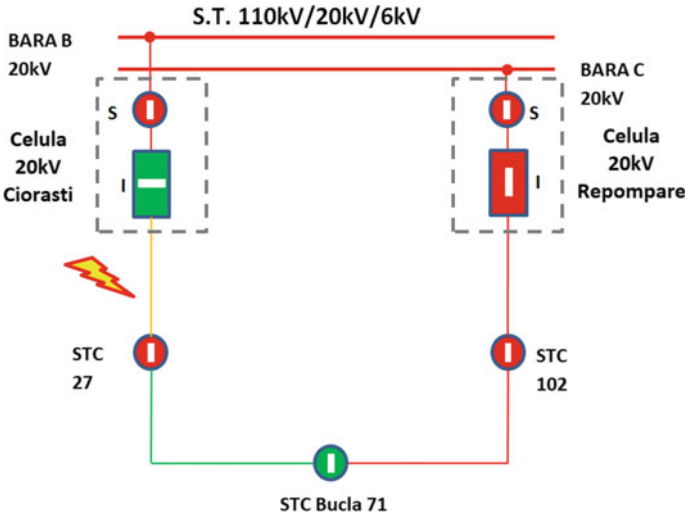

Fig. 28.2 Defect localization for *OPL* 20 kV Tecuci—Ciorasti loop with 20 kV Tecuci *OPL—Repump I*

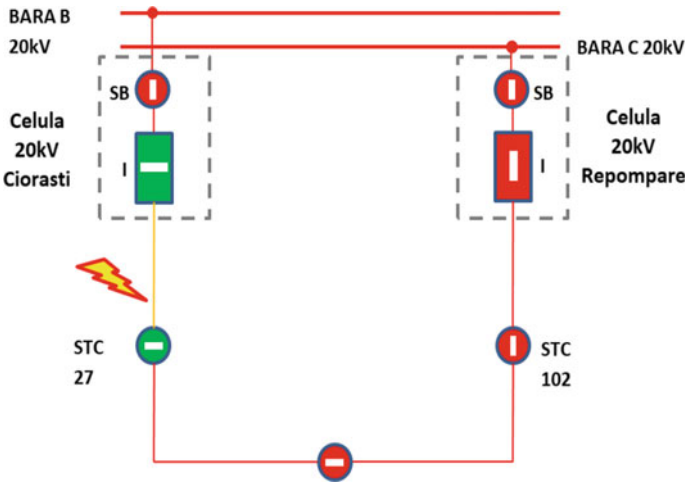

Fig. 28.3 Remotely control by dispatcher of the *OPL* 20 kV Tecuci—Ciorasti loop with 20 kV Tecuci *OPL—Repump I*

Following the triggering of the 20 kV Ciorasti Cell Switch, the entire 20 kV Tecuci—Ciorasti *OPL* is disengaged (between I and *STC* Circle 71). In order to remedy this problem and replenish the affected consumers, it is necessary to identify the defect. The time to locate the fault site is particularly high (hours), especially in extreme climatic conditions.

After identifying the defective site, the dispatcher can remotely open the *STC* 27 remote sectionalizer, and then remote the remote-controlled sectionalizer of the *STC* loop 71 (Fig. 28.3)

28.5 The Designed Situation by Using Remote-Controlled Reclosers Equipped with LOOP AUTOMATION Scheme

Next, a designed solution to reduce the detection and fault isolation times in the 20 kV *OPL* is presented, by using remote-controlled reclosers equipped with LOOP AUTOMATION.

The simplified electrical scheme in Fig. 28.1 is considerate, in which the *STC* 27, *STC* 102 and *STC Bucla 71* are replaced by remote control sectionalizers *RSH 1*, *RSH 2* and *RSH Bucla* (Fig. 28.4).

At the occurrence of a permanent defect, short-circuit or homopolar, on the same portion of the electrical network shown in Fig. 28.2 (between the 20 kV Ciorasti cell breaker I and the *RSH 1* recloser), the circuit breaker I will be triggered (Fig. 28.5).

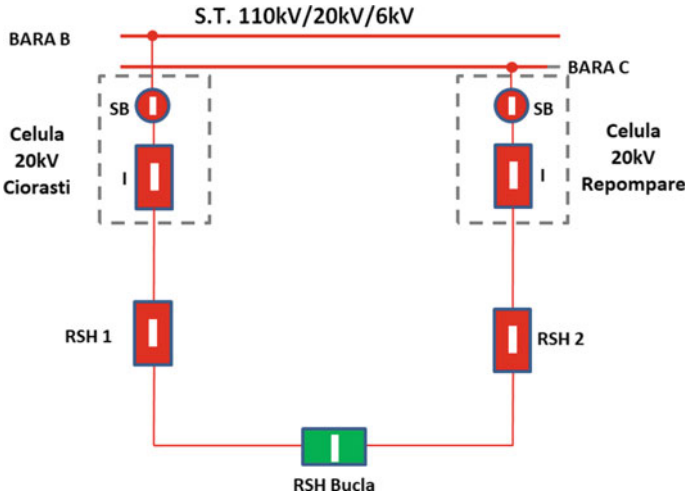

Fig. 28.4 Replacing of the *STC* 27, *STC* 102 and *STC Bucla* 71 by remote control sectionalizers *RSH 1*, *RSH 2*, and *RSH Bucla*

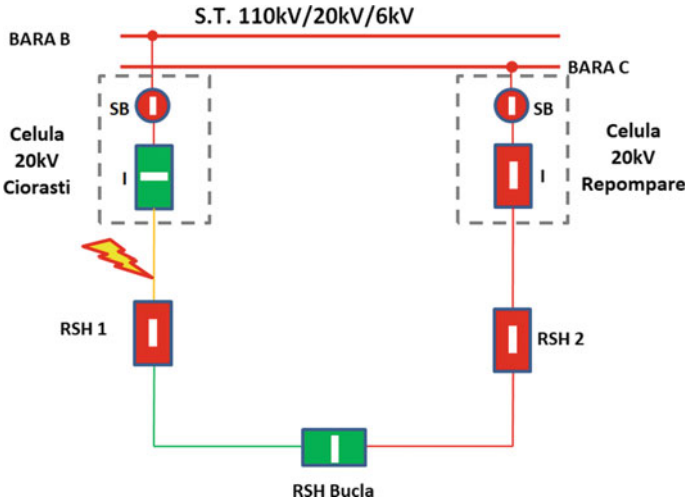

Fig. 28.5 Protection activation on a permanent defect, short-circuit or homopolar

The active protection functions on the numerical relay for the 20 kV Ciorasti cell are the following:

PMT $I_{pp} = 336$ A, $t = 1.2$ s.
PMR $I_{pp} = 600$ A, $t = 0.6$ s.
PH $I_{pp} = 30$ A, $t = 2$ s.
PHS $I_{pp} = 10$ A, $t = 1.8$ s.
RAR double cycle, $t_{p1} = 2$ s, $t_{p2} = 10$ s.

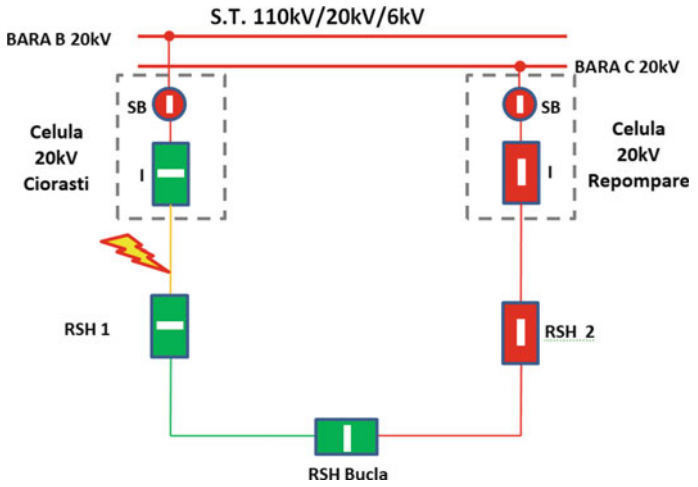

Fig. 28.6 Protection activation on a permanent defect, short-circuit or homopolar: reconfiguring the network

The automation LOOP AUTOMATION, implemented in the considered electric scheme, involves the following steps:

(a) At the occurrence of the permanent defect, there are two *RAR* cycles (unsuccessful) with pauses associated with *RAR* pauses equal to $t_{p1} = 2$ s, and $t_{p2} = 10$ s respectively. Depending on the type of fault type, the maximum time associated with the protection function is 2 s (corresponding to homopolar protection). After the two unsuccessful *RAR* cycles (maximum 17 s) have elapsed, the disconnected switching state of the circuit breaker (LOCKOUT) is activated in the 20 kV Ciorasti cell protection terminal;

(b) Upon activation of the LOCKOUT state of the circuit breaker by the protection terminal of the 20 kV Ciorasti cell, a Trip Request of the RSH 1 recloser is transmitted. On the *RSH 1* numerical relay, automatic self-timer automation is automatically cancelled rapid auto-reclosure (*RAR*) and change the direction of the source (by reconfiguring the network, the new source for the *RSH1* recloser becomes the 20 kV *Repumping* cell)-Fig. 28.6;

(c) The connection control of the *RSH Bucla Recloser* (Fig. 28.7) is send. The numerical relay for *RSH Recloser Bucla* automatically activates the set of protections corresponding to the 20 kV Replacing cell source. This autoconfiguration of the set of adjustments is possible due to the monitoring of the voltages on each phase upstream and downstream of the recloser assembly.

With the use of LOOP AUTOMATION automation, a significant reduction in defect detection and isolation time is achieved in MV over power lines, from several hours or even tens of hours (in the case of 20 kV *OPL* in which it increases significantly and the duration of the fault location) to about 20 s.

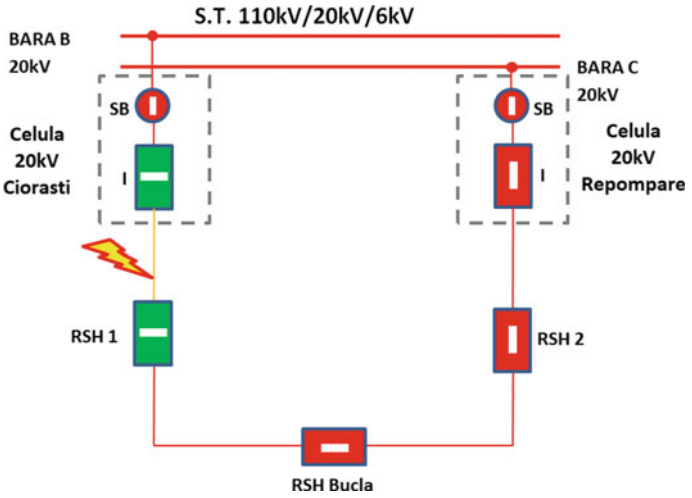

Fig. 28.7 The connection control of the *RSH Bucla Recloser*

Implementation of adaptive protection system of OPL MV network

(a) Configuration of tripping thresholds for maximum current protection, maximum timed current protection, homopolar current timing protection, timed homopolar sensitive current protection and *RAR* automation (two cycles of *RAR*).

In Fig. 28.8, the *WSOS* Configuration Interface is used to set the thresholds for triggering maximum current protection, maximum timed current protection, timed current homopolar protection, timed current sensitive homopolar protection for control group A (*Forward direction*) for the *RSH1* recloser. Similarly, the regulating groups for the *RSH2* and *RSH Bucla* reclosers are also parameterized, both in the *Forward* (to source) and *Reverse* (to consumer) directions.

In the "*Setting current*" box, the maximum phase current protection (Phase = 300 A), maximum homopolar current protection (Ground = 20 A) and sensible homopolar current maximum protection (*SGF* Sensible Ground Fault = 8 A) are set.

The number of cycles associated with *RAR* automation is set in the "*Trips to Lockout*" field and is set to 3 (corresponding to 3 triggers, i.e. 2 *RAR* cycles).

(b) Configuration of triggering characteristics corresponding to maximum fast current protection, maximum timed current protection, homopolar of timed current protection, homopolar sensitive current timed protection.

In Fig. 28.9 shows the configuration interface for operating the maximum current protections 50, 51 and 51N corresponding to *RAR* cycle 1.

In the "*Phase Protection*" field a trigger curve, previously defined, called "*50-51 RSH1 Forward*" is selected. By pressing the "View Curve" button, you can view the user-defined triggering feature (Fig. 28.10).

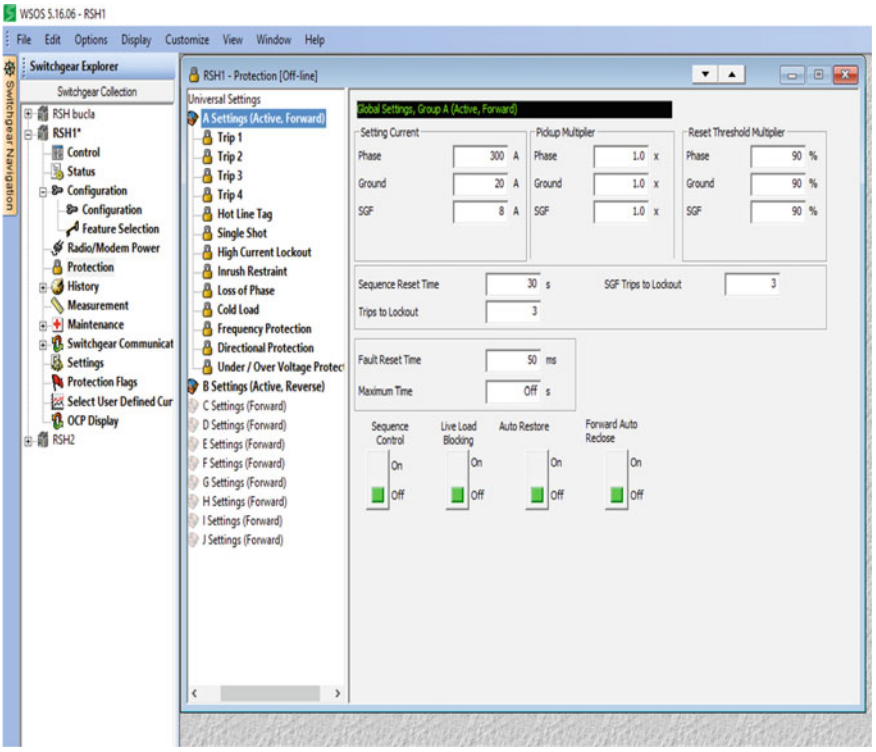

Fig. 28.8 *WSOS* Configuration Interface

The timing for the first *RAR* cycle (unsuccessful *RAR*) is parameterized in the "*Reclose Time*" field (2 s).

(c) Parameterization of the minimum and maximum voltage Protection (Fig. 28.11).

It is necessary to specify the phase voltage ($20\,\text{kV}/\sqrt{3} \approx 11565\,\text{V}$) in the "*Nominal Phase to Ground*" field. Minimum voltage protection is configured and activated (by selecting the Trip button) with a trigger threshold equal to $0.9 * U_{nom}$, i.e. a line voltage that is less than $0.9 \times 20\,\text{kV} = 18\,\text{kV}$. The triggering time is set to 0.5 s. The logical value of the $U_{\min}$ and $U_{\max}$ protections can be AND (it is necessary that all the phases are fulfilled) or OR (it is sufficient that on at least one phase whether the condition of the protection function is met).

The Fig. 28.11 is a screenshot of the specific interface for parameterization of the undervoltage and overvoltage protections.

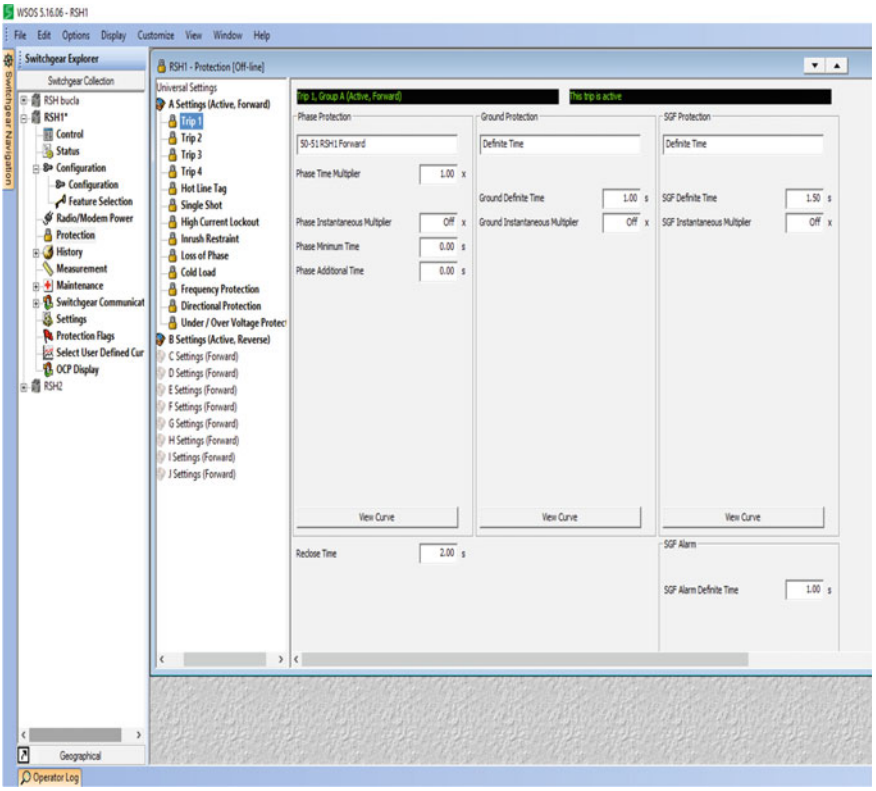

Fig. 28.9 The configuration interface for operating the maximum current protections 50, 51, and 51N

(d) Parameterization of the minimum and maximum frequency protections, and of the rate of change of frequency (Fig. 28.12).

The screenshot shown in Fig. 28.12 depicts the parameterization of the under frequency trip and over frequency trip for frequency protection tasks. At the same time, the rate of change of frequency trip protection is depicted.

(e) Definition and configuration of Loop Automation (Fig. 28.13).

In Fig. 28.13, the definition and configuration interface of Loop Automation is shown.

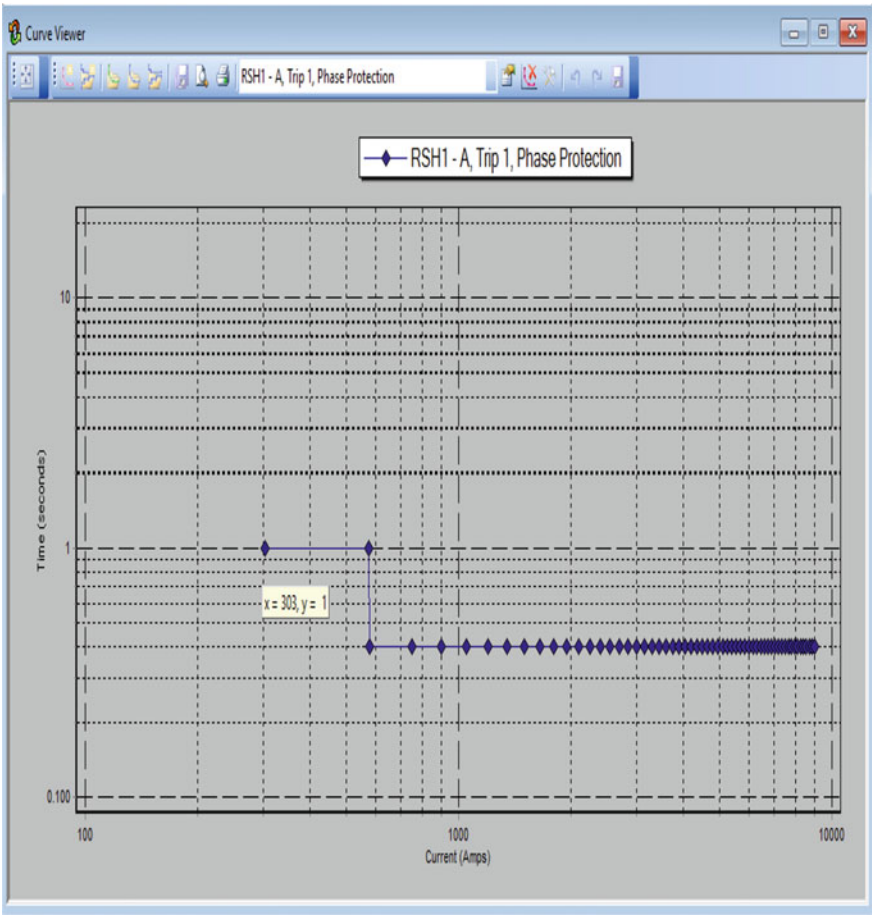

Fig. 28.10 "Phase Protection" field a trigger curve: the user-defined triggering feature

28.6 Conclusions

In this chapter, a modern adaptive protection solution is provided. The adaptive protections are the main challenges for the future power systems with distributed power sources. The configuration of the adaptive protection system to implement the Loop Automation Scheme is largely described by the authors through a case study in the Galati distribution operator activity area (from Romania). The *IED* equips in this case a remote-line sectionalizer. It should be noted that this solution determines the direction of the current flow through a real-time analysis of phase difference between current and voltage. This breaker is installed on a medium voltage line between a wind turbine and the rest of the electrical distribution in the area network. In this

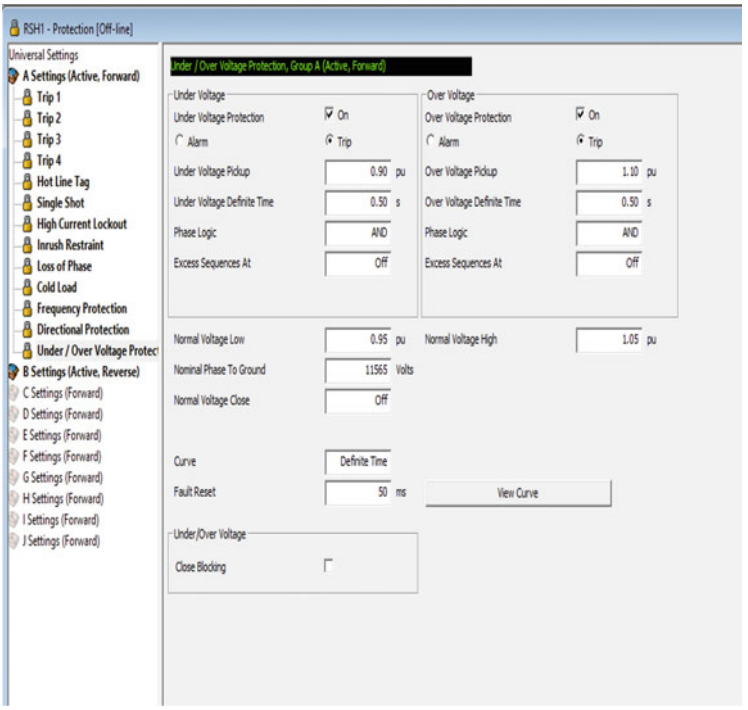

Fig. 28.11 Parameterization of the minimum and maximum voltage protection

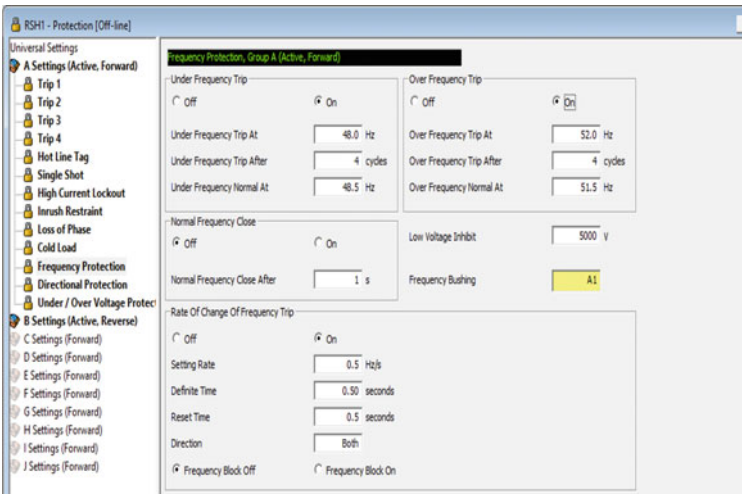

Fig. 28.12 Parameterization of the minimum and maximum frequency protections, and of the rate of change frequency

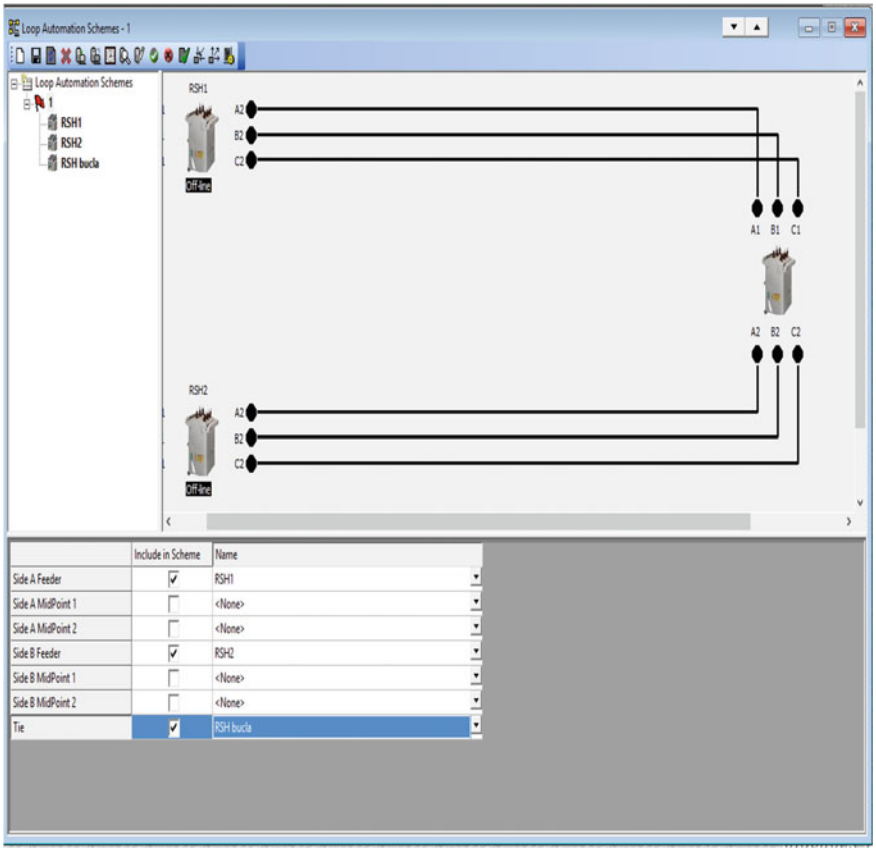

Fig. 28.13 Definition and configuration of Loop Automation

chapter the sectionalizer operation function is enabled in order to show the feasibility of the presented solution. The screenshots of the monitoring system is shown.

References

1. A. Yasir Saleem, N. Crespi, M. Husain Rehmani, R. Copeland, Internet of Things-aided smart grid: technologies, architectures, applications, prototypes, and future. Res. Dir. (2017), https://arxiv.org/abs/1704.08977. Accessed 2018
2. B. Kasztenny, N. Fischer, Advanced protection, automation, and control functions, in *1st Annual Protection, Automation and Control World Conference* (Schweitzer Engineering Laboratories, Inc., June 2010)
3. N. Zlatanov, AC *Power Distribution Systems and Standards* (2017)

4. http://www2.schneider-electric.com/resources/sites/SCHNEIDER_ELECTRIC/content/live/FAQS/307000/FA307978/en_US/VIP%2045%20trip%20time%20calculation.pdf. Accessed 2018
5. http://www2.schneider-electric.com/documents/electrical-distribution/en/shared/interactive-catalogue/seped307026enV2/pdfs/page_009.pdf. Accessed 2018
6. http://www.quad-industry.com/titan_img/ecatalog/Appl_14_ANSI_67_in%20Distance%20relay_en.pdf
7. https://new.abb.com/docs/librariesprovider27/default-document-library/gt_criteri-protezione-mt(en)b_1vcp000280-01-2016.pdf?sfvrsn=2. Accessed 2018
8. https://library.e.abb.com/public/29d8dfb6f07f249ec1257b480047e9da/1SDC007409G0201.pdf. Accessed 2018
9. http://www2.schneider-electric.com/documents/electrical-distribution/en/shared/interactive-catalogue/seped303005en/seped303005en/pdfs/page_102.pdf. Accessed 2018
10. https://myelectrical.com/notes/entryid/148/ansi-ieee-protective-device-numbering. Accessed 2018
11. http://www.csanyigroup.com/ansi-standards-for-protection-devices. Accessed 2018
12. https://electrical-engineering-portal.com/protection-relay-ansi-standards. Accessed 2018
13. https://store.gegridsolutions.com/faq/documents/general/get-8048a.pdf. Accessed 2018
14. https://en.wikipedia.org/wiki/ANSI_device_numbers. Accessed 2018

Chapter 29
IEC 61850 Based Protection Systems

Marian Gaiceanu and Iulian Nicusor Arama

Abstract The chapter includes protection power systems based on the IEC 61850 protocol for data communication systems between substations. The IEC 61850 is adequate for real time communication between *IED* based on GOOSE messages. The chapter includes the case study from the Romanian power systems: implementation of protection and remote control system in transformer station 110 kV/20 kV *Laminor*, using IEC 61850.

Keywords IEC 61850 · Protection · IED · SBO · GOOSE

29.1 Introduction

The protection and automation system of a station depends on the development and availability of microprocessor-based systems. Thus, the equipment from the power station transformation have been evolved from simple electromechanical devices to the digital robust terminals namely intelligent electronic devices (*IED*—Intelligent Equipment Device) used to perform specific required functions (for example, protection, monitoring and local/remote control). Until now, the specific proprietary communication protocols have been used, developed by each manufacturer in particular manner, requiring complex protocol converters and expensive when *IED*s are used from different suppliers. Therefore, there was need to develop an effective protocol for communication between the *IED*s, in order to ensure the interoperability.

IEC 61850 is a standard protocol for the automation, design of the transformer power stations developed by the International Electrotechnical Commission (IEC),

M. Gaiceanu (✉) · I. N. Arama
Department of Automation and Electrical Engineering, Dunarea de Jos University of Galati, Galati, Romania
e-mail: marian.gaiceanu@ugal.ro

I. N. Arama
e-mail: iulian.arama@ugal.ro

N. Mahdavi Tabatabaei et al. (eds.), *Microgrid Architectures, Control and Protection Methods*, Power Systems,
https://doi.org/10.1007/978-3-030-23723-3_29

Technical Committee 57 (TC57), which defines the reference architecture for energetic systems.

Thanks to the architectural design, inspired by the OSI 7 model and based on the abstraction of the entity definition, independent of the basic protocols, the IEC 61850 protocol allows mapping of objects and services.

IEC Standard 61850 contains a set of documents focusing on the following major issues:

- Functional model for *SA* (*Simulated Annealing*)—Part 5;
- Data model for *SAS* (*Substation Automation System*);
- Communications protocols and related services—Part 7 and Parts 8 and 9;
- *Substation Configuration Language* based on XML (*SCL*)—Part 6.

The primary requirements of IEC 61850 are [1]:

- Interoperability, the standard must support all the functions in the station applications. Interoperability implies that different *IED*s from different manufacturers may be able to exchange and use real-time information without protocol converters;
- The open architecture allows an arbitrary allocation of functions to devices and supports centralized and decentralized systems;
- Long-term stability, referring to the lifetime of an electrical transformer station. Primary equipment has the operating life between 40 and 50 years, and the digital terminals used to automate the station have a service life between 10 and 20 years. Therefore, it is necessary to easily integrate new *IED*s from the same manufacturer or other manufacturers.

The *IED* is, according to IEC 61850 any equipment that includes one or more processors (microcontrollers) with the ability to receive or send data/control to or to an external source.

Standard communication protocol IEC 61850 revolutionized the automation of power stations at the very fast peer-to-peer messages, structured and object-oriented data.

It is intended to provide a unitary protocol for the variety of intelligent numerical relays used in the transformer station, to implement a common format for station description, to facilitate the modelling of necessary data, to define the basic services needed to transfer the data through different protocols and enable interoperability between different manufacturers' equipment.

All data model functions, including data structure for the primary equipment of the station, are divided into modules that can then be separately implemented into *IED*s.

The basic elements are called logical nodes (*LN*s). Each object will include attributes that can represent detailed equipment values or equipment features.

The operations implemented by the data model defined by the IEC standard 61850 are as follows [2]:

- reading given data as values of attributes;
- writing a value as a configuration attribute;
- control of switching devices and other objects by methods such as *Select Before Operation* (*SBO*) or direct operation;
- reporting an event that changes the values;
- storing event logs;
- the necessary file transfer to configure them and the event log;
- *GOOSE* (Generic Object Oriented Substation Event) stands for an event system generic object oriented and it is a service for critical information transmission between *IED*s, such as status changes to equipment monitoring, interlocking, implementing automation like *Automatic Transfer Switches* (*ATS*) for Global Positioning System (GPS), so on;
- sampling the analog values by transmitting a string of synchronized voltage and current values.

The IEC 61850 standard uses Ethernet as basic communications technology at a speed of 100 Mb/s or higher depending on available network components. Star network topologies and hybrid ring are used. The most commonly used network topology is ring-type with automatic reconfiguration in the event of communication interruption on one of the redundant *IED* ports.

The chapter includes the case study from the Romanian power systems.

The chapter ends with the Reference Section.

29.2 Overview of IEC 61850 Standard

IEC 61850 standard for communication networks and systems in substations, has been developed to ensure interoperability between intelligent electronic devices (*IED*—Equipment Intelligent Device) required to provide protection, monitoring, control and automation functions implemented in power stations/substations.

IEC 61850 refers not only to the communication process but also to the modelling of information, adapted to the needs of the electricity industry. In addition, it defines an XML-based configuration language that standardizes the automation and protection device configuration technology used in electrical stations.

Meta model of IEC 61850 presents concepts like logical nodes (*LN*s—Logical Nodes) and data classes, which are defined in Parts 7-1 and 7-2. The *Substation Configuration Language* (*SCL*) is defined in Part 6 and is used to configure data sources and how to access their information about these data. Mapping (addressing) technology is described in 8-1, 9-1 and 9-2 Sections. The first Part, 8-1, defines both a mapping/addressing conforming to the *MMS* (Manufacturing Messaging Specification) message specification standard and Ethernet communication needed for model transfer events *GOOSE* (Generic Object Oriented Substation Events).

The basic model, defined in Part 7-3, implements common data classes for information status and analogue units, analogue signals settings. This information hierarchically organized is defined at logical node level, and data class respectively.

In Section 7-4, the automation model of the power station is defined which implements the addressing of logic nodes related to circuit breakers, sectionalizers, transformers, etc. Information about shaping equipment can be accessed both *online* using the appropriate search and in *offline* mode using the equipment SCL language.

The Meta model contains constructors representing the information model (measured value, reference value, sequence of events) as well as communication configuration constructors (called information exchange model in IEC 61850 Part 7-1), such as setting a report which can be used by a single client or associated applications.

Each physical equipment (*PD—Physical Device*) may include several *logic devices* (*LD*). Each logical device is made up of several *LN*s, having at least one logical node 0 that contains general device information. The logical node is defined based on a class of logical nodes.

The classes of logical nodes are defined in the information model standards for IEC 61850, such as 7-4, 7-410, and 7-420. The classes of logical nodes are generically defined from a semantic point of view. For example, GGIO class representing the only *generic inputs/outputs* (*GGIO*) and XCBR class defines the properties of a breaker (*Circuit Breaker—CB*). Additional details regarding the classes of logical nodes are set out in Part 3.2.1 (logical node types). The logical nodes contain several constructors of the information exchange model and, moreover, at least one data object. The data objects are defined both in the common data classes (Section 7-3), and in a new class of specific data. Common data classes are defined to implement common functions, for example, obtaining the state of a full-size digital variable, reading values and of an analogue signal, etc.

Case Study—Implementation of Protection and Remote Control System in TS 110 kV/20 kV *Laminor*, Using IEC 61850

29.3 Overview of the Schneider Micom P139 Digital Relay

Schneider digital protective relay *Micom P139* (Fig. 29.1), it was used to implement protection functions, remote control, tele-signalling and tele-measurement within the mill transformer station (TS) 20 kV cells of 110 kV/20 kV. The main protective functions available for 20 kV cells are: maximum current protection (50/51 P/Q/N), maximum short-circuit and homopolar directional protection (67 and 67 N), minimum and maximum frequency protections (81), minimum and maximum voltage protections (27 and 59) [3–6].

Fig. 29.1 The Micom P139 relay [3]

The *Micom P139* relay (Fig. 29.1) can be used in power systems with earthed neutral by resistance, inductor compensation or with the isolated neutral. The multitude of protection functions founded into *P139* relay allows the user to cover a wide range of applications designed to protect MV/HV electrical networks, transformers and their electrical motors. The protection parameters can be stored in four independent groups.

The control functions are designed to control a maximum of six electric switching equipment, which can be equipped with a medium/high voltage (MV/HV) cell within the electric transformer station. The numeric relay shows about 300 predefined types of medium and high voltage cells stored, depending on the desired configuration.

During operation, the operator interface is easy to use, facilitates the setting of the device parameters, ensuring safe operation by preventing accidental actuation operations of the switching equipment.

The *P139* is equipped with a large number of protection and control functions. These can be individually configured and cancelled. The flexible programming logic implemented by the device protection, allows the *P139* digital relay to be used in special applications.

29.4 Configuration of the IEC 61850 Standard with Easergy Micom S1 Studio [7]

In order to configure the IEC 61850 standard and to integrate the *Schneider Micom P139* digital relay into the SCADA system, the use of *Data Model Manager Application* (*DMMA*) is mandatory. The application is launched in execution and will be enabled Graphical User Interface (GUI) shown in Fig. 29.2. Within the GUI the following operations are possible: to add, delete, export or import a data model. Because the required data model has been previously saved, the "*Import*" option will be used and then the "*Next*" button will be activated.

Fig. 29.2 The GUI of the data model manager application

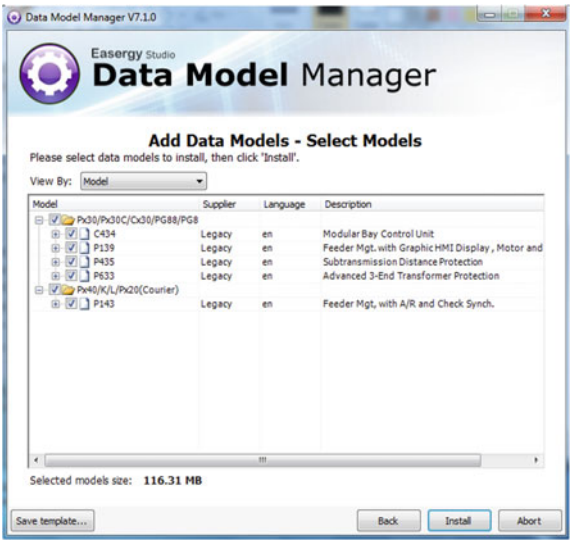

Fig. 29.3 Archive selection associated to the properly data model

After archive election associated to the properly data model, a new interface is activated (Fig. 29.3), which shows, in tabular form, related data models of digital relays types specified in the "*Model*" column and described in the "*Description*" column. The "*Install*" button will be activated. In this manner, new data models are installed corresponding to the different types of digital relays that can be configured in *Easergy Micom S1 Studio*.

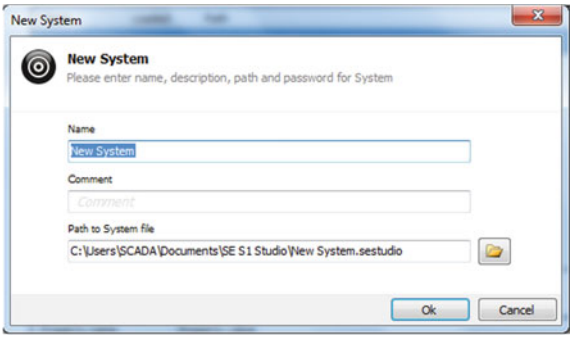

Fig. 29.4 Interface for definition of a new system

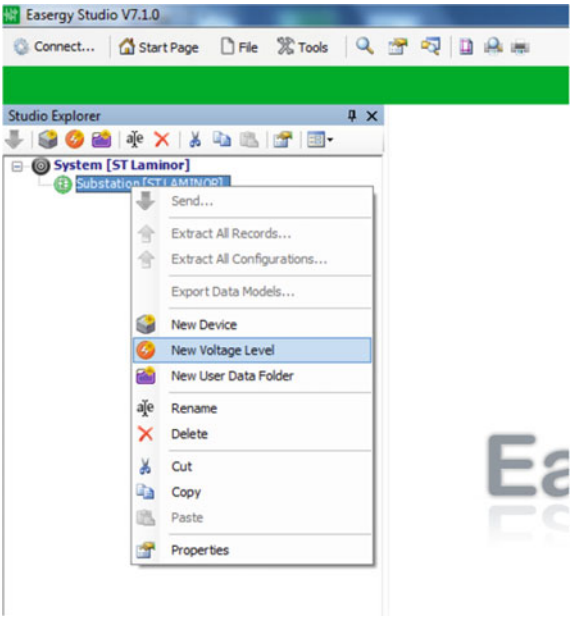

Fig. 29.5 Adding new substation to the project ST *Laminor* (ST Mill)

For definition of a new system/project, the "*New System*" command will be used. The command will enable the new interface as shown in Fig. 29.4. In the field "*Name*" the name of the project is specified and choose, if desired, another path way specified in the "*Path to file system*" field.

The next step is needed to define properly the transformer electric station. From the context menu (obtained by making a left click on the name system previously established), the command "*New Substation*" will be used (Fig. 29.5).

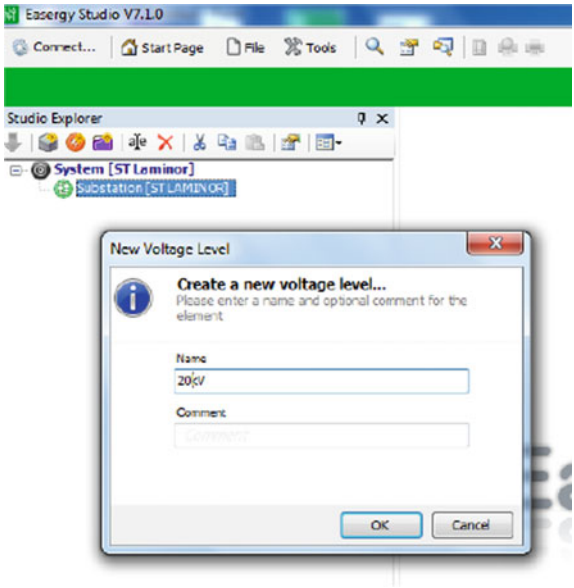

Fig. 29.6 Interface for creating of the new transformer substation

The new interface will be activated (Fig. 29.6) where it will be specifying the name of the transformer substation in the field "*Name*".

The next step is to define the voltage levels existing within transformer station, by using the command "*New Voltage Level*" (Fig. 29.7). As could be seen, in the Fig. 29.8 a graphical interface is enabled in order to specify the voltage levels of 110, 20 and 0.4 kV respectively (required for numerical relays definition used for monitoring different signalling related to DSI AC, DSI DC, AAR 0.4 kV, so on).

In Fig. 29.9, a new numeric terminal associated with the 20 kV voltage level is defined. The command "*New Device*" from the *Voltage Level*, generates a new box shown in Fig. 29.10, where it must specify the class of digital relays that belong to the equipment we want to define.

Depending on the class of selected numerical relays in the previous interface, a new dialog box is generated in order to select the type of the digital relay. In the presented case, the digital relay *P139* will be selected (Fig. 29.11). The "*Next*" button will be pressed. Depending on the imported data model into the *Schneider Easergy Micom S1 Studio*, according to the digital relays model that should be IEC 61850 configured, in the generated interface (Fig. 29.12) the *P139 Relay* type will be selected.

In Fig. 29.13, the last stage in the defining process of the new equipment is shown. The entities name should be specified (usually, they represent the name of a cells within transformer station). By pressing the "*Finish*" button, new equipment is generated (Fig. 29.14). The structure of the new equipment is loaded with appropriate predefined configuration files: the used Communication interfaces (section "*Connections*"), parameterization of the protection functions, types of automation,

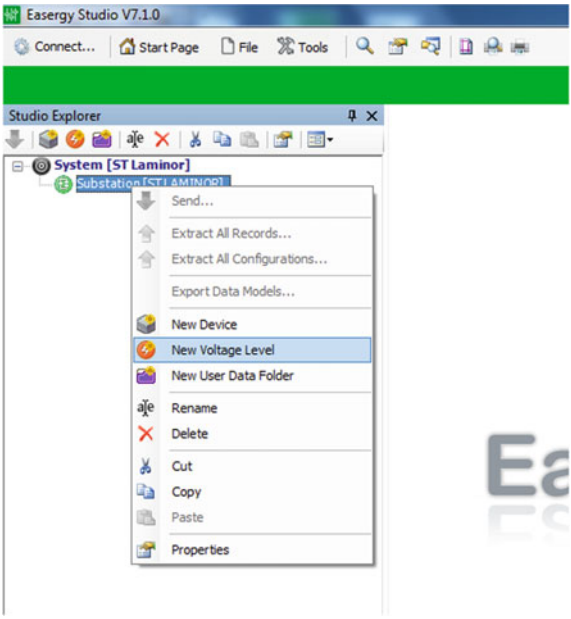

Fig. 29.7 Command selection to define the voltage levels existing within transformer station

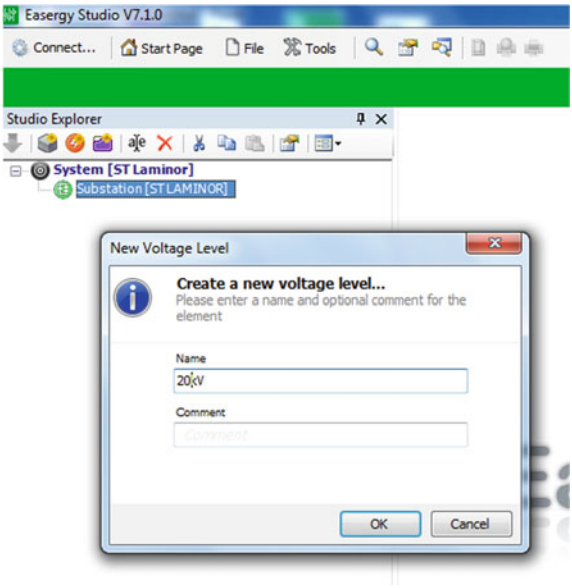

Fig. 29.8 Define the voltage levels values

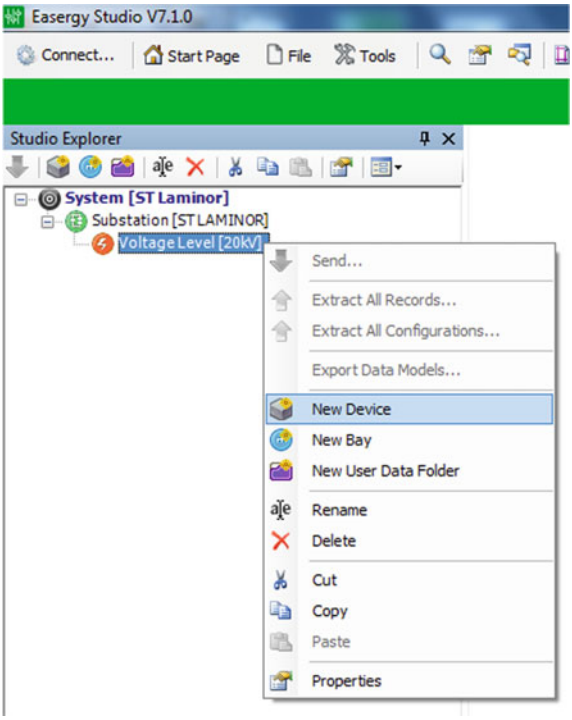

Fig. 29.9 Selection of the *New Device* command

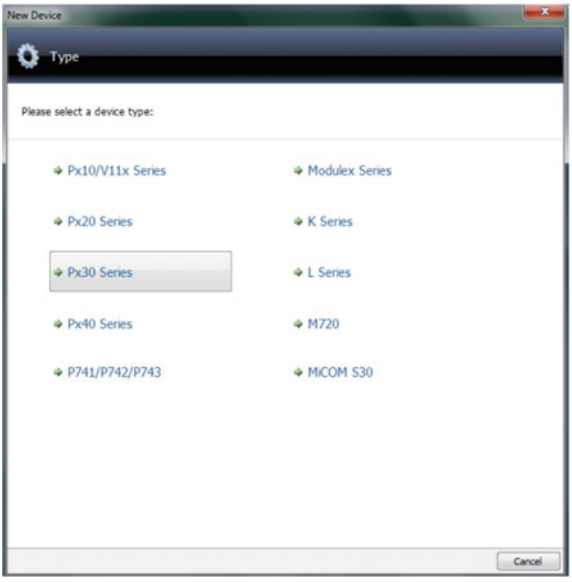

Fig. 29.10 The device type selection

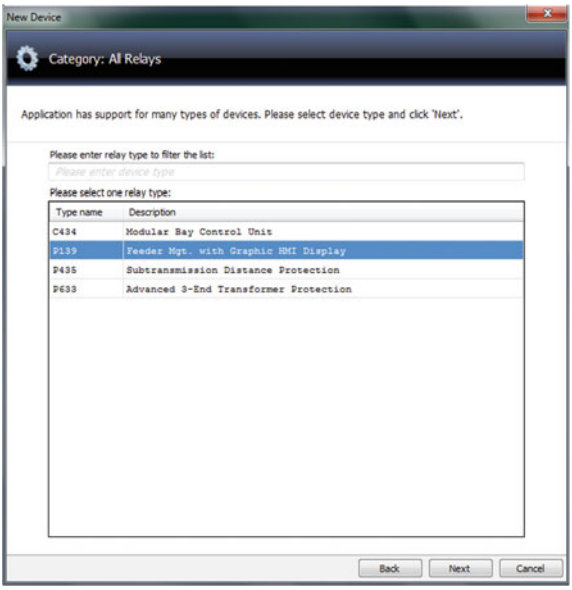

Fig. 29.11 Selection interface of the digital relay *P139*

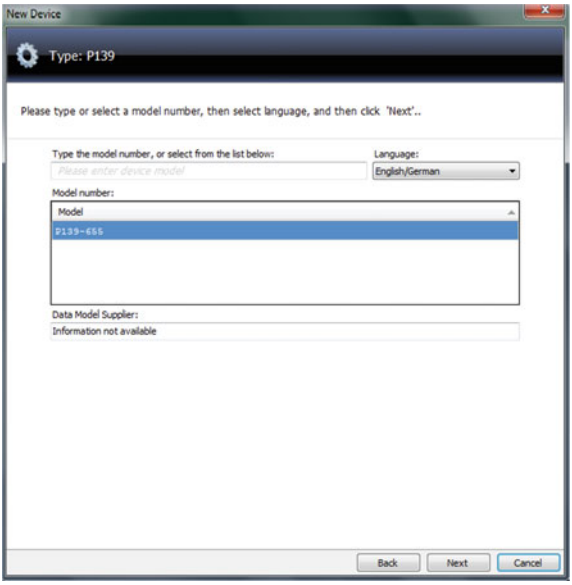

Fig. 29.12 Digital relays model that should be IEC 61850 configured

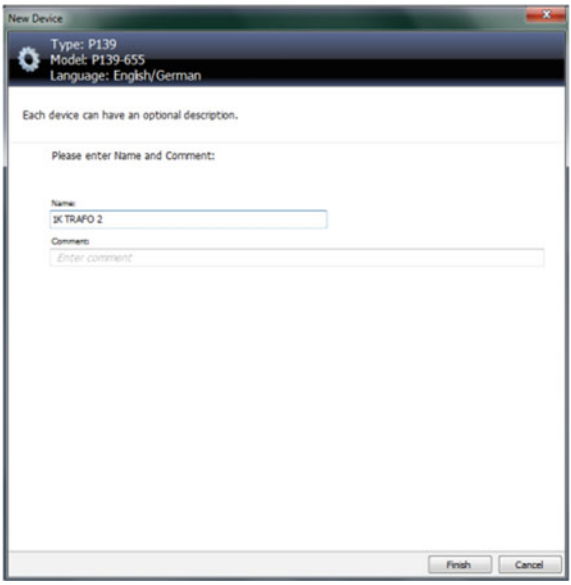

Fig. 29.13 Name specification of the new equipment

communication protocols (the "*Settings*" Section), *sinoptic/Mimic* presented on *P139* digital relay LCD screen (the "*BTC*" Section—*Bay Template Configurator*—editor and configurator of the 20 kV cell model), signalling menus parameterization available on numerical relay screen (Section "*Menu Text*"), respectively, configuration of the *Micom Configuration Language* (*MCL*), and implementation of IEC 61850 standard. Moreover, view log values analogue measured (*Measurement*), event log (*Log Recorder*) respectively *Disturbance Recorder* are available.

For definition a new IEC 61850 configuration file left click on "*MCL 61850*" will be executed and in the contextual menu shown in Fig. 29.14, command "*New File*" will be used.

A new IEC 61850 configuration file is created with the implicit name 000.mcl that will contain the corresponding configuration of the active digital relay. The name file can be modified through the "*Rename*" command. The file can be exported in *SCL* format for later importing in the case of IEC 61850 configuration definition for the new digital equipment, through the "*Export SCL File*" command. More *MCL* configuration files can be created, but only one single may be active. By using "*Set as default*" command, the changes on the active *mcl* file can be achieved. In order to enable IEC 61850 configuration editor the "*Open*" command is used (Fig. 29.15).

IED Configurator interface is activated (as shown in Fig. 29.16). In the title bar of the editor the name the *mcl* file to be configured it is specified.

In order to enable the editing mode of the *MCL* configuration file, right click on Template is executed (Fig. 29.17), and command "*Enter Manual Editing Mode*" is selected.

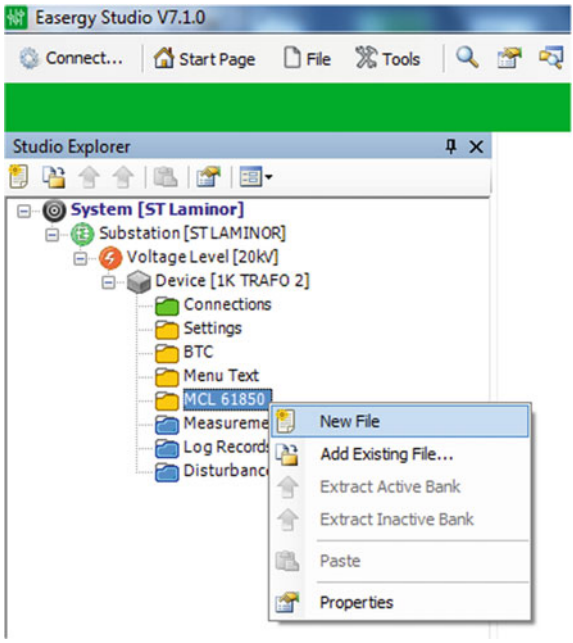

Fig. 29.14 New equipment is generated

Remark: After finishing of the IEC 61850 configuration, if the digital relay is in online mode, in order to use the write the file *MCL* into the digital relay memory the command "*Send to Device*" is used.

Within the "*IED Details*" section, shown in Fig. 29.18, the name of the digital equipment is defined (in the "*Name*" field). It is recommended that this name does not contain characters special or spaces. Typically, the name describes as efficiently *IED* the cell where digital relay is installed (2K_TR_2—it is the 20 kV 2K cell, i.e. 20 kV Trafo no. 2cell). The name should not have more than 10 characters (there are different types of RTUs at electric station level, as a SCADA protocol concentrator, which does not allow defining the "*IED name server*" that are longer than 10 characters).

Within the "*Communications*" Section, shown in Fig. 29.19, TCP/IP communication parameters are configured in the "*Address Configuration*" IP address, subnet mask, and IP gateway address. In the "*General Configuration*" box, the "*Media*" "*Copper or redundant board*" selection option has great importance if the provided digital relay has two ports (assure redundancy in the communication architecture, whether it is about the ring or double star configuration), even if these two ports are FO type. The "*TCP Keepalive*" parameter allows definition of a timer that determines whether the TCP connection is active or interrupted.

Within the "*SNTP*" Section, shown in Fig. 29.20, can be configured time synchronization of the digital relay up to a maximum of 2 external *Simple Network Time Protocol* (*SNTP*) servers. It is necessary the IP address specification of the *SNTP*

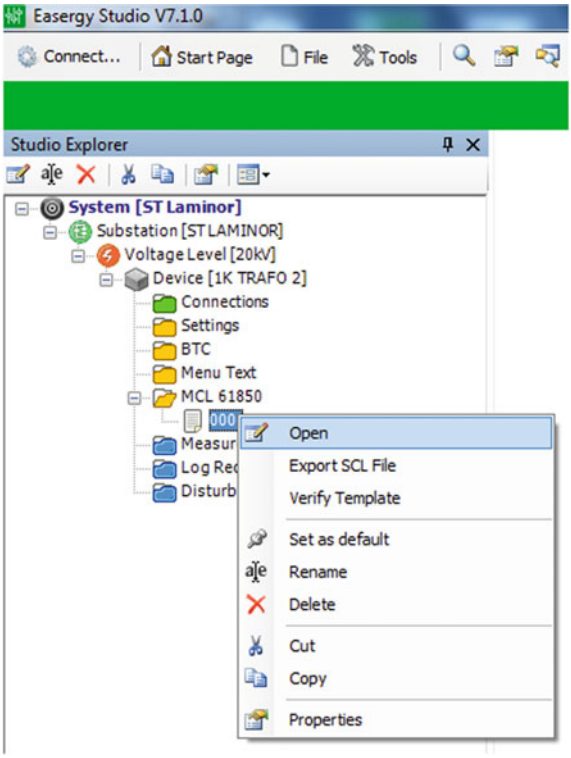

Fig. 29.15 The "*Open*" command is used to enable IEC 61850 configuration editor

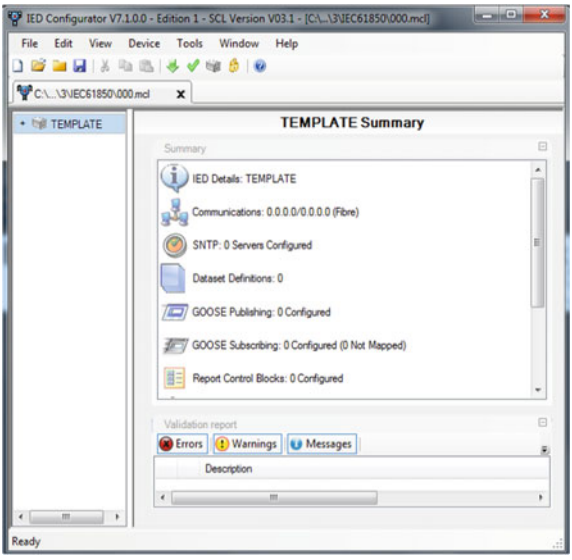

Fig. 29.16 *IED* Configurator interface

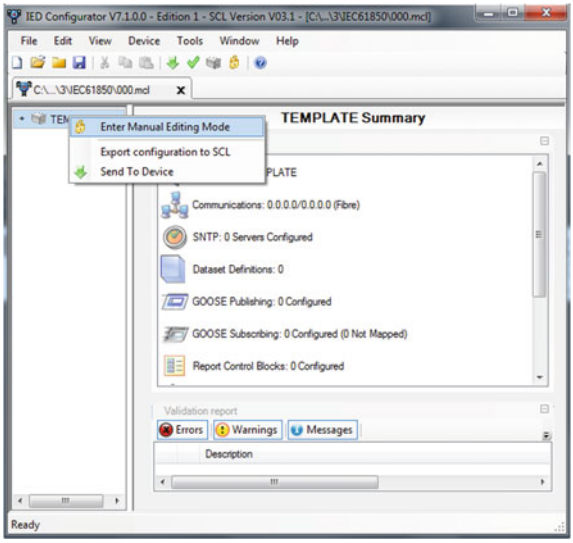

Fig. 29.17 The activation of the editing mode of the *MCL* configuration file

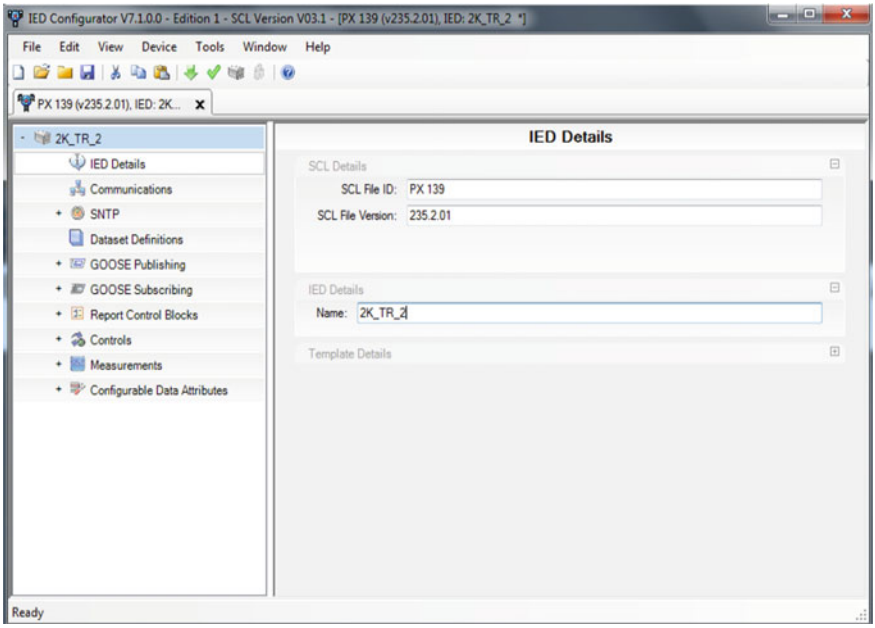

Fig. 29.18 "*IED Details*" Section

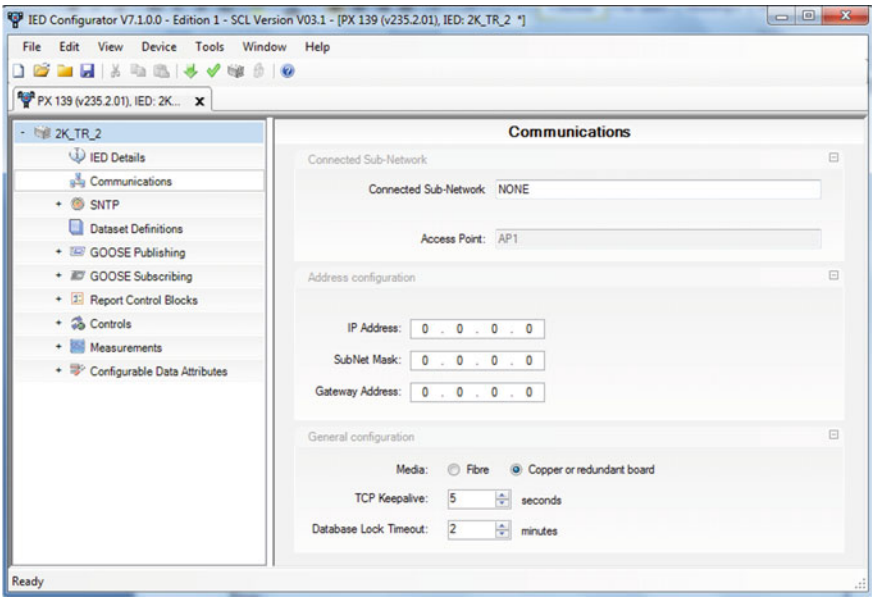

Fig. 29.19 "Communications" Section

server or selection name server in the *Server Name* list and the name port ("*Access Port Name*").

The "*Dataset Definitions*" Section, shown in Fig. 29.21, allows *definition* (press the "*Add Dataset*"), *change* (by making double-click left on an existing set) or *delete* (the "*Delete Dataset*" button is pressed) to a data set.

For each new data set created, the name (field "*Name*"), and the location (field "*Location*") should be specified (Figs. 29.22 and 29.23).

For each new data set created, a list of data objects will be added. This list can be changed lately by adding new objects or deletion of existing data objects. In Fig. 29.23, add in *Dataset1* set the object *Protection/DtpPhsPTOC1.ST.Op.general* (Fig. 29.24) that will allow monitoring of the signalling operation state of the maximal overcurrent protection timer.

Section "*GOOSE Publishing*", presented in Fig. 29.25, allows definition mechanism of publishing/editing *GOOSE* messages. The field "*Multicast MAC Address*" allows MAC address configuration for multicast/broadcast, used for the transmission of the *GOOSE* generic posts. The VLAN Identifier parameter (expressed in hexadecimal numeric code), and VLAN Priority parameter allow to apply a filter in accordance with the communication network in which is intended to be visible the sent *GOOSE* message. Box "*Repeat message parameters*" contains the needed parameters configuration time delays permissible transmission *GOOSE* messages. The "*GOOSE* Identifier" parameter contains ID the *GOOSE* message needed for implementation mechanism or publication and subscription. The *GOOSE* message

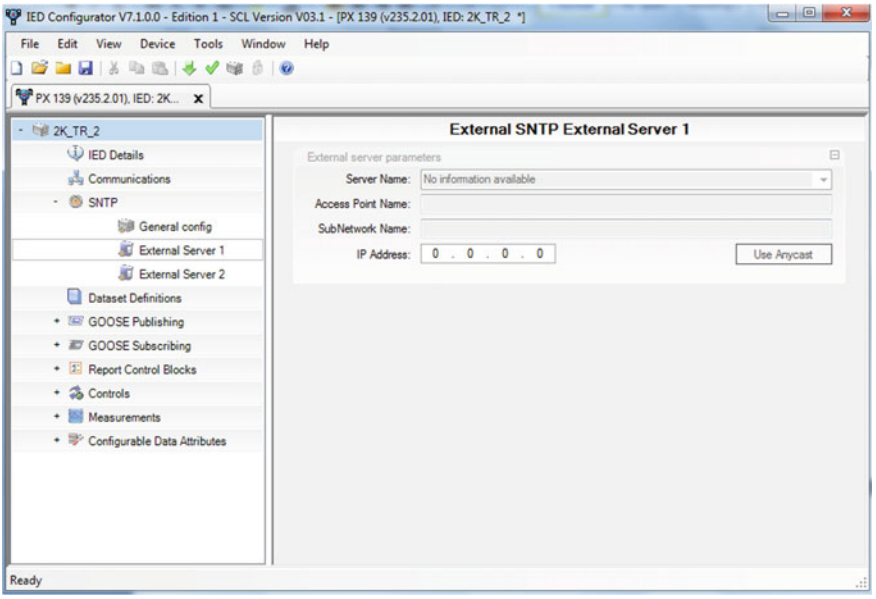

Fig. 29.20 "*SNTP*" Section

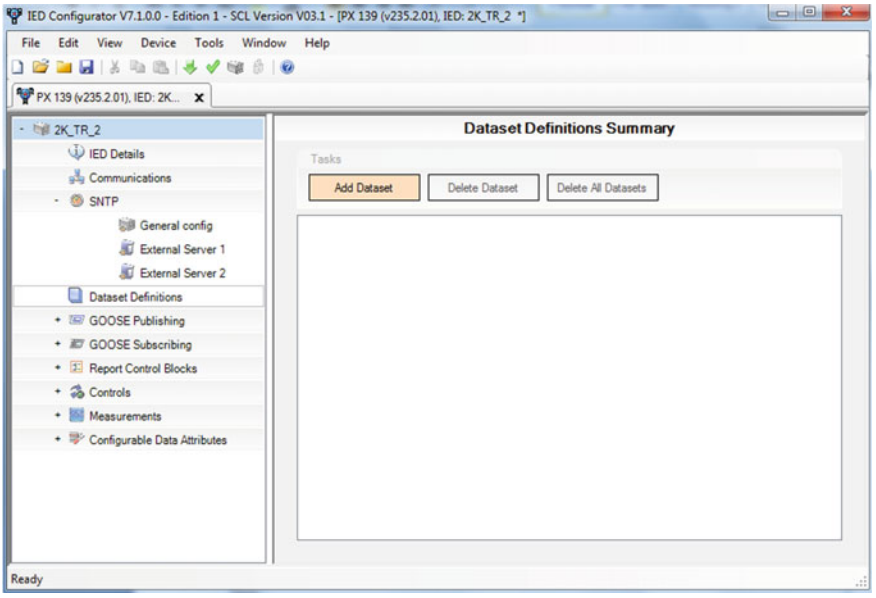

Fig. 29.21 "*Dataset Definitions*" Section

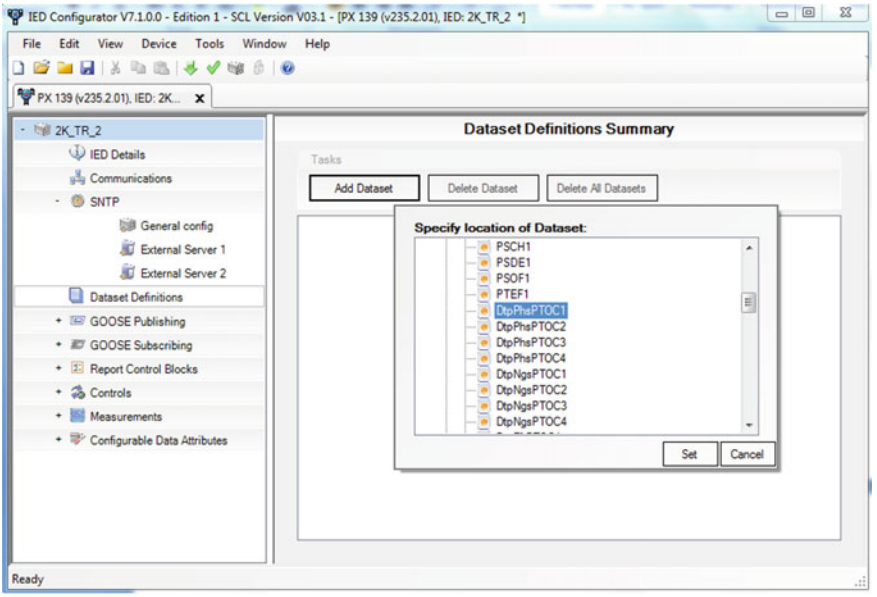

Fig. 29.22 Specification of the name (field "*Name*") and the location (field "*Location*")

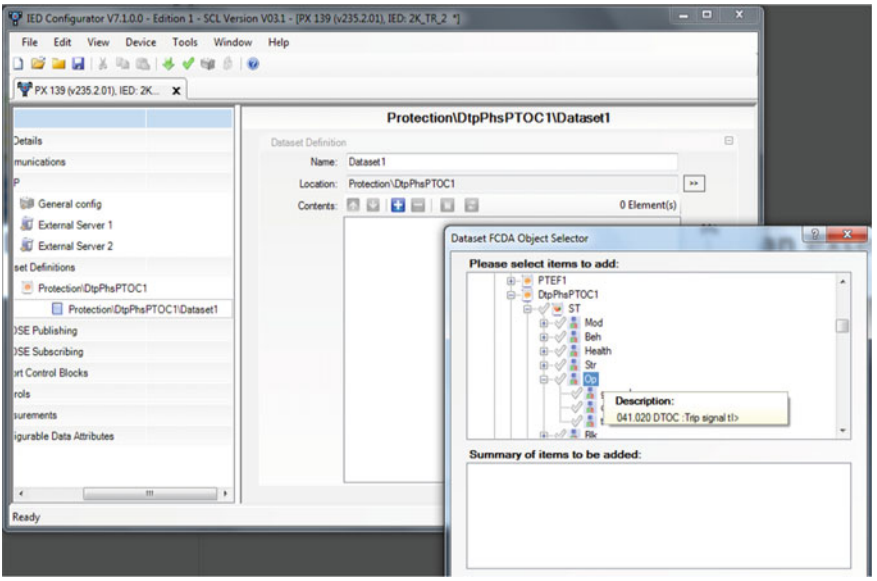

Fig. 29.23 Adding in *Dataset1* set the object *Protection/DtpPhsPTOC1.ST.Op.general*

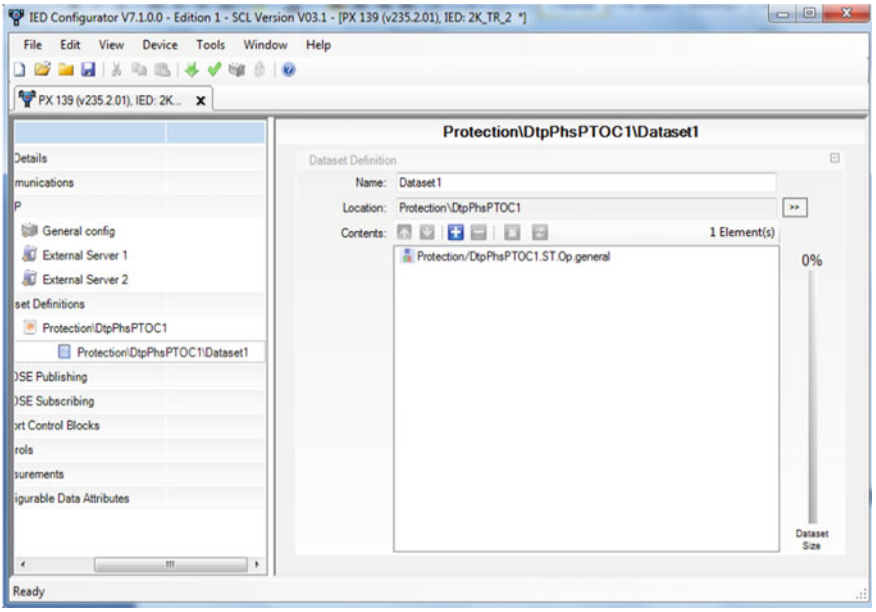

Fig. 29.24 The implemented object *Protection/DtpPhsPTOC1.ST.Op.general* in *Dataset1* set

will contain information about the state of the specified objects through the data set specified in the "*Dataset Reference*" list.

In order to define the IEC 61850 control reports, the "*Report Control Blocks*" Section is used. In Fig. 29.26, a report identified via *TR2_1 Ksystem/LLN0 $ RP $ urcbA* (specified in the "*Report ID*" field) that allows transmission (through the IEC 61850 protocol) of the state objects contained in the *Dataset2* data set (selected in the "*Dataset Reference*" list) is defined.

In Fig. 29.27, it is presented the single-phase scheme of TS 110 kV/20 kV *Laminor* that can be viewed in the SCADA system. Through the modern digital relays Schneider MICOM P139, by using the IEC 61850 standard, the increased features of the protection and remote control system are obtained: the state knowledge of the switching equipment, the knowledge of the analogue values, the digital input states (corresponding to the functioning of the protections, the control and signalling loops, the automations—*RAR*, *AAR*, *DRRI*, so on), remote control of the switching equipment, and protection functions.

In Fig. 29.28, the synoptic interface corresponding to the 20 kV 1 K *Trafo cell no. 2* is presented.

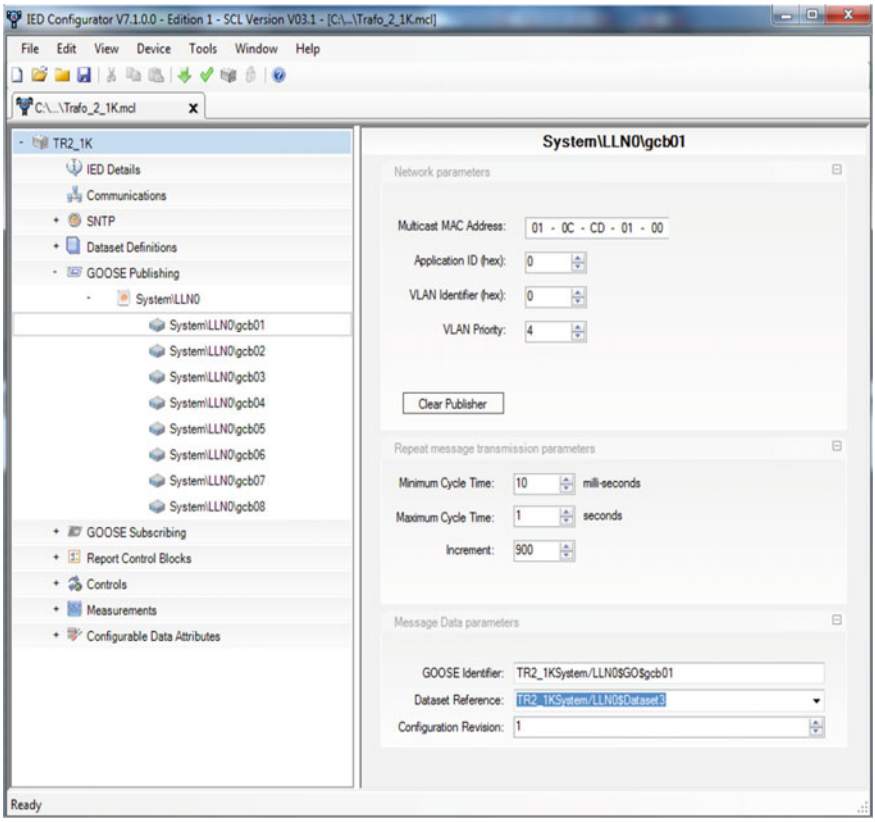

Fig. 29.25 Section "*GOOSE Publishing*"

29.5 Conclusions

The introduction of the advanced digital relays in power system allows a better control, protection (fast and selective) and communication for future power development. In this chapter, the *Schneider Micom P139* digital relay has been described, and a useful configuration of the IEC 61850 standard with *Easergy Micom S1 Studio* applied to transformer station 110 kV/20 kV *Laminor* have been presented.

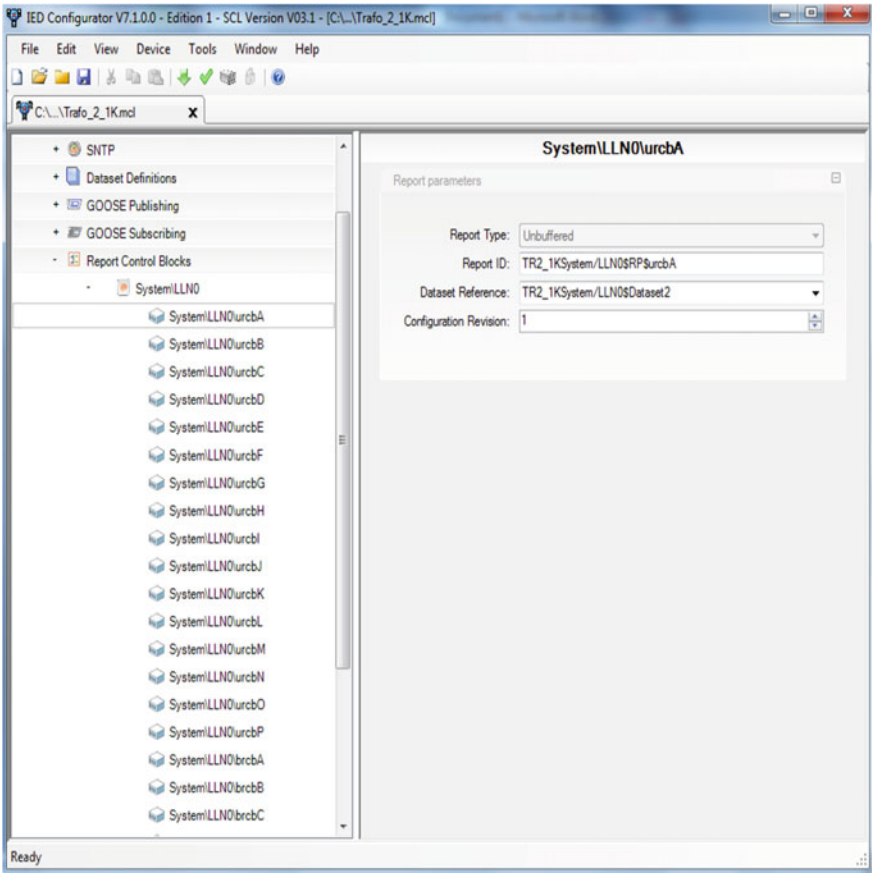

Fig. 29.26 "*Report Control Blocks*" Section

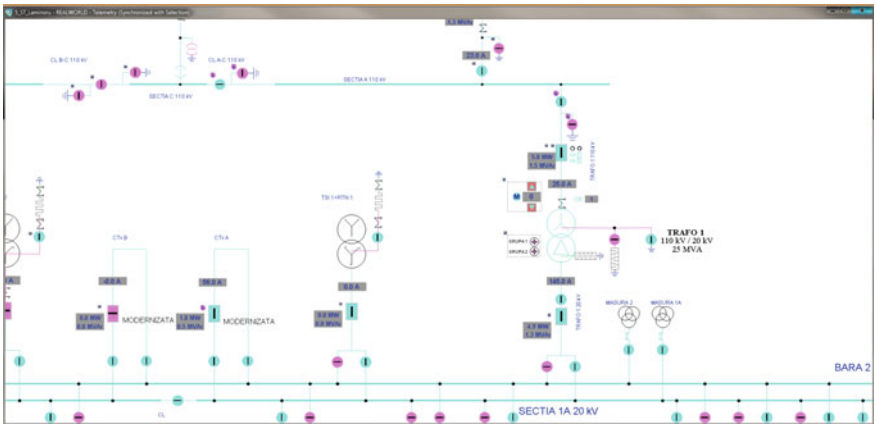

Fig. 29.27 Single phase scheme of TS 110 kV/20 kV *Laminor*

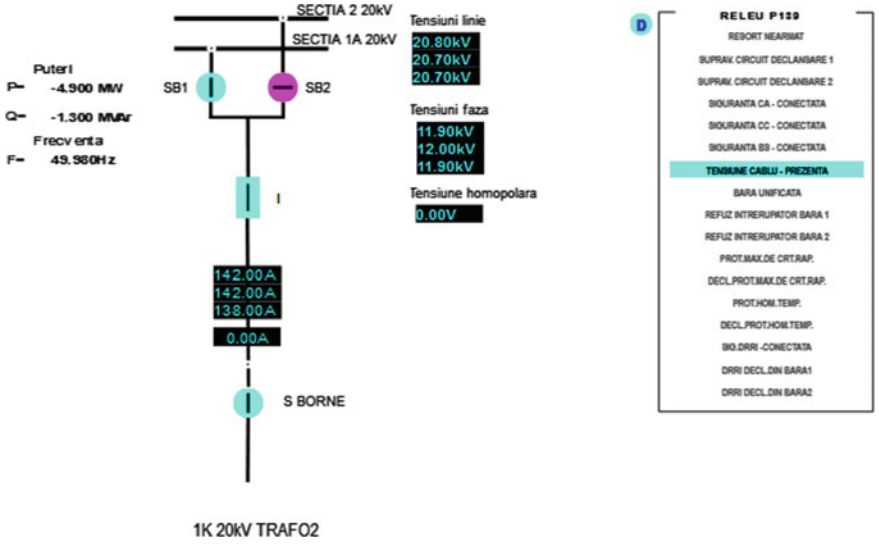

Fig. 29.28 The synoptic interface corresponding to the 20 kV 1K Trafo cell no. 2

References

1. H. Leon, C. Montez, M.R. Stemmer, F. Vasques, Simulation models for IEC 61850 communication in electrical substations using GOOSE and SMV time-critical messages, in *IEEE World Conference on Factory Communication Systems (WFCS)*, May 2016
2. http://www02.abb.com/global/sgabb/sgabb005.nsf/bf177942f19f4a98c1257148003b7a0a/e81bb489e5ae0b68482574d70020bf42/$FILE/B5_G2_Enhanced+protection+functionality+with+IEC+61850+and+GOOSE.pdf. Accessed 2018
3. MiCOM P139 Feeder Management and Bay Control, SW Version-651. Manual (global file) P139/EN M/R-21-A, 2014. Accessed 2018; B. Kasztenny, N. Fischer, Advanced protection, automation, and control functions. Schweitzer Engineering Laboratories, Inc., in *1st Annual Protection, Automation and Control World Conference*, June 2010
4. MiCOM P139 Feeder Management and Bay Control, SW Version- 651. Manual (global file) P139/EN M/R-21-A (2014)
5. M. Vadiati, M. Abbas Ghorbani, A.R. Ebrahimi, M. Arshia, Future trends of substation automation system by applying IEC 61850, in *43rd International Universities Power Engineering Conference* (2008)
6. U-Series Three-Phase Recloser/W-Series Single-Phase Recloser Medium Voltage Distribution. Whitepaper (08/2017), http://www.ariaatlas.org/userfiles/files/product/179/ADVC_U_&_W_Series_Whitepaper.pdf. Accessed 2018
7. https://www.schneider-electric.com/en/product-range-presentation/61035-easergy-studio/. Accessed 2018

Chapter 30
Power Quality Issues and Mitigation Techniques in Microgrid

Rajendrasinh Jadeja, Nicu Bizon, Tapankumar Trivedi, Amit Ved and Mrudurajsinh Chudasama

Abstract The most desirable characteristics of today's power system with distributed energy resources (DER) forming the microgrid is the reliability of the power supply and immunity to various power quality(PQ) issues. It is important to examine PQ issues arising from the introduction of DER and behavior of microgrid with penetration of various loads. In this chapter, reader is introduced to major power quality issues in the microgrid. A number of solutions to tackle these issues and their operating principle are also explained. In addition to the conventional power quality issues, load pulses are frequently encountered and need to be tackled with great care in microgrid. Hence, the hybridization of Energy Storage System (ESS) with different power storage devices such as the ultracapacitors (UCs), Superconducting Magnetic Energy Storage (SMES) devices, and high speed Flywheel Energy Systems (FESs) is proposed to dynamically compensate the power flow balance.

Keywords Harmonics · Load pulses · Power quality issues · Unified power quality conditioner

R. Jadeja (✉) · T. Trivedi · A. Ved · M. Chudasama
Marwadi University, Rajkot, India
e-mail: rajendrasinh.jadeja@marwadieducation.edu.in

T. Trivedi
e-mail: tapankumar.trivedi@marwadieducation.edu.in

A. Ved
e-mail: amit.ved@marwadieducation.edu.in

M. Chudasama
e-mail: mrudurajsinh.chudasama@marwadieducation.edu.in

N. Bizon
Department of Electronics, Computers and Electrical Engineering, Faculty of Electronics, Communications and Computers, University of Pitesti, Pitesti, Romania
e-mail: nicu.bizon@upit.ro

N. Mahdavi Tabatabaei et al. (eds.), *Microgrid Architectures, Control and Protection Methods*, Power Systems,
https://doi.org/10.1007/978-3-030-23723-3_30

30.1 Introduction

A microgrid is the composition of electrical systems along with conventional or renewable energy sources constituting a grid which feeds a significant number of small distributed loads [1]. Although all sources are primarily electrical sources, their operating characteristics and nature of supply depend largely on the load connected to them. As a result, the overall system can have highly nonlinear characteristics of operation. While this is not a point of great concern when several distributed generations (DGs) are tied to the grid; The changeover of the microgrid from on- grid to the isolated (islanded) mode or, the islanded mode to on-grid condition also introduces certain PQ issues and reliability issues [2]. The nonlinear loads connected to the microgrid can have deteriorating effect on system in comparison to the conventional grid and hence issues must be tackled with great concern.

The commonly found power quality issues in AC microgrid systems are Voltage Sags/Swells due to sudden change in loading, Interruptions due to changeover of from on- grid to the isolated mode, flicker, reactive power, and harmonics generated during the conversion from AC system to DC system and vice versa. DC systems are considered superior to the AC with respect to power quality issues since harmonics and reactive power do not have effect in case of DC microgrids. However, DC microgrids have unique issues of [3]

- Appearance of transient from AC grid
- Electromagnetic Compatibility
- Inrush current
- Overvoltage
- Unbalance in Voltages of bipolar DC links.

In the islanded mode of microgrid, the Power Electronic controller has to maintain the required reactive power demanded by the generating sources such as Wind Energy Conversion Systems (WECS) [4] and loads e.g. fans and pumps [5, 6]. For utilization purposes, the conversion of AC power to the DC requires power electronic converters. The soft starters installed for Wind Energy Systems use AC-AC voltage controllers. These converters are primarily responsible for the generation of harmonics in the system. The microturbine technology also requires the additional reactive power support. The voltage sag support is required in microturbine as well as WECS systems to ascertain the reliability of operation. The grid interface between AC grid and DC microgrid can be carried out using

1. Active Front End Converter
2. Uncontrolled converters
3. Power Factor Correction circuits [7].

It is evident that Active Front End Converters and Power Factor Corrections circuits maintain current THD within the specified limits [8]. However, uncontrolled converter-based conversion is capable to inject significant harmonics into the AC grid [9].

All above-stated problems lead to the conclusion that microgrid operation requires the ancillary support of custom power devices for power quality improvement. A DSTATCOM is tied in parallel to the Point of Common Coupling (PCC) of the AC microgrid [10]. The device ensures necessary reactive power support for the DERs and load. In case of Singly Excited Induction Generator system with small Hydro turbines, these devices provide zero voltage regulation (ZVR) [11] and hence standard voltages within ±5% tolerance limits are maintained. A DSTATCOM also provides compensation of harmonics generated by power electronic converters used in conjunction with the load. However, DSTATCOM cannot support voltage sag/swell during the transient condition.

During the transient conditions, voltage sag/swell and flickers occur due to the sudden removal of load. In such cases, the necessary voltage is provided using Dynamic Voltage Restorer(DVR) [12]. A DVR can also reduce the risk of a chain reaction that may occur during the ride through. The active power requirement of the DVR is either supported by Battery Energy Storage Systems (BESS) or additional power supply. More recently, a solution which is capable of performing the operation of DSTATCOM and DVR has become popular. The solution is well known for operability under wide range of PQ problems and is recognized as Unified Power Quality Conditioner(UPQC) [13]. It is interesting to note that these devices can be customized to tackle one or more power quality issues depending on the requirement of the microgrid [14, 15]. We shall start the discussion with harmonics and its impact on the microgrid.

30.2 Harmonics and Its Impact in Microgrid

Harmonics are present in power system since the first-time electricity has been transmitted, but it took years for the power system to experience the adverse effect of harmonics. Harmonics in power system increased considerably with evolution in semiconductor devices.

Nowadays, as everyone is demanding more efficient and compact household electrical appliances. So, It is compelling for product developer to go for power electronics converters and electronics devices to reduce the size and improve the efficiency of household appliances. In household appliances, a ceiling fan is a familiar appliance in which an AC regulator is connected with fan to control fan speed. Earlier fan regulators were of resistive type. In this conventional regulator, the voltage was controlled by means of a resistor to regulate speed, which led to power loss. As a solution to this, a TRIAC base electronics regulator was developed. This regulator solves the power loss issue but draws non-linear current and hence injects harmonics in the system. This increased use of power electronics converters will increase harmonics in the system.

In a microgrid, major loads are non-linear loads such as switch mode power supply (SMPS), adjustable speed drives, inverter air conditioners, different battery chargers, fan regulators, etc., which inject harmonics in the system. These harmonics

have more pernicious effect in microgrid then a large power system. So to have a study of harmonics in context with microgrid is very necessary.

30.2.1 Harmonics in Microgrid

As discussed earlier various non-linear loads such as drives, voltage regulators, Switch mode supplies, voltage regulators and etc. affects microgrid adversely. In industrial automation, the usage of AC Adjustable Speed Drive has increased significantly. Figure 30.1 shows a general diagram of adjustable speed drive. The discussion is on the resonant effect and current harmonics produced by two drives in the microgrid. For analysis, a pure sinusoidal three-phase balanced supply system is assumed. It is also assumed that each distribution line is having line inductance of L_s. Figure 30.1 shows general diagram of adjustable speed drive with two different intermediate circuits [9]. One intermediate circuit is of conventional drive and the other is small dc link capacitor drive. When considering conventional drive, as working of uncontrolled diode rectifier at any instant of time any two phase are connected to dc link through diodes of rectifier, so it is possible to represent this system as RLC circuit. Therefore, from the grid side, the equivalent impedance of conventional drive can be given as mention in Eq. (30.1).

$$Z_{eq} = \frac{\left(1 - 2\omega^2(L_s + L_d)C_{dc1} + j\omega\left(\frac{2(L_s+L_d)}{R_L}\right)\right)}{j\omega C_{dc1} + \frac{1}{R_L}} \tag{30.1}$$

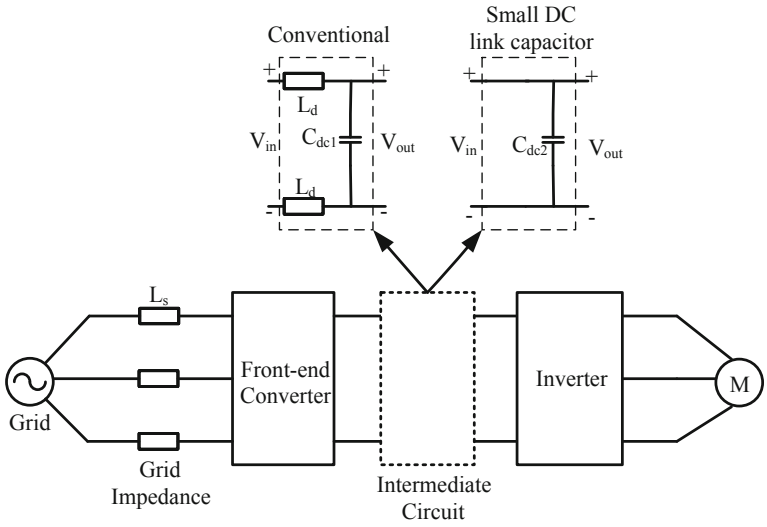

Fig. 30.1 Adjustable speed drive

$$f_r = \frac{1}{2\pi\sqrt{2(L_s + L_d)C_{dc1}}} \tag{30.2}$$

$$\xi_d = \frac{1}{2R_L}\sqrt{\frac{2(L_s + L_d)}{C_{dc1}}} \tag{30.3}$$

where, R_L is load resistor for load power modeling, L_d is equivalent inductance of positive and negative branch of dc link, C_{dc1} is dc link capacitor, and L_s is equivalent line inductance of transmission line.

For comparison, the same analysis is done for small dc link capacitor drive. Working of small dc link capacitor drive will remain same as a conventional drive but the difference is in dc link capacitor. A small dc link capacitor is used in this drive as compared to a conventional drive. Therefore, from the grid side, the equivalent impedance of small dc link capacitor drive can be given as mention in Eq. (30.4).

$$Z_{eq} = \frac{\left(1 - 2\omega^2 L_s C_{dc1} + j\omega\left(\frac{2L_s}{R_L}\right)\right)}{j\omega C_{dc2} + \frac{1}{R_L}} \tag{30.4}$$

$$f_r = \frac{1}{2\pi\sqrt{2L_s C_{dc2}}} \tag{30.5}$$

$$\xi_d = \frac{1}{2R_L}\sqrt{\frac{2L_s}{C_{dc2}}} \tag{30.6}$$

From above equations of the resonant frequency and damping factor for conventional and small dc link capacitor drive, it is clear that both damping factor and resonant frequency have changed considerably.

For example, a conventional drive has dc link inductance of 1.25 mH, dc link capacitor of 500 μF and a grid line impedance of 128 μH. The resonant frequency for the conventional drive is 136 Hz [9] whereas in small dc link capacitor drive line impedance is of 128 μH and dc link capacitor is of 30 μF. Therefore the resonant frequency of small dc link capacitor drive is 1816 Hz [9]. As resonant frequency in conventional drive is closer to lower order harmonics, it will result into amplification of lower order harmonics. Resonant frequency in small dc link capacitor is toward higher order harmonics, it will result into amplification of higher order harmonics. As a result, other electronics loads which are tied to same PCC will be affected by the resonant frequency of small dc link capacitor drive.

Production of harmonics is less affected by variation in load in case of the conventional drive as compared to small dc link capacitor drive. Harmonics emission by two different drives at different load capacity in microgrid can be seen from Fig. 30.2. Simulation results of two drives of 10 kW have been shown for understanding the effect of harmonics. It is clear from below Fig. 30.2 that operating drive on full power will inject less harmonics. When drives are operated at 10% of full load, harmonics injected in AC side is more *e.g.* for conventional drive *THD* is 111.25% and for small dc link capacitor drive, *THD* is 131.53%. When drives are operated at full load,

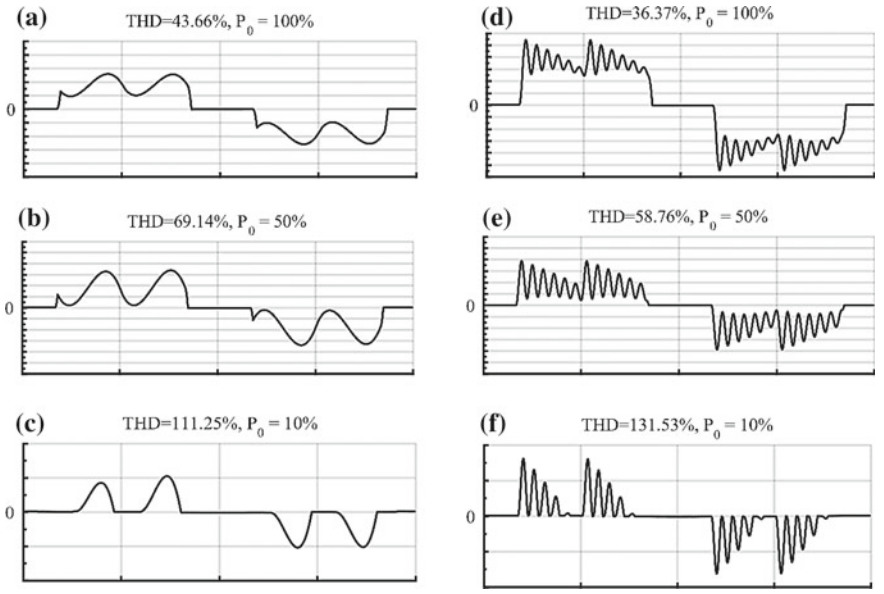

Fig. 30.2 **a** Input Current for conventional and small DC link capacitor drive **a** conventional—100% loading, **b** conventional—50% loading, **c** conventional—10% loading, **d** small DC link—100% loading, **e** small DC link—50% loading, **f** small DC link—10% loading (scale: Current Axis: 5A/div, Time axis: 5 ms/div)

harmonics injection in microgrid is lesser in comparison to operation at 10% load. For conventional drive *THD* at full load is 43.66% and for small dc link capacitor drive *THD* is 36.37%. Hence, we can say that variation in the *THD* level is highly dependent on the loading condition of the drive. For line with higher inductance, the variation can be reduced. However, the source voltage is distorted by higher inductance of the line and hence appropriate compensation mechanism must be adopted for overall improvement of the system.

30.3 Power Quality Issues in Microgrid

A microgrid can operate in isolated mode and/or grid-tied mode. In either case, it faces PQ issue which is different in both modes. In literature, AC microgrid and DC microgrid, both have emerged as alternative of each other. It is observed that DC microgrid has characteristics which eliminates many power quality problems. However, the DC microgrid suffers from unique power quality issues. It is important to address issues separately because both systems have different issues and require different treatment to mitigate these issues. These are issues are introduced in the next section.

30.3.1 Issues in AC Microgrid

AC microgrid is a small grid system which is connected with different types of distributed generators and different types of loads. With all these varities of generation and load it is difficult to maintain stability and power balance in the system. There are several issues concerned with AC microgrid. These issues are voltage stability, the reliability of the system, power quality, protection and control of system [16]. Some of the power quality issues in AC microgrid are defined as follows:

30.3.1.1 Imbalance in Power

Power imbalance occurs whenever there is transition from grid-tied mode to isolated mode of operation of the microgrid. A different micropower station connected to microgrid supplies power in the grid isolated mode. As these power stations have slow dynamic response, energy storage devices are used to maintain power imbalance occuring during the transition period in the microgrid. When normal mode is again restored, it is necessary to maintain the phase sequence and voltage magnitude to synchronize with the grid.

30.3.1.2 Low Voltage Stability

In distributed generation and microgrid power distribution support is lower as compared to the large grid, therefore low voltage stability issue occurs. As controlling of DGs and microgrid is done through power converter, the power transfer is limited in these converters in comparison to regular power plants. During high power demand condition in grid, these converters provide less support than regular power plants. The conventional power plants work with high kinetic energy stored in their rotating generators, and hence they can meet high power demand during transient conditions. When large grid is in power crisis and microgrid is transferred in islanded mode of operation, power-sharing support from microgrid to the large grid is zero. This isolated operation in power crisis will lead to imbalance in supply-demand ratio and in-turn rejecting voltage profile of grid [17].

30.3.1.3 Voltage Sag/Swell

When microgrid faces voltage sag, the functionality of power electronics converter based distributed generation may face different problems. During sag time when grid-connected load demands reactive power and trying to inject the reactive power, power electronics converter based distributed generators face over current in one or many phases. The other problem is crossing maximum voltage limit, which can cause tripping of generators and leads to blackout [18].

30.3.2 Issues in DC Microgrid

In many articles, power quality issues on AC microgrid system are highlighted but little attention is paid to study PQ issues in DC microgrid. DC microgrid also operates in grid-connected mode to consume and supply power to the grid and from the grid. Additionally, it operates in islanded mode of operation. Some of the typical power quality issues in DC microgrid are Unbalance in voltage of bipolar DC bus, appearance of voltage transient occurring in the AC grid, inrush current, and harmonics in DC microgrid.

30.3.2.1 Voltage Transient

Voltage transients frequently occur in AC microgrid but it affects the DC microgrid in same way. The main cause of voltage transient is switching of the capacitor bank, startup and shut down of distributed generation connected in DC microgrid and load change. When capacitor bank switching occurs a voltage transient moves from low voltage AC side through a rectifier to DC side of a microgrid, it has been found that the transient voltage reaches up to 194% of operating voltage [19]. It is also found that after this transient this voltage will stabilize at a higher voltage level than before, it is of the order of 111% of operating voltage [19].

30.3.2.2 Harmonics in DC Microgrid

As there is no AC-DC converter in DC microgrid lower order of harmonics are absent in the system, but increased use of DC-DC converter will cause electromagnetic interference issue. Though many time it has been discussed that DC system does not have harmonics in it, the term harmonics means multiple frequency of fundamental which is the operating frequency of power electronic converter. In DC system, the term harmonics means oscillatory voltage and oscillatory current caused by operating frequency of the device. In DC microgrid system many PWM based converters are used in different load, generating station in which capacitors are connected on both the side of converter. The impedance of DC bus and impedance of various capacitors will cause multiple resonance frequency [20]. If any of the resonant frequency matches with particular harmonics then the effect of this harmonics can cause serious problem to DC microgrid.

30.3.2.3 Inrush Current

The reason of inrush current in AC system is transformer, induction motor and other heavy inductive load but in case of DC microgrid the reason is different. When different load, distributed generating station and different storage devices connected

through power electronics converter, these converters produce harmonics Hence, suitable filters are placed on the load side. In addition to this, EMI filters are also added on AC side. The capacitor in this EMI filter draws high inrush current in DC microgrid. The magnitude of inrush current depends on voltage level of DC system, impedance of capacitor and converter capacitance. The other reason of having inrush current in DC microgrid is, when de-energized load is turned ON into a system, the large filter capacitor of these loads will draw heavy inrush current. The amount of the inrush current is so high that it can cause physical welding at point of contact.

30.3.2.4 Fault Current

The fault current in DC microgrid either flows from the capacitors connected to grid through converters or different distributed generating stations or from EMI filter capacitor. Since all power electronic converters are controlled in closed loop, the amount of fault current is restricted by rating of the converters. When limited fault current flows from DC microgrid because of power electronics converter, it is difficult for protection devices to distinguish between overload condition and fault condition. Thus, design of a proper protection system for DC microgrid poses serious challenge [21].

DC system does not have natural zero crossing of voltage and current like an AC system. This implies in DC system if arc fault occurs, it will not quench as quickly as it does in AC system. As this fault is self-sustaining fault and no surge current occur in DC system, it will continue for longer period of time and can cause a serious problem in the system. On the other hand, lower fault current can also increase voltage unbalance condition during fault occurrence in DC microgrid.

30.4 Mitigation of Current Related Issues

As discussed in the previous section, the microgrid faces a serious challenge from certain PQ issues such as harmonics, unbalance in currents, reactive power etc. irrespective of its operation in islanded or grid-connected mode. A no. of Distributed Energy Resources (DER) is connected to the microgrid with Power Electronic Converter Interface. The presence of harmonics and/or unbalance currents does not only affect the operation of distribution system but also affects the source in which it produces low-frequency oscillation. In addition to this, reactive power if left uncompensated in the line can create grave voltage regulation issues. The standard set for interconnection of DER into Electric Power System does not allow voltage fluctuation beyond the limit of $\pm 5\%$. A large of no. of solutions have been presented in literature and are categorized as shown in Fig. 30.3. In the present section, we will discuss some of the solutions in the context of microgrid. The primary function of these solutions is to intercept power quality issues and eliminate them in such a manner that they do not affect the overall system.

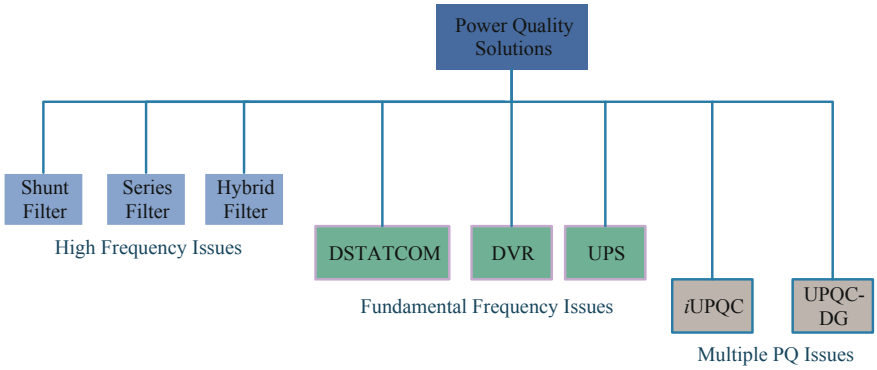

Fig. 30.3 Classification of power quality compensation devices for microgrid

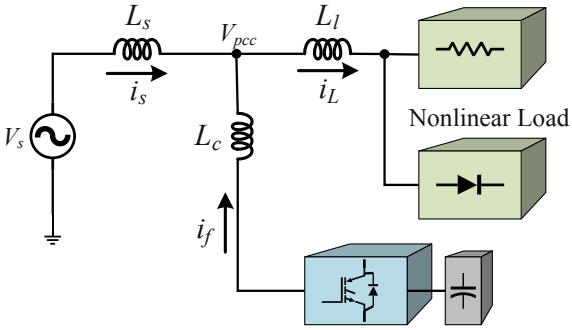

Fig. 30.4 Schematic diagram of shunt active power filter

30.4.1 Shunt Active Power Filter (SAPF)

As we know that current harmonics in the local distribution system can significantly distort the voltage of the line. Hence, they must be compensated at the local level. One such solution is the shunt active power filter. The device compensates for harmonics in the grid by injecting the harmonic current with the same magnitude but out of phase to the load (Fig. 30.4). Mathematically, the function of active filter can be expressed as,

$$i_f^{ref} = Y_h v_h \tag{30.7}$$

where, i_f^{ref} is reference active power filter current determined by the SAPF algorithm and Y_h is admittance offered by SAPF to the harmonic currents. Post compensation, the source current carried by distribution line becomes nearly sinusoidal and is exactly in phase with the PCC voltage. The performance of one such SAPF is for compensation of current harmonics is shown in Fig. 30.5.

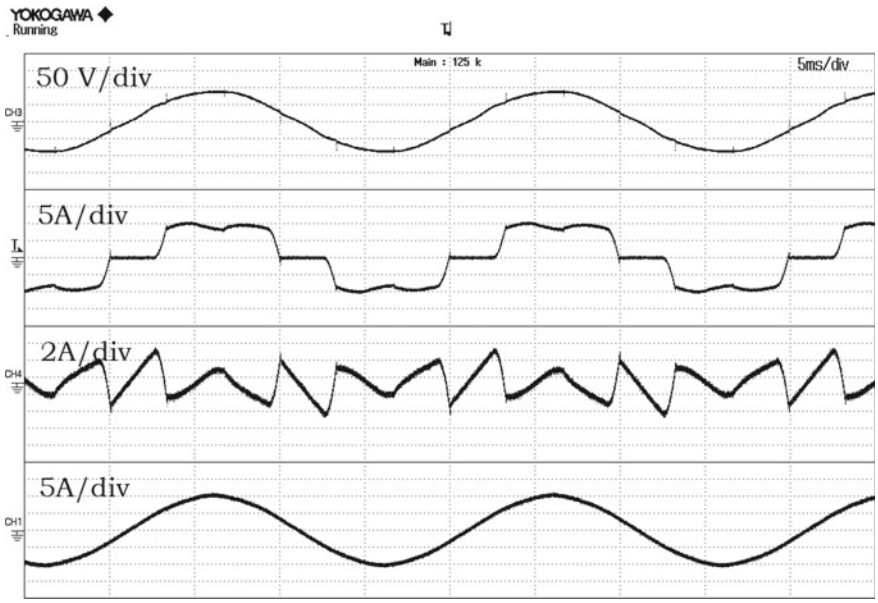

Fig. 30.5 Performance of shunt active power filter under ideal mains. *Source* Voltage, load current, compensating current, source current

However, distributed generators installed at various points in the microgrid contribute to the voltage fluctuation near the point of installation of shunt active power filter. Under such conditions, the role of SAPF cannot be restricted to the harmonic mitigation but voltage regulation can also be attributed by compensating for reactive power in the system.

Figure 30.6a shows a simplified circuit diagram of a shunt active power filter connected to a distribution line fed from the distributed generator connected at the end of the line. It is assumed that the distributed generator is injecting current i_g into the line and the change in the current causes voltage fluctuation at the terminal. This voltage fluctuation is dependent upon the impedance seen by the active power filter and distributed generators and is given by Thevenin equivalent,

$$Z_s = (r_s + j\omega L_s) \left\| \left(\frac{1}{j\omega C_{sh}} \right) \right. \tag{30.8}$$

$$Z_s = \frac{r_s + j\omega L_s}{1 - \omega^2 L_s C_{sh} + j\omega r_s C_{sh}} \tag{30.9}$$

At the fundamental frequency, the impedance is inductive irrespective of the value of filter capacitor connected across the PCC. The phasor diagram of the system is given in Fig. 30.6b. In normal case, the distributed generator produces only active power and injects the current which maintains zero phase difference with the terminal

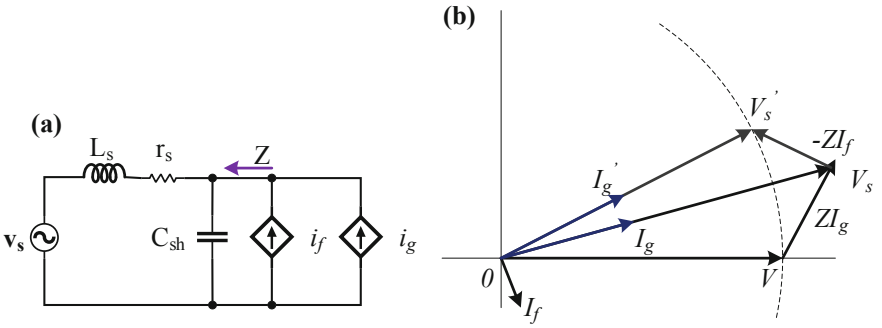

Fig. 30.6 Circuit diagram of SAPF with distribution generator

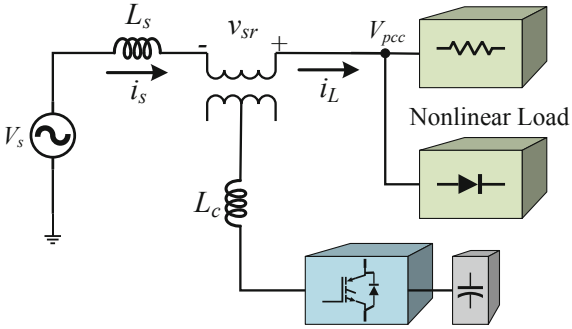

Fig. 30.7 Block diagram of series active power filter

voltage V. Due to the injected grid current, the source voltage amplitude increases to V_s as shown in Fig. 30.6a. The increases in the amplitude of voltage can only be compensated by injecting the filter current equivalent to the drop caused by line impedance. This is possible since the shunt active power filter can draw any amount of lagging or leading current so as to reduce the line voltage drop.

30.4.2 Series Active Power Filter

It has been observed many times that the total fraction of nonlinear loads such as SMPS, LED power supplies, and drives operating at light load condition can account to more than 50% of the demanded current in small systems. In this condition, the compensation of current harmonic will demand larger ratings of the overall SAPF system. Such loads are alternatively called as voltage harmonic producing load.

A series APF is a PQ solution which injects harmonic voltage in series with the source voltage and thereby source current becomes sinusoidal (Fig. 30.7).

The control of series APF is done based on the Eq. (30.10):

$$v_{sr}^{ref} = K_{sr} i_{sh} \tag{30.10}$$

In comparison to the shunt active power filter which requires current control technique to synthesize the compensation current, the series filter will require linear PWM controlled operating at high frequency. The major disadvantage of the series APF is the requirement of the series transformer (CT) which has larger ratings. In addition to this, the protection of the series connected transformer will be a major issue in the case of maloperation of the converter.

30.5 Mitigation of Voltage Related Issues

A microgrid suffers from voltage fluctuations as well as voltage unbalance. In addition to this, short time transients, voltage sag/swells, flickers are also prevalent in the microgrid operating in conjunction with the grid and several DERs. These phenomena normally occur due to variations in the loading pattern, uneven distribution of the line currents, impedance variation in devices and sudden introduction or removal of the large load or DG in the system. For reliable operation of sensitive loads as well as preventing the overall system from the malfunction, these issues must be mitigated. In this section, we discuss the operating principle and typical configurations of some of the popular solutions proposed in the literature.

30.5.1 Distribution STATCOM (DSTATCOM)

DSTATCOM is a device that is capable of mitigating multiple power quality issues. It absorbs or injects reactive power into the distribution system and thereby regulates the voltage at the load end.

A DSTATCOM consists of Voltage Source Inverter, coupling inductor or an optional transformer, ripple filter and DC link capacitor or Battery as shown in Fig. 30.9. The VSI synthesizes output voltage which injects the current in quadrature with the source voltage and hence feeds reactive power into the system. In addition to this, DSTATCOM manages the exchange of active power between DC link and grid to maintain the necessary voltage across the DC link. A single phase equivalent circuit diagram and relevant phasor diagram presented in Fig. 30.8 reveal the conventional operation of DSTATCOM.

The phasor diagram illustrates operation of DSTATCOM at fundamental frequency considering all the state vectors of VSI. Let us assume that amplitude and angle of the converter voltage vector V_c and voltage at the PCC V_{pcc} are as shown in Fig. 30.8. The magnitude $|V_c|$ and angle δ of converter voltage with respect to the PCC voltage vector determines the exchange of power between DSTATCOM and the grid.

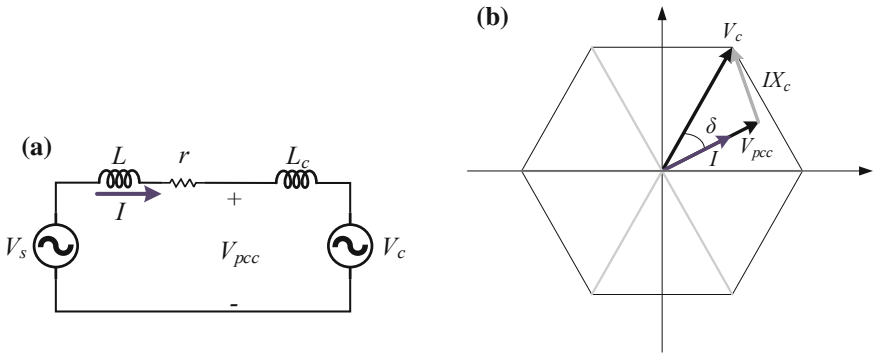

Fig. 30.8 **a** Single phase line diagram and, **b** phasor diagram of DSTATCOM operation with VSI

In the most simplified manner, the relationship of active and reactive power with given nomenclature is expressed as,

$$P = \frac{V_{pcc}V_c}{X_c}\sin\delta$$
$$Q = \frac{V_{pcc}^2}{X_c} - \frac{V_{pcc}V_c}{X_c}\cos\delta \tag{30.11}$$

30.5.1.1 Role of DSTATCOM for Voltage Regulation in Microgrid

As shown in Fig. 30.9, a DSTATCOM is connected at the PCC where one or more than one DERs are connected through the distribution line. The local loads have an intermittent demand for power. Additionally, the WECS system demands reactive power. This causes the voltage at the PCC to fluctuate over a wide range especially in the case of variable generation of power. It is needless say that a local DERs have capability to supply reactive power. Such a control requires a secondary control unit which regulates the amount of instantaneous active and reactive power fed by DERs. At present, most of the DERs are not equipped with such a facility. A DSTATCOM is applied to supply the reactive power demand of the load DERs as well as loads. In addition to this, it regulates the voltage at the PCC so that Zero Voltage Regulation (ZVR) is achieved [22]. The control scheme of DSTATCOM for compensation of reactive and achieving voltage regulation is shown in Fig. 30.10 below. A commonly used strategy for control is Instantaneous Reactive Control Theory (IRPT) which is explained as follows:

The IRPT theory is based on the instantaneous p-q theory where instantaneous active and reactive powers are defined as:

$$p = v_{La}i_a + v_{Lb}i_b + v_{Lc}i_c$$

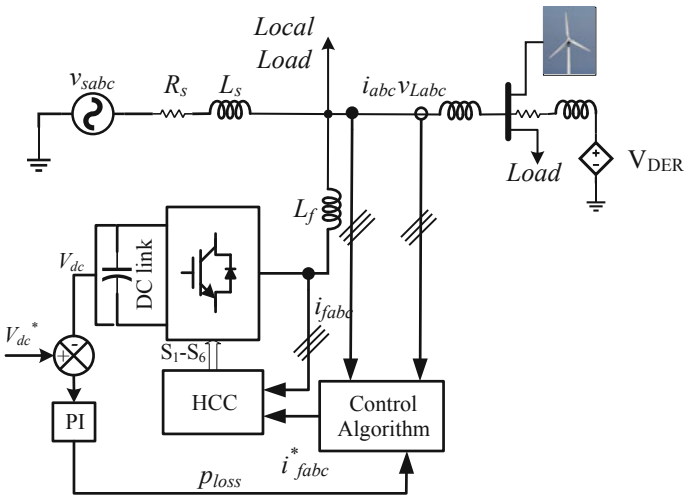

Fig. 30.9 Schematic of DSTATCOM connected for voltage regulation

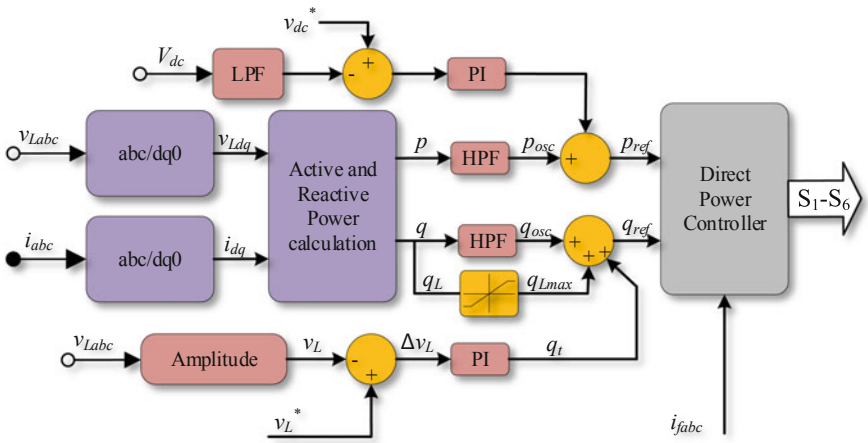

Fig. 30.10 Control algorithm for DSTATCOM used in simultaneous compensation of harmonics and voltage regulation

$$q = \frac{i_a(v_{Lb} - v_{Lc}) + i_b(v_{Lc} - v_{La}) + i_c(v_{La} - v_{Lb})}{\sqrt{3}} \tag{30.12}$$

The power thus calculated can be divided into the harmonic/negative sequence power as well as average power

$$\begin{aligned} p &= p_{dc} + p_{osc} \\ q &= q_{dc} + q_{osc} \end{aligned} \tag{30.13}$$

The oscillating component is obtained with application of either High Pass Filter with cut off frequency of 25 Hz or Notch Filter (for selected phenomena). These oscillating components are compensated in order to avoid critical issues such as harmonics and unbalance. In addition to this, reactive power required to maintain zero voltage regulation is obtained from

$$q_{ref} = q_{L\max} + \left(K_p \Delta v_L + \frac{K_I}{s} \Delta v_L\right) + q_{osc} \tag{30.14}$$

where, $q_{L\max}$ is the maximum reactive power support provided by the DSTATCOM. The value of $q_{L\max}$ depends upon reactive power required to meet the rating requirement of the overall system.

While average instantaneous active power requirement supplied by the device is zero, certain amount of active power is drawn from PCC to maintain the voltage across DC link. The value of the overall active power requirement is

$$p_{ref} = p_{osc} + \left(K_p \Delta V_{dc} + \frac{K_I}{s} \Delta V_{dc}\right) \tag{30.15}$$

The reference compensating power thus obtained can be realized using either conventional control strategies or the Direct Power Control strategy as realized in [23].

30.5.2 Dynamic Voltage Restorer

The Dynamic Voltage Restorer (DVR) is a PQ solution which protects the sensitive loads against voltage fluctuations in the grid. The DVR can inject series voltage in phase or quadrature with the source current and hence control active and reactive power flow into the system. The block diagram of the DVR is shown in Fig. 30.11.

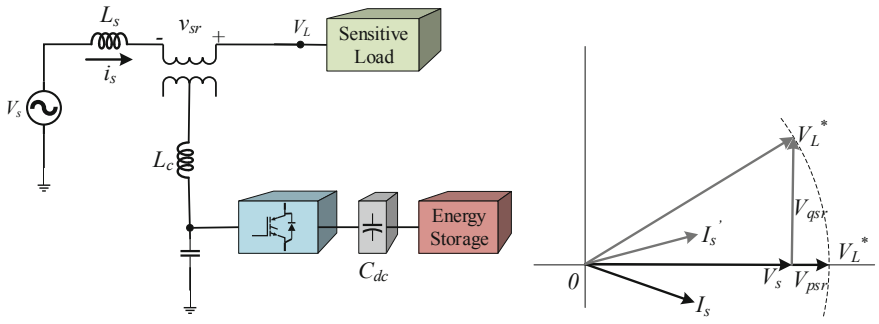

Fig. 30.11 Schematic diagram of DVR and phasor diagram for operation

In order to inject active power into the system, the DVR is equipped with Energy Storage System (ESS). This ESS can be a battery, Photovoltaic source or ultracapacitor etc. A properly configured matching transformer (CT) is employed in the DVR such that voltage unbalance and/or voltage sag/swell is effectively compensated in the system.

The energy requirement from the Energy Source is dependent on the amplitude and phase of the injected voltage. The requirement of energy based on strategies is explained in Fig. 30.11. In first case, the voltage is injected without phase displacement in reference to the source current and hence significant amount of active power i.e. component of source which is in phase with the series voltage V_{psr} is required. In another method, the injected voltage maintains quadrature relationship with the source current and is denoted by V_{qsr}. Due to injection of voltage, the load voltage occupies a new position V_L^* (shown by grey line).

As phase angle of the load voltage is advanced, the line current also attains a new position in the space plane and is shown as I_L'. The phenomena is known as phase jump in the line current. The energy requirement from the energy source is reduced significantly in comparison to the in-phase voltage injection. This is due to the fact that the phase angle between the injected voltage and source current is nearly 90°.

30.5.3 Control of DVR for Compensation of Voltage Unbalance and Voltage Sag

The control algorithm of the DVR senses the source voltage, decides the reference load voltage and calculates the voltage to be injected in series. Figure 30.12 shows the scheme for compensation of imbalance in source voltages and sag/swell in the system. The angular information θ_e of the source voltage is obtained using Double Decoupled SRF based PLL. The direct and quadrature axis component of the source voltage is obtained using three phase to two-phase transformation.

These components are further divided into the average and oscillating components i.e.

$$\begin{aligned} v_{ds} &= \bar{v}_{ds} + \tilde{v}_{ds} \\ v_{qs} &= \bar{v}_{qs} + \tilde{v}_{qs} \end{aligned} \tag{30.16}$$

The average component of the source voltage determines the voltage to be injected by DVR during the sag/swell. In addition to this, voltage unbalance is determined from the oscillating component of the source voltage. Mathematically, this is expressed as

$$\begin{aligned} v_{Cd}^* &= v_{Ld}^* - v_{sd} \quad \text{for in phase injection} \\ v_{Cq}^* &= \sqrt{{v_{Ld}^*}^2 - v_{sd}^2} \quad \text{for quadrature injection} \end{aligned} \tag{30.17}$$

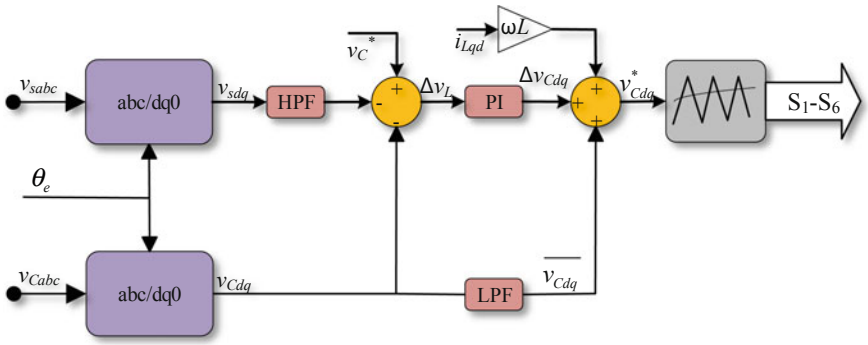

Fig. 30.12 Control algorithm for DVR used for simultaneous compensation of voltage unbalance and voltage sag

The difference of reference voltage and injected voltage across the secondary of the CT are compared and processed by the linear controller. The reference voltage to be compensated by the series converter in the DVR is determined by the feedforward controller shown in Fig. 30.12. The value of compensating voltage is determined by,

$$\begin{aligned} v_{cd}^* &= \overline{v_{cd}} + \omega L i_{sq} + \Delta v_{cd} \\ v_{cq}^* &= \overline{v_{cq}} - \omega L i_{sd} + \Delta v_{cq} \end{aligned} \tag{30.18}$$

30.6 Unified Power Quality Conditioner for Compensation of Multiple Power Quality Issues in Microgrid

UPQC is a combination of two important types of compensators namely shunt and series compensators. The shunt compensator is normally designed to mitigate current related issues and the series converter is most suitable for voltage related issues e.g. voltage harmonics sag/swell, flicker.

However, installing two separate devices may not be a cost-effective solution as DVR always demands a source for active power. Hence, back to back configuration of DSTATCOM and DVR was introduced and named Unified Power Quality Conditioner. UPQC mitigates reactive power as well as oscillating components of real power.

Figure 30.13 shows a block diagram of one such UPQC in which series converter is connected before the shunt converter. The UPQC is used for power quality issues encountered in the AC microgrid. In addition to this, DC microgrid is connected in parallel with the DC link of the UPQC. Depending upon the requirement, series converter and shunt converter may be interchanged. The behavior of a typical UPQC for compensation of harmonics, reactive power, and voltage sag is shown in Fig. 30.14.

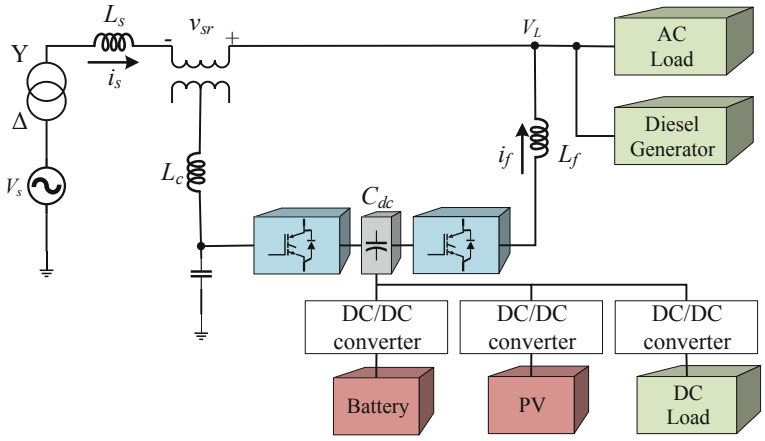

Fig. 30.13 Block diagram of unified power quality conditioner

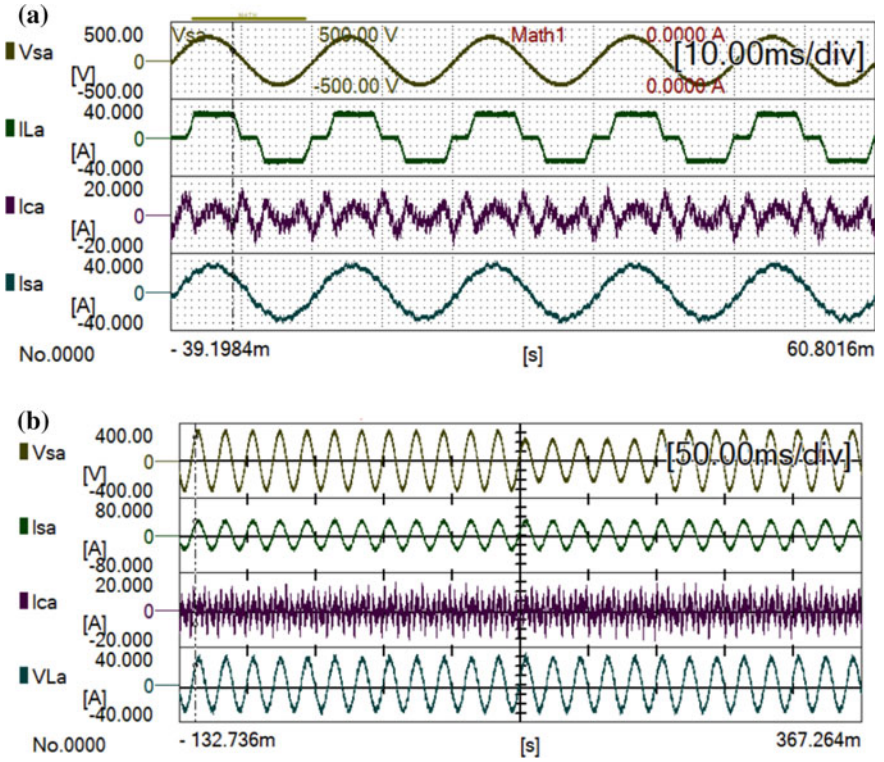

Fig. 30.14 Experimental results of UPQC for simultaneous compensation of current harmonics, reactive power and voltage sag, **a** compensation of harmonics by DSTATCOM, **b** compensation of voltage sag using DVR

Conventionally, the UPQC is employed for AC microgrid in which two back to back connected converters share a common DC link. The possibility of connecting UPQC DC link with the with DC microgrid has also been explored. The DC microgrid is constituted of Battery Energy Storage System, PV arrays and DC loads all connected to the DC link of the UPQC with appropriate DC-DC converter configuration. This system forms a hybrid AC/DC microgrid. While the compensation of the phenomena related to current and voltage on the AC side can be done using approach discussed in previous sections, the coordination with the DC microgrid requires additional control in which active power should be exchanged between the DC and AC microgrid based on the droop characteristics. Such a relationship is governed by the Eqs. (30.19)–(30.22) [24]:

$$P_{d\_raf} = \frac{1}{K_d}\left(V_{d\_ref} - V_{d\_cal}\right) \tag{30.19}$$

$$K_d = \frac{1}{P_{d\_\max}}\left(V_{d\_\max} - V_{d\_\min}\right) \tag{30.20}$$

$$\begin{aligned} V_{d\_cal} &= \sqrt{V_{d\_ref}^2 - \frac{1}{K_{S\_AD}}(\Delta\omega)} \\ \Delta\omega &= 2\pi f - \omega \\ K_{S\_AD} &= K_{S\_AC}\left(\frac{1}{2}\frac{C_d}{T_{smp}}\right) \\ K_{S\_AC} &= D_l + \left(\frac{1}{a_1} + \frac{1}{a_2} + \cdots + \frac{1}{a_n}\right) \end{aligned} \tag{30.21}$$

$$\begin{aligned} P_{a\_ref} &= \frac{1}{K_a}(\Delta\omega_0) \\ \Delta\omega_0 &= K_{S\_AD}(V_{d\_ref}^2 - V_d^2) \\ K_a &= \frac{1}{P_{a\_\max}}(\omega_{\max} - \omega_{\min}) \\ P_R &= P_S + P_{d\_ref} + P_{a\_ref} \end{aligned} \tag{30.22}$$

where,

P_s	Set point for power sharing
P_{d_ref}	DC microgrid to AC microgrid power exchange rate
P_{a_ref}	AC microgrid to DC microgrid power exchange rate
P_R	Power exchange reference signal between the two microgrid
$P_{d\_\max}$	maximum power supplied by DC side
$P_{a\_\max}$	AC source maximum power
K_d	DC droop characteristic slope
K_a	AC droop characteristic slope

K_{S_AD} AC-DC droop characteristic slope
K_{S_AC} AC microgrid droop characteristic slope

and

V_{d_cal} DC link calculated voltage
V_{d}_max DC link maximum allowable voltage
V_{d}_min DC link minimumm allowable voltage
a_n The nth generator droop coefficient
D_l AC microgrid load damping factor
C_d DC microgrid capacitance
T_{smp} Simulation sampling time
ω AC microgrid angular frequency
$\Delta\omega$ Deflection of angular frequency from the reference value
$\Delta\omega_0$ AC microgrid calculated frequency change
ωmax AC microgrid maximum allowable frequency
ωmin AC microgrid minimum allowable frequency.

30.7 Control to Mitigate the Load Pulses

The control to mitigate the load pulses in microgrids is a challenging subject for the researchers. For this, the hybridization of Energy Storage System (ESS) with different power storage devices such as the ultracapacitors (UCs), Superconducting Magnetic Energy Storage (SMES) devices, and high-speed Flywheel Energy Systems (FESs) is mandatory for supplying load pulses in order to dynamically compensate the power flow balance. In this section, the Li-Ion battery/SMES Hybrid Storage Systems (HSS) is used in a grid-connected Hybrid Power System (HPS) based on Renewable Energy Sources (RESs) and Fuel Cell (FC) system as a backup energy source (called below as FC/RES/ELZ HPS).

The details of HPS design can be found in [25]. The filtering-based control to split the power spectrum into the low and high-frequency bands will be used in this study [26]. The FC/RES/ELZ HPS is presented in Fig. 30.15, the battery/SMES HSS in Fig. 30.16, and the proposed mitigation control is presented in Fig. 30.17.

The voltage on the DC bus (VDC) will be regulated to $V_{DCref} = 200$ V by the DC voltage regulation loop on the Li-ion battery side (see the signal $V_{DCcorrection}$ in Fig. 30.17). This can assure an acceptable error $eV_{dc} = V_{DC} - V_{DCref}$ based on the Proportional-Integral (PI) controller, without affecting the Load-Following (LF) control [27, 28] applied to boost converter to generate the needed power on the DC bus (PDC).

On the DC bus, the power flow balance is Eq. (30.23):

$$C_{DC} u_{dc} du_{dc}/dt \cong \eta_{boost} p_{AES} + p_{ESS} + p_{RES} - p_{ELZ} - p_{Load} \tag{30.23}$$

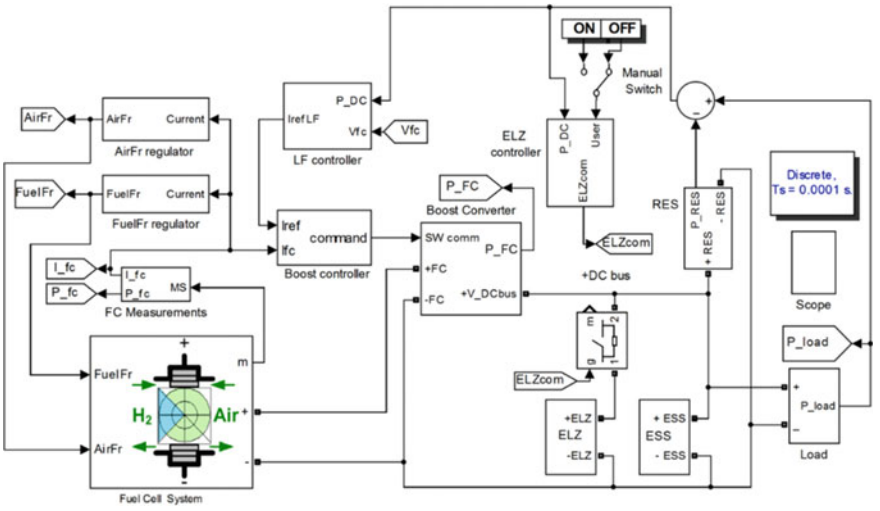

Fig. 30.15 The HPS

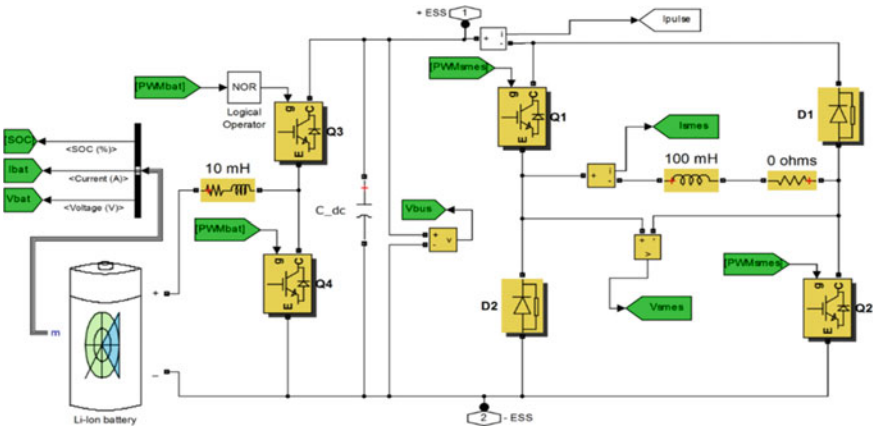

Fig. 30.16 The HSS

where, p_{AES} is the FC net power, p_{ELZ} is ELZ power, p_{ESS} is ESS power, p_{RES} is RES power, and p_{Load} is load demand, respectively. Also, η_{boost} is the energy efficiency of the boost DD-DC converter, and C_{DC} is the filtering capacitor of the DC voltage (u_{dc}).

Because the LF control is used, the battery will operate in charge-sustaining mode ($P_{ESS(AV)} = 0$; Fig. 30.18). So, $P_{FC(AV)}$ requested will be given by Eq. (30.24):

$$\begin{aligned} 0 &\cong \eta_{boost(AV)} P_{AES(AV)} + P_{RES(AV)} - P_{ELZ(AV)} - P_{Load(AV)} \\ &\Rightarrow P_{AES(AV)} = P_{DC(AV)} / \eta_{boost(AV)} \end{aligned} \tag{30.24}$$

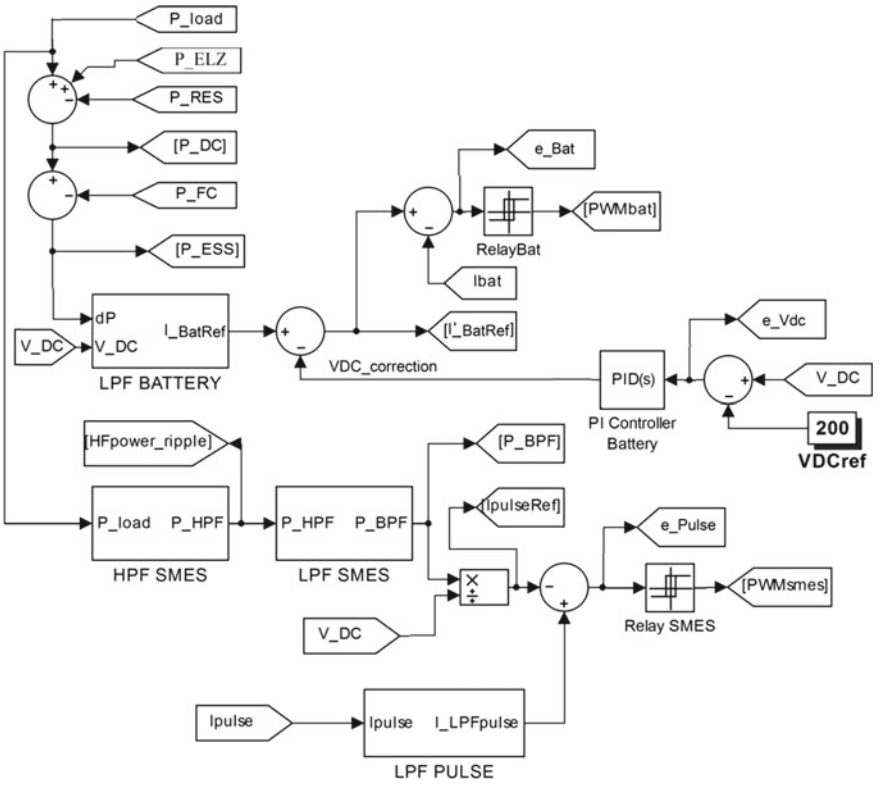

Fig. 30.17 Control proposed to generate the anti-ripple I_{pulse}

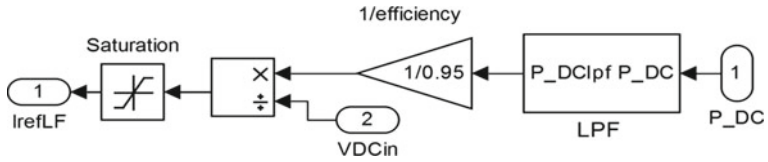

Fig. 30.18 Load-following (LF) control

where, $P_{DC(AV)} = P_{Load(AV)} + P_{ELZ(AV)} - P_{RES(AV)}$ is the average (AV) value of power needed on the DC bus.

In this study, the values of boost energy efficiency $\eta_{boost(AV)}$ is set to 95%, and the initial voltage on the capacitor C_{DC} and the battery are set to $V_{DCref} = 200$ V and 100 V. The electrolyzer (ELZ) could be supplied with power only if $P_{Load(AV)} < P_{RES(AV)}$. The FC system, Li-ion battery and SMES device are modeled using 6 kW Proton Exchange Membrane Fuel Cell (PEMFC) system and 100 Ah/100 V battery from the Matlab & Simulink toolboxes. The 10 mH/0 Ω inductance was used to model the SMES.

The initial State-Of-Charge (SOC) is set at 80%, the time constants for PEMFC and battery were set at 0.1 and 10 s, and the values of the remaining parameters for PEMFC and battery are the default ones [29].

The signal *PWMbat*, which is the output of the hysteresis current-mode controller ("Relay_bat" in Fig. 30.17) controls via the half-bridge DC-DC converter the battery's power flow to DC bus. The signal *PWMsmes*, which is the output of the hysteresis current-mode controller ("Relay_smes" in Fig. 30.17) controls via the asymmetric full-bridge DC-DC converter the SMES's power flow to DC bus.

By neglecting the voltage ripple on the DC bus, the power flow balance (a) can be rewritten to estimate the power deviation ΔP on the DC bus:

$$\begin{aligned} 0 \cong p_{DC} + p_{ESS} + p_{RES} - p_{ELZ} - p_{Load} \quad \Rightarrow \\ \Rightarrow p_{ESS} \cong \Delta P = p_{ELZ} + p_{Load} - p_{DC} - p_{RES} \end{aligned} \tag{30.25}$$

In this study the load power (P_{load}) was modeled by two current controlled sources: one for pulses of load (P_{load2}) and the other one for an unknown profile of the dynamic load (P_{load1}). The proposed control uses the filtering blocks "BPF_{SMES}" and "LPF_{Bat}" (see Fig. 30.17) to generate the reference currents $I_{Pulse(ref)}$ and $I_{Bat(ref)}$ based on P_{Load} and $\Delta P \cong p_{ESS,}$ which is given by (30.25). So, the reference currents $I_{Pulse(ref)}$ and $I_{Bat(ref)}$ are set by Eqs. (30.26) and (30.27):

$$I_{Pulse(ref)} = BPF_{SMES}(P_{Load}/V_{DC}) \tag{30.26}$$

$$I_{Bat(ref)} = LPF_{Bat}(\Delta P/V_{DC}) \tag{30.27}$$

The filtering blocks, "HPF_{SMES}" and "LPF_{SMES}", filter the load power, resulting P_{BPF} and the reference for SMES controller, $I_{pulse(ref)} = P_{BPF}/V_{DC}$. So, the load pulses ($p_{load2}$) will be mitigated by appropriate command of the SMES power converter based on the current error given by Eq. (30.28):

$$e_{Pulse} = I_{Pulse(ref)} - I_{Pulse(LPF)} \tag{30.28}$$

where, $I_{Pulse(LPF)}$ is the output of the "LPF_{Pulse}" block:

$$I_{Pulse(LPF)} = LPF_{Pulse}(I_{Pulse}) \tag{30.29}$$

and I_{Pulse} is the anti-ripple current. Considering Eqs. (30.26) and (30.29), if $e_{Pulse} \cong 0$, then:

$$I_{Pulse} \cong P_{Load2}/V_{DC} \tag{30.30}$$

So, the SMES power converter generates the anti-ripple current that mitigates the load pulses P_{load2}/V_{DC}. A 0.1 A hysteresis band for the SMES hysteresis current-mode controller can ensure $e_{Pulse} \cong 0$ with sufficient precision (see next Section

of results). The values of cut-off frequency of filters "HPF_{SMES}", "LPF_{SMES}", and "LPF_{Pulse}" are set at 0.1, 1000, 1000 Hz as well.

The battery hysteresis current-mode controller (the block "Relay_Bat" of Fig. 30.17) based on the errors $e_{Bat} = I'_{Bat(ref)} - I_{Bat}$, where

$$I'_{Bat(ref)} = I_{Bat(ref)} - V_{DC(correction)} \tag{30.31}$$

and $I_{Bat(ref)} = LPF_{Bat}(dP/V_{DC})$ will compensate possible deviations to power flow balance. The power flow balance Eq. (30.23) can be rewritten as:

$$0 \cong \eta_{boost(AV)} I_{ref(LF)} V_{FC(AV)} - P_{DC(AV)} \tag{30.32}$$

So, the reference of the LF control will be given by:

$$I_{ref(LF)} = P_{DC(AV)}/(V_{FC(AV)} \cdot \eta_{boost(AV)}) \tag{30.33}$$

where, $P_{DC(AV)} = P_{Load(AV)} + P_{ELZ(AV)} - P_{RES(AV)}$.

The behavior of the FC/RES/ELZ HPS under control loops mentioned above will be presented in the next section.

30.7.1 Simulation Results of the FC/RES/ELZ Hybrid Power System

Figure 30.19 shows the behavior of the FC HPS. The first plots present the dynamic profile of the load power (P_{load1}), the RES power (P_{RES}), and the battery power (P_{Bat}). Note that the battery operates in charge-sustained mode ($P_{Bat} \cong 0$) after the startup phase of the FC system (see Fig. 30.20). Until the FC system is able to generate the needed power to ensure the power flow balance (30.23), the battery ensures this power. The 4th plot presents the FC current represented which follows I_{refLF} given by (30.33). The ELZ will not operate because $P_{load} > P_{RES}$. The I_{FC} current controls the fueling flow rates (FuelFr and AirFr) in the same manner as in static Feed-Forward (sFF) control [30]. The fuel economy of the FC system can be improved by using real time strategies (RTOs) to optimize the operation of the FC system [27, 31]. Different optimization functions are used in the literature, as mix of the performance indicators such as the fuel consumption efficiency ($Fuel_{eff} \cong P_{FCnet}/FuelFr$) and the FC system efficiency (η_{sys}). These performance indicators are represented in next two plots of Fig. 30.19. As an example,, the efficient operation of FC/Wind Turbine system under turbulent wind is analyzed in [32], but note that the objective of this chapter is not related to optimal operation of the FC/RES/ELZ HPS.

The DC voltage (V_{DC}) and its zoom during the startup phase are shown in last two plots of Fig. 30.19. The voltage ripples are not observed so the load pulsed were

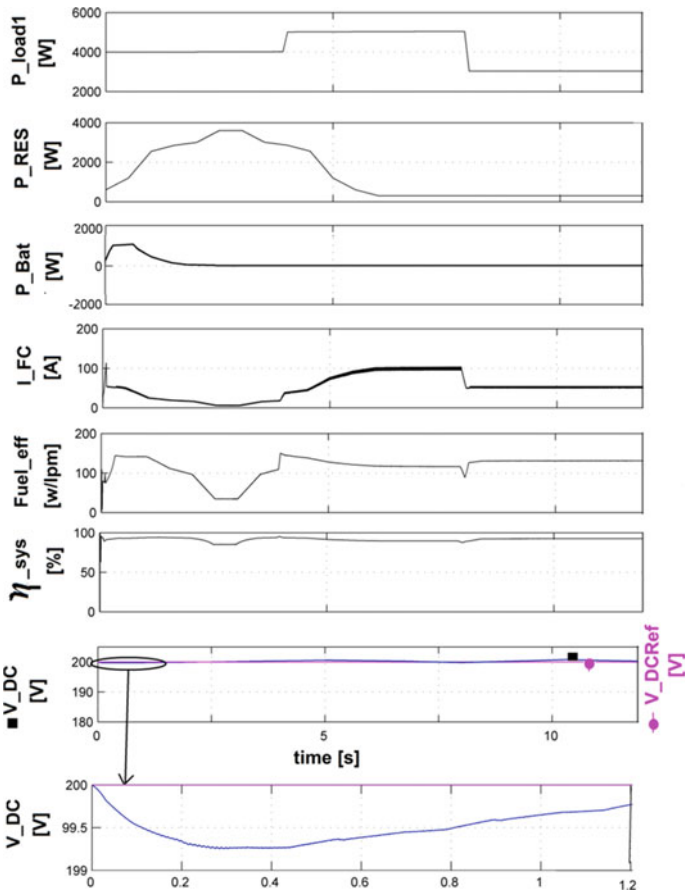

Fig. 30.19 Behavior of the HPS

mitigated by I_{pulse} (the generated anti-ripple current). The shape of the anti-ripple I_{pulse} is close to ripple on the DC bus ($I_{Pulse(ref)}$) given by Eq. (30.26).

The signals $I_{Pulse(ref)}$, I_{pulse}, $e_{Pulse} = I_{Pulse(ref)} - I_{Pulse(LPF)}$, and PWM_SMES (mentioned in Fig. 30.17) are represented in Figs. 30.20, 30.21 and 30.22 during the startup phase and have the same structure of plots as Fig. 30.20. These signals represent the load pulse and the low-frequency load ripple. Note that the error e_{Pulse} is set by the hysteresis band, being lower than $0.1A_{p\text{-}p}$ except the startup phase. The proposed control to mitigate the load ripple gives better results compared to those obtained with double-buck topology used for FC/UC HPS [33].

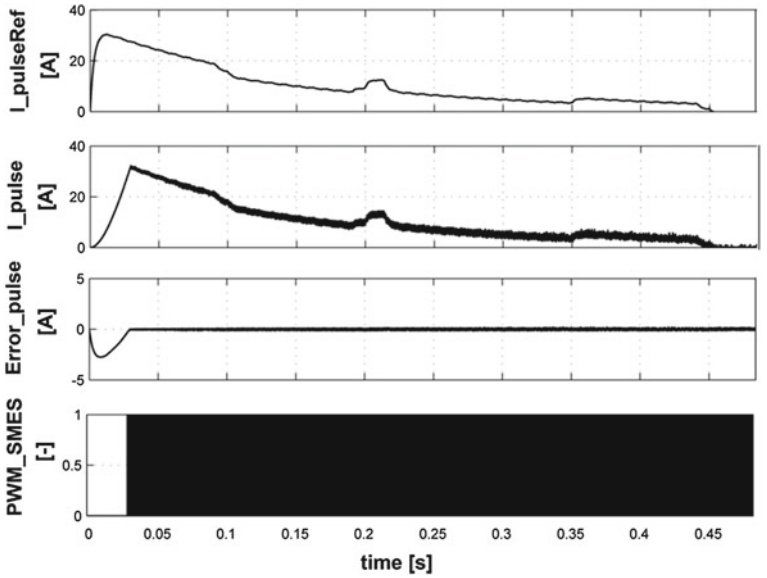

Fig. 30.20 The startup phase for the anti-ripple I_{pulse}

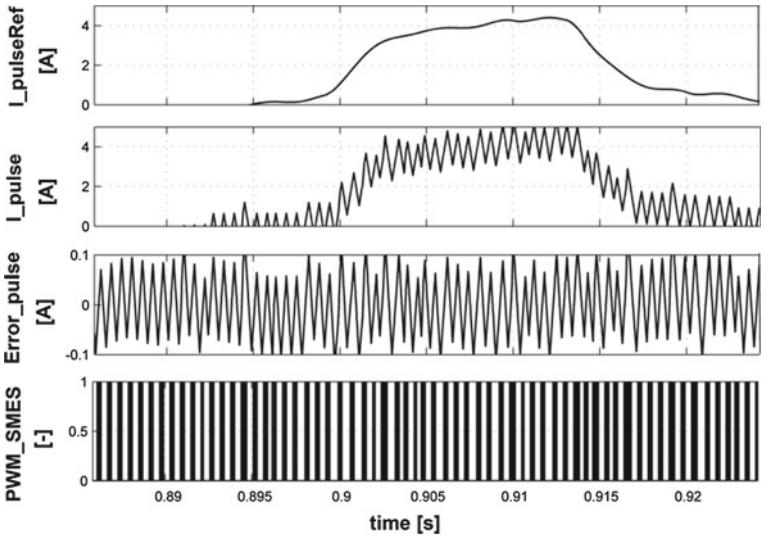

Fig. 30.21 Zooming of the load pulse and the anti-ripple I_{pulse}

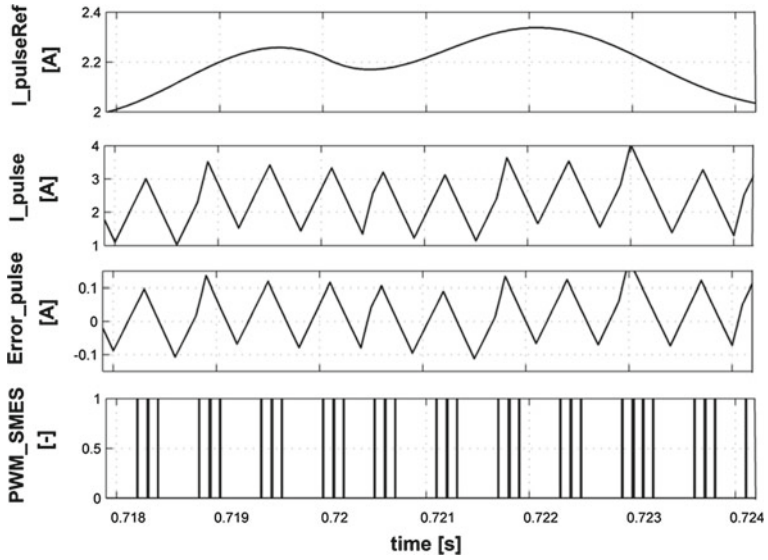

Fig. 30.22 Zooming of the low-frequency load ripple and the anti-ripple I_{pulse}

30.8 Conclusion

The ever-increasing complexity of the microgrid with deep penetration of linear and non-linear load as well as no. of Distributed Energy Sources has aggravated power quality issues and poses a serious challenge for the large user as well as utility. Harmonics are found to have deteriorating effects on the microgrid. Hence, investigation on harmonics generated due to various filtering and loading conditions of adjustable speed drives is carried out. It has been found that the input current *THD* of Adjustable Speed Drive ranges from 40 to 130%. Additionally, various power quality issues occurring in the microgrid are studied. A number of solutions have been reported in the literature for the mitigation of power quality issues in the microgrid. The most commonly employed solutions such as Active Power Filters, DSTATCOM, DVR, and UPQC are discussed with their operating principle and control algorithm. The mitigation of load pulses using proposed hybridization of Energy Storage System is examined with the detailed control scheme and necessary results. The solution to power quality issues are not limited to the primary compensation devices. Multifunctional DGs can compensate for many PQ issues in addition to the active power transfer between source and grid. A study on the role of multifunctional DGs is left to the interest of the reader.

References

1. E. Planas, J. Andreu, J.I. Garate, I. Martinez de Alegria, E. Ibarra, AC and DC technology in microgrids: a review. Renew. Sustain. Energy Rev. **43**, 726–749 (2015)
2. J.J. Justo, F. Mwasilu, J. Lee, J.W. Jung, AC-microgrids versus DC-microgrids with distributed energy resources: a review. Renew. Sustain. Energy Rev. **24**, 387–405 (2013)
3. D. Kumar, F. Zare, A. Ghosh, DC microgrid technology: system architectures, AC grid interfaces, grounding schemes, power quality, communication networks, applications, and standardizations aspects. IEEE Access **5**, 12230–12256 (2017)
4. N. Mahdavi Tabatabaei, A. Jafari Aghbolaghi, N. Bizon, F. Blaabjerg, *Reactive Power Control in AC Power Systems* (Cham, Switzerland, Springer International Publishing, 2017)
5. P. Aristidou, G. Valverde, T.V. Cutsem, Contribution of distribution network control to voltage stability: a case study. IEEE Trans. on Smart Grid **8**(1), 106–116 (2017)
6. M.T.L. Gayatri, A.M. Parimi, A.V. Pavan Kumar, A review of reactive power compensation techniques in microgrids. Renew. Sustain. Energ. Rev. **81**, 1030–1036 (2018)
7. R. Gundabathini, N.M. Pindoriya, Improved control strategy for bidirectional single phase AC-DC converter in hybrid AC/DC microgrid. Electr. Power Compon. Syst. **45**(20), 2293–2303 (2017)
8. B. Singh, S. Singh, A. Chandra, K. Al Haddad, Comprehensive study of single-phase AC-DC power factor corrected converters with high-frequency isolation. IEEE Trans. Ind. Inf. **7**(4), 540–556 (2011)
9. F. Zare, H. Soltani, D. Kumar, P. Davari, H.A.M. Delpino, F. Blaabjerg, Harmonic emissions of three-phase diode rectifiers in distribution networks. IEEE Access **5**, 2819–2833 (2017)
10. M.B. Latran, A. Teke, Y. Yoldas, Mitigation of power quality problems using distribution static synchronous compensator: a comprehensive review. IET Power Electron. **8**(7), 1312–1328 (2015)
11. S.R. Arya, B. Singh, A. Chandra, K. Al Haddad, Power Factor Correction and Zero Voltage Regulation in Distribution System Using DSTATCOM, in *IEEE International Conference on Power Electronics, Drives and Energy Systems (PEDES)*, 16–19 Dec 2012
12. Z. Li, W. Li, T. Pan, An optimized compensation strategy of DVR for micro-grid voltage sag. Prot. Control Mod. Power Syst. **1**(1), 10 (2016)
13. V. Khadkikar, Enhancing electric power quality using UPQC: a comprehensive overview. IEEE Trans. Power Electron. **27**, 2284–2297 (2012)
14. H. Hafezi, G. D'Antona, A. Dede, D.D. Giustina, R. Faranda, G. Massa, Power quality conditioning in LV distribution networks: results by field demonstration. IEEE Trans. Smart Grid **8**(1), 418–427 (2017)
15. J. He, B. Liang, Y.W. Li, C. Wang, Simultaneous microgrid voltage and current harmonics compensation using coordinated control of dual-interfacing converters. IEEE Trans. Power Electron. **32**(4), 2647–2660 (2017)
16. W. Al Saedi, S.W. Lachowicz, D. Habibi, O. Bass, Power flow control in grid-connected microgrid operation using particle swarm optimization under variable load conditions. Int. J. Electr. Power Energ. Syst. **49**, 76–85 (2013)
17. P. Gopakumar, M.J.B. Reddy, D.K. Mohanta, Stability concerns in smart grid with emerging renewable energy technologies. Electr. Power Compon. Syst. **42**(3–4), 418–425 (2014)
18. Y. Liu, Y. Li, Y. Chi, W. Wang, Analysis on a Large Scale Wind Turbines Cascading Trip-off Accident in North China, in *IEEE Grenoble Conference*, 16–20 June 2013 (2013), pp. 1–6
19. E. Taylor, M. Korytowski, G. Reed, Voltage transient propagation in AC and DC datacenter distribution architectures, in *IEEE Energy Conversion Congress and Exposition (ECCE)* (September 2012), pp. 15–20
20. A.D. Graham, AD The Importance of a DC Side Harmonic Study for a DC Distribution System, in *6th IET International Conference on Power Electronics, Machines and Drives (PEMD)*, 27–29 Mar 2012

21. A. Kwasinski, Advanced Power Electronics Enabled Distribution Architectures: Design, Operation, and Control, in *8th International Conference on Power Electronics (ECCE Asia)*, 30 May–3 June 2011
22. V. Rajagopal, B. Singh, G.K. Kasal, Electronic load controller with power quality improvement of isolated induction generator for small hydro power generation. IET Renew. Power Gener. **5**(2), 202–213 (2010)
23. T. Trivedi, R. Jadeja, P. Bhatt, Improved direct power control of shunt active power filter with minimum reactive power variation and minimum apparent power variation approaches. J. Electr. Eng. Technol. **12**(3), 1124–1136 (2017)
24. P.G. Khorasani, M. Joorabian, S.G. Seifossadat, Smart grid realization with introducing unified power quality conditioner integrated with DC microgrid. Electr. Power Syst. Res. **151**, 68–85 (2017)
25. N. Bizon, Effective mitigation of the load pulses by controlling the battery/SMES hybrid energy storage system. Appl. Energy **229**, 459–473 (2018)
26. C. Turpin, B. Morin, E. Bru, O. Rallieres, X. Roboam, B. Sareni, M.G. Arregui, N. Roux, Power for aircraft emergencies: a hybrid proton-exchange membrane H_2\/O_2 fuel cell and ultracapacitor system. IEEE Electrification Mag. **5**(4), 72–85 (2017)
27. N. Bizon, Real-time optimization strategy for fuel cell hybrid power sources with load-following control of the fuel or air flow. Energy Convers. Manag. **157**, 13–27 (2018)
28. N. Bizon, P. Thounthong, Fuel economy using the global optimization of the Fuel Cell Hybrid Power Systems. Energy Convers. Manag. **173**, 665–678 (2018)
29. Hydro-Quebec and the MathWorks I, *Sim Power Systems Reference* (Mathworks Inc, 2010)
30. J.T. Pukrushpan, A.G. Stefanopoulou, H. Peng, *Control of Fuel Cell Power Systems: Principles, Modeling, Analysis and Feedback Design* (Springer Science & Business Media, 2004)
31. N. Bizon, A.G. Mazare, L.M. Ionescu, F.M. Enescu, Optimization of the proton exchange membrane fuel cell hybrid power system for residential buildings. Energy Convers. Manag. **163**, 22–37 (2018)
32. N. Bizon, Optimal operation of fuel cell/wind turbine hybrid power system under turbulent wind and variable load. Appl. Energ. **212**, 196–209 (2018)
33. N. Bizon, A new topology of fuel cell hybrid power source for efficient operation and high reliability. J. Power Sources **196**(6), 3260–3270 (2011)

Chapter 31
Control and Protection of the Smart Microgrids Using Internet of Things: Technologies, Architecture and Applications

Fernando Georgel Birleanu and Nicu Bizon

Abstract With the everyday technological growing and updates of the Internet of Things (IoT), smart microgrids, as the building foundations of the future smart grid, are integrating more and more different IoT architectures and technologies for applications intended to develop, control, monitor and protect microgrids. A smart microgrid consists of a smaller grid that can function independently or in conjunction with the main power grid and it is suitable for institutional, commercial and industrial consumers and also for urban and rural communities. A microgrid can operate in two modes, stand-alone mode and grid-connected mode, with the possibility to switch between modes because of faults in the local grid, scheduled maintenance and upgrade, shortages and outages in the host grid or for other reasons. With various distributed energy resources (DER) and interconnected loads in the microgrid, IoT is intended to provide solutions for high energy management, security mechanisms and control methods and applications. The basic components of a microgrid refer to local generation, consumption, energy storage and point of coupling to the main power grid. Local generation consists of different energy resources that provide electricity to users, from single residential house to commercial and industrial centers, which represent consumption. Energy storage is where the power is stored and comes with multiple functions such as voltage and frequency regulation, power backup or cost optimization. A coupling point refers to the junction between a smaller smart microgrid and the main smart grid. The main purposes of this chapter are to show the role of Internet of Things in creating and developing smart microgrids including benefits, challenges and risks and to reveal a variety of mechanisms, methods and procedures built to control and protect smart microgrids. Different technologies, architectures and applications using IoT, as the main key features, with the major goal of protect-

F. G. Birleanu (✉)
Faculty of Electronics, Communications and Computers, Doctoral School, University of Pitesti, Pitesti, Romania
e-mail: birleanu.fernando@gmail.com

N. Bizon
Department of Electronics, Computers and Electrical Engineering, Faculty of Electronics, Communications and Computers, University of Pitesti, Pitesti, Romania
e-mail: nicu.bizon@upit.ro

N. Mahdavi Tabatabaei et al. (eds.), *Microgrid Architectures, Control and Protection Methods*, Power Systems,
https://doi.org/10.1007/978-3-030-23723-3_31

ing and controlling innovative smart microgrids in line with modern optimization features and policies are intended to upgrade and improve efficiency, resiliency and economics. Microgrids represent a large IoT opportunity because they are composed of equipment that demands sensing, connectivity and analytics technologies to operate at the highest level.

Keywords Smart microgrid · Internet of Things · Distributed energy resources · Control · Protection

31.1 Introduction

There are many ways to define and describe a microgrid and its behavior, from the definition given by the U.S. Department of Energy [1–6]. In short terms, a microgrid refers to a compact group of interrelated power sources and loads that can function either connected to the main grid, either independently.

Usually, a microgrid architecture, as shown in Fig. 31.1, relies on the energy sources used to generate energy, on the storage systems and on the local loads with all the control systems for microgeneration and loads, Microgeneration Control (MC) and Local Control (LC) [7]. The microgrid is connected to the main grid via a Microgrid Central Control System (MCCS) and this junction is called the Point of Common Coupling (PCC). While the solid line shows the power flow between the main grid and the generators, storage systems and loads, the dot line reveals the information exchange between the control systems in the communication network thanks to the Internet of Things technology.

With different microgrid topologies, such as radial, ring or meshed, there are many types of microgrids [8–10]:

- Customer microgrids, also called the true microgrids;
- Institutional microgrids;
- Community microgrids, also called the milligrids;
- Remote off-grid microgrids, that never connect to the main grid because of geographical and economic concerns;
- Military base microgrids;
- Industrial and commercial microgrids.

With the purpose to sustain the energy for a small surface, a microgrid can generate and consume power of the order of kilowatts while the total amount of energy for a smart grid can reach up to tens or hundreds of gigawatts. While the possibilities to generate the energy for a microgrid, refer to fuel cells, photovoltaic cells or microturbines, the storage of this energy can be ensured using batteries, regenerative fuel cells or kinetic energy storage solutions [3, 11–16].

Microgrids, viewed as smaller versions of the main power grid that is the smart grid, are more and more becoming a reality through the everyday growing of the Internet of Things technology [17–24]. And, with the next generation of wireless

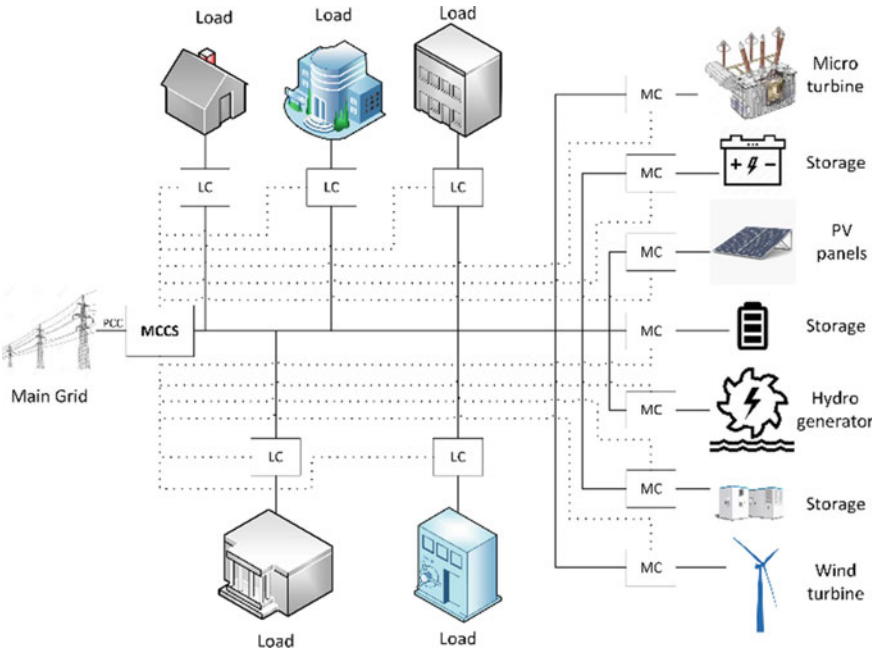

Fig. 31.1 A microgrid architecture

communication, the 5G, which is very close to us, the capabilities, features and services provided by microgrids and the smart grid via IoT are extremely wide.

Therefore, microgrids, through Internet of Things, are intended to bring several benefits such as reliability, cost efficiency, power quality, enhanced integration of renewable and distributed energy sources, and increased security for operators and users of the power grid and clean local energy generation.

But all these benefits must face various design and development challenges. So, the most important challenges for microgrid control and protection using IoT that arise with the development of these intelligent power networks include modeling, stability issues, bidirectional energy flows, week inertia and uncertainty.

This chapter is organized in five parts as follows. The first part of this chapter is an introduction in smart microgrids based on Internet of Things technology regarding their behavior and operation. The second part illustrates the impact of IoT in smart microgrids and smart grid over the last years with all the main challenges, approaches and benefits that this technology of interconnecting all the" things" in the world brought with it. The next two parts of this chapter will review the main applications, architectures and technologies using Internet of Things to manage microgrids through control and protection mechanisms. The last part concludes the chapter and draws some goals for future research directions.

31.2 Impact of Internet of Things (Iot) in Smart Microgrids

Over the years there had been several industrial revolutions along with the technological evolution. While the first industrial revolution refers at the steam-based machines and instruments, the second industrial revolution relies on the energy-based tools mass production. After these innovations, a huge step in the mankind evolution is the computer and internet-based learning which is the third industrial revolution. Internet of Things, in line with the 5G and Artificial Intelligence (AI), is right in the middle of the fourth industrial revolution that reveals the intelligence-based business models [25, 26].

Internet of Things technology aims for the interconnection of anything, anytime, anyone, any place, any service and any network through sensors and actuators with the purpose to develop smart domains [27–31].

To see what IoT means and how big it is meant to be, below is a short history of how "things" were connected in the last decades and what to expect to in the near future [25]:

- In 1975 there were 1 billion connected places thanks to invention of the telephone that started approximately a century ago;
- In 2000 there were 5 billion connected people thanks to the evolution of wireless communications;
- In 2020, few years from now, it is expected that over 50 billion devices to be connected thanks to IoT.

As a comparison, Fig. 31.2 pictures the main purpose of the IoT versus Machine to Machine (M2M) [26, 32]. From many M2M independent systems, the technology of Internet of Things brings these into one big connected structure. While M2M has vertical applications and it is hardware-based, IoT has horizontal functions and it is software-based. More, the IoT means not only a communication between machines, it means also a communication humans-machines and machines-humans that uses the cloud and Internet Protocol (IP) protocols. Therefore, M2M is essential for IoT, but M2M does not require IoT.

Internet of Things has applications in many domains as in Fig. 31.3 and here we focus on what this technology means for smart microgrids [25, 26, 33].

First of all, IoT is possible due to the fifth generation of wireless mobile technology, 5G, the so called "driver of the next generation smart grid" [34].

The 5G evolved as in Fig. 31.4 and its expectations include many features and updates as [25, 33]:

- Data rate—between 1 and 20 Gbps;
- Latency—1 to 10 ms;
- Availability—99.999% of time;
- Reliability—99.999% of packets;
- Security—network security, strong authentication, user privacy;
- Connection density—between 10 thousand and 1 million device per square kilometer;

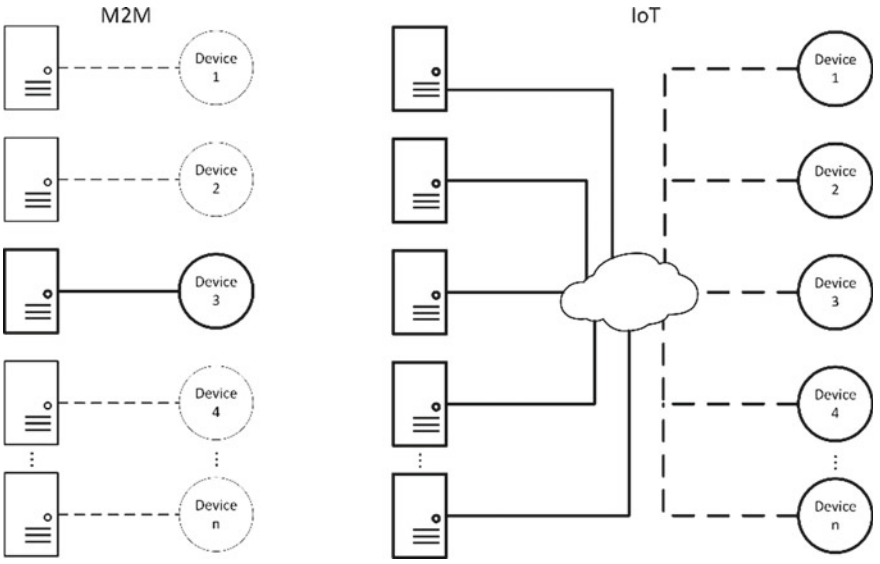

Fig. 31.2 M2M versus IoT

- Battery life—up to 10 years for low power IoT devices;
- Area traffic capacity—between 0.1 and 10 Mbps per square meter;
- User experienced data rate—between 10 and 100 Mbps.

Currently, a smart microgrid is about smart meters, e-billing and electronic communication platform. On the way to 5G, smart microgrid will have intelligent systems in order to ensure the management for generation, DER management in a secure shape and distribution automation. When 5G will be on, smart grid and smart microgrid will be about power generation and distribution automation through real-time load balancing and large-scale distributed generation services.

The impact of IoT and 5G technologies in smart microgrids translates in a list of confrontations that microgrids must face with [35]:

- Energy saving;
- Real-time power flow and statistics data;
- Reliable power system network;
- Advanced security and privacy;
- High flexibility;
- Big data to process and filter;
- Interoperability between standard energy and renewable energies;
- Self-healing techniques and systems.

More, according to [36], at a first look at the architecture of the 5G and its expectations, smart grid and smart microgrids must ensure three critical demands that are:

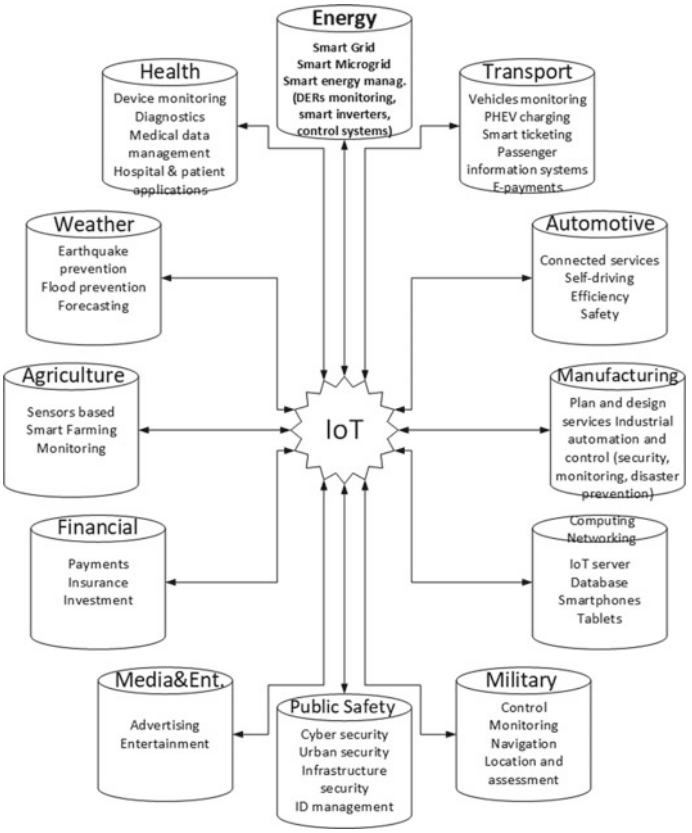

Fig. 31.3 Domains of applications for the Internet of Things concept

- Gigantic machine-type communication that interfaces billion of devices (50 billion expected in 2020);
- Gigantic broadband that distributes bandwidth of the order of gigaoctets or more when requested;
- Critical machine-type communication that must ensure prompt feedback with advanced reliability.

In line with all these challenges and requirements that a microgrid must face with, a report from 2015 [37], when the studies and tests for the 5G started, there are some aspects of commercial and technical changes in the social usage that will appear once with the infiltration of 5G and IoT in the power generation and distribution sector:

- Data is going to bey the key element for the industry of smart electricity. IoT will produce huge amount of real-time data and Big Data systems will analyze, process and filter this data up to each individual consumer. The junction between these two technologies will produce efficient energy management through low cost services;

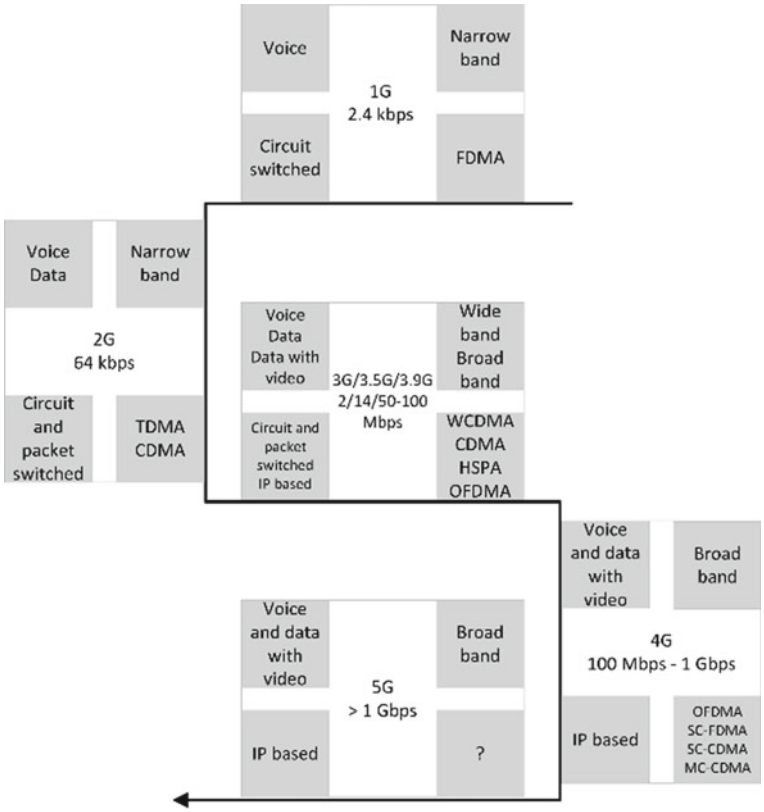

Fig. 31.4 Standards in the evolution of wireless communication systems

- The costs for consumers power storage will be affordable, while the management of this storage remains a challenge at microgrid level;
- "Individual" electricity will become "shared" electricity because users will not only produce their own power, they will probably share it to the demanders of the next levels;
- There will be a significant number of small power producers in line with the big utility companies, all for a decentralized system;
- The carbon dioxide emission will be reduced thanks to the efficient usage of local resources and to the diminution of non-renewable resources usage;
- The pricing strategies will be more flexible through, for example, real-time peak pricing or pas as you go;
- There will be different levels for the power supply, as low-cost supply, back-up supply, eco-friendly supply or classical supply and different level for data management and services;
- New services will be provided, such as predictive maintenance or consumption optimization;

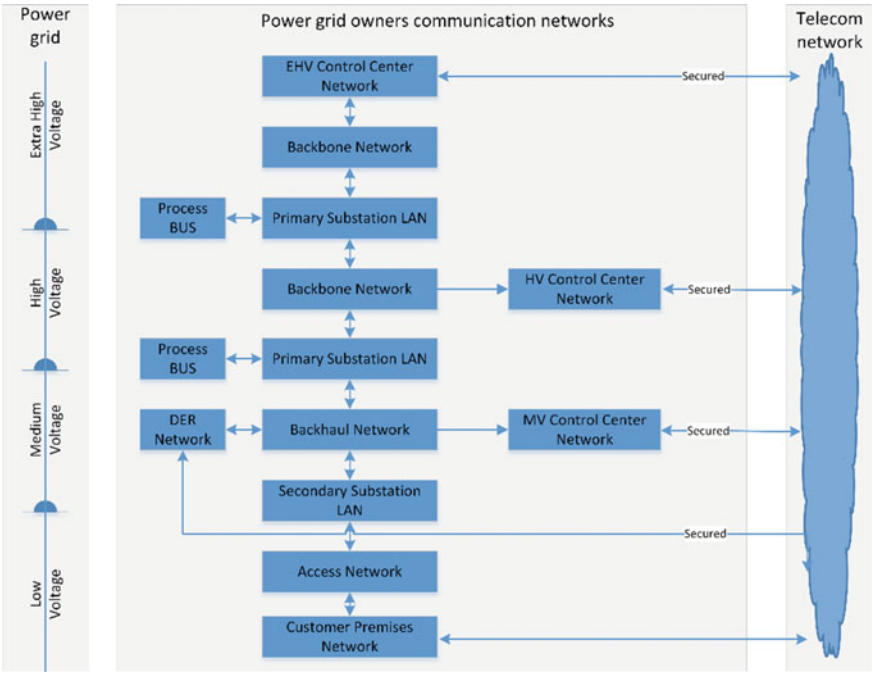

Fig. 31.5 A 5G communication network architecture for an intelligent power grid

- The intelligent grid will possess features as high efficiency and flexibility with the demanding dependency on the transmission quality, on the availability of high-quality data and on the analysis for transactions.

If we take a look at an intelligent power grid with accent on the communications network, there are two main communications networks:

- The communications network of the power grid owners;
- The telecommunications network via IoT and 5G;

Such an intelligent grid is illustrated (Fig. 31.5) [37]:

As a short summary, there are four impact challenges that the future communication network must deal with so that microgrids will function at the highest parameters:

- Resilience;
- Security;
- Robustness;
- Costs stability.

Smart microgrids via Internet of Things will have a huge impact on the control network and on the future power grid, that is the smart grid, because there will be a new perspective to produce, deliver and manage electricity either in island mode, either in grid-connected mode.

31.3 Controlling the Smart Microgrids via IoT

Usually, at a large scale, smart microgrids are viewed as individual items that can connect or disconnect to the main power grid, that is the smart grid, through different control mechanisms. Figure 31.6 reveals a general connection of a microgrid to the main grid with all the main components that need to be controlled via IoT [33].

Internet of Things has a very important role in controlling smart microgrids because these systems are very complex and require a two-way communication method [38–44]. As we are going to see in Fig. 31.7, IoT comes right in the key points of the diagram using different sensing technology and the latest communication protocols to understand, correct, improve and maintain the efficient behavior of the smart microgrids.

The control and monitor solution, proposed by [45], includes four monitor points (circles in Fig. 31.7) and a monitor center through sensor wires. In this way, the generation, the distribution, the energy storage and the loads are controlled in order to maintain a robust and resilient smart microgrid.

For each type of microgrid, regarding the distribution network current, either Alternative Current (AC), Direct Current (DC) or hybrid, there are three layers of control for almost every control mechanism depending on the time to perform certain actions and commands, as follows [46]:

- The primary layer—operations of the order of seconds and below;
- The second layer—operations of the order of seconds to minutes;
- The third layer—operations of the order of minutes to hours.

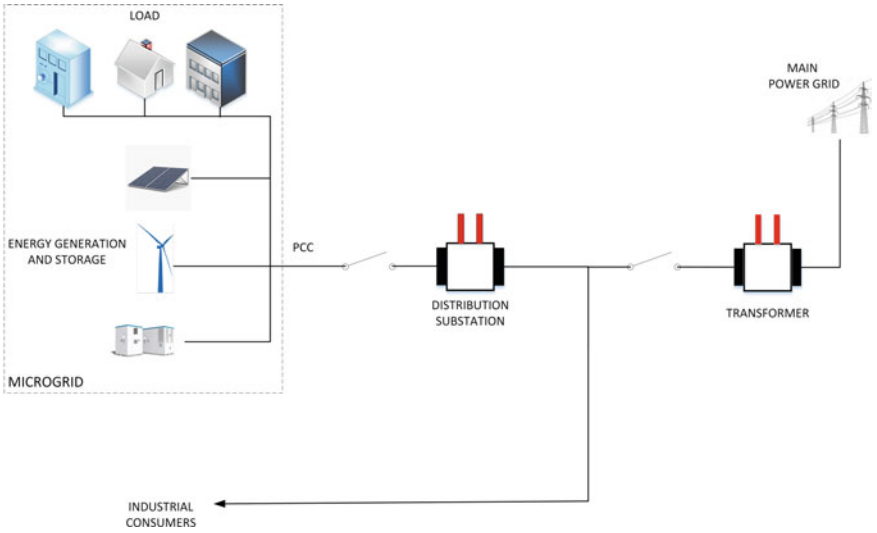

Fig. 31.6 A general microgrid diagram

The primary control manages the synergies between the single components of a microgrid (as sources, loads and storage) and the main grid. In this layer, each item sets and follows its own functioning parameters, such as frequency, voltage or power generation/consumption. The response time in this layer for different control actions has an average of milliseconds.

The second control layer deals with interactions between the components in the microgrid for adapting general microgrid voltages and frequencies that are managed by the first control layer.

The third layer interfaces the microgrid with the out world for certain control actions, such as load balancing, the time to enter in grid-connected mode or in stand-alone mode (island mode), economic dispatch of energy sources and so on.

All the control methods for smart microgrids, based on the three layers above, divide in three fundamental categories [38, 46]:

- Centralized control approaches—data is collected from the entire microgrid (Fig. 31.8) and then this data is analyzed in a central control unit that sends data to each sensor or item. On one hand, this approach is easy to design and implement and its maintenance is not very hard to manage, but only in case of concentrated and low-damaging failures. On the other hand, this approach is unstable, demands an increased level of connectivity and it is not easy to enlarge;
- Decentralized control approaches—in this case each subsystem of the microgrid has its own control unit to take different parametric decisions (Fig. 31.9). So, in this case there is no need for the information and data about the entire grid in order to take a decision. This method cannot promise to offer optimum stability and efficiency, but the biggest advantage relies in the privacy protection of subsystems. The pros of such methods are the parallel computation and the fact that there is no need for a two-way communication network. The cons are the medium scalability

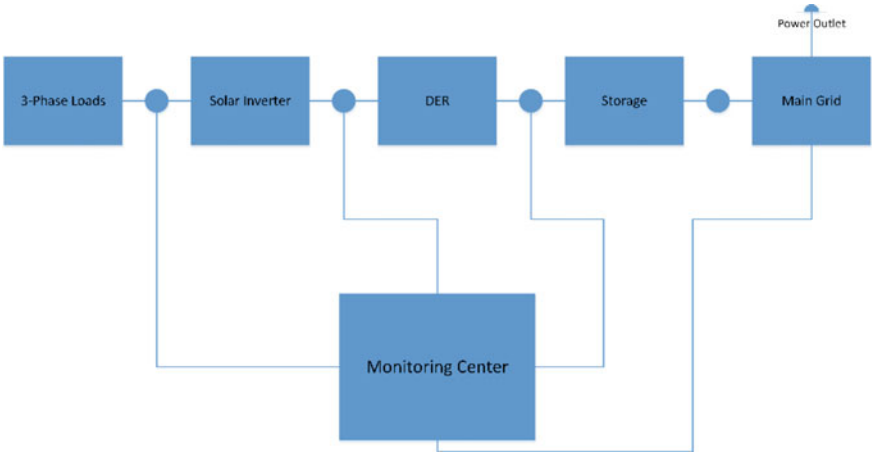

Fig. 31.7 Microgrid control and monitor

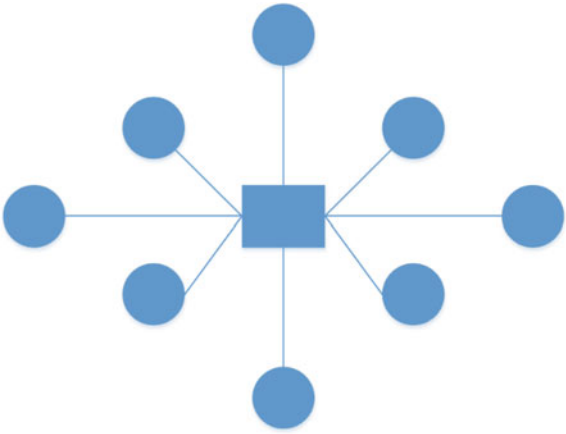

Fig. 31.8 Centralized control approach

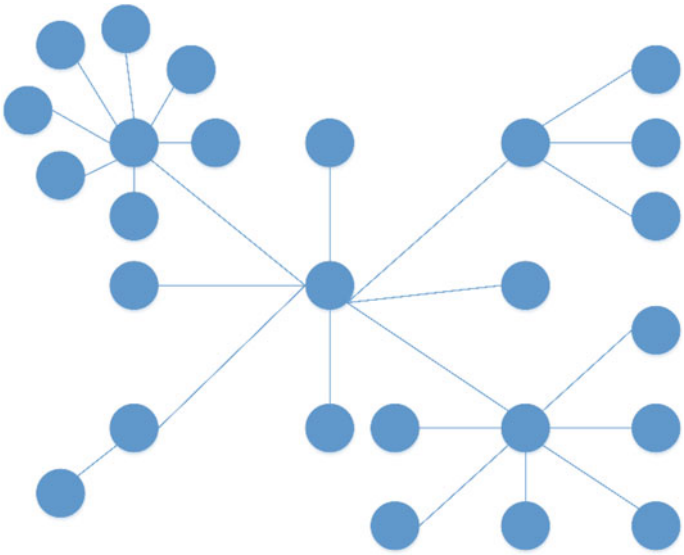

Fig. 31.9 Decentralized control approach

and low performance because of the lack of communication between important parts of the microgrid;

- Distributed control approaches—in these approaches, each part of the microgrid, such as users or DERs, handles information and data provided by its neighbors and locally measured parameters (Fig. 31.10). These methods are about information sharing so that the smart microgrid can achieve global optimization. The advantages of this case are: parallel calculation, easy to enlarge, there can be made

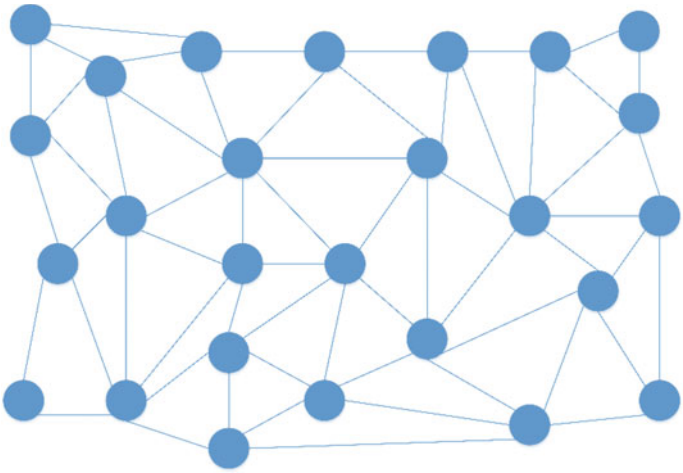

Fig. 31.10 Distributed control approach

any changes in the system topology and it is suitable for large scale systems. The disadvantages are the costs for upgrading the communication network, the need for synchronization and the need for the two-way communication network.

As an example, based on these control methods architectures, Fig. 31.11 shows a smart microgrid with a distributed control method where all the elements are connected via Internet of Things and 5G.

Apart from these control techniques that involve parameter and behavior control, there is another important aspect that requires advanced control: the power management of a smart microgrid. This management can be ensured through Demand Response (DR) and Demand Side Management (DSM) systems that are more and more feasible, due to the technological advances in the wireless communications, in DERs and in Distributed Energy Storage (DES) tools.

Most of the DR or DSM mechanisms are developed in order to minimize the power peak demand by switching from peak hours demand to non-peak hours demand. These systems can be seen as energy optimizers or energy balancers by reprogramming the energy request according to smart microgrids or according to the main grid.

A DR can either give feedbacks to changes in power prices over time, either give incentives from utilities that can have as a result the peak adjustment, for example. So, there are two DR methods: price-based and incentive-based. To implement such methods, the DSM scheme is used, that depends on the two-way communication methods between Wide Area Network (WAN), for the main grid side, and Home Area Network (HAN), for the customer side, as in Fig. 31.12.

After these control tools and mechanisms of smart microgrids it is necessary to see which are the protection challenges for a microgrid and also, what issues

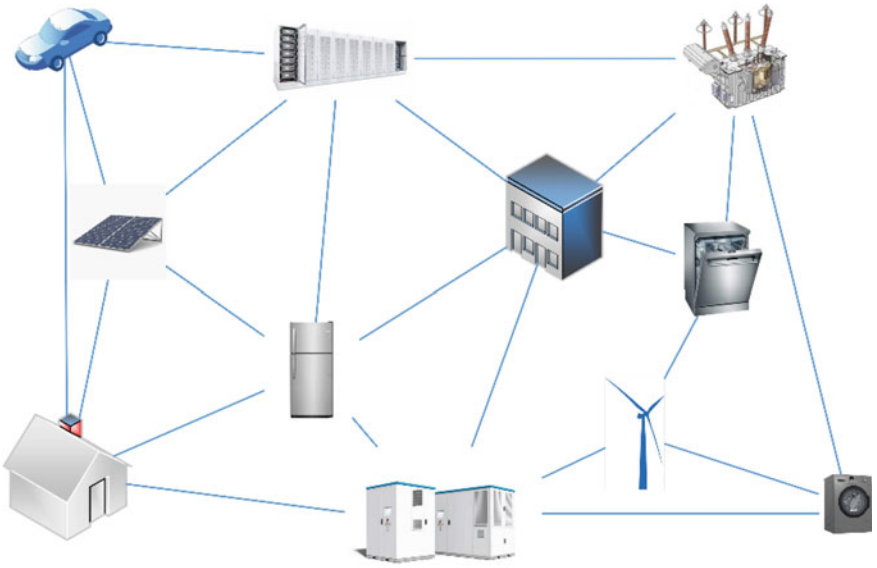

Fig. 31.11 Smart microgrid—distributed control method

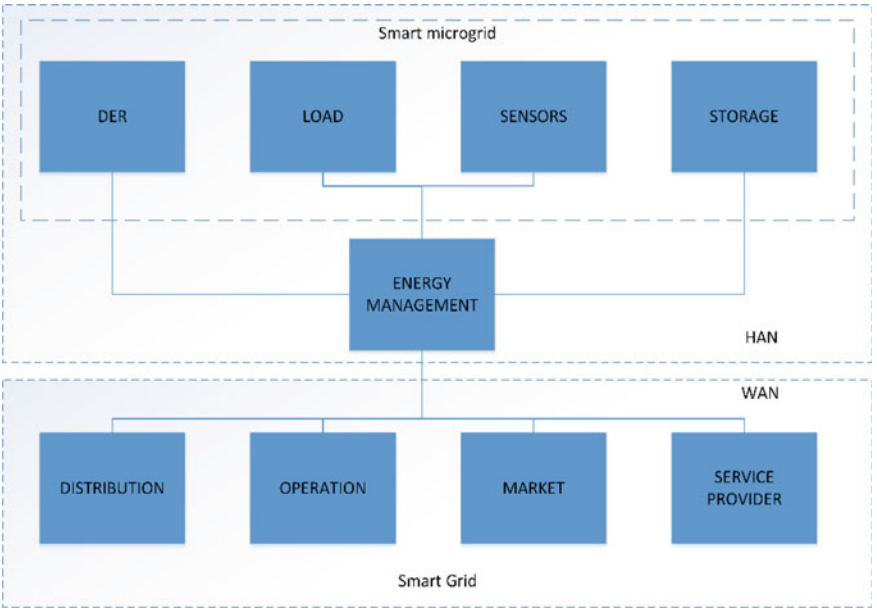

Fig. 31.12 DSM scheme

these systems encounter when trying to develop and implement different protecting mechanisms.

31.4 Protecting the Smart Microgrids via IoT

The protection system in a microgrid is the biggest challenge to achieve because of the complexity of interconnections and multiple power sources and loads. This protection system [47–54] must face microgrid faults as well as main grid faults and it must separate the microgrid from the main grid as soon as possible.

In order to an efficient protection of the microgrid, there is a must in pointing the main protection issues and threats that occur during the life-cycle of such a system [55, 56]:

- Islanding—this issue occurs when there are various faults in the power network and DER still generates power, although the microgrid is disconnected;
- Alterations in fault current level—this happens when multiple DERs that utilizes induction or synchronous generators are connected to the grid;
- Reverse power flow—because energy can flow in both directions, two DERs in the grid located in both sides of a load will generate energy that flows in opposite direction towards the load.
- Device discrimination—classical current protection method that uses the variation in magnitude of fault current for discrimination is not suitable for the microgrid;
- Single phase connection—when a DER generates single phase current that can affect three phase currents in the power network.

For IoT-based smart microgrids and smart grid there are different security issues and challenges because of the intelligent technologies' involvement in the old power grid. These security issues and challenges can slow down the development and integration of IoT-based power services.

The security issues that the intelligent grids and the main smart grid must deal with are listed below:

- Authorization and control access—attackers or even insiders, as it can be seen in [57] can try to access and manipulate different devices, sensors and tools since IoT-based energy grid is about remote-based configuration and monitoring methods;
- Availability—in case of Denial-of-Service (DoS) or Distributed Denial-of-Service (DDoS) attacks, important and vital parts of the grid will be totally or partially unavailable, because of the IoT and Internet Protocol (IP) protocol;
- Data tampering—this issue refers in changing sensitive data about power peak intervals and prices that can cause customer material damages or even overloads in the microgrid;
- Eavesdropping—attackers can try to access information between "things" in the network, since the public communication infrastructure is going to be used and not proprietary ones;

- Spoofing—a "thing" identity can be used in order to gain several advantages such as avoiding own power consumption payments or receiving sensitive data;
- Malicious code—this refers to infections that are built to affect devices and objects in the grid;
- Privacy—this issue is on the customers side because some smart appliances can use backdoors or hidden functions to monitor more that energy services;
- Cyber-attacks—these attacks are meant to affect physical entities and elements of the power grid and the IoT system.

Apart from security issues, when dealing with such a complex system, there are some serious challenges that must be considered, for an efficient and robust IoT-based intelligent grid:

- Mobility—nonstop authentication with the need of highly secured communication;
- Latency—some assets require real-time operations;
- Interoperability and heterogeneity—the addition of some tools so that different object can communicate. This will affect the end-to-end communication security;
- Constrained resources—most of the devices and tools in the smart microgrid are resource constrained dependent and there should be proper solutions adopted;
- Trust management—the need in a minimal trust level implementation for the communication of objects and devices controlled by different entities;
- Scalability—scalable security mechanisms is a serious challenge because of the large number of devices and "things" involved;
- Deployment—as a consequence of the scalability challenge, some devices will have zero physical protection as they will be controlled and monitored through remote methods.

In [58] there is a conceptual framework used to identify security challenges and threats for the intelligent power grid, illustrated in Fig. 31.13.

For a more technological approach, Table 31.1 reveals a detailed classification of the technical and non-technical security source of threats based on all the devices, tools and objects that defines and connects an IoT-based smart microgrid.

For all these protection issues, there are a series of solutions, through different technologies and architectures, meant to overpass and correct the presented issues, such as [55, 56]:

- Adaptive protection for microgrid;
- Inverter controller design;
- Differential protection scheme;
- Balanced combination of different types of DER units;
- Protection of inverter interfaced DER units;
- Protection scheme using differential and symmetrical of currents;
- Voltage-based protection;
- Distance protection;
- Pattern recognition-based protection.

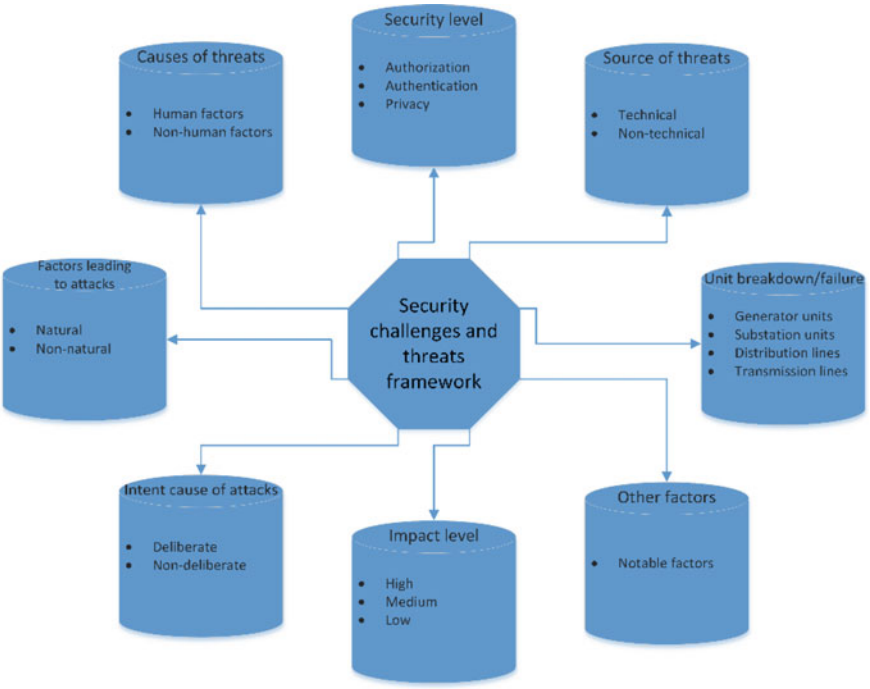

Fig. 31.13 Conceptual framework used to identify security threats and challenges of smart microgrids and smart grid

All these security challenges and issues are leading to a number of five security services, absolutely necessarily, that in an IoT-based intelligent grid must be developed, implemented and ensured:

- Authentication;
- Data confidentiality;
- Data integrity;
- Privacy;
- Authorization/access control.

Based on the information above, Fig. 31.14 shows a topology for intelligent protection of a microgrid, where the relays (R1–R9) and the DERs communicate with the central control and protections unit to record and monitor their status [59]. This topology must meet some safety requirements for an efficient control and protection of the microgrid regarding six important parameters, as in Fig. 31.15. These parameters are meant to detect and correct any situations that are not normal, to avoid equipment and tools damage, to provide backup protection and to maintain stability, either in island mode, either in grid-connected mode.

Table 31.1 Sources of threats classification for smart microgrids and smart grid

Technical source of threats	Infrastructural security	Cyber attacks
		Terrorism, theft
		Protection of power plants, transmission and distribution lines, Information and Communications Technology (ICT) devices, power
		Smart meter bypass
	Technical operational security	Operations reliability and resilience
		Security of data and analysis of the system
		Level of intelligence
		Routine check and maintenance
		Infrastructural installations and operations plan
		Control initiations
		Technical skills and qualification of the personnel
	Systems' data management security	Rules and regulations data policy
		Real time monitoring
		Data security against cyber attacks
		Customer privacy assurance
		Personnel privacy loyalty
Non-technical source of threats	Environmental security	Natural disasters
		Smart response in case of climate hazards
		Considerations in installation
	Government regulatory policies	Regulatory planning and policies
		Market operations
		Investment in the Research and Development (R&D) sector
		Economic, politic and social involvements in policy implementations

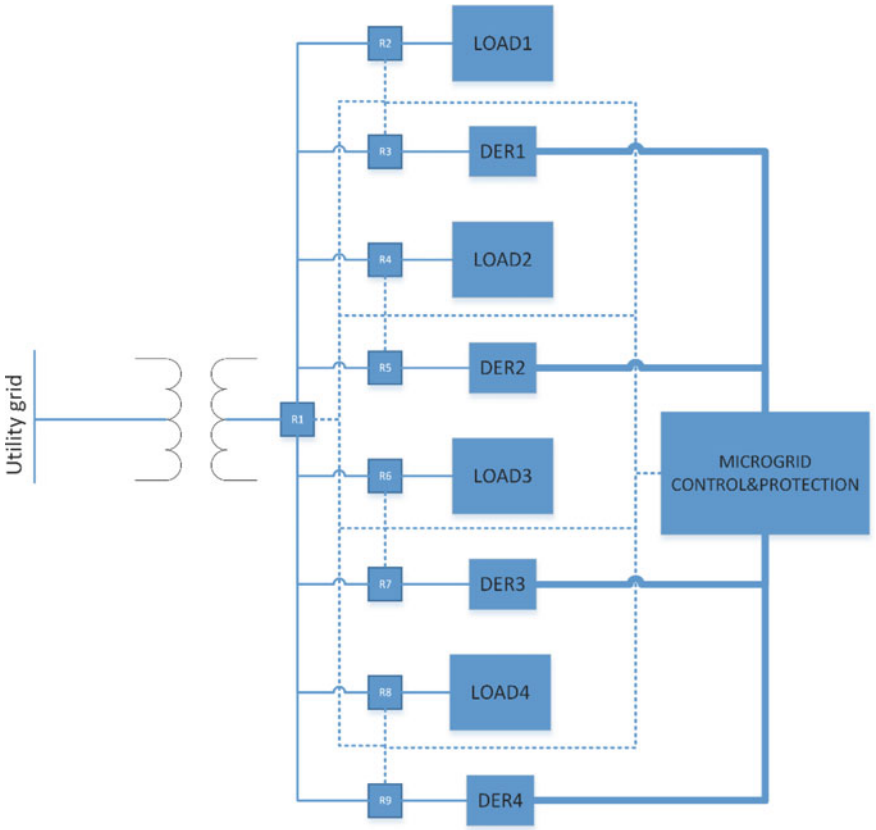

Fig. 31.14 Topology for a microgrid control and protection system

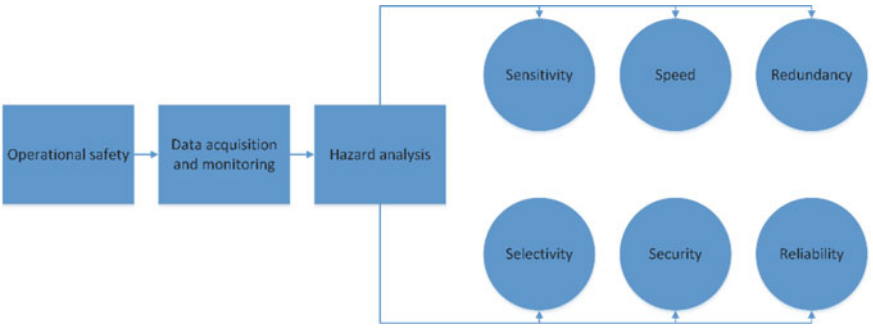

Fig. 31.15 Microgrid safety design

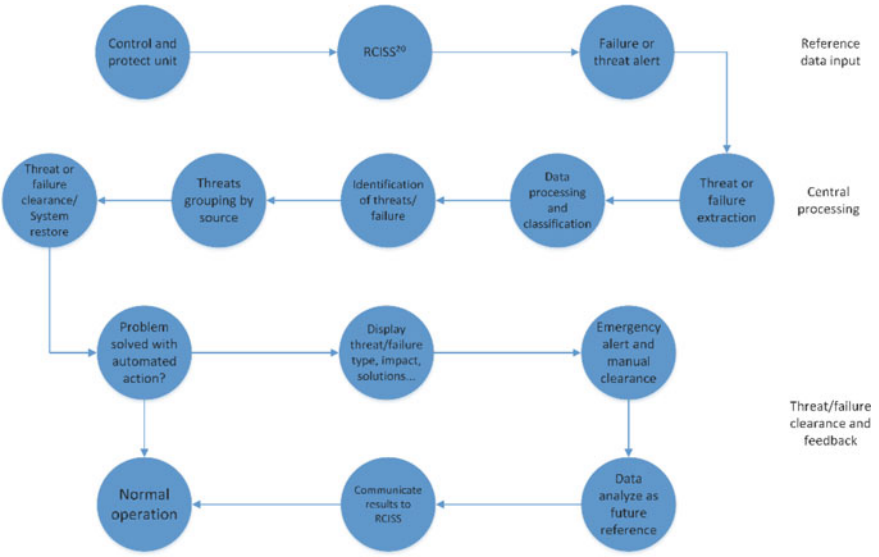

Fig. 31.16 Framework for the smart grid and smart microgrids security used to detect and clear threats and failures (reference control input and support system)

In [60] there are presented four principles to secure and protect a microgrid:

- Harden the microgrid—physical protection (tamper-proof devices, walls, surveillance), mitigation of insider threats, interoperability, standardization;
- Complete ongoing assessments of interconnection security mechanisms;
- Plan and prepare for each type of disaster recovery;
- Resource the security strategy—security operations and engineering, incident response operations, compliance, awareness.

Another framework for the microgrids security (Fig. 31.16) helps to identify and clear detected threats for a proper behavior of the power grid through IoT via different intelligent mechanisms used to detect, display and respond to the specific fault or threat [58].

All these methods, architectures and applications are built with the purpose to build robust, highly secured and resilient smart microgrids that can face to various failures and challenges such as complex cyber-attacks or different other factors and causes.

31.5 Conclusion

Internet of Things has a very important role in developing smart microgrids due to the technological impact that comes with and to the endless smart possibilities that

are arising every day. In energy terms, IoT via 5G means smart grid, smart microgrid and smart energy management with the big challenge in handling a huge number of devices and a huge amount of data.

An important provocation remains and it will persist many years from now, the need in controlling and protecting these intelligent power grid with the help of Internet of Things.

Different architectures were presented during this chapter for efficient control and intelligent protection for the microgrids, with capabilities in detecting and responding through many threats and failures.

Microgrids, through Internet of Things, are aiming for a variety of benefits including the enhanced integration of renewable and distributed energy sources, power quality, clean local energy generation, reliability, cost efficiency and increased security for operators and users of the power grid.

References

1. D.T. Ton, M.A. Smith, The US department of energy's microgrid initiative. Electricity J. **25**, 84–94 (2012)
2. https://www.energy.gov/sites/prod/files/2016/06/f32/The%20US%20Department%20of%20Energy%27s%20Microgrid%20Initiative.pdf
3. A. Hirsch, Y. Parag, J. Guerrero, Microgrids: a review of technologies, key drivers, and outstanding issues. Renew. Sustain. Energy Rev. **90**, 402–411 (2018)
4. S. Chowdhury, S.P. Chowdhury, P. Crossley, *Microgrids and Active Distribution Networks*. IET Renewable Energy Series (2009)
5. F. Martin Martinez, A. Sanchez Miralles, M. Rivier, A review of the technologies involved in microgrid that has a small section dedicated to the definitions of the microgrid. Renew. Sustain. Energy Rev. **62(C)**, 1133–1153 (2016), https://doi.org/10.1016/j.rser.2016.05.025, https://www.google.com/url?sa=t&rct=j&q=&esrc=s&source=web&cd=4&ved=2ahUKEwizs52XhvPiAhUCLlAKHcK0DAAQFjADegQIAhAC&url=https%3A%2F%2Fvbn.aau.dk%2Ffiles%2F287478138%2F1_s2.0_S136403211830128X_main.pdf&usg=AOvVaw3N5Xieg15IqQsDKavmgEpI
6. https://building-microgrid.lbl.gov/about-microgrids
7. https://www.hindawi.com/journals/je/2013/937614/
8. https://building-microgrid.lbl.gov/types-microgrids
9. https://en.wikipedia.org/wiki/Microgrid
10. https://dspace.cc.tut.fi/dpub/bitstream/handle/123456789/23938/turunen.pdf?sequence=1
11. F. Georgel Birleanu, P. Anghelescu, N. Bizon, E. Pricop, in *Handbook of Smart Grid Communications*, ed. by E. Kabalci, Y. Kabalci. Cyber Security Objectives and Requirements for Smart Grid (Springer London Limited, 2019)
12. N. Bizon, N. Mahdavi Tabatabaei, F. Blaabjerg, E. Kurt (Ed.), *Energy Harvesting and Energy Efficiency: Technology, Methods and Applications* (Springer London Limited, 2017)
13. N. Mahdavi Tabatabaei, N. Bizon, A.J. Aghbolaghi, F. Blaabjerg (eds.), *Fundamentals and Contemporary Issues of Reactive Power Control in AC Power Systems* (Springer London Limited, 2017)
14. N. Bizon, L. Dascalescu, N. Mahdavi Tabatabaei (eds.), *Autonomous Vehicles: Intelligent Transport Systems and Smart Technologies* (Nova Science Publishers Inc., USA, 2014)
15. N. Bizon, N. Mahdavi Tabatabaei (eds.), *Advances in Energy Research: Energy and Power Engineering* (Nova Science Publishers Inc., USA, 2013)

16. N. Bizon (ed.), *Advances in Energy Research: Distributed Generation systems integrating Renewable Energy Resources*, 3 chapters by N. Bizon (Nova Science Publishers Inc., USA, 2012)
17. L. Davoli, L. Belli, A. Cilfone, G. Ferrari, Integration of Wi-Fi mobile nodes in a Web of Things Testbed. KICS – ICT Express **2**, 96–99 (2016)
18. A. Carvallo, J. Cooper, *The Advanced Smart Grid—Edge Power Driving Sustainability* (Artech House 2011)
19. F.P. Sioshansi, *Smart Grid—Integrating Renewable, Distributed, & Efficient Energy* (Springer, 2012)
20. D.E. Kouicem, A. Bouabdallah, H. Lakhlef, A lab demonstration from national instruments to control and monitor the behaviour of microgrids that includes a demo block diagram in order to achieve the proposed goal. Comput. Netw. **141**, 199–221 (2018), https://doi.org/10.1016/j.comnet.2018.03.012, https://www.sciencedirect.com/science/article/abs/pii/S1389128618301208, https://www.google.com/url?sa=t&rct=j&q=&esrc=s&source=web&cd=1&ved=2ahUKEwivp6ibifPiAhVJsKQKHVg7BAIQFjAAegQIARAC&url=http%3A%2F%2Fdownload.ni.com%2Fpub%2Fiot%2FIIoT_Lab_Control_and_Monitor_Microgrids.pdf&usg=AOvVaw3rauNlcAiQ3aHhRCo-y_M7
21. S.S. Reka, T. Dragicevic, Future effectual role of energy delivery: a comprehensive review of Internet of Things and smart grid. Renew. Sustain. Energy Rev. **91**, 90–108 (2018)
22. B. Hong, W. Zhang, Y. Zhou, J. Chen, Y. Xiang, Y. Mu, Energy-Internet-oriented microgrid energy management system architecture and its application in China. Appl. Energy **228**, 2153–2164 (2018)
23. H. Hellaoui, M. Koudil, A. Bouabdallah, Energy-efficient mechanisms in security of the internet of things: a survey. Comput. Netw. **127**, 173–189 (2017)
24. H. Boyes, B. Hallaq, J. Cunningham, T. Watson, The industrial internet of things (IIoT): an analysis framework. Comput. Ind. **101**, 1–12 (2018)
25. V. Tsiatsis, S. Karnouskos, J. Holler, D. Boyle, C. Mulligan, Internet of Things, 2nd edn. *Technologies and Applications for a New Age of Intelligence*. 26th November 2018, eBook ISBN: 9780128144367, Paperback ISBN: 9780128144350 (Academic Press, 2018)
26. M. Tornqvist, Energy, *IoT and 5G—Everything is Connected* (Ericsson, 2018)
27. C. Pfister, *Getting Started with the Internet of Things* (Maker Media, Inc, May 2011) ISBN: 9781449301972, https://www.oreilly.com/library/view/getting-started-with/9781449301972/, https://www.google.com/url?sa=t&rct=j&q=&esrc=s&source=web&cd=1&ved=2ahUKEwiRk6X2vPPiAhXoAxAIHRLfC1sQFjAAegQIBRAC&url=https%3A%2F%2Fwww.accenture.com%2F_acnmedia%2FPDF-27%2FAccenture_DEG-Microgrid-Security_POV_FINAL.pdf&usg=AOvVaw31CsU4PI_gy-8G2izyoaS3
28. A.R. Al Ali, Internet of Things role in the renewable energy resources. Energy Procedia **100**, 34–38 (2016)
29. F.F. Wu, P.P. Varaiya, R.S.Y. Hui, Smart grids with intelligent periphery: an Architecture for the energy internet. Engineering **1**(4), 436–446 (2015)
30. A. Magruk, The most important aspects of uncertainty in the Internet of Things field—context of smart buildings. Procedia Eng. **122**, 220–227 (2015)
31. E. Borgia, The Internet of Things vision: key features, applications and open issues. Comput. Commun. **54**, 1–31 (2014)
32. https://internetofthingsagenda.techtarget.com/definition/machine-to-machine-M2M
33. https://www.researchgate.net/publication/301573997_Microgrid_State_Estimation_Using_the_IoT_with_5G_Technology
34. https://www.engerati.com/transmission-and-distribution/article/communications-networks-technologies/5g-%E2%80%93-driver-next
35. https://www.slideshare.net/SenZationsSummerSchoolonIoTNo1/iot-and-5g-opportunities-and-challenges-senzations-2015
36. H.C. Leligou, T. Zahariadis, L. Sarakis, E. Tsampasis, A. Voulkidis, T. Velivassaki, Smart Grid: A Demanding Use Case for 5G Technologies, in *IEEE PerCom Workshop on Pervasive Sensing for Sustainable Smart Cities and Smart Buildings* (Athens, Greece, March 2018)

37. G Infrastructure Association, 5G and Energy (2015), https://5g-ppp.eu/wp-content/uploads/2014/02/5G-PPP-White_Paper-on-Energy-Vertical-Sector.pdf
38. H. Pourbabak, T. Chen, B. Zhang, W. Su, *Control and Energy Management System in Microgrids* (2017), https://doi.org/10.1049/pbpo090e_ch3
39. S. Park, B. Kang, M. Choi, S. Jeon, A micro-distributed ESS-based smart LED streetlight system for intelligent demand management of the micro grid. Sustain. Cities Soc. **39**, 801–813 (2018)
40. I. Khajenasiri, A. Estebsari, M. Verhelst, G. Gielen, A review on Internet of Things solutions for intelligent energy control in buildings for smart city applications. Energy Procedia **111**, 770–779 (2017)
41. A. Chakrabortty, M.D. Ilie, *Control and Optimization Methods for Electric Smart Grids* (Springer, 2012)
42. C.W. Gellings, *The Smart Grid: Enabling Energy Efficiency and Demand Response* (The Fairmont Press, 2009)
43. S.H. Nandipati, P.T. Babu, M. Chigurupati, C. Vaithilingam, Interface protection and energy management system for microgrid using Internet of Things. Energy Procedia **117**, 201–208 (2017)
44. J. Schulz, R.S.H. Popp, V.M. Scharmer, F. Zaeh, An IoT based approach for energy flexible control of production systems. Procedia CIRP **69**, 650–655 (2018)
45. National Instruments, *Control and Monitor Microgrids—An NI Industrial IoT Lab Demonstration* (2017)
46. L. Shaver, *Implementation of a DC Microgrid* (University of Wisconsin-Madison, 2017)
47. Y. Song, J. Lin, M. Tang, S. Dong, An Internet of energy things based on wireless LPWAN. Engineering **3**, 460–466 (2017)
48. S.N. Islam, M.A. Mahmud, A.M.T. Oo, Impact of optimal false data injection attacks on local energy trading in a residential microgrid. KICS—ICT Express **4**, 30–34 (2018)
49. M. Banerjee, J. Lee, K.K.R. Choo, A Blockchain future to Internet of Things security: a position paper. Digit. Commun. Netw. (2017)
50. L. Urquhart, D. McAuley, Avoiding the internet of insecure industrial things. Comput. Law Secur. Rev. (2017)
51. K. Friansa, I.N. Haq, B.M. Santi, D. Kurniadi, E. Leksono, B. Yuliarto, Development of battery monitoring system in smart microgrid based on Internet of Things (IoT). Procedia Eng. **170**, 482–487 (2017)
52. S. Bennati, E. Pournaras, Privacy-enhancing aggregation of Internet of Things data via sensors grouping. Sustain. Cities Soc. **39**, 387–400 (2018)
53. M. Jaradat, M. Jarrah, A. Bousseelham, Y. Jararweh, M. Al Ayyoub, The internet of energy: smart sensor networks and big data management for smart grid. Procedia Comput. Sci. **56**, 592–597 (2015)
54. F. Birleanu, N. Bizon, Principles, architectures and challenges for ensuring the integrity, internal control and security of embedded systems. J. Electr. Eng. Electron. Control Comput. Sci. (JEEECCS) **3**(7), 37–45 (2017)
55. S. Turunen, *Protection of Microgrids and Distributed Energy Resources Based on IEC 61850* (Tampere University of Technology, 2016)
56. P.A. Kumar, J. Shankar, Y. Nagaraju, Protection issues in microgrid. Int. J. Appl. Control Electr. Electron. Eng. **1**(1) (2013)
57. F. Georgel Birleanu, P. Anghelescu, N. Bizon, in *Handbook of Power Systems Resiliency: Modeling, Analysis and Practice*, ed. by N. Mahdavi Tabatabaei, S. Najafi Ravadanegh, N. Bizon. Malicious and Deliberate Attacks and Power System Resiliency (Springer London Limited, 2018)
58. A.O. Otuoze, M.W. Mustafa, R.M. Larik, Smart grids security challenges: classification by sources of threats. J. Electr. Syst. Inf. Technol. Sci. Direct (2017)
59. M.R. Islam, H.A. Gabbar, Study of micro grid safety & protection strategies with control system infrastructures. Smart Grid Renew. Energy **3**, 1–9 (2012)
60. Accenture, *Cyber-Physical Security for the Microgrid* (2016)

Correction to: Microgrid Planning and Modeling

Ali Jafari Aghbolaghi, Naser Mahdavi Tabatabaei, Morteza Kalantari Azad, Mozhgan Tarantash and Narges Sadat Boushehri

Correction to:
Chapter 2 in: N. Mahdavi Tabatabaei et al. (eds.), *Microgrid Architectures, Control and Protection Methods*, Power Systems, https://doi.org/10.1007/978-3-030-23723-3_2

The original version of this book was published with an older version of the abstract in Chapter 2. This has now been corrected and updated.

The updated version of this chapter can be found at https://doi.org/10.1007/978-3-030-23723-3_2

N. Mahdavi Tabatabaei et al. (eds.), *Microgrid Architectures, Control and Protection Methods*, Power Systems,
https://doi.org/10.1007/978-3-030-23723-3_32

Index

N. Mahdavi Tabatabaei et al. (eds.), *Microgrid Architectures, Control and Protection Methods*, Power Systems,
https://doi.org/10.1007/978-3-030-23723-3